IMMUNITY TO HUMAN FUNGAL PATHOGENS: MECHANISMS OF HOST RECOGNITION, PROTECTION, PATHOLOGY, AND FUNGAL INTERFERENCE

EDITED BY: Steven P. Templeton, Amariliz Rivera, Bernard Hube and Ilse D. Jacobsen

PUBLISHED IN: Frontiers in Immunology and Frontiers in Microbiology

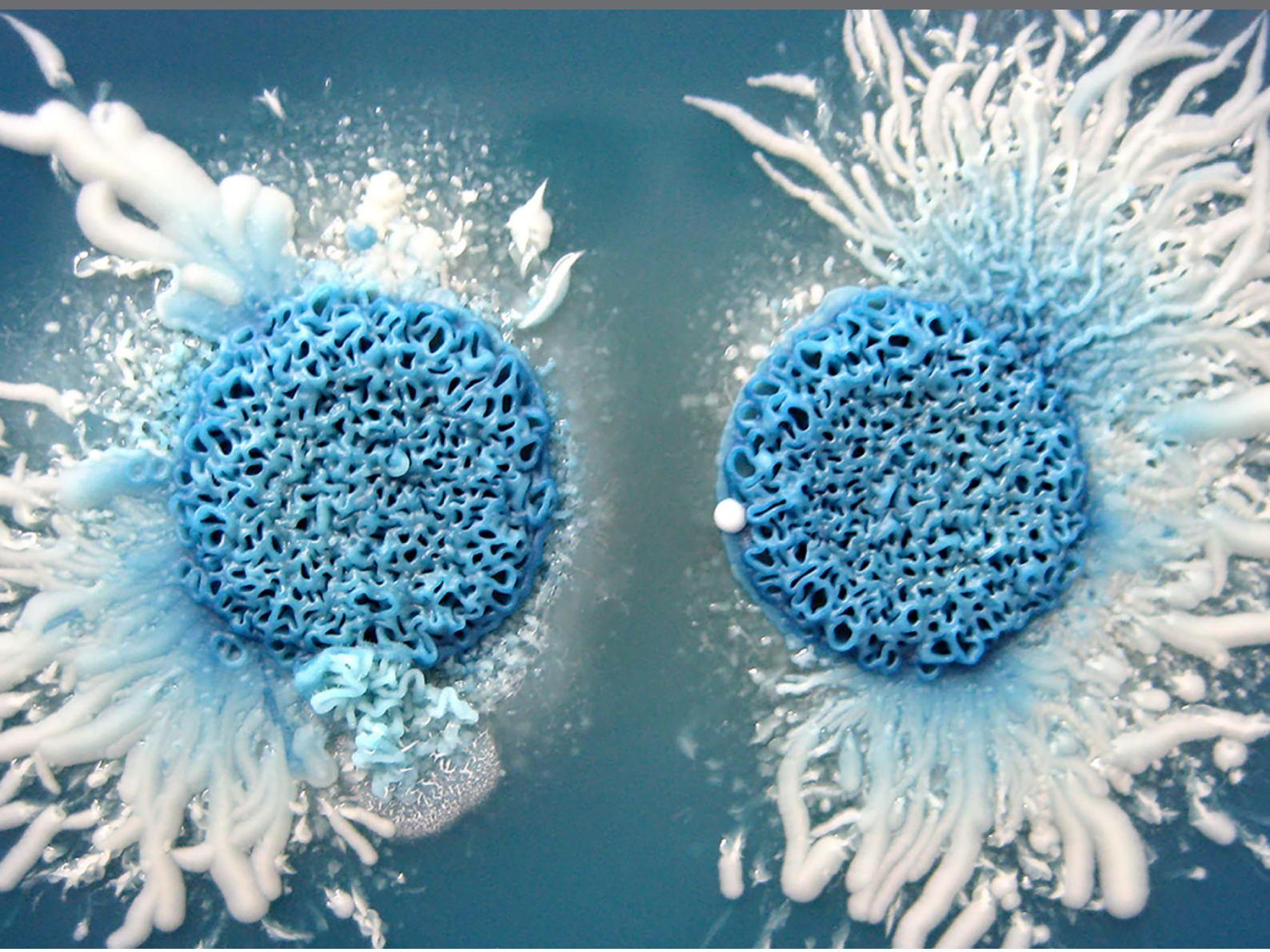

frontiers Research Topics

frontiers

Frontiers Copyright Statement

© Copyright 2007-2019 Frontiers Media SA. All rights reserved.

All content included on this site, such as text, graphics, logos, button icons, images, video/audio clips, downloads, data compilations and software, is the property of or is licensed to Frontiers Media SA ("Frontiers") or its licensees and/or subcontractors. The copyright in the text of individual articles is the property of their respective authors, subject to a license granted to Frontiers.

The compilation of articles constituting this e-book, wherever published, as well as the compilation of all other content on this site, is the exclusive property of Frontiers. For the conditions for downloading and copying of e-books from Frontiers' website, please see the Terms for Website Use. If purchasing Frontiers e-books from other websites or sources, the conditions of the website concerned apply.

Images and graphics not forming part of user-contributed materials may not be downloaded or copied without permission.

Individual articles may be downloaded and reproduced in accordance with the principles of the CC-BY licence subject to any copyright or other notices. They may not be re-sold as an e-book.

As author or other contributor you grant a CC-BY licence to others to reproduce your articles, including any graphics and third-party materials supplied by you, in accordance with the Conditions for Website Use and subject to any copyright notices which you include in connection with your articles and materials.

All copyright, and all rights therein, are protected by national and international copyright laws.

The above represents a summary only. For the full conditions see the Conditions for Authors and the Conditions for Website Use.

ISSN 1664-8714
ISBN 978-2-88945-682-6
DOI 10.3389/978-2-88945-682-6

About Frontiers

Frontiers is more than just an open-access publisher of scholarly articles: it is a pioneering approach to the world of academia, radically improving the way scholarly research is managed. The grand vision of Frontiers is a world where all people have an equal opportunity to seek, share and generate knowledge. Frontiers provides immediate and permanent online open access to all its publications, but this alone is not enough to realize our grand goals.

Frontiers Journal Series

The Frontiers Journal Series is a multi-tier and interdisciplinary set of open-access, online journals, promising a paradigm shift from the current review, selection and dissemination processes in academic publishing. All Frontiers journals are driven by researchers for researchers; therefore, they constitute a service to the scholarly community. At the same time, the Frontiers Journal Series operates on a revolutionary invention, the tiered publishing system, initially addressing specific communities of scholars, and gradually climbing up to broader public understanding, thus serving the interests of the lay society, too.

Dedication to Quality

Each Frontiers article is a landmark of the highest quality, thanks to genuinely collaborative interactions between authors and review editors, who include some of the world's best academicians. Research must be certified by peers before entering a stream of knowledge that may eventually reach the public - and shape society; therefore, Frontiers only applies the most rigorous and unbiased reviews.
Frontiers revolutionizes research publishing by freely delivering the most outstanding research, evaluated with no bias from both the academic and social point of view. By applying the most advanced information technologies, Frontiers is catapulting scholarly publishing into a new generation.

What are Frontiers Research Topics?

Frontiers Research Topics are very popular trademarks of the Frontiers Journals Series: they are collections of at least ten articles, all centered on a particular subject. With their unique mix of varied contributions from Original Research to Review Articles, Frontiers Research Topics unify the most influential researchers, the latest key findings and historical advances in a hot research area! Find out more on how to host your own Frontiers Research Topic or contribute to one as an author by contacting the Frontiers Editorial Office: researchtopics@frontiersin.org

IMMUNITY TO HUMAN FUNGAL PATHOGENS: MECHANISMS OF HOST RECOGNITION, PROTECTION, PATHOLOGY, AND FUNGAL INTERFERENCE

Topic Editors:
Steven P. Templeton, Indiana University School of Medicine—Terre Haute, United States
Amariliz Rivera, Rutgers—The State University of New Jersey, United States
Bernard Hube, Leibniz Institute for Natural Product Research and Infection Biology—Hans Knöll Institute, Friedrich Schiller University, Germany
Ilse D. Jacobsen, Leibniz Institute for Natural Product Research and Infection Biology—Hans Knöll Institute, Friedrich Schiller University, Germany

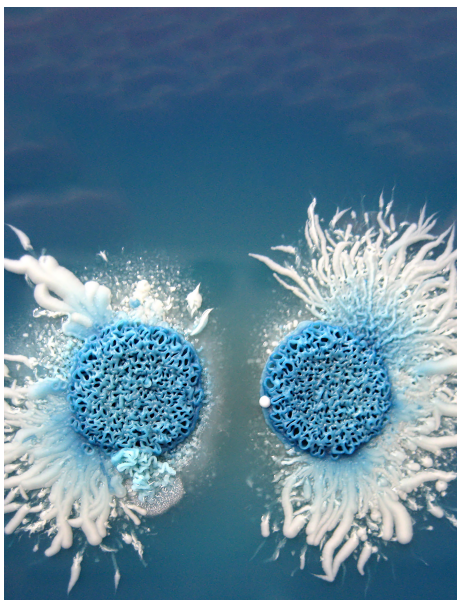

Candida albicans cultured on growth media containing bromocresol green to detect alkalinization (blue). Image: Mayer (2012).

Mayer, F., Wilson, D., Jacobsen, I., Miramón, P., Große, K., & Hube, B. (2012). The Novel Candida albicans Transporter Dur31 Is a Multi-Stage Pathogenicity Factor. *Plos Pathogens*, 8(3), e1002592. doi: 10.1371/journal.ppat.1002592
PMID: 22438810

Fungi are found in virtually every environment, and comprise a significant portion of the normal microflora of healthy individuals. Some species of fungi are aeroallergen sources capable of inducing sensitization and causing exacerbation of asthma and respiratory allergy. Others are transmissible between hosts and may cause no symptoms in healthy individuals. However, immune suppressed individuals may develop invasive disease marked by tissue invasion with a potential for widespread dissemination. Existing therapies for patients consist of antifungal drugs, yet these require prolonged administration with the possibility of adverse side effects, and may be rendered ineffective by the emergence of antifungal-resistant strains. It is therefore of interest to increase our understanding of host-pathogen interactions

in order to facilitate the development of new therapies for individuals suffering from fungal infection and disease. These early interactions are shaped by an array of constituent and secreted factors that stimulate or inhibit host immune responses toward protective or detrimental immunity. Likewise, an array of preformed factors and tissue-resident cells provide early protection from fungal infection and provide extracellular signals that result in localized recruitment of inflammatory cells and determine the character of subsequent adaptive antifungal immunity.

This Research Topic explores the host and fungal pathways that program innate and adaptive immunity and the immune cells, molecules, and regulatory pathways that comprise protective or detrimental responses to fungal exposure or infection. Over 200 authors contributed reviews, opinions, or original research focusing on antifungal immunity in humans and in experimental models. We believe that the results of these efforts provide a benchmark for further advances and improved antifungal therapies.

Citation: Templeton, S. P., Rivera, A., Hube, B., Jacobsen, I. D., eds. (2019). Immunity to Human Fungal Pathogens: Mechanisms of Host Recognition, Protection, Pathology, and Fungal Interference. Lausanne: Frontiers Media. doi: 10.3389/978-2-88945-682-6

Table of Contents

08 ***Editorial: Immunity to Human Fungal Pathogens: Mechanisms of Host Recognition, Protection, Pathology, and Fungal Interference***
Steven P. Templeton, Amariliz Rivera, Bernard Hube and Ilse D. Jacobsen

12 ***Regulation of C-Type Lectin Receptor-Mediated Antifungal Immunity***
Juan Tang, Guoxin Lin, Wallace Y. Langdon, Lijian Tao and Jian Zhang

24 ***The Syk-Coupled C-Type Lectin Receptors Dectin-2 and Dectin-3 are Involved in* Paracoccidioides brasiliensis *Recognition by Human Plasmacytoid Dendritic Cells***
Nycolas Willian Preite, Claudia Feriotti, Dhêmerson Souza de Lima, Bruno Borges da Silva, Antônio Condino-Neto, Alessandra Pontillo, Vera Lúcia Garcia Calich and Flávio Vieira Loures

38 ***The Major Chromoblastomycosis Etiologic Agent* Fonsecaea pedrosoi *Activates the NLRP3 Inflammasome***
Raffael Júnio Araújo de Castro, Isaque Medeiros Siqueira, Márcio Sousa Jerônimo, Angelina Maria Moreschi Basso, Paulo Henrique de Holanda Veloso Junior, Kelly Grace Magalhães, Luiza Chaves Leonhardt, Stephan Alberto Machado de Oliveira, Pedro Henrique Bürgel, Aldo Henrique Tavares and Anamélia Lorenzetti Bocca

54 ***NOD-Like Receptor P3 Inflammasome Controls Protective Th1/Th17 Immunity Against Pulmonary Paracoccidioidomycosis***
Claudia Feriotti, Eliseu Frank de Araújo, Flavio Vieira Loures, Tania Alves da Costa, Nayane Alves de Lima Galdino, Dario Simões Zamboni and Vera Lucia Garcia Calich

69 ***Canonical Stimulation of the NLRP3 Inflammasome by Fungal Antigens Links Innate and Adaptive B-Lymphocyte Responses by Modulating IL-1ß and IgM Production***
Mohamed F. Ali, Harika Dasari, Virginia P. Van Keulen and Eva M. Carmona

81 ***The Absence of NOD1 Enhances Killing of* Aspergillus fumigatus *Through Modulation of Dectin-1 Expression***
Mark S. Gresnigt, Martin Jaeger, R. K. Subbarao Malireddi, Orhan Rasid, Grégory Jouvion, Catherine Fitting, Willem J. G. Melchers, Thirumala-Devi Kanneganti, Agostinho Carvalho, Oumaima Ibrahim-Granet and Frank L. van de Veerdonk

95 ***FIBCD1 Binds* Aspergillus fumigatus *and Regulates Lung Epithelial Response to Cell Wall Components***
Christine Schoeler Jepsen, Lalit Kumar Dubey, Kimmie B. Colmorten, Jesper B. Moeller, Mark A. Hammond, Ole Nielsen, Anders Schlosser, Steven P. Templeton, Grith L. Sorensen and Uffe Holmskov

109 ***Innate Immunity Induced by the Major Allergen Alt a 1 From the Fungus* Alternaria *is Dependent Upon Toll-Like Receptors 2/4 in Human Lung Epithelial Cells***
Tristan Hayes, Amanda Rumore, Brad Howard, Xin He, Mengyao Luo, Sabina Wuenschmann, Martin Chapman, Shiv Kale, Liwu Li, Hirohito Kita and Christopher B. Lawrence

120 ***Tissue-Resident Macrophages in Fungal Infections***
Shengjie Xu and Mari L. Shinohara

127 ***Interaction of THP-1 Monocytes With Conidia and Hyphae of Different* Curvularia *Strains***
Eszter Judit Tóth, Éva Boros, Alexandra Hoffmann, Csilla Szebenyi, Mónika Homa, Gábor Nagy, Csaba Vágvölgyi, István Nagy and Tamás Papp

136 ***Involvement of Dihydrolipoyl Dehydrogenase in the Phagocytosis and Killing of* Paracoccidioides brasiliensis *by Macrophages***
Taise N. Landgraf, Marcelo V. Costa, Aline F. Oliveira, Wander C. Ribeiro, Ademilson Panunto-Castelo and Fabrício F. Fernandes

146 **Candida albicans *Yeast, Pseudohyphal, and Hyphal Morphogenesis Differentially Affects Immune Recognition***
Liliane Mukaremera, Keunsook K. Lee, Hector M. Mora-Montes and Neil A. R. Gow

158 ***Fluorescent Tracking of Yeast Division Clarifies the Essential Role of Spleen Tyrosine Kinase in the Intracellular Control of* Candida glabrata *in Macrophages***
Zeina Dagher, Shuying Xu, Paige E. Negoro, Nida S. Khan, Michael B. Feldman, Jennifer L. Reedy, Jenny M. Tam, David B. Sykes and Michael K. Mansour

167 ***Host-Derived Leukotriene B_4 is Critical for Resistance Against Invasive Pulmonary Aspergillosis***
Alayna K. Caffrey-Carr, Kimberly M. Hilmer, Caitlin H. Kowalski, Kelly M. Shepardson, Rachel M. Temple, Robert A. Cramer and Joshua J. Obar

177 ***Protein Deiminase 4 and CR3 Regulate* Aspergillus fumigatus *and ß-Glucan-Induced Neutrophil Extracellular Trap Formation, but Hyphal Killing is Dependent Only on CR3***
Heather L. Clark, Serena Abbondante, Martin S. Minns, Elyse N. Greenberg, Yan Sun and Eric Pearlman

188 ***Natural Killer Cells in Antifungal Immunity***
Stanislaw Schmidt, Lars Tramsen and Thomas Lehrnbecher

198 ***Antifungal Activity of Plasmacytoid Dendritic Cells and the Impact of Chronic HIV Infection***
Samuel Maldonado and Patricia Fitzgerald-Bocarsly

211 ***Exploitation of Scavenger Receptor, Macrophage Receptor With Collagenous Structure, by* Cryptococcus neoformans *Promotes Alternative Activation of Pulmonary Lymph Node CD11b$^+$ Conventional Dendritic Cells and Non-Protective Th2 Bias***
Jintao Xu, Adam Flaczyk, Lori M. Neal, Zhenzong Fa, Daphne Cheng, Mike Ivey, Bethany B. Moore, Jeffrey L. Curtis, John J. Osterholzer and Michal A. Olszewski

224 ***Leucine-Rich Repeat Kinase 2 Controls the Ca^{2+}/Nuclear Factor of Activated T Cells/IL-2 Pathway during* Aspergillus *Non-Canonical Autophagy in Dendritic Cells***
Alicia Yoke Wei Wong, Vasilis Oikonomou, Giuseppe Paolicelli, Antonella De Luca, Marilena Pariano, Jan Fric, Hock Soon Tay, Paola Ricciardi-Castagnoli and Teresa Zelante

238 ***Human and Murine Innate Immune Cell Populations Display Common and Distinct Response Patterns During Their* In Vitro *Interaction With the Pathogenic Mold* Aspergillus fumigatus**
Anna-Maria Hellmann, Jasmin Lother, Sebastian Wurster, Manfred B. Lutz, Anna Lena Schmitt, Charles Oliver Morton, Matthias Eyrich, Kristin Czakai, Hermann Einsele and Juergen Loeffler

249 ***Th17-Inducing Cytokines IL-6 and IL-23 are Crucial for Granuloma Formation During Experimental Paracoccidioidomycosis***
Fabrine Sales Massafera Tristão, Fernanda Agostini Rocha, Daniela Carlos, Natália Ketelut-Carneiro, Camila Oliveira Silva Souza, Cristiane Maria Milanezi and João Santana Silva

262 ***Contribution of IL-1RI Signaling to Protection Against* Cryptococcus neoformans *52D in a Mouse Model of Infection***
Mitra Shourian, Ben Ralph, Isabelle Angers, Donald C. Sheppard and Salman T. Qureshi

280 ***RIPK3/Fas-Associated Death Domain Axis Regulates Pulmonary Immunopathology to Cryptococcal Infection Independent of Necroptosis***
Zhenzong Fa, Qun Xie, Wei Fang, Haibing Zhang, Haiwei Zhang, Jintao Xu, Weihua Pan, Jinhua Xu, Michal A. Olszewski, Xiaoming Deng and Wanqing Liao

295 ***A Multifaceted Role of Tryptophan Metabolism and Indoleamine 2,3-Dioxygenase Activity in* Aspergillus fumigatus*–Host Interactions***
Tsokyi Choera, Teresa Zelante, Luigina Romani and Nancy P. Keller

306 ***Disease Tolerance Mediated by Phosphorylated Indoleamine-2,3 Dioxygenase Confers Resistance to a Primary Fungal Pathogen***
Eliseu Frank de Araújo, Flávio Vieira Loures, Cláudia Feriotti, Tania Costa, Carmine Vacca, Paolo Puccetti, Luigina Romani and Vera Lúcia Garcia Calich

320 ***The IDO–AhR Axis Controls Th17/Treg Immunity in a Pulmonary Model of Fungal Infection***
Eliseu Frank de Araújo, Claudia Feriotti, Nayane Alves de Lima Galdino, Nycolas Willian Preite, Vera Lúcia Garcia Calich and Flávio Vieira Loures

335 ***MicroRNA Regulation of Host Immune Responses Following Fungal Exposure***
Tara L. Croston, Angela R. Lemons, Donald H. Beezhold and Brett J. Gree

346 ***Autoimmune Regulator Deficiency Results in a Decrease in STAT1 Levels in Human Monocytes***
Ofer Zimmerman, Lindsey B. Rosen, Muthulekha Swamydas, Elise M. N. Ferre, Mukil Natarajan, Frank van de Veerdonk, Steven M. Holland and Michail S. Lionakis

354 ***The Interface Between Fungal Biofilms and Innate Immunity***
John F. Kernien, Brendan D. Snarr, Donald C. Sheppard and Jeniel E. Nett

364 ***Fungal Microbiota in Chronic Airway Inflammatory Disease and Emerging Relationships With the Host Immune Response***
Irene Zhang, Steven D. Pletcher, Andrew N. Goldberg, Bridget M. Barker and Emily K. Cope

371 ***Host Responses to* Malassezia *spp. in the Mammalian Skin***
Florian Sparber and Salomé LeibundGut-Landmann

378 ***Mechanisms of* Cryptococcus neoformans*-Mediated Host Damage***
Arturo Casadevall, Carolina Coelho and Alexandre Alanio

386 ***Immunology of Cryptococcal Infections: Developing a Rational Approach to Patient Therapy***
Waleed Elsegeiny, Kieren A. Marr and Peter R. Williamson

395 ***Induction of Broad-Spectrum Protective Immunity Against Disparate* Cryptococcus *Serotypes***
Marley C. Caballero Van Dyke, Ashok K. Chaturvedi, Sarah E. Hardison, Chrissy M. Leopold Wager, Natalia Castro-Lopez, Camaron R. Hole, Karen L. Wozniak and Floyd L. Wormley Jr.

412 ***The Elusive Anti-*Candida *Vaccine: Lessons From the Past and Opportunities for the Future***
Gloria Hoi Wan Tso, Jose Antonio Reales-Calderon and Norman Pavelka

425 ***Methods of Controlling Invasive Fungal Infections Using CD8$^+$ T Cells***
Pappanaicken R. Kumaresan, Thiago Aparecido da Silva and Dimitrios P. Kontoyiannis

frontiers in Immunology

EDITORIAL
published: 15 October 2018
doi: 10.3389/fimmu.2018.02337

Editorial: Immunity to Human Fungal Pathogens: Mechanisms of Host Recognition, Protection, Pathology, and Fungal Interference

Steven P. Templeton[1]*, *Amariliz Rivera*[2,3], *Bernard Hube*[4,5] and *Ilse D. Jacobsen*[4,5,6]

[1] Department of Microbiology and Immunology, Indiana University School of Medicine—Terre Haute, Terre Haute, IN, United States, [2] Center for Immunity and Inflammation, New Jersey Medical School, Rutgers—The State University of New Jersey, Newark, NJ, United States, [3] Department of Pediatrics, New Jersey Medical School, Rutgers—The State University of New Jersey, Newark, NJ, United States, [4] Department of Microbial Pathogenicity Mechanisms, Leibniz Institute for Natural Product Research and Infection Biology—Hans Knöll Institute, Jena, Germany, [5] Institute of Microbiology, Friedrich Schiller University, Jena, Germany, [6] Research Group Microbial Immunology, Leibniz Institute for Natural Product Research and Infection Biology—Hans Knöll Institute, Jena, Germany

Keywords: human fungal pathogens, fungal infection, antifungal immunity, fungal pathology, immune recognition

Editorial on the Research Topic

Immunity to Human Fungal Pathogens: Mechanisms of Host Recognition, Protection, Pathology, and Fungal Interference

Fungi are eukaryotic heterotrophs present in virtually every environment, with potentially more than 5 million individual species (1). Despite this impressive biodiversity, only about 300 species are capable of causing disease in humans (2). The most successful human pathogens among these share the ability to grow at the physiologic temperature of endothermic vertebrates and consequently colonize or infect only susceptible hosts (3). Immune-competent humans are largely resistant to fungal infections that throughout much of human history were considered rare and remained poorly understood. However, since 1980, the prevalence of opportunistic fungal diseases has steadily increased in parallel with increases in individuals with acquired immune deficiencies or those receiving immune suppressive or myeloablative therapies (4–6). Worse yet, current options for antifungal therapies remain limited and the continued emergence of resistant strains threatens to further erode antifungal drug efficacy (7, 8). The pressing need for novel therapies has thus resulted in increasing interest in studies in fungal biology and host-fungal interactions that may identify novel antifungal targets or alternative antifungal therapies.

The constant exposure of humans to both commensal and environmental fungi requires a competent immune system for tolerance, protection, and/or clearance, while limiting collateral damage caused by excessive or detrimental inflammation. Innate responses to fungal pathogens are initiated by fungal component recognition via an array of pathogen-associated molecular pattern recognition receptors (PRRs) (9–11). Recognition of fungal ligands by these receptors initiates a cascade of signaling events that result in activation of inflammatory cytokine and chemokine expression, driving recruitment and activation of innate phagocytic cells such as neutrophils and monocytes to the site of infection. Dendritic cells take up fungal particles in this cytokine-rich microenvironment, integrate these activating signals through PRRs and cytokine/chemokine receptors, migrate to site-draining lymph nodes, and subsequently activate naïve fungal-specific T cells. In this manner, early fungal recognition and inflammation provide critical signals that drive adaptive antifungal immunity. However, significant variation encountered by the host innate immune system, and co-evolutionary adaptation of pathogenic

OPEN ACCESS

Edited and reviewed by:
Ian Marriott,
University of North Carolina at Charlotte, United States

***Correspondence:**
Steven P. Templeton
sptemple@iupui.edu

Specialty section:
This article was submitted to Microbial Immunology, a section of the journal Frontiers in Immunology

Received: *28 August 2018*
Accepted: *20 September 2018*
Published: *15 October 2018*

Citation:
Templeton SP, Rivera A, Hube B and Jacobsen ID (2018) Editorial: Immunity to Human Fungal Pathogens: Mechanisms of Host Recognition, Protection, Pathology, and Fungal Interference. Front. Immunol. 9:2337. doi: 10.3389/fimmu.2018.02337

fungi, drive diverse disease outcomes ranging from tolerance, clearance and resolution to dissemination and excessive inflammation.

Increased understanding of these host-fungal interactions and the mechanisms that favor protective immunity over immune pathology could provide targets for novel therapeutic approaches that complement the limited repertoire of existing antifungal drugs. The aim of this research topic is to explore the host and fungal pathways that program innate and adaptive immunity and the immune cells, molecules, and regulatory pathways that comprise protective or detrimental responses to fungal exposure or infection. Researchers from 15 countries in North and South America, Europe, Asia, and Australia contributed 36 review and original research articles that cover a wide range of fungal pathogens, disease models, and effector and regulatory cell and molecular pathways of host immune responses to fungal exposure and infection. Here, we present an outline of the findings, perspectives, and reviews contained in this research topic.

The major class of pattern recognition receptors, the C-type lectin receptors (CLRs), including molecules critical for the initiation of inflammation and the development of adaptive immunity to fungi, are reviewed by Tang et al.. Although the important role of the β-1,3-glucan receptor dectin-1 in antifungal immunity is well appreciated, the α-mannan-binding dectin-2 and dectin-3 also influence responses to fungal exposure and infection and their roles are less clear. In support of these studies, Preite et al. show that dectin-2 and dectin-3 mediate antifungal activity and cytokine secretion of human plasmacytoid dendritic cells (pDCs) in response to the endemic dimorphic fungal pathogen *Paracoccidioides brasiliensis* via a pathway mediated by the CLR-associated signaling molecule Syk. In addition, de Castro et al. show that mouse bone marrow-derived macrophages (BMMs) and DCs (BMDCs) produce IL-1β and IL-18 in response to *Fonsecaea pedrosoi*, the main causative agent of chromoblastomycosis, in a dectin−1, −2, and −3-dependent manner. A role for the NOD-Like Receptor P3 (NLRP3), an intracellular protein complex that controls activation of inflammatory caspases and cytokine production, is shown by Feriotti et al. as important for the development of protective immunity to pulmonary infection with *P. brasiliensis*. β-glucan stimulation of NLRP3 inflammasome-mediated IL-1β secretion in B cells reported by Ali et al. shows innate antifungal cytokine production in an adaptive lymphocytes that were also capable of producing IgM in an NLRP3-dependent manner.

In contrast to the protective role for the NLRP3 inflammasome in invasive infection with the filamentous opportunistic mold *Aspergillus fumigatus* (12), Gresnigt et al. report that NOD1-deficient mice exhibit increased protection from invasive aspergillosis compared to wild-type controls. Another potential fungal PRR is the fibrinogen-binding domain receptor FIBCD1, and Schoeler Jepsen et al. demonstrate suppression of IL-8 secretion, mucin production, and airway inflammatory gene transcription in FIBCD1-transfected human lung epithelial cells in response to *A. fumigatus*. Lung epithelial cells are shown by Hayes et al. to produce IL-8 and MCP-1 in response to the *Alternaria* allergen Alt a 1 in a TLR2/4-dependent manner. Collectively, these studies support fungal pattern recognition by an increasing number of receptor families with diverse roles in the development of protective or detrimental immunity to fungal exposure and infection.

PRR-expressing tissue-resident macrophages are part of the first line of defense against fungal infections (reviewed by Xu and Shinohara). Circulating monocytes are subsequently recruited to sites of infection in response to inflammatory signals produced by tissue-resident macrophages. Tóth et al. report that the exposure of hyphae of the dematiaceous mold *Curvularia lunata* to human THP-1 monocytes resulted in increased inflammatory IL-8 and regulatory/anti-inflammatory IL-10, suggesting a possible mechanism for the ability of this species to cause chronic infections in immune competent individuals. Landgraf et al. report that dihydrolipoyl dehydrogenase secreted by *P. brasiliensis* may act as an exoantigen that enhances macrophage phagocytosis. Mukaremera et al. report that hypha of the yeast *Candida albicans* induced low levels of cytokine secretion from human monocytes, with the highest levels from yeast and intermediate levels from pseudohypha, and cell wall mannan depletion partially reversed these responses. Using fluorescence yeast cell wall-labeling to measure yeast division within macrophages, Dagher et al. show that activation of the tyrosine kinase Syk is critical for macrophage control of phagocytosed *C. glabrata*. Together, these studies provide new insights into the roles for monocytes and macrophages in induction and regulation of antifungal inflammation and fungal clearance.

Inflammatory cytokine production by macrophages leads to localized inflammation with production of chemokines that attract additional innate immune cells. Caffrey-Carr et al. report that antifungal protection and recruitment of neutrophils and eosinophils in response to *A. fumigatus* inhalation is dependent on the lipid inflammatory mediator Leukotriene β4. Clark et al. show that a key mediator of chromatin decondensation, protein deaminase 4, and the complement receptor CR3, are critical for neutrophil extracellular trap formation in response to *A. fumigatus*, while hyphal killing required only CR3. The role of innate lymphoid natural killer (NK) cells in innate antifungal immunity is reviewed by Schmidt et al.. These works further illustrate diverse mechanisms and roles for innate myeloid and lymphoid cells in antifungal immunity.

Dendritic cells (DCs) are multifaceted professional antigen presenting cells that integrate antigen uptake and local inflammatory signals in order to effectively prime adaptive antifungal immune responses upon migration to site-draining lymph nodes (9). The role of type I interferon-producing plasmacytoid DCs in antifungal immunity in the context of chronic HIV infection is reviewed by Maldonado and Fitzgerald-Bocarsly. Xu et al. investigated the role of macrophage receptor with collagenous structure (MARCO) on pDC recruitment and induction of antifungal adaptive immunity to *C. neoformans* infection, and report that expression of MARCO promoted recruitment of lymph node DCs and skewed local

and systemic T helper cell responses away from protective Th1 responses and toward non-protective Th2 responses. Wong et al. demonstrate a role for leucine-rich repeat kinase 2 (LRRK2) in translocation of NFAT to the nucleus in DCs in the early stages of the non-canonical autophagic response to *A. fumigatus* conidia, thus connecting LRRK2 with NFAT-mediated IL-2 expression in early antifungal immunity. Hellmann et al. compared immune responses to *A. fumigatus* in human and mouse DCs, macrophages, and neutrophils, and observed that human DCs exhibited more significant increases in maturation markers and phagocytic ability than murine DCs, while murine neutrophils and macrophages displayed more reactive oxygen species production after *A. fumigatus* exposure. Collectively, these works provide support for additional mediators of DC function that shape antifungal adaptive immunity, and suggest distinct roles for these cells in human fungal disease and experimental animal models.

After DCs migrate to draining lymph nodes, they present fungal antigen to naïve T cells, inducing antifungal adaptive immunity. This process is influenced by cytokines in the microenvironment. Formation of the antifungal Th17 subset of T helper cells is promoted by the inflammatory cytokines IL-6 and IL-23, and Tristão et al. report that these cytokines, along with the IL-17 receptor A, were necessary for protective lung granuloma formation in mice infected with *P. brasiliensis*. IL-1α/β also influence adaptive immune responses to fungi, such as the dimorphic *Cryptococcus* spp., as Shourian et al. observed that IL-1 receptor type 1-deficient mice had increased cryptococcal burden, eosinophilia, M2 macrophage polarization, and recruitment of CD4+IL-13+ T cells, with a concomitant reduction in pro-inflammatory Th1 and Th17 cytokines. However, excessive inflammation and Th1 activation in *C. neoformans* infection is also detrimental, and was reported by Fa et al. to be mediated by the cell death regulatory genes FADD (Fas-associated death domain) and RIP3K (receptor interacting protein kinase 3). The results of these studies support roles for Th1 and Th17 responses in antifungal immunity, as well as a requirement for regulation of cell death to limit excessive inflammation.

Cell and molecular regulation of immunity occurs at multiple levels from induction to resolution of immune responses. An enzyme that limits available tryptophan and thus dampens immune cell proliferation and effector function, indoleamine 2,3-dioxygenase (IDO), is produced by mammalian hosts and the fungal pathogen *A. fumigatus*; findings that shed light on this host-pathogen dynamic are reviewed by Choera et al.. De Araújo et al. report that DCs from an infected *P. brasiliensis*-susceptible mouse strain exhibit IDO activity and promote inflammation, while DCs from resistant mice phosphorylate IDO and promote a tolerogenic phenotype. The same group further compared *P. brasiliensis* infection in IDO-deficient and wild-type mice, and observed increased mortality, fungal burden, histopathology, and Th17 cell recruitment and activation in IDO-deficient mice with concomitant decreases in Th1 and Treg cells de Araújo et al.. In addition to the enzymatic activity and signaling by IDO, antifungal immune responses are regulated at the post-transcriptional level by microRNAs (miRNAs); these molecules and their associated pathways are reviewed by Croston et al.. Zimmerman et al. report that patients with autoimmune polyendocrinopathy-candidiasis-ectodermal dystrophy (APECED) exhibit decreased levels of the signaling molecule STAT1, in contrast with patients with STAT1 gain-of-function mutations, despite similar disease phenotypes. These works highlight findings of enzymatic, post-translational, and signal transduction in the regulation of antifungal immunity and fungal disease susceptibility.

Although spore/hyphal recognition by innate cells drives the development of immunity to fungal pathogens, host-fungal pathogen interactions are also considered at the macroscopic level of microbial communities (e.g., biofilms) and host tissues. Kernien et al. review host immune recognition of fungal biofilms and biofilm properties that inhibit host recognition and clearance. Zhang et al. explore how immune interactions with respiratory and gastrointestinal fungal microbiota contribute to chronic airway inflammatory disease. Sparber and LeibundGut-Landmann more specifically discuss host immune responses to skin-colonizing *Malassezia* species, yeasts that are involved in a variety of skin disorders. Finally, Casadevall et al. review the evidence that *C. neoformans* mediates host damage at the molecular, cellular, tissue, and organism levels, in some instances with formation of large fungal masses in brain tissue. These reviews highlight emerging areas of fungal immunology that consider fungal interactions with the host immune system beyond the level of cell and molecular recognition.

Despite significant advances in our understanding of host immunity to fungal exposure and infection, treatment of fungal diseases has not progressed beyond the use of a limited repertoire of antifungal drugs that are rendered increasingly ineffective by emerging fungal resistance. Since appropriate antifungal immunity is critical for protection from fungal disease, complementary therapies that target immune pathways represent areas of considerable interest for fungal immunologists. Elsegeiny et al. review studies of immune pathology in cryptococcal infection and discuss the need for immune targeting therapies that suppress immune-mediated damage without further compromising host protection. Van Dyke et al. demonstrate that combining non-lethal *C. neoformans* challenge with local IFN-γ production elicits an immune response that protects mice from subsequent lethal infection. Tso et al. summarize efforts and obstacles in the development of anti-*Candida* vaccines, and discuss the potential use of trained immunity in the development of strategies against opportunistic fungal infections. Finally, Kumaresan et al. review the development of CD8+ T cell therapy for the control of invasive fungal infections, with a focus on the use of chimeric antigen receptor (CAR) T cells that target β-glucan. These reviews underscore the importance of current and future efforts to enhance immune protection while limiting immune pathology in patients that may not respond to traditional antifungal therapies.

Collectively, the studies described in original research and review articles in this topic provide optimism

for the future of antifungal immune therapy. Recent advances by fungal immunologists have greatly increased our understanding of the basic mechanisms of innate immune recognition, inflammation, adaptive immunity, and regulation of antifungal immune responses at molecular, cell, tissue, and organismal levels. We hope these articles will stimulate further research with the ultimate goal of improving outcomes for patients with fungal diseases.

AUTHOR CONTRIBUTIONS

All authors listed have made a substantial, direct and intellectual contribution to the work, and approved it for publication.

REFERENCES

1. O'brien HE, Parrent JL, Jackson JA, Moncalvo JM, Vilgalys R. Fungal community analysis by large-scale sequencing of environmental samples. *Appl Environ Microbiol.* (2005) 71:5544–50. doi: 10.1128/AEM.71.9.5544-5550.2005
2. Taylor LH, Latham SM, Woolhouse ME. Risk factors for human disease emergence. *Philos Trans R Soc Lond B Biol Sci.* (2001) 356:983–9. doi: 10.1098/rstb.2001.0888
3. Robert VA, Casadevall A. Vertebrate endothermy restricts most fungi as potential pathogens. *J Infect Dis.* (2009) 200:1623–6. doi: 10.1086/644642
4. Fridkin SK, Jarvis WR. Epidemiology of nosocomial fungal infections. *Clin Microbiol Rev.* (1996) 9:499–511.
5. Richardson M, Lass-Florl C. Changing epidemiology of systemic fungal infections. *Clin Microbiol Infect. (2008) 14* (*Suppl. 4*)*:5–24.* doi: 10.1111/j.1469-0691.2008.01978.x
6. Lehrnbecher T, Frank C, Engels K, Kriener S, Groll AH, Schwabe D. Trends in the postmortem epidemiology of invasive fungal infections at a university hospital. *J Infect.* (2010) 61:259–65. doi: 10.1016/j.jinf.2010.06.018
7. Ostrosky-Zeichner L, Casadevall A, Galgiani JN, Odds FC, Rex JH. An insight into the antifungal pipeline: selected new molecules and beyond. *Nat Rev Drug Discov.* (2010) 9:719–27. doi: 10.1038/nrd3074
8. Fisher MC, Hawkins NJ, Sanglard D, Gurr SJ. Worldwide emergence of resistance to antifungal drugs challenges human health and food security. *Science* (2018) 360:739–42. doi: 10.1126/science.aap7999
9. Wuthrich M, Deepe GSJr, Klein B. Adaptive immunity to fungi. *Annu Rev Immunol.* (2012) 30:115–48. doi: 10.1146/annurev-immunol-020711-074958
10. Plato A, Hardison SE, Brown GD. Pattern recognition receptors in antifungal immunity. *Semin Immunopathol.* (2015) 37:97–106. doi: 10.1007/s00281-014-0462-4
11. Stappers MHT, Clark AE, Aimanianda V, Bidula S, Reid DM, Asamaphan P, et al. Recognition of DHN-melanin by a C-type lectin receptor is required for immunity to Aspergillus. *Nature* (2018) 555:382–6. doi: 10.1038/nature25974
12. Karki R, Man SM, Malireddi RKS, Gurung P, Vogel P, Lamkanfi M, et al. Concerted activation of the AIM2 and NLRP3 inflammasomes orchestrates host protection against Aspergillus infection. *Cell Host Microbe* (2015) 17:357–68. doi: 10.1016/j.chom.2015.01.006

Conflict of Interest Statement: The authors declare that the research was conducted in the absence of any commercial or financial relationships that could be construed as a potential conflict of interest.

Copyright © 2018 Templeton, Rivera, Hube and Jacobsen. This is an open-access article distributed under the terms of the Creative Commons Attribution License (CC BY). The use, distribution or reproduction in other forums is permitted, provided the original author(s) and the copyright owner(s) are credited and that the original publication in this journal is cited, in accordance with accepted academic practice. No use, distribution or reproduction is permitted which does not comply with these terms.

frontiers in Immunology

REVIEW
published: 01 February 2018
doi: 10.3389/fimmu.2018.00123

Regulation of C-Type Lectin Receptor-Mediated Antifungal Immunity

Juan Tang[1†], Guoxin Lin[2,3†], Wallace Y. Langdon[4], Lijian Tao[1] and Jian Zhang[2]*

[1] Department of Nephrology, Xiangya Hospital, Central South University, Changsha, Hunan, China, [2] Department of Pathology, The University of Iowa, Iowa City, IA, United States, [3] Department of Anesthesiology, The Third Xiangya Hospital, Central South University, Changsha, Hunan, China, [4] School of Biological Sciences, University of Western Australia, Perth, WA, Australia

Of all the pathogen recognition receptor families, C-type lectin receptor (CLR)-induced intracellular signal cascades are indispensable for the initiation and regulation of antifungal immunity. Ongoing experiments over the last decade have elicited diverse CLR functions and novel regulatory mechanisms of CLR-mediated-signaling pathways. In this review, we highlight novel insights in antifungal innate and adaptive-protective immunity mediated by CLRs and discuss the potential therapeutic strategies against fungal infection based on targeting the mediators in the host immune system.

Keywords: C-type lectin receptor, fungal infection, signaling pathways, posttranslational modifications, immunity

OPEN ACCESS

Edited by:
Ilse Denise Jacobsen, Leibniz-Institut für Naturstoff-Forschung und Infektionsbiologie, Hans Knöll Institut, Germany

Reviewed by:
Salomé LeibundGut-Landmann, University of Zurich, Switzerland
Dr Betty Hebecker, University of Aberdeen, United Kingdom

***Correspondence:**
Jian Zhang
jian-zhang@uiowa.edu

†These authors have contributed equally to this work.

Specialty section:
This article was submitted to Microbial Immunology, a section of the journal Frontiers in Immunology

Received: *31 October 2017*
Accepted: *16 January 2018*
Published: *01 February 2018*

Citation:
Tang J, Lin G, Langdon WY, Tao L and Zhang J (2018) Regulation of C-Type Lectin Receptor-Mediated Antifungal Immunity. Front. Immunol. 9:123. doi: 10.3389/fimmu.2018.00123

INTRODUCTION

Fungi are ubiquitously present in the mucosal and epidermal surfaces in healthy individuals and often cause infections in immune-compromised patients. These include HIV-positive patients, recipients of organ transplants, and cancer patients treated with chemotherapy. In healthy individuals, fungal infections can also develop including vulvovaginal candidiasis, tinea pedis, fungal keratitis, and chromoblastomycosis (1–6). Invasive fungal infections, particularly with *Candida albicans* (*C. albicans*), demonstrate high mortality rates and kill more than 1.5 million people worldwide annually (7). Moreover, other identified pathogenic fungi such as *Aspergillus fumigatus* (*A. fumigatus*), *C. auris*, and *Cryptococcus gattii* (*C. gattii)* also pose a great threat to public health (1, 8, 9). Toxicity and resistance to the limited number of antifungal agents that are currently available contributes to high morbidity and mortality associated with fungal sepsis. Therefore, there is an urgent need to better understand the immune response during fungal infection and develop new immuno-therapeutic approaches.

C-type lectin receptors (CLRs), including transmembrane and soluble forms, are characterized by containing at least one C-type lectin-like domain (CTLD). They have been shown to recognize both endogenous and exogenous ligands (10). As the most important pattern recognition receptor (PRR) family for the detection of fungi, CLRs are recognized to play a critical role in tailoring immune responses against fungal exposure (11–14). In this review, we will focus on the roles and mechanisms of membrane-bound CLR-mediated-signaling pathways in host defense against fungal infections, with an emphasis on *C. albicans*. *C. albicans* is the most common fungal species isolated from biofilms, formed either on implanted devices or on human tissues, which become pathogenic in immune-compromised patients. We will also discuss the role of posttranslational modifications (PTMs) of CLR-signaling pathway components in anti-fungal immunity. In addition, we will also summarize the recent progress on the potential host-derived immune therapies for disseminated candidiasis.

FUNGAL RECOGNITION

The pathogen-associated molecular patterns (PAMPs) on the fungal cell wall are crucial for the initiation of innate immune responses against fungal pathogens. The fungal cell wall is predominantly composed of carbohydrate polymers interspersed with glycoproteins (15–17). The three major components, found in almost all fungi, are β-glucans, which are anchored in the inner core of the cell wall, chitin, which is a robust β-1,4-linked homopolymer of N-acetylglucosamine (GlcNac) located in the inner cell wall, and mannans, which are localized in the outer layer of the fungal yeast cell wall. The central core of the cell wall is branched β-1,3/1,6-glucans that are linked to chitin *via* β-1,4 linkages (15, 18). Mannans are chains of up to several hundred mannoses that are added to fungal proteins *via* N- or O-linkages. Mannoproteins can covalently attach to glucans or chitin *via* either their sugar residues or glycosylphosphatidylinositol (17). In addition, O-linked glycoproteins containing mannobiose-rich structures from *Malassezia* function as distinct ligands to induce immune responses (19). Another crucial component on the fungal cell wall is melanin, which is involved in fungal virulence, resistance to antifungal drugs, and protection against insults from the environment (20, 21).

The recognition of PAMPs expressed in pathogens involves four families of PRRs, including Toll-like receptors (TLRs), NOD-like receptors (NLRs), retinoic acid-inducible gene I (RIG-I)-like receptors (RLRs), and CLRs, each of which shows notable differences regarding pathogen recognitions, signal transduction, and intracellular downstream pathways (14, 22). Among these PRRs, CLRs have been shown to be essential for fungal recognition, either alone or in conjunction with TLRs (23–25). The family of CLRs comprises a subset of CTLD-containing proteins, including some Ca^{2+}-dependent and Ca^{2+}-independent carbohydrate-binding membrane-bound receptors. They are preferentially expressed by myeloid cells (26, 27). Ca^{2+}-dependent carbohydrate binding is the most common CTLD function in vertebrates. Under these circumstances, the CTLD is therefore named as a carbohydrate recognition domain (CRD) (27). CLRs can recognize an array of molecules such as carbohydrates, proteins, and lipids.

Several PRRs have been reported to recognize β-glucans, including Dectin-1, complement receptor 3 (CR3), and three members of the scavenger receptor family, CD5, CD36, and SCARF1 (28–33). Recent studies have revealed that Dectin-2, Dectin-3, macrophage mannose receptor (MR), macrophage-inducible C-type lectin (Mincle), and dendritic cell (DC)-specific ICAM3-grabbing non-integrin (DC-SIGN) can recognize mannans and mannoproteins (12, 13, 34–37). It has been shown that Dectin-1 specifically recognizes β-1, 3-glucans (11, 38), whereas Dectin-2 and Dectin-3 specifically recognize α-mannans (12, 13). The receptor(s) that recognizes chitin is still unknown, although NOD2, MR, and TLR9 were proposed to recognize chitin (39).

CLRs IN ANTIFUNGAL IMMUNE RESPONSE

The major CLRs that are recognized to be involved in antifungal immune responses are Dectin-1, Dectin-2, Dectin-3, MR, Mincle, and DC-SIGN. Dectin-1, Dectin-2, Dectin-3, Mincle, and DC-SIGN share a similar molecular structure consisting of a CRD, a stalk region, a transmembrane domain, and a cytoplasmic domain (40–42). By contrast, MR is composed of an amino terminal cysteine-rich domain, a single fibronectin type II domain, eight CRDs, a transmembrane domain, and a cytoplasmic tail (43, 44) (**Figure 1**). These CLRs can be divided into two main groups based on their intracellular-signaling motifs: CLRs with immunoreceptor tyrosine-based activation motifs (ITAMs) or ITAM-like (also named hem-ITAM) domains and CLRs containing non-immunoreceptor tyrosine-based motifs such as MR and DC-SIGN (27, 45). The activation of these receptors can transduce intracellular-signaling pathways directly through integral ITAM-like motif(s) within the cytoplasmic tails (such as Dectin-1), or indirectly through association with ITAM-containing FcR-γ chains, including Dectin-2, Dectin-3, and Mincle (25, 27, 46). Upon ligand binding, the activation of receptors induces the tyrosine phosphorylation of ITAM-like/ITAM motif(s) by Src family kinases, leading to the recruitment and activation of Syk kinase. This subsequently initiates downstream-signaling pathways. The activation of Syk signaling requires its interaction with two phosphorylated tyrosines within ITAM-like/ITAM motifs. However, unlike canonical ITAM motifs within FcR-γ adaptors which contain a repeat of YxxI/L, the ITAM-like motif located in the cytoplasmic tail of Dectin-1 has only a single YxxI/L; thus, the signaling from Syk may involve the receptor dimerization of Dectin-1 containing a single phosphotyrosine (25, 47) (**Figure 1**). Signals from the CLRs initiate and modulate not only innate immune responses but also the development of adaptive immunity, especially T_H1 and T_H17 responses, which are crucial for the control of fungal infections. The role of Dectin-1, Dectin-2, and Dectin-3 in antifungal immunity is of considerable interest and has been extensively studied during the last decade.

Signaling Pathways Mediated by Dectin-1

Dectin-1 (encoded by *Clec7a*), which is mostly expressed by myeloid phagocytes (macrophages, DCs, and neutrophils), recognizes β-1,3-glucans in a calcium-independent manner (40). The engagement of Dectin-1 by β-1,3-glucans induces the activation of Src protein tyrosine kinase (PTK). Src phosphorylates the single cytoplasmic ITAM-like domain of Dectin-1, which subsequently results in the recruitment and activation of Syk (25, 48, 49). The activated Syk then phosphorylates protein kinase C δ (PKC-δ), which phosphorylates caspase activation and recruitment domain-containing protein 9 (CARD9) (50, 51). This facilitates complex formation with Bcl-10 and MALT1 (51, 52), thus eliciting NF-κB activation (24, 51) (**Figure 1**). In addition, Dectin-1-induced activation of extracellular signal-regulated protein kinase (ERK) is also mediated through CARD9, which links Ras-GRF1 to H-Ras (53). In addition to the Syk-dependent pathways, signaling from Dectin-1 also involves Syk-independent pathways mediated by Raf-1, resulting in noncanonical NF-κB activation by collaboration with the Syk-dependent NF-κB-inducing kinase (NIK) pathway (24). The activation of NF-κB and ERK mediates the inflammatory responses against fungal infections and directs T_H1/T_H17 differentiation for antifungal immunity (24, 54–56).

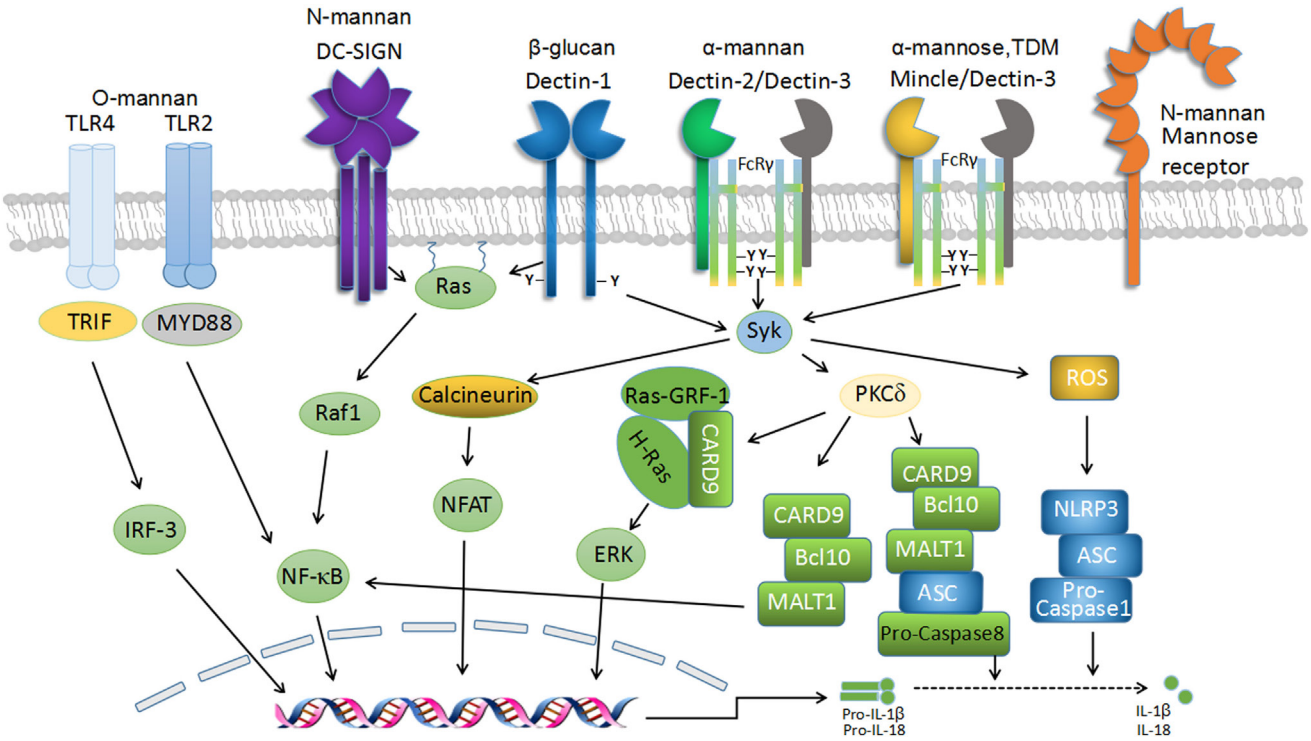

FIGURE 1 | C-type lectin receptor (CLR) signaling in fungal recognition. Schematic representation of the transmembrane CLRs associated with antifungal immunity and their intracellular-signaling networks. The recognition of fungal components by several CLRs, including Dectin-1, Dectin-2, Dectin-3, macrophage-inducible C-type lectin (Mincle), and dendritic cell-specific ICAM3-grabbing non-integrin (DC-SIGN), induces downstream signaling *via* Syk-dependent and Raf-1-dependent pathways to mediate antifungal immunity. Dectin-1 homodimers, Dectin-2-Dectin-3 heterodimers, and Mincle-Dectin-3 heterodimers couple with immunoreceptor tyrosine-based activation motif (ITAM)-like and FcR-γ-associated ITAM motifs, respectively, to recruit Syk to initiate downstream signaling, which leads to reactive oxygen species (ROS) production and caspase activation and recruitment domain-containing protein 9 (CARD9)/Bcl-10/MALT1 complex-mediated activation of NF-κB pathway. ROS triggers NLRP3 inflammasome assembly and activation, which cleave pro-IL-1β and pro-IL-18 into mature forms to elicit protective roles in anti-fungi immunity. Dectin-1-signaling pathway also induces Syk-dependent activation of Ras-GRF1, which recruits H-Ras *via* the CARD9 adaptor and ultimately leads to extracellular signal-regulated protein kinase (ERK) activation. Furthermore, signaling by Syk results in nuclear factor of activated T cells (NF-AT) activation in a calcineurin-dependent fashion, which integrates with NF-κB signaling to regulate gene transcription. Moreover, Dectin-1-signaling activation seems to be essential for the formation of noncanonical caspase-8 inflammasome, which is responsible for active IL-1β production.

Dectin-1 signaling induces numerous signaling events characterized by phagocytosis, respiratory burst, and the production of various inflammatory mediators, including cytokines, chemokines, and inflammatory lipids (40, 47, 57, 58). It is well established that the production of IL-1β, together with IL-6 and IL-23, is essential for antifungal immune responses partly through priming adaptive immunity to differentiate $CD4^+$ T cells to T_H1/T_H17 cells (24, 56, 59). Moreover, the production of type I interferons (IFNs) can be induced after fungal recognition and require Dectin-1/Syk signaling and transcription factor IRF5 involvement (49). In mouse models, enhanced IFN-β secretion is critical for protection from fungal challenge (49, 60). Importantly, consistent with animal studies, type I IFNs exert a protective role against *C. albicans* infection in humans (61). Dectin-1 signaling also triggers the activation of nuclear factor of activated T cells (NF-AT) through the Syk/calcineurin pathway, leading to the production of inflammatory cytokines, such as IL-2, IL-10, and IL-12 p70, and the regulation of T cell development and differentiation (62–64) (**Figure 1**).

CARD9 is considered to be essential for tailoring immune responses to fungal pathogens (51). The survival of *Card9*$^{-/-}$ mice is greatly impaired following systemic *C. albicans* infection (51, 53). In addition, NF-κB-mediated cytokine production is severely defective in the absence of CARD9 (51, 53). Notably, human CARD9 deficiency, which is referred to as an autosomal-recessive disorder, is associated with a spectrum of fungal diseases caused by various fungal pathogens (65). Currently, 16 human CARD9 mutations, including nonsense and missense mutations, have been reported in patients worldwide (66). CARD9 mutations result in the impairment of mucosal fungal defense, partly by inhibiting T_H17-induced immune responses, which are responsible for the susceptibility to chronic mucocutaneous candidiasis (67). However, the underlying mechanism regarding how human CARD9 mutations affect T_H17 immunity deserves further investigation.

Strikingly, CARD9 serves as the only currently known human gene in regulating the dissemination of *C. albicans* to the central nervous system (CNS). CARD9 deficiency in both mice and humans results in vulnerability to fungal infection in the CNS, owing to impaired neutrophil accumulation in the fungal-infected CNS, which correlates with the lack of CXC-chemokine induction (68). Consistent with these findings, decreased neutrophil

recruitment to the lungs was reported in *Card9*$^{-/-}$ mice infected with *A. fumigatus* (69). CARD9 deficiency may also predispose to extrapulmonary *A. fumigatus* infection in humans as a result of impaired neutrophil recruitment (70). Nevertheless, the CARD9-dependent-protective role seems less necessary for pulmonary mold infections. Thus, future studies are required to decipher the role of CARD9 in other immune cells to explain its "organ-specific" and "species-specific" function in antifungal immunity. Moreover, the effects of genetic mutations in CARD9-coupled receptors (Dectin-1, Dectin-2, and Dectin-3) and CARD9-binding partners (MALT1 and Bcl-10) in human antifungal host defense require more in-depth studies.

Vav proteins, the key upstream regulators of CARD9, are critical in CLR/CARD9-induced-inflammatory responses similar to CARD9 (71). Indeed, humans with polymorphisms in *DECTIN-1 and VAV3* show increased susceptibility to invasive *C. albicans* infection (71, 72). Interestingly, one recent study illustrated that neutrophilic myeloid-derived suppressor cells (MDSCs) are induced *in vitro* upon infection with various *Candida* species, which functionally inhibit T cell responses *via* Dectin-1/CARD9 signaling and subsequently suppress ROS generation, indicating that CARD9 seems to function as a negative modulator in fungal immune response (73). It is unknown whether this is true *in vivo*. The contribution of MDSCs to fungal infections requires further investigation.

Signaling Pathways Mediated by Dectin-2, Dectin-3, and Mincle

Dectin-2 (encoded by *Clec4n*), Dectin-3 (MCL, encoded by *Clec4d*), and Mincle (encoded by *Clec4e*) belong to the Dectin-2 family of CLRs, whose encoding genes are grouped closely at the telomeric end of the NK-gene cluster. They all have a single extracellular CTLD, short cytoplasmic tails, and trigger intracellular signaling indirectly through association with the ITAM-containing FcR-γ chain (55, 74–76). Signaling from Dectin-2, Dectin-3, and Mincle is mediated *via* the Syk/PKCδ-dependent CARD9/Bcl-10/MALT1 pathway, resulting in the activation of the transcription factor NF-κB and the subsequent production of inflammatory cytokines and chemokines (13, 75, 77). Dectin-2 recognizes high-mannose structures and binds *Candida* α-mannans in a calcium-dependent manner (12, 78). It can also recognize O-linked mannobiose-rich glycoprotein from *Malassezia*, glycans containing mannose from house dust mite extracts (19, 79). Dectin-2 has been implicated in the defense against numerous pathogens, including *C. albicans, C. neoformans, A. fumigatus*, *Saccharomyces cerevisiae, Paracoccidioides brasiliensis, Histoplasma capsulatum, Microsporum audouinii, Trichophyton rubrum, Mycobacterium tuberculosis,* and *Schistosoma mansoni* (75, 78, 80). Dectin-2 and Dectin-3 can form heterodimers to recognize the hyphal forms of *C. albicans* to induce pro-inflammatory production (13), although the involvement of Dectin-3 in *C. neoformans* infection is still controversial (81).

Mice deficient for Dectin-2 are highly susceptible to systemic candidiasis (12). Further study indicates that Dectin-2 and Dectin-3, two similar CLRs, form a constitutive heterodimeric PRR for sensing α-mannans on the surface of *C. albicans* and induce Syk-mediated activation of NF-κB to combat fungal invasion (13). Blocking either Dectin-2 or Dectin-3 with antibodies dramatically eliminates NF-κB-mediated-inflammatory responses upon *C. albicans* stimulation. The genetic deletion of Dectin-3, or mice receiving Dectin-3-blocking antibodies, showed high susceptibility to systemic candidiasis (13). Therefore, Dectin-2 coupled with Dectin-3 displays protective antifungal immunity in animal models. Recently, two studies also showed that Dectin-3 is constitutively expressed in myeloid cells and functions as an FcR-γ-coupled receptor for sensing trehalose-6,6'-dimycolate (TDM), a potent mycobacterial adjuvant (76, 82). In addition, Dectin-3 is also essential for inducing Mincle expression upon TDM stimulation (82). Dectin-3 has been shown to interact with Mincle *via* the stalk region of Dectin-3, thus enhancing the protein expression of Mincle (83).

Emerging evidence showed that the engagement of the T_H17/IL-17 pathway plays a critical role in host defense against mucosal fungal infection (84). Both Dectin-2 and Dectin-3 are of great importance for T_H17 cell differentiation in host defense against *C. albicans* or *Blastomyces dermatitidis* (12, 85). Furthermore, PI3K-δ, a proximal Syk-dependent-signaling intermediate downstream of Dectin-2, plays an important role in the generation of T_H2 and T_H17 immunities against infection with *Dermatophagoides farina* (*D. farina*) (86). In addition, a recent study showed that NF-κB subunit c-Rel-dependent cytokine induction relies on the Dectin-2/MALT1-signaling cascade to trigger T_H17-polarizing cytokines IL-1β and IL-23 secretion, thus possessing T_H17-protective immunity against pathogenic fungal invasion (52). The expression of IL-17RC on humans and murine neutrophils has been identified in a Dectin-2-dependent pathway (87). Dectin-2-induced autocrine IL-17 secretion has also been implicated with ROS generation and fungal killing (87).

Mincle has been shown to recognize *mycobacteria*, *C. albicans*, *Malasezzia,* and *Fonsecaea species* (36, 88–90). It is the sensor for α-mannose, glycolipid trehalose-6, 6′-dimycolate (TDM), and the self-ribonucleoprotein SAP-130 (74, 88, 91). Mincle is expressed constitutively at low levels in myeloid cells, and its expression is dependent on Dectin-3 (76, 83, 92). The expression pattern of Mincle suggests that it may not be the major fungal recognition receptor. In support of this notion, although mice lacking Mincle display increased fungal burden in the kidneys, the survival rate of *Mincle*$^{-/-}$ mice is similar to wild-type mice upon systemic *C. albicans* infection (89). It has been shown that Mincle is not a phagocytic receptor but modestly potentiates pro-inflammatory cytokine production (89). Mincle has been shown to inhibit Dectin-1-induced T_H1 responses to *F. monophora* infection by inducing IRF1 degradation through the E3 ubiquitin ligase Mdm2, which impairs the polarization of T_H1 cells. Defective T_H1 responses contribute to the chronic infection of *F. monophora* which causes chromoblastomycosis, a chronic fungal skin infection (93). In addition, Mincle has been demonstrated to specifically recognize *Malassezia* species and play a crucial role in host defense against this fungus (36).

Other Fungal Recognition Receptors

MR (CD206, encoded by *Mrc1*): MR recognizes N-linked mannan of infectious *Candida* and mediates endocytosis and phagocytosis (94). Recent studies indicate that MR might promote the secretion of pro-inflammatory cytokines through the activating intracellular signal cascades. Although non-ITAM motifs are identified within the MR, a recent study reports that human MR becomes tyrosine phosphorylated upon *M. tuberculosis* (*M. tb*) infection, and this phosphorylation mediates a sequential association of Grb-2 and SHP-1 (95), suggesting that human MR itself can transduce downstream signaling. However, no known signaling motifs in murine MR have been identified, and no signaling has been induced directly from murine MR in response to fungal infections. Using human peripheral blood mononuclear cells, MR was found to be the main receptor pathway for the induction of T_H17 cells by *C. albicans in vitro* (34). However, the importance of MR in fungal recognition is challenged by the fact that normal host defense is not altered during systemic candidiasis or *Pneumocystis carinii* infection in $Mr^{-/-}$ mice (96). In support of this, MR is also not required for resistance to *Coccidioides immitis* infection (97). Therefore, MR may not be the major fungal recognition receptor in mice. It is possible that the human and murine MRs may behave differently. This notion is supported by a recent report that human but not mouse MR signaling induced by *M. tb* regulates macrophage recognition and vesicle trafficking (95).

DC-SIGN (encoded by *Cd209a*): DC-SIGN is a transmembrane receptor for pathogen binding and uptake, which is mainly expressed in a subset of macrophages and DCs (98, 99). It has been demonstrated that DC-SIGN can bind and internalize soluble ligands effectively, which facilitates antigen processing and presentation to T cells (100). DC-SIGN has a high affinity to detect varied carbohydrate-based ligands, including mannose structures and fucose-bearing glycans, to recognize diverse organisms including HIV-1, *M. tb*, *Helicobacter pylori*, or fungi such as *C. albicans*, *A. fumigatus,* and *C. tropicum* (35, 37, 101–103). The polymorphisms of both Dectin-1 and DC-SIGN were reported to associate with invasive pulmonary Aspergillosis infection (104). It has been demonstrated that DC-SIGN can recognize *Candida* mannan and that *N*-linked mannosyl residues are essential for this interaction (37). In particular, the *N*-mannosylation is required for the binding, phagocytosis, and immune sensing of *C. albicans* by human DCs (37). Upon high-mannose recognition, the signalosome leads to Raf-1 activation and subsequent p65 acetylation, which facilitates gene-transcriptional expression, especially amplifying TLR-induced cytokine production such as IL-10, IL-6, and IL-12 (23). However, DC-SIGN in collaboration with MR seems to suppress Dectin-1-mediated T_H17 responses, but potentiate T_H1 responses in β-glucan- or *M. tb*-treated DCs (105). Moreover, DC-SIGN, which contains abundant galactomannan, is also found to play an important role in the recognition and binding of *A. fumigatus* conidia in human DCs (103). The ligation of DC-SIGN by the glycoprotein fimbriae of *Porphyromonas gingivalis* promotes the evasion of antibacterial autophagy and lysosome fusion, resulting in intracellular persistence in myeloid DCs, whereas TLR2 activation can overcome autophagy evasion and pathogen persistence in DCs (106). However, the importance of DC-SIGN in antifungal immunity has not been verified by a gene-targeting approach.

CD23 (encoded by *Fcer2a*): CD23 is the low-affinity receptor for IgE and is also a novel CLR which binds to α-mannans and β-glucans (107). A recent study illustrated that c-Jun N-terminal kinase 1 (JNK1) deficiency exerts a protective effect in systemic candidiasis. The expression of CD23 is negatively regulated through a Dectin-1-induced NF-AT pathway (107). Antifungal effector NOS2 is dramatically augmented through the recognition of α-mannans and β-glucans with CD23 in mice lacking JNK1. Likewise, the genetic deletion of CD23 abrogates the protection of $Jnk1^{-/-}$ mice from disseminated candidiasis. JNK inhibitors boost antifungal innate immunity *in vivo* and *in vitro* (107). Taken together, JNK inhibition may also be a novel therapeutic strategy to combat disseminated candidiasis (**Figure 2**).

CR3 (Mac-1, $\alpha_{M\beta2}$, or CD11b/CD18): CR3 is mainly expressed in leukocytes. CR3 consists of an I domain and a specific lectin domain, which bind to protein ligands such as iC3b, fibronectin and ICAM-1, and complement deposited on β-1,6-glucans (108). CR3 has been shown to cooperate with Dectin-1 for the detection of β-glucans and the regulation of innate immune responses during fungal pathogen exposure (109). Recent studies identified that CR3 and Dectin-1 collaboratively induce cytokine responses in macrophages in an Syk/JNK/AP-1 manner upon disseminated *H. capsulatum* infection (110), which further facilitates fungal-adaptive immune responses. Still, the underlying molecular mechanisms of crosstalk among other fungal PRRs will be of great interest for future investigations.

Collaboration between CLRs and TLRs

There is emerging evidence that signaling from CLRs in collaboration with other PRRs, especially TLRs, is indispensable for optimal antifungal immunity. It has been reported that the cooperative interaction between Dectin-1 and TLR2 or TLR4 synergistically facilitates the production of TNF, IL-23, and IL-10, but reduces IL-12 (59, 111). Dectin-1/TLR2 can amplify MR-mediated Th17 responses and IL-17 production upon *C. albicans* infection (34). In addition, DC-SIGN modulates the signaling from multiple TLRs on human DCs through activating Raf-1-dependent acetylation of NF-κB, which can promote the transcription of IL-10 and enhance antifungal-inflammatory response (23).

Recent studies have shown the importance of costimulation of Mincle and TLRs in protective antifungal response to *F. pedrosoi*, the most common fungus associated with chromoblastomycosis. Normally, *F. pedrosoi* is recognized by CLRs, but not TLRs, leading to the defective production of costimulatory cytokines and impaired fungal clearance. Intriguingly, the exogenous application of TLR7 ligand, imiquimod, restores the induction of inflammatory responses mediated *via* both Syk/CARD9- and MyD88-dependent-signaling pathways, as well as facilitates *F. pedrosoi* clearance in mice (90). In support of this finding, the topical administration of imiquimod to several patients with chromoblastomycosis also results in rapid infection resolution and greatly improved the lesions (112).

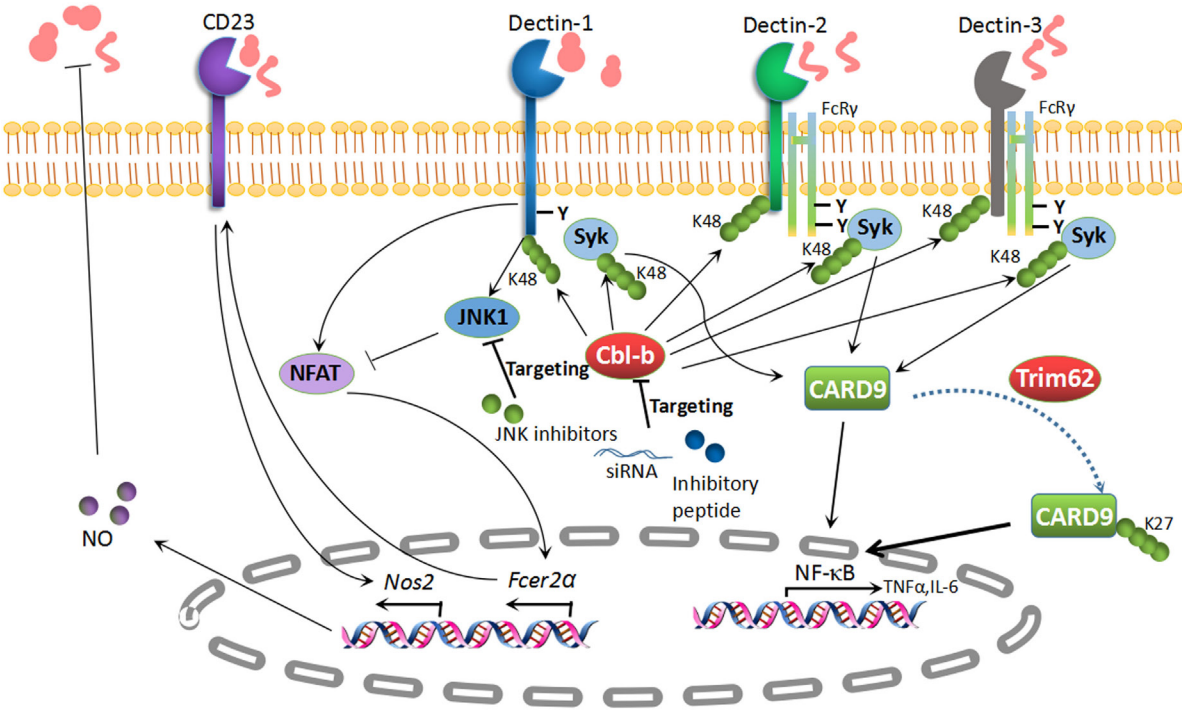

FIGURE 2 | Potential targets in antifungal immunity. K48-linked polyubiquitination of Dectin-1, Dectin-2, Dectin-3, and Syk is mediated by the E3 ubiquitin ligase Cbl-b, which results in the degradation of these molecules. Subsequently, the pro-inflammatory cytokines are impaired in the presence of Cbl-b. The inhibition of Cbl-b with an inhibitory peptide or *Cbl-b* siRNA can boost antifungal immunity, which provides a potential treatment strategy for fungal invasion. CD23 is a novel C-type lectin receptor for fungal recognition, which is elevated in parallel with NO production in *Jnk1*$^{-/-}$ mice. The inhibition of c-Jun N-terminal kinase 1 (JNK1) has revealed its potential as a therapeutic target for enhancing antifungal immunity. TRIM62, another E3 ubiquitin ligase, is responsible for K27-linked polyubiquitination of caspase activation and recruitment domain-containing protein 9 (CARD9) to elicit its antifungal immunity. TRIM62 or CARD9 variants appear to be potential therapeutic targets for fungal infections.

INFLAMMASOMES IN ANTIFUNGAL IMMUNITY

Emerging evidence shows that the engagement of inflammasomes plays a critical role in host defense against fungal infection, which can lead to the processing and activation of IL-1β and IL-18 (113). Both cytokines are implicated in mediating antifungal cellular responses, especially the promotion of adaptive T_H1/T_H17 responses.

NLRP3 has been proposed to be the main inflammasome involved in protective fungal immunity (114). Several CLRs and TLRs can induce the priming of inflammasomes and the activation of NF-κB *via* the recognition of fungal PAMPs, resulting in the expression of pro-IL-1β and pro-IL-18 (115–117). Both Dectin-1/Syk- and TLR2/MYD88-signaling pathways have been shown to induce NLRP3 priming in murine macrophages infected with *C. albicans* (114). In addition, the production of pro-IL-1β in response to *A. fumigatus, M. canis, Malassezia* spp., *P. brasiliensis*, and *C. neoformans* requires Dectin-1/Syk-dependent signaling (118–122). A more recent study indicates that Dectin-2 is the primary receptor for NLRP3 inflammasome activation in DCs in response to *H. capsulatum* (117). It is unknown whether Dectin-2 and other CLRs such as Dectin-3, Mincle, and MR are also involved in the activation of inflammasomes.

The canonical NLRP3 inflammasome can be triggered by ROS, K^+ efflux, and lysosomal cathepsins release induced by various fungal species. Upon infection with *C. albicans* and *A. fumigatus*, it has been shown that the activation of the NLRP3 inflammasome requires transition from the yeast to the filamentous phase (123), which may be attributed to the differential exposure of β-glucans on the fungal surface and thus the differential recognition by Dectin-1 (124). Upon phagocytosis by host macrophages, *C. albicans* filaments trigger lysosomal rupture, which is required for the particulate activation of the NLRP3 inflammasome (124, 125). In addition, *C. albicans*-secreted aspartic proteases Sap2 and Sap6 are thought to activate the caspase-1-dependent NLRP3 inflammasome by inducing ROS production and K^+ efflux (126). Recent evidence has shown that NLRP3 coupling with AIM2 receptors is required to activate caspase-1- and caspase-8-dependent inflammasomes and induce protective antifungal responses in DCs challenged with *A. fumigatus* (127). Mice deficient in both NLRP3 and AIM2 are more susceptible to invasive Aspergillosis than mice lacking a single inflammasome receptor, suggesting the importance of cooperative activation and dual cytoplasmic surveillance of these two inflammasomes against *A. fumigatus* infection (127). Interestingly, mucosal *Candida* infection induces the activation of an NLRC4-dependent inflammasome, which can utilize caspase-1 to process IL-1β and IL-18 (128). The NLRC4

inflammasome protects against mucosal fungal overgrowth and facilitates inflammatory cytokine secretion and neutrophil influx in a murine model of oropharyngeal candidiasis (128).

Recently, an NLR-independent and caspase-8-dependent inflammasome have been identified (115). It seems that Dectin-1 signaling induces the formation of a CARD9/Bcl-10/MALT1/caspase-8/ASC complex which is dependent on Syk (115). Interestingly, caspase-8 in this complex is only partially cleaved to generate a p43 intermediate, which averts the triggering of caspase-3 and apoptosis (115). Dectin-1-mediated activation of caspase-8 appears to be involved in the cleavage of pro-IL-1β and the production of its bioactive form to defend against fungi (115). A subsequent study reported that this noncanonical caspase-8 inflammasome can be activated and modulated by Tec, an intracellular non-receptor PTK, which acts as a novel signaling mediator between Dectin-1/Syk and PLC-γ2 in macrophages upon infection with *Candida* (116). The genetic ablation or the chemical inhibition of Tec results in a dramatic reduction of inflammatory responses and protects from fatal fungal sepsis (116). Interestingly, it has been shown that caspase-8, coordinating with caspase-1, plays a crucial role in promoting NLRP3 inflammasome-dependent maturation of IL-1β mediated by Dectin-1 and CR3 in DCs during β-glucan sensing and *C. albicans* infection (109). In addition, the same group also showed that there is crosstalk between CR3 and Dectin-1 during *H. capsulatum* yeast infection in macrophage TNF and IL-6 responses in an Syk/JNK/AP-1-dependent manner (110). However, it was reported that *H. capsulatum* α-(1,3)-glucan blocks innate immune recognition by Dectin-1 (129). The importance of Dectin-1 in *H. capsulatum* infection, in particular *in vivo*, remains to be determined. Furthermore, the role of caspase-8 in controlling antifungal immunity has not been confirmed by a gene-targeting approach.

CLR-MEDIATED PTMS IN ANTIFUNGAL IMMUNITY

Recent literature has shed additional light on novel molecules engaged in antifungal immunity and PTMs in CLR-signaling cascades, thus opening new avenues for innovative therapeutic approaches (107, 130–133). It has been increasingly recognized that PTMs serve as modulators to tailor fungal evasion by targeting innate sensors, adaptors, signaling components, and transcription factors. Subsequently, PTMs regulate the activation, survival, and stability of potent proteins by linking covalent bonds to functional groups (134). To date, several PTMs including phosphorylation and ubiquitination have been characterized in the regulation of immune responses against fungi.

Protein Kinases and Phosphatases in Antifungal Innate Immunity

Two major cytoplasmic kinase families in innate cells, including the Src family kinases and the Syk, are involved in intracellular-signaling cascades upon fungal pathogen exposure. Signaling involving the phosphorylation of tyrosine residues within the ITAM(s) by Src family kinases leads to the recruitment and activation of Syk, which then phosphorylates phospholipase Cγ2 (PLC-γ2). Activated PLC-γ2 initiates the hydrolysis of membrane-bound phosphatidylinositol-3,4,5-triphosphate (PIP_3) to soluble inositol triphosphate (IP_3) and diacylglycerol, both of which result in the influx of calcium and the activation of PKC-δ, the latter mediating the phosphorylation of CARD9 and the subsequent activation of the CARD9/Bcl-10/MALT1 complex. Downstream signaling through the Syk/PLCγ2 pathway from Dectin-1 and Dectin-2 involves the activation of NF-κB, ERK, and NF-AT (24, 53, 135, 136).

Numerous studies have shown that the balance between phosphorylation and dephosphorylation is of great importance in orchestrating fungal immune responses. In addition to Src kinases phosphorylating ITAM(s) within Dectin-1 and FcR-γ, recent literature has shown that two members of Src family kinases, Fyn and Lyn, facilitate the *cryptococcal*-killing capacity in NK cells by mediating PI3K/ERK1/2-signaling activity, which further directs the traffic of perforin-containing granules to synapses for pathogen clearance (137). Whether other Src family kinases are involved in the regulation of fungal invasion remains to be determined.

The CARD9/Bcl-10/MALT1 complex in Dectin-1 signaling upon *Candida* infection has been known to activate the IKK complex, leading to the phosphorylation of IκB and the activation of all canonical NF-κB subunits including p50, p65, and c-Rel (24, 51, 138). Importantly, Syk activation in response to Dectin-1 stimulation is also able to activate noncanonical subunits of NF-κB (p52 and RelB) through NIK and IKKα, leading to the nuclear translocation of p52–RelB dimers (24). In addition, Dectin-1 signaling can induce Syk-independent phosphorylation and activation of Raf-1 *via* Ras. Activated Ras leads to the activation of Raf-1, which then phosphorylates NF-κB p65, and facilitates p65–RelB dimer formation that sequesters active RelB and potentiates T_H1 responses by inducing IL-12p40 and IL-1β (24). Interestingly, another group recently found that Dectin-1 stimulated with *C. albicans* triggers Syk-dependent phosphorylation of Ras-GRF1, which mediates the recruitment and activation of H-Ras through CARD9 alone, but not the CARD9/Bcl-10/MALT1 complex, leading to the phosphorylation and activation of ERK, but not NF-κB and subsequent pro-inflammatory responses (53). This suggests that upon Dectin-1 signaling, CARD9 is required for ERK activation but is dispensable for NF-κB activation.

CLR (Dectin-1, Dectin-2/3, or Mincle) signaling has been reported to phosphorylate and activate SHP-2, which is able to recruit Syk to Dectin-1 or to the adaptor FcR-γ, thus resulting in the activation of Syk and downstream signaling and mediate antifungal innate immune responses and T_H17 responses (139). In addition, the phosphatase SHIP-1 has been recently identified to co-localize with Dectin-1-phosphorylated hem-ITAM and to negatively modulate ROS production in a Dectin/Syk/PI3K/PDK1/NADPH oxidase-dependent manner in response to *C. albicans* infection (140). Thus, a novel role of SHIP-1 in selectively controlling the balance of effectors in the Syk/PI3K pathway has been identified. Phosphatase and tensin homolog deleted on chromosome 10 also serves as a negative modulator to regulate the PGE2/cAMP/PKA-signaling cascade *via* blocking F-actin-mediated cytoskeletal remodeling and dephosphorylating

cofilin-1 during immune defense against pathogenic *C. albicans* (141). Therefore, phosphorylation- and dephosphorylation-mediated protein kinases and phosphatases are crucial for controlling antifungal immunity.

Ubiquitin Ligases and Deubiquitinating Enzymes in Antifungal Innate Immunity

PTM of target proteins by polyubiquitination has been intensively studied in numerous biological systems (142–146). Seven lysine residues in ubiquitin determine the specific type of polyubiquitination. Lysine 48 (K48)-linked polyubiquitination is involved in proteasome-mediated protein degradation, whereas lysine 63-linked polyubiquitination is usually engaged in signal pathway transmission (145). In addition to K48- and K63-linked polyubiquitination, K6-, K11-, K27-, K29-, and K33-linked polyubiquitination are being exploited to address their roles in immune responses and inflammatory diseases (145). Recently, a number of studies have highlighted an important role for ubiquitination of the CLR-signaling pathway in fungal immunity (130–133).

TRIM62

TRIM62, also named DEAR1, is a member of the TRIM/RBCC family, which includes proteins with conserved RING finger, B-box, and coiled-coil domains (147). It has been well established that CARD9 positively modulates host immune responses following fungal infection. TRIM62 has been shown to function as a CARD9-binding component and to mediate K27-linked polyubiquitination of CARD9 at K125 to facilitate its protective role in anti-fungi immune responses (130). Similar to *Card9*$^{-/-}$ mice, *Trim62*$^{-/-}$ mice also show increased susceptibility, as well as impaired cytokine responses, in a *C. albicans* infection model (130). Therefore, TRIM62 acts as a positive regulator essential for CARD9-mediated antifungal immunity. TRIM62 or CARD9 variants are therefore potential therapeutic targets for fungal infections (**Figure 2**).

Cbl-b

Cbl-b is a member of Cbl family RING finger E3 ubiquitin ligases (142, 148). Several other groups including ours identified RING finger-type E3 ubiquitin ligase Cbl-b as a key E3 ubiquitin ligase mediating host antifungal innate immunity (131–133). The genetic deletion of Cbl-b renders mice less susceptible to systemic *C. albicans* infection, which is in line with the hyperproduction of pro-inflammatory cytokines TNF-α and IL-6, the robust release of reactive oxygen species (ROS), and improved fungal killing. At the molecular level, Cbl-b targets Dectin-1, Dectin-2, Dectin-3, and SYK for K48-linked polyubiquitination and proteasome-mediated degradation, which further facilitates its anti-inflammatory response (131–133). Interestingly, Cbl-b small-inhibitory peptides and *Cbl-b*-specific siRNA provide protective efficacy against disseminated candidiasis (131, 132). Therefore, targeting Cbl-b may be a potential therapeutic strategy for disseminated candidiasis (**Figure 2**).

A20

A20 is a deubiquitination enzyme which is pivotal for tailoring innate immune responses by inhibiting the NF-κB-signaling cascade (149). IKKγ and TRAF6 activities are dampened in a non-catalytic manner by A20 (149, 150). A recent study showed that A20 is removed by autophagy, which further boosts NF-κB capacity in F4/80^{hi} tissue-resident macrophages to facilitate the pathogen clearance during disseminated *Candida* infection (151).

CONCLUSION

Much progress has been made to unveil the underlying mechanisms of fungal immunity. CLRs are considered to be pivotal in orchestrating innate and adaptive immunity against fungal pathogens based on animal and some human genetic studies. The discovery of novel molecules such as Cbl-b and JNK in anti-fungi immune responses has laid the foundation for potential treatment strategies. Yet, the exact crosstalk between innate and adaptive antifungal immunities, and the yet-to-be-defined PTMs, needs to be resolved in future studies. Moreover, translational studies of newly identified molecular targets are essential for future clinical application. Thus, the studies described in this review provide direction for the rational design of therapeutic strategies in disseminated candidiasis; however, further translational studies with animal models remain to be performed before moving forward into clinical application.

AUTHOR CONTRIBUTIONS

JT, GL, and JZ conceptualized the scope of the review; JT, GL, and JZ wrote the review; and LT and WYL edited the review.

FUNDING

This work is supported by the US National Institutes of Health (grants R01 AI090901, AI121196, and 123253; all to Jian Zhang) and the American Heart Association (AHA Great Rivers Associate Grant-in-Aid grant 16GRT2699004 to Jian Zhang).

REFERENCES

1. Brown GD, Denning DW, Levitz SM. Tackling human fungal infections. *Science* (2012) 336(6082):647. doi:10.1126/science.1222236
2. Gudlaugsson O, Gillespie S, Lee K, Vande Berg J, Hu J, Messer S, et al. Attributable mortality of nosocomial candidemia, revisited. *Clin Infect Dis* (2003) 37(9):1172–7. doi:10.1086/378745
3. Alter SJ, McDonald MB, Schloemer J, Simon R, Trevino J. Common child and adolescent cutaneous infestations and fungal infections. *Curr Probl Pediatr Adolesc Health Care* (2018) 48(1):3–25. doi:10.1016/j.cppeds.2017.11.001
4. Falagas ME, Betsi GI, Athanasiou S. Probiotics for prevention of recurrent vulvovaginal candidiasis: a review. *J Antimicrob Chemother* (2006) 58(2):266–72. doi:10.1093/jac/dkl246
5. Ansari Z, Miller D, Galor A. Current thoughts in fungal keratitis: diagnosis and treatment. *Curr Fungal Infect Rep* (2013) 7(3):209–18. doi:10.1007/s12281-013-0150-110.1007/s12281-013-0150-1
6. Seyedmousavi S, Netea MG, Mouton JW, Melchers WJ, Verweij PE, de Hoog GS. Black yeasts and their filamentous relatives: principles of pathogenesis and host defense. *Clin Microbiol Rev* (2014) 27(3):527–42. doi:10.1128/CMR.00093-13

7. Brown GD, Denning DW, Gow NA, Levitz SM, Netea MG, White TC. Hidden killers: human fungal infections. *Sci Transl Med* (2012) 4(165):165rv13. doi:10.1126/scitranslmed.3004404
8. Byrnes EJ III, Li W, Lewit Y, Ma H, Voelz K, Ren P, et al. Emergence and pathogenicity of highly virulent *Cryptococcus gattii* genotypes in the northwest United States. *PLoS Pathog* (2010) 6(4):e1000850. doi:10.1371/journal.ppat.1000850
9. Sears D, Schwartz BS. *Candida auris*: an emerging multidrug-resistant pathogen. *Int J Infect Dis* (2017) 63:95–8. doi:10.1016/j.ijid.2017.08.017
10. Geijtenbeek TB, Gringhuis SI. Signalling through C-type lectin receptors: shaping immune responses. *Nat Rev Immunol* (2009) 9(7):465–79. doi:10.1038/nri2569
11. Taylor PR, Tsoni SV, Willment JA, Dennehy KM, Rosas M, Findon H, et al. Dectin-1 is required for beta-glucan recognition and control of fungal infection. *Nat Immunol* (2007) 8(1):31–8. doi:10.1038/Ni1408
12. Saijo S, Ikeda S, Yamabe K, Kakuta S, Ishigame H, Akitsu A, et al. Dectin-2 recognition of alpha-mannans and induction of Th17 cell differentiation is essential for host defense against *Candida albicans*. *Immunity* (2010) 32(5):681–91. doi:10.1016/j.immuni.2010.05.001
13. Zhu LL, Zhao XQ, Jiang C, You Y, Chen XP, Jiang YY, et al. C-type lectin receptors dectin-3 and dectin-2 form a heterodimeric pattern-recognition receptor for host defense against fungal infection. *Immunity* (2013) 39(2):324–34. doi:10.1016/j.immuni.2013.05.017
14. Dambuza IM, Brown GD. C-type lectins in immunity: recent developments. *Curr Opin Immunol* (2015) 32:21–7. doi:10.1016/j.coi.2014.12.002
15. Gow NAR, Latge J-P, Munro CA. The fungal cell wall: structure, biosynthesis, and function. *Microbiol Spectr* (2017) 5(3). doi:10.1128/microbiolspec.FUNK-0035-2016
16. Latge JP. The cell wall: a carbohydrate armour for the fungal cell. *Mol Microbiol* (2007) 66(2):279–90. doi:10.1111/j.1365-2958.2007.05872.x
17. Levitz SM. Innate recognition of fungal cell walls. *PLoS Pathog* (2010) 6(4):e1000758. doi:10.1371/journal.ppat.1000758
18. Bowman SM, Free SJ. The structure and synthesis of the fungal cell wall. *Bioessays* (2006) 28(8):799–808. doi:10.1002/bies.20441
19. Ishikawa T, Itoh F, Yoshida S, Saijo S, Matsuzawa T, Gonoi T, et al. Identification of distinct ligands for the C-type lectin receptors Mincle and dectin-2 in the pathogenic fungus *Malassezia*. *Cell Host Microbe* (2013) 13(4):477–88. doi:10.1016/j.chom.2013.03.008
20. Gomez BL, Nosanchuk JD. Melanin and fungi. *Curr Opin Infect Dis* (2003) 16(2):91–6. doi:10.1097/01.aco.0000065076.06965.04
21. Nosanchuk JD, Stark RE, Casadevall A. Fungal melanin: what do we know about structure? *Front Microbiol* (2015) 6:1463. doi:10.3389/fmicb.2015.01463
22. Kawai T, Akira S. The roles of TLRs, RLRs and NLRs in pathogen recognition. *Int Immunol* (2009) 21(4):317–37. doi:10.1093/intimm/dxp017
23. Gringhuis SI, den Dunnen J, Litjens M, van Het Hof B, van Kooyk Y, Geijtenbeek TB. C-type lectin DC-SIGN modulates toll-like receptor signaling *via* Raf-1 kinase-dependent acetylation of transcription factor NF-kappaB. *Immunity* (2007) 26(5):605–16. doi:10.1016/j.immuni.2007.03.012
24. Gringhuis SI, den Dunnen J, Litjens M, van der Vlist M, Wevers B, Bruijns SC, et al. Dectin-1 directs T helper cell differentiation by controlling noncanonical NF-kappaB activation through Raf-1 and Syk. *Nat Immunol* (2009) 10(2):203–13. doi:10.1038/ni.1692
25. Rogers NC, Slack EC, Edwards AD, Nolte MA, Schulz O, Schweighoffer E, et al. e Sousa: Syk-dependent cytokine induction by dectin-1 reveals a novel pattern recognition pathway for C type lectins. *Immunity* (2005) 22(4):507–17. doi:10.1016/j.immuni.2005.03.004
26. Zelensky AN, Gready JE. The C-type lectin-like domain superfamily. *FEBS J* (2005) 272(24):6179–217. doi:10.1111/j.1742-4658.2005.05031.x
27. Sancho D, Reis C. e Sousa: signaling by myeloid C-type lectin receptors in immunity and homeostasis. *Annu Rev Immunol* (2012) 30:491–529. doi:10.1146/annurev-immunol-031210-101352
28. Brown GD, Gordon S. Immune recognition. A new receptor for beta-glucans. *Nature* (2001) 413(6851):36–7. doi:10.1038/35092620
29. Ross GD, Cain JA, Myones BL, Newman SL, Lachmann PJ. Specificity of membrane complement receptor type three (CR3) for beta-glucans. *Complement* (1987) 4(2):61–74. doi:10.1159/000463010
30. Xia Y, Vetvicka V, Yan J, Hanikyrova M, Mayadas T, Ross GD. The beta-glucan-binding lectin site of mouse CR3 (CD11b/CD18) and its function in generating a primed state of the receptor that mediates cytotoxic activation in response to iC3b-opsonized target cells. *J Immunol* (1999) 162(4):2281–90.
31. Vera J, Fenutria R, Canadas O, Figueras M, Mota R, Sarrias MR, et al. The CD5 ectodomain interacts with conserved fungal cell wall components and protects from zymosan-induced septic shock-like syndrome. *Proc Natl Acad Sci U S A* (2009) 106(5):1506–11. doi:10.1073/pnas.0805846106
32. Brown GD, Taylor PR, Reid DM, Willment JA, Williams DL, Martinez-Pomares L, et al. Dectin-1 is a major beta-glucan receptor on macrophages. *J Exp Med* (2002) 196(3):407–12. doi:10.1084/Jem.20020470
33. Means TK, Mylonakis E, Tampakakis E, Colvin RA, Seung E, Puckett L, et al. Evolutionarily conserved recognition and innate immunity to fungal pathogens by the scavenger receptors SCARF1 and CD36. *J Exp Med* (2009) 206(3):637–53. doi:10.1084/jem.20082109
34. van de Veerdonk FL, Marijnissen RJ, Kullberg BJ, Koenen HJ, Cheng SC, Joosten I, et al. The macrophage mannose receptor induces IL-17 in response to *Candida albicans*. *Cell Host Microbe* (2009) 5(4):329–40. doi:10.1016/j.chom.2009.02.006
35. Cambi A, Gijzen K, de Vries J, Torensma R, Joosten B, Adema GJ, et al. The C-type lectin DC-SIGN (CD209) is an antigen-uptake receptor for *Candida albicans* on dendritic cells. *Eur J Immunol* (2003) 33(2):532–8. doi:10.1002/immu.200310029
36. Yamasaki S, Matsumoto M, Takeuchi O, Matsuzawa T, Ishikawa E, Sakuma M, et al. C-type lectin Mincle is an activating receptor for pathogenic fungus, *Malassezia*. *Proc Natl Acad Sci U S A* (2009) 106(6):1897–902. doi:10.1073/pnas.0805177106
37. Cambi A, Netea MG, Mora-Montes HM, Gow NA, Hato SV, Lowman DW, et al. Dendritic cell interaction with *Candida albicans* critically depends on N-linked mannan. *J Biol Chem* (2008) 283(29):20590–9. doi:10.1074/jbc.M709334200
38. Saijo S, Fujikado N, Furuta T, Chung SH, Kotaki H, Seki K, et al. Dectin-1 is required for host defense against *Pneumocystis carinii* but not against *Candida albicans*. *Nat Immunol* (2007) 8(1):39–46. doi:10.1038/ni1425
39. Wagener J, Malireddi RK, Lenardon MD, Koberle M, Vautier S, MacCallum DM, et al. Fungal chitin dampens inflammation through IL-10 induction mediated by NOD2 and TLR9 activation. *PLoS Pathog* (2014) 10(4):e1004050. doi:10.1371/journal.ppat.1004050
40. Brown GD. Dectin-1: a signalling non-TLR pattern-recognition receptor. *Nat Rev Immunol* (2006) 6(1):33–43. doi:10.1038/Nri1745
41. Graham LM, Brown GD. The dectin-2 family of C-type lectins in immunity and homeostasis. *Cytokine* (2009) 48(1–2):148–55. doi:10.1016/j.cyto.2009.07.010
42. Guo Y, Feinberg H, Conroy E, Mitchell DA, Alvarez R, Blixt O, et al. Structural basis for distinct ligand-binding and targeting properties of the receptors DC-SIGN and DC-SIGNR. *Nat Struct Mol Biol* (2004) 11(7):591–8. doi:10.1038/nsmb784
43. Kruskal BA, Sastry K, Warner AB, Mathieu CE, Ezekowitz RA. Phagocytic chimeric receptors require both transmembrane and cytoplasmic domains from the mannose receptor. *J Exp Med* (1992) 176(6):1673–80. doi:10.1084/jem.176.6.1673
44. Boskovic J, Arnold JN, Stilion R, Gordon S, Sim RB, Rivera-Calzada A, et al. Structural model for the mannose receptor family uncovered by electron microscopy of Endo180 and the mannose receptor. *J Biol Chem* (2006) 281(13):8780–7. doi:10.1074/jbc.M513277200
45. Svajger U, Anderluh M, Jeras M, Obermajer N. C-type lectin DC-SIGN: an adhesion, signalling and antigen-uptake molecule that guides dendritic cells in immunity. *Cell Signal* (2010) 22(10):1397–405. doi:10.1016/j.cellsig.2010.03.018
46. Kerrigan AM, Brown GD. Syk-coupled C-type lectins in immunity. *Trends Immunol* (2011) 32(4):151–6. doi:10.1016/j.it.2011.01.002
47. Goodridge HS, Reyes CN, Becker CA, Katsumoto TR, Ma J, Wolf AJ, et al. Activation of the innate immune receptor dectin-1 upon formation of a 'phagocytic synapse'. *Nature* (2011) 472(7344):471–5. doi:10.1038/nature10071
48. Leibundgut-Landmann S, Osorio F, Brown GD, Reis C. e Sousa: stimulation of dendritic cells *via* the dectin-1/Syk pathway allows priming of cytotoxic T-cell responses. *Blood* (2008) 112(13):4971–80. doi:10.1182/blood-2008-05-158469

49. del Fresno C, Soulat D, Roth S, Blazek K, Udalova I, Sancho D, et al. Interferon-beta production *via* dectin-1-Syk-IRF5 signaling in dendritic cells is crucial for immunity to *C. albicans*. *Immunity* (2013) 38(6):1176–86. doi:10.1016/j.immuni.2013.05.010
50. Strasser D, Neumann K, Bergmann H, Marakalala MJ, Guler R, Rojowska A, et al. Syk kinase-coupled C-type lectin receptors engage protein kinase C-sigma to elicit Card9 adaptor-mediated innate immunity. *Immunity* (2012) 36(1):32–42. doi:10.1016/j.immuni.2011.11.015
51. Gross O, Gewies A, Finger K, Schafer M, Sparwasser T, Peschel C, et al. Card9 controls a non-TLR signalling pathway for innate anti-fungal immunity. *Nature* (2006) 442(7103):651–6. doi:10.1038/nature04926
52. Gringhuis SI, Wevers BA, Kaptein TM, van Capel TM, Theelen B, Boekhout T, et al. Selective C-Rel activation *via* Malt1 controls anti-fungal T(H)-17 immunity by dectin-1 and dectin-2. *PLoS Pathog* (2011) 7(1):e1001259. doi:10.1371/journal.ppat.1001259
53. Jia XM, Tang B, Zhu LL, Liu YH, Zhao XQ, Gorjestani S, et al. CARD9 mediates dectin-1-induced ERK activation by linking Ras-GRF1 to H-Ras for antifungal immunity. *J Exp Med* (2014) 211(11):2307–21. doi:10.1084/jem.20132349
54. LeibundGut-Landmann S, Gross O, Robinson MJ, Osorio F, Slack EC, Tsoni SV, et al. e Sousa: Syk- and CARD9-dependent coupling of innate immunity to the induction of T helper cells that produce interleukin 17. *Nat Immunol* (2007) 8(6):630–8. doi:10.1038/ni1460
55. Robinson MJ, Osorio F, Rosas M, Freitas RP, Schweighoffer E, Gross O, et al. e Sousa: dectin-2 is a Syk-coupled pattern recognition receptor crucial for Th17 responses to fungal infection. *J Exp Med* (2009) 206(9):2037–51. doi:10.1084/jem.20082818
56. Zielinski CE, Mele F, Aschenbrenner D, Jarrossay D, Ronchi F, Gattorno M, et al. Pathogen-induced human TH17 cells produce IFN-gamma or IL-10 and are regulated by IL-1beta. *Nature* (2012) 484(7395):514–8. doi:10.1038/nature10957
57. Goodridge HS, Underhill DM, Touret N. Mechanisms of Fc receptor and dectin-1 activation for phagocytosis. *Traffic* (2012) 13(8):1062–71. doi:10.1111/j.1600-0854.2012.01382.x
58. Underhill DM, Rossnagle E, Lowell CA, Simmons RM. Dectin-1 activates Syk tyrosine kinase in a dynamic subset of macrophages for reactive oxygen production. *Blood* (2005) 106(7):2543–50. doi:10.1182/blood-2005-03-1239
59. Dennehy KM, Willment JA, Williams DL, Brown GD. Reciprocal regulation of IL-23 and IL-12 following co-activation of dectin-1 and TLR signaling pathways. *Eur J Immunol* (2009) 39(5):1379–86. doi:10.1002/Eji.200838543
60. Bourgeois C, Majer O, Frohner IE, Lesiak-Markowicz I, Hildering KS, Glaser W, et al. Conventional dendritic cells mount a type I IFN response against *Candida* spp. requiring novel phagosomal TLR7-mediated IFN-beta signaling. *J Immunol* (2011) 186(5):3104–12. doi:10.4049/jimmunol.1002599
61. Smeekens SP, Ng A, Kumar V, Johnson MD, Plantinga TS, van Diemen C, et al. Functional genomics identifies type I interferon pathway as central for host defense against *Candida albicans*. *Nat Commun* (2013) 4:1342. doi:10.1038/ncomms2343
62. Goodridge HS, Simmons RM, Underhill DM. Dectin-1 stimulation by *Candida albicans* yeast or zymosan triggers NFAT activation in macrophages and dendritic cells. *J Immunol* (2007) 178(5):3107–15. doi:10.4049/jimmunol.178.5.3107
63. Fric J, Zelante T, Wong AY, Mertes A, Yu HB, Ricciardi-Castagnoli P. NFAT control of innate immunity. *Blood* (2012) 120(7):1380–9. doi:10.1182/blood-2012-02-404475
64. Macian F. NFAT proteins: key regulators of T-cell development and function. *Nat Rev Immunol* (2005) 5(6):472–84. doi:10.1038/nri1632
65. Lanternier F, Pathan S, Vincent QB, Liu L, Cypowyj S, Prando C, et al. Deep dermatophytosis and inherited CARD9 deficiency. *N Engl J Med* (2013) 369(18):1704–14. doi:10.1056/NEJMoa1208487
66. Drummond RA, Lionakis MS. Mechanistic insights into the role of C-type lectin receptor/CARD9 signaling in human antifungal immunity. *Front Cell Infect Microbiol* (2016) 6:39. doi:10.3389/fcimb.2016.00039
67. Glocker EO, Hennigs A, Nabavi M, Schaffer AA, Woellner C, Salzer U, et al. A homozygous CARD9 mutation in a family with susceptibility to fungal infections. *N Engl J Med* (2009) 361(18):1727–35. doi:10.1056/NEJMoa0810719
68. Drummond RA, Collar AL, Swamydas M, Rodriguez CA, Lim JK, Mendez LM, et al. CARD9-dependent neutrophil recruitment protects against fungal invasion of the central nervous system. *PLoS Pathog* (2015) 11(12):e1005293. doi:10.1371/journal.ppat.1005293
69. Jhingran A, Kasahara S, Shepardson KM, Junecko BA, Heung LJ, Kumasaka DK, et al. Compartment-specific and sequential role of MyD88 and CARD9 in chemokine induction and innate defense during respiratory fungal infection. *PLoS Pathog* (2015) 11(1):e1004589. doi:10.1371/journal.ppat.1004589
70. Rieber N, Gazendam RP, Freeman AF, Hsu AP, Collar AL, Sugui JA, et al. Extrapulmonary *Aspergillus* infection in patients with CARD9 deficiency. *JCI Insight* (2016) 1(17):e89890. doi:10.1172/jci.insight.89890
71. Roth S, Bergmann H, Jaeger M, Yeroslaviz A, Neumann K, Koenig PA, et al. Vav proteins are key regulators of Card9 signaling for innate antifungal immunity. *Cell Rep* (2016) 17(10):2572–83. doi:10.1016/j.celrep.2016.11.018
72. Fischer M, Spies-Weisshart B, Schrenk K, Gruhn B, Wittig S, Glaser A, et al. Polymorphisms of dectin-1 and TLR2 predispose to invasive fungal disease in patients with acute myeloid leukemia. *PLoS One* (2016) 11(3):e0150632. doi:10.1371/journal.pone.0150632
73. Rieber N, Singh A, Oz H, Carevic M, Bouzani M, Amich J, et al. Pathogenic fungi regulate immunity by inducing neutrophilic myeloid-derived suppressor cells. *Cell Host Microbe* (2015) 17(4):507–14. doi:10.1016/j.chom.2015.02.007
74. Yamasaki S, Ishikawa E, Sakuma M, Hara H, Ogata K, Saito T. Mincle is an ITAM-coupled activating receptor that senses damaged cells. *Nat Immunol* (2008) 9(10):1179–88. doi:10.1038/ni.1651
75. Sato K, Yang XL, Yudate T, Chung JS, Wu J, Luby-Phelps K, et al. Dectin-2 is a pattern recognition receptor for fungi that couples with the Fc receptor gamma chain to induce innate immune responses. *J Biol Chem* (2006) 281(50):38854–66. doi:10.1074/jbc.M606542200
76. Miyake Y, Toyonaga K, Mori D, Kakuta S, Hoshino Y, Oyamada A, et al. C-type lectin MCL is an FcRgamma-coupled receptor that mediates the adjuvanticity of mycobacterial cord factor. *Immunity* (2013) 38(5):1050–62. doi:10.1016/j.immuni.2013.03.010
77. Kerscher B, Willment JA, Brown GD. The dectin-2 family of C-type lectin-like receptors: an update. *Int Immunol* (2013) 25(5):271–7. doi:10.1093/intimm/dxt006
78. McGreal EP, Rosas M, Brown GD, Zamze S, Wong SY, Gordon S, et al. The carbohydrate-recognition domain of dectin-2 is a C-type lectin with specificity for high mannose. *Glycobiology* (2006) 16(5):422–30. doi:10.1093/glycob/cwj077
79. Barrett NA, Maekawa A, Rahman OM, Austen KF, Kanaoka Y. Dectin-2 recognition of house dust mite triggers cysteinyl leukotriene generation by dendritic cells. *J Immunol* (2009) 182(2):1119–28. doi:10.4049/jimmunol.182.2.1119
80. Ritter M, Gross O, Kays S, Ruland J, Nimmerjahn F, Saijo S, et al. da Costa: schistosoma mansoni triggers dectin-2, which activates the Nlrp3 inflammasome and alters adaptive immune responses. *Proc Natl Acad Sci U S A* (2010) 107(47):20459–64. doi:10.1073/pnas.1010337107
81. Campuzano A, Castro-Lopez N, Wozniak KL, Leopold Wager CM, Wormley FL Jr. Dectin-3 is not required for protection against *Cryptococcus neoformans* infection. *PLoS One* (2017) 12(1):e0169347. doi:10.1371/journal.pone.0169347
82. Zhao XQ, Zhu LL, Chang Q, Jiang C, You Y, Luo T, et al. C-type Lectin receptor dectin-3 mediates trehalose 6,6'-dimycolate (TDM)-induced Mincle expression through CARD9/Bcl10/MALT1-dependent nuclear factor (NF)-kappaB activation. *J Biol Chem* (2014) 289(43):30052–62. doi:10.1074/jbc.M114.588574
83. Miyake Y, Masatsugu OH, Yamasaki S. C-type lectin receptor MCL facilitates Mincle expression and signaling through complex formation. *J Immunol* (2015) 194(11):5366–74. doi:10.4049/jimmunol.1402429
84. Hernandez-Santos N, Gaffen SL. Th17 cells in immunity to *Candida albicans*. *Cell Host Microbe* (2012) 11(5):425–35. doi:10.1016/j.chom.2012.04.008
85. Wang H, Li M, Lerksuthirat T, Klein B, Wuthrich M. The C-type lectin receptor MCL mediates vaccine-induced immunity against infection with *Blastomyces dermatitidis*. *Infect Immun* (2015) 84(3):635–42. doi:10.1128/IAI.01263-15
86. Lee MJ, Yoshimoto E, Saijo S, Iwakura Y, Lin X, Katz HR, et al. Phosphoinositide 3-kinase delta regulates dectin-2 signaling and the generation of Th2 and Th17 immunity. *J Immunol* (2016) 197(1):278–87. doi:10.4049/jimmunol.1502485

87. Taylor PR, Roy S, Leal SM Jr, Sun Y, Howell SJ, Cobb BA, et al. Activation of neutrophils by autocrine IL-17A-IL-17RC interactions during fungal infection is regulated by IL-6, IL-23, RORgammat and dectin-2. *Nat Immunol* (2014) 15(2):143–51. doi:10.1038/ni.2797
88. Ishikawa E, Ishikawa T, Morita YS, Toyonaga K, Yamada H, Takeuchi O, et al. Direct recognition of the mycobacterial glycolipid, trehalose dimycolate, by C-type lectin Mincle. *J Exp Med* (2009) 206(13):2879–88. doi:10.1084/jem.20091750
89. Wells CA, Salvage-Jones JA, Li X, Hitchens K, Butcher S, Murray RZ, et al. The macrophage-inducible C-type lectin, Mincle, is an essential component of the innate immune response to *Candida albicans*. *J Immunol* (2008) 180(11):7404–13. doi:10.4049/jimmunol.180.11.7404
90. Sousa Mda G, Reid DM, Schweighoffer E, Tybulewicz V, Ruland J, Langhorne J, et al. Restoration of pattern recognition receptor costimulation to treat chromoblastomycosis, a chronic fungal infection of the skin. *Cell Host Microbe* (2011) 9(5):436–43. doi:10.1016/j.chom.2011.04.005
91. Bugarcic A, Hitchens K, Beckhouse AG, Wells CA, Ashman RB, Blanchard H. Human and mouse macrophage-inducible C-type lectin (Mincle) bind *Candida albicans*. *Glycobiology* (2008) 18(9):679–85. doi:10.1093/glycob/cwn046
92. Kerscher B, Wilson GJ, Reid DM, Mori D, Taylor JA, Besra GS, et al. Mycobacterial receptor, Clec4d (CLECSF8, MCL), is coregulated with Mincle and upregulated on mouse myeloid cells following microbial challenge. *Eur J Immunol* (2016) 46(2):381–9. doi:10.1002/eji.201545858
93. Wevers BA, Kaptein TM, Zijlstra-Willems EM, Theelen B, Boekhout T, Geijtenbeek TB, et al. Fungal engagement of the C-type lectin Mincle suppresses dectin-1-induced antifungal immunity. *Cell Host Microbe* (2014) 15(4):494–505. doi:10.1016/j.chom.2014.03.008
94. Porcaro I, Vidal M, Jouvert S, Stahl PD, Giaimis J. Mannose receptor contribution to *Candida albicans* phagocytosis by murine E-clone J774 macrophages. *J Leukoc Biol* (2003) 74(2):206–15. doi:10.1189/jlb.1202608
95. Rajaram MVS, Arnett E, Azad AK, Guirado E, Ni B, Gerberick AD, et al. *M. tuberculosis*-initiated human mannose receptor signaling regulates macrophage recognition and vesicle trafficking by FcRgamma-chain, Grb2, and SHP-1. *Cell Rep* (2017) 21(1):126–40. doi:10.1016/j.celrep.2017.09.034
96. Lee SJ, Zheng NY, Clavijo M, Nussenzweig MC. Normal host defense during systemic candidiasis in mannose receptor-deficient mice. *Infect Immun* (2003) 71(1):437–45. doi:10.1128/IAI.71.1.437-445.2003
97. Viriyakosol S, Jimenez Mdel P, Saijo S, Fierer J. Neither dectin-2 nor the mannose receptor is required for resistance to *Coccidioides immitis* in mice. *Infect Immun* (2014) 82(3):1147–56. doi:10.1128/IAI.01355-13
98. van Kooyk Y, Geijtenbeek TB. DC-SIGN: escape mechanism for pathogens. *Nat Rev Immunol* (2003) 3(9):697–709. doi:10.1038/nri1182
99. Tassaneetrithep B, Burgess TH, Granelli-Piperno A, Trumpfheller C, Finke J, Sun W, et al. DC-SIGN (CD209) mediates dengue virus infection of human dendritic cells. *J Exp Med* (2003) 197(7):823–9. doi:10.1084/jem.20021840
100. Engering A, Geijtenbeek TB, van Vliet SJ, Wijers M, van Liempt E, Demaurex N, et al. The dendritic cell-specific adhesion receptor DC-SIGN internalizes antigen for presentation to T cells. *J Immunol* (2002) 168(5):2118–26. doi:10.4049/jimmunol.168.5.2118
101. Hodges A, Sharrocks K, Edelmann M, Baban D, Moris A, Schwartz O, et al. Activation of the lectin DC-SIGN induces an immature dendritic cell phenotype triggering Rho-GTPase activity required for HIV-1 replication. *Nat Immunol* (2007) 8(6):569–77. doi:10.1038/ni1470
102. Gringhuis SI, den Dunnen J, Litjens M, van der Vlist M, Geijtenbeek TB. Carbohydrate-specific signaling through the DC-SIGN signalosome tailors immunity to *Mycobacterium tuberculosis*, HIV-1 and *Helicobacter pylori*. *Nat Immunol* (2009) 10(10):1081–8. doi:10.1038/ni.1778
103. Serrano-Gomez D, Leal JA, Corbi AL. DC-SIGN mediates the binding of *Aspergillus fumigatus* and keratinophylic fungi by human dendritic cells. *Immunobiology* (2005) 210(2–4):175–83. doi:10.1016/j.imbio.2005.05.011
104. Sainz J, Lupianez CB, Segura-Catena J, Vazquez L, Rios R, Oyonarte S, et al. Dectin-1 and DC-SIGN polymorphisms associated with invasive pulmonary Aspergillosis infection. *PLoS One* (2012) 7(2):e32273. doi:10.1371/journal.pone.0032273
105. Zenaro E, Donini M, Dusi S. Induction of Th1/Th17 immune response by *Mycobacterium tuberculosis*: role of dectin-1, Mannose receptor, and DC-SIGN. *J Leukoc Biol* (2009) 86(6):1393–401. doi:10.1189/jlb.0409242
106. El-Awady AR, Miles B, Scisci E, Kurago ZB, Palani CD, Arce RM, et al. Porphyromonas gingivalis evasion of autophagy and intracellular killing by human myeloid dendritic cells involves DC-SIGN-TLR2 crosstalk. *PLoS Pathog* (2015) 10(2):e1004647. doi:10.1371/journal.ppat.1004647
107. Zhao X, Guo Y, Jiang C, Chang Q, Zhang S, Luo T, et al. JNK1 negatively controls antifungal innate immunity by suppressing CD23 expression. *Nat Med* (2017) 23(3):337–46. doi:10.1038/nm.4260
108. Brown GD. Innate antifungal immunity: the key role of phagocytes. *Annu Rev Immunol* (2011) 29:1–21. doi:10.1146/annurev-immunol-030409-101229
109. Ganesan S, Rathinam VAK, Bossaller L, Army K, Kaiser WJ, Mocarski ES, et al. Caspase-8 modulates dectin-1 and complement receptor 3-driven IL-1beta production in response to beta-glucans and the fungal pathogen, *Candida albicans*. *J Immunol* (2014) 193(5):2519–30. doi:10.4049/jimmunol.1400276
110. Huang JH, Lin CY, Wu SY, Chen WY, Chu CL, Brown GD, et al. CR3 and dectin-1 collaborate in macrophage cytokine response through association on lipid rafts and activation of Syk-JNK-AP-1 pathway. *PLoS Pathog* (2015) 11(7):e1004985. doi:10.1371/journal.ppat.1004985
111. Brown GD, Herre J, Williams DL, Willment JA, Marshall ASJ, Gordon S. Dectin-1 mediates the biological effects of beta-glucans. *J Exp Med* (2003) 197(9):1119–24. doi:10.1084/Jem.20021890
112. de Sousa Mda G, Belda W Jr, Spina R, Lota PR, Valente NS, Brown GD, et al. Topical application of imiquimod as a treatment for chromoblastomycosis. *Clin Infect Dis* (2014) 58(12):1734–7. doi:10.1093/cid/ciu168
113. Tavares AH, Burgel PH, Bocca AL. Turning up the heat: inflammasome activation by fungal pathogens. *PLoS Pathog* (2015) 11(7):e1004948. doi:10.1371/journal.ppat.1004948
114. Hise AG, Tomalka J, Ganesan S, Patel K, Hall BA, Brown GD, et al. An essential role for the NLRP3 inflammasome in host defense against the human fungal pathogen *Candida albicans*. *Cell Host Microbe* (2009) 5(5):487–97. doi:10.1016/j.chom.2009.05.002
115. Gringhuis SI, Kaptein TM, Wevers BA, Theelen B, van der Vlist M, Boekhout T, et al. Dectin-1 is an extracellular pathogen sensor for the induction and processing of IL-1beta *via* a noncanonical caspase-8 inflammasome. *Nat Immunol* (2012) 13(3):246–54. doi:10.1038/ni.2222
116. Zwolanek F, Riedelberger M, Stolz V, Jenull S, Istel F, Koprulu AD, et al. The non-receptor tyrosine kinase Tec controls assembly and activity of the non-canonical caspase-8 inflammasome. *PLoS Pathog* (2014) 10(12):e1004525. doi:10.1371/journal.ppat.1004525
117. Chang TH, Huang JH, Lin HC, Chen WY, Lee YH, Hsu LC, et al. Dectin-2 is a primary receptor for NLRP3 inflammasome activation in dendritic cell response to *Histoplasma capsulatum*. *PLoS Pathog* (2017) 13(7):e1006485. doi:10.1371/journal.ppat.1006485
118. Tavares AH, Magalhaes KG, Almeida RD, Correa R, Burgel PH, Bocca AL. NLRP3 inflammasome activation by *Paracoccidioides brasiliensis*. *PLoS Negl Trop Dis* (2013) 7(12):e2595. doi:10.1371/journal.pntd.0002595
119. Guo C, Chen M, Fa Z, Lu A, Fang W, Sun B, et al. Acapsular *Cryptococcus neoformans* activates the NLRP3 inflammasome. *Microbes Infect* (2014) 16(10):845–54. doi:10.1016/j.micinf.2014.08.013
120. Said-Sadier N, Padilla E, Langsley G, Ojcius DM. *Aspergillus fumigatus* stimulates the NLRP3 inflammasome through a pathway requiring ROS production and the Syk tyrosine kinase. *PLoS One* (2010) 5(4):e10008. doi:10.1371/journal.pone.0010008
121. Mao L, Zhang L, Li H, Chen W, Wang H, Wu S, et al. Pathogenic fungus *Microsporum canis* activates the NLRP3 inflammasome. *Infect Immun* (2014) 82(2):882–92. doi:10.1128/IAI.01097-13
122. Kistowska M, Fenini G, Jankovic D, Feldmeyer L, Kerl K, Bosshard P, et al. *Malassezia* yeasts activate the NLRP3 inflammasome in antigen-presenting cells *via* Syk-kinase signalling. *Exp Dermatol* (2014) 23(12):884–9. doi:10.1111/exd.12552
123. Joly S, Ma N, Sadler JJ, Soll DR, Cassel SL, Sutterwala FS. Cutting edge: *Candida albicans* hyphae formation triggers activation of the Nlrp3 inflammasome. *J Immunol* (2009) 183(6):3578–81. doi:10.4049/jimmunol.0901323
124. Gow NA, van de Veerdonk FL, Brown AJ, Netea MG. *Candida albicans* morphogenesis and host defence: discriminating invasion from colonization. *Nat Rev Microbiol* (2011) 10(2):112–22. doi:10.1038/nrmicro2711
125. Krysan DJ, Sutterwala FS, Wellington M. Catching fire: *Candida albicans*, macrophages, and pyroptosis. *PLoS Pathog* (2014) 10(6):e1004139. doi:10.1371/journal.ppat.1004139

126. Pietrella D, Pandey N, Gabrielli E, Pericolini E, Perito S, Kasper L, et al. Secreted aspartic proteases of *Candida albicans* activate the NLRP3 inflammasome. *Eur J Immunol* (2013) 43(3):679–92. doi:10.1002/eji.201242691
127. Karki R, Man SM, Malireddi RK, Gurung P, Vogel P, Lamkanfi M, et al. Concerted activation of the AIM2 and NLRP3 inflammasomes orchestrates host protection against *Aspergillus* infection. *Cell Host Microbe* (2015) 17(3):357–68. doi:10.1016/j.chom.2015.01.006
128. Tomalka J, Ganesan S, Azodi E, Patel K, Majmudar P, Hall BA, et al. A novel role for the NLRC4 inflammasome in mucosal defenses against the fungal pathogen *Candida albicans*. *PLoS Pathog* (2011) 7(12):e1002379. doi:10.1371/journal.ppat.1002379
129. Rappleye CA, Eissenberg LG, Goldman WE. *Histoplasma capsulatum* alpha-(1,3)-glucan blocks innate immune recognition by the beta-glucan receptor. *Proc Natl Acad Sci U S A* (2007) 104(4):1366–70. doi:10.1073/pnas.0609848104
130. Cao Z, Conway KL, Heath RJ, Rush JS, Leshchiner ES, Ramirez-Ortiz ZG, et al. Ubiquitin ligase TRIM62 regulates CARD9-mediated anti-fungal immunity and intestinal inflammation. *Immunity* (2015) 43(4):715–26. doi:10.1016/j.immuni.2015.10.005
131. Xiao Y, Tang J, Guo H, Zhao Y, Tang R, Ouyang S, et al. Targeting CBLB as a potential therapeutic approach for disseminated candidiasis. *Nat Med* (2016) 22(8):906–14. doi:10.1038/nm.4141
132. Wirnsberger G, Zwolanek F, Asaoka T, Kozieradzki I, Tortola L, Wimmer RA, et al. Inhibition of CBLB protects from lethal *Candida albicans* sepsis. *Nat Med* (2016) 22(8):915–23. doi:10.1038/nm.4134
133. Zhu LL, Luo TM, Xu X, Guo YH, Zhao XQ, Wang TT, et al. E3 ubiquitin ligase Cbl-b negatively regulates C-type lectin receptor-mediated antifungal innate immunity. *J Exp Med* (2016) 213(8):1555–70. doi:10.1084/jem.20151932
134. Leach MD, Brown AJ. Posttranslational modifications of proteins in the pathobiology of medically relevant fungi. *Eukaryot Cell* (2012) 11(2):98–108. doi:10.1128/EC.05238-11
135. Kingeter LM, Lin X. C-type lectin receptor-induced NF-kappaB activation in innate immune and inflammatory responses. *Cell Mol Immunol* (2012) 9(2):105–12. doi:10.1038/cmi.2011.58
136. Gorjestani S, Yu M, Tang B, Zhang D, Wang D, Lin X. Phospholipase Cgamma2 (PLCgamma2) is key component in dectin-2 signaling pathway, mediating anti-fungal innate immune responses. *J Biol Chem* (2011) 286(51):43651–9. doi:10.1074/jbc.M111.307389
137. Oykhman P, Timm-McCann M, Xiang RF, Islam A, Li SS, Stack D, et al. Requirement and redundancy of the Src family kinases Fyn and Lyn in perforin-dependent killing of *Cryptococcus neoformans* by NK cells. *Infect Immun* (2013) 81(10):3912–22. doi:10.1128/IAI.00533-13
138. Dennehy KM, Ferwerda G, Faro-Trindade I, Pyz E, Willment JA, Taylor PR, et al. Syk kinase is required for collaborative cytokine production induced through dectin-1 and toll-like receptors. *Eur J Immunol* (2008) 38(2):500–6. doi:10.1002/Eji.200737741
139. Deng Z, Ma S, Zhou H, Zang A, Fang Y, Li T, et al. Tyrosine phosphatase SHP-2 mediates C-type lectin receptor-induced activation of the kinase Syk and anti-fungal TH17 responses. *Nat Immunol* (2015) 16(6):642–52. doi:10.1038/ni.3155
140. Blanco-Menendez N, Del Fresno C, Fernandes S, Calvo E, Conde-Garrosa R, Kerr WG, et al. SHIP-1 couples to the dectin-1 hemITAM and selectively modulates reactive oxygen species production in dendritic cells in response to *Candida albicans*. *J Immunol* (2015) 195(9):4466–78. doi:10.4049/jimmunol.1402874
141. Serezani CH, Kane S, Medeiros AI, Cornett AM, Kim SH, Marques MM, et al. PTEN directly activates the actin depolymerization factor cofilin-1 during PGE2-mediated inhibition of phagocytosis of fungi. *Sci Signal* (2012) 5(210):ra12. doi:10.1126/scisignal.2002448
142. Liu Q, Zhou H, Langdon WY, Zhang J. E3 ubiquitin ligase Cbl-b in innate and adaptive immunity. *Cell Cycle* (2014) 13(12):1875–84. doi:10.4161/cc.29213
143. Liu YC. Ubiquitin ligases and the immune response. *Annu Rev Immunol* (2004) 22:81–127. doi:10.1146/annurev.immunol.22.012703.104813
144. Reyes-Turcu FE, Ventii KH, Wilkinson KD. Regulation and cellular roles of ubiquitin-specific deubiquitinating enzymes. *Annu Rev Biochem* (2009) 78:363–97. doi:10.1146/annurev.biochem.78.082307.091526
145. Zinngrebe J, Montinaro A, Peltzer N, Walczak H. Ubiquitin in the immune system. *EMBO Rep* (2014) 15(1):28–45. doi:10.1002/embr.201338025
146. Bhoj VG, Chen ZJ. Ubiquitylation in innate and adaptive immunity. *Nature* (2009) 458(7237):430–7. doi:10.1038/nature07959
147. Huang F, Xiao H, Sun BL, Yang RG. Characterization of TRIM62 as a RING finger E3 ubiquitin ligase and its subcellular localization. *Biochem Biophys Res Commun* (2013) 432(2):208–13. doi:10.1016/j.bbrc.2013.02.012
148. Zhang J. Ubiquitin ligases in T cell activation and autoimmunity. *Clin Immunol* (2004) 111(3):234–40. doi:10.1016/j.clim.2004.02.003
149. Shembade N, Ma A, Harhaj EW. Inhibition of NF-kappaB signaling by A20 through disruption of ubiquitin enzyme complexes. *Science* (2010) 327(5969):1135–9. doi:10.1126/science.1182364
150. Skaug B, Chen J, Du F, He J, Ma A, Chen ZJ. Direct, noncatalytic mechanism of IKK inhibition by A20. *Mol Cell* (2011) 44(4):559–71. doi:10.1016/j.molcel.2011.09.015
151. Kanayama M, Inoue M, Danzaki K, Hammer G, He YW, Shinohara ML. Autophagy enhances NFkappaB activity in specific tissue macrophages by sequestering A20 to boost antifungal immunity. *Nat Commun* (2015) 6:5779. doi:10.1038/ncomms6779

Conflict of Interest Statement: The authors declare that the research was conducted in the absence of any commercial or financial relationships that could be construed as a potential conflict of interest.

Copyright © 2018 Tang, Lin, Langdon, Tao and Zhang. This is an open-access article distributed under the terms of the Creative Commons Attribution License (CC BY). The use, distribution or reproduction in other forums is permitted, provided the original author(s) and the copyright owner are credited and that the original publication in this journal is cited, in accordance with accepted academic practice. No use, distribution or reproduction is permitted which does not comply with these terms.

frontiers in Immunology

ORIGINAL RESEARCH
published: 20 March 2018
doi: 10.3389/fimmu.2018.00464

The Syk-Coupled C-Type Lectin Receptors Dectin-2 and Dectin-3 Are Involved in *Paracoccidioides brasiliensis* Recognition by Human Plasmacytoid Dendritic Cells

Nycolas Willian Preite, Claudia Feriotti, Dhêmerson Souza de Lima, Bruno Borges da Silva, Antônio Condino-Neto, Alessandra Pontillo, Vera Lúcia Garcia Calich and Flávio Vieira Loures†*

Departamento de Imunologia, Instituto de Ciências Biomédicas, Universidade de São Paulo, São Paulo, Brazil

Plasmacytoid dendritic cells (pDCs), which have been extensively studied in the context of the immune response to viruses, have recently been implicated in host defense mechanisms against fungal infections. Nevertheless, the involvement of human pDCs during paracoccidioidomycosis (PCM), a fungal infection endemic to Latin America, has been scarcely studied. However, pDCs were found in the cutaneous lesions of PCM patients, and in pulmonary model of murine PCM these cells were shown to control disease severity. These findings led us to investigate the role of human pDCs in the innate phase of PCM. Moreover, considering our previous data on the engagement of diverse Toll-like receptors and C-type lectin receptors receptors in *Paracoccidioides brasiliensis* recognition, we decided to characterize the innate immune receptors involved in the interaction between human pDCs and yeast cells. Purified pDCs were obtained from peripheral blood mononuclear cells from healthy donors and they were stimulated with *P. brasiliensis* with or without blocking antibodies to innate immune receptors. Here we demonstrated that *P. brasiliensis* stimulation activates human pDCs that inhibit fungal growth and secrete pro-inflammatory cytokines and type I IFNs. Surprisingly, *P. brasiliensis*-stimulated pDCs produce mature IL-1β and activate caspase 1, possibly *via* inflammasome activation, which is a phenomenon not yet described during pDC engagement by microorganisms. Importantly, we also demonstrate that dectin-2 and dectin-3 are expressed on pDCs and appear to be involved (*via* Syk signaling) in the pDC-*P. brasiliensis* interaction. Moreover, *P. brasiliensis*-stimulated pDCs exhibited an efficient antigen presentation and were able to effectively activate $CD4^+$ and $CD8^+$ T cells. In conclusion, our study demonstrated for the first time that human pDCs are involved in *P. brasiliensis* recognition and may play an important role in the innate and adaptive immunity against this fungal pathogen.

Keywords: paracoccidioidomycosis, plasmacytoid dendritic cells, C-type lectin receptors, dectin-2, dectin-3, type I IFNs, inflammasome

OPEN ACCESS

Edited by:
Amariliz Rivera, Rutgers University, United States

Reviewed by:
Roland Lang, Universitätsklinikum Erlangen, Germany
Patricia Fitzgerald-Bocarsly, Rutgers University, United States

***Correspondence:**
Flávio Vieira Loures
loures@unifesp.br

†***Present address:***
Flávio Vieira Loures, Instituto de Ciência e Tecnologia, Universidade Ferderal de São Paulo, São José dos Campos, Brazil

Specialty section:
This article was submitted to Microbial Immunology, a section of the journal Frontiers in Immunology

Received: *08 August 2017*
Accepted: *21 February 2018*
Published: *20 March 2018*

Citation:
Preite NW, Feriotti C, Souza de Lima D, da Silva BB, Condino-Neto A, Pontillo A, Calich VLG and Loures FV (2018) The Syk-Coupled C-Type Lectin Receptors Dectin-2 and Dectin-3 Are Involved in Paracoccidioides brasiliensis Recognition by Human Plasmacytoid Dendritic Cells. Front. Immunol. 9:464. doi: 10.3389/fimmu.2018.00464

INTRODUCTION

Paracoccidioidomycosis (PCM), the most prevalent and endemic deep mycosis in Latin America, is caused by the thermally dimorphic fungus *Paracoccidioides brasiliensis*. The resistance to this disease was linked to the secretion of Th1 cytokines in humans and murine models of PCM, while reduced Th1 immunity and the predominant secretion of Th2 cytokines associate with systemic and progressive illness (1, 2). The role of Th17 immunity is poorly defined. Nevertheless, in PCM patients, IL-17-expressing cells have been observed in cutaneous and mucosal lesions and they have been associated with the development of granulomas (3). Moreover, the varied patterns of T cell responses in patients with PCM lead to diverse clinical manifestations. In infected asymptomatic individuals, the resistance to infection was shown to be mediated by the Th1 response, which is essential for macrophage activation and fungal killing, while the juvenile form, the most severe form of the disease, presents a dominant Th2/Th9 response and an elevated antibody response. In adult form of the disease, a chronic inflammatory response involving Th1 and Th17-mediated immunity was also described (2).

Plasmacytoid dendritic cells (pDCs) are a DC subset largely involved in immune responses against viruses (4, 5). Following Toll-like receptors (TLRs) stimulation, the pDCs mature and become potent antigen-presenting cells (APCs), upregulating MHC and costimulatory molecules, and secreting high levels of cytokines such as IFN-α and TNF-α. Activated mature pDCs prime naive T cells for Th1 or Th17 differentiation (6, 7). Outside of viral infections, important roles for pDCs have been described in the immune response against fungal infections (8–12). A pioneer study showed that human pDCs interact to and inhibit the growth of *Aspergillus fumigatus*-hyphae. Moreover, *in vivo* depletion of pDC confers hyper-susceptibility to aspergillosis in mice. In addition, it was also demonstrated that dectin-2, a C-type lectin receptor (CLR) expressed by human pDCs, acts in collaboration with the FcRγ chain to recognize hyphae of *A. fumigatus*. This interaction induces the synthesis of TNF-α and IFN-α, and facilitates efficient antifungal activity. Additionally, pDCs stimulated by *A. fumigatus* hyphae exhibit a characteristic gene expression signature, leading to the formation of extracellular traps (pETs) (10). *P. brasiliensis* was also shown to be recognized by murine pDCs. *In vitro* stimulation of bone marrow-derived DCs (BMDCs) from susceptible (B10.A) mice induces a prevalent inflammatory myeloid phenotype characterized by the secretion of high levels of IL-12, TNF-α, and IL-1β. In contrast, in BMDCs from the resistant (A/J) mice a varied population of myeloid cells and pDCs secreting inflammatory cytokines and expressing high levels of secreted and membrane-bound TGF-β were observed following BMDCs stimulation with fungal cells (8). Importantly, in 24 of 46 PCM patients, the presence of pDCs was verified when their cutaneous lesions were immunostained with anti-pDC specific antibodies (11). In addition, peripheral blood pDCs appeared in lower numbers in PCM patients compared to the number of blood pDCs found in health donors, suggesting that pDCs migrate to the lymph nodes, spleen, and target organs during a *P. brasiliensis* infection (12). Taking in account these findings and the fact that human innate immunity against *P. brasiliensis* infection is poorly defined, we aimed to investigate the interaction of human pDCs with *P. brasiliensis* yeast cells. Moreover, considering our previous data on the engagement of TLRs, complement receptor-3, and CLRs in *P. brasiliensis* recognition (13–17), we considered that it would be important to define the class of innate receptors involved in fungal recognition by human pDCs. Here, we show that when stimulated by *P. brasiliensis* yeast cells human pDCs are activated, produce inflammatory cytokines, and acquire enhanced fungicidal activity. In addition, we demonstrate that *P. brasiliensis* recognition by human pDCs is mediated by dectin-2 and dectin-3, and is regulated by Syk signaling. Our study of the secretion of mature IL-β and caspase-1 activation has also indicated that *P. brasiliensis* recognition triggers inflammasome activation in human pDC, a finding that, as far we know, has not been described previously. Finally, our data also suggested that *P. brasiliensis* activated pDCs can prime the activation of $CD4^+$ and $CD8^+$ T cells, and may participate in the acquired immunity to this pathogen.

MATERIALS AND METHODS

Ethics Statement

All research involving human participants was approved by the Institute of Biomedical Science Institutional Ethics Committee. Written informed consent was obtained from all human participants and all clinical investigations were conducted according to the principles expressed in the Declaration of Helsinki.

Isolation of Human pDCs, mDCs, and $CD3^+$ Cells

The human pDCs were isolated from healthy donors using magnetic beads as previously described (10). About 120 mL of the peripheral blood was collected by venipuncture. The blood samples was anticoagulated with heparin, and the peripheral blood mononuclear cells (PBMCs) were purified by Ficoll-Hypaque density gradient centrifugation. The PBMCs were stained with CD304-coated magnetic beads (Miltenyi Biotec) and the pDCs were isolated after two rounds of positive selection. For flow cytometric experiments in which pDCs were gated using an anti-CD123 antibody, only one round of positive selection was run. For some experiments, the flow-through cells (here called pDC^- cells), which consisted of PBMCs depleted of $CD304^+$ cells, were also collected. For coculture experiments, purified human myeloid dendritic cells (mDCs) and CD3 cells were obtained from PBMCs by positive selection using magnetic beads (Miltenyi Biotec). mDCs were also used in qPCR experiments. The purity of the cell populations was confirmed by assessing the expression of CD123, CD1c, and CD3 as pDC, mDC, and lymphocyte markers, respectively, by flow cytometry. The purity of pDCs, mDCs, and $CD3^+$ cells always exceeded 95%.

P. brasiliensis Yeast Cells and pDC Stimulation

Paracoccidioides brasiliensis yeast cells were maintained by weekly cultivation in Fava Netto culture medium at 37°C and used on day 7 of culture. The highly virulent *P. brasiliensis*

18 isolate was used in this study. To determine the viability of fungal cell suspensions we used Janus Green B vital dye (Merck), and the viability was always greater than 95%. For colony-forming units (CFU) and ELISA experiments, pDC (1×10^5) or flow through-cells (pDC$^-$) were challenged overnight with *P. brasiliensis* in different ratios of pDC:*P. brasiliensis*, such as 10:1, 25:1, and 50:1 (1×10^4, 4×10^3, and 2×10^3 yeasts, respectively) as indicated in the figure legends.

Reagents and Cell Culture

The RPMI-1640 media was obtained from GIBCO (Invitrogen) and was supplemented with 100 U/mL penicillin, 100 U/mL streptomycin, and 2 mM L-glutamine. IgG Rat monoclonal anti-dectin-1 (Biolegend), dectin-2 (R&D System), dectin-3 (Biolegend), and antimincle (InvivoGen) blocking antibodies were used in the concentration indicated in the figure legends. The TLR-9 antagonist (A151, TTAGGG oligonucleotide sequence,

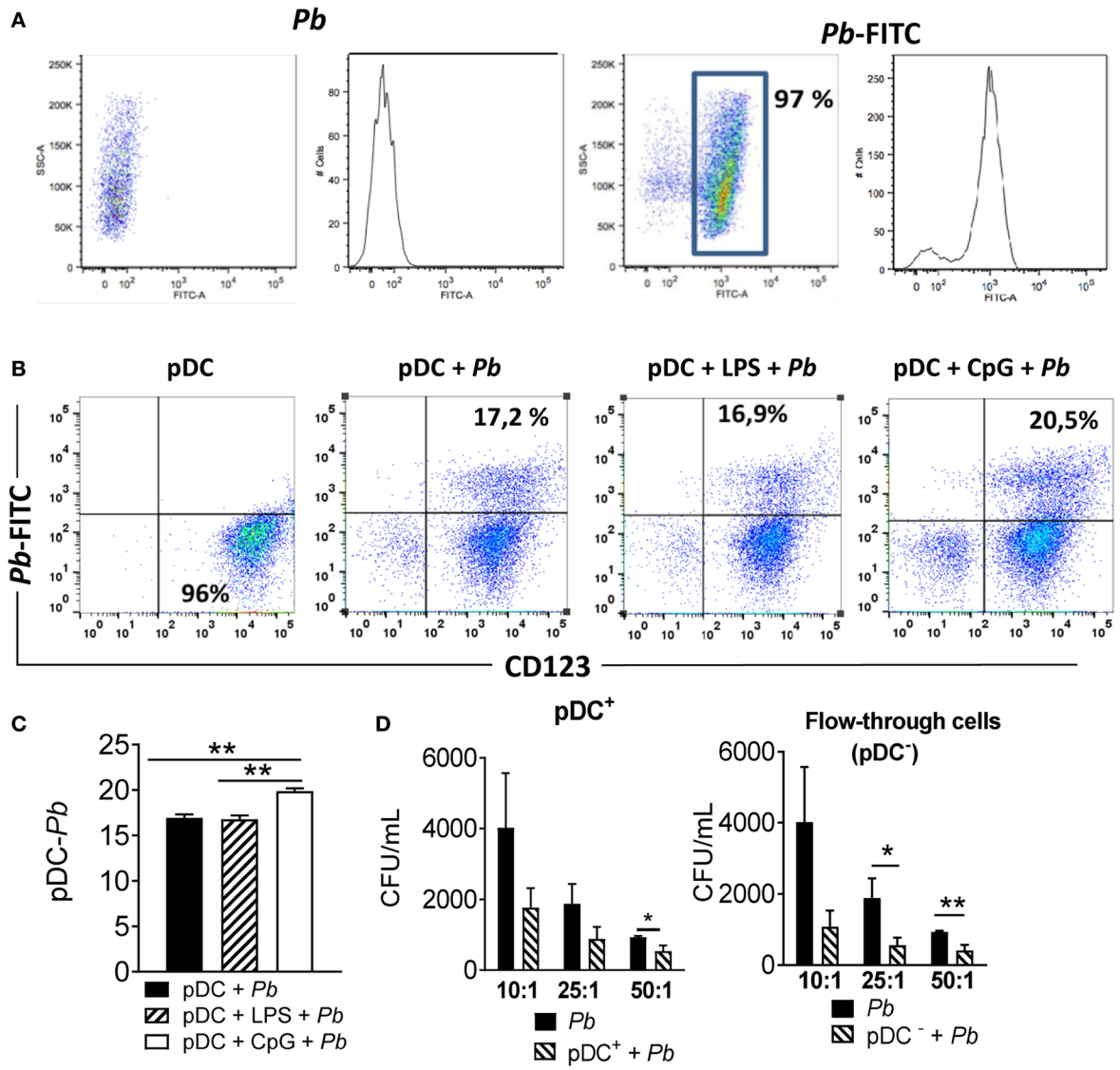

FIGURE 1 | Plasmacytoid dendritic cells (pDCs) interact with and control *Paracoccidioides brasiliensis* growth. **(A,B)** Peripheral blood mononuclear cells (PBMCs) were separated into pDC positive (pDCs+) using magnetic beads conjugated to an anti-CD304 antibody. The cells (2×10^5/well) were challenged for 4 h with *P. brasiliensis* yeast cells (2×10^5/well) previously labeled with FITC. Some wells were treated with CpG (100 ng/mL) or LPS (10 ng/mL) before the challenge. After 4 h of culture, the cells were labeled with an anti-CD123 antibody (specific to human pDCs) in the appropriate titration, and then 50,000 events were acquired by flow cytometry. **(B)** Dot plots are representative results for an experiment from three independents experiments. **(C)** Data represent means ± SE of the pDC–*P. brasiliensis* interaction from three donors, tested in triplicate $^{**}p < 0.01$. **(D)** For CFU analysis, PBMCs were separated into pDC-positive (pDCs$^+$) and pDC-negative (pDC$^-$) fractions using CD304-coated magnetic beads. The pDCs$^+$ and flow through-cells (1×10^5/well) were then challenged with *P. brasiliensis* yeast cells in different ratios of pDC: *Pb*, such as 10:1, 25:1 and 50:1 (1×10^4, 4×10^3, and 2×10^3 yeasts, respectively). After 18 h of culture, the plates were centrifuged and the supernatant was collected for cytokine measurements by ELISA. The pellet was lysed and suspended in 200 µL of phosphate-buffered saline. Next, 100 µL was transferred to BHI medium and the colonies (CFU) counted for 15 days. Data represent means ± SE of CFU from four donors, tested in triplicate. $^*p < 0.05$, $^{**}p < 0.01$, and $^{***}p < 0.001$.

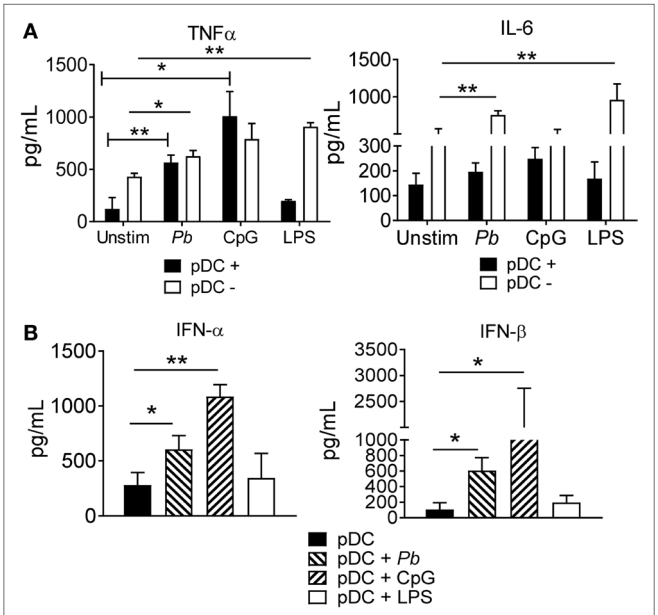

FIGURE 2 | Proinflammatory and type I IFNs cytokines released by plasmacytoid dendritic cells (pDCs) stimulated with *Paracoccidioides brasiliensis* yeast cells. Peripheral blood mononuclear cells (PBMCs) were separated into pDC-positive (pDCs$^+$) and pDC-negative (pDCs$^-$) populations using magnetic beads conjugated to anti-CD304 antibodies. The cells (1×10^5/well) were left without stimulation or challenged overnight with of *P. brasiliensis* yeast cells (2×10^3), CpG (100 ng/mL), or LPS (10 ng/mL). The supernatant was removed and the levels of IL-6, TNF-α **(A)**, and type I IFNs **(B)** were analyzed by ELISA. Data are represented as the mean ± SE of the average cytokine concentrations from five donors, tested in duplicate. ***$p < 0.001$ by comparing the data indicated by the bar.

10 μg/mL), TLR-7/9 inhibitor Bafilomycin A1 (10 μg/mL), and the immunostimulatory CpG 2336 oligonucleotide (100 ng/mL) were purchased from InvivoGen. Ultrapure *Escherichia coli* LPS (10 ng/mL) and the Syk inhibitor piceatannol (10 μM) was purchased from Sigma.

P. brasiliensis–pDC Interaction

Paracoccidioides brasiliensis yeast cells were labeled with fluorescein isothiocyanate (FITC) as previously described (18). Briefly, the yeasts were washed in phosphate-buffered saline (PBS, pH = 7.4) and heat-killed at 60°C for 1 h. To eliminate the aggregates, the yeast cells suspension was subjected to three cycles of sonication for 10 s each (21% amplitude) with Sonics (Vibra Cell VCX 750, Sonics & Materials). The yeasts were washed twice with PBS, counted and adjusted to 1×10^6 cells/mL, and then incubated with FITC (100 μg/mL, Sigma) for 25–30 min at 36°C. The yeast suspension was then washed with PBS twice. The pDCs (2×10^5) were challenged for 4 h with *P. brasiliensis*-FITC (1×10^5) at a ratio of 2:1 at 36°C in 5% CO_2 to permit fungi adhesion and ingestion. The cells were then harvested and the pDCs were labeled with anti-CD123 (eBioscience) antibody for 25 min at 4°C. Because *P. brasiliensis* yeast cells are highly variable in size and granularity (different sizes, number of buds, and number of nuclei), the granulocyte gates defined by size (FSC) and granularity (SSC) in order to determine the pDC population were not used. A minimum of 50,000 events were acquired on a FACScanto II flow cytometer (BD Biosciences) using the FACSDiva software (BD Biosciences). The data were analyzed using the FlowJo software (Tree Star).

Cytokine Measurements

The pDCs were cultured in 96-well plates in pDC media. The cells were left untreated or incubated with anti-dectin-1, dectin-2, dectin-3, or antimincle antibodies (100 μg/mL) for 30 min at 37°C. The pDCs were then challenged with *P. brasiliensis* yeast cells at a final volume of 200 μL in pDC media at the ratios indicated in the figure legends. Control wells contained pDCs only, pDCs and antibodies, pDCs and CpG, or pDCs and LPS. For the inhibition of TLR-9, pDCs were left untreated or incubated for 30 min with either 10 μg/mL of bafilomycin A1 or 10 μg/mL of the TLR-9 antagonist A151. After 18 h of incubation at 37°C, the supernatants were removed and the levels of TNF-α, IL-6, IL-1β, IFN-α, and IFN-β were measured by ELISA according to the manufacturers' protocols (eBioscience for TNF-α and IL-6; Biolegend for IL-1β; PBL Assay Science for IFN-α and IFN-β).

CFU Assays

The number of viable microorganisms in cell cultures was performed by counting the number of CFU as previously described (19). Briefly, after 18 h of coculture, the plates were centrifuged (400 *g*, 10 min, 4°C), and the supernatant was collected for cytokine measurements by ELISA. The wells were lysed with 200 μL of distilled water. The suspensions were collected in individual tubes and centrifuged (400 *g*, 10 min, 4°C). The pellet was suspended in 1 mL of PBS, and 100 μL of each lysate was spread onto BHI medium. The colonies (CFU) were counted for 15 days.

pDC Flow Cytometric Analysis

The pDC$^+$ populations (2×10^5/well) were either left unstimulated or challenged overnight with *P. brasiliensis* yeast cells (4×10^3). For cell-surface staining, the pDCs were washed and suspended at 2×10^5 cells/mL in staining buffer (PBS, 2% fetal calf serum, and 0.1% NaN_3) and then stained in the dark for 20 min at 4°C with the optimal dilution of anti-123, CD86, MHC-II antibodies. The cells were then washed twice with staining buffer, suspended in 200 μL of paraformaldehyde (PFA) to fix the cells. To measure caspase-1 activity, the pDCs were adjusted to 2×10^5 viable cells in 20 μL of apoptosis wash buffer. Cells were stained with FLICA probe according to the manufacturer's protocol (Immunochemistry Technologies) for 1 h at 37°C in 5% CO_2. Control wells contained untreated pDCs, pDC and CpG, or pDC and LPS. In some experiments, cells were treated with 1 mM ATP (Sigma-Aldrich) for 15 min and then stained with FLICA probe. Active caspase-1 was then measured by flow cytometry as previously described (16). To exclude dead cells, the Live/Dead Fixable Violet Cell Stain Kit (Life Technologies) was used according to the manufacturer's instructions. A minimum of 50,000 events were acquired on a FACScanto II flow cytometer (BD Biosciences) using the FACSDiva software (BD Biosciences). The pDCs were gated based upon their forward and side light scatter. The cell surface expression of pDC markers was analyzed using FlowJo software (Tree Star).

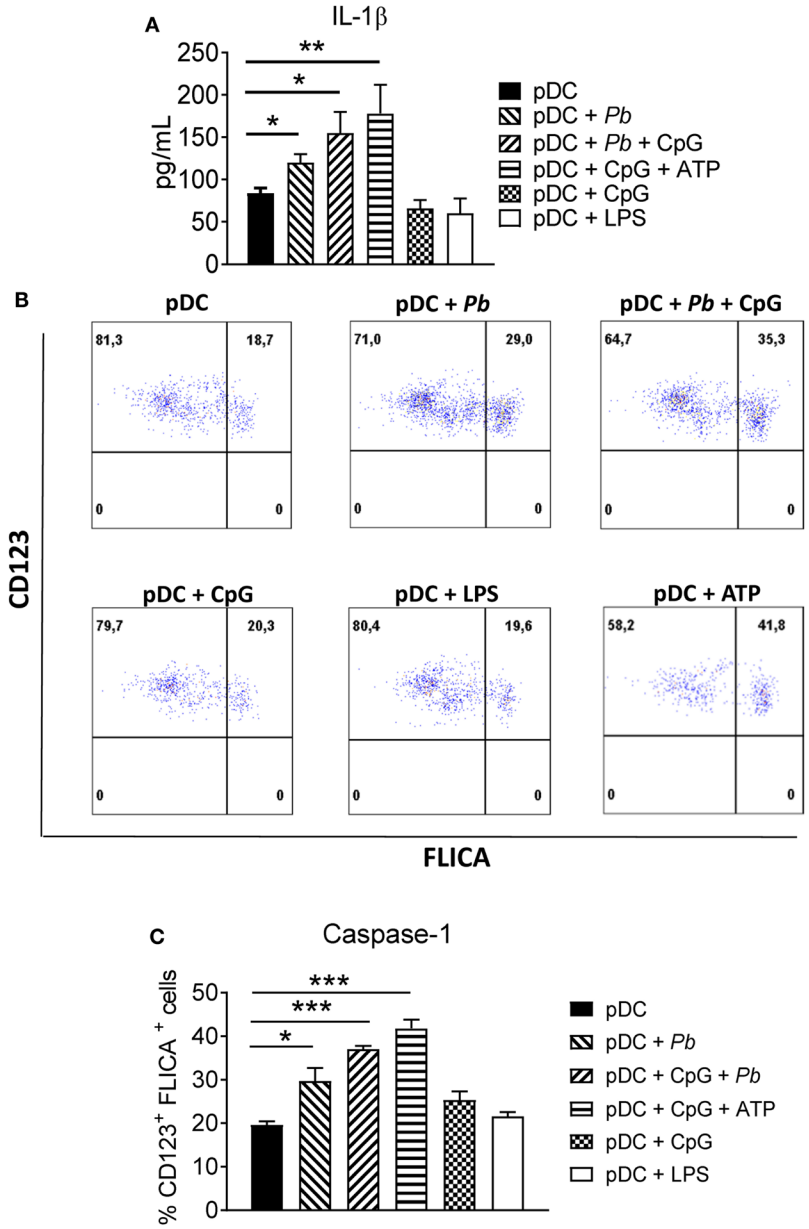

FIGURE 3 | Plasmacytoid dendritic cell (pDC) exposed to *Paracoccidioides brasiliensis* yeast cells secretes mature IL-1β and express activated caspase-1. **(A)** Peripheral blood mononuclear cells (PBMCs) were separated into pDC positive (pDCs+) cells using magnetic beads conjugated to anti-CD304 antibodies. The cells (1×10^5/well) were then left without stimulation or challenged overnight with *P. brasiliensis* yeast cells (2×10^3), CpG (100 ng/mL), or LPS (10 ng/mL). The supernatant was removed and the levels of IL-1β were analyzed by ELISA. Data are represented as the mean ± SE of the average cytokine concentrations from three donors, tested in duplicate. *$p < 0.05$ by comparing the data indicated by the bar. **(B,C)** Caspase-1 activity was evaluated by flow cytometry. PBMCs were separated into pDC positive (pDCs+) populations using magnetic beads conjugated to anti-CD304 antibodies. The cells (2×10^5/well) were left without stimulation or challenged overnight with *P. brasiliensis* yeast cells (4×10^3), CpG (100 ng/mL), or LPS (10 ng/mL). Cells were stained with FLICA probe for 1 h and the percentage of $CD123^+FLICA^+$ cells were determined by flow cytometry. **(B)** Dot plots are representative results of an experiment from two independent experiments. **(C)** Data are represented as the mean ± SE of $CD123^+FLICA^+$ cells from two donors, tested in duplicate. *$p < 0.05$, **$p < 0.01$, ***$p < 0.001$ by comparing the data indicated by the bars.

RNA Isolation and Relative Gene Expression Analysis

Total RNA was isolated and converted into cDNA from 2×10^5 purified pDC^+ and mDC^+, unstimulated or challenged overnight with *P. brasiliensis* yeast cells (4×10^3), using the TaqMan Gene Expression Cells-to-CT kit according to manufacturer's protocol (Applied Biosystems, Thermofisher Scientific). The expression of *CLEC7A/DECTIN1, CLEC6A/DECTIN2, CLEC4D/DECTIN3,*

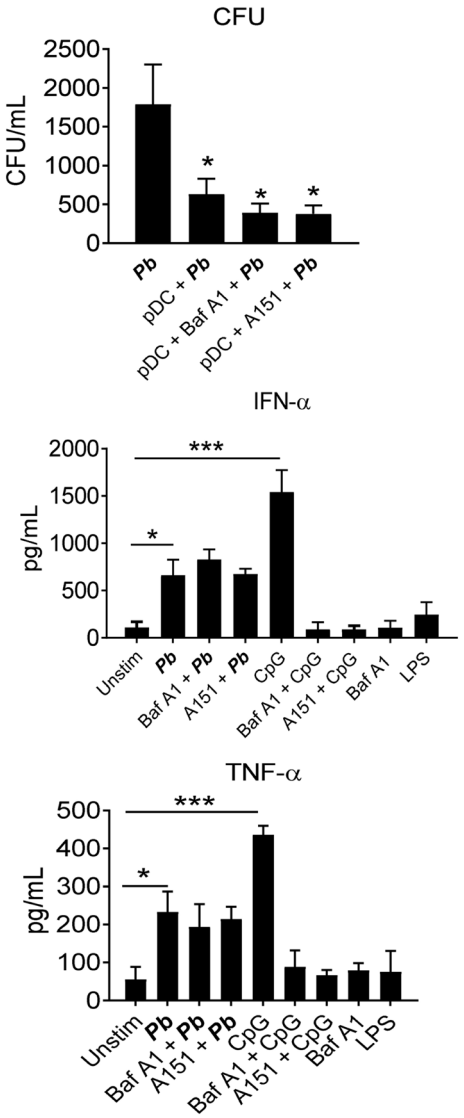

FIGURE 4 | Toll-like receptor (TLR)-9 is not used by plasmacytoid dendritic cells (pDCs) to sense *Paracoccidioides brasiliensis* yeast cells. peripheral blood mononuclear cells were separated into pDC-positive populations (pDCs$^+$) using magnetic beads conjugated to anti-CD304 antibody. The cells (1×10^5/well) were challenged overnight with *P. brasiliensis* yeast cells (2×10^3). Some wells were kept unstimulated, with only the yeasts, and LPS (100 ng/mL). Some cultures were treated with an TLR-9 antagonist (A151, TTAGGG, 10 μg/mL) or with the TLR-9 inhibitor Bafilomycin A1 (10 μg/mL) before challenging either with the yeasts or with the positive control for TLR-9 activation CpG (100 ng/mL). After 18 h of culture, the plates were centrifuged and the supernatant was collected for cytokine measurements by ELISA. The pellet was lysed and suspended in 200 μL of phosphate-buffered saline. Next, 100 μL was transferred to BHI medium, and the colonies (CFU) were counted for 15 days. Data represent the means ± SE of the CFU and cytokine concentrations from three donors, tested in triplicate. *$p < 0.05$ comparing the group maintained only with the fungus with the others.

CLEC4E/MINCLE was evaluated using gene-specific TaqMan assays (Applied Biosystems) and qPCR on a MxP3000P Real-Time PCR System (Stratagene). Raw expression data (Ct) were normalized with the expression of the housekeeping gene glyceraldehyde-3-phosphate dehydrogenase/*GAPDH* (ΔCt). Relative expression of the target genes was calculated as $2^{-\Delta Ct}$ according to Schmittgen and Livak (20), comparing stimulated and unstimulated cells ($\Delta\Delta Ct = \Delta Ct_{Pb} - \Delta Ct_{Unstimulated}$).

pDC/mDC and Lymphocyte Coculture

The pDCs$^+$ or mDCs$^+$ populations (1×10^5/well) were challenged with *P. brasiliensis* yeast cells (1×10^4) for 2 h and cocultured with CD3$^+$ cells (1×10^6) for 5 days at 37°C in 5% CO_2. All cells populations were isolated from the same donor. The ratio DCs to lymphocytes (1:10) was determined in a previous study (15). For cell-surface staining, the cocultured cells were washed and suspended at a concentration of 5×10^5 cells/mL in staining buffer (PBS, 2% fetal calf serum and 0.1% NaN_3). They were then stained in the dark for 20 min at 4°C with the optimal dilution of anti-CD4, CD8, CD25, and anti-CD69 antibodies. The cells were then washed twice with staining buffer, and suspended in 200 μL of PFA to fix the cells. A minimum of 50,000 events were acquired on FACScanto II flow cytometer (BD Biosciences) using the FACSDiva software (BD Biosciences). The lymphocytes were gated based upon forward and side light scatter. The cell surface expression of lymphocyte markers was analyzed using FlowJo software (Tree Star).

Statistical Analysis

For comparisons of two groups, the means ± SE were analyzed using the two-tailed unpaired Student's *t*-test with the Bonferroni correction applied when making multiple comparisons. For comparisons of more than two groups, significance was determined using the one- or two-way analysis of variance with the Tukey multiple corrections. Kruskal–Wallis test was applied in RT-PCR experiments. All data were collected and analyzed from at least three independent experiments. The levels of significance were $p < 0.05$ (*$p < 0.05$, **$p < 0.01$, and ***$p < 0.001$). Calculations were performed using a statistical software package (GraphPad Prism 6.0).

RESULTS

The *P. brasiliensis*–pDC Interaction and Fungicidal Activity

Initially, we investigated the ability of human pDCs to interact and phagocytose *P. brasiliensis* yeast cells. PBMC-isolated pDCs were challenged with FITC-conjugated *P. brasiliensis* (**Figure 1A**) for 4 h, and the frequency of adhered or ingested *P. brasiliensis* yeast cells by pDCs was determined by counting the number of labeled pDC (CD123$^+$ cells) containing *Pb*-FITC (CD123$^+$ *Pb*-FITC$^+$). **Figure 1B** shows that about 17% of the total pDCs were double-positive for CD123 and *Pb*-FITC, suggesting that pDCs interacted with *P. brasiliensis* yeast cells. Considering that human pDCs are TLR-9$^+$ and TLR-4$^-$ (21, 22), the TLR-4 bacterial LPS agonist and the TLR-9 CpG agonist were used in some experiments to specifically prime pDCs to enhance their phagocytic ability. As expected, the ability of pDCs to interact with the yeasts did not significantly change in the presence of LPS. However, the addition of CpG enhanced the *P. brasilienis*–pDC interaction (**Figures 1B,C**).

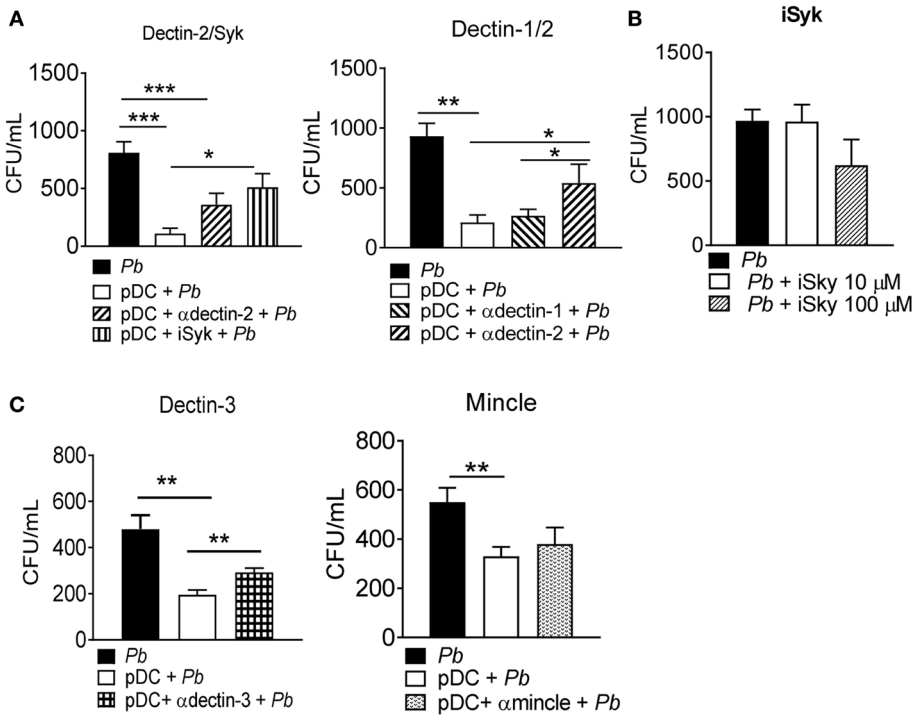

FIGURE 5 | Dectin2, dectin-3, and Syk signaling activate the fungicidal activity of plasmacytoid dendritic cells (pDCs). Peripheral blood mononuclear cells were separated into pDC-positive populations (pDCs+) using magnetic beads conjugated to anti-CD304 antibody. The cells (1×10^5/well) were challenged overnight with *P. brasiliensis* yeast cells (2×10^3). **(A)** Some cultures were treated with anti-dectin-1, dectin-2, or with a Syk pathway inhibitor, piceatannol (10 μM). **(B)** The Syk inhibitor (10 or 100 μM) was also cultured with *P. brasiliensis* yeast cells only. **(C)** Futher, anti-mincle and anti-dectin-3 antibodies (100 μg/mL) were also used, before challenging with *P. brasiliensis* yeast cells. After 18 h of culture, the plates were centrifuged, and the supernatant was collected for cytokine measurements by ELISA. The pellet was lysed and suspended in 200 μL of phosphate-buffered saline. Next, 100 μL was transferred to BHI medium, and the colonies (CFU) were counted for 15 days. Data represent the means ± SE of the CFU from three donors, tested in triplicate. $^*p < 0.05$, $^{**}p < 0.01$, $^{***}p < 0.001$ by comparing the data indicated by the bars.

To analyze the fungicidal ability of human pDCs, the PBMCs were separated into pDC^+ or pDC^- populations. The pDC^- fraction is composed of the flow-through cells resulting from the pDC isolation. This fraction, used as a control in some assays, contains mostly non-pDC PBMCs such as conventional DCs, monocytes, lymphocytes and small fractions of other cell subpopulations. The depletion of pDC was able to reduce the frequency of pDC on the PBMCs in about 90% (Figure S1 in Supplementary Material) resulting in less than 0.2% of pDC in the PBMCs. The cells were challenged overnight with *P. brasiliensis* yeast cells in different pDC: *Pb* ratios (10:1, 25:1, and 50:1). **Figure 1D** shows that only in the 50:1 ratio were pDCs able to control fungal growth. The pDC^- fractions, however, showed fungicidal activity at ratios of 25:1 and 50:1.

Cytokine Release by Human pDCs Stimulated by *P. brasiliensis* Yeast Cells

Next, we examined whether the interaction between the pDCs and *P. brasiliensis* yeast cells could induce the secretion of inflammatory cytokines. The pDCs were challenged with *P. brasiliensis* for 18 h, and the levels of TNF-α and IL-6 in the culture supernatants were determined. Both cytokines were secreted by pDCs, but only TNF-α levels were increased by *P. brasiliensis*-stimulated pDCs. The TLR-9 ligand, CpG, strongly stimulated the pDCs, whereas the TLR-4 ligand, LPS, failed to stimulate these cells to produce either TNF-α or IL-6. As expected, LPS stimulated the pDC^- fraction (which contained LPS-responsive monocytes) to release TNF-α and IL-6 (**Figure 2A**).

Next, we examined whether the interaction of pDCs with *P. brasiliensis* yeast cells could increase type I IFN release. Both IFN-α and IFN-β were secreted by $pDCs^+$ following stimulation with *P. brasiliensis* yeast cells. Once again, CpG strongly stimulated the pDCs, while LPS failed to activate these cells (**Figure 2B**).

P. brasiliensis Induces Production of IL-1β and Increases Caspase-1 Activity in Human pDCs

An emerging area of investigation examines the participation of the inflammasome in fungal infections (16, 23). The inflammasome is a multiprotein cytoplasmic complex assembled after an innate immune receptor [e.g., NOD-like receptor family, pyrin domain-containing (NLRP) 1, NLRP3, or absent in melanoma 2 (AIM2)] is activated by a pathogen-associated molecular pattern (PAMPs) or damage-associated molecular pattern. This results in a multi-protein platform that activates caspase-1, which processes

pro-IL-1β and pro-IL-18 into their biologically active or mature forms (24).

In our experiments, *P. brasiliensis* yeast cells induced a significant production of IL-1β by pDCs. Importantly, treatment with CpG or LPS alone did not significantly increase IL-1β production by these cells (**Figure 3A**). Accordingly, caspase-1 activation was strongly induced in *P. brasiliensis*-stimulated pDCs, more than in LPS-treated or CpG-treated pDCs (**Figures 3B,C**). However, when pDCs received both signals (CpG and yeasts), enhancement in the activity of caspase-1 was observed. Importantly, the addition of 1 mM ATP to the cultures increased caspase-1 activity and IL-1β production, suggesting that a purinergic signaling could be involved in inflammasome activation by *P. brasiliensis*. To our knowledge, increased extracellular ATP activates NLRP3-inflammasome through the binding on P2 × 7 purinergic receptor inducing a K^+ efflux which in turn activates NLRP3 (25). Deeper investigations are needed to confirm the involvement of ATP-P2 × 7-NLRP3 axis in pDC response to *P. brasiliensis*, although the involvement of P2 × 7 receptor in the immunoprotection of murine PCM was demonstrated in our previous studies (26).

The Role of TLR-9 in the *P. brasiliensis*–pDC Interaction

Several studies have demonstrated that TLR-9 is an important PRR used by pDCs during their interaction with microorganisms. We have assessed the role of TLR-9 in the sensing of *P. brasiliensis* by human pDCs using two reagents that inhibit this receptor. Thus, the influence of bafilomycin A1, an endosomal acidification inhibitor known to interfere with TLR-9 signaling (27), and the TLR-9 antagonist A151 (28), on the ability of pDCs to kill *P. brasiliensis* and release cytokines was determined. Both TLR-9 inhibitors showed no effects on *P. brasiliensis* growth or IFN-α secretion. Furthermore, bafilomycin A1 did not affect TNF-α production. As expected, both inhibitors abrogated CpG-stimulated type I IFN release (**Figure 4**). These data suggest that *P. brasiliensis* is recognized by human pDCs in a TLR-9-independent manner.

The Role of CLRs in the *P. brasiliensis*–pDC Interaction

Since *P. brasiliensis* recognition was observed to be TLR-9-independent, we assessed the role of some CLRs in fungal recognition by pDCs. CLRs are a large family of calcium-dependent carbohydrate binding molecules expressed by macrophages, DCs and other leukocytes (29). The mannose receptor (MR), dectin-1, dectin-2, dectin-3, and mincle receptors are examples of CLRs involved in antifungal immunity, although their function and signaling mechanisms are still being clarified (30). Anti-dectin-1, dectin-2, dectin-3, and mincle antibodies were used to block these receptors during the interaction of pDCs with *P. brasiliensis* yeast cells. We also used piceatannol (10 μM), which blocks the activity of the Syk enzyme, involved in CLR signaling. The specific blockade of dectin 2 and Syk, but not dectin 1, reduced the fungicidal ability of pDCs. This indicated the involvement of dectin-2/Syk signaling during fungal recognition and activation of pDCs (**Figure 5A**). Importantly, the Syk inhibitor piceatannol did not compromise fungal growth even when a high concentration (100 μM) was used in the *P. brasiliensis* culture (**Figure 5B**). We also investigated the role of dectin-3 and mincle receptors during the recognition of *P. brasiliensis* yeast cells by pDCs, because both CLRs were not previously studied in innate immunity against *P. brasiliensis* infection. Interestingly, dectin-3 but not mincle blocked by specific antibodies prior to *P. brasiliensis* stimulation, improved the recovery of yeast cells from the pDC-*P. brasiliensis* cocultures (**Figure 5C**).

Regarding cytokines released, an impaired production of TNF-α, IL-1β, and IFN-β was observed when dectin-2 or Syk were inhibited. No inhibition of IL-6 production was observed when the Syk pathway or dectin-2 were blocked (**Figure 6**). We also observed a reduction in the production of TNF-α and IL-1β following treatment with anti-dectin-3 antibody (**Figure 7A**). In line with the CFU results, treatment with the anti-mincle antibody did not influence cytokine production by *P. brasiliensis*-stimulated pDCs (**Figure 7B**). Again, treatment with both anti-dectin-3 and mincle antibodies did not alter IL-6 production. Importantly, in contrast with the absence of blocking activity on pDC, the anti-mincle antibody blocked mDC (Figure S2 in Supplementary Material).

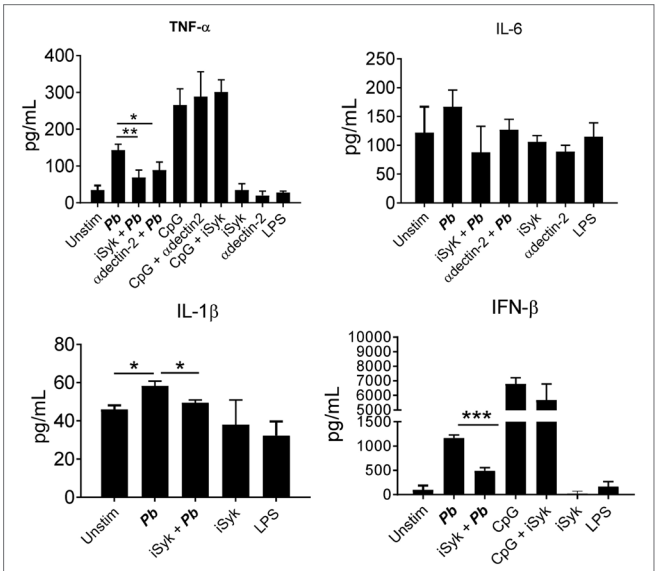

FIGURE 6 | Dectin-2/Syk signaling controls the secretion of cytokines by *Paracoccidioides brasiliensis* stimulated plasmacytoid dendritic cells (pDCs). Peripheral blood mononuclear cells were separated into pDC-positive populations ($pDCs^+$) using magnetic beads conjugated to anti-CD304 antibodies. The pDCs (1×10^5/well) were challenged overnight with of *P. brasiliensis* yeast cells (2×10^5). Some wells were kept only with the yeasts, CpG (100 ng/mL), or LPS (10 ng/mL). Some cultures were treated with anti-dectin-2 antibody (100 μg/mL) or with a Syk pathway inhibitor, piceatannol (10 μM), before challenging with *P. brasiliensis* yeast cells. After 18 h of culture, the plates were centrifuged and the supernatant was collected for cytokines measurements by ELISA. Data are represented by the means ± SE of the average cytokine concentrations from four donors, tested in duplicate. ***$p < 0.001$ and *$p < 0.05$ comparing the data indicated by the bars.

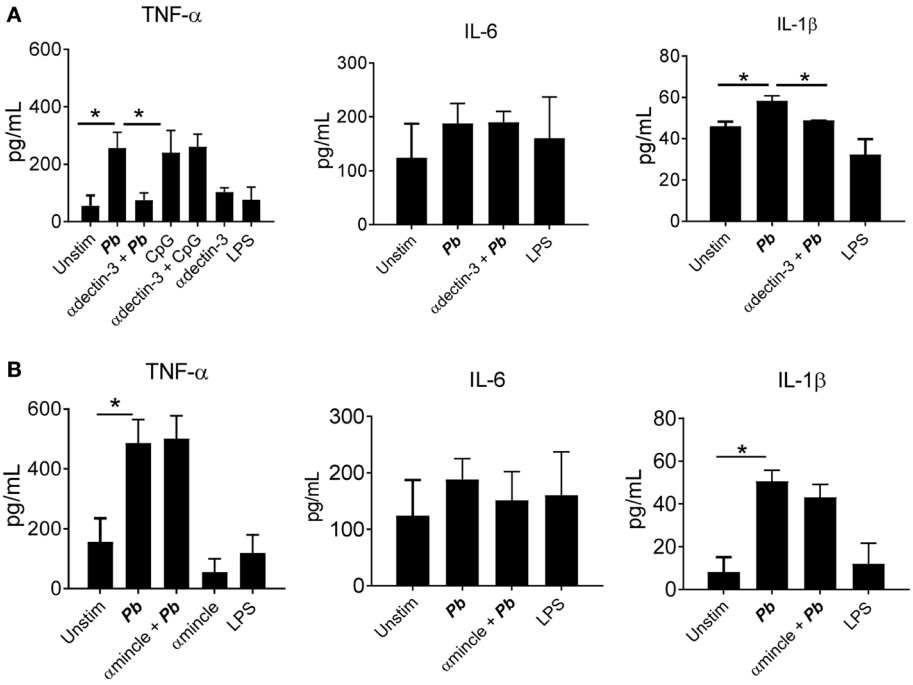

FIGURE 7 | Dectin-3, but not mincle, controls cytokine secretion by *Paracoccidioides brasiliensis* stimulated plasmacytoid dendritic cells (pDCs). Peripheral blood mononuclear cells were separated into pDC-positive populations (pDCs$^+$) using magnetic beads conjugated to anti-CD304 antibodies. The pDCs (1×10^5/well) were challenged overnight with *P. brasiliensis* yeast cells (2×10^3). Some wells were treated only with the yeasts or with LPS (10 ng/mL). Some cultures were treated with **(A)** anti-mincle (100 μg/mL) or **(B)** anti-dectin-3 antibody (100 μg/mL). After 18 h of culture, the plates were centrifuged, and the supernatant was collected for cytokine measurements by ELISA. Data are represented as the mean ± SE of the average of cytokine concentrations from four donors, tested in duplicate. ***$p < 0.001$ and *$p < 0.05$ comparing the data indicated by the bar.

When the expression of *DECTIN1*, *DECTIN2*, *DECTIN3* and *MINCLE* genes was investigated in mDCs and pDCs, we observed that while all genes were expressed in mDCs, only *DECTIN2* and *DECTIN3* were found on human pDCs, therefore explaining the previously mentioned lack of effect of blocking antibodies for dectin-1 and mincle in pDC activation. The basal expression of *DECTIN2* resulted significantly higher in pDC compared to mDC ($p = 0.005$) (**Figure 8A**). When DCs where stimulated by *P. brasiliensis* yeast cells, the expression of *DECTIN2* and *DECTIN3* resulted downregulated compared to unstimulated resting cells (FC < 1) (**Figure 8B**). Of note *P. brasiliensis* induced a statistically significant downregulation of *DECTIN2* in mDCs (FC = 0.10 ± 0.08; logFC = −1.49 ± 0.36; $p = 0.025$), and of *DECTIN2* (FC = 0.07 ± 0.02; logFC = −1.24 ± 0.17; $p = 0.005$) and *DECTIN3* (FC = 0.05 ± 0.02; logFC = −1.51 ± 0.24; $p = 0.009$) in pDCs. These results highlight the importance of CLRs in *P. brasiliensis* recognition by human pDCs.

pDC–Lymphocyte Interaction

Additional studies demonstrated that *P. brasiliensis*-challenged pDCs showed an increased expression of membrane molecules typically found in activated APCs. *P. brasiliensis*-stimulated pDCs presented a higher expression of both MHC-class II and the costimulatory molecule CD86 when compared with unstimulated counterparts (**Figures 9A,B**). Since this result indicated that the pDCs transitioned to a mature status upon *P. brasiliensis* stimulation, we investigated the role of pDCs as APCs. In this regard, we explored the priming of antigen-specific CD4$^+$ and CD8$^+$ T lymphocytes *in vitro*. The pDCs$^+$ and mDCs$^+$ populations were each challenged with *P. brasiliensis* yeast cells and cocultured with CD3$^+$ cells for 5 days. The mDC-CD3 coculture was used as a positive control because the priming ability of mDCs to specific T lymphocytes was previously described (15). We verified that both pDCs and mDCs recognized, processed, and presented *P. brasiliensis* antigens to the T lymphocytes. A higher frequency of activated CD4$^+$ T lymphocytes (CD4$^+$CD25$^+$) was observed in both cultures maintained with mDCs and pDCs compared to the group of lymphocytes cultured without *P. brasiliensis* stimulation. A similar response was found for CD8$^+$ T lymphocytes; however, the sensitized mDCs expanded a higher frequency of activated CD8$^+$ T lymphocytes (CD8$^+$CD69$^+$) compared to the pDCs (**Figures 9C,D**, right panel). Importantly, the CD3$^+$ cells did not respond to the DC stimulation in the absence of *P. brasiliensis* in the coculture (**Figure 9D**, left panel).

DISCUSSION

The involvement of pDCs has been prominently described in viral infections (5). However, recent studies have opened new roles of pDCs to other types of pathogens, indicating an important

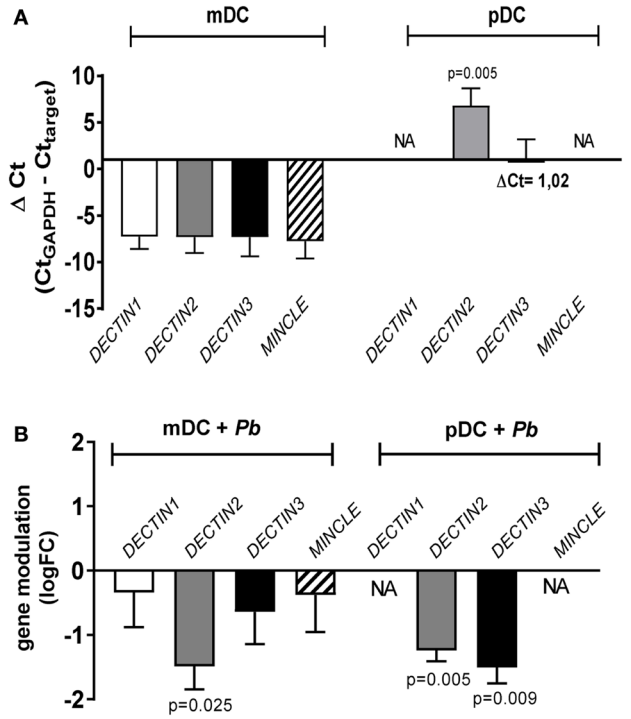

FIGURE 8 | DECTIN1/2/3 and MINCLE gene expression in myeloid dendritic cell (mDC) and plasmacytoid dendritic cell (pDC) stimulated with *Paracoccidioides brasiliensis*. mDCs and pDCs from four healthy individuals were either left unstimulated or challenged overnight with *P. brasiliensis* yeast cells. Then RNA was isolated from each condition and used to evaluate the expression of DECTIN1/2/3 and MINCLE genes by qPCR. GAPDH was used as housekeeping gene for raw data normalization. **(A)** Basal genes expression in mDC and pDC was calculated as ΔCt ($\Delta Ct = Ct_{GAPDH} - Ct_{target}$) as previously reported (31). Data are represented as mean (ΔCt) ± SE. Kruskal–Wallis test was applied to verify the significance of the difference between basal gene expression in mDC and pDC. When significant, the ΔCt of mDC versus pDC genes is indicated at the top of each bar (*p*). NA, not amplified. **(B)** The modulation of expression by *P. brasiliensis* was (20) calculated using the $2-\Delta\Delta Ct$ (fold-change, FC) method comparing stimulated and unstimulated cells ($\Delta\Delta Ct = \Delta CtPb - \Delta CtUnstimulated$). Data are represented as mean (logFC) ± SE. Student's *t*-test was applied to verify the significance of the FC. When significant, the fold-change of stimulated versus unstimulated cells is indicated at the top of each bar (*p*).

role for these cells in bacterial (32, 33) and fungal infections (8–12, 34). However, to our knowledge, no data are available regarding the role of human pDCs in innate and adaptive immunity against *P. brasiliensis*. Here, we show that human pDCs inhibit the growth of *P. brasiliensis* yeast cells. They also mature and produce cytokines upon stimulation with the yeasts. In addition, we have also demonstrated that dectin-2 and dectin-3 (*via* Syk signaling) are pattern receptors involved in *P. brasiliensis* sensing by human pDCs.

Studies with FITC labeled yeasts showed that about 15% of pDCs interact with yeast cells. As flow cytometric assays can not distinguish between adherent and ingested yeasts we can not guarantee that the yeasts were phagocytosed by the pDCs. However, our further experiments showed that the lymphocytes activation promoted by the pDCs was *P. brasiliensis*-specific indicating that pDCs can phagocytose, process and present fungal antigens to the lymphocytes. In addition, CpG, a TLR-9 agonist, has moderately increased the adhesion/engulfment of *P. brasiliensis* by pDCs. Although TLR-9 is not a phagocytic receptor, it is possible that the activation of pDCs *via* TLR-9 activates the cells and triggers mechanisms that promote the ability of pDCs to recognize the fungus. More importantly, we show in this study that human pDCs control fungal growth. Ramirez-Ortiz et al. (9) were the first authors to describe a non-redundant role for human pDCs during host defense against a human fungal pathogen. Human pDCs spread over *A. fumigatus* hyphae, inhibited their growth and released inflammatory cytokines (9). A recent report has also shown that mouse and human pDCs have cytotoxic activity against the opportunistic fungal pathogen *Cryptococcus neoformans*. The mechanism involves reactive oxygen species activity, which is distinct from that engaged by pDCs to control *A. fumigatus* infections (35).

The recognition of *P. brasiliensis* by human pDCs leads to TNF-α secretion. Although the pDCs were able to produce IL-6 in response to an infection (36), the levels of this cytokine did not increase following *P. brasiliensis* stimulation. The release of TNF-α by human pDCs is in agreement with the previous report regarding *A. fumigatus* hyphae stimulation (9, 10). In addition, in a mouse model of PCM, our group verified that *P. brasiliensis* infection induced BMDCs of resistant A/J mice to generate a population of pDCs that secreted inflammatory cytokines, including TNF-α (8). This was the first evidence that pDCs were involved in the host response to *P. brasiliensis*. We have also demonstrated that mouse pDCs release TNF-α and type I IFNs in response to *P. brasiliensis* yeast cells (34), a finding confirmed in the current study of human pDCs. Although the roles of type I IFN and pDCs are well known in DNA and RNA viral infections (36), their function in fungal infections is poorly defined. Romani et al. did not observed IFN-α secretion by pDCs stimulated by *A. fumigatus* resting conidia (37) but the tissue invasive hyphal morphotype was shown to stimulate human pDCs to release IFN-α (9, 10).

Our previous studies showed that dectin-1 and Syk signaling activate the NLRP3 inflammasome in *P. brasiliensis* stimulated macrophages (16). Furthermore, type I IFNs were shown to induce the expression of inflammasome components such as those of the NLRP3, retinoic acid-inducible gene 1, and AIM2 (38). This was in addition to the up-regulation of caspase-11, an enzyme required for the non-canonical activation of the NLRP3 inflammasome (39). These findings led us to investigate whether pDCs were able to activate the inflammasomes, activate caspase-1 and release IL-1β after *P. brasiliensis* stimulation. Our results showed that pDCs are capable of IL-1β release and caspase-1 activation, indicating that *P. brasiliensis* activates the pDCs inflammasome. This is a finding never described previously with regard to this DC subset during a host–microbe interaction.

Several PRRs, including dectin-1 (15, 17, 40), TLR-2 (13, 40), TLR-4 (14, 15, 40) and TLR-9 (41, 42) have been reported to recognize *P. brasiliensis* components. Human pDCs express several PPRs such as DC immunoreceptor, dectin-2, and siglec-H, but do not express TLR-2, TLR-4, and the CLRs dectin-1, MR, and

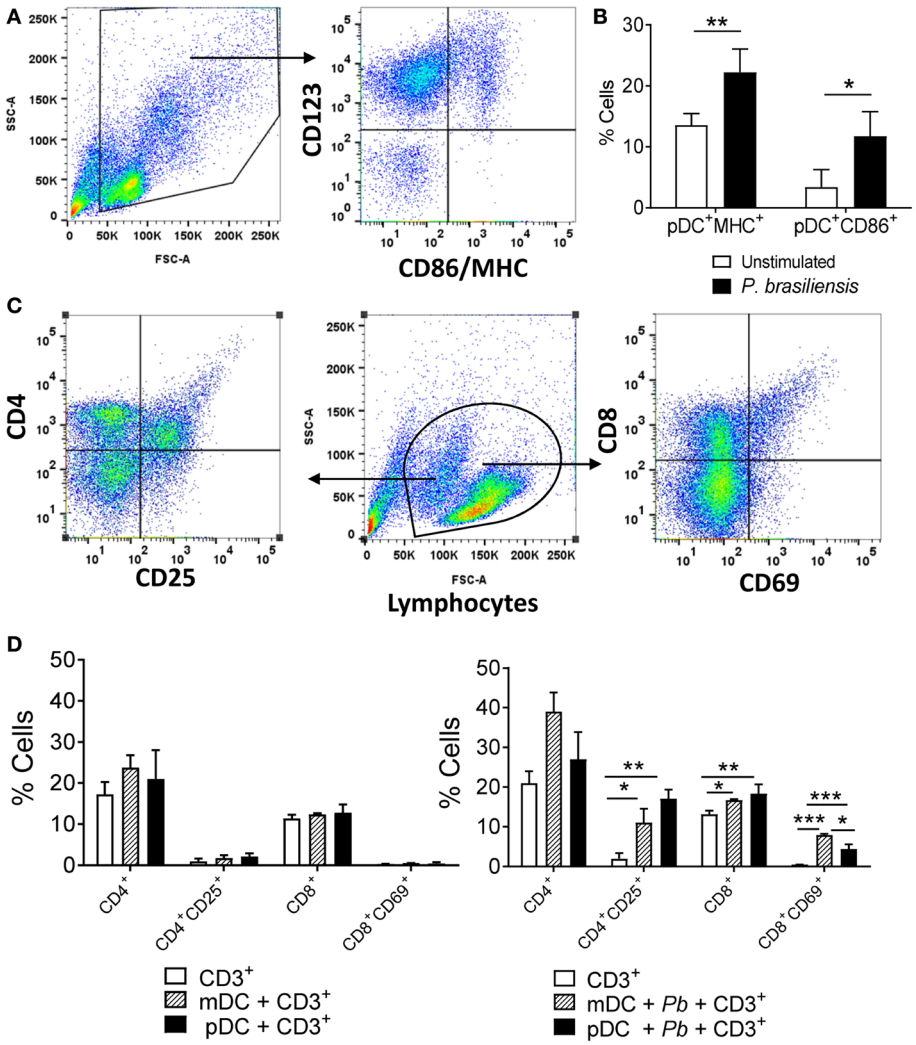

FIGURE 9 | *Paracoccidioides brasiliensis* stimulation induces a mature phenotype in plasmacytoid dendritic cells (pDCs) that become able to promote the activation of $CD4^+$ and $CD8^+$ T lymphocytes. Peripheral blood mononuclear cells (PBMCs) were separated into pDC-positive ($pDCs^+$) and myeloid dendritic cell (mDC)-positive (mDC^+) population using magnetic beads conjugated to anti-CD304 and anti-CD1c antibodies, respectively. **(A,B)** For characterization of pDCs activation, the cells were labeled with appropriate titers of anti-CD123, MHC-class II, and CD86 antibodies and then 50,000 events were acquired in the flow cytometer and gated as indicated in the dot plots **(A)**. As the pDC^+ population was stained with an specific pDC marker (anti-CD123), the characterization of cell maturation was performed by obtaining the pDCs from the PBMCs following one round of positive selection. Data are the means ± SE of the frequency of double-positive cells from three donors, tested in triplicate **(B). (C,D)** For coculture experiments, the pDCs and mDCs (1×10^5/well) were cultured with or without *P. brasiliensis* yeast cells (1×10^4) and after 2 h they were then placed in cocultured with lymphocytes (1×10^6), which were previously obtained from PBMCs of the same donor and separated with anti-CD3 magnetic beads. After 5 days of coculture, the lymphocytes were analyzed by flow cytometry using anti-CD4, CD8, CD25, and anti-CD69 antibodies. The control wells contained only $CD3^+$ cells. The lymphocyte population was gated by FSC/SSC analysis and the gated cells were then analyzed for expression of lymphocyte activation markers **(C).** Data are the means ± SE of the frequency of single positive ($CD4^+$/$CD8^+$) double-positive cells ($CD4^+CD25^+$ and $CD8^+CD69^+$) from three donors, tested in triplicate in cultures with [**(D)**, right panel] or without *P. brasiliensis* yeast cells [**(D)**, left panel]. $^*p < 0.05$, $^{**}p < 0.01$, $^{***}p < 0.001$ by comparing the data indicated by the bars.

DC-SIGN (43–46). In a previous study, we verified that dectin-2 participates in the interaction of pDC and *A. fumigatus*-hyphae and that this recognition leads to TNF-α and IFN-α release by the pDCs as well as improved antifungal resistance (10). In this study, we have also investigated the role of some PRRs in *P. brasiliensis* recognition by pDCs. Our studies show that TLR-9 does not play a role in the *P. brasiliensis*–pDC interaction. These results are similar to those found during the studies with *A. fumigatus* hyphae in which, the hyphae–pDC interaction was also TLR-9 independent (9). Although TLR-9 was reported as an important PRR in the control of murine PCM (41, 42), our data indicate that TLR-9 expressed by other innate immune cells was possibly responsible for this effect.

The cytoplasmic moieties of CLRs have an immunoreceptor tyrosine-based activation motif. These moieties engage the Syk tyrosine kinase, which transduces signals that activate the

transcription factor NF-kB and downstream gene expression. This results in increased phagocytosis and cytokine production by innate immune cells (47). During *C. albicans*-hyphae recognition, dectin-3 forms heterodimers with dectin-2, compared with their respective homodimers, the dectin-3-dectin-2 heterodimers bind α-mannans more effectively, leading to potent inflammatory responses (48). Our results showed the involvement of dectin-2/dectin-3/Syk signaling during *P. brasiliensis* recognition by human pDCs.

As studies regarding the expression of CLRs on human pDC are scarce and sometimes conflicting (49), we have decided to investigate the gene expression for the dectin-1, dectin-2, dectin-3, and mincle receptors on human pDC upon *P. brasiliensis* stimulation. While all genes studied were expressed on human mDCs, only *DECTIN2* and *DECTIN3* were found on human pDCs. Although some studies have demonstrated the expression of dectin-1 on human pDCs (50) the expression of this receptor was not observed in our study. The absent expression of *DECTIN1* and *MINCLE* explained the lack of effect of blocking antibodies during pDC activation by *P. brasiliensis* yeast cells. Importantly, a limitation of our study is that we did not analyze the expression of these receptors on cell membrane of DCs after stimulation with the fungus. However, it is known that the endocytosis of plasma membrane-localized PRRs after a microbial encounter hinders their detection (51, 52). Notably, our findings are in agreement with a previous study of *A. fumigatus* in which fungal hyphae were recognized by human pDCs through dectin-2 rather than dectin-1 or TLR-7/9 (9, 10). Although yeasts of *P. brasiliensis* and *A. fumigutus*-hyphae are composed of different PAMPs (53–56), the involvement of dectin-2 and dectin-3 receptors in triggering pDCs responses following fungal stimulation indicates that these receptors play an important role in the innate immune response to fungal infections. Importantly, dectin-3 has also been shown to participate in the inhibition of *C. neoformans* growth by human and mouse pDCs (35). These previous findings and those reported here highlight the importance of some CLRs (mainly dectin-2 and dectin-3) in the fungal recognition response by human pDCs. However, mincle, another receptor belonging to the dectin-2 family of CLRs (57) was not observed to participate in *P. brasiliensis* sensing by human pDCs even though it is involved in fungal recognition by conventional DCs (44).

Importantly, curdlan (an agonist of dectin-1) was previously shown to induce the production and secretion of mature IL-1β by activating the cytosolic NLRP3 inflammasome and this process requires the phosphorylation of Syk kinase (58, 59). However, as our study indicated that human pDCs do not express dectin-1, it is possible that other CLRs *via* Syk signaling can be used by *P. brasiliensis*-stimulated pDCs to activate the inflammasomes pathway.

Although the fungicidal activity of pDCs observed in this study occurred only at very high concentrations of pDCs relative to the fungus, our results of pDC–yeast interaction and cytokine production brought original clues to elucidate the biological function of human pDCs in the immune response against *P. brasiliensis*. In addition, using the pDC-lymphocyte coculture experiments, we could demonstrate that this cell population can trigger an antigen-specific adaptive immune response. Mittelbrunn et al. were the first to show that mature pDCs form canonical immune synapses that involve the relocation of the microtubule-organizing center, F-actin and protein kinase C to the contact site, in addition to the activation of early signaling molecules in T cells (60). In pulmonary PCM, our group previously demonstrated that mouse pDCs exert an important regulatory function during the host defense process by preferentially expanding regulatory T lymphocytes in a mechanism dependent on the enzyme indolamine 2,3-dioxygenase-1, which confers a tolerogenic profile to pDCs (34). To our knowledge, the current work is in agreement with previous data showing the presence of pDC in cutaneous lesions and in the blood of PCM patients (11, 12), and this is the first study describing the ability of human pDCs to trigger adaptive immune responses in a context of non-viral infectious disease. However, additional studies are necessary to elucidate the patterns of T cell immunity induced by fungi-sensitized pDCs.

In conclusion, our data show for the first time that *P. brasiliensis* activates human pDCs that inhibit fungal growth and secrete pro-inflammatory cytokines such as TNF-α and type I IFNs. Surprisingly, *P. brasiliensis*-stimulated pDCs activate caspase 1 and produce mature IL-1β, possibly *via* inflammasome activation. This phenomenon has not been previously described during pDC engagement by a microorganism. Importantly, dectin-2 and dectin-3 (acting *via* Syk signaling) are PRRs expressed on pDC and are involved in the pDC–*P. brasiliensis* interaction that results in pDCs activation. Therefore, our data support an important role for CLRs in *P. brasiliensis* recognition by pDCs, indicating that this DC subset actively participate in the mechanisms of innate and adaptive immunity against this primary fungal pathogen.

ETHICS STATEMENT

All research involving human participants was approved by the Institute of Biomedical Science Institutional Ethics Committee. Written informed consent was obtained from all human participants and all clinical investigations were conducted according to the principles expressed in the Declaration of Helsinki.

AUTHOR CONTRIBUTIONS

Conceived and designed experiments: NP, ACN, AP, VC, and FL. Contributed with reagent: AP. Performed the experiments: NP, CF, DSL, BS, and FL. Analyzed the data: NP, BS, and FL. Wrote the article: NP, DSL, AP, ACN, VC, and FL.

ACKNOWLEDGMENTS

We are grateful to Eliseu Frank de Araujo and Tânia A. Costa and for invaluable technical assistance.

FUNDING

This project was supported by Fundação de Amparo à Pesquisa do Estado de São Paulo (FAPESP) research grant

2014/04783-2 to FL and 2016/23189-0 to VLGC; FAPESP felowship 2017/00711-5 to NP and 2013/02396-9 to CF. The funders had no role in this study design, data collection and analysis, decision to publish, or preparation of the manuscript.

SUPPLEMENTARY MATERIAL

The Supplementary Material for this article can be found online at https://www.frontiersin.org/articles/10.3389/fimmu.2018.00464/full#supplementary-material.

REFERENCES

1. Kashino SS, Fazioli RA, Cafalli-Favati C, Meloni-Bruneri LH, Vaz CA, Burger E, et al. Resistance to *Paracoccidioides brasiliensis* infection is linked to a preferential Th1 immune response, whereas susceptibility is associated with absence of IFN-gamma production. *J Interferon Cytokine Res* (2000) 20:89–97. doi:10.1089/107999000312766
2. De Castro LF, Ferreira MC, da Silva RM, Blotta MH, Longhi LN, Mamoni RL. Characterization of the immune response in human paracoccidioidomycosis. *J Infect* (2013) 67:470–85. doi:10.1016/j.jinf.2013.07.019
3. Pagliari C, Fernandes ER, Stegun FW, da Silva WL, Seixas Duarte MI, Sotto MN. Paracoccidioidomycosis: cells expressing IL17 and Foxp3 in cutaneous and mucosal lesions. *Microb Pathog* (2011) 50:263–7. doi:10.1016/j.micpath.2010.12.008
4. Banchereau J, Steinman RM. Dendritic cells and the control of immunity. *Nature* (1998) 392:245–52. doi:10.1038/32588
5. Cao W, Liu YJ. Innate immune functions of plasmacytoid dendritic cells. *Curr Opin Immunol* (2007) 19:24–30. doi:10.1016/j.coi.2006.11.004
6. Yu CF, Peng WM, Oldenburg J, Hoch J, Bieber T, Limmer A, et al. Human plasmacytoid dendritic cells support Th17 cell effector function in response to TLR7 ligation. *J Immunol* (2010) 184:1159–67. doi:10.4049/jimmunol.0901706
7. Mouriès J, Moron G, Schlecht G, Escriou N, Dadaglio G, Leclerc C. Plasmacytoid dendritic cells efficiently cross-prime naive T cells in vivo after TLR activation. *Blood* (2008) 112:3713–22. doi:10.1182/blood-2008-03-146290
8. Pina A, de Araujo EF, Felonato M, Loures FV, Feriotti C, Bernardino S, et al. Myeloid dendritic cells (DCs) of mice susceptible to paracoccidioidomycosis suppress T cell responses whereas myeloid and plasmacytoid DCs from resistant mice induce effector and regulatory T cells. *Infect Immun* (2013) 81:1064–77. doi:10.1128/IAI.00736-12
9. Ramirez-Ortiz ZG, Lee CK, Wang JP, Boon L, Specht CA, Levitz SM. A nonredundant role for plasmacytoid dendritic cells in host defense. *Cell Host Microbe* (2011) 9:415–24. doi:10.1016/j.chom.2011.04.007
10. Loures FV, Röhm M, Lee CK, Santos E, Wang JP, Specht CA, et al. Recognition of *Aspergillus fumigatus* hyphae by human plasmacytoid dendritic cells is mediated by dectin-2 and results in formation of extracellular traps. *PLoS Pathog* (2015) 11:e1004643. doi:10.1371/journal.ppat.1004643
11. Pagliari C, Kanashiro-Galo L, Silva AA, Barboza TC, Criado PR, Duarte MI, et al. Plasmacytoid dendritic cells in cutaneous lesions of patients with chromoblastomycosis, lacaziosis, and paracoccidioidomycosis: a comparative analysis. *Med Mycol* (2014) 52:397–402. doi:10.1093/mmy/myt026
12. Venturini J, Cavalcante RS, Moris DV, Golim MA, Levorato AD, Reis KHD, et al. Altered distribution of peripheral blood dendritic cell subsets in patients with pulmonary paracoccidioidomycosis. *Acta Trop* (2017) 173:185–90. doi:10.1016/j.actatropica.2017.06.007
13. Loures FV, Pina A, Felonato M, Calich VL. TLR2 is a negative regulator of Th17 cells and tissue pathology in a pulmonary model of fungal infection. *J Immunol* (2009) 183:1279–90. doi:10.4049/jimmunol.0801599
14. Loures FV, Pina A, Felonato M, de Araújo EF, Leite KR, Calich VL. Toll-like receptor 4 signaling leads to severe fungal infection associated with enhanced proinflammatory immunity and impaired expansion of regulatory T cells. *Infect Immun* (2010) 78:1078–88. doi:10.1128/IAI.01198-09
15. Loures FV, Araújo EF, Feriotti C, Bazan SB, Calich VL. TLR-4 cooperates with dectin-1 and mannose receptor to expand Th17 and Tc17 cells induced by *Paracoccidioides brasiliensis* stimulated dendritic cells. *Front Microbiol* (2015) 6:261. doi:10.3389/fmicb.2015.00261
16. Feriotti C, Bazan SB, Loures FV, Araújo EF, Costa TA, Calich VL. Expression of dectin-1 and enhanced activation of NALP3 inflammasome are associated with resistance to paracoccidioidomycosis. *Front Microbiol* (2015) 6:913. doi:10.3389/fmicb.2015.00913
17. Loures FV, Araújo EF, Feriotti C, Bazan SB, Costa TA, Brown GD, et al. Dectin-1 induces M1 macrophages and prominent expansion of CD8+IL-17+ cells in pulmonary paracoccidioidomycosis. *J Infect Dis* (2014) 210:762–73. doi:10.1093/infdis/jiu136
18. Ribeiro LR, Loures FV, de Araújo EF, Feriotti C, Costa TA, Serezani CH, et al. Lipoxin inhibits fungal uptake by macrophages and reduces the severity of acute pulmonary infection caused by *Paracoccidioides brasiliensis*. *Mediators Inflamm* (2015) 2015:852574. doi:10.1155/2015/852574
19. Singers-Vermes LM, Ciavaglia MC, Kashino SS, Burguer E, Calich VL. The source of the growth-promoting factor(s) affects the plating efficiency of *Paracoccidioides brasiliensis*. *J Med Vet Mycol* (1992) 30:261–4. doi:10.1080/02681219280000331
20. Schmittgen TD, Livak KJ. Analyzing real-time PCR data by the comparative C(T) method. *Nat Protoc* (2008) 3:1101–8. doi:10.1038/nprot.2008.73
21. Gilliet M, Cao W, Liu YJ. Plasmacytoid dendritic cells: sensing nucleic acids in viral infection and autoimmune diseases. *Nat Rev Immunol* (2008) 8:594–606. doi:10.1038/nri2358
22. Pietras EM, Saha SK, Cheng G. The interferon response to bacterial and viral infections. *J Endotoxin Res* (2006) 12:246–50. doi:10.1179/096805106X118799
23. van de Veerdonk FL, Joosten LA, Netea MG. The interplay between inflammasome activation and antifungal host defense. *Immunol Rev* (2015) 265:172–80. doi:10.1111/imr.12280
24. Broz P, Dixit VM. Inflammasomes: mechanism of assembly, regulation and signalling. *Nat Rev Immunol* (2016) 16:407–20. doi:10.1038/nri.2016.58
25. Adinolfi E, Lisa Giuliani A, De Marchi E, Pegoraro A, Orioli E, Di Virgilio F. The P2X7 receptor: a main player in inflammation. *Biochem Pharmacol* (2017) 17:30733–5. doi:10.1016/j.bcp.2017.12.021
26. Feriotti C, de Araújo EF, Loures FV, da Costa TA, Galdino NAL, Zamboni DS, et al. NOD-like receptor P3 inflammasome controls protective Th1/Th17 immunity against pulmonary paracoccidioidomycosis. *Front Immunol* (2017) 8:786. doi:10.3389/fimmu.2017.00786
27. Rutz M, Metzger J, Gellert T, Luppa P, Lipford GB, Wagner H, et al. Toll-like receptor 9 binds single-stranded CpG-DNA in a sequence- and pH-dependent manner. *Eur J Immunol* (2004) 34:2541–50. doi:10.1002/eji.200425218
28. Krieg AM, Wu T, Weeratna R, Efler SM, Love-Homan L, Yang L, et al. Sequence motifs in adenoviral DNA block immune activation by stimulatory CpG motifs. *Proc Natl Acad Sci U S A* (1998) 95:12631–6. doi:10.1073/pnas.95.21.12631
29. Willment JA, Brown GD. C-type lectin receptors in antifungal immunity. *Trends Microbiol* (2008) 16:27–32. doi:10.1016/j.tim.2007.10.012
30. Drummond RA, Brown GD. Signalling C-type lectins in antimicrobial immunity. *PLoS Pathog* (2013) 9:e1003417. doi:10.1371/journal.ppat.1003417
31. Ostrop J, Jozefowski K, Zimmermann S, Hofmann K, Strasser E, Lepenies B, et al. Contribution of MINCLE-SYK signaling to activation of primary human APCs by mycobacterial cord factor and the novel adjuvant TDB. *J Immunol* (2015) 195:2417–28. doi:10.4049/jimmunol.1500102
32. Parcina M, Miranda-Garcia MA, Durlanik S, Ziegler S, Over B, Georg P, et al. Pathogen-triggered activation of plasmacytoid dendritic cells induces IL-10-producing B cells in response to *Staphylococcus aureus*. *J Immunol* (2013) 190:1591–602. doi:10.4049/jimmunol.1201222
33. Wu V, Smith AA, You H, Nguyen TA, Ferguson R, Taylor M, et al. Plasmacytoid dendritic cell-derived IFNα modulates Th17 differentiation during early *Bordetella pertussis* infection in mice. *Mucosal Immunol* (2016) 9:777–86. doi:10.1038/mi.2015.101
34. Araújo EF, Medeiros DH, Galdino NA, Condino-Neto A, Calich VL, Loures FV. Tolerogenic plasmacytoid dendritic cells control *Paracoccidioides brasiliensis* infection by inducting regulatory T cells in an IDO-dependent manner. *PLoS Pathog* (2016) 12:e1006115. doi:10.1371/journal.ppat.1006115
35. Hole CR, Leopold Wager CM, Mendiola AS, Wozniak KL, Campuzano A, Lin X, et al. Antifungal activity of plasmacytoid dendritic cells against *Cryptococcus neoformans* in vitro requires expression of dectin-3 (CLEC4D) and reactive oxygen species. *Infect Immun* (2016) 84:2493–504. doi:10.1128/IAI.00103-16

36. Lederle A, Su B, Holl V, Penichon J, Schmidt S, Decoville T, et al. Neutralizing antibodies inhibit HIV-1 infection of plasmacytoid dendritic cells by an FcγRIIa independent mechanism and do not diminish cytokines production. *Sci Rep* (2014) 4:5845. doi:10.1038/srep05845
37. Romani L, Bistoni F, Gaziano R, Bozza S, Montagnoli C, Perruccio K, et al. Thymosin alpha 1 activates dendritic cells for antifungal Th1 resistance through toll-like receptor signaling. *Blood* (2004) 103:4232–9. doi:10.1182/blood-2003-11-4036
38. Malireddi RK, Kanneganti TD. Role of type I interferons in inflammasome activation, cell death, and disease during microbial infection. *Front Cell Infect Microbiol* (2013) 3:77. doi:10.3389/fcimb.2013.00077
39. Case CL, Kohler LJ, Lima JB, Strowig T, de Zoete MR, Flavell RA, et al. Caspase-11 stimulates rapid flagellin-independent pyroptosis in response to *Legionella pneumophila*. *Proc Natl Acad Sci U S A* (2013) 110:5851–6. doi:10.1073/pnas.1211521110
40. Bonfim CV, Mamoni RL, Blotta MH. TLR-2, TLR-4 and dectin-1 expression in human monocytes and neutrophils stimulated by *Paracoccidioides brasiliensis*. *Med Mycol* (2009) 47:722–33. doi:10.3109/13693780802641425
41. Menino JF, Saraiva M, Gomes-Alves AG, Lobo-Silva D, Sturme M, Gomes-Rezende J, et al. TLR-9 activation dampens the early inflammatory response to *Paracoccidioides brasiliensis*, impacting host survival. *PLoS Negl Trop Dis* (2013) 7:e2317. doi:10.1371/journal.pntd.0002317
42. Morais EA, Chame DF, Melo EM, de Carvalho Oliveira JA, de Paula AC, Peixoto AC, et al. TLR 9 involvement in early protection induced by immunization with rPb27 against paracoccidioidomycosis. *Microbes Infect* (2016) 18:137–47. doi:10.1016/j.micinf.2015.10.005
43. Lande R, Gilliet M. Plasmacytoid dendritic cells: key players in the initiation and regulation of immune responses. *Ann N Y Acad Sci* (2010) 1183:89–103. doi:10.1111/j.1749-6632.2009.05152.x
44. Graham LM, Brown GD. The dectin-2 family of C-type lectins in immunity and homeostasis. *Cytokine* (2009) 48:148–55. doi:10.1016/j.cyto.2009.07.010
45. Meyer-Wentrup F, Benitez-Ribas D, Tacken PJ, Punt CJ, Figdor CG, de Vries IJ, et al. Targeting DCIR on human plasmacytoid dendritic cells results in antigen presentation and inhibits IFN-alpha production. *Blood* (2008) 111:4245–53. doi:10.1182/blood-2007-03-081398
46. Gavino AC, Chung JS, Sato K, Ariizumi K, Cruz PD Jr. Identification and expression profiling of a human C-type lectin, structurally homologous to mouse dectin-2. *Exp Dermatol* (2005) 14:281–8. doi:10.1111/j.0906-6705.2005.00312.x
47. Kerscher B, Willment JA, Brown GD. The dectin-2 family of C-type lectin-like receptors: an update. *Int Immunol* (2013) 25:271–7. doi:10.1093/intimm/dxt006
48. Zhu LL, Zhao XQ, Jiang C, You Y, Chen XP, Jiang YY, et al. C-type lectin receptors dectin-3 and dectin-2 form a heterodimeric patternrecognition receptor for host defense against fungal infection. *Immunity* (2013) 39:324–34. doi:10.1016/j.immuni.2013.05.017
49. Maldonado S, Fitzgerald-Bocarsly P. Antifungal activity of plasmacytoid dendritic cells and the impact of chronic HIV infection. *Front Immunol* (2017) 8:1705. doi:10.3389/fimmu.2017.01705
50. Joo H, Upchurch K, Zhang W, Ni L, Li D, Xue Y, et al. Opposing roles of dectin-1 expressed on human plasmacytoid dendritic cells and myeloid dendritic cells in Th2 polarization. *J Immunol* (2015) 195:1723–31. doi:10.4049/jimmunol.1402276
51. Zanoni I, Ostuni R, Marek LR, Barresi S, Barbalat R, Barton GM, et al. CD14 controls the LPS-induced endocytosis of toll-like receptor 4. *Cell* (2011) 147:868–80. doi:10.1016/j.cell.2011.09.051
52. Jiang W, Swiggard WJ, Heufler C, Peng M, Mirza A, Steinman RM, et al. The receptor DEC-205 expressed by dendritic cells and thymic epithelial cells is involved in antigen processing. *Nature* (1995) 375:151–5. doi:10.1038/375151a0
53. Latge JP, Beauvais A. Functional duality of the cell wall. *Curr Opin Microbiol* (2014) 20:111–7. doi:10.1016/j.mib.2014.05.009
54. Tomazett PK, Cruz AH, Bonfim SM, Soares CM, Pereira M. The cell wall of *Paracoccidioides brasiliensis*: insights from its transcriptome. *Genet Mol Res* (2005) 4:309–25.
55. Puccia R, Vallejo MC, Matsuo AL, Longo LV. The *Paracoccidioides* cell wall: past and present layers toward understanding interaction with the host. *Front Microbiol* (2011) 2:257. doi:10.3389/fmicb.2011.00257
56. de Oliveira HC, Assato PA, Marcos CM, Scorzoni L, de Paula E Silva AC, Da Silva Jde L, et al. *Paracoccidioides*-host interaction: an overview on recent advances in the paracoccidioidomycosis. *Front Microbiol* (2015) 6:1319. doi:10.3389/fmicb.2015.01319
57. Ishikawa T, Itoh F, Yoshida S, Saijo S, Matsuzawa T, Gonoi T, et al. Identification of distinct ligands for the C-type lectin receptors mincle and dectin-2 in the pathogenic fungus *Malassezia*. *Cell Host Microbe* (2013) 13:477–88. doi:10.1016/j.chom.2013.03.008
58. Kankkunen P, Teirilä L, Rintahaka J, Alenius H, Wolff H, Maitikainen S. (1,3)-beta-glucans activate both dectin-1 and NLRP3 inflammasome in human macrophages. *J Immunol* (2010) 184:6335–42. doi:10.4049/jimmunol.0903019
59. Gross O, Poeck H, Bscheider M, Dostert C, Hannesschläger N, Endres S, et al. Syk kinase signaling couples to the Nlrp3 inflammasome for anti-fungal host defense. *Nature* (2009) 459:433–6. doi:10.1038/nature07965
60. Mittelbrunn M, Martínez del Hoyo G, López-Bravo M, Martín-Cofreces NB, Scholer A, Hugues S, et al. Imaging of plasmacytoid dendritic cell interactions with T cells. *Blood* (2009) 113:75–84. doi:10.1182/blood-2008-02-139865

Conflict of Interest Statement: The authors declare that the research was conducted in the absence of any commercial or financial relationships that could be construed as a potential conflict of interest.

The reviewer PF and handling Editor declared their shared affiliation.

Copyright © 2018 Preite, Feriotti, Souza de Lima, da Silva, Condino-Neto, Pontillo, Calich and Loures. This is an open-access article distributed under the terms of the Creative Commons Attribution License (CC BY). The use, distribution or reproduction in other forums is permitted, provided the original author(s) and the copyright owner are credited and that the original publication in this journal is cited, in accordance with accepted academic practice. No use, distribution or reproduction is permitted which does not comply with these terms.

frontiers in Immunology

ORIGINAL RESEARCH
published: 20 November 2017
doi: 10.3389/fimmu.2017.01572

The Major Chromoblastomycosis Etiologic Agent *Fonsecaea pedrosoi* Activates the NLRP3 Inflammasome

Raffael Júnio Araújo de Castro[1], Isaque Medeiros Siqueira[1], Márcio Sousa Jerônimo[1], Angelina Maria Moreschi Basso[1], Paulo Henrique de Holanda Veloso Junior[1], Kelly Grace Magalhães[2], Luiza Chaves Leonhardt[1], Stephan Alberto Machado de Oliveira[1], Pedro Henrique Bürgel[1], Aldo Henrique Tavares[1†] and Anamélia Lorenzetti Bocca[1†]*

[1] Laboratory of Applied Immunology, Department of Cellular Biology, Institute of Biological Sciences, University of Brasília, Brasília, Brazil, [2] Laboratory of Immunology and Inflammation, Department of Cellular Biology, Institute of Biological Sciences, University of Brasília, Brasília, Brazil

OPEN ACCESS

Edited by:
Ilse Denise Jacobsen, Leibniz-Institut für Naturstoff-Forschung und Infektionsbiologie, Hans Knöll Institut, Germany

Reviewed by:
Etienne Meunier, UMR5089 Institut de Pharmacologie et de Biologie Structurale (IPBS), France
Leonardo H. Travassos, Federal University of Rio de Janeiro, Brazil

***Correspondence:**
Anamélia Lorenzetti Bocca
albocca@unb.br

†These authors have contributed equally and share senior authorship.

Specialty section:
This article was submitted to Microbial Immunology, a section of the journal Frontiers in Immunology

Received: *30 August 2017*
Accepted: *01 November 2017*
Published: *20 November 2017*

Citation:
Castro RJA, Siqueira IM, Jerônimo MS, Basso AMM, Veloso Junior PHH, Magalhães KG, Leonhardt LC, Oliveira SAM, Bürgel PH, Tavares AH and Bocca AL (2017) The Major Chromoblastomycosis Etiologic Agent Fonsecaea pedrosoi Activates the NLRP3 Inflammasome. Front. Immunol. 8:1572. doi: 10.3389/fimmu.2017.01572

Fonsecaea pedrosoi is the main etiologic agent of chromoblastomycosis (CBM), one of the most prevalent subcutaneous mycosis in tropical and subtropical countries. CBM is a poorly characterized chronic infection that commonly starts after transcutaneous inoculation of conidia and saprophytic hyphae of *F. pedrosoi*. Recently, we have shown that unlike conidia, hyphae and muriform cells (the parasitic morphotype) of *F. pedrosoi* promotes an intense inflammatory response pattern *in vivo*, which comprises the production of an inflammasome-derived cytokine, IL-1β. Nonetheless, the mechanisms underlying IL-1β production and maturation upon *F. pedrosoi* infection and its functional output in the course of CBM remains unknown. We show here that *F. pedrosoi* hyphae, differently from conidia, induce IL-1β secretion in both bone marrow-derived dendritic cells and macrophages. Using inhibitors and knockout cells, we demonstrated that the mechanisms underlying IL-1β production by hyphae-infected macrophages were dependent on dectin-1, -2, and -3 receptors and the Syk-NF-kB signaling pathway. Furthermore, *F. pedrosoi* promoted a NLRP3-dependent inflammasome activation, which required potassium efflux, reactive oxygen species production, phagolysosomal acidification, and cathepsin B release as triggers. IL-1β processing and release was mediated primarily by caspase-1 and, to a lesser extent, by caspase-8-dependent cleavage. Finally, we showed using a murine CBM model that *F. pedrosoi* elicits a NLRP3-regulated IL-1β and interleukin-18 release *in vivo*, but without NLRP3 inflammasome activation interfering in the course of the experimental infection.

Keywords: NLRP3 inflammasome, *Fonsecaea pedrosoi*, chromoblastomycosis, hyphae, macrophages, dendritic cells

INTRODUCTION

Chromoblastomycosis (CBM) is a chronic, granulomatous, suppurative, and often debilitating cutaneous and subcutaneous mycosis, caused by dimorphic filamentous fungi belonging to the *Dematiaceous* family (1–3). Multiple dematiaceous fungi are related to the disease etiology; of these, *Fonsecaea pedrosoi* and *Cladophialophora carrionii* are the most frequently identified fungal species in human CBM skin lesions. This disease occurs worldwide; however, it is mostly

prevalent in tropical and subtropical areas (4, 5). Clinically, CBM is characterized by the slow development of polymorphic skin lesions, such as nodules, warts, tumors, plaques, and scars, after inoculation of fungal propagules consisting of conidia and hyphal fragments into host skin, more frequently into lower limbs (6–8). During infection of mammalian host, these primarily saprophyte fungal forms undergo transformation into the intensely melanized and thick-walled muriform (sclerotic) cells, the parasitic morphotype of *F. pedrosoi* (4).

Although little is known about the immune response of the host to infection by *F. pedrosoi*, it has been credited that an adaptive response mediated by T helper (Th) cell types 1 and 17 might be protective against *F. pedrosoi* infection (9–11). In this scenario, the abrogation of IL-12p35 transcription in human dendritic cells, leading to Th1-deficient development by several *Fonsecaea* species, and the Th17-mediated response suppression in experimentally infected mice, suggest that this fungal pathogen evade host immune response by complex mechanisms. These mechanisms usually encompass the evasion or subversion of the function of innate pattern recognition receptors (PRRs) in the detection of conserved fungal components or pathogen-associated molecular patterns (PAMPs) by phagocytes (10–12). A number of PRRs families have been associated with *F. pedrosoi* sensing, including the C-type lectin receptors (CLRs) mincle, dectin-1 and dectin-2, as well as toll-like receptors (TLRs). Besides these cytoplasmic membrane-bound receptors, fungal sensing by cytosolic PRRs, such as NOD-like receptors (NLRs) and AIM2-like receptors, is becoming increasingly apparent.

The members of the NLR protein family typically share three functional domains: a C-terminal leucine-rich-repeat putative ligand-binding domain, a central NACHT nucleotide-binding and oligomerization domain and an N-terminal signaling domain (13). The latter consists of different domains, most notably a pyrin domain (PYD) or a caspase recruitment domain (CARD). Certain NLRP (NLR subfamily with an N-terminal PYD), such as NLRP1 and NLRP3, and the NLR family CARD domain-containing protein 4 (NLRC4) associate with inflammatory caspase-1 (in the form of pro-caspase-1) to assemble the inflammasome, a large cytosolic multiprotein complex. Notably, NLRP3-containing inflammasome formation is dependent on the adaptor protein ASC (apoptosis-associated speck-like protein containing a CARD), which promotes the recruitment of pro-caspase-1 through CARD–CARD interactions (13). The assembly of the inflammasome complex leads to the cleavage of pro-caspase-1 into an active cysteine protease, which cleaves the proinflammatory cytokines interleukin-1β (IL-1β) and interleukin-18 (IL-18) into their mature forms. NLRP3 inflammasome, the most studied and the main inflammasome associated with fungal infection, is activated by a typical two-step mechanism: priming and activation (14, 15). The priming signal is generated by the recognition of PAMPs by PRRs, usually leading to NF-kB activation and, as a result, production of pro-IL-1β, pro-IL-18, and NLRP3. The activation step is associated with the assembly of the multiprotein complex induced by a broad variety of endogenous danger-associated molecules (DAMPs), such as potassium efflux, production of reactive oxygen species (ROS), phagolysosome acidification, and cathepsin B release. Several conditions may lead to DAMPs production, including metabolic disorders, inflammatory diseases, and infections.

The inflammasome-dependent release of IL-1β and IL-18 cytokines has a striking importance in the regulation of innate and adaptive response against many different fungal pathogens, including significant protective roles against *Candida albicans*, *Aspergillus fumigatus*, *Cryptococcus neoformans*, *Paracoccidioides brasiliensis*, and *Histoplasma capsulatum* (16–22). One aspect associated with inflammasome activation is fungal morphotype diversity and complexity. *C. albicans* hyphae are better inducers and the only fungal form of *A. fumigatus* that activates the NLRP3 inflammasome (16, 17, 23). Indeed, we have recently showed that unlike conidia, the hyphae and muriform (sclerotic) cells of *F. pedrosoi* promote intense production of proinflammatory cytokines *in vitro* and *in vivo* (24). Among these cytokines, we observed IL-1β production, suggesting that *F. pedrosoi* could activate the inflammasome. In this context, we aimed to evaluate the inflammasome activation by *F. pedrosoi* infective propagules and the role of the inflammasome in CBM experimental disease.

We show here that *F. pedrosoi* hyphae, differently from conidia, induce IL-1β secretion in both bone marrow-derived dendritic cells and macrophages. The mechanisms underlying IL-1β production by macrophage-infected hyphae were dependent on dectin-1, -2, and -3 receptors and the Syk-NF-kB signaling pathway. *F. pedrosoi* promoted a NLRP3-dependent inflammasome activation, which required K^+ efflux, ROS production, phagolysosomal acidification, and cathepsin B release. IL-1β processing and release were mediated by caspase-1 and, to a lesser extent, caspase-8-dependent cleavage. Furthermore, we demonstrated using an experimental CBM model that *F. pedrosoi* elicits a NLRP3-regulated IL-1β and IL-18 release *in vivo*. However, we did not observe an influence of the NLRP3 inflammasome on the control of the fungal infection.

MATERIALS AND METHODS

Fungal Culture and Preparation

Fonsecaea pedrosoi ATCC 46428 were maintained in Sabouraud dextrose agar medium (SDA) at 37°C after serial animal passages to enhance fungal virulence. In order to obtain purified conidia and hyphae for experiments, virulent *F. pedrosoi* propagules were grown in potato dextrose medium in a rotary shaker (120 rpm) at 30°C. A 15-day-old suspension containing conidia and hyphal fragments was submitted to successive filtrations on 70 and 40 μm cell strainers (BD), respectively. The 40 μm filter-retained cells (ranging between 40 and 70 μm) were re-suspended in phosphate-buffered saline (PBS) and consisted of more than 98% of purified hyphae. The suspension of cells smaller than 40 μm was further filtered using a 14 μm filter paper (J. Prolab) to remove small hyphal fragments and achieve a minimum of 98% purified conidia. A mix of purified hyphae and conidia at a 3:1 rate was used as *F. pedrosoi* fungal

propagules for *in vivo* assays. For assays with inactivated fungi, conidia, and hyphae were heat-killed by boiling for 40 min, or fixed with 3% paraformaldehyde (PFA) for 6 h. *F. pedrosoi* cells were washed twice, counted using a hemocytometer, and used for experiments.

Cell Culture

Bone marrow-derived macrophages (BMDMs) and dendritic cells (BMDCs) were generated by a previously described method (25). Briefly, bone marrow cells were flushed out of murine femurs and tibias and submitted to erythrocyte lysis using tris-buffered ammonium chloride. Cells (2×10^6) were plated onto non-tissue culture-treated Petri dishes in 10 mL of RPMI-1640 medium (Sigma-Aldrich) supplemented with 10% heat-inactivated FBS (Gibco), 50 μM 2-mercaptoethanol, 50 μg/mL of gentamicin, and 20 ng/mL GM-CSF (Peprotech), and cultured for 8 days in a humidified 5% CO_2 atmosphere at 37°C. On day 3, another 10 mL of fresh complete medium was added to the culture. On day 6, half of the medium was exchanged. On day 8, loosely adherent/suspended BMDCs and firmly adherent BMDMs stripped with TrypLE™ Express (Gibco) were separately collected and plated at a density of 10^6 cells/mL in RPMI medium containing 10% FBS and 50 μg/mL of gentamicin, for experimental use. THP-1 cells were maintained and used under the same experimental use conditions.

In Vitro F. pedrosoi Challenge and Cell Treatments

Bone marrow-derived macrophages derived from wild-type (WT) or knockout mice were infected with *F. pedrosoi* for 6 (RT-qPCR analysis) and 24 h (other assays) at a multiplicity of infection (MOI) of 3 for conidial infection (except for fungicidal assays, performed with a MOI of 1) and of 1 for hyphal. For inhibition assays, BMDMs received 2 h prior to the infection a Myd88 inhibitor peptide (50 μM) (InvivoGen), Syk inhibitor R406 (5 μM) (InvivoGen), NF-kB inhibitor celastrol (5 μM) (InvivoGen), caspase-1 inhibitor AC-YVAD-CHO (50 μM) (Santa Cruz Biotechnology), caspase-8 inhibitor Z-IETD-FMK (50 μM) (Santa Cruz Biotechnology), intracellular potassium efflux inhibitors glyburide (150 μM) (InvivoGen) and KCl (50 mM) (Sigma-Aldrich), ROS inhibitor DPI (diphenyleneiodonium chloride) (20 μM) (Sigma-Aldrich), endosomal acidification inhibitor bafilomycin A (250 nM) (InvivoGen) or cathepsin B inhibitor CA-074 Me (50 μM) (Sigma-Aldrich). In some experiments, BMDMs and BMDCs were treated 2 h previously to the fungal infection with 500 ng/mL of LPS (Sigma-Aldrich) and/or 20 μM of nigericin (InvivoGen) during the last 40 min of incubation (1 h for fungicidal assays). Cells stimulated with both LPS and nigericin served as a positive control for NLRP3-mediated inflammasome activation.

Analysis of Fungal Cell Morphology by Flow Cytometry

In order to induce and evaluate conidial swelling, *F. pedrosoi* conidia (5×10^6 cells/mL) were incubated for 6 h with PBS or RPMI supplemented with 20% of heat-inactivated FBS at 37°C, under 120 rpm. In addition, conidia were incubated with BMDMs at a MOI of 3, for 6 and 24 h. Infected BMDMs were washed to discard nonphagocyted fungus and lysed with 0.05% SDS to release intracellular fungi. Then, fungal were fixed with PFA treatment, washed twice, and evaluated by flow cytometry analysis. Micron-size beads of 2 and 3 μm (CS&T Research Beads, BD) were used as control. Cell acquisition was performed using a FACSVerse (BD) flow cytometry, and data were analyzed with FlowJo v.10 software.

In Vitro Fungicidal Assay

Bone marrow-derived macrophages derived from WT, *Nlrp3*$^{-/-}$, and *Caspase-1/11*$^{-/-}$ mice were infected for 24 h with *F. pedrosoi* conidia or hyphae. In addition, WT macrophages were also treated, or not, with nigericin as described above, or stimulated 3 h before the infection with LPS and IFN-γ (both from Sigma-Aldrich) (500 and 20 ng/mL, respectively) to activate the mechanisms of macrophage killing [e.g., nitric oxide (NO) production]. After infection, the cell culture supernatant was harvested for NO determination. The remaining cell monolayers were carefully washed to remove non-adherent cells, lysed as described above, and re-suspended in PBS. After serial dilutions, cell suspension was plated on SDA and incubated at 30°C for 5–7 days for colony-forming unit (CFU) evaluation.

Detection of Activated Caspase-1 by Fluorochrome-Labeled Inhibitor of Caspases (FLICA)

After 24 h of infection with *F. pedrosoi* conidia or hyphae, BMDMs were detached (as mentioned above) and incubated for 1 h with a caspase-1 fluorochrome-labeled inhibitor of caspases (FLICA), FAM-YVAD-FMK (Immunochemistry Technologies), according to the manufacturer's instructions. Next, cells were washed and stained with APC-conjugated anti-CD11b antibody (eBioscience) in PBS with 2% heat-inactivated FBS (Gibco) to distinguish macrophages from non-internalized fungus. Then, cells were washed and samples were analyzed by flow cytometry as described above.

Quantitative Real-time PCR (qRT-PCR)

Total RNA from BMDMs was extracted using the TRIzol reagent (Invitrogen) and cDNA was synthesized using the high capacity RNA-to-cDNA kit (Applied Biosystems), according to manufacturer's protocols. qRT-PCR was performed using SYBR green incorporation (Applied Biosystems) and real-time PCR equipment (StepOne system) (Applied Biosystems). Expression of the genes of interest was normalized to the expression of the housekeeping gene *Rps9* and expressed as "Fold change," which was calculated by the $2^{-\Delta\Delta CT}$ method (26). The primers used were validated according Livak and Schmittgen (26) and listed in Table S1 in Supplementary Material.

Animals and *In Vivo F. pedrosoi* Infection

Clec7a$^{-/-}$ (*Dectin-1*$^{-/-}$) mice were supplied by Dr. Gordon Brown (University of Aberdeen, Scotland). *Clec4n*$^{-/-}$ (*Dectin-2*$^{-/-}$), *Clec4d*$^{+/+}$ (*Dectin-3*$^{+/+}$), *Clec4d*$^{-/-}$ (*Dectin-3*$^{-/-}$) mice were kindly provided by Dr. Bruce Klein (University of Wisconsin-Madison,

USA). All animals (C57BL/6 background), including *Nlrp3*$^{-/-}$, *Caspase-1/11*$^{-/-}$, and C57BL/6 WT mice, were maintained under pathogen-free conditions and used at 8 to 12 weeks old for experiments. For *in vivo* infection, WT, *Nlrp3*$^{-/-}$ and *Caspase-1/11*$^{-/-}$ mice were inoculated subcutaneously into the hind footpad with 50 µl (per foot) of a suspension containing 1×10^6 (2×10^7/mL) *F. pedrosoi* hyphae and conidia in the proportion of 3:1, respectively (fungal propagules). Mice were euthanized at 14, 21, and 28 days postinfection and the footpad was collected, weighed, and homogenized for ELISA assay and plated for CFU analysis.

Measurement of NO and Cytokine Production

Nitrite (NO_2^-) concentration in culture supernatants was applied as an indicator of NO generation and measured with the Griess reagent (1% sulfanilamide, 0.1% naphthylethylene diamine dihydrochloride, 2.5% H_3PO_4). For that, 50 µl of the culture supernatant was added to an equal volume (v/v) of Griess reagent and allowed to incubate at room temperature for 10 min. Absorbance was measured at 540 nm using a microplate reader. The NO_2^- concentration was determined using a standard curve of 1.56–100 µM of $NaNO_2$. Cytokine levels from the homogenized animal tissue and cell culture lysate and supernatants were determined by ELISA, according to the manufacturer's guidelines, for the following cytokines: human interleukin-1β (IL-1β) and murine IL-1β (both uncleaved and cleaved forms), IL-18 and tumor necrosis factor-α (TNF-α), all purchased from eBioscience. Results were expressed as cytokines pictogram per milliliters or per 100 mg of tissue, for samples obtained from *in vivo* assays.

Statistical Analysis

Statistical analysis was conducted using GraphPad Prism v.5.0 software. Data were analyzed by one-way ANOVA followed by Tukey's *post hoc* test. Two-way ANOVA and Bonferroni's *post hoc* test were used to compare different groups with more than one variable. *p*-Values of less than 0.05 were considered significant.

RESULTS

F. pedrosoi Hyphae, but Not Conidia, Induce IL-1β Secretion in BMDMs and THP-1 Cells

To determine whether *F. pedrosoi* could induce IL-1β secretion, we infected murine BMDMs with *F. pedrosoi* conidia or hyphae for 24 h. Hyphae cell infection resulted in IL-1β secretion, while conidia failed to induce significant levels of this cytokine (**Figure 1A**). In addition, THP-1, a human monocyte cell line, secreted IL-1β upon infection by *F. pedrosoi* hyphae, but not conidia (**Figure 1B**). To test if the size of conidia could affect the BMDM activation, we induced swollen-conidia (Figure S1 in Supplementary Material), an intermediate stage of conidia-into-hyphae transformation, and used it to stimulate BMDMs. Swollen conidia were equally unable to promote IL-1β secretion (**Figure 1A**).

Then, we evaluated if the lack of secreted IL-1β in BMDM-conidia coculture supernatant results primarily from the inability of BMDMs to trigger *Il1b* gene transcription after conidial infection. RT-qPCR analysis revealed that at 6 h of infection, hyphae and, to a lesser extent, conidia induce *Il1b* and *Tnfa*, but not *il18* transcripts in BMDMs (**Figure 1C**). ELISA assay performed with 24 h culture supernatant showed that, contrary to conidial, hyphal infection results in IL-18 and TNF-α secretion (**Figures 1D,E**), despite the observation that the *Il18* transcript is not upregulated. Further, we stimulated BMDMs with inactivated hyphae to determine whether the viability of this fungal form influences IL-1β secretion. Both PFA and heat-killed (HK) hyphae stimulus resulted in severe reduction of IL-1β in comparison to live fungus (**Figure 1F**), whereas the viability of the fungus did not significantly affect the levels of TNF-α production and only slighted affected the levels of pro-IL-1β only in the HK hyphae (**Figures 1G,H**). These finding suggest that that the viability of *F. pedrosoi* affects activation, but not priming of NLRP3 inflammasome.

Differential Inflammasome Activation Requirements in BMDMs and BMDCs Are Morphotype-Dependent in *F. pedrosoi* Infection

Since we previously showed that BMDCs differ from BMDMs regarding inflammasome activation requirements upon *P. brasiliensis* infection (27), we investigated whether this is also the case with *F. pedrosoi*. Differently from BMDM infection, conidia alone induced IL-1β secretion in BMDCs, suggesting that it acts as both the first and the second signal for inflammasome activation in this cell type (**Figures 2A,B**). When nigericin was added to BMDMs or BMDCs, these cells secreted a large amount of mature IL-1β, confirming that conidia elicit pro-IL-1β production (as indicated in **Figure 1C**), but fail to provide further inflammasome activating signals in BMDMs (**Figures 2A,B**). Regarding hyphae, this morphotype alone was able to induce IL-1β secretion not only in BMDMs (as shown in **Figure 1**) but also in BMDCs (**Figure 2B**).

The Syk-NF-kB Signaling Pathway, Coupled to Dectin-1, Dectin-2, and Dectin-3 Receptors, Enables Inflammasome Activation by BMDMs Challenged with *F. pedrosoi* Hyphae

Macrophages play central roles in host immune response against fungal infections (28). Likewise, these phagocytes are not only ubiquitous in CBM lesions but are also actively involved in the recognition of fungal cells and in the modulation of inflammatory responses against *F. pedrosoi* (4, 29, 30). In this context, we performed subsequent assays focused on macrophage-hyphae interaction, since we show here that hyphae are the *F. pedrosoi* infective morphotype most likely to be responsible for initiating the inflammatory response observed in CBM. In order to determine the mechanisms underlying BMDMs inflammasome priming in *F. pedrosoi* infection, we treated BMDMs with celastrol, an inhibitor of IKK activity, which results in the inactivation of NF-kB, the main transcriptional factor associated with pro-IL-1β

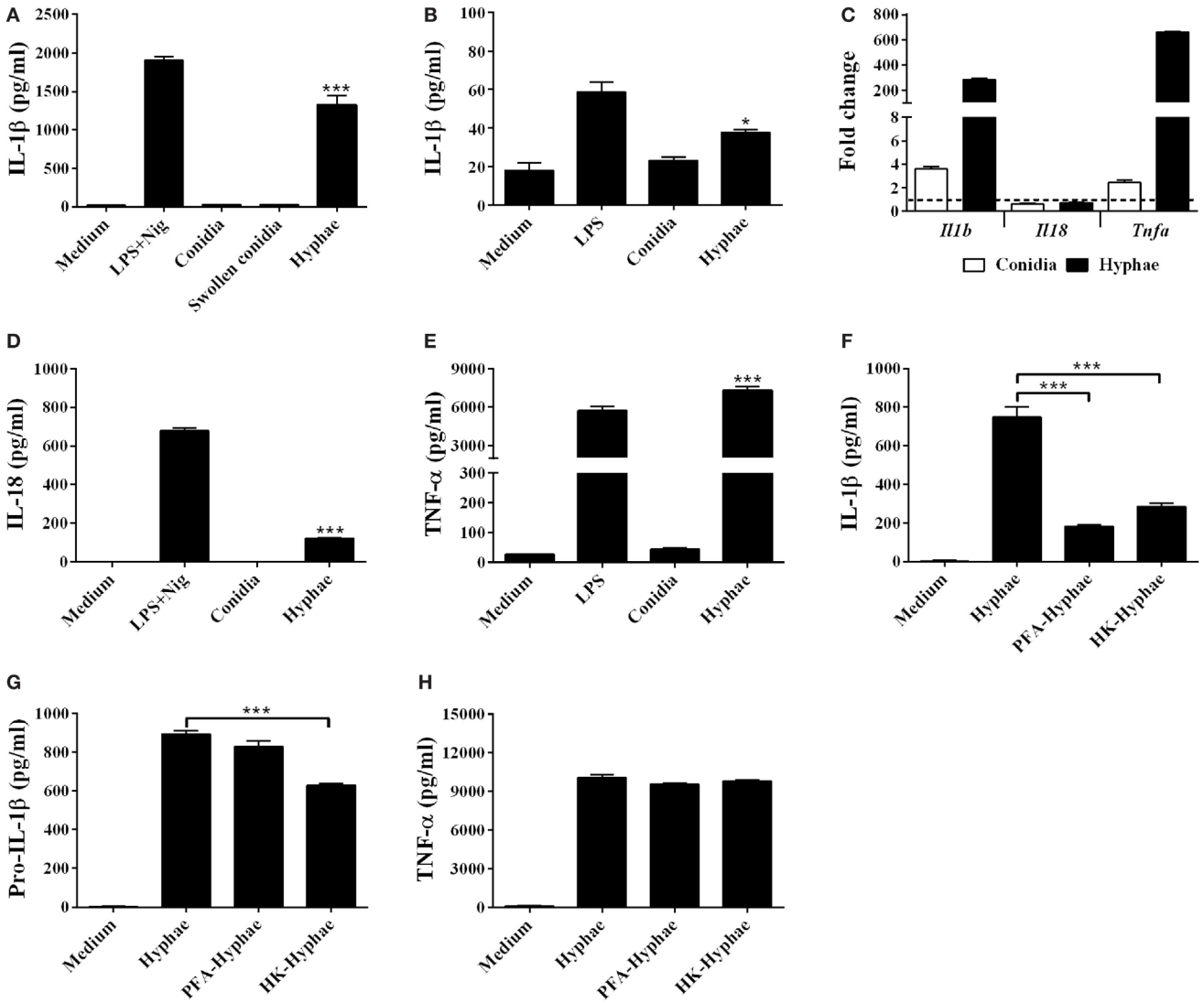

FIGURE 1 | *Fonsecaea pedrosoi* hyphae, but not conidia, induce IL-1β secretion in bone marrow-derived macrophages (BMDMs) and THP-1 cells. IL-1β levels after 24 h of BMDMs incubation with medium, *F. pedrosoi* conidia, swollen conidia, or hyphae **(A)**. IL-1β secretion after 24 h of THP-1 cell incubation with medium, *F. pedrosoi* conidia, or hyphae **(B)**. Intracellular *Il1b*, *Il18*, and *Tnfa* gene transcription of BMDMs after 6 h stimulation with hyphae or conidia were analyzed by RT-qPCR **(C)**. Interleukin-18 (IL-18) **(D)** and tumor necrosis factor-α (TNF-α) **(E)** secretion of BMDMs co-cultivated with medium, conidia, or hyphae. BMDMs were stimulated also with live, paraformaldehyde-killed, or heat-killed (HK) hyphae for IL-β **(F)**, pro-IL-β **(G)**, and TNF-α measurement **(H)**. Pro-IL-1β was evaluated in the cell lysate after 12 h of infection, while the others cytokines were assayed in the cell supernatant after 24 h. IL-1β, pro-IL-1β, IL-18, and TNF-α levels were evaluated by ELISA. Data shown are mean ± SEM and are representative of two to three independent experiments. $^{*}p < 0.05$; $^{***}p < 0.001$, compared to cells with only medium or between groups indicated by brackets.

transcription. As expected, NF-kB inhibition led to a complete abolition of IL-1β, as well as a strong reduction of TNF-α secretion in cell supernatant (**Figures 3A,B**, respectively). Furthermore, it is known that NF-kB-activating PRRs license inflammasome activation by providing both pro-IL-1β and inflammasome receptors expression (31). To clarify the nature of the PRRs that are involved in the *F. pedrosoi* recognition that led to NF-kB-dependent BMDMs priming, we evaluated the transcription of *Myd88* and *Syk*, which are pivotal signal transducers of TLRs and CLRs, respectively. We observed that hyphae not only induced *Syk* and *Nfkb1* upregulation (**Figure 3C**), but also depend on Syk activity to induce IL-1β secretion, as shown in BMDMs treated with Syk inhibitor R406 (**Figure 3A**). *Myd88*, however, was poorly transcribed in BMDMs upon hyphal infection (**Figure 3C**), and its activity was indifferent to IL-1β secretion in cells treated with a Myd88 inhibitory peptide (**Figure 3A**).

It is known that CLRs, such as dectin-1, dectin-2, and dectin-3, signaling *via* Syk kinase promote NF-kB activation (32). To test whether these CLRs were responsible for recruiting Syk to signal inflammasome priming in BMDMs challenged with hyphae, we used cells from mice deficient in these receptors, and observed that *Dectin-1*$^{-/-}$, *Dectin-2*$^{-/-}$, and *Dectin-3*$^{-/-}$ BMDMs

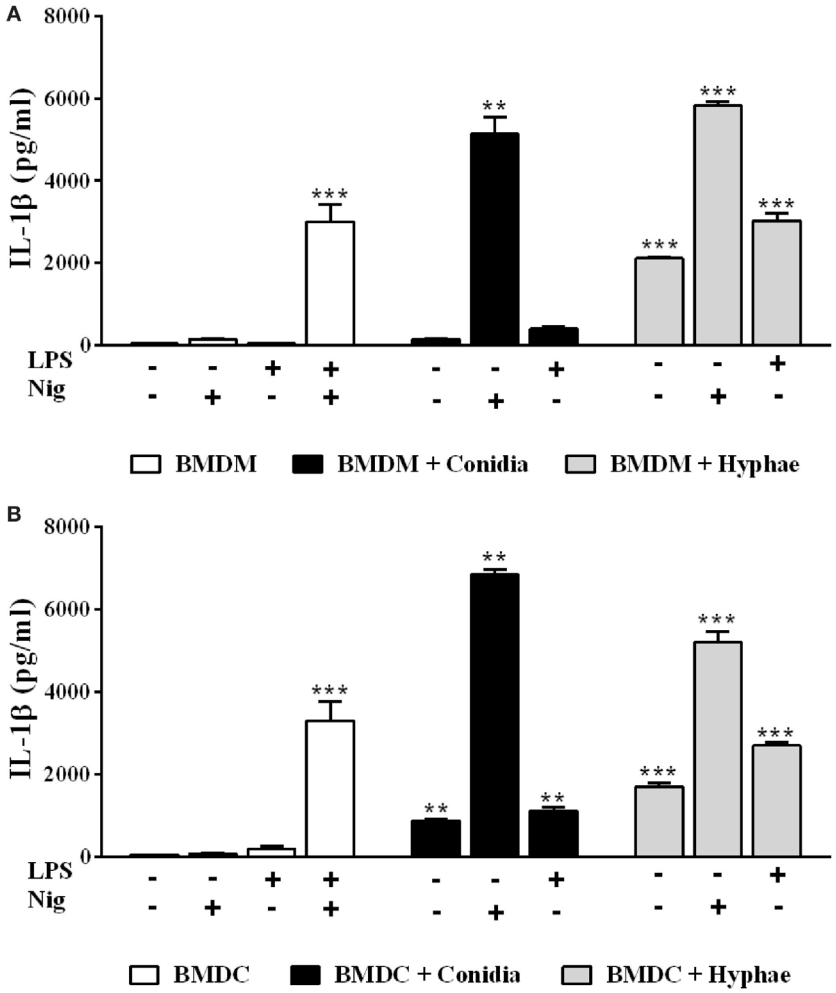

FIGURE 2 | Differential inflammasome activation requirements in bone marrow-derived macrophages (BMDMs) and dendritic cells (BMDCs) are morphotype-dependent in *Fonsecaea pedrosoi* infection. IL-1β detection by ELISA in supernatants of BMDMs **(A)** and BMDCs **(B)** incubated for 24 h with medium, *F. pedrosoi* conidia or hyphae, and co-stimulated (or not) with LPS (500 ng/mL added 2 h before fungal infection), nigericin (20 μM during the last 40 min of incubation), or both (as a positive control). Data shown are mean ± SEM and are representative of three independent experiments. $^{**}p < 0.01$; $^{***}p < 0.001$, compared to cells with only medium.

show reduced IL-1β secretion when compared to their respective controls (**Figure 3D**). Except for *Dectin-3*$^{-/-}$ cells, all tested knockout cells also exhibited a slight reduction in TNF-α levels (**Figure 3E**). Dectin-1 KO cells had the strongest depletion of IL-1β (**Figure 3D**), although WT BMDMs did not present differential regulation of *Dectin-1* transcription—only *Dectin-2* and *Dectin-3* genes were upregulated (**Figure 3F**). Further, since the inhibition of Syk signaling did not completely abrogate the IL-1B secretion (**Figure 3A**), we reasoned that an alternative Syk-independent dectin-1-NF-kB signaling pathway would be in use. To evaluate this hypothesis, we inhibited Raf-1 kinase signaling, an adaptor protein that dectin-1 engages to signal NF-kB activation independently of Syk (33); however, IL-1β levels were unaffected (data not shown). The results indicate that the Syk-NF-kB signaling pathway, coupled to dectin-1, dectin-2, and dectin-3 receptors, enables inflammasome activation by BMDMs challenged with *F. pedrosoi* hyphae.

Inflammasome Activation by *F. pedrosoi* Hyphae Is Dependent on Caspase-1 and Caspase-8

IL-1β secretion requires proteolytic cleavage of its inactive proform, canonically performed by caspase-1 enzyme. To assess whether *F. pedrosoi* infective morphotypes were able to activate caspase-1, we used a fluorescent probe, FAM-YVAD-FMK, which specifically binds the active protease, and analyzed stained BMDMs using flow cytometry. As expected, only hyphae, but not conidia, were able to induce caspase-1 activation (**Figure 4A**), which corroborates our ELISA data showing that only hyphae infection led to IL-1β processing and secretion in BMDMs (**Figure 2A**). Then, to confirm that IL-1β secretion was caspase-1 dependent, we challenged BMDMs from WT and *Caspase-1/11* knockout mice with hyphae. In addition, we also treated WT BMDMs with AC-YVAD-CHO, a specific caspase-1 inhibitor. Both *Caspase-1/11*$^{-/-}$ BMDMs and WT BMDMs treated with

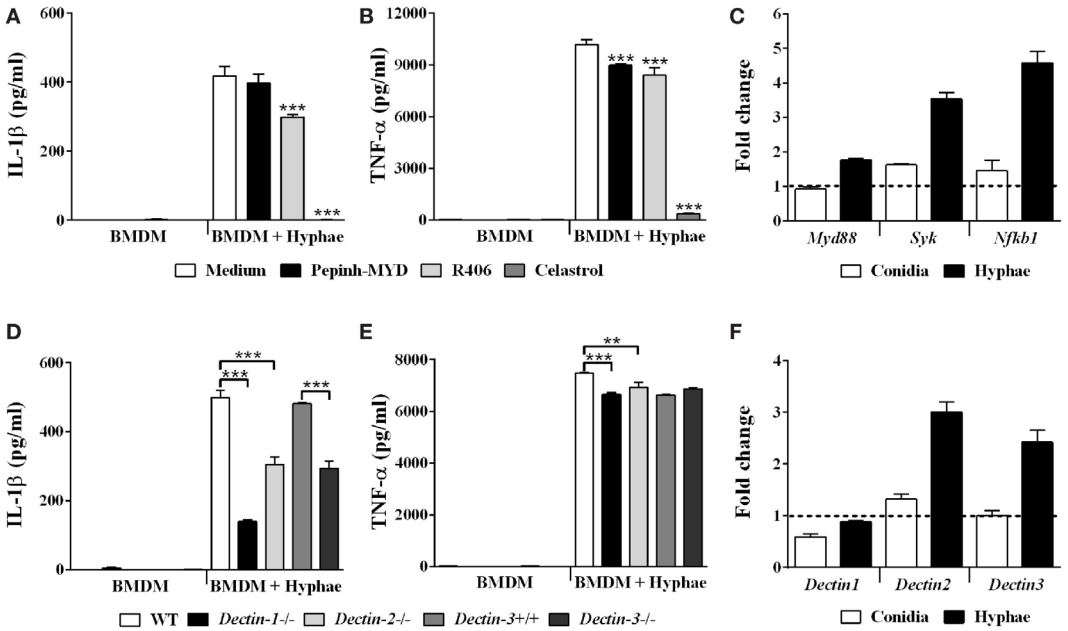

FIGURE 3 | The Syk-NF-kB signaling pathway, coupled to dectin-1, dectin-2, and dectin-3 receptors, enables inflammasome activation by bone marrow-derived macrophages (BMDMs) challenged with *Fonsecaea pedrosoi* hyphae. BMDMs were pretreated for 2 h with Myd88 inhibitor peptide (50 μM), R406 (5 μM), and celastrol (5 μM) and thereafter infected with *F. pedrosoi* hyphae for 24 h **(A,B)**. BMDMs were infected with conidia or hyphae for 6 h, and then were lysed for RT-qPCR analysis to quantify gene expression of indicated genes **(C,F)**. BMDMs obtained from wild-type (WT), *Dectin-1*$^{-/-}$, *Dectin-2*$^{-/-}$, *Dectin-3*$^{+/+}$, and *Dectin-3*$^{-/-}$ mice were infected with *F. pedrosoi* hyphae for 24 h **(D,E)**. The supernatant of 24 h cell culture assays were evaluated for IL-1β and TNF-α by ELISA. Data shown are mean ± SEM and are representative of two to three independent experiments. $^{**}p < 0.01$; $^{***}p < 0.001$, compared to infected untreated cells or between groups indicated by brackets.

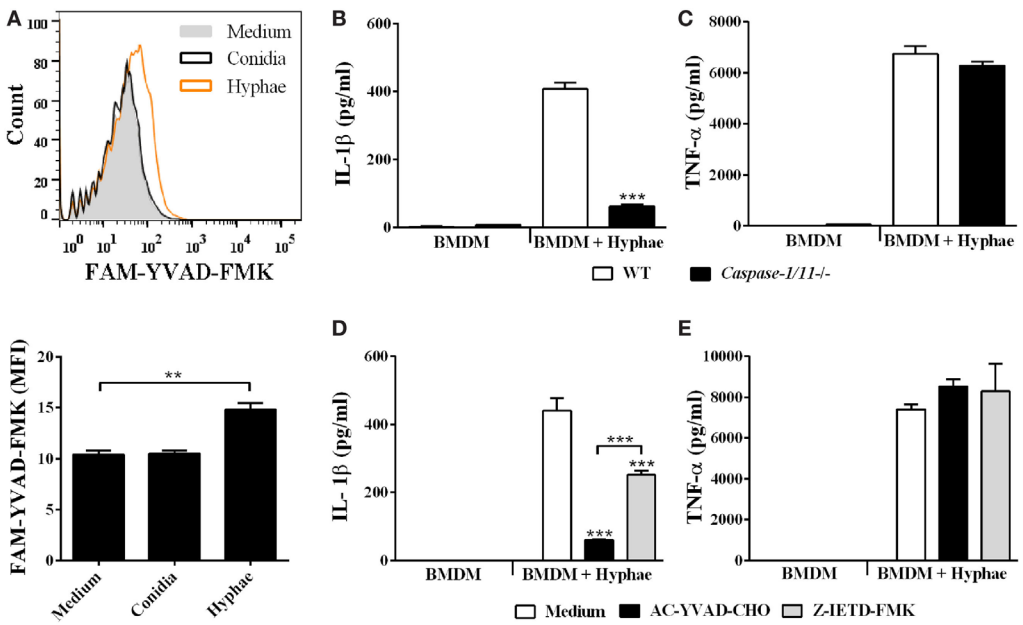

FIGURE 4 | Inflammasome activation by *Fonsecaea pedrosoi* hyphae is dependent on caspase-1 and caspase-8. Bone marrow-derived macrophages (BMDMs) were incubated with medium, *F. pedrosoi* conidia or hyphae for 24 h, and thereafter stained with anti-CD11b-APC antibody and FAM-YVAD-FMK-FITC probe to perform flow cytometry analysis. Caspase-1 activity (indicated by intensity of FAM-YVAD-FMK-FITC binding) of CD11b^{+} cells is represented in histogram and by cell mean fluorescence intensity (MFI) **(A)**. BMDMs obtained from wild-type (WT) or *Caspase-1/11*$^{-/-}$ mice were infected with *F. pedrosoi* hyphae for 24 h **(B,C)**. WT BMDMs were pretreated for 2 h with 50 μM of AC-YVAD-CHO (caspase-1 inhibitor) or Z-IETD-FMK (caspase-8 inhibitor) and then infected with *F. pedrosoi* hyphae for 24 h **(D,E)**. The supernatant of cell culture assays **(B–E)** was evaluated for IL-1β and tumor necrosis factor-α by ELISA. Data shown are mean ± SEM and are representative of two to three independent experiments. $^{**}p < 0.01$; $^{***}p < 0.001$, compared to WT-infected untreated cells or between groups indicated by brackets.

caspase-1 inhibitor showed a severe reduction in IL-1β secretion (**Figures 4B,D**, respectively). Moreover, as caspase-8 has been associated with the non-canonical processing of IL-1β in response to *C. albicans*, *A. fumigatus*, and *C. neoformans* infection, we further tested caspase-8 inhibitor Z-IETD-FMK with WT BMDMs infected with *F. pedrosoi* hyphae (34, 35). Interestingly, cells treated with caspase-8 inhibitor decreased IL-1β production, although not as dramatically as cells undergoing caspase-1 inhibition (**Figure 4D**). TNF-α secretion was not affected in the inhibition/absence of the aforementioned caspases (**Figures 4C,E**). In addition to its role in maturing inflammasome-derived cytokines, caspase-1 mediate an inflammasome-dependent cell death mechanism termed pyroptosis, which leads to plasma membrane lysis and release of cytoplasmic content, including lactate dehydrogenase (LDH). Interestingly, we observed no extracellular release of LDH from BMDMs infected with *F. pedrosoi* hyphae nor conidia, which suggests that pyroptosis does not occur in our model (data not shown). Thus, our data demonstrate that IL-1β secretion by BMDMs in response to *F. pedrosoi* hyphae infection depends on caspase-1 and, to a lesser extent, on caspase-8 activity.

F. pedrosoi Hyphae Activate the NLRP3 Inflammasome, Which Depends on K^+ Efflux, ROS Production, Phagolysosomal Acidification/Disruption, and Cathepsin B Release

With respect to inflammasome activation upon fungal infections, only the inflammasome receptors AIM2, NLRC4 and, mainly, NLRP3, are related to engaging and triggering IL-1β caspase-dependent cleavage (36). Thus, we first evaluated the gene transcription of these receptors in BMDMs upon hyphal infection, and only *Nlrp3* was upregulated (**Figure 5A**). To evaluate whether NLRP3 participates in IL-1β secretion in BMDMs stimulated with hyphae, we used BMDMs obtained from NLRP3-deficient mice. In NLRP3 absence, IL-1β secretion was almost completely abolished (**Figure 5B**), whereas inflammasome-independent TNF-α production remained unchanged (**Figure 5C**).

NLRP3 is activated in response to a myriad of microbial infections through the sensing of their common-induced cellular disturbances, principally potassium efflux, ROS production, phagolysosomal acidification, and cathepsin B release (37). In order to assess whether the aforementioned mechanisms of NLRP3-inflammasome activation are required for our model, we impaired cell potassium efflux by cell treatment with glyburide, an ATP-sensitive K^+ channel inhibitor, and also by addition of exogenous KCl. Under both conditions, we observed a drastic decrease in IL-1β levels (**Figure 5D**). To verify the role of ROS production, we used DPI, a blocker of ROS derived from the phagosome and mitochondria. In response, IL-1β secretion was impaired (**Figure 5E**). However, reduction in TNF-α secretion was also observed (data not shown). Furthermore, we measured IL-1β levels in cultures of BMDMs treated with bafilomycin A and CA-074Me, inhibitors of phagolysosomal acidification and cathepsin B cytosolic activity, respectively, which succeeds phagolysosomal damage and subsequent disruption. This inhibitory assay indicated that IL-1β secretion is strongly dependent on cathepsin B release and influenced by phagolysosomal

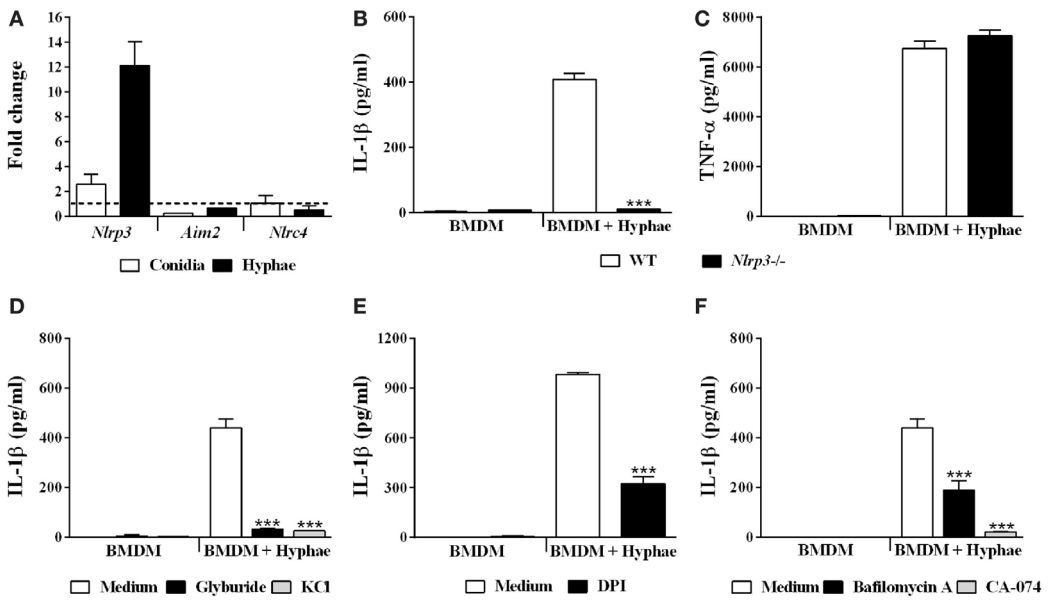

FIGURE 5 | *Fonsecaea pedrosoi* hyphae activate the NLRP3 inflammasome, which depends on K^+ efflux, ROS production, phagolysosomal acidification, and cathepsin B release. Bone marrow-derived macrophages (BMDMs) were infected with conidia or hyphae for 6 h and, thereafter, were lysed for RT-qPCR analysis to quantify gene expression of indicated genes **(A)**. BMDMs obtained from wild-type (WT) or *NLRP3*$^{-/-}$ mice were infected with *F. pedrosoi* hyphae for 24 h **(B,C)**. WT BMDMs were pretreated for 2 h with glyburide (150 μM) or KCl (50 mM) **(D)**, DPI (20 μM) **(E)**, and bafilomycin A (250 nM) or CA-074 (50 μM) **(F)**. Then, cells were infected with *F. pedrosoi* hyphae for 24 h. The supernatant of 24 h cell culture assays **(B–F)** was evaluated for IL-1β by ELISA. Data shown are mean ± SEM and are representative of two to three independent experiments. ***$p < 0.001$, compared to WT-infected untreated cells.

acidification (**Figure 5F**). Furthermore, since cathepsin B release requires phagolysosome membrane permeabilization, we incubated BMDMs with FITC-dextran and evaluated whether it leaks into the cytosol (Figure S2 in Supplementary Material). Internalized FITC-dextran diffused into the cytosol after *F. pedrosoi* challenge, as previously described for *C. neoformans* infection (35), which suggests that disruption of the phagolysosome caused by *F. pedrosoi* preceded cathepsin B release in order to induce IL-1β secretion. Altogether, our data show that *F. pedrosoi* hyphae activate the NLRP3 inflammasome in BMDMs, which depends on K^+ efflux, ROS production, phagolysosomal acidification, and disruption followed by cathepsin B release. All cell treatments used above were previously successfully tested (27) to exclude the reduction of IL-1β due to cytotoxic effects.

Inflammasome Activation Does Not Promote *In Vitro* Fungicidal Activity of BMDMs Challenged with *F. pedrosoi* Conidia or Hyphae

Some studies have demonstrated that inflammasome activation drives host protective immune responses against fungal pathogens, such as *C. albicans*, *C. neoformans*, and *P. brasiliensis* (36). Thus, after clarifying the mechanisms of inflammasome activation in BMDMs infected with *F. pedrosoi*, we aimed to verify whether this is reflected in enhanced fungicidal activity by BMDMs against *F. pedrosoi* conidia and hyphae. To this end, we infected WT, *Caspase-1/11*$^{-/-}$ and *Nlrp3*$^{-/-}$ BMDMs for 24 h and thereafter performed the CFU assay. We observed no differences in fungal burden among experimental groups (**Figures 6A,E**), which we already expected for infection with conidia, since this morphotype alone is unable to activate the inflammasome in BMDMs, as demonstrated in the present study (**Figure 2A**). We did not observe NO production in these groups (**Figures 6C,G**). Therefore, we went further and co-stimulated infected BMDMs with nigericin to promote strong inflammasome activation, as shown in **Figure 2A**, and then performed the CFU assay. Nevertheless, the inducible burst in inflammasome activity was not accompanied by diminished recovery of viable fungus from BMDMs infected with conidia or hyphae (**Figures 6B,F**). Interestingly, a control group treated simultaneously with LPS and IFN-γ showed no difference in fungal killing (**Figures 6B,F**), despite the induced NO production (**Figures 6D,H**). This can be explained in part because *F. pedrosoi* morphotypes, especially hyphae, inhibited NO production (**Figures 6D,H**).

NLRP3 Inflammasome Does Not Contribute to Fungal Clearance in a Murine CBM Model

In order to verify whether *F. pedrosoi* could activate the inflammasome *in vivo*, and to further investigate the functional role

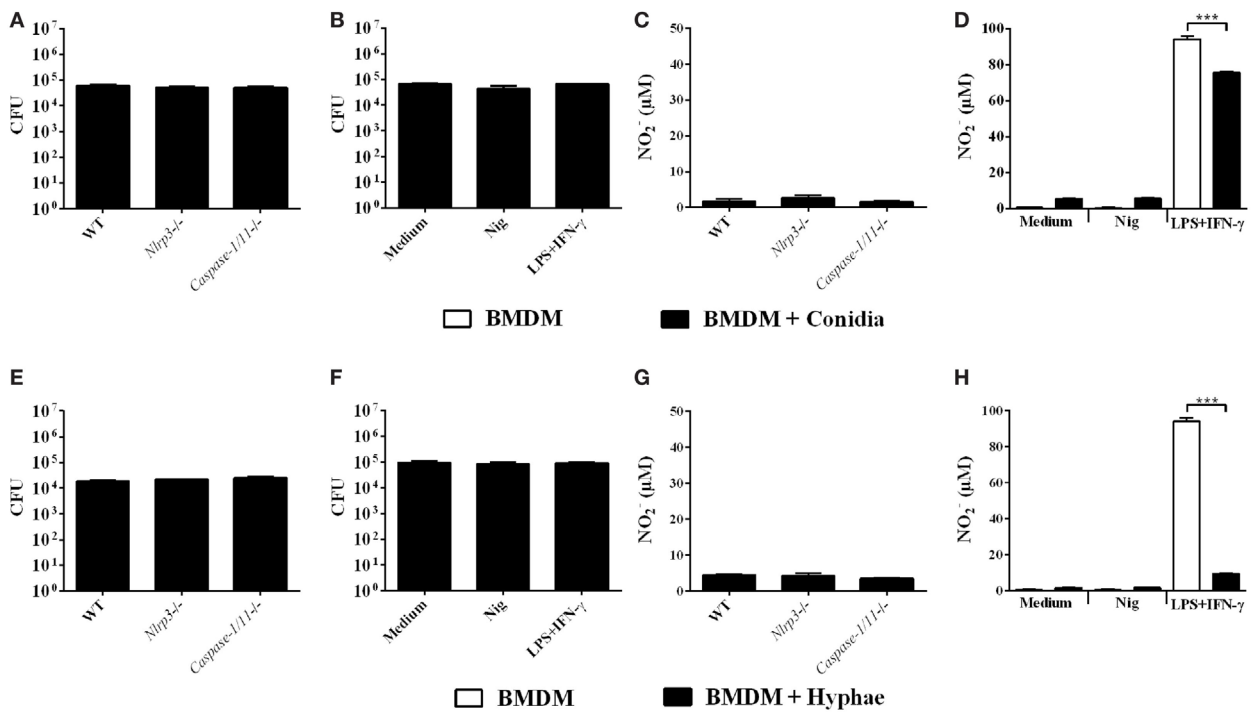

FIGURE 6 | Inflammasome activation does not promote *in vitro* fungicidal activity of bone marrow-derived macrophages (BMDMs) challenged with *Fonsecaea pedrosoi* conidia or hyphae. BMDMs were infected for 24 h with *F. pedrosoi* conidia **(A–D)** or hyphae **(E–H)**. Then, culture supernatant was collected for nitrite measurement by Griess reagent, whereas infected cells were lysed to perform colony-forming unit (CFU) analysis. CFU **(A,E)** and NO_2^- **(C,G)** values of an assay with infected wild-type (WT), *NLRP3*$^{-/-}$ and *Caspase-1*$^{-/-}$ BMDMs. CFU **(B,F)** and NO_2^- **(D,H)** values of an assay with non-infected (white bars) and infected (black bars) WT BMDMs co-stimulated (or not) with both LPS and IFN-γ (500 and 20 ng/mL added 3 h before fungal infection, respectively) or nigericin (20 μM during the last 60 min of incubation). Data shown are mean ± SEM and are representative of three independent experiments. ***$p < 0.001$, between groups indicated by brackets.

of the inflammasome in an experimental model of CBM, we infected WT, *Nlrp3* and *Caspase-1/11*-deficient mice subcutaneously in the footpad with a mixed inoculum of fungal propagules consisting of conidia and hyphae. WT-infected mice showed a sustained production of IL-1β at all the time points analyzed, which was reduced at 21 and 28 days postinfection (d.p.i.) in *Nlrp3*$^{-/-}$ mice (**Figure 7A**). In addition, we observed significant levels of IL-18 only in an advanced stage of remission of the disease, at 28 d.p.i., with defective cytokine production in *Nlrp3*$^{-/-}$ mice (**Figure 7B**). There was no difference in the production of both cytokines between WT and *Caspase-1/11*$^{-/-}$ mice (**Figures 7A,B**). Interestingly, the production of IL-1β and IL-18, regulated by NLRP3 and Caspase-1/11 in response to *F. pedrosoi* hyphae (**Figures 4** and **5**), did not affect the fungal load of the footpad, as we did not observe statistical differences in CFU assays among WT and both groups of knockout mice, at any of the times analyzed (**Figure 7C**). Histological examination of infected tissues from all groups show similar features as indicated by the presence of exudative areas and inflammatory infiltrates early as 14 d.p.i., which diminished over time and was accompanied by tissue remodeling and repair (Figure S3A in Supplementary Material). Consistently with CFU and histological analysis, there was no difference in morphometric measurements of the injured footpad among experimental groups (Figure S3B in Supplementary Material).

These data indicate that *F. pedrosoi* induces the production of IL-1β and IL-18 in the course of a subcutaneous experimental infection model, but this production does not affect the fungal clearance.

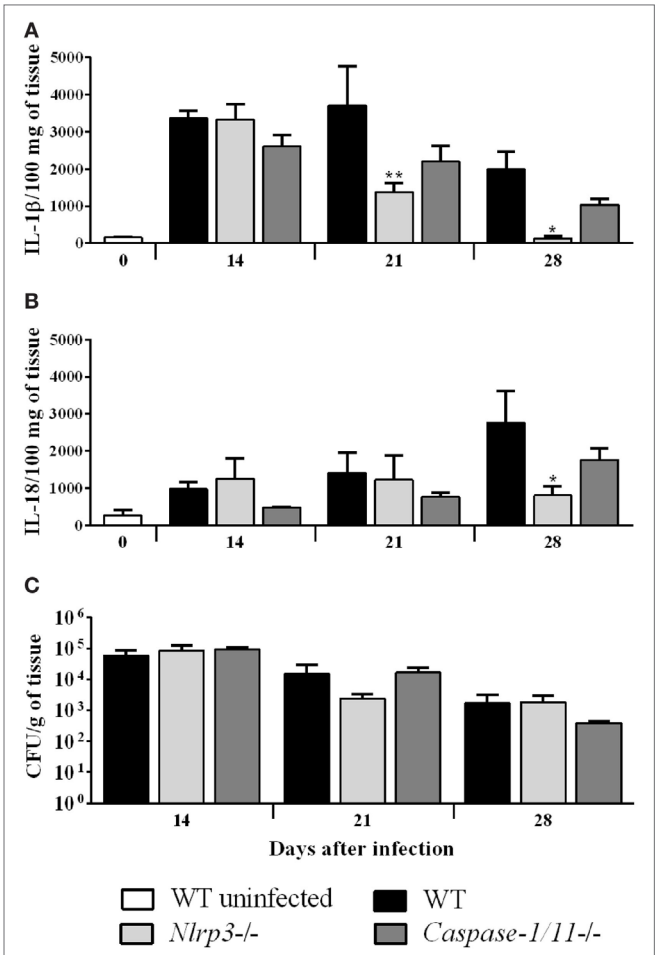

FIGURE 7 | NLRP3 inflammasome does not contribute to fungal clearance in a murine chromoblastomycosis model. Wild-type (WT), *Nlrp3*$^{-/-}$ and *Caspase-1/11*$^{-/-}$ C57BL/6 mice ($n = 4$) were infected in both hind footpads with 1×10^6 *Fonsecaea pedrosoi* propagules. WT uninfected mice were used as control. Mice were euthanized at the indicated days postinfection, and the footpad tissue homogenate was assessed for both cleaved and uncleaved IL-1β **(A)** and interleukin-18 **(B)** by ELISA, and plated for colony-forming unit analysis **(C)**. Data shown are mean ± SEM and are representative of two independent experiments. *$p < 0.05$; **$p < 0.01$, compared to WT infected.

DISCUSSION

Studies examining innate immune cell recognition of *F. pedrosoi* are scarce. Although the involvement of CLRs and TLRs in this process is relatively well known, cytoplasmic NLRs had never been considered. In this study, we demonstrate that the main agent of CBM, *F. pedrosoi*, activates NLRP3 inflammasome-dependent secretion of IL-1β and IL-18 in phagocytes and *in vivo*. Moreover, the mechanisms underlying this process encompass Syk-coupled CLR receptors, caspase-1 and caspase 8 proteolytic activity and several DAMPs.

One key aspect shown to determine NLRP3 inflammasome activation during fungal infection is morphogenesis. We show here that live *F. pedrosoi* hyphae, and not conidia, were able to induce the production of mature IL-1β and IL-18 in BMDMs, despite the fact that both cell types prompted the upregulation of IL-1β transcripts (pro-IL-1β). In addition, only hyphal cells induced IL-1β secretion in human monocytic THP-1 cells. Similarly, activation of NLRP3 inflammasome and cytokine secretion in macrophages challenged with *A. fumigatus* was achieved only with hyphae. This suggests that an invading aggressive hyphal form may be necessary to trigger the inflammatory response (23). Actually, in lung tissues of NLRP3-deficient mice, minimal inflammatory reaction to *Aspergillus* hyphae infection is observed (19). Further, *F. pedrosoi* swollen conidia, an intermediate stage of conidia-into-hyphae germination, were not able to induce mature IL-1β production, as also shown in *A. fumigatus*-infected macrophages (23). Interestingly, inflammasome-independent cytokines, such as TNF-α, are more induced by *Aspergillus* swollen conidia compared to inactive conidia, and cell wall PAMPs are transiently displayed and detected by macrophage PRRs (38, 39). In this context, future studies are warranted for the identification of cell wall composition/PAMPs exposure modification during *F. pedrosoi* germination. In *C. albicans*, although the switch from yeast to hyphal morphogenesis was initially believed to be indispensable for the activation of the NLRP3 inflammasome (17), recent studies have showed that the remodeling of its cell wall leading to PAMPs exposure during phagocytosis is the main factor associated with inflammasome activation (40, 41).

Another important aspect that influences NLRP3 inflammasome activation during infectious processes is the host cell type. Indeed, differently from what is shown in macrophages,

F. pedrosoi conidia alone were able to induce mature IL-1β production in dendritic cells. In addition, when nigericin (bacterial pore formation toxin) was added to macrophage cell culture, a significant amount of IL-1β secretion was observed, corroborating the fact that conidia induce pro-IL-1β production but fail to provide inflammasome-activating second signal in macrophages. Consistent with this observation, our group previously showed that *P. brasiliensis* can trigger pro-IL-1β production in macrophages and dendritic cells, but it was only in the latter that infection resulted in IL-1β maturation and release (27). Also, activation of NLRP3 inflammasome and production of mature IL-1β in macrophages infected with *C. albicans* yeast occurred only after a priming step with LPS (17, 42) whereas the fungus alone induced mature cytokine release in the dendritic cell (16). These results are in line with the fact that NLRP3 concentration is critical to the efficacy of inflammasome activation (31), and NLRP3 protein levels under steady-state conditions and after PRR engagement are higher in dendritic cells when compared with macrophages (43, 44). Furthermore, *in vivo* murine splenic conventional dendritic cells reveal constant high *Nlrp3* transcript levels (45). Thus, both fungal form and phagocyte type are critical factors that dictate NLRP3 inflammasome activation in fungal infections.

Priming is the first step required for inflammasome activation, and this process is generally associated with PRRs engagement by PAMPs leading to pro-IL-1β, pro-IL-18, and NLRP3 production. CLRs are the major PRRs family for the recognition of fungal carbohydrate residues and have been associated with the priming step of inflammasome activation in several fungal infections (46). For instance, the dectin-1 receptor is necessary for the production of pro-IL-1β and IL-1 β in murine and human macrophages and dendritic cells infected with *Microsporum canis*, *C. albicans*, and *Malassezia* spp. (42, 47, 48). Also, signaling mediated by dectin-2 is required for the production of IL-1β in dendritic cells infected with both hyphae and conidia of *C. albicans* (49). Interestingly, dectin-1 and dectin-2 have been associated with the induction of cytokine secretion, including inflammasome-dependent IL-1β, in a collaborative manner. Dectin-1 and dectin-2 double-deficient dendritic cells infected with *Trichophyton rubrum* or *H. capsulatum* have impaired secretion of IL-1β when compared to WT cells and cells with either receptor deficiency alone (21, 50). Moreover, using blocking antibodies for dectin-1 or dectin-2 in single or double dectin-1/dectin-2 deficient cells, Chang et al. (21) elegantly demonstrated that dectin-2 was the major receptor for inflammasome activation in *H. capsulatum*-infected dendritic cells. Although we did not employ double deficient cells, our results using cells lacking dectin-1 or dectin-2 clearly show that these CLRs play a significant role in inducing the secretion of IL-1β by macrophages infected with *F. pedrosoi* hyphae. This is in line with the fact that dectin-1 and dectin-2 are required for the development of Th17 cells in mice subcutaneously infected with *F. pedrosoi*, since IL-1β associated with IL-23 favors a Th17 response (11, 51).

Besides dectin-1 and dectin-2, we also demonstrated a role for dectin-3 in the induction of IL-1β secretion by BMDMs infected with *F. pedrosoi* hyphae. It is noteworthy that dectin-3 can form heterodimers with dectin-2 for sensing and mediation of host protective anti-*C. albicans* defense (32). In addition, dectin-3 is necessary for the development of vaccine-induced Th17 cells that are associated with protection against the fungal pathogen *Blastomyces dermatitidis* (52). The role of dectin-3 in the recognition of *F. pedrosoi* conidia has been evaluated using lacZ activity measurement in reporter cells coexpressing dectin-2/dectin-3 or expressing dectin-2 or dectin-3 alone (11). Only a weak response was detected in dectin-3 expressing cells, and cells coexpressing dectin-2/dectin-3 did not show an enhanced dectin-2 induced reporter activity. Furthermore, IL-6 production was not significantly altered in dectin-3-deficient cells. In this context, our results suggest that, contrary to conidia, *F. pedrosoi* hyphae may expose dectin-3 ligands leading to recognition and pro-inflammatory cytokine production by macrophages.

Upon PAMP binding, all three aforementioned CLRs initiate intracellular signaling pathways, and the Syk-CARD9-NFkB pathway is the best characterized and the most common during fungal infections (36, 46). For instance, Syk-dependent NLRP3 priming occurs in *C. albicans*, *A. fumigatus*-, *C. neoformans*- and *P. brasiliensis*-infected cells (16, 18, 23, 27). Indeed, a significant reduction in IL-1β secretion was shown here in macrophages infected with *F. pedrosoi* and treated with chemical inhibitors of Syk kinase and NFkB activity. This result parallels those showing *Syk* and *Nfkb1* upregulated transcripts induced by *F. pedrosoi* hyphae. It was noted that *Myd88* transcripts were also significantly induced by hyphae in macrophages, but their inhibition did not affect the production of IL-1β. Conversely, the secretion of the inflammasome-independent cytokine TNF-α relied upon dectin-1 and both Syk- and Myd88-mediated signaling, which is in accordance with previous studies showing that TNF-α production in macrophages treated with β-glucans (i.e., dectin-1 ligand) requires that Syk-dependent signaling synergizes with the Myd88 pathway (53).

Followed by priming, the proteolytic cleavage of pro-IL-1β into its mature form is canonically performed by the protease caspase-1, and this process is largely dependent on the assembly of the NLRP3 inflammasome in fungal infections (36, 54). Using a fluorescence-based assay, we demonstrated that only *F. pedrosoi* hyphae were directly able to activate caspase-1 in macrophages. In addition, caspase-1/11-deficient macrophages and macrophages treated with caspase-1 peptide inhibitor produced a significant, but not total, impairment in mature IL-1β secretion, suggesting that caspase-1-independent processes may also be involved. In fact, non-canonical processing of IL-1β has been shown to operate in phagocytes infected with fungal pathogens. *C. albicans* triggers caspase-8-mediated cleavage of pro-IL-1β independently of a NLR-containing inflammasome. This occurs *via* assembly of the CARD9–Bcl-10–MALT1 scaffold mediated by Syk signaling, followed by the recruitment of caspase-8 into this scaffold for direct IL-1β processing (34). Caspase-8 can also function in a NLRP3-dependent inflammasome activation manner, as demonstrated in phagocytes infected with *A. fumigatus* and *C. neoformans* (19, 35). The use of a specific caspase-8 peptide inhibitor shows here that this protease has a role in the processing of IL-1β in *F. pedrosoi*-infected macrophages. Given the fact that NLRP3-deficient

macrophages completely failed to produce IL-1β upon *F. pedrosoi* challenge, the function of caspase-8 in our model probably relies on the NLRP3 inflammasome assembly instead of a direct processing activity.

Along with NLRP3, NLRC4 and AIM2-containing-inflammasomes have been implicated in the antifungal response (36, 54). Specifically, *C. albicans* triggers NLCR4 inflammasome exclusively in mucosal cells, and deficiency in this NLR results in impaired neutrophil infiltration in the mucosa in a murine model of oral infection (55). Conversely, the NLRP3 inflammasome is strictly required in phagocytes infected with *C. albicans* (16). Regarding *A. fumigatus*, this fungus induces cooperative and synergistic activation of the NLRP3 and AIM2 inflammasomes in phagocytes and in an experimental murine model of intranasal infection (19). Similarly, NLRP3 and AIM2 inflammasomes are activated by plasmodium hemozoin and DNA (56). In this context, we evaluated the transcript levels of *Nlrp3*, *Nlrc4*, and *Aim2* genes in BMDMs infected with the infective forms of *F. pedrosoi*. Hyphae induced the upregulation of *Nlrp3* transcripts only. These data, coupled with the fact that NLRP3-deficient infected macrophages do not produce IL-1β, as mentioned above, indicate that multiple inflammasome activation is probably not in use in our fungal model. At the same time, these results also suggest that, unlike in *A. fumigatus*, there is a poor availability of *F. pedrosoi* dsDNA (the main AIM2 ligand) in the cytosol of infected cells. Nevertheless, the use of mice deficient in NLRC4 and AIM2 would shed light on this issue.

Although not fully characterized, cellular stresses that induce endogenous DAMPs have been associated with NLRP3 assembly and inflammatory caspase activation. Among them, K^+ efflux due to stimulation of the ATP-sensitive K^+ channel, ROS generation, and lysosome rupture are usually presented (15). Using chemical inhibitors, we demonstrated that *F. pedrosoi* hyphae promote these intracellular disturbances in macrophages, leading to inflammasome activation. Both K^+ efflux and ROS are the main cellular disturbances associated with NLRP3 activation in phagocytes infected with diverse fungi, encompassing those causing dermathophytoses (47, 48, 57), and invasive mycosis (16, 18, 21, 27). Specifically, potassium efflux is considered a common unifying pathway for NLRP3 inflammasome complex activation triggered by numerous NLRP3 stimuli (58). As such, we tested two inhibitors of K^+ efflux, glyburide and KCl. Both treatments resulted in a significant impairment of IL-1β secretion by macrophages, reinforcing the central role of intracellular K^+ level reduction in the regulation of NLRP3 inflammasome activation. Similarly, the use of DPI, an inhibitor of NADPH oxidase-dependent and mitochondria-derived ROS production, also led to diminished IL-1β production. It is noteworthy that ROS generation is apparently not directly associated with the NLRP3 activation (i.e., inflammasome assembly) step. Instead, it may affect the priming step, as several inhibitors of ROS generation or scavengers of ROS have been shown to inhibit NFκB-mediated transcription of NLRP3 and pro-IL-1β (16, 59). Indeed, besides IL-1β, the production of the inflammasome-independent NFκB-dependent TNF-α was abrogated with the treatment with DPI in macrophages infected with *F. pedrosoi* (data not shown). In addition to ROS and K^+ efflux, disruption of the phagolysosomal membrane, leading to impairment of phagolysosomal acidification and leakage of enzymes such as cathepsin B into the cytoplasm results in NLRP3 activation (15). Therefore, macrophages infected with *F. pedrosoi* were treated with bafilomycin, which inhibits the vacuolar H^+ ATPase, or CA-074, which in turn inhibits cathepsin B activity. The treatments resulted in a significant reduction in IL-1β secretion, similar to the activation of the inflammasome by several bacteria and particulate matter (15, 36). Regarding fungi, cathepsin B is not required for IL-1β production in dendritic cells infected with *C. albicans* or *A. fumigatus* (16, 19). Conversely, the production of this cytokine in macrophages infected with *C. albicans* is dependent on cathepsin B (17). In phagocytes infected with *P. brasiliensis*, dendritic cells, but not macrophages, require phagolysosomal disruption for NLRP3 inflammasome activation (27, 60). Thus, the requirement for phagolysosomal disruption in the assembly of NLRP3 inflammasome is not universal, as it is dependent on the cell type and fungal pathogen.

Macrophages are essential innate immunity cells that are critical for direct antifungal response. Macrophages, along with neutrophils and lymphocytes, are regularly observed within the chronic granulomatous lesions of CBM patients, displaying different degrees of maturation and activation, and they also form multinucleated giant cells that harbor fungi (29, 30). In addition, *F. pedrosoi* cells can be detected in intracytoplasmic vacuoles of skin macrophages (61). Thus, we investigated whether NLRP3 inflammasome activation would play a part in the microbicidal capacity of macrophages infected with *F. pedrosoi*. In BMDMs lacking NLRP3 or Caspase-1 and infected with hyphae or conidia, no significant difference in the fungal burden was observed. Since conidia alone are not able to induce inflammasome activation, we treated macrophages with nigericin for the induction of the second signal for inflammasome activation and consequently production of mature IL-1β. Macrophages infected with hyphae were also treated with nigericin, leading to enhanced IL-1β secretion. Again, fungal viability was not affected, reinforcing the supposition that the NLRP3 inflammasome has no role in modulating the ability of macrophages to kill *F. predosoi.* In fact, the killing process of *F. pedrosoi* by macrophages is rarely efficient, and it is neutrophils that are considered the main phagocyte cell with microbicidal activity against this fungus (62, 63). Several studies have demonstrated that *F. pedrosoi* is able to survive and proliferate in murine macrophages, and activated macrophages are only fungistatic (62, 64–66). One important factor associated with the inability of macrophages to kill *F. pedrosoi* is the inhibition of NO production by macrophages (66). In line with this finding, no significant levels of nitrite were detected in the supernatant of macrophage cultures infected with *F. pedrosoi* cells. Furthermore, macrophages infected with either conidia or hyphae and treated with IFN-γ and LPS were not fungicidal and their nitrite production was significantly impaired. Lack of properly activated macrophages may serve *F. pedrosoi* intracellular parasitism, leading to disease establishment and progression in susceptible hosts.

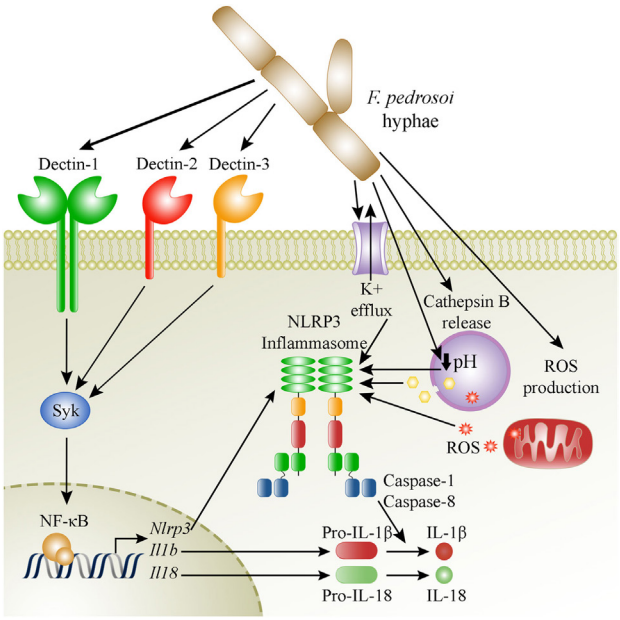

FIGURE 8 | Suggested model of activation of the NLRP3 inflammasome by *Fonsecaea pedrosoi* hyphae in macrophages. *F. pedrosoi* hyphae induce macrophage priming by a canonical Syk-NF-kB signaling pathway coupled to dectin-1, dectin-2, and dectin-3 recognition of the fungus. This leads to NLRP3, pro-IL-1β, and pro-IL-18 production. Then, the NLRP3-inflammasome is activated as a result of potassium efflux, phagolysosome acidification, cathepsin B release, and ROS production, which subsequently leads to IL-1β and IL-18 processing and secretion by caspase-1 and caspase-8 dependent cleavage.

Since *F. pedrosoi* activates the NLRP3 inflammasome *in vitro*, we investigated whether *in vivo* activation occurs and the possible role of this process in controlling fungal infection. Employing a mouse model of subcutaneous *F. pedrosoi* infection (24, 67), WT-infected mice showed a sustained production of IL-1β at all the time points analyzed, which was significantly reduced in mice lacking NLRP3. In addition, the NLRP3 inflammasome was also required for the production of IL-18, as assessed in the footpad macerate at 28 d.p.i. These results suggest that NLRP3 sensing is required for the maturation of IL-1β and IL-18 in mice infected with *F. pedrosoi*. Surprisingly, the production of these cytokines was not significantly different in the footpad of caspase-1/11-deficient mice, although there was a tendency for IL-1β and IL-18 to be lower than in control mice. In macrophages infected with *F. pedrosoi*, caspase-1, and caspase-8 were required for the production of IL-1β. It is possible that *in vivo*, caspase-8 compensates for the lack of caspase-1. For instance, *C. neoformans* activates NLRP3-caspase-8 inflammasome in the absence of caspase-1 (35). Also, caspase-independent cleavage of pro-IL-1β may ensue, especially *via* neutrophil-derived serine proteases (68). This is in line with the fact that the chronic inflammatory response observed in murine and human CBM is characterized by a mononuclear granuloma modified by the influx of neutrophils, giving rise to a suppurative neutrophilic infiltrate (5, 24). In this context, in disseminated candidiasis where neutrophils are the main component of the infiltrates in inflammatory organs, IL-1β processing is probably mainly achieved by neutrophil-derived protease, rather than by caspase-1 (69, 70).

Differently from several models of systemic mycosis where NLRP3 inflammasome activation is associated with host protection and impairment of fungal growth (16–22), NLRP3 and caspase-1 deficient mice subcutaneously infected with *F. pedrosoi* developed to be self-healing in 30–40 days with a progressive fungal clearance. This finding is in accordance with the fact that infected mice lacking NLRP3 or Caspase-1 had similar histological and morphometric analyses of the footpad tissue when compared with control mice.

In conclusion, we revealed here the mechanisms of NLRP3 inflammasome activation in macrophages and in mice infected with the most important CBM etiologic agent *F. pedrosoi,* as depicted in our proposed model in **Figure 8**. Future studies employing other causative agents of CBM will contribute to a better understanding on the role of inflammasome activation in the pathogenesis of this neglected disease.

ETHICS STATEMENT

All experimental procedures were approved by the Animal Ethics Committee of the University of Brasilia (UnBDoc number 134976/2014), and conducted according to the Brazilian Council for the Control of Animal Experimentation (CONCEA) guidelines.

AUTHOR CONTRIBUTIONS

Conceived and designed the experiments: RJAC, IMS, PHB, AHT, and ALB. Performed the experiments: RJAC, IMS, MSJ, AMMB, PHHVJ, SAMO, and LCL. Analyzed the data: RJAC, IMS, AHT, and ALB. Contributed to reagents/material/analysis tools: AHT and ALB. Contributed to Caspase-1 and NLRP3 KO mice: KGM. Wrote the paper: RJAC, AHT, and ALB.

FUNDING

Funding for this research was provided by Fundação de Apoio à Pesquisa do Distrito Federal (FAPDF Project 193.00805/2015), Conselho Nacional de Pesquisa (CNPq Project 302752/2015-3) for financial support and Coordenação de Aperfeiçoamento de Pessoal de Nível Superior (CAPES) for graduate students' grants.

SUPPLEMENTARY MATERIAL

The Supplementary Material for this article can be found online at http://www.frontiersin.org/article/10.3389/fimmu.2017.01572/full#supplementary-material.

FIGURE S1 | *Fonsecaea pedrosoi* conidia reaches the swelling stage of germination. Flow cytometry analysis of *F. pedrosoi* conidia incubed for 6 h with phosphate-buffered saline, RPMI supplemented with 20% of SBF (R20 medium) or bone marrow-derived macrophages (BMDMs) for 6 and 24 h. Infected BMDMs were washed to discard nonphagocyted fungus and lysed to release intracellular fungi. After, conidia were fixed and evaluated by flow cytometry analysis. Commercial 2 and 3 μm sized-cytometry-beads were used as control. Dot plot side scatter (FSC) vs forward scatter (FSC) analysis of conidia **(A)**. Histogram analyses of conidia size **(B)**. Average conidia size using the

median FSC and expressed as arbitrary units (au) **(C)**. Data shown are mean ± SEM and are representative of three independent experiments. ***$p < 0.001$, between groups indicated by brackets; n.s., not significantly.

FIGURE S2 | *Fonsecaea pedrosoi* hyphae infection cause phagolysosome membrane permeabilization contributing to inflammasome activation. Bone marrow-derived macrophages were seeded on glass bottom culture dishes with RPMI for 1 h for cell adhesion. After wash of unbound cells with warm RPMI, cells were incubated with 70 kDa FITC-dextran (Sigma-Aldrich; 2 mg/mL) in RPMI with 10% FBS for 2 h. The cells were washed and infected or not (medium) with *F. pedrosoi* hyphae (MOI 1) or *Cryptococcus neoformans* yeasts (MOI 2) opsonized with anti-GXM Ab. After 4 h of infection, non-phagocytosed fungi were washed and infection proceeded up to 20 h. After infection, cells were washed again, incubated with RPMI medium without phenol red supplemented with 10% FBS and stained with DAPI. Cells were washed, incubated with medium, and visualized by fluorescence microscopy. White arrowhead indicates internalized fungi.

FIGURE S3 | NLRP3 or caspase-1/11 absence do not affect tissue response to *Fonsecaea pedrosoi* infection. Wild-type, *Nlrp3*$^{-/-}$ and *Caspase-1/11*$^{-/-}$ mice were injected subcutaneously with 1×10^6 *F. pedrosoi* propagules into the hind footpad. For histology evaluation, infected mice were euthanized at the indicated days after infection and fragments of tissues were fixed with 10% phosphate-buffered formalin and embedded in paraffin. Paraffin-sectioned samples were stained with Hematoxilin and Eosin (H&E) and analyzed under a Zeiss inverted microscope **(A)**. During infection, the injured tissue was measured every 3 days with a caliper for morphometric examination **(B)**. Data shown are mean ± SEM (n = 4) and are representative of two independent experiments.

REFERENCES

1. McGinnis MR, Hilger AE. Infections caused by black fungi. *Arch Dermatol* (1987) 123:1300–2. doi:10.1001/archderm.1987.01660340062020
2. López Martínez R, Méndez Tovar LJ. Chromoblastomycosis. *Clin Dermatol* (2007) 25:188–94. doi:10.1016/j.clindermatol.2006.05.007
3. Queiroz-Telles F. Chromoblastomycosis: a neglected tropical disease. *Rev Inst Med Trop São Paulo* (2015) 57(Suppl 1):46–50. doi:10.1590/S0036-46652015000700009
4. Santos ALS, Palmeira VF, Rozental S, Kneipp LF, Nimrichter L, Alviano DS, et al. Biology and pathogenesis of *Fonsecaea pedrosoi*, the major etiologic agent of chromoblastomycosis. *FEMS Microbiol Rev* (2007) 31:570–91. doi:10.1111/j.1574-6976.2007.00077.x
5. Queiroz-telles F, de Hoog S, Santos WCL, Salgado CG, Vicente VA, Bonifaz A, et al. Chromoblastomycosis. *Clin Microbiol Rev* (2017) 30: 233–76. doi:10.1128/CMR.00032-16
6. Bonifaz A, Carrasco-Gerard E, Saúl A. Chromoblastomycosis: clinical and mycologic experience of 51 cases. *Mycoses* (2001) 44:1–7. doi:10.1046/j.1439-0507.2001.00613.x
7. Salgado CG, da Silva JP, Diniz JAP, da Silva MB, da Costa PF, Teixeira C, et al. Isolation of *Fonsecaea pedrosoi* from thorns of *Mimosa pudica*, a probable natural source of chromoblastomycosis. *Rev Inst Med Trop Sao Paulo* (2004) 46:33–6. doi:10.1590/S0036-46652004000100006
8. Queiroz-Telles F, Esterre P, Perez-Blanco M, Vitale RG, Salgado CG, Bonifaz A. Chromoblastomycosis: an overview of clinical manifestations, diagnosis and treatment. *Med Mycol* (2009) 47:3–15. doi:10.1080/13693780802538001
9. Teixeira de Sousa MDG, Ghosn EEB, Almeida SR. Absence of CD4+ T cells impairs host defence of mice infected with *Fonsecaea pedrosoi*. *Scand J Immunol* (2006) 64:595–600. doi:10.1111/j.1365-3083.2006.01846.x
10. Wevers BA, Kaptein TM, Zijlstra-Willems EM, Theelen B, Boekhout T, Geijtenbeek TBH, et al. Fungal engagement of the C-type lectin mincle suppresses dectin-1-induced antifungal immunity. *Cell Host Microbe* (2014) 15:494–505. doi:10.1016/j.chom.2014.03.008
11. Wüthrich M, Wang H, Li M, Lerksuthirat T, Hardison SE, Brown GD, et al. *Fonsecaea pedrosoi*-induced Th17-cell differentiation in mice is fostered by dectin-2 and suppressed by mincle recognition. *Eur J Immunol* (2015) 45:2542–52. doi:10.1002/eji.201545591
12. Sousa MDG, Reid DM, Schweighoffer E, Tybulewicz V, Ruland J, Langhorne J, et al. Restoration of pattern recognition receptor costimulation to treat chromoblastomycosis, a chronic fungal infection of the skin. *Cell Host Microbe* (2011) 9:436–43. doi:10.1016/j.chom.2011.04.005
13. Schroder K, Tschopp J. The inflammasomes. *Cell* (2010) 140:821–32. doi:10.1016/j.cell.2010.01.040
14. Wen H, Miao EA, Ting JP. Review mechanisms of NOD-like receptor-associated inflammasome activation. *Immunity* (2013) 39:432–41. doi:10.1016/j.immuni.2013.08.037
15. Jo EK, Kim JK, Shin DM, Sasakawa C. Molecular mechanisms regulating NLRP3 inflammasome activation. *Cell Mol Immunol* (2016) 13:148–59. doi:10.1038/cmi.2015.95
16. Gross O, Poeck H, Bscheider M, Dostert C, Hannesschläger N, Endres S, et al. Syk kinase signalling couples to the Nlrp3 inflammasome for anti-fungal host defence. *Nature* (2009) 459:433–6. doi:10.1038/nature07965
17. Joly S, Ma N, Sadler JJ, Soll DR, Cassel SL, Sutterwala FS. Cutting edge: *Candida albicans* hyphae formation triggers activation of the Nlrp3 inflammasome. *J Immunol* (2009) 183:3578–81. doi:10.4049/jimmunol.0901323
18. Guo C, Chen M, Fa Z, Lu A, Fang W, Sun B, et al. Acapsular *Cryptococcus neoformans* activates the NLRP3 inflammasome. *Microbes Infect* (2014) 16:845–54. doi:10.1016/j.micinf.2014.08.013
19. Karki R, Man SM, Malireddi RKS, Gurung P, Vogel P, Lamkanfi M, et al. Concerted activation of the AIM2 and NLRP3 inflammasomes orchestrates host protection against *Aspergillus* infection. *Cell Host Microbe* (2015) 17:357–68. doi:10.1016/j.chom.2015.01.006
20. Feriotti C, de Araújo EF, Loures FV, da Costa TA, de Lima GNA, Zamboni DS, et al. NOD-like receptor P3 inflammasome controls protective Th1/Th17 immunity against pulmonary paracoccidioidomycosis. *Front Immunol* (2017) 8:1–15. doi:10.3389/fimmu.2017.00786
21. Chang TH, Huang JH, Lin HC, Chen WY, Lee YH, Hsu LC, et al. Dectin-2 is a primary receptor for NLRP3 inflammasome activation in dendritic cell response to *Histoplasma capsulatum*. *PLoS Pathog* (2017) 13:e1006485. doi:10.1371/journal.ppat.1006485
22. Lei G, Chen M. Biofilm from a clinical strain of *Cryptococcus neoformans* activates the NLRP3 inflammasome. *Cell Res* (2013) 23:965–8. doi:10.1038/cr.2013.49
23. Saïd-Sadier N, Padilla E, Langsley G, Ojcius DM. *Aspergillus fumigatus* stimulates the NLRP3 inflammasome through a pathway requiring ROS production and the Syk tyrosine kinase. *PLoS One* (2010) 5:e10008. doi:10.1371/journal.pone.0010008
24. Siqueira IM, de Castro RJA, Leonhardt LCdM, Jerônimo MS, Soares AC, Raiol T, et al. Modulation of the immune response by *Fonsecaea pedrosoi* morphotypes in the course of experimental chromoblastomycosis and their role on inflammatory response chronicity. *PLoS Negl Trop Dis* (2017) 11:e0005461. doi:10.1371/journal.pntd.0005461
25. Lutz MB, Kukutsch N, Ogilvie ALJ, Roßner S, Koch F, Romani N, et al. An advanced culture method for generating large quantities of highly pure dendritic cells from mouse bone marrow. *J Immunol Methods* (1999) 223:77–92. doi:10.1016/S0022-1759(98)00204-X
26. Livak KJ, Schmittgen TD. Analysis of relative gene expression data using real-time quantitative PCR and the $2^{-\Delta\Delta CT}$ method. *Methods* (2001) 408:402–8. doi:10.1006/meth.2001.1262
27. Tavares AH, Magalhães KG, Almeida RDN, Correa R, Burgel PH, Bocca AL. NLRP3 inflammasome activation by *Paracoccidioides brasiliensis*. *PLoS Negl Trop Dis* (2013) 7:e2595. doi:10.1371/journal.pntd.0002595
28. Erwig LP, Gow NAR. Interactions of fungal pathogens with phagocytes. *Nat Rev Microbiol* (2016) 14:163–76. doi:10.1038/nrmicro.2015.21
29. Esterre P, Peyrol S, Sainte-Marie D, Pradinaud R, Grimaud JA. Granulomatous reaction and tissue remodelling in the cutaneous lesion of chromomycosis. *Virchows Arch A Pathol Anat Histopathol* (1993) 422:285–91. doi:10.1007/BF01608337
30. Minotto R, Edelweiss MIA, Scroferneker ML. Study on the organization of cellular elements in the granulomatous lesion caused by chromoblastomycosis. *J Cutan Pathol* (2017) 44:915–8. doi:10.1111/cup.13014
31. Bauernfeind FG, Horvath G, Stutz A, Alnemri ES, MacDonald K, Speert D, et al. Cutting edge: NF-kappaB activating pattern recognition and cytokine receptors license NLRP3 inflammasome activation by regulating NLRP3 expression. *J Immunol* (2009) 183:787–91. doi:10.4049/jimmunol.0901363

32. Zhu L-L, Zhao X-Q, Jiang C, You Y, Chen X-P, Jiang Y-Y, et al. C-type lectin receptors dectin-3 and dectin-2 form a heterodimeric pattern-recognition receptor for host defense against fungal infection. *Immunity* (2013) 39:324–34. doi:10.1016/j.immuni.2013.05.017
33. Gringhuis SI, den Dunnen J, Litjens M, van der Vlist M, Wevers B, Bruijns SCM, et al. Dectin-1 directs T helper cell differentiation by controlling noncanonical NF-kappaB activation through Raf-1 and Syk. *Nat Immunol* (2009) 10:203–13. doi:10.1038/ni.1692
34. Gringhuis SI, Kaptein TM, Wevers BA, Theelen B, van der Vlist M, Boekhout T, et al. Dectin-1 is an extracellular pathogen sensor for the induction and processing of IL-1β via a noncanonical caspase-8 inflammasome. *Nat Immunol* (2012) 13:246–54. doi:10.1038/ni.2222
35. Chen M, Xing Y, Lu A, Fang W, Sun B, Chen C, et al. Internalized *Cryptococcus neoformans* activates the canonical caspase-1 and the noncanonical caspase-8 inflammasomes. *J Immunol* (2015) 195:4962–72. doi:10.4049/jimmunol.1500865
36. Tavares AH, Bürgel PH, Bocca AL. Turning up the heat: inflammasome activation by fungal pathogens. *PLoS Pathog* (2015) 11:e1004948. doi:10.1371/journal.ppat.1004948
37. Bauernfeind F, Hornung V. Of inflammasomes and pathogens – sensing of microbes by the inflammasome. *EMBO Mol Med* (2013) 5:814–26. doi:10.1002/emmm.201201771
38. Hohl TM, Van Epps HL, Rivera A, Morgan LA, Chen PL, Feldmesser M, et al. *Aspergillus fumigatus* triggers inflammatory responses by stage-specific beta-glucan display. *PLoS Pathog* (2005) 1:e30. doi:10.1371/journal.ppat.0010030
39. Luther K, Torosantucci A, Brakhage AA, Heesemann J, Ebel F. Phagocytosis of *Aspergillus fumigatus* conidia by murine macrophages involves recognition by the dectin-1 beta-glucan receptor and toll-like receptor 2. *Cell Microbiol* (2007) 9:368–81. doi:10.1111/j.1462-5822.2006.00796.x
40. Wellington M, Koselny K, Krysan DJ. *Candida albicans* morphogenesis is not required for macrophage interleukin 1β production. *MBio* (2012) 4:e00433–12. doi:10.1128/mBio.00433-12
41. Wellington M, Koselny K, Sutterwala FS, Krysan DJ. *Candida albicans* triggers NLRP3-mediated pyroptosis in macrophages. *Eukaryot Cell* (2014) 13:329–40. doi:10.1128/EC.00336-13
42. Hise AG, Tomalka J, Ganesan S, Patel K, Hall BA, Brown GD, et al. An essential role for the NLRP3 inflammasome in host defense against the human fungal pathogen *Candida albicans*. *Cell Host Microbe* (2009) 5:487–97. doi:10.1016/j.chom.2009.05.002
43. Bauernfeind F, Rieger A, Schildberg FA, Knolle A, Schmid-burgk JL, Hornung V, et al. NLRP3 inflammasome activity is negatively controlled by miR-223. *J Immunol* (2012) 189:4175–81. doi:10.4049/jimmunol.1201516
44. He Y, Franchi L, Núñez G. TLR agonists stimulate Nlrp3-dependent IL-1β production independently of the purinergic P2X7 receptor in dendritic cells and in vivo. *J Immunol* (2013) 190:334–9. doi:10.4049/jimmunol.1202737
45. Guarda G, Zenger M, Yazdi AS, Ferrero I, Menu P, Tardivel A, et al. Differential expression of NLRP3 among hematopoietic cells. *J Immunol* (2011) 186:2529–34. doi:10.4049/jimmunol.1002720
46. Hardison SE, Brown GD. C-type lectin receptors orchestrate anti-fungal immunity. *Nat Immunol* (2012) 13:817–22. doi:10.1038/ni.2369
47. Mao L, Zhang L, Li H, Chen W, Wang H, Wu S, et al. Pathogenic fungus *Microsporum canis* activates the NLRP3 inflammasome. *Infect Immun* (2014) 82:882–92. doi:10.1128/IAI.01097-13
48. Kistowska M, Fenini G, Jankovic D, Feldmeyer L, Kerl K, Bosshard P, et al. Malassezia yeasts activate the NLRP3 inflammasome in antigen-presenting cells via Syk-kinase signalling. *Exp Dermatol* (2014) 23:884–9. doi:10.1111/exd.12552
49. Saijo S, Ikeda S, Yamabe K, Kakuta S, Ishigame H, Akitsu A, et al. Dectin-2 recognition of α-mannans and induction of Th17 cell differentiation is essential for host defense against *Candida albicans*. *Immunity* (2010) 32:681–91. doi:10.1016/j.immuni.2010.05.001
50. Yoshikawa FSY, Yabe R, Iwakura Y, De Almeida SR, Saijo S. Dectin-1 and dectin-2 promote control of the fungal pathogen *Trichophyton rubrum* independently of IL-17 and adaptive immunity in experimental deep dermatophytosis. *Innate Immun* (2016) 22:316–24. doi:10.1177/1753425916645392
51. Dong B, Li D, Li R, Chen SC, Liu W, Liu W, et al. A chitin-like component on sclerotic cells of *Fonsecaea pedrosoi* inhibits dectin-1-mediated murine Th17 development by masking β-glucans. *PLoS One* (2014) 9:e114113. doi:10.1371/journal.pone.0114113
52. Wang H, Li M, Lerksuthirat T, Klein B. The C-type lectin receptor MCL mediates vaccine-induced immunity against infection with *Blastomyces dermatitidis*. *Infect Immun* (2016) 84:635–42. doi:10.1128/IAI.01263-15
53. Gantner BN, Simmons RM, Canavera SJ, Akira S, Underhill DM. Collaborative induction of inflammatory responses by dectin-1 and toll-like receptor 2. *J Exp Med* (2003) 197:1107–17. doi:10.1084/jem.20021787
54. Van De Veerdonk FL, Joosten LAB, Netea MG. The interplay between inflammasome activation and antifungal host defense. *Immunol Rev* (2015) 265:172–80. doi:10.1111/imr.12280
55. Tomalka J, Ganesan S, Azodi E, Patel K, Majmudar P, Hall BA, et al. A novel role for the NLRC4 inflammasome in mucosal defenses against the fungal pathogen *Candida albicans*. *PLoS Pathog* (2011) 7:e1002379. doi:10.1371/journal.ppat.1002379
56. Kalantari P, Deoliveira RB, Chan J, Corbett Y, Rathinam V, Stutz A, et al. Dual engagement of the NLRP3 and AIM2 inflammasomes by plasmodium-derived hemozoin and DNA during malaria. *Cell Rep* (2013) 6:196–210. doi:10.1016/j.celrep.2013.12.014
57. Li H, Wu S, Mao L, Lei G, Zhang L, Lu A, et al. Human pathogenic fungus *Trichophyton schoenleinii* activates the NLRP3 inflammasome. *Protein Cell* (2013) 4:529–38. doi:10.1007/s13238-013-2127-9
58. Muñoz-Planillo R, Kuffa P, Martínez-Cólon G, Smith BL, Rajendiran TM, Kuffa P, et al. K+ efflux is the common trigger of NLRP3 inflammasome activation by bacterial toxins and particulate matter. *Immunity* (2013) 38:1142–53. doi:10.1016/j.immuni.2013.05.016
59. Bauernfeind F, Bartok E, Rieger A, Franchi L, Núñez G, Hornung V. Cutting edge: reactive oxygen species inhibitors block priming, but not activation, of the NLRP3 inflammasome. *J Immunol* (2011) 187:613–7. doi:10.4049/jimmunol.1100613
60. Ketelut-Carneiro N, Silva GK, Rocha FA, Milanezi CM, Cavalcanti-Neto FF, Zamboni DS, et al. IL-18 triggered by the Nlrp3 inflammasome induces host innate resistance in a pulmonary model of fungal infection. *J Immunol* (2015) 194:4507–17. doi:10.4049/jimmunol.1402321
61. Walter P, Garin Y, Richard-Lenoble D. Chromoblastomycosis. A morphological investigation of the host-parasite interaction. *Virchows Arch A Pathol Anat Histol* (1982) 397:203–14. doi:10.1007/BF00442390
62. Rozental S, Alviano CS, de Souza W. The in vitro susceptibility of *Fonsecaea pedrosoi* to activated macrophages. *Mycopathologia* (1994) 126:85–91. doi:10.1007/BF01146200
63. Rozental S, Alviano CS, de Souza W. Fine structure and cytochemical study of the interaction between *Fonsecaea pedrosoi* and rat polymorphonuclear leukocyte. *J Med Vet Mycol* (1996) 34:323–30. doi:10.1080/02681219680000551
64. Farbiarz SR, de Carvalho TU, Alviano C, De Souza W. Fine structure and cytochemistry of the interaction between *Fonsecaea pedrosoi* and mouse resident macrophages. *J Med Vet Mycol* (1990) 28:373–83. doi:10.1080/02681219080000481
65. Hayakawa M, Ghosn EEB, da Gloria Teixeria de Sousa M, Ferreira KS, Almeida SR. Phagocytosis, production of nitric oxide and pro-inflammatory cytokines by macrophages in the presence of dematiaceous [correction of dematiaceus] fungi that cause chromoblastomycosis. *Scand J Immunol* (2006) 64:382–7. doi:10.1111/j.1365-3083.2006.01804.x
66. Bocca AL, Brito PPMS, Figueiredo F, Tosta CE. Inhibition of nitric oxide production by macrophages in chromoblastomycosis: a role for *Fonsecaea pedrosoi* melanin. *Mycopathologia* (2006) 161:195–203. doi:10.1007/s11046-005-0228-6
67. Ahrens J, Graybill JR, Abishawl A, Tio FO, Rinaldi MG. Experimental murine chromomycosis mimicking chronic progressive human disease. *Am J Trop Med Hyg* (1989) 40:651–8. doi:10.4269/ajtmh.1989.40.651
68. Netea MG, Joosten LAB. Inflammasome inhibition: putting out the fire. *Cell Metab* (2015) 21:513–4. doi:10.1016/j.cmet.2015.03.012
69. Vonk AG, Netea MG, Van Krieken JH, Iwakura Y, Van Der Meer JWM, Kullberg BJ. Endogenous interleukin (IL)-1α and IL-1β are crucial for host defense against disseminated candidiasis. *J Infect Dis* (2006) 193:1419–26. doi:10.1086/503363

70. Mencacci A, Cenci E, Bacci A, Montagnoli C, Bistoni F, Romani L. Cytokines in candidiasis and aspergillosis. *Curr Pharm Biotechnol* (2010) 1:235–51. doi:10.2174/1389201003378924

Conflict of Interest Statement: The authors declare that the research was conducted in the absence of any commercial or financial relationships that could be construed as a potential conflict of interest.

Copyright © 2017 Castro, Siqueira, Jerônimo, Basso, Veloso Junior, Magalhães, Leonhardt, Oliveira, Bürgel, Tavares and Bocca. This is an open-access article distributed under the terms of the Creative Commons Attribution License (CC BY). The use, distribution or reproduction in other forums is permitted, provided the original author(s) or licensor are credited and that the original publication in this journal is cited, in accordance with accepted academic practice. No use, distribution or reproduction is permitted which does not comply with these terms.

frontiers in Immunology

ORIGINAL RESEARCH
published: 10 July 2017
doi: 10.3389/fimmu.2017.00786

NOD-Like Receptor P3 Inflammasome Controls Protective Th1/Th17 Immunity against Pulmonary Paracoccidioidomycosis

*Claudia Feriotti[1], Eliseu Frank de Araújo[1], Flavio Vieira Loures[1], Tania Alves da Costa[1], Nayane Alves de Lima Galdino[1], Dario Simões Zamboni[2] and Vera Lucia Garcia Calich[1]**

[1]Department of Immunology, University of São Paulo, São Paulo, Brazil, [2]Department of Cell Biology, School of Medicine of Ribeirão Preto, University of São Paulo, São Paulo, Brazil

The NOD-like receptor P3 (NLRP3) inflammasome is an intracellular multimeric complex that triggers the activation of inflammatory caspases and the maturation of IL-1β and IL-18, important cytokines for the innate immune response against pathogens. The functional NLRP3 inflammasome complex consists of NLRP3, the adaptor protein apoptosis-associated speck-like protein, and caspase-1. Various molecular mechanisms were associated with NLRP3 activation including the presence of extracellular ATP, recognized by the cell surface P2X7 receptor (P2X7R). Several pattern recognition receptors on innate immune cells recognize *Paracoccidioides brasiliensis* components resulting in diverse responses that influence adaptive immunity and disease outcome. However, the role of NLRP3 inflammasome was scantily investigated in pulmonary paracoccidioidomycosis (PCM), leading us to use an intratracheal (i.t.) model of infection to study the influence of this receptor in anti-fungal immunity and severity of infection. For *in vivo* studies, *C57BL/6* mice deficient for several NLRP3 inflammasome components (*Nlrp3*$^{-/-}$, *Casp1/11*$^{-/-}$, *Asc*$^{-/-}$) as well as deficient for ATP receptor (*P2x7r*$^{-/-}$) were infected *via* i.t. with *P. brasiliensis* and several parameters of immunity and disease severity analyzed at the acute and chronic periods of infection. Pulmonary PCM was more severe in *Nlrp3*$^{-/-}$, *Casp1/11*$^{-/-}$, *Asc*$^{-/-}$, and *P2x7r*$^{-/-}$ mice as demonstrated by the increased fungal burdens, mortality rates and tissue pathology developed. The more severe disease developed by NLRP3, ASC, and Caspase-1/11 deficient mice was associated with decreased production of IL-1β and IL-18 and reduced inflammatory reactions mediated by PMN leukocytes and activated CD4$^+$ and CD8$^+$ T cells. The decreased T cell immunity was concomitant with increased expansion of CD4$^+$CD25$^+$Foxp3 regulatory T (Treg) cells. Characterization of intracellular cytokines showed a persistent reduction of CD4$^+$ and CD8$^+$ T cells expressing IFN-γ and IL-17 whereas those producing IL-4 and TGF-β appeared in increased frequencies. Histopathological studies showed that all deficient mouse strains developed more severe lesions containing elevated numbers of budding yeast cells resulting in increased mortality rates. Altogether, these findings led us to conclude that the activation of the NLRP3 inflammasome has a crucial role in the immunoprotection against pulmonary PCM by promoting the expansion of Th1/Th17 immunity and reducing the suppressive control mediated by Treg cells.

Keywords: pulmonary paracoccidioidomycosis, NOD-like receptor P3 inflammasome, Th1/Th17 immunity, regulatory T cells, immunoregulation

OPEN ACCESS

Edited by:
Steven Templeton, Indiana University School of Medicine – Terre Haute, United States

Reviewed by:
Paolo Puccetti, University of Perugia, Italy
Robson Coutinho-Silva, Federal University of Rio de Janeiro, Brazil

****Correspondence:***
Vera Lucia Garcia Calich
vlcalich@icb.usp.br

Specialty section:
This article was submitted to Microbial Immunology, a section of the journal Frontiers in Immunology

Received: *15 March 2017*
Accepted: *21 June 2017*
Published: *10 July 2017*

Citation:
Feriotti C, de Araújo EF, Loures FV, da Costa TA, Galdino NAdL, Zamboni DS and Calich VLG (2017) NOD-Like Receptor P3 Inflammasome Controls Protective Th1/Th17 Immunity against Pulmonary Paracoccidioidomycosis. Front. Immunol. 8:786. doi: 10.3389/fimmu.2017.00786

INTRODUCTION

Paracoccidioides brasiliensis is the etiological agent of paracoccidioidomycosis (PCM), the most prevalent systemic mycosis in Latin America (1). The pattern recognition receptors (PRRs) expressed on phagocytic cells recognize pathogen-associated molecular patterns (PAMPs) on *P. brasiliensis* surface and regulate the innate and adaptive phases of immunity. The different signaling pathways used by these PRRs to activate immune cells result in different patterns of cell activation, production of diverse pools of cytokines and chemokines triggering diverse immune mechanisms. In human PCM and experimental models, the prevalent expansion of Th1/Th17 cells with reduced expansion of Treg cells characterize the benign disease, whereas elevated proliferation of Th2/Th9 and Treg cells is associated with severe PCM (2–11).

The toll-like receptors (TLRs) play a crucial role in the recognition of fungal pathogens such as *P. brasiliensis*, *Candida albicans*, *Aspergillus fumigatus*, *Cryptococcus neoformans*, and others (8, 12–16). TLR2 and TLR4 sense *P. brasiliensis* mediated by MyD88-dependent signaling that leads to cytokines production by alveolar and peritoneal macrophages (6, 7, 17, 18). These components were also seen to control the adaptive immunity and severity of disease developed by *P. brasiliensis* infected mice (6, 7, 18). In addition, C-type lectin receptors (CLRs) like mannose receptor (MR) and dectin-1 as well as the complement receptors 3 play an important role in *P. brasiliensis* recognition and activation of immune cells (8, 19–22). Altogether, these studies have demonstrated that in pulmonary PCM, as in other infectious pathologies, PRRs are key elements that govern protective immunity, which must be tightly controlled by anti-inflammatory mechanisms as those mediated by Treg cells and their products (5–7).

The NOD-like receptor P3 (NLRP3) belongs to the NOD family of cytosolic PRRs that detect intracellular PAMPs well as danger signals, named danger associated molecular patterns (DAMPs). Under cell activation, components of NLR family can aggregate into large cytoplasmic complexes called inflammasomes (23). The members of this family have a LRR (leucine-rich repeat) domain in the C-terminal structure, a nucleotide-binding and oligomerization domain containing a neuronal apoptosis inhibitory protein, and a N-terminal caspase recruitment domain (CARD) or pyrin (PYD) domain. In the canonical pathway of NLRP3 inflammasome activation, NLRP3 oligomerization is initiated through the apoptosis-associated speck-like protein (ASC) containing C-terminal CARD that is recruited to the complex *via* NLRP3-PYD-ASC-PYD interaction. ASC associates with procaspase-1 *via* CARD interaction, leading to caspase-1 activation that promotes the processing of pro-IL-1β and pro-IL-18 into their mature forms (24–26). The NLRP3 inflammasome is activated by a large repertoire of PAMPs and DAMPs, including ATP, uric acid crystals, silica, aluminum hydroxide, asbestos, reactive oxygen species (ROS), and bacterial or viral RNA (27, 28). Besides the canonical pathway, a non-canonical pathway that utilizes caspase-11 has been shown to activate NLRP3 inflammasome (29, 30). The non-canonical NLRP3 inflammasome can be directly activated by LPS derived from Gram-negative bacteria and by some fungi, which are delivered into the cytosol and activate caspase-11. This, in turn, triggers the opening of the pannexin-1 channel that induces the K + efflux required for NLRP3 inflammasome activation and release of mature IL-1β (30, 31). The first signal for pro-IL-1β processing is through pro-IL-1β and NLRP3 expression mediated by NF-kB transcription that is potentially activated by TLRs and CLRs, and the second signal is the proteolytic processing of pro-caspase-1 by activated NLRP3 (25). NLRP3 is the NLR mostly involved in the immunity against fungal infections (32–34). In *C. albicans* infection, the canonical and non-canonical pathways of NLRP3 inflammasome activation were shown to be essential for mediating IL-1β secretion (29, 35). *In vivo* studies of disseminated *C. albicans* infection showed that NLRP3, Syk, ASC, and caspase-1 are fundamental to control disease severity and regulate the adaptive antifungal immune response through the induction of Th1 and Th17 development (36, 37). In an invasive pulmonary model of aspergillosis, NLRP3 and AIM2 were required to engage the inflammasome to trigger innate immune responses against *A. fumigatus*; mice lacking both AIM2 and NLRP3, but not mice lacking a single inflammasome receptor, were hyper susceptible to invasive aspergillosis (38). The pioneer study of Tavares et al. demonstrated that following *P. brasiliensis* infection, the production of mature IL-1β by bone marrow-derived dendritic cells depends on NLRP3 and caspase-1 activation (39), although the fungal molecules associated with this process are still unknown. However, K + efflux, ROS generation, lysosomal acidification, and cathepsin B release to the cytosol were seen to be required to the NLRP3 inflammasome activation by *P. brasiliensis* (39). Furthermore, a recent work of our lab showed that a dectin-1-Syk mediated mechanism controls NLRP3 inflammasome activation by *P. brasiliensis* infected macrophages of resistant A/J mice (21). In another study using a murine model of systemic PCM induced by intravenous infection, the susceptibility of NLRP3 and caspase-1 knockout mice to *P. brasiliensis* infection was evaluated and their increased susceptibility was associated with reduced IL-18 production and Th1 immunity (40).

Because the human disease is thought to be acquired by the pulmonary route, and diverse routes of infection induce different patterns of immunity and disease severity (41), in the present study, we sought to investigate the role of NLRP3 inflammasome in the pulmonary infection caused by *P. brasiliensis.* Therefore, several C57BL/6 mouse strains deficient for NLRP3 inflammasome components (*Nlrp3*$^{-/-}$, *Casp1/11*$^{-/-}$, *Asc*$^{-/-}$ mice) as well as deficient for the ATP receptor (*P2x7r*$^{-/-}$ mice) were intratracheally infected with 1×10^6 *P. brasiliensis* yeasts and compared with their wild type (WT) controls. Several parameters of pulmonary infection and immune response were evaluated at the acute and chronic phases of the disease. Our results indicated that NLRP3 inflammasome plays a crucial role in the control of the innate and adaptive immunity against *P. brasiliensis* infection. This control was associated with IL-1β and IL-18 secretion induced by caspase-1 activity starting at an early phase of infection. The activation of NLRP3 inflammasome was seen to be essential to control fungal growth and activate protective T cell immunity. This protective inflammatory response was composed of increased

numbers of PMN leukocytes and activated $CD4^+$ and $CD8^+$ T lymphocytes that migrate to the site of infection. Furthermore, NLRP3 inhibited the expansion and migration of regulatory T (Treg) cells resulting in a well-balanced and protective Th1/Th17 immunity.

MATERIALS AND METHODS

Mice

Wild type (*WT*), *Nlrp3*$^{-/-}$, *Casp1/11*$^{-/-}$, *P2x7r*$^{-/-}$, and *Asc*$^{-/-}$ *C57BL/6* mouse strains were obtained from our Isogenic Unit (Immunology Department of Institute of Biomedical Sciences of University of São Paulo, Brazil). *Casp1/11*$^{-/-}$ mice (42) were provided by Dr. Flavell, R. (Howard Hughes Medical Institute, Yale University School of Medicine), *Asc*$^{-/-}$ mice (43) were provided by Dr. Zamboni, D. S. (University of São Paulo, Ribeirão Preto, São Paulo, Brazil), *Nlrp3*$^{-/-}$ mice (44) and *P2x7r*$^{-/-}$ (45) mice were obtained from Jackson Laboratories and used at 8–11 weeks of age. Specific pathogen free mice were fed with sterilized laboratory chow and water *ad libitum*. Animal experiments were performed in strict accordance with the Brazilian Federal Law 11,794 establishing procedures for the scientific use of animals, and the State Law establishing the Animal Protection Code of the State of São Paulo. All efforts were made to minimize suffering, and all animal procedures were approved by the Ethics Committee on Animal Experiments of the Institute of Biomedical Sciences of University of São Paulo (Proc.76/04/CEUA).

Fungus

Paracoccidioides brasiliensis (Pb 18 strain), isolated from a young patient in 1929, was maintained by weekly subcultivation in semisolid Fava Netto's medium at 35°C (46). Yeast cells were collected, washed, and adjusted to 20×10^6 cells/mL. Viability was determined with Janus Green B vital dye (Merck Frankfurter Straße, Darmstadt, GER) and was always higher than 85%. The presence of LPS in all used solutions was determined by the Limulus amebocyte lysate chromogenic assay (Sigma-Aldrich, St. Louis, MO, USA) and always showed LPS levels <0.015 EU/mL.

Intratracheal Fungal Infection

Mice were anesthetized and submitted to intratracheal (i.t.) *P. brasiliensis* infection as previously described (47). Briefly, after intraperitoneal injection of ketamine (90 mg/kg) and xylazine (10 mg/kg), animals were infected with 1×10^6 Pb18 yeast cells, contained in 50 µL of PBS, by surgical i.t. inoculation, which allowed dispensing of the fungal cells directly into the lungs. The skin was then sutured, and mice were placed under a heat lamp until they recovered from anesthesia.

Colony Forming Units (CFUs) Assays

To assess the viable number of CFU in target organs, lungs, and livers from *C57BL/6*, *Nlrp3*$^{-/-}$, *Casp1/11*$^{-/-}$, *P2x7r*$^{-/-}$ and *Asc*$^{-/-}$ mice were aseptically removed, weighted, and homogenized in 5 ml PBS using tissue grinders as previously described (48). In brief, 100 µL aliquots of 50- and 100-fold dilutions from organ homogenates were plated onto petri dishes containing brain heart infusion agar (Difco) supplemented with 5% *P. brasiliensis* 192 culture filtrate and 4% (v/v) horse serum (Instituto Butantan, São Paulo, Brazil) and incubated at 36°C. The fungal counting started at day 5 after plating, which is the period when the fungus starts to grow. Thereafter, the counting was performed daily and number of CFUs per gram of tissue determined.

Mortality Rates

Mortality studies were done with groups of 8 *C57BL/6*, *Nlrp3*$^{-/-}$, *Casp1/11*$^{-/-}$, *P2xR7*$^{-/-}$, and *Asc*$^{-/-}$ mice inoculated i.t. with 1×10^6 yeast cells. Deaths were registered daily and experiments were repeated twice.

Histopathological Analysis

Histopathological analysis of lungs and livers was performed as previously described (49). Briefly, lungs and livers from *C57BL/6*, *Nlrp3*$^{-/-}$, *Casp1/11*$^{-/-}$, *P2x7r*$^{-/-}$, and *Asc*$^{-/-}$ mice were fixed in formalin (10%) and embedded in paraffin. Tissues sections were stained with hematoxylin–eosin (H&E) for analysis of the lesions and Grocott for fungal evaluation. Morphometrical analysis was performed using Nikon DXM 1200c digital camera and Nikon NIS Elements AR 2.30 software. Results were expressed as the mean ± SD for the total area of lesions.

Cytokines Detection

The levels of IL-1β, IL-18, TNF-α, and IL-6 were measured in lung homogenates by ELISA with antibodies pairs purchased from eBioscience according to the manufacturer's protocol. The absorbance values were determined using a spectrophotometric plate reader (VersaMax, Molecular Devices).

Flow Cytometry Analysis

Cells obtained from lung homogenates at 48 h, 2, 4, and 10 weeks after i.t. infection were isolated as previously described (50). In brief, the lungs were excised, minced, and digested with collagenase (1 mg/ml, Sigma) and DNase (30 µg/mL, Sigma) in RPMI buffer (5% fetal calf serum, Sigma). Leukocytes were isolated with Percoll (20%, Sigma). The numbers of leukocytes were adjusted to 1×10^6 cells/mL and suspended in staining buffer (PBS, 2% fetal calf serum and 0.1% NaN3). Fc receptors were blocked using unlabeled anti-CD16/32 antibodies (1 µg/ml; BD Biosciences), and cells were stained for 20 min at 4°C with the monoclonal antibodies diluted at optimal concentration: pacific blue (PB)-labeled anti-CD45, anti-CD25, anti-IL-1β, anti-F4/80 (5 µg/ml); phycoerythrin (PE)-labeled anti-CD4, anti-Ly6G, anti-Syk kinase (2 µg/ml); PECy7-labeled anti-CD8, anti-CD4, anti-IL-4 (2 µg/ml); allophycocyanin (APC)-labeled anti-CD44, anti-FoxP3, anti-CD8, anti-CD86, anti-IFN-γ (5 µg/ml); APC-Cy7-labeled, anti-CD45 (2 µg/ml); Brilliant Violet 510 (BV)-labeled anti-IL-17 (2 µg/ml); peridinin chlorophyll protein (PerCP)-labeled anti-TGF-β, anti-CD62L, anti-MHCII (2 µg/ml); fluorescein isothiocyanate-labeled anti-CD11b, anti-CD3 (5 µg/ml); (from BD Biosciences or BioLegend). Cells were washed twice with staining buffer, fixed with 1% paraformaldehyde (Sigma), and acquired using a FACSCanto II equipment and software FlowJo (Tree-Star).

Intracellular Cytokines Measurement

The intracellular detection of cytokines was performed as previously described (49). Briefly, cells were labeled for surface molecules with monoclonal antibodies: anti-CD45, anti-CD8 (PB), anti-CD4 (PE), and anti-CD25 (PB) (BD Biosciences). For intracellular staining, cells were treated with Cytofix/Cytoperm kit (BD Biosciences), according to manufacturer's protocol and labeled with anti-IL-1β (PECY7), anti-IFN-γ (APC), anti-IL-17 (BV), anti-IL-4 (PECy7), anti-TGF-β (PerCP) monoclonal antibodies. For Treg characterization, plots were gated on $CD4^+CD25^+$ cells. Cells were fixed with 1% paraformaldehyde (Sigma) and acquired at 50,000 events using a FACSCanto II equipment and FACSDiva software (BD Biosciences) using software FlowJo (Tree-Star).

RNA Isolation and cDNA Synthesis

Lungs were homogenized in TRIzol reagent using tissue grinders. RNA isolation and purification was performed as described (49) using Ultraclean Tissue & Cells RNA Isolation Kit (MO BIO Laboratories) according to the manufacturer's protocol. RNA concentration was assessed on a NanoDrop ND-1000 spectrophotometer. c-DNA synthesis was performed using the High Capacity RNA-to-cDNA kit (Applied Biosystems) following the manufacturer's instructions.

Real-time Quantitative Polymerase Chain Reaction

The cDNA was amplified using TaqMan Universal PCR Master Mix (Applied Biosystems) according to manufacturer's protocol. The primers used were: IL-1β Mm01336189_m1; IL-18 Mm00434225_m1; ASC (Pycard) Mm00445747_ g1; Syk (Sykb) Mm01333032_m1; Casp-1 Mm00438023_m1; Nlrp3 Mm00840904_m1 (Applied Biosystems). Data were normalized to GAPDH gene expression. TaqMan PCR assays were performed on a MxP3000P QPCR System, and data were developed using the MxPro QPCR software (Stratagene). The average threshold cycle (CT) values of samples were normalized to CT value of GAPDH gene. The relative expression was determined by the $2^{-\Delta\Delta}$CT method.

Statistics

Values represent means ± SD. Comparison among multiple groups was done with ANOVA non-pared test, and multiple comparisons according Bonferroni Differences between survivals were compared by log-rank test. All statistical analyses were performed using the software GraphPad Prism (GraphPad Software, Inc.).

RESULTS

NLRP3 Inflammasome Controls the Pulmonary and Hepatic Fungal Loads of Mice i.t. Infected with *P. brasiliensis* Yeasts

To evaluate the function of NLRP3 inflammasome in pulmonary PCM, we first investigated the control of fungal burdens by WT and NLRP3 inflammasome deficient (*Nlrp3*$^{-/-}$, *Casp1/11*$^{-/-}$, and *Asc*$^{-/-}$) mice i.t. infected with (1×10^6) yeasts cells. Mice deficient for the ATP receptor (*P2x7r*$^{-/-}$) were also studied. Lung and liver of mice were excised, macerated, and the homogenates were diluted at 1:100 and plated in Petri dishes. The fungal counting started at day 5 after plating, which is the period when the fungus starts to grow. Thereafter, the counting was performed daily. The degree of infection was analyzed from the acute to the late phases (48 h, 2, 4, and 10 weeks) of infection. In the acute phase (48 h p.i.), no differences in the pulmonary and hepatic fungal loads between WT and NLRP3 deficient mice were seen. In contrast, increased fungal recovery at weeks 2, 4, and 10 of infection were observed in the lungs of *Nlrp3*$^{-/-}$, *Casp1/11*$^{-/-}$, *P2x7r*$^{-/-}$, and *Asc*$^{-/-}$ mice, that was more prominent at 10 weeks of infection (**Figure 1A**). At weeks 4 and 10 after infection increased, fungal burdens were seen in the liver of all deficient mice (**Figure 1B**). These data demonstrate that NLRP3 played an important role in the control of pulmonary fungal load and its dissemination to the liver.

P. brasiliensis Infection Induces the Expression of mRNA from NLRP3-Inflammasome Related Components That Is Abolished in *Nlrp3*$^{-/-}$, *Casp1/11*$^{-/-}$, and *Asc*$^{-/-}$ Mice

The activation of NLRP3 inflammasome requires two steps, the first mediated by PRRs and NFkB activation. Pathogen components, which are TLRs agonists as well as inflammatory cytokines such as TNF-α and IL-1β can trigger NFκB activation through diverse signaling pathways (51, 52). Therefore, caspase-1 can trigger NFkB activity *via* activity of pro-inflammatory cytokines produced by ASC-dependent inflammasome activation. Additionally, recent studies have shown that caspase-1 and ASC can direct NFkB activation, and this process is independent on the enzymatic activity of caspase-1 (52, 53). Indeed, caspase-1 can trigger TLR2- and TLR4-mediated NFκB activation *via* MyD88 adaptor like (MAL) for signal transduction (54). This led us to hypothesize that the absence of NLRP3 components might reduce the mRNA expression of cytokines and other NLRP3-related components. Therefore, the expression of IL-1β, IL-18, NLRP3, Caspase-1, ASC, and Syk mRNA was characterized in lung macerates of *WT*, *Nlrp3*$^{-/-}$, *Casp1/11*$^{-/-}$, and *Asc*$^{-/-}$ mice at week 4 after infection. Increased expression of IL-1β, IL-18, NLRP3, Caspase-1, ASC, and Syk mRNA was detected in the lungs of WT mice compared to knockouts mice and uninfected mice as a control (**Figures 2A,B**) demonstrating that *P. brasiliensis* infection induces an increased synthesis of components associated with NLRP3 inflammasome. In addition, the increased expression of Syk mRNA suggests the contribution of this enzyme in the activation process of NLRP3 as shown in our previous study (21).

Secretion of IL-1β and IL-18 but Not TNF-α and IL-6 Depends on NLRP3 Activation

The cytokines levels in lung homogenates of *WT*, *Nlrp3*$^{-/-}$, *Casp1/11*$^{-/-}$, *P2x7r*$^{-/-}$, and *Asc*$^{-/-}$ mice were analyzed at 48 h, 2, 4, and 10 weeks of *P. brasiliensis* infection. High levels of IL-1β

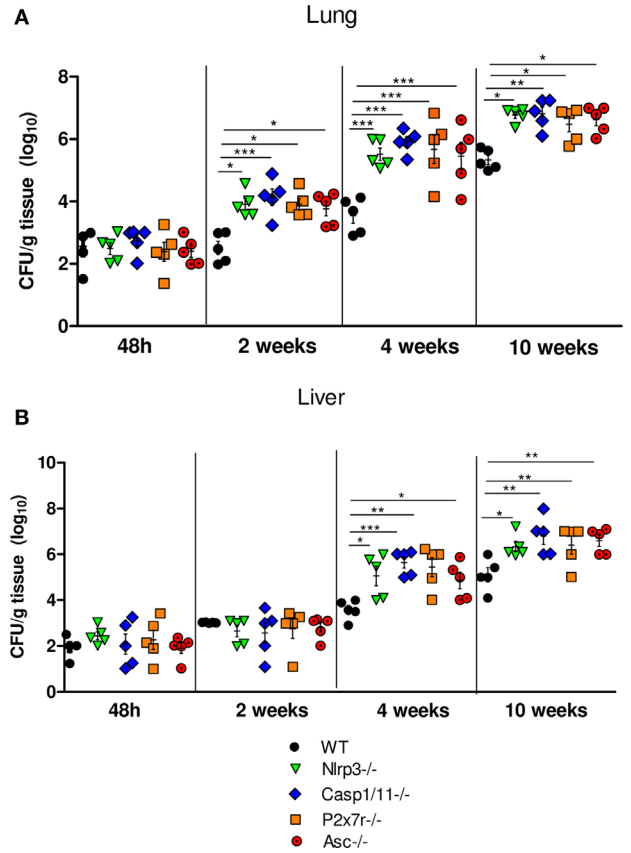

FIGURE 1 | NOD-like receptor P3 (NLRP3) inflammasome controls the pulmonary and hepatic fungal loads of mice i.t. infected with *P. brasiliensis* yeasts. Disease severity was assessed by a CFU assay using macerated lungs **(A)** and livers **(B)** of *WT* mice, *Nlrp3*$^{-/-}$, *Casp1/11*$^{-/-}$, *P2x7r*, and *Asc*$^{-/-}$ mice infected with 1 × 10^6 yeasts cells *via* i.t. at 48 h, 2, 4, and 10 weeks of infection. Data are expressed as the number of CFU/g tissue of an experiment using five mice. Equivalent results were obtained in a second experiment using the same number of infected animals (*$P < 0.05$, **$P < 0.01$, and ***$P < 0.001$).

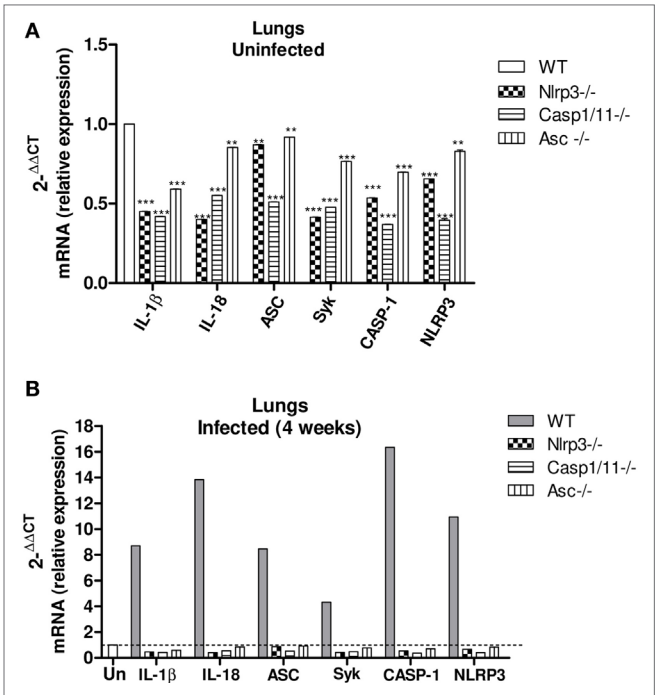

FIGURE 2 | *Paracoccidioides brasiliensis* infection induces an increased expression of mRNA from NLRP3 inflammasome-related components, which is abolished in *Nlrp3*$^{-/-}$, *Casp1/11*$^{-/-}$, and *Asc*$^{-/-}$ mice. Real-time quantitative polymerase chain reaction analysis of the IL-1β, IL-18, Asc, Casp-1, Nlrp3, and Syk genes expression in the lung macerates of *Nlrp3*$^{-/-}$, *Casp1/11*$^{-/-}$, *Asc*$^{-/-}$, and WT uninfected mice **(A)** and at week 4 of infection **(B)**.

and IL-18 secretion were observed in the lungs of *WT* mice at all postinfection periods studied, but a more robust production was observed at weeks 4 and 10 postinfection. Equivalent reduced levels of these cytokines were detected in the lung supernatants of *Nlrp3*$^{-/-}$, *Casp1/11*$^{-/-}$, *P2x7r*$^{-/-}$, and *Asc*$^{-/-}$ mice (**Figures 3A,B**). From 48 h up to 10 weeks of infection a modest increase of TNF-α and IL-6 secretion was observed in the lungs of all mouse strains studied, but no significant differences were observed at any period of infection (**Figures 3C,D**). These findings showed that in pulmonary PCM, TNF-α, and IL-6 production is independent on NLRP3 activation.

NLRP3 Induces Increased Influx of PMN Leukocytes, into the Lungs of *P. brasiliensis* Infected Mice

The pulmonary cellular infiltrates in *WT*, *Nlrp3*$^{-/-}$, *Casp1/11*$^{-/-}$, and *Asc*$^{-/-}$ mice were analyzed by flow cytometry at several periods of *P. brasiliensis* infection (**Figure 4A**). An increased influx of total leukocytes characterized as CD45$^+$ cells was detected in the lungs of *WT* mice compared with *Nlrp3*$^{-/-}$, *Casp1/11*$^{-/-}$, and *Asc*$^{-/-}$ mice, which was more expressive in the acute phase (48 h) of infection (**Figure 4B**). After 48 h and 2 weeks of infection, a high number of CD11b$^+$F4/80$^+$ macrophages were seen in the lungs of infected mice, that decreases at later periods, but no significant differences between *WT* and deficient mice were detected (**Figure 4C**). Interestingly, an increased influx of GR1$^+$Ly6G$^+$ PMN cells was seen in the lungs of *WT* mice in comparison with *Nlrp3*$^{-/-}$, *Casp1/11*$^{-/-}$, and *Asc*$^{-/-}$ mice at 48 h, 2 and 4 weeks of infection (**Figure 4D**). These data showed that NLRP3 actively regulates the cell infiltration that occurs in the lungs of *P. brasiliensis* infected mice.

NLRP3 Induces Increased Influx of Activated CD4$^+$ and CD8$^+$ T Cells into the Lungs of Infected Mice

The profile of CD4$^+$ cell activation was characterized by flow cytometry (**Figure 5A**). From week 2 onward, CD4$^+$ T lymphocytes appeared in increased numbers in the lungs of WT when compared with *Nlrp3*$^{-/-}$, *Casp1/11*$^{-/-}$, and *Asc*$^{-/-}$ mice (**Figure 5B**). The subpopulations of naïve (CD4$^+$CD44^{low}CD62L^{high}) and effector/memory (CD4$^+$CD44^{high}CD62L^{low}) T cells were also determined. Our data showed increased numbers of naïve CD4$^+$ T cells in the lungs of *Nlrp3*$^{-/-}$, *Casp1/11*$^{-/-}$, and *Asc*$^{-/-}$ compared with WT mice at weeks 2, 4, and 10 of infection (**Figure 5C**). In

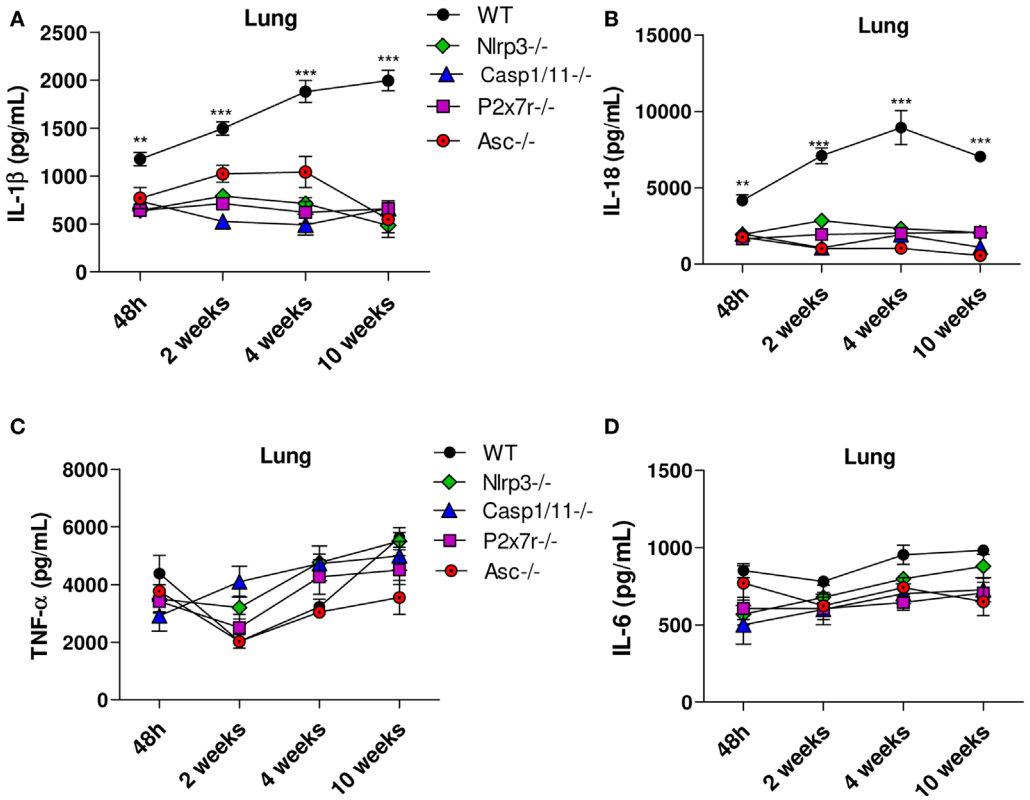

FIGURE 3 | Secretion of IL-1β and IL-18 but not TNF-α and IL-6 is controlled by NLRP3 inflammasome activation. The supernatants of macerated lungs from *WT*, *Nlrp3*$^{-/-}$, *Casp1*$^{-/-}$ *P2x7r*$^{-/-}$, and *Asc*$^{-/-}$ mice infected *via* i.t. with 1 × 10^6 *Paracoccidioides brasiliensis* yeasts were used to assess IL-1β, IL-18, TNF-α and IL-6 production by ELISA. Levels of IL-1β and IL-18 **(A,B)** and TNF-α and IL-6 **(C,D)** in the lungs of mice 48 h, 2, 4, and 10 weeks after infection with *P. brasiliensis* yeasts. Data represents one of two independent experiments using five mice per group ($n = 5$). Experiment was performed in triplicates represented as Mean ± SEM (**$P < 0.01$ and ***$P < 0.001$ compared with deficient mice).

contrast, WT mice presented increased numbers of pulmonary effector/memory CD4$^+$ T cells at the same postinfection periods (**Figure 5D**). When the presence of activated CD8$^+$ T cells was evaluated, an increased number of activated CD8$^+$CD69$^+$ T cells were detected in the lungs of WT mice at weeks 2, 4, and 10 of infection. In contrast, *Nlrp3*$^{-/-}$, *Casp1/11*$^{-/-}$, and *Asc*$^{-/-}$ mice had diminished numbers of activated CD8+ CD9+ T cells at 2 and 4 weeks that were totally abolished at 10 weeks of infection (**Figures 5E,F**).

NLRP3 Inhibits the Presence of Treg Cells into the Lungs of Infected Mice

Regulatory T cells were characterized by the CD4$^+$CD25$^+$FOXP3$^+$ phenotype as shown in the **Figure 6A**. An increased number of Treg cells was observed in the lungs of *Nlrp3*$^{-/-}$, *Casp1/11*$^{-/-}$, and *Asc*$^{-/-}$ at 4 and 10 weeks of infection, compared with WT mice, which also showed increased number of these cells, although lower than NLRP3 components deficient mice (**Figure 6B**). These data showed that NLRP3 played a role in the control of adaptive immunity to *P. brasiliensis* infection by increasing the number of activated T cells in WT mice, as shown in **Figure 5D**, and reducing the presence of Treg cells that migrate to the lung of WT mice.

NLRP3 Signaling Induces a Prevalent Expansion CD4$^+$ and CD8$^+$ T Cells Expressing IFN-γ and IL-17 with Concomitant Reduction of IL-4$^+$ and TGF-β T Cells

We have further studied the expression of intracellular pro-IL-1β, IFN-γ, IL-4, IL-17, and TGF-β cytokines by CD4$^+$ and CD8$^+$ T cells in the lungs of infected *WT*, *Nlrp3*$^{-/-}$, *Casp1/11*$^{-/-}$, and *ASC*$^{-/-}$ mice at 48 h, 2, 4, and 10 weeks of infection. Our data showed that in the acute phase of infection (48 h) there was an elevated frequency of CD4$^+$ and CD8$^+$ T cells expressing intracellular pro-IL-1β, IFN-γ, and IL-4 in the lungs of WT and deficient (*Nlrp3*$^{-/-}$, *Casp1/11*$^{-/-}$, and *ASC*$^{-/-}$) mice, but no significant differences were observed between the mouse strains. At this period, no significant expression of IL-17 and TGF-β was detected in CD4$^+$ and CD8$^+$ T cells (**Figures 7A,E**). From 2 to 10 weeks of infection, increased frequencies of IFN-γ$^+$ and IL-17$^+$ CD4$^+$ T cells were seen in the lungs of *WT* mice when compared with *Nlrp3*$^{-/-}$, *Casp1/11*$^{-/-}$, and *Asc*$^{-/-}$ mice. In contrast, there was an increased percentage of IL-4$^+$ and TGF-β$^+$ CD4$^+$ T cells in the lungs of *Nlrp3*$^{-/-}$, *Casp1/11*$^{-/-}$, and *Asc*$^{-/-}$ compared with WT mice (**Figures 7B–D**). Generally,

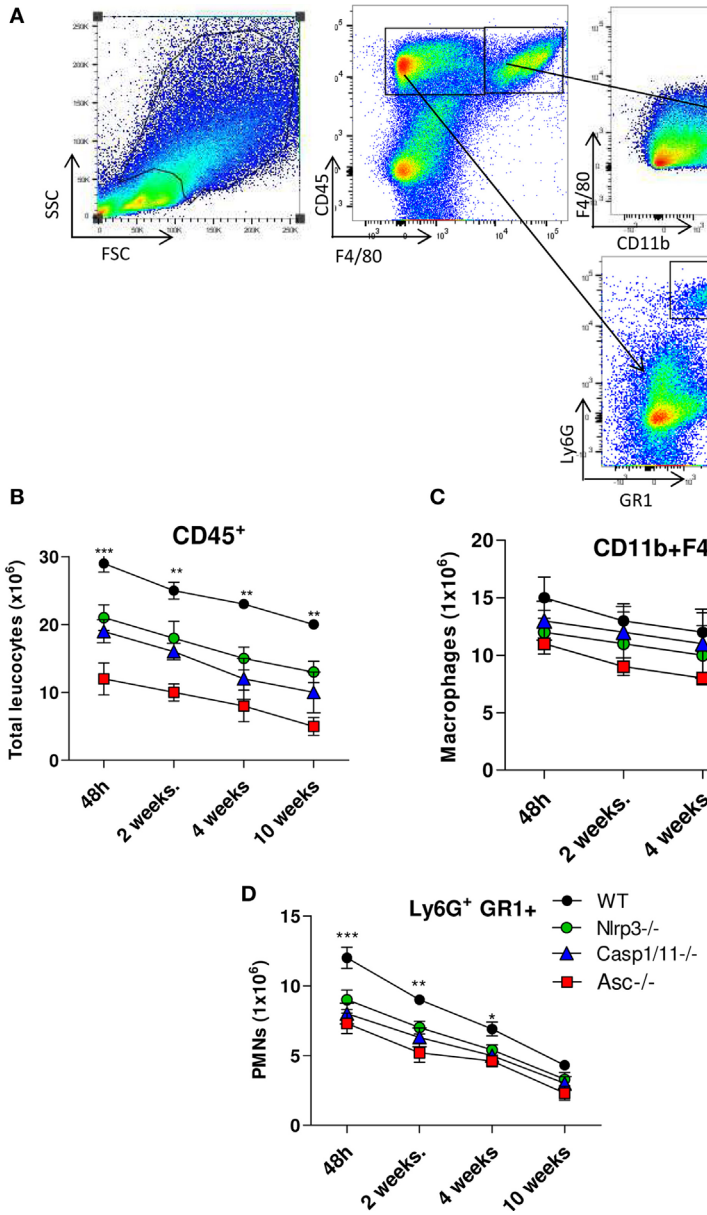

FIGURE 4 | Activation of NLRP3 inflammasome induces increased influx of PMN leukocytes into the lungs of *Paracoccidioides brasiliensis* infected mice. Inflammatory cell infiltrates in the lungs of *WT*, *Nlrp3*$^{-/-}$, *Casp1*$^{-/-}$, and *Asc*$^{-/-}$ mice infected with 1 × 10^6 *P. brasiliensis* yeasts were analyzed at different postinfection periods (48 h, 2, 4, and 10 weeks) by flow cytometry. **(A)** Gates strategy using WT cells, **(B)** total leukocytes, **(C)** macrophages, and **(D)** PMN leukocytes were phenotyped by anti-CD45, F4/80, CD11b, GR1, and anti-Ly6G fluorochromes-labeled antibodies. Data represents one of two independent experiments using five mice per group ($n = 5$). Experiment was performed in triplicates represented as Mean ± SEM (*$P < 0.05$, **$P < 0.01$, and ***$P < 0.001$, compared with deficient mice).

CD8$^+$ T cells appeared in decreased frequencies when compared with CD4$^+$ T cells, but a similar profile of cytokines expression was observed in both T cell subpopulations (**Figures 7E–H**). Interestingly, differences in IL-17 synthesis by CD8 T cell were only seen at week 10 postinfection. These data showed that NLRP3 played an important role in the polarization of type-1 and type-17 T cell responses in WT mice resulting in a better control of *P. brasiliensis* infection. In contrast, *Nlrp3*$^{-/-}$, *Casp1/11*$^{-/-}$, and *Asc*$^{-/-}$ mice showed a prevalent Th2/Th3/Treg profile of response that was unable to control the fungal infection.

P. brasiliensis Infected *Nlrp3*$^{-/-}$, *Casp1/11*$^{-/-}$, *P2x7r*$^{-/-}$, and *Asc*$^{-/-}$ Mice Show Increased Tissue Pathology and Decreased Survival Rates

To better clarify the importance of NLRP3 in the severity of *P. brasiliensis* infection, the histopathological analysis of the

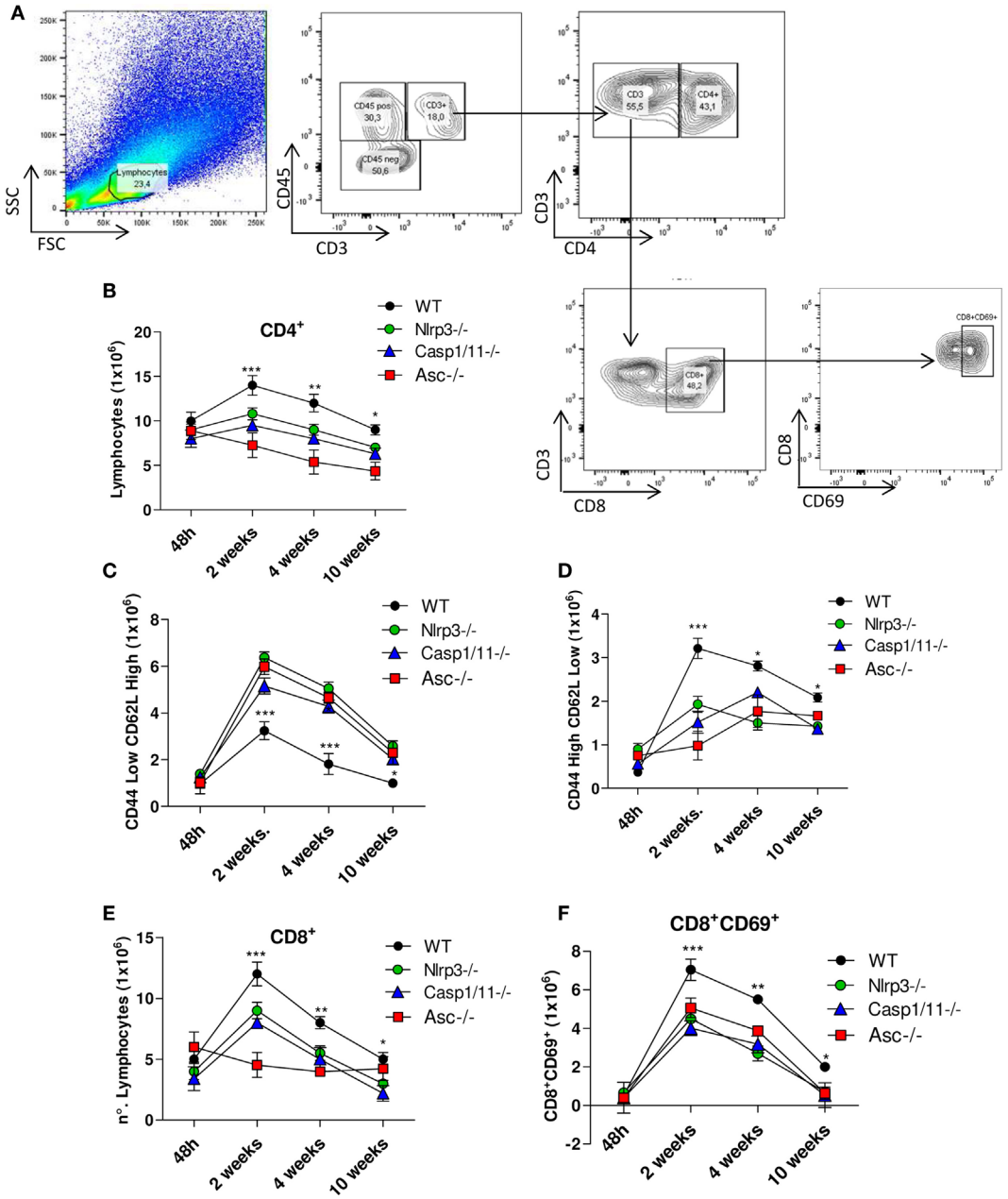

FIGURE 5 | NOD-like receptor P3 (NLRP3) inflammasome induces the migration of activated CD4+ and CD8+ T cells into the lungs of *Paracoccidioides brasiliensis* infected mice. Inflammatory cell infiltrates in the lungs of *WT*, *Nlrp3*$^{-/-}$, *Casp1*$^{-/-}$, and *Asc*$^{-/-}$ mice infected with 1 × 10^6 *P. brasiliensis* yeasts were analyzed at different postinfection periods (48 h, 2, 4, and 10 weeks) by flow cytometry. **(A)** Gates strategy using lung leukocytes from WT mice. **(B)** CD4$^+$ T cells were characterized using anti-CD4 labeled antibodies. **(C)** Naïve (CD44^{low}CD62L^{high}) and **(D)** memory/effector (CD44^{high}CD62L^{low}) CD4$^+$ T lymphocytes were characterized using adequate gates and fluorochromes-labeled anti-CD4, CD44, and CD62L antibodies. **(E)** CD8$^+$ and **(F)** CD8$^+$CD69$^+$-activated T cells were characterized using anti-CD8 and CD69 fluorochromes-labeled antibodies. Data represents one of two independent experiments using five mice per group (n = 5). Experiment was performed in triplicates represented as Mean ± SEM (*P < 0.05, **P < 0.01, and ***P < 0.001, compared with deficient mice).

lung tissues of *WT* and *Nlrp3*$^{-/-}$, *Casp1/11*$^{-/-}$, *P2x7*$^{-/-}$, and *Asc*$^{-/-}$ mice was performed at weeks 4 and 10 of i.t. infection. The histological sections were stained with hematoxylin–eosin (H&E) for cellular identification and with Groccot stain for fungal identification and localization in the tissue (**Figure 8**). The degree of infection was evaluated based in the size and morphology of lung lesions as well as fungal presence and intensity of inflammatory infiltrates. At 4 weeks of infection, less extensive and severe pulmonary lesions were observed in the lungs of *WT* in comparison with *Nlrp3*$^{-/-}$, *Casp1/11*$^{-/-}$, *P2x7r*$^{-/-}$, and *Asc*$^{-/-}$ mice. The lungs of WT mice showed an inflammatory process that spread over the entire area of the

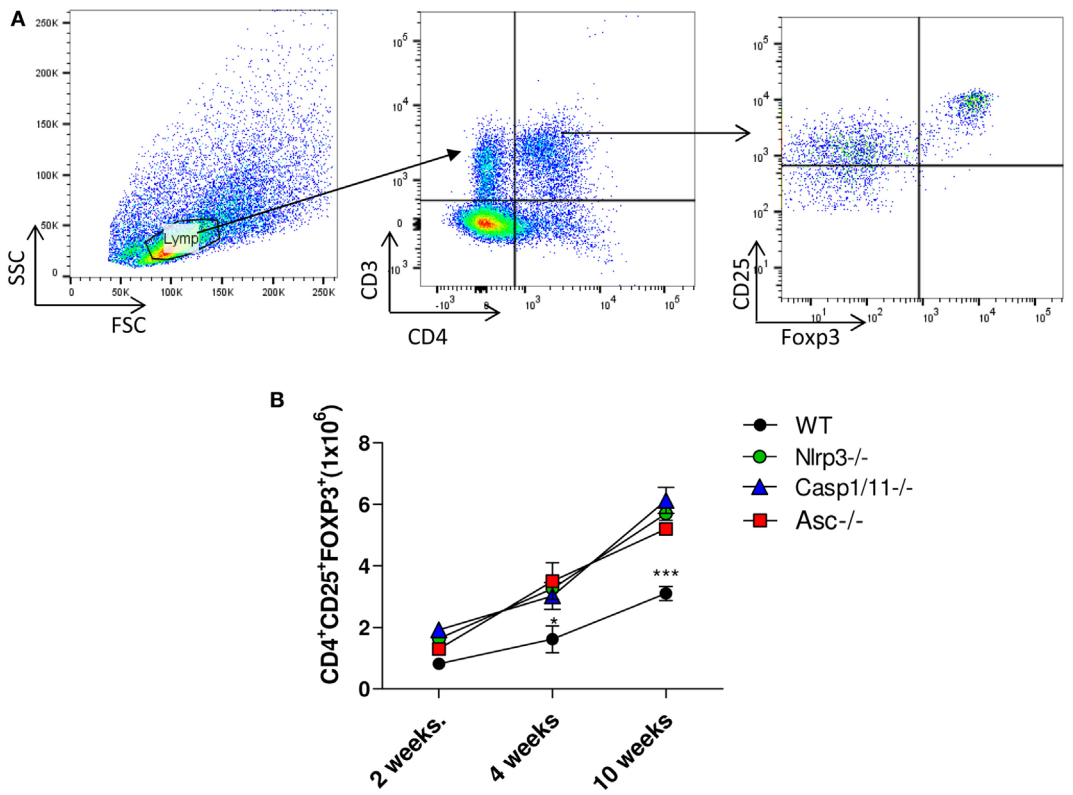

FIGURE 6 | NOD-like receptor P3 (NLRP3) inflammasome inhibits the presence of regulatory T (Treg) cells in the lungs of infected mice. The number of Treg cells ($CD4^+CD25^+FOXP3^+$) was determined in the lungs of *WT*, *Nlrp3*$^{-/-}$, *Casp1/11*$^{-/-}$, and *Asc*$^{-/-}$ mice infected with 1×10^6 *Paracoccidioides brasiliensis* yeasts at different postinfection periods (48 h, 2, 4, and 10 weeks) by flow cytometry. **(A)** Gates strategy using lung leukocytes from WT mice. **(B)** Treg cells ($CD4^+CD25^+FOXP3^+$) were characterized using adequate gates and fluorochromes-labeled anti CD4, CD25, and FOXP3 antibodies. Data represents one of two independent experiments using five mice per group ($n = 5$). Experiment was performed in triplicates represented as Mean ± SEM (*$P < 0.05$, **$P < 0.01$, and ***$P < 0.001$, compared with deficient mice).

organ. Large fungal loads were restricted to the center of lesions. The granulomas were large and coalescent, but there were some preserved organ areas. In *Nlrp3*$^{-/-}$, *Casp1/11*$^{-/-}$, *P2x7r*$^{-/-}$, and *Asc*$^{-/-}$ mice the extension and cellularity of the lesions as well as the presence of fungi were larger than in *WT* mice (**Figure 8A**). By 10 weeks of infection (**Figure 8B**), a similar pattern of lesions was detected, but at higher intensity. In comparison with week 4, a higher content of fungi within the granulomas and increased necrotic areas were seen at this postinfection period. In summary, the pathology developed by *Nlrp3*$^{-/-}$, *Casp1/11*$^{-/-}$, *P2x7r*$^{-/-}$, and *Asc*$^{-/-}$ mice was much more severe than that presented by *WT* mice corroborating the data of the increased fungal burden and impaired T cell immunity demonstrated by these mouse strains.

The extent of lesions areas in the lungs (**Figures 9A,B**) reveals that mice deficient for NLRP3, Caspase-1/11, P2X7R, and ASC showed significantly larger lesions occupying higher tissue area than those present in WT animals. Mortality studies were done with groups of eight mice i.t. infected with one million *P. brasiliensis* yeasts. Infected mice were monitored daily for a period of 250 days to determine the survival time. As can be seen, *Nlrp3*$^{-/-}$, *Casp1/11*$^{-/-}$, *P2x7r*$^{-/-}$, and *Asc*$^{-/-}$ mice had a significantly shorter survival time than WT mice (**Figure 9C**), further confirming the crucial importance of NLRP3 in the immunoprotection of pulmonary PCM.

DISCUSSION

The role of NLRP3 inflammasome and the cooperation of TLRs and CLRs in the modulation of immune response against *P. brasiliensis* infection in macrophages and dendritic cells have been studied in our lab (8, 15, 18, 22). Using our murine model of resistance and susceptibility to PCM, it was verified that the activation of NLRP3 inflammasome by *P. brasiliensis* infection of macrophages from resistant A/J mice is dependent on dectin-1-Syk signaling (21). Other studies showed the role of TLR2, TLR4, dectin-1, and MyD88 signaling in the secretion of pro-inflammatory cytokines (IL-1β, TNF-α, and IL-6) and control of protective Th1/Th17 immune responses (5, 18, 20). Mice and patients infected with *P. brasiliensis* secrete IL-1β and IL-18, suggesting that NLRP3 is an important player in the recognition of this fungal pathogen (55, 56). The role of NLRP3 using *in vivo* models of PCM were less explored; however, a recent study using

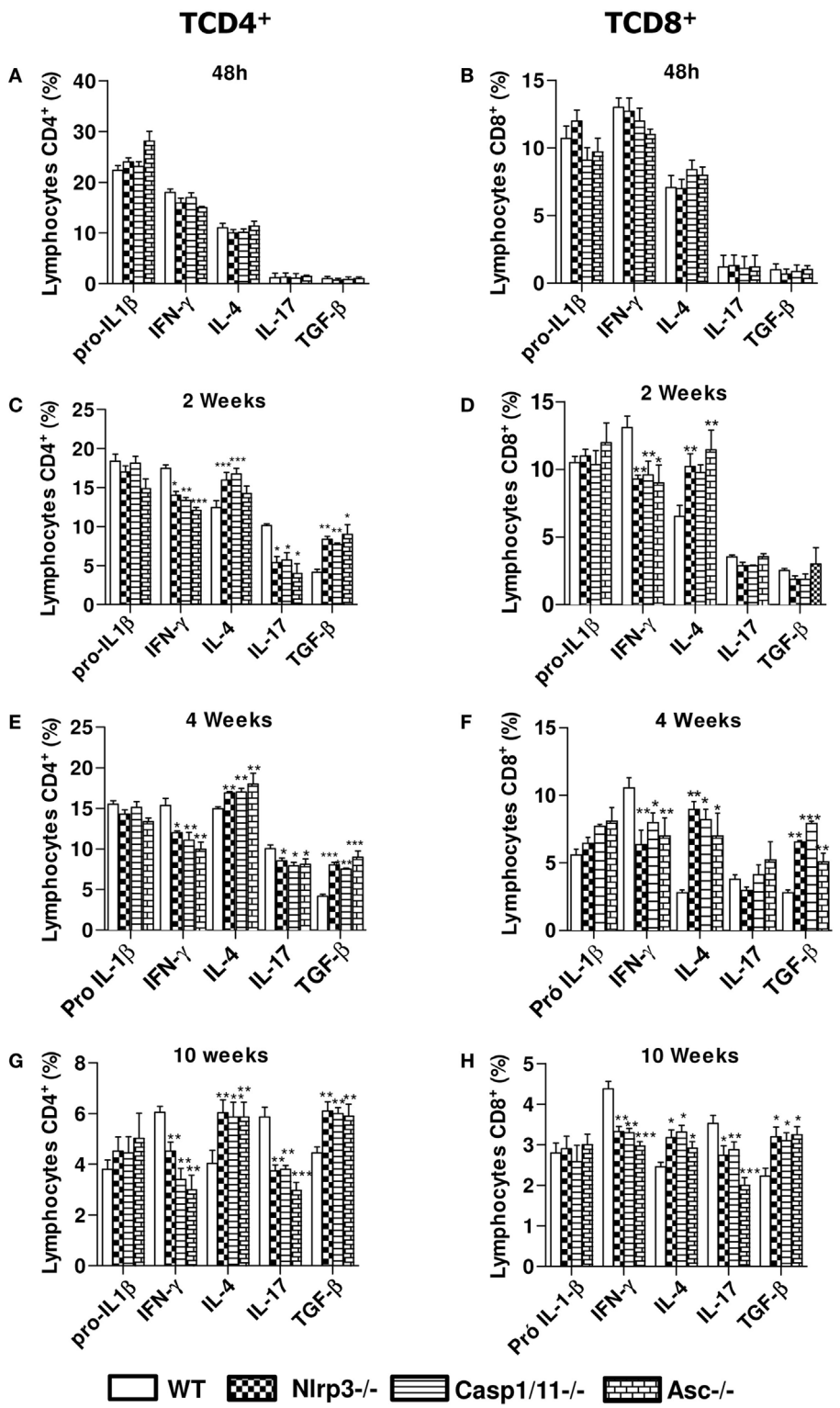

FIGURE 7 | NOD-like receptor P3 (NLRP3) inflammasome induces a Th1/Th17 profile of immune response. Intracellular cytokine analysis from inflammatory infiltrates of lungs of *WT*, *Nlrp3*$^{-/-}$, *Casp1/11*$^{-/-}$, and *Asc*$^{-/-}$ mice infected with 1 × 10^6 *Paracoccidioides brasiliensis* yeasts was performed at 48 h **(A,E)**, 2 weeks **(B,F)**, 4 weeks **(C,G)**, and 10 weeks **(D,H)** by flow cytometry. CD4$^+$ and CD8$^+$ T cells were labeled with anti-CD4 and anti-CD8 antibodies, permeabilized and intracellular cytokines determined using fluorochromes-labeled anti- IL-1β, IFN-γ, IL-4, IL-17, and TGF-β antibodies. Data represents one of two independent experiments using five mice per group (n = 5). Experiment was performed in triplicates represented as Mean ± SEM (*P < 0.05, **P < 0.01, and ***P < 0.001, compared with WT mice).

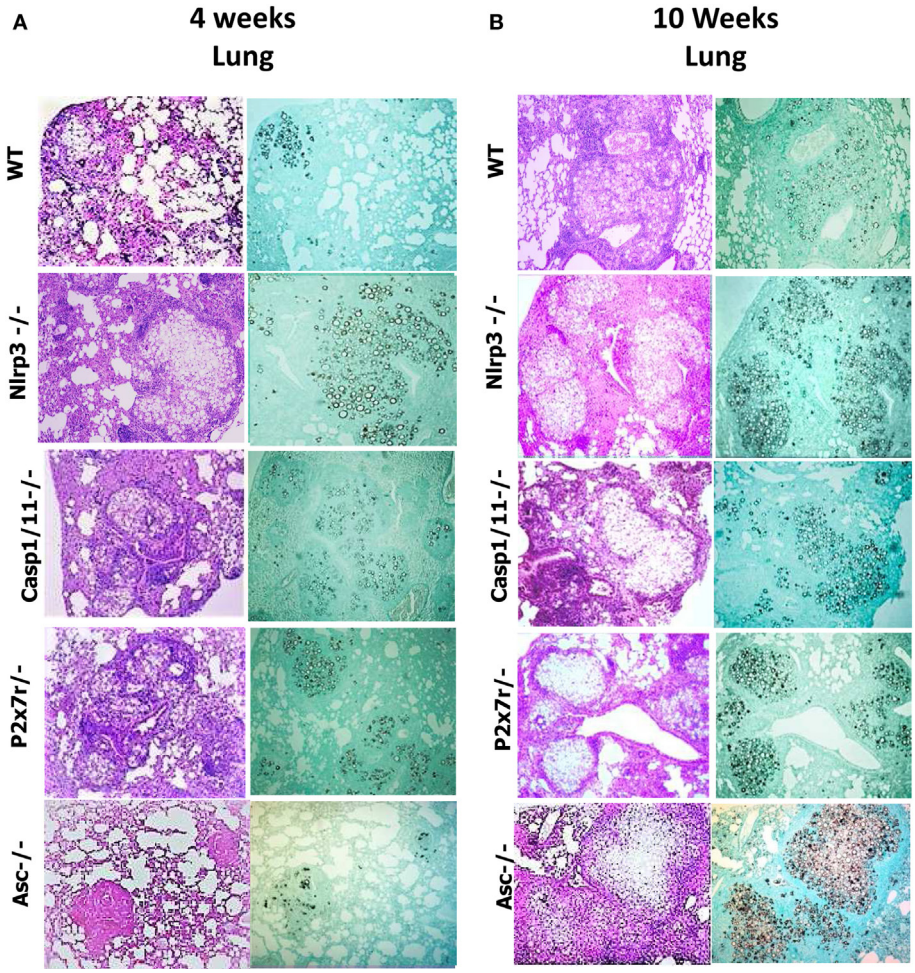

FIGURE 8 | NOD-like receptor P3 (NLRP3) inflammasome activation leads to less severe lung pathology. Photomicrographs of lungs of *WT*, *Nlrp3*$^{-/-}$, *Casp1/11*$^{-/-}$, *P2x7r*$^{-/-}$, and *Asc*$^{-/-}$ mice infected i.t. with 1 × 10^{6} *Paracoccidioides brasiliensis* yeasts after 4 and 10 weeks of infection. **(A,B)** Histological lung sections were stained with hematoxylin–eosin [H&E, left panels of **(A,B)**] or Groccot [right panels of **(A,B)**].

mice systemically infected with *P. brasiliensis* demonstrated that NLRP3 controls host resistance by inducing a prevalent Th1 immunity associated with IL-18 secretion (40). Because human PCM is acquired by the pulmonary route of infection, in the present study, we sought to characterize the role of NLRP3 inflammasome in i.t. infected mice whose response involves pulmonary-mediated immunological mechanisms. Several parameters of disease severity and host response were evaluated at several postinfection periods. Increased numbers of viable yeasts were recovered from lungs and livers of *Nlrp3*$^{-/-}$, *Casp1/11*$^{-/-}$, *P2x7r* $^{-/-}$, and *Asc*$^{-/-}$ mice. Our CFU data corroborate with those of Ketelut-Carneiro et al. that found increased fungal loads in the lungs and livers of *Asc*$^{-/-}$ and *Casp1/11*$^{-/-}$ mice infected by the i.v. route (40). Our study has also revealed for the first time the importance of the purinergic P2X7 receptor (P2X7R) in NLRP3 activation by *P. brasiliensis* infection, in agreement with recent studies that demonstrated the participation of this receptor in the activation of the NLRP3 inflammasome and immunity against intracellular infections caused by *Mycobacterium*, *Chlamydia*, *Leishmania*, and *Toxoplasma* (57–60). In our pulmonary model of PCM, a marked influence of P2X7R in the immune response and disease severity of mice was clearly shown by the deficient fungicidal activity, decreased cytokines production, high tissue damage and decreased survival rates developed by P2X7R deficient mice. As expected, NLRP3 activation exerted a profound influence in the levels of IL-1β and IL-18 present in the lung tissue and subsequent polarization of immune response. This finding indicates that the new equilibrium in the pool of pulmonary cytokines were responsible by the diverse immunity developed by NLRP3 deficient mice, once the levels of other cytokines such as TNF-α and IL-6 remained in the control levels. It is well known that IL-1β and IL-18 contribute to the induction of the adaptive immune response by stimulation of T cell proliferation, differentiation of Th1/Th17 immunity and increased activity of NKT cytotoxic cells (61). NLRP3 and pro-IL-1β mRNAs are highly expressed in the first signal of NLRP3 activation, as a result of the engagement of PRRs and PAMPs on phagocytes (25, 62). Our findings demonstrated that the genetic deficiency

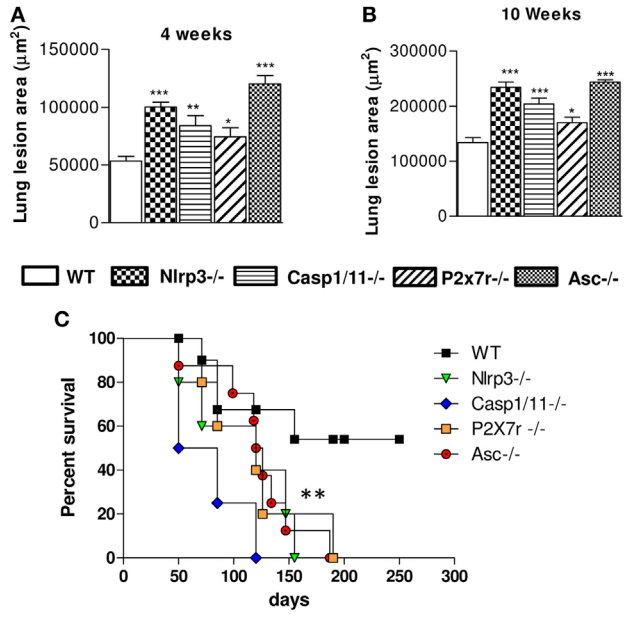

FIGURE 9 | NOD-like receptor P3 (NLRP3) inflammasome activation determines decreased pulmonary pathology and increased survival rates of *Paracoccidioides brasiliensis* infected mice. The total areas of lung lesions were calculated in the periods of 4 **(A)** and 10 weeks **(B)** after infection. Data are expressed as the mean ± SEM of triplicates from two independent experiments. **(C)** The mortality studies were conducted with groups of 8 *WT*, *Nlrp3*$^{-/-}$, *Casp1/11* $^{-/-}$, *Asc*$^{-/-}$, and *P2x7r*$^{-/-}$ mice i.t. infected with 1 × 10^6 *P. brasiliensis*. Mice were monitored daily for a period of 250 days to determine the survival time (*$P < 0.05$, **$P < 0.01$, and ***$P < 0.001$, compared with WT mice).

of NLRP3, Casp1/11, and Asc totally impaired the expression of IL-1β, IL-18, NLRP3, Casp1, and ASC mRNA in the lungs of infected mice at week 4 of infection. Besides the control of NLRP3 inflammasome components, *P. brasiliensis* infection induced an increased expression of Syk, confirming our previous studies demonstrating the crucial role of dectin-1-Syk signaling in the activation of this receptor (21). It is well known that the definition of the inflammatory infiltrates that accompanies an infectious process helps to define the type and intensity of the established immune response. Here, the expression of NLRP3 inflammasome-associated components was concomitant with increased infiltration of PMNs but not macrophages into the lungs of mice, indicating the selective influence of NLRP3 activation on this important effector cell in fungal infections. PMN-rich inflammatory reactions characterize the function of Th17 cells that, besides the typical production of IL-17 and IL-22, are committed with the secretion of chemokines involved in the migration and activation of PMN leukocytes (8, 63–66). In agreement, an enhanced differentiation of Th17 and Tc17 cells were seen during the infection of NLRP3 sufficient mice. The NLRP3 inflammasome activation has also induced an increased influx and activation of CD4$^+$ and CD8$^+$ T cells to the lungs of mice that were probably involved in the control of fungal loads, and subsequent control of lung pathology. Indeed, decreased numbers of CD4$^+$- and CD8$^+$-activated T cells were consistently seen in the lungs of *Nlrp3*$^{-/-}$, *Casp1/11*$^{-/-}$, and *Asc*$^{-/-}$ mice that developed increased fungal burdens associated with increased lung pathology and mortality rates. In pulmonary PCM, both T cell subsets participate in the protective mechanisms, with an intense and prominent contribution of CD8$^+$ T cells (67, 68). Although in less number, CD8$^+$ T cells were here shown to participate in the immunity associated with NLRP3 activation, a relevant observation added to the role of this receptor in the host defense mechanisms against *P. brasiliensis* infection.

The caspase-1-dependent cytokines exert important effects in the initiation of the adaptive Th1 and Th17 cellular responses to fungal infections (37). IL-1β has been suggested to promote inflammatory diseases by inducing the expansion of differentiated T cells (69) and has been implicated, alone or in combination with IL-6 and TGF-β, in driving murine and human Th17 priming and phenotype stabilization (66, 69). IL-18 was initially discovered as an IFN-γ-inducing factor, which together with IL-12 promotes the development of Th1 cells (70). Here, we assessed the intracellular cytokines production to define the effect of NLRP3 activation in the Th1, Th2, and Th17 defense mechanisms of *P. brasileinsis* infected mice. A new balance of Th cells subsets was seen in the absence of NLRP3 inflammasome components: an increased expression of IL-4 and TGF-β that accompanied a reduced number of IFN-γ$^+$ and IL-17$^+$ CD4$^+$ and CD8$^+$ T cells. In murine PCM, we previously demonstrated that IL-4 can exert protective or deleterious roles, depending on the mouse strain studied (71). It can dampen excessive inflammatory reactions of B10.A mice but suppresses the protective Th1 immunity of *C57BL/6* mice. A recent report showed that IL-4 suppresses NLRP3-dependent caspase-1activation and subsequent IL-1β secretion (72). These data show a mutual control between NLRP3 inflammasome and IL-4, as here observed. Our study also showed a clear association between NLRP3 activation and decreased synthesis of TGF-β and Treg cells development suggesting that the predominant pro-inflammatory milieu produced by this receptor significantly reduced the regulatory anti-inflammatory mechanisms. Interestingly, in a model of chronic kidney disease, the expression of NLRP3 was linked to the control of TGF-β-dependent signaling (73) although in our model enhanced TGF-β expressing cells were allied with absence of NLRP3 activation.

The analysis of intracellular cytokines revealed that NLRP3 played an important role in the induction of Th1 and Th17 responses with concomitant reduction of Th2/Treg expansion, a process of immune regulation associated with regressive disease in both humans and experimental models of PCM (2, 3, 5–8, 10). In addition, an important contribution of CD8$^+$ T cells to IL-17 and IFN-γ production was also seen. Although no studies have directly addressed the role of IL-17 in PCM, several indirect findings clearly demonstrated that a well-balanced production of pro- and anti-inflammatory cytokines is crucial to determine a protective immunity. The evaluation of cytokines production by patients with polar forms of PCM has shown that the prevalent synthesis of Th1/Th17 cytokines characterized the mild forms of chronic PCM, whereas an elevated production of IL-4 and IL-9, associated with high numbers of Treg cells, were linked with the severe forms of the disease (10). Our previous

studies have also demonstrated that a balanced differentiation of Th1/Th17/Treg cells is fundamental to achieve immunoprotection in pulmonary PCM. Indeed, the absence of TLR2 signaling induces excessive pathology associated with increased Th17 differentiation an impaired Treg development (6). In contrast, in TLR4 deficiency the excessive proliferation of Treg cells and reduced Th17 differentiation led to more severe disease (7). Importantly, the absence of dectin-1 signaling induced a critical reduction in all IL-17 secreting cells, particularly IL-17^{+}CD8^{+} T cells and a severe PCM (20). These findings, and those here reported clearly indicate that the equilibrium in the expansion of T cell subpopulations is fundamental to immunoprotection against PCM.

The findings here reported are in contrast with those of Ketelut-Carneiro et al. showing that an enhanced Th1 immunity controlled by increase production of IL-18 was responsible by the protective role of NLRP3 inflammasome in a murine model of PCM (40). These discrepancies, however, could be attributed to the route of infection used. Indeed, the study of Ketelut-Carneiro et al. used i.v. infected mice (40), whereas our studies were done with i.t. infected animals. In this aspect, our previous studies have clearly shown the influence of the route of infection in the severity of the disease and immune response of *P. brasiliensis* infected mice (41). We verified that the s.c. route induces a self-healing infection in several mouse strains allied with elevated delayed hypersensitivity reactions. Interestingly, the previous s.c. infection of B10.A mice led to immunoprotection or disease exacerbation depending on the route of fungal challenge. Immunoprotection was achieved after intraperitoneal challenge and was associated with persistent cell-mediated immunity and a mixed type-1/type-2 immunity. Exacerbated disease was found after intravenous challenge and was linked with anergy of cellular immunity and prevalent type-2 immune response (41). In contrast to the prevalent Th1/Th17 immunity induced by NLRP3 inflammasome activation in *WT* mice, *Nlrp3*$^{-/-}$, *Casp1/11*$^{-/-}$, and *Asc*$^{-/-}$ mice showed increase expansion and migration of Treg cells to the site of infection that possibly have contributed to the deficient control of fungal loads and non-protective inflammatory reactions. In agreement, the survival studies showed increased mortality rates among *Nlrp3*$^{-/-}$, *Casp1/11*$^{-/-}$, *Asc*$^{-/-}$, and *P2x7r*$^{-/-}$ mice accompanying increased fungal burdens and areas of lung lesions. In conclusion, the more efficient immunity mediated by Th1 and Th17 cells associated with NLRP3 inflammasome activation is highly protective to pulmonary PCM and this intracellular receptor appears to be significantly involved in the control of signaling pathways that led to the integration of innate and adaptive host immune responses to *P. brasiliensis* infection.

ETHICS STATEMENT

Animal experiments were performed in strict accordance with the Brazilian Federal Law 11,794 establishing procedures for the scientific use of animals and the State Law establishing the Animal Protection Code of the State of São Paulo. All efforts were made to minimize suffering, and all animal procedures were approved by the Ethics Committee on Animal Experiments of the Institute of Biomedical Sciences of University of São Paulo (Proc.76/04/CEUA).

AUTHOR CONTRIBUTIONS

Conceived and designed experiments: VC and CF. Contributed with reagent: DZ. Performed the experiments: CF, TC, EA, FL, and NG. Analyzed the data: CF, VC, FL, EA, and DZ. Wrote the paper: CF and VC.

ACKNOWLEDGMENTS

We thank Paulo Albe for processing the histological samples. This work was supported by Fundação de Amparo à Pesquisa do Estado de São Paulo (FAPESP, grants 2013/23536-3 and 2013/02396-9) and Conselho Nacional de Pesquisas (CNPq, grants 471317/2012-8 and 306812/2014-2).

REFERENCES

1. Brummer E, Castaneda E, Restrepo A. Paracoccidioidomycosis: an update. *Clin Microbiol Rev* (1993) 6:89–117. doi:10.1128/CMR.6.2.89
2. Franco MF. Host parasite relationship in paracoccidioidomycosis. *J Med Vet Mycol* (1987) 25:5–18. doi:10.1080/02681218780000021
3. Benard G. An overview of the immunopathology of human paracoccidioidomycosis. *Mycopathologia* (2008) 165:209–21. doi:10.1007/s11046-007-9065-0
4. Felonato M, Pina A, Bernardino S, Loures FV, de Araujo EF, Calich VL. CD28 exerts protective and detrimental effects in a pulmonary model of paracoccidioidomycosis. *Infect Immun* (2010) 78:4922–35. doi:10.1128/IAI.00297-10
5. Felonato M, Pina A, de Araujo EF, Loures FV, Bazan SB, Feriotti C, et al. Anti-CD25 treatment depletes Treg cells and decreases disease severity in susceptible and resistant mice infected with *Paracoccidioides brasiliensis*. *PLoS One* (2012) 7:e51071. doi:10.1371/journal.pone.0051071
6. Loures FV, Pina A, Felonato M, Calich VL. TLR2 is a negative regulator of Th17 cells and tissue pathology in a pulmonary model of fungal infection. *J Immunol* (2009) 183:1279–90. doi:10.4049/jimmunol.0801599
7. Loures FV, Pina A, Felonato M, Araújo EF, Leite KRM, Calich VLG. TLR4 signaling leads to a more severe fungal infection associated with enhanced proinflammatory immunity and impaired expansion of regulatory T cells. *Infect Immun* (2010) 78:1078–88. doi:10.1128/IAI.01198-09
8. Loures FV, Araújo EF, Feriotti C, Bazan SB, Calich VLG. TLR-4 cooperates with dectin-1 and mannose receptor to expand Th17 and Tc17 cells induced by *Paracoccidioides brasiliensis* stimulated dendritic cells. *Front Microbiol* (2015) 6:261. doi:10.3389/fmicb.2015.00261
9. Bernardino S, Pina A, Felonato M, Costa TA, Frank de Araújo E, Feriotti C, et al. TNF-α and CD8+ T cells mediate the beneficial effects of nitric oxide synthase-2 deficiency in pulmonary paracoccidioidomycosis. *PLoS Negl Trop Dis* (2013) 7(8):e2325. doi:10.1371/journal.pntd.0002325
10. de Castro LF, Ferreira MC, da Silva RM, Blotta MH, Longhi LN, Mamoni RL. Characterization of the immune response in human paracoccidioidomycosis. *J Infect* (2013) 67:470–85. doi:10.1016/j.jinf.2013.07.019
11. Ferreira MC, de Oliveira RT, da Silva RM, Blotta MH, Mamoni RL. Involvement of regulatory T cells in the immunosuppression characteristic of patients with paracoccidioidomycosis. *Infect Immun* (2010) 78:4392–401. doi:10.1128/IAI.00487-10
12. Shoham S, Huang C, Chen JM, Golenbock DT, Levitz SM. Toll-like receptor 4 mediates intracellular signaling without TNF-alpha release in response to *Cryptococcus neoformans* polysaccharide capsule. *J Immunol* (2001) 166:4620–6. doi:10.4049/jimmunol.166.7.4620

13. Netea MG, Van Der Graaf CA, Vonk AG, Verschueren I, Van Der Meer JW, Kullberg BJ. The role of toll-like receptor (TLR) 2 and TLR4 in the host defense against disseminated candidiasis. *J Infect Dis* (2002) 185:1483–9. doi:10.1086/340511
14. Netea MG, Ferwerda G, van der Graaf CA, van der Meer JW, Kullberg BJ. Recognition of fungal pathogens by toll-like receptors. *Curr Pharm Des* (2006) 12:4195–201. doi:10.2174/138161206778743538
15. Calich VLG, Costa TA, Felonato M, Arruda C, Bernardino S, Loures FV, et al. Innate immunity to *Paracoccidioides brasiliensis* infection. *Mycopathologia* (2008) 165:223–36. doi:10.1007/s11046-007-9048-1
16. Chai LY, Vonk AG, Kullberg BJ, Verweij PE, Verschueren I, van der Meer JW, et al. *Aspergillus fumigatus* cell wall components differentially modulate host TLR2 and TLR4 responses. *Microbes Infect* (2011) 13:151–9. doi:10.1016/j.micinf.2010.10.005
17. Bonfim CV, Mamoni RL, Blotta MH. TLR-2, TLR-4 and dectin-1 expression in human monocytes and neutrophils stimulated by *Paracoccidioides brasiliensis*. *Med Mycol* (2009) 47:722–33. doi:10.3109/13693780802641425
18. Loures FV, Pina A, Felonato M, Feriotti C, de Araújo EF, Calich VL. MyD88 signaling is required for efficient innate and adaptative immune responses to *Paracoccidioides brasiliensis* infection. *Infect Immun* (2011) 79:2470–80. doi:10.1128/IAI.00375-10
19. Feriotti C, Loures FV, De Araujo EF, Costa TA, Calich VLG. Mannosyl-recognizing receptors induce an M1-like phenotype in macrophages of susceptible mice but an M2-like phenotype in mice resistant to a fungal infection. *PLoS One* (2013) 8:e54845. doi:10.1371/journal.pone.0054845
20. Loures FV, Araújo EF, Feriotti C, Bazan SB, Costa TA, Brown GD, et al. Dectin-1 induces M1 macrophages and prominent expansion of CD8+IL-17+ cells in pulmonary Paracoccidioidomycosis. *J Infect Dis* (2014) 210:762–73. doi:10.1093/infdis/jiu136
21. Feriotti C, Bazan SB, Loures FV, Araújo EF, Costa TA, Calich VLG. Expression of dectin-1 and enhanced activation of NALP3 inflammasome are associated with resistance to paracoccidioidomycosis. *Front Microbiol* (2015) 6:913. doi:10.3389/fmicb.2015.00913
22. Pina A, Bernardino S, Calich VLG. Alveolar macrophages from susceptible mice are more competent than those of resistant mice to control initial *Paracoccidioides brasiliensis* infection. *J Leukoc Biol* (2008) 83:1088–93. doi:10.1189/jlb.1107738
23. Matzinger P. The danger model: a renewed sense of self. *Science* (2002) 296(5566):301–5. doi:10.1126/science.1071059
24. Kumar H, Kawai T, Akira S. Pathogen recognition by the innate immune system. *Int Rev Immunol* (2011) 30:16–34. doi:10.3109/08830185.2010.529976
25. Schroder K, Tschopp J. The inflammasomes. *Cell* (2010) 140:821–32. doi:10.1016/j.cell.2010.01.040
26. Vanaja SK, Rathinam VA, Fitzgerald KA. Mechanisms of inflammasome activation: recent advances and novel insights. *Trends Cell Biol* (2015) 25:308–15. doi:10.1016/j.tcb.2014.12.009
27. Pétrilli V, Dostert C, Muruve DA, Tschopp J. The inflammasome: a danger sensing complex triggering innate immunity. *Curr Opin Immunol* (2007) 19:615–22. doi:10.1016/j.coi.2007.09.002
28. Fritz JH, Ferrero RL, Philpott DJ, Girardin SE. Nod-like proteins in immunity, inflammation and disease. *Nat Immunol* (2006) 7:1250–7. doi:10.1038/ni1412
29. Gabrielli E, Pericolini E, Luciano E, Sabbatini S, Roselletti E, Perito S, et al. Induction of caspase-11 by aspartyl proteinases of *Candida albicans* and implication in promoting inflammatory response. *Infect Immun* (2015) 83:1940–8. doi:10.1128/IAI.02895-14
30. He Y, Hara H, Núñez G. Mechanism and regulation of NLRP3 inflammasome activation. *Trends Biochem Sci* (2016) 41:1012–21. doi:10.1016/j.tibs.2016.09.002
31. Man SM, Kanneganti TD. Regulation of inflammasome activation. *Immunol Rev* (2015) 265:6–21. doi:10.1111/imr.12296
32. Said-Sadier N, Padilla E, Langsley G, Ojcius DM. *Aspergillus fumigatus* stimulates the NLRP3 inflammasome through a pathway requiring ROS production and the Syk tyrosine kinase. *PLoS One* (2010) 5:e10008. doi:10.1371/journal.pone.0010008
33. Wellington M, Koselny K, Sutterwala FS, Krysan DJ. *Candida albicans* triggers NLRP3-mediated pyroptosis in macrophages. *Eukaryot Cell* (2014) 13:329–40. doi:10.1128/EC.00336-13
34. Plato A, Hardison SE, Brown GD. Pattern recognition receptors in antifungal immunity. *Semin Immunopathol* (2015) 37:97–106. doi:10.1007/s00281-014-0462-4
35. Joly S, Sutterwala FS. Fungal pathogen recognition by the NLRP3 inflammasome. *Virulence* (2010) 1:276–80. doi:10.4161/viru.1.4.11482
36. Gross O, Poeck H, Bscheider M, Dostert C, Hannesschläger N, Endres SJ, et al. Syk kinase signalling couples to the Nlrp3 inflammasome for anti-fungal host defence. *Nature* (2009) 459:433–6. doi:10.1038/nature07965
37. Van De Veerdonk FL, Joosten LA, Shaw PJ, Smeekens SP, Malireddi RK, Van Der Meer JW, et al. The inflammasome drives protective Th1 and Th17 cellular responses in disseminated candidiasis. *Eur J Immunol* (2011) 41:2260–8. doi:10.1002/eji.201041226
38. Karki R, Man SM, Malireddi RK, Gurung P, Vogel P, Lamkanfi M, et al. Concerted activation of the AIM2 and NLRP3 inflammasomes orchestrates host protection against *Aspergillus* infection. *Cell Host Microbe* (2015) 17:357–68. doi:10.1016/j.chom.2015.01.006
39. Tavares AH, Magalhães KG, Almeida RD, Correa R, Burgel PH, Bocca AL. NLRP3 inflammasome activation by *Paracoccidioides brasiliensis*. *PLoS Negl Trop Dis* (2013) 7:e2595. doi:10.1371/journal.pntd.0002595
40. Ketelut-Carneiro N, Silva GK, Rocha FA, Milanezi CM, Cavalcanti-Neto FF, Zamboni DS, et al. IL-18 triggered by the Nlrp3 inflammasome induces host innate resistance in a pulmonary model of fungal infection. *J Immunol* (2015) 194:4507–17. doi:10.4049/jimmunol.1402321
41. Arruda C, Kashino SS, Fazioli RA, Calich VL. A primary subcutaneous infection with *Paracoccidioides brasiliensis* leads to immunoprotection or exacerbated disease depending on the route of challenge. *Microbes Infect* (2007) 9:308–16. doi:10.1016/j.micinf.2006.12.005
42. Kuida K, Lippke JA, Ku G, Harding MW, Livingston DJ, Su MS, et al. Altered cytokine export and apoptosis in mice deficient in interleukin-1 beta converting enzyme. *Science* (1995) 267:2000–3. doi:10.1126/science.7535475
43. Lara-Tejero M, Sutterwala FS, Ogura Y, Grant EP, Bertin J, Coyle AJ, et al. Role of the caspase-1 inflammasome in *Salmonella typhimurium* pathogenesis. *J Exp Med* (2006) 203:1407–12. doi:10.1084/jem.20060206
44. Sutterwala FS, Ogura Y, Szczepanik M, Lara-Tejero M, Lichtenberger GS, Grant EP, et al. Critical role for NALP3/CIAS1/cryopyrin in innate and adaptive immunity through its regulation of caspase-1. *Immunity* (2006) 24:317–27. doi:10.1016/j.immuni.2006.02.004
45. Solle M, Labasi J, Perregaux DG, Stam E, Petrushova N, Koller BH, et al. Altered cytokine production in mice lacking P2X(7) receptors. *J Biol Chem* (2001) 276:125–32. doi:10.1074/jbc.M006781200
46. Netto CF, Vegas VS, Sciannaméa IM, Guarnieri DB. The polysaccharidic antigen from *Paracoccidioides brasiliensis*. Study of the time of cultivation necessary for the preparation of the antigen. *Rev Inst Med Trop Sao Paulo* (1969) 11:177–81.
47. Cano LE, Singer-Vermes LM, Vaz CA, Russo M, Calich VLG. Pulmonary paracoccidioidomycosis in resistant and susceptible mice, relationship among progression of infection, bronchoalveolar cell activation, cellular immune response, and specific isotype patterns. *Infect Immun* (1995) 63:1777–83.
48. Singer-Vermes LM, Ciavaglia MC, Kashino S, Burger E, Calich VLG. The source of the growth-promoting factor(s) affects the plating efficiency of *Paracoccidioides brasiliensis*. *J Med Vet Mycol* (1992) 30:261–4. doi:10.1080/02681219280000331
49. Bazan SB, Costa TA, de Araújo EF, Feriotti C, Loures FV, Pretel FD, et al. Loss- and gain-of-function approaches indicate a dual role exerted by regulatory T cells in pulmonary paracoccidioidomycosis. *PLoS Negl Trop Dis* (2015) 9:e0004189. doi:10.1371/journal.pntd.0004189
50. Ribeiro LR, Loures FV, de Araújo EF, Feriotti C, Costa TA, Serezani CH, et al. Lipoxin inhibits fungal uptake by macrophages and reduces the severity of acute pulmonary infection caused by *Paracoccidioides brasiliensis*. *Mediators Inflamm* (2015) 2015:852574. doi:10.1155/2015/852574
51. Sollberger G, Strittmatter GE, Garstkiewicz M, Sand J, Beer HD. Caspase-1: the inflammasome and beyond. *Innate Immun* (2014) 20:115–25. doi:10.1177/1753425913484374
52. Lamkanfi M, Kalai M, Saelens X, Declercq W, Vandenabeele P. Caspase-1 activates nuclear factor of the kappa-enhancer in B cells independently of

its enzymatic activity. *J Biol Chem* (2004) 279:24785–93. doi:10.1074/jbc.M400985200
53. Sarkar A, Duncan M, Hart J, Hertlein E, Guttridge DC, Wewers MD. Asc directs NF-kappaB activation by regulating receptor interacting protein-2 (Rip2) caspase-1 interactions. *J Immunol* (2006) 176:4979–86. doi:10.4049/jimmunol.176.8.4979
54. Miggin SM, Pålsson-McDermott E, Dunne A, Jefferies C, Pinteaux E, Banahan K, et al. NF- kappaB activation by the toll-IL-1 receptor domain protein MyD88 adapter-like is regulated by caspase-1. *Proc Natl Acad Sci U S A* (2007) 104:3372–7. doi:10.1073/pnas.0608100104
55. Kurokawa CS, Araujo JP Jr, Soares AM, Sugizaki MF, Peraçoli MT. Pro- and anti-inflammatory cytokines produced by human monocytes challenged in vitro with *Paracoccidioides brasiliensis*. *Microbiol Immunol* (2007) 51:421–8. doi:10.1111/j.1348-0421.2007.tb03929.x
56. Peraçoli M, Kurokawa CS, Calvi SA, Mendes RP, Pereira PC, Marques SA, et al. Production of pro- and anti-inflammatory cytokines by monocytes from patients with paracoccidioidomycosis. *Microbes Infect* (2003) 5:413–8. doi:10.1016/S1286-4579(03)00040-6
57. Amaral EP, Ribeiro SC, Lanes VR, Almeida FM, de Andrade MR, Bomfim CC, et al. Pulmonary infection with hypervirulent mycobacteria reveals a crucial role for the P2X7 receptor in aggressive forms of tuberculosis. *PLoS Pathog* (2014) 10(7):e1004188. doi:10.1371/journal.ppat.1004188
58. Darville T, Welter-Stahl L, Cruz C, Sater AA, Andrews CW Jr, Ojcius DM. Effect of the purinergic receptor P2X7 on *Chlamydia* infection in cervical epithelial cells and vaginally infected mice. *J Immunol* (2007) 179(3):707–14. doi:10.4049/jimmunol.179.6.3707
59. Figliuolo VR, Chaves SP, Savio LEB, Thorstenberg MLP, Salles EM, Takiya CM, et al. The role of the P2X7 receptor in murine cutaneous leishmaniasis: aspects of inflammation and parasite control. *Purinergic Signal* (2017) 13:143–52. doi:10.1007/s11302-016-9544-1
60. Lees MP, Fuller SJ, McLeod R, Boulter NR, Miller CM, Zakrzewski AM, et al. P2X7 receptor-mediated killing of an intracellular parasite, *Toxoplasma gondii*, by human and murine macrophages. *J Immunol* (2010) 184:7040–6. doi:10.4049/jimmunol.1000012
61. Mishra A, Guo Y, Zhang L, More S, Weng T, Chintagari NR, et al. A critical role for P2X7 receptor-induced VCAM-1 shedding and neutrophil infiltration during acute lung injury. *J Immunol* (2016) 197:2828–37. doi:10.4049/jimmunol.1501041
62. Dostert C, Ludigs K, Guarda G. Innate and adaptive effects of inflammasomes on T cell responses. *Curr Opin Immunol* (2013) 25:359–65. doi:10.1016/j.coi.2013.02.008
63. Bauernfeind F, Ablasser A, Bartok E, Kim S, Hornung V. Inflammasome: current understanding and open questions. *Cell Mol Life Sci* (2011) 68:765–83. doi:10.1007/s00018-010-0567-4
64. De Luca A, Zelante T, D'Angelo C, Zagarella S, Fallarino F, Spreca A, et al. IL-22 defines a novel immune pathway of antifungal resistance. *Mucosal Immunol* (2010) 3:361–73. doi:10.1038/mi.2010.22
65. Manel N, Unutmaz D, Littman DR. The differentiation of human T(H)-17 cells requires transforming growth factor-beta and induction of the nuclear receptor RORgammat. *Nat Immunol* (2008) 9:641–9. doi:10.1038/ni.1610
66. Acosta-Rodriguez EV, Rivino L, Geginat J, Jarrossay D, Gattorno M, Lanzavecchia A, et al. Surface phenotype and antigenic specificity of human interleukin 17-producing T helper memory cells. *Nat Immunol* (2007) 8:639–46. doi:10.1038/ni1467
67. Cano LE, Singer-Vermes LM, Mengel JA, Xidieh CF, Arruda C, André DC, et al. Depletion of CD8+ T cells in vivo impairs host defense of resistant and susceptible mice to pulmonary paracoccidioidomycosis. *Infect Immun* (2000) 68:352–9. doi:10.1128/IAI.68.1.352-359.2000
68. Chiarella AP, Arruda C, Pina A, Costa TA, Ferreira RC, Calich VL. The relative importance of CD4+ and CD8+ T cell in immunity to pulmonary paracoccidioidomycosis. *Microbes Infect* (2007) 9:1078–88. doi:10.1016/j.micinf.2007.04.016
69. Ben-Sasson SZ, Hu-Li J, Quiel J, Cauchetaux S, Ratner M, Shapira I, et al. IL-1 acts directly on CD4 T cells to enhance their antigen-driven expansion and differentiation. *Proc Natl Acad Sci U S A* (2009) 106:7119–24. doi:10.1073/pnas.0902745106
70. Nakanishi K, Yoshimoto T, Tsutsui H, Okamura H. Interleukin-18 is a unique cytokine that stimulates both Th1 and Th2 responses depending on its cytokine milieu. *Cytokine Growth Factor Rev* (2001) 12:53–72. doi:10.1016/S1359-6101(00)00015-0
71. Arruda C, Valente-Ferreira RC, Pina A, Kashino SS, Fazioli RA, Vaz CA. Dual role of interleukin-4 (IL-4) in pulmonary paracoccidioidomycosis: endogenous IL-4 can induce protection or exacerbation of disease depending on the host genetic pattern. *Infect Immun* (2004) 72:3932–40. doi:10.1128/IAI.72.7.3932-3940.2004
72. Hwang I, Yang J, Hong S, Ju Lee E, Lee SH, Fernandes-Alnemri T, et al. Non-transcriptional regulation of NLRP3 inflammasome signaling by IL-4. *Immunol Cell Biol* (2015) 93:591–9. doi:10.1038/icb.2014.125
73. Wang W, Wang X, Chun J, Vilaysane A, Clark S, French G, et al. Inflammasome-independent NLRP3 augments TGF-β signaling in kidney epithelium. *J Immunol* (2013) 190:1239–49. doi:10.4049/jimmunol.1201959

Conflict of Interest Statement: The authors declare that the research was conducted in the absence of any commercial or financial relationships that could be construed as a potential conflict of interest.

Copyright © 2017 Feriotti, de Araújo, Loures, da Costa, Galdino, Zamboni and Calich. This is an open-access article distributed under the terms of the Creative Commons Attribution License (CC BY). The use, distribution or reproduction in other forums is permitted, provided the original author(s) or licensor are credited and that the original publication in this journal is cited, in accordance with accepted academic practice. No use, distribution or reproduction is permitted which does not comply with these terms.

frontiers in Immunology

ORIGINAL RESEARCH
published: 09 November 2017
doi: 10.3389/fimmu.2017.01504

Canonical Stimulation of the NLRP3 Inflammasome by Fungal Antigens Links Innate and Adaptive B-Lymphocyte Responses by Modulating IL-1β and IgM Production

*Mohamed F. Ali, Harika Dasari, Virginia P. Van Keulen and Eva M. Carmona**

The Thoracic Diseases Research Unit and the Division of Pulmonary and Critical Care, Department of Medicine Mayo Clinic and Foundation, Rochester, MN, United States

OPEN ACCESS

Edited by:
Steven Templeton, Indiana University School of Medicine, United States

Reviewed by:
Vera Lucia Garcia Calich, University of São Paulo, Brazil
Grith Lykke Sorensen, University of Southern Denmark Odense, Denmark

****Correspondence:***
Eva M. Carmona
carmona.eva@mayo.edu

Specialty section:
This article was submitted to Microbial Immunology, a section of the journal Frontiers in Immunology

Received: *06 September 2017*
Accepted: *25 October 2017*
Published: *09 November 2017*

Citation:
Ali MF, Dasari H, Van Keulen VP and Carmona EM (2017) Canonical Stimulation of the NLRP3 Inflammasome by Fungal Antigens Links Innate and Adaptive B-Lymphocyte Responses by Modulating IL-1β and IgM Production. Front. Immunol. 8:1504. doi: 10.3389/fimmu.2017.01504

The NLRP3 inflammasome is activated in response to different bacterial, viral, and fungal pathogens and serves as modulator of different pattern recognition receptors signaling pathways. One of the main functions of NLRP3 is to participate in IL-1β maturation which is important in the host defense against *Pneumocystis* and other fungal infections. However, dysregulation of NLRP3 and IL-1β secretion are also implicated in the pathophysiology of many auto-inflammatory disorders. Often time's inflammatory flares are preceded by infectious illnesses questioning the role of infection in autoimmune exacerbations. However, we still do not fully understand the exact role that infection or even colonization plays as a trigger of inflammation. Herein, we investigated the role of NLRP3 in circulating B-lymphocytes following activation with two major microbial antigens (β-glucan and CpG). NLRP3 was determined essential in two independent B-lymphocytes processes: pro-inflammatory cytokine secretion and antibody regulation. Our results show that the β-glucan fungal cell wall carbohydrate stimulated B-lymphocytes to secrete IL-1β in a process partially mediated by Dectin-1 activation *via* SYK and the transcription factors NF-κB and AP-1. This IL-1β secretion was regulated by the NLRP3 inflammasome and was dependent on potassium efflux and Caspase-1. Interestingly, B-lymphocytes activated by unmethylated CpG motifs, found in bacterial and fungal DNA, failed to induce IL-1β. However, B-lymphocyte stimulation by CpG resulted in NLRP3 and Caspase-1 activation and the production and secretion of IgM antibodies. Furthermore, CpG-stimulated IgM secretion, unlike β-glucan-mediated IL-1β production, was mediated by the mammalian target of rapamycin (mTOR). Inhibition of NLRP3 and the mTOR pathway in CpG activated B-lymphocytes resulted in impaired IgM secretion suggesting their participation in antibody regulation. In conclusion, this study describes a differential response of NLRP3 to β-glucan and CpG antigens and identifies the NLRP3 inflammasome of human circulating B-lymphocytes as a modulator of the innate and adaptive immune systems.

Keywords: β-glucan, B-lymphocytes, inflammasome, fungi, CpG, NLRP3, IL-1β, IgM

INTRODUCTION

The host immune system greatly determines the severity of fungal diseases. In patients with an intact immune system, fungal infections are often clinically asymptomatic or manifest as a mild respiratory illness. In the immunocompromised host, however, fungal infections can disseminate and result in a life-threatening event with high morbidity and mortality. Fungal diseases are on the rise, likely as a result of increasing use of immunosuppressive agents to treat malignancies and autoimmune diseases. Better understanding of fungal immunity will help with the development of alternative antifungal therapeutic strategies that enhance specific aspects of host immunity.

B-lymphocytes, well-known players of the adaptive immune response, react to fungal pathogens by generating antibodies and by releasing inflammatory cytokines (1, 2). In the presence of T cells, B-lymphocyte responses are characterized by isotype class switch and generation of memory and long-lived plasma cells leading to the production of high affinity immunoglobulins (Igs) mostly of the IgG subtype. In the absence of T cells, B-lymphocytes still generate Igs but these are of low affinity and mostly IgM. T-cell independent activation of B-lymphocytes also results in the release of a variety of cytokines and chemokines which are mostly triggered by the activation of pattern recognition receptors (PRRs) such as toll-like receptors (TLRs) and C-lectin receptors (3). PRRs are expressed by most innate immune effector cells, including B-lymphocytes and play a critical role in the detection of pathogens by recognizing conserved pathogen-associated molecular patterns like β-glucan and CpG. β-glucans are highly immunogenic carbohydrates found in the cell wall of many fungi including *Aspergillus* spp., *Candida* spp., and *Pneumocystis* while CpG are highly immunoreactive unmethylated motifs found in bacterial and fungal DNA (4, 5). While each signal using specific PRRs, both have potent immunomodulatory properties and can activate B-lymphocytes directly without the participation of T cells. B-lymphocyte activation by β-glucan and CpG results in the secretion of a specific profile of pro-inflammatory cytokines and chemokines important for the orchestration and activation of monocytes, macrophages, and neutrophils and therefore essential for host defense against fungal and other infections (6–8).

The NLRP3 inflammasome is generally triggered by infection or tissue damage and participates in the processing of mature and bioactive IL-1β from its precursor and inactive form (pro-IL-1β) (9, 10). Since increased production of IL-1β is known to be important for the clearance of fungal infections and little is known about the contribution of B-lymphocytes to the innate immune fungal defense, we sought to investigate the role of NLRP3 activation in B-lymphocytes upon fungal β-glucan stimulation and compare it with B-lymphocyte responses to CpG.

The assembly of the inflammasome classically involves the recruitment of a Nod-like receptor (NLR), an adaptor protein (ASC) and a protease (pro-caspase-1). Depending on the stimuli, the activation of NLRP3 can follow a canonical pathway that involves caspase-1 activation or a non-canonical pathway that is independent of caspase-1. In the particular case of β-glucans, the data are contradictory and both pathways have been described (11–13). In B-lymphocytes, however, the participation of NLRP3 in cytokine regulation and other processes has not been well characterized.

Herein, we describe a dual function of the NLRP3 inflammasome in activated peripheral human B-lymphocytes as a modulator of IL-1β secretion as well as antibody production. While fungal β-glucans andCpG were both able to elicit activation of the NLRP3 inflammasome, the mechanisms of activation were divergent with β-glucan inducing IL-1β secretion and CpG an increase of IgM. Furthermore, CpG activation of NLRP3 was dependent on the activation of the mammalian target of rapamycin (mTOR) pathway while β-glucan activation was mTOR-independent.

MATERIALS AND METHODS

Reagents and Antibodies

Endotoxin-free buffers and reagents were scrupulously used in all experiments. Curdlan, Zymosan, and Laminarin were purchased from Sigma Chemical Co. (St. Louis, MO, USA). *Aspergillus fumigatus* β-glucan preparations were isolated as previously described (14). To ensure that all glucan preparations were free of endotoxin prior to use in culture, Curdlan, Zymosan, and *A. fumigatus* glucans were vigorously washed 10 times with distilled physiological saline, incubated rotating overnight with polymyxin B (Sigma, St. Louis, MO, USA) at 4°C, then vigorously washed again with distilled physiological saline. The final preparations were assayed for endotoxin with the limulus amebocyte lysate method using Pyrosate Rapid Endotoxin Detection Kit (Associates of Cape Cod, East Falmouth, MA, USA) and found to consistently contain less than 0.25 EU/ml. Glucans were pulse sonicated 10 times using a Branson digital sonifier (VWR Scientific, Radnor, PA, USA) at 35% amplitude immediately before addition to the cultures. The Erk 1/2 inhibitor (PD98059), SYK inhibitors (Piceatannol and R406), and NF-κB inhibitor (Bay11-7085) were all obtained from Calbiochem, Inc. (San Diego, CA, USA). AP-1 inhibitor (SR 11302) was from R&D Systems, Inc. (Minneapolis, MN, USA). Caspase inhibitors (Ac-YVAD-CMK and Ac-YVAD-CHO) were purchased from Cayman Chemical (Ann Arbor, MI, USA), VX-765 was from AdooQ Bioscience (Irvine, CA, USA), and Rapamycin was purchased from Selleck Chemicals (Houston, TX, USA). KCl and Adenosine 5′-triphosphate (ATP) were from Sigma and oxidized ATP (oxATP) and MCC950 were from EMD Millipore (Billerica, MA, USA). Phosphorothioate-protected CpG oligonucleotide (5′-TCGTCGTTTTGTCGTTTTGTCGTT-3′) ODN 2006 and *A. fumigatus* oligonucleotides; AF1 (5′-TCGTC GTTGTCGTCGTC-3′) and AF2 (5′-TCGTCGTTGTCGTC-3′) were commercially synthesized by Integrated DNA Technologies, Inc. For most of the experiments, we used CpG ODN 2006 (CpG) unless otherwise specified. Antibodies recognizing the inflammasome components caspase-1 and IL-1β were purchased from Santa Cruz Inc. (Dallas, TX, USA), while NLRP3, ASC, and the mTOR pathway antibodies; mTOR, phospho-mTOR, S6K, and phospho-S6K were from Cell Signaling Technology, Inc. (Danvers, MA, USA). The neutralizing antibody for Dectin-1 was purchased from AbD Serotec (Raleigh, NC, USA) and Isotype control antibody was from R&D Systems, Inc. (Minneapolis,

MN, USA). All other reagents were obtained from Sigma-Aldrich (St. Louis, MO, USA) unless specified otherwise.

Leukocyte Isolation and Culture

All methods were carried out in accordance with relevant guidelines and regulations. Human B-lymphocytes were isolated as previously described (7). Briefly, B-lymphocytes were isolated from acid citrate dextrose anticoagulated blood obtained from de-identified healthy volunteer platelet donors in accordance with the current regulations by the AABB and the US Food and Drug Administration (15) and by the Mayo Clinic Institutional Review Board (IRB). Ethics committee approval was not required according to the local and national and guidelines. Cells were isolated using RosetteSep B-cell enrichment cocktail according to the manufacturer's protocol (StemCell Technologies, Vancouver, BC, Canada). The enriched B-lymphocyte population was repeatedly observed to contain an average of 93.1% ± 2.3% B-lymphocytes. Sorting of human CD19+ B-lymphocytes into naïve (CD27−) and memory (CD27+) B-lymphocytes was performed using mouse anti-human CD27-APC-Vio770 and mouse anti-human CD19-PE antibodies from Miltenyi Biotec (San Diego, CA, USA), on a FACSAria II SORP flow cytometer running FACSDiva v 6.1.3 software.

RNA Isolation and Real-time qPCR Analysis

Total cellular RNA was isolated from B-lymphocytes using RNeasy Plus Universal Mini Kit (Qiagen) according to the manufacturer's instructions. For cDNA synthesis, total RNA concentrations and purity were determined using a Nanodrop ND-1000 spectrophotometer, and 1 µg RNA was used in a 20 µl reaction mixture using a Verso cDNA Synthesis Kit (Thermo Scientific). Quantitative real-time PCR was performed in 10 µl reaction in a 96-well plate using 2 µl of diluted cDNA with SYBR Premix Ex Taq (Clontech Laboratories, Inc.) on a ViiA7 Real-Time PCR Detection System (Life Technologies). The data were analyzed with ViiA7 software, version 1.2.4 (Life Technologies). Relative transcript expression of IL-1β was determined using the comparative Ct method, and was normalized to GAPDH transcripts of the same cDNA samples. The results were expressed as % of the target gene relative to that of GAPDH and plotted as the mean ± SEM. Experimental reproducibility was confirmed using three biological replicates from independent experiments which used B-lymphocytes from three different donors. The primers used for amplification were: IL-1β, 5′-ATGCACCTGTACGATCACTG-3′ and 5′-ACAAAGGACA TGGAGAACACC-3′; GAPDH, 5′-ACATCGCTCAGACACCA TG-3′ and 5′-TGTAGTTGAGGTCAATGAAGGG-3′.

Cytokines and IgM Detection

B-lymphocytes (4×10^5 cells/well in 96-well plates) were cultured with 1 µg/ml of CpG (ODN 2006), or with 1 µg/ml AF1, 1 µg/ml AF2, 200 µg/ml of Curdlan (Curd), 200 µg/ml Zymosan (Zym), 200 µg/ml or 200 µg/ml*A. fumigatus* β-glucan (AspG) in culture medium for 24 h for IL-1β and other cytokines and 5 days for IgM unless otherwise indicated. Cell supernatants were then analyzed for IL-1β, TNFα, IL-6, MMP7, and IgM production using human DuoSet ELISA kit for MMP-7 from R&D Systems, Inc. (Minneapolis, MN, USA), BD OptEIA human ELISA kit for IL-1β and Ready-Set-Go ELISA kit for TNFα, IL-6, and IgM from Thermo Fisher (Rochester, NY, USA). ELISAs were performed according to each manufacturer's instructions. Inhibitors [50 and 100 µM Caspase-1 inhibitors (VX-765 and YVAD.CMK), 50 mM KCl, 50 µM oxATP, 100 µM MCC950, 40 µM Piceatannol, 5 µM R406, 10 µM Bay11-7085, 10 µM SR11302 or 1 mg/ml Laminarin] and neutralizing antibodies (5 µg/ml anti-Dectin-1 IgG or mouse IgG) were incubated with B-lymphocytes for 1 h prior to addition of CpG or β-glucan preparations. Inhibitors were dissolved in dimethyl sulfoxide unless otherwise indicated. Solvents were added to all treatments to assure that solvents concentrations are the same in all treatment conditions.

Caspase-1 Activity Assay

Caspase-1 activity was determined by a Caspase-1 Fluorometric Assay (BioVision, Mountain View, CA, USA), according to the manufacturer's instruction. Briefly, 10^7 B-lymphocytes were stimulated with Curdlan and CpG in the presence of the caspase inhibitor YVAD-CMK, incubated at 37°C for 24 h and lysed with cell lysis buffer on ice for 10 min. Then, equal volumes of 2× reaction buffer and YVAD-AFC were added to the 200 µg of lysates in a 96-well plate and incubated for 2 h at 37°C. The samples were read on a Softmax microplate reader (Molecular Devices, Sunnyvale, CA, USA) with a 400 nm excitation filter and 505 nm emission filter. The caspase-1 activity is expressed relative to the unstimulated control.

Cellular Viability

Cell viability was assessed using the XTT Cell Proliferation Kit II (Roche Molecular Biochemicals, Indianapolis, IN, USA) according to the manufacturer's protocol. This assay measures the conversion of sodium-3′-[1-(phenylaminocarbonyl)-3, 4-tetrazolium]-bis(4-methoxy-6-nitro) benzenesulfonic acid hydrate (XTT) to a formazan dye through electron coupling in metabolically active mitochondria using the coupling reagent *N*-methyldibenzopyrazine methyl sulfate. Only metabolically active cells are capable of mediating this reaction, which is detected by absorbance of the dye at 450–500 nm. Briefly, 50 µl of the XTT labeling mixture was added to the 100 µl of growth medium containing B-lymphocytes and different concentrations of the inhibitors. The XTT labeling mixture was added in parallel samples 24 h after the addition of the various inhibitors. A set of blanks was also included that did not contain cells and was treated identically as the normal samples. In addition, a set of solvent controls was also included for each inhibitor. Absorbance was measured at 6 h after XTT addition. All treatments were performed in three replicates. Only inhibitor concentrations that elicited less than 20% net toxicity were used in these assays.

Preparation of Cell Lysates, Electrophoresis, and Immunoblotting

Total cellular proteins were obtained from B-lymphocytes following the described culture conditions. Briefly, the cells were

washed with cold PBS twice and lysed in RIPA buffer (50 mM Tris–HCl pH 7.4, 15 mM NaCl, 0.25% deoxycholic acid, 1% NP-40) freshly supplemented with 1 mM phenylmethylsulfonyl fluoride, mammalian protease inhibitor mixture, 10 mM Na Fluoride, and 1 mM Na Orthovanadate. Cells were kept on ice for 15 min and then the lysates were centrifuged at 12,000 × *g* for 10 min at 4°C. The resultant soluble supernatant contained total cellular protein. Protein concentrations were determined with the Bio-Rad protein assay (Hercules, CA, USA) using BSA as the standard. Equal amounts of total cellular proteins were separated on SDS-10% polyacrylamide gels with Precision Plus Protein Dual Color Standards (Bio-Rad; Hercules, CA, USA) being used as the molecular weight standards. Proteins were transferred to Immobilon-P membranes (Millipore, Bedford, MA, USA). Membranes were then blocked at room temperature for 30 min with 1% BSA/TBST (TBS, pH 7.4, 1% BSA, 0.1% Tween 20) and incubated overnight at 4°C in a blocking solution containing primary antibodies at the appropriate dilutions. After washing with TBST, the membranes were incubated with horseradish peroxidase-conjugated secondary antibodies for 1 h. Immunoreactive bands were detected with SuperSignal West PicoChemiluminescent Substrate from Thermo Scientific (Rockford, IL, USA). Actin was used as loading control for the cell lysates and a non-specific protein for the cell supernatant.

Statistical Analyses

All data are presented as the mean ± SEM, from at least three independent experiments from different biological donors, unless otherwise specified. An experimental run included at least three different donors. The data were first analyzed using one-way ANOVA, the differences between the individual groups were compared using multiple comparisons post-test unless otherwise indicated. Statistical analysis was performed using GraphPad Prism Version 5 (GraphPad Software, La Jolla, CA, USA).

RESULTS

IL-1β Is Induced by Fungal β-Glucans in a T-Cell Independent Manner

B-lymphocytes respond to fungal β-glucans and bacterial DNA in a T-cell independent manner by releasing cytokines and chemokines important for the acute inflammatory response (8, 16). We have previously shown that β-glucan-stimulated peripheral human B-lymphocytes are a source of IL-8, IL-6, and TNFα (7). Additionally, supernatant from β-glucan-stimulated B-lymphocytes was able to significantly increase neutrophil chemotaxis suggesting the contribution of B-lymphocytes in the acute inflammatory process (7). To further understand the role of B-lymphocytes in fungal defense and since IL-1β has been shown to participate in fungal clearance and neutrophil recruitment (17, 18), freshly isolated peripheral B-lymphocytes from normal donors were stimulated with either β-glucan (Curdlan) or CpG (CpG ODN 2006) and assessed for IL-1β expression. RNA levels of IL-1β were significantly elevated in β-glucan-stimulated cells but not in those stimulated with CpG (**Figure 1A**). Protein levels of IL-1β were next confirmed in the cell supernatants by ELISA. As expected, β-glucan-stimulated cells secreted significant amounts of active IL-1β in a dose and time responsive manner (**Figures 1B,C**). The addition of β-glucan to CpG did not enhance IL-1β stimulation (**Figure 1D**). Furthermore, IL-1β secretion was not restricted to curdlan β-glucans as other β-glucan preparation such as zymosan and β-glucan from *Aspergillus* were also potent inducers of IL-1β (**Figure 1E**). Similarly, failure to induce IL-1β secretion was not restricted to CpG ODN 2006, since two different CpG motifs present in *A. fumigatus* DNA (AF1 and AF2) (4) also failed to stimulate IL-1β secretion (**Figure 1F**). The differential response of B-lymphocytes to β-glucan and CpG was intriguing, though similarly observed by our group in the setting of IL-8 and IgM (7). Our published studies demonstrated that β-glucan-induced IL-8 secretion had no effect on IgM while CpG stimulated IgM secretion did not participate in IL-8 secretion (7).

β-Glucan and CpG Induce Activation of the NLRP3 Inflammasome in Human Circulating B-Lymphocytes

The NLRP3 inflammasome is crucial for the processing of biologically inactive IL-1β (pro-IL-1β) into the mature and biologically active form (IL-1β). It was therefore important for us to determine its role in β-glucan-mediated IL-1β secretion. Protein expression of NLRP3, ASC, caspase-1, and pro-IL-1β as well as caspase-1 activity were therefore assessed and found to increase significantly upon β-glucan stimulation (**Figures 2A,C**). CpG stimulation did not induce pro-IL-1β, a required step needed for mature IL-1β production (**Figure 2B**). However, despite the lack of increase in pro-IL-1β, CpG also resulted in activation of the NLRP3 inflammasome (**Figures 2B,C**).

To further demonstrate that Caspase-1 and NLRP3 were indeed important in β-glucan-mediated IL-1β secretion and since primary human B-lymphocytes are not suitable for lentivirus infection or transfection with other forms of interfering RNA, IL-1β was measured in the cell supernatant of stimulated cells in the presence of different Caspase-1 and NLRP3 inhibitors. As shown in **Figures 2D–F**, the use of the caspase-1 inhibitors VX765 and YVAD-CMK, KCL, oxATP, and the specific NLRP3 inhibitor, MCC950 (19), resulted in significant decreases of IL-1β secretion, confirming the participation of the canonical NLRP3 inflammasome pathway in β-glucan-mediated IL-1β secretion. Absence of cell toxicity was confirmed for all the inhibitors as shown in Supplement S1 in Supplementary Material.

Since prior data suggested that in NLRP3 deficient mice IgM secretion and antibody production are impaired (8, 20–22), we hypothesized that NLRP3 may regulate IgM secretion. We and others have additionally shown that peripheral B-lymphocytes secrete IgM in response to CpG (ODN 2006) (7, 23) (Supplement S2 in Supplementary Material). To better understand the role of NLRP3 activation in CpG-stimulated B-lymphocytes we further investigated if IgM was also triggered in response to AF1 and AF2. As shown in **Figure 3A** IgM was similarly induced by all forms of CpG tested. Next, we evaluated IgM levels after CpG stimulation in the presence of different concentrations of MCC950. Interestingly, the levels of IgM decreased in the presence of MCC950 in a dose-dependent manner (**Figure 3B**; Supplement S3A

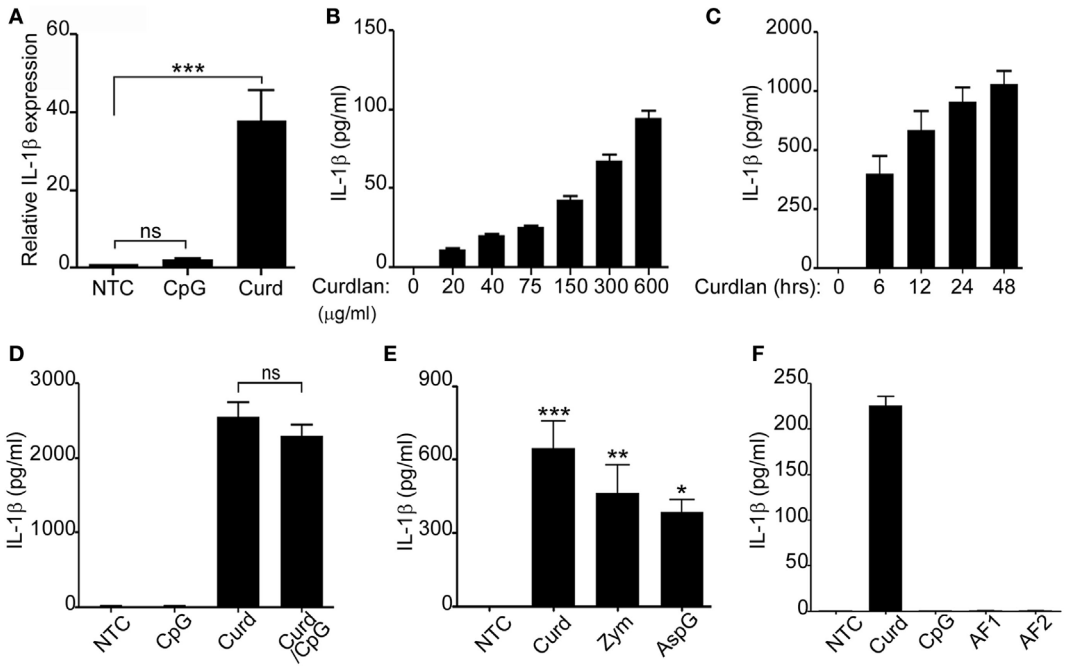

FIGURE 1 | Fungal β-glucans elicit IL-1β secretion in B-lymphocytes. Quantitative real-time PCR for IL-1β mRNA was determined in non-treated cells (NTC) or B-cells stimulated with CpG or Curdlan (Curd). Expression was normalized to GAPDH **(A)**. IL-1β levels were measured by ELISA in the cell supernatant of curdlan stimulated cells at different concentrations **(B)**, for different periods of time **(C)**, with CpG and Curdlan as indicated **(D)** with different β-glucan preparations: Curdlan, Zymosan (Zym), and *Aspergillus fumigatus* (AspG) **(E)** and with different CpG motifs from *A. fumigatus*: AF1 and AF2 **(F)**. Stimulation was done overnight unless otherwise indicated. 200 μg/ml β-glucan and 1 μg/ml CpG, AF1, and AF2 were used unless otherwise specified. Data are representative of at least three donors in each independent experiment ($n = 3$). $^{*}p < 0.05$, $^{**}p < 0.01$, $^{***}p < 0.0001$, ns, not significant ($p > 0.05$).

in Supplementary Material). To ensure that this effect was specific to inhibition of the NLRP3 inflammasome, IL-6, MMP-7, and TNFα were also assessed in the presence of MCC950. As shown in **Figure 3C,** none of the other cytokines and metalloproteases were affected by the presence of the inhibitor further supporting the specific role of the NLRP3 inflammasome in IgM secretion. Additionally, IgM release was also impaired in the presence of KCL, oxATP, and caspase inhibitors (**Figures 3D,E**; Supplement S3A in Supplementary Material), all well-known agents that affect the functioning of the NLRP3 inflammasome.

Dectin-1 and Syk-Participate in NLRP3 Activation by β-Glucans While CpG Signaling Activation of NLRP3 Regulates IgM *via* mTOR

Since the inflammasome was activated by both β-glucan and CpG and both are known to signal through very different PRRs, we next explored the specific signaling pathways that lead to IL-1β and IgM secretion upon β-glucan and CpG, respectively.

β-Glucans are known to signal predominantly through the C-lectin receptor Dectin-1 (6, 7, 24, 25) while CpG is the natural ligand for TLR9 (4, 26). Hence, we first explored the contribution of Dectin-1 in β-glucan-induced IL-1β signaling. B-lymphocytes were pre-incubated with either laminarin (a soluble β-glucan known to bind to Dectin-1 acting as a competitive inhibitor) or a specific Dectin-1 blocking antibody prior to β-glucan stimulation. IL-1β levels were significantly reduced in the presence of both, laminarin and the Dectin-1 antibody, confirming the role of Dectin-1 in β-glucan-mediated IL-1β secretion (**Figures 4A,B**). β-glucan-mediated IL-1β was also dependent on Syk and the transcription factors NF-κB and AP-1 (**Figures 4C,D**).

TLR9 is the main receptor for CpG motifs found in bacterial and fungal DNA (4, 26) and it is known that stimulation by CpG also involves mTOR (4, 6, 27–29). In contrast, β-glucan stimulation does not seem to require mTOR (6). Thus, to additionally understand the potential involvement of mTOR activation in IgM and IL-1β regulation, phosphorylation of mTOR and other mTOR-related proteins were assessed after cells were stimulated for different period of time with CpG or β-glucan. mTOR and other mTOR-related proteins (S6K, S6, and 4EBP1) tested were phosphorylated upon CpG but not after β-glucan stimulation with the exception of 4EBP1 which seemed to be phosphorylated by both (**Figure 5A**; Supplement S3B in Supplementary Material). β-glucan activation of 4EBP1 was inhibited in the presence of PD98059, a specific ERK1/2 inhibitor, and not by Rapamycin, a well-known mTOR inhibitor, suggesting that 4EBP1 activation, in β-glucan-stimulated cells, was mTOR-independent and required ERK1/2 (Supplement S4 in Supplementary Material), consistent with prior observations (30).

As our data suggested that NLRP3 regulates IgM *via* mTOR, we measured IgM levels after CpG-stimulation in the presence

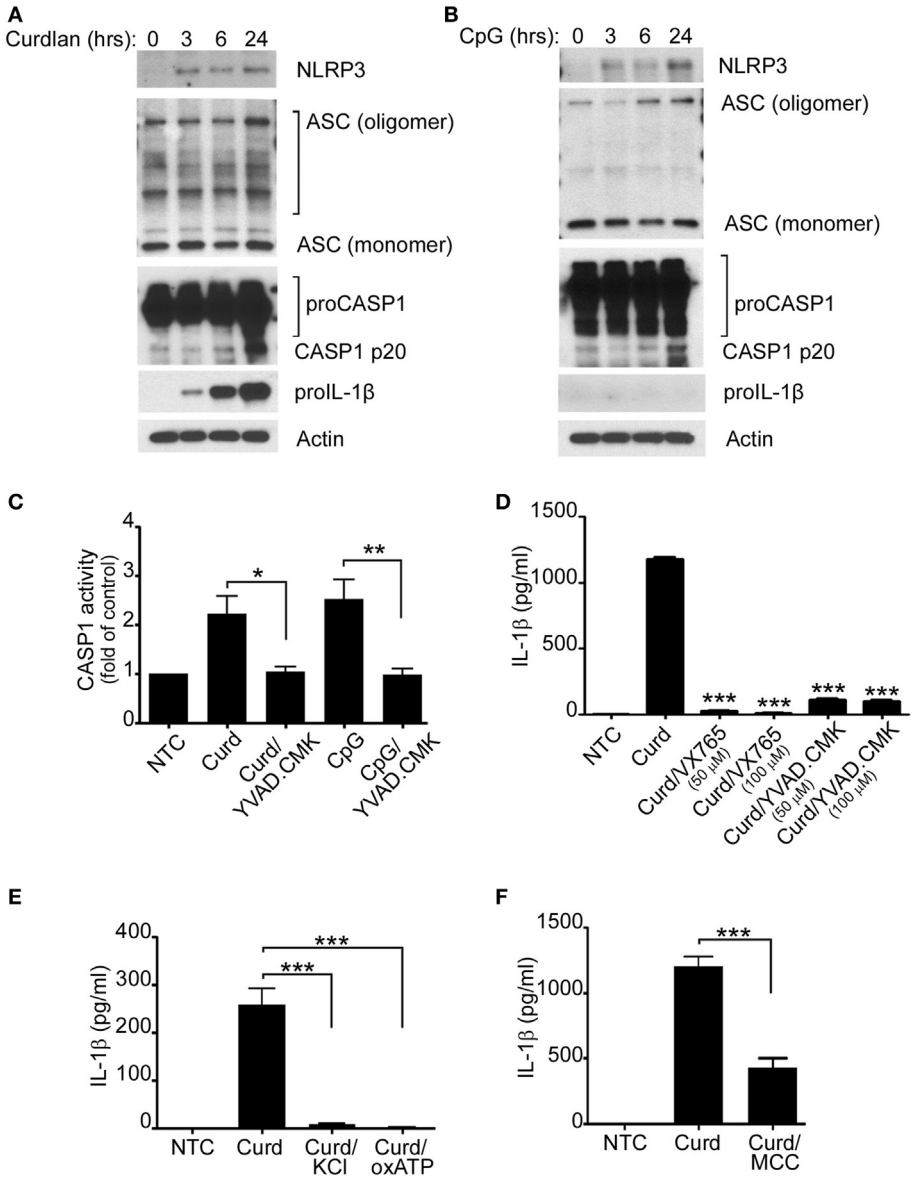

FIGURE 2 | IL-1β secretion requires the NLRP3 inflammasome. Immunoblot analysis of NLRP3, ASC, proCaspase-1, Caspase-1 p20, pro-IL-1β, and actin after curdlan **(A)** or CpG stimulation **(B)** for different periods of time, as indicated. **(C)** Capase1 activity was determined in unstimulated cells (NTC), after Curdlan (Curd) and CpG stimulation. In some cases, the stimulation was performed in the presence of the caspase inhibitor YVAD-CMK (50 μM) as indicated. IL-1β ELISA measured in the cell supernatant of NTC, after curdlan stimulation and after curdlan stimulation of cells pretreated with VX-765 and YVAD-CMK **(D)**, 50 mM KCL and 50 μM oxidized ATP (oxATP) **(E)** and 100 μM MCC950 **(F)** as indicated. 200 μg/ml curdlan and 1 μg/ml CpG were used for stimulation. Data are representative of at least three independent experiments. $^{*}p < 0.05$, $^{**}p < 0.01$, $^{***}p < 0.0001$.

and absence of Rapamycin. The use of Rapamycin resulted in significant reduction of IgM thus confirming the role of mTOR signaling in IgM regulation (**Figure 5B**; Supplement S3A in Supplementary Material). The levels of IgM in the presence of Rapamycin were comparably reduced to the levels of IgM after MCC950. In contrast, β-glucan stimulation of IL-1β, while reduced in the presence of MCC950, was not affected by the use of Rapamycin confirming that this is an mTOR-independent process (**Figure 5C**). Interestingly, Rapamycin inhibition of the NLRP3 inflammasome seemed to affect Caspase-1 activation as shown in **Figure 5D**. Similar observations were made for MCC950, consistent with prior published observations (31).

Memory B-Lymphocytes Are the Main Producers of IL-1β and IgM

Peripheral B-lymphocytes can be divided into naïve and memory cells. In order to further understand the subtype of B-lymphocytes responsible for the secretion of IL-1β and IgM,

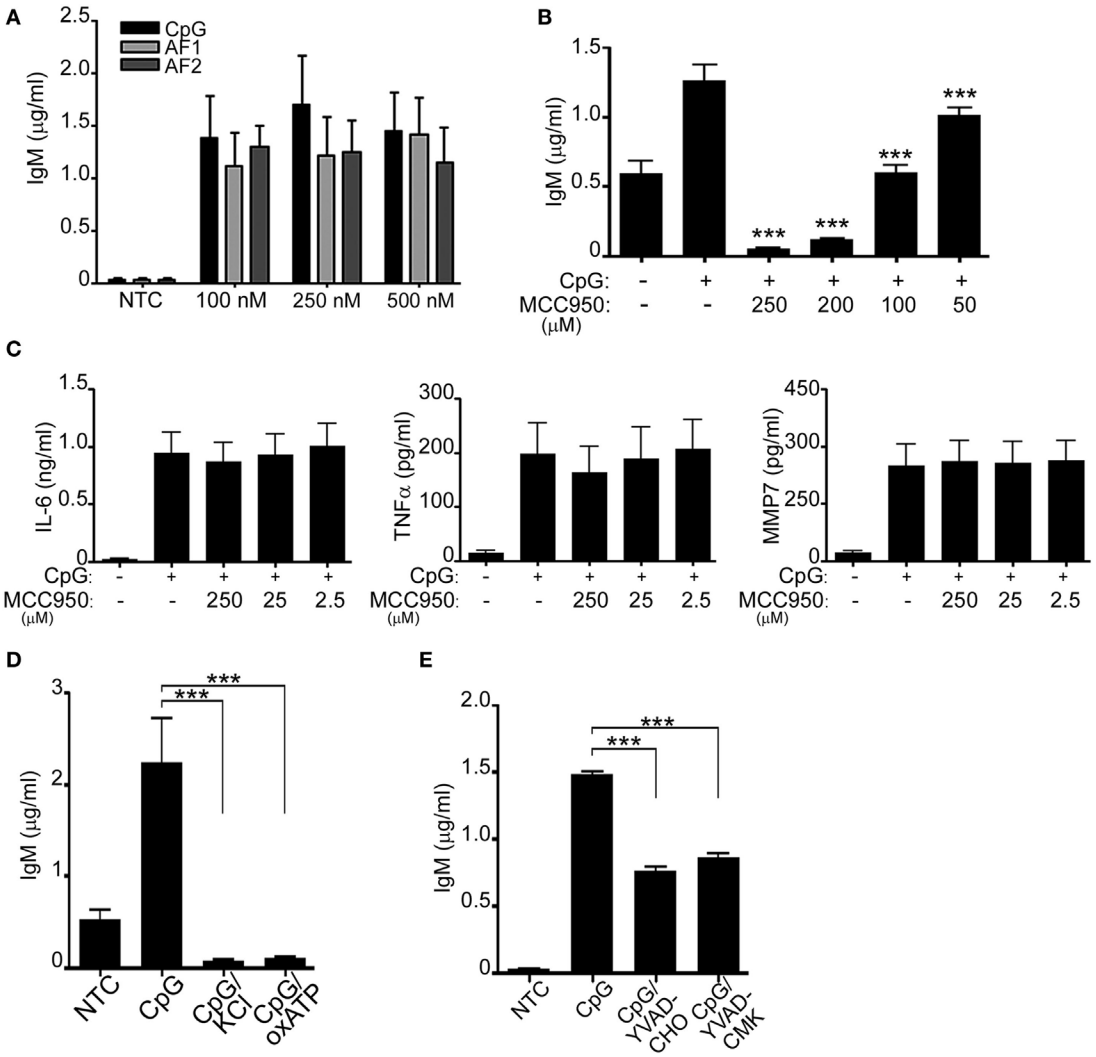

FIGURE 3 | CpG induces NLRP3-mediated antibody production. IgM **(A,B)**, IL-6, TNF-α, and MMP-7 **(C)** were measured by ELISA in the cell supernatant of unstimulated (NTC), CpG, AF1 and AF2 stimulated cells, and CpG stimulated cells in the presence of different concentrations of MCC950 as indicated. Cells were left untreated (NTC) or pre-incubated with 50 mM KCL, 50 μM oxidized ATP (oxATP) **(D)**, and the caspase-1 inhibitors, YVAD-CHO and YVAD-CMK, at a concentration of 50 μM each **(E)** prior to stimulation with CpG as indicated. 1 μg/ml CpG was used unless otherwise specified. Data are representative of at least three donors in each independent experiments ($n = 3$). ***$p < 0.0001$.

and since it is clearly established that naïve and memory cells produce different cytokine patterns upon stimulation (32, 33). We isolated B-lymphocytes by negative selection and then sorted them into $CD20^+CD27^-$ (naïve) and $CD20^+CD27^+$ (memory) cells. The two different subtypes of B-lymphocytes were independently stimulated with either β-glucan or CpG. IL-1β and IgM levels in the cell supernatant were then measured by ELISA. As **Figure 6A** shows, we observed that IL-1β was mostly secreted by memory cells whereas IgM production was greater from the sorted memory cells and significantly higher than naïve cells ($p < 0.001$), but was still seen at significant levels in the naïve cells upon CpG stimulation. Co-stimulation of the BCR receptor resulted in an increase in IgM secretion but it did not have a significant effect on IL-1β secretion (**Figure 6B**).

DISCUSSION

In this study, we demonstrate that in human peripheral B-lymphocytes the NLRP3 inflammasome is differentially activated by fungal β-glucan and CpG antigens. Activation of NLRP3 by fungal β-glucan resulted in the cleavage of pro-IL-1β into its active form. While this is a well-known function of the NLRP3 in other cell types such as macrophages and dendritic cells, its role in peripheral human B-lymphocytes was not yet clearly understood. Furthermore, herein we have shown that IL-1β secretion was mediated through the major β-glucan receptor Dectin-1 and required signaling through Syk, consistent with our prior observations of β-glucan signaling in B-lymphocytes and current knowledge in other immune cells (6, 7, 11, 34–36). IL-1β

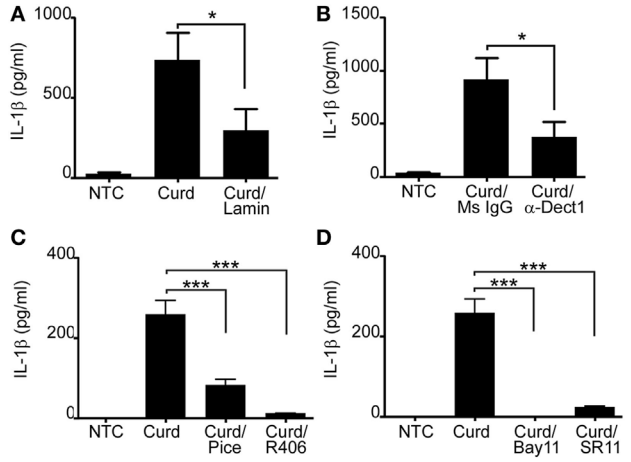

FIGURE 4 | Dectin-1 partially mediates IL-1β secretion and requires SYK and the transcriptions factors AP-1 and NF-κB. IL-1β ELISA measured in the cell supernatant of curdlan (Curd) stimulated cells in the presence or absence of 1 mg/ml Laminarin (Lamin) **(A)**, 5 μg/ml anti-dectin-1 antibody (α-Dect1) or 5 μg/ml isotype control (Ms IgG) **(B)**, 40 μM of the SYK inhibitor, piceatannol (pice) and 5 μM of the SYK inhibitor, R406 **(C)**, and 10 μM of the NF-κB inhibitor, Bay11, and 10 μM of the AP-1 inhibitor, SR11 **(D)**. Data are representative of at least three donors in each independent experiments ($n = 3$). $^{*}p < 0.05$, $^{***}p < 0.0001$.

regulation was mediated by the transcription factors NF-κB and AP-1 known to be necessary for the transcription of pro-IL-1β (35, 37). Once pro-IL-1β is formed then subsequent activation of the NLRP3 inflammasome is necessary for the processing of the inactive pro-IL-1β into the active or mature form. Activation of the inflammasome *via* the canonical and non-canonical pathways has been described in other cell types (13, 35, 38). For instance, in dendritic cells, Dectin-1 participates not only in the activation of NF-κB and synthesis of pro-IL-1β by curdlan-activated dendritic cells but also in the production of mature IL-1β through a non-canonical inflammasome that recruits ASC and caspase-8 to the complex CARD-Malt-BCL10 (38). Caspase-8 has also been reported as an effector and regulator molecule of the canonical NLRP3 inflammasome that drives IL-1β production (13). Herein, we demonstrate that stimulation of B-lymphocytes with β-glucan and CpG resulted in the activation of the canonical NLRP3 pathway and involved both ASC and caspase-1 activation. Interestingly, while β-glucan-mediated IL-1β secretion via Dectin-1-Syk-NF-κB/AP-1 pathways and canonical NLRP3 activation, CpG stimulation of B-lymphocytes also resulted in the activation of the canonical NLRP3 inflammasome, but triggered the secretion of IgM and not IL-1β. The lack of IL-1β was likely due to the absence of pro-IL-1β which limited the production of the active form since no substrate was available.

Studies have shown that host immunity against disseminated *candida*, *aspergillosis*, and *pneumocystis* infection relies on IL-1β to clearly mount an adequate immune response, particularly in early stages of disease (17, 39–41). Impaired IL-1β secretion results in decreased recruitment of neutrophils, macrophages, and lymphocytes to the lungs, affecting the phagocytosis and killing of the fungi (17). IL-1β also acts by activating the release of other inflammatory cytokines, like IL-6 and TNFα as well as inducing Th17 polarization, all important mediators in antifungal defense (42). Furthermore, IL-1β is also involved in the pathogenesis of many inflammatory diseases such as familial mediterranean fever, familial cold-induced auto-inflammatory syndrome, steroid-resistant asthma, and rheumatoid arthritis (43–46). In most of these diseases, blocking IL-1β by monoclonal antibodies or blocking the NLRP3 inflammasome provide symptomatic relief and are currently the standard clinical treatment strategies. Understanding IL-1β regulation in B-lymphocytes offers a new way to potentially develop treatments that will continue to improve the clinical course of patients, not only during the acute infectious process, but potentially by ameliorating these chronic inflammatory conditions as well.

Over the last decade, microbiome studies have clearly demonstrated that the lower respiratory tract is colonized by many organisms and is not sterile as initially assumed. It is very likely that the lung microbiome, similar to the intestinal microbiome, plays an important role in maintaining the well-functioning defense mechanisms of the respiratory mucosa (47). It is also highly probable that bacterial and fungal antigens, through activation of PRRs, help to keep the immune system in a basal activation state that ultimately results in the well-being of the host. However, if this balance is disrupted, and the microbiota loses diversity, the more prevalent microbial antigens through the same PRR would have no regulatory negative feedback resulting in an exaggerated inflammatory response. In the clinical setting, single or paucity fungal colonization in the airway is not uncommon, particularly in immunosuppressed patients. While the clinical significance of this finding is unknown, in the majority of the cases it gets overlooked, as the thought is that it does not result in a clinically significant illness. While this may be true, our observations suggest that fungal antigens are potential triggers of IgM, IL-1β, and other inflammatory cytokines (IL-8, IL-6, and TNFα) that can potentially act as chronic stimuli for B-lymphocytes. Thus, it is important to recognize that fungal activated B-lymphocytes, while they can contribute to host protection against fungal diseases in the right clinical setting, they can also result in a source of chronic inflammation.

Contrary to what we observed in β-glucan-stimulated B-lymphocytes, our data also showed that CpG, while activating the NLRP3 inflammasome, did not result in IL-1β secretion, but upregulated IgM secretion *via* the mTOR signaling pathway (see proposed mechanism in **Figure 7**). The role of NLRP3 in antibody production has been suggested in animal models (8); however it has not been investigated in human B-lymphocytes. Herein, we showed that inhibition of NLRP3 decreased IgM production in a dose-dependent manner while not affecting the secretion of other cytokines such as TNF-α, IL-6, and MMP-7, suggesting that the production of IgM is seemingly controlled by the NLRP3 inflammasome.

The mTOR pathway is ubiquitously expressed in immune cells, including B-lymphocytes (48, 49). Upon activation it regulates important cell processes such as protein translation, cell growth and proliferation (50). mTOR functions as two signaling complexes, mTOR complex 1 (mTOR1) and mTOR complex 2 (mTOR2).

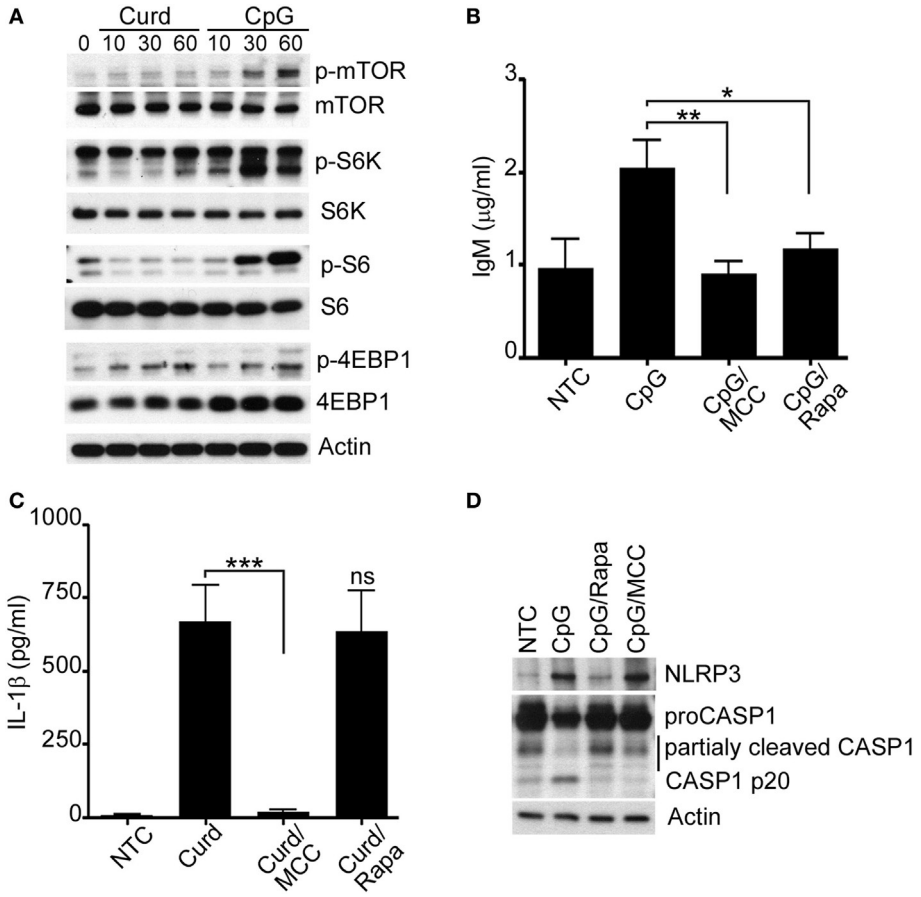

FIGURE 5 | Mammalian target of rapamycin (mTOR) regulates IgM production. **(A)** Immunoblot analysis of p-mTOR, p-S6K, p-S6, p-4EBP1 after curdlan (Curd) or CpG stimulation, for the indicated periods of time. Total mTOR, S6K, S6, 4EBP1 and actin were used as protein control. IgM **(B)** and IL-1β **(C)** ELISA were measured in the cell supernatant of unstimulated cells (NTC), CpG stimulated cells, and CpG stimulated cells in the presence of MCC950 (MCC) and Rapamycin (Rapa) for 24 h. **(D)** Immunoblot analysis of NLRP3, and Caspase-1 in NTC, after CpG stimulation in the presence and absence of MCC950 (MCC) and Rapamycin (Rapa). Actin was used as protein loading control. Cells were stimulated with 200 μg/ml curdlan and 1 μg/ml CpG and pre-incubated with 100 μM of MCC950 and 100 nM Rapamycin. Data are representative of at least three donors in each independent experiments ($n = 3$). $^{*}p < 0.05$, $^{**}p < 0.01$, $^{***}p < 0.0001$.

Activation of mTOR1 results in phosphorylation of p70-s6K (S6K), S6, and eukaryotic initiation factor 4E-binding protein (4E-BP1) which is important for the regulation of protein synthesis (50). Herein, we found phosphorylation of S6, S6K, and 4EBP-E after CpG stimulation. Furthermore, the use of Rapamycin, a well-described mTOR1 inhibitor, decreased IgM secretion. The use of Rapamycin also affected NLRP3 and caspase-1 activation, therefore impairing the function of NLRP3 inflammasome complex and suggesting that IgM regulation is not only mediated by NLRP3 but also by mTOR. Prior observations in macrophages also suggest that mTOR inhibition suppresses NLRP3 inflammasome activation in macrophages (31). In their study, mTOR regulated HK1-dependent glycolysis was critical for NLRP3 activation. While further investigations are needed in B-lymphocytes, studies to deeply understand the specific mechanism by which mTOR and NLRP3 are controlling antibody regulation in B-lymphocytes studies have shown that mTOR participates in the regulation of high affinity antibodies (51). Furthermore, in animal models, impaired mTOR signaling in follicular and marginal B-lymphocytes stimulated by LPS show a marked reduction of IgM and IgG (50, 52). That mTOR is important for germinal center formation is known (48) however, little is known about the unique function of mTOR in circulating human B-lymphocytes. Here, we have demonstrated the participation of mTOR in NLRP3 function and regulation of IgM. Interestingly, while β-glucans are able to trigger different cytokines and chemokines, they fail to induce IgM in human peripheral B-lymphocytes (7). These data differ from prior studies in murine models in which curdlan stimulation seemed to induce IgM secretion (8). While the differences seen between the two experimental models could be explained by the differences in the experimental methodology and the lack of β-glucan to induce proliferation in the human cells; herein, we have shown the inability of curdlan to trigger mTOR activation, a step found to be important for IgM secretion. Our observations are novel and raise awareness of the role of NLRP3 as regulator not only of IL-1β and IL-18 but also of IgM. Interestingly, despite NLRP3 activation, IL-18 was not induced by β-glucan or CpG in peripheral B-lymphocytes (7).

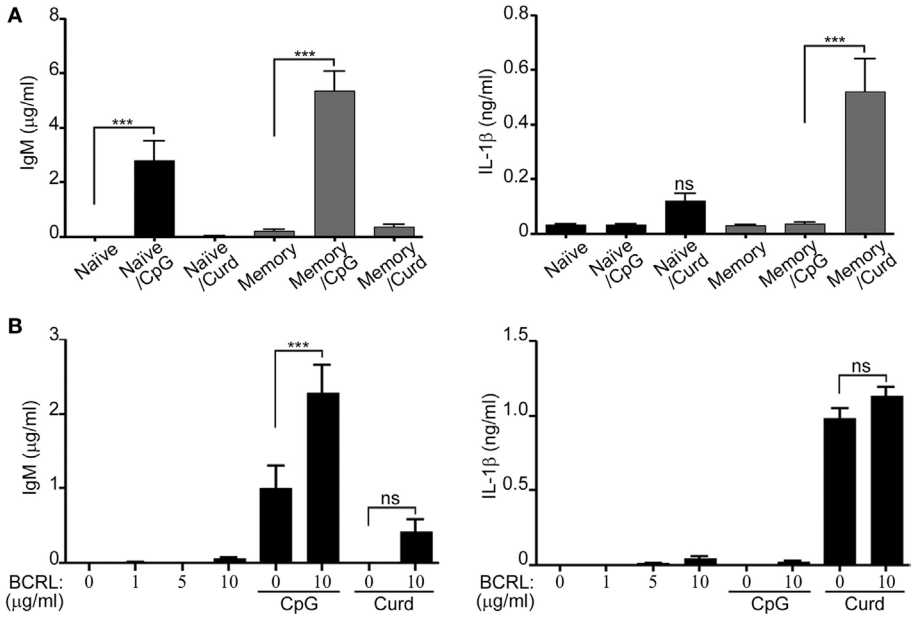

FIGURE 6 | Different levels of IL-1β and IgM secretion by stimulated naïve and memory B-lymphocytes. B-lymphocytes were isolated by negative selection, stained for 30 min with anti-CD20 and anti-CD27 antibodies, and sorted into ($CD20^+CD27^+$ and $CD20^+CD27^-$). Sorted cells were then plated at 2×10^6/ml and stimulated with CpG and curdlan (Curd) **(A)** or with B cell receptor ligand (BCRL) alone or in combination with CpG or curdlan **(B)** as indicated. IgM and IL-1β ELISA were measured in the cell supernatant 72 h later. 200 μg/ml curdlan and 1 μg/ml CpG were used unless otherwise specified. Data are representative of at least three donors in each independent experiment ($n = 2$) $^{***}p < 0.0001$, ns, not significant ($p > 0.05$).

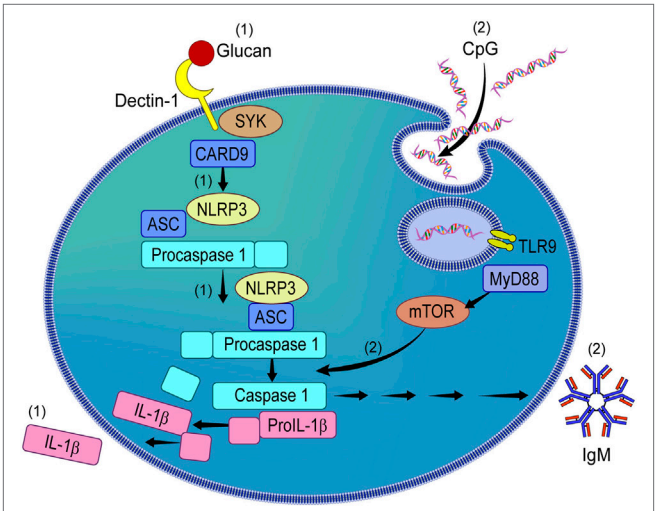

FIGURE 7 | Proposed mechanism of NLRP3 activation by β-glucan and CpG in circulating human B-lymphocytes. β-glucan and CpG activate NLRP3 in peripheral B-lymphocytes. While β-glucan activated B-lymphocytes secrete IL-1β *via* NLRP3 activation **(1)**, CpG does not induce IL-1β but IgM **(2)**. CpG-induced IgM *via* NLRP3 is mammalian target of rapamycin (mTOR)-dependent but not β-glucan-mediated IL-1β secretion.

Beyond their antibody-producing role, B-lymphocytes can affect the local immune environment through the release of cytokines and other proteins; however, how they modulate and contribute to the orchestration of the innate immune system is not clearly understood. Our group has recently shown that activated B-lymphocytes participate in the recruitment of neutrophils by releasing IL-8 and indirectly by contributing to the release of syndecan-4 *via* MMP-7 (6, 7). Syndecan proteins are expressed on the cell membrane and can be shed into the extracellular space by metalloproteases (53). Upon shedding they are free to bind to different cytokines participating in the regulation of cytokine influx and neutrophil recruitment (54–56). Herein, we further demonstrated that B-lymphocytes also contribute to the pool of IL-1β, a pro-inflammatory cytokine very important for antimicrobial host defense (42) and to the secretion of IgM antibodies. Naïve and memory B-lymphocytes play different roles in the regulation of the immune response by releasing different cytokine profiles (2). Here, we investigated the specific B-lymphocyte subtype responsible for IL-1β and IgM secretion and contrary to what we have observed with MMP-7, which was mostly released by naïve cells, memory cells were found to be the main source for both IL-1β and IgM (6). While the exact mechanisms by which different B-lymphocyte subtypes seem to preferentially secrete a specific cytokine milieu is not totally understood, these patterns are not fixed and can be influenced by the circumstances that surround their activation such as presence of T-lymphocytes and other inflammatory cells, by the integration of different signals from multiple receptors and by the proportion of the different B-lymphocytes compartments (2, 33, 57). These are important observations with therapeutic implications as B-lymphocyte reconstitution after Rituximab (B-lymphocyte depleted agent) treatment favors naïve B-lymphocytes (33). Increased numbers of naïve

B-lymphocytes, based on our observations, will result in a decrease of IL-1β and IgM levels potentially contributing to a less inflammatory milieu. How these changes may affect antimicrobial and anti-inflammatory host response need to be further investigated.

In summary, this study identified that the NLRP3 inflammasome is essential for two independent processes, pro-inflammatory cytokine secretion and antibody regulation. Whether NLRP3 activation resulted in cytokine or antibody regulation depended on the stimulating antigen with IL-1β secretion being triggered by fungal β-glucans and IgM by CpG. NLRP3 regulation was also differently regulated upon β-glucan or CpG antigens and was mTOR-independent when stimulated by β-glucans but mTOR-dependent upon CpG stimulation. The new role of the NLRP3 inflammasome and the mTOR pathway as regulators of IL-1β and IgM in activated B-lymphocytes studied here offers a potential new strategy to treat autoimmune disease in which IL-1β and pathogenic IgM antibodies may play a role, particularly if triggered by infectious agents. Further investigations are therefore needed to clarify the potential benefits of mTOR and NLRP3 inhibitors in these clinical settings.

AUTHOR CONTRIBUTIONS

Concept and design; data acquisition; and data interpretation/analysis: EC, MA, HD, and VV; manuscript drafting: EC, MA, and VV; manuscript review: all authors.

ACKNOWLEDGMENTS

We thank Dr. Peikert and Dr. Limper and all the members Dr. Limper's laboratory and the Mayo Clinic Thoracic Diseases Research Unit for their many helpful discussions.

FUNDING

Funded by NIH grants K08 (HL112849) to EC and funds from the Annenberg Foundation.

SUPPLEMENTARY MATERIAL

The Supplementary Material for this article can be found online at http://www.frontiersin.org/article/10.3389/fimmu.2017.01504/full#supplementary-material.

REFERENCES

1. Verma A, Wuthrich M, Deepe G, Klein B. Adaptive immunity to fungi. *Cold Spring Harb Perspect Med* (2014) 5:a019612. doi:10.1101/cshperspect.a019612
2. Lund FE. Cytokine-producing B lymphocytes-key regulators of immunity. *Curr Opin Immunol* (2008) 20:332–8. doi:10.1016/j.coi.2008.03.003
3. Mauri C, Bosma A. Immune regulatory function of B cells. *Annu Rev Immunol* (2012) 30:221–41. doi:10.1146/annurev-immunol-020711-074934
4. Ramirez-Ortiz ZG, Specht CA, Wang JP, Lee CK, Bartholomeu DC, Gazzinelli RT, et al. Toll-like receptor 9-dependent immune activation by unmethylated CpG motifs in *Aspergillus fumigatus* DNA. *Infect Immun* (2008) 76:2123–9. doi:10.1128/IAI.00047-08
5. Krieg AM. CpG motifs in bacterial DNA and their immune effects. *Annu Rev Immunol* (2002) 20:709–60. doi:10.1146/annurev.immunol.20.100301.064842
6. Ali MF, Dasari H, Van Keulen VP, Cornec D, Vasmatzis G, Peikert T, et al. Microbial antigens stimulate metalloprotease-7 secretion in human B-lymphocytes using mTOR-dependent and independent pathways. *Sci Rep* (2017) 7:3869. doi:10.1038/s41598-017-04199-2
7. Ali MF, Driscoll CB, Walters PR, Limper AH, Carmona EM. Beta-glucan-activated human B lymphocytes participate in innate immune responses by releasing proinflammatory cytokines and stimulating neutrophil chemotaxis. *J Immunol* (2015) 195:5318–26. doi:10.4049/jimmunol.1500559
8. Kumar H, Kumagai Y, Tsuchida T, Koenig PA, Satoh T, Guo Z, et al. Involvement of the NLRP3 inflammasome in innate and humoral adaptive immune responses to fungal beta-glucan. *J Immunol* (2009) 183:8061–7. doi:10.4049/jimmunol.0902477
9. Agostini L, Martinon F, Burns K, McDermott MF, Hawkins PN, Tschopp J. NALP3 forms an IL-1beta-processing inflammasome with increased activity in Muckle-Wells autoinflammatory disorder. *Immunity* (2004) 20:319–25. doi:10.1016/S1074-7613(04)00046-9
10. Franchi L, Eigenbrod T, Munoz-Planillo R, Nunez G. The inflammasome: a caspase-1-activation platform that regulates immune responses and disease pathogenesis. *Nat Immunol* (2009) 10:241–7. doi:10.1038/ni.1703
11. Gringhuis SI, den Dunnen J, Litjens M, van der Vlist M, Wevers B, Bruijns SC, et al. Dectin-1 directs T helper cell differentiation by controlling noncanonical NF-kappaB activation through Raf-1 and Syk. *Nat Immunol* (2009) 10:203–13. doi:10.1038/ni.1692
12. Gurung P, Kanneganti TD. Novel roles for caspase-8 in IL-1beta and inflammasome regulation. *Am J Pathol* (2015) 185:17–25. doi:10.1016/j.ajpath.2014.08.025
13. Antonopoulos C, Russo HM, El Sanadi C, Martin BN, Li X, Kaiser WJ, et al. Caspase-8 as an effector and regulator of NLRP3 inflammasome signaling. *J Biol Chem* (2015) 290:20167–84. doi:10.1074/jbc.M115.652321
14. Manners DJ, Masson AJ, Patterson JC. The heterogeneity of glucan preparations from the walls of various yeasts. *J Gen Microbiol* (1974) 80:411–7. doi:10.1099/00221287-80-2-411
15. Dietz AB, Bulur PA, Emery RL, Winters JL, Epps DE, Zubair AC, et al. A novel source of viable peripheral blood mononuclear cells from leukoreduction system chambers. *Transfusion* (2006) 46:2083–9. doi:10.1111/j.1537-2995.2006.01033.x
16. Klinman DM, Yi AK, Beaucage SL, Conover J, Krieg AM. CpG motifs present in bacteria DNA rapidly induce lymphocytes to secrete interleukin 6, interleukin 12, and interferon gamma. *Proc Natl Acad Sci U S A* (1996) 93:2879–83. doi:10.1073/pnas.93.7.2879
17. Chen W, Havell EA, Moldawer LL, McIntyre KW, Chizzonite RA, Harmsen AG. Interleukin 1: an important mediator of host resistance against *Pneumocystis carinii*. *J Exp Med* (1992) 176:713–8. doi:10.1084/jem.176.3.713
18. Vonk AG, Netea MG, van Krieken JH, Iwakura Y, van der Meer JW, Kullberg BJ. Endogenous interleukin (IL)-1 alpha and IL-1 beta are crucial for host defense against disseminated candidiasis. *J Infect Dis* (2006) 193:1419–26. doi:10.1086/503363
19. Coll RC, Robertson AA, Chae JJ, Higgins SC, Munoz-Planillo R, Inserra MC, et al. A small-molecule inhibitor of the NLRP3 inflammasome for the treatment of inflammatory diseases. *Nat Med* (2015) 21:248–55. doi:10.1038/nm.3806
20. Eisenbarth SC, Colegio OR, O'Connor W, Sutterwala FS, Flavell RA. Crucial role for the Nalp3 inflammasome in the immunostimulatory properties of aluminium adjuvants. *Nature* (2008) 453:1122–6. doi:10.1038/nature06939
21. Kool M, Petrilli V, De Smedt T, Rolaz A, Hammad H, van Nimwegen M, et al. Cutting edge: alum adjuvant stimulates inflammatory dendritic cells through activation of the NALP3 inflammasome. *J Immunol* (2008) 181:3755–9. doi:10.4049/jimmunol.181.6.3755
22. Li H, Willingham SB, Ting JP, Re F. Cutting edge: inflammasome activation by alum and alum's adjuvant effect are mediated by NLRP3. *J Immunol* (2008) 181:17–21. doi:10.4049/jimmunol.181.1.17
23. Krieg AM, Yi AK, Matson S, Waldschmidt TJ, Bishop GA, Teasdale R, et al. Cpg motifs in bacterial-DNA trigger direct B-cell activation. *Nature* (1995) 374:546–9. doi:10.1038/374546a0
24. Brown GD, Taylor PR, Reid DM, Willment JA, Williams DL, Martinez-Pomares L, et al. Dectin-1 is a major beta-glucan receptor on macrophages. *J Exp Med* (2002) 196:407–12. doi:10.1084/jem.20020470

25. Carmona EM, Vassallo R, Vuk-Pavlovic Z, Standing JE, Kottom TJ, Limper AH. Pneumocystis cell wall beta-glucans induce dendritic cell costimulatory molecule expression and inflammatory activation through a Fas-Fas ligand mechanism. *J Immunol* (2006) 177:459–67. doi:10.4049/jimmunol.177.1.459
26. Hemmi H, Takeuchi O, Kawai T, Kaisho T, Sato S, Sanjo H, et al. A toll-like receptor recognizes bacterial DNA. *Nature* (2000) 408:740–5. doi:10.1038/35047123
27. Cao W, Manicassamy S, Tang H, Kasturi SP, Pirani A, Murthy N, et al. Toll-like receptor-mediated induction of type I interferon in plasmacytoid dendritic cells requires the rapamycin-sensitive PI(3)K-mTOR-p70S6K pathway. *Nat Immunol* (2008) 9:1157–64. doi:10.1038/ni.1645
28. Takeshita F, Leifer CA, Gursel I, Ishii KJ, Takeshita S, Gursel M, et al. Cutting edge: role of toll-like receptor 9 in CpG DNA-induced activation of human cells. *J Immunol* (2001) 167:3555–8. doi:10.4049/jimmunol.167.7.3555
29. Bauer S, Kirschning CJ, Hacker H, Redecke V, Hausmann S, Akira S, et al. Human TLR9 confers responsiveness to bacterial DNA via species-specific CpG motif recognition. *Proc Natl Acad Sci U S A* (2001) 98:9237–42. doi:10.1073/pnas.161293498
30. Kawabata K, Murakami A, Ohigashi H. Citrus auraptene targets translation of MMP-7 (matrilysin) via ERK1/2-dependent and mTOR-independent mechanism. *FEBS Lett* (2006) 580:5288–94. doi:10.1016/j.febslet.2006.08.072
31. Moon JS, Hisata S, Park MA, DeNicola GM, Ryter SW, Nakahira K, et al. mTORC1-induced HK1-dependent glycolysis regulates NLRP3 inflammasome activation. *Cell Rep* (2015) 12:102–15. doi:10.1016/j.celrep.2015.05.046
32. Perez-Andres M, Paiva B, Nieto WG, Caraux A, Schmitz A, Almeida J, et al. Human peripheral blood B-cell compartments: a crossroad in B-cell traffic. *Cytometry B Clin Cytom* (2010) 78(Suppl 1):S47–60. doi:10.1002/cyto.b.20547
33. Duddy M, Niino M, Adatia F, Hebert S, Freedman M, Atkins H, et al. Distinct effector cytokine profiles of memory and naive human B cell subsets and implication in multiple sclerosis. *J Immunol* (2007) 178:6092–9. doi:10.4049/jimmunol.178.10.6092
34. Kankkunen P, Teirila L, Rintahaka J, Alenius H, Wolff H, Matikainen S. (1,3)-beta-glucans activate both dectin-1 and NLRP3 inflammasome in human macrophages. *J Immunol* (2010) 184:6335–42. doi:10.4049/jimmunol.0903019
35. Gross O, Poeck H, Bscheider M, Dostert C, Hannesschlager N, Endres S, et al. Syk kinase signalling couples to the Nlrp3 inflammasome for anti-fungal host defence. *Nature* (2009) 459:433–6. doi:10.1038/nature07965
36. Carmona EM, Kottom TJ, Hebrink DM, Moua T, Singh RD, Pagano RE, et al. Glycosphingolipids mediate pneumocystis cell wall beta-glucan activation of the IL-23/IL-17 axis in human dendritic cells. *Am J Respir Cell Mol Biol* (2012) 47:50–9. doi:10.1165/rcmb.2011-0159OC
37. Roman J, Ritzenthaler JD, Fenton MJ, Roser S, Schuyler W. Transcriptional regulation of the human interleukin 1beta gene by fibronectin: role of protein kinase C and activator protein 1 (AP-1). *Cytokine* (2000) 12:1581–96. doi:10.1006/cyto.2000.0759
38. Gringhuis SI, Kaptein TM, Wevers BA, Theelen B, van der Vlist M, Boekhout T, et al. Dectin-1 is an extracellular pathogen sensor for the induction and processing of IL-1beta via a noncanonical caspase-8 inflammasome. *Nat Immunol* (2012) 13:246–54. doi:10.1038/ni.2222
39. Hise AG, Tomalka J, Ganesan S, Patel K, Hall BA, Brown GD, et al. An essential role for the NLRP3 inflammasome in host defense against the human fungal pathogen *Candida albicans*. *Cell Host Microbe* (2009) 5:487–97. doi:10.1016/j.chom.2009.05.002
40. Sainz J, Perez E, Gomez-Lopera S, Jurado M. IL1 gene cluster polymorphisms and its haplotypes may predict the risk to develop invasive pulmonary aspergillosis and modulate C-reactive protein level. *J Clin Immunol* (2008) 28:473–85. doi:10.1007/s10875-008-9197-0
41. Wojtowicz A, Gresnigt MS, Lecompte T, Bibert S, Manuel O, Joosten LA, et al. IL1B and DEFB1 polymorphisms increase susceptibility to invasive mold infection after solid-organ transplantation. *J Infect Dis* (2015) 211:1646–57. doi:10.1093/infdis/jiu636
42. Netea MG, Simon A, van de Veerdonk F, Kullberg BJ, Van der Meer JW, Joosten LA. IL-1beta processing in host defense: beyond the inflammasomes. *PLoS Pathog* (2010) 6:e1000661. doi:10.1371/journal.ppat.1000661
43. Chae JJ, Wood G, Masters SL, Richard K, Park G, Smith BJ, et al. The B30.2 domain of pyrin, the familial Mediterranean fever protein, interacts directly with caspase-1 to modulate IL-1beta production. *Proc Natl Acad Sci U S A* (2006) 103:9982–7. doi:10.1073/pnas.0602081103
44. Hoffman HM, Rosengren S, Boyle DL, Cho JY, Nayar J, Mueller JL, et al. Prevention of cold-associated acute inflammation in familial cold autoinflammatory syndrome by interleukin-1 receptor antagonist. *Lancet* (2004) 364:1779–85. doi:10.1016/S0140-6736(04)17401-1
45. Kim RY, Pinkerton JW, Essilfie AT, Robertson AAB, Baines KJ, Brown AC, et al. Role for NLRP3 inflammasome-mediated, IL-1beta-dependent responses in severe, steroid-resistant asthma. *Am J Respir Crit Care Med* (2017) 196:283–97. doi:10.1164/rccm.201609-1830OC
46. Brennan FM, McInnes IB. Evidence that cytokines play a role in rheumatoid arthritis. *J Clin Invest* (2008) 118:3537–45. doi:10.1172/JCI36389
47. Man WH, de Steenhuijsen Piters WA, Bogaert D. The microbiota of the respiratory tract: gatekeeper to respiratory health. *Nat Rev Microbiol* (2017) 15:259–70. doi:10.1038/nrmicro.2017.14
48. Limon JJ, Fruman DA. Akt and mTOR in B cell activation and differentiation. *Front Immunol* (2012) 3:228. doi:10.3389/fimmu.2012.00228
49. Donahue AC, Fruman DA. Distinct signaling mechanisms activate the target of rapamycin in response to different B-cell stimuli. *Eur J Immunol* (2007) 37:2923–36. doi:10.1002/eji.200737281
50. Powell JD, Pollizzi KN, Heikamp EB, Horton MR. Regulation of immune responses by mTOR. *Annu Rev Immunol* (2012) 30:39–68. doi:10.1146/annurev-immunol-020711-075024
51. Keating R, Hertz T, Wehenkel M, Harris TL, Edwards BA, McClaren JL, et al. The kinase mTOR modulates the antibody response to provide cross-protective immunity to lethal infection with influenza virus. *Nat Immunol* (2013) 14:1266–76. doi:10.1038/ni.2741
52. Benhamron S, Tirosh B. Direct activation of mTOR in B lymphocytes confers impairment in B-cell maturation and loss of marginal zone B cells. *Eur J Immunol* (2011) 41:2390–6. doi:10.1002/eji.201041336
53. Manon-Jensen T, Itoh Y, Couchman JR. Proteoglycans in health and disease: the multiple roles of syndecan shedding. *FEBS J* (2010) 277:3876–89. doi:10.1111/j.1742-4658.2010.07798.x
54. Endo K, Takino T, Miyamori H, Kinsen H, Yoshizaki T, Furukawa M, et al. Cleavage of syndecan-1 by membrane type matrix metalloproteinase-1 stimulates cell migration. *J Biol Chem* (2003) 278:40764–70. doi:10.1074/jbc.M306736200
55. Li Q, Park PW, Wilson CL, Parks WC. Matrilysin shedding of syndecan-1 regulates chemokine mobilization and transepithelial efflux of neutrophils in acute lung injury. *Cell* (2002) 111:635–46. doi:10.1016/S0092-8674(02)01079-6
56. Park PW, Foster TJ, Nishi E, Duncan SJ, Klagsbrun M, Chen Y. Activation of syndecan-1 ectodomain shedding by *Staphylococcus aureus* alpha-toxin and beta-toxin. *J Biol Chem* (2004) 279:251–8. doi:10.1074/jbc.M308537200
57. Gray D, Gray M, Barr T. Innate responses of B cells. *Eur J Immunol* (2007) 37:3304–10. doi:10.1002/eji.200737728

Conflict of Interest Statement: The authors declare that the research was conducted in the absence of any commercial or financial relationships that could be construed as a potential conflict of interest.

Copyright © 2017 Ali, Dasari, Van Keulen and Carmona. This is an open-access article distributed under the terms of the Creative Commons Attribution License (CC BY). The use, distribution or reproduction in other forums is permitted, provided the original author(s) or licensor are credited and that the original publication in this journal is cited, in accordance with accepted academic practice. No use, distribution or reproduction is permitted which does not comply with these terms.

frontiers in Immunology

ORIGINAL RESEARCH
published: 13 December 2017
doi: 10.3389/fimmu.2017.01777

The Absence of NOD1 Enhances Killing of *Aspergillus fumigatus* Through Modulation of Dectin-1 Expression

Mark S. Gresnigt[1,2], Martin Jaeger[2], R. K. Subbarao Malireddi[3], Orhan Rasid[1], Grégory Jouvion[4], Catherine Fitting[1], Willem J. G. Melchers[5], Thirumala-Devi Kanneganti[3], Agostinho Carvalho[6,7], Oumaima Ibrahim-Granet[1†] and Frank L. van de Veerdonk[2†]*

[1] Unité de recherche Cytokines and Inflammation, Institut Pasteur, Paris, France, [2] Laboratory for Experimental Internal Medicine, Department of Internal Medicine, Radboud University Medical Center, Nijmegen, Netherlands, [3] Department of Immunology, St. Jude Children's Research Hospital, Memphis, TN, United States, [4] Unité Histopathologie Humaine et Modèles Animaux, Département Infection et Epidémiologie, Institut Pasteur, Paris, France, [5] Department of Medical Microbiology, Radboud University Medical Centre, Nijmegen, Netherlands, [6] Life and Health Sciences Research Institute (ICVS), School of Medicine, University of Minho, Braga, Portugal, [7] ICVS/3B's – PT Government Associate Laboratory, Braga/Guimarães, Portugal

OPEN ACCESS

Edited by:
Steven Templeton,
Indiana University School of Medicine, United States

Reviewed by:
Joshua J. Obar,
Dartmouth College, United States
Tiago W. P. Mineo,
Federal University of Uberlandia, Brazil

***Correspondence:**
Frank L. van de Veerdonk
frank.vandeveerdonk@radboudumc.nl

[†]These authors have contributed equally to this work.

Specialty section:
This article was submitted to Microbial Immunology, a section of the journal Frontiers in Immunology

Received: 26 September 2017
Accepted: 28 November 2017
Published: 13 December 2017

Citation:
Gresnigt MS, Jaeger M, Subbarao Malireddi RK, Rasid O, Jouvion G, Fitting C, Melchers WJG, Kanneganti T-D, Carvalho A, Ibrahim-Granet O and van de Veerdonk FL (2017) The Absence of NOD1 Enhances Killing of Aspergillus fumigatus Through Modulation of Dectin-1 Expression. Front. Immunol. 8:1777. doi: 10.3389/fimmu.2017.01777

One of the major life-threatening infections for which severely immunocompromised patients are at risk is invasive aspergillosis (IA). Despite the current treatment options, the increasing antifungal resistance and poor outcome highlight the need for novel therapeutic strategies to improve outcome of patients with IA. In the current study, we investigated whether and how the intracellular pattern recognition receptor NOD1 is involved in host defense against *Aspergillus fumigatus*. When exploring the role of NOD1 in an experimental mouse model, we found that *Nod1*$^{-/-}$ mice were protected against IA and demonstrated reduced fungal outgrowth in the lungs. We found that macrophages derived from bone marrow of *Nod1*$^{-/-}$ mice were more efficiently inducing reactive oxygen species and cytokines in response to *Aspergillus*. Most strikingly, these cells were highly potent in killing *A. fumigatus* compared with wild-type cells. In line, human macrophages in which NOD1 was silenced demonstrated augmented *Aspergillus* killing and NOD1 stimulation decreased fungal killing. The differentially altered killing capacity of NOD1 silencing versus NOD1 activation was associated with alterations in dectin-1 expression, with activation of NOD1 reducing dectin-1 expression. Furthermore, we were able to demonstrate that *Nod1*$^{-/-}$ mice have elevated dectin-1 expression in the lung and bone marrow, and silencing of *NOD1* gene expression in human macrophages increases dectin-1 expression. The enhanced dectin-1 expression may be the mechanism of enhanced fungal killing of *Nod1*$^{-/-}$ cells and human cells in which NOD1 was silenced, since blockade of dectin-1 reversed the augmented killing in these cells. Collectively, our data demonstrate that NOD1 receptor plays an inhibitory role in the host defense against *Aspergillus*. This provides a rationale to develop novel immunotherapeutic strategies for treatment of aspergillosis that target the NOD1 receptor, to enhance the efficiency of host immune cells to clear the infection by increasing fungal killing and cytokine responses.

Keywords: NOD1, *Aspergillus fumigatus*, nucleotide-binding oligomerization domain, dectin-1, fungal killing

INTRODUCTION

Invasive aspergillosis (IA) is an opportunistic fungal infection that globally affects hundreds of thousands severely immunocompromised patients on an annual basis (1). IA is associated with an unacceptable high mortality (2), yet modern antifungal drugs, patient isolation care, and prophylactic treatment strategies have not been able to reduce mortality over the past years. An increased knowledge of the antifungal host response is crucial for understanding the pathogenesis of the disease on one hand and on the other hand in the development of new immunomodulatory therapies, which are considered to be one of the few possibilities to decrease mortality associated with IA (3).

A fine-tuned interplay between recognition and signaling leads to the clearance of the fungus by the immune system, while defects in parts of these components or their absence have been associated with severe infections with the fungus. Although most types of PRRs, including toll-like receptors and C-type lectin receptors, have well-characterized roles in antifungal host defense (4, 5). Some PRRs have, however, not yet been evaluated for their role in antifungal host defense. Insights in these not yet explored PRRs might yield new insights in the pathogenesis of IA and provide potential candidate targets for novel treatment strategies.

The nucleotide-oligomerization domain (NOD) receptors play a crucial role in host defense against bacteria; however, only limited evidence is available regarding the role of these receptors in host defense against aspergillosis. One of the NOD receptors, NOD1, has been described to be able to activate NFκB in corneal epithelial cells in response to *Aspergillus fumigatus* (6). However, it is not yet investigated whether NOD1 plays a role in host defense against pulmonary aspergillosis. Overall, it is evident that NOD1 plays an important role in pulmonary host defense. NOD1 is highly expressed in the lung (7) and in lung epithelial cells (8). Human alveolar macrophages utilize NOD1 to induce proinflammatory cytokine responses and induce autophagy for an efficient host defense against *Mycobacterium tuberculosis* (9). Moreover, in host defense against *Legionella pneumophila*, NOD1 regulates neutrophil recruitment to the alveoli (10, 11). These studies of pulmonary host defense against bacteria reveal various mechanisms, induced by NOD1, that are known to play significant roles in host defense against *A. fumigatus*; e.g., autophagy machinery (12–15), neutrophil recruitment (16–18), and proinflammatory cytokines (19–21).

Therefore, the current study investigates the role of NOD1 in host defense against aspergillosis. Specifically, in a murine model representing immunocompromised hosts, we assess how NOD1 deficiency influences the host defense during aspergillosis. Using murine *Nod1*-deficient cells as well as silencing of *NOD1* gene expression in primary human cells, we systematically evaluated the importance of this receptor in the antifungal response. Novel insight into the exact biology of this receptor during aspergillosis can increase our understanding of the infection, which subsequently may lead to the development of immunotherapeutic strategies.

MATERIALS AND METHODS

Aspergillus fumigatus

A clinical isolate of *A. fumigatus* V05-27, which has been characterized previously (22), was used for all *ex vivo* and *in vitro* stimulations. Conidia and hyphae were prepared and heat-inactivated (HI) as previously described (23). A concentration of 1×10^7/mL was used in the experiments unless otherwise indicated. For *in vivo* experiments, the luciferase-expressing *A. fumigatus* 2/7/1 strain was used, which has been described previously (24); this strain has been reported to have a similar antifungal susceptibility and demonstrates no growth defects under various *in vitro* cultivation conditions such as different temperatures and carbon sources (24). In corticosteroid immunosuppressed mouse models of aspergillosis (25), the 2/7/1 strain demonstrated a similar virulence as observed for its parental strain CBS144.85 (26, 27).

In Vivo Experiments

Mice for *in vivo* experiments were supplied by the breeding center R. Janvier (Le Genest Saint-Isle, France). For the survival experiment in an immunosuppressed background C57/BL6 wild type (WT), and *Nod1*$^{-/-}$ mice (28 to 31 g, 10 weeks old) were used. Mice were immunosuppressed at day 4 and day 1 before infection by intraperitoneal injection of 200-µL cyclophosphamide (Sigma Aldrich) at 4 mg/mL. At the day of infection, mice were anesthetized by intramuscular injection (150 µL) of ketamine (10 mg/mL) and xylasine (10 mg/mL) hair was shaved from the ventral lung area and subsequently mice were inoculated intranasally with 5×10^4 luciferase-expressing *A. fumigatus* 2/7/1 conidia (24) in 25-µL PBS.

In all experiments, survival and weight was monitored during the course of infection. Bioluminescence imaging was acquired at day 1 post-infection (pi) and was continued on days 2, 3, 6, and 8 pi. Images were acquired using an IVIS 100 system (PerkinElmer, Waltham, MA, USA) as previously described (25).

For immunological and histological assessment female C57/BL6 and *Nod1*$^{-/-}$ mice (19–22 g, 8 weeks old) were used. They received similar immunosuppression regimen and were similarly infected as the mice for survival. Weight and bioluminescence were monitored daily during the course of infection. At day 3, the mice were euthanized. Serum and BAL were collected and lung homogenates were obtained following disruption in saline using the Retsch Mixer Mill 301 homogenizer. Cytokine concentrations in BAL and plasma were determined by ELISA as specified by the manufacturer (DuoSet; R&D Systems).

The fungal burden was determined by amplification of *Aspergillus* ITS2 regions. Briefly, homogenized tissue samples were used for DNA isolation by using the automated MagNA Pure system and the MagNA Pure LC Total Nucleic Acid Isolation Kit according to manufacturer's protocol (Roche Applied Science). PhHV was added to all samples as an internal isolation control C.

The concentration of total isolated DNA was measured by using the Quantus Fluorometer (Promega). *Aspergillus* loads were determined by real-time PCR using the LC480 instrument and the probes master kit (Roche applied Science). Thermocycling conditions were as follows: 37°C for 10 min,

95°C for 10 min, and 50 cycles: 95°C for 15 s, and 60°C for 45 s. The rDNA ITS2 region of *A. fumigatus* was detected by using primers 5′-GCGTCATTGCTGCCCTCAAGC-3′, 5′-ATATGC TTAAGTTCAGCGGGT-3′ and probe Cy5-TCCTCGAGCGTA TGGGGCTT-BBQ. The PhHV isolation control was detected by using primers 5′-GGGCGAATCACAGATTGAATC-3′, 5′-GCG GTTCCAAACGTACCAA-3′ and probe LC610-TTTTTATGT GTCCGCCACCATCTGGATC- BBQ. For the ITS2 detection, a twofold dilution series of the cloned PCR product was included to calculate the number of copies per reaction.

PBMC Isolation and Stimulation

Venous blood samples from healthy controls and patients were obtained after written informed consent. PBMCs were isolated as previously described (23). Briefly, blood was diluted in PBS (1:1) and fractions were separated by Ficoll (Ficoll-Paque Plus, GE Healthcare) density gradient centrifugation. Cells were washed twice with PBS and resuspended in RPMI-1640$^+$ (RPMI1640 Dutch modification supplemented with 10-μg/mL gentamycin, 2mM glutamax and 1mM pyruvate; Thermofisher).

PBMCs were plated in 96-well round-bottom plates (Corning) at a final concentration of 2.5×10^6 cells/mL and in a total volume of 200 μL and stimulated with medium (negative control) or live *Aspergillus* at a final concentration of 1×10^7/mL for 24 h. PBMCs in costimulation experiments were exposed to 10-μg/mL TriDAP (Invivogen) and subsequently stimulated with medium or live resting conidia (1×10^7/mL). After stimulation, culture supernatants were collected and stored at −20°C until cytokine measurement. Cells were either analyzed for surface receptor expression by flow cytometry or assessed for the fungal killing capacity.

Flow Cytometry

Surface pattern recognition receptor expression on human monocytes was assessed following stimulation of PBMCs with TriDAP as described above. Monocytes were stained with anti-human CD14 conjugated with FITC (BD) and anti-human CD45 conjugated with PE-Cy7 in combination with, anti-human CD282 (TLR2) Alexa647 (BD) and anti-human CD284 (TLR4) PE (Biolegend), or anti-human CD206 (Mannose Receptor) PE (Biolegend) and anti-human dectin-1 APC (R&D). CD14$^+$ monocytes were gated within the population of CD45$^+$ cells and subsequently, the mean fluorescence intensity (MFI) of TLR2, TLR4, Mannose receptor, and dectin-1 were assessed on the CD14$^+$/CD45$^+$ cells. For dectin-1 also a negative population was observed and the percentage of dectin-1$^+$ cells was assessed in addition to the MFI. The cells were measured on an FC500 flow cytometer (Beckman Coulter) and the data were analyzed using CXP analysis software v2.2 (Beckman Coulter).

Ex Vivo Stimulation of WT and *Nod1*$^{-/-}$ Murine Splenocytes and Bone Marrow-Derived Macrophages (BMDMs)

Wild-type and *Nod1*$^{-/-}$ C57Bl/6 mice were bred and maintained in the St. Jude Children's Research Hospital, Memphis, TN, USA. Spleens were homogenized in 0.4-μM cell strainer (BD) and the cell number was adjusted to 1×10^7/mL. The cell suspensions (500 μL/well) were placed in 24-well plates (corning) and incubated with culture medium or *Aspergillus* conidia for 1 or 5 days at 37°C and 5% CO_2.

Bone marrow from mice (age between 8 and 20 weeks old) was flushed out after dissecting mouse legs. Differentiation into macrophages (BMDMs) occurred in 5 days at 37°C (5% CO_2) in Dulbecco's modified eagles medium (DMEM) supplemented with 30% of L929 supernatant containing 10% fetal bovine serum (HI, Invitrogen), 100-U/mL penicillin and 100-mg/mL streptomycin. The BMDMs (1×10^5 /well) were placed in 96-well plates (corning) and incubated with culture medium or live *Aspergillus* conidia for 1 day at 37°C and 5% CO_2. After stimulation, culture supernatants were collected and stored at −20°C until cytokine measurement.

Silencing NOD1

Freshly isolated PBMCs were differentiated to macrophages using 6-day differentiation in 10% human serum (serum differentiated macrophages) or 10% human serum supplemented with 5-ng/mL GM-CSF (R&D Systems). After differentiation (1×10^5) macrophages were seeded in 96-well plates and left for 2 h at 37°C to subsequently transfect them with 25-nM NOD1 siRNA (on target) or scrambled (non-targeted siRNA) control siRNA (smartpool, Thermo Scientific) for 48 h at 37°C (Dharmafect, Thermo Scientific). Subsequently, the culture medium was refreshed and cells were used for killing, ROS assays, and PCR analysis.

Killing of *Aspergillus* by BMDMs, Human Macrophages, or PBMCs

Following differentiation, the mouse BMDMs (1×10^5), human MDMs (1×10^5), or freshly isolated PBMCs (5×10^5) were exposed to *Aspergillus* conidia (2×10^6) in 96-well plates a final volume of 200 μL. In several experiments dectin-1 was blocked using laminarin (100 μg/mL; Sigma Aldrich) or with a mouse dectin-1 blocking antibody (GE2; Thermo Fisher) or its isotype control. After 24 hat 37°C and 5% CO_2, the cells were washed in water and plated in serial dilution on Sabouraud agar plates. CFUs were counted after 24 h incubation at 37°C.

Quantitative Reverse Transcriptase PCR

RNA was isolated according to the protocol supplied with the TRIzol reagent. Isolated mRNA (1 μg) was reverse transcribed into cDNA using the iScript cDNA synthesis kit (BIORAD). Quantitative real-time PCR (qPCR) was performed using power SYBR Green PCR master mix (Applied Biosystems) and following primers for human samples hNOD1 Fwd 5′-AGAGGCTCTGCGGAACCA-3′ and Rev 5′-TGTGGAGATGCCGTTGGA-3′, hGAPDH Fwd 5′-AGGGGAGATTCAGTGTGGTG-3′ and Rev 5′-CGACC ACTTTGTCAAGCTCA-3′ hCLEC7A Fwd 5′-ACAATGCTG GCAACTGGGCT-3′ and Rev 5′-GCCGAGAAAGGCCTATC CAAAA-3′ hTLR2 Fwd 5′-GAATCCTCCAATCAGGCTTC TCT-3′ and Rev 5′-GCCCTGAGGGAATGGAGTTTA-3′ and the following primer sets form mouse samples mClec7a Fwd 5′-AGGTTTTTCTCAGCCTTGCCTTC-3′ and Rev 5′-GGG AGCAGTGTCTCTTACTTCC-3′, mGapdh Fwd 5′-AGGTC

GGTGTGAACGGATTTG-3′ and Rev 5′-TGTAGACCATGT AGTTGAGGTCA-3′. PCR was performed using an Applied Biosystems 7300 real-time PCR system using PCR conditions 2 min 50°C, 10 min 95°C followed by 40 cycles at 95°C for 15 s and 60°C for 1 min. The RNA genes of interest were corrected for differences in loading concentration using the signal of the housekeeping protein GAPDH.

IκBa Phosphorylation

For analysis of NFκB signaling pathways, the BMDMs were subcultured in 12-well cell culture plates for 16 h, and stimulated with live *Aspergillus* spores at 25 MOI of infection for indicated times. Protein lysates were prepared using the lysis buffer (10-mM Tris–HCl, 150-mM NaCl, 1% Nonidet P-40, supplemented with protease and phosphatase inhibitor cocktails; Roche). Protein samples were denatured by boiling in sample loading buffer-containing SDS and 100-mM DTT for 5 min and separated in denaturing SDS-PAGE. Separated proteins were transferred to PVDF membranes and immunoblotted with rabbit antibodies against total IκBa, Phospho-IκBa. All antibodies were purchased from Cell Signaling followed by secondary anti-rabbit HRP antibodies (JacksonImmunoResearch Laboratories).

Cytokine Measurements

The cytokine levels were measured using commercially available ELISA assays according to the protocol supplied by the manufacturer. IL-1β, TNFα, IL-17, and IL-22 assays were from R&D Systems and IFNγ was from Sanquin. Mouse IL-1β, TNFα, IL-6, KC, IL-17, IL-22, and IFNγ in splenocyte stimulations were measured using the Luminex multiplex platform (Millipore). In the *in vivo* experiments mouse IL-1β, TNFα, IL-6, KC, and G-CSF were measured using commercially available ELISA assays from R&D Systems according to the protocol supplied by the manufacturer.

NOD1 Immunofluorescence Staining

$CD14^+$ cells were isolated from PBMCs using magnetic bead isolation (MACS Miltenyi) according to the protocol supplied by the manufacturer. $CD14^+$ cells (1×10^5) were allowed to adhere for 1 h to 12-mm Ø glass coverslips. After adherence, the $CD14^+$ monocytes were exposed for 30 min to FITC labeled *Aspergillus* conidia in a ratio of (5:1/conidia/CD14 cells), after which the cells were fixed in Methanol. NOD1 was stained using rabbit anti-NOD1 and secondary stained with Goat anti-rabbit IgG H/L Alexa594 (Invitrogen). The coverslips were mounted in Vectashield with DAPI (Vector Laboratories) and immunofluorescence was observed at 1,000× magnification using a Zeiss LSM510 confocal microscope (Carl Zeiss).

Statistical Analysis

Data are presented as the mean ± SEM, or as scatterplots representing individual data points and a line indicating the median value of all the data obtained in experiments. Experiments were conducted at least twice and the number of biological replicates (mice/human donors) is indicated in the figure legends for each graph. Unless otherwise indicated the Mann–Whitney *U* test was used to determine statistical significant differences between experimental groups with $p < 0.05 = *$, $p < 0.01 = **$, $p < 0.001 = ***$, and $p < 0.0001 = ****$. All data were analyzed using Graphpad Prism v6.0.

RESULTS

NOD1 Localizes to *Aspergillus*-Containing Phagosomes

Since NOD1 is an intracellular pattern recognition receptor for bacterial ligands, we wanted to investigate at which cellular level NOD1 interacts with *Aspergillus*. To assess the location of NOD1 during the interaction of monocytes with *Aspergillus*, the monocytes of healthy human volunteers were allowed to engulf *Aspergillus*, both resting and swollen conidia, for 1 h. Subsequently, NOD1 was stained by immunofluorescence staining. We observed that engulfed *A. fumigatus* resting or swollen conidia demonstrate a halo of NOD1 surrounding the conidia, suggestion colocalization to the phagosomes containing *Aspergillus* (**Figure 1**). In addition to the halo surrounding the conidia, a diffuse cytoplasmic staining of NOD1 could be observed.

NOD1-Deficient Mice Do Not Develop IA

To investigate whether NOD1 plays a role in the susceptibility to aspergillosis, we subjected WT C57Bl6 and *Nod1*$^{-/-}$ mice to lethal *Aspergillus* infection. Survival experiments were performed in mice immunosuppressed with cyclophosphamide and subsequently infected with the bioluminescent *Aspergillus* strain 2/7/1 (24). In contrast to WT mice, *Nod1*$^{-/-}$ mice showed a significant improvement in 14-day survival (**Figure 2A**). Nine out of 12 *Nod1*$^{-/-}$ mice survived, whereas 12 out of 13 WT mice did not survive the infection. Bioluminescence imaging of the luciferase-expressing *Aspergillus* within the mice suggests that *Nod1*$^{-/-}$ mice more efficiently clear the fungi from the lung, whereas WT mice developed a progressing infection as indicated by the increasing luminescence signal (**Figure 2B**). When comparing the weight loss of mice post-infection we observed that *Nod1*$^{-/-}$ mice and a single-surviving WT mouse started to recover their weight from day 4 post-infection (pi), whereas all other WT mice sharply declined in weight and succumbed to the infection and the three non-surviving *Nod1*$^{-/-}$ mice demonstrated a similar weight loss as WT mice (**Figure 2C**).

Reduced Inflammation and Improved Fungal Clearance in Nod1-Deficient Mice

To investigate differences in fungal burden, histological damage and inflammation in a standardized fashion, an experiment was performed where cyclophosphamide immunosuppressed mice were infected with the bioluminescent *Aspergillus* strain 2/7/1, but were sacrificed at day 3 pi. The luminescence signal from the lung reveals that *Nod1*$^{-/-}$ mice have a significantly reduced fungal burden compared with WT mice (**Figure 3A**). This observation could be confirmed by a quantitative *Aspergillus* PCR, which revealed the absence of *Aspergillus* DNA in the lung homogenates of *Nod1*$^{-/-}$ mice. However, in the lung homogenates of WT mice *Aspergillus* could be detected (**Figure 3B**). To assess how fungal burden correlates with pathological

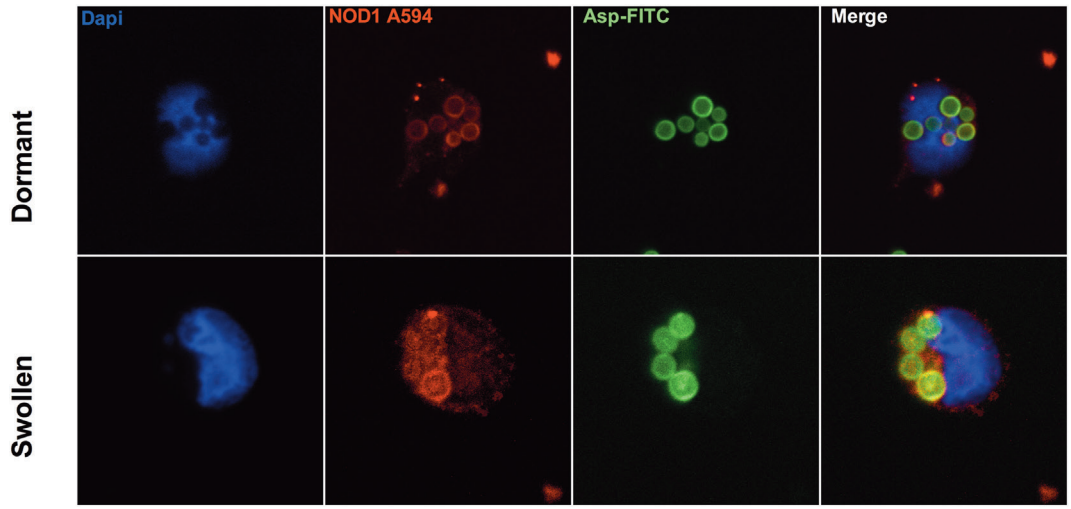

FIGURE 1 | NOD1 localizing to *Aspergillus*-containing phagosomes. Representative confocal immunofluorescence images at 100× magnification demonstrating co-localization of NOD1 (stained with rabbit-anti-humanNOD1, conjugated with Goat-anti-RabbitIgG-Alexa594) with engulfed FITC-labeled dormant or swollen *Aspergillus fumigatus* spores in human monocytes (nuclear stain: DAPI).

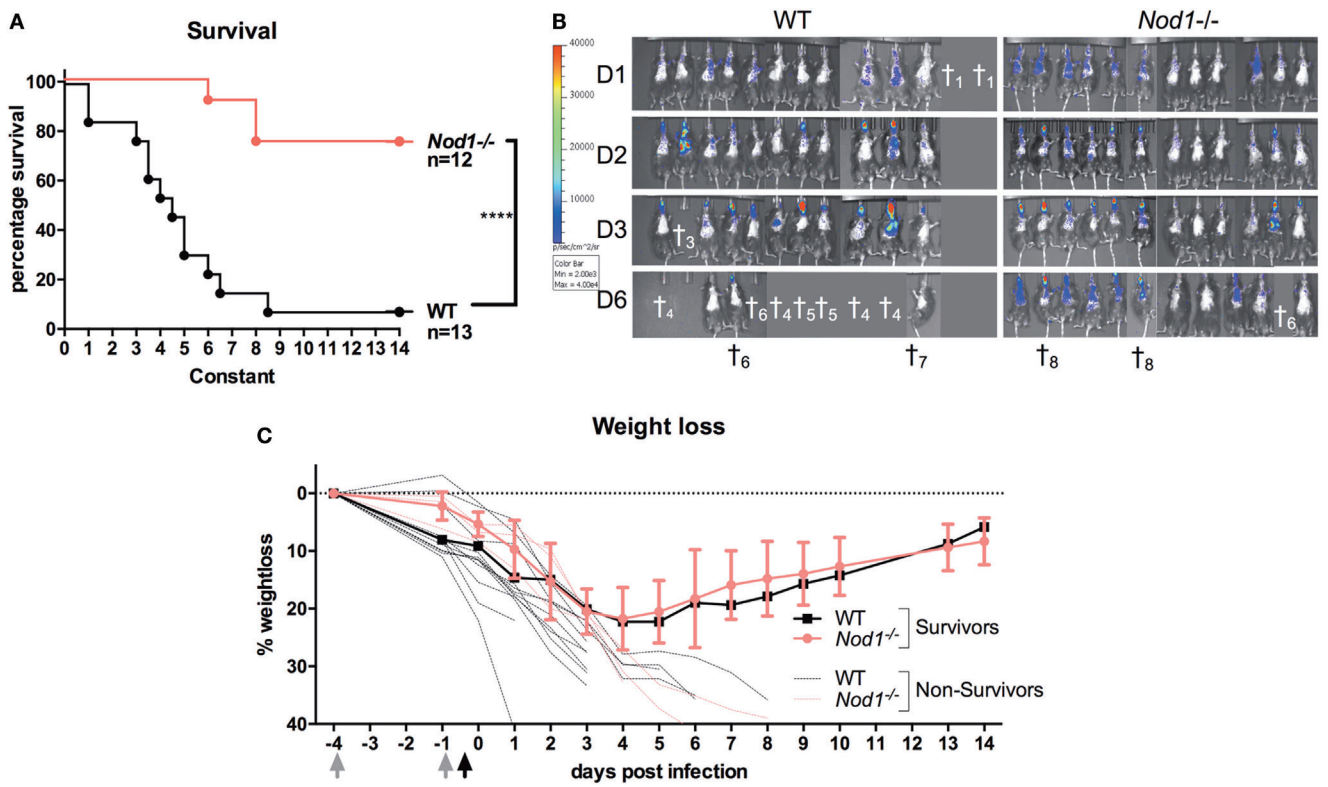

FIGURE 2 | Immunocompromised *Nod1*$^{-/-}$ mice protected against invasive aspergillosis. Assessment of survival, fungal burden and weight in cyclophosphamide immunosuppressed wild-type (WT) (n = 13) and *Nod1*$^{-/-}$ (n = 12) mice infected intranasally with 5 × 10^4 conidia in three separate experiments (WT:*Nod1*$^{-/-}$ 5:6; 3:3; 5:3). **(A)** Kaplan–Meier survival curve of WT (n = 13) and *Nod1*$^{-/-}$ (n = 12) mice. P-values of the Kaplan–Meier curve were determined using the log-rank test. Data represent the cumulative data of three separate experiments. **(B)** Bioluminescence imaging representing the fungal burden in the lungs of the mice during the course of the infection. **(C)** Representative graph of percentage weight loss of surviving mice in one of the experiments where survival of WT (n = 5; 4 died; n = 1 shown) and *Nod1*$^{-/-}$ (n = 6; 1 died; n = 5 shown) mice was compared.

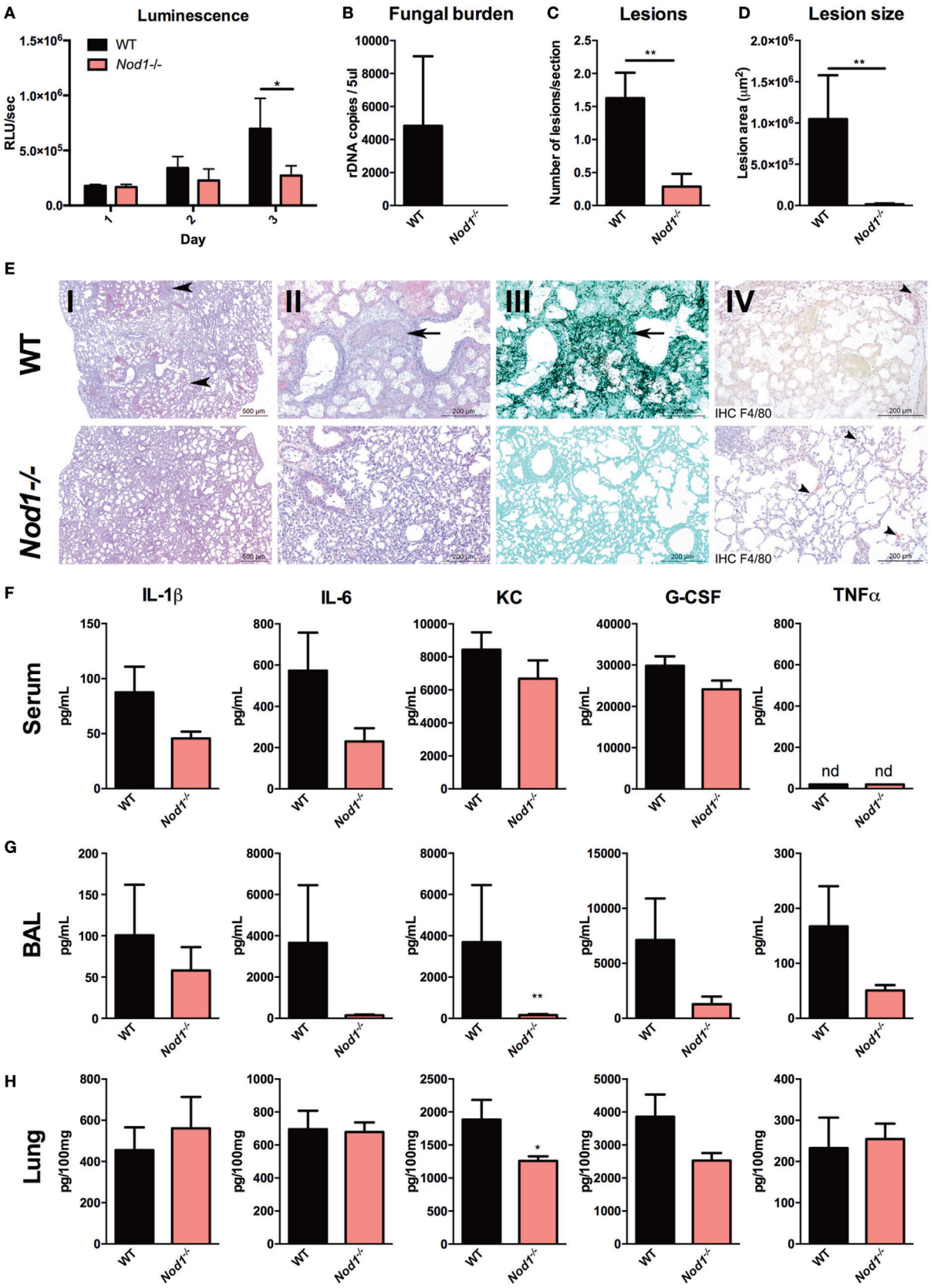

FIGURE 3 | Continued

FIGURE 3 | *Nod1*$^{-/-}$ mice reducing fungal burden, histological damage, and inflammation. Assessment of fungal burden, histopathological damage, and inflammation in *A. fumigatus*-infected wild-type (WT; $n = 8$) and *Nod1*$^{-/-}$ ($n = 7$) mice in two separate experiments (WT:*Nod1*$^{-/-}$ = 4:4 and 4:3). **(A)** Luminescence signal at day 1 to 3 post-infection revealing the fungal burden represented by the luminescence signal from live *Aspergillus* within infected WT and *Nod1*$^{-/-}$ mice. **(B)** Fungal burden as determined by amplification of *Aspergillus* ITS2 regions from lung homogenates. **(C–E)** Histology of lung sections of WT and *Nod1*$^{-/-}$ mice at day 3 pi, and morphometric analysis of the lesions in the whole lung sections using Image J software to quantify the lesions in **(C)** number and **(D)** size. Slides were stained by HE staining at [**(E)**; I] 2× and [**(E)**; II] 10x magnification, [**(E)**; III] Grocott's Methenamine Silver staining at 10× magnification or [**(E)**; IV] immunohistochemistry with anti-F4/80 antibody counterstained with HE staining. **(F–H)** IL-1β, IL-6, KC, G-CSF, and TNFα levels in **(F)** serum, **(G)** broncheoalveolar lavage (BAL), and **(H)** lung homogenates measured at day 3 pi. Data are represented as mean ± SEM and means were compared using the Mann–Whitney *U* test. *P*-values of statistical tests are shown within the graphs.

damage to the lungs, a histopathological analysis was performed. Morphometric analysis of the histology revealed significantly fewer lesions in the lung sections of *Nod1*$^{-/-}$ mice compared with WT mice (**Figure 3C**). Moreover, the size of the lesions affected a significantly smaller part of the lungs (**Figure 3D**). The morphometric analysis of pulmonary lesions corresponds with the finding that practically no fungi could be detected with Grocott methamine silver staining (**Figure 3E**, III). Based on immunohistochemistry for F4/80^{+} no differences in the presence of macrophages could be determined between WT and *Nod1*$^{-/-}$ mice (**Figure 3E**, IV). Systemic inflammation in the WT and *Nod1*$^{-/-}$ mice was assessed by measuring serum cytokine levels, and pulmonary inflammation was assessed by measuring cytokines in the BAL and in lung homogenates. Although *Nod1*$^{-/-}$ mice have a slight reduction in the levels of circulating proinflammatory cytokines, this was not significant compared with the WT mice (**Figure 3F**). In the BAL and lung homogenates, only a significant reduction in KC (CXCL1) levels were found when comparing *Nod1*$^{-/-}$ to the control group (**Figures 3G,H,** respectively). However, it must be noted that levels of other cytokines also tend to be lower in *Nod1*$^{-/-}$, but due to a large variation in the control group the differences are not significant.

Improved Cytokine Responses, Oxidative Burst, and Fungal Killing in Nod1 Deficient cells

Ex vivo cytokine responses to *Aspergillus* were investigated in *Nod1*-deficient cells to identify the underlying mechanisms of the phenotypes observed in *Nod1*$^{-/-}$ mice. Cytokine responses by WT and *Nod1*$^{-/-}$ BMDMs were investigated. *Nod1*$^{-/-}$ BMDMs demonstrated significantly higher cytokine responses, compared with WT BMDMs (**Figure 4A**). Moreover, splenocytes were isolated from naive *Nod1*$^{-/-}$ and WT C57Bl/6 mice and stimulated with *Aspergillus*. Although the cytokine responses produced by splenocytes in response to *Aspergillus* were generally low, *Nod1*$^{-/-}$ splenocytes produced significantly more TNFα and KC in response to *Aspergillus* (**Figure 4B**). The *Aspergillus*-induced, T-helper cell cytokines IL-17, and IFNγ were undetectable (ud) and IL-22 was very poorly induced by WT splenocytes, while these cytokines were significantly elevated in culture supernatants of *Nod1*$^{-/-}$ splenocytes (**Figure 4C**). In addition to cytokine release, zymosan- and *Aspergillus*-induced ROS by BMDMs was significantly higher in *Nod1*$^{-/-}$ BMDMs (**Figure 4D**). The area under the curve was calculated to illustrate the quantitative difference in ROS release, with zymosan or *Aspergillus*. We also investigated whether this increased responsiveness of *Nod1*$^{-/-}$ BMDMs correlated with an altered capacity to kill *A. fumigatus* conidia. *Nod1*$^{-/-}$ BMDMs were significantly more efficient in killing *Aspergillus* conidia than WT BMDMs (**Figure 4E**). Subsequently, we investigated whether the differential cytokine induction and activation of *Nod1*$^{-/-}$ cells was due to differences in the capacity of these cells to activate NFκB signaling. BMDMs were exposed to live *Aspergillus* spores and subsequently lysed to assess IκBa phosphorylation as a marker for NFκB activation by Western Blot. WT macrophages show a steady increase in IκBa phosphorylation after stimulation, whereas the level of IκBa phosphorylation varies over time in *Nod1*$^{-/-}$ BMDMs with a significant increase after 1 and 2 h (**Figure 4F**).

NOD1 Silencing Augments Oxidative Burst and Fungal Killing

Since *Nod1* deficiency impacts the killing capacity and ROS production in murine BMDMs, we validated these findings within a human background by silencing *NOD1* gene expression in human monocyte-derived macrophages (MDMs). *NOD1* silencing by siRNA targeting NOD1 (siNOD1) was confirmed by qPCR and a significant reduction of *NOD1* mRNA expression could be detected in both serum- and GM-CSF-differentiated MDMs (**Figure 5A**). Treatment with siNOD1 increased the killing capacity of MDMs when compared with cells that were transfected with scrambled siRNA (**Figure 5B**). ROS release was undetectable in the serum-differentiated MDMs; however, in GM-CSF-differentiated MDMs treated with siNOD1 the capacity to induce an oxidative burst was also slightly, yet significantly increased (**Figures 5C,D**).

NOD1 Signaling Suppresses Fungal Killing Capacity

Since we observed that NOD1 deficiency or silencing resulted in an increased capacity to eliminate *A. fumigatus* conidia, we investigated whether activation of NOD1 could thus have an inhibitory effect on the host response to *Aspergillus*. To assess the effect of NOD stimulation on oxidative burst, PBMCs were stimulated with TriDAP and subsequently exposed to zymosan. Oxidative burst induced by zymosan was also reduced by pre-stimulation with the NOD1 ligand (**Figure 6A**). NOD ligands could potentially induce an oxidative burst thereby exhausting the cells; however, we found no detectable oxidative burst induced by NOD ligands (**Figure 6B**). Monocytes were differentiated with GM-CSF into MDMs and exposed to the NOD1 ligand

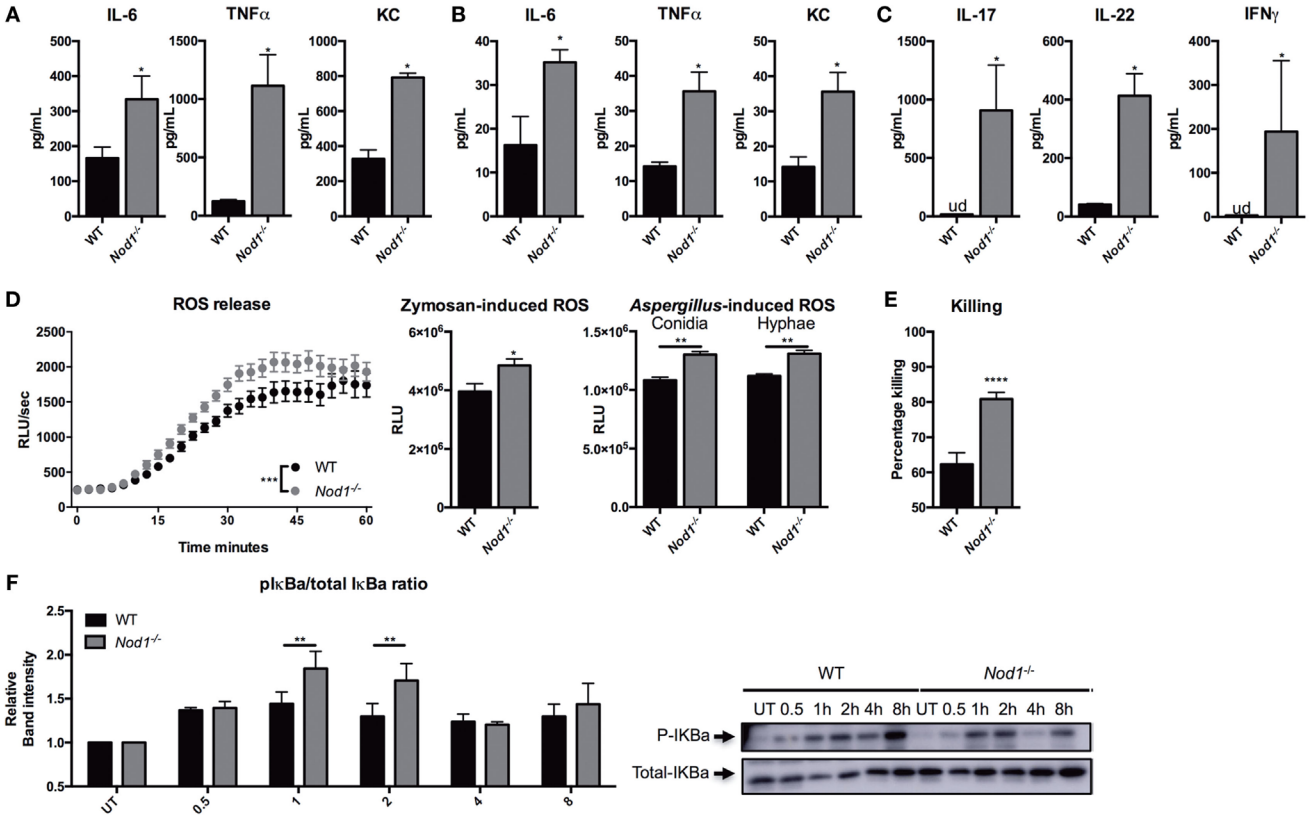

FIGURE 4 | *Nod1*-deficient cells showing an augmented antifungal host response. **(A)** IL-6, TNFα, KC, in culture supernatants of bone marrow-derived macrophages (BMDMs) (1×10^5) from wild-type (WT) and *Nod1*$^{-/-}$ mice ($n = 6$) that were stimulated for 24 h with heat inactivated *Aspergillus* conidia (2×10^6). **(B)** IL-6, TNFα, KC, and **(C)** IL-17, IL-22, and IFNγ levels in culture supernatants of splenocytes (1×10^6) from WT and *Nod1*$^{-/-}$ mice ($n = 5$ mice per group) that were stimulated for 5 days with heat inactivated *Aspergillus* conidia (2×10^7). **(D)** ROS release by WT and *Nod1*$^{-/-}$ BMDMs following exposure to zymosan ($n = 6$). Time points were compared for significance by two-way ANOVA. Area under the curve of the ROS luminescence data of *Aspergillus* spores ($n = 6$) and swollen conidia ($n = 6$) (1×10^7/mL) opsonized in 10% human serum and zymosan stimulated BMDMs. **(E)** CFU remaining of *A. fumigatus* plotted as percentage of input (2×10^6) following exposure for 24 h to WT ($n = 30$) and *Nod1*$^{-/-}$ ($n = 24$) BMDMs (1×10^5). **(F)** Representative Western Blot for phosphorylated and total IκBa in WT and *Nod1*$^{-/-}$ BMDMs following 0.5, 1, 2, 4, and 8 h of exposure to live *A. fumigatus spores*. IκBa phosphorylation measured as mean band intensity and corrected for total IκBa ($n = 3$). Data in bar plots are represented as mean ± SEM, data in scatter plots are represented as individual data points and median, and means were compared using the Mann–Whitney *U* test. ud = undetectable.

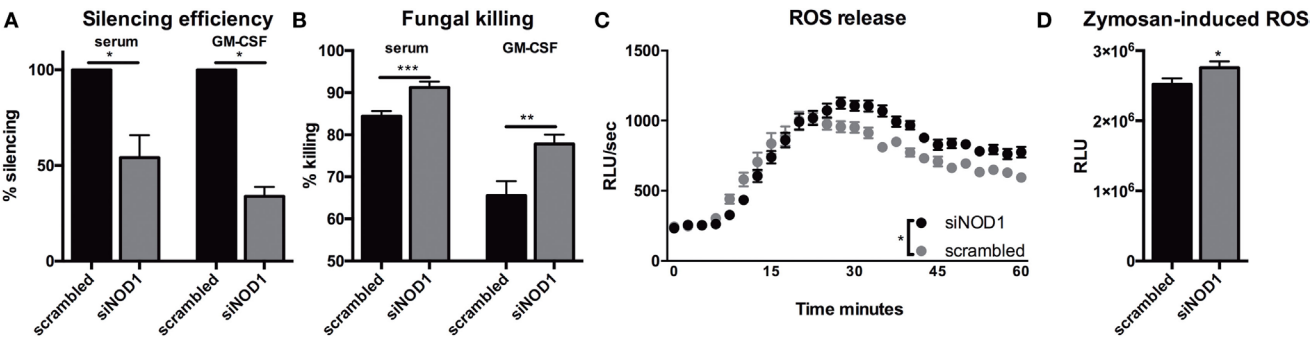

FIGURE 5 | Silencing of NOD1 gene expression in human monocyte-derived macrophages improves fungal killing and oxidative burst. **(A)** Silencing efficiency of siRNA targeting NOD1(siNOD1) compared with scrambled siRNA in human macrophages (1×10^5) differentiated in 10% serum ($n = 6$) or 10% serum with 5 ng/mL GM-CSF ($n = 7$). **(B)** CFU remaining of *A. fumigatus* plotted as percentage of input (2×10^6) following exposure for 24 h to human macrophages (1×10^5) differentiated in 10% serum or 10% serum with 5 ng/mL GM-CSF that were treated with scrambled siRNA or siNOD1. **(C,D)** ROS release by GM-CSF differentiated macrophages treated with scrambled siRNA or siNOD1following exposure to zymosan ($n = 5$). Time points were compared for significance by two-way ANOVA. Data in scatter plots are represented as individual data points and median. Means were compared using the Wilcoxon signed rank test. ud = undetectable.

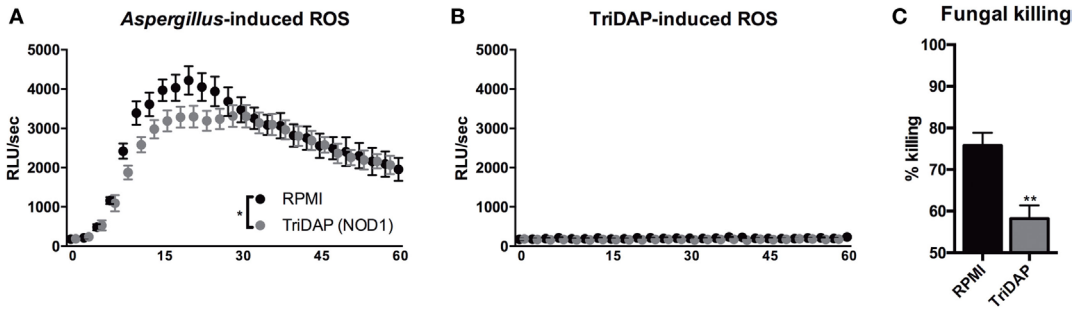

FIGURE 6 | NOD1 activation dampening protective antifungal effector functions in human cells. **(A,B)** ROS release by human PBMCs following exposure to **(A)** Zymosan, when cells were pre-stimulated for 24 h in presence or absence of (10 μg/mL) TriDAP ($n = 5$), or **(B)** culture medium or (10 μg/mL) TriDAP alone ($n = 3$). **(C)** Fungal killing capacity of human GM-CSF differentiated monocytes-derived macrophages assessed as CFU remaining of *A. fumigatus* plotted as percentage of input (2×10^6) following exposure for 24 h to (1×10^5), after 24-h pre-stimulation in the presence or absence of (10 μg/mL) TriDAP ($n = 9$). All plots represent mean ± SEM. Means were compared using the Wilcoxon signed rank test, except for ROS curves, which were compared for significance using two-way ANOVA.

TriDAP. MDMs that were exposed to TriDAP demonstrated a significantly reduced killing capacity compared with control cells (**Figure 6C**).

NOD1 Activation or Deficiency Modulates Expression of Dectin-1

Nucleotide-oligomerization domain receptors are known to interplay with TLRs *via* their downstream kinase RICK, and in particular with TLR2 (28–31). NOD1 deficiency or stimulation of NOD1 could very well impact killing, cytokine release, and ROS *via* modulation of PRRs. Therefore, surface expression of several PRRs, known to be involved in host defense against *Aspergillus*, were assessed by flow cytometry on PBMCs. Stimulation with TriDAP did not significantly affect TLR4 and MR expression on monocytes. dectin-1, however, was differentially regulated by NOD1 stimulation with a decrease of its expression (**Figure 7A**). This observation was also reflected by the number of dectin-1 positive monocytes (**Figure 7B**). To validate whether the reduced dectin-1 surface expression was regulated on a transcriptional level, RNA expression of *CLEC7A* (the gene encoding dectin-1) was assessed. Similarly, a decreased dectin-1 (*CLEC7A*) expression was observed (**Figure 7C**). In addition, siRNA treatment with siNOD1 of MDMs resulted in an increased dectin-1 (*CLEC7A*) expression (**Figure 7D**). To assess whether *Nod1*-deficient mice have altered dectin-1 expression, RNA was isolated from the lung, spleen, and bone marrow and dectin-1 (*Clec7A*) expression was measured. Compared with wild-type mice, *Nod1*-deficient mice had significantly elevated *Clec7A* expression in the lung and bone marrow, while only a trend toward increased *Clec7A* expression was observed in the spleen (**Figure 7E**). To determine whether the augmented killing capacity of human MDMs in which NOD1 is silenced is due to a functional enhancement of dectin-1 we systematically blocked dectin-1 using laminarin and dectin-1-blocking antibodies. The augmented killing capacity of human macrophages treated with *NOD1* targeting siRNA was abolished by dectin-1 blockade using laminarin or anti-human dectin-1 (**Figure 7F**). Similarly, laminarin mediated blockade of dectin-1 reversed the augmented fungal killing of *Nod1*$^{-/-}$ BMDMs (**Figure 7G**).

DISCUSSION

PRRs regulate the induction of an effective host defense against *A. fumigatus* through recognition of molecules present on the fungal cell wall and induction of potent antifungal effector mechanisms (4, 32). However, little is known about receptors that have a direct inhibitory effects on the induction of antifungal effector mechanisms. Here we demonstrate that the intracellular pattern recognition receptor NOD1 plays an inhibitory role in host response against *A. fumigatus*. We observed that NOD1 activation reduces fungal killing and the induction of oxidative burst. Conversely, murine *Nod1*-deficient cells or human cells in which *NOD1* gene expression was silenced show augmented fungal killing, oxidative burst, and cytokine responses. Most striking, despite being immunocompromised, *Nod1*$^{-/-}$ mice were observed to be less susceptible to *Aspergillus* infection, with reduced fungal burden, and pathological damage to the lungs. Finally, we demonstrate that the activity of NOD1 is inversely correlated with dectin-1 expression, where NOD1 stimulation reduces the expression of dectin-1, while *NOD1* silencing in human macrophages or murine *Nod1* deficiency was associated with increased *CLEC7A* (dectin-1) mRNA expression.

It is rarely observed that deficiency of a receptor is associated with decreased antifungal effector mechanisms. *Tlr9*$^{-/-}$ mice were found to be less susceptible to *Aspergillus* infection with reduced fungal burden (33). However, why TLR9 deficiency is protective is difficult to understand since TLR9 stimulation by CpG enhances the capacity of DCs to induce protective Th1 responses (34). Modulation of TLR5 in THP-1 cells is shown to negatively impact killing of *Aspergillus* conidia, with silencing of *TLR5* gene expression associated with increased fungal killing and activation of TLR5 with reduced fungal killing (35), reduced fungal killing was also observed in neutrophils (36). This modulation of fungal killing is similar to our data with NOD1 activation or siNOD1 in MDMs. However, a mutation in *TLR5* leading to a stop codon was identified as a risk factor for aspergillosis (37). Other than these PRRs, we are not aware of other receptors that negatively impact host defense against *Aspergillus*.

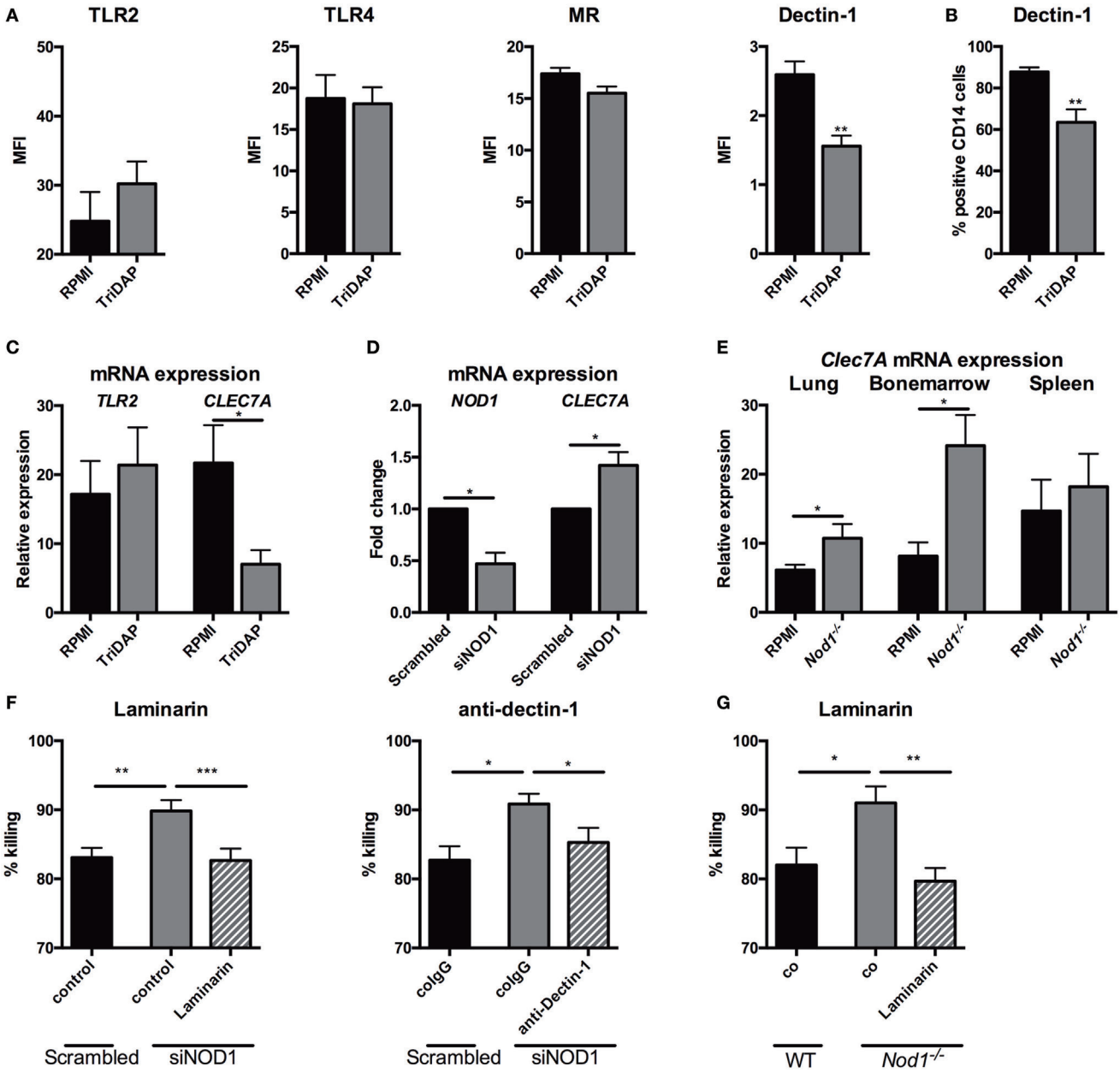

FIGURE 7 | NOD1 suppresses dectin-1 expression and NOD1 deficiency augmenting fungal killing through dectin-1. **(A)** Surface expression of TLR2 ($n = 6$), TLR4 ($n = 6$), MR ($n = 9$) and dectin-1 ($n = 9$) on human CD14$^+$ monocytes measured by flowcytometry following 24-h stimulation in the presence or absence of (10 μg/mL) TriDAP. **(B)** Percentage of dectin-1$^+$ CD14$^+$ monocytes following 24-h stimulation in the presence or absence of (10 μg/mL) TriDAP ($n = 9$). **(C)** mRNA expression of *TLR2* ($n = 8$) and *CLEC7A* (dectin-1) ($n = 6$) in human PBMCs following 24-h stimulation in the presence or absence of (10 μg/mL) TriDAP. **(D)** *NOD1* and *CLEC7A* (dectin-1) mRNA expression following siRNA treatment with scrambled siRNA or siRNA targeting NOD1(siNOD1) ($n = 6$). **(E)** *Clec7A* (dectin-1) expression in the lung, bone marrow and spleen of wild type (WT) ($n = 8$) and *Nod1*$^{-/-}$ ($n = 6$) at day 3 following *Aspergillus*-infection. Means were compared using the Mann–Whitney *U* test. **(F,G)** Fungal killing capacity assessed as CFU remaining of *A. fumigatus* plotted as percentage of input (2×10^6). **(F)** Fungi killed by human GM-CSF differentiated monocytes-derived macrophages treated with scrambled siRNA or NOD1 targeting siRNA, the latter in the presence or absence of Laminarin (100 μg/mL) or a dectin-1 blocking antibody. Means were compared using the Wilcoxon signed rank test. **(G)** Fungi were killed by murine BMDMs of WT and *Nod1*$^{-/-}$ mice, the latter in the presence or absence of laminarin. Means were compared using the Mann–Whitney *U* test. All plots represent mean ± SEM.

Following an otherwise lethal *Aspergillus* infection, *Nod1*-deficient mice demonstrated rapid fungal clearance, which was associated with an almost complete absence of pathological damage and fungal outgrowth in the lungs. In contrast, WT mice succumbed to the infection with severe fungal outgrowth in the lungs and significant pathological damage detected by histopathology. In contrast to our aspergillosis model, the NOD1 receptor is non-redundant in numerous bacterial infection

models, such as *Mycobacterium tuberculosis* (9), *Pseudomonas aeruginosa* (38), *Shigella flexineri* (39), and *Helicobacter pylori* (40). In these models, NOD1 was required for an efficient cytokine response (38, 39) and killing of the pathogen (9, 38, 40). In contrast to these latter studies with bacteria, our data suggest that NOD1 has an inhibitory role on the antifungal host defense against *Aspergillus*. *Nod1* deficiency results in an increased capacity of BMDMs to kill live *Aspergillus* and an enhanced oxidative burst upon stimulation with zymosan. Strikingly, we also observe increased cytokine responses and enhanced NFκB translocation in murine *Nod1*-deficient cells. This is in contrast to a previous study that shows NOD1 to be required for NFκB translocation in the response of corneal epithelial cells to *A. fumigatus* (6). The fact that we observe similar results when we silence *NOD1* gene expression in human MDMs validates that the observed effects are due to the absence of NOD1. In contrast, we observed that NOD1 activation has the opposite effect of *NOD1* deficiency and silencing. Taken together, these data suggest that NOD1 inhibits crucial pathways in recognition of *Aspergillus* that limits the induction of protective antifungal effector mechanisms.

Mechanistically, we were able to demonstrate that activation of the NOD1 receptor by its ligand TriDAP reduces surface expression of the C-type lectin receptor dectin-1 on human monocytes, one of the most crucial receptors in host defense against *Aspergillus* (41–51). We found that the reduced surface expression was the result of a downregulation of *CLEC7A* mRNA expression when human monocytes were stimulated with the NOD1 ligand. Contrariwise, NOD1 silencing increased *CLEC7A* mRNA expression. Therefore, the activity of NOD1 seems to show a reverse correlation with *CLEC7A* transcription. Extending this to the *in vivo* model we observed increased *Clec7A* mRNA levels in the lungs and bone marrow of *Nod1*$^{-/-}$ mice, compared with WT controls. Dectin-1 is crucial for the induction of ROS by *Aspergillus*, which is in line with our data showing increased ROS by *Nod1*-deficient murine BMDMs or in human MDM where *NOD1* gene expression was silenced, which express more dectin-1 (52). We were able to pinpoint that the increased *dectin-1* expression, in the absence of NOD1, was responsible for augmented fungal killing by *Nod1*$^{-/-}$ BMDMs and human MDM in which NOD1 was silenced, as blockade of dectin-1 reversed the augmented killing.

ROS is essential for the host defense against *Aspergillus* and its importance is illustrated by patients with chronic granulomatous disease who are highly susceptible to infections with *Aspergillus* due to a defect in NADPH-dependent ROS production (53, 54). *Aspergillus* and Zymosan, which are used in our study to study the oxidative burst by murine and human macrophages, are both recognized by dectin-1 (55). We suggest that the modulation of dectin-1 expression by NOD1 could be the responsible mechanism for alterations in the capacity to induce an oxidative burst. Similarly we found that *Nod1*$^{-/-}$ BMDMs and human MDMs wherein *NOD1* gene expression was silenced have an increased capacity to kill conidia and a decreased conidial killing was observed in human MDMs when NOD1 was stimulated. These changes in conidial killing can also be explained by the differences in dectin-1 expression, as dectin-1 expression is required for efficient phagocytosis (45, 50, 51) and killing of *A. fumigatus* (48, 49) [reviewed in Ref. (42)].

In our *in vitro* studies, we observed that the absence of NOD1 improved fungal killing through enhancement of dectin-1 expression in BMDMs or human MDMs. Although it is evident that in host defense against *A. fumigatus* these cells employ dectin-1 to induce their antifungal effector functions, it is becoming increasingly evident that other cells also use dectin-1 to recognize *Aspergillus.* For example, the role of the pulmonary epithelium is an important tissue that must be taken into account, since these cells can also play an important role in anti-Aspergillus host defense. Dectin-1 on bronchial epithelial cells plays a role in the induction of innate immune responses to *Aspergillus* including the release of antimicrobial peptides such as defensins (51). Moreover, it has been demonstrated that enhancing dectin-1 on only the pulmonary epithelium promotes the resistance to IA (52). The role of dectin-1 in non-myeloid derived tissues is also highlighted by the observation that dectin-1 polymorphisms in the genotype of the recipients of hematopoietic stem cell transplants, which represent the non-myeloid tissues in the patient, predisposes to the development of aspergillosis (56). It cannot be concluded that the protection against aspergillosis that we observe in *Nod1*$^{-/-}$ mice is solely due to the increased dectin-1 expression on macrophages. We observed that dectin-1 expression in these mice is increased in both the bone marrow as well as the lung. Although resident macrophages in the lung could account for the changed dectin-1 expression, from our data it cannot be excluded that enhanced dectin-1 expression on the pulmonary epithelium does not play an additional role in the protection against *Aspergillus* infection.

Most interestingly, we were able to demonstrate that, in addition to its cytoplasmic expression, the NOD1 receptor localizes to *Aspergillus*-containing phagosome. Due to this localization to the phagosome, we suggest that NOD1 may also recognize fungal PAMPs that are exposed in the phagosome. Nevertheless, further studies are warranted to explore whether cytoplasmic sensing of fungal PAMPs or sensing of fungal PAMPs in the phagosome triggers the effects mediated by NOD1. Although NOD1 is crucial for recognition of bacterial cell wall products (57, 58) and activation of downstream protective immune mechanisms, we suggest that upon engagement of NOD1 with fungi, deleterious mechanisms are induced. Therefore, the potent protective effect of *Nod1* deficiency and beneficial effects of NOD1 silencing makes it tempting to suggest the blockade of NOD1 as a novel treatment strategy for IA. Currently, no pharmacological inhibitors are available to block NOD1 *in vivo*, but small molecule inhibitors that could potentially be used for therapy have been identified (59).

Collectively, we conclude that NOD1 induces a detrimental effect on protective antifungal mechanisms in host defense against *A. fumigatus*. The absence of NOD1 enhances the protective effector mechanisms such as cytokine production, oxidative burst, fungal killing, and dectin-1 expression. This observation paves the way for the development of new treatment strategies for IA that target NOD1.

ETHICS STATEMENT

The human study was carried out in accordance with the recommendations of the guidelines for human research from the Arnhem-Nijmegen Medical Ethical Committee, with written informed consent from all subjects. All subjects gave written informed consent in accordance with the Declaration of Helsinki. The protocol was approved by the Arnhem-Nijmegen Medical Ethical Committee. The animal study was carried out in accordance with the recommendations of Institut Pasteur guidelines, in compliance with European animal welfare regulation and under regulations of the St. Jude Children's Research Hospital Committee on Use and Care of Animals. The protocols were approved by the by the ethical committee for animal experimentation CETEA (Comité d'éthique en experimentation animale, Project license number 2013-0020) and by St. Jude Children's Research Hospital Committee on Use and Care of Animals (protocol no 482-100265-1-/13), respectively.

AUTHOR CONTRIBUTIONS

MG, OI-G, and FV conceived and designed the experiments. MG, MJ, RM, OR, GJ, CF, WM, and OI-G performed the experiments. MG, MJ, RM, OR, GJ, WM, TK, and OI-G analyzed the data. TK provided valuable reagents. MG, AC, OI-G, and FV wrote the manuscript. MG, MJ, WM, TK, AC, OI-G, and FV amended the manuscript.

ACKNOWLEDGMENTS

Part of this work was the doctoral thesis of M.S. Gresnigt, Recognition and Cytokine Signaling Pathways in Host Defense Against *Aspergillus fumigatus* (60). The authors thank C. Wertz and M. Fanton D'Andon for providing *Nod1*-deficient mice K. Schraa for her assistance with culturing BMDMs, B. Briard for help with western blot analysis.

FUNDING

MG was supported by the Erasmus lifelong learning program. FV was supported by the E-rare project EURO-CMC. TK was supported by the National Institutes of Health [grant numbers AI101935, AI124346, AR056296, and CA163507]. AC was supported by the Northern Portugal Regional Operational Programme (NORTE 2020), under the Portugal 2020 Partnership Agreement, through the European Regional Development Fund (FEDER) (NORTE-01-0145-FEDER-000013), and the Fundação para a Ciência e Tecnologia (FCT) (IF/00735/2014).

SUPPLEMENTARY MATERIAL

The Supplementary Material for this article can be found online at http://www.frontiersin.org/articles/10.3389/fimmu.2017.01777/full#supplementary-material.

REFERENCES

1. Brown GD, Denning DW, Gow NA, Levitz SM, Netea MG, White TC. Hidden killers: human fungal infections. *Sci Transl Med* (2012) 4(165): 165rv13. doi:10.1126/scitranslmed.3004404
2. Ben-Ami R, Lewis RE, Kontoyiannis DP. Enemy of the (immunosuppressed) state: an update on the pathogenesis of *Aspergillus fumigatus* infection. *Br J Haematol* (2010) 150(4):406–17. doi:10.1111/j.1365-2141.2010.08283.x
3. Armstrong-James D, Brown GD, Netea MG, Zelante T, Gresnigt MS, van de Veerdonk FL, et al. Immunotherapeutic approaches to treatment of fungal diseases. *Lancet Infect Dis* (2017) 17(12):e393–402. doi:10.1016/S1473-3099(17)30442-5
4. Gresnigt MS, Netea MG, van de Veerdonk FL. Pattern recognition receptors and their role in invasive aspergillosis. *Ann N Y Acad Sci* (2012) 1273:60–7. doi:10.1111/j.1749-6632.2012.06759.x
5. Lamoth F, Rubino I, Bochud PY. Immunogenetics of invasive aspergillosis. *Med Mycol* (2011) 49(Suppl 1):S125–36. doi:10.3109/13693786.2010.516408
6. Zhang Y, Wu J, Xin Z, Wu X. *Aspergillus fumigatus* triggers innate immune response via NOD1 signaling in human corneal epithelial cells. *Exp Eye Res* (2014) 127:170–8. doi:10.1016/j.exer.2014.07.025
7. Su AI, Wiltshire T, Batalov S, Lapp H, Ching KA, Block D, et al. A gene atlas of the mouse and human protein-encoding transcriptomes. *Proc Natl Acad Sci U S A* (2004) 101(16):6062–7. doi:10.1073/pnas.0400782101
8. Opitz B, Puschel A, Schmeck B, Hocke AC, Rosseau S, Hammerschmidt S, et al. Nucleotide-binding oligomerization domain proteins are innate immune receptors for internalized *Streptococcus pneumoniae*. *J Biol Chem* (2004) 279(35):36426–32. doi:10.1074/jbc.M403861200
9. Juarez E, Carranza C, Hernandez-Sanchez F, Loyola E, Escobedo D, Leon-Contreras JC, et al. Nucleotide-oligomerizing domain-1 (NOD1) receptor activation induces pro-inflammatory responses and autophagy in human alveolar macrophages. *BMC Pulm Med* (2014) 14:152. doi:10.1186/1471-2466-14-152
10. Berrington WR, Iyer R, Wells RD, Smith KD, Skerrett SJ, Hawn TR. NOD1 and NOD2 regulation of pulmonary innate immunity to *Legionella pneumophila*. *Eur J Immunol* (2010) 40(12):3519–27. doi:10.1002/eji.201040518
11. Frutuoso MS, Hori JI, Pereira MS, Junior DS, Sonego F, Kobayashi KS, et al. The pattern recognition receptors Nod1 and Nod2 account for neutrophil recruitment to the lungs of mice infected with *Legionella pneumophila*. *Microbes Infect* (2010) 12(11):819–27. doi:10.1016/j.micinf.2010.05.006
12. Sprenkeler EG, Gresnigt MS, van de Veerdonk FL. LC3-associated phagocytosis: a crucial mechanism for antifungal host defence against *Aspergillus fumigatus*. *Cell Microbiol* (2016) 18(9):1208–16. doi:10.1111/cmi.12616
13. Chamilos G, Akoumianaki T, Kyrmizi I, Brakhage A, Beauvais A, Latge JP. Melanin targets LC3-associated phagocytosis (LAP): a novel pathogenetic mechanism in fungal disease. *Autophagy* (2016) 12(5):888–9. doi:10.1080/15548627.2016.1157242
14. Kanayama M, Shinohara ML. Roles of autophagy and autophagy-related proteins in antifungal immunity. *Front Immunol* (2016) 7:47. doi:10.3389/fimmu.2016.00047
15. Tam JM, Mansour MK, Acharya M, Sokolovska A, Timmons AK, Lacy-Hulbert A, et al. The role of autophagy-related proteins in *Candida albicans* infections. *Pathogens* (2016) 5(2):E34. doi:10.3390/pathogens5020034
16. Bonnett CR, Cornish EJ, Harmsen AG, Burritt JB. Early neutrophil recruitment and aggregation in the murine lung inhibit germination of *Aspergillus fumigatus* conidia. *Infect Immun* (2006) 74(12):6528–39. doi:10.1128/iai.00909-06
17. Mehrad B, Strieter RM, Moore TA, Tsai WC, Lira SA, Standiford TJ. CXC chemokine receptor-2 ligands are necessary components of neutrophil-mediated host defense in invasive pulmonary aspergillosis. *J Immunol* (1999) 163(11):6086–94.
18. Cunha C, Kurzai O, Loffler J, Aversa F, Romani L, Carvalho A. Neutrophil responses to aspergillosis: new roles for old players. *Mycopathologia* (2014) 178(5–6):387–93. doi:10.1007/s11046-014-9796-7
19. Phadke AP, Mehrad B. Cytokines in host defense against *Aspergillus*: recent advances. *Med Mycol* (2005) 43(Suppl 1):S173–6. doi:10.1080/13693780500052099
20. Gresnigt MS, van de Veerdonk FL. The role of interleukin-1 family members in the host defence against *Aspergillus fumigatus*. *Mycopathologia* (2014) 178(5–6):395–401. doi:10.1007/s11046-014-9776-y

21. Mencacci A, Cenci E, Bacci A, Montagnoli C, Bistoni F, Romani L. Cytokines in candidiasis and aspergillosis. *Curr Pharm Biotechnol* (2000) 1(3):235–51. doi:10.2174/1389201003378924
22. Netea MG, Warris A, Van der Meer JW, Fenton MJ, Verver-Janssen TJ, Jacobs LE, et al. *Aspergillus fumigatus* evades immune recognition during germination through loss of toll-like receptor-4-mediated signal transduction. *J Infect Dis* (2003) 188(2):320–6. doi:10.1086/376456
23. Chai LY, Kullberg BJ, Vonk AG, Warris A, Cambi A, Latge JP, et al. Modulation of toll-like receptor 2 (TLR2) and TLR4 responses by *Aspergillus fumigatus*. *Infect Immun* (2009) 77(5):2184–92. doi:10.1128/IAI.01455-08
24. Galiger C, Brock M, Jouvion G, Savers A, Parlato M, Ibrahim-Granet O. Assessment of efficacy of antifungals against *Aspergillus fumigatus*: value of real-time bioluminescence imaging. *Antimicrob Agents Chemother* (2013) 57(7):3046–59. doi:10.1128/AAC.01660-12
25. Brock M, Jouvion G, Droin-Bergere S, Dussurget O, Nicola MA, Ibrahim-Granet O. Bioluminescent *Aspergillus fumigatus*, a new tool for drug efficiency testing and in vivo monitoring of invasive aspergillosis. *Appl Environ Microbiol* (2008) 74(22):7023–35. doi:10.1128/AEM.01288-08
26. Dubourdeau M, Athman R, Balloy V, Huerre M, Chignard M, Philpott DJ, et al. *Aspergillus fumigatus* induces innate immune responses in alveolar macrophages through the MAPK pathway independently of TLR2 and TLR4. *J Immunol* (2006) 177(6):3994–4001. doi:10.4049/jimmunol.177.6.3994
27. Philippe B, Ibrahim-Granet O, Prevost MC, Gougerot-Pocidalo MA, Sanchez Perez M, Van der Meeren A, et al. Killing of *Aspergillus fumigatus* by alveolar macrophages is mediated by reactive oxidant intermediates. *Infect Immun* (2003) 71(6):3034–42. doi:10.1128/IAI.71.6.3034-3042.2003
28. Joosten LA, Heinhuis B, Abdollahi-Roodsaz S, Ferwerda G, Lebourhis L, Philpott DJ, et al. Differential function of the NACHT-LRR (NLR) members Nod1 and Nod2 in arthritis. *Proc Natl Acad Sci U S A* (2008) 105(26):9017–22. doi:10.1073/pnas.0710445105
29. Netea MG, Ferwerda G, de Jong DJ, Jansen T, Jacobs L, Kramer M, et al. Nucleotide-binding oligomerization domain-2 modulates specific TLR pathways for the induction of cytokine release. *J Immunol* (2005) 174(10):6518–23. doi:10.4049/jimmunol.174.10.6518
30. Watanabe T, Kitani A, Murray PJ, Strober W. NOD2 is a negative regulator of toll-like receptor 2-mediated T helper type 1 responses. *Nat Immunol* (2004) 5(8):800–8. doi:10.1038/ni1092
31. Oosting M, Berende A, Sturm P, Ter Hofstede HJ, de Jong DJ, Kanneganti TD, et al. Recognition of *Borrelia burgdorferi* by NOD2 is central for the induction of an inflammatory reaction. *J Infect Dis* (2010) 201(12):1849–58. doi:10.1086/652871
32. Becker KL, Ifrim DC, Quintin J, Netea MG, van de Veerdonk FL. Antifungal innate immunity: recognition and inflammatory networks. *Semin Immunopathol* (2015) 37(2):107–16. doi:10.1007/s00281-014-0467-z
33. Bellocchio S, Montagnoli C, Bozza S, Gaziano R, Rossi G, Mambula SS, et al. The contribution of the toll-like/IL-1 receptor superfamily to innate and adaptive immunity to fungal pathogens in vivo. *J Immunol* (2004) 172(5):3059–69. doi:10.4049/jimmunol.172.5.3059
34. Bozza S, Gaziano R, Lipford GB, Montagnoli C, Bacci A, Di Francesco P, et al. Vaccination of mice against invasive aspergillosis with recombinant *Aspergillus* proteins and CpG oligodeoxynucleotides as adjuvants. *Microbes Infect* (2002) 4(13):1281–90. doi:10.1016/S1286-4579(02)00007-2
35. Rodland EK, Ager-Wick E, Halvorsen B, Muller F, Froland SS. Toll-like receptor 5 (TLR5) may be involved in the immunological response to *Aspergillus fumigatus* in vitro. *Med Mycol* (2011) 49(4):375–9. doi:10.3109/13693786.2010.531772
36. Bellocchio S, Moretti S, Perruccio K, Fallarino F, Bozza S, Montagnoli C, et al. TLRs govern neutrophil activity in aspergillosis. *J Immunol* (2004) 173(12):7406–15. doi:10.4049/jimmunol.173.12.7406
37. Grube M, Loeffler J, Mezger M, Kruger B, Echtenacher B, Hoffmann P, et al. TLR5 stop codon polymorphism is associated with invasive aspergillosis after allogeneic stem cell transplantation. *Med Mycol* (2013) 51(8):818–25. doi:10.3109/13693786.2013.809630
38. Chung D, Barker BM, Carey CC, Merriman B, Werner ER, Lechner BE, et al. ChIP-seq and in vivo transcriptome analyses of the *Aspergillus fumigatus* SREBP SrbA reveals a new regulator of the fungal hypoxia response and virulence. *PLoS Pathog* (2014) 10(11):e1004487. doi:10.1371/journal.ppat.1004487
39. Kroll K, Pahtz V, Hillmann F, Vaknin Y, Schmidt-Heck W, Roth M, et al. Identification of hypoxia-inducible target genes of *Aspergillus fumigatus* by transcriptome analysis reveals cellular respiration as an important contributor to hypoxic survival. *Eukaryot Cell* (2014) 13(9):1241–53. doi:10.1128/ec.00084-14
40. Ben-Ami R. Angiogenesis at the mold-host interface: a potential key to understanding and treating invasive aspergillosis. *Future Microbiol* (2013) 8(11):1453–62. doi:10.2217/fmb.13.114
41. Chamilos G, Ganguly D, Lande R, Gregorio J, Meller S, Goldman WE, et al. Generation of IL-23 producing dendritic cells (DCs) by airborne fungi regulates fungal pathogenicity via the induction of T(H)-17 responses. *PLoS One* (2010) 5(9):e12955. doi:10.1371/journal.pone.0012955
42. Drummond RA, Brown GD. The role of dectin-1 in the host defence against fungal infections. *Curr Opin Microbiol* (2011) 14(4):392–9. doi:10.1016/j.mib.2011.07.001
43. Gessner MA, Werner JL, Lilly LM, Nelson MP, Metz AE, Dunaway CW, et al. Dectin-1-dependent interleukin-22 contributes to early innate lung defense against *Aspergillus fumigatus*. *Infect Immun* (2012) 80(1):410–7. doi:10.1128/IAI.05939-11
44. Hohl TM, Van Epps HL, Rivera A, Morgan LA, Chen PL, Feldmesser M, et al. *Aspergillus fumigatus* triggers inflammatory responses by stage-specific beta-glucan display. *PLoS Pathog* (2005) 1(3):e30. doi:10.1371/journal.ppat.0010030
45. Kyrmizi I, Gresnigt MS, Akoumianaki T, Samonis G, Sidiropoulos P, Boumpas D, et al. Corticosteroids block autophagy protein recruitment in *Aspergillus fumigatus* phagosomes via targeting dectin-1/Syk kinase signaling. *J Immunol* (2013) 191(3):1287–99. doi:10.4049/jimmunol.1300132
46. Said-Sadier N, Padilla E, Langsley G, Ojcius DM. *Aspergillus fumigatus* stimulates the NLRP3 inflammasome through a pathway requiring ROS production and the Syk tyrosine kinase. *PLoS One* (2010) 5(4):e10008. doi:10.1371/journal.pone.0010008
47. Sainz J, Lupianez CB, Segura-Catena J, Vazquez L, Rios R, Oyonarte S, et al. Dectin-1 and DC-SIGN polymorphisms associated with invasive pulmonary aspergillosis infection. *PLoS One* (2012) 7(2):e32273. doi:10.1371/journal.pone.0032273
48. Steele C, Rapaka RR, Metz A, Pop SM, Williams DL, Gordon S, et al. The beta-glucan receptor dectin-1 recognizes specific morphologies of *Aspergillus fumigatus*. *PLoS Pathog* (2005) 1(4):e42. doi:10.1371/journal.ppat.0010042
49. Werner JL, Metz AE, Horn D, Schoeb TR, Hewitt MM, Schwiebert LM, et al. Requisite role for the dectin-1 beta-glucan receptor in pulmonary defense against *Aspergillus fumigatus*. *J Immunol* (2009) 182(8):4938–46. doi:10.4049/jimmunol.0804250
50. Luther K, Torosantucci A, Brakhage AA, Heesemann J, Ebel F. Phagocytosis of *Aspergillus fumigatus* conidia by murine macrophages involves recognition by the dectin-1 beta-glucan receptor and toll-like receptor 2. *Cell Microbiol* (2007) 9(2):368–81. doi:10.1111/j.1462-5822.2006.00796.x
51. Gersuk GM, Underhill DM, Zhu L, Marr KA. Dectin-1 and TLRs permit macrophages to distinguish between different *Aspergillus fumigatus* cellular states. *J Immunol* (2006) 176(6):3717–24. doi:10.4049/jimmunol.176.6.3717
52. Underhill DM, Rossnagle E, Lowell CA, Simmons RM. Dectin-1 activates Syk tyrosine kinase in a dynamic subset of macrophages for reactive oxygen production. *Blood* (2005) 106(7):2543–50. doi:10.1182/blood-2005-03-1239
53. Antachopoulos C. Invasive fungal infections in congenital immunodeficiencies. *Clin Microbiol Infect* (2010) 16(9):1335–42. doi:10.1111/j.1469-0691.2010.03289.x
54. Segal BH, DeCarlo ES, Kwon-Chung KJ, Malech HL, Gallin JI, Holland SM. *Aspergillus nidulans* infection in chronic granulomatous disease. *Medicine (Baltimore)* (1998) 77(5):345–54. doi:10.1097/00005792-199809000-00004
55. Gantner BN, Simmons RM, Canavera SJ, Akira S, Underhill DM. Collaborative induction of inflammatory responses by dectin-1 and toll-like receptor 2. *J Exp Med* (2003) 197(9):1107–17. doi:10.1084/jem.20021787
56. Cunha C, Di Ianni M, Bozza S, Giovannini G, Zagarella S, Zelante T, et al. Dectin-1 Y238X polymorphism associates with susceptibility to invasive aspergillosis in hematopoietic transplantation through impairment of both recipient- and donor-dependent mechanisms of antifungal immunity. *Blood* (2010) 116(24):5394–402. doi:10.1182/blood-2010-04-279307
57. Chamaillard M, Hashimoto M, Horie Y, Masumoto J, Qiu S, Saab L, et al. An essential role for NOD1 in host recognition of bacterial

peptidoglycan containing diaminopimelic acid. *Nat Immunol* (2003) 4(7):702–7. doi:10.1038/ni945

58. Girardin SE, Boneca IG, Carneiro LA, Antignac A, Jehanno M, Viala J, et al. Nod1 detects a unique muropeptide from gram-negative bacterial peptidoglycan. *Science* (2003) 300(5625):1584–7. doi:10.1126/science.1084677
59. Shepardson KM, Ngo LY, Aimanianda V, Latge JP, Barker BM, Blosser SJ, et al. Hypoxia enhances innate immune activation to *Aspergillus fumigatus* through cell wall modulation. *Microbes Infect* (2013) 15(4):259–69. doi:10.1016/j.micinf.2012.11.010
60. Gresnigt MS. *Recognition and Cytokine Signalling Pathways in Host Defence against Aspergillus fumigatus [Doctoral Dissertation]*. Radboud University Nijmegen (2015). Available from: http://repository.ubn.ru.nl

Conflict of Interest Statement: The authors declare that the research was conducted in the absence of any commercial or financial relationships that could be construed as a potential conflict of interest.

Copyright © 2017 Gresnigt, Jaeger, Subbarao Malireddi, Rasid, Jouvion, Fitting, Melchers, Kanneganti, Carvalho, Ibrahim-Granet and van de Veerdonk. This is an open-access article distributed under the terms of the Creative Commons Attribution License (CC BY). The use, distribution or reproduction in other forums is permitted, provided the original author(s) or licensor are credited and that the original publication in this journal is cited, in accordance with accepted academic practice. No use, distribution or reproduction is permitted which does not comply with these terms.

frontiers in Immunology

ORIGINAL RESEARCH
published: 18 September 2018
doi: 10.3389/fimmu.2018.01967

FIBCD1 Binds *Aspergillus fumigatus* and Regulates Lung Epithelial Response to Cell Wall Components

Christine Schoeler Jepsen[1†], Lalit Kumar Dubey[1,2†], Kimmie B. Colmorten[1], Jesper B. Moeller[1,3], Mark A. Hammond[1], Ole Nielsen[4], Anders Schlosser[1], Steven P. Templeton[5], Grith L. Sorensen[1] and Uffe Holmskov[1]*

[1] Cancer and Inflammation Research, Department of Molecular Medicine, University of Southern Denmark, Odense, Denmark, [2] Global Health Institute, School of Life Sciences, École Polytechnique Fédérale de Lausanne, Lausanne, Switzerland, [3] Jill Roberts Institute for Research in Inflammatory Bowel Disease, Weill Cornell Medicine, Cornell University, New York, NY, United States, [4] Department of Clinical Pathology, Odense University Hospital, Odense, Denmark, [5] Department of Microbiology and Immunology, Indiana University School of Medicine-Terre Haute, Terre Haute, IN, United States

OPEN ACCESS

Edited by:
Amariliz Rivera, Rutgers, The State University of New Jersey, United States

Reviewed by:
Georgios Chamilos, University of Crete, Greece
Agostinho Carvalho, University of Minho, Portugal
Joshua J. Obar, Dartmouth College, United States

***Correspondence:**
Uffe Holmskov
uholmskov@health.sdu.dk

[†] These authors have contributed equally to this work

Specialty section:
This article was submitted to Microbial Immunology, a section of the journal Frontiers in Immunology

Received: *31 January 2018*
Accepted: *09 August 2018*
Published: *18 September 2018*

Citation:
Jepsen CS, Dubey LK, Colmorten KB, Moeller JB, Hammond MA, Nielsen O, Schlosser A, Templeton SP, Sorensen GL and Holmskov U (2018) FIBCD1 Binds Aspergillus fumigatus and Regulates Lung Epithelial Response to Cell Wall Components. Front. Immunol. 9:1967. doi: 10.3389/fimmu.2018.01967

Aspergillus fumigatus (*A. fumigatus*) is a ubiquitous fungus of clinical importance associated with development of various pulmonary diseases and allergic hypersensitivity reactions. It is protected against environmental stress by a cell wall that contains polysaccharides such as chitin. We previously demonstrated that fibrinogen C domain-containing protein 1 (FIBCD1) is a membrane-bound protein that binds chitin through a conserved S1 binding site and is expressed in intestinal epithelium and salivary glands. Here, we further localized FIBCD1 protein expression at the surface of bronchial and alveolar human lung epithelium, observed recognition of *A. fumigatus* cell wall with S1 site-independent recognition. We observed FIBCD1-mediated suppression of IL-8 secretion, mucin production, and transcription of genes associated with airway inflammation and homeostasis in FIBCD1-transfected lung epithelial cells. These modulations were generally enforced by stimulation with *A. fumigatus* cell wall polysaccharides. In parallel, we demonstrated a FIBCD1-mediated modulation of IL-8 secretion induced by TLR2,−4, and −5. Collectively, our findings support FIBCD1 as a human lung epithelial pattern recognition receptor that recognizes the complex *A. fumigatus* cell wall polysaccharides and modulates the lung epithelial inflammatory response by suppressing inflammatory mediators and mucins.

Keywords: FIBCD1, *Aspergillus fumigatus*, human, A549, lung, inflammation, IL-8, epithelium

INTRODUCTION

Aspergillus fumigatus (*A. fumigatus*) is a ubiquitous, filamentous fungus with the ability to cause invasive and allergic pulmonary diseases that is partly attributed to its ability to circumvent host immune defenses at airway mucosal sites (1–4). Humans inhale several hundred *A. fumigatus* conidia every day and their small size make them easily aerosolized and capable of reaching the lung alveoli. In healthy, immune-competent hosts, inhaled *A. fumigatus* conidia are cleared by innate defense mechanisms including mucociliary transport mechanisms and phagocytic activity of leukocytes, primarily residential macrophages and neutrophils recruited by epithelial secretion

of chemotactic factors such as IL-8. Additionally, epithelial secretion of opsonizing mediators such as ficolins and complement components support the activity of these mechanisms (5, 6).

A cell wall, mainly composed of polysaccharides and secretory antigens, protects *A. fumigatus* conidia and hyphae against environmental stress (7). The structural skeleton of the cell wall is composed of chitin and galactomannan covalently bound to β-1,3-glucan (8), which are polysaccharide structures absent in mammals. Therefore, they serve as pathogen-associated molecular patterns (PAMPs) recognized by pattern recognition receptors (PRRs) on mammalian cells (9). The *A. fumigatus* cell wall is continuously remodeled during morphogenesis from inhaled, resting conidia to fully-grown hyphae (10). In resting conidia, the cell wall is protected by an additional layer of hydrophobic proteins and pigments, not produced in germ tubes and hyphae. This layer shields *A. fumigatus* cell wall PAMPs, which makes the resting conidia immunologically inert (9). During the first stages of germination, cell wall polysaccharides are hydrolyzed and *de novo* synthesis of cell wall components, e.g. chitin and β-1,3-glucan, is initiated (10). This causes the conidia to swell, disintegrating the outer layer and exposing cell wall PAMPs to host PRRs (9). Various PRRs are involved in the initiation, control, and resolution of the anti-*A. fumigatus* inflammatory response (11), including Toll-Like Receptors (TLRs) (5, 6) and the β-1,3-glucan receptor Dectin-1 (12). Several studies report a TLR-regulated anti-*A. fumigatus* response dependent on the fungus' morphotype (5, 6, 13). However, the underlying mechanisms remain unknown and may involve interplay between other PRRs that recognize *A. fumigatus*-associated PAMPs.

We have previously identified fibrinogen C domain-containing protein 1 (FIBCD1) as the first membrane-bound protein of the fibrinogen-related domain (FReD) superfamily (14). FIBCD1 is expressed as a tetramer on the apical surface of small and large intestinal epithelium and is composed of a cytoplasmic tail with three potential phosphorylation sites, a transmembrane region, and an ectodomain containing a coiled-coil region, a polycationic region, and a FReD (14). FIBCD1 exhibits calcium-dependent binding of acetylated structures including crab shell chitin through a conserved S1 binding site in FReD and facilitates endocytosis of bound ligands (14, 15). The crystal structure of FIBCD1-FReD (16) is homologous to FReD superfamily members involved in immune regulation, including ficolin-1 and −2 (17, 18). Both ficolin-1 and −2 recognize *A. fumigatus*-associated PAMPs (19, 20) and binds directly or indirectly to resting *A. fumigatus* conidia (21).

The aim of this study is to investigate the potential role of FIBCD1 in the immune response against *A. fumigatus*. We hypothesize that FIBCD1 is expressed in human lung epithelium and interacts with *A. fumigatus* by binding fungal cell wall chitin in the S1 binding site of FIBCD1-FReD. We hypothesize that interaction between FIBCD1 and ligand(s) modulates TLR- and lung epithelial cell-mediated inflammatory response to fungal cell wall components.

Abbreviations: acBSA, acetylated BSA; *A. fumigatus, Aspergillus fumigatus*; AIF, alkali-insoluble fraction; CNRQ, calibrated normalized relative quantity; DPBS, Dulbecco's PBS; FIBCD1, fibrinogen C domain-containing protein 1; FReD, fibrinogen-related domain; IAA, iodoacetamide; IHC, Immunohistochemical; MBL, mannan-binding lectin; MOPS, 3-(N-morpholino)propanesulfonic acid; MUC, mucin; PAMPs, pathogen-associated molecular patterns; PRR, pattern recognition receptor; qPCR, quantitative PCR; RT, room temperature; SD, sabouraud dextrose; WGA, wheat germ agglutinin.

METHODS AND MATERIALS

Buffers and Reagents

PBS: 140 mM NaCl, 3 mM KCl, 8 mM Na_2HPO_4, 1.5 mM KH_2PO_4. TBS: 10 mM Tris-base, 140 mM NaCl. SDS-PAGE sample buffer: 374 mM Tris-base, 40% (v/v) glycerol, 3 mM bromophenol blue, 8% (w/v) SDS. Acetylated BSA (acBSA), BSA, citric acid, EDTA, glycine, glycerol, silver nitrate ($AgNO_3$), SDS, sodium azide (NaN_3), Tris-base, Triton X-100, H_2SO_4, iodoacetamide (IAA), DTT, $CaCl_2$, sodium acetate, $NaHCO_3$, sterile PBS, curdlan (β-1,3-glucan, from *Alcaligenes faecalis*), RNase ZAP®, M-MLV reverse transcriptase, and oligo-dT primers were ordered from Sigma-Aldrich Co., St Louis, MO, United States. Alexa Fluor 488, Alexa Fluor 633-labeled wheat germ agglutinin (WGA), Gateway Technology® pDONR™-221 vector, 3-(N-morpholino)-propanesulfonic acid (MOPS) running buffer, RPMI media, FBS, L-glutamine, penicillin/streptomycin, hygromycin B, trypsin/EDTA, Dulbecco's PBS (DPBS), DMSO, TRIzol reagent, and RNaseOUT™ recombinant ribonuclease inhibitor were ordered from Invitrogen™, Thermo Fisher Scientific Inc., Waltham, MA, United states. Sabouraud dextrose (SD) agar, SD broth media, and 40-μm cell strainer were ordered from BD Biosciences, Franklin Lakes, NJ, United States. Acetic acid, bromophenol blue, formaldehyde, KCl, KH_2PO_4, NaCl, Na_2HPO_4, Na_2CO_3, NaOH, Tween 20, and mira cloth were ordered from Merck KGaA, Darmstadt, Germany. Four to twelve percent of polyacrylamide gradient gels, Precision Plus Protein™ KaleidoscopeTM Standards, and non-fat dry milk were ordered from Bio-Rad Laboratories, Inc., Hercules, CA, United States. Chitin beads were ordered from New England Biolabs Inc., Ipswich, Massachusetts, USA, and Dectin-1Fc was kindly provided by Prof Gordon Brown, Aberdeen University. HRP-conjugated rabbit anti-mouse Ig (#P0260), FITC-conjugated goat anti-mouse antibody (#F0479), and HRP-conjugated goat anti-rabbit Ig (#P0448) were ordered from Dako, Glostrup, Denmark. D-galacto-D-mannan (from Ceratonia Siliqua) and mouse monoclonal anti-GAPDH antibody (#sc32233) were ordered from Santa Cruz Biotechnologies, Inc., Dallas, TX, United States.

The anti-mucin (MUC) antibodies rabbit monoclonal anti-MUC-1 antibody (#ab45167), rabbit polyclonal anti-MUC-13 antibody (#ab65109), and mouse monoclonal anti-MUC-5AC antibody (#ab11335) were ordered from Abcam plc, Cambridge, United Kingdom. Protein G column, polyvinylidene difluoride membrane, filter paper, and ECL kit were ordered from GE Healthcare, Little Chalfont, United Kingdom. Ambion® nuclease-free water, custom TaqMan® array 96-well plates, and 2 X TaqMan® fast advanced master mix were ordered from Thermo Fisher Scientific Inc., Waltham, MA, United states.

The human TLR agonist kit was ordered from InvivoGen, San Diego, CA, United States. Alphazyme was ordered from PAA Laboratories GmbH, Pasching, Austria. O-phenylendiamid was ordered from Kem-En-Tec Diagnostics A/S, Taastrup, Denmark. Human CXCL8/IL-8 DuoSet kit was ordered from R&D Systems, Inc., Minneapolis, MN, United states. Limulus amebocyte lysate assay (QCL-1000™) was ordered from Lonza Group Ltd., Basel, Switzerland. Protease inhibitor cocktail tablets were ordered from Roche Diagnostics, Basel, Switzerland. Commercial cDNA library and FIBCD1 PerfectProbe™ assay were ordered from Primerdesign Ltd., United Kingdom. JetPEI transfection reagents were ordered from Polyplus transfection SA, Illkirch, France. Monoclonal anti-ovalbumin antibody was ordered from SSI, Copenhagen, Denmark. The murine Sp2/mIl-6 (CRL-2016) myeloma cells and human lung carcinoma type II epithelial-like A549 cell line were purchased from the American type culture collection (Rockville, MD, USA).

Real Time Analysis of FIBCD1 Expression in Human Tissues

The relative tissue distribution of human FIBCD1 mRNA was quantitated using a commercial cDNA library and a custom made FIBCD1 PerfectProbe™ assay with the primer sequences 5′-CACCGTGGCTGACTATTCC-3′ and 5′-TTCTCTGAATGGTCGCTGTC-3′. Analysis was performed in triplicates using the cycling conditions: 95°C for 10 min, followed by 50 cycles of 95°C for 15 s, 60°C for 30 s and 72°C for 15 s. The study was performed on a 7500 Real-time PCR system (Applied Biosystems®, Thermo Fisher Scientific Inc., Waltham, MA, USA) using 18S RNA for normalization.

Expression and Purification of Recombinant FIBCD1-FReD (rfibcd1-FReD)

rFIBCD1-FReD was expressed in insect cells and purified on N-acetylated immobilized resin as described previously (15).

Production of Monoclonal Anti-FIBCD1 Antibodies

Mouse monoclonal anti-FIBCD1 antibodies HG-HYB-12-2,−12-5, and −12-6 were produced as previously described (14). Mouse monoclonal anti-FIBCD1-FReD antibody HYB-11-14-25 was produced by immunization of *Fibcd1*$^{-/-}$ C57BL6/n mice. The mice were immunized twice with 20 μg of rFIBCD1-FReD using GERBU as adjuvant with more than 2 weeks between each immunization. The mice were boosted once by an intra-peritoneal injection with 20 μg rFIBCD1-FReD without adjuvant 3 days before isolation of B cells. Hybridoma cells were produced by fusion between isolated B cells and myeloma cells and adapted for serum-free media. Secreted antibodies were purified using a protein G column on a fast protein liquid chromatography apparatus (ÄKTA, GE Healthcare, Little Chalfont, United Kingdom). These experiments were performed under license from the National Animal Experiments Inspectorate (reference no. 2012–15–2934–00076).

Immunohistochemical Analysis of FIBCD1 in Human Lung Tissue

Human tissues were obtained from the tissue bank at the Department of Pathology, Odense University Hospital (Odense, Denmark). The tissues were fixed in 4% formalin in PBS for 24 h and then conventionally dehydrated and embedded in paraffin. A biotin-streptavidin immunoperoxidase technique was used on paraffin sections. Paraffin sections were pre-treated in TEG buffer (10 mmol/L Tris, 0.5 mmol/L EGTA, pH 9) in a microwave oven for three 5 min periods at 650 W. The sections were left in TEG buffer for 15 min, washed in TBS, pre-incubated with 2% (w/v) BSA in TBS for 10 min, and incubated for 30 min with the mouse anti-human FIBCD1 (HG-HYB-12-2, 0.5 mg/mL) in TBS containing 15% (w/v) BSA and otherwise processed as described by Madsen et al. (22). The specificity of the immuno-staining was verified by replacing the primary antibody with a non-specific antibody. The local ethical committee in Odense approved the use of human tissue samples (ref. no: VF20050070).

Fungal Strain and Growth Conditions

A. fumigatus conidia (101355, Centraalbureau von Schimmelcultures, Utrecht, Netherlands) were cultivated on SD agar plates at 37°C for 5 days and harvested using PBS/0.5% Tween, washed, and used immediately or stored at 4°C. *A. fumigatus* germination was obtained by inoculating SD broth media with freshly-harvested conidia (less than a week after harvest) and incubating at 37°C. For production of a 1-week-culture, 10^4 freshly-harvested conidia were added per mL media in an Erlenmeyer flask containing 1:4 volume media and incubating at 37°C, 100–140 rpm for 7 days.

Alexa Fluor 488-Labeling of rFIBCD1-FReD

Purified protein (2 mg/mL) was labeled with Alexa Fluor 488 in a 1:9 molar ratio at RT for 1–2 h according to manufacturer's recommendations followed by extensive dialysis against PBS to remove excess dye. Activity of labeled rFIBCD1-FReD was tested by binding to acBSA. Labeled protein was stored at 4°C until used.

Staining of *A. fumigatus*

Staining of *A. fumigatus* was performed by a modification of previously described methods (23) and imaged using an Olympus IX71 fluorescence microscope equipped with four laser optics and F-view fluorescence CCD camera (Olympus Corporation, Tokyo, Japan). All images were acquired and processed using Cell^F soft imaging software (Olympus Corporation, Tokyo, Japan).

Preparation of *A. fumigatus* Alkali-Insoluble Fraction (AIF)

A. fumigatus cell wall component suspension (i.e., alkali-insoluble fraction) was prepared as previously described with minor modifications (8). Briefly, mycelium was harvested from one-week-culture by filtration through mira cloth, washed with distilled PBS, and subjected to three hot alkali treatments (distilled 1 M NaOH, 65°C heat bath, 30 min), each followed by five washes with distilled water and one with distilled TBS at

10,000 × g for 10 min. The product was grinded with mortar and pestle, washed with sterile PBS, forced through a 40 μm cell strainer, pH adjusted to ∼7, added 0.05% NaN_3, and the final product stored at 4°C. AIF was tested for endotoxin contamination using a limulus amebocyte lysate assay revealing an endotoxin level below 0.25 endotoxin units per mL. The absence of protein was confirmed by boiling AIF 1:2 in SDS-PAGE sample buffer on a 99°C heating block for 1 min and separating eluted protein on a 4–12% polyacrylamide gradient gel using MOPS running buffer and subsequently silver staining the gel as described in the following section. The concentration was determined by vacuum drying using a MAXI-dry vacuum centrifuge (Heto-Holten A/S, Alleroed, Denmark) at 55°C, 1,300 rpm.

Pull Down Assay

For protein staining, 2 mg of AIF was washed three times with TBS/0.05% Tween/5 mM $CaCl_2$ and incubated at 4°C overnight with 20 μg/mL Dectin-1Fc, recombinant mannan-binding lectin (rMBL), WGA, and rFIBCD1-FReD in a total volume of 1 mL. Pull down was performed by centrifugation at 4°C, 10,000 × g for 5 min. The insoluble pellets were washed three times with TBS/0.05% Tween/5 mM $CaCl_2$ and bound protein was eluted by boiling the pellets in SDS-PAGE sample buffer for 1 min. For Western blotting, 2 mg AIF and β-1,3-glucan and 200 μL chitin beads were washed three times with TBS/0.05% Tween and incubated at 4°C overnight with 5 μg/mL rFIBCD1-FReD in a total volume of 1 mL TBS/0.05% Tween supplemented with 5 mM $CaCl_2$, 10 mM EDTA, or 100 mM sodium acetate. Pull down was performed by centrifugation at 5,000 rpm (Minispin, Eppendorf AG, Hamburg, Germany) for 5 min. The insoluble pellets were washed three times with TBS/0.05% Tween supplemented with 5 mM $CaCl_2$, 10 mM EDTA, or 100 mM sodium acetate and bound protein was eluted by boiling the pellets in SDS-PAGE sample buffer on a 99°C heating block for 1 min. Pull down of mutant FIBCD1-FReD (A432V) by AIF and chitin beads was performed as previously described (15). Eluted protein was separated by SDS-PAGE on a 4–12% polyacrylamide gradient gel using MOPS running buffer and analyzed by silver staining or Western blotting as described in the following section.

Silver Staining

Silver staining of proteins separated by SDS-PAGE was performed as previously described (24) with some modifications (**Supplementary Datasheet 2**).

Generation of A549 Cells Expressing Full Length of FIBCD1

To generate A549 cells stably expressing full length FIBCD1, the cells were transfected with the expression vector pDEST-FIBCD1 using JetPEI transfection reagents according to manufacturer's instructions. The pDEST-FIBCD1 vector was constructed using Gateway Technology® and keeping to the recommendations of the manufacturer using cDNA containing the open reading frame of FIBCD1, donor vector pDONR™-221, and destination vector pDEST. A corresponding sham-transfected isogenic control cell type was constructed using a pDEST-sham vector. Cells were selected for stable integration of vectors using 500 μg/mL of hygromycin B. Successful expression of FIBCD1 protein was confirmed by Western blotting of cell lysates (**Supplementary Datasheet 2**) and surface expression of FIBCD1 was confirmed by flow cytometry. Unless otherwise stated, A549 cells were maintained in serial passages at 37°C, 5% CO_2 humidity in RPMI media supplemented with 10% FBS, 2 mM L-glutamine, 250 μg/mL hygromycin B, 50 U/mL penicillin, and 50 μg/mL streptomycin. When confluent, cells were subcultured by washing twice in sterile DPBS, detaching with 1 mL 0.5% trypsin/EDTA/sterile DPBS, and diluted using fresh complete media.

Flow Cytometry

A549 cells were harvested by incubation with alphazyme and centrifugation at 350 × g for 5 min. Cells were suspended in media, counted using a haemocytometer, portioned out in minisorp tubes (10^6 cells/tube), pelleted by centrifugation, and supernatant removed. The cells were incubated on ice for 2 h with 0.1 mg/mL monoclonal mouse anti-FIBCD1 antibody HG-HYB-12-5 in PBS/0.5% BSA diluted 1:2 in 100 μL cell suspension. Monoclonal anti-ovalbumin antibody was used as an isotype control. Then, the cells were washed three times and incubated in darkness on ice for 1 h with FITC-conjugated goat anti-mouse antibody diluted 1:10 in PBS/0.5% BSA and 1:2 in 100 μL cell suspension. Finally, the cells were washed three times, diluted in 1.5 mL PBS/0.5% BSA, and analyzed on a Benson Dickinson FACS Calibur (BD Biosciences, Franklin Lakes, NJ, United States) using CELL Quest™ (BD Biosciences, Franklin Lakes, NJ, United States) and FlowJo 8.8.6 software (FlowJo, LLC, Ashland, OR, United States).

Cell Culture Stimulation Conditions, Relative Gene Expression, and Protein Expression

For stimulations of transfected cells, A549 cells transfected with sham and FIBCD1, respectively, were harvested by incubation with 0.5% trypsin/EDTA in DPBS and centrifugation at 350 × g for 5 min. Cells were suspended in media, counted using a haemocytometer, and seeded at a density of 10^6 cells/well/2 mL media in 6-well culture plates or 250,000 cells/well/0.5 mL media in 24-well culture plates (80% confluence). After ∼8 h, the adherent cells were washed with sterile DPBS, added 2 or 0.5 mL serum-free media, and incubated overnight. Then, cells were stimulated by removing the media and adding 2 mL of fresh serum-free media containing 100 μL conidia, AIF, β-1,3-glucan, chitin, galactomannan, or acBSA (ligand control) diluted in sterile DPBS or 0.5 mL of fresh serum-free media containing 22.2 μL human TLR agonist diluted in endotoxin-free water to each well and incubating 0, 4, and 8 h. All stimulations were performed as technical duplicates and biological triplicates.

At each time point, culture supernatant was removed from the cells and used for detection of secreted IL-8 by use of the human CXCL8/IL-8 DuoSet kit and keeping to the recommendations of the manufacturer. For RNA analysis, the cells were washed with DPBS, added TRIzol Reagent, and stored

at −20°C. Total RNA was isolated from cells stimulated 8 h with 500 μg/mL AIF, β-1,3-glucan, or chitin, and cells incubated with DPBS for 8 h as a reference. TRIzol Reagent from technical duplicates of stimulated cells was pooled together, while five biological replicates from DPBS-incubated cells were pooled together to three independent samples. Total RNA was isolated from TRIzol Reagent according to the recommendations of the manufacturer in a fume cupboard treated with RNase ZAP®. cDNA synthesis by M-MLV reverse transcriptase and oligo-dT primers was subsequently performed in keep with manufacturer's instructions. The RNA concentration and purity (260/280) was determined by NanoDrop® ND-1000 spectrophotometry (Thermo Fisher Scientific Inc., Waltham, MA, United states). Then, quantitative PCR (qPCR) was performed targeting 21 different genes involved in immunological response and barrier function (CCL2, CCL5, CCL20, CXCL2, CSF2RA, TNF, TSLP, IL1B, IL6 IL8, IL10, IL12B, IL13, IL25, IL33, MUC1, MUC13, MUC5AC, TJP1, OCLN, ICAM1) and two housekeeping genes (GAPDH, TBP) for normalization. Custom TaqMan® Array 96-well Plates containing dried assay of these genes were added 10 μL cDNA diluted 1:2 in 2 X TaqMan® fast advanced master mix as single copies and qPCR was performed according to the recommendations of the manufacturer using a StepOnePlus™ Real-Time PCR System (Applied Biosystems®, Thermo Fisher Scientific Inc., Waltham, MA, USA) and StepOne™ v2.1 software (Applied Biosystems®, Thermo Fisher Scientific Inc., Waltham, MA, USA). A no-template control was included to exclude DNA contamination. Relative expression of the genes was calculated by qBase plus software (Biogazelle, Gent, Belgium), which uses threshold cycle values of target genes and reference genes to determine calibrated normalized relative quantities (CNRQs). For protein analysis, cells were washed twice with DPBS, added 11 μL/cm^2 RIPA buffer/protease inhibitors (1 tablet per 50 mL)/phosphatase inhibitors (1 tablet per 10 mL), and incubated on a shaker at 4°C for 60 min. Cellular debris were sedimented by centrifugation at 4°C, 10,000 rpm (Sigma 1–16 k refrigerated centrifuge, Sigma-Aldrich Co., St Louis, MO, United States) for 5 min and supernatants were stored at −20°C. Protein concentrations were determined by Bradford in accordance with the recommendations of the manufacturer and samples were prepared for SDS-PAGE by boiling three parts cell lysate with one part SDS-PAGE sample buffer on a 99°C heating block for 1 min. The samples were alkylated by adding one tenth 1.4 M IAA, separated on a 4–12% polyacrylamide gradient gel (19 μg protein per well) using MOPS running buffer, and analyzed by Western blotting as described in the following section.

Western Blotting

Proteins separated by SDS-PAGE were transferred onto a polyvinylidene difluoride membrane by semidry electroblotting (1.2 mA/cm^2 for 1 h or 0.2 mA/cm^2 overnight) using transfer buffer (75 mM Tris-base/39 mM glycine/0.037% (w/v) SDS/20% ethanol) and blocked with TBS/0.5 M NaCl/0.1% Tween/5% non-fat dry milk at 4°C for several hours. FIBCD1 was detected by probing the blot with 2 μg/mL mouse monoclonal anti-FIBCD1 antibody HG-HYB-12-2 or mouse monoclonal anti-FIBCD1-FReD antibody HYB-11-14-25 diluted in TBS/0.5 M NaCl/0.1 % Tween/2.5% non-fat dry milk at 4°C overnight. Mucins were detected by probing the blot with 0.22 μg/mL rabbit monoclonal anti-MUC-1 antibody, 2 μg/mL rabbit polyclonal anti-MUC-13 antibody, or 6.6 μg/mL mouse monoclonal anti-MUC-5AC antibody in 20 mL TBS/0.5 M NaCl/0.1% Tween/2.5% non-fat dry milk at 4°C overnight. Mouse monoclonal anti-GAPDH antibody (0.01 μg/mL) was used as control. Excess antibody was removed by extensive washing with TBS/0.5 M NaCl/0.1% Tween and the blot was incubated 1 h with either HRP-conjugated rabbit anti-mouse antibody diluted 1:10,000 or HRP-conjugated goat anti-rabbit antibody diluted 1:20,000 in TBS/0.5 M NaCl/0.1% Tween. The blot was washed, developed using ECL standard method, detected by Fusion Fx7 (Vilber Lourmat, Collégien, France), and depicted using FUSION-CAPT version 15.18 software (Vilber Lourmat, Collégien, France). Precision Plus Protein™ Kaleidoscope™ Standards were used as size markers. Between incubations with anti-mucin and -GAPDH antibodies, the membrane was stripped and blocked. Stripping was achieved by washing once with TBS/0.5 M NaCl/0.1% Tween, boiling in deionized water for 10 min, and washing twice with TBS/0.5 M NaCl/0.1% Tween.

Expression of Results and Statistics

Unless otherwise stated, data are expressed as mean ± SEM and differences were considered to be statistically significant when $p < 0.05$. Log2-transformed IL-8 secretion data was analyzed by one- or two-way ANOVA with Tukey's *post-hoc* tests depending on the number of independent variables using Prism software (version 6.0d, Graphpad, San Diego, CA, USA). Multilevel mixed-effects linear regression models were used to determine whether changed RNA expression of various genes was associated with stimulant, genotype, or a combined effect of these variables using the XTMIXED function of STATA13 (STATA Corp, College Station, TX, USA). Genes were analyzed separately using multilevel mixed-effects linear regression models to compensate for random effects. Log2 (CNRQ) was outcome, while stimulant, genotype, and interaction between these were fixed effects, and biological triplicate and culture plate variation were random effects (**Table S1**). Final models were evaluated for normality by prediction of residuals and assessment of their normal distribution by graphic (qq-plot, histogram, and box plot) and numeric methods (Skewness/Kurtosis and Shapiro-Wilk tests). *P*-values were extracted from the models using the LINCOM function.

RESULTS

FIBCD1 Is Expressed on the Apical Surface of Human Bronchial and Alveolar Epithelial Cells

We have previously shown that FIBCD1 is expressed apically by epithelial cells of mucous membranes, i.e. the small and large intestine and salivary glands (14), and therefore hypothesized that it is also expressed in the lung mucosal membrane. First, we determined FIBCD1 mRNA expression in a series of human tissues (**Figure 1A**). The highest expressional levels were found

in the respiratory tract (lung and trachea), gastrointestinal tract (colon and small intestine), testis, placenta, and brain. Then, we performed an immunohistochemical (IHC) analysis of human, non-cancerous lung tissue (control) from patients with lung cancer (**Figures 1B–E**) and from patients with pulmonary *A. fumigatus* infection (**Figures 1F–I**). FIBCD1 immunostaining was detected in submucosal glands, alveoli, and bronchioles with more intense staining coincident with areas of inflammation (**Figures 1G,H**). Bronchiolar FIBCD1 was restricted to the apical surface of ciliated epithelial cells (**Figures 1E,I**) similar to the expression observed in the gastrointestinal tract (14). Similar results were observed by von Huth et al. (25) in non-malignant, non-inflammatory, and histologically normal, human tissues. Thus, FIBCD1 is expressed apically in the lung mucosal membrane and seemingly increased in areas of inflammation.

FIBCD1 Binds to *A. fumigatus* Dependent on Cell Wall PAMP Availability

We next examined if FIBCD1 is capable of recognizing *A. fumigatus* hyphae. Fluorescence microscopy revealed FIBCD1 recognition of fully-grown hyphae (**Figures 2A,B**), including chitin-rich septum regions (**Figures 2C,D**) and mycelial frame of budding hyphae (**Figures 2E,F**). We further examined co-localization between the chitin-binding fluorescent-labeled WGA and FIBCD1 in different morphological stages. Co-localization was observed in all stages characterized by exposed cell wall polysaccharides including swollen conidia, germ tubes, budding regions, and growing hyphae (**Figure 2G**), while no binding of FIBCD1 observed on resting conidia (**Figure S1**). Thus, FIBCD1 binds to *A. fumigatus* dependent on cell wall PAMP availability.

FIBCD1 Recognizes a Composite Structure in AIF Not Exclusively Through the S1 Binding Site

To evaluate if FIBCD1 binds fungal chitin, we isolated the chitin-containing structural skeleton of the *A. fumigatus* cell wall (AIF) and performed a pull-down assay (**Figure 3A**). We show that rFIBCD1-FReD binds AIF and pull-down using Dectin-1 fc, rMBL, and WGA demonstrated that cell wall components β-1,3-glucan, galactomannan, and chitin, respectively, were preserved after treatment (12, 26). We observed bands corresponding to FIBCD1-FReD monomeric, dimeric, trimeric, and tetrameric structures, at ∼25, 50, 75, and 100 kDa, respectively, and large Dectin-1 fc structures of ∼120 and 300 kDa. We observed bands corresponding to higher polymeric structures of rMBL, which assembles into trimers and hexamers of trimers. The smallest rMBL band is ∼30 kDa, which is comparable to the rMBL monomer. Finally, we observed a band corresponding to the WGA monomer at ∼18 kDa.

FIBCD1 exhibits calcium-dependent binding of chitin and other acetylated compounds through a conserved S1 hydrophobic pocket of the FReD (14, 15). Therefore, we hypothesized that FIBCD1 binds *A. fumigatus* AIF through a similar mechanism. To investigate this, we performed a pull-down assay using AIF in the presence or absence of calcium and

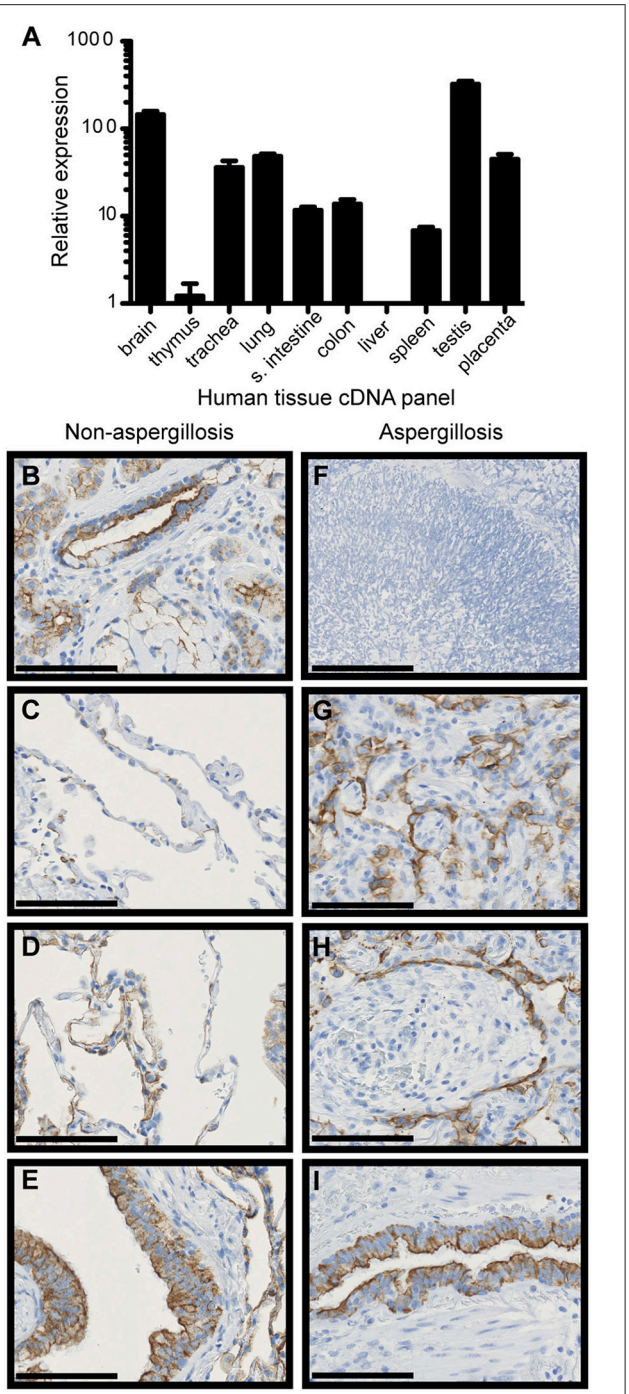

FIGURE 1 | FIBCD1 RNA is expressed in various human tissues and FIBCD1 protein is expressed on the apical site of lung epithelium and within submucosal glands. **(A)** Relative expression of FIBCD1 mRNA in various human tissues relative to expression in thymus. Technical triplicates. **(B–E)** IHC staining of FIBCD1 in non-cancerous lung tissue from a 68-year-old female patient with adenocarcinoma (scale bars: 100 μm, magnification: 40X). FIBCD1 was detected in submucosal glands **(B)**, non-inflamed alveoli **(C)**, inflamed alveoli **(D)**, and inflamed bronchioles **(E)**. **(G–I)** IHC staining of FIBCD1 in lung tissue from a 63-year-old male patient with *A. fumigatus* infiltration (scale bars: 100 μm, magnification: 40X). Formation of aspergilloma was observed (**F**, scale bar: 200 μm, magnification: 20X) and FIBCD1 was detected in alveoli with atelectasis **(G)** and pneumonia **(H)** and in bronchioles **(I)**.

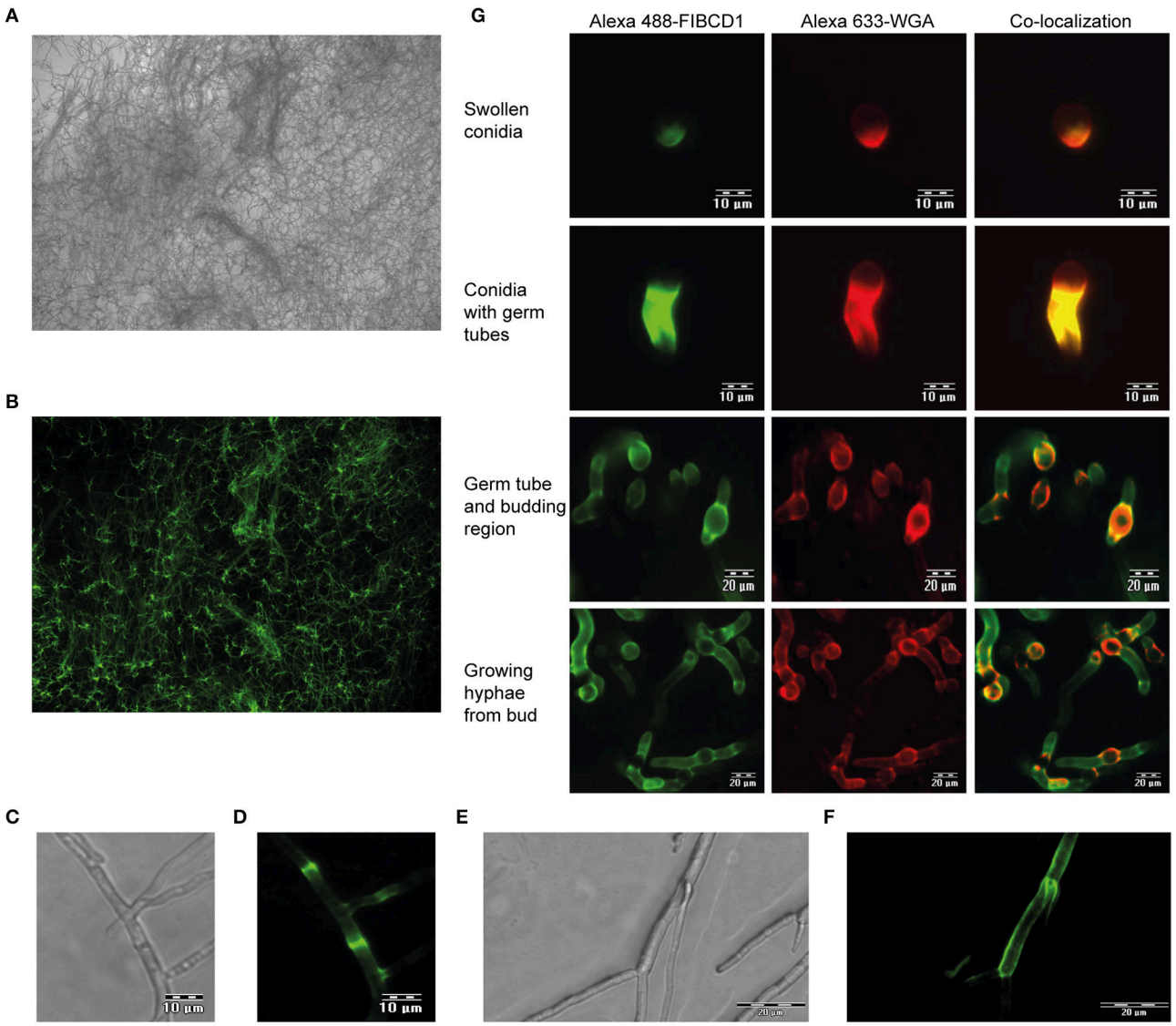

FIGURE 2 | FIBCD1 recognizes chitin-rich regions of *A. fumigatus* during different life stages. Bright field **(A,C,E)** and fluorescence **(B,D,F,G)** microscopy of *A. fumigatus*. **(A,B)** A total of 10^7 *A. fumigatus* conidia/mL was grown in SD medium to form fungal hyphae followed by staining with Alexa 488-labeled FIBCD1 as described in materials and methods. A clear recognition of fungal hyphae by FIBCD1 was observed. Image: 10X objective. **(C–F)** $5{\cdot}10^6$ *A. fumigatus* conidia/mL were grown in SD broth medium and stained with Alexa 488-labeled FIBCD1. rhFIBCD1 recognized the chitin-rich *A. fumigatus* septum of fully-grown hyphae. Image 40X and 20X objectives. **(G)** 10^4 *A. fumigatus* conidia/mL was grown in SD medium for various time points (6, 8, and 12 h) at 37°C and stained with Alexa 633-labeled WGA and Alexa 488-labeled FIBCD1. FIBCD1 failed to bind resting conidia (**Figure S1**). We observed co-localization of regions recognized by Alexa 488-labeled FIBCD1 and Alexa 633-labeled WGA.

acetate (**Figure 3B**). The insoluble, separate cell wall components β-1,3-glucan and chitin (beads) were used as negative and positive control, respectively (14). Surprisingly, our results show that FIBCD1 binding of AIF is calcium-independent and less sensitive to acetate than purified chitin, suggesting that FIBCD1 binds AIF through additional binding sites outside the S1 binding pocket, potentially involving other polysaccharide structures found in AIF. Therefore, we performed a pull-down assay of wild type FIBCD1-FReD and FIBCD1-FReD with a site-directed mutagenesis abolishing the binding properties of the S1 binding site, A432V (15), using AIF and chitin beads (positive control) (**Figure 3C**). Our results show that FIBCD1-FReD is capable of binding AIF when the binding activity of the S1 binding site is disrupted.

FIBCD1 Overexpression Suppresses IL-8 Secretion After Stimulation With *A. fumigatus* AIF and Galactomannan

A549 lung epithelial cells secrete IL-8 after exposure to *A. fumigatus* irradiated conidia and mycelium (27), and we confirmed a time- and dose-dependent induction of IL-8

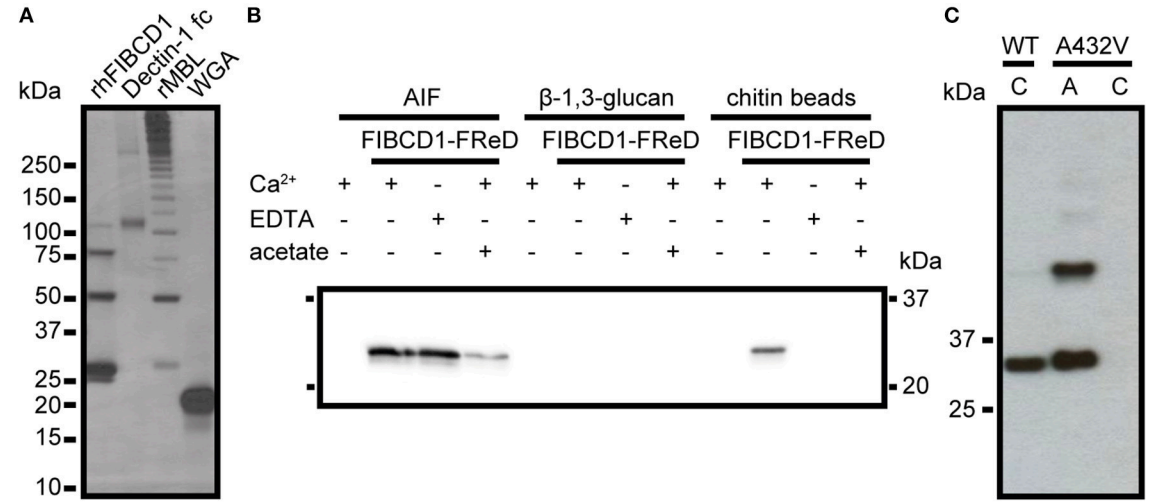

FIGURE 3 | rFIBCD1-FReD binds *A. fumigatus* AIF calcium- and acetate-independently. **(A)** The presence and binding activity of β-1,3-glucan, galactomannan, and chitin in AIF was validated by pull down of know ligands Dectin-1 fc, rMBL, and WGA. The samples were subjected to SDS-PAGE and analyzed by silver staining. Color is adjusted to gray scale. **(B)** Western blot showing FIBCD1-FReD pull down by AIF-associated polysaccharides in the presence of calcium (5 mM $CaCl_2$), EDTA (10 mM), and acetate (100 mM). 2 mg of AIF, β-1,3-glucan, and chitin beads were incubated with 5 μg/mL FIBCD1-FReD and pull down was performed as described. Data represent three independent experiments. **(C)** Western blot showing wild type and A432V mutant FIBCD1-FReD pull down by chitin beads and AIF. Color is adjusted to gray scale. Lane 1, 3: chitin beads, Lane 2: AIF.

following stimulation with live conidia and AIF (**Figure S2**). Since A549 cells constitutively expressed low or non-detectable levels of FIBCD1 protein (**Figure 4B**, top panel), we increased FIBCD1 expression by transfecting A549 cells with the full-length human *fibcd1* gene and compared these to sham-transfected A549 cells. In A549 FIBCD1-transfected cells, FIBCD1 protein expression was confirmed by Western blot analysis (**Figure 4A**) and surface expression by flow cytometry (**Figure 4B**, bottom panel). Stimulation of the transfected A549 cells with AIF, β-1,3-glucan, chitin, or galactomannan (**Figures 4C–L**) resulted in time- and dose-dependent IL-8 secretion. FIBCD1 over-expression mediated basal suppression of IL-8 secretion in cells without stimulus (DPBS alone). This FIBCD1-mediated IL-8 suppression was abolished during stimulation with β-1,3-glucan (**Figures 4E,F**) and chitin (**Figures 4G,H**). Chitin induced a very low IL-8 response, while β-1,3-glucan induced a high IL-8 response in both cell types. However, FIBCD1-mediated suppression of IL-8 secretion was increased by stimulation with AIF (**Figures 4C,D**) and galactomannan (**Figures 4I,J**). A similar response was observed against the positive control ligand acBSA (**Figures 4K,L**). Hence, FIBCD1 overexpression suppresses IL-8 secretion and maintains this suppression after stimulation with *A. fumigatus* AIF and galactomannan.

FIBCD1 Suppresses Mucin and Inflammatory Gene Expression and Increases Expression of Genes Involved in Mucosal Barrier Function

Next, we investigated the effect of FIBCD1 transfection on lung epithelial and immune response gene expression after incubation with AIF, β-1,3-glucan, and chitin (**Figure 5** and **Table S1**). Transfected FIBCD1 expression suppressed the RNA expression of proinflammatory cytokines, chemokines, and mucins (CCL20, CSF2RA, TNF, IL1B, IL8, MUC1, MUC13, and MUC5AC) and increased RNA expression of barrier function proteins (OCLN and ICAM1). FIBCD1-mediated suppression of CCL20, IL1B, IL8, and ICAM1 was reversed in the presence of β-1,3-glucan or chitin. In contrast, stimulation with AIF generally increased FIBCD1-mediated suppression of CCL2, CSF2RA, IL1B, IL8, MUC13, and MUC5AC and FIBCD1-mediated induction of the Th2-associated cytokine IL12B. CXCL2, IL6, IL10, IL25, and IL33 were not detected (data not shown). We further evaluated the protein expression of genes with threshold cycle values below 25 (data not shown) regulated at least 2-fold by FIBCD1 expression and not already examined (MUC-1, MUC-13, and MUC-5AC) (**Figure 6**). In keep with the qPCR data, we observed FIBCD1-mediated suppression of MUC-1,−13, and −5AC in the presence or absence of AIF. Increased FIBCD1-mediated suppression in the presence of AIF was only observed on MUC-13 and −5AC. Thus, FIBCD1 overexpression suppresses mucins and inflammatory gene expression and increases expression of genes involved in mucosal barrier function.

FIBCD1 Influences IL-8 Secretion From A549 Lung Epithelial Cells in Response to TLR2, TLR4, and TLR5 Agonists

Finally, we examined whether FIBCD1 expression modulated TLR-induced IL-8 secretion by stimulating A549 sham- and FIBCD1-transfected cells with 10 different TLR agonists and measuring IL-8 levels in culture supernatants (**Figure 7**). We found that FIBCD1 in particular suppressed TLR2 and −4 agonist-induced IL-8 secretion and that TLR5 agonist

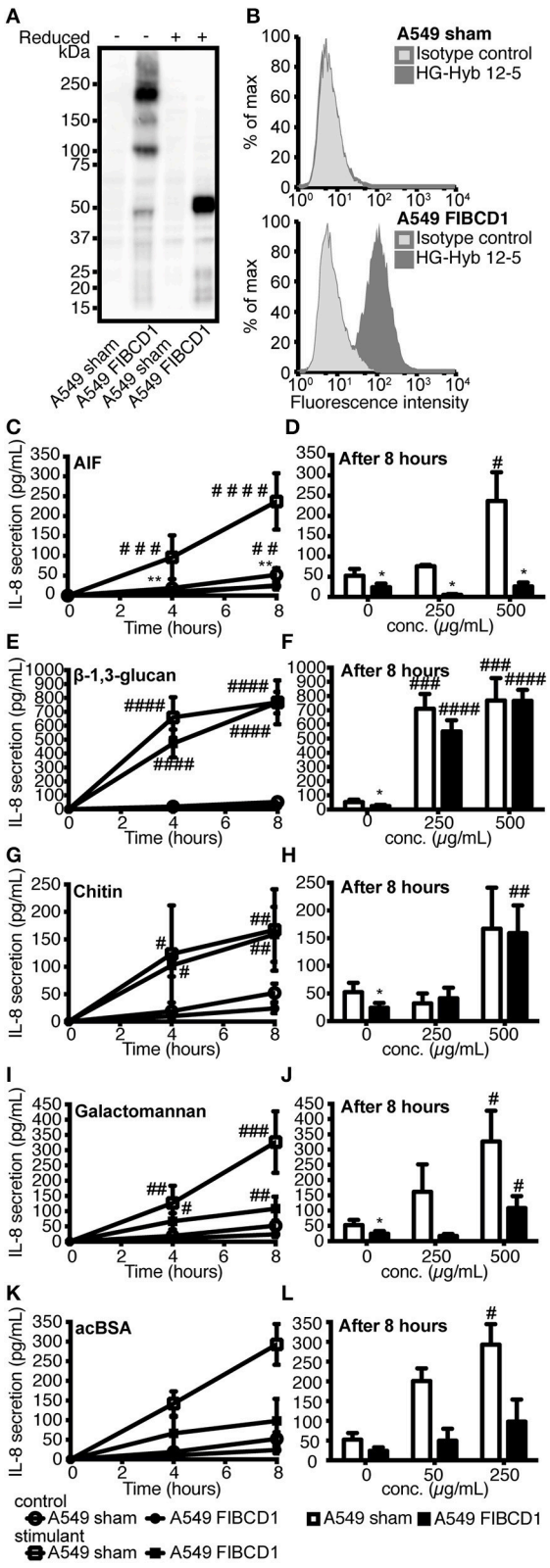

FIGURE 4 | Overexpression of FIBCD1 on the surface of A549 cells inhibits secretion of IL-8. The phenotype of sham- and FIBCD1-transfected A549 cells *(Continued)*

FIGURE 4 | was analyzed by Western blotting **(A)** and flow cytometry **(B)**. **(A)** Western blot of cell lysate from sham- and FIBCD1-transfected A549 cells under reducing and non-reducing conditions revealed the presence of four known oligomeric forms of FIBCD1 in the FIBCD1-transfected cells when probed with the anti-FIBCD1 mAb clone HG-HYB 12-2. **(B)** Flow cytometry of sham- and FIBCD1-transfected A549 cells showed surface expression of FIBCD1 on FIBCD1-transfected cells and none on sham-transfected cells when using anti-FIBCD1 antibody HG-HYB 12-5 for detection. **(C–L)** A549 sham- and FIBCD1-transfected cells were seeded at a density of one million cells in 2 mL of media per well of a 6-well tissue culture plate and serum-starved overnight prior to stimulation with two different concentrations of several components associated with *A. fumigatus* or FIBCD1 for 0, 4, and 8 h and the concentration of secreted IL-8 was determined by sandwich ELISA as described. Left column: Time-dependent IL-8 secretion to 1,000 μg AIF **(C)**, 1,000 μg β-1,3-glucan **(E)**, 1,000 μg chitin **(G)**, 1,000 μg galactomannan **(I)**, or 500μg acBSA **(K)** per 2 mL medium. Right column: Dose-dependent IL-8 secretion after 8 h of stimulation with AIF **(D)**, β-1,3-glucan **(F)**, chitin **(H)**, galactomannan **(J)**, or acBSA **(L)**. Data are presented as mean ± SEM from three independent experiments. Duplicate cell cultures were used for each of the three independent experiments and ELISA measurements were performed in duplicates on each of these. Data were analyzed by two-way ANOVA, following Tukey's test, $\#p < 0.05$, $\#\#p < 0.01$, $\#\#\#p < 0.001$, and $\#\#\#\#$ $p < 0.0001$ relative to 0 h or DPBS-treated cells. $^{*}p < 0.05$ and $^{**}p < 0.01$, relative to A549 sham cells stimulated with the same stimulant for the same time period.

circumvented IL-8 suppression. These findings are supported by qPCR (**Figure S4**). Though TLR6/2,−7,−8, and −9 agonist-induced IL-8 secretion was suppressed by FIBCD1 expression, it differed little from the basal suppression. Contrary to this, TLR2,−4, and −5 agonist-induced IL-8 secretion was changed at least 2-fold from basal suppression. Similar results were observed after 4 h of stimulation (**Figure S3**). Hence, FIBCD1 expression influences TLR2,−4, and −5 agonist-induced IL-8 secretion.

DISCUSSION

We previously reported FIBCD1 protein expression at the brush border of human intestinal epithelium and identified binding of crab shell chitin in the S1 binding site of FIBCD1-FReD (14, 15). In the current study, we observed FIBCD1 protein expression at the apical site of human bronchial and alveolar epithelium and binding between FIBCD1 and *A. fumigatus* dependent on cell wall availability, as well as an S1 site-independent AIF recognition. We observed FIBCD1-mediated suppression of IL-8 secretion, mucin production, and transcription of genes involved in inflammatory signaling and FIBCD1-mediated induction of tight junction and cell adhesion molecule transcription. Additionally, we show that this regulation was modulated by stimulation with *A. fumigatus* cell wall and individual cell wall components, i.e., β-1,3-glucan and chitin, and FIBCD1 expression effected TLR agonist-induced IL-8 secretion.

Fluorescence microscopy of different *A. fumigatus* morphotypes (**Figure 2**) showed that soluble FIBCD1 binding was dependent on conidial germination and concomitant exposure of cell wall polysaccharides. Thus, FIBCD1's role in the immune response against *A. fumigatus* may be associated with the expanded immune response, i.e. opsonization

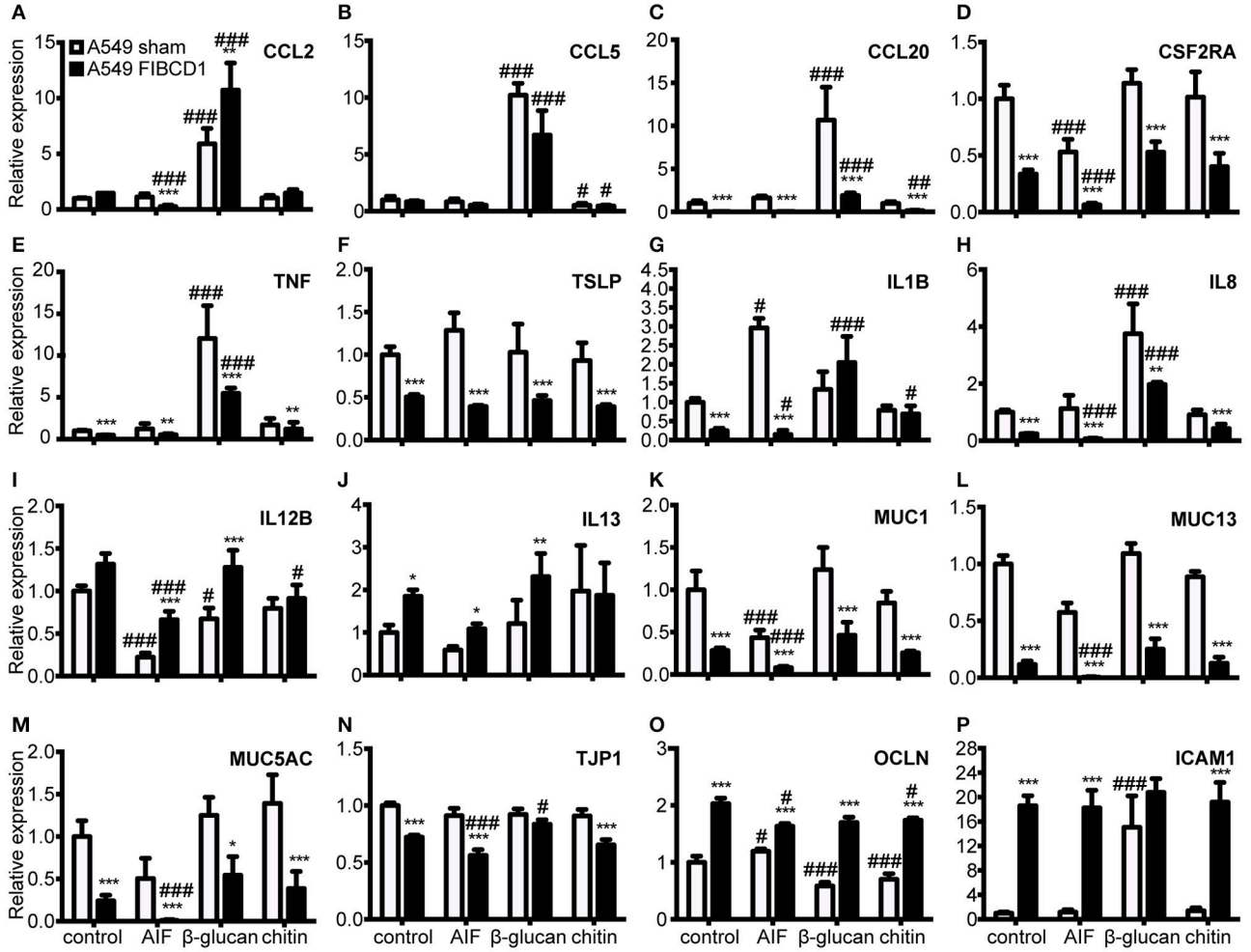

FIGURE 5 | Overexpression of FIBCD1 affects RNA expression of genes associated with immunological responses at mucosal sites. Relative RNA expression of cytokines **(A-J)**, mucins **(K-M)**, TJ proteins **(N-O)**, and adhesion protein **(P)** by A549 sham and A549 FIBCD1 cells in response to stimulation. One million A549 lung epithelial cells transfected with sham and hFIBCD1, respectively, were incubated with DPBS, 500 μg/mL AIF, β-1,3-glucan, and chitin in 2 mL serum-free complete medium for 8 h. The culture supernatants were removed, 1 mL TRIzol added to each well, RNA isolated, cDNA synthetized and tested, and qPCR performed. Data are presented as mean ± SEM from three independent experiments. *P*-values are extracted from the multilevel linear regression models. $^{\#}p < 0.05$, $^{\#\#}p < 0.01$, and $^{\#\#\#}p < 0.001$ relative to DPBS-treated cells. $^{*}p < 0.05$, $^{**}p < 0.01$, and $^{***}p < 0.001$ relative to A549 sham cells stimulated with the same stimulant.

and chemotactic attraction of neutrophils to the site of inflammation (1). Furthermore, we observed co-localization between chitin-rich zones and areas recognized by FIBCD1, which led us to investigate interaction between FIBCD1 and the chitin-containing structural skeleton of the *A. fumigatus* cell wall (AIF). Pull-down experiments (**Figure 3**) revealed that FIBCD1 recognizes AIF independently of calcium and the S1 binding site with less sensitivity to acetate compared to that of chitin.

Chitin is the only component of the cell wall known as a FIBCD1 ligand, which it binds through the S1 binding site (14). These findings support that FIBCD1 recognizes fungal chitin through the S1 binding site, but also recognizes other cell wall structures found in AIF, possibly through conjunctional binding sites or separately in other unknown binding sites.

Similar to a previous study using A549 lung epithelial cells (27), we observed a time- and dose-dependent secretion of IL-8, a proinflammatory chemokine that attracts neutrophils and thereby plays an important role in the inflammatory response against *A. fumigatus* hyphae (1). Stimulation of A549 lung epithelial cells overexpressing FIBCD1 (**Figure 4**) revealed a suppression of IL-8 secretion, which is abolished by stimulation with β-1,3-glucan and chitin and increased by AIF, galactomannan, and acBSA. As a non-FIBCD1 binding ligand, we expect the observed effect of β-1,3-glucan on FIBCD1-mediated suppression of IL-8 secretion to be caused by the activation of pathways that either deactivate FIBCD1, decrease its expression, or induce IL-8 production through circumventing pathways, possibly through the well-known β-1,3-glucan PRR Dectin-1 (12). Different effects of the FIBCD1

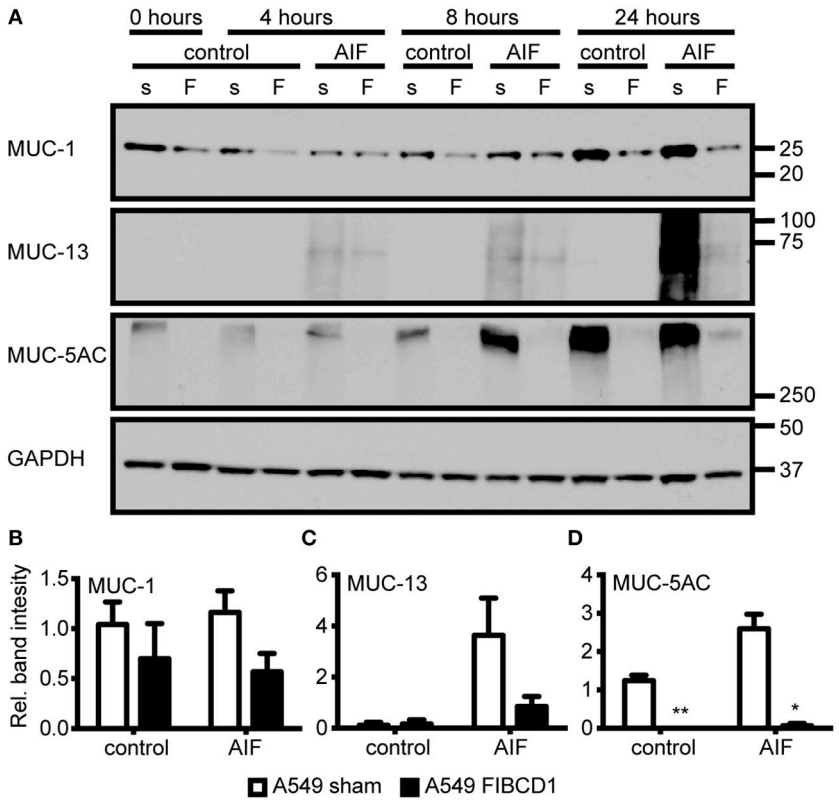

FIGURE 6 | Overexpression of FIBCD1 modulates mucin protein production. A549 sham- and FIBCD1-transfected cells were seeded at a density of one million cells in 2 mL of media per well of a 6-well tissue culture plate and serum-starved over night prior to incubation with DPBS or 500 μg/mL AIF in 2 mL serum-free media for 0, 4, 8, and 24 h. **(A)** Western blot analysis was performed as described using 19 μg of cell lysate per well. Lane 1, 3, 5, 7, 9, 11, 13: A549 sham-transfected cells, Lane 2, 4, 6, 8, 10, 12, 14: A549 FIBCD1-transfected cells. The Western blot shown is from one of three independent experiments yielding similar results. Color is adjusted to gray scale. **(B–D)** Western blots were quantified using ImageJ software. The values obtained after 8 h are expressed as mean ± SEM of the ratio of MUC-1 **(B)**, MUC-13 **(C)**, and MUC-5AC **(D)** to GAPDH from three independent experiments. Data were analyzed by two-way ANOVA, following Tukey's test, $^{\#}p < 0.05$, $^{\#\#}p < 0.01$, and $^{\#\#\#}p < 0.001$ relative to control cells. $^{*}p < 0.05$, $^{**}p < 0.01$, and $^{***}p < 0.001$ relative to A549 sham cells stimulated with the same stimulant.

ligands AIF, chitin, and acBSA were observed, which is likely caused by particle size and source differences known to impact epithelial responses against chitin (28, 29). Previous studies have shown that large particles fail to induce an inflammatory response, while intermediate and small particles protect against Th2-associated allergy (28, 29). In the current study, the exact size of the chitin particles is unknown, however, large, insoluble fragments were observed by bright field microscopy during the stimulation study, which may have effected the interaction between FIBCD1 and chitin. Contrary to this, AIF was administered in intermediate particle size (<40 μm) and acBSA and galactomannan are both soluble molecules. It is currently unclear if the FIBCD1-mediated suppression of IL-8 secretion in response to galactomannan is caused by mere particle size, intersections of signaling pathways or by direct or indirect interaction between FIBCD1 and galactomannan. It is, however, clear that galactomannan does not bind to the S1 binding site of FIBCD1-FReD (**Figure S5**).

We observed a FIBCD1-mediated transcriptional suppression of proinflammatory cytokines, chemokines, and mucins and an induction of barrier function gene expression (**Figure 5**). During the anti-fungal response, several proteins of the genes suppressed by FIBCD1 are released from epithelium to aid in the response. They cause increased inflammation, recruitment of neutrophils, monocytes, and mast cells to the site of inflammation, stimulation of naïve Th cell polarization to Th2 cells, and facilitate homing of these cells. Finally, they induce secretion of MUC-5AC and epithelial expression of MUC-1 and −13, and disrupt epithelial apical junctional complexes, which further enhances inflammation and antigen presentation by dendritic cells (30–40). Thus, FIBCD1 may serve as a general suppressor of airway inflammation. Similar to the IL-8 secretion observations, stimulation with β-1,3-glucan and chitin diminish and AIF increases FIBCD1-mediated suppression.

Mucociliary clearance is the primary defense mechanism against *A. fumigatus* in the bronchioles (6) and is highly dependent on the synthesis, glycosylation, and release of secreted and membrane-bound mucins (37, 41). FIBCD1-mediated suppression of MUC-1 and MUC-5AC and an AIF-increased

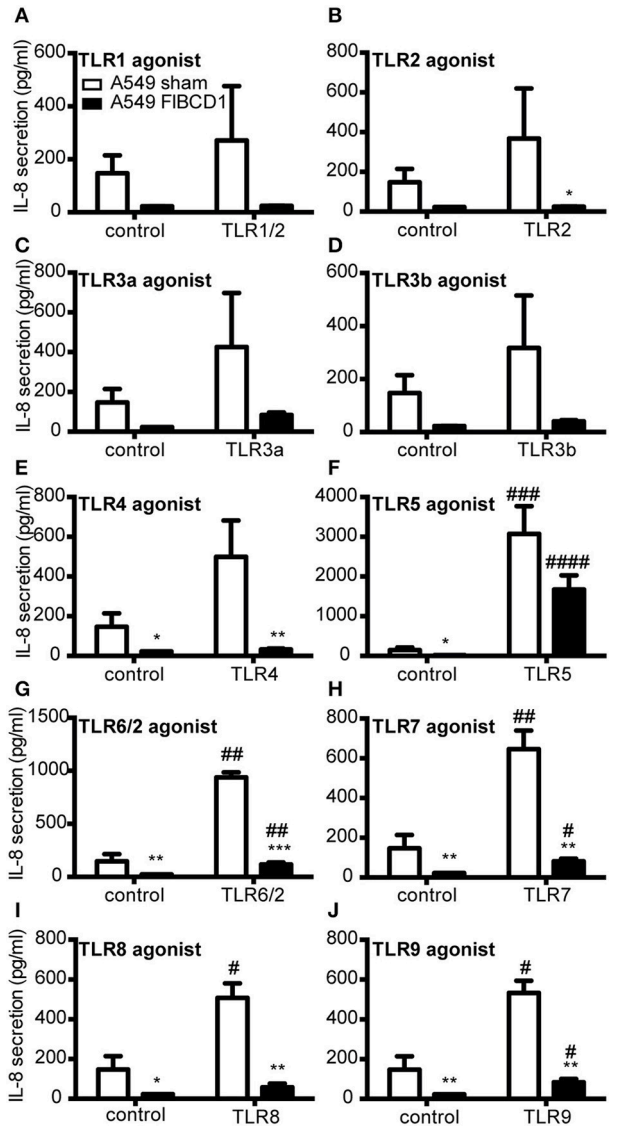

FIGURE 7 | Overexpression of FIBCD1 on the surface of A549 cells inhibits TLR agonist effects. A549 sham- and FIBCD1-transfected cells were seeded at a density of 250,000 cells in 0.5 mL of media per well of a 24-well tissue culture plate and serum-starved overnight prior to stimulation. The cells were stimulated with TLR1/2 **(A)**, 5 **(F)**, and 6/2 **(G)** agonists (0.67 μg/mL), TLR2 **(B)** agonist (6.7·107 cells/mL), TLR3a **(C)** and 3b **(D)** agonists (8.9 μg/mL), TLR4 **(E)** agonist (4.4 μg/mL), TLR7 **(H)** and 8 **(I)** agonists (1.8 μg/mL), and TLR9 **(J)** agonist (0.068 μg/mL) for 8 h and the concentration of secreted IL-8 was determined by sandwich ELISA as described in methods. Data are presented as mean ± SEM from three independent experiments. Duplicate cell cultures were used for each of the three independent experiments and ELISA measurements were performed in duplicates on each of these. Data were analyzed by two-way ANOVA, followed by Tukey's post-test, $^{\#}p < 0.05$, $^{\#\#}p < 0.01$, $^{\#\#\#}p < 0.001$, and $^{\#\#\#\#}p < 0.0001$ relative to DPBS-treated cells. $^{*}p < 0.05$, $^{**}p < 0.01$, and $^{***}p < 0.001$ relative to A549 sham cells stimulated with the same stimulant.

FIBCD1-mediated suppression of MUC-13 and MUC-5AC were observed by Western blotting of cell lysates from A549 lung epithelial cells (**Figure 6**). This indicates that FIBCD1 expression impacts mucus composition and thereby fungal clearance. However, whether these alterations are beneficial for fungi or host is unclear. Additionally, MUC-5AC is a secretory mucin (41) and the lack of vesicle storage in the A549 FIBCD1-transfected cells compared to the A549 sham-transfected cells may reflect increased release as well as decreased production.

Finally, we observed that FIBCD1 overexpression affects the inflammatory response mediated by TLRs in A549 lung epithelial cells (**Figure 7**). The overexpression decreases TLR2- and TLR4-induced IL-8 secretion and increases TLR5-induced IL-8 secretion. Intriguingly, these TLRs are associated with different outcomes of fungal infections. Several studies have investigated the role of TLR2 and TLR4 in the immunological response against *A. fumigatus* and found that their expression is required for optimal host defense (6, 42, 43). The investigation of TLR5's involvement in anti-*A. fumigatus* responses is fairly limited, and it has early been demonstrated that TLR5 have no influence on the anti-*A. fumigatus* response (42). However, Rodland et al. (44) observed an increased RNA expression of the receptor in human monocytes challenges with *A. fumigatus* and later found that TLR5 has an enhancing effect on the viability of conidia (45).

Collectively, our findings demonstrate FIBCD1 as human lung epithelial PRR that recognizes the cell wall of *A. fumigatus* and suppresses epithelial inflammatory signaling and mucin production. FIBCD1 activation may have a beneficial effect by decreasing inflammatory damage or an adverse effect by diminishing anti-fungal responses such as recruitment of neutrophils and mucin production.

AUTHOR CONTRIBUTIONS

The experiments were designed by CJ, LD, AS, GS, ST, and UH. CJ, LD, KC, JM, MH, and ON performed the experiments. CJ performed statistical analysis of the data. The reagents, materials, and analysis tools were provided by ON, AS, GS, and UH. CJ, ST, and UH wrote the paper.

FUNDING

This work was supported by The Danish Medical Research Council, The Independent Research Fund Denmark, The Novo Nordisk Foundation, The Lundbeck Foundation, Fonden til Lægevidenskabens Fremme, The Beckett foundation, and The Gangsted Foundation.

ACKNOWLEDGMENTS

We thank René Holst for help with the multilevel linear regression models, Theresa Thomsen for providing the FIBCD1 deletion mutants, and Jan Mollenhauer for providing the pDEST vector.

SUPPLEMENTARY MATERIAL

The Supplementary Material for this article can be found online at: https://www.frontiersin.org/articles/10.3389/fimmu.2018.01967/full#supplementary-material

Figure S1 | FIBCD1 does not recognizes *A. fumigatus* resting conidia. Bright field **(A)** and fluorescence **(B)** microscopy of *A. fumigatus*. **(A,B)** *A. fumigatus* conidia/mL was grown in SD medium to form fungal hyphae followed by staining with Alexa 488-labeled FIBCD1 as described in materials and methods. A clear recognition of fungal hyphae by FIBCD1 was observed while no staining was seen of the resting conidia indicated by arrows was seen. Image: 20X objective.

Figure S2 | *A. fumigatus* conidia and AIF induce IL-8 secretion by A549 wild type cells time- and dose-dependently. Wild type A549 cells were seeded at a density of $3{\cdot}10^5$ cells in 2 mL of media per well of a 12-well tissue culture plate and serum-starved over night prior to stimulation and the concentration of secreted IL-8 was determined by sandwich ELISA as described in methods. Left panels: Time-dependent IL-8 secretion to $3{\cdot}10^5$ conidia **(A)** and 800 μg AIF **(C)** per 2 mL medium. Right panels: Dose-dependent IL-8 secretion after 8 h of stimulation with conidia **(B)** and AIF **(D)**. Data are presented as mean ± SEM from three independent experiments. ELISA measurements were performed in triplicates **(A,C)** and duplicates **(B,D)** for each of the three independent experiments. Data were analyzed by two-way **(A,C)** and one-way **(B,D)** ANOVA, followed by Tukey's post-test. $*p < 0.05$, $**p < 0.01$, $***p < 0.001$, and $****p < 0.0001$ relative to previous time or dosage.

Figure S3 | Overexpression of FIBCD1 on the surface of A549 cells influences TLR agonist effects after 4 h. A549 sham- and FIBCD1-transfected cells were seeded at a density of 250,000 cells in 0.5 mL of media per well of a 24-well tissue culture plate and serum-starved overnight prior to stimulation. The cells were stimulated with TLR1/2 **(A)**, 5 **(F)**, and 6/2 **(G)** agonists (0.67 μg/mL), TLR2 **(B)** agonist (6.7·107 cells/mL), TLR3a **(C)** and 3b **(D)** agonists (8.9 μg/mL), TLR4 **(E)** agonist (4.4 μg/mL), TLR7 **(H)** and 8 **(I)** agonists (1.8 μg/mL), and TLR9 **(J)** agonist (0.068 μg/mL) for 4 h and the concentration of secreted IL-8 was determined by sandwich ELISA as described in methods. Data are presented as mean ± SEM from three independent experiments. Duplicate cell cultures were used for each of the three independent experiments and ELISA measurements were performed in duplicates on each of these. Data were analyzed by two-way ANOVA, following Tukey's test, $\#p < 0.05$, $\#\#p < 0.01$, $\#\#\#p < 0.001$, and $\#\#\#\#p < 0.001$ relative to DPBS-treated cells. $*p < 0.05$, $**p < 0.01$, and $***p < 0.001$ relative to A549 sham cells stimulated with the same stimulant.

Figure S4 | Overexpression of FIBCD1 on the surface of A549 cells influences TLR agonist effects. A549 sham- and FIBCD1-transfected cells were seeded at a density of 250,000 cells in 0.5 mL of media per well of a 24-well tissue culture plate and serum-starved overnight prior to stimulation. The cells were stimulated with TLR1/2 and 5 agonists (0.67 μg/mL), TLR2 agonist ($6.7{\cdot}10^7$ cells/mL), and TLR4 agonist (4.4 μg/mL) for 4 h **(A)** and 8 h **(B)**. The culture supernatants were removed, 0.5 mL TRIzol added to each well, RNA isolated, cDNA synthetized, and qPCR performed. Data are presented as mean ± SEM from three independent experiments and qPCR measurements were performed in duplicates on each of these. Data were analyzed by two-way ANOVA, following Tukey's test, $\#p < 0.05$, $\#\#p < 0.01$ and $\#\#\#p < 0.001$, relative to DPBS-treated cells. $**p < 0.01$, and relative to A549 sham cells stimulated with the same stimulant.

Figure S5 | Competitive ELISA showing galactomannan's effect on binding between acBSA and FIBCD1-FReD. A maxisorp immuno plate was coated with 1 μg/mL acBSA in ELISA coating buffer overnight. PBS, acetate, mannan, and galactomannan were loaded in a 2-fold dilution series in TBS/0.05% tween/5 mM $CaCl_2$ starting at 100 mM, 2 mg/mL, and 2 mg/mL, respectively, along with 0.5 μg/mL FIBCD1-FReD. PBS was used as a control for decreased Ca^{2+} presence by the addition of polysaccharides suspended in PBS, calcium content started at 2.5 mM $CaCl_2$. FIBCD1-FReD was detected by 1 μg/mL HG-HYB-12-6 in TBS/0.05% tween/5 mM $CaCl_2$ and HRP-conjugated rabbit anti-mouse antibody. Data represent three independent experiments and is shown as mean ± SEM. ELISA measurements were performed in duplicates for each of the three independent experiments.

Table S1 | Multilevel linear regression models. Results of the multilevel linear regression models used to analyze relative mRNA expression of cytokines, mucins, adhesion proteins, and TJ proteins in A549 sham and A549 FIBCD1 cells in response to stimulation (**Figure 6**).

REFERENCES

1. Latge JP. *Aspergillus fumigatus* and aspergillosis. *Clin Microbiol Rev.* (1999) 12:310–50.
2. Zmeili OS, Soubani AO. Pulmonary aspergillosis: a clinical update. *QJM* (2007) 100:317–34. doi: 10.1093/qjmed/hcm035
3. Simon-Nobbe B, Denk U, Poll V, Rid R, Breitenbach M. The spectrum of fungal allergy. *Int Arch Allergy Immunol.* (2008) 145:58–86. doi: 10.1159/000107578
4. Chaudhary N, Marr KA. Impact of *Aspergillus fumigatus* in allergic airway diseases. *Clin Transl Allergy* (2011) 1:4. doi: 10.1186/2045-7022-1-4
5. Balloy V, Chignard M. The innate immune response to *Aspergillus fumigatus*. *Microbes Infect*. (2009)11:919–27. doi: 10.1016/j.micinf.2009.07.002
6. Park SJ, Mehrad B. Innate immunity to Aspergillus species. *Clin Microbiol Rev.* (2009) 22:535–51. doi: 10.1128/cmr.00014-09
7. Bernard M, Latge JP. *Aspergillus fumigatus* cell wall: composition and biosynthesis. *Med Mycol.* (2001) 39:9–17. doi: 10.1080/714030981
8. Fontaine T, Simenel C, Dubreucq G, Adam O, Delepierre M, Lemoine J, et al. Molecular organization of the alkali-insoluble fraction of *Aspergillus fumigatus* cell wall. *J Biol Chem.* (2000) 275:41528. doi: 10.1074/jbc.M909975199
9. Latge JP. Tasting the fungal cell wall. *Cell Microbiol.* (2010) 12:863–72. doi: 10.1111/j.1462-5822.2010.01474.x
10. Latge JP, Mouyna I, Tekaia F, Beauvais A, Debeaupuis JP, Nierman W. Specific molecular features in the organization and biosynthesis of the cell wall of *Aspergillus fumigatus*. *Med Mycol.* (2005) 43:S15–S22. doi: 10.1080/13693780400029155
11. Romani L. Immunity to fungal infections. *Nat Rev Immunol.* (2004) 4:1–23. doi: 10.1038/nri1255.
12. Steele C, Rapaka RR, Metz A, Pop SM, Williams DL, Gordon S, et al. The beta-glucan receptor dectin-1 recognizes specific morphologies of *Aspergillus fumigatus*. *PLoS Pathog.* (2005) 1:e42. doi: 10.1371/journal.ppat.0010042
13. Netea MG, Warris A, Van der Meer JWM, Fenton MJ, Verver-Janssen TJG, Jacobs LEH, et al. *Aspergillus fumigatus* evades immune recognition during germination through loss of toll-like receptor-4-mediated signal transduction. *J Infect Dis.* (2003) 188:320–6. doi: 10.1086/376456
14. Schlosser A, Thomsen T, Moeller JB, Nielsen O, Tornoe I, Mollenhauer J, et al. Characterization of FIBCD1 as an acetyl group-binding receptor that binds chitin. *J Immunol.* (2009) 183:3800–9. doi: 10.4049/jimmunol.0901526
15. Thomsen T, Moeller JB, Schlosser A, Sorensen GL, Moestrup SK, Palaniyar N, et al. The recognition unit of FIBCD1 organizes into a noncovalently linked tetrameric structure and uses a hydrophobic funnel (S1) for acetyl group recognition. *J Biol Chem.* (2010) 285:1229–38. doi: 10.1074/jbc.M109.061523
16. Shrive AK, Moeller JB, Burns I, Paterson JM, Shaw AJ, Schlosser A, et al. Crystal structure of the tetrameric fibrinogen-like recognition domain of fibrinogen c domain containing 1 (FIBCD1) protein. *J Biol Chem.* (2014) 289:2880–7. doi: 10.1074/jbc.M113.520577
17. Lynch NJ, Roscher S, Hartung T, Morath S, Matsushita M, Maennel DN, et al. L-ficolin specifically binds to lipoteichoic acid, a cell wall constituent of Gram-positive bacteria, and activates the lectin pathway of complement. *J Immunol.* (2004) 172:1198–202. doi: 10.4049/jimmunol.172.2.1198
18. Liu Y, Endo Y, Iwaki D, Nakata M, Matsushita M, Wada I, et al. Human M-ficolin is a secretory protein that activates the lectin complement pathway. *J Immunol.* (2005) 175:3150–6. doi: 10.4049/jimmunol.175.5.3150

19. Ma YG, Cho MY, Zhao MY, Park JW, Matsushita M, Fujita T, et al. Human mannose-binding lectin and L-ficolin function as specific pattern recognition proteins in the lectin activation pathway of complement. *J Biol Chem.* (2004) 279:25307–12. doi: 10.1074/jbc.M400701200
20. Jensen K, Lund KP, Christensen KB, Holm AT, Dubey LK, Moeller JB, et al. M-ficolin is present in *Aspergillus fumigatus* infected lung and modulates epithelial cell immune responses elicited by fungal cell wall polysaccharides. *Virulence* (2017) 8:1870–9. doi: 10.1080/21505594.2016.1278337
21. Ma YJ, Doni A, Hummelshoj T, Honore C, Bastone A, Mantovani A, et al. Synergy between ficolin-2 and pentraxin 3 boosts innate immune recognition and complement deposition. *J Biol Chem.* (2009) 284:28263–75. doi: 10.1074/jbc.M109.009225
22. Madsen J, Tornoe I, Nielsen O, Koch C, Steinhilber W, Holmskov U. Expression and localization of lung surfactant protein A in human tissues. *Am J Respir Cell Mol Biol.* (2003) 29:591–7. doi: 10.1165/rcmb.2002-0274OC
23. Fortwendel JR, Panepinto JC, Seitz AE, Askew DS, Rhodes JC. *Aspergillus fumigatus* rasA and rasB regulate the timing and morphology of asexual development. *Fung Genet Biol.* (2004) 41:129–39. doi: 10.1016/j.fgb.2003.10.004
24. Nesterenko MV, Tilley M, Upton SJ. A simple modification of blums silver stain method allows for 30 minute detection of proteins in polyacrylamide gels. *J Biochem Biophys Methods* (1994) 28:239–242. doi: 10.1016/0165-022x(94)90020-5
25. von Huth S, Moeller JB, Schlosser A, Marcussen N, Nielsen O, Nielsen V, et al. Immunohistochemical localization of fibrinogen c domain containing 1 on epithelial and mucosal surfaces in human tissues. *J Histochem Cytochem.* (2017) 66:85–97. doi: 10.1369/0022155417743694
26. Raikhel NV, Lee HI, Broekaert WF. Structure and function of chitin-binding proteins. *Ann Rev Plant Phys Plant Mol Biol.* (1993) 44:591–615. doi: 10.1146/annurev.pp.44.060193.003111
27. Zhang Z, Liu R, Noordhoek JA, Kauffman HF. Interaction of airway epithelial cells (A549) with spores and mycelium of *Aspergillus fumigatus*. *J Infect.* (2005) 51:375–82. doi: 10.1016/j.jinf.2004.12.012
28. Da Silva CA, Chalouni C, Williams A, Hartl D, Lee CG, Elias JA. Chitin is a size-dependent regulator of macrophage TNF and IL-10 production. *J Immunol.* (2009) 182:3573–82. doi: 10.4049/jimmunol.0802113
29. Alvarez FJ. The effect of chitin size, shape, source and purification method on immune recognition. *Molecules* (2014) 19:4433–51. doi: 10.3390/molecules19044433
30. Stadnyk AW. Cytokine production by epithelial cells. *FASEB J.* (1994) 8:1041–7. doi: 10.1096/fasebj.8.13.7926369
31. Duong M, Ouellet N, Simard M, Bergeron Y, Olivier M, Bergeron MG. Kinetic study of host defense and inflammatory response to *Aspergillus fumigatus* in steroid-induced immunosuppressed mice. *J Infect Dis.* (1998) 178:1472–82. doi: 10.1086/314425
32. Eisenbarth SC, Piggott DA, Huleatt JW, Visintin I, Herrick CA, Bottomly K. Lipopolysaccharide-enhanced, toll-like receptor 4-dependent T helper cell type 2 responses to inhaled antigen. *J Exp Med.* (2002) 196:1645–51. doi: 10.1084/jem.20021340.
33. Bruewer M, Luegering A, Kucharzik T, Parkos CA, Madara JL, Hopkins AM, et al. Proinflammatory cytokines disrupt epithelial barrier function by apoptosis-independent mechanisms. *J Immunol.* (2003) 171:6164–72. doi: 10.4049/jimmunol.171.11.6164
34. Li X, Wang L, Nunes DP, Troxler RF, Offner GD. Pro-inflammatory cytokines up-regulate MUC1 gene expression in oral epithelial cells. *J Dental Res.* (2003) 82:883–7. doi: 10.1177/154405910308201107
35. Song KS, Lee WJ, Chung KC, Koo JS, Yang EJ, Choi JY, et al. Interleukin-1 beta and tumor necrosis factor-alpha induce MUC5AC overexpression through a mechanism involving ERK/p38 mitogen-activated protein kinases-MSK1-CREB activation in human airway epithelial cells. *J Biol Chem.* (2003) 278:23243–50. doi: 10.1074/jbc.M300096200
36. Al-Sadi RM, Ma TY. IL-1beta causes an increase in intestinal epithelial tight junction permeability. *J Immunol.* (2007) 178:4641–9. doi: 10.4049/jimmunol.178.7.4641
37. Linden SK, Sutton P, Karlsson NG, Korolik V, McGuckin MA. Mucins in the mucosal barrier to infection. *Mucosal Immunol.* (2008) 1:183–97. doi: 10.1038/mi.2008.5
38. Bellanger AP, Millon L, Khoufache K, Rivollet D, Bieche I, Laurendeau I, et al. *Aspergillus fumigatus* germ tube growth and not conidia ingestion induces expression of inflammatory mediator genes in the human lung epithelial cell line A549. *J Med Microbiol.* (2009) 58(*Pt* 2):174–179. doi: 10.1099/jmm.0.005488-0
39. Capaldo CT, Nusrat A. Cytokine regulation of tight junctions. *Biochim Biophys Acta* (2009) 1788:864–71. doi: 10.1016/j.bbamem.2008.08.027
40. Ito T, Carson WF, Cavassani KA, Connett JM, Kunkel SL. CCR6 as a mediator of immunity in the lung and gut. *Exp Cell Res.* (2011) 317:613–9. doi: 10.1016/j.yexcr.2010.12.018
41. Fahy JV, Dickey BF. Airway mucus function and dysfunction. *N Engl J Med.* (2010) 363:2233–47. doi: 10.1056/NEJMra0910061
42. Meier A, Kirschning CJ, Nikolaus T, Wagner H, Heesemann J, Ebel F. Toll-like receptor (TLR) 2 and TLR4 are essential for Aspergillus-induced activation of murine macrophages. *Cell Microbiol.* (2003) 5:561–70. doi: 10.1046/j.1462-5822.2003.00301.x
43. Balloy V, Si-Tahar M, Takeuchi O, Philippe B, Nahori MA, Tanguy M, et al. Involvement of toll-like receptor 2 in experimental invasive pulmonary aspergillosis. *Infect Immunol.* (2005) 73:5420–5. doi: 10.1128/iai.73.9.5420-5425.2005
44. Rodland EK, Mattingsdal M, Olstad OK, Ovstebo R, Kierulf P, Muller F, et al. Expression of genes in normal human monocytes in response to *Aspergillus fumigatus*. *Med Mycol.* (2008) 46:327–36. doi: 10.1080/13693780701874507
45. Ernst KRO, Ager-Wick E, Halvorsen B, Muller F, Froland SS. Toll like receptor 5 (TLR5) may be involved in the immunological response to *Aspergillus fumigatus in vitro*. *Med Mycol.* (2011) 49:375–9. doi: 10.3109/13693786.2010.531772

Conflict of Interest Statement: The authors declare that the research was conducted in the absence of any commercial or financial relationships that could be construed as a potential conflict of interest.

The handling editor is currently co-organizing a Research Topic with one of the authors ST, and confirms the absence of any other collaboration.

Copyright © 2018 Jepsen, Dubey, Colmorten, Moeller, Hammond, Nielsen, Schlosser, Templeton, Sorensen and Holmskov. This is an open-access article distributed under the terms of the Creative Commons Attribution License (CC BY). The use, distribution or reproduction in other forums is permitted, provided the original author(s) and the copyright owner(s) are credited and that the original publication in this journal is cited, in accordance with accepted academic practice. No use, distribution or reproduction is permitted which does not comply with these terms.

frontiers in Immunology

ORIGINAL RESEARCH
published: 30 July 2018
doi: 10.3389/fimmu.2018.01507

Innate Immunity Induced by the Major Allergen Alt a 1 From the Fungus *Alternaria* Is Dependent Upon Toll-Like Receptors 2/4 in Human Lung Epithelial Cells

Tristan Hayes[1,2†], Amanda Rumore[3†], Brad Howard[1], Xin He[1], Mengyao Luo[1], Sabina Wuenschmann[4], Martin Chapman[4], Shiv Kale[5], Liwu Li[1], Hirohito Kita[6] and Christopher B. Lawrence[1*]*

[1] Department of Biological Sciences, Virginia Tech, Blacksburg, VA, United States, [2] Department of Pediatrics, School of Medicine, Indiana University Bloomington, Indianapolis, IN, United States, [3] Department of Biology, Randolph College, Lynchburg, VA, United States, [4] Indoor Biotechnologies, Charlottesville, VA, United States, [5] Biocomplexity Institute, Virginia Tech, Blacksburg, VA, United States, [6] Division of Allergic Diseases, Internal Medicine, Mayo Clinic, Rochester, MN, United States

OPEN ACCESS

Edited by:
Steven Templeton,
Indiana University School of Medicine-Terre Haute, United States

Reviewed by:
Ana Serezani,
Vanderbilt University Medical Center, United States
Emily K. Cope,
Northern Arizona University, United States
Matthew Poynter,
University of Vermont, United States

***Correspondence:**
Hirohito Kita
kita.hirohito@mayo.edu;
Christopher B. Lawrence
cblawren@vt.edu

[†]These authors have contributed equally to this work.

Specialty section:
This article was submitted to Microbial Immunology, a section of the journal Frontiers in Immunology

Received: 09 February 2018
Accepted: 18 June 2018
Published: 30 July 2018

Citation:
Hayes T, Rumore A, Howard B, He X, Luo M, Wuenschmann S, Chapman M, Kale S, Li L, Kita H and Lawrence CB (2018) Innate Immunity Induced by the Major Allergen Alt a 1 From the Fungus Alternaria Is Dependent Upon Toll-Like Receptors 2/4 in Human Lung Epithelial Cells. Front. Immunol. 9:1507. doi: 10.3389/fimmu.2018.01507

Allergens are molecules that elicit a hypersensitive inflammatory response in sensitized individuals and are derived from a variety of sources. Alt a 1 is the most clinically important secreted allergen of the ubiquitous fungus, *Alternaria*. It has been shown to be a major allergen causing IgE-mediated allergic response in the vast majority of *Alternaria*-sensitized individuals. However, no studies have been conducted in regards to the innate immune eliciting activities of this clinically relevant protein. In this study, recombinant Alt a 1 was produced, purified, labeled, and incubated with BEAS-2B, NHBE, and DHBE human lung epithelial cells. Alt a 1 elicited strong induction of IL-8, MCP-1, and Gro-a/b/g. Using gene-specific siRNAs, blocking antibodies, and chemical inhibitors such as LPS-RS, it was determined that Alt a 1-induced immune responses were dependent upon toll-like receptors (TLRs) 2 and 4, and the adaptor proteins MYD88 and TIRAP. Studies utilizing human embryonic kidney cells engineered to express single receptors on the cell surface such as TLRs, further confirmed that Alt a 1-induced innate immunity is dependent upon TLR4 and to a lesser extent TLR2.

Keywords: *Alternaria*, allergen, innate immunity, toll-like receptors, mold, fungus–host interaction

INTRODUCTION

Besides being a common cause of allergic rhinitis, sensitivity to the airborne fungus *Alternaria alternata* is believed to be a common cause of allergic/atopic asthma. Epidemiological studies from locations worldwide indicate that *Alternaria* sensitivity is closely linked with the development of asthma and up to 70% of mold-allergic patients have skin prick test (SPT) reactivity to *Alternaria* (1–3). *Alternaria* sensitivity has been shown to not only be a risk factor for asthma but can also directly lead to the development of severe and potentially fatal asthma often more than any other fungus (1–5). In addition, *Alternaria* sensitization has been determined to be one of the most important factors in the onset of childhood asthma in the southwest desert regions of the US and other arid regions in the world (2, 6, 7). *Alternaria* spores are ubiquitous, routinely found in atmospheric surveys in the US

and in other countries and are the most frequently encountered fungal spore type (8). Airborne spore counts are often 1,000-fold greater than pollen counts, and exposures are often longer in duration. Indeed, it has long been speculated that this type of exposure may be partially responsible for both the chronic nature and severity of asthma in *Alternaria*-sensitized individuals (9). Indeed, in a survey by the National Institute of Environmental Health & Safety of 831 homes, containing 2,456 individuals, it was found that the prevalence of current symptomatic asthma correlated with increasing indoor *Alternaria* concentrations (3). Higher levels of *Alternaria* antigens in the environment significantly increased odds of having had asthma symptoms during the preceding year, more so than other examined antigens.

Although some research has been performed on the physiological and molecular identification of *Alternaria* allergens, approximately three major and five minor allergenic proteins have been described to date (10, 11). In general, the biological role of these allergens and other fungal products in the development of allergy and asthma is poorly understood. There is clearly a need to elucidate the role of *Alternaria* immunoreactive proteins and other molecules in the development of asthma from mechanistic perspectives.

Many of the known *Alternaria* allergens are intracellular proteins with clinically relevant homologs being reported in other fungi with known functions such as enolase, ribosomal proteins, nuclear transport factor, and aldehyde dehydrogenase to name a few (11–13). Alt a 1, the major allergen produced by *Alternaria* spp. namely *A. alternata*, is a relatively small (157 amino acids) secreted protein with no clear function in fungal metabolism or ecology (14, 15). Its protein sequence and β-barrel structure is unique among fungal allergens with no known cross reactivity to other allergens (16–20). Diagnosis of *A. alternata* sensitization is often hampered by the variability and complexity of fungal extracts, and thus simplification of the diagnostic procedures with purified allergens has been investigated. Currently, in some allergy clinics in the US, pure Alt a 1 protein is often used to assess sensitization in SPTs in lieu of total fungal extract because it produces the same reaction as total antigen extracts in the majority (80–90%) of human subjects (21–23). Furthermore, Alt a 1, either in its natural or recombinant form, is sufficient for a reliable diagnosis of *A. alternata* sensitization and induces skin prick reactivity comparable with that produced by commercially available *A. alternata* extract (21–23).

In this study, we investigated and report for the first time the innate immunostimulatory activities of Alt a 1 in human bronchial epithelial cells. We found Alt a 1 has potent cytokine and chemokine inducing activity. Moreover, this activity was found to be dependent upon toll-like receptors (TLR2 and TLR4) and associated signaling pathways. This study is the very first in regards to defining the potential role of a single purified *Alternaria* product or protein in innate immunity. Results of these studies are discussed.

MATERIALS AND METHODS

Vector Construction and Transformation of *Pichia pastoris*

An Alt a 1 cDNA harboring vector (pGAPZ, Thermo Fisher Scientific, Waltham, MA, USA) for expression in *P. pastoris* was provided as a generous gift from Dr. Martin Chapman (Indoor Biotechnologies, Charlottesville, VA, USA). Briefly, the pGAPZ-Alt a 1 vector contained a 6× poly-histidine tag for purification *via* immobilized metal ion affinity chromatography (IMAC) and allowed for zeocin to be used for selection. The pGAPZ-Alt a 1 plasmid was transformed into *P. pastoris* GS115 (Thermo Fisher Scientific, Waltham, MA, USA) *via* heat shock and plated on media containing zeocin according to the manufacturer's protocols (Thermo Fisher Scientific, Waltham, MA, USA). Next, as per the manufacturer's protocols, zeocin-resistant *P. pastoris* colonies were then screened for the presence of Alt a 1 using colony-based PCR using forward primer 5′-gtctggaagatctccgagttttacggacg-caag-3′ and the reverse primer 5′-cttgcgtccgtaaaactcggagatcttcca-gac-3′. Positive colonies were selected and used for downstream expression and production of rAlt a 1 in *P. pastoris* GS115.

Protein Expression and Purification

The rAlt a 1 protein was expressed in *P. pastoris* GS115 according to the manufacturer's instructions (Thermo Fisher Scientific, Waltham, MA, USA) and purification followed a typical IMAC protocol (Qiagen Inc., Valencia, CA, USA). Briefly, yeast was grown in 500 mL yeast extract peptone dextrose broth at 22°C while shaking at 180 RPM. After 60 h, the culture media was separated into cells and supernatant by centrifuge at 5,000 × *g* for 10 min. The supernatant was then buffer exchanged with 2 L of lysis buffer (50 mM NaH_2PO_4, 500 mM NaCl, 30 mM Imidazole, pH 8.0). After concentrating to 25 mL, supernatant was then applied to NiNTA resin (Qiagen Inc., Valencia, CA, USA) that had been washed and equilibrated in lysis buffer per manufacturer's protocols. Four column volumes of lysis buffer were flowed through the column. Next, 5 mL elution buffer (50 mM NaH_2PO_4, 500 mM NaCl, 50 mM imidazole, pH 8.0) was applied to the column. Elution buffer with increasing imidazole concentrations (100, 150, and 200 mM, respectively) was then applied. rAlt a 1 protein eluted at 200 mM imidazole concentration.

Purity was assessed *via* 15% SDS-polyacrylamide gel electrophoresis. As expected, the rAlt a 1 protein appeared to be a heterodimer consisting of 14.4 and 17 kDa bands under denaturing conditions. Amicon Ultra Centrifugal Filters MWCO 10 kDA (Sigma-Aldrich, St. Louis, MO, USA) were used to concentrate proteins, and proteins were buffer exchanged with endotoxin-free PBS, pH 7.4 (Thermo Fisher Scientific, Waltham, MA, USA) for downstream endotoxin removal and applications. Approximately 20 mg/L of rAlt a 1 was typically obtained following purification.

Endotoxin Removal and Quantification of rAlt a 1

Even though protein was produced in yeast, potential endotoxin contamination was removed from purified Alt a 1 using endotoxin removal columns (Detoxi-Gel endotoxin removing columns, Thermo Fisher Scientific, Waltham, MA, USA). Briefly, resin was equilibrated in 1% sodium deoxycholate followed by five volume washes of PBS. 1 mL of protein was loaded onto the column and incubated for 1 h. Protein was eluted by addition of endotoxin-free PBS, pH7.4 (Thermo Fisher Scientific, Waltham, MA, USA).

Quantification of endotoxin levels was performed using an enzyme-linked immunosorbent assay (ELISA) Kit (Biomatik,

ON, Canada). Briefly, 50 μL of protein was assessed following the manufacturer's protocol. Samples were run in duplicate in 96-well plate format and were read on a Versa MAX ELISA Microplate Reader (Molecular Devices, Sunnyvale, CA, USA) at room temperature. Measurements at OD_{450} were corrected against values obtained at OD_{570} following the manufacturer's suggestions. A standard curve was generated for each reading and generated using R software. Endotoxin/LPS concentration was determined using the standard curve and tabulated in ng/mL of LPS. Experiments were performed at least five times/protein preparation. In all experiments, purified rAlt a 1 contained below the detectable limit of endotoxin (<0.01 ng/mL). After testing for homogeneity of variances, Tukey's HSD was performed and adjusted (if applicable).

Membrane-Based Cytokine Arrays

Human cell culture supernatants were assayed for general secretion of different cytokines and chemokines using the RayBio C-Series Human Cytokine Antibody Array C1 per manufacturer's protocols (RayBiotech, Norcross, GA, USA). BEAS-2B cells were grown in DMEM + 1% Pen/Strep/10% FBS. NHBE/DHBE were grown in BEGM media per the manufacturer's protocols (Lonza, Walkersville, MD, USA). Cells were incubated at 37°C/5% CO_2. Approximately 4×10^6 BEAS-2B (ATCC CRL 9609, Manassas, VA, USA) or 4×10^6 NHBE/DHBE (Lonza, Walkersville, MD, USA) cells were starved for 4 h prior to the addition of 50 μg rAlt a 1 and incubated for 24 h. Supernatants were collected and used in downstream experiments per the manufacturer's protocols (RayBiotech, Norcross, GA, USA). Briefly, membranes were blocked with the blocking buffer and then washed. The membranes were then treated with the samples for 2 h at RT shaking at 90 RPM. After an additional wash, the biotinylated antibody cocktail was used to cover the membranes. After a 2-h incubation at RT with shaking at 90 RPM another wash step was conducted. Afterward, the membranes were covered with horseradish peroxidase streptavidin concentrate and incubated for 2 h at RT with shaking at 90 RPM. The membranes were then washed and signals were detected using chemiluminescence. Briefly, membranes were washed with two detection buffers provided by RayBiotech (Norcross, GA, USA) and exposed continuously from 5 to 600 s with images taken at multiple intervals in between using BioRad Chemi Doc CRS+ System with Image Lab Software (BioRad, Berkeley, CA, USA). Images were then exported with no correction or image modification.

Enzyme-Linked Immunosorbent Assays

Enzyme-linked immunosorbent assays were performed using Human IL-8, MCP-1, and GRO (a/b/g) ELISA MAX (BioLegend, San Diego, CA, USA) kits. Supernatants from cells treated with rAlt a 1 were examined following the manufacturer's protocol. Samples were run in duplicate in 96-well plate format and were read on a Versa MAX ELISA Microplate Reader (Molecular Devices, Sunnyvale, CA, USA) at room temperature. Measurements at OD_{450} were corrected against values obtained at OD_{570} following the manufacturer's suggestions. A standard curve was generated for each reading and generated using R software. Cytokine/chemokine concentrations were determined using the standard curve and tabulated in pg/mL. Experiments were performed at least five times. After testing for homogeneity of variances, Tukey's HSD was performed and adjusted (if applicable).

Human Embryonic Kidney (HEK) 293 Cells Engineered to Express TLRs and Measurement of NF-κB Activity

Human embryonic kidney 293-Blue hTLR4 cells expressing TLR4, MD2/CD14 co-receptor genes and a secreted embryonic alkaline phosphatase (SEAP) reporter gene under control of an IL-12 promoter and HEK-Blue Null 2 cells lacking TLR4 receptor but expressing the IL-12 promoter and SEAP reporter gene (Invivogen, San Diego, CA, USA) were seeded in a 96-well plate. The final volume of culture media was 200 μL DMEM + 1% Pen/Strep/10% FBS. After 16 h at 37°C/5% CO_2, the media was removed from the cells. Cells were then starved for 2 h in 200 μL DMEM + 1% Pen/Strep. Cells were pretreated with 5 ng/mL ultrapure LPS-RS (Invivogen, San Diego, CA, USA), 10 μg/mL anti-hTLR4-IgG or 10 μg/mL mouse IgG 1 control antibody (antibodies from Invivogen, San Diego, CA, USA) for 1 h. Then cells were treated with 1 μg rAlt a 1. Cells were then incubated at 37°C/5% CO_2 for 24 h. Afterward 20 μL of the cell supernatant was added to 180 μL QUANTI-Blue reagent (Invivogen, San Diego, CA, USA). After incubation for 3 h at 37°C, the plate was read at 655 nM (VersaMax ELISA microplate reader) at RT. After testing for homogeneity of variances, Tukey's HSD was performed and adjusted (if applicable).

Human embryonic kidney 293-Blue hTLR2 cells expressing TLR2 and CD14 co-receptor genes and an SEAP reporter gene under control of the interferon $(IFN)_\beta$ minimal promoter were seeded in a 96-well plate, final volume was 200 μL DMEM + 1% Pen/Strep/10% FBS. After 16 h at 37°C/5% CO_2, the media was removed from the cells. Cells were then starved for 2 h in 200 μL DMEM + 1% Pen/Strep. Cells were pretreated with 10 μg/mL human IgA2-control, 10 μg/mL anti-hCD14-IgA, and 1 μg/mL Mab-hMD2 (all from Invivogen, San Diego, CA, USA), for 2 h. Then cells were treated with 1 μg rAlt a 1. Cells were then incubated at 37°C/5% CO_2, for 24 h. Afterward 20 μL of the cell supernatant was added to 180 μL QUANTI-Blue reagent (Invivogen, San Diego, CA, USA). After incubation for 3 h at 37°C, the plate was read at 655 nM (VersaMax ELISA microplate reader) at RT. After testing for homogeneity of variances, Tukey's HSD was performed and adjusted (if applicable).

Human embryonic kidney 293-Blue hTLR5 cells expressing TLR5 gene and an SEAP reporter gene under control of an AP-1 promoter were seeded on a 96-well plate. Cells were treated with 100 ng/mL of FLA-ST Ultrapure (Invivogen, San Diego, CA, USA) or 1 μg rAlt a 1. This purified flagellin from *Salmonella typhimurium* is detected by TLR5 resulting in MyD88-mediated NF-κB activation. Cells were incubated overnight at 37°C/5% CO_2. After incubation, 20 μL of the cell supernatant was added to 180 μL QUANTI-Blue reagent (Invivogen). After incubation for 3 h at 37°C, the plate was read at 655 nM (VersaMax ELISA microplate reader) at RT. After testing for homogeneity of variances, Tukey's HSD was performed and adjusted (if applicable).

Blocking Antibodies in BEAS-2B Cells

2.5×10^5 BEAS-2B cells were plated in 1 mL DMEM + 1% Pen/Strep/10% FBS. After 24 h, 10 μg/mL of either anti-hTLR2-IgA, 10 μg/mL anti-hTLR4-IgG, 10 μg/mL human IgA2-control, or 10 μg/mL mouse-IgG1-control (all from Invivogen, San Diego, CA, USA) was added. After 2 h, 100 μg rAlt a 1 was added. Cells were then incubated for 24 h at 37°C/5% CO_2. Supernatants were then collected and assayed for cytokines *via* ELISA as described previously.

Gene Knockdown Using siRNAs in BEAS-2B Cells

3.0×10^5 BEAS-2B cells were seeded and cultured to 70% confluency in 24-well plates containing DMEM with 10% FBS. The cells were then transfected with 10 nM of either scrambled control, TLR2, TLR4, TIRAP, or MyD88 siRNAs (Santa Cruz Biotechnology, Santa Cruz, CA, USA) in serum-free Opti-MEM medium (Invitrogen, Carlsbad, CA, USA) using Lipofectamine RNA iMAX Reagent (Invitrogen, Carlsbad, CA, USA) according to the manufacturer's protocols. After 24 h, cells were treated with either 50 μg rAlt a 1 or where appropriate, 5 ng/mL of LPS (Sigma-Aldrich, St. Louis, MO, USA). To determine efficacy of gene silencing, western blot analysis was performed 24 h after transfection.

Statistical Analysis

Data are expressed as means and SDs. Data were tested for homogeneity of variances and appropriated analysis of variances tests were performed and adjusted accordingly. Downstream analysis of all numerical data utilized R software and packages. Packages used for analyzing data included Coin, Car, Drc, Multcomp, and Sandwich (24–28).

RESULTS

Alt a 1 Induces Innate Immune Responses in BEAS-2B Bronchial Epithelial Cells

To initially characterize the innate immune response induced by rAlt a 1 in bronchial epithelial cells *in vitro*, we used human cytokine/chemokine arrays harboring antibodies corresponding to 23 target molecules. Our results indicated that Alt a 1 induced the secretion of several cytokines and chemokines in BEAS-2B human bronchial epithelial airway cells—primarily MCP-1 (CCL2), IL-8, and GRO-a/b/g (CXCL1/2/3) (**Figure 1**). Similar results were obtained in experiments using NHBE and DHBE cells (data not shown). There were no marked differences between responses in BEAS-2B, NHBE, and DHBE cells. There was some indication that IL-15 may also be inducible by Alt a 1 in our array studies but was not explored further.

After finding that rAlt a 1 induces the secretion of several innate immune cytokines and chemokines *via* array blots, determining if there was a time-dependent secretion of IL-8 in BEAS-2B cells was conducted *via* ELISA assay (**Figure 2**). The goal of this experiment was to characterize the temporal aspects of IL-8 secretion and to determine if 24 h post treatment was optimal for supernatant collection. Human cells were incubated with Alt a 1 for time periods ranging from 15 min to 24 h. Significant increases of IL-8 secretion occurred after cells were incubated with Alt a 1 for 12 h. However, 24 h was the time point at which IL-8 secretion was the highest (**Figure 2A**). We also determined if Alt a 1 induces IL-8 in a dose-dependent manner and found this to be the case (**Figure 2B**). We found very strong induction of IL-8 with as little as 10 μg of rAlt a 1 with a maximum induction using 150 μg of protein. This indicates Alt a 1 is quite potent at inducing IL-8 in BEAS-2B cells even at lower concentrations.

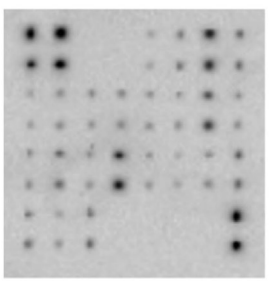

Alt a 1							
POS	POS	NEG	NEG	GCSF	GM-CSF	**GRO a/b/g**	GRO alpha
POS	POS	NEG	NEG	GCSF	GM-CSF	**GRO a/b/g**	GRO alpha
IL-1 alpha	IL-2	IL-3	IL-5	IL-6	IL-7	**IL-8**	IL-10
IL-1 alpha	IL-2	IL-3	IL-5	IL-6	IL-7	**IL-8**	IL-10
IL-13	IL-15	IFN-gamma	**MCP-1**	MCP-2	MCP-3	MIG	RANTES
IL-13	IL-15	IFN-gamma	**MCP-1**	MCP-2	MCP-3	MIG	RANTES
TGF-beta 1	TNF alpha	TNF beta	BLANK	BLANK	BLANK	BLANK	POS
TGF-beta 1	TNF alpha	TNF beta	BLANK	BLANK	BLANK	BLANK	POS

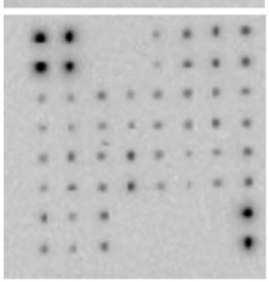

PBS Treated Cells							
POS	POS	NEG	NEG	GCSF	GM-CSF	GRO a/b/g	GRO alpha
POS	POS	NEG	NEG	GCSF	GM-CSF	GRO a/b/g	GRO alpha
IL-1 alpha	IL-2	IL-3	IL-5	IL-6	IL-7	IL-8	IL-10
IL-1 alpha	IL-2	IL-3	IL-5	IL-6	IL-7	IL-8	IL-10
IL-13	IL-15	IFN-gamma	MCP-1	MCP-2	MCP-3	MIG	RANTES
IL-13	IL-15	IFN-gamma	MCP-1	MCP-2	MCP-3	MIG	RANTES
TGF-beta 1	TNF alpha	TNF beta	BLANK	BLANK	BLANK	BLANK	POS
TGF-beta 1	TNF alpha	TNF beta	BLANK	BLANK	BLANK	BLANK	POS

FIGURE 1 | Cytokine profiling of rAlt a 1 treated BEAS-2B cells. 5.0×10^5 BEAS-2B cells were treated with 50 μg rAlt a 1 or 50 μL of endotoxin-free, sterile PBS (negative control). Cytokine array blots (*top left*) and corresponding maps of targets (*top right*) derived from cells treated with rAlt a 1, cytokine array blot (*bottom left*) and corresponding map of targets derived from cells treated with PBS (*bottom right*). Comparisons were made between the two blots and cytokines and chemokines highlighted in blue are those that were found to be qualitatively stronger in cells treated with rAlt a 1.

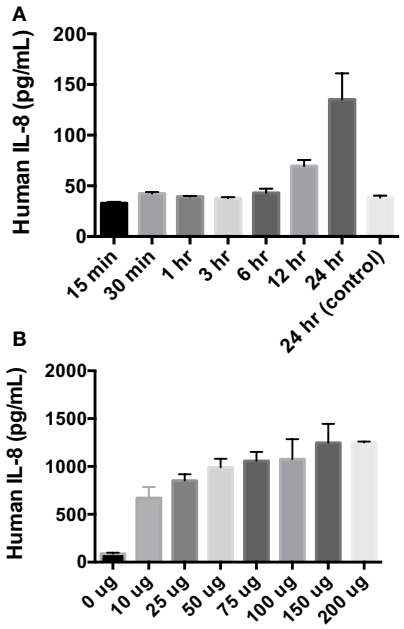

FIGURE 2 | Temporal and dose dependency of Alt a 1 induced IL-8 in BEAS-2B cells. **(A)** 2.0×10^5 BEAS-2B cells were grown in RPMI + FBS + 1% Pen Strep. Cells were starved for 6 h prior to induction with rAlt a 1 or endotoxin-free sterile PBS. The starve media consisted of RPMI + 1% Pen Strep without FBS. Cells were treated with 50 μg rAlt a 1 for the specified time. Supernatants were collected and assayed *via* BIOLEGEND IL-8 ELISAMAX. After testing for homogeneity of variances, Tukey's HSD was performed and adjusted (*$p < 0.001$). Data are represented as mean (SD). Comparisons were made between rAlt a 1 treated and untreated cells (PBS-treated 24 h control). **(B)** 5×10^5 BEAS-2B cells were grown in RPMI + FBS + 1% Pen Strep. They were then starved for 6 h. The starve media was RPMI + 1% Pen Strep. Cells were treated with rAlt a 1 or PBS (0 μg) for 24 h. Media was collected and assayed *via* BIOLEGEND IL-8 ELISAMAX. Data are represented as mean (SD). Comparisons were made between Alt a 1-treated and control PBS-treated cells (*$p < 0.001$).

Additional ELISA assays were next used instead to quantify and confirm the levels of secreted cytokines/chemokines, MCP-1 (CCL2), IL-8, and GRO-a/b/g (CXCL1/2/3). Human BEAS-2B cells were treated with rAlt a 1 for 24 h (**Figure 3**). The ELISA results confirmed the cytokine array blots and showed that levels of human IL-8, MCP-1, and GRO-a/b/g were significantly increased in rAlt a 1 treated cells.

Gene Knockdown Approaches Using siRNAs Indicate Alt a 1 Induction of Innate Immune Responses Is Dependent Upon TLR Signaling in BEAS-2B Cells

To determine the potential role of known pattern recognition receptors (PRRs) such as TLRs and associated signaling pathways in Alt a 1-induced innate immune responses in bronchial epithelial cells (BEAS-2B), a gene knockdown approach using siRNAs was used initially. A suite of gene-specific siRNAs (MyD88, PI-3-K, TIRAP, TLR2, TLR3, TLR4) or scrambled control siRNA (scRNA) were transfected into BEAS-2B cells, then treated with rAlt a 1 for 24 h. We confirmed knockdown of target genes using quantitative reverse transcription PCR. We typically obtained >70% gene-specific knockdown efficiency (data not shown). Supernatants were then collected and assayed for IL-8 levels. These cells showed no consistent reduction in IL-8 secretion when PI-3-K and TLR3 were knocked down (data not shown). In repeated experiments, Alt a 1-treated cells showed decreased IL-8 secretion following incubation with siRNAs corresponding to MyD88, TIRAP, TLR2, and TLR4, compared to scRNA controls (**Figure 4**). We found that silencing of TLR4 resulted in complete abolishment of Alt a 1 induced IL-8 when compared to scRNA control treated cells. In comparison to silencing of TLR4, the effect of silencing TLR2 was statistically significant but was not as robust in these experiments. Interestingly, akin to our results with TLR4-specific siRNAs, we found that silencing of TIRAP or MyD88 resulted in virtually complete abolishment of Alt a 1 induced IL-8 when compared to scRNA control treated cells indicating the importance of these adaptor proteins downstream of TLR-receptors. Collectively, this data indicated that Alt a 1-induced innate immune responses are dependent upon these receptors and downstream adaptors in BEAS-2B cells (**Figure 4**).

Blocking Antibody and Antagonist Approaches Demonstrate Alt a 1 Induction of Innate Immune Responses Is Dependent Upon TLR Signaling in BEAS-2B Cells

We confirmed the results of our siRNA gene knockdown experiments using TLR2 and TLR4 blocking antibodies. In preliminary experiments using TLR4 blocking antibodies, results indicated that TLR4 is important for Alt a 1 induction of MCP-1 (CCL2), IL-8, and GRO-a/b/g (CXCL1/2/3) in BEAS-2B cells (data not shown).

Next we incorporated control antibodies (non-blocking), and TLR4 and TLR2 specific blocking antibodies (**Figure 5**). Blocking TLR4 resulted in a much more pronounced reduction in Alt a 1-induced IL-8 compared to blocking TLR2. We also examined if combining TLR2 and TLR4 blocking antibodies would have an additive effect in regards to dampening Alt a 1 induced IL-8 and found this to be the case. Pretreating cells with both TLR2 and TLR4 blocking antibodies completely abolished Alt a 1-induced IL-8 but was not statistically significant when compared to blocking TLR4 alone and may warrant further investigation. Collectively, these results suggested that Alt a 1-induced IL-8 in BEAS-2B cells is primarily dependent upon TLR4 with a minor contribution from TLR2.

Engineered HEK 293 Cells Demonstrate Alt a 1-Induced NF-κB Signaling Is TLR 2 and 4 Dependent

To further examine the importance of TLR4 in the initiation of the innate immune response to Alt a 1, we used HEK 293 cells engineered to express specific cell surface receptors such as TLR2, TLR4, or TLR5. These cells are also engineered with a reporter system whereby an NF-κB-dependent gene promoter is fused to a

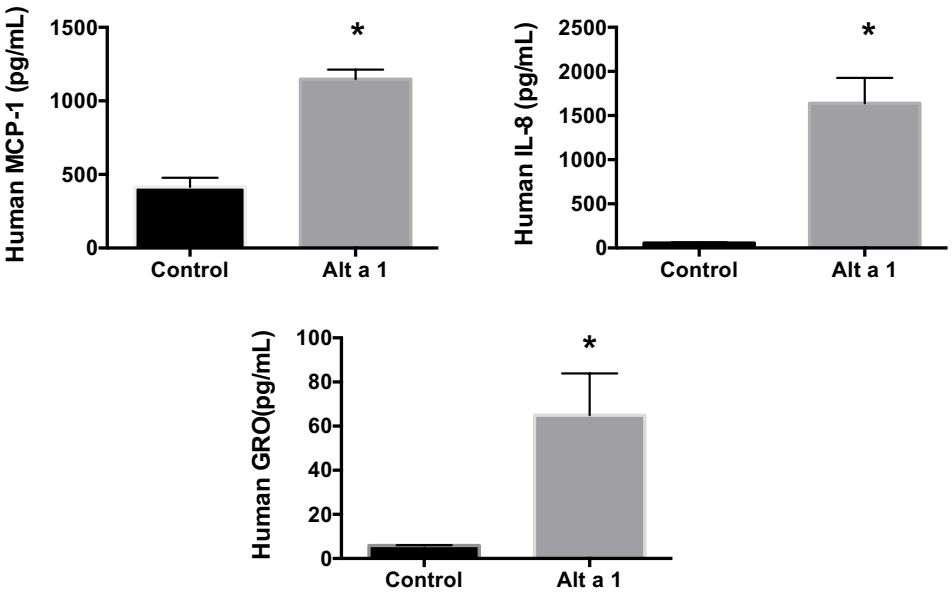

FIGURE 3 | Induction of cytokines and chemokines in BEAS-2B cells treated with Alt a 1. 5.0×10^5 human BEAS-2B cells were treated with 50 μg rAlt a 1 for 24 h. Supernatant was collected and cytokine/chemokine levels were determined using BIOLEGEND ELISAMAX [MCP-1 (CCL2), IL-8, and GRO-a/b/g (CXCL1/2/3)]. Data are represented as mean (SD). After testing for homogeneity of variances, Tukey's HSD was performed and adjusted (*$p < 0.001$).

gene encoding a secreted form of alkaline phosphatase (SEAP). In initial experiments, HEK-Blue hTLR4 cells were used to determine if Alt a 1 could activate NF-κB signaling *via* TLR4 (**Figure 6**). We first optimized the systems using cells treated with a TLR4-specific agonist LPS (ultrapure TLR4-specific LPS-EB) and this resulted in high levels of SEAP (**Figure 6A**). This activity could be reduced when cells were pretreated with a TLR4 antagonist (LPS-RS which binds to TLR4 but does not induce a downstream signal), or with TLR4 blocking antibodies (**Figure 6A**).

Using this system, cells were pretreated with antibodies and then treated with rAlt a 1. Directly supporting our data from experiments with TLR4-specific siRNAs and blocking antibodies in BEAS-2B cells, the HEK-hTLR4 cells but not corresponding HEK-null control cells were responsive to rAlt a 1 (**Figure 6B**). Furthermore, this response could be almost completely abolished by directly blocking the TLR4 receptor using both TLR4 blocking antibodies and the TLR4 antagonistic ligand, LPS-RS. Non-blocking control antibodies had no effect on rAlt a 1-induced SEAP. We also performed similar experiments in hTLR2 HEK-blue cells. Results of these experiments indicated that Alt a 1 induced SEAP activity was dependent upon TLR2 (**Figure 6C**).

The specific mechanism for how Alt a 1 triggers both TLR2 and TLR4 is unclear. One explanation could lie in the requirement of co-receptor molecules for the receptors, such as CD14 and MD2. Experiments focusing upon co-receptor molecules for both TLRs were explored in HEK-hTLR2 and HEK-hTLR4 cells. CD14 associates with both TLR2 and TLR4 upon signaling. Another receptor, MD2, is more specific to TLR4. Therefore, we tested to see if these adaptors/co-receptors may be important for signaling using CD14 and MD2 blocking antibodies first in hTLR4 HEK-blue cells.

When CD14 was blocked in hTLR4 HEK-blue cells, signaling appeared to be reduced only slightly and was not statistically significant (Figure S1 in Supplementary Material). This suggested that Alt a 1 may trigger immunity in a CD14-independent manner to a large degree through TLR4. Results of these experiments also suggested that MD2 may not be important for the ability of Alt a 1 to signal through TLR4.

By contrast, blocking CD14 in HEK-hTLR2-blue cells treated with Alt a 1 appeared to cause a small but significant reduction in SEAP (Figure S2 in Supplementary Material). This indicated CD14 may be required for optimal signaling by Alt a 1 *via* TLR2. Blocking MD2 had no effect on HEK-hTLR2-blue cells treated with Alt a 1 indicating unlike CD14, MD2 is most likely not involved in Alt a 1 induced signaling *via* TLR2.

Finally, we investigated the MyD88-dependent TLR5 receptor using a similar approach. To ensure that the conditions of our system were compatible with HEK-hTLR5 cells, we first used bacterial flagellin from *S. typhimurium* (FLA-ST), a canonical ligand for TLR5 as a positive control. As expected, FLA-ST induced robust TLR5-dependent SEAP activity. In contrast to HEK-hTLR2 and HEK-hTLR4, HEK-hTLR5 cells treated with Alt a 1 showed no response indicating that Alt a 1 does not trigger a TLR5–MyD88-dependent response (data not shown).

DISCUSSION

Alt a 1 is the most relevant allergen from the fungus *A. alternata*. Over 90% of patients sensitized to *Alternaria* typically have specific IgE to Alt a 1, indicating that it is a major allergen (29, 30). Sequence and structural studies have indicated that Alt a 1 is a species-specific allergen with no known cross reactivity with other allergens. Its sequence and β-barrel structure is unique among fungal allergens (16–20). Insights into its function have been hypothesized. Because Alt a 1 localizes to the cell wall of

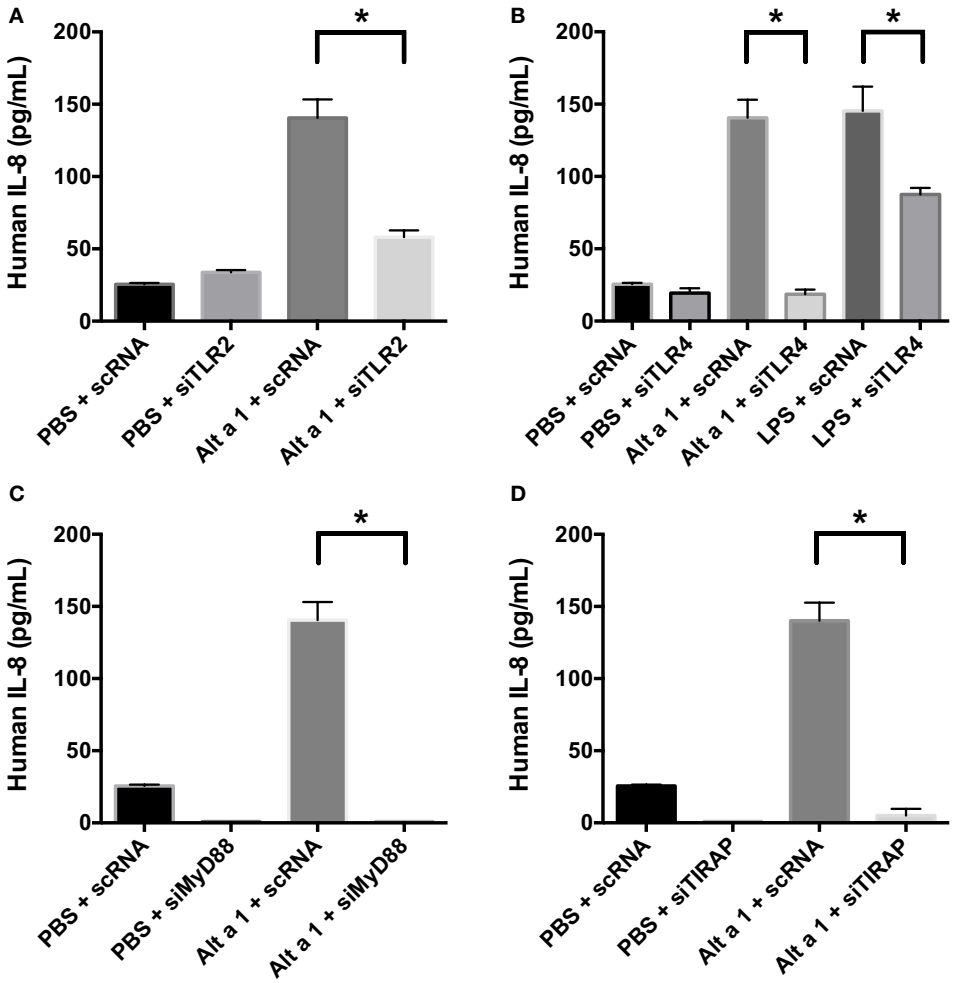

FIGURE 4 | Alt a 1 induces signaling in BEAS-2B cells *via* toll-like receptor (TLR)2, TLR4, MyD88, and TIRAP. 3.0×10^4 human BEAS-2B cells in DMEM + 10% FBS were cultured to 70% confluency in 24-well plates. The cells were transfected with 10 nM of either scrambled control or gene-specific siRNAs in serum-free Opti-MEM medium using Lipofectamine RNA iMAX Reagent according to the manufacturer's protocols. After 24 h, cells were treated with either 50 μg rAlt a 1 or an equivalent volume of PBS. Media was collected and assayed *via* BIOLEGEND IL-8 ELISAMAX. Data are represented as mean (SD). After testing for homogeneity of variances, Tukey's HSD was performed and adjusted (if applicable) (*$p < 0.001$). **(A)** TLR2, **(B)** TLR4, **(C)** MyD88, and **(D)** TIRAP.

spores, it has been predicted to play a role in the stability of the spore (31). *Alternaria* spores isolated from schools, libraries, and offices have been shown to be capable of secreting detectable levels of Alt a 1 (32). On plants, this protein may play a role in the pathogenesis of *Alternaria* spp. (33). This protein has the potential to bind quercetin/flavonol like molecules of plant and fungal origin (34). Alt a 1 has been shown to be localized in the cytoplasm and cell wall of spores and secreted extremely rapidly in media of physiologically relevant pH especially slightly acidic conditions (34). This suggests that following spore inhalation, Alt a 1 may be secreted into the airways quite rapidly. Based on these recent secretion studies it is possible that all individuals are chronically exposed to Alt a 1 even in the absence of fungal colonization of the airways. Studies examining the importance of Alt a 1 beyond the scope of its capability of being used in diagnostic procedures have not been conducted (21).

In this study, we report for the first time that Alt a 1 induces innate immune responses in bronchial epithelial cells *in vitro*. A combination of cell lines and primary cells (BEAS-2B, NHBE, DHBE) with complementary experimental approaches were used to determine that at least some aspects of Alt a 1 signaling are dependent upon PRRs and adaptor molecules including TLR2, TLR4, MYD88, and TIRAP. Moreover, this is the first study to show that a single, highly purified molecule from *Alternaria* induces innate immune responses.

Previously, most immunological studies surrounding *Alternaria* have employed potent extracts consisting of a complex mixture of proteins and speculatively other molecules from *Alternaria* which could include mycotoxins, other secondary metabolites, and cell wall fragments such as chitin, mannans, and β-1,3-glucans. The complexity and inconsistency of extract composition has made it challenging to define specific components contributing to the

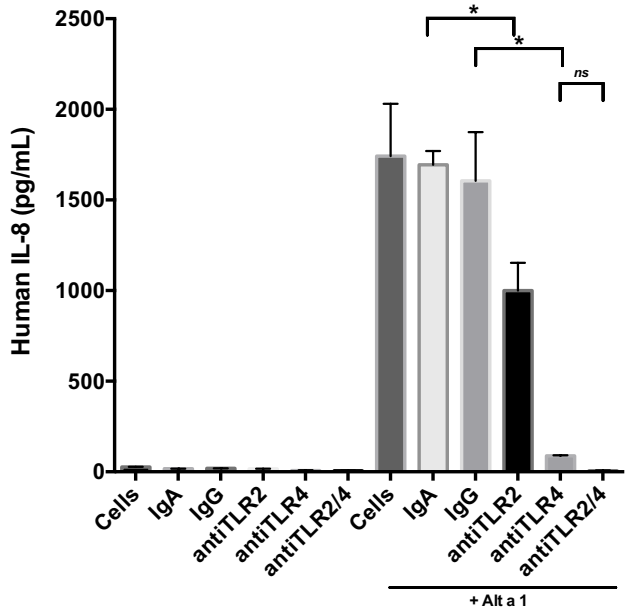

FIGURE 5 | Alt a 1 primarily induces innate immunity through toll-like receptor (TLR)4 in BEAS-2B cells. 2.5×10^5 BEAS-2B cells were grown in RPMI + FPS + 1% Pen Strep. Cells were washed 24 h before use. They were then starved for 6 h. The starve media was RPMI + 1% Pen Strep. Some cells were pretreated with 10 μg/mL anti-hTLR2-IgA, 10 μg/mL anti-hTLR4-IgG, 10 μg/mL human IgA2-control, or 10 μg/mL mouse-IgG1-control for 1 h, then given 50 μg rAlt a 1. Cells incubated for 24 h. Media was collected and assayed *via* BIOLEGEND IL-8 ELISAMAX. Data are represented as mean (SD). After testing for homogeneity of variances, Tukey's HSD was performed and adjusted (if applicable) (*$p < 0.001$). The anti-hTLR2-IgA Alt a 1 treatment was compared to the Alt a 1-IgG treated control. The anti-hTLR4-IgG treatment was compared to the Alt a 1-IgG treated control. Alta1 + TLR2/4 treatment is significant when compared to the Alt a 1-IgG treated control or Alta1 + hTLR2 and is designated with an asterisk. However, Alta1 + hTLR2/4 is not significant when compared to Alta1 + TLR4.

proinflammatory nature of these products. It is widely accepted that different culture and extraction conditions can lead to the variability in airway cell response to extracts (22, 35). In addition, extracts can have widely different allergen content (36). Expression of fungal allergens can even vary by strain (37).

It has been reported in several studies that protease activities in *Alternaria* extracts, especially serine, aspartic, and cysteine protease activity, are potent inducers of cytokines *in vitro* and *in vivo* (38–40). Using inhibitors, it was preciously shown that serine proteases activity from *Alternaria* induced TSLP and IL-33, potentially playing an important role in the development of allergic inflammation, airway disease, and severe asthma exacerbations (38). Aspartic protease activity was shown to activate eosinophils leading to degranulation (39). Aspartic protease activity was shown to induce the release of several other cytokines, including IL-6 and IL-8 (40). Despite the evidence for the role of *Alternaria* proteases found in extracts to be potent inducers of cytokines, no single purified protease has been identified and correlated with these activities. It is important to note that Alt a 1 has not been reported to possess any protease activity. Alt a 1's enzymatic activity has been reported to be primarily esterase and phosphatase (14). While extracts have clearly defined a potential role that proteases play in the immune response of the airway to fungi, they have not allowed for the determination of the role that individual proteins of *Alternaria*, such as Alt a 1 may play in the context of allergic inflammation, sensitization, and development of more complex disorders such as asthma (41). It is interesting to speculate how Alt a 1 may contribute to the overall inflammatory response of *Alternaria* spores and hyphae in the context of other proinflammatory molecules found in *Alternaria* including proteases mentioned above, chitin, glucans, mannans, and other yet to be identified molecules. In this regard, we have created Alt a 1 knockout (KO) and overexpression mutants in *A. alternata* and have recently initiated *in vitro* and *in vivo* experiments comparing these mutants and wild-type (WT) spores for their ability to induce immune responses. Preliminary data from our lab indicate that mutant spores lacking Alt a 1 induce an overall lower innate immune response when compared to WT spores both *in vitro* (BEAS-2B cells) and in mouse *in vivo* models (Rumore et al., unpublished). Moreover, Alt a 1 overexpression mutants (secreting ~2.5 times as much Alt a 1 compared to WT) induce a dramatically higher innate immune response in these systems compared to Alt a 1 KO mutants or WT spores. Future experiments investigating the role of Alt a 1 in adaptive immunity *in vivo* are certainly warranted using these tools.

Although tremendous progress has been made over the past few decades regarding determining the mechanistic aspects of allergic inflammation, more research needs to be performed in innate immunity and its role in sensitization and exacerbation aspects of allergic diseases. Published studies have increasingly made it clear that TLRs are key players in innate immunity to a growing number of allergens. For example, the dust mite allergen, Der p 2, has been shown to mimic the activity of human and mouse MD2 in the presence of LPS to trigger a response through TLR4 (42) *in vitro* and *in vivo*. Der p 2 has been shown to induce TLR2–MYD88-dependent mediated innate immune signaling in nasal fibroblasts (43). In this study, we found the induction of several cytokines and chemokines by Alt a 1 in bronchial epithelial cells including GRO-a/b/g (CXCL1/2/3), IL-8, and MCP-1 (CCL2) and this was TLR2/4, MyD88, and TIRAP dependent. These cytokines and chemokines have been shown in many studies to play a role in monocyte, neutrophil, and fibroblast recruitment and angiogenesis in asthma and innate allergic inflammation (44–46). Studying if other cytokines and chemokines such as TSLP, IL-33, and IL-25 are induced by Alt a 1 and/or in different cell types may be the subject of future research. Our preliminary data strongly suggest that Alt a 1 is capable of inducing the release of IL-33 from NHBE cells and warrants further investigation in the future (data not shown).

More specifically, using gene knockdown approaches and complementary studies with blocking antibodies, we found that the ability of Alt a 1 to induce a potent cytokine response was dependent upon TLR2, TLR4, MyD88, and TIRAP. Treatment of engineered HEK-Blue Null, TLR2, TLR4, and TLR5 cells with Alt a 1 showed that TLR2 and TLR4-associated NF-κB signaling but not TLR5 is activated. Furthermore, incubation with TLR4 blocking antibodies and LPS-RS caused the abolishment of signaling

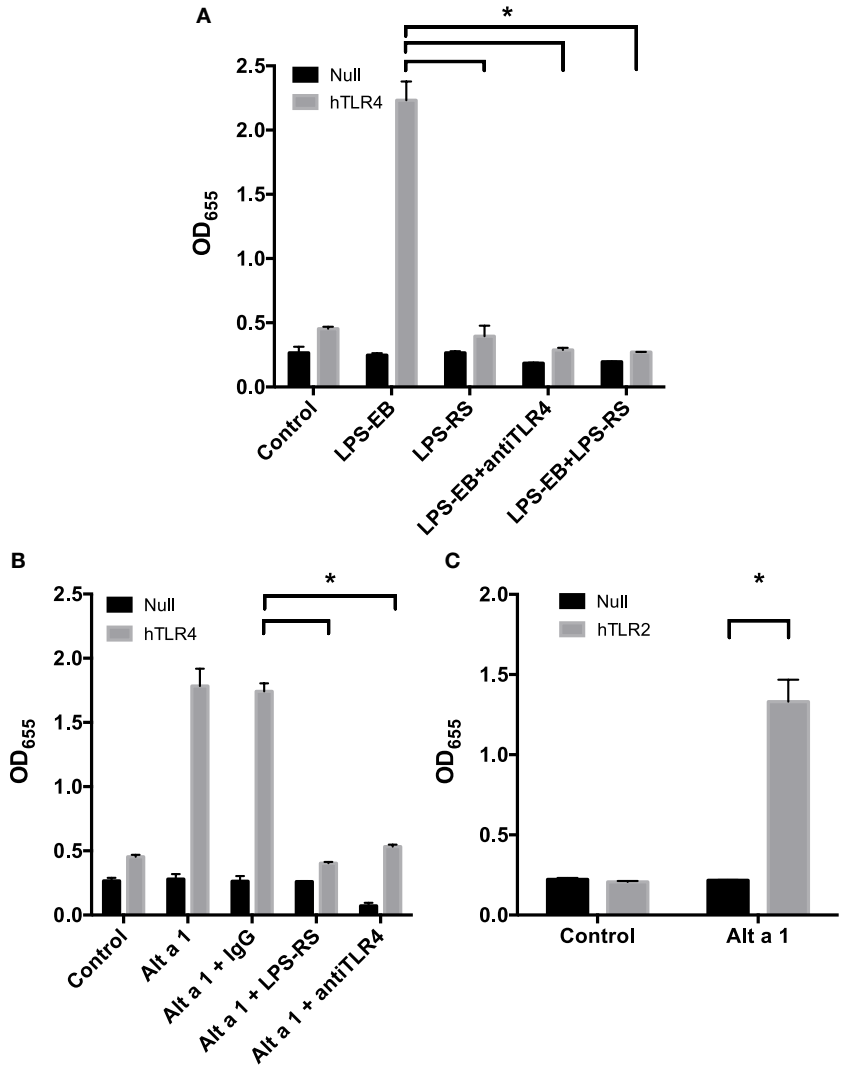

FIGURE 6 | Alt a 1 activates toll-like receptor (TLR)2/4-dependent NF-κB signaling in engineered human embryonic kidney (HEK) cells. 2.5×10^4 HEK-Blue hTLR4 **(A,B)**, HEK-Blue hTLR2 **(C)**, and HEK-Blue null cells **(A–C)** were plated in 96-well plates in 200 µL DMEM + 1% Pen/Strep/10% FBS. After 16 h at 37°C/5% CO_2, the media was removed from the cells. Cells were then starved for 2 h in DMEM + 1% Pen/Strep. **(A)** Cells were pretreated with 5 ng/mL ultrapure LPS-RS, 10 µg/mL anti-hTLR4-IgG, or 10 µg/mL mouse IgG 1 control for an hour. Then cells were treated with 5 ng/mL ultrapure LPS-EB. Cells incubated with treatments in the incubator for 24 h. Afterward 20 µL of the cell supernatant was added to 180 µL QUANTI-Blue reagent. After incubation for 3 h at 37°C, the plate was read at 655 nM room temperature. Data are represented as mean (SD). After testing for homogeneity of variances, Tukey's HSD was performed and adjusted (if applicable) (*$p < 0.001$). Comparisons shown are against LPS-EB (*$p < 0.001$). **(B)** Cells were pretreated with 5 ng/mL ultrapure LPS-RS, 10 µg/mL anti-hTLR4-IgG, or 10 µg/mL mouse IgG 1 control for an hour. Then cells were treated with 1 µg rAlt a 1. Cells incubated with treatments in the incubator for 24 h. Afterward, 20 µL of the cell supernatant was added to 180 µL QUANTI-Blue reagent. After incubation for 3 h at 37°C, the plate was read at 655 nM room temperature. Data are represented as mean (SD). After testing for homogeneity of variances, Tukey's HSD was performed and adjusted (if applicable) (*$p < 0.001$). Comparisons shown are against Alt a 1 + IgG (*$p < 0.001$). **(C)** Cells were treated with 1 µg rAlt a 1. Data are represented as mean (SD). After testing for homogeneity of variances, Tukey's HSD was performed and adjusted (if applicable) (*$p < 0.001$). Comparisons shown are against **(A)** LPS-EB, **(B)** Alt a 1 alone or Alt a 1 + IgG, and **(C)** Alt a 1 untreated null and hTLR2 cells and Alt a 1 treated null cells.

in both HEK-Blue TLR4 and human bronchial epithelial airway (BEAS-2B) cells. In contrast to studies with Der p 2, the MD2 mimic that presents LPS to TLR4, our studies suggest that Alt a 1 does not function as an MD2 mimic because it is structurally unrelated to MD2 or Der p 2. Furthermore, we had virtually undetectable amounts of LPS in our protein preparation. LPS was a requirement for Der p 2 signaling *via* TLR4 (42).

In addition to MD2 and CD14, another important protein in TLR4 signaling is lipopolysaccharide-binding protein (LBP). LBP is mainly found in the serum and has been found to facilitate TLR4 signaling by carrying LPS to the receptor. In a study by Kato et al. comparing gene expression profiles in the presence and absence of serum, it was found that induction of cytokines like IL-8 and members of the GRO family in PBMCs was not dependent upon

LBP being present, however, a subset of IFN-inducible genes was dependent upon LBP (47). The data from this study suggested that MyD88-dependent genes did not require LBP to be present but IRF-3 associated genes required LBP. In our experiments, we starved cells of serum prior to challenges with Alt a 1 and other ligands thus, most likely removing the vast majority of LBP present but still observed TLR4- and MyD88-dependent expression of cytokines like IL-8. If Alt a 1 functions as an LBP mimic, one would most likely not detect this in the context of our experimental design. As mentioned previously, we did not detect LPS in our protein preparations thus most likely ruling out the possibility that Alt a 1 could be an LPS carrier or binding protein mimicking MD2, CD14, or LBP. However, it is important to point out that even though our experiments using engineered HEK cells indicated that MD2 and CD14 are probably not major components of Alt a 1 induced signaling, overexpression of TLR2 and TLR4 receptors could mask the role of CD14 and MD2. Future experiments in BEAS-2B or other cell types are warranted to further elucidate the role of these adaptors in Alt a 1 induced immunity.

Another possibility to consider is contamination of our *Pichia*-produced protein preparations with ligands that may activate TLR2. However, there are no reports of *Pichia*-produced proteins harboring contaminants that activate TLR2. It has been shown that the allergen Der p 21 can induce IL-8 in BEAS-2B cells in a TLR2-dependent manner (48). However, rDer p 21 protein preparations used in this study were analyzed by MS and the authors did not report any contamination. The authors speculated that because Der p 21 is predicted to be a lipid binding protein it may carry an unknown ligand to TLR2. In the context of our study, it is possible that Alt a 1 directly binds to and activates TLR2 and TLR4 or liberates a ligand from the cell surface *via* its esterase and/or phosphatase enzymatic activity and will be the focus of future investigations.

Collectively, these findings provide new avenues for the study of allergic inflammation, the sensitization process, and the development of asthma and other allergic airway diseases especially to *Alternaria*.

AUTHOR CONTRIBUTIONS

TH and AR contributed equally to the manuscript (co-first authors), TH and AR designed and performed experiments, analyzed data, and contributed to writing of the paper, BH and XH designed and performed experiments and analyzed data, ML performed experiments and analyzed data, MC and SW created and provided experimental reagents critical for the study, LL and HK designed experiments and provided reagents, CL designed experiments, analyzed data, and contributed to writing of the paper.

FUNDING

Awards from the National Institute of Allergy and Infectious Diseases 5R01AI071106 to HK and CL, 5R21AI115986 to CL, and 1R21AI094071 to CL supported this research.

SUPPLEMENTARY MATERIAL

The Supplementary Material for this article can be found online at https://www.frontiersin.org/articles/10.3389/fimmu.2018.01507/full#supplementary-material.

REFERENCES

1. Gergen PJ, Turkeltaub PC. The association of individual allergen reactivity with respiratory disease in a national sample: data from the second National Health and Nutrition Examination Survey, 1976-80 (NHANES II). *J Allergy Clin Immunol* (1992) 90:579–88. doi:10.1016/0091-6749(92)90130-T
2. Halonen M, Stern DA, Wright AL, Taussig LM, Martinez FD. *Alternaria* as a major allergen for asthma in children raised in a desert environment. *Am J Respir Crit Care Med* (1997) 155:1356–61. doi:10.1164/ajrccm.155.4.9105079
3. Salo PM, Arbes SJ Jr, Sever M, Jaramillo R, Cohn RD, London SJ, et al. Exposure to *Alternaria alternata* in US homes is associated with asthma symptoms. *J Allergy Clin Immunol* (2006) 118:892–8. doi:10.1016/j.jaci.2006.07.037
4. O'Hollaren MT, Yunginger JW, Offord KP, Somers MJ, O'Connell EJ, Ballard DJ, et al. Exposure to an aeroallergen as a possible precipitating factor in respiratory arrest in young patients with asthma. *N Engl J Med* (1991) 324:359–63. doi:10.1056/NEJM199102073240602
5. Andersson M, Downs S, Mitakakis T, Leuppi J, Marks G. Natural exposure to *Alternaria* spores induces allergic rhinitis symptoms in sensitized children. *Pediatr Allergy Immunol* (2003) 14:100–5. doi:10.1034/j.1399-3038.2003.00031.x
6. Peat JK, Tovey E, Mellis CM, Leeder SR, Woolcock AJ. Importance of house dust mite and *Alternaria* allergens in childhood asthma: an epidemiological study in two climatic regions of Australia. *Clin Exp Allergy* (1993) 23:812–20. doi:10.1111/j.1365-2222.1993.tb00258.x
7. Peat JK, Toelle BG, Gray EJ, Haby MM, Belousova E, Mellis CM, et al. Prevalence and severity of childhood asthma and allergic sensitisation in seven climatic regions of New South Wales. *Med J Aust* (1995) 163:22–6.
8. Hoffman DR. Mould allergens. In: Al-Doory Y, Domson JE, editors. *Mould Allergy*. Philadelphia: Lea and Febiger (1984). p. 104–16.
9. van Leeuwen WS. Bronchial asthma in relation to climate. *Proc R Soc Med* (1924) 17:19–26.
10. Sanchez H, Bush RK. A review of *Alternaria alternata* sensitivity. *Rev Iberoam Micol* (2001) 18:56–9.
11. Breitenbach M, Simon-Nobbe B. The allergens of *Cladosporium herbarum* and *Alternaria alternata*. *Chem Immunol* (2002) 81:48–72. doi:10.1159/000058862
12. Simon-Nobbe B, Probst G, Kajava AV, Oberkofler H, Susani M, Crameri R, et al. IgE-binding epitopes of enolases, a class of highly conserved fungal allergens. *J Allergy Clin Immunol* (2000) 106:887–95. doi:10.1067/mai.2000.110799
13. Weichel M, Schmid-Grendelmeier P, Flückiger S, Breitenbach M, Blaser K, Crameri R. Nuclear transport factor 2 represents a novel cross-reactive fungal allergen. *Allergy* (2003) 58:198–206. doi:10.1034/j.1398-9995.2003.23822.x
14. Barnes CS, Pacheco F, Landuyt J, Rosenthal D, Hu F, Portnoy J. Production of a recombinant protein from *Alternaria* containing the reported N-terminal of the Alt a1 allergen. *Adv Exp Med Biol* (1996) 409:197–203. doi:10.1007/978-1-4615-5855-2_26
15. Sáenz-de-Santamaría M, Guisantes JA, Martínez J. Enzymatic activities of *Alternaria alternata* allergenic extracts and its major allergen (Alt a 1). *Mycoses* (2006) 49:288–92. doi:10.1111/j.1439-0507.2006.01238.x
16. Twaroch TE, Curin M, Sterflinger K, Focke-Tejkl M, Swoboda I, Valenta R. Specific antibodies for the detection of *Alternaria* allergens and the identification of cross-reactive antigens in other fungi. *Int Arch Allergy Immunol* (2016) 170:269–78. doi:10.1159/000449415
17. Bowyer P, Fraczek M, Denning DW. Comparative genomics of fungal allergens and epitopes shows widespread distribution of closely related allergen and epitope orthologues. *BMC Genomics* (2006) 7:251. doi:10.1186/1471-2164-7-251
18. Crameri R. Structural aspects of fungal allergens. *Semin Immunopathol* (2014) 37:117–21. doi:10.1007/s00281-014-0458-0

19. Chruszcz M, Chapman MD, Osinski T, Solberg R, Demas M, Porebski PJ, et al. *Alternaria alternata* allergen Alt a 1: a unique β-barrel protein dimer found exclusively in fungi. *J Allergy Clin Immunol* (2012) 130:241–7.e9. doi:10.1016/j.jaci.2012.03.047
20. Wagner GE, Gutfreund S, Fauland K, Keller W, Valenta R, Zangger K. Backbone resonance assignment of Alt a 1, a unique β-barrel protein and the major allergen of *Alternaria alternata*. *Biomol NMR Assign* (2014) 8:229–31. doi:10.1007/s12104-013-9489-z
21. Asturias JA, Ibarrola I, Ferrer A, Andreu C, López-Pascual E, Quiralte J, et al. Diagnosis of *Alternaria alternata* sensitization with natural and recombinant Alt a 1 allergens. *J Allergy Clin Immunol* (2005) 115:1210–7. doi:10.1016/j.jaci.2005.02.012
22. Paris S, Fitting C, Ramirez E, Latgé JP, David B. Comparison of different extraction methods of *Alternaria* allergens. *J Allergy Clin Immunol* (1990) 85:941–8. doi:10.1016/0091-6749(90)90081-E
23. Aden E, Weber B, Bossert J, Teppke M, Frank E, Wahl R, et al. Standardization of *Alternaria alternata*: extraction and quantification of alt a 1 by using an mAb-based 2-site binding assay. *J Allergy Clin Immunol* (1999) 104:128–35. doi:10.1016/S0091-6749(99)70124-7
24. Implementing a Class of Permutation Tests. The coin Package | Hothorn. *J Stat Softw* (2017). Available from: https://www.jstatsoft.org/article/view/v028i08 (accessed January 8, 2017).
25. *An R Companion to Applied Regression* | SAGE Publications Inc (2017). Available from: https://us.sagepub.com/en-us/nam/an-r-companion-to-applied-regression/book233899 (accessed January 8, 2017).
26. Ritz C, Baty F, Streibig JC, Gerhard D. Dose-response analysis using R. *PLoS One* (2015) 10:e0146021. doi:10.1371/journal.pone.0146021
27. Hothorn T, Bretz F, Westfall P. Simultaneous inference in general parametric models. *Biom J* (2008) 50:346–63. doi:10.1002/bimj.200810425
28. Object-oriented computation of sandwich estimators. *J Stat Softw* (2017). Available from: https://www.jstatsoft.org/article/view/v016i09 (accessed January 8, 2017).
29. Yunginger JW, Jones RT, Nesheim ME, Geller M. Studies on *Alternaria* allergens. *J Allergy Clin Immunol* (1980) 66:138–47. doi:10.1016/0091-6749(80)90061-5
30. Kleine-Tebbe J, Worm M, Jeep S, Matthiesen F, Løwenstein H, Kunkel G. Predominance of the major allergen (Alt a I) in *Alternaria* sensitized patients. *Clin Exp Allergy* (1993) 23:211–8. doi:10.1111/j.1365-2222.1993.tb00884.x
31. Twaroch TE, et al. Predominant localization of the major *Alternaria* allergen Alt a 1 in the cell wall of airborne spores. *J Allergy Clin Immunol* (2012) 129:1148–9. doi:10.1016/j.jaci.2011.10.008
32. Skóra J, Otlewska A, Gutarowska B, Leszczyńska J, Majak I, Stępień Ł. Production of the allergenic protein Alt a 1 by *Alternaria* isolates from working environments. *Int J Environ Res Public Health* (2015) 12:2164–83. doi:10.3390/ijerph120202164
33. Cramer RA, Lawrence CB. Cloning of a gene encoding an Alt a 1 isoallergen differentially expressed by the necrotrophic fungus *Alternaria brassicicola* during *Arabidopsis* infection. *Appl Environ Microbiol* (2003) 69:2361–4. doi:10.1128/AEM.69.4.2361-2364.2003
34. Garrido-Arandia M, Silva-Navas J, Ramírez-Castillejo C, Cubells-Baeza N, Gómez-Casado C, Barber D, et al. Characterisation of a flavonoid ligand of the fungal protein Alt a 1. *Sci Rep* (2016) 6:33468. doi:10.1038/srep33468
35. Kim JH, Harvey LA, Evans AL, Byfield GE, Betancourt DA, Dean TR. Biological responses of Raw 264.7 macrophage exposed to two strains of *Stachybotrys chartarum* spores grown on four different wallboard types. *Inhal Toxicol* (2016) 28:303–12. doi:10.3109/08958378.2016.1170909
36. De Vouge MW, Thaker AJ, Zhang L, Muradia G, Rode H, Vijay HM. Molecular cloning of IgE-binding fragments of *Alternaria alternata* allergens. *Int Arch Allergy Immunol* (1998) 116:261–8. doi:10.1159/000023954
37. Martínez J, Gutiérrez A, Postigo I, Cardona G, Guisantes J. Variability of Alt a 1 expression by different strains of *Alternaria alternata*. *J Investig Allergol Clin Immunol* (2006) 16:279–82.
38. Snelgrove RJ, Gregory LG, Peiró T, Akthar S, Campbell GA, Walker SA, et al. *Alternaria*-derived serine protease activity drives IL-33–mediated asthma exacerbations. *J Allergy Clin Immunol* (2014) 134:583–92.e6. doi:10.1016/j.jaci.2014.02.002
39. Matsuwaki Y, Wada K, White TA, Benson LM, Charlesworth MC, Checkel JL, et al. Recognition of fungal protease activities induces cellular activation and eosinophil-derived neurotoxin release in human eosinophils. *J Immunol* (2009) 183:6708–16. doi:10.4049/jimmunol.0901220
40. Matsuwaki Y, Wada K, White T, Moriyama H, Kita H. *Alternaria* fungus induces the production of GM-CSF, interleukin-6 and interleukin-8 and calcium signaling in human airway epithelium through protease-activated receptor 2. *Int Arch Allergy Immunol* (2012) 158:19–29. doi:10.1159/000337756
41. Kustrzeba-Wójcicka I, Siwak E, Terlecki G, Wolańczyk-Mędrala A, Mędrala W. *Alternaria alternata* and its allergens: a comprehensive review. *Clin Rev Allergy Immunol* (2014) 47:354–65. doi:10.1007/s12016-014-8447-6
42. Trompette A, Divanovic S, Visintin A, Blanchard C, Hegde RS, Madan R, et al. Allergenicity resulting from functional mimicry of a toll-like receptor complex protein. *Nature* (2009) 457:585–8. doi:10.1038/nature07548
43. Chiou Y-L, Lin C-Y. Der p2 activates airway smooth muscle cells in a TLR2/MyD88-dependent manner to induce an inflammatory response. *J Cell Physiol* (2009) 220:311–8. doi:10.1002/jcp.21764
44. Keglowich L, Roth M, Philippova M, Resink T, Tjin G, Oliver B, et al. Bronchial smooth muscle cells of asthmatics promote angiogenesis through elevated secretion of CXC-chemokines (ENA-78, GRO-α, and IL-8). *PLoS One* (2013) 8:e81494. doi:10.1371/journal.pone.0081494
45. Singh SR, Sutcliffe A, Kaur D, Gupta S, Desai D, Saunders R, et al. CCL2 release by airway smooth muscle is increased in asthma and promotes fibrocyte migration. *Allergy* (2014) 69:1189–97. doi:10.1111/all.12444
46. Roy RM, Wüthrich M, Klein BS. Chitin elicits CCL2 from airway epithelial cells and induces CCR2-dependent innate allergic inflammation in the lung. *J Immunol* (2012) 189:2545–52. doi:10.4049/jimmunol.1200689
47. Kato A, Ogasawara T, Homma T, Saito H, Matsumoto K. Lipopolysaccharide-binding protein critically regulates lipopolysaccharide-induced IFN-beta signaling pathway in human monocytes. *J Immunol* (2004) 172(10):6185–94. doi:10.4049/jimmunol.172.10.6185
48. Pulsawat P, Theeraapisakkun M, Nony E, Le Mignon M, Jain K, Buaklin A, et al. Characterization of the house dust mite allergen Der p 21 produced in *Pichia pastoris*. *Protein Expr Purif* (2014) 101:8–13. doi:10.1016/j.pep.2014.05.001

Conflict of Interest Statement: MC and SW were employed by the company Indoor Biotechnologies Inc., Charlottesville, VA. All other authors declare no competing interests.

The handling Editor declared a shared affiliation, though no other collaboration, with one of the authors TH.

Copyright © 2018 Hayes, Rumore, Howard, He, Luo, Wuenschmann, Chapman, Kale, Li, Kita and Lawrence. This is an open-access article distributed under the terms of the Creative Commons Attribution License (CC BY). The use, distribution or reproduction in other forums is permitted, provided the original author(s) and the copyright owner are credited and that the original publication in this journal is cited, in accordance with accepted academic practice. No use, distribution or reproduction is permitted which does not comply with these terms.

frontiers in Immunology

MINI REVIEW
published: 12 December 2017
doi: 10.3389/fimmu.2017.01798

Tissue-Resident Macrophages in Fungal Infections

Shengjie Xu[1] *and Mari L. Shinohara*[1,2]*

[1] Department of Immunology, Duke University School of Medicine, Durham, NC, United States, [2] Department of Molecular Genetics and Microbiology, Duke University School of Medicine, Durham, NC, United States

Invasive fungal infections result in high morbidity and mortality. Host organs targeted by fungal pathogens vary depending on the route of infection and fungal species encountered. *Cryptococcus neoformans* infects the respiratory tract and disseminates throughout the central nervous system. *Candida albicans* infects mucosal tissues and the skin, and systemic *Candida* infection in rodents has a tropism to the kidney. *Aspergillus fumigatus* reaches distal areas of the lung once inhaled by the host. Across different tissues in naïve hosts, tissue-resident macrophages (TRMs) are one of the most populous cells of the innate immune system. Although they function to maintain homeostasis in a tissue-specific manner during steady state, TRMs may function as the first line of defense against invading pathogens and may regulate host immune responses. Thus, in any organs, TRMs are uniquely positioned and specifically programmed to function. This article reviews the current understanding of the roles of TRMs during major fungal infections.

Keywords: tissue-resident macrophages, fungal infections, microglia, alveolar macrophages, *Candida*, *Cryptococcus*, *Aspergillus*

OPEN ACCESS

Edited by:
Amariliz Rivera, New Jersey Medical School, United States

Reviewed by:
Ilse Denise Jacobsen, Leibniz-Institut für Naturstoff-Forschung und Infektionsbiologie, Hans Knöll Institut, Germany
Joshua J. Obar, Dartmouth College, United States
George So Yap, Rutgers University, Unites States

***Correspondence:**
Mari L. Shinohara
mari.shinohara@duke.edu

Specialty section:
This article was submitted to Microbial Immunology, a section of the journal Frontiers in Immunology

Received: *27 September 2017*
Accepted: *30 November 2017*
Published: *12 December 2017*

Citation:
Xu S and Shinohara ML (2017) Tissue-Resident Macrophages in Fungal Infections. Front. Immunol. 8:1798. doi: 10.3389/fimmu.2017.01798

INTRODUCTION

Macrophages were initially discovered in the late nineteenth century by Metchnikoff and named for its phagocytic activity as "devouring cells" in Greek (1, 2). They are capable of engulfing and digesting cellular debris, foreign substances, and microorganisms, which are critical for tissue remodeling and immune defense against pathogens. Based on the morphology, function, origin, and kinetics of these phagocytes, macrophages were categorized into the "mononuclear phagocytes system (MPS)" (3). Even after a century since the discovery of macrophages, research efforts have continuously focused on the origins and functions of macrophages for their significant impact on tissue homeostasis and disease pathogenesis.

Tissue-resident macrophages (TRMs) consist of heterogeneous subsets of macrophages distributed in tissues across the body and contribute to tissue homeostasis and immunosurveillance (4, 5). Depending on which organs they reside, some TRMs have specific names, such as alveolar macrophages (AMs) (lung), microglia (brain), Kupffer cells (liver), renal macrophages (kidney), and osteoclasts (skeletal system). As such specific names indicate, TRMs are considered to have specific functions due to various tissue microenvironments (6, 7). This mini-review provides an outline of several major TRMs in fungal infections, mainly focusing on murine studies, by which a majority of mechanistic insights about TRMs have been obtained.

ORIGINS OF TRMs

Developmental Origins of TRMs

Tissue-resident macrophages used to be considered as cells derived from circulating monocytes during the early establishment of the MPS (3). However, a series of recent studies drastically changed this notion, particularly through the technical advancement of *in vivo* cellular lineage-tracing by employing the "fate-mapping" technique using the mouse Cre-lox genetic system. Such *in vivo* lineage-tracing approaches have shown, for example, that microglia arise early in mouse development and are derived from primitive macrophages in the yolk sac (YS) (8). These studies suggested that microglia are ontogenically distinct from monocyte-derived macrophages (MDMs), which are of the hematopoietic origin. In addition to microglia, F4/80^{hi} Kupffer cells and epidermal Langerhans cells were demonstrated to be YS-derived and do not require Myb, a transcription factor required for the development of hematopoietic stem cells (HSCs) (9). By employing the conditional CX_3CR1 fate-mapping system, another study showed that origins of Kupffer cells, AMs, splenic, and peritoneal macrophages, are also embryonic, at least in part (10). Introduction of fate-mapping markers other than CX_3CR1 further clarified that TRMs in many tissues consist of mixed populations of the embryonic (YS and/or fetal liver) and the BM hematopoietic origins, except for microglia that are exclusively of the YS-origin (11–13).

A majority of TRMs are self-maintained throughout adult life with minimal contribution from circulating monocytes (14). However, populations of TRMs can also be replaced. For example, intestinal macrophages in mouse neonates are derived from YS and fetal liver, but do not persist into adulthood and are replaced by MDMs around the time of weaning (15). Cardiac macrophages are established from YS and fetal monocyte progenitors, but disruption of homeostasis replaces the population with MDMs (11). These murine studies strongly suggested that TRMs, in general, are derived from diverse precursors including YS macrophages, fetal liver monocytes, and even circulating HSC-derived monocytes; and ontogenic origins of TRMs greatly vary depending on tissues.

TRMs Reflecting Organ-Specific Microenvironments

Tissue-resident macrophages develop locally and adapt to tissue microenvironments during embryogenesis and beyond. Distinct gene expression patterns were identified among local TRMs from various tissues (6, 7, 16, 17), and are often reflected at the epigenetic level, particularly indicated by differential histone marks on the enhancer landscape (6, 7). Multiple pieces of evidence have suggested that such tissue-specific patterns of gene expression in TRMs are influenced by tissue-specific environmental factors, including heme (18), retinoic acid (6, 17), and TGF-β (6, 19). Interestingly, macrophage "precursors" derived from YS, fetal liver, and adult monocytes appear to have the plasticity to become certain TRMs, based on tissue-specific gene expression profiles. For example, macrophages precursors from various origins develop into functional and self-maintaining AMs, when transplanted to an empty alveolar niche (20). However, once differentiated into organ-specific macrophages, TRMs, except for Kupffer cells, cannot efficiently colonize the empty AM niche (20), suggesting that the plasticity would be lost after the precursor stage. Thus, functions of TRMs are actively shaped by their local tissue microenvironment.

TRMs IN ANTIFUNGAL RESPONSES

Critical steps to protect hosts from infections include; early recognition of the fungi, activation of host immunity, and killing of the spores and vegetative fungal cells to contain fungal dissemination (21–24). During early stages of fungal infections, infected hosts rely on tissue-resident "cells," not necessarily TRMs alone, to function as the first line of defense. Here, despite the tissue-specific functions of TRMs from various organs, a general expectation for TRMs is to function as immune sentinels to detect infections at the front line. In fact, TRMs express a wide array of cell surface receptors that sense intruding microbes and produce chemokines and cytokines to recruit and activate other cell subsets for further help (25, 26). However, do TRMs always work to protect hosts? We will visit this topic in the following subsections. As some backgrounds for this section, we would like to mention that TRMs are not considered to play a role in T cell priming with microbe-derived antigens in draining lymph nodes because they are not migratory cells (27). It is also of note that CCR2$^+$ inflammatory MDMs play critical role in fungal clearance (28–32). Here, CCR2$^+$ MDMs are recruited from circulation by chemoattractants secreted by sentinel cells. In the following subsections and **Table 1**, we focus on the early interaction of TRMs with fungi.

Lung—AMs

Because lungs are exposed to the outer environment, they constantly inhale microbes, which enter the distal airway to bronchioles and alveoli. AMs are lung-resident macrophages considered to be largely derived from fetal liver monocytes (10, 13, 51) and represent more than 90% of leukocytes in a bronchoalveolar lavage in healthy animals (52). Since fungal infections through the pulmonary route have been intensively studied, AMs may be the best-documented TRMs in fungal infections. Here, we discuss AMs and two major pulmonary fungal pathogens, *Cryptococcus neoformans* and *Aspergillus fumigatus*, which can cause serious invasive cryptococcosis and aspergillosis, respectively (21, 53–55).

C. neoformans spores and *A. fumigatus* conidia enter into the lungs by inhalation and encounter lung-resident cells first, including AMs. Although AMs are not effective in antigen presentation to T cells due to their low level of costimulatory molecules (56), AMs are considered to be at the first line of immune defense against pulmonary pathogens (57). AMs express complement receptor 3 (CR3) and Fcγ receptors (FcγR) to opsonize and phagocytose *C. neoformans* spores (33, 34, 58, 59). Phagocytosis of *C. neoformans* spores is enhanced by extracellular sphingosine-1-phosphate, which upregulates FcγR expression on AMs (35). In *A. fumigatus* infection, AMs can trap dormant *A. fumigatus* conidia with pseudopods and endocytose

TABLE 1 | Tissue-resident macrophage antifungal response.

Cell type	Fungal pathogen	Macrophage responses	Experimental approaches
Alveolar macrophages	*C. neoformans*	Take up spores which are opsonized by complement and antibodies through CR3 and Fcγ receptors (33, 34) mediated by S1PR2 (35)	Stimulating adherent murine bronchoalveolar lavage (BAL) cells in tissue culture (35)
		Produce TNFα, CXCL1, CXCL2, CCL2, and IL-1β (36)	Stimulating adherent murine BAL cells in tissue culture (36)
	A. fumigatus	Trap *A. fumigatus* conidia by pseudopods and take up conidia in actin-dependent manner (37)	Stimulating MH-S murine AM cell line in tissue culture (38)
		Kill *A. fumigatus* conidia through phagolysosome acidification (37) and production of reactive oxidant species (39)	Stimulating adherent murine BAL cells in tissue culture (39)
		Bind and uptake *A. fumigatus* conidia through SP-A and SP-D (40)	Stimulating BAL cells from aspergillosis patients in tissue culture (40)
		Detect cell wall β-1,3-glucans through Dectin-1 (41) and NOD2 receptors (42)	Murine *A. fumigatus* pulmonary infection model: AMs identified as $CD45^+Ly6G^-$ $CD11c^+$ cells (41)
		Induce proinflammatory cytokines and chemokines (38)	Stimulating MH-S cell line and adherent murine BAL cells in tissue culture (38)
Microglia	*C. albicans*	Detect cell wall β-glucan through Dectin-1 and activate Syk, Vav1, and PI3K (43) required for phagocytosis (44), and superoxide production (45)	Stimulating murine microglia primary cell culture and BV-2 microglial cell line (43)
		Increase CD11b expression and change morphology (46)	Invasive murine candidiasis model: evaluating $MHC\text{-}II^+Iba1^+$ microglia *in situ* or $CD45^+CD11b^+MHC\text{-}II^+$ microglia by flow cytometry (46)
	C. neoformans	Produce chemokines, MCP-1, MIP-1α, and MIP-1β through FcR-mediated activation by antibody-bound *C. neoformans* (47)	Stimulating human fetal microglia cells with *C. neoformans* and antifungal antibodies in tissue culture (47)
		Require IFNγ or LPS priming to eliminate *C. neoformans* through nitric oxide production (48)	Stimulating BV-2 microglial cell line (48)
	A. fumigatus	Require complement system for phagocytosis of *A. fumigatus* conidia (49, 50)	Stimulating human primary microglia in tissue culture (50)
Kidney macrophages	*C. albicans*	Internalize conidia and pseudohyphae (29)	Invasive murine candidiasis model: evaluating $CX3CR1^+$ renal macrophages *in situ* (29)
		Produce chemokines, CXCL1, and CXCL2 (25)	Invasive murine candidiasis model: evaluating $SSC^{lo}CD45^+Ly6G^-CD11b^+F4/80^{hi}$ renal macrophages by flow cytometry (25)

conidia in an actin-dependent manner (37, 60). Although neutrophils are the main population involved in complement-dependent opsonization, phagocytosis, and killing of the fungi (61, 62), AMs can also kill internalized *A. fumigatus* conidia by detection of conidia swelling and the endosome–phagosome fusion, resulting in acidification of the organelles (37). Activation of NADPH oxidase in AMs was also reported (39), suggesting AMs to gain an "M1" phenotype. Alternatively, another study showed that *A. fumigatus* infection promotes AMs to gain an alternative activated macrophage phenotype, or also known as the M2 phenotype, based on upregulation of M2 macrophage markers, such as gene transcripts encoding arginase-1 (Arg1), Ym1, and CD206 (63). Interestingly, the study did not observe the induction of *Nos2*, a major M1 macrophage marker (63). It was suggested that Arg1-expressing AMs potentially deprive L-arginine, a substrate of arginase. Since L-arginine is an essential nutrient source of fungi, the expression of Arg1 may result in inhibiting fungal growth through arginine deprivation (63). These studies suggested the presence of multiple mechanisms by which AMs protects hosts from fungal infections.

Failure in the initial clearance of invaded fungi allows them to take advantage of the humid and nutrient-rich milieu in the lung to disseminate. As the next layer to contain fungal dissemination, inflammatory neutrophils and monocytes need to be recruited in the lung. Here, it is possible that AMs play a sentinel role to recruit such inflammatory cells by secreting cytokines and chemokines to fight against fungi. For example, dectin-1 on AMs detects β-glucans on the fungal cell surface (41, 64) and stimulates the production of proinflammatory cytokines TNFα, IL-6, and IL-18 (65). Intracellular receptor NOD2 in AMs can also induce the synthesis of cytokines, such as IL-12, IFN-γ, GM-CSF, CCL2/MCP-1, CXCL2/MIP-2, and CXCL1/KC (38, 42). It is of note that the majority of these studies on cytokine and chemokine expression were performed with isolated AMs or cell lines in tissue culture. Thus, *in vivo* protein expression patterns of AMs to *A. fumigatus* and *C. neoformans* infections need to be studied.

Neutrophil chemoattractants, such as CXCL1 and CXCL2, have a great impact on the host protection from *A. fumigatus* infection (66, 67), and the main source of the chemoattractants in *A. fumigatus* infection was reported to be epithelial cells, rather than AMs (68). Indeed, AM depletion by clodronate does not alter neutrophil recruitment and host mortality in pulmonary *A. fumigatus* infection (69). Thus, a role of AMs in

A. fumigatus may be minor. In contrast in *C. neoformans* infection, AMs highly express CXCL1 and CXCL2, as well as TNFα (36), but *C. neoformans* can survive in AMs and contribute to latent infection (70). However, it is puzzling that depletion of AMs and DCs "together," by using CD11c-DTR mice (AMs and DCs are CD11c positive), resulted in more neutrophil infiltration in the lung 4 days after *C. neoformans* infection and enhanced mortality with severe lung inflammation (71). Although it is not clear which cell type, DCs, or AMs, is dominant in inhibiting neutrophil recruitment in the lung, questions that can be brought up are how DCs and/or AMs inhibit neutrophil recruitment and whether the inhibition occurs only under some conditions. Since it is technically difficult to deplete AMs alone, we still need to wait to understand if and how AMs are detrimental or protective in fungal infections.

Central Nervous System (CNS)—Microglia

Fungal infections in the CNS are usually secondary to infections in peripheral tissues. Yet, once fungal pathogens reach to the CNS, it can be fatal to hosts. Some species of *Candida*, *Cryptococcus*, and *Aspergillus* can cause life-threatening CNS infections in immunocompromised patients (72–74). Microglia reside in the CNS parenchyma and are poised to provide the first line of defense against invading pathogens. Through the expression of various pattern-recognition receptors, microglia can recognize a wide range of pathogens that colonize the CNS (75, 76). In this section, we discuss responses of microglia during CNS infection by these fungi.

Candida albicans commonly colonizes the mucocutaneous locations in the host, and can also invade the bloodstream to cause systemic candidiasis. Innate immunity is the dominant protective mechanism against disseminated candidiasis. Microglia detect β-glucans through dectin-1, resulting in phosphorylation of Syk (43), and activation of Vav1 and PI3K, which are required for phagocytosis and superoxide production (45). However, dectin-1 stimulation alone is not sufficient for microglia to induce cytokines or chemokine production (43). This suggests a unique mechanism of dectin-1 signaling in microglia distinct from other types of TRMs and MDMs, in which dectin-1 signaling is sufficient for production of cytokines and chemokines. Microglia are also found in the retina and activated by invasive candidiasis, resulting in enhanced expression of cell surface CD11b, and morphological change (46), as well as phagocytosis of *C. albicans* conidia through dectin-1 activation (44).

In contrast to *Candida*, *C. neoformans* spores are not effectively cleared by microglia. Thus, microglia require other immune cells and mechanisms to effectively combat *C. neoformans* infection in the CNS (77, 78). Opsonization of *C. neoformans* spores by antibodies plays a critical role in the induction of cytokine and chemokine expression in microglia (48). For example, opsonizing antibodies induce microglial expression of chemokines, such as CCL2/MCP-1, CCL3/MIP-1α, and CCL4/MIP-1β, but the response is also known to be inhibited by cryptococcal capsular polysaccharides (47). In addition to antibodies, LPS and IFNγ promote the killing of opsonized and unopsonized *C. neoformans* by augmenting nitric oxide production without inducing phagocytosis in a microglial cell line (48). Another study showed that IFNγ is required for enhanced anticryptococcal responses when microglia are activated by intracranial injection of IL-2 and a CD40 agonistic antibody (79). Taken together, IFNγ appears to be critical for microglia to respond to *C. neoformans*.

Aspergillus fumigatus also causes meningitis, but little is known about responses of microglia to *A. fumigatus*. One study showed that CR3 expression of microglia is reduced by an *A. fumigatus*-derived protease, resulting in a significant decrease in phagocytosis by primary human microglia (49). The high frequency of host mortality by cerebral aspergillosis suggests that antifungal responses of microglia are not efficient, although it might be possible that IFNγ also enhances the response against *Aspergillus* by microglia.

Taken together, these studies suggest that microglia are not efficient in fungal clearance. Although it is not clear why microglia are not effective cells among the MPS, the specific microenvironment of the CNS, which is known as an immune-privileged site, may be involved in shaping the character of microglia. The CNS is isolated from other peripheral organs because it is separated from blood circulation by the blood–brain barrier. The physical separation of the CNS from the immune system in the rest of organs, at least in part, may contribute to the specific development and functions of microglia, distinct from the rest of TRMs.

Kidney—Renal Macrophages

In healthy kidneys, immune cells are rarely found except for resident DCs and macrophages (80). Renal macrophages are found in the tubulointerstitium (81), a compartment of the kidney bounded by the vasculature and nephrons, and comprising about 80% of kidney volume (80). Renal macrophages in adult mice are largely derived from fetal liver monocytes (11, 82) and have been extensively studied due to their involvement in immune homeostasis (83–85) and host defense against infections (29, 86).

The kidney is a main target organ in murine systemic candidiasis (87, 88), but not necessarily a primary target in human systemic candidiasis (89). Nevertheless, host resistance heavily depends on the immune system in the kidney. For example, renal macrophages, as well as possibly splenic and liver macrophage, are considered to be protective in host defense against *Candida* (29, 87, 90). CX_3CR1-deficient mice are susceptible to *Candida* infection, possibly due to reduced numbers of kidney-resident and -infiltrated macrophages (91). As early as 2 h after *Candida* infection, renal macrophages elicit their protective responses by internalizing conidia and encasing pseudohyphal elements (91). In addition to their phagocytic ability, renal macrophages isolated from naïve mice are shown to kill *Candida* conidia in tissue culture (91). Besides their endogenous fungal-killing ability, kidney $F4/80^{hi}$ macrophages also recruit neutrophils by secreting high levels of chemokine CXCL2 in the first 24 h of systemic *Candida* infection in an autophagy-dependent manner (25), indeed playing a role as immune sentinels. In summary, kidney macrophages are important players in fungal clearance in murine candidiasis model.

CLOSING REMARKS

Our knowledge on TRMs identities and functions has been greatly expanded in the last decade. Depending on the physical

locations and fungal pathogens, TRMs respond in different ways. Tissue-specific factors may also have impacts on the antifungal outcome of TRMs. However, there are still many unanswered questions and technical hurdles to further advance the field. Here, we close our discussion with six questions.

(A) *Do the functions of TRMs from various organs share something in common?* Because TRMs are shaped by tissue-specific environments to acquire unique intracellular gene expression profile and assisted by tissue factors to enhance their antifungal response, previous studies have focused on the dissimilarity among TRMs from various organs. Yet, all TRMs are expected to play a similar role in maintaining immune surveillance and behaving as sentinels when infections occur. Thus, despite their organ-specific environments, TRMs could potentially share some functions, particularly as sentinels during infections. (B) *To which extent can result from tissue culture experiments be applied to TRMs' functions in vivo?* Majority of functional studies on TRMs have been performed in tissue culture or even with cell lines. It is not clear if *ex vivo* behaviors of TRMs reflect those *in vivo*. (C) *Do human TRMs behave similarly to murine TRMs?* Due to the technical limits to isolate TRMs from humans, a majority of TRM studies have been carried out by using animals. Therefore, it is again not clear if and to what extent TRMs from human and murine share similar responses. (D) *Are TRMs involved in allowing fungi to switch from commensal/non-pathogenic to pathogenic?* TRMs' involvement in the switching might be possible because of the localization of TRMs in tissues where commensal fungi are homed. (E) *Are TRMs heterogeneous if they are within a single organ?* For example, the presence of microglia subsets has been identified (92, 93). It is intriguing to explore possible cellular subsets within TRMs in a single tissue and their possibly distinct functions. To answer the question, new technologies, such as single-cell sequencing or CyTOF would be very powerful tools to answer the question. (F) *How can we "specifically" deplete a certain TRM population?* One of the most significant technical challenges in studying TRMs may be depleting a certain population of TRMs. Clodronate-liposome is used to deplete TRMs, but it is not specific depletion. There are genetically modified mice and antagonists of certain receptors used to particularly deplete microglia. However, what is the best method to deplete AMs or Kupffer cells, for example? These are at least several questions and challenges to overcome to better understand TRMs in fungal infections and even other pathogenic conditions.

AUTHOR CONTRIBUTIONS

All authors listed have made a substantial, direct, and intellectual contribution to the work and approved it for publication.

ACKNOWLEDGMENTS

We thank M. Elizabeth Deerhake and William E. Barclay for critical reading and editing of the manuscript. This study was supported by an NIH grant to M.L.S. (R01-AI088100).

REFERENCES

1. Cavaillon JM. The historical milestones in the understanding of leukocyte biology initiated by Elie Metchnikoff. *J Leukoc Biol* (2011) 90:413–24. doi:10.1189/jlb.0211094
2. Kaufmann SH. Immunology's foundation: the 100-year anniversary of the Nobel Prize to Paul Ehrlich and Elie Metchnikoff. *Nat Immunol* (2008) 9:705–12. doi:10.1038/ni0708-705
3. van Furth R, Cohn ZA, Hirsch JG, Humphrey JH, Spector WG, Langevoort HL. The mononuclear phagocyte system: a new classification of macrophages, monocytes, and their precursor cells. *Bull World Health Organ* (1972) 46: 845–52.
4. Taylor PR, Martinez-Pomares L, Stacey M, Lin HH, Brown GD, Gordon S. Macrophage receptors and immune recognition. *Annu Rev Immunol* (2005) 23:901–44. doi:10.1146/annurev.immunol.23.021704.115816
5. Varol C, Mildner A, Jung S. Macrophages: development and tissue specialization. *Annu Rev Immunol* (2015) 33:643–75. doi:10.1146/annurev-immunol-032414-112220
6. Gosselin D, Link VM, Romanoski CE, Fonseca GJ, Eichenfield DZ, Spann NJ, et al. Environment drives selection and function of enhancers controlling tissue-specific macrophage identities. *Cell* (2014) 159:1327–40. doi:10.1016/j.cell.2014.11.023
7. Lavin Y, Winter D, Blecher-Gonen R, David E, Keren-Shaul H, Merad M, et al. Tissue-resident macrophage enhancer landscapes are shaped by the local microenvironment. *Cell* (2014) 159:1312–26. doi:10.1016/j.cell.2014.11.018
8. Ginhoux F, Greter M, Leboeuf M, Nandi S, See P, Gokhan S, et al. Fate mapping analysis reveals that adult microglia derive from primitive macrophages. *Science* (2010) 330:841–5. doi:10.1126/science.1194637
9. Schulz C, Gomez Perdiguero E, Chorro L, Szabo-Rogers H, Cagnard N, Kierdorf K, et al. A lineage of myeloid cells independent of Myb and hematopoietic stem cells. *Science* (2012) 336:86–90. doi:10.1126/science.1219179
10. Yona S, Kim KW, Wolf Y, Mildner A, Varol D, Breker M, et al. Fate mapping reveals origins and dynamics of monocytes and tissue macrophages under homeostasis. *Immunity* (2013) 38:79–91. doi:10.1016/j.immuni.2012.12.001
11. Epelman S, Lavine KJ, Beaudin AE, Sojka DK, Carrero JA, Calderon B, et al. Embryonic and adult-derived resident cardiac macrophages are maintained through distinct mechanisms at steady state and during inflammation. *Immunity* (2014) 40:91–104. doi:10.1016/j.immuni.2013.11.019
12. Guilliams M, De Kleer I, Henri S, Post S, Vanhoutte L, De Prijck S, et al. Alveolar macrophages develop from fetal monocytes that differentiate into long-lived cells in the first week of life via GM-CSF. *J Exp Med* (2013) 210: 1977–92. doi:10.1084/jem.20131199
13. Hoeffel G, Chen J, Lavin Y, Low D, Almeida FF, See P, et al. C-Myb(+) erythro-myeloid progenitor-derived fetal monocytes give rise to adult tissue-resident macrophages. *Immunity* (2015) 42:665–78. doi:10.1016/j.immuni.2015.03.011
14. Hashimoto D, Chow A, Noizat C, Teo P, Beasley MB, Leboeuf M, et al. Tissue-resident macrophages self-maintain locally throughout adult life with minimal contribution from circulating monocytes. *Immunity* (2013) 38:792–804. doi:10.1016/j.immuni.2013.04.004
15. Bain CC, Bravo-Blas A, Scott CL, Gomez Perdiguero E, Geissmann F, Henri S, et al. Constant replenishment from circulating monocytes maintains the macrophage pool in the intestine of adult mice. *Nat Immunol* (2014) 15: 929–37. doi:10.1038/ni.2967
16. Gautier EL, Shay T, Miller J, Greter M, Jakubzick C, Ivanov S, et al. Gene-expression profiles and transcriptional regulatory pathways that underlie the identity and diversity of mouse tissue macrophages. *Nat Immunol* (2012) 13:1118–28. doi:10.1038/ni.2419
17. Okabe Y, Medzhitov R. Tissue-specific signals control reversible program of localization and functional polarization of macrophages. *Cell* (2014) 157:832–44. doi:10.1016/j.cell.2014.04.016
18. Haldar M, Kohyama M, So Alex Y-L, Kc W, Wu X, Briseño Carlos G, et al. Heme-mediated SPI-C induction promotes monocyte differentiation into iron-recycling macrophages. *Cell* (2014) 156:1223–34. doi:10.1016/j.cell.2014.01.069
19. Butovsky O, Jedrychowski MP, Moore CS, Cialic R, Lanser AJ, Gabriely G, et al. Identification of a unique TGF-beta-dependent molecular and functional signature in microglia. *Nat Neurosci* (2014) 17:131–43. doi:10.1038/nn.3599

20. van de Laar L, Saelens W, De Prijck S, Martens L, Scott CL, Van Isterdael G, et al. Yolk sac macrophages, fetal liver, and adult monocytes can colonize an empty niche and develop into functional tissue-resident macrophages. *Immunity* (2016) 44:755–68. doi:10.1016/j.immuni.2016.02.017
21. Buchanan KL, Murphy JW. What makes *Cryptococcus neoformans* a pathogen? *Emerg Infect Dis* (1998) 4:71–83. doi:10.3201/eid0401.980109
22. Hasenberg M, Behnsen J, Krappmann S, Brakhage A, Gunzer M. Phagocyte responses towards *Aspergillus fumigatus*. *Int J Med Microbiol* (2011) 301: 436–44. doi:10.1016/j.ijmm.2011.04.012
23. Schaffner A, Douglas H, Braude A. Selective protection against conidia by mononuclear and against mycelia by polymorphonuclear phagocytes in resistance to *Aspergillus*. Observations on these two lines of defense in vivo and in vitro with human and mouse phagocytes. *J Clin Invest* (1982) 69:617–31. doi:10.1172/JCI110489
24. Shoham S, Levitz SM. The immune response to fungal infections. *Br J Haematol* (2005) 129:569–82. doi:10.1111/j.1365-2141.2005.05397.x
25. Kanayama M, Inoue M, Danzaki K, Hammer G, He YW, Shinohara ML. Autophagy enhances NFkappaB activity in specific tissue macrophages by sequestering A20 to boost antifungal immunity. *Nat Commun* (2015) 6:5779. doi:10.1038/ncomms6779
26. Zhang L, Wang CC. Inflammatory response of macrophages in infection. *Hepatobiliary Pancreat Dis Int* (2014) 13:138–52. doi:10.1016/S1499-3872(14)60024-2
27. Mildner A, Jung S. Development and function of dendritic cell subsets. *Immunity* (2014) 40:642–56. doi:10.1016/j.immuni.2014.04.016
28. Hohl TM, Rivera A, Lipuma L, Gallegos A, Shi C, Mack M, et al. Inflammatory monocytes facilitate adaptive CD4 T cell responses during respiratory fungal infection. *Cell Host Microbe* (2009) 6:470–81. doi:10.1016/j.chom.2009.10.007
29. Lionakis MS, Swamydas M, Fischer BG, Plantinga TS, Johnson MD, Jaeger M, et al. CX3CR1-dependent renal macrophage survival promotes *Candida* control and host survival. *J Clin Invest* (2013) 123:5035–51. doi:10.1172/JCI71307
30. Ngo LY, Kasahara S, Kumasaka DK, Knoblaugh SE, Jhingran A, Hohl TM. Inflammatory monocytes mediate early and organ-specific innate defense during systemic candidiasis. *J Infect Dis* (2014) 209:109–19. doi:10.1093/infdis/jit413
31. Serbina NV, Jia T, Hohl TM, Pamer EG. Monocyte-mediated defense against microbial pathogens. *Annu Rev Immunol* (2008) 26:421–52. doi:10.1146/annurev.immunol.26.021607.090326
32. Shi C, Pamer EG. Monocyte recruitment during infection and inflammation. *Nat Rev Immunol* (2011) 11:762–74. doi:10.1038/nri3070
33. Griffin FM Jr. Roles of macrophage Fc and C3b receptors in phagocytosis of immunologically coated *Cryptococcus neoformans*. *Proc Natl Acad Sci U S A* (1981) 78:3853–7. doi:10.1073/pnas.78.6.3853
34. Zaragoza O, Taborda CP, Casadevall A. The efficacy of complement-mediated phagocytosis of *Cryptococcus neoformans* is dependent on the location of C3 in the polysaccharide capsule and involves both direct and indirect C3-mediated interactions. *Eur J Immunol* (2003) 33:1957–67. doi:10.1002/eji.200323848
35. McQuiston T, Luberto C, Del Poeta M. Role of sphingosine-1-phosphate (S1P) and S1P receptor 2 in the phagocytosis of *Cryptococcus neoformans* by alveolar macrophages. *Microbiology* (2011) 157:1416–27. doi:10.1099/mic.0.045989-0
36. Guillot L, Carroll SF, Homer R, Qureshi ST. Enhanced innate immune responsiveness to pulmonary *Cryptococcus neoformans* infection is associated with resistance to progressive infection. *Infect Immun* (2008) 76:4745–56. doi:10.1128/IAI.00341-08
37. Ibrahim-Granet O, Philippe B, Boleti H, Boisvieux-Ulrich E, Grenet D, Stern M, et al. Phagocytosis and intracellular fate of *Aspergillus fumigatus* conidia in alveolar macrophages. *Infect Immun* (2003) 71:891–903. doi:10.1128/IAI.71.2.891-903.2003
38. Dubourdeau M, Athman R, Balloy V, Huerre M, Chignard M, Philpott DJ, et al. *Aspergillus fumigatus* induces innate immune responses in alveolar macrophages through the MAPK pathway independently of TLR2 and TLR4. *J Immunol* (2006) 177:3994–4001. doi:10.4049/jimmunol.177.6.3994
39. Philippe B, Ibrahim-Granet O, Prevost MC, Gougerot-Pocidalo MA, Sanchez Perez M, Van der Meeren A, et al. Killing of *Aspergillus fumigatus* by alveolar macrophages is mediated by reactive oxidant intermediates. *Infect Immun* (2003) 71:3034–42. doi:10.1128/IAI.71.6.3034-3042.2003
40. Madan T, Eggleton P, Kishore U, Strong P, Aggrawal SS, Sarma PU, et al. Binding of pulmonary surfactant proteins A and D to *Aspergillus fumigatus* conidia enhances phagocytosis and killing by human neutrophils and alveolar macrophages. *Infect Immun* (1997) 65:3171–9.
41. Hohl TM, Van Epps HL, Rivera A, Morgan LA, Chen PL, Feldmesser M, et al. *Aspergillus fumigatus* triggers inflammatory responses by stage-specific beta-glucan display. *PLoS Pathog* (2005) 1:e30. doi:10.1371/journal.ppat.0010030
42. Zhang HJ, Qu JM, Shao CZ, Zhang J, He LX, Yuan ZH. *Aspergillus fumigatus* conidia upregulates NOD2 protein expression both in vitro and in vivo. *Acta Pharmacol Sin* (2008) 29:1202–8. doi:10.1111/j.1745-7254.2008.00860.x
43. Shah VB, Huang Y, Keshwara R, Ozment-Skelton T, Williams DL, Keshvara L. Beta-glucan activates microglia without inducing cytokine production in dectin-1-dependent manner. *J Immunol* (2008) 180:2777–85. doi:10.4049/jimmunol.180.5.2777
44. Maneu V, Yanez A, Murciano C, Molina A, Gil ML, Gozalbo D. Dectin-1 mediates in vitro phagocytosis of *Candida albicans* yeast cells by retinal microglia. *FEMS Immunol Med Microbiol* (2011) 63:148–50. doi:10.1111/j.1574-695X.2011.00829.x
45. Shah VB, Ozment-Skelton TR, Williams DL, Keshvara L. Vav1 and PI3K are required for phagocytosis of beta-glucan and subsequent superoxide generation by microglia. *Mol Immunol* (2009) 46:1845–53. doi:10.1016/j.molimm.2009.01.014
46. Maneu V, Noailles A, Megias J, Gomez-Vicente V, Carpena N, Gil ML, et al. Retinal microglia are activated by systemic fungal infection. *Invest Ophthalmol Vis Sci* (2014) 55:3578–85. doi:10.1167/iovs.14-14051
47. Goldman D, Song X, Kitai R, Casadevall A, Zhao ML, Lee SC. *Cryptococcus neoformans* induces macrophage inflammatory protein 1alpha (MIP-1alpha) and MIP-1beta in human microglia: role of specific antibody and soluble capsular polysaccharide. *Infect Immun* (2001) 69:1808–15. doi:10.1128/IAI.69.3.1808-1815.2001
48. Blasi E, Barluzzi R, Mazzolla R, Tancini B, Saleppico S, Puliti M, et al. Role of nitric oxide and melanogenesis in the accomplishment of anticryptococcal activity by the BV-2 microglial cell line. *J Neuroimmunol* (1995) 58:111–6. doi:10.1016/0165-5728(95)00016-U
49. Rambach G, Hagleitner M, Mohsenipour I, Lass-Florl C, Maier H, Wurzner R, et al. Antifungal activity of the local complement system in cerebral aspergillosis. *Microbes Infect* (2005) 7:1285–95. doi:10.1016/j.micinf.2005.04.014
50. Rambach G, Dum D, Mohsenipour I, Hagleitner M, Wurzner R, Lass-Florl C, et al. Secretion of a fungal protease represents a complement evasion mechanism in cerebral aspergillosis. *Mol Immunol* (2010) 47:1438–49. doi:10.1016/j.molimm.2010.02.010
51. Kopf M, Schneider C, Nobs SP. The development and function of lung-resident macrophages and dendritic cells. *Nat Immunol* (2015) 16:36–44. doi:10.1038/ni.3052
52. Lohmann-Matthes ML, Steinmuller C, Franke-Ullmann G. Pulmonary macrophages. *Eur Respir J* (1994) 7:1678–89.
53. Denning DW. Invasive aspergillosis. *Clin Infect Dis* (1998) 26:781–803; quiz 804–5. doi:10.1086/513943
54. Hohl TM, Feldmesser M. *Aspergillus fumigatus*: principles of pathogenesis and host defense. *Eukaryot Cell* (2007) 6:1953–63. doi:10.1128/EC.00274-07
55. Latge JP. *Aspergillus fumigatus* and aspergillosis. *Clin Microbiol Rev* (1999) 12:310–50.
56. Chelen CJ, Fang Y, Freeman GJ, Secrist H, Marshall JD, Hwang PT, et al. Human alveolar macrophages present antigen ineffectively due to defective expression of B7 costimulatory cell surface molecules. *J Clin Invest* (1995) 95:1415–21. doi:10.1172/JCI117796
57. Fels AO, Cohn ZA. The alveolar macrophage. *J Appl Physiol (1985)* (1986) 60:353–69.
58. Luo Y, Cook E, Fries BC, Casadevall A. Phagocytic efficacy of macrophage-like cells as a function of cell cycle and Fcgamma receptors (FcgammaR) and complement receptor (CR)3 expression. *Clin Exp Immunol* (2006) 145:380–7. doi:10.1111/j.1365-2249.2006.03132.x
59. Luo Y, Tucker SC, Casadevall A. Fc- and complement-receptor activation stimulates cell cycle progression of macrophage cells from G1 to S. *J Immunol* (2005) 174:7226–33. doi:10.4049/jimmunol.174.11.7226

60. Marr KA, Koudadoust M, Black M, Balajee SA. Early events in macrophage killing of *Aspergillus fumigatus* conidia: new flow cytometric viability assay. *Clin Diagn Lab Immunol* (2001) 8:1240–7. doi:10.1128/CDLI.8.6.1240-1247.2001
61. Braem SG, Rooijakkers SH, van Kessel KP, de Cock H, Wosten HA, van Strijp JA, et al. Effective neutrophil phagocytosis of *Aspergillus fumigatus* is mediated by classical pathway complement activation. *J Innate Immun* (2015) 7:364–74. doi:10.1159/000369493
62. Jaillon S, Peri G, Delneste Y, Fremaux I, Doni A, Moalli F, et al. The humoral pattern recognition receptor PTX3 is stored in neutrophil granules and localizes in extracellular traps. *J Exp Med* (2007) 204:793–804. doi:10.1084/jem.20061301
63. Bhatia S, Fei M, Yarlagadda M, Qi Z, Akira S, Saijo S, et al. Rapid host defense against *Aspergillus fumigatus* involves alveolar macrophages with a predominance of alternatively activated phenotype. *PLoS One* (2011) 6:e15943. doi:10.1371/journal.pone.0015943
64. Dague E, Alsteens D, Latge JP, Dufrene YF. High-resolution cell surface dynamics of germinating *Aspergillus fumigatus* conidia. *Biophys J* (2008) 94:656–60. doi:10.1529/biophysj.107.116491
65. Gersuk GM, Underhill DM, Zhu L, Marr KA. Dectin-1 and TLRs permit macrophages to distinguish between different *Aspergillus fumigatus* cellular states. *J Immunol* (2006) 176:3717–24. doi:10.4049/jimmunol.176.6.3717
66. Braedel S, Radsak M, Einsele H, Latge JP, Michan A, Loeffler J, et al. *Aspergillus fumigatus* antigens activate innate immune cells via toll-like receptors 2 and 4. *Br J Haematol* (2004) 125:392–9. doi:10.1111/j.1365-2141.2004.04922.x
67. Mehrad B, Wiekowski M, Morrison BE, Chen SC, Coronel EC, Manfra DJ, et al. Transient lung-specific expression of the chemokine KC improves outcome in invasive aspergillosis. *Am J Respir Crit Care Med* (2002) 166:1263–8. doi:10.1164/rccm.200204-367OC
68. Jhingran A, Kasahara S, Shepardson KM, Junecko BA, Heung LJ, Kumasaka DK, et al. Compartment-specific and sequential role of MyD88 and CARD9 in chemokine induction and innate defense during respiratory fungal infection. *PLoS Pathog* (2015) 11:e1004589. doi:10.1371/journal.ppat.1004589
69. Mircescu MM, Lipuma L, van Rooijen N, Pamer EG, Hohl TM. Essential role for neutrophils but not alveolar macrophages at early time points following *Aspergillus fumigatus* infection. *J Infect Dis* (2009) 200:647–56. doi:10.1086/600380
70. McQuiston TJ, Williamson PR. Paradoxical roles of alveolar macrophages in the host response to *Cryptococcus neoformans*. *J Infect Chemother* (2012) 18:1–9. doi:10.1007/s10156-011-0306-2
71. Osterholzer JJ, Milam JE, Chen GH, Toews GB, Huffnagle GB, Olszewski MA. Role of dendritic cells and alveolar macrophages in regulating early host defense against pulmonary infection with *Cryptococcus neoformans*. *Infect Immun* (2009) 77:3749–58. doi:10.1128/IAI.00454-09
72. Goodman JS, Kaufman L, Koenig MG. Diagnosis of cryptococcal meningitis. Value of immunologic detection of cryptococcal antigen. *N Engl J Med* (1971) 285:434–6. doi:10.1056/NEJM197108192850804
73. Gottfredsson M, Perfect JR. Fungal meningitis. *Semin Neurol* (2000) 20:307–22. doi:10.1055/s-2000-9394
74. Kleinschmidt-DeMasters BK. Central nervous system aspergillosis: a 20-year retrospective series. *Hum Pathol* (2002) 33:116–24. doi:10.1053/hupa.2002.30186
75. Kielian T. Toll-like receptors in central nervous system glial inflammation and homeostasis. *J Neurosci Res* (2006) 83:711–30. doi:10.1002/jnr.20767
76. Larsen PH, Holm TH, Owens T. Toll-like receptors in brain development and homeostasis. *Sci STKE* (2007) 2007:e47. doi:10.1126/stke.4022007pe47
77. Aguirre K, Miller S. MHC class II-positive perivascular microglial cells mediate resistance to *Cryptococcus neoformans* brain infection. *Glia* (2002) 39:184–8. doi:10.1002/glia.10093
78. Hill JO, Aguirre KM. CD4+ T cell-dependent acquired state of immunity that protects the brain against *Cryptococcus neoformans*. *J Immunol* (1994) 152:2344–50.
79. Zhou Q, Gault RA, Kozel TR, Murphy WJ. Protection from direct cerebral *Cryptococcus* infection by interferon-gamma-dependent activation of microglial cells. *J Immunol* (2007) 178:5753–61. doi:10.4049/jimmunol.178.9.5753
80. Kaissling B, Hegyi I, Loffing J, Le Hir M. Morphology of interstitial cells in the healthy kidney. *Anat Embryol (Berl)* (1996) 193:303–18. doi:10.1007/BF00186688
81. Hume DA, Gordon S. Mononuclear phagocyte system of the mouse defined by immunohistochemical localization of antigen F4/80. Identification of resident macrophages in renal medullary and cortical interstitium and the juxtaglomerular complex. *J Exp Med* (1983) 157:1704–9. doi:10.1084/jem.157.5.1704
82. Hoeffel G, Chen J, Lavin Y, Low D, Almeida Francisca F, See P, et al. C-Myb+ erythro-myeloid progenitor-derived fetal monocytes give rise to adult tissue-resident macrophages. *Immunity* (2015) 42:665–78. doi:10.1016/j.immuni.2015.03.011
83. Cao Q, Wang Y, Wang XM, Lu J, Lee VW, Ye Q, et al. Renal F4/80+ CD11c+ mononuclear phagocytes display phenotypic and functional characteristics of macrophages in health and in adriamycin nephropathy. *J Am Soc Nephrol* (2015) 26:349–63. doi:10.1681/ASN.2013121336
84. Ginhoux F, Jung S. Monocytes and macrophages: developmental pathways and tissue homeostasis. *Nat Rev Immunol* (2014) 14:392–404. doi:10.1038/nri3671
85. Kim MG, Boo CS, Ko YS, Lee HY, Cho WY, Kim HK, et al. Depletion of kidney CD11c+ F4/80+ cells impairs the recovery process in ischaemia/reperfusion-induced acute kidney injury. *Nephrol Dial Transplant* (2010) 25:2908–21. doi:10.1093/ndt/gfq183
86. Hochheiser K, Heuser C, Krause TA, Teteris S, Ilias A, Weisheit C, et al. Exclusive CX3CR1 dependence of kidney DCs impacts glomerulonephritis progression. *J Clin Invest* (2013) 123:4242–54. doi:10.1172/JCI70143
87. Lionakis MS, Lim JK, Lee CC, Murphy PM. Organ-specific innate immune responses in a mouse model of invasive candidiasis. *J Innate Immun* (2011) 3:180–99. doi:10.1159/000321157
88. Spellberg B, Ibrahim AS, Edwards JE Jr, Filler SG. Mice with disseminated candidiasis die of progressive sepsis. *J Infect Dis* (2005) 192:336–43. doi:10.1086/430952
89. Lionakis MS. New insights into innate immune control of systemic candidiasis. *Med Mycol* (2014) 52:555–64. doi:10.1093/mmy/myu029
90. Hebecker B, Vlaic S, Conrad T, Bauer M, Brunke S, Kapitan M, et al. Dual-species transcriptional profiling during systemic candidiasis reveals organ-specific host-pathogen interactions. *Sci Rep* (2016) 6:36055. doi:10.1038/srep36055
91. Lionakis MS, Netea MG. *Candida* and host determinants of susceptibility to invasive candidiasis. *PLoS Pathog* (2013) 9:e1003079. doi:10.1371/journal.ppat.1003079
92. Hickey WF, Kimura H. Perivascular microglial cells of the CNS are bone marrow-derived and present antigen in vivo. *Science* (1988) 239:290–2. doi:10.1126/science.3276004
93. Keren-Shaul H, Spinrad A, Weiner A, Matcovitch-Natan O, Dvir-Szternfeld R, Ulland TK, et al. A unique microglia type associated with restricting development of Alzheimer's disease. *Cell* (2017) 169:1276–90.e17. doi:10.1016/j.cell.2017.05.018

Conflict of Interest Statement: The authors declare that the research was conducted in the absence of any commercial or financial relationships that could be construed as a potential conflict of interest.

Copyright © 2017 Xu and Shinohara. This is an open-access article distributed under the terms of the Creative Commons Attribution License (CC BY). The use, distribution or reproduction in other forums is permitted, provided the original author(s) or licensor are credited and that the original publication in this journal is cited, in accordance with accepted academic practice. No use, distribution or reproduction is permitted which does not comply with these terms.

frontiers in Immunology

ORIGINAL RESEARCH
published: 18 October 2017
doi: 10.3389/fimmu.2017.01369

Interaction of THP-1 Monocytes with Conidia and Hyphae of Different *Curvularia* Strains

*Eszter Judit Tóth[1,2], Éva Boros[3], Alexandra Hoffmann[2], Csilla Szebenyi[1,2], Mónika Homa[1,2], Gábor Nagy[1], Csaba Vágvölgyi[2], István Nagy[3] and Tamás Papp[1,2]**

[1] MTA-SZTE Fungal Pathogenicity Mechanisms Research Group, Hungarian Academy of Sciences, University of Szeged, Szeged, Hungary, [2] Faculty of Science and Informatics, Department of Microbiology, University of Szeged, Szeged, Hungary, [3] Hungarian Academy of Sciences, Biological Research Centre, Szeged, Hungary

Interaction of the human monocytic cell line, THP-1 with clinical isolates of three *Curvularia* species were examined. Members of this filamentous fungal genus can cause deep mycoses emerging in both immunocompromised and immunocompetent patients. It was found that monocytes reacted only to the hyphal form of *Curvularia lunata.* Cells attached to the germ tubes and hyphae and production of elevated levels of interleukin (IL)-8 and IL-10 and a low level of TNF-α were measured. At the same time, monocytes failed to produce IL-6. This monocytic response, especially with the induction of the anti-inflammatory IL-10, correlates well to the observation that *C. lunata* frequently cause chronic infections even in immunocompetent persons. Despite the attachment to the hyphae, monocytes could not reduce the viability of the fungus and the significant decrease in the relative transcript level of HLA-DRA assumes the lack of antigen presentation of the fungus by this cell type. *C. spicifera* and *C. hawaiiensis* failed to induce the gathering of the cells or the production of any analyzed cytokines. Monocytes did not recognize conidia of *Curvularia* species, even when melanin was lacking in their cell wall.

Keywords: *Curvularia*, monocyte, invasive mycosis, melanin, quantitative reverse transcription PCR, ELISA, interleukin-10

OPEN ACCESS

Edited by:
Ilse Denise Jacobsen, Leibniz-Institut für Naturstoff-Forschung und Infektionsbiologie—Hans Knöll Institut, Germany

Reviewed by:
Roland Lang, Universitätsklinikum Erlangen, Germany
Mario M. D'Elios, University of Florence, Italy

****Correspondence:***
Tamás Papp
pappt@bio.u-szeged.hu

Specialty section:
This article was submitted to Microbial Immunology, a section of the journal Frontiers in Immunology

Received: *21 June 2017*
Accepted: *05 October 2017*
Published: *18 October 2017*

Citation:
Tóth EJ, Boros É, Hoffmann A, Szebenyi C, Homa M, Nagy G, Vágvölgyi C, Nagy I and Papp T (2017) Interaction of THP-1 Monocytes with Conidia and Hyphae of Different Curvularia Strains. Front. Immunol. 8:1369. doi: 10.3389/fimmu.2017.01369

INTRODUCTION

Members of the ascomycete genus, *Curvularia* includes primarily saprotrophic and plant pathogenic filamentous fungi. Some of them, such as *Curvularia lunata*, *C. hawaiiensis*, and *C. spicifera*, however, are also considered as emerging agents of local and invasive human phaeohyphomycoses (1), i.e., infections caused by melanin producing molds. *Curvularia* species are frequently reported as agents of allergic fungal sinusitis and bronchopulmonary disease (2–4) but they can also be associated with mycotic keratitis (5, 6), cutaneous and subcutaneous mycoses (7, 8), and infections of the central nervous system (2, 9). Deep and disseminated *Curvularia* infections have been described in both immunocompromised and immunocompetent patients (4, 10–13). Increasing prevalence of these infections has been reported during recent years (4, 14, 15). Despite that *Curvularia* species are among the most common dematiaceous fungi isolated from clinical samples (16), experimental data concerning the background of their pathogenicity and interactions with the host are very limited (2).

Human monocytes are circulating cells of innate immunity that can further differentiate into macrophages or dendritic cells and capable of phagocytoses, cytokine production, and antigen

presentation. They play a pivotal role in the host response to fungal infections and their activity against the conidia, germlings, and hyphae of *Aspergillus fumigatus* was proven and analyzed previously (17, 18).

THP-1 is a human monocytic cell line isolated from a patient with acute monocytic leukemia. This cell line can be differentiated into macrophages and are widely used to study monocyte and macrophage functions and in immune modulation studies (19). For example, THP-1 monocytes treated with LPS, showed altered expression of several inflammation related genes, such as *IL1B*, *IL6*, *IL8*, *IL10*, and *TNFA* (19, 20). Several studies have compared the responses of THP-1 monocytes and human peripheral blood mononuclear cell derived monocytes to a variety of stimuli and the two cell types showed relatively similar response patterns in most cases (19). THP-1 monocytes and macrophages has also been used successfully as *in vitro* models to examine host–pathogen interactions for various fungal agents, such as *A. fumigatus* (18, 21–23), *Candida albicans* (24), *Candida glabrata* (25), and *Cryptococcus neoformans* (26).

In this study, interactions of THP-1 monocytes with conidia and hyphae of three fungal strains representing *C. hawaiiensis*, *C. lunata,* and *C. spicifera* were analyzed to get a first insight into the host response to *Curvularia* species. For comparison, an *A. fumigatus* strain from a clinical origin was also involved in the study.

MATERIALS AND METHODS

Fungal Strains, Culture Conditions, and Inoculum Preparation

Curvularia lunata SZMC 23759 and *C. spicifera* SZMC 13064, *A. fumigatus* SZMC 23245 isolated from human eye infections and *C. hawaiiensis* CBS 103.97 isolated from human sinusitis with ophthalmic and cerebral involvement were used in the study. Strains were grown on potato dextrose agar (PDA; VWR International) at room temperature. To block melanin synthesis, PDA was supplemented with 20 µg/ml tricyclazole (Sigma-Aldrich) and 1% of agar (Merck). For the interaction studies, conidial suspensions (10^5 conidia/ml) were prepared in phosphate buffer saline (PBS; 137 mM NaCl, 2.7 mM KCl, 10 mM Na_2HPO_4, 2 mM KH_2PO_4, pH 7.4) by washing the conidia from 14 and 7 days old fungal cultures in case of the *Curvularia* strains and the *Aspergillus* strain, respectively. To get rid of hyphal debris, spore suspensions were filtered through a filter paper with a pore size of 45 µm (Millipore). Heat inactivation of the conidia was performed at 125°C for 25 min.

Culturing and Infection of the THP-1 Cells

THP-1 cells were maintained in RPMI 1640 medium (Gibco) supplemented with 10% (v/v) heat inactivated fetal bovine serum (FBS; Gibco) and 1% (v/v) antibiotic/antimycotic solution containing 10,000 U/ml of penicillin, 10,000 µg/ml of streptomycin and 25 µg/ml of Amphotericin B (Gibco) at 37°C in a humidified incubator with 5% CO_2. For interaction studies, THP-1 cells (10^5 cells/ml) were placed on 6-well or 12-well cell culture plates with flat bottoms (Sarstedt) in 3 or 1 ml RPMI 1640 medium supplemented with 10% heat inactivated FBS and without antibiotic the day before infection, respectively.

Number of the *Curvularia* conidia and cells were set to maintain an effector (THP-1) to target (conidia) (E:T) ratio of 20:1, while for *A. fumigatus* E:T ratio was 20:1 or 1:2. Because of the small size of the conidia of *A. fumigatus*, an E:T ratio of 1:2 proved to be optimal for this fungus in agreement with the literature data (18). For the *Curvularia* strains, we tested various E:T ratios and that of 20:1 proved to be applicable, mainly because of the large size and the relatively short germination time (approx. 1.5 h) of their conidia. Cells were incubated with or without the fungi at 37°C in a humidified incubator with 5% CO_2 for 3, 9, or 24 h. When monocytes were treated with lipopolysaccharide (LPS, *Escherichia coli* Q26:B6; Sigma-Aldrich), 1 µg/ml final concentration of LPS was used. Microscopic examination of the interactions was performed using a Leica DMI4000 B inverse microscope (Leica Microsystems). All experiments were performed in two technical and three biological replicates.

Phagocytosis Assay

THP-1 cells (10^5 cells/ml) were seated on a 12-well plate one day before the experiment. Four hours before the assay, cells were stained with CellMask Deep Red Plasma Membrane stain (Thermo Scientific) in a 0.5-fold concentration for 15 min and washed twice with PBS. Conidia were stained with AlexaFluor 488 carboxylic acid, succinimidyl ester (Thermo Scientific) for 15 min and washed twice with PBS at 4°C to prevent germination. The E:T ratio was 1:2 or 20:1. For analysis, collected samples were centrifuged with 1,000 rpm for 15 min and resuspended in 200 µl PBS supplemented with 0.05% Tween-20 (Reanal). Interaction and phagocytosis were measured after 1 or 3 h using a FlowSight Imaging Flow Cytometer (Amnis) and evaluated with the IDEAS Software (Amnis).

Real-time Quantitative Reverse Transcription PCR (qRT-PCR) Analysis

Total RNA was extracted from the THP-1 cells using the RNeasy Mini kit (Qiagen) according to the instructions of the manufacturer. The final elution volume was 20 µl. cDNA was synthesized using the SuperScript VILO Master Mix (Invitrogen) following the protocol of the manufacturer. qRT-PCR was carried out using StepOne Plus Real-Time PCR System (Applied Biosystems). Reactions were performed by either the TaqMan Gene expression Master Mix (Applied Biosystems) or the Sybr Select Master Mix (Applied Biosystems) using the probes and primers listed in **Tables 1** and **2**, respectively, according to the manufacturer's

TABLE 1 | TaqMan probe details (Applied Biosystems) used in the qRT-PCR analyses.

Target gene	TaqMan assay ID
18S rDNA	Hs99999901_s1
IL10	Hs00961522_m1
IL6	Hs00174131_m1
IL8	Hs00174103_m1
TNFA	Hs00174128_m1
NLRC3	Hs01054716_m1

TABLE 2 | Primer pairs used in the qRT-PCR analyses.

Target gene	Forward (5′–3′) primer	Reverse (5′–3′) primer	Product length (bp)
CCR1	TCTACGCCTTCGTTGGTGAG	TTTAACCAGGTGCACAGCCA	80
CCR2	TACCAACGAGAGCGGTGAAG	GCATGTTGCCCACAAAACCA	149
CCR5	TTACTGTCCCCTTCTGGGCT	AAGCAAACACAGCATGGACG	168
CXCR2	TTTCGCCATGGACTCCTCAA	GTAGTGGAAGTGTGCCCTGA	116
IL1B	AGCTGGAGAGTGTAGATCCCAA	GGGAACTGGGCAGACTCAAA	112
ITGAL	GCAAGGACATACCGCCCAT	TACTCAGGCTCAGCTCCACA	186
ITGAM	AGTCTGCCTCCATGTCCAGAA	CTGCGTGTGCTGTTCTTTGTC	144
ITGAX	AGTCTGCCTCCATGTCCAGAA	CTGCGTGTGCTGTTCTTTGTC	103
HLADRA	CCGATCACCAATGTACCTCCA	CGAAGCCACGTGACATTGAC	128

protocols. Relative transcript levels were calculated with the $\Delta\Delta C_T$ ($2^{-\Delta\Delta Ct}$) method (27) using a fragment of the 18S rRNA coding gene for normalization. All measurements were performed in two technical and three biological replicates.

Cytokine Assays

To confirm the cytokine concentrations in the culture supernatants, DuoSet ELISA Kits (R&D Systems) were used for tumor necrosis factor alpha (TNF-α), interleukin (IL)-6, and IL-8 according to the instructions of the manufacturer. To measure the IL-10 level, the Human IL-10 ELISA kit (Immunotools) was used. Cytokine titers were calculated by reference to standard curves generated by the four parameters logistic curve-fit method.

Viability Test

To measure the hyphal damage after the incubation with monocytes, a colorimetric assay using 3-(4,5-dimethylthiazol-2-yl)-2,5-diphenyltetrazolium bromide (MTT; Sigma-Aldrich) was performed (28) on 12-well culture plates. After incubation for 3, 6, or 24 h, monocytes were lysed with 0.5% sodium deoxycholate (Sigma-Aldrich) and the wells were washed three times with PBS. Then, 1 ml RPMI 1640 supplemented with 1% MTT was added to the wells and the plates were incubated at 37°C, under 5% CO_2 concentration for 3 h. After removing the supernatant, wells were washed two times with PBS and stored at −20°C overnight. Before detection, 1 ml acidic isopropanol (95% isopropanol and 5% 1 N HCl) was added into the wells and the plates were incubated until the blue color dissolved from hyphae. Absorbance of the supernatant was measured at the wavelength of 550 nm using a spectrophotometer (Spectrostar Nano, BMG Labtech). Viability of the hyphae was calculated using the following formula, where OD_{550} sample was the absorbance measured for the hyphae incubated with monocytes and OD_{550} control was the absorbance measured for the hyphae incubated without monocytes: $\text{Viability} = \left(\frac{OD550\ \text{sample}}{OD550\ \text{control}}\right) \times 100.$

Statistical Analysis

All measurements were performed in at least two technical and three biological replicates. Significance was calculated with paired *t*-test using Microsoft Excel of the Microsoft Office package. *P* values less than 0.05 were considered statistically significant.

RESULTS

THP-1 Cells Do Not Phagocytose *Curvularia* spp. Conidia and Hyphae

THP-1 cells were confronted with *C. lunata*, *C. hawaiiensis*, and *C. spicifera* by co-incubating heat inactivated or living conidia with the monocytes. Interactions were analyzed after 3 and 24 h of confrontation. In case of the living conidia, germination was already in progress and germ tubes were developed at 3 h postinoculation (**Figures 1A,B**) while branching hyphae were present at 24 h postinoculation (**Figures 1A,B**). Microscopic analysis revealed that the monocytes were not able to phagocytose the conidia of any tested strains; moreover, they did not attract to them at all (**Figures 1A,B**). The absence of the monocytic response did not depend on the melanin content as it also missed in case of those conidia of *C. lunata* where the melanin biosynthesis had been previously blocked. At the same time, THP-1 cells aggregated around and attached to the hyphae of *C. lunata* (**Figures 1C,D**). However, monocytes did not block the germination of the conidia and MTT assay did not detect hyphal damage in the tested *Curvularia* strains (**Figure 2**). For comparison, MTT assay was also performed with *A. fumigatus* under the same co-incubation conditions. In this case, viability of the hyphae decreased to 12.9% after 24 h of interaction with the THP-1 cells.

For quantification and a more detailed analysis, phagocytosis was also examined by imaging flow cytometry in case of *C. lunata* and *A. fumigatus* (**Figure 3**). THP-1 cells actively phagocytosed the living conidia of *A. fumigatus* already at 1 h after their confrontation; the mean ratio of the phagocyting cells counted from three biological replicates was found to be 2.4 (±0.4)% and 20.7 (±2.5)% at E:T ratios of 20:1 (**Figure 3C**) and 1:2 (**Figure 3B**), respectively. At the same time, the number of interacting cells and conidia proved to be insignificant in the case of *C. lunata*. Only 0.12 (±0.1)% of the monocytes were attached to or ingesting the conidia at 1 h after the start of the interaction (the E:T ratio was 20:1). Similar values were measured for heat inactivated and melanin blocked conidia, 0.35 (±0.2)% and 0.69 (±0.1)% after 1 h of interaction, respectively. Image analysis revealed that majority of these small numbers of interactions detected by flow cytometry was only attachment of the monocytes to the conidia instead of real phagocytosis (**Figure 3A**).

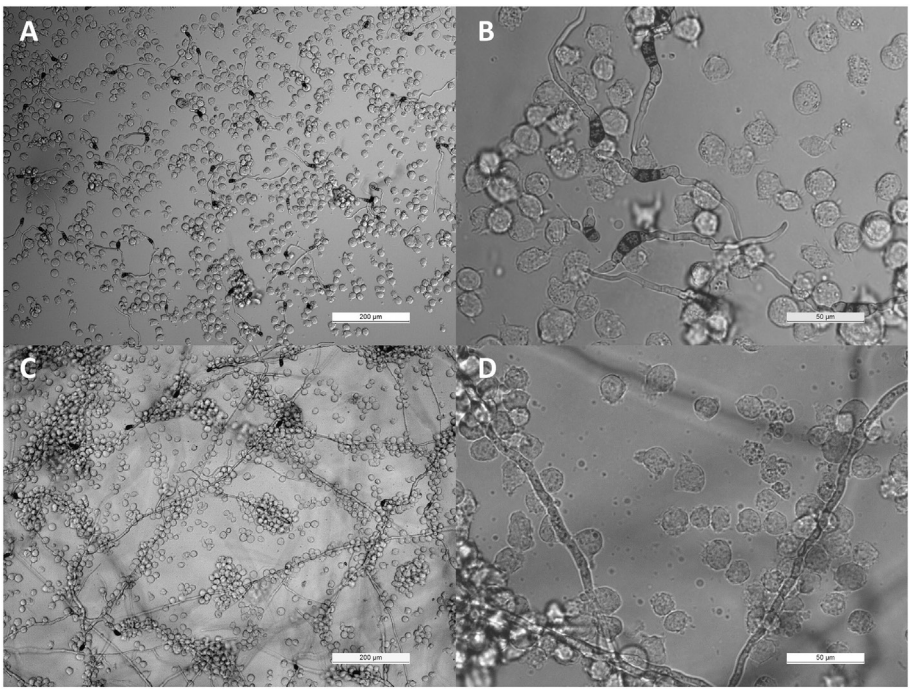

FIGURE 1 | Interaction of THP-1 monocytes with *Curvularia lunata*. Light micrographs were taken at 3 [panels **(A,B)**] and 24 h [panels **(C,D)**] postinoculation; the E:T ratio was 20:1.

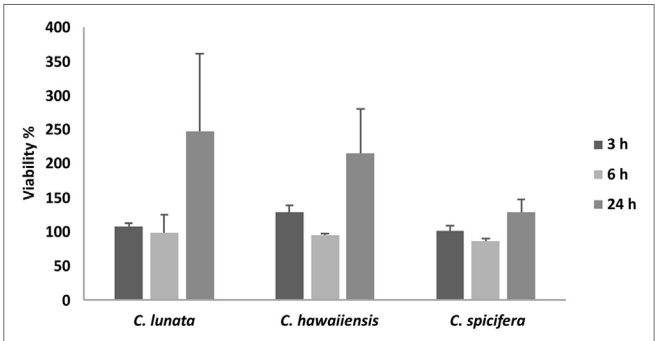

FIGURE 2 | Cell viability (MTT) assay of the three *Curvularia* strains incubated together with THP-1 monocytes for 3 and 24 h. Results are presented as averages of three independent experiments; error bars represent SDs.

qRT-PCR Analysis of Immune-Relevant Genes Induced by Germinating Conidia and Hyphae of *Curvularia* Species

Three and 24 h after the infection of THP-1 monocytes with conidia, cells were harvested and the relative transcript level of certain activation related and cytokine or chemokine coding genes were measured. Significant changes were not detected in the transcription of the genes encoding the chemokine receptors CCR5 (C-C chemokine receptor type 5), CXCR2 (IL-8 receptor, beta) and the cytokine IL-6 at both tested times in any interactions. Decreased relative transcript levels were detected for the genes of the chemokine receptors CCR1 (C-C chemokine receptor type 1) and CCR2 (C-C chemokine receptor type 2) after 24-h interaction with the tested *Curvularia* strains (**Figure 4**). Similarly, slightly decreased transcript levels were measured for the genes encoding the adhesion molecules ITGAL (integrin subunit alpha L), ITGAM (integrin subunit alpha M) and ITGAX (integrin subunit alpha X) after 24 h of co-incubation. In case of the gene encoding IL-1β, NLRC3 (NLR family CARD domain containing 3) either no significant changes in the transcription or decreased transcript levels were detected after 24 h of interaction (**Figure 4**). Transcription of gene of HLA-DRA (HLA class II histocompatibility antigen, DR alpha chain) showed significant reduction in case of *C. lunata*. Increased transcription of the gene encoding TNF-α was observed in response to all tested strains after both 3 and 24 h (**Figure 4**). A trend for increased transcript levels was detected for the genes of IL-8 and IL-10 but significant changes were detected only in interactions with certain strains (i.e., with *C. spicifera* for IL-8 and with *C. hawaiiensis* and *C. spicifera* for IL-10) (**Figure 4**).

In case of *A. fumigatus*, transcript levels were measured after 3, 9, and 24 h of interaction, because this fungus starts to germinate at about 7 h after inoculation. In accordance with the literature data (18), conidia did not induce the transcription of *IL6*, *IL8*, *IL10*, and *TNFA* while significantly increased relative transcript levels were measured for *TNFA* after 9 h of interaction (67.66 ± 10.9) and *IL8* at 9 (8.86 ± 0.73) and 24 h (24.03 ± 2.93) (see Figure S1 in Supplementary Material).

As control, THP-1 cells were also stimulated with LPS and the relative transcript levels of *IL1b*, *IL6*, *IL8*, *IL10*, *TNFA*, *CCR1*, and *CCR2* were measured as above. As expected, all tested genes showed significantly altered expression after LPS treatment. Expression of *IL1b*, *IL6*, *IL8*, *IL10*, and *TNFA* was induced showing

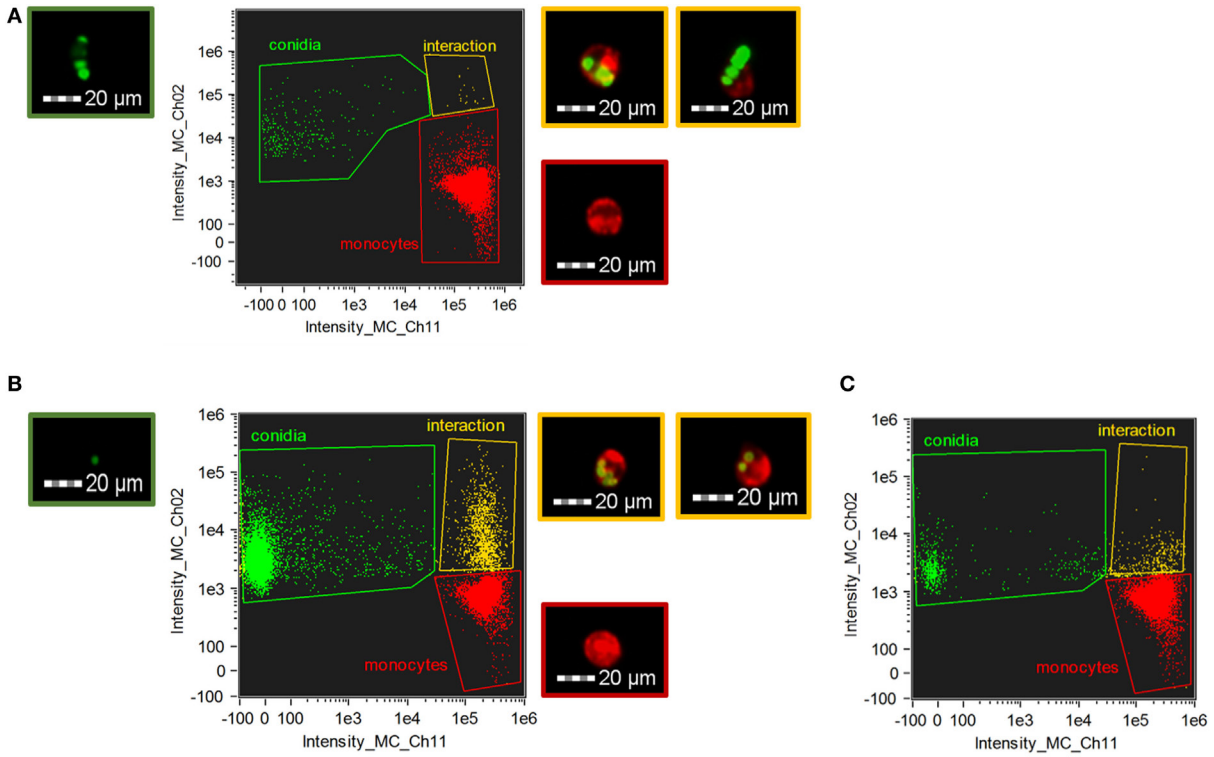

FIGURE 3 | Phagocytosis of *Curvularia lunata* **(A)** and *Aspergillus fumigatus* **(B,C)** conidia by THP-1 monocytes. THP-1 cells and conidia were stained with CellMask Deep Red Plasma Membrane Stain and Alexa Fluor 488 carboxylic acid, succinimidyl ester, respectively. Number of the *Curvularia* conidia and cells were set to maintain an E:T ratio of 20:1 **(A)**, while for *A. fumigatus* E:T ratio was 1:2 **(B)** or 20:1 **(C)**. Monocytes were identified by detecting fluorescence intensity on channel 11 (Intensity_MC_CH_11) while channel 2 (Intensity_MC_CH_2) was used to detect the conidia. Cells and conidia were co-incubated for 1 h. Fluorescent micrographs showing conidia (green border) and THP-1 cells alone (red border) and in interaction (i.e., phagocytosis or attachment) (yellow border) were recorded during the imaging flow cytometry.

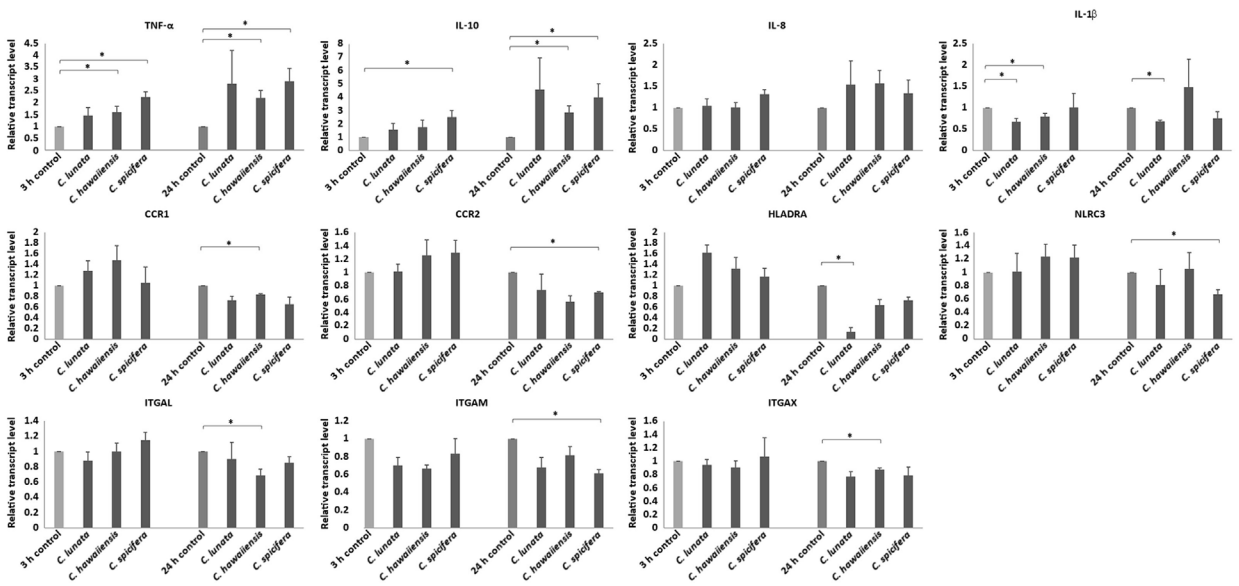

FIGURE 4 | Relative transcript levels of pro- and anti-inflammatory cytokines, activation and antigen presentation related genes. THP-1 monocytes were confronted with *Curvularia* strains for 3 and 24 h. After total RNA extraction from the monocytes, cDNA synthesis, and quantitative reverse transcription PCR were carried out. Relative transcript levels were calculated by the $2^{-\Delta\Delta Ct}$ method. Presented values are averages of the results of three independent experiments; error bars represent SDs. Relative transcript values followed by * significantly differed from the control (taken as 1), according to the paired *t*-test ($p < 0.05$).

significantly increased relative transcript levels compared to the untreated control, in contrast, relative transcript levels of *CCR1* and *CCR2* were found to be significantly decreased (see Figure S2 in Supplementary Material).

IL-6, IL-8, IL-10, and TNF-α Production in Response to Germinating Conidia and Hyphae of *Curvularia* Species

In agreement with the results of the transcription analysis, no significant IL-6 production was observed in all interactions (**Figure 5**). In response to *C. lunata*, THP-1 cells showed significant IL-8 (340 pg/ml) and IL-10 (318 pg/ml) production after 24 h of interaction (**Figure 5**). Confronting with *A. fumigatus*, monocytes displayed similar IL-8 production (376 pg/ml) but only a low amount of IL-10 (43 pg/ml) could be detected. Infection with the other two *Curvularia* strains did not cause significant change in the IL-8 and IL-10 level. In case of *C. lunata*, a moderate increase in the TNF-α level (45 pg/ml) was also measured at 24 h postinoculation (**Figure 5**).

Response of THP-1 Cells to the Conidia of *C. lunata*

Response of monocytes to non-germinating and germinating conidia were compared in case of *C. lunata*. In this experiment, activation of cytokine and chemotactic genes and cytokine production was analyzed by qRT-PCR and ELISA assays, respectively, after interactions of THP-1 cells with heat inactivated conidia (see Figures S3 and S4 in Supplementary Material). As melanin content may hamper the monocyte response, non-melanized and heat inactivated conidia, which were harvested after blocking the melanin biosynthesis during cultivation, were also tested. Compared to the germinating conidia and hyphae (**Figures 4** and **5**), presence of heat inactivated conidia, either melanized or non-melanized, did not affect the transcription of the examined genes and the production of any tested cytokines suggesting that only the germ tubes and the hyphae are able to activate the monocytes (Figures S3 and S4 in Supplementary Material).

DISCUSSION

Considering that activation of the innate immune system has a crucial role in recognition and control of filamentous fungal infections (18), present study was carried out to obtain information about the response of monocytic cell line THP-1 to the dematiaceous fungus *C. lunata* and related species.

THP-1 monocytes were not able to phagocytose the large and melanized conidia of any tested *Curvularia* species. Despite the lack of attraction to the conidia, monocytes recognized *C. lunata*,

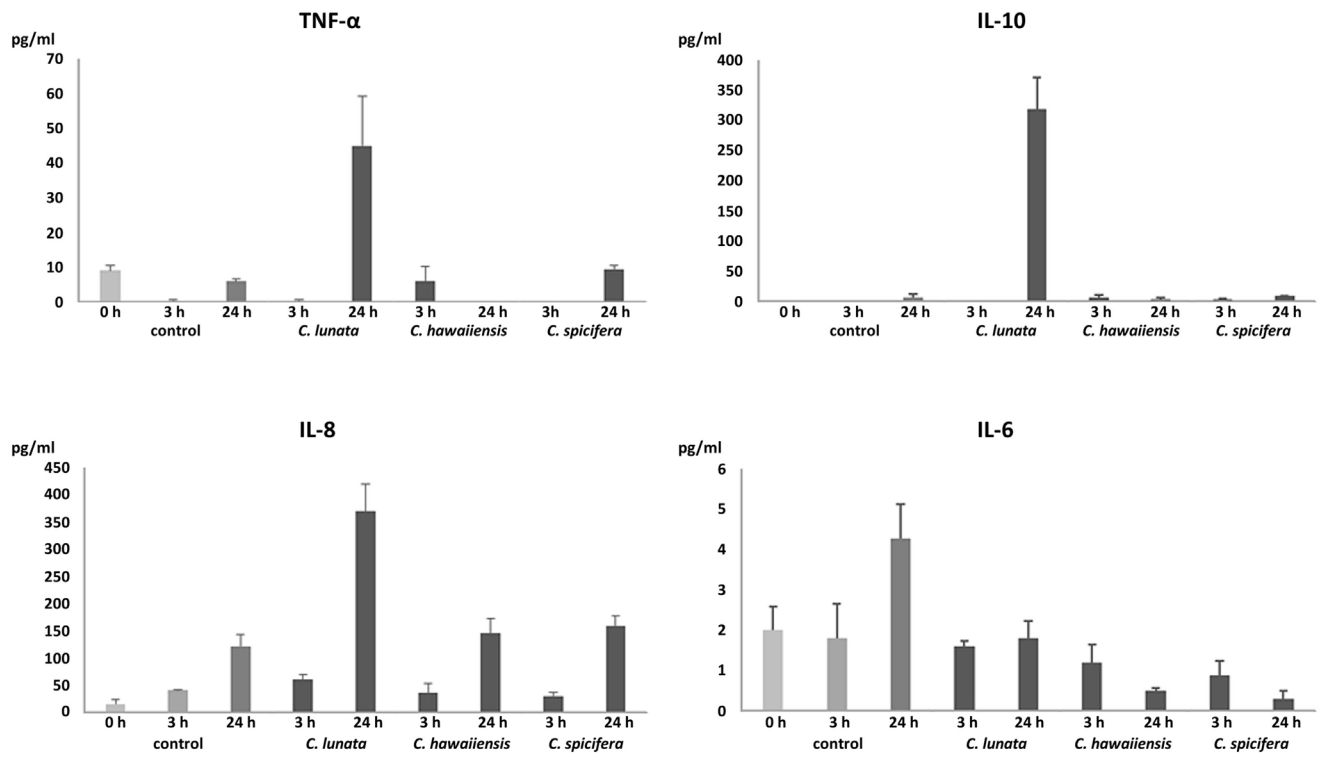

FIGURE 5 | Quantity of produced pro- and anti-inflammatory cytokines (pg/ml) after interaction with *Curvularia* strains for 3 and 24 h. THP-1 cells were interacted with the fungal conidia in an E:T ratio of 20:1. In case of the control, monocytes were incubated without the fungi. Concentrations of IL-6, IL-8, IL-10, and TNF-α in the culture supernatant were measured by ELISA. Cytokine titers were calculated by reference to standard curves generated by the four parameters logistic curve-fit method. Results are presented as averages from three independent experiments; error bars represent SDs.

but not *C. hawaiiensis* and *C. spicifera*, and preferably attached to the hyphae. In contrast to the *Curvularia* conidia, those of *A. fumigatus* were actively phagocytosed by the THP-1 cells in agreement with the results of previous studies (18). Different cell wall composition and highly distinct size of their conidia can explain this different affinity of the monocytes to the *Curvularia* and *Aspergillus* conidia. Although there are no available data about the response of monocytes to any similar dematiaceous mold, there are a few studies discussing the interaction of these fungi with other cell types. Recently, Reedy et al. (29) found that macrophages could not phagocytose the conidia of *Exserohilum rostratum*, another dematiaceous mold related to *Curvularia*. At the same time, macrophages also showed an attraction and attachment to the hyphae of *Exserohilum*. The different affinity of macrophages to the conidia and the hyphae was explained by the possibly different polysaccharide composition of the cell walls (29). Besides phagocytosis, only touching and dragging of the fungal cells, conidia and hyphal elements by macrophages to prevent the spread of the fungus into the different tissues was proven in cases of *A. fumigatus* and *C. albicans* (30).

Melanin is present in the cell wall of a wide range of fungal pathogens. Like Aspergilli, *Curvularia* species produce dihydroxynaphthalene-type melanin (DHN-melanin) (16). Melanin is generally considered as a virulence factor having role in the prevention of the immune recognition by masking the pathogen-associated molecular patterns on the surface of the conidia, as it was found in *A. fumigatus* (31–33). However, in our experiments, there was no difference in the response of monocytes to melanized and non-melanized conidia of *C. lunata* indicating that melanin content of the conidia has no significant effect on the recognition of this fungus by the THP-1 cells. Previously, comparison of killing rates of numerous dematiaceous yeasts by human neutrophils suggested that only melanization is not sufficient to assure the virulence (34).

MTT assay indicated that THP-1 cells did not damage significantly the *Curvularia* strains. Similarly, macrophages could not inhibit conidial germination and hyphal growth of *E. rostratum* (29). At the same time, THP-1 cells effectively decreased the viability of *A. fumigatus* during their interaction, as expected based on previous studies (20).

Transcription of immune-relevant genes of the monocytes during interaction with *C. lunata*, *C. hawaiiensis* and *C. spicifera* was examined by qRT-PCR analysis. A decrease in the transcription of the gene encoding CCR2, which is downregulated during monocytic differentiation (35), suggests the activation of THP-1 cells in response to *C. spicifera*. However, the unaltered or decreased expression of most tested genes, such as those encoding IL-6, IL-1β, CCR1, ITGAL, ITGAM, and ITGAX, suggests that *Curvularia* hyphae induce a moderate response in this cell type. After confrontation with *C. lunata*, transcription of HLA-DRA was significantly downregulated, assuming the lack of antigen presentation by monocytes despite of the attachment to the hyphae. In case of *A. fumigatus*, it was previously found that phagocytosis of the conidia did not induce the immediate expression of cytokine and chemokine genes in THP-1, which were activated only in the presence of the hyphae (18, 36). Similarly, we detected the induction of certain immune-relevant genes at 9 h postinoculation when the hyphae formation had already started.

In addition to the transcription analysis, production of certain cytokine proteins was measured after confrontation with the examined *Curvularia* strains. To the hyphae of *C. lunata*, THP-1 cells responded with intense IL-8 and IL-10 and moderate TNF-α production while they failed to produce IL-6. The chemokine IL-8 or CXCL8 is known to be involved in the immune response to fungal pathogens and it has a primary role in recruiting neutrophils to the site of infection (37, 38). IL-8 production and release by monocytes (including THP-1 cells) in response to confrontation with *A. fumigatus* is well documented by several studies (17, 18, 22). The low levels of the pro-inflammatory cytokines after interaction with *Curvularia* strains is somewhat surprising. These cytokines are involved in the effective immunity to fungal infections and their role has been studied and proven among others in response to *C. albicans*, *A. fumigatus*, and *C. neoformans* (37). In case of *C. lunata*, this situation can be partly explained by the high expression of the anti-inflammatory cytokine IL-10, which can repress pro-inflammatory responses and can inhibit the production of TNF-α, IL-6, and even IL-8 (39–41). In case of the THP-1 cells confronted with the *A. fumigatus* strain involved for comparison, this relatively high IL-10 production was not detected. Induction of IL-10 production in monocytes correlates well to that *Curvularia* strains and especially *C. lunata* can cause chronic infections even in immunocompetent persons (4) and are among the most frequent agents of allergic sinusitis and allergic bronchopulmonary disease (2, 4). It is known that certain pathogenic organisms possess mechanisms to modulate the immune response by enhancing IL-10 production and/or exploit the anti-inflammatory properties of IL-10 for their survival (42, 43). In the cases of *Histoplasma capsulatum* and *C. albicans*, the absence of IL-10 expression led to enhanced clearance of the fungi (44–46). Similarly, increased levels of serum IL-10 due to single nucleotide polymorphism in the *IL10* gene is associated with an increased susceptibility to *A. fumigatus* colonization and allergic bronchopulmonary aspergillosis (47). Despite the high IL-10 production, increased IL-8 level was measured after co-incubation with *C. lunata* that may suggest that neutrophils may have an important role in the immune response to this fungus as it was found in case of several other fungal species (33, 38). Interestingly, significantly increased relative transcript levels were measured for the genes encoding TNF-α and IL-10 in response to *C. spicifera* and *C. hawaiiensis* while secretion of these proteins by the monocytes could not be detected. Although the relative transcript level of *IL8* showed similar values as in case of *C. lunata*, there was no significant increase in protein release either. Considering that secretion of IL-10 and IL-8 is regulated primarily at a transcriptional level (48, 49), this is a surprising phenomenon. TNF-α production is regulated at a transcriptional and translational level as well (50, 51). Immune cells can display different attraction even to closely related fungal species. For example, different recognition of *C. albicans* and *C. glabrata* was observed by Netea et al. (52) and a distinct IL-1β release and ROS production of macrophages induced by *C. albicans* and *C. parapsilosis* (53). *Aspergillus* species (i.e., *A. fumigatus*, *A. flavus*, *A. niger,* and *A. terreus*) also induced significantly different release of IL-6 and TNF-α by human monocytes (54).

As a conclusion, our results show that THP-1 monocytes cannot effectively phagocytose the conidia of *Curvularia* species and there is a clear difference in response of these cells to the three investigated strains. They attach to the hyphae and respond to those of *C. lunata* by IL-10 and IL-8 production. Further studies to clarify the mechanisms in the background of the enhanced IL-10 production and the possible association of this phenomenon with the chronic mycoses caused by this fungus are needed. Considering the upregulation of IL-8, the role of neutrophils in the clearance of *Curvularia* infections is also worth to examine.

AUTHOR CONTRIBUTIONS

ET carried out most of the experimental work, performed the statistical analysis, and participated in the evaluation of the results and drafting the manuscript. ÉB, AH, CS, and MH performed experiments, analyzed data, and participated in the writing of the manuscript. GN performed experiments and participated in the evaluation of the results. IN, CV, and TP designed and coordinated the study and participated in the writing and the edition of the manuscript.

ACKNOWLEDGMENTS

The authors would like to thank Erik Zajta and Katalin Csonka for her help in the cell culturing and ELISA tests.

FUNDING

The study was supported by the "Lendület" Grant of the Hungarian Academy of Sciences (LP2016-8/2016) and the project GINOP-2.3.2-15-2016-00035. ÉB was funded by the European Union and the State of Hungary, co-financed by the European Social Fund in the framework of "National Excellence Program" (grant number A2-ELMH-12-0082); IN was supported by the János Bolyai Research Scholarship of the Hungarian Academy of Sciences. EJT is supported by the UNKP-17-3 New National Excellence Program of the Ministry of Human Capacities.

SUPPLEMENTARY MATERIAL

The Supplementary Material for this article can be found online at http://www.frontiersin.org/article/10.3389/fimmu.2017.01369/full#supplementary-material.

REFERENCES

1. Manamgoda DS, Cai L, Bahkali AH, Chukeatirote E, Hyde KD. Cochliobolus: an overview and current status of species. *Fungal Divers* (2011) 51(1):3–42. doi:10.1007/s13225-011-0139-4
2. Paredes K, Capilla J, Sutton DA, Mayayo E, Fothergill AW, Guarro J. Virulence of *Curvularia* in a murine model. *Mycoses* (2013) 56(5):512–5. doi:10.1111/myc.12064
3. Cavanna C, Seminari E, Pusateri A, Mangione F, Lallitto F, Esposto MC, et al. Allergic fungal rhinosinusitis due to *Curvularia lunata*. *New Microbiol* (2014) 37(2):241–5.
4. Krizsán KPT, Manikandan P, Shobana S, Chandrasekaran M, Vágvölgyi C, Kredics L. Clinical importance of the genus *Curvularia*. In: Razzaghi-Abyaneh M, Shams-Ghahfarokhi M, Rai M, editors. *Medical Mycology: Current Trends and Future Prospects*. Boca Raton, FL: CRC Press (2015). p. 147–204.
5. Bashir G, Hussain W, Rizvi A. *Bipolaris hawaiiensis* keratomycosis and endophthalmitis. *Mycopathologia* (2009) 167(1):51–3. doi:10.1007/s11046-008-9144-x
6. Mythili A, Babu Singh YR, Priya R, Shafeeq Hassan A, Manikandan P, Panneerselvam K, et al. In vitro and comparative study on the extracellular enzyme activity of molds isolated from keratomycosis and soil. *Int J Ophthalmol* (2014) 7(5):778–84. doi:10.3980/j.issn.2222-3959.2014.05.07
7. Moody MN, Tschen J, Mesko M. Cutaneous *Curvularia* infection of the forearm. *Cutis* (2012) 89(2):65–8.
8. Gunathilake R, Perera P, Sirimanna G. *Curvularia lunata*: a rare cause of black-grain eumycetoma. *J Mycol Med* (2014) 24(2):158–60. doi:10.1016/j.mycmed.2013.09.005
9. Skovrlj B, Haghighi M, Smethurst ME, Caridi J, Bederson JB. *Curvularia* abscess of the brainstem. *World Neurosurg* (2014) 82(1–2):e9–13. doi:10.1016/j.wneu.2013.07.014
10. Revankar SG, Patterson JE, Sutton DA, Pullen R, Rinaldi MG. Disseminated phaeohyphomycosis: review of an emerging mycosis. *Clin Infect Dis* (2002) 34(4):467–76. doi:10.1086/338636
11. Kobayashi H, Sano A, Aragane N, Fukuoka M, Tanaka M, Kawaura F, et al. Disseminated infection by *Bipolaris spicifera* in an immunocompetent subject. *Med Mycol* (2008) 46(4):361–5. doi:10.1080/13693780701883490
12. Balla A, Pierson J, Hugh J, Wojewoda C, Gibson P, Greene L. Disseminated cutaneous *Curvularia* infection in an immunocompromised host; diagnostic challenges and experience with voriconazole. *J Cutan Pathol* (2016) 43(4):383–7. doi:10.1111/cup.12648
13. Peghin M, Monforte V, Martin-Gomez MT, Ruiz-Camps I, Berastegui C, Saez B, et al. Epidemiology of invasive respiratory disease caused by emerging non-*Aspergillus* molds in lung transplant recipients. *Transpl Infect Dis* (2016) 18(1):70–8. doi:10.1111/tid.12492
14. El Khizzi NBS, Parvez S. *Bipolaris*: a plant pathogen causing human infections: an emerging problem in Saudi Arabia. *Res J Microbiol* (2010) 5(3):212–7. doi:10.3923/jm.2010.212.217
15. da Cunha KC, Sutton DA, Fothergill AW, Cano J, Gene J, Madrid H, et al. Diversity of *Bipolaris* species in clinical samples in the United States and their antifungal susceptibility profiles. *J Clin Microbiol* (2012) 50(12):4061–6. doi:10.1128/JCM.01965-12
16. Perfect JR, Alexander BD, Schell WA. Phaeohyphomycoses (brown–black moulds). 2nd ed. In: Kauffman C, Pappas P, Sobel JD, Dismukes WE, editors. *Essentials of Clinical Mycology*. New York, NY: Springer Science & Business Media (2011). p. 305–17.
17. Cortez KJ, Lyman CA, Kottilil S, Kim HS, Roilides E, Yang J, et al. Functional genomics of innate host defense molecules in normal human monocytes in response to *Aspergillus fumigatus*. *Infect Immun* (2006) 74(4):2353–65. doi:10.1128/IAI.74.4.2353–2365.2006
18. Loeffler J, Haddad Z, Bonin M, Romeike N, Mezger M, Schumacher U, et al. Interaction analyses of human monocytes co-cultured with different forms of *Aspergillus fumigatus*. *J Med Microbiol* (2009) 58(Pt 1):49–58. doi:10.1099/jmm.0.003293-0
19. Chanput W, Mes JJ, Wichers HJ. THP-1 cell line: an in vitro cell model for immune modulation approach. *Int Immunopharmacol* (2014) 23(1):37–45. doi:10.1016/j.intimp.2014.08.002
20. Sharif O, Bolshakov VN, Raines S, Newham P, Perkins ND. Transcriptional profiling of the LPS induced NF-kappaB response in macrophages. *BMC Immunol* (2007) 8:1. doi:10.1186/1471-2172-8-1
21. Marr KA, Koudadoust M, Black M, Balajee SA. Early events in macrophage killing of *Aspergillus fumigatus* conidia: new flow cytometric viability assay. *Clin Diagn Lab Immunol* (2001) 8(6):1240–7. doi:10.1128/CDLI.8.6.1240-1247.2001
22. Shalit I, Halperin D, Haite D, Levitov A, Romano J, Osherov N, et al. Anti-inflammatory effects of moxifloxacin on IL-8, IL-1beta and TNF-alpha secretion and NFkappaB and MAP-kinase activation in human monocytes stimulated with *Aspergillus fumigatus*. *J Antimicrob Chemother* (2006) 57(2):230–5. doi:10.1093/jac/dki441
23. Simitsopoulou M, Roilides E, Paliogianni F, Likartsis C, Ioannidis J, Kanellou K, et al. Immunomodulatory effects of voriconazole on monocytes challenged

with *Aspergillus fumigatus*: differential role of toll-like receptors. *Antimicrob Agents Chemother* (2008) 52(9):3301–6. doi:10.1128/AAC.01018-07
24. Barker KS, Liu T, Rogers PD. Coculture of THP-1 human mononuclear cells with *Candida albicans* results in pronounced changes in host gene expression. *J Infect Dis* (2005) 192(5):901–12. doi:10.1086/432487
25. Rai MN, Borah S, Bairwa G, Balusu S, Gorityala N, Kaur R. Establishment of an in vitro system to study intracellular behavior of *Candida glabrata* in human THP-1 macrophages. *J Vis Exp* (2013) 82:e50625. doi:10.3791/50625
26. Srikanta D, Yang M, Williams M, Doering TL. A sensitive high-throughput assay for evaluating host-pathogen interactions in *Cryptococcus neoformans* infection. *PLoS One* (2011) 6(7):e22773. doi:10.1371/journal.pone.0022773
27. Livak KJ, Schmittgen TD. Analysis of relative gene expression data using real-time quantitative PCR and the 2(-Delta Delta C(T)) method. *Methods* (2001) 25(4):402–8. doi:10.1006/meth.2001.1262
28. Levitz SM, Diamond RD. A rapid colorimetric assay of fungal viability with the tetrazolium salt MTT. *J Infect Dis* (1985) 152(5):938–45. doi:10.1093/infdis/152.5.938
29. Reedy JL, Negoro PE, Feliu M, Lord AK, Khan NS, Lukason DP, et al. The carbohydrate lectin receptor dectin-1 mediates the immune response to *Exserohilum rostratum*. *Infect Immun* (2017) 85(3):e903–16. doi:10.1128/IAI.00903-16
30. Behnsen J, Narang P, Hasenberg M, Gunzer F, Bilitewski U, Klippel N, et al. Environmental dimensionality controls the interaction of phagocytes with the pathogenic fungi *Aspergillus fumigatus* and *Candida albicans*. *PLoS Pathog* (2007) 3(2):e13. doi:10.1371/journal.ppat.0030013
31. Pihet M, Vandeputte P, Tronchin G, Renier G, Saulnier P, Georgeault S, et al. Melanin is an essential component for the integrity of the cell wall of *Aspergillus fumigatus* conidia. *BMC Microbiol* (2009) 9:177. doi:10.1186/1471-2180-9-1771471-2180-9-177
32. Chai LY, Netea MG, Sugui J, Vonk AG, van de Sande WW, Warris A, et al. *Aspergillus fumigatus* conidial melanin modulates host cytokine response. *Immunobiology* (2010) 215(11):915–20. doi:10.1016/j.imbio.2009.10.002
33. Erwig LP, Gow NA. Interactions of fungal pathogens with phagocytes. *Nat Rev Microbiol* (2016) 14(3):163–76. doi:10.1038/nrmicro.2015.21
34. Peltroche-Llacsahuanga H, Schnitzler N, Jentsch S, Platz A, De Hoog S, Schweizer KG, et al. Analyses of phagocytosis, evoked oxidative burst, and killing of black yeasts by human neutrophils: a tool for estimating their pathogenicity? *Med Mycol* (2003) 41(1):7–14. doi:10.1080/mmy.41.1.7.14
35. Fantuzzi L, Borghi P, Ciolli V, Pavlakis G, Belardelli F, Gessani S. Loss of CCR2 expression and functional response to monocyte chemotactic protein (MCP-1) during the differentiation of human monocytes: role of secreted MCP-1 in the regulation of the chemotactic response. *Blood* (1999) 94(3):875–83.
36. Said-Sadier N, Padilla E, Langsley G, Ojcius DM. *Aspergillus fumigatus* stimulates the NLRP3 inflammasome through a pathway requiring ROS production and the Syk tyrosine kinase. *PLoS One* (2010) 5(4):e10008. doi:10.1371/journal.pone.0010008
37. Antachopoulos C, Roilides E. Cytokines and fungal infections. *Br J Haematol* (2005) 129(5):583–96. doi:10.1111/j.1365-2141.2005.05498.x
38. Morton CO, Bouzani M, Loeffler J, Rogers TR. Direct interaction studies between *Aspergillus fumigatus* and human immune cells; what have we learned about pathogenicity and host immunity? *Front Microbiol* (2012) 3:413. doi:10.3389/fmicb.2012.00413
39. de Waal Malefyt R, Abrams J, Bennett B, Figdor CG, de Vries JE. Interleukin 10(IL-10) inhibits cytokine synthesis by human monocytes: an autoregulatory role of IL-10 produced by monocytes. *J Exp Med* (1991) 174(5):1209–20. doi:10.1084/jem.174.5.1209
40. Couper KN, Blount DG, Riley EM. IL-10: the master regulator of immunity to infection. *J Immunol* (2008) 180(9):5771–7. doi:10.4049/jimmunol.180.9.5771
41. Ouyang W, Rutz S, Crellin NK, Valdez PA, Hymowitz SG. Regulation and functions of the IL-10 family of cytokines in inflammation and disease. *Annu Rev Immunol* (2011) 29:71–109. doi:10.1146/annurev-immunol-031210-101312
42. Cyktor JC, Turner J. Interleukin-10 and immunity against prokaryotic and eukaryotic intracellular pathogens. *Infect Immun* (2011) 79(8):2964–73. doi:10.1128/IAI.00047-11
43. Iyer SS, Cheng G. Role of interleukin 10 transcriptional regulation in inflammation and autoimmune disease. *Crit Rev Immunol* (2012) 32(1):23–63. doi:10.1615/CritRevImmunol.v32.i1.30
44. Romani L, Puccetti P, Mencacci A, Cenci E, Spaccapelo R, Tonnetti L, et al. Neutralization of IL-10 up-regulates nitric oxide production and protects susceptible mice from challenge with *Candida albicans*. *J Immunol* (1994) 152(7):3514–21.
45. Deepe GS Jr, Gibbons RS. Protective and memory immunity to *Histoplasma capsulatum* in the absence of IL-10. *J Immunol* (2003) 171(10):5353–62. doi:10.4049/jimmunol.171.10.5353
46. Netea MG, Sutmuller R, Hermann C, Van der Graaf CA, Van der Meer JW, van Krieken JH, et al. Toll-like receptor 2 suppresses immunity against *Candida albicans* through induction of IL-10 and regulatory T cells. *J Immunol* (2004) 172(6):3712–8. doi:10.4049/jimmunol.172.6.3712
47. Romani L. Immunity to fungal infections. *Nat Rev Immunol* (2004) 4(1):1–23. doi:10.1038/nri1255
48. Le T, Leung L, Carroll WL, Schibler KR. Regulation of interleukin-10 gene expression: possible mechanisms accounting for its upregulation and for maturational differences in its expression by blood mononuclear cells. *Blood* (1997) 89(11):4112–9.
49. Roebuck KA. Regulation of interleukin-8 gene expression. *J Interferon Cytokine Res* (1999) 19(5):429–38. doi:10.1089/107999099313866
50. Spriggs DR, Deutsch S, Kufe DW. Genomic structure, induction, and production of TNF-alpha. *Immunol Ser* (1992) 56:3–34.
51. Parameswaran N, Patial S. Tumor necrosis factor-alpha signaling in macrophages. *Crit Rev Eukaryot Gene Expr* (2010) 20(2):87–103. doi:10.1615/CritRevEukarGeneExpr.v20.i2.10
52. Netea MG, Joosten LA, van der Meer JW, Kullberg BJ, van de Veerdonk FL. Immune defence against *Candida* fungal infections. *Nat Rev Immunol* (2015) 15(10):630–42. doi:10.1038/nri3897nri3897
53. Toth A, Zajta E, Csonka K, Vagvolgyi C, Netea MG, Gacser A. Specific pathways mediating inflammasome activation by *Candida parapsilosis*. *Sci Rep* (2017) 7:43129. doi:10.1038/srep43129
54. Warris A, Netea MG, Verweij PE, Gaustad P, Kullberg BJ, Weemaes CM, et al. Cytokine responses and regulation of interferon-gamma release by human mononuclear cells to *Aspergillus fumigatus* and other filamentous fungi. *Med Mycol* (2005) 43(7):613–21. doi:10.1080/13693780500088333

Conflict of Interest Statement: The authors declare that the research was conducted in the absence of any commercial or financial relationships that could be construed as a potential conflict of interest.

Copyright © 2017 Tóth, Boros, Hoffmann, Szebenyi, Homa, Nagy, Vágvölgyi, Nagy and Papp. This is an open-access article distributed under the terms of the Creative Commons Attribution License (CC BY). The use, distribution or reproduction in other forums is permitted, provided the original author(s) or licensor are credited and that the original publication in this journal is cited, in accordance with accepted academic practice. No use, distribution or reproduction is permitted which does not comply with these terms.

frontiers in Microbiology

ORIGINAL RESEARCH
published: 20 September 2017
doi: 10.3389/fmicb.2017.01803

Involvement of Dihydrolipoyl Dehydrogenase in the Phagocytosis and Killing of *Paracoccidioides brasiliensis* by Macrophages

*Taise N. Landgraf[1], Marcelo V. Costa[2], Aline F. Oliveira[3], Wander C. Ribeiro[1], Ademilson Panunto-Castelo[2] and Fabrício F. Fernandes[3]**

[1] Department of Biochemistry and Immunology, Ribeirão Preto Medical School, University of São Paulo, Ribeirão Preto, Brazil, [2] Department of Biology, Faculty of Philosophy, Sciences and Letters of Ribeirão Preto, University of São Paulo, Ribeirão Preto, Brazil, [3] Department of Cell and Molecular Biology, Ribeirão Preto Medical School, University of São Paulo, Ribeirão Preto, Brazil

OPEN ACCESS

Edited by:
Ilse Denise Jacobsen, Leibniz-Institut für Naturstoff-Forschung und Infektionsbiologie, Hans Knöll Institut, Germany

Reviewed by:
Mario M. D'Elios, University of Florence, Italy
Sascha Brunke, Leibniz-Institut für Naturstoff-Forschung und Infektionsbiologie, Hans Knöll Institut, Germany

***Correspondence:**
Fabrício F. Fernandes
fabsff@yahoo.com.br

Specialty section:
This article was submitted to Microbial Immunology, a section of the journal Frontiers in Microbiology

Received: *26 April 2017*
Accepted: *05 September 2017*
Published: *20 September 2017*

Citation:
Landgraf TN, Costa MV, Oliveira AF, Ribeiro WC, Panunto-Castelo A and Fernandes FF (2017) Involvement of Dihydrolipoyl Dehydrogenase in the Phagocytosis and Killing of Paracoccidioides brasiliensis by Macrophages. Front. Microbiol. 8:1803. doi: 10.3389/fmicb.2017.01803

Paracoccidioides brasiliensis and *Paracoccidioides lutzii* are fungi causing paracoccidioidomycosis (PCM), an autochthonous systemic mycosis found in Latin America. These microorganisms contain a multitude of molecules that may be associated with the complex interaction of the fungus with the host. Here, we identify the enzyme dihydrolipoyl dehydrogenase (DLD) as an exoantigen from *P. brasiliensis* (Pb18_Dld) by mass spectrometry. Interestingly, the DLD gene expression in yeast form showed higher expression levels than those in mycelial form and transitional phases. Pb18_Dld gene was cloned, and the recombinant protein (rPb18_Dld) was expressed and purified for subsequent studies and production of antibodies. Immunogold labeling and transmission electron microscopy revealed that the Pb18_Dld is also localized in mitochondria and cytoplasm of *P. brasiliensis*. Moreover, when macrophages were stimulated with rPb18Dld, there was an increase in the phagocytic and microbicidal activity of these cells, as compared with non-stimulated cells. These findings suggest that Pb18_Dld can be involved in the pathogen-host interaction, opening possibilities for studies of this protein in PCM.

Keywords: *Paracoccidioides brasiliensis*, dihydrolipoyl dehydrogenase, exoantigen, subcellular localization, microbicidal activity

INTRODUCTION

Paracoccidioidomycosis (PCM) is a chronic granulomatous mycosis caused by thermally dimorphic fungi *Paracoccidioides lutzii* and *P. brasiliensis*, which contain a complex of at least four different cryptic species, S1, PS2, PS3, and PS4 (Matute et al., 2006; Carrero et al., 2008; Teixeira et al., 2009, 2014; Theodoro et al., 2012). PCM is the most important systemic mycosis in Latin America with high prevalence in Brazil, Colombia, Argentina, and Venezuela. The mean annual mortality rate is 1.65 per million inhabitants, the highest for any systemic mycosis, making PCM the eighth most important cause of mortality among chronic or recurrent infectious, parasitic diseases, and infectious diseases in Brazil (Coutinho et al., 2002; Colombo et al., 2011; Bocca et al., 2013).

Fungi of the genus *Paracoccidioides* are asexual and dimorphic, growing as mycelial forms at 25°C and as yeast form at 37°C (da Silva et al., 1994; de Almeida, 2005). Transformation of the fungus from mycelia to yeast is responsible for establishing the infectious process (Bagagli et al., 2008) as well as for the initial interaction of the fungus with the immune system, which determines the fate of the infecting forms. Secretion of antimicrobial proteins by the pulmonary epithelium and phagocytic activity of resident alveolar macrophages mediates the initial response to infection (Calich et al., 2008). Infections can stimulate different subsets of T cells and consequently induce the production of distinct patterns of cytokines that are responsible for the protection or susceptibility of the host to pathogens (Della Bella et al., 2017), including fungal infections (Calich and Kashino, 1998; Oliveira et al., 2002; Romani, 2004).

The ability of this pathogenic fungus to develop a multi-faceted response to a wide variety of stressors found in the host is extremely important for its virulence and pathogenesis. Many of these extracellular molecules are secreted by or are associated with the fungal wall (Casotto, 1990; Diniz et al., 1999, 2001). Numerous proteins or glycoproteins that are common to different strains of *P. brasiliensis* are secreted in culture, and these are recognized, to varying degrees, by the serum of the patients (Panunto-Castelo et al., 2003). The most studied exoantigen (ExoAg) of *P. brasiliensis* is the 43-kDa glycoprotein (gp43), which is a molecule involved in binding of *P. brasiliensis* to the extracellular matrix and surface of epithelial cells (Vicentini et al., 1994; Gesztesi et al., 1996). More recently, Torres et al. (2013) showed that *P. brasiliensis* cell lines in which gp43 was silenced were less internalized by macrophages.

Some studies have been carried out in order to elucidate the complex programs of gene expression that *Paracoccidioides* spp. uses to survive when exposed to conditions similar to those found in the host. Tavares et al. (2007) showed, for instance, that *P. brasiliensis* regulates expression of 119 genes during phagocytosis. These genes were first associated with glucose and amino acid limitation, cell wall building, and oxidative stress. Subsequent studies also elucidated the molecules involved in the adaptation of the fungus. In addition to the activation of enzymes involved in the defense against oxidative stress (Derengowski et al., 2008; de Arruda Grossklaus et al., 2013; Parente-Rocha et al., 2015), other metabolic modifications have been suggested to occur in yeast cells, such as gluconeogenesis, ethanol production, and degradation of fatty acids and amino acids (Lima et al., 2014).

In this study, we aimed to identify the proteins that were secreted/excreted by *P. brasiliensis*. We also attempted to evaluate whether these molecules could have any association with the phagocytosis and killing activity, contributing to the pathogenic process. Although *P. brasiliensis* secretes a number of different proteins into the basal medium, one protein in particular drew our attention because it was present in high amount. The protein was identified as dihydrolipoyl dehydrogenase (Pb18_Dld), which was expressed at high levels in the pathogenic form, and was located in and outside the mitochondria, which improved the macrophage-mediated phagocytic and microbicidal activity.

MATERIALS AND METHODS

Ethics Statement and Mice

This work was conducted according to the ethical principles of animal research adopted by the Brazilian Society of Laboratory Animal Science, and received approval from the Ethics Committee on Animal Use of the Ribeirão Preto Medical School, USP. The Protocol number is 105/2007. Male BALB/c mice, aged 6–8 weeks, were purchased from the Central Animal House of the Ribeirão Preto Campus of University de São Paulo (USP), and were maintained in the Animal Facilities of the Department of Biology, Faculty of Philosophy, Sciences and Letters of Ribeirão Preto, USP.

Growth Conditions of the *P. brasiliensis* Isolate

Virulent yeast cells of *P. brasiliensis* strain 18 (Pb18) were cultured for 15 days at 37°C in DMEM (Sigma-Aldrich, St Louis, USA), in a shaking incubator at 100 rpm. The yeast cells were maintained by culturing at 37°C, while the mycelial forms were obtained by culturing at 25°C. Both cultures were maintained under these conditions for 7 days. The transition phase from mycelium-to-yeast was induced by culturing the mycelia at 25°C for 72 h, changing the temperature to 37°C, and incubating for 24 h. The transition from yeast to mycelium was induced by growing yeast for 72 h at 37°C, changing the temperature to 25°C, and incubating for 24 h. One aliquot of each *P. brasiliensis* culture was treated with 50 μg/mL Calcofluor white stain (Sigma-Aldrich) for 30 min at 37°C to analyze the fungal morphological forms by fluorescence microscopy.

Preparation of Extracellular Extract and Total Soluble Antigen from *P. brasiliensis* and Pb18_Dld Identification

Supernatants of the cultures containing ExoAgs were recovered by centrifugation at 10,000 × g, concentrated and diafiltrated against 10 mM phosphate-buffered saline (PBS, pH 7.2) using centrifugal filtration devices with a molecular weight cut-off of 10,000 kDa (Millipore, Billerica, USA). The ExoAgs were analyzed using 12% sodium dodecyl sulfate-polyacrylamide gel electrophoresis (SDS-PAGE). The gels were stained with Coomassie brilliant blue G250 (USB Corporation, Cleveland, USA). The relative amount of the 60-kDa protein band was calculated with the ImageJ 1.37v software (National Institutes of Health, Bethesda, USA) and the values were normalized against the total amount of loaded proteins. Next, the 60-kDa band was excised from the gel, and mass spectrometry was performed at the FingerPrint Proteomics and Mass Spectrometry Facility, College of Life Sciences, University of Dundee. Mascot (version 2.3; Matrix, United Kingdom) analysis was performed to identify peptides and to search for proteins in the NCBI non-redundant (nr) database. Total soluble antigen derived from *P. brasiliensis* yeast cells was prepared according to reported by Fernandes et al. (Panunto-Castelo et al., 2003).

In Silico Analysis

The *in silico* analyses were performed based on Pb18_Dld amino acid sequence (GenBank accession no. EEH50415.1) that was submitted to NetOGlyc 3.1 Server (http://www.cbs.dtu.dk/services/NetOGlyc-3.1/), NetNGlyc 1.0 Server (http://www.cbs.dtu.dk/services/NetNGlyc/), SignalP 4.1 Server (http://www.cbs.dtu.dk/services/SignalP/), and TargetP v1.1 Server (http://www.cbs.dtu.dk/services/TargetP/). Protein conserved domains are available in the CDD NCBI's conserved domain database (https://www.ncbi.nlm.nih.gov/Structure/cdd/wrpsb.cgi).

Differential Expression of Dld mRNA from Different Morphological Forms of *P. brasiliensis*

The gene expression profile of *P. brasiliensis* was analyzed in mycelium, yeast, and transition forms from mycelium-to-yeast and yeast-to-mycelium, which were cultivated as described previously. The total RNA from the *P. brasiliensis* morphological forms was extracted using *TRIzol* (Thermo Fisher Scientific Inc., Waltham, USA). Briefly, cells were harvested, disrupted by grinding in liquid nitrogen, and mixed with TRizol, according to the manufacturer's instructions. Total RNA was treated with DNase I (Thermo Fisher Scientific Inc.). The concentration of RNA was measured with the help of a spectrophotometer at 260 nm and the quality of RNA was evaluated by the ratio of absorbance at 260 and 280 nm. In order to ensure RNA integrity, samples were electrophoresed in 1.5% agarose gel. In addition, the absence of contaminating chromosomal DNA was confirmed, after the treatment of the RNA with DNaseI, by the absence of the HSP60 gene amplification (Fernandes et al., 2016) after PCR. cDNA was synthesized using 1 μg of total RNA with oligo-dT_{12-18} primer (Thermo Fisher Scientific Inc.) and SuperScript III reverse transcriptase (Thermo Fisher Scientific Inc.), according to the manufacturer's instructions. Real-time PCR was performed using *Kit Platinum SYBR Green qPCR SuperMix-UDG with ROX* (Thermo Fisher Scientific Inc.), according to the manufacturer's instructions. Next, specific primers were used for Pb18_DLD: 5′-GGTTTGGACAAGGTCGG-3′ (sense) and 5′-CATGGCCGTAGCCCTTC-3′ (antisense). To measure the gene expression levels, we used CFX96 real-time PCR detection system (Bio-Rad, Hercules, USA). Fold changes in mRNA expression were calculated using the $2^{-\Delta Cq}$ formula, where ΔCq is the difference in the threshold cycle (*Cq*) between the DLD (target) gene and the β-actin (Sequence ID: ref |XM_010763641.1|) or α-tubulin references (housekeeping) genes (Goldman et al., 2003). The reaction of the genes β-actin and α-tubulin was done using a couple of primers: 5′-GGATGAGGAGATGGATTATGG-3′ (sense) and 5′-GAAACACTCGACGCACACGAC-3′ (antisense); and 5′-GTGGACCAGGTGATCGATGT-3′ (sense) and 5′-ACCCTGGAGGCAGTCACA-3′ (antisense), respectively. All experiments were performed using biological and experimental triplicates.

Cloning of the Pb18_Dld Gene Transcript

The cDNA obtained from the mRNA of yeast cells of *P. brasiliensis* was used to amplify the region encoding Pb18_Dld using oligonucleotide primers 5′-CATATGTTTCGGCCCCTTCTCCC-3′ (sense) and 5′-GGATCCCTAGAAATGAATCGCTTTCG-3′ (antisense), and high-fidelity Taq DNA polymerase (Thermo Fisher Scientific Inc.). The amplified fragment was cloned into pCR 2.1-TOPO vector (Thermo Fisher Scientific Inc.), and was sequenced at the Laboratory of Plant Molecular Biology from the *Faculty of Philosophy, Sciences, and Letters of Ribeirão* Preto—USP. Next, the fragment was removed from the pCR 2.1-TOPO vector using restriction enzymes *NdeI* and *BamHI* (Fermentas, Carlsbad, USA), and was sub-cloned into pET-28a vector (Addgene, Cambridge, USA).

Expression and Purification of rPb18_Dld

The pET-28a vector, containing the gene transcript of Pb18_Dld, was transformed into *Escherichia coli* BL21 cells for expression of the Pb18_Dld recombinant protein (rPb18_Dld). Briefly, cultures were grown in LB medium supplemented with kanamycin sulfate (50 μg/mL) at 37°C until an absorbance of 0.4–0.5 was observed at 600 nm. Then, rPb18_rDld expression was induced with 0.8 mM isopropyl-D-thiogalactopyranoside (IPTG) for 6 h. The bacterial cells were then harvested by centrifugation at 10,000 × g, at 25°C for 10 min, resuspended in buffer containing 50 mM NaH_2PO_4, 300 mM NaCl, and 20 mM imidazole (pH 8.0), and lysed by sonication. The pellet containing the insoluble fractions was washed five times with a washing buffer [50 mM NaH_2PO_4, 300 mM NaCl, 2 M urea, 2 mM 2-mercaptoethanol, 20 mM imidazole, and 1% Triton X-100 (pH 8.0)]. Then, the pellet was resuspended in solubilization buffer [50 mM NaH_2PO_4, 300 mM NaCl, 20 mM imidazole, 7 M urea (pH 8.0)], followed by incubation for 1 h at room temperature. The solubilized material was recovered by centrifugation at 10,000 × g at 4°C for 10 min, and was filtered through Millex-GV PVDF (pore size, 0.22 μm; Millipore). The rPb18_Dld was purified by performing metal chelate affinity chromatography with a Ni^{2+}–Sepharose affinity column (His-Trap; GE Healthcare, Piscataway, USA). Next, the rPb18_Dld was eluted using elution buffer (50 mM NaH_2PO_4, 300 mM NaCl, 300 mM imidazole, 7 M urea), refolded by dialysis against PBS, and concentrated by ultrafiltration. Protein concentration was determined using BCA kit (Pierce Chemical Co., Rockford, USA) and purity, size, and identity of the rPb18_Dld protein were evaluated using SDS-PAGE (12%). In addition, the recombinant protein samples were analyzed for endotoxin contamination by using Limulus amebocyte lysate (LAL) assay (Sigma-Aldrich), and were found to contain <0.05 ng/mL of bacterial endotoxin.

Mice Immunization

We used purified rPb18_Dld protein to generate specific anti-rPb18_Dld polyclonal antibody in mice serum. Male BALB/c mice were immunized by subcutaneous injection of 50 μL of purified protein (10 μg/mice) with 50 μL of complete Freund's adjuvant (CFA, Sigma-Aldrich) at first administration. Animals were boosted twice, at 1-week intervals, with the same amount of antigen emulsified in 50 μL of incomplete Freund's adjuvant. One week after the last boost, the serum containing polyclonal antibody to rPb18_rDld was aliquoted and stored at −20°C.

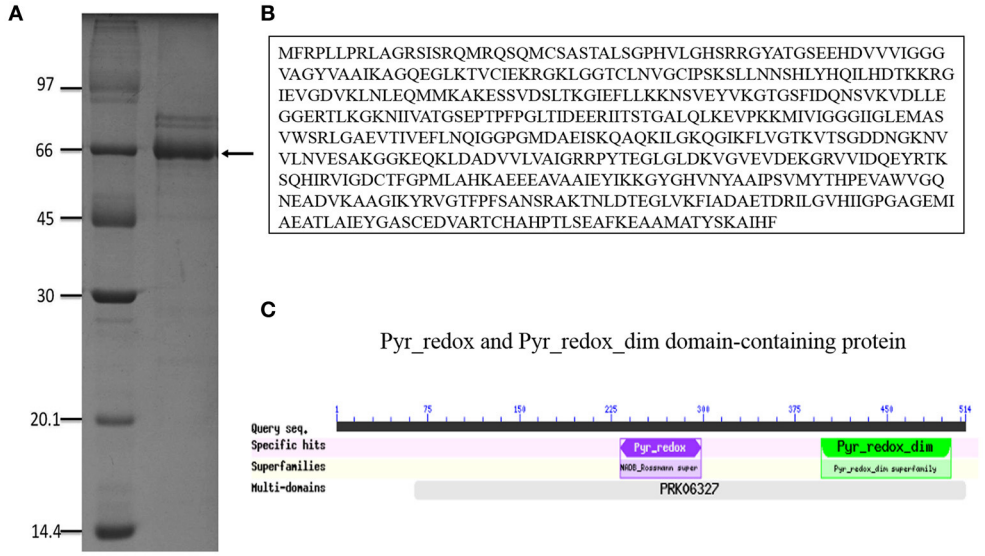

FIGURE 1 | Pb18_Dld identification. **(A)** SDS-PAGE result of *P. brasiliensis* exoantigens grown in DMEM, for 15 days at 37°C. After this period, cultures were centrifuged, and the supernatant was dialyzed and analyzed. The band indicated by the arrow was excised from the gel and analyzed by mass spectrometry. SDS-PAGE was stained with Coomassie brilliant blue. **(B)** Pb18_Dld amino acid sequence. **(C)** Conserved domains (available on CDD NCBI's conserved domain database).

Western Blotting

The electrophoresis analyses were performed on 12% SDS–PAGE, and transferred to polyvinylidene fluoride membranes (PVDF)—Hybond membranes Amersham 0.45 P PVDF (GE Healthcare). Thereafter, membranes were incubated with Tris-buffered saline (TBS-T) [20 mM Tris-HCl, 150 mM NaCl and 0.1% (v/v) Tween-20 (pH 7.6)] containing 3% gelatin for 1 h at 25°C, and incubated for 4 h at room temperature with anti-Pb18_rDld polyclonal antibody diluted 1:1,000 in TBS-T containing 1% gelatin. Thereafter, membranes were washed five times with TBS-T and incubated for 2 h at room temperature with the anti-mouse IgG rabbit secondary antibody conjugated to peroxidase (Sigma-Aldrich) diluted 1:500 in TBS-T containing 1% gelatin. Blots were washed five times with TBS-T and then immersed in a fresh mixture of 4-chloro-1-naphthol (4C1N) (Sigma-Aldrich) and 3⁄3-diaminobenzidine tetrahydrochloride (Sigma-Aldrich) or ECL reagent for 1 min to detection of protein using a ChemiDoc MP Imaging System (Bio-Rad, Hercules, USA).

Electron Microscopy

The Pb18_Dld subcellular localization was performed with yeast and mycelia washed with PBS and fixed in 3.7% formaldehyde buffered with PBS at 25°C for 1 h. After fixation, cells were washed with PBS and resuspended in 0.05% glutaraldehyde buffered with PBS and incubated at 25°C. After 15 min, the cells were centrifuged at 5,000 × g for 5 min at 25°C and washed three times with 1 mL of PBS. Then, the cells were resuspended in PBS containing 0.1% Triton X-100 and incubated at 25°C for 45 min. The cells were recovered by centrifugation at 5,000 × *g* for 5 min and washed with 1 mL PBS. Samples were incubated with 1 mL PBS-1% BSA at 25°C. After 45 min, anti-Pb18_rDld polyclonal antibody (1:500) was added for 1 h, followed by incubation at 25°C under gentle agitation. After washing with PBS-1% BSA, colloidal gold-conjugated anti-mouse IgG (Nanoprobes Inc., NY, USA) was added to the cells for 1 h at 25°C under gentle agitation. The cells were washed five times with PBS, with 5 min incubation for each wash and fixed with 2.5% glutaraldehyde in 100 mM cacodylate buffer (pH 7.4) (EM Sciences, Hatfield, USA) at 25°C for 1 h. Cells were washed with cacodylate buffer and incubated at 4°C for 18 h, followed by washing five times with ultrapure water. Further processing of cells was conducted as per the manufacturer's instructions of GoldEnhancement (Nanoprobes). Subsequently, the fixed cells were incubated in 1% OsO_4 (EM Sciences) for 2 h, rinsed in ultrapure water, and incubated with a solution of saturated thiocarbohydrazide (EM Sciences), followed by 1% OsO_4. Yeast cells were dehydrated with ethanol (30–100% v/v) and coated with gold in a BAL-TEC SCD 050 Sputter Coater (BAL-TEC AG, Balzers, Liechtenstein). Finally, the sections were observed with a transmission electron microscope Jeol JEM—100 CXII (JEOL, Peabody, MA, USA).

Macrophages Phagocytic and Microbicidal Activity Assays

Macrophages were obtained from the peritoneal cavity of BALB/c mice 72 h after an intraperitoneal injection of 1 mL of 3% sterile sodium thioglycollate medium (Sigma-Aldrich), according to the described protocol (Freitas et al., 2016). Peritoneal macrophages (1×10^6) were stimulated or not with 10 µg of rPb18_Dld and maintained in a 5% CO_2 humidified atmosphere incubator at 37°C. After 24 h, macrophages were infected with 3×10^5 yeast cells of *P. brasiliensis* and incubated for 4 h at 37°C.

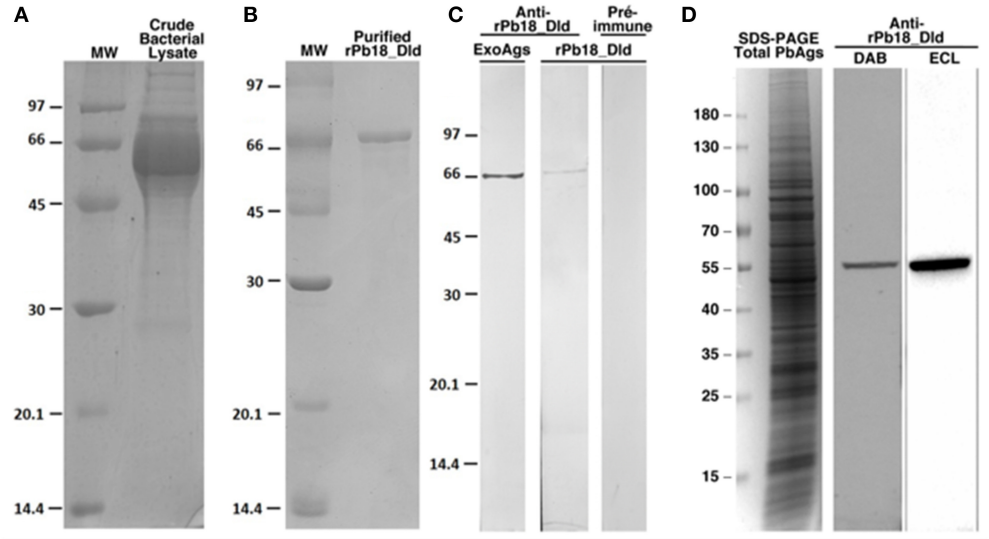

FIGURE 2 | Analysis of the expression and purification of rPb18_Dld, and production of anti-rPB18_Dld polyclonal antibody. SDS-PAGE results of **(A)** rPb18_Dld expression and **(B)** purified rPb18_Dld by affinity chromatography using a liquid chromatographic system, Akta Purifier in HisTrap Crude FF column. The purified protein was dialyzed against PBS. SDS-PAGE was stained with Coomassie brilliant blue. **(C)** Western blotting analysis of anti-rPb18_Dld polyclonal serum. Membranes containing rPb18_Dld or total exoantigens containing native Pb18_Dld (ExoAg) were incubated with serum containing polyclonal anti-rPb18_Dld antibodies. Negative control of the reaction was performed using the membrane containing rPb18_Dld incubated with preimmune serum. The membranes were visualized by peroxide substrate hydrogen and diaminobenzidine tetrahydrochloride. **(D)** SDS-PAGE stained with Coomassie brilliant blue of total soluble antigen from *P. brasiliensis* (Total PbAgs). Western blotting analysis of anti-rPb18_Dld polyclonal serum with membranes containing Total PbAgs were incubated with 1:1,000 containing polyclonal anti-rPb18_Dld antibodies. The membranes were visualized by peroxide substrate hydrogen and diaminobenzidine tetrahydrochloride (DAB) or by chemiluminescent with ECL reagent (ECL).

The cultures were washed with RPMI-incomplete medium. To evaluate the phagocytic activity, 1 mL of distilled water was added to the microplate wells to promote macrophage lysis. The samples were serially diluted and cultured for 10 days at 37°C in solid BHI medium supplemented with 1% glucose to determine the presence of colony forming units (CFU) of viable yeasts. To analyze microbicidal activity, the washed cultures were additionally incubated for 48 h. Macrophage lysis and yeast cultures were carried out as described above. The number of CFU were counted and expressed as CFU/well.

Statistical Analyses

Data are expressed as mean ± standard deviation from at least duplicate experiments. Statistical differences between the means of the experimental groups were determined using the Student's unpaired *t*-test (GraphPad Software, San Diego, USA). Differences with $P < 0.05$ were considered statistically significant.

RESULTS

Identification of Dihydrolipoyl Dehydrogenase (Pb18_Dld) as the Predominant Protein in the *P. brasiliensis* Culture Supernatant

Antigens secreted by *P. brasiliensis* could play an important role in fungus-host interactions. Therefore, we sought to identify new antigens from supernatants after centrifugation of *P. brasiliensis* cultured in DMEM, which is a basal medium that does not contain proteins. When the supernatants were analyzed by SDS-PAGE, we observed that a major band of 60 kDa was invariably present in all ExoAgs preparations (**Figure 1A**), comprising more than 85% of the total protein content. Some minor bands were observed in the supernatants, such as the proteins of 90-, 85-, and 43-kDa, the latter possibly being gp43. One-dimensional nano-LC-MS/MS analysis of tryptic fragments of the 60 kDa protein band revealed two unique peptides that matched the sequence of Pb18_Dld (GenBank accession number EEH50415.1). Pb18_Dld is a protein involved in fungal metabolism (Weber et al., 2012; Parente-Rocha et al., 2015), and is composed of 514 amino acids (**Figure 1B**), with a small NADH binding domain, a larger FAD-binding domain (Pyr_redox), and a dimerization domain (Pyr_redox_dim) (**Figure 1C**).

To confirm the presence of Pb18_DLD in the culture supernatant, we used anti-rPb18_Dld polyclonal antibody. First, we cloned the *Pb18_Dld* gene transcript in an expression plasmid, pET28-a, for the production of the recombinant protein in bacteria (rPb18_Dld) (**Figure 2A**). **Figure 2B** shows the recombinant protein, which was purified using a nickel column for the production of anti-rPb18_Dld polyclonal antibodies in mouse. Use of the anti-recombinant protein antibody revealed the presence of Dld in total soluble antigen from yeast cells, as well as, in *P. brasiliensis* DMEM culture supernatant (**Figures 2C,D**), suggesting that Pb18_Dld is a protein secreted by *P. brasiliensis*.

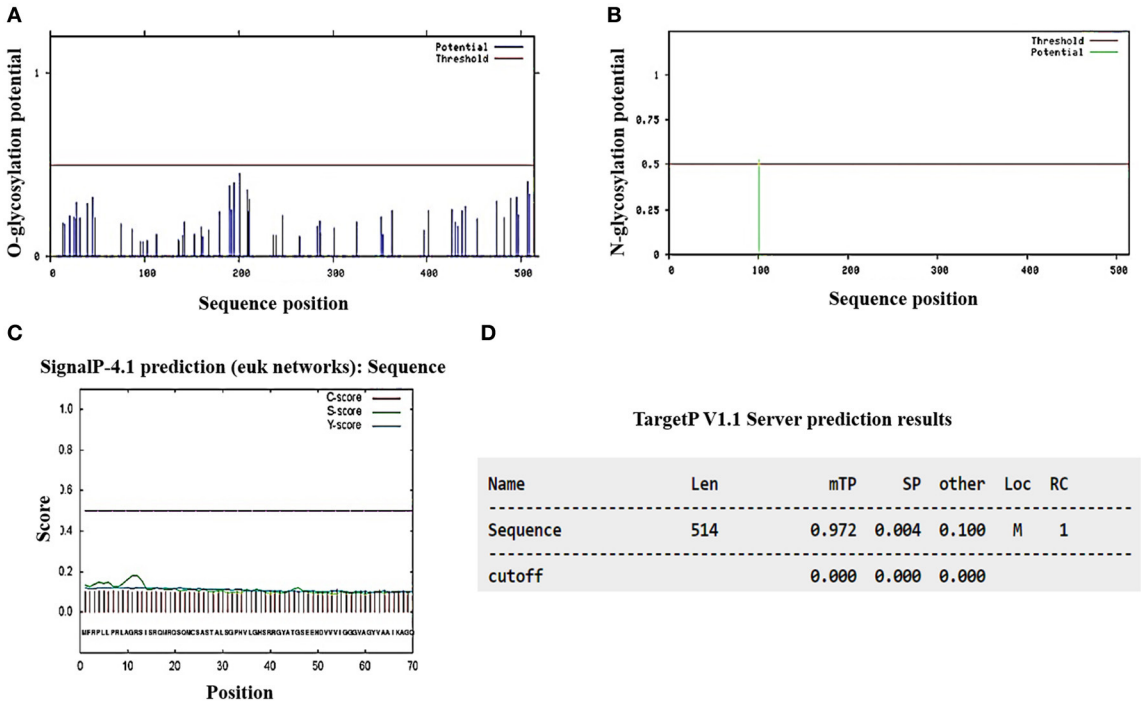

FIGURE 3 | *In silico* analysis of the presence of glycosylation potential sites, signal peptide, and prediction analysis of subcellular location from Pb18_Dld. The amino acid sequence of Pb18_Dld protein was used for analysis in different programs **(A,B)** NetOGlyc 1.0 and NetNGlyc 3.11 show graphics with horizontal lines that represent the reliability limits of the results and vertical lines that indicate the potential sites of O- and N-glycosylation. **(C)** SignalP-4.1 shows graphic with dotted line, representing the reliability limits of results. The lines C, S, and Y-score indicate possible signal peptide cleavage positions and signal peptide regions. **(D)** TargetP v1.1 shows the length (Len), mitochondrial target peptide (mTP), secretory pathway (SP), localization (Loc), mitochondria (M), and reliability class (RC).

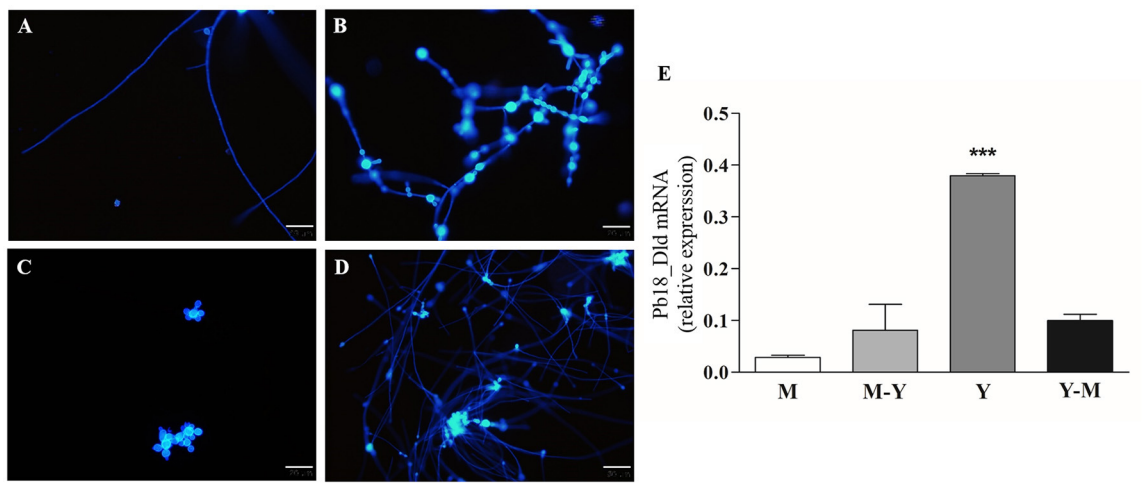

FIGURE 4 | Pb18_Dld mRNA differential expression in different morphological forms of *P. brasiliensis*. **(A–D)** Morphological analysis by fluorescence microscopy. An aliquot of each fungal culture was incubated with Calcofluor white stain solution (50 μg/mL) for labeling the fungal cells. The bars correspond to 20 μm. **(E)** Evaluation of Pb18_Dld mRNA differential expression by RT-qPCR using cDNA from mycelia **(A)**, mycelia-to-yeast **(B)**, yeast **(C)**, and yeast-to-mycelia **(D)**. The β-actin and α-tubulin reference genes were used as endogenous controls to normalize the relative Pb18_Dld mRNA expression.

In Silico Analysis of Pb18_Dld

As part of a complementary analysis to characterize Pb18_Dld, we conducted an *in silico* examination of the protein to check for the presence of putative N- and O-linked oligosaccharides and signal peptides in the amino acid sequence. The analysis revealed that this protein possessed only one putative N-glycosylation site

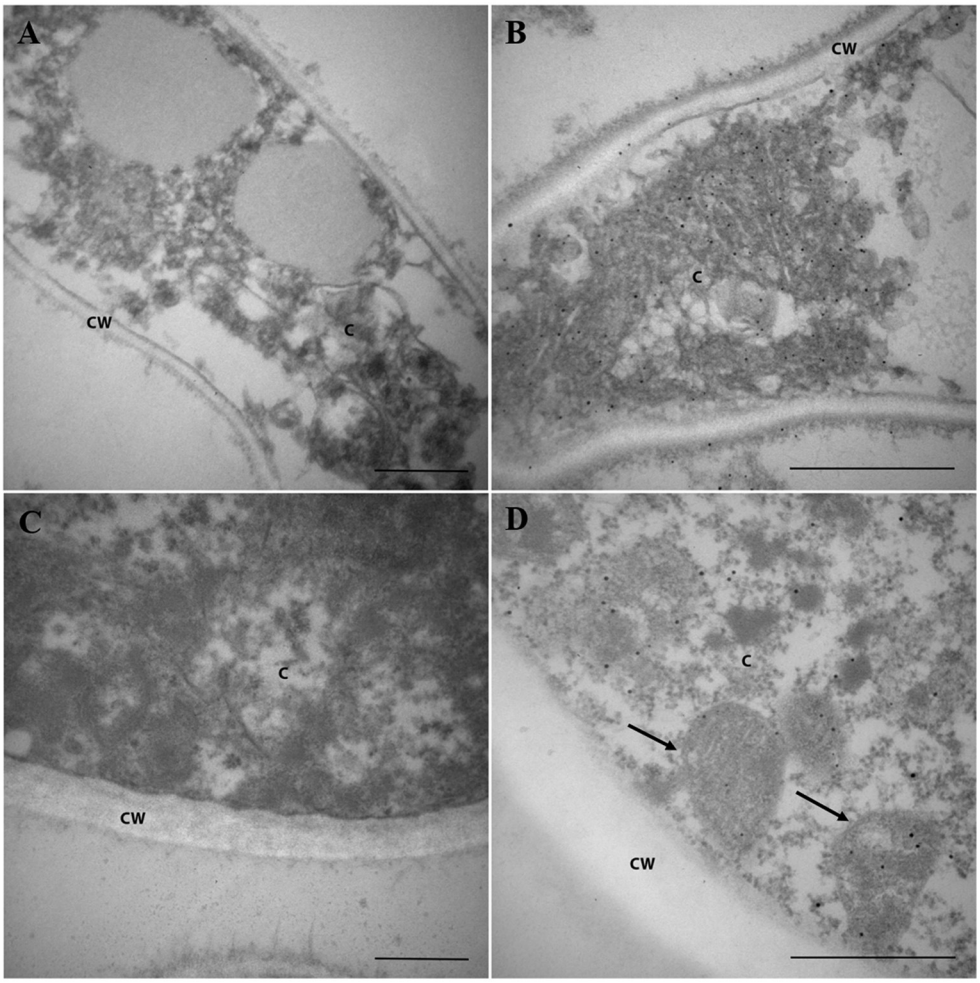

FIGURE 5 | Pb18_Dld localization in mycelia and yeast cells from *P. brasiliensis*, visualized by immunoelectron microscopy. **(A,B)** Mycelium and **(C,D)** yeast from *P. brasiliensis* were labeled with primary polyclonal antibody anti-rPb18_Dld **(B,D)** or pre-immune serum **(A,B)** and secondary antibody conjugated to colloidal gold. The staining of Pb18_Dld was analyzed by electron microscopy. Bars correspond to 2 μm. The C and CW identifications correspond to the cytoplasm and cell wall, respectively. The arrows indicate mitochondria.

in the asparagine residue at the 101 position, no potential site of O-glycosylation (**Figures 3A,B**) and no signal peptide that targeted the protein to the secretory pathway (**Figures 3C,D**). Moreover, the data obtained *in silico* by using TargetP predicted that Pb18_Dld was localized in mitochondria (**Figure 3D**), although it was also identified in the extracellular fraction. Together, these data suggest that Pb18_Dld is a mitochondrial protein that can be secreted via a non-conventional pathway.

Pb18_Dld from *P. brasiliensis* Is Expressed Primarily in Yeast Form

To determine if there were differences in expression levels of Pb18_Dld in yeast, mycelia, and transition forms, we compared normalized mRNA-expression levels among *in vitro* grown phases. Prior to mRNA extraction, we confirmed that the fungal morphology corresponded to expected forms by fluorescence microscopy of samples stained with Calcofluor white (**Figures 4A–D**). Pb18_Dld transcripts were detected in all evaluated morphological forms, although they showed higher expression in yeast, which is the pathogenic form, as compared with levels in transition phases (mycelium-to-yeast and yeast-to-mycelium) or the mycelial form (**Figure 4E**).

Pb18_Dld Subcellular Localization in *P. brasiliensis* Yeast and Mycelia

As Pb18_Dld was a component of ExoAgs and *in silico* analysis of its sequence did not show the signal peptide, we intended to investigate the localization of Pb18_Dld in fungal yeast. Yeast and mycelia of *P. brasiliensis* were fixed and incubated with anti-rPb18_Dld polyclonal mice antibody, and subsequently, incubated with secondary antibody, colloidal gold anti-mouse IgG conjugate, for immunodetection of the protein by electron microscopy. Control samples were obtained by incubation with pre-immune mice serum (**Figures 5A,C**). Electron microscopy assays revealed the ubiquitous distribution of gold particles in

cytoplasm and mitochondria of both forms of *P. brasiliensis* (**Figures 5B,D**). In addition, the protein was also present in the mycelial cell wall (**Figure 5B**). Together, these results are in accordance with the mitochondrial localization predicted by *in silico* analysis, and suggest that Pb18_Dld could be secreted by an alternative secretion pathway.

Phagocytosis of Macrophages is Increased in the Presence of rPb18_Dld

Macrophages comprise one of the primary defense mechanisms against infection by *P. brasiliensis* (Brummer et al., 1988a,b). Additionally, Pb18_Dld showed higher expression in the pathogenic form. Therefore, we evaluated whether this protein could have some effect on the phagocytic and microbicidal activity of macrophages. Phagocytosis and killing assays were performed using peritoneal macrophages. Interestingly, when the cells were pretreated with rPb18_Dld, we observed a significant increase in the phagocytic activity, i.e., after 4 h of co-culture, from 3.98×10^3 CFU/mL $\pm$ 1.28 to 6.9×10^3 CFU/mL $\pm$ 0.30. We also observed an increase in the microbicidal activity i.e., after 48 h of co-culture, with a reduction from 4.18×10^3 CFU/mL $\pm$ 0.71 to 2.6×10^3 CFU/mL $\pm$ 0.78 at rDld-Pb18 stimulated-macrophages, representing relative killing of 62% of yeast cells (**Figure 6**). Together, our data suggest that this protein may be important to improve fungicidal process by macrophages during infection.

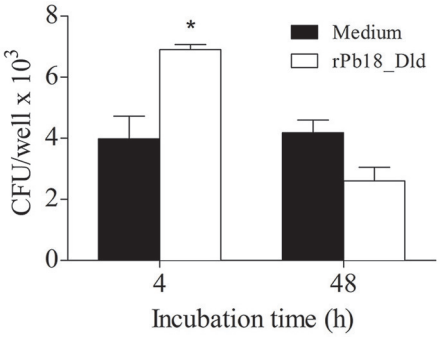

FIGURE 6 | Phagocytic and microbicidal activity of macrophages stimulated with rPb18_Dld. *P. brasiliensis* yeast cells were grown in DMEM medium at 37°C for 5 days and co-cultured with peritoneal macrophages, prestimulated or not with 10 μg of rPb18_rDld. Phagocytic and microbicidal activity were determined by counting the CFU of yeast recovered from the lysate of murine peritoneal macrophages after 4 and 48 h of incubation with yeast at 37°C, respectively. Results represent the mean ± standard deviation values of two independent experiments in triplicate. *$P < 0.05$ in relation to the other experimental groups, as determined by Student *t*-test.

DISCUSSION

In this study, to identify new antigens from *P. brasiliensis* that could be associated with the host, we focused on ExoAgs preparations and isolated a highly expressed protein, identified by mass spectrometry as Pb18_Dld. The fact that Pb18_Dld could be detected in the extracellular extract suggested that it was an ExoAg released by the fungus. This is an intriguing observation because orthologs of this protein were typically detected in the mitochondria. It is part of the machinery responsible for aerobic respiration, in which the pyruvate produced by glycolysis and via the phosphate pentose pathway is mainly oxidized and decarboxylated to acetyl-CoA by the pyruvate dehydrogenase complex (Lehninger et al., 2005). In accordance with its function, our electron microscopy data showed that this enzyme is located in the mitochondria and, interestingly, in the cytoplasm of mycelia and yeast and in the mycelial cell wall. Corroborating our findings, work published by Weber et al. (2012) showed that Dld from *P. lutzii* is a component of extracellular proteomics of mycelial and yeast forms.

The presence of Pb18_Dld and other proteins at the cell surface or outside the fungal cell wall, in the absence of a conventional N-terminal signal sequence responsible for targeting the protein to classical secretory pathway, is an intriguing question. To explain this occurrence, non-conventional secretory pathways, as well as unusual signal sequences, had been described. An example of unusual transport is the extracellular vesicles produced by fungi (Straus et al., 1996). In fact, some enzymes involved in the glycolytic pathway and tricarboxylic acid cycle were identified in the contents of these vesicles (Vallejo et al., 2012).

Carbohydrates are the primary and preferred carbon source used by most organisms (Askew et al., 2009). For survival of pathogens in the hostile host microenvironment, expression of virulence factors and their ability to assimilate various carbon sources for energy production are important (Lorenz et al., 2004; Barelle et al., 2006; Askew et al., 2009; Romani, 2011). Some studies indicate that metabolic remodeling observed in *Paracoccidioides* spp. infection is a survival strategy (Lima et al., 2014). *P. lutzii*, when grown under copper deprivation, showed induction of the pyruvate dehydrogenase complex, suggesting that availability of acetyl-CoA by the generated pyruvate could be important for the survival of *P. lutzii* in inhospitable conditions (de Oliveira et al., 2014). Parente-Rocha et al. (2015) demonstrated that the fungi could modify their metabolism when subjected to conditions that mimic macrophage infection by *P. brasiliensis*. In this study, we observed that there is an increase in the Dld expression in yeast cells, which is the pathogenic form of *P. brasiliensis*.

High Dld expression in the ExoAgs preparation of *P. brasiliensis* raised the possibility that this protein might be a potential virulence factor, facilitating the infection. A common approach for recognition of virulence factors in dimorphic fungi is the correlation with increased expression of the possible factor in the pathogenic form of the fungus (Rappleye and Goldman, 2006). Our results have shown that the expression of Pb18_Dld mRNA is the highest in the yeast morphology, which is the fungal pathogenic form. Similar to Dld, glyceraldehyde-3-phosphate dehydrogenase (GAPDH), a glycolytic enzyme from *P. brasiliensis*, was shown to be present in larger amounts in the parasitic yeast phase than in the mycelia, suggesting a putative role for GAPDH in the parasitic phase of the fungus (Barbosa et al., 2004). Subsequently, it was demonstrated that GAPDH is located at the outermost layer

in the cell wall of *P. brasiliensis* yeast forms, and has adhesive properties (Barbosa et al., 2006). The ability to perform biological functions unrelated to the protein canonical function is common for some metabolic enzymes of *Paracoccidioides* spp. that are frequently involved in virulence (Marcos et al., 2014). When we added rPb18_Dld to cultures of macrophages from the peritoneal cavity, it induced a higher phagocytosis rate. To date, there has been no report regarding the role of this metabolic protein in immune responses of the host. Although our results suggested that Pb18_Dld possibly displayed immunostimulatory effects in host cells, it was undeniable that many molecules induced the activation of macrophages and yet had a deleterious effect on the host (Medzhitov, 2008). Therefore, further experiments are needed before we reject the association of Pb18_Dld with *P. brasiliensis* virulence.

In summary, we demonstrated that Dld, a glycolytic enzyme, which is present in the mitochondria, cytoplasm, and cell wall and is secreted by *P. brasiliensis*, is more prominently expressed in the pathogenic form of the fungus. In addition, this protein stimulates the immune system by increasing the phagocytic and microbicidal activity of macrophages. Although the significance of this protein in disease progression has to be confirmed by virulence tests, for instance, using genetically Pb18_Dld deficient yeast, our work offers a new approach to studying Pb18_Dld as a potential therapeutic target in PCM.

AUTHOR CONTRIBUTIONS

Conceived and designed the experiments: TL, AP, and FF. Performed the experiments: TL, MC, AO, WR, and FF. Analyzed the data: TL, AP, and FF. Contributed reagents/materials/analysis tools: AP and FF. Wrote the paper: TL, AP, and FF.

FUNDING

This work was supported by Fundação de Amparo à Pesquisa de São Paulo (grant numbers 2012/08552-0, 2013/12278-3, and 2016/00629-4).

ACKNOWLEDGMENTS

We thank Andréa Carla Quiapim for technical support in sequencing. We thank Maria Dolores Seabra Ferreira and José Augusto Maulin for technical support in electron microscopy.

REFERENCES

Askew, C., Sellam, A., Epp, E., Hogues, H., Mullick, A., Nantel, A., et al. (2009). Transcriptional regulation of carbohydrate metabolism in the human pathogen *Candida albicans*. *PLoS Pathog.* 5:e1000612. doi: 10.1371/journal.ppat.1000612

Bagagli, E., Theodoro, R. C., Bosco, S. M., and McEwen, J. G. (2008). *Paracoccidioides brasiliensis*: phylogenetic and ecological aspects. *Mycopathologia* 165, 197–207. doi: 10.1007/s11046-007-9050-7

Barbosa, M. S., Bao, S. N., Andreotti, P. F., de Faria, F. P., Felipe, M. S., dos Santos Feitosa, L., et al. (2006). Glyceraldehyde-3-phosphate dehydrogenase of *Paracoccidioides brasiliensis* is a cell surface protein involved in fungal adhesion to extracellular matrix proteins and interaction with cells. *Infect. Immun.* 74, 382–389. doi: 10.1128/IAI.74.1.382-389.2006

Barbosa, M. S., Cunha Passos, D. A., Felipe, M. S., Jesuino, R. S., Pereira, M., and de Almeida Soares, C. M. (2004). The glyceraldehyde-3-phosphate dehydrogenase homologue is differentially regulated in phases of *Paracoccidioides brasiliensis*: molecular and phylogenetic analysis. *Fungal Genet. Biol.* 41, 667–675. doi: 10.1016/j.fgb.2004.02.002

Barelle, C. J., Priest, C. L., Maccallum, D. M., Gow, N. A., Odds, F. C., and Brown, A. J. (2006). Niche-specific regulation of central metabolic pathways in a fungal pathogen. *Cell. Microbiol.* 8, 961–971. doi: 10.1111/j.1462-5822.2005.00676.x

Bocca, A. L., Amaral, A. C., Teixeira, M. M., Sato, P. K., Shikanai-Yasuda, M. A., and Soares Felipe, M. S. (2013). Paracoccidioidomycosis: eco-epidemiology, taxonomy and clinical and therapeutic issues. *Future Microbiol.* 8, 1177–1191. doi: 10.2217/fmb.13.68

Brummer, E., Hanson, L. H., and Stevens, D. A. (1988a). Gamma-interferon activation of macrophages for killing of *Paracoccidioides brasiliensis* and evidence for nonoxidative mechanisms. *Int. J. Immunopharmacol.* 10, 945–952. doi: 10.1016/0192-0561(88)90041-0

Brummer, E., Hanson, L. H., Restrepo, A., and Stevens, D. A. (1988b). *In vivo* and *in vitro* activation of pulmonary macrophages by IFN-gamma for enhanced killing of *Paracoccidioides brasiliensis* or *Blastomyces dermatitidis*. *J. Immunol.* 140, 2786–2789.

Calich, V. L., and Kashino, S. S. (1998). Cytokines produced by susceptible and resistant mice in the course of *Paracoccidioides brasiliensis* infection. *Braz. J. Med. Biol. Res.* 31, 615–623. doi: 10.1590/S0100-879X1998000500003

Calich, V. L., da Costa, T. A., Felonato, M., Arruda, C., Bernardino, S., Loures, F. V., et al. (2008). Innate immunity to *Paracoccidioides brasiliensis* infection. *Mycopathologia* 165, 223–236. doi: 10.1007/s11046-007-9048-1

Carrero, L. L., Nino-Vega, G., Teixeira, M. M., Carvalho, M. J., Soares, C. M., Pereira, M., et al. (2008). New *Paracoccidioides brasiliensis* isolate reveals unexpected genomic variability in this human pathogen. *Fungal Genet. Biol.* 45, 605–612. doi: 10.1016/j.fgb.2008.02.002

Casotto, M. (1990). Characterization of the cellular antigens of *Paracoccidioides brasiliensis* yeast form. *J. Clin. Microbiol.* 28, 1188–1193.

Colombo, A. L., Tobon, A., Restrepo, A., Queiroz-Telles, F., and Nucci, M. (2011). Epidemiology of endemic systemic fungal infections in Latin America. *Med. Mycol.* 49, 785–798. doi: 10.3109/13693786.2011.577821

Coutinho, Z. F., Silva, D., Lazera, M., Petri, V., Oliveira, R. M., Sabroza, P. C., et al. (2002). Paracoccidioidomycosis mortality in Brazil (1980-1995). *Cad. Saúde Publica* 18, 1441–1454. doi: 10.1590/S0102-311X2002000500037

da Silva, A. M., Borba, C. M., and de Oliveira, P. C. (1994). Viability and morphological alterations of *Paracoccidioides brasiliensis* strains preserved under mineral oil for long periods of time. *Mycoses* 37, 165–169. doi: 10.1111/j.1439-0507.1994.tb00295.x

de Almeida, S. M. (2005). Central nervous system paracoccidioidomycosis: an overview. *Braz. J. Infect. Dis.* 9, 126–133. doi: 10.1590/S1413-86702005000200002

de Arruda Grossklaus, D., Bailao, A. M., Vieira Rezende, T. C., Borges, C. L., de Oliveira, M. A., Parente, J. A., et al. (2013). Response to oxidative stress in *Paracoccidioides* yeast cells as determined by proteomic analysis. *Microbes Infect.* 15, 347–364. doi: 10.1016/j.micinf.2012.12.002

de Oliveira, H. C., da Silva Jde, F., Matsumoto, M. T., Marcos, C. M., Peres da Silva, R., Moraes da Silva, R. A., et al. (2014). Alterations of protein expression in conditions of copper-deprivation for *Paracoccidioides lutzii* in the presence of extracellular matrix components. *BMC Microbiol.* 14:302. doi: 10.1186/s12866-014-0302-7

Della Bella, C., Benagiano, M., De Gennaro, M., Gomez-Morales, M. A., Ludovisi, A., D'Elios, S., et al. (2017). T-cell clones in human trichinellosis: evidence for a mixed Th1/Th2 response. *Parasite Immunol.* 39:e12412. doi: 10.1111/pim.12412

Derengowski, L. S., Tavares, A. H., Silva, S., Procopio, L. S., Felipe, M. S., and Silva-Pereira, I. (2008). Upregulation of glyoxylate cycle genes upon *Paracoccidioides brasiliensis* internalization by murine macrophages and *in vitro* nutritional

stress condition. *Med. Mycol.* 46, 125–134. doi: 10.1080/13693780701670509

Diniz, S. N., Cisalpino, P. S., Freire, A. T., Silva-Teixeira, D. N., Contigli, C., Rodrigues Junior, V., et al. (2001). *In vitro* granuloma formation, NO production and cytokines profile from human mononuclear cells induced by fractionated antigens of *Paracoccidioides brasiliensis*. *Hum. Immunol.* 62, 799–808. doi: 10.1016/S0198-8859(01)00268-3

Diniz, S. N., Cisalpino, P. S., Koury, M. C., Andrade, G. M., Nogueira, M. G., and Goes, A. M. (1999). *In vitro* human immune reactivity of fast protein liquid chromatography fractionated *Paracoccidioides brasiliensis* soluble antigens. *Microbes Infect.* 1, 353–360. doi: 10.1016/S1286-4579(99)80051-3

Fernandes, F. F., Oliveira, L. L., Landgraf, T. N., Peron, G., Costa, M. V., Coelho-Castelo, A. A., et al. (2016). A detrimental effect of fungal 60-kDa heat shock protein on experimental *Paracoccidioides brasiliensis* infection. *PLoS ONE* 11:e0162486. doi: 10.1371/journal.pone.0162486

Freitas, M. S., Oliveira, A. F., da Silva, T. A., Fernandes, F. F., Goncales, R. A., Almeida, F., et al. (2016). Paracoccin induces M1 polarization of macrophages via interaction with TLR4. *Front. Microbiol.* 7:1003. doi: 10.3389/fmicb.2016.01003

Gesztesi, J. L., Puccia, R., Travassos, L. R., Vicentini, A. P., de Moraes, J. Z., Franco, M. F., et al. (1996). Monoclonal antibodies against the 43,000 Da glycoprotein from *Paracoccidioides brasiliensis* modulate laminin-mediated fungal adhesion to epithelial cells and pathogenesis. *Hybridoma* 15, 415–422. doi: 10.1089/hyb.1996.15.415

Goldman, G. H., dos Reis Marques, E., Duarte Ribeiro, D. C., de Souza Bernardes, L. A., Quiapin, A. C., Vitorelli, P. M., et al. (2003). Expressed sequence tag analysis of the human pathogen *Paracoccidioides brasiliensis* yeast phase: identification of putative homologues of *Candida albicans* virulence and pathogenicity genes. *Eukaryotic Cell* 2, 34–48. doi: 10.1128/EC.2.1.34-48.2003

Lehninger, A. L., Nelson, D. L., and Cox, M. M. (2005). *Lehninger Principles of Biochemistry, 4th Edn*. New York, NY: W. H. Freeman.

Lima P. S., Casaletti, L., Bailao, A. M., de Vasconcelos, A. T., Fernandes Gda, R., and Soares, C. M. (2014). Transcriptional and proteomic responses to carbon starvation in *Paracoccidioides*. *PLoS Negl. Trop. Dis.* 8:e2855. doi: 10.1371/journal.pntd.0002855

Lorenz, M. C., Bender, J. A., and Fink, G. R. (2004). Transcriptional response of *Candida albicans* upon internalization by macrophages. *Eukaryotic Cell* 3, 1076–1087. doi: 10.1128/EC.3.5.1076-1087.2004

Marcos, C. M., de Oliveira, H. C., da Silva Jde, F., Assato, P. A., Fusco-Almeida, A. M., and Mendes-Giannini, M. J. (2014). The multifaceted roles of metabolic enzymes in the Paracoccidioides species complex. *Front. Microbiol.* 5:719. doi: 10.3389/fmicb.2014.00719

Matute, D. R., McEwen, J. G., Puccia, R., Montes, B. A., San-Blas, G., Bagagli, E., et al. (2006). Cryptic speciation and recombination in the fungus *Paracoccidioides brasiliensis* as revealed by gene genealogies. *Mol. Biol. Evol.* 23, 65–73. doi: 10.1093/molbev/msj008

Medzhitov, R. (2008). Origin and physiological roles of inflammation. *Nature* 454, 428–435. doi: 10.1038/nature07201

Oliveira, S. J., Mamoni, R. L., Musatti, C. C., Papaiordanou, P. M., and Blotta, M. H. (2002). Cytokines and lymphocyte proliferation in juvenile and adult forms of paracoccidioidomycosis: comparison with infected and non-infected controls. *Microbes Infect.* 4, 139–144. doi: 10.1016/S1286-4579(01)01521-0

Panunto-Castelo, A., Freitas-da-Silva, G., Bragheto, I. C., Martinez, R., and Roque-Barreira, M. C. (2003). *Paracoccidioides brasiliensis* exoantigens: recognition by IgG from patients with different clinical forms of paracoccidioidomycosis. *Microbes Infect.* 5, 1205–1211. doi: 10.1016/j.micinf.2003.07.008

Parente-Rocha, J. A., Parente, A. F., Baeza, L. C., Bonfim, S. M., Hernandez, O., McEwen, J. G., et al. (2015). Macrophage interaction with *Paracoccidioides brasiliensis* yeast cells modulates fungal metabolism and generates a response to oxidative stress. *PLoS ONE* 10:e0137619. doi: 10.1371/journal.pone.0137619

Rappleye, C. A., and Goldman, W. E. (2006). Defining virulence genes in the dimorphic fungi. *Annu. Rev. Microbiol.* 60, 281–303. doi: 10.1146/annurev.micro.59.030804.121055

Romani, L. (2004). Immunity to fungal infections. *Nat. Rev. Immunol.* 4, 1–23. doi: 10.1038/nri1255

Romani, L. (2011). Immunity to fungal infections. *Nat. Rev. Immunol.* 11, 275–288. doi: 10.1038/nri2939

Straus, A. H., Freymuller, E., Travassos, L. R., and Takahashi, H. K. (1996). Immunochemical and subcellular localization of the 43 kDa glycoprotein antigen of *Paracoccidioides brasiliensis* with monoclonal antibodies. *J. Med. Vet. Mycol.* 34, 181–186. doi: 10.1080/02681219680000301

Tavares, A. H., Silva, S. S., Dantas, A., Campos, E. G., Andrade, R. V., Maranhao, A. Q., et al. (2007). Early transcriptional response of *Paracoccidioides brasiliensis* upon internalization by murine macrophages. *Microbes Infect.* 9, 583–590. doi: 10.1016/j.micinf.2007.01.024

Teixeira, M. M., Theodoro, R. C., de Carvalho, M. J., Fernandes, L., Paes, H. C., Hahn, R. C., et al. (2009). Phylogenetic analysis reveals a high level of speciation in the *Paracoccidioides* genus. *Mol. Phylogenet. Evol.* 52, 273–283. doi: 10.1016/j.ympev.2009.04.005

Teixeira, M. M., Theodoro, R. C., Nino-Vega, G., Bagagli, E., and Felipe, M. S. (2014). *Paracoccidioides* species complex: ecology, phylogeny, sexual reproduction, and virulence. *PLoS Pathog.* 10:e1004397. doi: 10.1371/journal.ppat.1004397

Theodoro, R. C., Teixeira Mde, M., Felipe, M. S., Paduan Kdos, S., Ribolla, P. M., San-Blas, G., et al. (2012). Genus paracoccidioides: species recognition and biogeographic aspects. *PLOS ONE* 7:e37694. doi: 10.1371/journal.pone.0037694

Torres, I., Hernandez, O., Tamayo, D., Munoz, J. F., Leitao, N. P. Jr., Garcia, A. M., et al. (2013). Inhibition of PbGP43 expression may suggest that gp43 is a virulence factor in *Paracoccidioides brasiliensis*. *PLoS ONE*8:e68434. doi: 10.1371/journal.pone.0068434

Vallejo, M. C., Nakayasu, E. S., Matsuo, A. L., Sobreira, T. J., Longo, L. V., Ganiko, L., et al. (2012). Vesicle and vesicle-free extracellular proteome of *Paracoccidioides brasiliensis*: comparative analysis with other pathogenic fungi. *J. Proteome Res.* 11, 1676–1685. doi: 10.1021/pr200872s

Vicentini, A. P., Gesztesi, J. L., Franco, M. F., de Souza, W., de Moraes, J. Z., Travassos, L. R., et al. (1994). Binding of *Paracoccidioides brasiliensis* to laminin through surface glycoprotein gp43 leads to enhancement of fungal pathogenesis. *Infect. Immun.* 62, 1465–1469.

Weber, S. S., Parente, A. F., Borges, C. L., Parente, J. A., Bailao, A. M., and de Almeida Soares, C. M. (2012). Analysis of the secretomes of *Paracoccidioides mycelia* and yeast cells. *PLoS ONE* 7:e52470. doi: 10.1371/journal.pone.0052470

Conflict of Interest Statement: The authors declare that the research was conducted in the absence of any commercial or financial relationships that could be construed as a potential conflict of interest.

The reviewer SB and handling Editor declared their shared affiliation, and the handling Editor states that the process nevertheless met the standards of a fair and objective review.

Copyright © 2017 Landgraf, Costa, Oliveira, Ribeiro, Panunto-Castelo and Fernandes. This is an open-access article distributed under the terms of the Creative Commons Attribution License (CC BY). The use, distribution or reproduction in other forums is permitted, provided the original author(s) or licensor are credited and that the original publication in this journal is cited, in accordance with accepted academic practice. No use, distribution or reproduction is permitted which does not comply with these terms.

frontiers in Immunology

ORIGINAL RESEARCH
published: 07 June 2017
doi: 10.3389/fimmu.2017.00629

Candida albicans Yeast, Pseudohyphal, and Hyphal Morphogenesis Differentially Affects Immune Recognition

Liliane Mukaremera[1,2†], Keunsook K. Lee[1†], Hector M. Mora-Montes[3] and Neil A. R. Gow[1]*

[1]*Aberdeen Fungal Group, Institute of Medical Sciences, Foresterhill, University of Aberdeen, Aberdeen, United Kingdom,*
[2]*Department of Microbiology and Immunology, Medical School, University of Minnesota, Minneapolis, MN, United States,*
[3]*Departamento de Biología, División de Ciencias Naturales y Exactas, Universidad de Guanajuato, Guanajuato, Mexico*

OPEN ACCESS

Edited by:
Steven Templeton, Indiana University School of Medicine – Terre Haute, United States

Reviewed by:
Michael K. Mansour, Massachusetts General Hospital, United States
Michail Lionakis, National Institute of Allergy and Infectious Diseases, United States

***Correspondence:**
Neil A. R. Gow
n.gow@abdn.ac.uk

[†]These authors have contributed equally to this work.

Specialty section:
This article was submitted to Microbial Immunology, a section of the journal Frontiers in Immunology

Received: *10 March 2017*
Accepted: *12 May 2017*
Published: *07 June 2017*

Citation:
Mukaremera L, Lee KK, Mora-Montes HM and Gow NAR (2017) Candida albicans Yeast, Pseudohyphal, and Hyphal Morphogenesis Differentially Affects Immune Recognition. Front. Immunol. 8:629. doi: 10.3389/fimmu.2017.00629

Candida albicans is a human opportunist pathogen that can grow as yeast, pseudohyphae, or true hyphae *in vitro* and *in vivo*, depending on environmental conditions. Reversible cellular morphogenesis is an important virulence factor that facilitates invasion of host tissues, escape from phagocytes, and dissemination in the blood stream. The innate immune system is the first line of defense against *C. albicans* infections and is influenced by recognition of wall components that vary in composition in different morphological forms. However, the relationship between cellular morphogenesis and immune recognition of this fungus is not fully understood. We therefore studied various vegetative cell types of *C. albicans*, singly and in combination, to assess the consequences of cellular morphogenesis on selected immune cytokine outputs from human monocytes. Hyphae stimulated proportionally lower levels of certain cytokines from monocytes per unit of cell surface area than yeast cells, but did not suppress cytokine response when copresented with yeast cells. Pseudohyphal cells induced intermediate cytokine responses. Yeast monomorphic mutants had elevated cytokine responses under conditions that otherwise supported filamentous growth and mutants of yeast and hyphal cells that were defective in cell wall mannosylation or lacking certain hypha-specific cell wall proteins could variably unmask or deplete the surface of immunostimulatory ligands. These observations underline the critical importance of *C. albicans* morphology and morphology-associated changes in the cell wall composition that affect both immune recognition and pathogenesis.

Keywords: ***Candida albicans*, cell wall, cytokine, immune recognition, morphogenesis**

INTRODUCTION

Fungal pathogens are associated with a wide range of human diseases from superficial infections of the skin and mucosal surfaces to life-threatening systemic infections, depending on host health and immunocompetence. *Candida* species account collectively for as many as 400,000 cases of systemic fungal disease with associated mortality rates of up to 40% (1–4). Of these species, *Candida albicans* is the most common agent of disease and is characterized by its morphological plasticity. It is capable of vegetative growth *in vitro* and *in vivo* as ovoid budding yeast-like cells and as branching filamentous cells that exist as more or less elongated and constricted chains of yeast cells called pseudohyphae

or parallel-sided hyphal cells (5–10). Other cell types, such as GUT, gray, and opaque cells, are a tristable system of specialized cells involved in colonization of specific body sites and in mating competence (10). We set out to characterize differences in the immune response by human peripheral blood mononuclear cells (PBMCs) to yeast cells, hyphae, and pseudohyphae as the three major morphological forms of *C. albicans*.

The innate immune system is the first line of defense against all invading organisms and plays a major role in resistance to infectious diseases in immunocompetent hosts (11). Phagocytes detect microbial pathogen-associated molecular patterns (PAMPs) *via* pattern-recognition receptors (PRRs), resulting in signaling-mediated transcription and secretion of inflammatory mediators, such as chemokines and cytokines that recruit neutrophils and other immune cells to the site of infection, resulting in localized killing of the pathogen and activation of the adaptive immune response (11–13).

C. albicans PAMPs that activate the inflammatory response are located in both the outer and inner layers of the intact cell wall (4, 11, 14–16). Mannans and glucans are the main elicitors of both cytokine production and phagocytosis and are recognized by a range of C-type lectins and toll-like receptors (TLRs) (4, 17–21). The *O*-linked mannans are sensed through the TLR4 receptor (17), β-mannan is recognized by galectin-3 (22–25), and α-linked *N*-mannans are recognized by the mannose receptor (MR), dectin-2, mincle, and DC-SIGN (21, 26). Opsonized β1,6-glucan acts as an immune agonist (27), and chitin is taken up by the MR and induces TLR9- and NOD2-dependent IL-10 production (4, 28).

Most immune recognition studies have focused on *C. albicans* yeast cells as the cell target; however, it is known that filamentous hyphal cells induce an altered immune response (4, 6, 8, 21, 29–32). The switch between yeast and hyphal growth is critical for virulence (6, 8, 33, 34), affecting numerous properties including the expression of morphology-dependent cell wall adhesins, invasins, proteases, and a raft of other phenotypic and biochemical properties, including the recently discovered candidalysin toxin (35). Mutants locked in either the yeast or hypha form are avirulent, suggesting that the ability to transit reversibly between these morphotypes potentiate the virulence of this fungus (7, 33, 35–40). Pseudohyphae are a distinct growth form that differs from both yeast cells and parallel-sided hyphae and are characterized by synchronously dividing elongated yeast cells (5, 7, 41, 42). Although pseudohyphal forms are generated by a wide range of *Candida* species, we know little about the immune response to pseudohyphal cells.

It is therefore important to understand the consequences of cellular morphogenesis of *C. albicans* on immune recognition and the activation of inflammation. Here, we demonstrate that *C. albicans* hyphae stimulated lower levels of cytokine production from human PBMCs than did yeast cells, but did not suppress the immune response of yeast cells in trans. Pseudohyphae elicited intermediate cytokine profiles between those of yeast and hyphae and again did not suppress yeast-induced cytokines. We also demonstrate that cell wall mannosylation and certain hypha-specific cell wall proteins affect morphology-dependent recognition by PBMCs.

MATERIALS AND METHODS

Strains, Media, and Culture Conditions Inducing Cellular Morphogenesis

Strains used in this work are listed in Table S1 in Supplementary Material. Cells were maintained and propagated at 30°C in either Sabouraud broth [1% (w/v) mycological peptone, 4% (w/v) glucose] or YPD broth [1% (w/v) yeast extract, 2% (w/v) mycological peptone, 2% (w/v) glucose]. The immune reposes to hyphae induced by multiple independent growth conditions were compared. Hyphae were generated using multiple independent methods: (i) 20% (v/v) fetal calf serum (FCS) or in RPMI 1640 supplemented with 2.5% (v/v) FCS, (ii) in YPD broth supplemented with 20% (v/v) FCS, (iii) in SC broth [0.68% (w/v) yeast nitrogen base without amino acids, 0.074% (w/v) amino acids buffered with 0.378% (w/v) PIPES] supplemented with 0.012% (w/v) fresh *N*-acetylglucosamine (GlcNAc), or (iv) in Lee's medium (43). Cultures were collected for use when greater 90–95% filamentation was obtained (typically after 3.5 h of incubation at 37°C). Hyphae were then washed twice in PBS and stored frozen at −20°C until used in cytokine induction experiments.

C. albicans pseudohyphae were produced using conditions published previously with modifications (41). Overnight cultures of *C. albicans* were collected by centrifugation, washed twice with 0.15 M NaCl, resuspended in 0.15 M NaCl, and incubated at room temperature for 24 h to induce starvation. After 24-h starvation, cells were inoculated into RPMI 1640 at a final concentration of 1×10^6 cells/ml and incubated at 25, 30, or 37°C with shaking for 6 h. Under these conditions, the vegetative morphology could be regulated by growth temperature alone, with yeast cells formed at 25°C, pseudohyphae at 30°C, and true hyphae at 37°C. Heat-killed (HK) cells were prepared after incubation at 56°C for 1 h, with killing verified by plating on YPD.

Samples of cells were fixed in 5% (v/v) formalin for morphological and microscopical analyses. All photomicrographs were taken on an Olympus BX50 outfitted with an Infinity 1 digital camera. Morphology indices, which are a measure of the extent of cellular elongation and hence discrimination of constricted pseudohyphae from parallel-sided hyphae, were determined as published (41). All measurements were made using the measurement tool in ImageJ 1.47v (http://imagej.nih.gov/ij), and MIs were calculated in Microsoft Excel.

Calculation of the Surface Area (SA) of Fungal Cells

The SA of all cells was based on microscopical measurements made from DIC images using a Zeiss Axioplan 2 microscope and captured by a Hamamatsu C4742-95 digital camera (Hamamatsu Photonics, Hamamatsu, Japan). All measurements created by ImageJ were exported in Microsoft Excel. The SA of yeast cells was calculated based on measurements of the radius calculated from the average of the largest and smallest cell diameters of yeast cells ($4\pi r^2$). Germ tube SA was taken as the SA of the mother yeast plus the SA of the daughter germ tube (true hypha). Hypha SA based on SA ($2\pi r^2 + 2\pi rl$) where the germ tube length (l) was measured from the base of the mother cell and the germ tube diameter was the average

of the narrowest and widest diameter measurements made along each germ tube. At least 50 measurements, and 3–4 biological replicates, of SA of individual yeast and hyphal cells grown were made.

Cytokine Stimulation Assays

Blood samples were collected from healthy volunteers according to local guidelines and regulations, as approved by the College Ethics Review Board of the University of Aberdeen (CERB/2012/11/676). The PBMCs were used in this study and isolated using Ficoll-Paque™ PLUS (GE Healthcare) as previously described (44), with slight modifications. Unless otherwise indicated, 5×10^5 PBMCs in 100 µl were incubated in a round-bottom 96-well plate (Nunc) with 100 µl of fungal cells at 1×10^6 cells/ml. After incubation for 24 h at 37°C under 5% (v/v) CO_2, plates were centrifuged at 1,000 *g* for 10 min at room temperature, and supernatants were saved and kept at −20°C until use. For cytokine assays using mixed *C. albicans* cell types, PBMCs were first pre-incubated with 50 µl of cells of one morphology at 2×10^6 cells/ml for 1 h at 37°C under 5% (v/v) CO_2. Subsequently, 50 µl of a sample containing a second sample of yeast or hyphae cells at 2×10^6 cells/ml were added to PBMCs. Plates were then incubated for a further 24 h at 37°C, before supernatant collection and assay of induced cytokines. In experiments with PBMCs, the inoculum of hyphal cells was more or less aggregated. To assess the effect of cell aggregates on the cytokine stimulation, control experiments where hyphae were dispersed by ultrasonication before interaction with immune cells were performed, but theses did not show any significant differences with cultures of non-sonicated cells (data not shown). Therefore, steric blocking of monocyte access to fungal material did not explain the reduced response to hyphae that was observed.

TNFα, IL-1α, IL-1β, IL-6, and IL-10 concentrations were determined from coculture supernatants. For IL-1α quantification, stimulated PBMCs were disrupted by three sequential temperature shock cycles, and homogenates used for cytokine determination. All cytokine concentrations were determined using enzyme-linked immunosorbent assays (R&D Systems) according to the manufacturer's instructions.

Cell Wall Extraction and Analysis

C. albicans cells of different morphology were prepared as described above. Cells were collected by low-speed centrifugation and washed with ultrapure water, then broken using glass beads and a FastPrep machine (Qbiogene), homogenates were centrifuged at 13,000 *g* for 3 min, and pellets, containing the cell debris and walls, were washed five times with 1 M NaCl, resuspended in cell wall extraction buffer [50 mM Tris–HCl buffer pH 7.5, 2% (w/v) SDS, 0.3 M β-mercaptoethanol, and 1 mM EDTA], then boiled for 10 min, and washed three times with ultrapure water. Cell walls were freeze dried and stored at −20°C until used. The β-glucan, mannan, and chitin contents of cell wall preparations were determined by acid hydrolysis of the polymers and quantification of glucose, mannose, and glucosamine. Freeze-dried cell walls were hydrolyzed with 2 M trifluoroacetic acid as described previously (45), and acid hydrolyzates were analyzed by HPAEC-PAD (high-performance anion-exchange chromatography with pulsed amperometric detection) (46).

hPBMC Cell Damage Assay

Human PBMC damage was assessed by lactate dehydrogenase (LDH) released into the supernatant in the culture medium. After 24 h stimulation with *C. albicans* either heat-killed yeast (HKY) or HKH over a range of MOIs (*Candida* cells:hPBMCs) from 0.002:1 to 2:1. The LDH release was determined using the cytotoxicity detection kit (Roche Applied Science), according to the manufacturer's instructions. As a negative control for LDH release, 5×10^5 cells of hPBMCs were incubated with only the cell culture medium and incubated at 37°C with 5% CO_2 for 24 h. For the positive control maximum LDH release, 5×10^5 cells of hPBMCs was obtained by treatment with 2% Triton X-100 and incubated under the same conditions. The percentage of LDH release was calculated relative to the value for 100% cell death.

Statistical Analyses

The Mann–Whitney *U* test, *t*-test, or one-way ANOVA with a Dunnett's *post hoc* test in an appropriate parameter was used to analyze data. Results are presented as means ± SDs or SEMs and levels of significance determined at $p < 0.05$.

RESULTS

Differential Cytokine Induction by Yeast and Filamentous Cell Types

We used the cytokine response of human PBMCs as a read out to investigate the role of *C. albicans* morphogenesis on immune recognition. The cytokine profile of human PBMCs was compared when these immune cells were exposed to yeast cells and filamentous forms (true hyphae and pseudohyphae) of *C. albicans*. Yeast, pseudohyphal, and hyphal cells could all be induced *in vitro* using various culture conditions that preferentially stimulated a specific *C. albicans* cell morphology. Live and HK cells of different cell morphologies were also analyzed in our study. Across a wide range of conditions, heat killing increased the total amount of TNFα and other cytokines induced by yeast cells, and to a lesser extent, filamentous cells (**Figure 1**), suggesting that heat-treatment unmasks cytokine inducing PAMPs due to thermal disruption of components of the outer layer of the cell wall, thus exposing internal cytokine inductive cell layers to PRRs found on the surface of human PBMCs.

Under the conditions employed, more than 99% of yeast cells were obtained at 25°C and more than 94% of hyphae with at least two cell compartments were generated at 37°C (data not shown). Cell for cell, HK yeast cells induced significantly more TNFα than hyphal cells (**Figure 1A**). Germ tubes/hyphae induced less TNFα despite the presence of the parent yeast cell, implying that hypha formation may suppress TNFα production that would be normally associated with the cell surface of HK yeast cells (**Figures 1A–C** and **3**).

TNFα production induced by *C. albicans* was dose dependent (**Figure 1B**). Live yeast cells stimulated lower cytokine production compared to HK yeast cells—a difference that was less apparent when comparing live and HK true hyphal cells (**Figure 1B**). Both live and HK hyphae stimulated poor TNFα production compared to that of HK yeast cells (**Figures 1B,C**). In addition, LDH activity

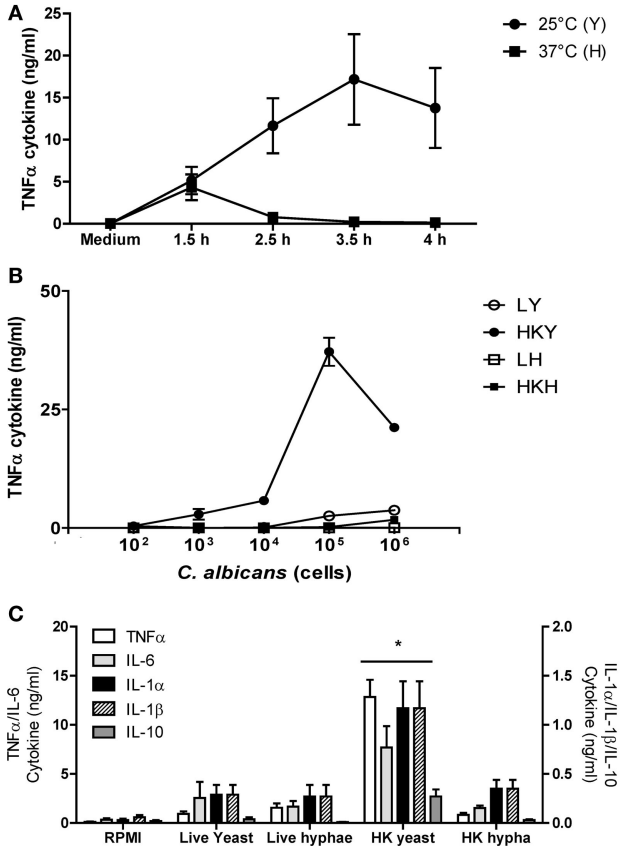

FIGURE 1 | TNFα stimulation with *Candida albicans* yeast and hyphal cells by human peripheral blood mononuclear cells (PBMCs). **(A)** Cytokine production by human PBMCs stimulated with yeasts cells (Y) of *C. albicans* NGY152 grown at 25°C (closed circles) or hyphae (H) grown at 37°C (closed squares) in RPMI 1640 + 2.5% fetal calf serum (FCS). Error bars = SEM ($n = 3$). **(B)** Dose-dependent stimulation of TNFα production by human PBMCs when stimulated with different forms of *C. albicans* NGY152 grown in RPMI 1640 + 2.5% FCS. Heat-killed yeasts (HKY), closed circles; live yeasts (LY), open circles; HK hyphae (HKH), closed squares; live hyphae (LH), open squares. Error bars = SEM ($n = 6$). In these experiments, a total of 5×10^5 PBMCs were used in each treatment and so the MOI varied from 0.0002:1 to 2:1. **(C)** Cytokine production by human PBMCs stimulated with the different morphological forms of *C. albicans* NGY152. In each treatment, an inoculum of 1×10^6 cells/ml was used. Results are means ± SEM ($n = 6$; $^*p < 0.05$).

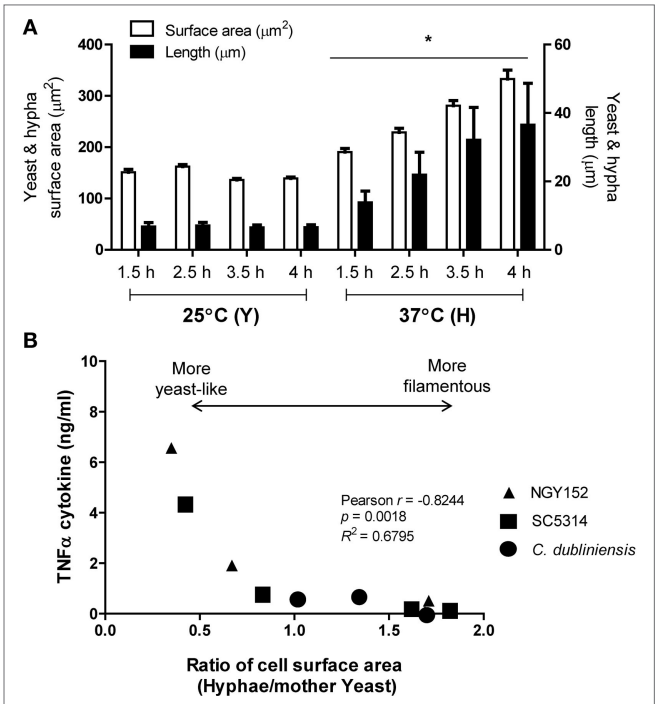

FIGURE 2 | Cell surface area (SA) of hyphal forming cells negatively correlated with TNFα stimulation. **(A)** Cell SA and cell size of *Candida albicans* SC5314 yeast (Y) or hyphae (H) grown at either 25 or 37°C for 1.5, 2.5, 3.5, and 4 h ($^*p < 0.05$). Error bars are SEM ($n > 50$ individual cells). **(B)** Relationship between TNFα production and extent of cell elongation expressed as the ratio of the hyphal cell area and the mother yeast cell area for *C. albicans* SC5314 and NGY152, and *Candida dubliniensis* CD36.

released into the supernatant was measured after 24 h stimulation with *C. albicans* HKY or HKH. There was no significant difference between *C. albicans* stimulated and non-stimulated hPBMCs (Figure S1 in Supplementary Material). Therefore, although TNFα production by hPBMCs incubated with 1×10^6 cells of HKY was significantly reduced, this was not due a loss of viability of hPBMCs. Similar results were obtained for a range of other cytokines, including IL-1α, IL-1β, IL-6, and IL-10 (**Figure 1C**).

We next investigated how hypha cell SA correlated with TNFα production by human PBMCs. Cell SA and cell size (diameter or length) of *C. albicans* yeast and hyphae were calculated assuming yeast cells were elliptical spheres, and germ tubes were parallel-sided cylinders. The size and SA of yeast plus associated germ tubes cells grown at 25 and 37°C are shown in **Figure 2A**. SA and length of hyphae increased by time. Under these conditions (at 3.5 h) of growth, yeasts had a mean diameter of 6.6 ± 0.1 μm (mean ± SEM) and mean SA of 136 ± 3.1 μm², respectively (**Figure 2A**). Hyphae had approximately twofold increased SA and were fivefold longer than the yeast cell diameter at the time cells were harvested. These values are comparable with those in previous reports (47). The average growth rate of hyphae grown in RPMI1640 plus 2.5% serum was 9.0 ± 1.1 μm/h. For *C. albicans* strains SC5314, NGY152, and the hypha-forming species *Candida dubliniensis* (strain CD36), there was a negative correlation between hypha to yeast cell surface ratio and TNFα production by human PBMCs (**Figure 2B**). Longer hyphae induced progressively less TNFα production per unit of cell surface (data not shown). We conclude that hyphae induce less TNFα than yeast cells and that the hypha surface may in some way suppress TNFα production by the cell wall of the attached parent yeast cell or that the yeast cell wall may be modified during the process of germ tube formation, so that it becomes less inductive of cytokine formation.

Hypha Formation and Cytokine Induction by Human PBMCs

In order to confirm whether this observation was indeed related to cell morphology rather than the growth conditions used to

generate yeast and hyphae, we compared the immune response of hyphae generated in different growth media. Live and HK hyphae generated in either YPD medium supplement with FCS, Lee's medium, minimal medium (SC) added with GlcNAc, or in dilute FCS, were universally poorer inducers of TNFα, IL-1α, IL-1β, IL-6, and IL-10 (Table S1 in Supplementary Material) than yeast cells. Therefore, the reduced ability of *C. albicans* hyphae to stimulate cytokine production was independent of the hyphal-inducing growth conditions used.

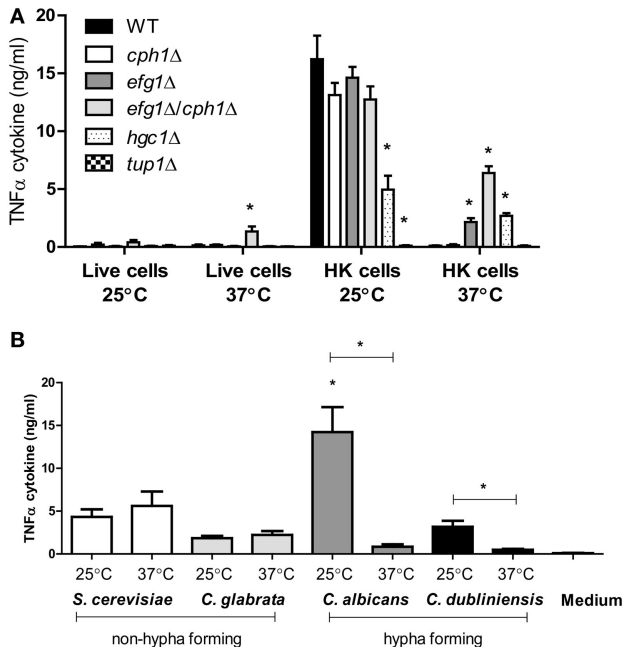

FIGURE 3 | TNFα production by human peripheral blood mononuclear cells stimulated with morphological mutants of *Candida albicans* mutants or other yeast species. **(A)** *C. albicans* NGY152 (WT), JKC19 (*cph1*Δ), HLC52 (*efg1*Δ), HLC54 (*cph1*Δ/*efg1*Δ), WYZ12.2 (*hgc1*Δ), and Bca2-10 (*tup1*Δ). Results are means ± SEM ($n = 6$; *$p < 0.05$). **(B)** TNFα stimulation by non-hypha-forming species *Saccharomyces cerevisiae* (S288C) and *Candida glabrata* (ATCC 2001) compared to hypha-forming species *C. albicans* (NGY152) and *Candida dubliniensis* (CD36) (*$p < 0.05$). Error bars = SEM ($n = 9$).

Next, we investigated the TNFα simulation by yeast cells of *Candida glabrata* and *Saccharomyces cerevisiae* (48), which, unlike *C. albicans* and *C. dubliniensis*, are not able to form hyphae or pseudohyphae. Yeast cells of *S. cerevisiae*, *C. glabrata*, and *C. dubliniensis* stimulated comparable levels of TNFα cytokine when grown at 25 and 37°C (**Figure 3B**). *C. dubliniensis* yeast cells induced less TNFα than *C. albicans*, when grown at 25°C. However, as with *C. albicans*, *C. dubliniensis* yeast grown at 25°C induced more cytokine than hyphae grown at 37°C. Therefore, the hyphae of both *C. albicans* and *C. dubliniensis* stimulated less TNFα than the respective yeast form.

We then assessed the ability of various mutants that regulate morphogenesis to stimulate cytokine production. The *cph1*Δ mutant was still able to form hyphae under the experimental conditions used (93% hypha production), and these cells did not stimulate a high level of TNFα by human PBMCs (**Figure 3A**). In comparison, the *efg1*Δ mutant mainly produced pseudohyphae (more than 90%) and stimulated only about 15% of TNFα of the control HK wild-type yeast cells. The *cph1*Δ/*efg1*Δ double mutant was unable to form hyphae at 37°C and stimulated significantly higher amounts of TNFα at 37°C than the hyphal wild-type parent (**Figure 3A**). Another yeast-locked *hgc1*Δ mutant also induced higher levels of TNFα at 37°C, although surprisingly this was also reduced at 25°C, indicating that Hgc1 influences TNFα stimulation in human PBMCs for both yeast and hyphae. By contrast, the pseudohypha-locked *tup1*Δ mutant stimulated a poor cytokine production at both 25 and 37°C (**Figure 3A**). Similar results for TNFα were observed for IL-1α, IL-1β, IL-6, and IL-10 (data not shown).

Next, we investigated the apparent ability of the germ tube to inhibit the ability of the mother yeast cells to stimulate TNFα cytokine production. PBMCs were pretreated with live or HK yeast or hyphae for 1 h, then a second stimulus of the same or another morphotype was added. PBMCs preincubated with HK yeast cells and then stimulated with either live or HK hyphae were not compromised in their ability to produce TNFα (**Figure 4**). Reciprocally when HK hyphae were preincubated with PBMCs

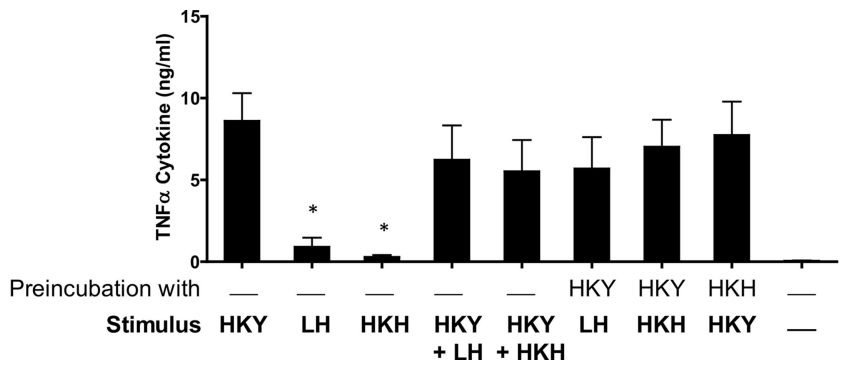

FIGURE 4 | Stimulation of cytokine production by human peripheral blood mononuclear cells (PBMCs) interacting with *Candida albicans* yeast cells and hyphae. Human PBMCs in RPMI 1640 were preincubated 1 h with either *C. albicans* NGY152 yeast cells or hyphae and then stimulated with a second cell type for 24 h. HKY, heat-killed yeast; LH, live hyphae; HKH, heat-killed hyphae (*$p < 0.05$; $n = 12$).

and then stimulated with HK yeast cells, there was a no significant reduction in the cytokine response (**Figure 4**). When yeast cells and hyphae were mixed together in a ratio 1:1, there was a strong cytokine production comparable to that elicited with HK yeast cells alone. Therefore, germ tubes with an attached parent yeast cell did not induce a response that would normally be associated with free yeast cells; however, hyphae did not block cytokine stimulation by yeast cells presented in trans.

The possibility that *C. albicans* reduced cytokine production by hyphae was due to blocking receptors on immune cells was tested by coincubating hyphal cells with various TLR ligands including Pam_3CSk_4, LPS, zymosan, flagellin, and curdlan. However, *C. albicans* hyphae did not block nor reduce TNFα, IL-1β, or IL-1α stimulated by these TLRs ligands used (Figure S2 in Supplementary Material).

Cell Wall Composition and the Immune Response

The fungal cell wall contains most of the PAMPs recognized by the innate immune cells (4, 11). Thus, we next assessed the ability of yeast and hyphal cells with specific cell wall defects to stimulate cytokine production by human PBMCs. A *chs3*Δ null mutant with a low chitin content at the cell wall (49), and a *mnn4*Δ mutant (50) lacking cell wall mannosylphosphate, were unaffected in the PBMC-induced cytokine production, compared to wild-type control cells (**Figure 5A**). A *pmr1*Δ mutant (51), which is deficient in yeast and hyphal cell wall *N*- and *O*-linked mannan, induced a reduced cytokine response by HK yeast cells, but an increased cytokines response from live and HK hyphae. This suggests that for yeast cells the lack of mannan reduced the overall immune response, while in hyphae the major effect of mannan depletion was to reveal subsurface immunostimulatory ligands such as β-glucan. In the *O*-mannosylation *mnt1/mnt2*Δ mutant (52), and the core *N*-mannan *mns1*Δ mutant (45) the secretion of most cytokines was enhanced or not affected in yeast or hyphal cells. IL-1α secretion from monocytes was enhanced to the greatest extend in the *pmr1*Δ, *mnt1/mnt2*Δ, and *mns1*Δ mutants in both yeast and hyphal cells (**Figure 5B**).

We compared the cytokine levels produced by a number of mutants that lacked hypha-associated cell wall proteins including *als3*Δ (53), *hwp1*Δ (54), *hyr1*Δ (55), and *ece1*Δ (56) with those stimulated with wild-type control cells. Only the *hwp1*Δ HK mutant hyphae stimulated a higher cytokine production than wild-type control cells (**Figure 5C**). Unexpectedly, despite the hypha-specific expression pattern for *HYR1* (55), the *hyr1*Δ mutant yeast cells stimulated a slightly reduced cytokine response from human PBMCs compared to wild-type control cells (**Figure 5C**). The *hwp1*Δ mutant showed no significant differences in mannan, glucan, and chitin content of the cell wall, when compared to wild-type control cells in both morphologies (**Table 1**), suggesting that this proteins may act in masking cytokine stimulating PAMPs in the cell wall. By contrast, yeast and hyphal cells of the *mns1*Δ and *pmr1*Δ mutants displayed a significant reduction in cell wall mannan and increased levels of glucan (**Table 1**). Therefore, cell wall mannosylation and the presence of Hwp1 were important for the reduced ability of hyphae of *C. albicans* to induce cytokines by human PBMCs.

We also tested the effect of deletion of the yeast-specific gene *PGA29* on cytokine production by human PBMCs and noted that this HK mutant induced less TNFα under conditions of yeast growth (Figure S3 in Supplementary Material). The reconstituted heterozygous *pga29/PGA29* mutant restored the TNFα induction to normal levels. Therefore, morphology-specific cell wall proteins of both yeast and hyphae influenced immune recognition.

C. albicans Pseudohyphae Stimulate Intermediate Cytokine Levels from Human PBMCs

We then examined the ability of pseudohyphae to induce cytokine production. We deployed a method in which changes in temperature alone could generate yeast cells, pseudohyphae, or hyphae (41, 57). When *C. albicans* NGY152 was grown in RPMI 1640 medium at a neutral pH and at 30°C for 6 h (**Figure 6A**), it reproducibly resulted in a largely pseudohyphal population (~90%). For this strain, growth at 25°C yielded yeast cells (MI = 0.65 ± 0.06, mean ± SEM), 30°C yielded pseudohyphae (MI = 2.34 ± 0.19), and 37°C yielded hyphal forms (MI = 8.65 ± 0.73) (**Figure 6B**).

Next, we investigated cytokine production of human PBMCs stimulated with pseudohyphae in comparison to yeast and hyphae. In a range of experiments pseudohyphal cell populations generated reproducibly intermediate levels of TNFα and other cytokines from live and HK cells, although the differences were not always significant at $p < 0.05$ and the level of significance varied depending on whether the average MI of a given population of pseudohyphae was sufficiently distinct from that of populations of yeast cells or hyphae (**Figures 6A–D**). There was a statistically significant correlation between the level of TNFα and IL-1β cytokine from PBMCs and the MI of *C. alb*icans cells inducing these cytokines (**Figure 6E**).

DISCUSSION

Multiple independent studies have proposed a positive correlation between the formation of *C. albicans* hyphae and an enhanced capacity for tissue invasion, damage, and virulence (6, 33, 39). However, the significance of *C. albicans* morphogenesis on the innate immune response has not been fully characterized. Here, the interaction of yeasts, pseudohyphae, and hyphae of this fungus with cells of the human innate immune system was investigated using cytokine production by human PBMCs as an immunoassay readout. We demonstrate that yeast cells generated more inflammatory cytokines from PBMCs than hyphae, and that pseudohyphae generated intermediate cytokine levels. These differences were observed in independent strains for cells generated in different growth media. Heat killing of cells has been used frequently in immunological studies of *C. albicans* to prevent cells undergoing filamentation in response to serum components of cell culture media when exposing *Candida* to immune cells during cytokine induction assays (58, 59). HK cells had enhanced immune responses, which has been interpreted as being due to heat-induced permeabilization of the cell wall and subsequent exposure of the underlying β1,3-glucan layer, which is strongly immunogenic (18). Our data support this hypothesis and suggest that HK cells generate a greater cytokine signal because more

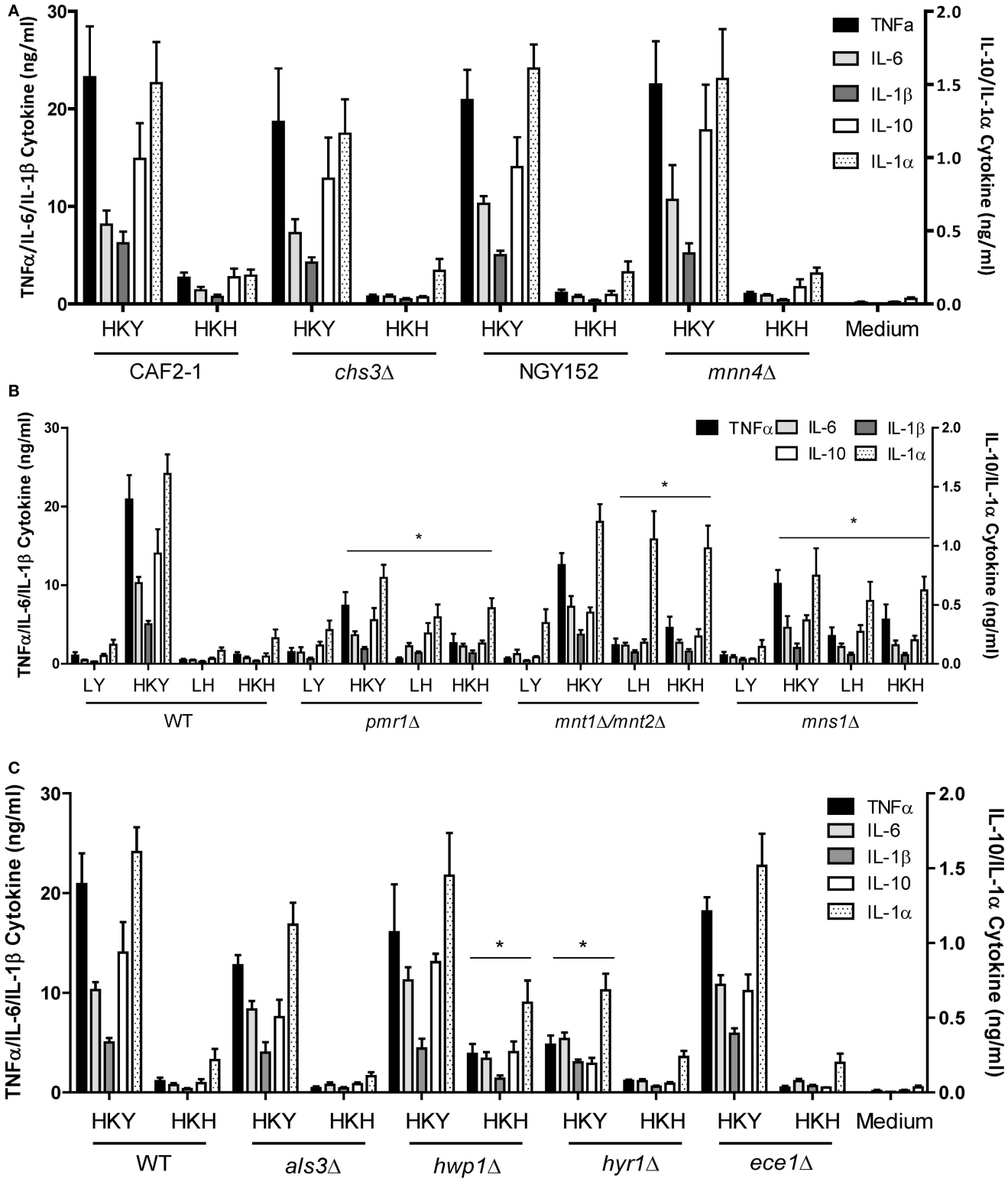

FIGURE 5 | **Cytokine production stimulated by cell wall mutants of yeast and hyphal cells**. **(A)** Cytokine production stimulated by human PBMCs with LY—live yeast; HKY—heat-killed yeast; LH—live hyphae; HKH—heat-killed hyphae; *Candida albicans mnn4*Δ and *chs3*Δ and control strains, NGY152 and CAF2-1. **(B)** Cytokine stimulation with mannosylation defective mutants, *pmr1*Δ, *mnt1*Δ/*mnt2*Δ, and *mns1*Δ. **(C)** *als3*Δ, *hwp1*Δ, *hyr1*Δ, and *ece1*Δ. Results presented as mean ± SEM ($n = 6$), and the asterisks indicate comparison of the wild-type values and the mutant strains ($^*p < 0.05$).

TABLE 1 | Cell wall composition of *Candida albicans* strains.

Strain	Glucosamine	Glucose	Mannose
Yeast morphology			
WT	1.01 ± 0.4	58.31 ± 2.25	40.68 ± 2.19
*hwp1*Δ	0.77 ± 0.46	52.99 ± 0.77*	46.24 ± 0.34*
*mns1*Δ	0.91 ± 1.18	88.71 ± 2.34*	10.38 ± 0.96*
*pmr1*Δ	1.50 ± 2.05	99.55 ± 3.63*	0.50 ± 1.33*
Hypha morphology			
WT	4.77 ± 0.32#	87.18 ± 1.54#	8.06 ± 0.99#
*hwp1*Δ	5.63 ± 0.93#	83.68 ± 2.57#	10.68 ± 1.75#
*mns1*Δ	6.10 ± 1.34#	87.61 ± 1.59	6.29 ± 0.18#
*pmr1*Δ	1.48 ± 0.74*	97.72 ± 2.01*	0.80 ± 0.68*,#

*Means ± SD (n = 3) *p < 0.05 when comparing the mutant strain with the wild-type control cells.*

#p < 0.05 when comparing hyphae with yeast cells.

PAMPs can engage collaboratively with PRRs, thus resulting in coreceptor amplification of the cytokine response (18, 60–62).

Although the hyphae used in these experiments also had a parental yeast cell, the combined cytokine signal due to the hypha plus parent yeast cell was significantly less than that expected from the yeast cell alone. This may suggest that either the yeast cell surface of germ tube matures to become different from that of a free yeast cell or that an unknown mechanism operates in germ tubes that are able to block cytokine induction due to the mother yeast cell. However, if a blocking signal is present, it does not operate in "trans" since hyphae added after free yeast cells were used to stimulate PBMCs did not interfere with the ensuing yeast cell stimulated cytokine response. Interestingly, hyphae of *C. dubliniensis* also stimulated less cytokine from PBMCs than yeast cells. The genomes of *C. albicans* and *C. dubliniensis* are 95% identical, and the cell walls are also thought to be of similar composition, although there are notable differences in the cell wall proteome (63). These closely related *Candida* species therefore show both common aspects and some differences in the nature of the immune response to yeast and hyphal cells.

Different immune cell types respond differently to *C. albicans* yeast and hyphae. For example, *C. albicans* hyphae induce higher levels of TNFα than yeast cells in macrophages (64, 65), while yeast and hyphae stimulate comparable levels of IL-8 cytokine by human neutrophils (47). It was shown that *C. albicans* induced different cytokine responses from oral and vaginal epithelial cells, and that hyphae induced higher cytokine levels than yeast cells in both epithelial cell types (32, 66). However, our findings reinforce previous studies where *C. albicans* filaments (hyphae and pseudohyphae) were reported to stimulate the production of less IL-12, IFN-γ, IL-1β, and IL-12p70 by human PBMCs and murine splenic lymphocytes than *C. albicans* yeast cells (30, 58, 67–69). It was also previously reported that TLR4-mediated pro-inflammatory signals were diminished during the germination of *C. albicans* yeast cells into hyphae (30). Supporting this, we show that *C. albicans* cells grown at 37°C have a progressively reduced TNFα cytokine response. In addition, it was reported that *C. albicans* hyphal cell walls also stimulated less chemokines than yeast cell walls (68), and it was suggested that this may be due to surface expression of β1,6-glucan being lower on hyphae compared to yeast cells. The cell SA of each individual hyphal compartment is larger than that of a yeast cell, and hyphae have no bud scars where inner wall layers are exposed (29). Therefore, it is possible that the density of certain immune agonists is less concentrated on the hyphal surface than on yeast cells. Also, progressive elongation of hyphae *in vivo* has been shown to result in increasing exposures of β1,3-glucan (70). Hence, cellular morphogenesis leading to filamentous growth of *C. albicans* leads to important progressive modifications of cell wall composition and architecture that has profound and differing effects on the immune response.

Cell wall polysaccharide analysis showed that yeast cell walls contained significantly higher amounts of mannan but lower amounts chitin and glucan compared to that of hyphal cell walls (**Table 1**). The reduction of mannan and increase in chitin content of hyphal cell walls might also be related to the lower cytokine responses to *C. albicans* hyphae (28, 45, 71, 72). Our results underline the importance of *N*- and *O*-linked mannans in the recognition of *C. albicans* hyphae by human PBMCs (**Figure 5**) since *N*- and *O*-mannan mutants (45, 52), but not chitin and phosphomannan mutants, stimulated the production of higher levels of cytokines that wild-type hyphae.

Although the primary polysaccharides in the cell wall are likely to have a major influence on immune recognition, it was noted that a HK *hwp1*Δ cell wall protein deletion mutant induced an increased cytokine signal, despite having no measurable alteration in hyphal mannan or glucan content. Similarly, a mutant lacking *MNS1* grown under hyphal-inducing conditions showed insignificant changes in cell wall components, but substantial reduction in cytokine production. However, the *mns1* yeast cells had 34% increased glucan as a compensation of 70% reduction in mannan, and a reduced cytokine profile. Therefore, there was no direct or universal correlation between cytokine induction and gross cell wall polysaccharide composition.

Our observations suggest that surface proteins, polysaccharides, and virulence factors are regulated or modified during filamentous growth resulting in changes in the immune response. Such changes in the incorporation of surface cell wall proteins on cells of different morphology could mask or unmask PAMPs, thereby blocking or promoting PRR engagement.

The presence of *C. albicans* hyphae could potentially compete with yeast cells for the ability to bind PRRs and stimulate immune cells. This would be important if specific yeast cell wall proteins are important for immune recognition and activation. We observed that a *pga29* mutant grown in the yeast form stimulated less TNFα from human PBMCs. This cell wall protein Pga29 has homologs in several pathogenic *Candida* spp. and is abundant in yeast cell walls in *C. albicans* but not in hyphae (73). Deletion of *PGA29* resulted in decreased glucan–mannan in the cell wall, and reduction of TNFα, IL-6, and IL-8 stimulated by oral reconstituted human epithelial cells (74). Therefore, both yeast and hypha-specific cell wall proteins may directly modulate immune responses.

It is also possible that *C. albicans* hyphal cells may produce secreted molecules that suppress immune recognition. Quorum-sensing molecules, such as farnesol, tyrosol, phenylethanol, and tryptophol, produced by *C. albicans*, play a key role in morphogenesis (75–77), and tyrosol acts negatively on cytokine production stimulated by RAW 264.7 macrophages induced

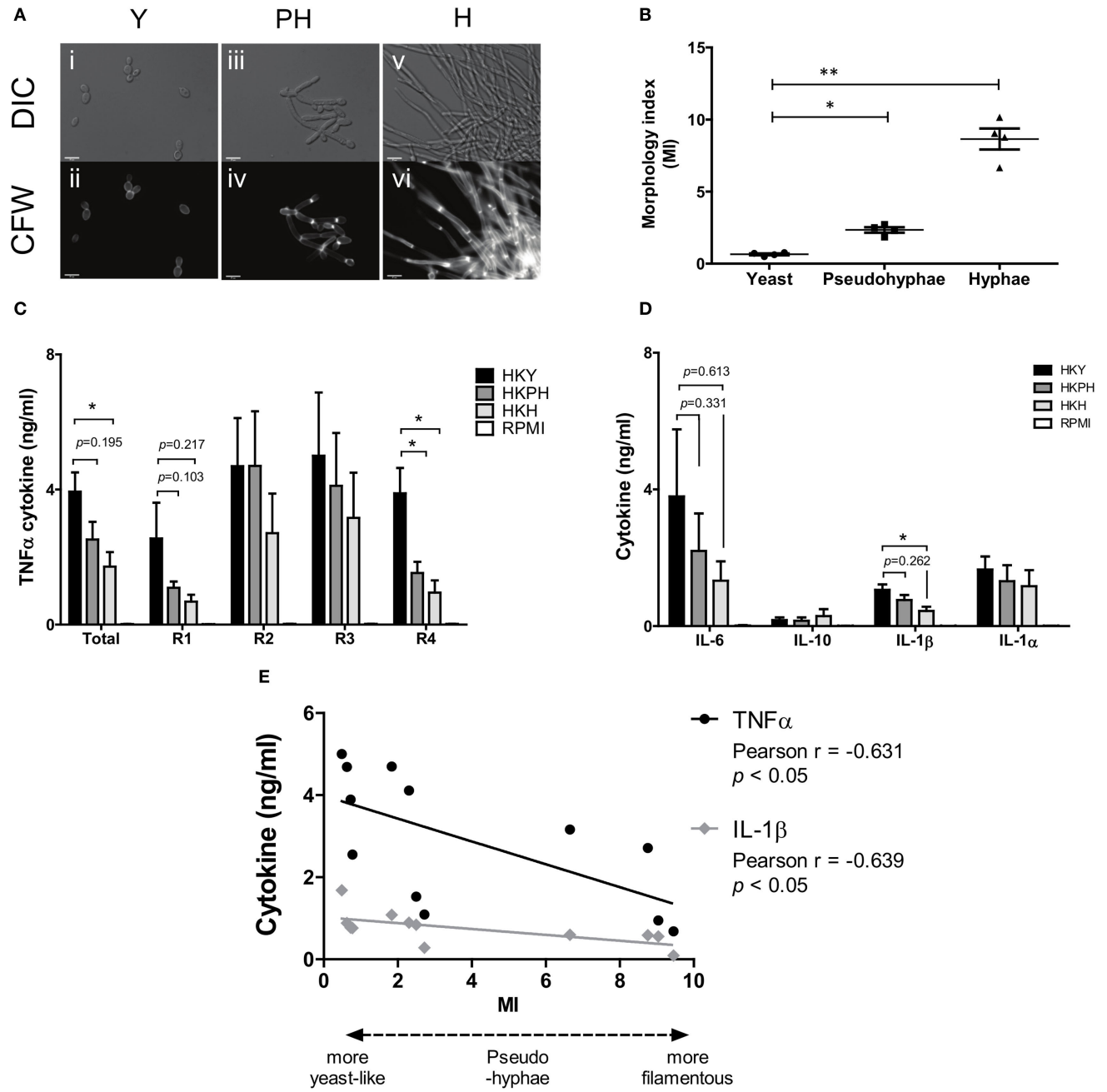

FIGURE 6 | Cytokine production by hPBMCs stimulated by different *Candida albicans* morphological forms. **(A)** Yeasts (i–ii), pseudohyphae (iii–iv), or hyphae (v–vi) of *C. albicans* NGY152 were grown in RPMI 1640 (pH 7) for 6 h at 25, 30, and 37°C, respectively, fixed, and stained with 25 μg/ml CFW to visualize the cell wall. Scale bars = 10 μm. **(B)** Morphological index (MI) of yeast, pseudohyphal, and hyphal cells was measured. Error bars are SEMs (averages from 50 cell measurements and 4 biological replicates) (*$p < 0.05$; **$p < 0.01$). **(C)** TNFα cytokine production elicited by human peripheral blood mononuclear cells (PBMCs) with HK NGY152 of yeast (Y), pseudohypha (PH), and hypha (H) cells. Each replicate (R1–R4) were averaged as total values. Data are means ± SEM ($n > 6$; *$p < 0.05$). **(D)** IL-6, IL-1β, IL-1α, and IL-10 cytokine production elicited by human PBMCs with HK of yeast (Y), pseudohypha (PH), and hypha (H) cells. Data are means ± SEM ($n > 6$; *$p < 0.05$). **(E)** Correlation between TNFα or IL-1β cytokine and MI. Results are Person *R* values ($n = 4$ biological replica).

by lipopolysaccharide (78). However, we showed that neither live nor HK hyphae could suppress yeast cell-induced cytokine production in trans; therefore, soluble factors were not suggested as playing a significant role in our experiments.

Our observations and those of previous studies (30, 58, 68, 69) demonstrate that *C. albicans* hyphae stimulated lower cytokine production by PBMCs than *C. albicans* yeast cells, thus indicating that *C. albicans* hyphae may help to evade or

alter the host immune response. However, it is clear that *C. albicans* hyphae induced strong cytokine responses and caused more damage to epithelial cells, while yeast cells did not trigger cytokine responses (66, 79, 80). Also, *C. albicans* hyphae induce stronger cytokine responses that yeast cells from macrophages (64, 65). The common denominator of these various reports is that cellular morphogenesis plays an important role in determining the immune response to *C. albicans*, but the nature of this response is both host cell type specific and pathogen morphotype dependent. These data underline the perspective that *C. albicans* presents a moving target to the cells of the innate immune response.

ETHICS STATEMENT

Blood samples were used in this study to generate human peripheral blood monocytes. Samples were collected from healthy volunteers according to local guidelines and regulations, as approved by the College Ethics Review Board of the University of Aberdeen (CERB/2012/11/676).

AUTHOR CONTRIBUTIONS

LM and KL performed experiments. NG, HM-M, LM, and KL conceived and designed experiments and analyzed the data. NG and HM-M supervised the project. LM, KL, and NG contributed to writing of the manuscript. All the authors reviewed the manuscript.

ACKNOWLEDGMENTS

The authors thank Amy Whittington for preliminary experiments on *in vitro* induction of pseudohyphae and Mihai Netea for discussions. The authors also thank Michael Weig for the pga29 strains.

FUNDING

NG and AW were supported by the Wellcome Trust (086827, 075470, 097377, 101873, and 200208); the European Union ALLFUN (FP7/2007 2013, HEALTH-2010-260338), and the MRC Centre for Medical Mycology for funding (N006364/1). LM was supported by a SORSAS (Scottish Overseas Research Students Award Scheme) from the University of Aberdeen and Funding from the Rwandan Government.

SUPPLEMENTARY MATERIAL

The Supplementary Material for this article can be found online at http://journal.frontiersin.org/article/10.3389/fimmu.2017.00629/full#supplementary-material.

FIGURE S1 | **Cell damage assay of hPBMC stimulated with *Candida albicans***. Lactate dehydrogenase activity released from 5×10^5 hPBMCs into the culture medium was determined after 24 h stimulated with either *C. albicans* heat-killed yeast or HKH at the different number of cells from 1×10^2 to 1×10^6 cells. The result represented as a percentage relative to 100% cell death of hPBMCs when killed with 2% Triton-X-100. Error bars = SEM ($n = 4$).

FIGURE S2 | **Cytokine production by hPBMCs stimulated by different *Candida albicans* coincubated with toll-like receptors (TLRs) ligands**. Human peripheral blood mononuclear cells were stimulated using a mixture of *C. albicans* cells and TLRs ligands. Cells were either live (L) or heat-killed (HK), and yeast (Y) or hyphae (H). TLRs ligands used were flagellin (for TLR5), LPS (for TLR4), Pam_3CSK_4 (for TLR2/TLR1), zymosan, and curdlan (for Dectin-1). The cytokines measured were TNF-α **(A)**, IL-6 **(B)**, IL-1β **(C)**, IL-1α **(D)**, and IL-10 **(E)**. IL-10 was barely detectable and could not be evaluated. Data are means ± SEM ($n > 3$; $^*p < 0.05$). ND, not detectable.

FIGURE S3 | **TNFα cytokine production by hPBMCs incubated with *Candida albicans* lacking *PGA29***. *C. albicans* cells lacking *PGA29* was grown in RPMI 1640 + 2.5% fetal calf serum at 25 or 37°C for 3.5 h. Cells were collected and heat killed. The mutant was incubated with hPBMCs for 24 h. Then, TNFα cytokine production was determined (see Methods and Materials). Data are means ± SEM (n > 9; *p < 0.05; ***p < 0.001).

TABLE S1 | ***C. albicans* and other fungal strains used in this study.**

REFERENCES

1. Gudlaugsson O, Gillespie S, Lee K, Vande Berg J, Hu J, Messer S, et al. Attributable mortality of nosocomial candidemia, revisited. *Clin Infect Dis* (2003) 37:1172–7. doi:10.1086/378745
2. Pappas PG, Rex JH, Lee J, Hamill RJ, Larsen RA, Powderly W, et al. A prospective observational study of candidemia: epidemiology, therapy, and influences on mortality in hospitalized adult and pediatric patients. *Clin Infect Dis* (2003) 37:634–43. doi:10.1086/376906
3. Kullberg BJ, Arendrup MC. Invasive candidiasis. *N Engl J Med* (2015) 373:1445–56. doi:10.1056/NEJMra1315399
4. Erwig LP, Gow NAR. Interactions of fungal pathogens with phagocytes. *Nat Rev Microbiol* (2016) 14:163–76. doi:10.1038/nrmicro.2015.21
5. Sudbery PE, Gow NAR, Berman J. The distinct morphogenic states of *Candida albicans*. *Trends Microbiol* (2004) 12:317–24. doi:10.1016/j.tim.2004.05.008
6. Gow NAR, van de Veerdonk FL, Brown AJP, Netea MG. *Candida albicans* morphogenesis and host defence: discriminating invasion from colonization. *Nat Rev Microbiol* (2011) 10:112–22. doi:10.1038/nrmicro2711
7. Sudbery PE. Growth of *Candida albicans* hyphae. *Nat Rev Microbiol* (2011) 9:737–48. doi:10.1038/nrmicro2636
8. Gow NAR, Hube B. Importance of the *Candida albicans* cell wall during commensalism and infection. *Curr Opin Microbiol* (2012) 15:406–12. doi:10.1016/j.mib.2012.04.005
9. Kullberg BJ, Arendrup MC. Invasive candidiasis. *N Engl J Med* (2016) 374:793–5. doi:10.1056/NEJMc1514201
10. Sellam A, Whiteway M. Recent advances on *Candida albicans* biology and virulence. *F1000Res* (2016) 5:2582. doi:10.12688/f1000research.9617.1
11. Netea MG, Brown GD, Kullberg BJ, Gow NAR. An integrated model of the recognition of *Candida albicans* by the innate immune system. *Nat Rev Microbiol* (2008) 6:67–78. doi:10.1038/nrmicro1815
12. Hoebe K, Janssen E, Beutler B. The interface between innate and adaptive immunity. *Nat Immunol* (2004) 5:971–4. doi:10.1038/ni1004-971
13. Medzhitov R. Recognition of microorganisms and activation of the immune response. *Nature* (2007) 449:819–26. doi:10.1038/nature06246
14. Cheng SC, Joosten LA, Kullberg BJ, Netea MG. Interplay between *Candida albicans* and the mammalian innate host defense. *Infect Immun* (2012) 80:1304–13. doi:10.1128/IAI.06146-11
15. Netea MG, Joosten LA, van der Meer JW, Kullberg BJ, van de Veerdonk FL. Immune defence against *Candida* fungal infections. *Nat Rev Immunol* (2015) 15:630–42. doi:10.1038/nri3897
16. Gow NAR, Netea MG. Medical mycology and fungal immunology: new research perspectives addressing a major world health challenge. *Philos Trans R Soc Lond B Biol Sci* (2016) 371. doi:10.1098/rstb.2015.0462
17. Netea MG, Gow NAR, Munro CA, Bates S, Collins C, Ferwerda G, et al. Immune sensing of *Candida albicans* requires cooperative recognition of mannans and glucans by lectin and toll-like receptors. *J Clin Invest* (2006) 116:1642–50. doi:10.1172/JCI27114
18. Gow NAR, Netea MG, Munro CA, Ferwerda G, Bates S, Mora-Montes HM, et al. Immune recognition of *Candida albicans* beta-glucan by dectin-1. *J Infect Dis* (2007) 196:1565–71. doi:10.1086/523110

19. Cambi A, Netea MG, Mora-Montes HM, Gow NAR, Hato SV, Lowman DW, et al. Dendritic cell interaction with *Candida albicans* critically depends on *N*-linked mannan. *J Biol Chem* (2008) 283:20590–9. doi:10.1074/jbc.M709334200
20. Heinsbroek SEM, Taylor PR, Martinez FO, Martinez-Pomares L, Brown GD, Gordon S. Stage-specific sampling by pattern recognition receptors during *Candida albicans* phagocytosis. *PLoS Pathog* (2008) 4:e1000218. doi:10.1371/journal.ppat.1000218
21. McKenzie CGJ, Koser U, Lewis LE, Bain JM, Mora-Montes HM, Barker RN, et al. Contribution of *Candida albicans* cell wall components to recognition by and escape from murine macrophages. *Infect Immun* (2010) 78:1650–8. doi:10.1128/IAI.00001-10
22. Jouault T, El Abed-El Behi M, Martínez-Esparza M, Breuilh L, Trinel PA, Chamaillard M, et al. Specific recognition of *Candida albicans* by macrophages requires galectin-3 to discriminate *Saccharomyces cerevisiae* and needs association with TLR2 for signaling. *J Immunol* (2006) 177:4679–87. doi:10.4049/jimmunol.177.7.4679
23. Kohatsu L, Hsu DK, Jegalian AG, Liu FT, Baum LG. Galectin-3 induces death of *Candida* species expressing specific beta-1,2-linked mannans. *J Immunol* (2006) 177:4718–26. doi:10.4049/jimmunol.177.7.4718
24. Linden JR, De Paepe ME, Laforce-Nesbitt SS, Bliss JM. Galectin-3 plays an important role in protection against disseminated candidiasis. *Med Mycol* (2013) 51:641–51. doi:10.3109/13693786.2013.770607
25. Courjol F, Jouault T, Mille C, Hall R, Maes E, Sendid B, et al. Beta-1,2-mannosyltransferases 1 and 3 participate in yeast and hyphae *O*- and *N*-linked mannosylation and alter *Candida albicans* fitness during infection. *Open Forum Infect Dis* (2015) 2:ofv116. doi:10.1093/ofid/ofv116
26. Harris M, Mora-Montes HM, Gow NAR, Coote PJ. Loss of mannosylphosphate from *Candida albicans* cell wall proteins results in enhanced resistance to the inhibitory effect of a cationic antimicrobial peptide via reduced peptide binding to the cell surface. *Microbiology* (2009) 155:1058–70. doi:10.1099/mic.0.026120-0
27. Rubin-Bejerano I, Abeijon C, Magnelli P, Grisafi P, Fink GR. Phagocytosis by human neutrophils is stimulated by a unique fungal cell wall component. *Cell Host Microbe* (2007) 2:55–67. doi:10.1016/j.chom.2007.06.002
28. Wagener J, Malireddi RKS, Lenardon MD, Köberle M, Vautier S, MacCallum DM, et al. Fungal chitin dampens inflammation through IL-10 induction mediated by NOD2 and TLR9 activation. *PLoS Pathog* (2014) 10. doi:10.1371/journal.ppat.1004050
29. Gantner BN, Simmons RM, Underhill DM. Dectin-1 mediates macrophage recognition of *Candida albicans* yeast but not filaments. *EMBO J* (2005) 24:1277–86. doi:10.1038/sj.emboj.7600594
30. Van Der Graaf CAA, Netea MG, Verschueren I, Van Der Meer JWM, Kullberg BJ. Differential cytokine production and toll-like receptor signaling pathways by *Candida albicans* blastoconidia and hyphae. *Infect Immun* (2005) 73:7458–64. doi:10.1128/IAI.73.11.7458-7464.2005
31. Cheng SC, van de Veerdonk FL, Lenardon M, Stoffels M, Plantinga T, Smeekens S, et al. The dectin-1/inflammasome pathway is responsible for the induction of protective T-helper 17 responses that discriminate between yeasts and hyphae of *Candida albicans*. *J Leukoc Biol* (2011) 90:357–66. doi:10.1189/jlb.1210702
32. Moyes DL, Murciano C, Runglall M, Islam A, Thavaraj S, Naglik JR. *Candida albicans* yeast and hyphae are discriminated by MAPK signaling in vaginal epithelial cells. *PLoS One* (2011) 6:e26580. doi:10.1371/journal.pone.0026580
33. Lo HJ, Köhler JR, Didomenico B, Loebenberg D, Cacciapuoti A, Fink GR. Nonfilamentous *C. albicans* mutants are avirulent. *Cell* (1997) 90:939–49. doi:10.1016/S0092-8674(00)80358-X
34. Gow NAR, Brown AJP, Odds FC. Fungal morphogenesis and host invasion. *Curr Opin Microbiol* (2002) 5:366–71. doi:10.1016/S1369-5274(02)00338-7
35. Moyes DL, Wilson D, Richardson JP, Mogavero S, Tang SX, Wernecke J, et al. Candidalysin is a fungal peptide toxin critical for mucosal infection. *Nature* (2016) 532:64–8. doi:10.1038/nature17625
36. Ghannoum MA, Spellberg B, Saporito-Irwin SM, Fonzi WA. Reduced virulence of *Candida albicans PHR1* mutants. *Infect Immun* (1995) 63:4528–30.
37. Calera JA, Zhao XJ, Calderone R. Defective hyphal development and avirulence caused by a deletion of the *SSK1* response regulator gene in *Candida albicans*. *Infect Immun* (2000) 68:518–25. doi:10.1128/IAI.68.2.518-525.2000
38. Murad AMA, Leng P, Straffon M, Wishart J, Macaskill S, MacCallum D, et al. NRG1 represses yeast-hypha morphogenesis and hypha-specific gene expression in *Candida albicans*. *EMBO J* (2001) 20:4742–52. doi:10.1093/emboj/20.17.4742
39. Saville SP, Lazzell AL, Monteagudo C, Lopez-Ribot JL. Engineered control of cell morphology in vivo reveals distinct roles for yeast and filamentous forms of *Candida albicans* during infection. *Eukaryot Cell* (2003) 2:1053–60. doi:10.1128/EC.2.5.1053-1060.2003
40. Zheng X, Wang Y, Wang Y. Hgc1, a novel hypha-specific G1 cyclin-related protein regulates *Candida albicans* hyphal morphogenesis. *EMBO J* (2004) 23:1845–56. doi:10.1038/sj.emboj.7600195
41. Merson-Davies LA, Odds FC. A morphology index for characterization of cell shape in *Candida albicans*. *J Gen Microbiol* (1989) 135:3143–52.
42. Berman J, Gow NAR. Chapter 3. Cell cycle of fungal pathogens. In: San-Blas G, Calderone RA, editors. *Pathogenic Fungi: Structural Biology and Taxonomy*. Norfolk, UK: Caster Academic Press (2004). p. 101–25.
43. Lee KL, Buckley HR, Campbell CC. An amino acid liquid synthetic medium for the development of mycelial and yeast forms of *Candida albicans*. *Sabouraudia* (1975) 13:148–53. doi:10.1080/00362177585190271
44. Endres S, Ghorbani R, Lonnemann G, van der Meer JWM, Dinarello CA. Measurement of immunoreactive interleukin-1ß from human mononuclear cells: optimization of recovery, intrasubject consistency, and comparison with interleukin-1a and tumor necrosis factor. *Clin Immunol Immunopathol* (1988) 49:424–38. doi:10.1016/0090-1229(88)90130-4
45. Mora-Montes HM, Bates S, Netea MG, Diaz-Jimenez DF, Lopez-Romero E, Zinker S, et al. Endoplasmic reticulum alpha-glycosidases of *Candida albicans* are required for N glycosylation, cell wall integrity, and normal host-fungus interaction. *Eukaryot Cell* (2007) 6:2184–93. doi:10.1128/EC.00350-07
46. Plaine A, Walker L, Da Costa G, Mora-Montes HM, McKinnon A, Gow NA, et al. Functional analysis of *Candida albicans* GPI-anchored proteins: roles in cell wall integrity and caspofungin sensitivity. *Fungal Genet Biol* (2008) 45:1404–14. doi:10.1016/j.fgb.2008.08.003
47. Hosseinzadeh A, Urban CF. Novel insight into neutrophil immune responses by dry mass determination of *Candida albicans* morphotypes. *PLoS One* (2013) 8:e77993. doi:10.1371/journal.pone.0077993
48. Fidel PL Jr, Vazquez JA, Sobel JD. *Candida glabrata*: review of epidemiology, pathogenesis, and clinical disease with comparison to *C. albicans*. *Clin Microbiol Rev* (1999) 12:80–96.
49. Bulawa CE, Miller DW, Henry LK, Becker JM. Attenuated virulence of chitin-deficient mutants of *Candida albicans*. *Proc Natl Acad Sci U S A* (1995) 92:10570–4. doi:10.1073/pnas.92.23.10570
50. Hobson RP, Munro CA, Bates S, MacCallum DM, Cutler JE, Heinsbroek SE, et al. Loss of cell wall mannosylphosphate in *Candida albicans* does not influence macrophage recognition. *J Biol Chem* (2004) 279:39628–35. doi:10.1074/jbc.M405003200
51. Bates S, MacCallum DM, Bertram G, Munro CA, Hughes HB, Buurman ET, et al. *Candida albicans* Pmr1p, a secretory pathway P-type Ca^{2+}/Mn^{2+}-ATPase, is required for glycosylation and virulence. *J Biol Chem* (2005) 280:23408–15. doi:10.1074/jbc.M502162200
52. Munro CA, Bates S, Buurman ET, Hughes HB, Maccallum DM, Bertram G, et al. Mnt1p and Mnt2p of *Candida albicans* are partially redundant alpha-1,2-mannosyltransferases that participate in *O*-linked mannosylation and are required for adhesion and virulence. *J Biol Chem* (2005) 280:1051–60. doi:10.1074/jbc.M411413200
53. Zhao X, Oh SH, Cheng G, Green CB, Nuessen JA, Yeater K, et al. *ALS3* and *ALS8* represent a single locus that encodes a *Candida albicans* adhesin; functional comparisons between Als3p and Als1p. *Microbiology* (2004) 150:2415–28. doi:10.1099/mic.0.26943-0
54. Sundstrom P, Balish E, Allen CM. Essential role of the *Candida albicans* transglutaminase substrate, hyphal wall protein 1, in lethal oroesophageal candidiasis in immunodeficient mice. *J Infect Dis* (2002) 185:521–30. doi:10.1086/338836
55. Bailey DA, Feldmann PJF, Bovey M, Gow NAR, Brown AJP. The *Candida albicans HYR1* gene, which is activated in response to hyphal development,

belongs to a gene family encoding yeast cell wall proteins. *J Bacteriol* (1996) 178:5353–60. doi:10.1128/jb.178.18.5353-5360.1996
56. Birse CE, Irwin MY, Fonzi WA, Sypherd PS. Cloning and characterization of *ECE1*, a gene expressed in association with cell elongation of the dimorphic pathogen *Candida albicans*. *Infect Immun* (1993) 61:3648–55.
57. Hornby JM, Dumitru R, Nickerson KW. High phosphate (up to 600 mM) induces pseudohyphal development in five wild type *Candida albicans*. *J Microbiol Methods* (2004) 56:119–24. doi:10.1016/j.mimet.2003.09.021
58. Chiani P, Bromuro C, Torosantucci A. Defective induction of interleukin-12 in human monocytes by germ-tube forms of *Candida albicans*. *Infect Immun* (2000) 68:5628–34. doi:10.1128/IAI.68.10.5628-5634.2000
59. Beaussart A, Alsteens D, El-Kirat-Chatel S, Lipke PN, Kucharíková S, Van Dijck P, et al. Single-molecule imaging and functional analysis of Als adhesins and mannans during *Candida albicans* morphogenesis. *ACS Nano* (2012) 6:10950–64. doi:10.1021/nn304505s
60. Brown GD, Herre J, Williams DL, Willment JA, Marshall ASJ, Gordon S. Dectin-1 mediates the biological effects of ß-glucans. *J Exp Med* (2003) 197:1119–24. doi:10.1084/jem.20021890
61. Gantner BN, Simmons RM, Canavera SJ, Akira S, Underhill DM. Collaborative induction of inflammatory responses by dectin-1 and toll-like receptor 2. *J Exp Med* (2003) 197:1107–17. doi:10.1084/jem.20021787
62. Dennehy KM, Willment JA, Williams DL, Brown GD. Reciprocal regulation of IL-23 and IL-12 following co-activation of Dectin-1 and TLR signaling pathways. *Eur J Immunol* (2009) 39:1379–86. doi:10.1002/eji.200838543
63. Jackson AP, Gamble JA, Yeomans T, Moran GP, Saunders D, Harris D, et al. Comparative genomics of the fungal pathogens *Candida dubliniensis* and *Candida albicans*. *Genome Res* (2009) 19:2231–44. doi:10.1101/gr.097501.109
64. Blasi E, Pitzurra L, Puliti M, Bartoli A, Bistoni F. *Candida albicans* hyphal form enhances tumor necrosis factor mRNA levels and protein secretion in murine ANA-1 macrophages. *Cell Immunol* (1992) 142:137–44. doi:10.1016/0008-8749(92)90275-T
65. Matuschak GM, Lechner AJ. The yeast to hyphal transition following hematogenous candidiasis induces shock and organ injury independent of circulating tumor necrosis factor-alpha. *Crit Care Med* (1997) 25:111–20. doi:10.1097/00003246-199701000-00022
66. Moyes DL, Runglall M, Murciano C, Shen C, Nayar D, Thavaraj S, et al. A biphasic innate immune MAPK response discriminates between the yeast and hyphal forms of *Candida albicans* in epithelial cells. *Cell Host Microbe* (2010) 8:225–35. doi:10.1016/j.chom.2010.08.002
67. d'Ostiani CF, Del Sero G, Bacci A, Montagnoli C, Spreca A, Mencacci A, et al. Dendritic cells discriminate between yeasts and hyphae of the fungus *Candida albicans*. Implications for initiation of T helper cell immunity in vitro and in vivo. *J Exp Med* (2000) 191:1661–74. doi:10.1084/jem.191.10.1661
68. Torosantucci A, Chiani P, Cassone A. Differential chemokine response of human monocytes to yeast and hyphal forms of *Candida albicans* and its relation to the ß-1,6 glucan of the fungal cell wall. *J Leukoc Biol* (2000) 68(6):923–32.
69. Van De Veerdonk FL, Joosten LAB, Devesa I, Héctor MM, Kanneganti T, Dinarello CA, et al. Bypassing pathogen-induced inflammasome activation for the regulation of interleukin-1ß production by the fungal pathogen *Candida albicans*. *J Infect Dis* (2009) 199:1087–96. doi:10.1086/597274
70. Wheeler RT, Kombe D, Agarwala SD, Fink GR. Dynamic, morphotype-specific *Candida albicans* β-glucan exposure during infection and drug treatment. *PLoS Pathog* (2008) 4:e1000227. doi:10.1371/journal.ppat.1000227
71. Bates S, De La Rosa JM, MacCallum DM, Brown AJP, Gow NAR, Odds FC. *Candida albicans* Iff11, a secreted protein required for cell wall structure and virulence. *Infect Immun* (2007) 75:2922–8. doi:10.1128/IAI.00102-07
72. Mora-Montes HM, Netea MG, Ferwerda G, Lenardon MD, Brown GD, Misura AS, et al. Recognition and blocking of innate immunity cells by *Candida albicans* chitin. *Infect Immun* (2011) 79:1961–70. doi:10.1128/IAI.01282-10
73. De Boer AD, De Groot PWJ, Weindl G, Schaller M, Riedel D, Diez-Orejas R, et al. The *Candida albicans* cell wall protein Rhd3/Pga29 is abundant in the yeast form and contributes to virulence. *Yeast* (2010) 27:611–24. doi:10.1002/yea.1790
74. Vavala E, Mignogna G, Spano F, Stringaro A, Colone M, Sanguinetti M, et al. The cell wall protein Rhd3/Pga29 is over-expressed in *Candida albicans* upon micafungin treatment. *J Chemother* (2013) 25:332–40. doi:10.1179/1973947813Y.0000000091
75. Hornby JM, Jensen EC, Lisec AD, Tasto JJ, Jahnke B, Shoemaker R, et al. Quorum sensing in the dimorphic fungus *Candida albicans* is mediated by farnesol. *Appl Environ Microbiol* (2001) 67:2982–92. doi:10.1128/AEM.67.7.2982-2992.2001
76. Chen H, Fujita M, Feng Q, Clardy J, Fink GR. Tyrosol is a quorum-sensing molecule in *Candida albicans*. *Proc Natl Acad Sci U S A* (2004) 101:5048–52. doi:10.1073/pnas.0401416101
77. Chen H, Fink GR. Feedback control of morphogenesis in fungi by aromatic alcohols. *Genes Dev* (2006) 20:1150–61. doi:10.1101/gad.1411806
78. Lu J, Huang G, Wang Z, Zhuang S, Xu L, Song B, et al. Tyrosol exhibits negative regulatory effects on LPS response and endotoxemia. *Food Chem Toxicol* (2013) 62:172–8. doi:10.1016/j.fct.2013.08.031
79. Dalle F, Wächtler B, L'Ollivier C, Holland G, Bannert N, Wilson D, et al. Cellular interactions of *Candida albicans* with human oral epithelial cells and enterocytes. *Cell Microbiol* (2010) 12:248–71. doi:10.1111/j.1462-5822.2009.01394.x
80. Moyes DL, Murciano C, Runglall M, Kohli A, Islam A, Naglik JR. Activation of MAPK/c-Fos induced responses in oral epithelial cells is specific to *Candida albicans* and *Candida dubliniensis* hyphae. *Med Microbiol Immunol* (2012) 201:93–101. doi:10.1007/s00430-011-0209-y

Conflict of Interest Statement: The authors declare that the research was conducted in the absence of any commercial or financial relationships that could be construed as a potential conflict of interest.

Copyright © 2017 Mukaremera, Lee, Mora-Montes and Gow. This is an open-access article distributed under the terms of the Creative Commons Attribution License (CC BY). The use, distribution or reproduction in other forums is permitted, provided the original author(s) or licensor are credited and that the original publication in this journal is cited, in accordance with accepted academic practice. No use, distribution or reproduction is permitted which does not comply with these terms.

frontiers in Immunology

ORIGINAL RESEARCH
published: 16 May 2018
doi: 10.3389/fimmu.2018.01058

Fluorescent Tracking of Yeast Division Clarifies the Essential Role of Spleen Tyrosine Kinase in the Intracellular Control of *Candida glabrata* in Macrophages

*Zeina Dagher[1], Shuying Xu[1], Paige E. Negoro[1], Nida S. Khan[1,2], Michael B. Feldman[3], Jennifer L. Reedy[1], Jenny M. Tam[1], David B. Sykes[4] and Michael K. Mansour[1]**

[1] Division of Infectious Disease, Massachusetts General Hospital, Harvard Medical School, Boston, MA, United States, [2] Biomedical Engineering and Biotechnology, University of Massachusetts Medical School, Worcester, MA, United States, [3] Division of Pulmonary and Critical Care, Massachusetts General Hospital, Boston, MA, United States, [4] Center for Regenerative Medicine, Massachusetts General Hospital, Boston, MA, United States

OPEN ACCESS

Edited by:
Steven Templeton,
Indiana University School of Medicine-Terre Haute, United States

Reviewed by:
Jeniel E. Nett,
University of Wisconsin-Madison, United States
Attila Gacser,
University of Szeged, Hungary

***Correspondence:**
Michael K. Mansour
mkmansour@mgh.harvard.edu

Specialty section:
This article was submitted to Microbial Immunology, a section of the journal Frontiers in Immunology

Received: 06 March 2018
Accepted: 27 April 2018
Published: 16 May 2018

Citation:
Dagher Z, Xu S, Negoro PE, Khan NS, Feldman MB, Reedy JL, Tam JM, Sykes DB and Mansour MK (2018) Fluorescent Tracking of Yeast Division Clarifies the Essential Role of Spleen Tyrosine Kinase in the Intracellular Control of Candida glabrata in Macrophages. Front. Immunol. 9:1058. doi: 10.3389/fimmu.2018.01058

Macrophages play a critical role in the elimination of fungal pathogens. They are sensed *via* cell surface pattern-recognition receptors and are phagocytosed into newly formed organelles called phagosomes. Phagosomes mature through the recruitment of proteins and lysosomes, resulting in addition of proteolytic enzymes and acidification of the microenvironment. Our earlier studies demonstrated an essential role of Dectin-1-dependent activation of spleen tyrosine kinase (Syk) in the maturation of fungal containing phagosomes. The absence of Syk activity interrupted phago-lysosomal fusion resulting in arrest at an early phagosome stage. In this study, we sought to define the contribution of Syk to the control of phagocytosed live *Candida glabrata* in primary macrophages. To accurately measure intracellular yeast division, we designed a carboxyfluorescein succinimidyl ester (CFSE) yeast division assay in which bright fluorescent parent cells give rise to dim daughter cells. The CFSE-labeling of *C. glabrata* did not affect the growth rate of the yeast. Following incubation with macrophages, internalized CFSE-labeled *C. glabrata* were retrieved by cellular lysis, tagged using ConA-647, and the amount of residual CFSE fluorescence was assessed by flow cytometry. *C. glabrata* remained undivided (CFSE bright) for up to 18 h in co-culture with primary macrophages. Treatment of macrophages with R406, a specific Syk inhibitor, resulted in loss of intracellular control of *C. glabrata* with initiation of division within 4 h. Delayed Syk inhibition after 8 h was less effective indicating that Syk is critically required at early stages of macrophage–fungal interaction. In conclusion, we demonstrate a new method of tracking division of *C. glabrata* using CFSE labeling. Our results suggest that early Syk activation is essential for macrophage control of phagocytosed *C. glabrata*.

Keywords: *Candida*, *Candida glabrata*, macrophages, spleen tyrosine kinase, phagosome, carboxyfluorescein succinimidyl ester

INTRODUCTION

The fungal pathogen *Candida glabrata* is a common cause of invasive bloodstream infections in immunocompromised patients (1). With the rise of organ transplantation, immunosuppressive chemotherapy, implanted medical devices, and antibacterial use, *C. glabrata* has emerged as a frequently isolated species, accounting for 20% of systemic bloodstream *Candida*-related infections in North America (2, 3).

In vitro, following interaction with human or murine macrophages, *C. glabrata* undergoes phagocytosis. Despite being internalized, *C. glabrata* survives and replicates inside host immune cells (4, 5). Intracellular killing of *C. glabrata* by macrophages is only about 10% effective (6). The capacity of this *Candida* species to evade the innate immune system complicates evaluation of intracellular pathogen control by simple phagocytosis assays. A more sensitive and accurate approach to quantifying *C. glabrata* intracellular proliferation is required to understand and identify the relevant pathogen–host interactions.

The carboxyfluorescein diacetate succinimidyl ester (CFSE) assay is a well-established method to fluorescently track lymphocyte cellular division (7, 8). The succinimidyl moiety of the dye covalently attaches to cellular aliphatic amine groups, forming stable amide bonds (9). This covalent-coupling dye allows for tracking of lymphocyte proliferation; each progressive cell division results in a twofold dilution of the fluorescent signal between daughter cells (10, 11). Unlike labeling techniques that rely on microscopic evaluation, CFSE can be visualized by both fluorescence microscopy and can be formally quantitated by flow cytometry (12). CFSE is highly fluorescent, has an excitation/emission profile at 491/518 nm, is stable in long-term tracking, and can be used *in vitro* and *in vivo* (10).

Although most published reports have used CFSE to monitor lymphocyte proliferation, recent studies have also used the dye to follow proliferation of other mammalian and non-mammalian cell types, such as bacterial cells and parasites (13, 14). CFSE also successfully labeled *Paracoccidioides* yeast in a flow cytometry based phagocytosis study, although the tracking of proliferation was not evaluated (15).

Here, we have applied the CFSE proliferation-tracking properties to *C. glabrata*, though several factors require special consideration. Unlike animal cells, fungi possess a cell wall composed of extracellular carbohydrate-rich polymers. CFSE brightly labels the cell wall, though does not permeate the yeast to label intracellular structures. Additionally, unlike mammalian cells where the cell membrane is shared symmetrically (in equal amounts) between daughter cells (16), the yeast cell wall is shared asymmetrically, with the budding yeast generating an almost-entirely new cell wall (17). This new (and CFSE-unlabeled) cell wall is synthesized at growing cell tips through the localization and activation of cell wall carbohydrate synthases (18, 19). Thus, unlike CFSE assays in lymphocytes, the CFSE labeling of yeast such as *C. glabrata* does not allow one to track beyond a single division.

Following infection, tissue macrophages sense fungi through the expression of pattern-recognition receptors (PRRs), such as Dectin-1 and Dectin-2, which recognize fungal cell wall carbohydrates (5, 20). Recognition through PRRs triggers phagocytosis, engulfing microorganisms within phagosomes, eventually fusing with additional subcellular compartments including lysosomes for acidification and killing (21). The process of acidification is termed phagosomal maturation, which in response to fungal cell wall ligands, is spleen tyrosine kinase (Syk)-dependent (22). Syk activation and signal transduction is central for immune activation in several immune cells (23). PRRs share the ability to associate with immunoreceptor tyrosine-based activation motifs (ITAM) in their cytoplasmic domains, leading to Syk recruitment and phosphorylation, resulting in downstream events including phagocytosis, and the production of reactive oxygen species (ROS) and proinflammatory cytokines (24–26). The central role of Syk in activation of several innate and adaptive immune cells has made this kinase a promising target for the development of anti-inflammatory therapeutics (27, 28).

Although the role of Syk in intracellular signaling has been studied extensively, its involvement in the response to intracellular pathogens in innate immune cells, such as macrophages, is not delineated (23, 26). In this study, we introduce a CFSE-labeling assay that allows for intracellular tracking of yeast proliferation in macrophage phagosomes. We demonstrate that CFSE is a reliable method of evaluating *C. glabrata* division by fluorescence microscopy and quantitatively by flow cytometry. Employing the CFSE assay, we show that Syk inhibition in macrophages results in the loss of the ability to control *C. glabrata* proliferation. This loss of *C. glabrata* division control is independent of phagocytosis and is not a result of failure to activate the Dectin-1 and Dectin-2 pathways. These observations highlight CFSE live labeling as a useful and convenient tool for measuring yeast proliferation accurately and support further investigation into the role of Syk in antifungal immunity.

MATERIALS AND METHODS

Reagents

R406 was purchased from Santa Cruz Biotechnology (Dallas, TX, USA), Nonidet P40 (NP40) and peptone from American Bioanalytical (Natick, MA, USA), CFSE dye, and all other chemicals from Sigma (St. Louis, MO, USA) unless otherwise stated. Wild type *C. glabrata* (ATCC2001) was purchased from the American Type Culture Collection (ATCC, Manassas, VA, USA). Cell lysis buffer consisted of 4× NP40 containing 40 mM Tris–hydrochloric acid, 600 mM sodium chloride, 20 mM magnesium chloride, and 4% NP40 titrated to pH 7.5. Yeast culture media liquid YPD contained 1% yeast extract (BD Biosciences, San Jose, CA, USA), 2% peptone, and 2% dextrose. Cell culture media (RPMI-complete) was composed of RPMI 1640 (Corning, Tewksbury, MA, USA) with 2 mM L-glutamine, 10% heat-inactivated fetal bovine serum, and 1% penicillin–streptomycin (ThermoFisher Scientific, Waltham MA, USA).

Yeast Culture and CFSE Staining

Candida glabrata were grown overnight shaking in liquid YPD at 30°C, washed three times in phosphate buffered saline (PBS), counted using a Luna automated cell counter (Logos Biosystems, Annandale, VA, USA), and resuspended in PBS at the desired inoculum.

To stain yeast with CFSE, wild type *C. glabrata* were grown to log phase in liquid YPD, washed twice in 1 mL PBS, and 160 million yeast were stained with 25 μg/mL CFSE for 30 min in 4 mL PBS at 30°C on a vertical rotator. Yeasts were washed twice in 10 mL PBS containing 2% bovine serum albumin (BSA) to remove excess CFSE. Stained yeast cells were resuspended in 1 mL PBS and passed through a 25G 7/8-inch needle 10 times to dissociate clumps into single cell suspension.

Calcofluor White Staining

To stain all intracellular yeast cells, macrophages were fixed and permeabilized with 4% paraformaldehyde (Electron Microscopy Sciences, Hatfield, PA, USA) for 20 min at room temperature in the dark. Cells were washed three times with PBS and incubated in 10% calcofluor white solution in PBS for 15 min and imaged using confocal microscopy with 405 nm laser excitation.

Collection of Murine Peritoneal Macrophages

Eight-week-old inbred C57BL/6 mice (Jackson Laboratory, ME, USA), Dectin-1$^{-/-}$ (B6 background, a gift from Dr. Gordon Brown, University of Aberdeen, UK) (29), or Dectin-2$^{-/-}$ (B6 background, a gift from Dr. Marcel Wuethrich, University of Wisconsin) (30) were housed in a specific pathogen-free facility at the Massachusetts General Hospital (MGH, Boston, MA, USA). All animal experiments were approved by the MGH Institutional Animal Care and Use Committee. Peritoneal macrophages were isolated from mice following intraperitoneally instillation of 2 mL thioglycollate (Northeast Laboratory, Waterville, ME, USA). After 3 days, the mice were euthanized and the peritoneum lavaged with 10 mL RPMI-complete to retrieve cells. Intraperitoneal cells were washed and plated at a density of 300,000 cells per well in 500 μL RPMI-complete in 24-well dishes and allowed to adhere overnight. Non-adherent contaminating cells were washed away after 24 h resulting in a >95% pure, viable macrophage population as determine by anti-Mac 1 staining using flow cytometry (data not shown).

Co-Culture of Peritoneal Macrophages and CFSE-*C. glabrata*

The media in each 24-well was reduced to 250 μL and wells were treated with R406 dissolved in DMSO or DMSO only either 10 min prior to *C. glabrata* inoculation or 2, 4, or 8 h after *C. glabrata* inoculation. A total of 200,000 CFSE-labeled *C. glabrata* were added for a final MOI of 0.6. Plates were centrifuged for 1 min at 700 × *g* to facilitate cell-ligand contacts and incubated at 37°C with 5% CO_2. After the time indicated, the macrophages were lysed with 100 μL of 4× NP40 on ice for 5 min. Well contents were centrifuged for 7.5 min at 10,000 rpm. The pellets were then fixed with 4% formaldehyde for 10 min in the dark and washed with PBS/2% BSA. Concanavalin A conjugated to Alexa Fluor 647 (ThermoFisher, Waltham, MA, USA) at a final concentration 3 μg/mL was added for 20 min in the dark to stain *C. glabrata*. Yeast were washed and resuspended in PBS/2% BSA for flow cytometry.

Macrophage Phagocytosis of *C. glabrata*

To assess macrophage phagocytosis, CFSE-*C. glabrata* were co-incubated with macrophages in the presence or absence of inhibitor for the time indicated. Plates were transferred onto ice, wells washed with PBS, then macrophages mechanically lifted, and strained through a 40-μm filter and immediately subjected to flow cytometry gating on the macrophage population. The phagocytosis percent was measured as the number of CFSE positive macrophages over the total macrophage cell number.

Reactive Oxygen Species

Reactive oxygen species was measured as described (31), briefly macrophages were plated at 5×10^4 cells/well in white wall 96-well plate (Costar, Cambridge, MA, USA). Cells were placed on ice and washed three times with PBS. Lucigenin solution (0.9 mM $CaCl_2$, 0.5 mM $MgCl_2$, 20 mM dextrose, and 20 μM lucigenin) was added, and cells were incubated on ice for 10 min. Heat-killed *C. glabrata* for 10 min were added at an effector to target ratio of 25, and then the plate was centrifuged at 750 × *g* for 1 min to facilitate cell-ligand contacts. An initial reading was then taken immediately after centrifugation for baseline. The plate was then incubated at 37°C and read with SpectraMax i3x reader (Molecular Devices, Sunnyvale, CA, USA) for total luminescence every 10 min for 2 h.

Confocal Microscopy

2×10^4 peritoneal macrophages were plated onto eight-chambered coverslip slides (LabTek, Thermo Scientific, Rochester, NY, USA) in RPMI-complete. CFSE-labeled *C. glabrata* were added at MOI 1:1, spun at 700 *g* × 1 min for immediate co-culture and slides mounted on a Nikon Ti-E inverted microscope equipped with an EM-CCD camera (Hamamatsu Photonics K.K., Hamamatsu, Japan). The excitation source was an 89 North MultiLine LaserBank (89 North, Burlington, VT, USA) A piezo stage (Prior Instruments, Rockland, MA, USA) capable of *X*, *Y*, and *Z* movement was used for acquisition. A polarizer (Nikon, MEN 51941) and Wollaston prisms (Nikon, MBH76190) were used to acquire differential interference contrast (DIC) images. Emission light from the samples was collected after passage through the appropriate emission filters (Semrock, Rochester, NY, USA) (32). Images were acquired using MetaMorph software (Molecular Devices, Downingtown, PA, USA), and processed using Adobe Photoshop CS5 and assembled in Adobe Illustrator, version CS5 (Adobe Systems, San Jose, CA, USA).

Flow Cytometric Analysis of CFSE

Carboxyfluorescein succinimidyl ester-labeled *C. glabrata* that were fixed and stained with concanavalin A-Alexa Fluor 647 were flowed using FACS Calibur flow cytometer (Becton-Dickinson, San Jose, CA, USA) and CellQuest software (Becton-Dickinson). ConA-647 (FL4) was plotted on the *y*-axis and CFSE (FL1) on the *x*-axis and the percentage of CFSE bright undivided population was determined with FlowJo 10 (FlowJo, Ashland, OR, USA).

Statistics

Statistical calculations were performed using GraphPad Prism 7 software. Data were analyzed by two-tailed, unpaired *t* test and were considered significantly different when $p \leq 0.05$.

RESULTS

CFSE Labeling Tracks Division of *C. glabrata*

We evaluated CFSE staining of *C. glabrata* using fluorescence microscopy. *C. glabrata* were homogenously fluorescent throughout the cell wall, likely due to the high content of fungal cell wall esterases that permit CFSE activation and labeling. The CFSE-labeled *C. glabrata* retained normal cell shape and morphology (**Figure 1**). Following 6 h in culture, CFSE-labeled *C. glabrata* were counter-stained with calcofluor white for chitin to delineate all yeast cells and visualized using confocal microscopy. All yeast cells were evenly stained with calcofluor white. Parent yeast cells were brightly CFSE-fluorescent, while daughter cells exhibited diluted CFSE leading to reduced fluorescence intensity as identified by flow cytometry (**Figure 2A**).

The consistent and predictable decrease in fluorescence permits quantitation of *C. glabrata* intracellular division as a marker of control by macrophages. While calcofluor allows visualization of all yeast cells using 405 nm laser excitation under confocal microscopy, our FACSCalibur is fitted with a blue and red laser incapable of exciting calcofluor. For these reasons, the total number of yeast were identified by labeling with concanavalin A conjugated to AF647 for flow cytometry. Therefore, a *C. glabrata* parent cell population is double-positive for CFSE and ConA-647, while divided daughter cells are CFSE-dim, but remain ConA-647 (**Figure 2B**).

With each cell division, the percent of the parent cells decrease, as daughter cell numbers rise and are easily distinguished *via* CFSE intensity. In fact, the diminished CFSE-bright parent cells was inversely proportional to the increase in the optical density of the growing yeast, confirming that the percentage of CFSE-bright cells accurately reflects yeast proliferation (**Figure 2C**). Moreover, CFSE-labeled and unlabeled *C. glabrata* proliferated at the same rate (as measured by OD_{600}) indicating that the CFSE-labeling process does not affect yeast proliferation.

Macrophages Control Intracellular *C. glabrata* Proliferation Using Syk

To evaluate the role of Syk in macrophages following exposure to *C. glabrata*, we used an *in vitro* co-culture system. Peritoneal macrophages were co-cultured with CFSE-labeled *C. glabrata* parent cells and monitored for evidence of intracellular proliferation. In wild type murine macrophages, yeast cells were phagocytosed by macrophages with high efficiency. There were rare numbers of extracellular yeast remaining as measured by microscopy (**Figure 3A**) and flow cytometry analysis of co-culture supernatant (data not shown). Following co-culture incubation, analysis of CFSE intensity of *C. glabrata* from lysed macrophages revealed that yeast did not divide for up to 16 h as measured by retained parent CFSE-bright (**Figure 3B**, top panel). However, in the presence of the reversible Syk inhibitor, R406, macrophages were unable to control *C. glabrata* division (**Figure 3B** bottom panel). Compared to untreated controls, R406-treated macrophages resulted in a diminished number of parent yeast and in a growing numbers of divided daughter population. While these yeast remained intracellular, they had escaped control and undergone division as noted by loss of CFSE (**Figure 3C**). To ensure that R406 does not alter growth kinetics of *C. glabrata*, division rates of *C. glabrata* in the presence of R406 and was not different from yeast control conditions (data not shown). These data suggest that loss of Syk activity significantly impaired the ability of macrophages to control *C. glabrata* intracellular division.

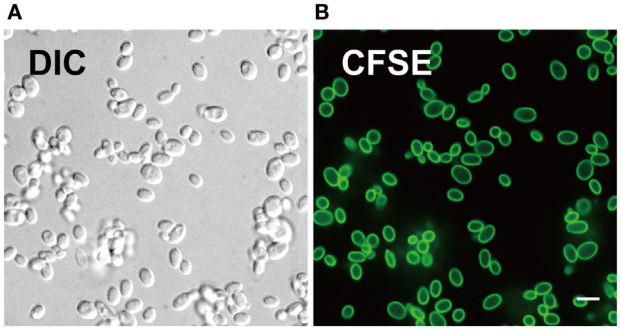

FIGURE 1 | Carboxyfluorescein succinimidyl ester (CFSE) labels cell wall of *Candida glabrata*. **(A)** Differential interference contrast and **(B)** fluorescence confocal microscopy image of live *C. glabrata* stained with CFSE showing labeling of all yeast cells prior to cell division. Scale bar represents 5 μm.

Early Syk Activity Is Required for Intracellular *C. glabrata* Control

Given that Syk is essential for control of *C. glabrata* division, we next sought to define the temporal relationship between Syk activity and yeast control. Macrophages that had engulfed *C. glabrata* were exposed to R406 continuously or following a 2, 4, or 8-h delay from time of coincubation. Syk inhibition at the start, or 2- or 4-h resulted in a loss of macrophage control as evidenced by the significant decrease in the percent of undivided yeast (**Figure 4**). The delayed addition of R406 to 8 h, and beyond, did not have an influence *C. glabrata* division. These data suggest that it is the early Syk activity following macrophage phagocytosis of yeast that is required for intracellular *C. glabrata* control.

Syk Inhibition Does Not Affect Macrophage Phagocytosis

In certain cell types, Syk has been shown to play a role in cytoskeletal rearrangement and endocytosis (33). If the process of macrophage phagocytosis was impaired by Syk inhibition (R406), this might leave extracellular *C. glabrata* in an actively dividing state. To determine if Syk inhibition impacts the process of phagocytosis of *C. glabrata* by peritoneal macrophages, we measured phagocytosis by flow cytometry in the presence and absence of R406. Cytochalasin D, an actin polymerization inhibitor, was used as a positive control inhibitor of phagocytosis.

We first determined the percent of macrophages that were associated with CFSE-bright *C. glabrata*. There was no difference in the ability of macrophages to phagocytose *C. glabrata* in the presence of R406 after 5 min (**Figure 5**). Macrophages that were treated with cytochalasin D showed dramatically reduced phagocytosis. The small percentage of yeast associated with cytochalasin D-treated macrophages as detected by flow possibly represents CFSE-bright *C. glabrata* attached extracellularly to the macrophage membrane or incomplete inhibition of

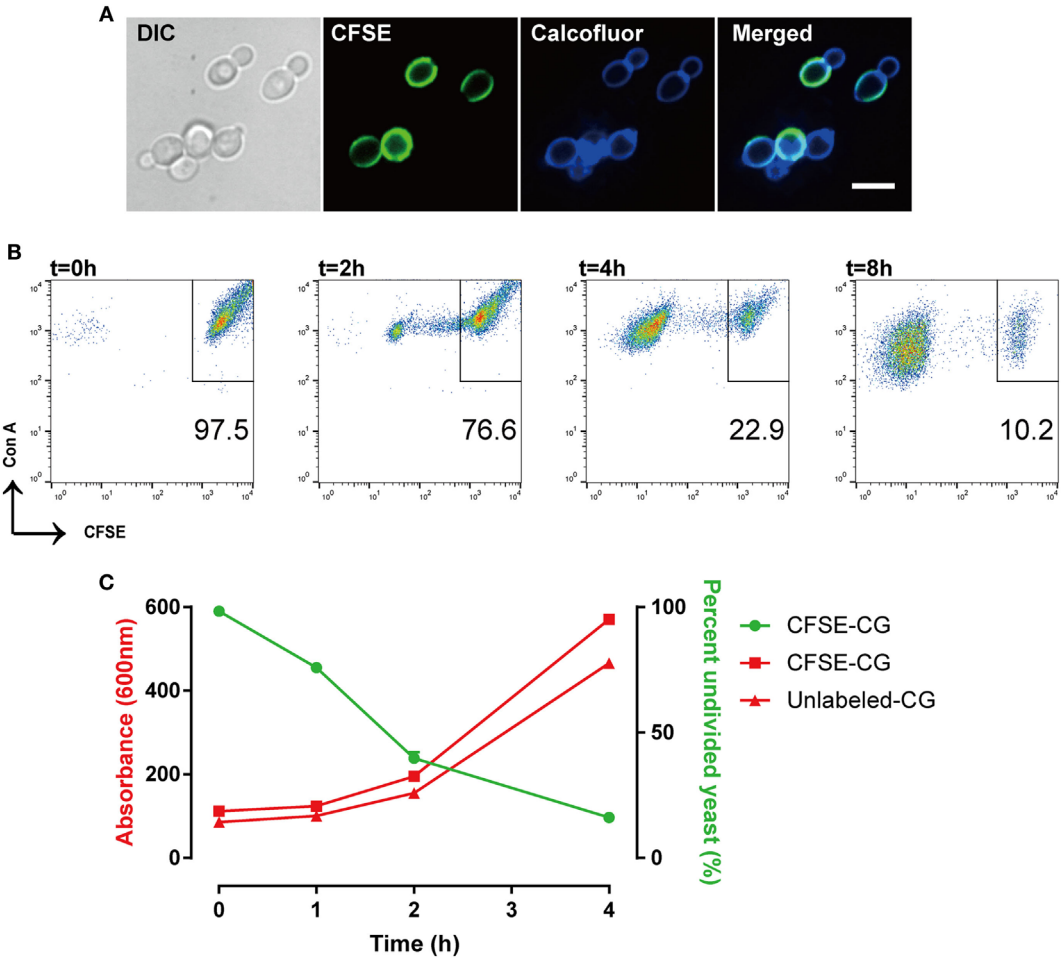

FIGURE 2 | Carboxyfluorescein succinimidyl ester (CFSE)-labeling marks *Candida glabrata* yeast division. **(A)** Differential interference contrast and fluorescence microscopy image of CFSE-labeled *C. glabrata* that have undergone division and stained with calcofluor white. Parental cells exhibit full CFSE labeling, while daughter cells have diluted CFSE labeling leading to dimmer fluorescence signal. Scale bar represents 5 μm. **(B)** Scatter plot of Con A-AF647 and CFSE fluorescence. CFSE-bright parental yeast population in upper right quadrant gate. Percent (scatter plot inset) of undivided CFSE-bright population was determined over time indicated. **(C)** Correlation of percent CFSE-bright population to OD_{600} nm of proliferating yeast. Data represent a minimum of three independent triplicate experiments.

phagocytosis by cytochalasin D. These findings indicate that Syk plays a minor role in the process of macrophage phagocytosis of *C. glabrata*.

R406 Inhibition of Syk Does Not Result in Permanent Macrophage Impairment

Given that Syk-mediated pathways are involved in multiple macrophage functions, we sought to determine if chemical Syk inhibition might result in a persistent hyporesponsive state. Given that ROS is a key mechanism in the response of macrophage to fungi, we evaluated ROS production in primary macrophages treated with R406 as compared to macrophages pulsed with R406 and then washed free of the inhibitor.

With constant R406, ROS production was completely suppressed (**Figure 6**). However, removal of R406 (following 2 h of exposure) restored ROS production to baseline levels. The observation that R406-pulsed macrophages were capable of generating robust ROS mirroring those of untreated control cells suggests that inhibition of Syk does not permanently alter the viability or biological activity of macrophages.

Dectin-1 and Dectin-2-Dependent Syk Activity Are Dispensable for Control of Intracellular *C. glabrata* Growth

Dectin-1 and Dectin-2 are upstream carbohydrate lectin PRRs that rely on Syk to regulate intracellular macrophage responses. To determine if the Syk activity required for intracellular *C. glabrata* control was derived through activation of Dectin-1 or Dectin-2, we compared peritoneal macrophages derived from wild type, to those derived from Dectin-1-deficient and Dectin-2-deficient mice. Following macrophage co-culture with CFSE-labeled *C. glabrata*, there was no difference in the control of intracellular *C. glabrata* growth between the macrophage genotypes signifying that the critical Syk activity required for yeast control is not related to individual Dectin-1 or Dectin-2 function (**Figure 7**).

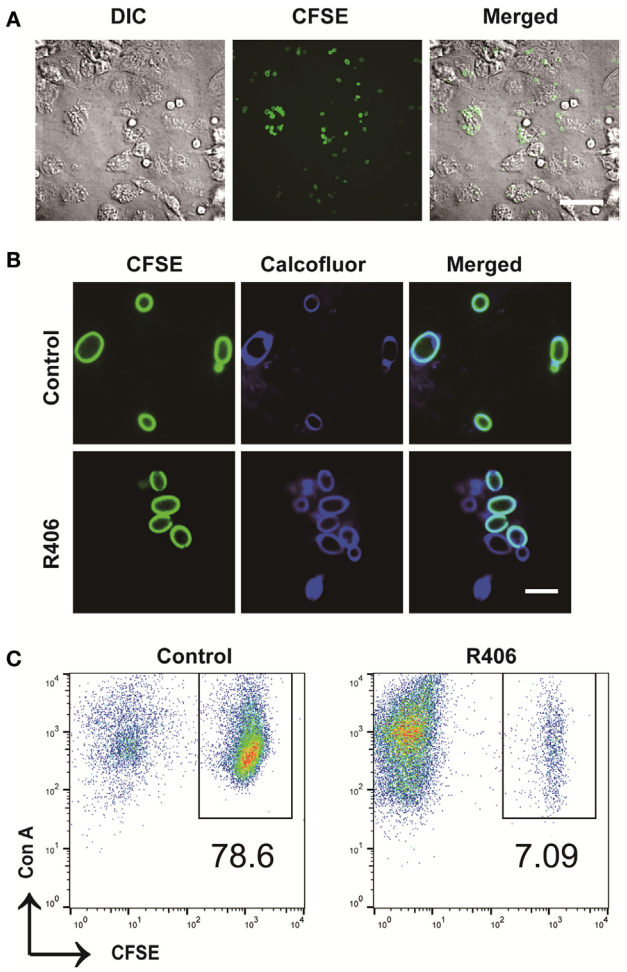

FIGURE 3 | Spleen tyrosine kinase is required for peritoneal macrophage control of *Candida glabrata*. **(A)** Differential interference contrast (DIC) and fluorescence microscopy image of carboxyfluorescein succinimidyl ester (CFSE)-*C. glabrata* and macrophage after 1 h of coculture indicating complete uptake of the yeast by the macrophages. Scale bar represents 50 µm. **(B)** DIC and fluorescence microscopy image of CFSE *C. glabrata* infected macrophages 16 h post inoculation. Macrophages control *C. glabrata* division in CFSE-bright undivided state, while treatment with R406 impaired the macrophages' ability in controlling *C. glabrata*. Scale bar represents 5 µm. **(C)** Flow cytometry scatter plots of Con A and CFSE showing macrophage controlling *C. glabrata* division and loss of control in R406-treated cells. Data represent three independent experiments.

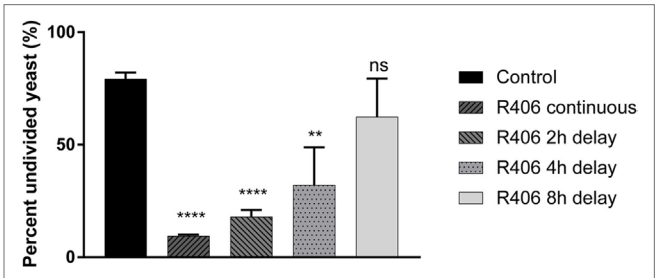

FIGURE 4 | Spleen tyrosine kinase (Syk) is required at an early stage for macrophage control of *Candida glabrata*. Macrophages were treated with chemical Syk inhibitor, R406, prior to addition of *C. glabrata* for 2, 4, and 8 h after infection. All wells were lysed after 16 h of co-culture and the yeast retrieved and stained with ConA-AF647. Percent of parental CFSE-bright population was assessed *via* flow cytometry, with R406 treatments initiated at indicated time. $^{**}p \leq 0.01$, $^{***}p \leq 0.001$, $^{****}p \leq 0.0001$. Data represent a minimum of three independent experiments.

DISCUSSION

Though the importance of the innate immune system in protecting against fungal pathogens has been articulated, defining the mechanisms responsible for the intracellular control of *C. glabrata* have yet to be defined. In this study, we define the role of Syk in the intracellular control of *C. glabrata* division in macrophages. Our approach outlines the CFSE-labeling technique as a new tool to track yeast division. We demonstrate that in macrophages, early Syk activity is essential for controlling *C. glabrata* division, and that this role is not solely dependent on the contribution of Dectin-1 or Dectin-2, both of which rely principally on Syk for intracellular signaling following ligand engagement.

We delineated a method of CFSE labeling that allows tracking of yeast multiplication. This process involved conjugating the cell wall of *C. glabrata* cells with CFSE, a fluorescent dye that links to amine groups through covalent bonds, and that can be visualized using confocal microscopy and flow cytometry. Microscopy demonstrated that CFSE does not change the morphology of *C. glabrata* cells. CFSE stained only the cell walls of parent yeasts, which permitted us to distinguish CFSE-bright parent populations and CFSE-dim daughter populations. The increase of CFSE-dim yeast cells, indicative of cell division and a growing daughter population, could be accurately measured by flow cytometry.

While CFSE assays have historically been used to follow the division of lymphocytes, our adaptation to track yeast division does face limitations. CFSE stains only the fungal cell wall rather than the contents of the cytoplasm, which allows us to track only a single generation of daughter cells. This observation is likely due to the presence of the esterase-rich fungal cell wall. Esterases are necessary for the activation of CFSE for covalent conjugation to amino groups on proteins. In mammalian cells, esterases are abundant within the cytoplasm, whereas in yeast, high levels of esterases are found within the fungal cell wall (34). This esterase distribution clarifies the reason for concentrated CFSE conjugation to the cell wall ultrastructure as opposed to homogenous cytoplasmic staining as seen in lymphocytes. Given the high concentration of CFSE in the cell wall, we confirmed that labeling did not alter the fungal cell wall or yeast division. By monitoring growth *via* optical density at 600 nm, we show that CFSE-labeled *C. glabrata* are capable of proliferating with normal kinetics as compared to unlabeled controls. While this method allows tracking of intracellular yeast division, it does not confirm killing of the yeast by macrophages.

Using CFSE-labeled yeast, we defined the role of Syk in the intracellular control of *C. glabrata* by macrophages. We hypothesized that Syk is indeed necessary for macrophages to maintain growth control of *C. glabrata* given its described contribution to phagolysosomal maturation (22) and autophagy (31). The downstream Syk-dependent molecular mechanisms critical for control of *C. glabrata* will require additional investigation and may involve sequestration of essential nutrients or disrupted

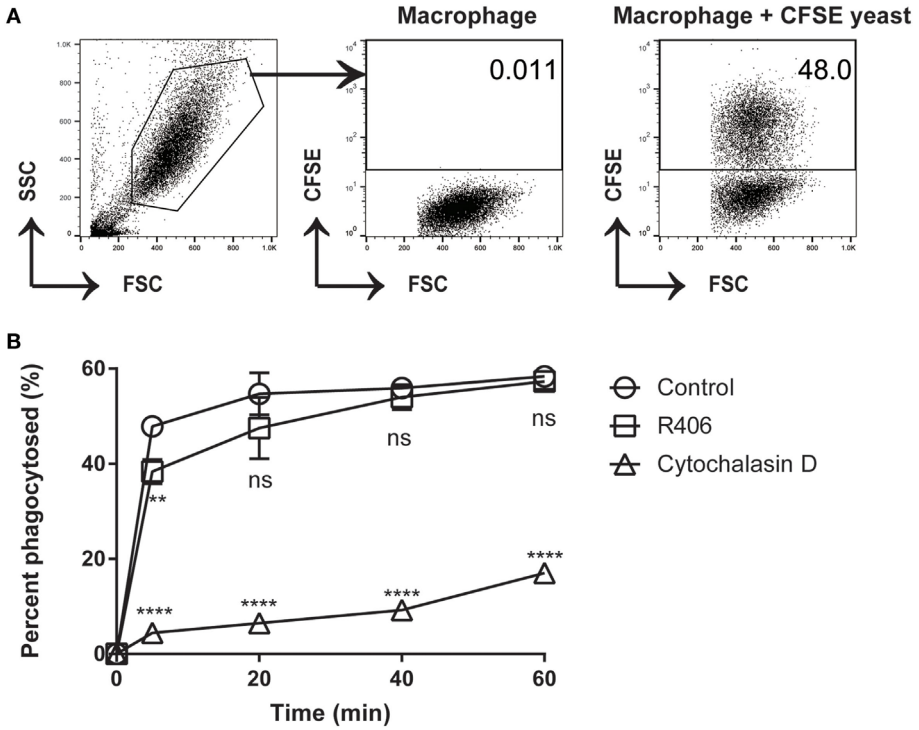

FIGURE 5 | R406-induced spleen tyrosine kinase inhibition does not affect macrophage phagocytosis of *C. glabrata*. **(A)** Gating scheme for calculated percentage of macrophages that have phagocytosed CFSE-labeled *C. glabrata* by flow cytometry. **(B)** Percent phagocytosis of *C. glabrata* by macrophages over time incubated with control, R406, or cytochalasin D by flow cytometry. $^{**}p \leq 0.01$, $^{****}p < 0.0001$. Data represent three independent experiments.

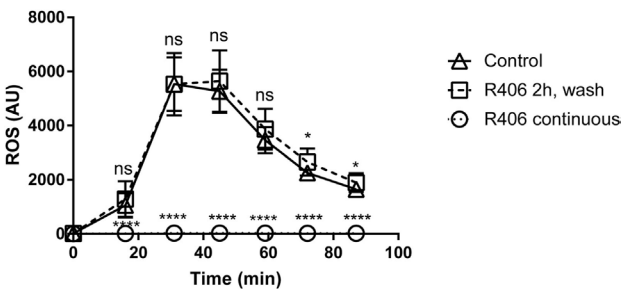

FIGURE 6 | R406 does not result in permanent macrophage response defects to fungal stimuli as measured by reactive oxygen species (ROS) production. Plated macrophages were treated with R406 for 2 h, and then washed to remove the inhibitor. ROS production measured by lucigenin after addition of heat-killed *Candida*. Arbitrary light unites (AU) represents total luminescence corresponding with ROS production. $^{*}p \leq 0.05$, $^{****}p \leq 0.0001$. Data represent a minimum of three independent experiments.

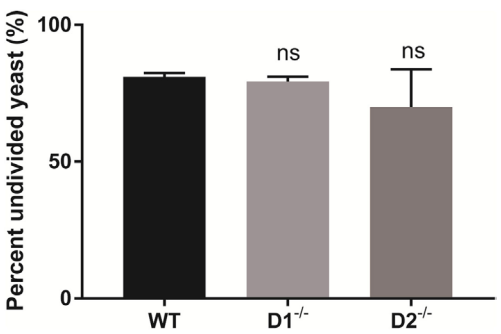

FIGURE 7 | Spleen tyrosine kinase-mediated control of *Candida glabrata* is independent of Dectin-1 and Dectin-2. Percent undivided carboxyfluorescein succinimidyl ester-bright *C. glabrata* population from peritoneal macrophages-yeast co-cultures. Macrophages were obtained from wild type, Dectin-1$^{-/-}$, and Dectin-2$^{-/-}$ mice. Comparisons between all groups are non-significant. Data represent a minimum of three independent experiments.

fusion of lysosomal content. The C-type lectin receptors, Dectin-1 and Dectin-2, recognize fungi and are linked through Syk for intracellular signaling (35). We determined the contribution of each receptor to Syk activity in macrophages following *Candida* exposure. Data reveal that loss of either receptor does not impact the control of intracellular *C. glabrata* suggesting that Syk activity is stimulated through redundant pathways.

In addition to Syk being important for *C. glabrata* control, we also demonstrates the importance of timing of Syk activity. Early Syk activation, within the first 4 h after macrophage phagocytosis *C. glabrata,* is the essential window for effective control of *C. glabrata* division. Macrophages in which Syk was inhibited 2 or 4 h after addition of *C. glabrata* enabled the yeast to divide unchecked. Syk may have less relevance when inhibited 8 h after co-infection because the macrophages retain their ability to control yeast division in similar fashion to untreated macrophages. These observations may be due to time-dependent phagosomal mechanisms, which have no further consequence on *C. glabrata*

division at later stages following phagocytosis. In addition, *C. glabrata*-specific immune evasion pathways may be upregulated at later time points, and these may bypass Syk-related control mechanisms. In this study, we have only evaluated chemical Syk inhibition, and have yet to test Syk knockout models.

Spleen tyrosine kinase has an established role in cytoskeletal changes, which could potentially impact phagocytosis. To control for this possibility, we measured uptake of *C. glabrata* by macrophages and found no difference in phagocytosis between control and R406-treated macrophages. This observation is in line with our previous observation using tyrosine mutations in the hemi-ITAM of Dectin-1, which result in complete loss of Syk phosphorylation, yet maintains near normal rates of phagocytosis (22). In addition, to address the likelihood of a lasting effect triggered through Syk inhibition, we utilized ROS activity as a surrogate marker of macrophage activity. After washout of R406, ROS activity is fully restored, indicating that transient Syk inhibition does not result in a long-lasting inhibition of macrophages, and does not account for loss of intracellular *C. glabrata* activity.

In conclusion, our results demonstrate that macrophages control the division of *C. glabrata* in a Syk-dependent manner. A limitation of this observation is the use of a single ATCC strain and further investigation is required to determine if Syk-dependent control is generalizable to other *Candida* species. These observations were verified by a CFSE-labeling technique that accurately distinguished CFSE-bright parent and CFSE-dim daughter cell populations through flow cytometric analysis or microscopy. We show that Syk in macrophages is essential in the early stages of *C. glabrata* infection and that Dectin-1 or Dectin-2 are not individual contributors to Syk activity. Further investigations are required to define the precise downstream mechanisms of Syk activity in the intracellular control of fungal pathogens.

ETHICS STATEMENT

This study was carried out in accordance with the recommendations of Massachusetts General Hospital Institutional Animal Care and Use Committee. The protocol was approved by the Massachusetts General Hospital Institutional Animal Care and Use Committee.

AUTHOR CONTRIBUTIONS

ZD, SX, PN, MM, and DS contributed to experimental design. ZD, SX, PN, JT, and MM executed the experiments. ZD, SX, PN, NK, MF, JR, JT, DS, and MM performed analysis and interpretation of experiments. ZD, SX, PN, and MM contributed in writing the manuscript.

FUNDING

This work was supported, in whole or in part, by NIH NIAID T32 AI007061 (to JR), NIH NIAID K08 AI110655 (to MM), and K08 CA201640 (to DS).

REFERENCES

1. Sardi JC, Scorzoni L, Bernardi T, Fusco-Almeida AM, Mendes Giannini MJ. *Candida* species: current epidemiology, pathogenicity, biofilm formation, natural antifungal products and new therapeutic options. *J Med Microbiol* (2013) 62(Pt 1):10–24. doi:10.1099/jmm.0.045054-0
2. Rodrigues CF, Silva S, Henriques M. *Candida glabrata*: a review of its features and resistance. *Eur J Clin Microbiol Infect Dis* (2014) 33(5):673–88. doi:10.1007/s10096-013-2009-3
3. Silva S, Henriques M, Hayes A, Oliveira R, Azeredo J, Williams DW. *Candida glabrata* and *Candida albicans* co-infection of an in vitro oral epithelium. *J Oral Pathol Med* (2011) 40(5):421–7. doi:10.1111/j.1600-0714.2010.00981.x
4. Kaur R, Ma B, Cormack BP. A family of glycosylphosphatidylinositol-linked aspartyl proteases is required for virulence of *Candida glabrata*. *Proc Natl Acad Sci U S A* (2007) 104(18):7628–33. doi:10.1073/pnas.0611195104
5. Kasper L, Seider K, Hube B. Intracellular survival of *Candida glabrata* in macrophages: immune evasion and persistence. *FEMS Yeast Res* (2015) 15(5):fov042. doi:10.1093/femsyr/fov042
6. Ifrim DC, Bain JM, Reid DM, Oosting M, Verschueren I, Gow NA, et al. Role of Dectin-2 for host defense against systemic infection with *Candida glabrata*. *Infect Immun* (2014) 82(3):1064–73. doi:10.1128/IAI.01189-13
7. Filby A, Begum J, Jalal M, Day W. Appraising the suitability of succinimidyl and lipophilic fluorescent dyes to track proliferation in non-quiescent cells by dye dilution. *Methods* (2015) 82:29–37. doi:10.1016/j.ymeth.2015.02.016
8. Tario JD Jr, Humphrey K, Bantly AD, Muirhead KA, Moore JS, Wallace PK. Optimized staining and proliferation modeling methods for cell division monitoring using cell tracking dyes. *J Vis Exp* (2012) (70):e4287. doi:10.3791/4287
9. Weston SA, Parish CR. New fluorescent dyes for lymphocyte migration studies. Analysis by flow cytometry and fluorescence microscopy. *J Immunol Methods* (1990) 133(1):87–97. doi:10.1016/0022-1759(90)90322-M
10. Hawkins ED, Hommel M, Turner ML, Battye FL, Markham JF, Hodgkin PD. Measuring lymphocyte proliferation, survival and differentiation using CFSE time-series data. *Nat Protoc* (2007) 2(9):2057–67. doi:10.1038/nprot.2007.297
11. Lastovicka J, Rataj M, Bartunkova J. Assessment of lymphocyte proliferation for diagnostic purpose: comparison of CFSE staining, Ki-67 expression and (3)H-thymidine incorporation. *Hum Immunol* (2016) 77(12):1215–22. doi:10.1016/j.humimm.2016.08.012
12. Parish CR. Fluorescent dyes for lymphocyte migration and proliferation studies. *Immunol Cell Biol* (1999) 77(6):499–508. doi:10.1046/j.1440-1711.1999.00877.x
13. Ludington JG, Ward HD. The *Cryptosporidium parvum* C-type lectin CpClec mediates infection of intestinal epithelial cells via interactions with sulfated proteoglycans. *Infect Immun* (2016) 84(5):1593–602. doi:10.1128/IAI.01410-15
14. Ueckert JE, Nebe von-Caron G, Bos AP, ter Steeg PF. Flow cytometric analysis of *Lactobacillus plantarum* to monitor lag times, cell division and injury. *Lett Appl Microbiol* (1997) 25(4):295–9. doi:10.1046/j.1472-765X.1997.00225.x
15. Batista VG, Toledo MS, Straus AH, Mendes-Giannini MJ, Duarte AJ, Takahashi HK, et al. Glycolipid sensing and innate immunity in paracoccidioidomycosis. *Mycopathologia* (2014) 178(3–4):153–62. doi:10.1007/s11046-014-9783-z
16. Bocharov G, Luzyanina T, Cupovic J, Ludewig B. Asymmetry of cell division in CFSE-based lymphocyte proliferation analysis. *Front Immunol* (2013) 4:264. doi:10.3389/fimmu.2013.00264
17. Seider K, Brunke S, Schild L, Jablonowski N, Wilson D, Majer O, et al. The facultative intracellular pathogen *Candida glabrata* subverts macrophage cytokine production and phagolysosome maturation. *J Immunol* (2011) 187(6):3072–86. doi:10.4049/jimmunol.1003730
18. Davi V, Minc N. Mechanics and morphogenesis of fission yeast cells. *Curr Opin Microbiol* (2015) 28:36–45. doi:10.1016/j.mib.2015.07.010
19. Piel M, Tran PT. Cell shape and cell division in fission yeast. *Curr Biol* (2009) 19(17):R823–7. doi:10.1016/j.cub.2009.08.012
20. Hohl TM, Rivera A, Pamer EG. Immunity to fungi. *Curr Opin Immunol* (2006) 18(4):465–72. doi:10.1016/j.coi.2006.05.003
21. Collette JR, Lorenz MC. Mechanisms of immune evasion in fungal pathogens. *Curr Opin Microbiol* (2011) 14(6):668–75. doi:10.1016/j.mib.2011.09.007

22. Mansour MK, Tam JM, Khan NS, Seward M, Davids PJ, Puranam S, et al. Dectin-1 activation controls maturation of beta-1,3-glucan-containing phagosomes. *J Biol Chem* (2013) 288(22):16043–54. doi:10.1074/jbc.M113.473223
23. Turner M, Schweighoffer E, Colucci F, Di Santo JP, Tybulewicz VL. Tyrosine kinase SYK: essential functions for immunoreceptor signalling. *Immunol Today* (2000) 21(3):148–54. doi:10.1016/S0167-5699(99)01574-1
24. Miller YI, Choi SH, Wiesner P, Bae YS. The SYK side of TLR4: signalling mechanisms in response to LPS and minimally oxidized LDL. *Br J Pharmacol* (2012) 167(5):990–9. doi:10.1111/j.1476-5381.2012.02097.x
25. Underhill DM, Rossnagle E, Lowell CA, Simmons RM. Dectin-1 activates Syk tyrosine kinase in a dynamic subset of macrophages for reactive oxygen production. *Blood* (2005) 106(7):2543–50. doi:10.1182/blood-2005-03-1239
26. Yi YS, Son YJ, Ryou C, Sung GH, Kim JH, Cho JY. Functional roles of Syk in macrophage-mediated inflammatory responses. *Mediators Inflamm* (2014) 2014:270302. doi:10.1155/2014/270302
27. Geahlen RL. Getting Syk: spleen tyrosine kinase as a therapeutic target. *Trends Pharmacol Sci* (2014) 35(8):414–22. doi:10.1016/j.tips.2014.05.007
28. Ruzza P, Biondi B, Calderan A. Therapeutic prospect of Syk inhibitors. *Expert Opin Ther Pat* (2009) 19(10):1361–76. doi:10.1517/13543770903207039
29. Taylor PR, Tsoni SV, Willment JA, Dennehy KM, Rosas M, Findon H, et al. Dectin-1 is required for beta-glucan recognition and control of fungal infection. *Nat Immunol* (2007) 8(1):31–8. doi:10.1038/ni1408
30. Saijo S, Ikeda S, Yamabe K, Kakuta S, Ishigame H, Akitsu A, et al. Dectin-2 recognition of alpha-mannans and induction of Th17 cell differentiation is essential for host defense against *Candida albicans*. *Immunity* (2010) 32(5):681–91. doi:10.1016/j.immuni.2010.05.001
31. Tam JM, Mansour MK, Khan NS, Seward M, Puranam S, Tanne A, et al. Dectin-1-dependent LC3 recruitment to phagosomes enhances fungicidal activity in macrophages. *J Infect Dis* (2014) 210(11):1844–54. doi:10.1093/infdis/jiu290
32. Reedy JL, Negoro PE, Feliu M, Lord AK, Khan NS, Lukason DP, et al. The carbohydrate lectin receptor dectin-1 mediates the immune response to *Exserohilum rostratum*. *Infect Immun* (2017) 85(3):e903–16. doi:10.1128/IAI.00903-16
33. Le Roux D, Lankar D, Yuseff MI, Vascotto F, Yokozeki T, Faure-Andre G, et al. Syk-dependent actin dynamics regulate endocytic trafficking and processing of antigens internalized through the B-cell receptor. *Mol Biol Cell* (2007) 18(9):3451–62. doi:10.1091/mbc.E06-12-1114
34. Peter J, Armstrong D, Lyman CA, Walsh TJ. Use of fluorescent probes to determine MICs of amphotericin B and caspofungin against *Candida* spp. and *Aspergillus* spp. *J Clin Microbiol* (2005) 43(8):3788–92. doi:10.1128/JCM.43.8.3788-3792.2005
35. Netea MG, Brown GD, Kullberg BJ, Gow NA. An integrated model of the recognition of *Candida albicans* by the innate immune system. *Nat Rev Microbiol* (2008) 6(1):67–78. doi:10.1038/nrmicro1815

Conflict of Interest Statement: The authors declare that the research was conducted in the absence of any commercial or financial relationships that could be construed as a potential conflict of interest.

Copyright © 2018 Dagher, Xu, Negoro, Khan, Feldman, Reedy, Tam, Sykes and Mansour. This is an open-access article distributed under the terms of the Creative Commons Attribution License (CC BY). The use, distribution or reproduction in other forums is permitted, provided the original author(s) and the copyright owner are credited and that the original publication in this journal is cited, in accordance with accepted academic practice. No use, distribution or reproduction is permitted which does not comply with these terms.

frontiers in Immunology

ORIGINAL RESEARCH
published: 11 January 2018
doi: 10.3389/fimmu.2017.01984

Host-Derived Leukotriene B_4 Is Critical for Resistance against Invasive Pulmonary Aspergillosis

*Alayna K. Caffrey-Carr[1,2], Kimberly M. Hilmer[1], Caitlin H. Kowalski[2], Kelly M. Shepardson[1,2], Rachel M. Temple[2], Robert A. Cramer[2] and Joshua J. Obar[2]**

[1] Department of Microbiology and Immunology, Montana State University, Bozeman, MT, United States, [2] Department of Microbiology and Immunology, Geisel School of Medicine at Dartmouth, Lebanon, NH, United States

Aspergillus fumigatus is a mold that causes severe pulmonary infections. Our knowledge of how immune competent hosts maintain control of fungal infections while constantly being exposed to fungi is rapidly emerging. It is known that timely neutrophil recruitment to and activation in the lungs is critical to the host defense against development of invasive pulmonary aspergillosis, but the inflammatory sequelae necessary remains to be fully defined. Here, we show that 5-Lipoxygenase (5-LO) and Leukotriene B_4 (LTB_4) are critical for leukocyte recruitment and resistance to pulmonary *A. fumigatus* challenge in a fungal-strain-dependent manner. 5-LO activity was needed in radiosensitive cells for an optimal anti-fungal response and *in vivo* LTB_4 production was at least partially dependent on myeloid-derived hypoxia inducible factor-1α. Overall, this study reveals a role for host-derived leukotriene synthesis in innate immunity to *A. fumigatus*.

Keywords: ***Aspergillus fumigatus*, leukotrienes, leukotriene B_4, neutrophils, eosinophils, hypoxia inducible factor-1α, respiratory tract infections, fungal infection**

OPEN ACCESS

Edited by:
Steven Templeton, Indiana University School of Medicine, United States

Reviewed by:
Michail Lionakis, National Institute of Allergy and Infectious Diseases (NIH), United States
Teresa Zelante, University of Perugia, Italy

****Correspondence:***
Joshua J. Obar
joshua.j.obar@dartmouth.edu

Specialty section:
This article was submitted to Microbial Immunology, a section of the journal Frontiers in Immunology

Received: *29 September 2017*
Accepted: *20 December 2017*
Published: *11 January 2018*

Citation:
Caffrey-Carr AK, Hilmer KM, Kowalski CH, Shepardson KM, Temple RM, Cramer RA and Obar JJ (2018) Host-Derived Leukotriene B_4 Is Critical for Resistance against Invasive Pulmonary Aspergillosis. Front. Immunol. 8:1984. doi: 10.3389/fimmu.2017.01984

INTRODUCTION

Aspergillus fumigatus is a ubiquitous mold that causes severe infections, such as invasive pulmonary aspergillosis (IPA), in the immunocompromised population. Due to a combination of (i) difficulty in diagnosis, (ii) limited efficacy of anti-fungal drugs coupled with the emergence of drug resistance, and (iii) a lack of an effective vaccine against *Aspergillus* spp., mortality rates of IPA are extremely high (1, 2). To this end, development of novel immunomodulatory strategies that can potentially be combined with current anti-fungal treatments is an active area of research.

On a day-to-day basis, inhaled spores are removed from the body through physical barriers encountered within the respiratory tract. If spores are deposited in the lung, resident alveolar macrophages and $CCR2^+$ monocytes, together with alveolar epithelial cells, phagocytose, and kill fungal conidia (3, 4). However, in individuals that lack this immune response, conidia are able to germinate and grow within the lung causing tissue damage and disease. These initial encounters are important in the recruitment and activation of neutrophils, inflammatory monocytes, NK cells, and CD4 T cells to further control fungal growth within the lung (5). Of these, neutrophils have long been recognized as one of the key effector cells necessary for resistance against *Aspergillus* infection and neutropenia is a key risk factor for patients that will develop IPA (6).

Neutrophil recruitment and activation is a highly controlled process that is regulated by a number of different inflammatory mediators including C5a, PAF, fMLP, Leukotriene B_4 (LTB_4), CXCR2 ligands, CCR1 ligands, TNFα, and IL-17 (7, 8). However, our understanding of the inflammatory mediators driving neutrophil accumulation and activation following *A. fumigatus* challenge remains incomplete. Following *A. fumigatus* challenge, IL-1RI/MyD88 signaling is essential for optimal

production of CXCL1 that is necessary for early neutrophil recruitment through CXCR2 (6, 9, 10). In addition, an unknown CARD9-dependent pathway is critical for late neutrophil accumulation following *A. fumigatus* challenge (9). Additionally, a TLR9/Btk/calcineurin/NFAT-dependent pathway regulates neutrophil accumulation during aspergillosis through its regulation of TNFα (11). Moreover, further complexity exists in that *A. fumigatus* isolates with differing virulence depend on distinct inflammatory responses to maintain host resistance (12, 13). Thus, greater knowledge about the inflammatory pathways which contribute to the anti-*Aspergillus* neutrophil response is required.

Regulation of inflammatory responses by lipid mediators is an emerging area. Particularly, LTB$_4$ has a critical role in the early recruitment and activation of neutrophils in other inflammatory models (14). Additionally, lipid mediators have been shown to be critical regulators of the host immune response against pathogenic fungi. Following challenge of alveolar macrophages or resident mouse peritoneal macrophages with *Candida albicans* arachidonic acid is effectively mobilized by cPLA2 (15–17), which is necessary for production of both prostaglandins and leukotrienes. cPLA2 is critical for host resistance against *C. albicans* challenge, through the regulation of macrophage transcriptional responses and likely through increased anti-fungal activity of alveolar macrophages (17, 18). Moreover, exogenous LTB$_4$ and LTD$_4$ can enhance phagocytosis and killing of *C. albicans* by macrophages (19). Finally, LTB$_4$-mediated inflammation is critical for host resistance and neutrophil recruitment during *Histoplasma capsulatum* (20, 21), and *Paracoccidioides brasiliensis* (22, 23) infection. Moreover, LTB$_4$-mediated inflammation is critical for establishing memory T cells for the prevention of histoplasmosis (24). Thus, we asked whether LTB$_4$ was crucial in the neutrophil response following pulmonary *A. fumigatus* challenge. Here, we show that leukotrienes are produced rapidly after *A. fumigatus* challenge by host cells and play a critical role in the anti-fungal neutrophil response necessary for host resistance against pulmonary *A. fumigatus* challenge.

MATERIALS AND METHODS

Mice

C57BL/6J (Stock #000664), C57BL/6NJ (Stock #005304), B6.129S2-*Alox5*^{tm1Fun} (*Alox5*$^{-/-}$; Stock #004155), and B6.129S4-*Ltb4r1*^{tm1Adl} (*Ltb4r1*$^{-/-}$; Stock #008102) were purchased from Jackson Laboratories. Mice with a targeted deletion of *Hif1a* in myeloid cells were created via crosses into a background of lysozyme M-driven cre-recombinase (*Hif1a*$^{LysM/LysM}$), as previously done (30). All mice were 8–10 weeks of age at the time of infection. All animal experiments were approved by the Montana State University Institutional Animal Care and Use Committee or Dartmouth College Institutional Animal Care and Use Committee.

Preparation of *A. fumigatus* and Pulmonary Challenge Model

Aspergillus fumigatus strains CEA10 and Af293 were grown and harvested as previously described (10). For fungal inoculation, mice were anesthetized with isoflurane and challenged by the intratracheally (i.t.) route with 4–7 × 10^7 *A. fumigatus* conidia in 100 µl sterile PBS. At the indicated time after challenge, mice were euthanized using an overdose of pentobarbital. Samples were collected and analyzed for inflammatory cell recruitment, fungal growth, lung damage, and vascular/epithelial leakage as previously described (10). For survival studies, mice were challenged with 4–7 × 10^7 conidia of either CEA10 or Af293 and monitored daily using a humane endpoint scoring system. Mice were humanely euthanized once they met endpoint criteria.

Bone Marrow Chimeric Mice

Bone marrow chimeric mice were made by lethal irradiation of C57BL/6 mice followed by intravenous reconstitution with either C57BL/6 bone marrow or *Alox5*$^{-/-}$ bone marrow. Mice were rested 6–8 weeks prior to challenge with 4 × 10^7 conidia of CEA10 i.t. At the indicated time-points, mice were euthanized using an overdose of pentobarbital, and samples collected and analyzed for inflammatory cell recruitment and fungal growth as previously described (10).

Leukotriene Quantification

Lipids were extracted from bronchoalveolar lavage fluid (BALF) using a hot-methanol extraction. Briefly, three parts HPLC-grade methanol were added to one part BALF sample. Samples were then vortexed for 30 s and placed into an 80°C water bath for 2 min. Tubes were spun at 14,000 RPM for 15 min and supernatant was collected then dried using a vacuum concentrator. Pellets were resuspended in HPLC-grade water in a volume equal to the starting volume of BALF sample. Extracted samples were then analyzed using enzyme immunoassay kits for LTB$_4$, cysteinyl leukotrienes (cysLT) (Cayman Chemical). Plates were read using a SpectraMax® Paradigm® plate reader (Molecular Devices).

Statistical Analysis

Statistical significance between experimental groups was determined using a Mann–Whitney *U* test (comparison of two experimental groups that are not normally distributed) or an one-way ANOVA with a Dunn's post-test (comparison of greater than two experimental groups that are not normally distributed), using the GraphPad Prism 6 software. For survival studies, Mantel–Cox log-rank test was used to determine whether there were significant differences in survival between C57BL/6, Hif1a$^{LysM/LysM}$, *Ltb4r1*$^{-/-}$, and *Alox5*$^{-/-}$ mice for each *A. fumigatus* strain.

RESULTS

Leukotriene Production following Pulmonary Challenge with *A. fumigatus*

In order to determine whether leukotrienes are produced following *A. fumigatus* challenge, we challenged C57BL/6 wild-type mice with the CEA10 strain of *A. fumigatus*. Throughout a time course of 6–48 h post-infection (hpi), we collected BALF and measured leukotriene production. We found that LTB$_4$ and cysLT showed increased production after *A. fumigatus* CEA10 challenge. The production of these inflammatory lipid mediators followed

a similar trend early after infection in which their expression peaked at 6 hpi, followed by decreased levels at 12 hpi. At 24 and 48 hpi LTB$_4$ increased from the 12 hpi levels, while the cysLT levels continue to decrease (**Figure 1**). These data demonstrate that both LTB$_4$ and cysLTs are synthesized following challenge of immunocompetent mice with *A. fumigatus*.

Ltb4r1$^{-/-}$ Mice Have a Defect in Inflammatory Cell Recruitment and Resistance to IPA

LTB$_4$ is known to be important in the recruitment of neutrophils in numerous inflammatory settings (14), but whether it is crucial in regulating the innate immune response following *A. fumigatus* challenge is unknown. To address whether LTB$_4$ was critical for neutrophil recruitment and resistance against IPA, we challenged *Ltb4r1*$^{-/-}$ and C57BL/6 mice with *A. fumigatus*. At 12 hpi, we analyzed BALF *via* differential cytospins stained with Diff-Quik™ to assess early inflammatory cell recruitment to the airways. Compared with the C57BL/6 mice, *Ltb4r1*$^{-/-}$ mice had a significant defect in neutrophil and eosinophil numbers, while macrophage numbers was similar (**Figure 2A**). Because the early recruitment of neutrophils is needed for host resistance to invasive *A. fumigatus* infection (6), we next addressed whether fungal growth was enhanced in the *Ltb4r1*$^{-/-}$ animals. At 24 hpi, Grocott-Gomori methenamine silver (GMS) staining of lung sections revealed the presence of an increased proportion of germinated *A. fumigatus* in *Ltb4r1*$^{-/-}$ mice compared with C57BL/6 mice (**Figure 2B**) demonstrating *Ltb4r1*$^{-/-}$ mice were impaired in their ability to clear the fungi (**Figure 2C**). Lastly, lung damage and endothelial/epithelial leakage induced by *A. fumigatus* challenge were assessed by quantifying lactate dehydrogenase (LDH) and albumin in the BALF, respectively. Albumin levels were significantly elevated in *Ltb4r1*$^{-/-}$ mice compared with C57BL/6 mice, indicating an increase in protein leakage from the vascular system (**Figure 2D**). In contrast, LDH levels were only mildly elevated suggesting induction of similar degrees of cell damage (**Figure 2D**). Taken together, these data demonstrate that LTB$_4$ signaling through its high-affinity receptor LTB4R1 is important in mediating neutrophil and eosinophil recruitment to the airways, which was ultimately necessary for host resistance to *A. fumigatus* growth.

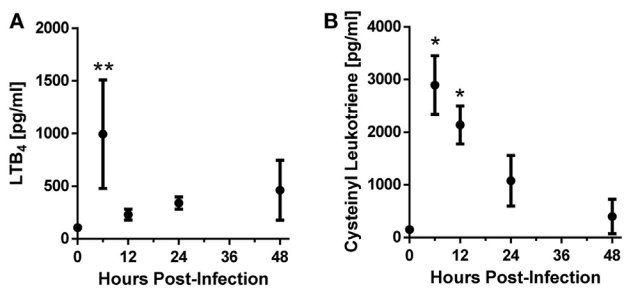

FIGURE 1 | C57BL/6 mice produce leukotrienes after pulmonary challenge with the CEA10 isolate of *Aspergillus fumigatus*. Mice were infected intratracheally with 5×10^7 CEA10 conidia and at indicated time-points, mice were euthanized and bronchoalveolar lavage fluid (BALF) collected. Lipids were then extracted from BALF using a hot-methanol extraction procedure, and LTB4 **(A)** and cysteinyl leukotriene **(B)** levels in the extracted BALF samples were measured using Cayman Chemical enzyme immunoassay kits. Data are representative of five mice per time-point. Each dot represents the mean ± 1 SEM. Statistically significant differences were determined using an one-way ANOVA with a Dunn's post-test (*$p < 0.05$ and **$p < 0.01$).

Alox5$^{-/-}$ Mice Are Impaired in Inflammatory Cell Recruitment and Resistance to IPA

Aspergillus fumigatus itself is known to be capable of producing eicosanoids (25), which results in an infection system in which both the mammalian and fungal cells could be the source of bioactive LTB$_4$. Thus, to address whether LTB$_4$ production coming from the murine cells was necessary for host resistance against *A. fumigatus*, we challenged 5-lipoxygenase (5-LO) (*Alox5*$^{-/-}$) deficient mice with *A. fumigatus*. *Alox5*$^{-/-}$ mice cannot convert arachidonic acid to LTA$_4$ and, therefore, lack all leukotriene synthesis (22). After *A. fumigatus* challenge, inflammatory cell recruitment to the airways was quantified at 12 hpi *via* cytospins and Diff-Quik™ staining. Similar to what we found with the *Ltb4r1*$^{-/-}$ mice, *Alox5*$^{-/-}$ mice had a significant defect in both neutrophil and eosinophil recruitment, while macrophage accumulation remained largely similar to C57BL/6 (**Figure 3A**). This defect in neutrophil and eosinophil recruitment correlated with an impairment in the ability of *Alox5*$^{-/-}$ mice to control fungal growth within the lung, demonstrated by a significantly higher germination rate (**Figures 3B,C**). We also measured LDH and albumin levels in the BALF of the *Alox5*$^{-/-}$ mice to assess lung damage and vascular/epithelial permeability, respectively. Interestingly, unlike the *Ltb4r1*$^{-/-}$ mice, LDH and albumin levels in BALF from *Alox5*$^{-/-}$ mice were not significantly different than C57BL/6 levels (**Figure 3D**). Together, these data indicate that leukotriene synthesis by host cells is critical for neutrophil and eosinophil recruitment, as well as host resistance against *A. fumigatus* growth.

Radiosensitive Cells Contribute to 5-LO Activity following Pulmonary *A. fumigatus* Challenge

To begin to determine the cells that contribute to 5-LO activity after *A. fumigatus* challenge, we utilized a bone marrow chimera approach. C57BL/6 mice were lethally irradiated then reconstituted with either C57BL/6 or *Alox5*$^{-/-}$ bone marrow intravenously to develop the following groups: C57BL/6 mice possessing C57BL/6 bone marrow and C57BL/6 mice possessing *Alox5*$^{-/-}$ bone marrow. Mice were then rested for 6–8 weeks prior to challenge with 4×10^7 conidia of CEA10. At 36 hpi, mice were euthanized, BAL collected for analysis of leukocyte recruitment to the airways, and lungs saved for histological analysis to assess fungal growth by GMS staining. Compared with C57BL/6 mice possessing C57BL/6 bone marrow, C57BL/6 mice possessing *Alox5*$^{-/-}$ bone marrow had a significant defect in neutrophil and eosinophil recruitment to the airways at 36 hpi, while macrophage accumulation was not significantly altered (**Figure 4A**). Moreover, at 36 hpi, C57BL/6

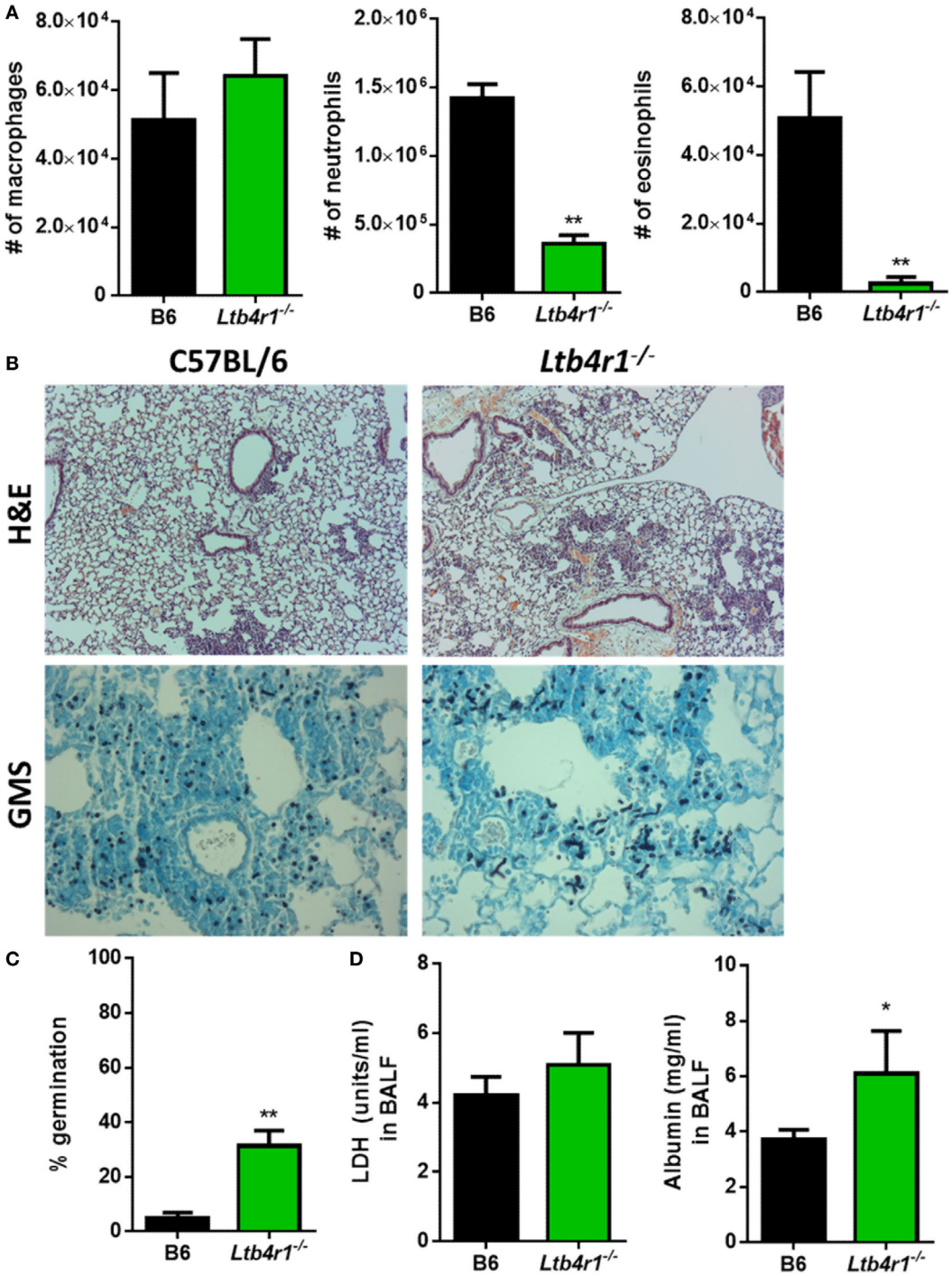

FIGURE 2 | *Ltb4r1*-deficient mice have a defect in neutrophil and eosinophil recruitment and increased fungal burden after pulmonary *Aspergillus fumigatus* challenge. Age-matched C57BL/6 or *Ltb4r1*-deficient mice were infected intratracheally with 5×10^7 CEA10 conidia and at indicated time-points, mice were euthanized, bronchoalveolar lavage fluid (BALF) collected, and lungs saved for histological analysis. **(A)** Total macrophage (left panel), neutrophil (middle panel), and eosinophil (right panel) numbers in the BALF was measured at 12 h post-infection (hpi). **(B)** Formalin-fixed lungs were paraffin embedded, sectioned, and stained with hematoxylin and eosin (H&E) (top) or Grocott-Gomori methenamine silver (GMS) (bottom) for analysis by microscopy. Representative lung sections from C57BL/6 and *Ltb4r1*-deficient mice infected with CEA10 are shown using the 10× objective for H&E staining or 40× objective for GMS staining. **(C)** *A. fumigatus* germination rates were assessed at 24 hpi by microscopically counting the number of conidia and germlings in GMS-stained sections from C57BL/6 and *Ltb4r1*-deficient mice. **(D)** Lung damage (left panel) and leakage (right panel) were assessed at 24 hpi by measuring lactate dehydrogenase (LDH) and albumin levels in the BALF, respectively. Data are representative of at least two independent experiments consisting of five to eight mice per group. Bar graphs show the group mean ± 1 SEM. Statistically significant differences were determined using Mann–Whitney *U* test (*$p < 0.05$, **$p < 0.01$).

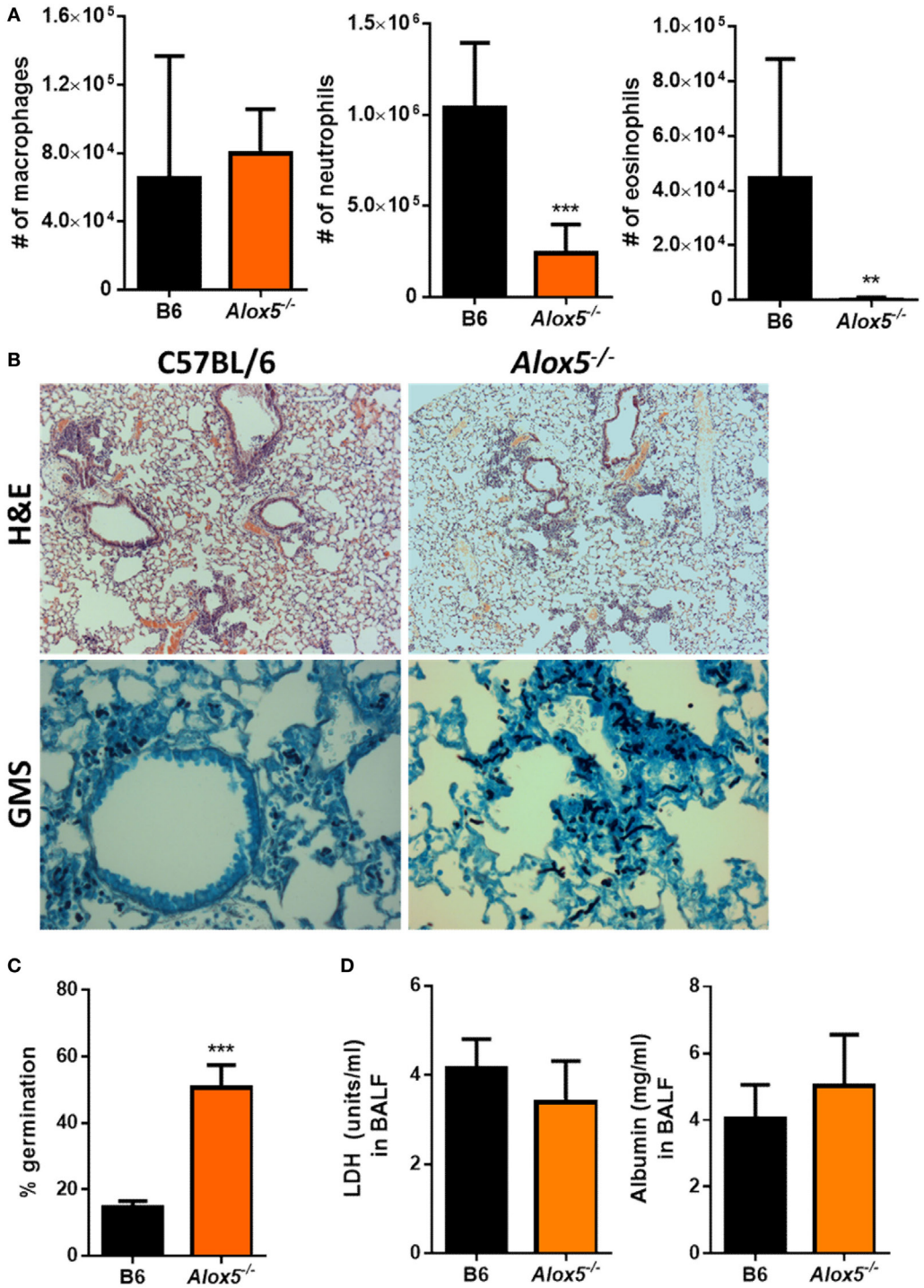

FIGURE 3 | *Alox5*-deficient mice have a defect in neutrophil and eosinophil recruitment and increased fungal burden after pulmonary *Aspergillus fumigatus* challenge. Age-matched C57BL/6J or *Alox5*-deficient mice were infected intratracheally with 5 × 10^7 CEA10 conidia and at indicated time-points, mice were euthanized [bronchoalveolar lavage fluid (BALF)] collected, and lungs saved for histological analysis. **(A)** Total macrophage (left panel), neutrophil (middle panel), and eosinophil (right panel) numbers in the BALF was measured at 12 hpi. **(B)** Formalin-fixed lungs were paraffin embedded, sectioned, and stained with hematoxylin and eosin (H&E) (top) or Grocott-Gomori methenamine silver (GMS) (bottom) for analysis by microscopy. Representative lung sections from C57BL/6J and *Alox5*-deficient mice infected with CEA10 are shown using the 10× objective for H&E staining or 40× objective for GMS staining. **(C)** *A. fumigatus* germination rates were assessed at 36 hpi by microscopically counting the number of conidia and germlings in GMS-stained sections from C57BL/6J and *Alox5*-deficient mice. **(D)** Lung damage (left panel) and leakage (right panel) were assessed at 36 hpi by measuring lactate dehydrogenase (LDH) and albumin levels in the BALF, respectively. Data are representative of at least two independent experiments consisting of five to eight mice per group. Bar graphs show the group mean ± 1 SEM. Statistically significant differences were determined using Mann–Whitney *U* test (**$p < 0.01$ and ***$p < 0.001$).

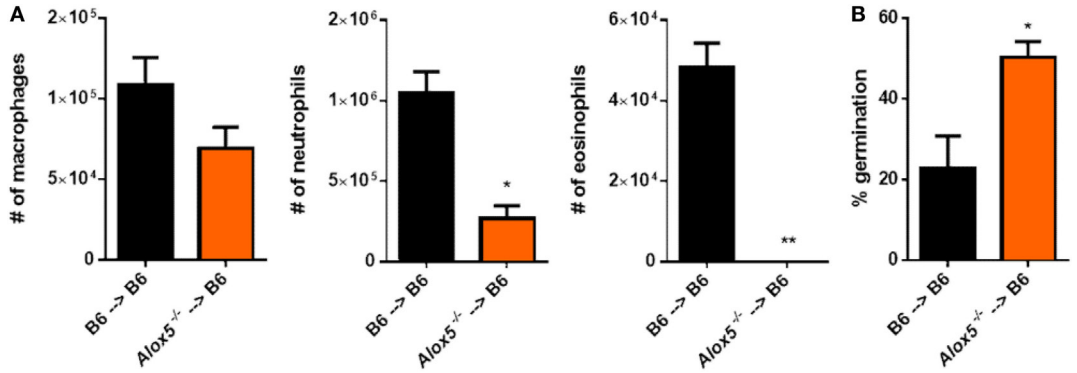

FIGURE 4 | Radiosensitive cells contribute to 5-lipoxygenase activity after pulmonary *Aspergillus fumigatus* challenge. Bone marrow chimeric mice were made by lethally irradiating C57BL/6 mice and reconstituting the mice with bone marrow from either C57BL/6 or *Alox5*$^{-/-}$ mice. These mice were challenged intratracheally with 4 × 10^7 conidia of CEA10 and at 36 hpi, mice were euthanized and **(A)** bronchoalveolar lavage fluid collected for quantification of leukocyte numbers to the airways and **(B)** lungs saved for histological analysis in which formalin-fixed lung were paraffin embedded, sectioned, and stained with Grocott-Gomori methenamine silver for analysis by microscopy. Data consist of four to five mice per group. Bar graphs show the group mean ± 1 SEM. Statistical significance was determined using a Mann–Whitney *U* test (*$p < 0.05$ and **$p < 0.01$).

mice possessing *Alox5*$^{-/-}$ bone marrow were impaired in their ability to control fungal germination compared with C57BL/6 mice possessing C57BL/6 bone marrow (**Figure 4B**). Taken together, these data suggest that radiosensitive cells contribute to 5-LO activity which is needed for neutrophil and eosinophil recruitment to the airways and control of fungal germination following pulmonary *A. fumigatus* challenge.

Leukotriene Synthesis Is Critical for Host Survival following Challenge with the CEA10 Strain of *A. fumigatus*, but Not the Af293 Strain

Thus far, we have shown that in response to the CEA10 strain of *A. fumigatus*, host-derived leukotriene synthesis is critical for timely neutrophil recruitment and control of fungal germination within the lung. Due to studies that demonstrate fungal-strain dependency on the host immune response, we next sought to determine if leukotriene-dependent immunity was reliant on the strain of *A. fumigatus* used for challenge (12, 13, 26). Inflammatory responses against the hypervirulent CEA10 isolate are highly inflammatory and heavily dependent on IL-1α for maintaining host resistance (12). Additionally, we showed that IL-1α release from macrophages following CEA10 challenge required calpain, which is a Ca^{2+}-dependent protease. Since, cPLA2 release of arachidonic acid is also a Ca^{2+}-dependent event, we hypothesized that strain-specific LTB_4 responses might be likely. To test this, we challenged C57BL/6 and *Alox5*$^{-/-}$ mice intratracheally with 5 × 10^7 conidia of either CEA10 or Af293. We monitored health and survival of mice in the 192 h following fungal challenge. *Alox5* (5-LO) was dispensable for survival of mice challenged with the Af293 strain of *A. fumigatus*, which is demonstrated by 100% survival of all mice challenged with Af293 (**Figure 5**). Conversely, *Alox5*$^{-/-}$ mice challenged with CEA10 displayed significantly higher mortality than C57BL/6 mice. Similar mortality trends were observed in the *Ltb4r1*$^{-/-}$ mice (data not shown). Overall, these data are in agreement with several other studies demonstrating that innate immune responses necessary for host resistance against *A. fumigatus* are highly dependent on the fungal strains used.

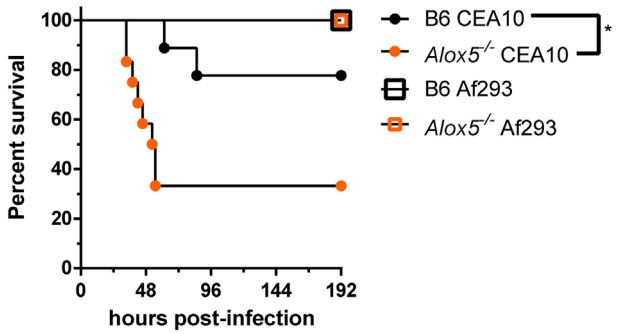

FIGURE 5 | Leukotriene-mediated immunity is fungal-strain dependent. C57BL/6 and *Alox5*-deficient were challenged with 5 × 10^7 conidia of CEA10 or Af293 intratracheal. Mice were monitored daily using a humane endpoint scoring system (based on weight loss, inactivity, ruffled fur, difficulty breathing, and neurological symptoms), and when the humane endpoint criteria was reached mice were humanely euthanized. Data are representative of 9–12 mice per group. Survival was plotted on Kaplan–Meier curves, and statistical significance between curves determined using the Mantel–Cox log rank (ns, not significant, *$p < 0.05$).

Hif1a-Deficient Mice Show a Defect in LTB4 Production following Challenge with CEA10, but Not with Af293

Under hypoxic conditions, the transcription factor hypoxia inducible factor-1α (HIF-1α) is activated, which allows translocation to the nucleus where it can bind to hypoxia response elements in the promoter region of target genes (27). HIF-1α is involved in controlling expression of 5-LO activating protein, a protein critical for the biosynthesis of LTB_4 and cysLTs, after hypoxic challenge

(28). Previous work has shown that hypoxic microenvironments form within the lung in multiple murine models of IPA (29). In an immune competent model of fungal bronchopneumonia, myeloid-derived HIF-1α was shown to be critical for neutrophil recruitment and ultimately, survival of mice challenged with *A. fumigatus* CEA10 strain (30). Given the link between HIF-1α and leukotriene biosynthesis, we sought to determine if HIF-1α contributes to LTB_4 production following *A. fumigatus* challenge. To test this, C57BL/6 or myeloid-specific lysozyme-M cre-recombinase driven HIF-1α null mice (*Hif1a*$^{LysM/LysM}$) mice were challenged with 5×10^7 conidia of either CEA10 or Af293, and LTB_4 protein levels measured in the BALF at 8 hpi. Following challenge with CEA10, there was a significant decrease in LTB_4 protein released into the airways of *Hif1a*$^{LysM/LysM}$ mice compared with C57BL/6 mice (**Figure 6A**). Interestingly, following Af293 challenge LTB_4 levels remained unchanged between C57BL/6 and *Hif1a*$^{LysM/LysM}$ mice (**Figure 6A**). Overall, this suggests that HIF-1α contributes to control of LTB_4 release following pulmonary *A. fumigatus* challenge in a fungal-strain-dependent manner.

Due to strain-specific release of LTB_4 in *Hif1a*$^{LysM/LysM}$ mice (**Figure 6A**), we next sought to determine if *Hif1a*$^{LysM/LysM}$ mice displayed a strain-specific susceptibility to *A. fumigatus* challenge. To test this, we challenged C57BL/6 and *Hif1a*$^{LysM/LysM}$ mice intratracheally with 7×10^7 conidia of either CEA10 or Af293. We monitored health and survival of mice in the 11 days following fungal challenge. HIF-1α expression in LysM-expressing cells was dispensable for survival of mice challenged with the Af293 strain of *A. fumigatus*, which is demonstrated by 90% survival of all mice challenged with Af293 (**Figure 6B**). Conversely, *Hif1a*$^{LysM/LysM}$ mice challenged with CEA10 displayed significantly higher mortality (10% survival), as previously reported (**Figure 6B**). Overall, these data are in agreement with the survival analysis of the *Alox5*$^{-/-}$ mice and reiterate that the innate immune responses necessary for host resistance against highly virulent *A. fumigatus* isolates, such as CEA10, are highly dependent on a robust inflammatory response.

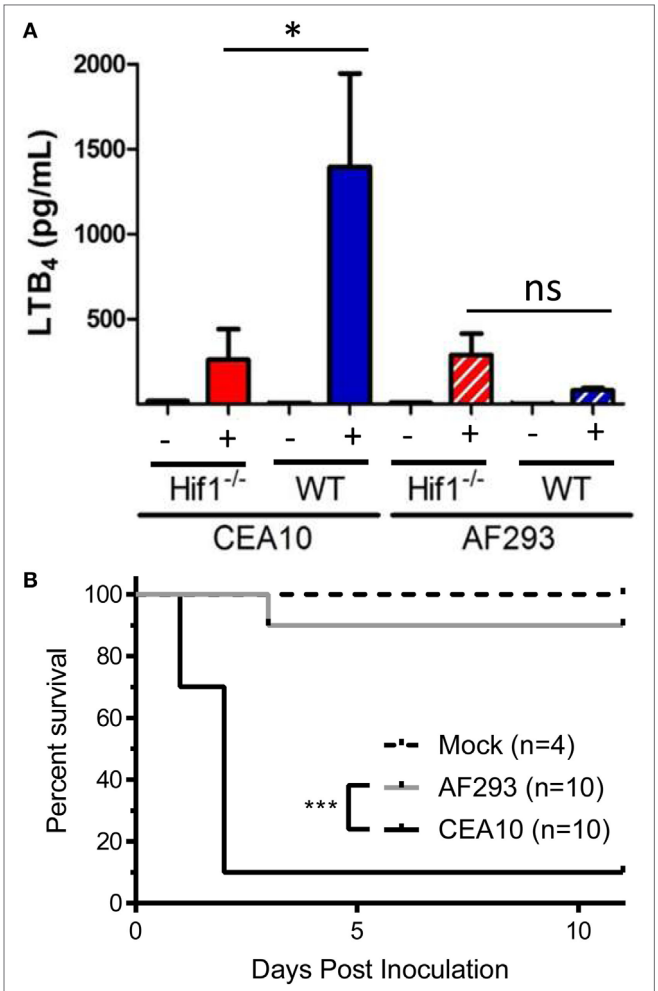

FIGURE 6 | LTB_4 production following *Aspergillus fumigatus* challenge is dependent on hypoxia inducible factor-1α (HIF-1α). **(A)** C57BL/6 or myeloid-specific lysozyme-M cre-recombinase driven HIF-1α null mice (Hif1$^{LysM/LysM}$) were challenged with either 5×10^7 CEA10 or Af293 by the intratracheal (i.t.) route. At 8 hpi, mice were euthanized, bronchoalveolar lavage fluid collected and LTB_4 measured. Data consist of four mice per group for *A. fumigatus*-challenged mice and one mouse per group challenged with PBS. Statistically significant differences were determined by a one-way ANOVA with a Dunn's post-test (ns, not significant, $*p < 0.05$). **(B)** C57BL/6 or myeloid-specific lysozyme-M cre-recombinase driven HIF-1α null mice (Hif1$^{LysM/LysM}$) were challenged with either 7×10^7 CEA10 or Af293 by the i.t. route. Mice were monitored daily using a humane endpoint scoring system (based on weight loss, inactivity, ruffled fur, difficulty breathing, and neurological symptoms), and when the humane endpoint criteria was reached mice were humanely euthanized. Data are representative of 10 mice per experimental group or 4 mice in the uninfected control group. Survival was plotted on Kaplan–Meier curves, and statistical significance between curves determined using the Mantel–Cox log rank ($***p < 0.0001$).

DISCUSSION

This study reveals an essential role for host-derived LTB_4 in the recruitment of both neutrophils and eosinophils through its high-affinity chemotactic receptor LTB4R1 following pulmonary challenge with high-virulent *A. fumigatus* strain CEA10. Ultimately, 5-LO and LTB_4 were crucial for host resistance to *A. fumigatus* challenge. In addition to recruitment of neutrophils, it was recently shown that LTB_4-treated neutrophils have enhanced anti-fungal activity against *A. fumigatus* (31). Thus, LTB_4 will not only recruit neutrophils to the site of *A. fumigatus* infection, but also simultaneously activates their anti-fungal armory. While our data are the first to demonstrate a critical role for LTB_4 in regulating neutrophil recruitment following challenge with a mold, others have reported leukotrienes are critical for leukocyte recruitment and activation following infection with the dimorphic fungi, *H. capsulatum* and *P. brasiliensis* (20, 22, 32). In these systems, it is unknown how leukotriene synthesis is initiated, but with the yeast *C. albicans* treatment of macrophages *in vitro* results in the synthesis of leukotrienes through a Dectin1-, Dectin2-, and MyD88-dependent pathway (16). Given that Dectin1, Dectin2, and MyD88 play a role in recognizing not only *A. fumigatus* (9, 10, 33, 34), but a range of fungal pathogens, it is likely this pathway will be important in the induction of the inflammatory eicosanoid pathway universally following challenge with fungal pathogens.

While it is well known that neutrophils are one of the most important effector cells against *A. fumigatus* (5), a recent study demonstrated a potential role for eosinophils in limiting the development of IPA (35). Our data demonstrate that LTB$_4$ is also critical for the recruitment of eosinophils to the airways of *A. fumigatus*-challenged mice. In immunocompetent mice, the absence of eosinophils resulted in a defect in *A. fumigatus* clearance *in vivo* which did not correlate with a defect in recruitment or function of other inflammatory cells, but rather the potential direct anti-fungal activity of eosinophils (35). In contrast, with repeated administration of *A. fumigatus* eosinophils were shown to have a detrimental effect on disease outcome and eosinophilia was associated with a decrease in neutrophil recruitment (36). Thus, more studies are needed to determine the exact role eosinophils play in different experimental models of IPA, and whether crosstalk between eosinophils and neutrophils regulate anti-fungal immunity.

Clinically, patients with chronic granulomatous disease have a higher risk of developing invasive *Aspergillus* infections, which is mirrored in mice lacking the NADPH oxidases. In these mice, IPA is characterized by excessive inflammation and tissue damage (37, 38). Interestingly, when *gp91^{phox}*-deficient mice were exposed subcutaneously to *A. fumigatus* there is an early neutrophilic response which is associated with elevated LTB$_4$ levels (38). Thus, it will be intriguing whether limiting LTB$_4$ signaling can ameliorate IPA in *gp91^{phox}*-deficient mice, similarly to what was observed with anakinra treatment to limit IL-1 signaling (37). This is plausible because in a *Mycobacterium tuberculosis* model, eicosanoid and IL-1 signaling regulate *M. tuberculosis* growth and pathogenicity (39). Furthermore, LTB$_4$ antagonism is an attractive treatment, because there are a number of clinically available inhibitors of this pathway. Another patient population at high risk of developing IPA is individuals receiving long-term corticosteroid treatment. Treatment with glucocorticoids leads to inhibition of cytosolic phospholipase A2α through the induction of lipocortin-1, blocking the conversion of phospholipids to arachidonic acid (40). Given this link between glucocorticoid treatment and the arachidonic acid pathway, it would be interesting to see the overall impact the presence or absence of leukotrienes has on the outcome of disease during a corticosteroid model of IPA. Moreover, in mice challenged with *A. fumigatus* corticosteroid treatment inhibited HIF-1α translocation to the nucleus, where it binds to target genes to regulate transcription (30). Due to the HIF-1α-dependent production of LTB$_4$ (**Figure 5**), it will be important to determine if the impaired HIF-1α translocation to the nucleus contributes to impaired LTB4 production, which results in enhanced susceptibility to IPA in those patients. Finally, these data suggest that the susceptibility of *Hif1*α-deficient mice to IPA may also be fungal-strain dependent, which warrants further dissection.

In conclusion, we have shown that during the inflammatory response of immunocompetent mice following pulmonary challenge with *A. fumigatus*, leukotriene production from hematopoietic cells is induced. In the absence of all leukotriene synthesis, and specifically in the absence of LTB4R1 signaling, there is a significant defect in neutrophil and eosinophil recruitment to the airways. This defect in leukocyte recruitment correlated with an elevated susceptibility of these mice to developing IPA, as measured by enhanced fungal germination in the lungs and enhanced mortality of mice devoid of leukotriene synthesis. Furthermore, the enhanced susceptibility of mice lacking leukotriene synthesis was fungal-strain dependent. Overall, these data reveal that the leukotriene pathway is critical in maintaining host resistance against *A. fumigatus* infection. Interestingly, prostaglandin E2 was recently shown to be involved in the anti-*Aspergillus* immune response (41), demonstrating a generally important role for arachidonic acid metabolites in regulating anti-fungal immunity.

ETHICS STATEMENT

All animal experiments were approved by the Montana State University Institutional Animal Care and Use Committee or Dartmouth College Institutional Animal Care and Use Committee.

AUTHOR CONTRIBUTIONS

AC-C, CK, KS, RC, and JO conceived and designed the experiments. AC-C, KH, CK, KS and RT performed the experiments. AC-C, KH, CK, KS, RT, RC, and JO analyzed the data. AC-C and JO wrote the paper. AC-C, RC, and JO edited the paper.

ACKNOWLEDGMENTS

The authors wish to thank Dr. David Leib for use of their microscope. Research in this study was funded in part by NIH R01 AI081838 (RC). JO and RC were supported in part by institutional startup funds and in part through the Dartmouth Lung Biology Center for Molecular, Cellular, and Translational Research grant P30 GM106394 (PI: Bruce A. Stanton) and Center for Molecular, Cellular, and Translational Immunological Research grant P30 GM103415 (PI: William R. Green). RC is an Investigators in the Pathogenesis of Infectious Diseases supported by the Burroughs Wellcome Fund. JO was partially supported by funding from National Institutes of Health NIGMS grant P20-GM1035000 (PI: Mark T. Quinn), the MSU Agricultural Experiment Station, and an equipment grant from the M. J. Murdock Charitable Trust. The funders had no role in study design, data collection and analysis, decision to publish, or preparation of the manuscript.

REFERENCES

1. Segal BH. Aspergillosis. *N Engl J Med* (2009) 360(18):1870–84. doi:10.1056/NEJMra0808853
2. Brown GD, Denning DW, Gow NA, Levitz SM, Netea MG, White TC. Hidden killers: human fungal infections. *Sci Transl Med* (2012) 4(165): 165rv13. doi:10.1126/scitranslmed.3004404
3. Obar JJ, Hohl TM, Cramer RA. New advances in invasive aspergillosis immunobiology leading the way towards personalized therapeutic approaches. *Cytokine* (2016) 84:63–73. doi:10.1016/j.cyto.2016.05.015
4. Espinosa V, Rivera A. First line of defense: innate cell-mediated control of pulmonary aspergillosis. *Front Microbiol* (2016) 7:272. doi:10.3389/fmicb.2016.00272

5. Cramer RA, Rivera A, Hohl TM. Immune responses against *Aspergillus fumigatus*: what have we learned? *Curr Opin Infect Dis* (2011) 24(4):315–22. doi:10.1097/QCO.0b013e328348b159
6. Park SJ, Mehrad B. Innate immunity to *Aspergillus* species. *Clin Microbiol Rev* (2009) 22(4):535–51. doi:10.1128/CMR.00014-09
7. Kolaczkowska E, Kubes P. Neutrophil recruitment and function in health and inflammation. *Nat Rev Immunol* (2013) 13(3):159–75. doi:10.1038/nri3399
8. Williams M, Azcutia V, Newton G, Alcaide P, Luscinskas FW. Emerging mechanisms of neutrophil recruitment across endothelium. *Trends Immunol* (2011) 32(10):461–9. doi:10.1016/j.it.2011.06.009
9. Jhingran A, Kasahara S, Shepardson KM, Junecko BA, Heung LJ, Kumasaka DK, et al. Compartment-specific and sequential role of MyD88 and CARD9 in chemokine induction and innate defense during respiratory fungal infection. *PLoS Pathog* (2015) 11(1):e1004589. doi:10.1371/journal.ppat.1004589
10. Caffrey AK, Lehmann MM, Zickovich JM, Espinosa V, Shepardson KM, Watschke CP, et al. IL-1α signaling is critical for leukocyte recruitment after pulmonary *Aspergillus fumigatus* challenge. *PLoS Pathog* (2015) 11(1):e1004625. doi:10.1371/journal.ppat.1004625
11. Herbst S, Shah A, Mazon Moya M, Marzola V, Jensen B, Reed A, et al. Phagocytosis-dependent activation of a TLR9-BTK-calcineurin-NFAT pathway co-ordinates innate immunity to *Aspergillus fumigatus*. *EMBO Mol Med* (2015) 7(3):240–58. doi:10.15252/emmm.201404556
12. Caffrey-Carr AK, Kowalski CH, Beattie SR, Blaseg NA, Upshaw CR, Thammahong A, et al. IL-1α is critical for resistance against highly virulent *Aspergillus fumigatus* isolates. *Infect Immun* (2017) 85(12):e00661–17. doi:10.1128/IAI.00661-17
13. Rizzetto L, Giovannini G, Bromley M, Bowyer P, Romani L, Cavalieri D. Strain dependent variation of immune responses to *A. fumigatus*: definition of pathogenic species. *PLoS One* (2013) 8(2):e56651. doi:10.1371/journal.pone.0056651
14. Sadik CD, Luster AD. Lipid-cytokine-chemokine cascades orchestrate leukocyte recruitment in inflammation. *J Leukoc Biol* (2012) 91(2):207–15. doi:10.1189/jlb.0811402
15. Parti RP, Loper R, Brown GD, Gordon S, Taylor PR, Bonventre JV, et al. Cytosolic phospholipase A(2) activation by *Candida albicans* in alveolar macrophages: role of dectin-*1*. *Am J Respir Cell Mol Biol* (2010) 42(4):415–23. doi:10.1165/rcmb.2009-0110OC
16. Suram S, Gangelhoff TA, Taylor PR, Rosas M, Brown GD, Bonventre JV, et al. Pathways regulating cytosolic phospholipase A(2) activation and eicosanoid production in macrophages by *Candida albicans*. *J Biol Chem* (2010) 285(40):30676–85. doi:10.1074/jbc.M110.143800
17. Suram S, Silveira LJ, Mahaffey S, Brown GD, Bonventre JV, Williams DL, et al. Cytosolic phospholipase A(2)α and eicosanoids regulate expression of genes in macrophages involved in host defense and inflammation. *PLoS One* (2013) 8(7):e69002. doi:10.1371/journal.pone.0069002
18. Jayaraja S, Dakhama A, Yun B, Ghosh M, Lee H, Redente EF, et al. Cytosolic phospholipase A(2) contributes to innate immune defense against *Candida albicans* lung infection. *BMC Immunol* (2016) 17:27. doi:10.1186/s12865-016-0165-9
19. Morato-Marques M, Campos MR, Kane S, Rangel AP, Lewis C, Ballinger MN, et al. Leukotrienes target F-actin/cofilin-1 to enhance alveolar macrophage anti-fungal activity. *J Biol Chem* (2011) 286(33):28902–13. doi:10.1074/jbc.M111.235309
20. Secatto A, Soares EM, Locachevic GA, Assis PA, Paula-Silva FWG, Serezani CH, et al. The leukotriene B$_4$/BLT1 axis is a key determinant in susceptibility and resistance to histoplasmosis. *PLoS One* (2014) 9(1):e85083. doi:10.1371/journal.pone.0085083
21. Secatto A, Rodrigues LC, Serezani CH, Ramos SG, Dias-Baruffi M, Faccioli LH, et al. 5-lipoxygenase deficiency impairs innate and adaptive immune responses during fungal infection. *PLoS One* (2012) 7(3):e31701. doi:10.1371/journal.pone.0031701
22. Santos PC, Santos DA, Ribeiro LS, Fagundes CT, de Paula TP, Avila TV, et al. The pivotal role of 5-lipoxygenase-derived LTB(4) in controlling pulmonary paracoccidioidomycosis. *PLoS Negl Trop Dis* (2013) 7(8):e2390. doi:10.1371/journal.pntd.0002390
23. Balderramas HA, Ribeiro OG, Soares ÂMVC, Oliveira SL. The role of leukotriene B$_4$ in early stages of experimental paracoccidioidomycosis induced in phenotypically selected mouse strains. *Med Mycol* (2013) 51(6):625–34. doi:10.3109/13693786.2013.777163
24. Medeiros AI, Sá-Nunes A, Turato WM, Secatto A, Frantz FG, Sorgi CA, et al. Leukotrienes are potent adjuvant during fungal infection: effects on memory T cells. *J Immunol* (2008) 181(12):8544–51. doi:10.4049/jimmunol.181.12.8544
25. Noverr MC, Toews GB, Huffnagle GB. Production of prostaglandins and leukotrienes by pathogenic fungi. *Infect Immun* (2002) 70(1):400–2. doi:10.1128/IAI.70.1.400-402.2002
26. Kowalski CH, Beattie SR, Fuller KK, McGurk EA, Tang Y-W, Hohl TM, et al. Heterogeneity among isolates reveals that fitness in low oxygen correlates with *Aspergillus fumigatus* virulence. *MBio* (2016) 7(5):e1515–6. doi:10.1128/mBio.01515-16
27. Nizet V, Johnson RS. Interdependence of hypoxic and innate immune responses. *Nat Rev Immunol* (2009) 9(9):609–17. doi:10.1038/nri2607
28. Gonsalves CS, Kalra VK. Hypoxia-mediated expression of 5-lipoxygenase-activating protein involves HIF-1α and NF-κB and microRNAs 135a and 199a-5p. *J Immunol* (2010) 184(7):3878–88. doi:10.4049/jimmunol.0902594
29. Grahl N, Puttikamonkul S, Macdonald JM, Gamcsik MP, Ngo LY, Hohl TM, et al. *In vivo* hypoxia and a fungal alcohol dehydrogenase influence the pathogenesis of invasive pulmonary aspergillosis. *PLoS Pathog* (2011) 7(7):e1002145. doi:10.1371/journal.ppat.1002145
30. Shepardson KM, Jhingran A, Caffrey A, Obar JJ, Suratt BT, Berwin BL, et al. Myeloid derived hypoxia inducible factor 1-alpha is required for protection against pulmonary *Aspergillus fumigatus* infection. *PLoS Pathog* (2014) 10(9):e1004378. doi:10.1371/journal.ppat.1004378
31. Jones CN, Dimisko L, Forrest K, Judice K, Poznansky MC, Markmann JF, et al. Human neutrophils are primed by chemoattractant gradients for blocking the growth of *Aspergillus fumigatus*. *J Infect Dis* (2016) 213(3):465–75. doi:10.1093/infdis/jiv419
32. Medeiros AI, Sá-Nunes A, Soares EG, Peres CM, Silva CL, Faccioli LH. Blockade of endogenous leukotrienes exacerbates pulmonary histoplasmosis. *Infect Immun* (2004) 72(3):1637–44. doi:10.1128/IAI.72.3.1637-1644.2004
33. Steele C, Rapaka RR, Metz A, Pop SM, Williams DL, Gordon S, et al. The beta-glucan receptor dectin-1 recognizes specific morphologies of *Aspergillus fumigatus*. *PLoS Pathog* (2005) 1(4):e42. doi:10.1371/journal.ppat.0010042
34. Sun H, Xu X-Y, Shao H-T, Su X, Wu X-D, Wang Q, et al. Dectin-2 is predominately macrophage restricted and exhibits conspicuous expression during *Aspergillus fumigatus* invasion in human lung. *Cell Immunol* (2013) 284(1–2):60–7. doi:10.1016/j.cellimm.2013.06.013
35. Lilly LM, Scopel M, Nelson MP, Burg AR, Dunaway CW, Steele C. Eosinophil deficiency compromises lung defense against *Aspergillus fumigatus*. *Infect Immun* (2014) 82(3):1315–25. doi:10.1128/IAI.01172-13
36. O'Dea EM, Amarsaikhan N, Li H, Downey J, Steele E, Van Dyken SJ, et al. Eosinophils are recruited in response to chitin exposure and enhance Th2-mediated immune pathology in *Aspergillus fumigatus* infection. *Infect Immun* (2014) 82(8):3199–205. doi:10.1128/IAI.01990-14
37. de Luca A, Smeekens SP, Casagrande A, Iannitti R, Conway KL, Gresnigt MS, et al. IL-1 receptor blockade restores autophagy and reduces inflammation in chronic granulomatous disease in mice and in humans. *Proc Natl Acad Sci U S A* (2014) 111(9):3526–31. doi:10.1073/pnas.1322831111
38. Petersen JE, Hiran TS, Scott Goebel W, Johnson C, Murphy RC, Azmi FH, et al. Enhanced cutaneous inflammatory reactions to *Aspergillus fumigatus* in a murine model of chronic granulomatous disease. *J Invest Dermatol* (2002) 118(3):424–9. doi:10.1046/j.0022-202x.2001.01691.x
39. Mayer-Barber KD, Andrade BB, Oland SD, Amaral EP, Barber DL, Gonzales J, et al. Host-directed therapy of tuberculosis based on interleukin-1 and type I interferon crosstalk. *Nature* (2014) 511(7507):99–103. doi:10.1038/nature13489
40. Rhen T, Cidlowski JA. Antiinflammatory action of glucocorticoids—new mechanisms for old drugs. *N Engl J Med* (2005) 353(16):1711–23. doi:10.1056/NEJMra050541
41. Garth JM, Reeder KM, Godwin MS, Mackel JJ, Dunaway CW, Blackburn JP, et al. IL-33 signaling regulates innate IL-17A and IL-22 production via suppression of prostaglandin E2 during lung fungal infection. *J Immunol* (2017) 199(6):2140–8. doi:10.4049/jimmunol.1602186

Conflict of Interest Statement: The authors declare that the research was conducted in the absence of any commercial or financial relationships that could be construed as a potential conflict of interest.

Copyright © 2018 Caffrey-Carr, Hilmer, Kowalski, Shepardson, Temple, Cramer and Obar. This is an open-access article distributed under the terms of the Creative Commons Attribution License (CC BY). The use, distribution or reproduction in other forums is permitted, provided the original author(s) or licensor are credited and that the original publication in this journal is cited, in accordance with accepted academic practice. No use, distribution or reproduction is permitted which does not comply with these terms.

frontiers in Immunology

ORIGINAL RESEARCH
published: 29 May 2018
doi: 10.3389/fimmu.2018.01182

Protein Deiminase 4 and CR3 Regulate *Aspergillus fumigatus* and β-Glucan-Induced Neutrophil Extracellular Trap Formation, but Hyphal Killing Is Dependent Only on CR3

Heather L. Clark[1,2,3], *Serena Abbondante*[2,3], *Martin S. Minns*[2,3], *Elyse N. Greenberg*[2,3], *Yan Sun*[1] *and Eric Pearlman*[2,3]*

[1] Department of Ophthalmology and Visual Sciences, Case Western Reserve University, Cleveland, OH, United States, [2] Department of Ophthalmology, University of California Irvine, Irvine, CA, United States, [3] Department of Physiology and Biophysics, University of California Irvine, Irvine, CA, United States

OPEN ACCESS

Edited by:
Amariliz Rivera, Rutgers, The State University of New Jersey, United States

Reviewed by:
Joshua J. Obar, Dartmouth College, United States
Michail Lionakis, National Institute of Allergy and Infectious Diseases (NIAID), United States

***Correspondence:**
Eric Pearlman
eric.pearlman@uci.edu

Specialty section:
This article was submitted to Microbial Immunology, a section of the journal Frontiers in Immunology

Received: *24 December 2017*
Accepted: *11 May 2018*
Published: *29 May 2018*

Citation:
Clark HL, Abbondante S, Minns MS, Greenberg EN, Sun Y and Pearlman E (2018) Protein Deiminase 4 and CR3 Regulate Aspergillus fumigatus and β-Glucan-Induced Neutrophil Extracellular Trap Formation, but Hyphal Killing Is Dependent Only on CR3. Front. Immunol. 9:1182. doi: 10.3389/fimmu.2018.01182

Neutrophil extracellular trap (NET) formation requires chromatin decondensation before nuclear swelling and eventual extracellular release of DNA, which occurs together with nuclear and cytoplasmic antimicrobial proteins. A key mediator of chromatin decondensation is protein deiminase 4 (PAD4), which catalyzes histone citrullination. In the current study, we examined the role of PAD4 and NETosis following activation of neutrophils by *A. fumigatus* hyphal extract or cell wall β-glucan (curdlan) and found that both induced NET release by human and murine neutrophils. Also, using blocking antibodies to CR3 and Dectin-1 together with CR3-deficient CD18$^{-/-}$ and Dectin-1$^{-/-}$ murine neutrophils, we found that the β-glucan receptor CR3, but not Dectin-1, was required for NET formation. NETosis was also dependent on NADPH oxidase production of reactive oxygen species (ROS). Using an antibody to citrullinated histone 3 (H3Cit) as an indicator of PAD4 activity, we show that β-glucan stimulated NETosis occurs in neutrophils from C57BL/6, but not PAD4$^{-/-}$ mice. Similarly, a small molecule PAD4 inhibitor (GSK484) blocked NET formation by human neutrophils. Despite these observations, the ability of PAD4$^{-/-}$ neutrophils to release calprotectin and kill *A. fumigatus* hyphae was not significantly different from C57BL/6 neutrophils, whereas CD18$^{-/-}$ neutrophils exhibited an impaired ability to perform both functions. We also detected H3Cit in *A. fumigatus* infected C57BL/6, but not PAD4$^{-/-}$ corneas; however, we found no difference between C57BL/6 and PAD4$^{-/-}$ mice in either corneal disease or hyphal killing. Taken together, these findings lead us to conclude that although PAD4 together with CR3-mediated ROS production is required for NET formation in response to *A. fumigatus*, PAD4-dependent NETosis is not required for *A. fumigatus* killing either *in vitro* or during infection.

Keywords: ***Aspergillus,*** **neutrophil extracellular trap, protein deiminase 4, CR3, keratitis**

INTRODUCTION

Neutrophil extracellular trap (NET) formation is a coordinated form of neutrophil cell death, first described by Zychlinsky and colleagues in which genomic DNA is released from neutrophils and traps and mediates killing of pathogenic bacteria, fungi, and parasites (1–3). The molecular events in this process involve protein kinase C, Raf, Mek, and Erk activation, which leads to activation of NADPH oxidase, production of reactive oxygen species (ROS), and mobilization of neutrophil elastase (NE) into the nucleus, where it functions to degrade histones, resulting in chromatin decondensation (1). NETosis also requires activation of protein deiminase 4 (PAD4) in the nucleus, which converts positively charged arginine residues to neutral citrulline. Histone citrullination also mediates chromatin decondensation and nuclear swelling (4–8).

We reported that neutrophils play a critical role in fungal killing and in corneal infections with the pathogenic molds *Aspergillus* and *Fusarium*, which are major causes of blindness and visual impairment worldwide (9, 10). We demonstrated an essential role for neutrophil NADPH oxidase and for the antimicrobial peptide calprotectin (CP) in fungal killing *in vitro* and in murine models of fungal keratitis (11, 12).

In the current study, we examined the role of PAD4 in NET formation in response to *Aspergillus fumigatus* or cell wall β-glucan and show that although PAD4 is required for NET formation *in vitro* and during corneal infection, it is not required for hyphal killing *in vitro* or during infection. Instead, we demonstrate that CR3 (CD11b/CD18), which also binds β-glucan, is required for production of reactive oxygen, hyphal killing, and CP release. We conclude that although NETs are generated by *A. fumigatus* hyphae, they are not required for hyphal killing *in vitro* or during corneal infection.

RESULTS

A. fumigatus and β-Glucan Induce Neutrophil Extracellular Traps From Human and Mouse Neutrophils

Although NETs have a distinctive appearance in fixed cells, NETs in live cell cultures are more diffuse (7), which we also found after incubating human peripheral blood neutrophils with *A. fumigatus* hyphal extract (AspHE), particulate β-glucan (curdlan), or phorbol myristic acid (PMA) when incubated with the cell-impermeable DNA stain SYTOX Green (**Figure 1A**).

Quantification of SYTOX Green showed that extracellular DNA increased over time (**Figure 1B**). Total DNA released over 20 h (area under the curve of **Figure 1B**) showed that all three stimuli induced a significant increase in DNA release from human peripheral blood neutrophils compared with media alone (**Figure 1C**). Similarly, mouse bone marrow neutrophils released DNA in response to AspHE and curdlan (**Figures 1D,E**), although PMA did not stimulate murine bone marrow neutrophils (not shown).

β-Glucan-Induced NETosis Requires Production of ROS

Reactive oxygen species is required for NETosis in human neutrophils following stimulation with PMA, although ROS-independent NET formation has also been reported (13–15). To examine if ROS has a role in NET formation in response to *A. fumigatus*, human neutrophils were incubated with PMA, curdlan, or AspHE in the presence of the NADPH oxidase inhibitor diphenyl iodonium (DPI). We found that DPI inhibited DNA release in response to all stimuli (**Figures 2A,B**), indicating a requirement for NADPH oxidase-generated ROS in NET formation in response to fungal cell wall components.

CR3 Mediates NET Formation and ROS Production in Response to β-Glucan

C-type lectin receptors, including Dectin-1, Dectin-2, and Dectin-3 (also called macrophage c-type lectin) on murine macrophages recognize fungal cell wall components, including β-glucan and α-mannose (16). Neutrophils constitutively express the C-type lectin Dectin-1 and the β2-integrin CR3 (Mac-1, CD11b/CD18), which in addition to the complement binding I-domain, has a lectin binding domain that recognizes β-glucan (17). The lectin binding domain mediates ROS production in response to *Candida* and *Aspergillus* (11, 13), although maximal production of ROS and NETs depends on activation of both domains of this unique receptor in the presence of complement (15).

To determine the relative contribution of CR3 and Dectin-1 in ROS production and NET formation, human peripheral blood neutrophils were incubated with particulate β-glucan (curdlan) together with antibodies to either Dectin-1 or CR3. We found significantly reduced extracellular DNA in the presence of anti-CR3 (**Figure 3A**), whereas anti-Dectin-1 resulted in increased DNA release (**Figure 3B**), which is consistent with an earlier report on NETosis induced by *Candida* hyphae compared with yeast (18). As ROS is required for NET formation, we also examined the role of CR3 and Dectin-1 in ROS production, and found that curdlan-induced ROS production was inhibited by anti-CR3, but not anti-Dectin-1 (**Figure 3C**).

These findings were reproduced in bone marrow neutrophils from Dectin-1$^{-/-}$ and from CD18$^{-/-}$ mice, where NETosis was dependent on CD18 expression, and there was no effect of Dectin-1 deletion on β-glucan-induced NET formation or ROS production (**Figures 3D,E**). We therefore conclude that CR3 rather than Dectin-1 is the predominant β-glucan receptor required for ROS production and NET release in human and murine neutrophils.

PAD4 Is Required for NET Formation Induced by β-Glucan

Conversion of arginines to neutral citrullines is mediated by the protein deimidase family of enzymes (19); however, only PAD4 is present in the nucleus, where it mediates citrullination of histones and subsequent chromatin decondensation.

To examine if PAD4 has a role in NET formation in response to fungal cell wall components, we visualized NET formation

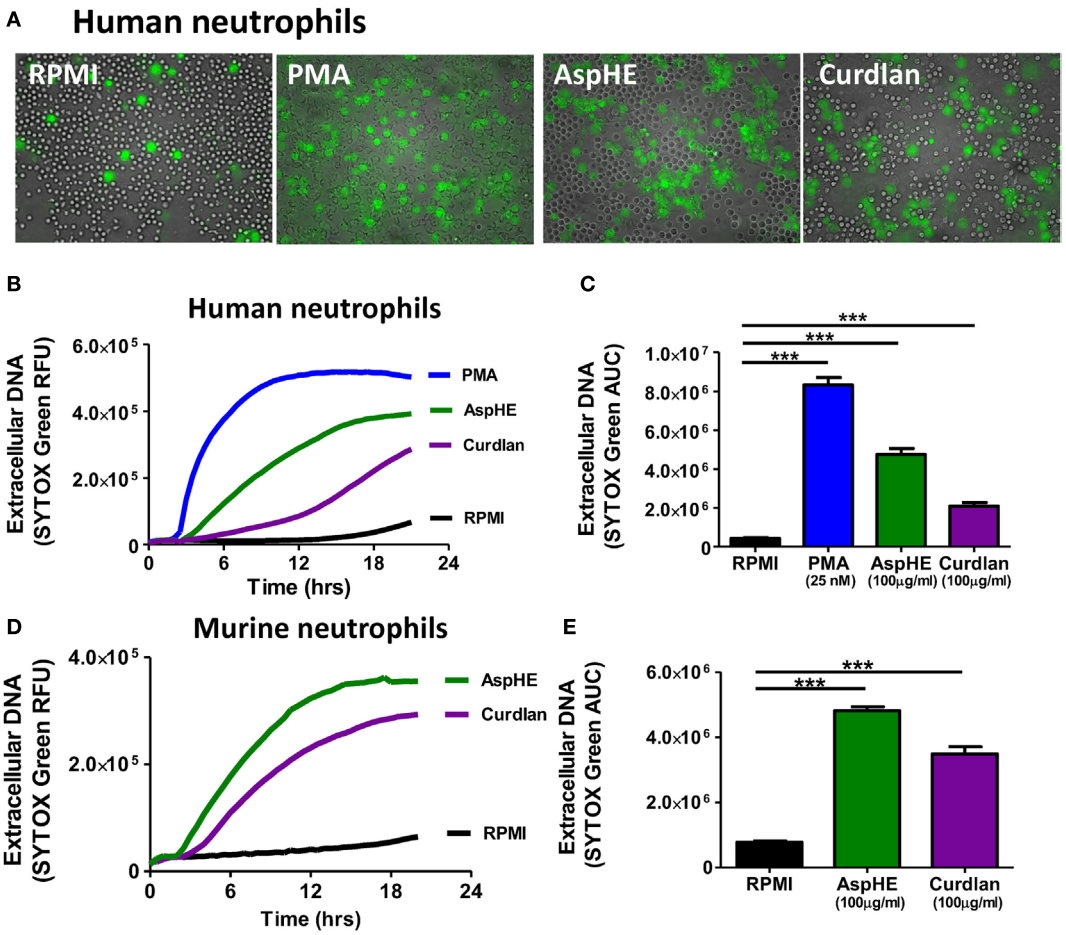

FIGURE 1 | *Aspergillus fumigatus* and β-glucan induce neutrophil extracellular trap formation in human and murine neutrophils. **(A)** Representative images showing DNA release by SYTOX Green staining in human peripheral blood neutrophils 20 h after stimulation with 25 nM phorbol myristic acid (PMA), 100 μg/ml *A. fumigatus* hyphal extract (AspHE), or 100 μg/ml particulate β-glucan (curdlan); original magnification is 200×. **(B)** DNA release overtime shown as relative fluorescent units (RFU) measured by SYTOX Green; **(C)** total extracellular DNA after 20 h calculated as area under the curve (AUC). **(D,E)** Extracellular DNA from mouse peritoneal neutrophils incubated with AspHE or curdlan and quantified by SYTOX Green RFU and AUC. Asterisks (***) indicate $p < 0.001$ based on one way ANOVA with Tukey post hoc analysis. Experiments were repeated five times with similar results.

in β-glucan stimulated neutrophils from C57BL/6 and PAD4$^{-/-}$ mice using antibodies to citrullinated histone H3 (H3Cit). We found that in response to curdlan, neutrophils from C57BL/6 mice generated characteristic NET structures that were also H3Cit^{+} (**Figures 4A–E**). In contrast, stimulated PAD4$^{-/-}$ neutrophils retain their lobular nuclei and were negative for H3Cit (**Figures 4C,F**). An early stage of NETosis is NE translocation to the nucleus (4), which is clearly detected in C57BL/6 neutrophils; however, elastase remained in the cytoplasm of PAD4$^{-/-}$ neutrophils (**Figures 4C,F**).

Protein deiminase 4-dependent NET formation by murine and human neutrophils was quantified by SYTOX green. Consistent with representative images, PAD4$^{-/-}$ neutrophils released significantly less DNA than C57BL/6 neutrophils following incubation with curdlan (**Figure 5A**). To investigate if there is a role for PAD4 in NET formation by human neutrophils, we used small molecule PAD4 inhibitors that inhibit NET formation *in vitro* (19). Curdlan-stimulated human neutrophils were incubated with the PAD4 inhibitor GSK484 or with the negative control compound GSK106. As shown in **Figures 5B,C**, DNA release in response to *Aspergillus* was significantly reduced in the presence of GSK484, whereas the negative control GSK106 did not inhibit DNA release.

Together, these findings clearly demonstrate that PAD4 citrullination is required for NET formation by murine and human neutrophils.

CR3 but Not PAD4 Is Required for Calprotectin Release *In Vitro*

The antimicrobial peptide calprotectin (CP; S100A8/A9) is a major component of NETs in response to *Candida albicans* and is required for NET-mediated killing (3). CP was found to be an essential NET component in controlling *A. fumigatus* following gene therapy for chronic granulomatous disease (20), and we

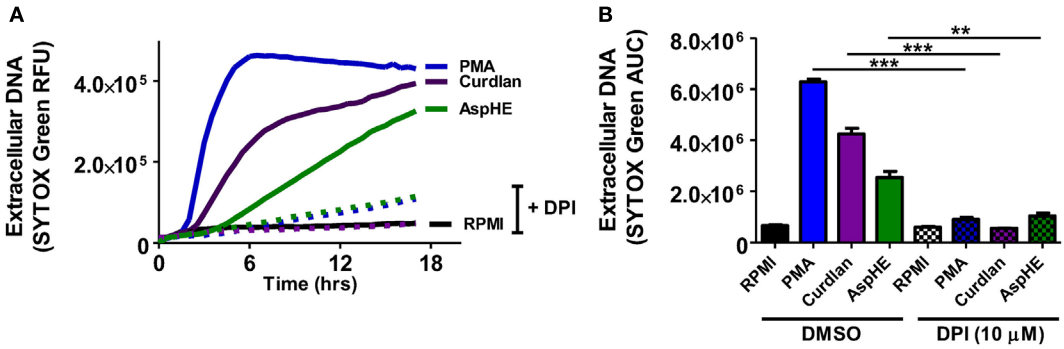

FIGURE 2 | Neutrophil extracellular trap (NET) formation is dependent on reactive oxygen species (ROS). Human neutrophils were stimulated 20 h with phorbol myristic acid (PMA), AspHE, or curdlan in the presence of the ROS inhibitor diphenyl iodonium (DPI) (10 μM). NET formation was quantified by SYTOX Green over time **(A)**, and total SYTOX over 18 h is shown as area under the curve (AUC) **(B)**. ANOVA with Tukey post hoc analysis showed ***$p < 0.001$ and **$p < 0.01$. Experiments were repeated four times with similar results.

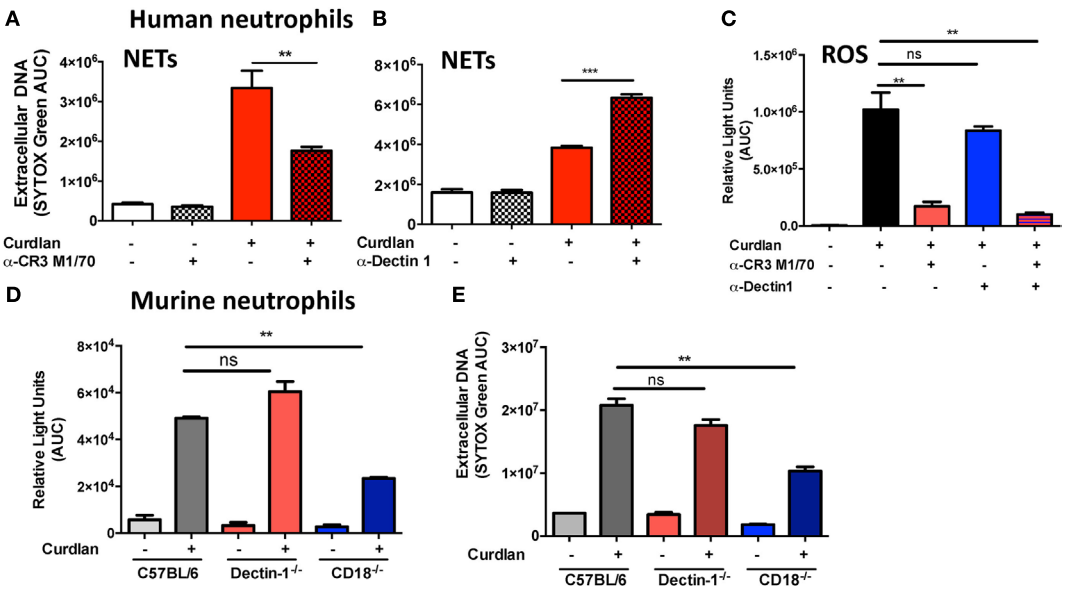

FIGURE 3 | Distinct roles for CR3 and Dectin-1 in β-glucan-induced reactive oxygen species (ROS) production and neutrophil extracellular trap (NET) formation. **(A–C)** Human neutrophils; **(D,E)** murine neutrophils. Neutrophils were incubated with β-glucan (curdlan) in the presence of the anti-CR3 blocking antibody M1/70 (30 μg/ml) **(A)** or with the anti-Dectin-1 blocking antibody 22H8 (Invivogen, 20 μg/ml) **(B)**. **(A,B)** DNA release was quantified by SYTOX Green and expressed as area under the curve. **(C)** ROS production measured by luminol. **(D,E)** DNA release and ROS production by mouse bone marrow neutrophils from C57BL/6, Dectin-1$^{-/-}$, and CD18$^{-/-}$ mice stimulated with curdlan. *p* Values are biological replicates of at least three repeat experiments and were calculated using ANOVA with Tukey post hoc analysis (***$p < 0.001$, **$p < 0.01$, and *$p < 0.05$).

reported that CP inhibits *A. fumigatus* hyphal growth by sequestering zinc *in vitro* and in *Aspergillus* keratitis (12).

To determine if CP is associated with NETs, we examined CP release in CR3 (CD18$^{-/-}$) and PAD4$^{-/-}$ neutrophils following stimulation with curdlan. Bone marrow neutrophils from C57BL/6, CD18$^{-/-}$, and PAD4$^{-/-}$ mice were incubated with curdlan 2h (prior to NET formation) or for 16 (after NET formation), and the CP subunit S100A8 was measured in cell-free supernatants by ELISA.

Whereas there was no significant difference in S100A8 between C57BL/6 and PAD4$^{-/-}$ neutrophils released in response to curdlan at either time point, CD18$^{-/-}$ neutrophils produced significantly less S100A8 at both time points (**Figure 6**). There was no difference in production of S100A8 in response to total hyphal extracts (Figure S1 in Supplementary Material).

These data indicate that CP is released from neutrophils in the absence of PAD4-dependent NET formation, and that release in response to curdlan requires CR3 activation.

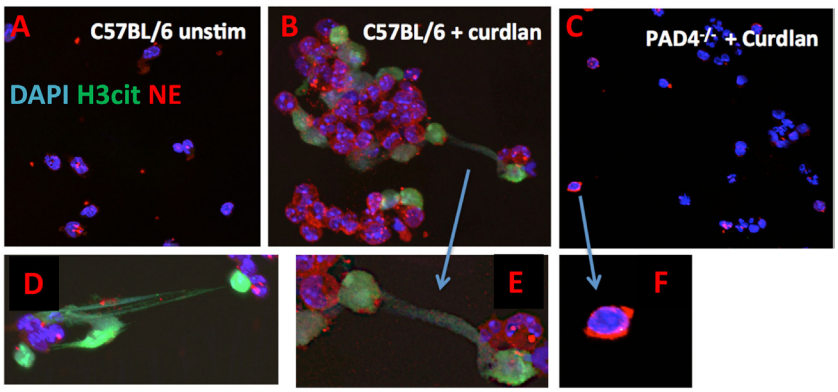

FIGURE 4 | β-Glucan-induced neutrophil extracellular trap formation. Curdlan-stimulated bone marrow neutrophils from C57BL/6 and PAD4$^{-/-}$ mice. Neutrophils were immunostained with antibodies to citrullinated histone 3 (H3Cit), neutrophil elastase (NE), and DAPI nuclear stain **(A–C)** 200×; **(D–F)** 400×.

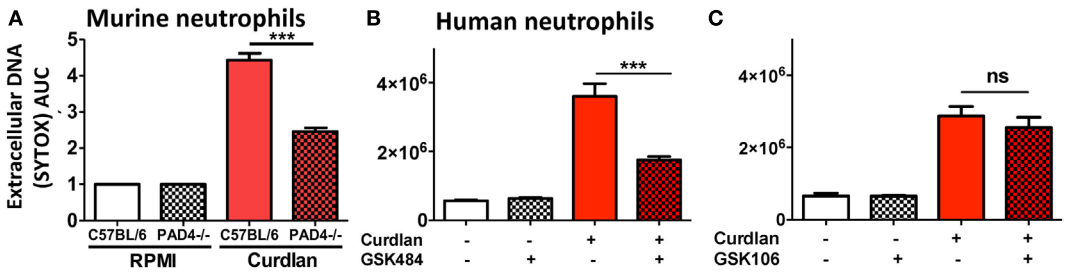

FIGURE 5 | Protein deiminase 4 (PAD4)-dependent neutrophil extracellular trap formation. **(A)** Bone marrow neutrophils from C57BL/6 and PAD4$^{-/-}$ mice were incubated 20 h with particulate β-glucan (curdlan) in RPMI, and DNA release was quantified by SYTOX Green. Values were normalized to unstimulated neutrophils (RPMI). **(B,C)** Human peripheral blood neutrophils incubated with curdlan and 10 μM specific PAD4 inhibitor GSK484 **(B)** or with the related, non-inhibitory compound GSK106 **(C)**. *p* Values are biological replicates of at least three repeat experiments and were calculated using ANOVA with Tukey post hoc analysis (***$p < 0.01$; **$p < 0.05$; ns, not significant). Experiments were repeated twice with similar results.

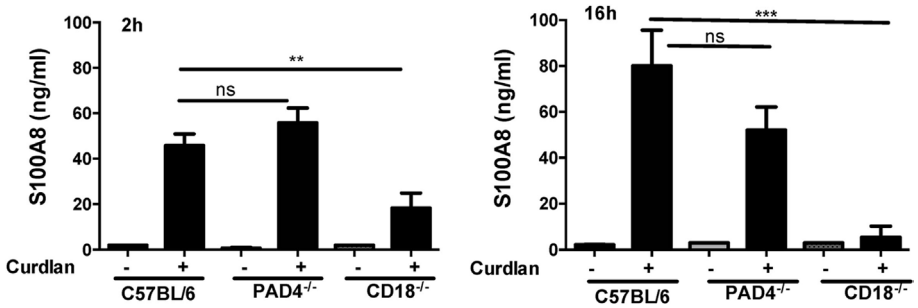

FIGURE 6 | CD18-dependent calprotectin (CP) (S100A8/A9) production. Bone marrow neutrophils from C57BL/6, PAD4$^{-/-}$, and CD18$^{-/-}$ mice were incubated 2 or 16 h with curdlan, and CP/S100A8 was quantified by ELISA. *p* Values are biological replicates of three repeat experiments and were calculated using ANOVA using a Tukey post hoc analysis (***$p < 0.001$; **$p < 0.01$; ns, not significant). S100A8 production to AspHE was similar in all groups (Figure S1 in Supplementary Material).

CR3, but Not PAD4, Is Required for Neutrophil Inhibition of *A. fumigatus* Hyphal Growth

To determine whether NETs regulate fungal growth *in vitro*, 2×10^5 human neutrophils were incubated with *A. fumigatus* hyphae in the presence of the anti-CR3 blocking antibody M1/70. Also, *A. fumigatus* hyphae were incubated with neutrophils from C57BL/6 and PAD4$^{-/-}$ mice. *A. fumigatus* hyphal growth over 18 h was quantified using calcofluor white, which binds cell wall chitin, and percent fungal mass was quantified based on hyphal growth in media alone (100%).

Human neutrophils significantly inhibited fungal growth compared with hyphae grown in media alone; however, this was reversed in the presence of blocking antibody to CR3 (**Figure 7A**). Similarly, hyphal growth was impaired when incubated with 2×10^5 C57BL/6 or PAD4$^{-/-}$ neutrophils, but not with neutrophils from CD18$^{-/-}$ mice (**Figure 7B**).

Together, these data demonstrate that CR3 signaling is required for fungal growth inhibition and/or killing by neutrophils *in vitro*, whereas there is no apparent role for PAD4.

PAD4 Is Not Required for *A. fumigatus* Killing, Corneal Disease, or Neutrophil Recruitment to Infected Corneas

Fungal keratitis is characterized by an early and profound infiltration of neutrophils to the corneal stroma in patients (21), and in murine models where these cells are required for hyphal killing and which mediate corneal opacification (9, 10).

To determine if PAD4 is required for NET formation in the cornea, and if NETs have a role in fungal killing at this site, corneas of C57BL/6 and PAD4$^{-/-}$ mice were infected with 1×10^5 RFP expressing *A. fumigatus* conidia (Af293), and after 48 h, corneal sections were examined for neutrophil infiltration and NET formation (H3Cit$^+$). H3Cit staining was evident in corneas of *A. fumigatus* infected C57BL/6, but not PAD4$^{-/-}$ mice (**Figure 8A**). Also, quantification of multiple sections showed a significant difference in H3Cit, but no significant difference in total Ly6G$^+$ cells between C57BL/6 and PAD4$^{-/-}$ mice (Figure S2 in Supplementary Material).

Total cells in infected corneas were examined by flow cytometry following collagenase digestion. As shown in **Figure 8B**, epithelial cells were identified as CD45$^-$, EpCam$^+$, which comprised <5% total cells, whereas >75% of total cells were CD45$^+$. Neutrophils were identified in the CD45$^+$ population as Ly6G/CD11b$^+$, with the remaining CD45$^+$ cells being Ly6C/CD11b$^+$ monocytes. Neutrophils comprised 40–60% total cells in infected corneas; however, there was no difference in the percentage of neutrophils between infected C57BL/6 and PAD4$^{-/-}$ corneas (**Figure 8C**; Figure S2 in Supplementary Material).

There were also no significant differences between infected C57BL/6 and PAD4$^{-/-}$ mice in the severity of corneal opacification, RFP-Af293 hyphal mass or CFU (**Figures 8D,E**). We also found no significant difference in CFU between C57BL/6 and PAD4$^{-/-}$ mice following infection with an *A. fumigatus* keratitis clinical isolate (Af BP) (**Figures 8F,G**). Collectively, these findings show that although PAD4-dependent NET formation is detected in infected corneas, they do not have an essential role in regulating fungal corneal infections.

DISCUSSION

A proposed sequence of events for NET formation by Zychlinsky and colleagues envisions an initial activation of neutrophils, assembly of the NADPH oxidase complex and production of ROS, resulting in bacterial entrapment and killing (1, 22). Human and mouse neutrophils with mutations or deletions in NADPH oxidase proteins cannot undergo NETosis *in vitro* or in a murine model of pulmonary aspergillosis (14). Elastase translocation to the nucleus is also required, and NETs are not detected following inhibition of elastase activity or in elastase deficient neutrophils (4).

Neutrophil extracellular traps have also been detected *in vivo* using two-photon microscopy, including in a murine model of pulmonary aspergillosis that shows hyphae in close association with neutrophils and extracellular DNA (23). These and other elegant studies leave little doubt that NETs are generated in response to bacteria, fungi and parasites. The controversy comes in to play in determining the role of NETs in killing pathogenic fungi. In the same pulmonary aspergillosis study, NETs did not kill *A. fumigatus*, although the authors suggest that NETs may have a role in inhibiting hyphal growth (23).

Human neutrophils from healthy, but not patients with chronic granulomatous disease (CGD) form NETs in response to *A. fumigatus* hyphae; however, DNAse treatment had no effect on hyphal killing in these patients, arguing against a role for NETs (24). Conversely, DNAse treatment inhibited the ability of human neutrophils to kill *A. fumigatus* germ tubes and hyphae (25, 26), thereby implicating a protective role for NETs in *A. fumigatus* infection.

In agreement with our current observations, the CGD study also showed that *A. fumigatus* conidia are recognized by CR3

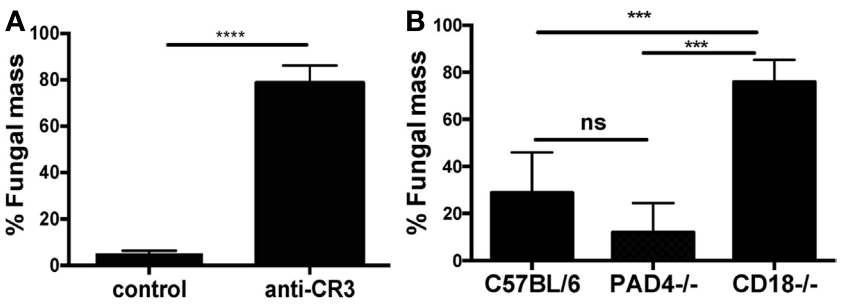

FIGURE 7 | CR3, but not protein deiminase 4 (PAD4), is required for neutrophil inhibition of *Aspergillus fumigatus* hyphal growth. **(A,B)** *A. fumigatus* hyphae incubated 18 h with human neutrophils in RPMI alone or with anti-CR3 M1/70 (20 μg/ml) **(A)**. Fungal mass was quantified by calcofluor white fluorescent chitin stain and presented as percent of total hyphae in the absence of neutrophils. **(B)** Percent fungal mass in bone marrow neutrophils from C57BL/6, CD18$^{-/-}$, or PAD4$^{-/-}$ mice following 18 h incubation with *A. fumigatus* hyphae. *p* Values are biological replicates of three repeat experiments and were calculated using Student's *t*-test **(A)** or ANOVA with a Tukey post hoc analysis **(B)** (****$p < 0.0001$; ***$p < 0.001$; ns, not significant).

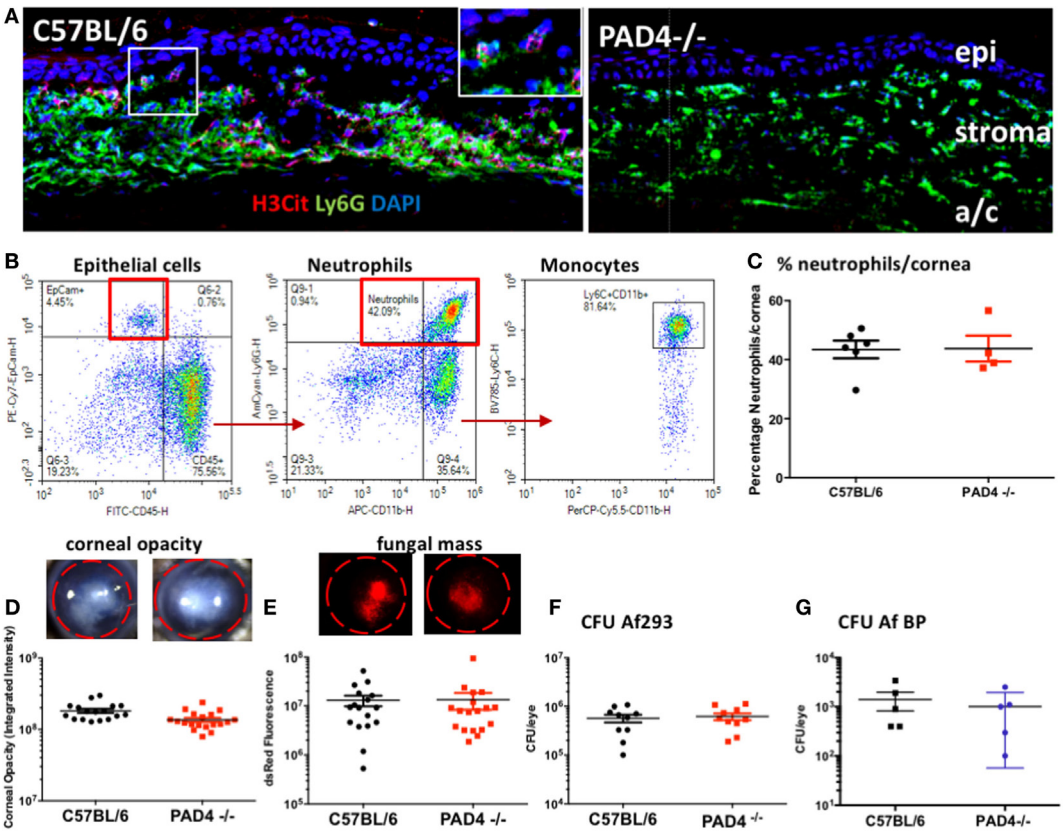

FIGURE 8 | *Aspergillus fumigatus* corneal infection in PAD4$^{-/-}$ mice. Corneas of C57BL/6 and PAD4$^{-/-}$ mice were infected with dsRed expressing *A. fumigatus*. **(A)** Corneal sections immunostained with antibodies to Ly6G and citrullinated histone 3 (H3Cit) and counterstained with DAPI nuclear stain. Epi, stroma = corneal epithelium and corneal stroma. Highlighted area shows H3Cit staining in neutrophils. Original magnification is 400×. **(B)** Representative flow cytometry scatter plots showing total cells from infected C57BL/6 corneas that include CD45^{-} epithelial cells, CD45^{+}Ly6G^{+} neutrophils, and Ly6C high monocytes. **(C)** Percent neutrophils in infected corneas from C57BL/6 and PAD4$^{-/-}$ mice [percent Ly6G^{+} neutrophils in infected corneas (representative scatter plots from C57BL/6 and PAD4$^{-/-}$ mice are shown in Figure S2 in Supplementary Material)]. **(D,E)** Representative corneas showing opacification and RFP expressing *A. fumigatus* hyphae. **(F,G)** Quantification of corneal opacity, dsRed as a measure of fungal mass, and CFU. Each data point represents an individual cornea. $p > 0.05$ using Student's *t*-test analyses for panels **(C–G)**, indicating that there are no statistically significant differences between C57BL/6 and PAD4$^{-/-}$ mice for any of these parameters. These data are representative of five repeat experiments.

rather than Dectin-1 on human neutrophils and mediates non-oxidative killing (24). This observation is supported by a report showing that Dectin-1 negatively regulates hyphae-induced NET formation by human neutrophils (18), and by an earlier study showing that human neutrophils use CR3 to form NETs in response to *C. albicans* (27). The latter study also reported that in murine neutrophils, Dectin-1 rather than CR3 mediates NETosis induced by *C. albicans*. However, we used neutrophils from Dectin-1$^{-/-}$ and CD18$^{-/-}$ mice to show that it is CR3 rather than Dectin-1 that mediates ROS production and NETosis, which is consistent with our earlier finding that CR3 rather than Dectin-1 that mediates ROS production by murine neutrophils (11).

Although this discrepancy may be a function of *Candida* vs. *Aspergillus*, Reichner and colleagues provide evidence of a second NETosis pathway in the presence of extracellular matrix components such as fibronectin (13, 15). Whereas the classical pathway of NETosis described by Zychlinsky requires chromatin decondensation mediated by elastase translocation to the nucleus that is ROS dependent and occurs over a period of hours (1, 22), Reichner describes a rapid process (<30 min) of NET formation induced by *Candida* hyphae, which is independent of ROS formation (15).

As our studies show elastase in the nucleus, that ROS is required for NET formation, and that this process occurs over a number of hours, we conclude that NETosis progresses through the classical pathway. However, it is possible that in the presence of extracellular matrix, the NETosis pathway regulated by matrix proteins may also be activated; indeed, this may in part explain why we found no role for PAD4 in infected corneas even while detecting PAD4-dependent H3Cit. Activation of both pathways could also explain discrepancies in the role of PAD4 described in other microbial infections (28–30).

In contrast to other NET-related mediators such as elastase and ROS, PAD4 specifically regulates histone citrullination and is unique among the protein deiminase family in being localized to the nucleus (31, 32). Therefore, the only phenotype of PAD4$^{-/-}$ neutrophils should be an inability to form NETs so we focused on the role of PAD4 in neutrophil responses to *A. fumigatus*. Furthermore, although PAD4-dependent NETosis has been reported in mouse models of bacterial and parasitic infections,

and in autoimmunity (4, 33), there are no reports on the role of PAD4 in fungal infections.

In this study, we visualized citrullinated histone H3 associated with NETs following β-glucan stimulation of C57BL/6, but not PAD4$^{-/-}$ neutrophils, and NETosis measured by SYTOX was also dependent on PAD4. Given that β-glucan is a major cell wall surface component of molds and yeast following germination, these findings indicate that most pathogenic fungi would stimulate NET formation. However, PAD4$^{-/-}$ neutrophils did not exhibit impaired CP release or have any role in hyphal killing *in vitro*; furthermore, although H3Cit was detected in *A. fumigatus* infected corneas, we found no difference in hyphal growth or corneal opacification between C57BL/6 and PAD4$^{-/-}$ mice. Therefore, at least under these experimental conditions, PAD4-dependent NET formation is not required to control hyphal growth or fungal infection.

Following corneal infection with *A. fumigatus*, we found only localized H3Cit staining compared with the large neutrophil infiltrate, so it is possible that the absence of a phenotype is a consequence of relatively few NETs being formed; however, it is more likely that even though antimicrobial peptides are associated with NETs, NETosis is not required for CP release, iron sequestration or ROS production, all of which are important in controlling hyphal growth *in vitro* and in infection models (11, 12, 34). These findings are consistent with other studies in which PAD4-dependent NETs were not required to control bacterial CFU in a cecal ligation model of peritonitis (30) or for controlling influenza (29), although PAD4$^{-/-}$ mice showed an impaired ability to control *Shigella flexneri* infection (4). Both ROS and PAD4 independent NETosis have been described for *Leishmania amazonensis* promastigotes (33).

Instead of PAD4, we found that CR3 was required for ROS production in response to curdlan and *A. fumigatus*, release of CP, and *A. fumigatus* hyphal killing. Although CR3 was also required for NET formation, these findings do not implicate NETs in fungal killing as production of ROS and CP may be independent of NETosis. Indeed, PAD4$^{-/-}$ neutrophils released comparable levels of CP as C57BL/6 neutrophils within 2 h, which is earlier than we can detect NET formation, and indicates that CP release is NETosis independent.

Taken together, CR3 appears to be the β-glucan receptor that leads to PAD4 activation and NETosis on human and murine neutrophils, which is dependent on ROS; however, although NETs contain antimicrobial peptides, we conclude that NET formation is not required for CP release or to regulate *A. fumigatus* hyphal growth *in vitro* or in the fungal keratitis model. Furthermore, because CD18 (LFA1) binding to ICAM-1 on capillary endothelial cells is required for neutrophil attachment and extravasation, CD18$^{-/-}$ neutrophils are not recruited to infected tissues; therefore, we were unable to examine CR3 recognition of *Aspergillus* in infected corneas.

Although the role of NETs in microbial killing appears to be controversial, NETs have also been implicated in tissue damage during infection and in autoimmune disease including rheumatoid arthritis, lupus, vasculitis, acute respiratory distress syndrome, and sepsis. This is due in part to release of histones that are abundant in NETs and which have direct cytotoxic activity (35). One example is intravenous injection of methicillin resistant *Staphylococcus aureus*, which resulted in PAD4-dependent NET formation in the liver and resulting hepatic injury (36). By contrast, we found that corneal opacity as a measure of tissue damage in fungal keratitis was not reduced in *A. fumigatus* infected PAD4$^{-/-}$ mice, indicating that NETs do not appear to regulate blinding corneal disease related to fungal infection. NETs have been reported in *Pseudomonas aeruginosa* keratitis, although ExoS-expressing strains are more susceptible than ExoU to NET-mediated bacterial killing (37).

A recent review of NETs proposes a clear distinction between ROS and elastase-dependent NETs, which have antimicrobial activity, and a second ROS independent, PAD4-mediated mechanism of DNA release termed leukotoxic hypercitrullination, which is triggered by elevated intracellular calcium (which activates PAD4) and is associated with autoimmunity (38). Our findings reveal β-glucan-induced NET formation that is both ROS and PAD4 dependent and is associated with intranuclear elastase, thereby suggesting this dichotomy is not so clear. The same review also notes that the main purpose of PAD4-mediated histone citrullination is to alter the chromatin and regulate gene transcription, whereas elastase digestion of chromatin is also required for NETosis. Our observations that release of extracellular DNA can be blocked by inhibiting PAD4 or ROS production makes it unlikely that we are seeing two distinct pathways.

In conclusion, this study demonstrates an essential role for CR3, ROS, and PAD4 in NET formation in response to *Aspergillus* and to β-glucan but shows that PAD4-dependent NETosis is not required for either hyphal killing or for tissue damage in the cornea.

MATERIALS AND METHODS

Ethics Statement

Human peripheral blood was collected from healthy donors between ages of 18 and 65 years in accordance with the Declaration of Helsinki guidelines and with the approval of the Institutional Review Board of the University of California (Irvine, CA, USA). Informed consent was obtained in writing from each volunteer.

All animals were treated in accordance with the guidelines provided in the Association for Research in Vision and Ophthalmology ARVO statement for the Use of Animals in Ophthalmic and Vision Research. All animal studies were conducted following approval of the Institutional Animal Care and Use Committee of Case Western Reserve University and the University of California, Irvine.

Human Peripheral Blood Neutrophils

Whole blood RBCs were separated in 3% dextran (Sigma-Aldrich, St. Louis, MO, USA) PBS, and neutrophils were purified from remaining cells by overlay on a Ficoll (GE Healthcare) density gradient and centrifugation at 500 × *g* for 25 min. Remaining RBCs were lysed, and neutrophils were resuspended in RPMI 1640 medium. Purity (~90%) was assessed by flow cytometry using antihuman D16 and CD66b Abs (eBioscience, San Diego, CA, USA).

Source of Mice

CD18$^{-/-}$ mice were originally provided by Claire Doerschuk (University of North Carolina, Chapel Hill, NC, USA). Age- and sex-matched C57BL/6 mice were purchased from Jackson Laboratories (Bar Harbor, ME, USA). PAD4$^{-/-}$ mice were originally provided by Dr. Kerri Mowen at Scripps Research Institute. All animal experiments were conducted with sex- and age-matched mice, and animal studies were compliant with all applicable provisions established by the Animal Welfare Act and the Public Health Services Policy on the Humane Care and Use of Laboratory Animals.

A. fumigatus Strains and Culture

The strain used in these studies was a keratitis clinical isolate obtained from the Bascom-Palmer Eye Institute, *A. fumigatus* BP, whereas the strain used for corneal infection experiments was the Af293-expressing red fluorescent protein used in our prior studies (12). Fungi were cultured on Sabouraud dextrose agar at 37°C for 3–5 days for sporulation, and conidia were isolated by disruption in PBS and filtration through sterile cotton gauze. For hyphal killing experiments, conidia were grown in Sabouraud dextrose broth (SDB), at 3,000 conidia/well of 96-well plate until germination (6 h), washed in sterile PBS and co-incubated with neutrophils. For AspHE preparation, conidia were grown in 500 ml SDB at 37°C for 5 days. SDB was removed from the fungi by vacuum filtration, and fungal mass was homogenized in a mortar and pestle under liquid nitrogen. Fungal homogenate was resuspended in RPMI 1640 without phenol red and filtered through a 70 μM cell strainer. Protein content was measured by BCA assay (ThermoFisher), and AspHE stocks were stored at −20°C.

Neutrophil Isolation

Human neutrophils were isolated from the blood of healthy donors age 18–50. All human studies were approved by the University of California, Irvine institutional review board. Whole blood was mixed 1:1 with 3% dextran-PBS for 20 min to sediment red blood cells. The upper layer was overlaid on Ficoll Hypaque (GE Healthcare) and centrifuged at 500 × *g* for 25 min. The pellet containing granulocytes and RBCs was treated with 1× RBC Lysis Buffer (eBioscience) and spun at 300 × *g* for 5 min to obtain a granulocyte pellet. Cells were resuspended in RPMI 1640 and counted. Typical purity was >95%. Total bone marrow was isolated from the tibias, and femurs of mice and neutrophils were purified using the EasySep mouse neutrophil enrichment kit (Stemcell), routinely yielding >90% neutrophil population.

SYTOX Green Assay for Extracellular DNA

Neutrophils were resuspended in RPMI 1640, no phenol red (Life Technologies) plus 10% FBS. Murine GM-CSF (20 ng/ml, R&D Systems) and 200 μM $CaCl_2$ were added to media for overnight mouse neutrophil experiments. In some assays, neutrophils were incubated at 37°C with inhibitors or blocking antibodies for 30 min before stimulation. Diphenyliodonium (DPI, Sigma-Aldrich) and a 10 mM stock solution in DMSO were prepared. The PAD4 inhibitors GSK484 and GSK106 described in Ref. (19) were purchased from Cayman chemical, and 40 mM of stock solutions was prepared in DMSO. Blocking antibody for CR3, LEAF purified antihuman/mouse CD11b, M1/70 was purchased from BioLegend. Anti-Dectin-1 22H8 blocking antibody was purchased from Invivogen. 2 × 10^5 cells/well for human or 1 × 10^5 cells/well for mice were added to black 96-well plates with optical bottoms (Corning) ± RPMI only, PMA (25 nM), particulate β-glucan (curdlan) (100 μg/ml) or AspHE (100 μg/ml) and 1 μM SYTOX Green nucleic acid stain (Life Technologies). Plates were incubated at 37°C, 5% CO_2 in a Biotek Cytation 5 imaging plate reader, and fluorescence was measured every 30 min at 504/523 nm for up to 24 h. Plates were imaged at 40–200× using brightfield or GFP filters.

Quantification of Reactive Oxygen

Neutrophils were resuspended in RPMI 1640 without phenol red (Life Technologies). In some assays neutrophils were incubated at 37°C with inhibitors or blocking antibodies for 30 min before stimulation. 2 × 10^5 cells/well were added to black 96-well plates with optical bottoms (Corning) ± RPMI only or curdlan (100 μg/ml) plus 500 μM luminol (Sigma-Aldrich) in the absence of serum, and luminescence was measured every 2 min for 2 h on a Biotek Cytation 5.

Immunocytochemistry and Fluorescence Imaging

Neutrophils were resuspended in RPMI 1640, no phenol red, 2% FBS at 2 × 10^6 cells/ml. In some assays, neutrophils were incubated at 37°C with cytokines, inhibitors or blocking antibodies for 30 min before stimulation. Cells were plated on glass bottom 8-well chamber slides (Ibidi) or poly-L-lysine coated glass coverslips (Neuvitro) ± RPMI only or curdlan (100 μg/ml) for up to 24 h. Media were removed, and cells were fixed for 30 min in 4% formaldehyde in PBS. Cells were permeabilized in 0.1% Triton-X100 in PBS for 15 min and washed in PBS. Cells were stained for H3Cit (Abcam 5103) 1:100 and NE (SCBT) at 1:50 overnight at 4°C. Slides were washed in PBST, and donkey anti-rabbit Alexafluor 488 or donkey anti-goat Alexafluor 568 (Life Technologies) was added for 1 h at RT. Slides were washed in PBST, and 100 μl of PBS-DAPI was added to slides. Slides were imaged at 200× on a Biotek Cytation 5 using GFP, RFP and DAPI filters and on a Leica confocal at 600×.

S100A8 ELISA

Mouse neutrophils were incubated in RPMI 1640 + 10% FBS + 20 ng/ml GM-CSF (R&D Systems) ± curdlan (100 μg/ml) or AspHE (100 μg/ml) at 1 × 10^5 cells/well in 96-well plates as described (12). Plates were incubated at 37°C for 2 or 16 h, centrifuged at 300 × *g* for 3 min, and cell-free supernatants were collected. S100A8 was measured by ELISA (R&D Systems) according to the manufacturer's directions.

Fungal Growth Inhibition Assay

These assays were performed as described recently (12). Briefly, *A. fumigatus* conidia were grown to a hyphal stage in 96-well plates and incubated 18 h at 37°C with 2 × 10^5 neutrophils/well. Following incubation, the supernatant was removed, and wells were stained with 50 μl Calcofluor white chitin stain (Sigma-Aldrich) for 10 min. Wells were washed three times in ddH_2O, and fluorescence was read on a Biotek Cytation 5 at 360/440 nM.

A. fumigatus Corneal Infection

Mice were anesthetized, the corneal epithelium was penetrated with a 30 G needle, and 2 μl containing 50,000 conidia (dsRed Af293) were injected into the corneal stroma using a 33 G Hamilton syringe as described (12).

After 48 h, mice were euthanized, and corneas were imaged by brightfield to detect corneal opacity, and by fluorescence to detect dsRed hyphae. Images were analyzed, and corneal opacity and dsRed were quantified using Metamorph with the parameters described by us in detail (11, 34). Whole eyes were homogenized using a Retsch Mixer Mill bead homogenizer (QIAGEN Sciences, Germantown, MD, USA), and colony forming units were counted manually.

Flow Cytometry

Corneas were carefully dissected to remove adherent iris material and digested 1 h in collagenase type 1 (80u/cornea; Sigma-Aldrich, cat no 234153). Total cells were collected and incubated with Fc block anti-mouse CD16/CD32 (clone 93, 16-0161-86; eBioscience), followed by anti-mouse neutrophil antibody (Ly6G, NIMP-R14-PE, ab125259; Abcam, Cambridge, MA, USA), and anti-CD11b-APC FAB1124A (R&D Systems, Minneapolis, MN, USA). We also used CD45-FITC (30-F11), Ly6C APC-Cy7 (HK1.4), and Ep-CAM-PECy7 (G8.8), all from BioLegend. Total cells were examined in an ACEA Novocyte™ flow cytometer and analyzed following appropriate compensation.

Immunofluorescence Staining of Mouse Corneas

Whole corneas were excised and immediately embedded in optimal cutting temperature (Thermo Fisher Scientific). Frozen sections (10 μm) were mounted on Superfrost™ Plus™ slides and stored at −80°C. Before staining, the slices were placed on a 37°C hot plate for 10 min followed by submersion in acetone for 10 min at −20°C. The slides were washed in PBS twice, permeabilized 5 min in 0.1% Triton-X/PBS, and incubated at room temperature for 1 h in blocking buffer containing 2% BSA and 0.1% Tween 20 with 1:200 Fc block (Anti-CD16/32; Tonbo Biosciences), and 10% donkey serum (Vector Labs).

Corneal sections (5 μm) were then stained at room temperature for 2 h with Ly6G antibody NIMPR14 at 40 μg/ml (Abcam) and 1:50 Rabbit polyclonal antibody to histone H3 (citrulline R2 + R8 + R17) (Abcam). Slides were rinsed three times in PBS, and then secondary antibodies, donkey anti-rabbit Alexa Fluor 555 or goat anti-rat Alexa Fluor 488, were applied at 1:1,000 (Invitrogen) for 1 h at room temperature. Slides were rinsed and mounted in Fluoromount with DAPI (Thermo Fisher Scientific). All images were acquired within 24 h.

Statistical Analysis

Experimental data from *in vitro* and *in vivo* studies were analyzed for significance from at least three independent experiments. Statistical significance for multiple parameters was determined using one-way ANOVA with Tukey *post hoc* analyses, or using Student's *t*-test when only two parameters were compared.

All statistical analyses were performed with GraphPad Prism software, v6.0c (La Jolla, CA, USA). A p value < 0.05 was considered significant as indicated in the figure legends ($^{*}p \leq 0.05$, $^{**}p \leq 0.01$, and $^{***}p \leq 0.001$).

ETHICS STATEMENT

All animals were used in accordance with the guidelines of the Case Western Reserve University and University of California, Irvine Institutional Animal Care and Use Committee (IACUC). Whole blood was collected from healthy donors between ages of 18 and 65 years in accordance with the Declaration of Helsinki guidelines and the Institutional Review Board of the University of California (Irvine, CA, USA).

AUTHOR CONTRIBUTIONS

HC, SA, MM, YS, and EG: experimental design, performance, and data analysis. HC and EP: manuscript preparation.

ACKNOWLEDGMENTS

We thank Laura Mendez-Luque and Michaela Marshall for excellent technical assistance. This work was supported by National Eye Institute Grant R01 EY18612 (to EP), the National Eye Institute National Research Service Award F30EY025548 (to HC), MSTP Grant T32 GM007250 (HC), and the Visual Sciences Research Center Core Grant P30EY011373. Studies were also supported by a grant from the Research to Prevent Blindness Foundation.

SUPPLEMENTARY MATERIAL

The Supplementary Material for this article can be found online at https://www.frontiersin.org/articles/10.3389/fimmu.2018.01182/full#supplementary-material.

REFERENCES

1. Brinkmann V, Reichard U, Goosmann C, Fauler B, Uhlemann Y, Weiss DS, et al. Neutrophil extracellular traps kill bacteria. *Science* (2004) 303(5663): 1532–5. doi:10.1126/science.1092385
2. Guimaraes-Costa AB, Nascimento MT, Froment GS, Soares RP, Morgado FN, Conceicao-Silva F, et al. *Leishmania amazonensis* promastigotes induce and are killed by neutrophil extracellular traps. *Proc Natl Acad Sci U S A* (2009) 106(16):6748–53. doi:10.1073/pnas.0900226106
3. Urban CF, Ermert D, Schmid M, Abu-Abed U, Goosmann C, Nacken W, et al. Neutrophil extracellular traps contain calprotectin, a cytosolic protein complex involved in host defense against *Candida albicans*. *PLoS Pathog* (2009) 5(10):e1000639. doi:10.1371/journal.ppat.1000639
4. Papayannopoulos V, Metzler KD, Hakkim A, Zychlinsky A. Neutrophil elastase and myeloperoxidase regulate the formation of neutrophil extracellular traps. *J Cell Biol* (2010) 191(3):677–91. doi:10.1083/jcb.201006052
5. Hakkim A, Fuchs TA, Martinez NE, Hess S, Prinz H, Zychlinsky A, et al. Activation of the Raf-MEK-ERK pathway is required for neutrophil extracellular trap formation. *Nat Chem Biol* (2011) 7(2):75–7. doi:10.1038/nchembio.496
6. Remijsen Q, Vanden Berghe T, Wirawan E, Asselbergh B, Parthoens E, De Rycke R, et al. Neutrophil extracellular trap cell death requires both

autophagy and superoxide generation. *Cell Res* (2011) 21(2):290–304. doi:10.1038/cr.2010.150
7. Neeli I, Radic M. Opposition between PKC isoforms regulates histone deimination and neutrophil extracellular chromatin release. *Front Immunol* (2013) 4:38. doi:10.3389/fimmu.2013.00038
8. Kenno S, Perito S, Mosci P, Vecchiarelli A, Monari C. Autophagy and reactive oxygen species are involved in neutrophil extracellular traps release induced by *C. albicans* morphotypes. *Front Microbiol* (2016) 7:879. doi:10.3389/fmicb.2016.00879
9. Tarabishy AB, Aldabagh B, Sun Y, Imamura Y, Mukherjee PK, Lass JH, et al. MyD88 regulation of *Fusarium keratitis* is dependent on TLR4 and IL-1R1 but not TLR2. *J Immunol* (2008) 181(1):593–600. doi:10.4049/jimmunol.181.1.593
10. Leal SM Jr., Cowden S, Hsia YC, Ghannoum MA, Momany M, Pearlman E. Distinct roles for Dectin-1 and TLR4 in the pathogenesis of *Aspergillus fumigatus* keratitis. *PLoS Pathog* (2010) 6:e1000976. doi:10.1371/journal.ppat.1000976
11. Leal SM Jr., Vareechon C, Cowden S, Cobb BA, Latge JP, Momany M, et al. Fungal antioxidant pathways promote survival against neutrophils during infection. *J Clin Invest* (2012) 122(7):2482–98. doi:10.1172/JCI63239
12. Clark HL, Jhingran A, Sun Y, Vareechon C, de Jesus Carrion S, Skaar EP, et al. Zinc and manganese chelation by neutrophil S100A8/A9 (calprotectin) limits extracellular *Aspergillus fumigatus* hyphal growth and corneal infection. *J Immunol* (2016) 196(1):336–44. doi:10.4049/jimmunol.1502037
13. Byrd AS, O'Brien XM, Johnson CM, Lavigne LM, Reichner JS. An extracellular matrix-based mechanism of rapid neutrophil extracellular trap formation in response to *Candida albicans*. *J Immunol* (2013) 190(8):4136–48. doi:10.4049/jimmunol.1202671
14. Rohm M, Grimm MJ, D'Auria AC, Almyroudis NG, Segal BH, Urban CF. NADPH oxidase promotes neutrophil extracellular trap formation in pulmonary aspergillosis. *Infect Immun* (2014) 82(5):1766–77. doi:10.1128/IAI.00096-14
15. O'Brien XM, Reichner JS. Neutrophil integrins and matrix ligands and NET release. *Front Immunol* (2016) 7:363. doi:10.3389/fimmu.2016.00363
16. Underhill DM, Pearlman E. Immune interactions with pathogenic and commensal fungi: a two-way street. *Immunity* (2015) 43(5):845–58. doi:10.1016/j.immuni.2015.10.023
17. Thornton BP, Vetvicka V, Pitman M, Goldman RC, Ross GD. Analysis of the sugar specificity and molecular location of the beta-glucan-binding lectin site of complement receptor type 3 (CD11b/CD18). *J Immunol* (1996) 156(3):1235–46.
18. Branzk N, Lubojemska A, Hardison SE, Wang Q, Gutierrez MG, Brown GD, et al. Neutrophils sense microbe size and selectively release neutrophil extracellular traps in response to large pathogens. *Nat Immunol* (2014) 15(11):1017–25. doi:10.1038/ni.2987
19. Lewis HD, Liddle J, Coote JE, Atkinson SJ, Barker MD, Bax BD, et al. Inhibition of PAD4 activity is sufficient to disrupt mouse and human NET formation. *Nat Chem Biol* (2015) 11(3):189–91. doi:10.1038/nchembio.1735
20. Bianchi M, Niemiec MJ, Siler U, Urban CF, Reichenbach J. Restoration of anti-*Aspergillus* defense by neutrophil extracellular traps in human chronic granulomatous disease after gene therapy is calprotectin-dependent. *J Allergy Clin Immunol* (2011) 127(5):1243–52.e7. doi:10.1016/j.jaci.2011.01.021
21. Karthikeyan RS, Priya JL, Leal SM Jr., Toska J, Rietsch A, Prajna V, et al. Host response and bacterial virulence factor expression in *Pseudomonas aeruginosa* and *Streptococcus pneumoniae* corneal ulcers. *PLoS One* (2013) 8(6):e64867. doi:10.1371/journal.pone.0064867
22. Fuchs TA, Abed U, Goosmann C, Hurwitz R, Schulze I, Wahn V, et al. Novel cell death program leads to neutrophil extracellular traps. *J Cell Biol* (2007) 176(2):231–41. doi:10.1083/jcb.200606027
23. Bruns S, Kniemeyer O, Hasenberg M, Aimanianda V, Nietzsche S, Thywissen A, et al. Production of extracellular traps against *Aspergillus fumigatus* in vitro and in infected lung tissue is dependent on invading neutrophils and influenced by hydrophobin RodA. *PLoS Pathog* (2010) 6(4):e1000873. doi:10.1371/journal.ppat.1000873
24. Gazendam RP, van Hamme JL, Tool AT, Hoogenboezem M, van den Berg JM, Prins JM, et al. Human neutrophils use different mechanisms to kill *Aspergillus fumigatus* conidia and hyphae: evidence from phagocyte defects. *J Immunol* (2016) 196(3):1272–83. doi:10.4049/jimmunol.1501811
25. McCormick A, Heesemann L, Wagener J, Marcos V, Hartl D, Loeffler J, et al. NETs formed by human neutrophils inhibit growth of the pathogenic mold *Aspergillus fumigatus*. *Microbes Infect* (2010) 12(12–13):928–36. doi:10.1016/j.micinf.2010.06.009
26. Lee MJ, Liu H, Barker BM, Snarr BD, Gravelat FN, Al Abdallah Q, et al. The fungal exopolysaccharide galactosaminogalactan mediates virulence by enhancing resistance to neutrophil extracellular traps. *PLoS Pathog* (2015) 11(10):e1005187. doi:10.1371/journal.ppat.1005187
27. Marcos V, Nussbaum C, Vitkov L, Hector A, Wiedenbauer EM, Roos D, et al. Delayed but functional neutrophil extracellular trap formation in neonates. *Blood* (2009) 114(23):4908–4911; author reply 4911–4902. doi:10.1182/blood-2009-09-242388
28. Li P, Li M, Lindberg MR, Kennett MJ, Xiong N, Wang Y. PAD4 is essential for antibacterial innate immunity mediated by neutrophil extracellular traps. *J Exp Med* (2010) 207(9):1853–62. doi:10.1084/jem.20100239
29. Hemmers S, Teijaro JR, Arandjelovic S, Mowen KA. PAD4-mediated neutrophil extracellular trap formation is not required for immunity against influenza infection. *PLoS One* (2011) 6(7):e22043. doi:10.1371/journal.pone.0022043
30. Martinod K, Fuchs TA, Zitomersky NL, Wong SL, Demers M, Gallant M, et al. PAD4-deficiency does not affect bacteremia in polymicrobial sepsis and ameliorates endotoxemic shock. *Blood* (2015) 125(12):1948–56. doi:10.1182/blood-2014-07-587709
31. Nakashima K, Hagiwara T, Yamada M. Nuclear localization of peptidylarginine deiminase V and histone deimination in granulocytes. *J Biol Chem* (2002) 277(51):49562–8. doi:10.1074/jbc.M208795200
32. Wang Y, Li M, Stadler S, Correll S, Li P, Wang D, et al. Histone hypercitrullination mediates chromatin decondensation and neutrophil extracellular trap formation. *J Cell Biol* (2009) 184(2):205–13. doi:10.1083/jcb.200806072
33. Rochael NC, Guimaraes-Costa AB, Nascimento MT, DeSouza-Vieira TS, Oliveira MP, Garcia e Souza LF. Classical ROS-dependent and early/rapid ROS-independent release of neutrophil extracellular traps triggered by *Leishmania* parasites. *Sci Rep* (2015) 5:18302. doi:10.1038/srep18302
34. Leal SM Jr, Roy S, Vareechon C, Carrion S, Clark H, Lopez-Berges MS, et al. Targeting iron acquisition blocks infection with the fungal pathogens *Aspergillus fumigatus* and *Fusarium oxysporum*. *PLoS Pathog* (2013) 9(7):e1003436. doi:10.1371/journal.ppat.1003436
35. Saffarzadeh M, Juenemann C, Queisser MA, Lochnit G, Barreto G, Galuska SP, et al. Neutrophil extracellular traps directly induce epithelial and endothelial cell death: a predominant role of histones. *PLoS One* (2012) 7(2):e32366. doi:10.1371/journal.pone.0032366
36. Kolaczkowska E, Jenne CN, Surewaard BG, Thanabalasuriar A, Lee WY, Sanz MJ, et al. Molecular mechanisms of NET formation and degradation revealed by intravital imaging in the liver vasculature. *Nat Commun* (2015) 6:6673. doi:10.1038/ncomms7673
37. Shan Q, Dwyer M, Rahman S, Gadjeva M. Distinct susceptibilities of corneal *Pseudomonas aeruginosa* clinical isolates to neutrophil extracellular trap-mediated immunity. *Infect Immun* (2014) 82(10):4135–43. doi:10.1128/IAI.02169-14
38. Konig MF, Andrade F. A critical reappraisal of neutrophil extracellular traps and NETosis mimics based on differential requirements for protein citrullination. *Front Immunol* (2016) 7:461. doi:10.3389/fimmu.2016.00461

Conflict of Interest Statement: None of the submitted work was carried out in the presence of any personal, professional, or financial relationships that could potentially be construed as a conflict of interest.

Copyright © 2018 Clark, Abbondante, Minns, Greenberg, Sun and Pearlman. This is an open-access article distributed under the terms of the Creative Commons Attribution License (CC BY). The use, distribution or reproduction in other forums is permitted, provided the original author(s) and the copyright owner are credited and that the original publication in this journal is cited, in accordance with accepted academic practice. No use, distribution or reproduction is permitted which does not comply with these terms.

frontiers in Immunology

REVIEW
published: 22 November 2017
doi: 10.3389/fimmu.2017.01623

Natural Killer Cells in Antifungal Immunity

*Stanislaw Schmidt, Lars Tramsen and Thomas Lehrnbecher**

Division for Pediatric Hematology and Oncology, Hospital for Children and Adolescents, Johann Wolfgang Goethe-University, Frankfurt, Germany

Invasive fungal infections are still an important cause of morbidity and mortality in immunocompromised patients such as patients suffering from hematological malignancies or patients undergoing hematopoietic stem cell transplantion. In addition, other populations such as human immunodeficiency virus-patients are at higher risk for invasive fungal infection. Despite the availability of new antifungal compounds and better supportive care measures, the fatality rate of invasive fungal infection remained unacceptably high. It is therefore of major interest to improve our understanding of the host–pathogen interaction to develop new therapeutic approaches such as adoptive immunotherapy. As experimental methodologies have improved and we now better understand the complex network of the immune system, the insight in the interaction of the host with the fungus has significantly increased. It has become clear that host resistance to fungal infections is not only associated with strong innate immunity but that adaptive immunity (e.g., T cells) also plays an important role. The antifungal activity of natural killer (NK) cells has been underestimated for a long time. *In vitro* studies demonstrated that NK cells from murine and human origin are able to attack fungi of different genera and species. NK cells exhibit not only a direct antifungal activity *via* cytotoxic molecules but also an indirect antifungal activity *via* cytokines. However, it has been show that fungi exert immunosuppressive effects on NK cells. Whereas clinical data are scarce, animal models have clearly demonstrated that NK cells play an important role in the host response against invasive fungal infections. In this review, we summarize clinical data as well as results from *in vitro* and animal studies on the impact of NK cells on fungal pathogens.

Keywords: natural killer cell, invasive fungal infection, *Aspergillus*, *Candida*, mucormycete, *Cryptococcus*, antifungal host response

OPEN ACCESS

Edited by:
Steven Templeton, Indiana University School of Medicine – Terre Haute, United States

Reviewed by:
Kerstin Hünniger, Leibniz-Institut für Naturstoff-Forschung und Infektionsbiologie, Hans Knöll Institut, Germany
Amir Horowitz, Icahn School of Medicine at Mount Sinai, United States

***Correspondence:**
Thomas Lehrnbecher
thomas.lehrnbecher@kgu.de

Specialty section:
This article was submitted to Microbial Immunology, a section of the journal Frontiers in Immunology

Received: *25 September 2017*
Accepted: *08 November 2017*
Published: *22 November 2017*

Citation:
Schmidt S, Tramsen L and Lehrnbecher T (2017) Natural Killer Cells in Antifungal Immunity. Front. Immunol. 8:1623. doi: 10.3389/fimmu.2017.01623

INTRODUCTION

Invasive fungal infections are still associated with significant morbidity and mortality. For example, a retrospective cohort study in the US demonstrated that as compared to patients without

Abbreviations: ADCC, antibody-dependent cell-mediated cytotoxicity; CD, cluster of differentiation; SRIR, self-recognizing inhibitory receptors; EBV, Epstein–Barr virus; CMV, cytomegalovirus; ALL, acute lymphoblastic leukemia; AML, acute myeloid leukemia; IFN, interferon; ILC, innate lymphoid cell; DCs, dendritic cells; RANTES, regulated upon activation, normal T-cell expressed, and secreted; CCL5, chemokine ligand 5; GM-CSF, granulocyte-macrophage colony-stimulating factor; TNF-α, tumor necrosis factor alpha; HSCT, hematopoietic stem cell transplantation; ROS, reactive oxygen species; CMCC, chronic mucocutaneous candidiasis; SLE, systemic lupus erythematosus; HIV, human immunodeficiency virus; IL, interleukin; TRAIL, tumor necrosis factor related apoptosis inducing ligand; IgG, immunoglobulin G; NADPH, nicotinamide adenine dinucleotide phosphate; Hsp, heat shock protein; NCR, natural cytotoxicity receptors; Gr-MDSC, granulocyte myeloid-derived suppressor cell; ITAM, immunoreceptor tyrosine-based activation motif.

invasive aspergillosis, patients suffering from the infection had a significant longer hospital stay, caused significantly higher costs, and, most importantly, had a significant higher mortality (1). A population-based analysis of invasive fungal infections in France revealed that between 2001 and 2010, the incidence of invasive fungal disease due to *Candida* spp., *Aspergillus* spp., and mucormycetes increased by 7.8, 4.4, and 7.3% per year, respectively, which was highly significant for each pathogen (2). In contrast to cryptococcosis, which often occurs in human immunodeficiency virus (HIV)-patients, the population at high risk for candidemia, invasive aspergillosis, and mucormycosis includes in particular patients with hematological malignancies, patients undergoing hematopoietic stem cell transplantation (HSCT) and solid organ recipients (2–6). These patient populations are characterized by the impairment of multiple arms of the immune system (7, 8), such as of natural barriers, the phagocyte system, innate immunity, and lymphocytes, all of which may increase the risk for an invasive fungal infection. Therefore, it is not surprising that the mortality rate of invasive fungal disease is extremely high in these patient populations, exceeding 70% in HSCT recipients suffering from invasive aspergillosis or mucormycosis (4).

It is well known that the recovery of the immune system has a major impact on the outcome of invasive fungal infection in an immunocompromised patient (9, 10). Unfortunately, to date, immunomodulation using cytokine and growth factor therapies, as well as adoptive immunotherapeutic strategies such as granulocyte transfusions or the administration of *Aspergillus*-specific T-cells did not significantly improve the prognosis of immunocompromised patients with invasive fungal disease (11). It is therefore of major interest to improve our understanding of the host–pathogen interaction to develop new therapeutic strategies for immunocompromised individuals suffering from fungal infection. This review will summarize available clinical data as well as results from *in vitro* and animal studies on the impact of natural killer (NK) cells on fungal pathogens.

THE HOST RESPONSE TO FUNGAL INFECTION

Over the last decades, we could witness major advances not only in the understanding of the complexity of the immune system but also in our knowledge on the immunopathogenesis of invasive fungal infections. The host response to a fungal pathogen includes, but is not restricted to various cells of the innate and adaptive immunity such as monocytes, neutrophils, dendritic cells (DCs), T and B lymphocytes, as well as multiple soluble molecules such as collectins, defensins, cytokines including interferons (IFNs) (12, 13). Although it is known for a long time that severe and prolonged neutropenia (e.g., absolute neutrophil count $\leq$500/μl and duration of neutropenia $\geq$10 days) is the single most important risk factor for invasive aspergillosis, invasive *Candida* infection, and mucormycosis in patients receiving cytotoxic chemotherapy or undergoing allogeneic HSCT (9, 14), recent studies refined our understanding how neutrophils are controlling in particular the early stages of invasive fungal infection. Neutrophils are attracted by cytokines released by endothelial cells and macrophages and are able to quickly migrate to a focus of infection. In addition to recruiting and activating other immune cells by the production of pro-inflammatory cytokines, neutrophils may attack as front-line defense invading pathogens by phagocytosis, the production of reactive oxygen intermediates, and the release antimicrobial enzymes to the formation of complex extracellular traps (NETs) that help in the elimination of the fungus (15). DCs transport fungal antigens to the draining lymph nodes, where they orchestrate T cell activation and differentiation (16). A number of lymphocyte subsets have an important impact in the antifungal immunity, such as Th1 cells (important for inflammation and fungal clearance), Th17 cells (neutrophil recruitment, defensins), Th22 cells (defensins, tissue homeostasis), and Treg cells (immunosuppression). In addition, a number of cytokines play important roles in the complex crosstalk between different cells of the immune system, which modify and regulate innate and adaptive immune responses, such as the induction of proliferation and differentiation, as well as the activation or suppression of different target cells (11–13). Still, many open questions have to be resolved, including the influence of the genetic background in the delicate interplay of immune cells, the interaction of the innate and adaptive immune system in balancing protection and immunopathology in fungal infections (12), and the influence of fungal microbiota or "mycobiota" on health and disease (17). More importantly, we have to learn how to modify the immune system in the combat against invasive fungal infections, in particular in the immunocompromised host, which includes not only the activation of the immune response to eliminate the pathogen but also its suppression to avoid collateral tissue damage.

NK CELL BIOLOGY

Human NK cells, which originate from the bone marrow, represent up to 15% of peripheral blood mononuclear cells. They are characterized by the expression of CD56 and by the absence of the T cell marker CD3. According to the surface expression density of CD56 and CD16, NK cells can be subdivided in two main subpopulations, namely the cytotoxic $CD56^{dim}CD16^{bright}$ and the immune regulatory $CD56^{bright}CD16^{dim}$ subsets (18). Although NK cells were originally considered as cells of innate immunity, they demonstrate qualities of the adaptive immunity such as immunological memory (19–22). In this regard, animal models and human studies indicate that NK cells are able to develop long-lasting antigen-specific memory (23–26). It has been demonstrated that memory-like NK cells display a less differentiated phenotype in $CD56^{dim}$ NK cells, which were $CD94^{+}NKG2A^{+}$ but $CD57^{-}KIR^{-}$ (27). The name "natural killer cell" originally came from their ability to kill tumor cells *in vitro* and *in vivo* without previous stimulation (22, 28–31). Their antitumor activity includes activity against acute lymphoblastic leukemia (32), acute myeloid leukemia (33), and neuroblastoma (34, 35). In addition to their antitumor activity, NK cells play an important role in the host response against various pathogens which includes viruses such as cytomegalovirus (CMV), Epstein–Barr virus (23, 36–38), or hepatitis B and C virus (37, 39, 40), and Gram-positive, Gram-negative, and intracellular bacteria, such as *Salmonella typhi*, *Escherichia coli* (41), or *Listeria monocytogenes* (42).

Natural killer cells eliminate their potential targets either by directly using cytotoxic molecules such as perforin or granzyme B, which are stored in granules, or by death receptor-mediated apoptosis (36). In addition, CD16 (FcγRIII) triggers antibody-dependent cell-mediated cytotoxicity on opsonized target cells (36). Education and differentiation are considered to be important mechanisms for both direct and antibody-dependent functionality of NK cells (43–45). Several models have been developed to explain the process of "education" (43, 45–49). In general, the expression of self-recognizing inhibitory receptors (SRIR) results in the development of NK cells toward fully functional mature form, which has been termed as "licensing" process (50). In contrast, the "disarming" model describes NK cells lacking SRIR that become anergic due to chronic activation (51). The more dynamic "rheostat model" has been used to describe that stronger inhibitory signaling through more SRIR interactions results in a greater functional responsiveness of NK cells (52, 53). Importantly, cytokine stimulation can prime SRIR-deficient NK cells to a functional state (50), and uneducated cells are also able to combat viral infections, as SRIR-deficient NK cells strongly respond toward murine CMV (54).

In addition to the direct cytotoxic abilities, NK cells have recently been classified closely to group 1 innate lymphoid cells, which are characterized by the production of IFN-γ, whereas type 2 cytokines are not produced (55). *Via* the release of chemokines and cytokines such as IFN-γ, tumor necrosis factor alpha (TNF-α), granulocyte-macrophage colony-stimulating factor (GM-CSF), or chemokine ligand 5 (CCL5) [regulated upon activation, normal T-cell expressed, and secreted (RANTES)], NK cells modulate the activity of various immune cells including neutrophils, DCs, and T cells (46, 56), which complements their direct anti-pathogen and antibody-mediated activities.

NK CELLS AND INVASIVE FUNGAL INFECTION: CLINICAL OBSERVATIONS

Although clinical data suggest the importance of NK cells in the risk and outcome of invasive fungal infection, the exact role of NK cells is difficult to determine as multiple cells are involved in the antifungal host response, and as these cells interact in a complex network with both positive and negative feedback mechanisms (7, 8). A recent study analyzed 51 patients undergoing allogeneic HSCT, among them 9 patients in whom proven or probable invasive aspergillosis occurred (10). The study evaluated both the quantitative and qualitative reconstitution of immune cells including polymorphonuclear cells, $CD4^+$ T cells, $CD8^+$ T cells, and NK cells, and the authors reported two important observations: first, transplant recipients suffering from invasive aspergillosis displayed insufficient NK cell recovery with cell counts remaining less than 200/μl as well as lower reactive oxygen species (ROS) production. Second, HSCT transplant recipients who were cured from invasive aspergillosis had significantly higher ROS production and higher NK cell counts as compared to those patients who had a poor outcome of the invasive fungal infection. As both cell count and ROS production were altered in each of the analyses, the importance of the NK cell count as single risk and single prognostic factor for invasive aspergillosis remains unresolved. Another study evaluated 396 patients undergoing solid organ transplantation (57). A total of 304 patients were kidney and 92 patients were liver transplant recipients, and median followed-up time was 504.5 days after transplantation. The analysis demonstrated that 1 month after transplantation, patients who did not develop invasive fungal disease at a later time point had significantly higher mean NK cell count as compared with those patients who developed fungal disease. In the non-transplant setting, larger clinical studies on the impact of NK cell-mediated immunity on fungal infections are lacking. Although it was observed that patients suffering from chronic mucocutaneous candidiasis (CMCC) have a decrease of both NK cell number and cytotoxic activity (58–60), the exact impact of NK cells in the pathogenesis of the infection or in the progression of the disease is hard to define, in particular as cell-mediated immunity is also impaired in patients with CMCC. Although it may very well be that the pathologic NK cell findings are a risk factor for CMCC, other possible explanations for the decreased NK cell count and NK cell activity include that the fungus had a negative impact on originally normal NK cells, or that the observation is an epiphenomenon only. Similarly, it was reported that a patient developed a *Trichophyton rubrum* infection during corticosteroid treatment for systemic lupus erythematosus (61). Although immunosuppressive therapy was stopped, the infection remained. Further evaluation demonstrated that both numbers and activity of NK cells were reduced. The authors speculated that the impairment of the NK cells was causing the infection, but again, one could also argue that the infection resulted in a decreased NK cell number and NK cell activity in this individual patient.

NK CELLS DAMAGE VARIOUS FUNGI *IN VITRO*

Multiple studies published over the last three decades demonstrate that both murine and human NK cells exhibit antifungal activity *in vitro* against various fungal pathogens, such as *Aspergillus fumigatus*, *Aspergillus niger*, *Candida albicans, Cryptococcus neoformans*, *Paracoccidioides brasiliensis*, *Rhizopus oryzae*, and other mucormycetes including *Lichthemia ramosa* or *Absidia corymbifera* (62–70) (**Figure 1**). NK cells damage the hyphal form of *A. fumigatus* and *R. oryzae*, but are not able to exhibit fungicidal activity toward conidia (62, 63, 65). In *C. albicans,* human NK cell are cytotoxic against germ tubes and additionally are able to phagocyte *C. albicans* yeasts (8 ± 0.5% of *C. albicans* yeasts were phagocytosed by NK cells within the first 2 h of interaction) (70). The lack of antifungal activity against conidia may be explained by the fact that conidia are often protected by capsules, by pigments such as melanin, or by hydrophobic layers, all of which may prevent recognition by various immune cells (71–74). For example, the rodlet/hydrophobin layer on dormant *A. fumigatus* conidia masks the recognition by the immune system and thus prevents an host immune response, whereas the genetical removal the rodlet/hydrophobin layer in dormant conidia of the *ΔrodA* mutant resulted in the induction of maturation and activation of human

DCs (71). Similarly, the lack of a capsule in the strain CAP67 of the yeast-like fungus *C. neoformans* leads to a higher expression of the cytotoxic molecule perforin by NK cells as compared to the encapsulated strain B3501 (75).

RECOGNITION OF FUNGI BY NK CELLS

Over the last years, there were major advances in the identification and characterization of receptors by which NK cells recognize fungal pathogens (**Figure 1**, **Table 1**). NK cells express unique activating receptors on their surface, which are called natural cytotoxicity receptors (NCR) 1–3 (NKp46, NKp44, and NKp30; CD335–CD337). Studies using blocking antibodies and siRNA to knockdown the NKp30 expression on the surface of the cell line YT demonstrated that NK cells are able to directly recognize *C. albicans* and *C. neoformans* by the NKp30 receptor, which further mediates killing of these fungi (68). However, polymorphonuclear neutrophils and granulocyte myeloid-derived suppressor cells may decrease the NKp30 expression on NK cells, which results in reduced cytotoxicity toward *A. fumigatus* and a

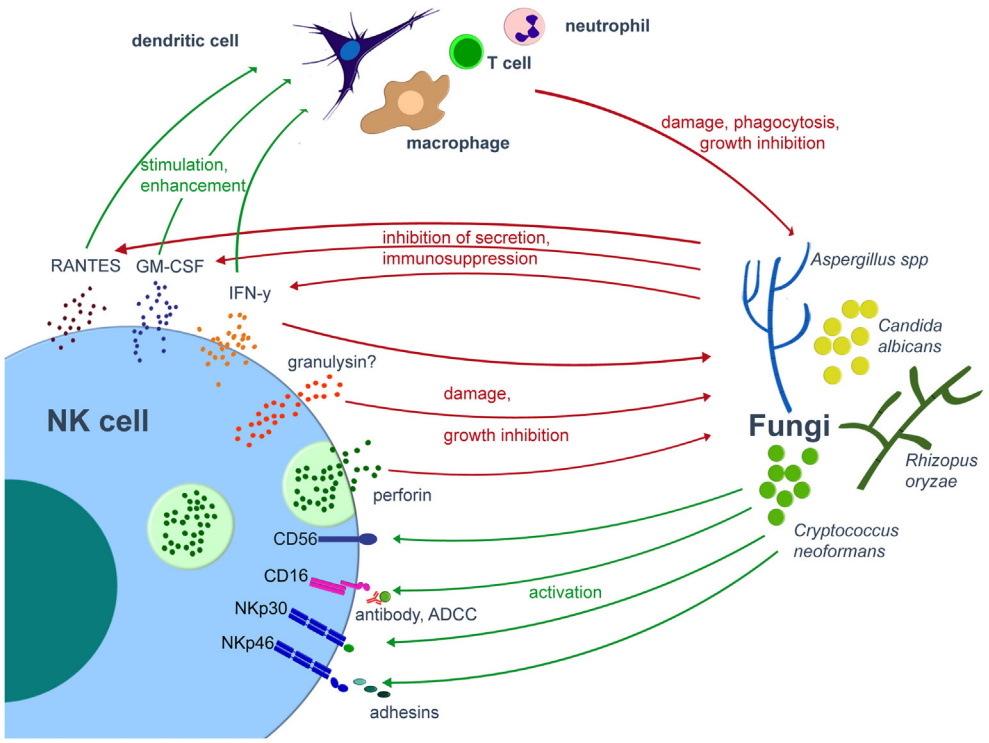

FIGURE 1 | Interplay of NK cells and fungal pathogens. Various fungal pathogens are able to activate NK cells. Once activated, NK cells directly damage fungi by cytotoxic molecules such as perforin or release cytokines, by which they modulate the antifungal host response *via* various immune cells. On the other hand, the fungus may compromise the host immune system. Green arrows indicate activation/stimulation, red arrows inhibition/damage. ADCC, antibody-dependent cell mediated cytotoxicity; IFN, interferon; GM-CSF, granulocyte-macrophage colony-stimulating factor; NK, natural killer.

TABLE 1 | Natural killer (NK) cell receptors in antifungal response.

Receptor	Origin	Ligand	Fungus	Remarks	Reference
NKp30	Human, YT cell line	Undefined pathogen-associated molecular pattern	*Candida albicans*, *Cryprococcus neoformans*	NKp30 required for YT cell cytotoxicity toward fungal pathogens *in vitro* siRNA knockdown of NKp30 results in decreased release of perforin Addition of anti-NKp30 antibody or inhibition of NKp30 via siRNA results in decreased antifungal activity	Li et al. (68)
NKp46 NCR1	Human Mouse	Fungal adhesins Epa1, Epa6, Epa7	*Candida glabrata*	Human NKp46 and mouse ortholog NCR1 bind *C. glabrata in vitro* Clearing of systemic *C. glabrata* infection *in vivo* depends on recognition of fungal adhesins by NCR1	Vitenshtein et al. (77)
CD56	Human	Unknown	*Aspergillus fumigatus*	Blocking of CD56 by inhibitory antibodies reduces fungal-mediated NK cell activation and inhibits amount of secreted cytokines *in vitro*	Ziegler et al. (80)
CD16	Mouse	Cryptococcal polysaccharide	*Cryptococcus neoformans*	Purified IgG fraction of rabbit anticryptococcal antibody augments growth inhibitory activity of murine splenic NK cells *in vitro*	Nabavi and Murphy (81)

decrease in IFN-γ secretion (76). Recently, the NKp46 receptor and its mouse ortolog NCR1 were identified to play an important role in the NK cell-mediated killing of *C. glabrata* (77). It was speculated whether NKp46/NCR1 may be a novel type of pattern recognition receptor, as these receptors not only recognize the *C. glabrata* adhesins Epa1, Epa6, and Epa7 but also bind viral adhesion receptors (77). The importance of the receptor is underlined by the observation that NCR1-deficient mice were unable to clear *C. glabrata* systemic infection (77). Because several fungi including *Aspergillus*, *Cryptococcus*, and *Coccidioides* express adhesins (78), further studies have to evaluate whether and to what extent these fungal adhesins are recognized by which of the NK cell receptors (79).

Recent studies suggested CD56 as pathogen recognition receptor, as it was demonstrated by flow cytometry that the fluorescence positivity of the surface receptor significantly decreased upon fungal contact (80). The authors could visualize the direct interaction of NK cells and *A. fumigatus via* CD56, which was reorganized and accumulated at this interaction site time dependently. Importantly, blocking of CD56 surface receptor reduced fungal-mediated NK cell activation and reduced cytokine secretion. Earlier studies have demonstrated that the low-affinity Fc-receptor CD16 [FcγRIIIa (CD16a) and FcγRIIIb (CD16b)] is also involved in the antifungal activity of NK cells, as NK cells inhibited the growth of *Cryptococci* more effectively in the presence of anti-cryptococcal IgG antibodies than in the presence of normal rabbit serum or medium (81). However, it is important to note that primary and pre-activated NK cells downregulate CD16 after contact with *C. albicans*, which has also been described for the cellular adhesin CD56 and immunoreceptor tyrosine-based activation motif-bearing receptors NKG2D (CD314) and NKp46 (CD335) (70). Taken together, we just begin to understand the complexity how NK cells are being activated by fungal pathogens.

DIRECT DAMAGE OF FUNGAL PATHOGENS BY NK CELLS

Various mechanisms are described by which NK cells directly kill tumor cells, which include the release of soluble cytotoxic molecules such as perforin or granzyme, or the induction of apoptosis by the Fas–FasL or the TNF pathway. Regarding fungal pathogens, several studies reported on the importance of lytic granules released by NK cells. For example, the use of monensin, which inhibits granule secretion, partially abrogated the growth inhibition of *C. neoformans* by human NK cells [reviewed in Ref. (79)]. It further became clear that mainly perforin and granulysin mediate the direct NK cell cytotoxicity toward fungal pathogens (67, 82). When pretreating human NK cells with concanamycin A (ConA), which induces accelerated perforin degradation *via* an increase of pH in the lytic granules, significantly less damage of *A. fumigatus* and *R. oryzae* hyphae can be observed as compared to the addition of untreated NK cells to the fungus (62, 63, 83). Other studies used purified perforin and reported on fungal damage of *A. fumigatus* hyphae (62), the inhibition of filamentation of *C. albicans* (84), and the inhibition of the metabolic activity of *C. albicans* and *R. oryzae* in a dose-dependent manner (63, 70). The fact that ConA did not totally abrogate NK cell-mediated fungal damage suggests that other molecules than perforin also participate in the antifungal activity of human NK cells, as reported for *A. fumigatus*, *C. albicans*, and *R. oryzae*. Interestingly, inhibition of perforin by ConA or by small interfering RNA decreased NK cell anti-cryptococcal activity, whereas inhibition of granulysin did not alter the antifungal effect (67). However, it has been shown that the defective anti-cryptococcal activity of NK cells from HIV-patients can be corrected by *ex vivo* treatment with interleukin (IL)-12 (68), as IL-12 restores the lower perforin expression in NK cells from HIV-infected patients as well as the defective granule polarization in response to *C. neoformans* (85). In tumor cells, perforin perforates the membrane of the target, which leads to an influx of water and a loss of intracellular molecules, resulting in cell lysis (86, 87). Similarly, granulysin disrupts the target cell membrane, which results in higher intracellular calcium and lower intracellular potassium concentrations, both of which ultimately activate caspases and programmed cell death (apoptosis) (88–92). However, it is important to note that the mechanisms of the antifungal effect of perforin and granulysin have not fully been elucidated to date.

There is an ongoing controversy on the direct antifungal effect of IFN-γ. One study reported on a direct IFN-γ-mediated antifungal activity of NK cells against *Aspergillus,* which was independent of degranulation of NK cells and their cytotoxic molecules (65). The authors suggested as explanation that "IFN-γ might cooperate with fungal ribotoxins, (…), transforming them into suicide molecules for fungus" (65). Similarly, it was demonstrated that IFN-γ at a concentration of 32 pg/ml exhibited a small but significant antifungal effect on *A. fumigatus*, *A. flavus*, and *Saccharomyces cerevisiae,* and inhibited the growth by 6, 11, and 17%, respectively (93). As higher concentrations of IFN-γ, e.g., 50 or 100 pg/ml, did not increase antifungal activity, and IFN-γ serum levels of 18 ± 30 pg/ml can be detected in healthy individuals (94), the importance of the direct antifungal effect *in vivo* is questionable. Corroborating the data of another report (70), no significant antifungal effects of IFN-γ were detected in *Candida* and *C. neoformans* (93). However, it is important to note that a combination of amphotericin B at a concentration of 1 μg/ml and IFN-γ at 32 pg/ml increased the efficacy of amphotericin B against *A. fumigatus*, which might be important for immunotherapeutic strategies.

Inducing apoptosis *via* the Fas–FasL or the TNF pathway is another mechanism by which NK cells are able to kill a target and has been described for various tumor cells as well as for pathogen infected cells (95, 96). Whereas data on apoptosis are missing for molds, apoptosis in yeast cells has been reported, but molecular mechanisms at the core of apoptotic execution is still unknown (97, 98). One recent study reported that blocking the death receptor ligands FasL and tumor necrosis factor-related apoptosis inducing ligand on the surface of human NK cells by antibodies did not have any impact on the antifungal activity (70). In addition, phagocytosis may be another mechanism of direct fungal damage by NK cells, which has been reported for *C. albicans* yeast (70). Notably, the IgG fraction of rabbit anti-cryptococcal serum enhanced the anti-cryptococcal activity of NK cells *via* their CD16 receptor (81).

MODULATION OF THE ANTIFUNGAL HOST RESPONSE BY NK CELLS

Upon stimulation, NK cells produce various cytokines, all of which modulate the host immunity against fungi. IFN-γ is one of the key molecules in the antifungal host response and is constitutively produced by NK cells (99). IFN-γ exhibits multiple effects on various immune cells. For example, IFN-γ is able to stimulate migration, adherence, phagocytosis, as well as oxidative killing by neutrophils and macrophages. Conditioned medium from co-incubation of NK cells and *C. albicans* enhanced polymorphonuclear neutrophil activation (70). In addition, data of a murine model demonstrated the pivotal role of IFN-γ-producing NK cells in inducing the phagocytic activity of splenic macrophages, thus mediating protection against systemic infection with *C. albicans* (100). As NK cells are the main source of IFN-γ in neutropenic mice suffering from aspergillosis, depletion of NK cells resulted in diminished IFN-γ levels in the lungs followed by an increased fungal load (101). Interestingly, the fungal load could be reduced by the transfer of wild-type IFN-γ producing NK cells, whereas this was not seen when transferring NK cells from IFN-γ-deficient mice. Because IFN-γ also enhances maturation of DCs and plays a pivotal role in the protective T_H1 cell response (11, 12, 102), the molecule was used as immunotherapy in invasive fungal disease. Whereas the administration of IFN-γ to mice with invasive aspergillosis was leading to reduced fungal burden and increased survival (103), available clinical data are inconclusive and do not allow a final conclusion on the usefulness of this strategy (11).

In addition to IFN-γ, NK cells produce soluble molecules such as GM-CSF and RANTES, both of which augment the host immune response *via* the stimulation of phagocytes and T cells, respectively (104–106).

INTERPLAY OF NK CELLS AND FUNGI

Fungi have developed strategies to counteract the complex and sophisticated antifungal immune response of the host. For example, *A. fumigatus* galactosaminogalactan induces apoptosis of polymorphonuclear neutrophils (107). Shedding of this molecule results in NK cell activation, which, in turn, leads to a Fas-dependent apoptosis-promoting signal in polymorphonuclear neutrophils (108). Galactosaminogalactan also induces IL-1 receptor antagonist, which leads to the suppression of IL-17 and IL-22 in peripheral blood mononuclear cells (109), and similar effects were observed with *Aspergillus* chitin (110). In addition, mycotoxins such as gliotoxin or aflatoxin (111) inhibit the phagocytic activity of macrophages, induce the apoptosis of monocytes, decrease the activation of nicotinamide adenine dinucleotide phosphate oxidase in neutrophils, and impair functional T cell responses (112–116), all of which hampers the host immune response toward the pathogen.

When NK cells are co-incubated with *A. fumigatus* or *R. oryzae*, lower levels of IFN-γ, GM-CSF, and RANTES are detected in the supernatant as compared to NK cells incubated alone (62, 63). Surprisingly, *A. fumigatus* increases the gene expression of IFN-γ in NK cells, but inhibits its release, thus leading to intracellular accumulation and decreased extracellular availability (117). Similarly, various mucormycetes affect the IFN-γ release by human NK cells (64). In contrast, earlier studies report that *C. neoformans* downregulates of the production of GM-CSF and TNF-α in unstimulated human NK cells, as assessed by gene expression and supernatant protein levels (118).

When looking at the fungal pathogen, it has been demonstrated that co-incubation of NK cells with *A. fumigatus* upregulated the expression of several stress-related fungal genes (117). This has been demonstrated for the heat shock protein *hsp90* or the ferric reductase *freB* (117). In *A. fumigatus*, Hsp90 plays an important role in the compensatory repair mechanisms of the cell wall in response to stress induced by antifungals, and Hsp90 has been described as a trigger for resistance to high concentrations of caspofungin, known as the paradoxical effect (119). FreB has recently been identified as an important enzyme in filamentous fungi which helps the fungus to adapt to iron starvation (120). Similarly, perforin-induced reduction of iron availability leads to the upregulation of the gene expression of *CSA2* in *C. albicans*, which is involved in the uptake of iron of human hemoglobin (84). Further characterization of specific interactions of the host immune system and fungal pathogens might identify novel targets for the antifungal armamentarium, e.g., the disruption of Hsp90 circuitry by Hsp90 inhibitors or anti-calcineurin drugs.

NK CELLS AND INVASIVE FUNGAL INFECTION: ANIMAL STUDIES

The few data of animal models clearly support the *in vitro* findings that NK cells play an important role in the antifungal host immune response. An early study in mice infected with *A. niger* demonstrated the association of the proliferation of NK cells and the inhibition of fungal growth (69). In addition, depletion of NK cells in mice inoculated with *C. neoformans* resulted in a considerably higher fungal load in the lungs as compared to untreated animals (121). In addition, antibody-mediated depletion of NK cells also decreased the phagocytosis of *C. albicans* by splenic macrophages as compared to controls (5.2 versus 21.5%) (100), and depletion of NK cells in mice *via* anti-asialo GM1 antibody resulted in enhanced susceptibility to *Histoplasma capsulatum* (122). Interestingly, in neutropenic mice, antibody-mediated depletion of NK cells also resulted in impaired clearance of the pathogen from the lungs and in a greater than twofold increase in mortality as compared to neutropenic mice with NK cells (123).

Importantly, the adoptive transfer of NK cells in mice lacking these cells can restore antifungal resistance. For example, in cyclophosphamide-pretreated mice suffering from cryptococcosis, the adoptive transfer of NK cell-enriched cell populations resulted in an enhanced clearance of the fungus as compared to controls receiving NK cell-depleted grafts (124, 125). As noted above, NK cell-derived IFN-γ plays an important role in the antifungal host response. NK cell depletion in neutropenic mice with invasive aspergillosis was leading to reduced lung IFN-γ levels and increased pulmonary fungal load, which was independent of T and B cell lymphocytes (101). However, the transfer of activated NK cells from wild-type, but not from IFN-γ-deficient mice

resulted in better clearance of *A. fumigatus* from the lungs of both IFN-γ-deficient and wild-type recipients. Based on these findings, future studies have to assess in which clinical circumstances the adoptive transfer of NK cells to an immunocomoromised host suffering from an invasive fungal infection will be of benefit.

CONCLUSION AND PERSPECTIVES

There is increasing evidence that NK cells play an important role in the antifungal host response. *In vitro* data show that multiple fungal pathogens are able to activate NK cells, and further research will hopefully shed more light in the characterization of the complex interplay of NK cell receptors and fungal ligands. Once activated, NK cells directly damage the fungus by soluble cytotoxic molecules such as perforin, whereas the role of other mechanisms such as the induction of apoptosis *via* different pathways is still relatively unclear. In addition to the direct fungal damage, NK cells release multiple cytokines and IFNs by which they modulate the immune system, e.g., *via* neutrophils and T cells. As cure from an infectious complication not only depends on the successful activation of the immune system but also from a timely downregulation and resolution of the inflammatory process, further research needs to characterize the release of pro- and anti-inflammatory molecules. How and to what extent the fungus itself alters its gene expression profile in the presence of NK cells remains another research gap. In this regard, we have to learn how the fungus compromises the host immune system, which might offer new targets in our combat against the pathogen. In addition, animal studies will help to clarify the benefit and potential risks of using NK cells as adoptive preventive or therapeutic strategy, which may be a significant step toward decreasing morbidity and mortality of invasive fungal infection in the clinical setting.

AUTHOR CONTRIBUTIONS

All authors were involved in the concept of the manuscript, search and analysis of the references, and writing the manuscript; read and approved the final version of the manuscript.

REFERENCES

1. Zaoutis TE, Heydon K, Chu JH, Walsh TJ, Steinbach WJ. Epidemiology, outcomes, and costs of invasive aspergillosis in immunocompromised children in the United States, 2000. *Pediatrics* (2006) 117:e711–6. doi:10.1542/peds.2005-1161
2. Bitar D, Lortholary O, Le Strat Y, Nicolau J, Coignard B, Tattevin P, et al. Population-based analysis of invasive fungal infections, France, 2001–2010. *Emerg Infect Dis* (2014) 20:1149–55. doi:10.3201/eid2007.140087
3. McNeil MM, Nash SL, Hajjeh RA, Phelan MA, Conn LA, Plikaytis BD, et al. Trends in mortality due to invasive mycotic diseases in the United States, 1980-1997. *Clin Infect Dis* (2001) 33:641–7. doi:10.1086/322606
4. Kontoyiannis DP, Marr KA, Park BJ, Alexander BD, Anaissie EJ, Walsh TJ, et al. Prospective surveillance for invasive fungal infections in hematopoietic stem cell transplant recipients, 2001-2006: overview of the transplant-associated infection surveillance network (TRANSNET) database. *Clin Infect Dis* (2010) 50:1091–100. doi:10.1086/651263
5. Horn DL, Fishman JA, Steinbach WJ, Anaissie EJ, Marr KA, Olyaei AJ, et al. Presentation of the PATH Alliance® registry for prospective data collection and analysis of the epidemiology, therapy, and outcomes of invasive fungal infections. *Diagn Microbiol Infect Dis* (2007) 59:407–14. doi:10.1016/j.diagmicrobio.2007.06.008
6. Azie N, Neofytos D, Pfaller M, Meier-Kriesche HU, Quan SP, Horn D. The PATH (prospective antifungal therapy) Alliance® registry and invasive fungal infections: update 2012. *Diagn Microbiol Infect Dis* (2012) 73:293–300. doi:10.1016/j.diagmicrobio.2012.06.012
7. Lehrnbecher T, Koehl U, Wittekindt B, Bochennek K, Tramsen L, Klingebiel T, et al. Changes in host defence induced by malignancies and antineoplastic treatment: implication for immunotherapeutic strategies. *Lancet Oncol* (2008) 9:269–78. doi:10.1016/S1470-2045(08)70071-8
8. Lehrnbecher T, Foster C, Vázquez N, Mackall CL, Chanock SJ. Therapy-induced alterations in host defense in children receiving therapy for cancer. *J Pediatr Hematol Oncol* (1997) 19:399–417. doi:10.1097/00043426-199709000-00001
9. Bodey GP. Infectious complications of acute leukemia. *Med Times* (1966) 94:1076–85.
10. Stuehler C, Kuenzli E, Jaeger VK, Baettig V, Ferracin F, Rajacic Z, et al. Immune reconstitution after allogeneic hematopoietic stem cell transplantation and association with occurrence and outcome of invasive aspergillosis. *J Infect Dis* (2015) 212:959–67. doi:10.1093/infdis/jiv143
11. Lehrnbecher T, Kalkum M, Champer J, Tramsen L, Schmidt S, Klingebiel T. Immunotherapy in invasive fungal infection – focus on invasive aspergillosis. *Curr Pharm Des* (2013) 19:3689–712. doi:10.2174/1381612811319200010
12. Romani L. Immunity to fungal infections. *Nat Rev Immunol* (2004) 4:1–23. doi:10.1038/nri1255
13. Romani L. Immunity to fungal infections. *Nat Rev Immunol* (2011) 11:275–88. doi:10.1038/nri2939
14. Fisher BT, Robinson PD, Lehrnbecher T, Steinbach WJ, Zaoutis TE, Phillips B, et al. Risk factors for invasive fungal disease in pediatric cancer and hematopoietic stem cell transplantation: a systematic review. *J Pediatric Infect Dis Soc* (2017). doi:10.1093/jpids/pix030
15. Cunha C, Kurzai O, Löffler J, Aversa F, Romani L, Carvalho A. Neutrophil responses to aspergillosis: new roles for old players. *Mycopathologia* (2014) 178:387–93. doi:10.1007/s11046-014-9796-7
16. Borghi M, Renga G, Puccetti M, Oikonomou V, Palmieri M, Galosi C, et al. Antifungal Th immunity: growing up in family. *Front Immunol* (2014) 5:506. doi:10.3389/fimmu.2014.00506
17. Limon JJ, Skalski JH, Underhill DM. Commensal fungi in health and disease. *Cell Host Microbe* (2017) 22:156–65. doi:10.1016/j.chom.2017.07.002
18. Cooper MA, Fehniger TA, Caligiuri MA. The biology of human natural killer-cell subsets. *Trends Immunol* (2001) 22:633–40. doi:10.1016/S1471-4906(01)02060-9
19. Sun JC, Lopez-Verges S, Kim CC, DeRisi JL, Lanier LL. NK cells and immune "memory". *J Immunol* (2011) 186:1891–7. doi:10.4049/jimmunol.1003035
20. Narni-Mancinelli E, Vivier E, Kerdiles YM. The "T-cell-ness" of NK cells: unexpected similarities between NK cells and T cells. *Int Immunol* (2011) 23:427–31. doi:10.1093/intimm/dxr035
21. Kleinnijenhuis J, Quintin J, Preijers F, Joosten LAB, Jacobs C, Xavier RJ, et al. BCG-induced trained immunity in NK cells: role for non-specific protection to infection. *Clin Immunol* (2014) 155:213–9. doi:10.1016/j.clim.2014.10.005
22. Kiessling R, Klein E, Wigzell H. "Natural" killer cells in the mouse. I. Cytotoxic cells with specificity for mouse Moloney leukemia cells. Specificity and distribution according to genotype. *Eur J Immunol* (1975) 5:112–7. doi:10.1002/eji.1830050208
23. Lam VC, Lanier LL. NK cells in host responses to viral infections. *Curr Opin Immunol* (2017) 44:43–51. doi:10.1016/j.coi.2016.11.003
24. Arase H, Mocarski ES, Campbell AE, Hill AB, Lanier LL. Direct recognition of cytomegalovirus by activating and inhibitory NK cell receptors. *Science* (2002) 296:1323–6. doi:10.1126/science.1070884
25. Adams EJ, Juo ZS, Venook RT, Boulanger MJ, Arase H, Lanier LL, et al. Structural elucidation of the m157 mouse cytomegalovirus ligand for Ly49 natural killer cell receptors. *Proc Natl Acad Sci U S A* (2007) 104:10128–33. doi:10.1073/pnas.0703735104
26. Kielczewska A, Kim H-S, Lanier LL, Dimasi N, Vidal SM. Critical residues at the Ly49 natural killer receptor's homodimer interface determine functional

recognition of m157, a mouse cytomegalovirus MHC class I-like protein. *J Immunol* (2007) 178:369–77. doi:10.4049/jimmunol.178.1.369
27. Romee R, Schneider SE, Leong JW, Chase JM, Keppel CR, Sullivan RP, et al. Cytokine activation induces human memory-like NK cells. *Blood* (2012) 120:4751–60. doi:10.1182/blood-2012-04-419283
28. Malmberg K-J, Carlsten M, Björklund A, Sohlberg E, Bryceson YT, Ljunggren H-G. Natural killer cell-mediated immunosurveillance of human cancer. *Semin Immunol* (2017) 31:20–9. doi:10.1016/j.smim.2017.08.002
29. Herberman RR, Ortaldo JR, Bonnard GD. Augmentation by interferon of human natural and antibody-dependent cell-mediated cytotoxicity. *Nature* (1979) 277:221–3. doi:10.1038/277221a0
30. Ortaldo JR, Bonnard GD, Kind PD, Herberman RB. Cytotoxicity by cultured human lymphocytes: characteristics of effector cells and specificity of cytotoxicity. *J Immunol* (1979) 122:1489–94.
31. Biron CA, Welsh RM. Activation and role of natural killer cells in virus infections. *Med Microbiol Immunol* (1982) 170:155–72. doi:10.1007/BF02298196
32. Liu LL, Béziat V, Oei VYS, Pfefferle A, Schaffer M, Lehmann S, et al. Ex vivo expanded adaptive NK cells effectively kill primary acute lymphoblastic leukemia cells. *Cancer Immunol Res* (2017) 5:654–65. doi:10.1158/2326-6066.CIR-16-0296
33. Schlegel P, Ditthard K, Lang P, Mezger M, Michaelis S, Handgretinger R, et al. NKG2D signaling leads to NK cell mediated lysis of childhood AML. *J Immunol Res* (2015) 2015:473175. doi:10.1155/2015/473175
34. Castriconi R, Dondero A, Corrias MV, Lanino E, Pende D, Moretta L, et al. Natural killer cell-mediated killing of freshly isolated neuroblastoma cells: critical role of DNAX accessory molecule-1-poliovirus receptor interaction. *Cancer Res* (2004) 64:9180–4. doi:10.1158/0008-5472.CAN-04-2682
35. Kloess S, Huenecke S, Piechulek D, Esser R, Koch J, Brehm C, et al. IL-2-activated haploidentical NK cells restore NKG2D-mediated NK-cell cytotoxicity in neuroblastoma patients by scavenging of plasma MICA. *Eur J Immunol* (2010) 40:3255–67. doi:10.1002/eji.201040568
36. Vivier E, Tomasello E, Baratin M, Walzer T, Ugolini S. Functions of natural killer cells. *Nat Immunol* (2008) 9:503–10. doi:10.1038/ni1582
37. Béziat V, Dalgard O, Asselah T, Halfon P, Bedossa P, Boudifa A, et al. CMV drives clonal expansion of NKG2C+ NK cells expressing self-specific KIRs in chronic hepatitis patients. *Eur J Immunol* (2012) 42:447–57. doi:10.1002/eji.201141826
38. Saghafian-Hedengren S, Sohlberg E, Theorell J, Carvalho-Queiroz C, Nagy N, Persson J-O, et al. Epstein-Barr virus coinfection in children boosts cytomegalovirus-induced differentiation of natural killer cells. *J Virol* (2013) 87:13446–55. doi:10.1128/JVI.02382-13
39. Shabani Z, Bagheri M, Zare-Bidaki M, Hassanshahi G, Arababadi MK, Mohammadi Nejad M, et al. NK cells in hepatitis B virus infection: a potent target for immunotherapy. *Arch Virol* (2014) 159:1555–65. doi:10.1007/s00705-013-1965-3
40. Werner JM, Heller T, Gordon AM, Sheets A, Sherker AH, Kessler E, et al. Innate immune responses in hepatitis C virus-exposed healthcare workers who do not develop acute infection. *Hepatology* (2013) 58:1621–31. doi:10.1002/hep.26353
41. Garcia-Peñarrubia P, Koster FT, Kelley RO, McDowell TD, Bankhurst AD. Antibacterial activity of human natural killer cells. *J Exp Med* (1989) 169:99–113. doi:10.1084/jem.169.1.99
42. Wherry JC, Schreiber RD, Unanue ER. Regulation of gamma interferon production by natural killer cells in scid mice: roles of tumor necrosis factor and bacterial stimuli. *Infect Immun* (1991) 59:1709–15.
43. Anfossi N, André P, Guia S, Falk CS, Roetynck S, Stewart CA, et al. Human NK cell education by inhibitory receptors for MHC class I. *Immunity* (2006) 25:331–42. doi:10.1016/j.immuni.2006.06.013
44. Parsons MS, Zipperlen K, Gallant M, Grant M. Killer cell immunoglobulin-like receptor 3DL1 licenses CD16-mediated effector functions of natural killer cells. *J Leukoc Biol* (2010) 88:905–12. doi:10.1189/jlb.1009687
45. Horowitz A, Djaoud Z, Nemat-Gorgani N, Blokhuis J, Hilton HG, Béziat V, et al. Class I HLA haplotypes form two schools that educate NK cells in different ways. *Sci Immunol* (2016) 1:eaag1672. doi:10.1126/sciimmunol.aag1672
46. Campbell KS, Hasegawa J. NK cell biology: an update and future directions. *J Allergy Clin Immunol* (2013) 132:536–44. doi:10.1016/j.jaci.2013.07.006
47. Yawata M, Yawata N, Draghi M, Little A-M, Partheniou F, Parham P. Roles for HLA and KIR polymorphisms in natural killer cell repertoire selection and modulation of effector function. *J Exp Med* (2006) 203:633–45. doi:10.1084/jem.20051884
48. Yawata M, Yawata N, Draghi M, Partheniou F, Little A-M, Parham P. MHC class I-specific inhibitory receptors and their ligands structure diverse human NK-cell repertoires toward a balance of missing self-response. *Blood* (2008) 112:2369–80. doi:10.1182/blood-2008-03-143727
49. Horowitz A, Strauss-Albee DM, Leipold M, Kubo J, Nemat-Gorgani N, Dogan OC, et al. Genetic and environmental determinants of human NK cell diversity revealed by mass cytometry. *Sci Transl Med* (2013) 5:208ra145. doi:10.1126/scitranslmed.3006702
50. Kim S, Poursine-Laurent J, Truscott SM, Lybarger L, Song Y-J, Yang L, et al. Licensing of natural killer cells by host major histocompatibility complex class I molecules. *Nature* (2005) 436:709–13. doi:10.1038/nature03847
51. Fernandez NC, Treiner E, Vance RE, Jamieson AM, Lemieux S, Raulet DH. A subset of natural killer cells achieves self-tolerance without expressing inhibitory receptors specific for self-MHC molecules. *Blood* (2005) 105:4416–23. doi:10.1182/blood-2004-08-3156
52. Brodin P, Lakshmikanth T, Johansson S, Kärre K, Höglund P. The strength of inhibitory input during education quantitatively tunes the functional responsiveness of individual natural killer cells. *Blood* (2009) 113:2434–41. doi:10.1182/blood-2008-05-156836
53. Joncker NT, Fernandez NC, Treiner E, Vivier E, Raulet DH. NK cell responsiveness is tuned commensurate with the number of inhibitory receptors for self-MHC class I: the rheostat model. *J Immunol* (2009) 182:4572–80. doi:10.4049/jimmunol.0803900
54. Orr MT, Murphy WJ, Lanier LL. "Unlicensed" natural killer cells dominate the response to cytomegalovirus infection. *Nat Immunol* (2010) 11:321–7. doi:10.1038/ni.1849
55. Spits H, Artis D, Colonna M, Diefenbach A, Di Santo JP, Eberl G, et al. Innate lymphoid cells – a proposal for uniform nomenclature. *Nat Rev Immunol* (2013) 13:145–9. doi:10.1038/nri3365
56. Orange JS, Ballas ZK. Natural killer cells in human health and disease. *Clin Immunol* (2006) 118:1–10. doi:10.1016/j.clim.2005.10.011
57. Fernández-Ruiz M, López-Medrano F, San Juan R, Allende LM, Paz-Artal E, Aguado JM. Low natural killer cell counts and onset of invasive fungal disease after solid organ transplantation. *J Infect Dis* (2016) 213:873–4. doi:10.1093/infdis/jiv552
58. Palma-Carlos AG, Palma-Carlos ML. Chronic mucocutaneous candidiasis revisited. *Allerg Immunol (Paris)* (2001) 33:229–32.
59. Chiu S-J, Tsao C-H, Chen L-C, Kao C-C, Lue K-H, Huang J-L. Chronic mucocutaneous candidiasis in a 6-year-old boy. *J Microbiol Immunol Infect* (2004) 37:196–9.
60. De Moraes-Vasconcelos D, Orii NM, Romano CC, Iqueoka RY, Duarte AJS. Characterization of the cellular immune function of patients with chronic mucocutaneous candidiasis. *Clin Exp Immunol* (2001) 123:247–53. doi:10.1046/j.1365-2249.2001.01430.x
61. Akiba H, Motoki Y, Satoh M, Iwatsuki K, Kaneko F. Recalcitrant trichophytic granuloma associated with NK-cell deficiency in a SLE patient treated with corticosteroid. *Eur J Dermatol* (2001) 11:58–62.
62. Schmidt S, Tramsen L, Hanisch M, Latgé J-P, Huenecke S, Koehl U, et al. Human natural killer cells exhibit direct activity against *Aspergillus fumigatus* hyphae, but not against resting conidia. *J Infect Dis* (2011) 203:430–5. doi:10.1093/infdis/jiq062
63. Schmidt S, Tramsen L, Perkhofer S, Lass-Florl C, Hanisch M, Roger F, et al. *Rhizopus oryzae* hyphae are damaged by human natural killer (NK) cells, but suppress NK cell mediated immunity. *Immunobiology* (2013) 218:939–44. doi:10.1016/j.imbio.2012.10.013
64. Schmidt S, Schneider A, Demir A, Lass-Flörl C, Lehrnbecher T. Natural killer cell-mediated damage of clinical isolates of mucormycetes. *Mycoses* (2016) 59:34–8. doi:10.1111/myc.12431
65. Bouzani M, Ok M, McCormick A, Ebel F, Kurzai O, Morton CO, et al. Human NK cells display important antifungal activity against *Aspergillus fumigatus*, which is directly mediated by IFN-γ release. *J Immunol* (2011) 187:1369–76. doi:10.4049/jimmunol.1003593
66. Hidore MR, Nabavi N, Reynolds CW, Henkart PA, Murphy JW. Cytoplasmic components of natural killer cells limit the growth of *Cryptococcus neoformans*. *J Leukoc Biol* (1990) 48:15–26.

67. Ma LL, Wang CLC, Neely GG, Epelman S, Krensky AM, Mody CH. NK cells use perforin rather than granulysin for anticryptococcal activity. *J Immunol* (2004) 173:3357–65. doi:10.4049/jimmunol.173.5.3357
68. Li SS, Kyei SK, Timm-McCann M, Ogbomo H, Jones GJ, Shi M, et al. The NK receptor NKp30 mediates direct fungal recognition and killing and is diminished in NK cells from HIV-infected patients. *Cell Host Microbe* (2013) 14:387–97. doi:10.1016/j.chom.2013.09.007
69. Benedetto N, Sabatini P, Sellitto C, Romano Carratelli C. Interleukin-2 and increased natural killer activity in mice experimentally infected with *Aspergillus niger*. *Microbiologica* (1988) 11:339–45.
70. Voigt J, Hünniger K, Bouzani M, Jacobsen ID, Barz D, Hube B, et al. Human natural killer cells acting as phagocytes against *Candida albicans* and mounting an inflammatory response that modulates neutrophil antifungal activity. *J Infect Dis* (2014) 209:616–26. doi:10.1093/infdis/jit574
71. Aimanianda V, Bayry J, Bozza S, Kniemeyer O, Perruccio K, Elluru SR, et al. Surface hydrophobin prevents immune recognition of airborne fungal spores. *Nature* (2009) 460:1117–21. doi:10.1038/nature08264
72. Chai LYA, Netea MG, Sugui J, Vonk AG, van de Sande WWJ, Warris A, et al. *Aspergillus fumigatus* conidial melanin modulates host cytokine response. *Immunobiology* (2010) 215:915–20. doi:10.1016/j.imbio.2009.10.002
73. Kozel TR, Gotschlich EC. The capsule of *Cryptococcus neoformans* passively inhibits phagocytosis of the yeast by macrophages. *J Immunol* (1982) 129:1675–80.
74. Rappleye CA, Goldman WE. Fungal stealth technology. *Trends Immunol* (2008) 29:18–24. doi:10.1016/j.it.2007.10.001
75. Marr KJ, Jones GJ, Zheng C, Huston SM, Timm-McCann M, Islam A, et al. *Cryptococcus neoformans* directly stimulates perforin production and rearms NK cells for enhanced anticryptococcal microbicidal activity. *Infect Immun* (2009) 77:2436–46. doi:10.1128/IAI.01232-08
76. Mueller-Leisse J, Brueggemann S, Bouzani M, Schmitt A-L, Einsele H, Loeffler J. Polymorphonuclear neutrophils and granulocytic myeloid-derived suppressor cells inhibit natural killer cell activity toward *Aspergillus fumigatus*. *Med Mycol* (2015) 53:622–9. doi:10.1093/mmy/myv030
77. Vitenshtein A, Charpak-Amikam Y, Yamin R, Bauman Y, Isaacson B, Stein N, et al. NK cell recognition of *Candida glabrata* through binding of NKp46 and NCR1 to fungal ligands Epa1, Epa6, and Epa7. *Cell Host Microbe* (2016) 20:527–34. doi:10.1016/j.chom.2016.09.008
78. de Groot PWJ, Bader O, de Boer AD, Weig M, Chauhan N. Adhesins in human fungal pathogens: glue with plenty of stick. *Eukaryot Cell* (2013) 12:470–81. doi:10.1128/EC.00364-12
79. Ogbomo H, Mody CH. Granule-dependent natural killer cell cytotoxicity to fungal pathogens. *Front Immunol* (2017) 7:692. doi:10.3389/fimmu.2016.00692
80. Ziegler S, Weiss E, Schmitt A-L, Schlegel J, Burgert A, Terpitz U, et al. CD56 is a pathogen recognition receptor on human natural killer cells. *Sci Rep* (2017) 7:6138. doi:10.1038/s41598-017-06238-4
81. Nabavi N, Murphy JW. Antibody-dependent natural killer cell-mediated growth inhibition of *Cryptococcus neoformans*. *Infect Immun* (1986) 51:556–62.
82. Obata-Onai A, Hashimoto S, Onai N, Kurachi M, Nagai S, Shizuno K, et al. Comprehensive gene expression analysis of human NK cells and CD8(+) T lymphocytes. *Int Immunol* (2002) 14:1085–98. doi:10.1093/intimm/dxf086
83. Kataoka T, Shinohara N, Takayama H, Takaku K, Kondo S, Yonehara S, et al. Concanamycin A, a powerful tool for characterization and estimation of contribution of perforin- and Fas-based lytic pathways in cell-mediated cytotoxicity. *J Immunol* (1996) 156:3678–86.
84. Hellwig D, Voigt J, Bouzani M, Löffler J, Albrecht-Eckardt D, Weber M, et al. *Candida albicans* induces metabolic reprogramming in human NK cells and responds to perforin with a zinc depletion response. *Front Microbiol* (2016) 7:750. doi:10.3389/fmicb.2016.00750
85. Kyei SK, Ogbomo H, Li S, Timm-mccann M, Xiang RF, Huston SM. Mechanisms by which interleukin-12 corrects defective NK cell anticryptococcal activity in HIV-infected patients. *MBio* (2016) 7:e00878–16. doi:10.1128/mBio.00878-16
86. Duke RC, Persechini PM, Chang S, Liu C-C, Cohen JJ, Young JD. Purified perforin induces target cell lysis but not DNA fragmentation. *J Exp Med* (1989) 170:1451–6. doi:10.1084/jem.170.4.1451
87. Law RHP, Lukoyanova N, Voskoboinik I, Caradoc-Davies TT, Baran K, Dunstone MA, et al. The structural basis for membrane binding and pore formation by lymphocyte perforin. *Nature* (2010) 468:447–51. doi:10.1038/nature09518
88. Ernst WA, Thoma-Uszynski S, Teitelbaum R, Ko C, Hanson DA, Clayberger C, et al. Granulysin, a T cell product, kills bacteria by altering membrane permeability. *J Immunol* (2000) 165:7102–8. doi:10.4049/jimmunol.165.12.7102
89. Gamen S, Hanson DA, Kaspar A, Naval J, Krensky AM, Anel A. Granulysin-induced apoptosis. I. Involvement of at least two distinct pathways. *J Immunol* (1998) 161:1758–64.
90. Kaspar AA, Okada S, Kumar J, Poulain FR, Drouvalakis KA, Kelekar A, et al. A distinct pathway of cell-mediated apoptosis initiated by granulysin. *J Immunol* (2001) 167:350–6. doi:10.4049/jimmunol.167.1.350
91. Krensky AM, Clayberger C. Biology and clinical relevance of granulysin. *Tissue Antigens* (2009) 73:193–8. doi:10.1111/j.1399-0039.2008.01218.x
92. Okada S, Li Q, Whitin JC, Clayberger C, Krensky AM. Intracellular mediators of granulysin-induced cell death. *J Immunol* (2003) 171:2556–62. doi:10.4049/jimmunol.171.5.2556
93. El-Khoury M, Ligot R, Mahoney S, Stack CM, Perrone GG, Morton CO. The in vitro effects of interferon-gamma, alone or in combination with amphotericin B, tested against the pathogenic fungi *Candida albicans* and *Aspergillus fumigatus*. *BMC Res Notes* (2017) 10:364. doi:10.1186/s13104-017-2696-4
94. Katti MK. Assessment of serum IL-1, IL-2 and IFN-γ levels in untreated pulmonary tuberculosis patients: role in pathogenesis. *Arch Med Res* (2011) 42:199–201. doi:10.1016/j.arcmed.2011.04.012
95. Screpanti V, Wallin RPA, Grandien A, Ljunggren HG. Impact of FASL-induced apoptosis in the elimination of tumor cells by NK cells. *Mol Immunol* (2005) 42:495–9. doi:10.1016/j.molimm.2004.07.033
96. Guerra C, Johal K, Morris D, Moreno S, Alvarado O, Gray D, et al. Control of *Mycobacterium tuberculosis* growth by activated natural killer cells. *Clin Exp Immunol* (2012) 168:142–52. doi:10.1111/j.1365-2249.2011.04552.x
97. Madeo F, Herker E, Wissing S, Jungwirth H, Eisenberg T, Fröhlich KU. Apoptosis in yeast. *Curr Opin Microbiol* (2004) 7:655–60. doi:10.1016/j.mib.2004.10.012
98. Fröhlich KU, Fussi H, Ruckenstuhl C. Yeast apoptosis – from genes to pathways. *Semin Cancer Biol* (2007) 17:112–21. doi:10.1016/j.semcancer.2006.11.006
99. Mah AY, Cooper MA. Metabolic regulation of natural killer cell IFN-γ production. *Crit Rev Immunol* (2016) 36:131–47. doi:10.1615/CritRevImmunol.2016017387
100. Algarra I, Ortega E, Serrano MJ, Alvarez de Cienfuegos G, Gaforio JJ. Suppression of splenic macrophage *Candida albicans* phagocytosis following in vivo depletion of natural killer cells in immunocompetent BALB/c mice and T-cell-deficient nude mice. *FEMS Immunol Med Microbiol* (2002) 33:159–63. doi:10.1111/j.1574-695X.2002.tb00586.x
101. Park SJ, Hughes MA, Burdick M, Strieter RM, Mehrad B. Early NK cell-derived IFN-γ is essential to host defense in neutropenic invasive aspergillosis. *J Immunol* (2009) 182:4306–12. doi:10.4049/jimmunol.0803462
102. Boehm U, Klamp T, Groot M, Howard JC. Cellular responses to interferon-gamma. *Annu Rev Immunol* (1997) 15:749–95. doi:10.1146/annurev.immunol.15.1.749
103. Nagai H, Guo J, Choi H, Kurup V. Interferon-gamma and tumor necrosis factor-alpha protect mice from invasive aspergillosis. *J Infect Dis* (1995) 172:1554–60. doi:10.1093/infdis/172.6.1554
104. Homey B, Müller A, Zlotnik A. Chemokines: agents for the immunotherapy of cancer? *Nat Rev Immunol* (2002) 2:175–84. doi:10.1038/nri748
105. Richardson MD, Brownlie CE, Shankland GS. Enhanced phagocytosis and intracellular killing of *Candida albicans* by GM-CSF-activated human neutrophils. *J Med Vet Mycol* (1992) 30:433–41. doi:10.1080/02681219280000591
106. Roilides E, Holmes A, Blake C, Venzon D, Pizzo PA, Walsh TJ. Antifungal activity of elutriated human monocytes against *Aspergillus fumigatus* hyphae: enhancement by granulocyte-macrophage colony-stimulating factor and interferon-gamma. *J Infect Dis* (1994) 170:894–9. doi:10.1093/infdis/170.4.894
107. Fontaine T, Delangle A, Simenel C, Coddeville B, van Vliet SJ, van Kooyk Y, et al. Galactosaminogalactan, a new immunosuppressive polysaccharide of *Aspergillus fumigatus*. *PLoS Pathog* (2011) 7:e1002372. doi:10.1371/journal.ppat.1002372

108. Robinet P, Baychelier F, Fontaine T, Picard C, Debré P, Vieillard V, et al. A polysaccharide virulence factor of a human fungal pathogen induces neutrophil apoptosis *via* NK cells. *J Immunol* (2014) 192:5332–42. doi:10.4049/jimmunol.1303180
109. Gresnigt MS, Bozza S, Becker KL, Joosten LAB, Abdollahi-Roodsaz S, van der Berg WB, et al. A polysaccharide virulence factor from *Aspergillus fumigatus* elicits anti-inflammatory effects through induction of interleukin-1 receptor antagonist. *PLoS Pathog* (2014) 10:e1003936. doi:10.1371/journal.ppat.1003936
110. Becker KL, Aimanianda V, Wang X, Gresnigt MS, Ammerdorffer A, Jacobs CW, et al. *Aspergillus* cell wall chitin induces anti- and proinflammatory cytokines in human PBMCs via the Fc-γ receptor/Syk/PI3K pathway. *MBio* (2016) 7:e01823–15. doi:10.1128/mBio.01823-15
111. Abad A, Fernández-Molina JV, Bikandi J, Ramírez A, Margareto J, Sendino J, et al. What makes *Aspergillus fumigatus* a successful pathogen? Genes and molecules involved in invasive aspergillosis. *Rev Iberoam Micol* (2010) 27:155–82. doi:10.1016/j.riam.2010.10.003
112. Müllbacher A, Eichner RD. Immunosuppression in vitro by a metabolite of a human pathogenic fungus. *Proc Natl Acad Sci U S A* (1984) 81:3835–7. doi:10.1073/pnas.81.12.3835
113. Sutton P, Newcombe NR, Waring P, Mullbacher A. In vivo immunosuppressive activity of gliotoxin, a metabolite produced by human pathogenic fungi. *Infect Immun* (1994) 62:1192–8.
114. Stanzani M, Orciuolo E, Lewis R, Kontoyiannis DP, Martins SLR, St. John LS, et al. *Aspergillus fumigatus* suppresses the human cellular immune response via gliotoxin-mediated apoptosis of monocytes. *Blood* (2005) 105:2258–65. doi:10.1182/blood-2004-09-3421
115. Tsunawaki S, Yoshida LS, Nishida S, Kobayashi T. Fungal metabolite gliotoxin inhibits assembly of the human respiratory burst NADPH oxidase fungal metabolite gliotoxin inhibits assembly of the human respiratory burst NADPH oxidase. *Infect Immun* (2004) 72:3373–82. doi:10.1128/IAI.72.6.3373-3382.2004
116. Yamada A, Kataoka T, Nagai K. The fungal metabolite gliotoxin: immunosuppressive activity on CTL-mediated cytotoxicity. *Immunol Lett* (2000) 71:27–32. doi:10.1016/S0165-2478(99)00155-8
117. Schneider A, Blatzer M, Posch W, Schubert R, Lass-Flörl C, Schmidt S, et al. *Aspergillus fumigatus* responds to natural killer (NK) cells with upregulation of stress related genes and inhibits the immunoregulatory function of NK cells. *Oncotarget* (2016) 7:71062–71. doi:10.18632/oncotarget.12616
118. Murphy JW, Zhou A, Wong SC. Direct interactions of human natural killer cells with *Cryptococcus neoformans* inhibit granulocyte-macrophage colony-stimulating factor and tumor necrosis factor alpha production. *Infect Immun* (1997) 65:4564–71.
119. Lamoth F, Juvvadi PR, Steinbach WJ. Heat shock protein 90 (Hsp90): a novel antifungal target against *Aspergillus fumigatus*. *Crit Rev Microbiol* (2014) 42:1–12. doi:10.3109/1040841X.2014.947239
120. Blatzer M, Binder U, Haas H. The metalloreductase FreB is involved in adaptation of *Aspergillus fumigatus* to iron starvation. *Fungal Genet Biol* (2011) 48:1027–33. doi:10.1016/j.fgb.2011.07.009
121. Lipscomb MF, Alvarellos T, Toews GB, Tompkins R, Evans Z, Koo G, et al. Role of natural killer cells in resistance to *Cryptococcus neoformans* infections in mice. *Am J Pathol* (1987) 128:354–61.
122. Tewari RP, Von Behren LA. Immune responses in histoplasmosis, a prototype of respiratory mycoses. *Indian J Chest Dis Allied Sci* (2000) 42:265–9.
123. Morrison BE, Park SJ, Mooney JM, Mehrad B. Chemokine-mediated recruitment of NK cells is a critical host defense mechanism in invasive aspergillosis. *J Clin Invest* (2003) 112:1862–70. doi:10.1172/JCI18125
124. Hidore MR, Murphy JW. Natural cellular resistance of beige mice against *Cryptococcus neoformans*. *J Immunol* (1986) 137:3624–31.
125. Hidore MR, Murphy JW. Correlation of natural killer cell activity and clearance of *Cryptococcus neoformans* from mice after adoptive transfer of splenic nylon wool-nonadherent cells. *Infect Immun* (1986) 51:547–55.

Conflict of Interest Statement: The authors declare that the research was conducted in the absence of any commercial or financial relationships that could be construed as a potential conflict of interest.

Copyright © 2017 Schmidt, Tramsen and Lehrnbecher. This is an open-access article distributed under the terms of the Creative Commons Attribution License (CC BY). The use, distribution or reproduction in other forums is permitted, provided the original author(s) or licensor are credited and that the original publication in this journal is cited, in accordance with accepted academic practice. No use, distribution or reproduction is permitted which does not comply with these terms.

frontiers in Immunology

REVIEW
published: 04 December 2017
doi: 10.3389/fimmu.2017.01705

Antifungal Activity of Plasmacytoid Dendritic Cells and the Impact of Chronic HIV Infection

Samuel Maldonado[1,2] *and Patricia Fitzgerald-Bocarsly*[1,2]*

[1] Rutgers School of Graduate Studies, Newark, NJ, United States, [2] Department of Pathology and Laboratory Medicine, New Jersey Medical School, Newark, NJ, United States

Due to the effectiveness of combined antiretroviral therapy, people living with HIV can control viral replication and live longer lifespans than ever. However, HIV-positive individuals still face challenges to their health and well-being, including dysregulation of the immune system resulting from years of chronic immune activation, as well as opportunistic infections from pathogenic fungi. This review focuses on one of the key players in HIV immunology, the plasmacytoid dendritic cell (pDC), which links the innate and adaptive immune response and is notable for being the body's most potent producer of type-I interferons (IFNs). During chronic HIV infection, the pDC compartment is greatly dysregulated, experiencing a substantial depletion in number and compromise in function. This immune dysregulation may leave patients further susceptible to opportunistic infections. This is especially important when considering a new role for pDCs currently emerging in the literature: in addition to their role in antiviral immunity, recent studies suggest that pDCs also play an important role in antifungal immunity. Supporting this new role, pDCs express C-type lectin receptors including dectin-1, dectin-2, dectin-3, and mannose receptor, and toll-like receptors-4 and -9 that are involved in recognition, signaling, and response to a wide variety of fungal pathogens, including *Aspergillus fumigatus*, *Cryptococcus neoformans, Candida albicans,* and *Pneumocystis jirovecii*. Accordingly, pDCs have been demonstrated to recognize and respond to certain pathogenic fungi, measured *via* activation, cytokine production, and fungistatic activity *in vitro*, while *in vivo* mouse models indicated a strikingly vital role for pDCs in survival against pulmonary *Aspergillus* challenge. Here, we discuss the role of the pDC compartment and the dysregulation it undergoes during chronic HIV infection, as well as what is known so far about the role and mechanisms of pDC antifungal activity.

Keywords: plasmacytoid dendritic cells, C-type lectin receptors, toll-like receptors, innate antifungal immunity, HIV

OPEN ACCESS

Edited by:
Steven Templeton, Indiana University School of Medicine, Terre Haute, United States

Reviewed by:
Rebecca Drummond, National Institutes of Health (NIH), United States
Paolo Puccetti, University of Perugia, Italy

***Correspondence:**
Patricia Fitzgerald-Bocarsly
Bocarsly@njms.rutgers.edu

Specialty section:
This article was submitted to Microbial Immunology, a section of the journal Frontiers in Immunology

Received: *02 October 2017*
Accepted: *20 November 2017*
Published: *04 December 2017*

Citation:
Maldonado S and Fitzgerald-Bocarsly P (2017) Antifungal Activity of Plasmacytoid Dendritic Cells and the Impact of Chronic HIV Infection. Front. Immunol. 8:1705. doi: 10.3389/fimmu.2017.01705

INTRODUCTION

An estimated 33 million people were living with HIV/AIDS worldwide in 2015 (1). Although the development of combined antiretroviral therapy has allowed HIV patients to suppress viral replication and live longer lifespans (2, 3), HIV evades the immune system and persists, causing chronic immune activation and inflammation (4). The persistence of infection and immune activation

leads to significant detrimental changes that occur in the body, and pose major threats to patients' well-being; in fact, in 2010, HIV/AIDS was still the fifth leading cause of disease burden worldwide (5).

Arguably the most significant pathological process faced by treated and untreated patients alike is the erosion of the immune system. HIV infection famously depletes $CD4^+$ T-helper (T_H) cells, first quickly in the acute phase of infection, followed by a near-total recovery in numbers, and finally a steady decline over a number of years (4) leaving the adaptive immune system at a tremendous disadvantage. T-cell depletion occurs *via* mechanisms such as direct infection, bystander effects due to chronic inflammation, and senescence (4, 6). The dysfunction of the immune system is also much broader; almost every known immune cell type has been associated with a dysfunction due to chronic HIV infection. Because HIV gains access to a cell *via* its interaction with CD4 and co-receptors CXCR4 and CCR5, it also has the capacity to infect other cells that express those receptors, including monocytes, macrophages, and plasmacytoid dendritic cells (pDCs) (4). In addition, the immune system may be further dysregulated due to chronic innate immune activation and the continued production of normally beneficial cytokines (7).

This erosion of the immune system leaves patients hypersusceptible to a variety of opportunistic infections, including fungal infections not commonly seen in the general population. For example, *Candida albicans* infection is the most common fungal infection in HIV patients. While it usually presents as oropharyngeal thrush, it can span a broad spectrum of severity from asymptomatic to invasive candidiasis (8). The most common systemic fungal infection in the HIV population is cryptococcal meningitis, caused by *Cryptococcus neoformans.* Cryptococcal meningitis causes 181,000 deaths a year in HIV-positive patients, accounting for 15% of global AIDS-related deaths (9, 10). *Aspergillus fumigatus* is the causative agent of invasive Aspergillosis, which is less common in the context of HIV infection but is particularly aggressive and difficult to treat, resulting in a median survival of only 3 months after diagnosis (11, 12). These and other pathogenic fungi take advantage of an HIV patient's impaired immune system. Studies early in the HIV epidemic suggested that HIV patients are much more likely to develop opportunistic infections when two events occur: absolute $CD4^+$ cell counts drop below 250 cells/mm^3, and interferon (IFN)-α production by virus-stimulated peripheral blood mononuclear cells (PBMCs) drops below 300 IU/ml (13). It is the latter that makes pDCs a cell type of great interest when studying HIV infection, as they are the body's most potent producers of type-I IFNs. pDCs produce up to 100-fold more IFN-α than any other cell type in response to viral stimulation and serve as an important link between the innate and the adaptive branches of the immune system (14–16). pDC IFN production and influence over the rest of the immune response has made these cells the subject of extensive investigation in human and mouse models. Importantly, murine systems do not perfectly represent human ones, and studies on mouse pDC function must also be investigated in humans. For example, toll-like receptor (TLR) 9 is broadly expressed by murine myeloid cells, but is more limited to pDCs and B-cells in humans (17). Similarly, murine pDCs commonly produce IL-12 while human pDCs rarely, if ever, produce IL-12 (18).

Plasmacytoid dendritic cell dysregulation during chronic HIV infection has garnered attention due to the potentially far-reaching effects on patient outcome and well-being. However, an interesting development in the field of pDC research is the investigation into their role in fungal infection. Studies have demonstrated that pDCs have the machinery needed to recognize and respond to fungal stimulation, that they in fact do respond with certain cellular functions, and that they are necessary *in vivo* for a successful antifungal immune response. In this review, we outline the current paradigm concerning pDCs' role in viral immunity and describe the dysregulation of the pDC compartment during chronic HIV infection. We then switch gears to the role of pDCs in antifungal immunity, where we highlight the components of fungal immunity that pDCs possess, and summarize what has been discovered to date concerning the mechanisms of pDC antifungal activity.

pDCs IN ANTIVIRAL IMMUNITY

Both the innate and the adaptive immune responses play active roles in combating viral infections such as HIV. The adaptive immune response includes a strong $CD4^+$ and $CD8^+$ T-cell response, as well as the production of neutralizing antibodies that begins during the acute phase of infection (19, 20). Mobilization of the adaptive immune response depends in part on pDCs, a lineage-negative subtype of dendritic cells that derives its name from a plasma-cell-like morphology. Although pDCs comprise only 0.2–0.8% of PBMC (14, 15, 21), their powerful immunomodulating capabilities make pDCs highly influential to the development of the immune response to HIV infection, and a lack of sufficient pDC numbers or function corresponds with high viral loads and opportunistic infections (22).

Human pDCs are generally found in peripheral blood and lymphoid tissue, so if an infection occurs in a different tissue (e.g., the lung or mucosa), they must migrate to sites of infection or inflammation by responding to chemokines. This occurs primarily *via* the chemokine receptors CMKLR1, CCR7, CXCR3, and CXCR4 (22–24) as well as through homing molecules, such as CD62L, which binds L-selectin and allows pDCs to track to high endothelial venules and the gut homing receptor α4β7 (25). Once at the site of infection, pDCs directly recognize and respond to viral stimulation. The initial interaction between pDCs and HIV virions is possible because pDCs express the surface molecules that are targeted by HIV: CD4, CCR4, and CXCR5, as reviewed in Ref. (16). The interaction between the virus and CD4 allows the pDC to endocytose the virus, which induces activation in a TLR-dependent or -independent manner.

In the TLR-dependent pathway, the endocytosed virus is delivered to endosomes in pDC that contain TLR-7 and 9. Acidification of the endosomes allows TLR-7 and 9 to access viral RNA or unmethylated CpG motifs, including that in viral DNA, respectively (26, 27). These TLRs have the capacity to recognize a host of viral, bacterial, and fungal nucleic acids, as well as small molecule artificial ligands such as imiquimod and resiquimod (28, 29). Ligation of TLR-7 or 9 induces a MyD88-dependent

activation pathway that ultimately leads to pDC activation and cytokine production (30). Although less well-characterized than the TLR-dependent pathway, evidence exists for a TLR-independent activation pathway in pDCs. For example, one study found that IFN-α production by murine pDCs in response to Sendai virus was not abrogated in MyD88$^{-/-}$ mice and was not dependent on endosomal acidification, both of which are required for TLR9 signaling (31). Another study found that murine pDC IFN-α production in response to HSV-1 was not completely dependent on TLR9 (32). However, specific mechanisms of TLR-independent pDC activation and cytokine production are still under investigation.

Both the TLR-dependent and -independent signaling pathways converge on interferon regulatory factor (IRF) 7, the master regulator of IFN production which is constitutively expressed by pDCs at uniquely high levels (30, 33, 34). Phosphorylation of IRF7 causes it to translocate into the nucleus and induce the transcription of IFN genes, producing high concentrations of type-I IFN (35). TLR-7 and -9 ligation also lead to the activation of transcription factor NF-κB, which induces the production of inflammatory cytokines/chemokines and the upregulation of co-stimulatory molecules (21, 36). Activated pDCs can then produce type-I IFNs, type-III IFNs, and a network of other cytokines and chemokines. They also have the ability to become antigen-presenting cells, at which point they develop a morphology resembling conventional DCs (cDCs) (36–38).

Perhaps the most significant contribution of pDCs to antiviral immunity is the production of massive amounts of type-I IFNs (mainly α and β) in response to viral stimulation. Most notably, pDCs can produce 100–1,000 times more type-I IFN than any other cell type (39–41). It has even been reported that as much as 60% of genes expressed in an activated pDC are dedicated to the production of type-I and type-III IFNs (42). Type-I IFNs all bind the same receptor, the IFN-α/β receptor, which is widely expressed by most nucleated cells in the body. The IFN-α/β receptor is composed of two subunits, IFNAR1 and IFNAR2, that form a heterodimer upon ligation of type-I IFN (43). IFNAR-associated Janus kinases then phosphorylate STAT1 and STAT2, which form a complex with IRF9 called the ISGF3 complex. The resulting signaling cascade activates gene transcription for factors that produce an antiviral state in surrounding tissues and mobilizes virtually all types of immune cells to combat viral infection (44, 45). For example, IFN-α acts as a survival, maturation, and cytokine/chemokine production factor for pDCs (46, 47) and cDCs (48), activates natural killer cells (26), biases the immune system toward a T_H1 response (49, 50), primes CD8$^+$ T-cells and induces memory CD8$^+$ T-cells (51–53), promotes the development of regulatory T (Treg) cells (54), and enhances antibody production against soluble antigen (55). These effects, among others, are critical for the inhibition of viral replication and are why type-I IFNs are arguably the most important cytokines in antiviral immunity.

In addition to type-I IFNs, pDCs also produce type-III IFNs (IFN-λ1–3) after viral stimulation (38). The IFN-λ receptor is expressed on a much more limited scale than the IFN-α/β receptor—primarily epithelial cells and pDCs (38, 56)—suggesting that the biological activity of IFN-λ is more narrow than that of type-I IFN. However, type-I and type-III IFN share many common features: their signaling pathways include many of the same factors, including STAT1, STAT2, and the formation of the ISGF3 complex; they also activate several common genes (57, 58). Functionally, IFN-λ also has antiviral effects, especially for the protection of epithelial cells (59), the enhancement of TLR-mediated signaling in pDCs (56), development of Treg cells (60), and biasing toward a T_H1 response by reducing IL-13 expression (61). However, it has also been reported that IFN-λ can be antagonistic to type-I IFN antiviral activity (62).

Other than IFNs, pDCs are able to produce several other cytokines and chemokines. NF-κB activation after viral stimulation induces pDCs to produce inflammatory cytokines and chemokines such as IL-12 (in murine but not human pDC), TNF-α, RANTES, IL-10, IP-10, IL-6, MIP-1α, and MIP-1β (36, 63). One study identified 12 chemokines that are produced in three distinct waves by pDCs in the hours following influenza virus infection (64). Furthermore, pDCs are also capable of other innate immune functions. Although resting pDCs are less efficient than myeloid DCs at capturing, processing, and presenting antigen (65, 66), activation of pDCs in response to influenza virus induces a change into a dendritic morphology and the upregulation of MHC-II, enhancing their ability to present antigen to naïve and memory T-cells (67, 68). In 2012, Tel et al. reported that pDCs could not only present tumor antigens but could also directly kill tumor cells. They termed these cells "killer pDCs" (69). Another interesting feature of the pDC is the expression of several surface receptors usually restricted to myeloid cells. On pDCs, these receptors include the C-type lectin receptors (CLRs) dectin-1, dectin-2, dectin-3, and mannose receptor (MR) (70–72), which will be discussed later. These receptors are of particular interest because they are involved in antifungal immunity.

pDC DYSREGULATION DURING CHRONIC HIV INFECTION

Despite the impressive antiviral functions of pDCs, HIV still manages to evade the immune system and persist in the body. The observation that HIV patient blood cells produced less IFN after stimulation led to the discovery of what were termed natural IFN-producing cells, which would later be known as pDCs (73–76). After the discovery of pDCs as the major IFN-α-producing cell, observations surfaced that showed chronic HIV infection leads to a decline in pDC number and function (77). The decline in absolute pDC numbers correlated directly with a decline in CD4$^+$ T-cell count and increased viral load (22, 78), while pDC functional decline (percent of IFN-α-producing pDC after viral stimulation) correlated with an increase in patient viral load, but not CD4$^+$ T-cell count (76). Although ART treatment results in a partial recovery of pDC numbers, they do not make a full recovery (79). The specific cause of this decline in pDC number is still under investigation. Studies on macaque models indicate that pDCs are recruited to lymph nodes where they die rapidly (80, 81); this was supported by a study that found higher numbers and accelerated pDC death in human lymph nodes (82). Other studies show that pDCs are susceptible to HIV infection, which can

cause syncytia formation and cell death (83, 84). Other possible mechanisms include recruitment to mucosal tissues, bystander apoptosis similar to T-cells, and bone marrow suppression (85).

Along with lower numbers, HIV also causes functional differences in pDCs. One of the earliest observations in HIV patients was the high levels of circulating IFN-α seen in some untreated patients, which was associated with disease progression (13, 86). The pDCs that accumulate in HIV patient lymph nodes were also described as producing significantly higher levels of IFN-α than non-infected healthy controls (82). This suggests that at certain points during infection, pDCs are chronically activated and are continuously producing IFN-α. This chronic immune activation may be driving pathology, including the immune exhaustion of T-cell compartments (7, 87). Supporting this hypothesis, one study found that humanized pDC-depleted mice infected with HIV-1 show dramatically reduced cell death and immune cell depletion, a phenomenon they suggested stems from the lack of persistent pDC activation and IFN production (88). In addition, other pDC functions are found to be dysregulated in HIV patients: pDCs become less able to stimulate T-cell proliferation in mixed lymphocyte reactions (89), show a partial activation phenotype (90), and have a reduced ability to respond to TLR7 and -9 agonists (91).

Another area of research concerns the possibility that pDCs may be inducing the differentiation of human Treg cells that lead to tolerogenicity and suppression of T-cell proliferation during chronic HIV infection. Human pDCs have been shown to induce both $CD8^+$ and $CD4^+$ Treg cell development in certain circumstances. For example, pDCs stimulated with type B CpG oligodeoxynucleotides (CpGb) induced $CD4^+CD25^-$ naïve T-cells to differentiate into $CD4^+CD25^+$ Treg cells, which suppressed T-cell proliferation and promoted tolerance (92). Another study found that pDCs activated with CD40L induced naïve $CD8^+$ T-cells to proliferate, but the resulting $CD8^+$ T-cells were poorly cytotoxic, had poor responses to secondary re-stimulation, and produced IL-10 (93). To that end, a study by Boasso et al. (94) found that T-cell proliferation in HIV-infected patients was being inhibited by pDCs through the expression of indoleamine-2,3-dioxygenase (IDO) (94). IDO is the first and rate-limiting enzyme in the catabolism of tryptophan, and its expression can be used by APCs as an immune modulator to limit T-cell proliferation (95). In the study, IDO mRNA expression in the blood of HIV-infected patients was directly correlated with viral load, and was responsible for impaired $CD4^+$ T-cell proliferation. Using flow cytometric analysis, they found that pDCs were the main producers of IDO, and that pDC IDO expression was a direct response to HIV that did not require the presence of other leukocytes. This phenomenon may represent yet another way that pDCs contribute to the dysfunction of the immune system during chronic HIV infection. In addition, another study found that IDO expression by pDCs blocks T-cell differentiation into T_H17 cells, which could further negatively impact adaptive immunity to fungal infection (96). This dysfunction, along with the dysregulation of virtually every immune cell type, leaves patients at higher risk of opportunistic infections and other comorbidities, including fungal infections with *C. albicans* and *C. neoformans*.

SELECT COMPONENTS OF THE IMMUNE RESPONSE TO FUNGAL INFECTION

A discussion of HIV patient susceptibility to fungal infections requires an understanding of normal antifungal immunity. Although some fungi are commensal with the human host, this review focuses on pathogenic fungal infections. Fungal pathogens, such as *A. fumigatus* and *C. neoformans*, tend to be ubiquitous to the environment and are introduced into the human host through inhalation of spores or small yeast cells (97, 98). In the case of *A. fumigatus* and other sporulating fungi, spores (termed "resting conidia," RC) that reach a suitable host begin to swell (termed "swollen conidia," SC), and germinate (termed "germinating conidia," GC), finally growing into filamentous hyphae (99). Fortunately, fungal pathogens express pathogen-associated molecular patterns (PAMPs), which are not found on mammalian cells and alert the immune system to the presence of non-self organisms (100). PAMPs can vary depending on the species, growth stage, and environment of the fungus (101, 102). Three significant PAMPs on fungal cell walls include β-glucans (polymers of glucose, typically with 1,3 linkages and occasional 1,6 branches), chitin (a polymer of *N*-acetylglucosamine), and mannans (polymers of mannose linked to fungal proteins) (97, 103). Fungi that make it into a human host can be recognized by innate immune cells through pattern recognition receptors (PRRs), such as TLRs and CLRs (100).

Once the PAMPs on fungi are recognized by cellular PRRs, a complex immune response begins that, incorporates both the innate and adaptive branches of the immune system (104). Phagocytes, such as monocytes, neutrophils, and macrophages, phagocytose and kill fungal pathogens directly (105), spread out over hyphae and kill them *via* oxidative and non-oxidative means, and in the case of neutrophils produce extracellular traps (106, 107). In addition to uptake and direct killing, cDCs also transport and present fungal antigen to T-cells and induce their differentiation into T_H1, T_H17, or Treg cells, depending on the environment and the fungus (108–110). While T_H1 cells are thought to be the most protective, patients with defects in the T_H1 compartment are not overly susceptible to certain fungal infections (97). This is because the T_H17 compartment is also protective and sometimes essential to fungal clearance, depending on the species and route of infection (111). Conversely, inborn errors in IL-17 immunity can result in chronic mucocutaneous candidiasis in humans (112), and more broad susceptibility to *C. albicans* infection in mice, including cutaneous and oropharyngeal infection (113). Finally, the development of protective antibodies after vaccination of mice with *C. albicans* adhesins suggests that humoral immunity may also get involved during fungal infection, although in those studies the main effector cells responsible for vaccine efficacy were CD4+ T-cells, and neither B-cell transfer nor passive immunization with serum of vaccinated mice were protective to unvaccinated mice (114).

The TLRs involved in fungal recognition that are expressed on pDCs are TLR4 and TLR9 (17, 35). TLR4 (CD284) is mainly known for recognizing bacterial lipopolysaccharide, but it also appears to recognize mannan structures of fungal cell walls, leading to cytokine/chemokine production and recruitment of neutrophils.

TLR4 is composed of a 608 residue extracellular domain, which contains 21 leucine-rich repeats and can be subdivided into N-, central, and C-terminal domains, and a 187-residue intracellular domain that signals *via* the TLR-associated adaptor MyD88 (115). Interruption of TLR4 signaling has been shown to increase susceptibility to *C. albicans* (116), *A. fumigatus* (117, 118), and *Pneumocystis jirovecii* (119) in mice. However, it is worth noting that TLR4 signaling did not induce cytokine production after recognizing mannans on *C. neoformans* cell walls (120), indicating fungal species-specific responses.

TLR9 (CD289) recognizes unmethylated CpG DNA sequences, which may allow it to recognize fungal DNA. As mentioned earlier, TLR9 is located in endosomes of pDCs, where it is known for responding to viral DNA in a MyD88-dependent manner. TLR9 has 25 intra-endosomal leucine-rich repeats, but a detailed structure for TLR9 has not yet been discovered (121). Studies show TLR9 induces IL-10 production by macrophages in response to *C. albicans* (120), pro-inflammatory cytokine secretion by mouse bone marrow-derived dendritic cells in response to *A. fumigatus* DNA (122), and IL-12p40 production and CD40 upregulation in DCs in response to *C. neoformans* (123). It is interesting to note that while MyD88 serves as a signaling adaptor for all of the TLRs except TLR3, patients with MyD88 deficiencies or mutations do not suffer from severe or recurrent fungal infections, suggesting that TLR signaling enhances but is not indispensable for antifungal immune responses (124).

C-type lectin receptors are a large family of receptors that contain C-type lectin-like domains (CTLDs), which, depending on the receptor, recognize a wide array of carbohydrates, proteins, or lipids (125). CLRs are a diverse family of receptors with a multitude of functions, but this review will focus on the four CLRs that have a role in fungal recognition and have been identified on human pDCs: dectin-1, dectin-2, dectin-3, and MR.

Dectin-1 (CLEC7A) recognizes β(1,3)- and β(1,6)-linked glucans, which are present on bacterial and fungal cell walls. B-glucans can comprise up to 50% of the cell walls of common pathogenic fungi, including *A. fumigatus*, *C. neoformans*, *P. jirovecii*, and *C. albicans* (126–130). Dectin-1 is composed of an extracellular CTLD, a single transmembrane domain, and an intracellular immunoreceptor tyrosine-based activation motif (ITAM) (126). The dimerization of dectin-1 and the phosphorylation of its intracellular ITAM recruits spleen tyrosine kinase (Syk), and induces a signaling cascade that includes the signaling adaptor caspase recruitment domain-containing protein 9 (CARD9). CARD9 is a major point of regulation within the signaling cascade of several CLRs, including dectin-1 and dectin-2, and is indispensable for the cell activation and cytokine production caused by dectin-1 and -2 ligation (131, 132). CARD9 deficiency has been linked to chronic and recurring fungal infections, especially by *C. albicans* (133, 134). In addition, pDCs from CARD9 knockout mice produced significantly less IL-6 and TNF-α than wild-type mice in response to influenza virus, while type-I IFN production was unaffected (135). Dectin-1/Syk/CARD9 signaling ultimately leads to the canonical activation and nuclear translocation of NF-κB subunits Rel-A (p65) and c-Rel. Dectin-1 also activates the NF-κB unit Rel-B through a non-canonical pathway, *via* Raf-1 instead of Syk (136). Dectin-1 has been shown to have an array of immune functions, including the recognition, uptake, and killing of fungi (137, 138), as well as cellular signaling leading to maturation, production of a respiratory burst, cytokine and chemokine production, enhanced survival and differentiation of T_H cells that helps control fungal infection in the GI tract, and cytotoxic T-lymphocyte priming (128, 139–143).

Dectin-2 (CLEC6A) recognizes α-mannose structures present on the surface of many viruses, bacteria, and fungal pathogens. Dectin-2 has been shown to have a role in immunity to fungi, including *C. albicans*, *A. fumigatus*, and non-encapsulated *C. neoformans*, with a preference for hyphal as opposed to yeast or conidial forms of fungal cell walls (144–146). It is composed of an extracellular CTLD and a short cytoplasmic tail, which couples with FcRγ to initiate downstream signaling. The phosphorylation of FcRγ again recruits Syk and CARD9 (147, 148). Dectin-2 signaling also induces the activation of NF-κB, but in contrast to dectin-1, dectin-2 selectively activates the c-Rel subunit of NF-κB *via* MALT1. This selectivity suggests that dectin-2 is more specific for the production of cytokines that induce T_H17 polarization (149). Dectin-2 signaling induces internalization of the fungus and the production of an array of cytokines, including TNF-α and IL-1β, 2, 6, 10, 12, and 23 (145, 147). Furthermore, blocking dectin-2 in mice abrogated the development of T_H1 and T_H17 cells, which left mice significantly more susceptible to *C. albicans* infection (150).

Similar to dectin-2, dectin-3 (CLEC4D, CLECSF8) also has a single extracellular CRD with a short cytoplasmic tail. The CRD of dectin-3 is highly homologous with that of dectin-2, and similarly recognizes α-mannans (151). In fact, dectin-3 was found to dimerize with dectin-2, and the resulting heterodimer was more adept at recognizing fungal PAMPs than the respective homodimers (152). Although the cytoplasmic tail of dectin-3 lacks a signaling motif and does not associate with any known signaling adaptor, including FcRγ, it does induce signaling *via* Syk and the CARD9/Bcl10/Malt1 complex and activates NF-κB (153). The cellular processes that are induced include phagocytosis, cytokine production, and a respiratory burst in macrophages (154). To illustrate its physiological relevance, murine bone marrow-derived macrophages pretreated with dectin-3-blocking monoclonal antibodies were inhibited from NF-κB nuclear translocation and cytokine production after *C. albicans* stimulation, and mice treated with dectin-3-blocking antibody succumbed rapidly to sub-lethal *C. albicans* IV challenge (152). Similarly, mice deficient in dectin-3 were more susceptible to DSS-induced colitis, and murine bone marrow-derived macrophages were impaired in phagocytic and fungicidal ability, NF-κB nuclear translocation, and cytokine production (155). Conversely, no role was found for dectin-3 in defense against *C. neoformans*, as dectin-3-deficient mice did not differ in pulmonary leukocyte recruitment, pulmonary cytokine profiles, or overall survival after pulmonary *C. neoformans* challenge. In addition, macrophages and DCs isolated from dectin-3 knockout mice did not differ in their phagocytic or fungicidal ability against *C. neoformans* (156).

Mannose receptor (CD206) is a highly endocytic receptor with three categories of extracellular binding domains, a single transmembrane domain, and a short cytoplasmic tail (157). The extracellular binding domains include an N-terminal cysteine-rich (CR) domain, which binds sulfated carbohydrates; a fibronectin

type II (FNII) domain, which binds collagen; and eight CTLDs, which bind carbohydrates that terminate in D-mannose, L-fucose, or *N*-acetyl glucosamine, as reviewed in Ref. (158, 159). While the CR and FNII extracellular domains are involved in glycoprotein homeostasis (160, 161), it is the CTLDs that are responsible for recognizing carbohydrate entities on pathogens (159). For one particularly interesting example, MR binds the gp120 glycoprotein on HIV and mediates binding of the virus by dendritic cells (70) and macrophages (162). In the context of fungal infection, the MR has been shown to enhance uptake and clearance of pathogenic fungi, including *A. fumigatus* (163) *C. albicans* (164, 165), *C. neoformans* (166), and *Pneumocystis carinii* (167). However, MR seems to not be phagocytic in its own right; MR was unable to induce phagocytosis of its ligands when transfected onto Chinese hamster ovary cells (168). MR instead influences the signaling of other receptors. For example, Tachado et al. (169) discovered that human embryonic kidney 293 cells required transfection of both TLR2 and the MR in order to produce IL-8 in response to *Pneumocystis*. Similarly, in alveolar macrophages, *Pneumocystis* challenge led to direct interaction of TLR2 and MR, while blocking MR and TLR2 simultaneously abrogated IL-8 production (169). The downstream results of MR signaling are varied and dependent on many factors, including signaling from other receptors and the route of ligand delivery (158). A summary of the TLRs and CLRs discussed here can be found in **Table 1**.

pDCs IN ANTIFUNGAL IMMUNITY

The involvement of pDCs in antifungal immunity is a topic of study currently emerging in the literature. An early indication came in 2004, when Romani et al. described how thymosin alpha 1, a peptide produced by the thymus, served to activate human cDCs and pDCs by enhancing their phagocytic capacity and IL-10 production in response to *A. fumigatus* stimulation (171). Later, Dan et al. found that mannoproteins from *C. neoformans* and CpG-containing DNA synergistically induced pDCs to produce greater amounts of pro-inflammatory cytokines, although stimulation with mannoproteins alone did not induce any cytokine production (170). This implied that pDCs were able to sense mannoproteins, which are classically recognized by CLRs, and that recognition of mannoproteins acted as an adjuvant for TLR9-dependent pDC activation by CpG. That same year, Ramirez-Ortiz et al. found that *A. fumigatus* DNA contained unmethylated CpG motifs, which triggered TLR9 in mouse and human pDCs and induced cytokine production *in vitro* (122). Perruccio et al. then confirmed that *A. fumigatus* DNA stimulated TLR-9 in pDCs and induced the production of IL-12p70, IL-10, and IFN-α (172).

The response of pDCs to fungal recognition is still under investigation, but a few studies have shed some light on mechanisms of pDC antifungal activity (summarized in **Figure 1**). Direct pDC antifungal activity was first demonstrated in 2011, when Ramirez-Ortiz et al. found that human pDCs directly inhibited growth of *A. fumigatus* hyphae and produced IFN-α and TNF-α in response to *in vitro* hyphal stimulation (173). They found that pDCs spread out over the surface of hyphae and inhibited hyphal viability by up to 80%. However, this strong antifungal activity was observed with a pDC:fungal ratio of 50:1, which seems highly unlikely to occur in a live organism. At a pDC-fungal ratio of 1:10, a 40% decrease in hyphal viability was still observed. At the

TABLE 1 | A summary of the pattern recognition receptors (PRRs) on plasmacytoid dendritic cells (pDCs) that have a role in antifungal immunity.

Receptor	Structure	Fungal ligand	Cellular functions	Fungal pathogen	Reference
TLR4 (CD284)	Extracellular 608 residue domain, composed of an N-, central, and C-terminal domain. 21 leucine-rich repeats	Mannan structures	Cytokine/chemokine production, recruitment of neutrophils	*Candida albicans, Aspergillus fumigatus, Pneumocystis.* Not TLR4-dependent in *C. neoformans* models.	(17, 35, 115–120)
TLR9 (CD289)	25 leucine-rich repeats. Detailed structure not yet described	Unmethylated CpG DNA	IL-10, pro-inflammatory cytokine production including IL-12p40 production by murine DCs	*C. albicans, A. fumigatus, Cryptococcus neoformans*	(120–123)
Dectin-1 (CLEC7A)	Single extracellular C-type lectin-like domain (CTLD), intracellular immunoreceptor tyrosine-based activation motif	β(1,3)- and β(1,6)-linked glucans	Phagocytosis, cell maturation, respiratory burst, cytokine/chemokine production, direction of T_H cell differentiation, CTL priming	*A. fumigatus, C. neoformans, C. albicans, Pneumocystis*	(126, 127, 129, 130, 136–139, 141, 142)
Dectin-2 (CLEC6A)	Single extracellular CTLD, short cytoplasmic tail (couples with FcRγ)	a-mannose structures	Cytokine production, T_H1 and T_H17 differentiation	*A. fumigatus, C. albicans, C. neoformans*	(144–147, 150)
Dectin-3 (CLEC4D, CLECSF8)	Single extracellular CTLD, short cytoplasmic tail (does not couple with FcRγ)	a-mannose structures	Phagocytosis, cytokine production, respiratory burst (macrophages)	*C. albicans, C. neoformans* (conflicting studies)	(151, 152, 155, 156, 163)
Mannose receptor (MR, CD206)	Extracellular CR domain, fibronectin type II domain, and 8 CTLDs. Short cytoplasmic tail	Carbohydrates that terminate in D-mannose, L-fucose, or *N*-acetyl glucosamine	Phagocytosis (possibly requires TLR2), fungal clearance, IL-8 production	*A. fumigatus, C. albicans, C. neoformans, Pneumocystis*	(155, 157, 158, 163–166, 168, 170)

Listed are receptors that have been shown to have a role in fungal infection and are expressed on pDCs. Each receptor is then summarized with a brief description of their structures, their fungal ligands, the major downstream cellular functions, and a selection of sources from which this information was gathered. TLR9, Dectin-1, Dectin-2, Dectin-3, and MR have been implicated specifically in pDC–fungal interaction, while TLR4 has been investigated on other cell types but not yet on pDCs.

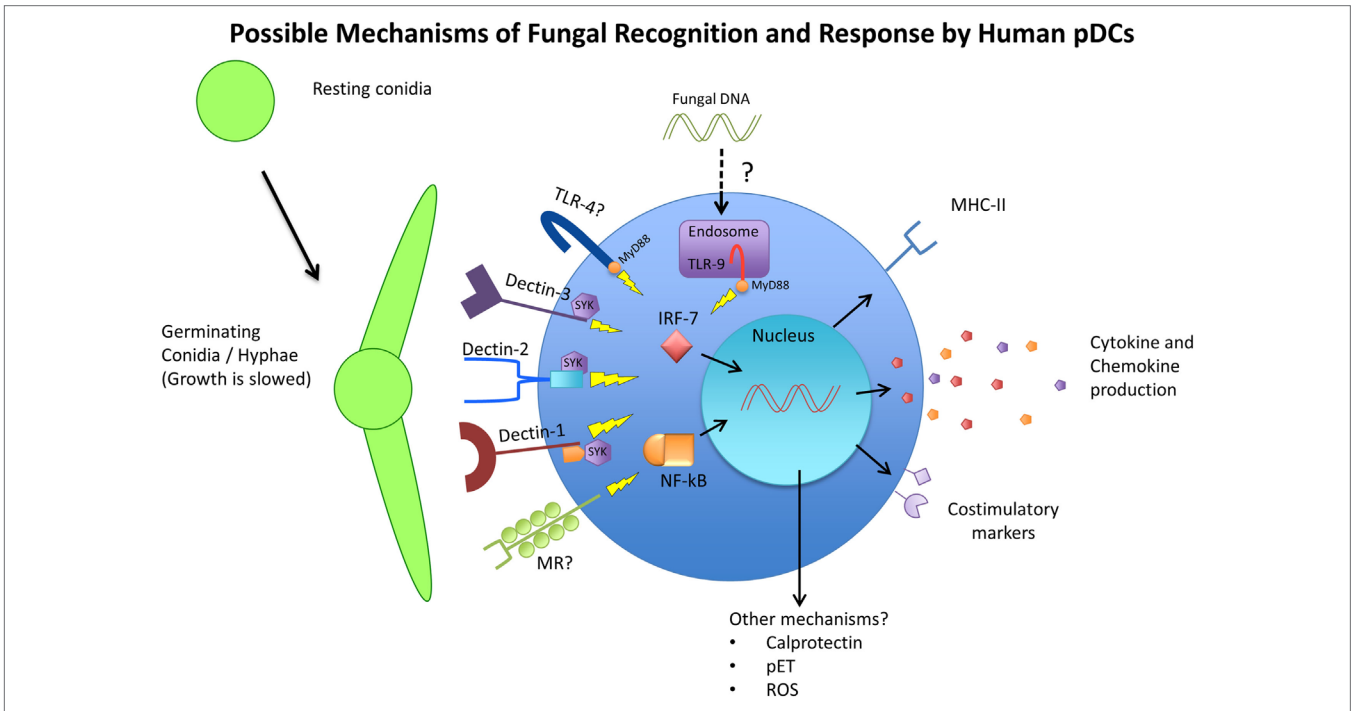

FIGURE 1 | Schematic representing the available receptors and cellular responses of plasmacytoid dendritic cells (pDCs) to fungal pathogens. Resting conidia (RC) or yeast cells are less immunogenic than germinating and hyphal forms of fungi due to the increased availability of ligands such as beta-glucans and alpha-mannan structures of the cell wall. The receptors TLR4, TLR9, Dectin-1, Dectin-2, Dectin-3, and MR have been implicated in antifungal immunity in various models and studies and have also been observed to be expressed by pDCs. The cellular responses of pDCs to fungal stimulation have only begun to be characterized, but include phagocytosis, activation/maturation, cytokine and chemokine production, and MHC-II upregulation. Other pDC antifungal mechanisms that have been proposed include the release of calprotectin by apoptotic pDCs, the production of pDC extracellular traps (pETs), and the production of reactive oxygen species (ROS).

same time, they found fungal stimulation lead to a large increase in pDC death, mediated partially by the production of gliotoxin by *A. fumigatus*. They also discovered that pDC lysates had the same antifungal activity as live cells, and implicated the release of calprotectin from dying pDCs as a contributor to the inhibition of fungal growth. Calprotectin has a documented role in antifungal immunity as a component of neutrophil extracellular traps (174). However, this was the first indication that pDCs may also use calprotectin. A later study by the same group indicated that pDC-*Aspergillus* interaction seemed to induce the production of pDC extracellular traps (pETs), similar to those extracellular traps laid by neutrophils (175). The production of extracellular traps by pDCs is a novel concept that has not been described elsewhere, and requires careful follow-up. Transcriptome analysis after *A. fumigatus* stimulation revealed the upregulation of several genes involved in activation, chemokine production, and antigen presentation, as well as genes associated with apoptosis. *In vivo*, mice depleted of pDCs were significantly more susceptible to *Aspergillus*-induced mortality, both after pulmonary and intravenous challenge (173). In addition, pulmonary challenge with *A. fumigatus* caused a six-fold increase in pDC number in the lungs. In a *C. neoformans* model, Hole et al. indicated that murine and human pDCs could phagocytose yeast cells and could directly inhibit *C. neoformans* growth through the use of reactive oxygen species (72).

As mentioned above, pDCs express receptors that are known to be involved in fungal recognition (summarized on **Figure 1**). As early as 2002, Taylor et al. mentioned that murine pDCs express dectin-1, although the data were not shown. Seeds et al. (71) later confirmed that finding, and added that murine pDCs also expressed the CLRs dectin-2 and MR (71). Because murine pDCs are not perfect representations of human pDCs, these receptors also needed to be investigated on human pDCs. Studies on human pDCs observed the expression of dectin-1 (176), dectin-2 (177), and MR (70, 178). However, attempts to identify which pDC receptor is responsible for fungal recognition have delivered mixed results. One study singled out dectin-2 as the main receptor responsible for recognition of *A. fumigatus* hyphae by human pDCs (175). They used laminarin and mannan to block dectin-1 and dectin-2, respectively, and found that while both blocking agents decreased the ability of pDCs to associate with fungal hyphae, only mannan's effect reached statistical significance. However, the definition and use of mannan as a dectin-2 blocker may be problematic, as it can be the ligand for other CLRs, including dectin-3 and MR. The study did follow-up by blocking with specific antibodies against dectin-1 and dectin-2, which recapitulated their results that dectin-2 was more responsible for pDC–hyphal association. Hole et al. observed the presence of dectin-3 on murine pDCs, and demonstrated that blocking dectin-3 on human pDCs resulted in a blunted

reaction to *C. neoformans* stimulation (72). In their study, pDCs from dectin-3 knockout mice experienced the greatest reduction in fungal uptake and growth inhibition, greater than dectin-1, dectin-2, and MR knockout mice. Accordingly, pDCs from dectin-3 knockout mice were greatly deficient in their ability to phagocytose *C. neoformans* yeast cells. It is interesting to note that these findings stand in contrast to the aforementioned study where dectin-3 was not required for protection against *C. neoformans* (156). Nevertheless, the data again indicated that while dectin-3 knockout mice were the most affected in their antifungal activity and the only ones to achieve significance, knocking out dectin-1, dectin-2, and MR also resulted in varying degrees of reduced antifungal activity. This allows the possibility that pDCs use a combination of receptors to recognize and respond to fungal pathogens and that these PRRs have a measure of redundancy.

Considered together, this evidence strongly indicates that pDCs play an important role in antifungal immunity. However, there remains much to be discovered concerning the mechanisms of pDC–fungal interaction, cellular responses to recognition, and the role of pDCs in the broader landscape of antifungal immunity.

CONCLUDING REMARKS

One of the most insidious threats to the health and well-being of immunocompromised individuals, including those living with HIV, is the threat of opportunistic infections. Opportunistic fungal infections can be particularly fast, lethal, and difficult to treat. The main contributing factor for increased susceptibility to fungal infection in immunocompromised patients is the depletion and dysregulation of many components of the immune system; even when infection is well-controlled with antiretroviral medication, over time this dysregulation is measurable in individuals chronically infected with HIV. The pDC is no exception; HIV patients have a decline in number and functionality of their pDC compartment. This is especially problematic when considering the role of pDCs in fungal infection that is currently emerging in the literature. Studies have shown that pDCs have the machinery to recognize and respond to fungal infection, and do so in a manner that indicates pDCs are involved in a successful antifungal immune response. Therefore, dysregulation of the pDC compartment may be a contributing factor to the increased susceptibility of fungal infections that afflict HIV patients and other immunocompromised populations.

AUTHOR CONTRIBUTIONS

SM performed all literature searches and writing of this review. PF-B provided focused expertise and guidance on the field of plasmacytoid dendritic cell and HIV biology, extensive revision of this manuscript, and final approval of the version for publication.

ACKNOWLEDGMENTS

The authors would like to acknowledge the contributions of fellow lab members PD, HH, ZR, and HD as well as past members JD, VS, TS, MP, MN, and DD.

FUNDING

SM is supported by National Institutes of Health Integrated T32 Training Program in *Infection, Immunity and Inflammation* (Grant # 5T32AI125185) and the MD/PhD program at Rutgers New Jersey Medical School. PF-B is funded by NIH grants AI026806 and AI106125.

REFERENCES

1. WHO. *Global Health Sector Strategy on HIV 2016–2021*. Geneva, Switzerland: WHO Press (2016). 60 p.
2. Zaidi J, Grapsa E, Tanser F, Newell ML, Barnighausen T. Dramatic increase in HIV prevalence after scale-up of antiretroviral treatment. *AIDS* (2013) 27(14):2301–5. doi:10.1097/QAD.0b013e328362e832
3. May MT, Gompels M, Delpech V, Porter K, Orkin C, Kegg S, et al. Impact on life expectancy of HIV-1 positive individuals of CD4+ cell count and viral load response to antiretroviral therapy. *AIDS* (2014) 28(8):1193–202. doi:10.1097/QAD.0000000000000243
4. Maartens G, Celum C, Lewin SR. HIV infection: epidemiology, pathogenesis, treatment, and prevention. *Lancet* (2014) 384(9939):258–71. doi:10.1016/S0140-6736(14)60164-1
5. Ortblad KF, Lozano R, Murray CJ. The burden of HIV: insights from the Global Burden of Disease Study 2010. *AIDS* (2013) 27(13):2003–17. doi:10.1097/QAD.0b013e328362ba67
6. Cooper A, Garcia M, Petrovas C, Yamamoto T, Koup RA, Nabel GJ. HIV-1 causes CD4 cell death through DNA-dependent protein kinase during viral integration. *Nature* (2013) 498(7454):376–9. doi:10.1038/nature12274
7. Boasso A, Shearer GM. Chronic innate immune activation as a cause of HIV-1 immunopathogenesis. *Clin Immunol* (2008) 126(3):235–42. doi:10.1016/j.clim.2007.08.015
8. Anwar KP, Malik A, Subhan KH. Profile of candidiasis in HIV infected patients. *Iran J Microbiol* (2012) 4(4):204–9.
9. Park BJ, Wannemuehler KA, Marston BJ, Govender N, Pappas PG, Chiller TM. Estimation of the current global burden of cryptococcal meningitis among persons living with HIV/AIDS. *AIDS* (2009) 23(4):525–30. doi:10.1097/QAD.0b013e328322ffac
10. Rajasingham R, Smith RM, Park BJ, Jarvis JN, Govender NP, Chiller TM, et al. Global burden of disease of HIV-associated cryptococcal meningitis: an updated analysis. *Lancet Infect Dis* (2017) 17(8):873–81. doi:10.1016/S1473-3099(17)30243-8
11. Denning DW, Follansbee SE, Scolaro M, Norris S, Edelstein H, Stevens DA. Pulmonary aspergillosis in the acquired immunodeficiency syndrome. *N Engl J Med* (1991) 324(10):654–62. doi:10.1056/NEJM199103073241003
12. Holding KJ, Dworkin MS, Wan PC, Hanson DL, Klevens RM, Jones JL, et al. Aspergillosis among people infected with human immunodeficiency virus: incidence and survival. Adult and Adolescent Spectrum of HIV Disease Project. *Clin Infect Dis* (2000) 31(5):1253–7. doi:10.1086/317452
13. Lopez C, Fitzgerald PA, Siegal FP. Severe acquired immune deficiency syndrome in male homosexuals: diminished capacity to make interferon-alpha in vitro associated with severe opportunistic infections. *J Infect Dis* (1983) 148(6):962–6. doi:10.1093/infdis/148.6.962
14. McKenna K, Beignon AS, Bhardwaj N. Plasmacytoid dendritic cells: linking innate and adaptive immunity. *J Virol* (2005) 79(1):17–27. doi:10.1128/JVI.79.1.17-27.2005
15. Fitzgerald-Bocarsly P, Dai J, Singh S. Plasmacytoid dendritic cells and type I IFN: 50 years of convergent history. *Cytokine Growth Factor Rev* (2008) 19(1):3–19. doi:10.1016/j.cytogfr.2007.10.006
16. Fitzgerald-Bocarsly P, Jacobs ES. Plasmacytoid dendritic cells in HIV infection: striking a delicate balance. *J Leukoc Biol* (2010) 87(4):609–20. doi:10.1189/jlb.0909635

17. Kadowaki N, Ho S, Antonenko S, Malefyt RW, Kastelein RA, Bazan F, et al. Subsets of human dendritic cell precursors express different toll-like receptors and respond to different microbial antigens. *J Exp Med* (2001) 194(6):863–9. doi:10.1084/jem.194.6.863
18. Krug A, Towarowski A, Britsch S, Rothenfusser S, Hornung V, Bals R, et al. Toll-like receptor expression reveals CpG DNA as a unique microbial stimulus for plasmacytoid dendritic cells which synergizes with CD40 ligand to induce high amounts of IL-12. *Eur J Immunol* (2001) 31(10):3026–37. doi:10.1002/1521-4141(2001010)31:10<3026::AID-IMMU3026>3.0.CO;2-H
19. McMichael AJ, Rowland-Jones SL. Cellular immune responses to HIV. *Nature* (2001) 410(6831):980–7. doi:10.1038/35073658
20. Douek DC, Picker LJ, Koup RA. T cell dynamics in HIV-1 infection. *Annu Rev Immunol*(2003)21:265–304.doi:10.1146/annurev.immunol.21.120601.141053
21. O'Brien M, Manches O, Bhardwaj N. Plasmacytoid dendritic cells in HIV infection. *Adv Exp Med Biol* (2013) 762:71–107. doi:10.1007/978-1-4614-4433-6_3
22. Schmidt B, Fujimura SH, Martin JN, Levy JA. Variations in plasmacytoid dendritic cell (PDC) and myeloid dendritic cell (MDC) levels in HIV-infected subjects on and off antiretroviral therapy. *J Clin Immunol* (2006) 26(1):55–64. doi:10.1007/s10875-006-8401-3
23. Zabel BA, Silverio AM, Butcher EC. Chemokine-like receptor 1 expression and chemerin-directed chemotaxis distinguish plasmacytoid from myeloid dendritic cells in human blood. *J Immunol* (2005) 174(1):244–51. doi:10.4049/jimmunol.174.1.244
24. Lande R, Gilliet M. Plasmacytoid dendritic cells: key players in the initiation and regulation of immune responses. *Ann N Y Acad Sci* (2010) 1183:89–103. doi:10.1111/j.1749-6632.2009.05152.x
25. Bargatze RF, Jutila MA, Butcher EC. Distinct roles of L-selectin and integrins alpha 4 beta 7 and LFA-1 in lymphocyte homing to Peyer's patch-HEV in situ: the multistep model confirmed and refined. *Immunity* (1995) 3(1):99–108. doi:10.1016/1074-7613(95)90162-0
26. Krug A, French AR, Barchet W, Fischer JA, Dzionek A, Pingel JT, et al. TLR9-dependent recognition of MCMV by IPC and DC generates coordinated cytokine responses that activate antiviral NK cell function. *Immunity* (2004) 21(1):107–19. doi:10.1016/j.immuni.2004.06.007
27. Beignon AS, McKenna K, Skoberne M, Manches O, DaSilva I, Kavanagh DG, et al. Endocytosis of HIV-1 activates plasmacytoid dendritic cells via toll-like receptor-viral RNA interactions. *J Clin Invest* (2005) 115(11):3265–75. doi:10.1172/JCI26032
28. Gibson SJ, Lindh JM, Riter TR, Gleason RM, Rogers LM, Fuller AE, et al. Plasmacytoid dendritic cells produce cytokines and mature in response to the TLR7 agonists, imiquimod and resiquimod. *Cell Immunol* (2002) 218(1–2):74–86. doi:10.1016/S0008-8749(02)00517-8
29. Colak E, Leslie A, Zausmer K, Khatamzas E, Kubarenko AV, Pichulik T, et al. RNA and imidazoquinolines are sensed by distinct TLR7/8 ectodomain sites resulting in functionally disparate signaling events. *J Immunol* (2014) 192(12):5963–73. doi:10.4049/jimmunol.1303058
30. Honda K, Yanai H, Negishi H, Asagiri M, Sato M, Mizutani T, et al. IRF-7 is the master regulator of type-I interferon-dependent immune responses. *Nature* (2005) 434(7034):772–7. doi:10.1038/nature03464
31. Hornung V, Schlender J, Guenthner-Biller M, Rothenfusser S, Endres S, Conzelmann KK, et al. Replication-dependent potent IFN-alpha induction in human plasmacytoid dendritic cells by a single-stranded RNA virus. *J Immunol* (2004) 173(10):5935–43. doi:10.4049/jimmunol.173.10.5935
32. Hochrein H, Schlatter B, O'Keeffe M, Wagner C, Schmitz F, Schiemann M, et al. Herpes simplex virus type-1 induces IFN-alpha production via toll-like receptor 9-dependent and -independent pathways. *Proc Natl Acad Sci U S A* (2004) 101(31):11416–21. doi:10.1073/pnas.0403555101
33. Izaguirre A, Barnes BJ, Amrute S, Yeow WS, Megjugorac N, Dai J, et al. Comparative analysis of IRF and IFN-alpha expression in human plasmacytoid and monocyte-derived dendritic cells. *J Leukoc Biol* (2003) 74(6):1125–38. doi:10.1189/jlb.0603255
34. O'Brien M, Manches O, Sabado RL, Baranda SJ, Wang Y, Marie I, et al. Spatiotemporal trafficking of HIV in human plasmacytoid dendritic cells defines a persistently IFN-alpha-producing and partially matured phenotype. *J Clin Invest* (2011) 121(3):1088–101. doi:10.1172/JCI44960
35. Dai J, Megjugorac NJ, Amrute SB, Fitzgerald-Bocarsly P. Regulation of IFN regulatory factor-7 and IFN-alpha production by enveloped virus and lipopolysaccharide in human plasmacytoid dendritic cells. *J Immunol* (2004) 173(3):1535–48. doi:10.4049/jimmunol.173.3.1535
36. Fuchsberger M, Hochrein H, O'Keeffe M. Activation of plasmacytoid dendritic cells. *Immunol Cell Biol* (2005) 83(5):571–7. doi:10.1111/j.1440-1711.2005.01392.x
37. Decalf J, Fernandes S, Longman R, Ahloulay M, Audat F, Lefrerre F, et al. Plasmacytoid dendritic cells initiate a complex chemokine and cytokine network and are a viable drug target in chronic HCV patients. *J Exp Med* (2007) 204(10):2423–37. doi:10.1084/jem.20070814
38. Yin Z, Dai J, Deng J, Sheikh F, Natalia M, Shih T, et al. Type III IFNs are produced by and stimulate human plasmacytoid dendritic cells. *J Immunol* (2012) 189(6):2735–45. doi:10.4049/jimmunol.1102038
39. Feldman M, Fitzgerald-Bocarsly P. Sequential enrichment and immunocytochemical visualization of human interferon-alpha-producing cells. *J Interferon Res* (1990) 10(4):435–46. doi:10.1089/jir.1990.10.435
40. Siegal FP, Kadowaki N, Shodell M, Fitzgerald-Bocarsly PA, Shah K, Ho S, et al. The nature of the principal type 1 interferon-producing cells in human blood. *Science* (1999) 284(5421):1835–7. doi:10.1126/science.284.5421.1835
41. Liu Y-J. IPC: professional type 1 interferon-producing cells and plasmacytoid dendritic cell precursors. *Annu Rev Immunol* (2005) 23:275–306. doi:10.1146/annurev.immunol.23.021704.115633
42. Ito T, Kanzler H, Duramad O, Cao W, Liu YJ. Specialization, kinetics, and repertoire of type 1 interferon responses by human plasmacytoid predendritic cells. *Blood* (2006) 107(6):2423–31. doi:10.1182/blood-2005-07-2709
43. Novick D, Cohen B, Rubinstein M. The human interferon alpha/beta receptor: characterization and molecular cloning. *Cell* (1994) 77(3):391–400. doi:10.1016/0092-8674(94)90154-6
44. Biron CA. Role of early cytokines, including alpha and beta interferons (IFN-a/b), in innate and adaptive immune responses to viral infections. *Semin Immunol* (1998) 10:383–90. doi:10.1006/smim.1998.0138
45. Fitzgerald-Bocarsly P, Feng D. The role of type I interferon production by dendritic cells in host defense. *Biochimie* (2007) 89(6–7):843–55. doi:10.1016/j.biochi.2007.04.018
46. Ito T, Amakawa R, Inaba M, Ikehara S, Inaba K, Fukuhara S. Differential regulation of human blood dendritic cell subsets by IFNs. *J Immunol* (2001) 166(5):2961–9. doi:10.4049/jimmunol.166.5.2961
47. Schmidt B, Ashlock BM, Foster H, Fujimura SH, Levy JA. HIV-infected cells are major inducers of plasmacytoid dendritic cell interferon production, maturation, and migration. *Virology* (2005) 343(2):256–66. doi:10.1016/j.virol.2005.09.059
48. Honda K, Sakaguchi S, Nakajima C, Watanabe A, Yanai H, Matsumoto M, et al. Selective contribution of IFN-alpha/beta signaling to the maturation of dendritic cells induced by double-stranded RNA or viral infection. *Proc Natl Acad Sci U S A* (2003) 100(19):10872–7. doi:10.1073/pnas.1934678100
49. Brinkmann V, Geiger T, Alkan S, Heusser CH. Interferon alpha increases the frequency of interferon gamma-producing human CD4+ T cells. *J Exp Med* (1993) 178(5):1655–63. doi:10.1084/jem.178.5.1655
50. Cella M, Facchetti F, Lanzavecchia A, Colonna M. Plasmacytoid dendritic cells activated by influenza virus and CD40L drive a potent TH1 polarization. *Nat Immunol* (2000) 1(4):305–10. doi:10.1038/79747
51. Rothenfusser S, Hornung V, Ayyoub M, Britsch S, Towarowski A, Krug A, et al. CpG-A and CpG-B oligonucleotides differentially enhance human peptide-specific primary and memory CD8+ T-cell responses in vitro. *Blood* (2004) 103(6):2162–9. doi:10.1182/blood-2003-04-1091
52. Yoneyama H, Matsuno K, Toda E, Nishiwaki T, Matsuo N, Nakano A, et al. Plasmacytoid DCs help lymph node DCs to induce anti-HSV CTLs. *J Exp Med* (2005) 202(3):425–35. doi:10.1084/jem.20041961
53. Niessner A, Sato K, Chaikof EL, Colmegna I, Goronzy JJ, Weyand CM. Pathogen-sensing plasmacytoid dendritic cells stimulate cytotoxic T-cell function in the atherosclerotic plaque through interferon-alpha. *Circulation* (2006) 114(23):2482–9. doi:10.1161/CIRCULATIONAHA.106.642801
54. Dikopoulos N, Bertoletti A, Kroger A, Hauser H, Schirmbeck R, Reimann J. Type I IFN negatively regulates CD8+ T cell responses through IL-10-producing CD4+ T regulatory 1 cells. *J Immunol* (2005) 174(1):99–109. doi:10.4049/jimmunol.174.1.99
55. Le Bon A, Schiavoni G, D'Agostino G, Gresser I, Belardelli F, Tough DF. Type I interferons potently enhance humoral immunity and can promote isotype switching by stimulating dendritic cells in vivo. *Immunity* (2001) 14(4):461–70. doi:10.1016/S1074-7613(01)00126-1
56. Ank N, Iversen MB, Bartholdy C, Staeheli P, Hartmann R, Jensen UB, et al. An important role for type III interferon (IFN-lambda/IL-28)

in TLR-induced antiviral activity. *J Immunol* (2008) 180(4):2474–85. doi:10.4049/jimmunol.180.4.2474
57. Ank N, West H, Bartholdy C, Eriksson K, Thomsen AR, Paludan SR. Lambda interferon (IFN-lambda), a type III IFN, is induced by viruses and IFNs and displays potent antiviral activity against select virus infections in vivo. *J Virol* (2006) 80(9):4501–9. doi:10.1128/JVI.80.9.4501-4509.2006
58. Onoguchi K, Yoneyama M, Takemura A, Akira S, Taniguchi T, Namiki H, et al. Viral infections activate types I and III interferon genes through a common mechanism. *J Biol Chem* (2007) 282(10):7576–81. doi:10.1074/jbc.M608618200
59. Sommereyns C, Paul S, Staeheli P, Michiels T. IFN-lambda (IFN-lambda) is expressed in a tissue-dependent fashion and primarily acts on epithelial cells in vivo. *PLoS Pathog* (2008) 4(3):e1000017. doi:10.1371/journal.ppat.1000017
60. Mennechet FJ, Uze G. Interferon-lambda-treated dendritic cells specifically induce proliferation of FOXP3-expressing suppressor T cells. *Blood* (2006) 107(11):4417–23. doi:10.1182/blood-2005-10-4129
61. Jordan WJ, Eskdale J, Srinivas S, Pekarek V, Kelner D, Rodia M, et al. Human interferon lambda-1 (IFN-lambda1/IL-29) modulates the Th1/Th2 response. *Genes Immun* (2007) 8(3):254–61. doi:10.1038/sj.gene.6364382
62. Bordi L, Lalle E, Lapa D, Caglioti C, Quartu S, Capobianchi MR, et al. Type III interferon (IFN-lambda) antagonizes the antiviral activity of interferon-alpha in vitro. *J Biol Regul Homeost Agents* (2013) 27(4):1001–9.
63. Megjugorac NJ, Young HA, Amrute SB, Olshalsky SL, Fitzgerald-Bocarsly P. Virally stimulated plasmacytoid dendritic cells produce chemokines and induce migration of T and NK cells. *J Leukoc Biol* (2004) 75(3):504–14. doi:10.1189/jlb.0603291
64. Piqueras B, Connolly J, Freitas H, Palucka AK, Banchereau J. Upon viral exposure, myeloid and plasmacytoid dendritic cells produce 3 waves of distinct chemokines to recruit immune effectors. *Blood* (2006) 107(7):2613–8. doi:10.1182/blood-2005-07-2965
65. Colonna M, Trinchieri G, Liu YJ. Plasmacytoid dendritic cells in immunity. *Nat Immunol* (2004) 5(12):1219–26. doi:10.1038/ni1141
66. Fanning SL, George TC, Feng D, Feldman SB, Megjugorac NJ, Izaguirre AG, et al. Receptor cross-linking on human plasmacytoid dendritic cells leads to the regulation of IFN-alpha production. *J Immunol* (2006) 177(9):5829–39. doi:10.4049/jimmunol.177.9.5829
67. Villadangos JA, Young L. Antigen-presentation properties of plasmacytoid dendritic cells. *Immunity* (2008) 29(3):352–61. doi:10.1016/j.immuni.2008.09.002
68. Sadaka C, Marloie-Provost MA, Soumelis V, Benaroch P. Developmental regulation of MHC II expression and transport in human plasmacytoid-derived dendritic cells. *Blood* (2009) 113(10):2127–35. doi:10.1182/blood-2008-10-178152
69. Tel J, Smits EL, Anguille S, Joshi RN, Figdor CG, de Vries IJ. Human plasmacytoid dendritic cells are equipped with antigen-presenting and tumoricidal capacities. *Blood* (2012) 120(19):3936–44. doi:10.1182/blood-2012-06-435941
70. Milone MC, Fitzgerald-Bocarsly P. The mannose receptor mediates induction of IFN-alpha in peripheral blood dendritic cells by enveloped RNA and DNA viruses. *J Immunol* (1998) 161(5):2391–9.
71. Seeds RE, Gordon S, Miller JL. Characterisation of myeloid receptor expression and interferon alpha/beta production in murine plasmacytoid dendritic cells by flow cytomtery. *J Immunol Methods* (2009) 350(1–2):106–17. doi:10.1016/j.jim.2009.07.016
72. Hole CR, Leopold Wager CM, Mendiola AS, Wozniak KL, Campuzano A, Lin X, et al. Antifungal activity of plasmacytoid dendritic cells against *Cryptococcus neoformans* in vitro requires expression of dectin-3 (CLEC4D) and reactive oxygen species. *Infect Immun* (2016) 84(9):2493–504. doi:10.1128/IAI.00103-16
73. Siegal FP, Lopez C, Fitzgerald PA, Shah K, Baron P, Leiderman IZ, et al. Opportunistic infections in acquired immune deficiency syndrome result from synergistic defects of both the natural and adaptive components of cellular immunity. *J Clin Invest* (1986) 78(1):115–23. doi:10.1172/JCI112539
74. Howell DM, Feldman SB, Kloser P, Fitzgerald-Bocarsly P. Decreased frequency of functional natural interferon-producing cells in peripheral blood of patients with the acquired immune deficiency syndrome. *Clin Immunol Immunopathol* (1994) 71(2):223–30. doi:10.1006/clin.1994.1076
75. Feldman SB, Milone MC, Kloser P, Fitzgerald-Bocarsly P. Functional deficiencies in two distinct interferon alpha-producing cell populations in peripheral blood mononuclear cells from human immunodeficiency virus seropositive patients. *J Leukoc Biol* (1995) 57(2):214–20.
76. Feldman S, Stein D, Amrute S, Denny T, Garcia Z, Kloser P, et al. Decreased interferon-alpha production in HIV-infected patients correlates with numerical and functional deficiencies in circulating type 2 dendritic cell precursors. *Clin Immunol* (2001) 101(2):201–10. doi:10.1006/clim.2001.5111
77. Soumelis V, Scott I, Gheyas F, Bouhour D, Cozon G, Cotte L, et al. Depletion of circulating natural type 1 interferon-producing cells in HIV-infected AIDS patients. *Blood* (2001) 98(4):906–12. doi:10.1182/blood.V98.4.906
78. Donaghy H, Pozniak A, Gazzard B, Qazi N, Gilmour J, Gotch F, et al. Loss of blood CD11c(+) myeloid and CD11c(-) plasmacytoid dendritic cells in patients with HIV-1 infection correlates with HIV-1 RNA virus load. *Blood* (2001) 98(8):2574–6. doi:10.1182/blood.V98.8.2574
79. Chehimi J, Azzoni L, Farabaugh M, Creer SA, Tomescu C, Hancock A, et al. Baseline viral load and immune activation determine the extent of reconstitution of innate immune effectors in HIV-1-infected subjects undergoing antiretroviral treatment. *J Immunol* (2007) 179(4):2642–50. doi:10.4049/jimmunol.179.4.2642
80. Malleret B, Maneglier B, Karlsson I, Lebon P, Nascimbeni M, Perie L, et al. Primary infection with simian immunodeficiency virus: plasmacytoid dendritic cell homing to lymph nodes, type I interferon, and immune suppression. *Blood* (2008) 112(12):4598–608. doi:10.1182/blood-2008-06-162651
81. Brown KN, Wijewardana V, Liu X, Barratt-Boyes SM. Rapid influx and death of plasmacytoid dendritic cells in lymph nodes mediate depletion in acute simian immunodeficiency virus infection. *PLoS Pathog* (2009) 5(5):e1000413. doi:10.1371/journal.ppat.1000413
82. Lehmann C, Lafferty M, Garzino-Demo A, Jung N, Hartmann P, Fatkenheuer G, et al. Plasmacytoid dendritic cells accumulate and secrete interferon alpha in lymph nodes of HIV-1 patients. *PLoS One* (2010) 5(6):e11110. doi:10.1371/journal.pone.0011110
83. Patterson S, Rae A, Hockey N, Gilmour J, Gotch F. Plasmacytoid dendritic cells are highly susceptible to human immunodeficiency virus type 1 infection and release infectious virus. *J Virol* (2001) 75(14):6710–3. doi:10.1128/JVI.75.14.6710-6713.2001
84. Schmidt B, Scott I, Whitmore RG, Foster H, Fujimura S, Schmitz J, et al. Low-level HIV infection of plasmacytoid dendritic cells: onset of cytopathic effects and cell death after PDC maturation. *Virology* (2004) 329(2):280–8. doi:10.1016/j.virol.2004.08.016
85. Wijewardana V, Brown KN, Barratt-Boyes SM. Studies of plasmacytoid dendritic cell dynamics in simian immunodeficiency virus infection of nonhuman primates provide insights into HIV pathogenesis. *Curr HIV Res* (2009) 7(1):23–9. doi:10.2174/157016209787048483
86. Barron MA, Blyveis N, Palmer BE, MaWhinney S, Wilson CC. Influence of plasma viremia on defects in number and immunophenotype of blood dendritic cell subsets in human immunodeficiency virus 1-infected individuals. *J Infect Dis* (2003) 187(1):26–37. doi:10.1086/345957
87. Khaitan A, Unutmaz D. Revisiting immune exhaustion during HIV infection. *Curr HIV/AIDS Rep* (2011) 8(1):4–11. doi:10.1007/s11904-010-0066-0
88. Li G, Cheng M, Nunoya J, Cheng L, Guo H, Yu H, et al. Plasmacytoid dendritic cells suppress HIV-1 replication but contribute to HIV-1 induced immunopathogenesis in humanized mice. *PLoS Pathog* (2014) 10(7):e1004291. doi:10.1371/journal.ppat.1004291
89. Donaghy H, Gazzard B, Gotch F, Patterson S. Dysfunction and infection of freshly isolated blood myeloid and plasmacytoid dendritic cells in patients infected with HIV-1. *Blood* (2003) 101(11):4505–11. doi:10.1182/blood-2002-10-3189
90. Dillon SM, Robertson KB, Pan SC, Mawhinney S, Meditz AL, Folkvord JM, et al. Plasmacytoid and myeloid dendritic cells with a partial activation phenotype accumulate in lymphoid tissue during asymptomatic chronic HIV-1 infection. *J Acquir Immune Defic Syndr* (2008) 48(1):1–12. doi:10.1097/QAI.0b013e3181664b60
91. Martinson JA, Roman-Gonzalez A, Tenorio AR, Montoya CJ, Gichinga CN, Rugeles MT, et al. Dendritic cells from HIV-1 infected individuals are less responsive to toll-like receptor (TLR) ligands. *Cell Immunol* (2007) 250(1–2):75–84. doi:10.1016/j.cellimm.2008.01.007
92. Moseman EA, Liang X, Dawson AJ, Panoskaltsis-Mortari A, Krieg AM, Liu YJ, et al. Human plasmacytoid dendritic cells activated by CpG oligodeoxynucleotides induce the generation of CD4+CD25+ regulatory T cells. *J Immunol* (2004) 173(7):4433–42. doi:10.4049/jimmunol.173.7.4433

93. Gilliet M, Liu YJ. Generation of human CD8 T regulatory cells by CD40 ligand-activated plasmacytoid dendritic cells. *J Exp Med* (2002) 195(6): 695–704. doi:10.1084/jem.20011603
94. Boasso A, Herbeuval JP, Hardy AW, Anderson SA, Dolan MJ, Fuchs D, et al. HIV inhibits CD4+ T-cell proliferation by inducing indoleamine 2,3-dioxygenase in plasmacytoid dendritic cells. *Blood* (2007) 109(8): 3351–9. doi:10.1182/blood-2006-07-034785
95. Munn DH, Shafizadeh E, Attwood JT, Bondarev I, Pashine A, Mellor AL. Inhibition of T cell proliferation by macrophage tryptophan catabolism. *J Exp Med* (1999) 189(9):1363–72. doi:10.1084/jem.189.9.1363
96. Baban B, Chandler PR, Sharma MD, Pihkala J, Koni PA, Munn DH, et al. IDO activates regulatory T cells and blocks their conversion into Th17-like T cells. *J Immunol* (2009) 183(4):2475–83. doi:10.4049/jimmunol.0900986
97. Romani L. Immunity to fungal infections. *Nat Rev Immunol* (2011) 11:275–88. doi:10.1038/nri2939
98. Vallabhaneni S, Mody RK, Walker T, Chiller T. The global burden of fungal diseases. *Infect Dis Clin North Am* (2016) 30(1):1–11. doi:10.1016/j.idc.2015.10.004
99. Tronchin G, Bouchara JP, Ferron M, Larcher G, Chabasse D. Cell surface properties of *Aspergillus fumigatus* conidia: correlation between adherence, agglutination, and rearrangements of the cell wall. *Can J Microbiol* (1995) 41(8):714–21. doi:10.1139/m95-098
100. van de Veerdonk FL, Kullberg BJ, van der Meer JW, Gow NA, Netea MG. Host-microbe interactions: innate pattern recognition of fungal pathogens. *Curr Opin Microbiol* (2008) 11(4):305–12. doi:10.1016/j.mib.2008.06.002
101. Hohl TM, Van Epps HL, Rivera A, Morgan LA, Chen PL, Feldmesser M, et al. *Aspergillus fumigatus* triggers inflammatory responses by stage-specific beta-glucan display. *PLoS Pathog* (2005) 1(3):e30. doi:10.1371/journal.ppat.0010030
102. Latge JP. Tasting the fungal cell wall. *Cell Microbiol* (2010) 12(7):863–72. doi:10.1111/j.1462-5822.2010.01474.x
103. Levitz SM. Innate recognition of fungal cell walls. *PLoS Pathog* (2010) 6(4):e1000758. doi:10.1371/journal.ppat.1000758
104. Hamad M. Innate and adaptive antifungal immune responses: partners on an equalfooting.*Mycoses*(2011)55:205–17.doi:10.1111/j.1439-0507.2011.02078.x
105. Brown GD. Innate antifungal immunity: the key role of phagocytes. *Annu Rev Immunol* (2011) 29:1–21. doi:10.1146/annurev-immunol-030409-101229
106. Hohl TM, Feldmesser M. *Aspergillus fumigatus*: principles of pathogenesis and host defense. *Eukaryot Cell* (2007) 6(11):1953–63. doi:10.1128/EC.00274-07
107. Bruns S, Kniemeyer O, Hasenberg M, Aimanianda V, Nietzsche S, Thywissen A, et al. Production of extracellular traps against *Aspergillus fumigatus* in vitro and in infected lung tissue is dependent on invading neutrophils and influenced by hydrophobin RodA. *PLoS Pathog* (2010) 6(4):e1000873. doi:10.1371/journal.ppat.1000873
108. Bozza S, Gaziano R, Spreca A, Bacci A, Montagnoli C, di Francesco P, et al. Dendritic cells transport conidia and hyphae of *Aspergillus fumigatus* from the airways to the draining lymph nodes and initiate disparate Th responses to the fungus. *J Immunol* (2002) 168(3):1362–71. doi:10.4049/jimmunol.168.3.1362
109. Huang H, Ostroff GR, Lee CK, Wang JP, Specht CA, Levitz SM. Distinct patterns of dendritic cell cytokine release stimulated by fungal beta-glucans and toll-like receptor agonists. *Infect Immun* (2009) 77(5):1774–81. doi:10.1128/IAI.00086-09
110. Roy RM, Klein BS. Dendritic cells in antifungal immunity and vaccine design. *Cell Host Microbe* (2012) 11(5):436–46. doi:10.1016/j.chom.2012.04.005
111. Peck A, Mellins ED. Precarious balance: Th17 cells in host defense. *Infect Immun* (2010) 78(1):32–8. doi:10.1128/IAI.00929-09
112. Puel A, Cypowyj S, Marodi L, Abel L, Picard C, Casanova JL. Inborn errors of human IL-17 immunity underlie chronic mucocutaneous candidiasis. *Curr Opin Allergy Clin Immunol* (2012) 12(6):616–22. doi:10.1097/ACI.0b013e328358cc0b
113. Ling Y, Puel A. IL-17 and infections. *Actas Dermosifiliogr* (2014) 105(Suppl 1): 34–40. doi:10.1016/S0001-7310(14)70016-X
114. Spellberg B, Ibrahim AS, Lin L, Avanesian V, Fu Y, Lipke P, et al. Antibody titer threshold predicts anti-candidal vaccine efficacy even though the mechanism of protection is induction of cell-mediated immunity. *J Infect Dis* (2008) 197(7):967–71. doi:10.1086/529204
115. Medzhitov R, Preston-Hurlburt P, Janeway CA Jr. A human homologue of the *Drosophila* toll protein signals activation of adaptive immunity. *Nature* (1997) 388(6640):394–7. doi:10.1038/41131
116. Netea MG, Van Der Graaf CA, Vonk AG, Verschueren I, Van Der Meer JW, Kullberg BJ. The role of toll-like receptor (TLR) 2 and TLR4 in the host defense against disseminated candidiasis. *J Infect Dis* (2002) 185(10):1483–9. doi:10.1086/340511
117. Mambula SS, Sau K, Henneke P, Golenbock DT, Levitz SM. Toll-like receptor (TLR) signaling in response to *Aspergillus fumigatus*. *J Biol Chem* (2002) 277(42):39320–6. doi:10.1074/jbc.M201683200
118. Bellocchio S, Montagnoli C, Bozza S, Gaziano R, Rossi G, Mambula SS, et al. The contribution of the toll-like/IL-1 receptor superfamily to innate and adaptive immunity to fungal pathogens in vivo. *J Immunol* (2004) 172(5):3059–69. doi:10.4049/jimmunol.172.5.3059
119. Ding K, Shibui A, Wang Y, Takamoto M, Matsuguchi T, Sugane K. Impaired recognition by toll-like receptor 4 is responsible for exacerbated murine *Pneumocystis* pneumonia. *Microbes Infect* (2005) 7(2):195–203. doi:10.1016/j.micinf.2004.10.010
120. Nakamura K, Miyagi K, Koguchi Y, Kinjo Y, Uezu K, Kinjo T, et al. Limited contribution of toll-like receptor 2 and 4 to the host response to a fungal infectious pathogen, *Cryptococcus neoformans*. *FEMS Immunol Med Microbiol* (2006) 47(1):148–54. doi:10.1111/j.1574-695X.2006.00078.x
121. Botos I, Segal DM, Davies DR. The structural biology of toll-like receptors. *Structure* (2011) 19(4):447–59. doi:10.1016/j.str.2011.02.004
122. Ramirez-Ortiz ZG, Specht CA, Wang JP, Lee CK, Bartholomeu DC, Gazzinelli RT, et al. Toll-like receptor 9-dependent immune activation by unmethylated CpG motifs in *Aspergillus fumigatus* DNA. *Infect Immun* (2008) 76(5):2123–9. doi:10.1128/IAI.00047-08
123. Nakamura K, Miyazato A, Xiao G, Hatta M, Inden K, Aoyagi T, et al. Deoxynucleic acids from *Cryptococcus neoformans* activate myeloid dendritic cells via a TLR9-dependent pathway. *J Immunol* (2008) 180(6):4067–74. doi:10.4049/jimmunol.180.6.4067
124. Picard C, von Bernuth H, Ghandil P, Chrabieh M, Levy O, Arkwright PD, et al. Clinical features and outcome of patients with IRAK-4 and MyD88 deficiency. *Medicine (Baltimore)* (2010) 89(6):403–25. doi:10.1097/MD.0b013e3181fd8ec3
125. Vautier S, Sousa Mda G, Brown GD. C-type lectins, fungi and Th17 responses. *Cytokine Growth Factor Rev* (2010) 21(6):405–12. doi:10.1016/j.cytogfr.2010.10.001
126. Brown GD, Gordon S. Immune recognition. A new receptor for beta-glucans. *Nature* (2001) 413(6851):36–7. doi:10.1038/35092620
127. Odabasi Z, Paetznick VL, Rodriguez JR, Chen E, McGinnis MR, Ostrosky-Zeichner L. Differences in beta-glucan levels in culture supernatants of a variety of fungi. *Med Mycol* (2006) 44(3):267–72. doi:10.1080/13693780500474327
128. Dennehy KM, Brown GD. The role of the beta-glucan receptor Dectin-1 in control of fungal infection. *J Leukoc Biol* (2007) 82(2):253–8. doi:10.1189/jlb.1206753
129. Seeds RE, Mukhopadhyay S, Jones IM, Gordon S, Miller JL. The role of myeloid receptors on murine plasmacytoid dendritic cells in induction of type I interferon. *Int Immunopharmacol* (2011) 11(7):794–801. doi:10.1016/j.intimp.2011.01.013
130. Rhein J, Bahr NC, Morawski BM, Schutz C, Zhang Y, Finkelman M, et al. Detection of high cerebrospinal fluid levels of (1 – >3)-beta-d-Glucan in cryptococcal meningitis. *Open Forum Infect Dis* (2014) 1(3):ofu105. doi:10.1093/ofid/ofu052.1014
131. Gross O, Gewies A, Finger K, Schafer M, Sparwasser T, Peschel C, et al. Card9 controls a non-TLR signalling pathway for innate anti-fungal immunity. *Nature* (2006) 442(7103):651–6. doi:10.1038/nature04926
132. Drummond RA, Lionakis MS. Mechanistic insights into the role of C-type lectin receptor/CARD9 signaling in human antifungal immunity. *Front Cell Infect Microbiol* (2016) 6:39. doi:10.3389/fcimb.2016.00039
133. Drewniak A, Gazendam RP, Tool AT, van Houdt M, Jansen MH, van Hamme JL, et al. Invasive fungal infection and impaired neutrophil killing in human CARD9 deficiency. *Blood* (2013) 121(13):2385–92. doi:10.1182/blood-2012-08-450551
134. Alves de Medeiros AK, Lodewick E, Bogaert DJ, Haerynck F, Daele S. Van, Lambrecht B, et al. Chronic and invasive fungal infections in a family with CARD9 deficiency. *J Clin Immunol* (2016) 36(3):204–9. doi:10.1007/s10875-016-0255-8

135. Uematsu T, Iizasa E, Kobayashi N, Yoshida H, Hara H. Loss of CARD9-mediated innate activation attenuates severe influenza pneumonia without compromising host viral immunity. *Sci Rep* (2015) 5:17577. doi:10.1038/srep17577
136. Gringhuis SI, den Dunnen J, Litjens M, van der Vlist M, Wevers B, Bruijns SC, et al. Dectin-1 directs T helper cell differentiation by controlling noncanonical NF-kappaB activation through Raf-1 and Syk. *Nat Immunol* (2009) 10(2):203–13. doi:10.1038/ni.1692
137. Herre J, Marshall AS, Caron E, Edwards AD, Williams DL, Schweighoffer E, et al. Dectin-1 uses novel mechanisms for yeast phagocytosis in macrophages. *Blood* (2004) 104(13):4038–45. doi:10.1182/blood-2004-03-1140
138. Hefter M, Lother J, Weiss E, Schmitt AL, Fliesser M, Einsele H, et al. Human primary myeloid dendritic cells interact with the opportunistic fungal pathogen *Aspergillus fumigatus* via the C-type lectin receptor Dectin-1. *Med Mycol* (2017) 55(5):573–8. doi:10.1093/mmy/myw105
139. Gantner BN, Simmons RM, Underhill DM. Dectin-1 mediates macrophage recognition of *Candida albicans* yeast but not filaments. *EMBO J* (2005) 24(6):1277–86. doi:10.1038/sj.emboj.7600594
140. Brown GD. Dectin-1: a signalling non-TLR pattern-recognition receptor. *Nat Rev Immunol* (2006) 6:33–43. doi:10.1038/nri1745
141. Werner JL, Metz AE, Horn D, Schoeb TR, Hewitt MM, Schwiebert LM, et al. Requisite role for the dectin-1 beta-glucan receptor in pulmonary defense against *Aspergillus fumigatus*. *J Immunol* (2009) 182(8):4938–46. doi:10.4049/jimmunol.0804250
142. Rivera A, Hohl TM, Collins N, Leiner I, Gallegos A, Saijo S, et al. Dectin-1 diversifies *Aspergillus fumigatus*-specific T cell responses by inhibiting T helper type 1 CD4 T cell differentiation. *J Exp Med* (2011) 208(2):369–81. doi:10.1084/jem.20100906
143. Drummond RA, Dambuza IM, Vautier S, Taylor JA, Reid DM, Bain CC, et al. CD4(+) T-cell survival in the GI tract requires dectin-1 during fungal infection. *Mucosal Immunol* (2016) 9(2):492–502. doi:10.1038/mi.2015.79
144. McGreal EP, Rosas M, Brown GD, Zamze S, Wong SY, Gordon S, et al. The carbohydrate-recognition domain of Dectin-2 is a C-type lectin with specificity for high mannose. *Glycobiology* (2006) 16(5):422–30. doi:10.1093/glycob/cwj077
145. Sato K, Yang XL, Yudate T, Chung JS, Wu J, Luby-Phelps K, et al. Dectin-2 is a pattern recognition receptor for fungi that couples with the Fc receptor gamma chain to induce innate immune responses. *J Biol Chem* (2006) 281(50):38854–66. doi:10.1074/jbc.M606542200
146. Kerscher B, Willment JA, Brown GD. The Dectin-2 family of C-type lectin-like receptors: an update. *Int Immunol* (2013) 25(5):271–7. doi:10.1093/intimm/dxt006
147. Bi L, Gojestani S, Wu W, Hsu YM, Zhu J, Ariizumi K, et al. CARD9 mediates dectin-2-induced IkappaBalpha kinase ubiquitination leading to activation of NF-kappaB in response to stimulation by the hyphal form of *Candida albicans*. *J Biol Chem* (2010) 285(34):25969–77. doi:10.1074/jbc.M110.131300
148. Drummond RA, Saijo S, Iwakura Y, Brown GD. The role of Syk/CARD9 coupled C-type lectins in antifungal immunity. *Eur J Immunol* (2011) 41(2):276–81. doi:10.1002/eji.201041252
149. Gringhuis SI, Wevers BA, Kaptein TM, van Capel TM, Theelen B, Boekhout T, et al. Selective C-Rel activation via Malt1 controls anti-fungal T(H)-17 immunity by dectin-1 and dectin-2. *PLoS Pathog* (2011) 7(1):e1001259. doi:10.1371/journal.ppat.1001259
150. Robinson MJ, Osorio F, Rosas M, Freitas RP, Schweighoffer E, Gross O, et al. Dectin-2 is a Syk-coupled pattern recognition receptor crucial for Th17 responses to fungal infection. *J Exp Med* (2009) 206(9):2037–51. doi:10.1084/jem.20082818
151. Arce I, Martinez-Munoz L, Roda-Navarro P, Fernandez-Ruiz E. The human C-type lectin CLECSF8 is a novel monocyte/macrophage endocytic receptor. *Eur J Immunol* (2004) 34(1):210–20. doi:10.1002/eji.200324230
152. Zhu LL, Zhao XQ, Jiang C, You Y, Chen XP, Jiang YY, et al. C-type lectin receptors Dectin-3 and Dectin-2 form a heterodimeric pattern-recognition receptor for host defense against fungal infection. *Immunity* (2013) 39(2):324–34. doi:10.1016/j.immuni.2013.05.017
153. Zhao XQ, Zhu LL, Chang Q, Jiang C, You Y, Luo T, et al. C-type lectin receptor dectin-3 mediates trehalose 6,6'-dimycolate (TDM)-induced Mincle expression through CARD9/Bcl10/MALT1-dependent nuclear factor (NF)-kappaB activation. *J Biol Chem* (2014) 289(43):30052–62. doi:10.1074/jbc.M114.588574
154. Graham LM, Gupta V, Schafer G, Reid DM, Kimberg M, Dennehy KM, et al. The C-type lectin receptor CLECSF8 (CLEC4D) is expressed by myeloid cells and triggers cellular activation through Syk kinase. *J Biol Chem* (2012) 287(31):25964–74. doi:10.1074/jbc.M112.384164
155. Wang T, Pan D, Zhou Z, You Y, Jiang C, Zhao X, et al. Dectin-3 deficiency promotes colitis development due to impaired antifungal innate immune responses in the Gut. *PLoS Pathog* (2016) 12(6):e1005662. doi:10.1371/journal.ppat.1005662
156. Campuzano A, Castro-Lopez N, Wozniak KL, Leopold Wager CM, Wormley FL Jr. Dectin-3 is not required for protection against *Cryptococcus neoformans* infection. *PLoS One* (2017) 12(1):e0169347. doi:10.1371/journal.pone.0169347
157. Ezekowitz RA, Sastry K, Bailly P, Warner A. Molecular characterization of the human macrophage mannose receptor: demonstration of multiple carbohydrate recognition-like domains and phagocytosis of yeasts in Cos-1 cells. *J Exp Med* (1990) 172(6):1785–94. doi:10.1084/jem.172.6.1785
158. Gazi U, Martinez-Pomares L. Influence of the mannose receptor in host immune responses. *Immunobiology* (2009) 214(7):554–61. doi:10.1016/j.imbio.2008.11.004
159. Martinez-Pomares L. The mannose receptor. *J Leukoc Biol* (2012) 92(6):1177–86. doi:10.1189/jlb.0512231
160. Lee SJ, Evers S, Roeder D, Parlow AF, Risteli J, Risteli L, et al. Mannose receptor-mediated regulation of serum glycoprotein homeostasis. *Science* (2002) 295(5561):1898–901. doi:10.1126/science.1069540
161. Napper CE, Drickamer K, Taylor ME. Collagen binding by the mannose receptor mediated through the fibronectin type II domain. *Biochem J* (2006) 395(3):579–86. doi:10.1042/BJ20052027
162. Nguyen DG, Hildreth JE. Involvement of macrophage mannose receptor in the binding and transmission of HIV by macrophages. *Eur J Immunol* (2003) 33(2):483–93. doi:10.1002/immu.200310024
163. Wang Q, Zhao G, Lin J, Li C, Jiang N, Xu Q, et al. Role of the mannose receptor during *Aspergillus fumigatus* infection and interaction with dectin-1 in corneal epithelial cells. *Cornea* (2016) 35(2):267–73. doi:10.1097/ICO.0000000000000710
164. Marodi L, Korchak HM, Johnston RB Jr. Mechanisms of host defense against *Candida* species. I. Phagocytosis by monocytes and monocyte-derived macrophages. *J Immunol* (1991) 146(8):2783–9.
165. Porcaro I, Vidal M, Jouvert S, Stahl PD, Giaimis J. Mannose receptor contribution to *Candida albicans* phagocytosis by murine E-clone J774 macrophages. *J Leukoc Biol* (2003) 74(2):206–15. doi:10.1189/jlb.1202608
166. Dan JM, Kelly RM, Lee CK, Levitz SM. Role of the mannose receptor in a murine model of *Cryptococcus neoformans* infection. *Infect Immun* (2008) 76(6):2362–7. doi:10.1128/IAI.00095-08
167. Ezekowitz RA, Williams DJ, Koziel H, Armstrong MY, Warner A, Richards FF, et al. Uptake of *Pneumocystis carinii* mediated by the macrophage mannose receptor. *Nature* (1991) 351(6322):155–8. doi:10.1038/351155a0
168. Le Cabec V, Emorine LJ, Toesca I, Cougoule C, Maridonneau-Parini I. The human macrophage mannose receptor is not a professional phagocytic receptor. *J Leukoc Biol* (2005) 77(6):934–43. doi:10.1189/jlb.1204705
169. Tachado SD, Zhang J, Zhu J, Patel N, Cushion M, Koziel H. *Pneumocystis*-mediated IL-8 release by macrophages requires coexpression of mannose receptors and TLR2. *J Leukoc Biol* (2007) 81(1):205–11. doi:10.1189/jlb.1005580
170. Dan JM, Wang JP, Lee CK, Levitz SM. Cooperative stimulation of dendritic cells by *Cryptococcus neoformans* mannoproteins and CpG oligodeoxynucleotides. *PLoS One* (2008) 3(4):e2046. doi:10.1371/journal.pone.0002046
171. Romani L, Bistoni F, Gaziano R, Bozza S, Montagnoli C, Perruccio K, et al. Thymosin alpha 1 activates dendritic cells for antifungal Th1 resistance through toll-like receptor signaling. *Blood* (2004) 103(11):4232–9. doi:10.1182/blood-2003-11-4036
172. Perruccio K, Bozza S, Montagnoli C, Bellocchio S, Aversa F, Martelli M, et al. Prospects for dendritic cell vaccination against fungal infections in hematopoietic transplantation. *Blood Cells Mol Dis* (2004) 33(3):248–55. doi:10.1016/j.bcmd.2004.08.011
173. Ramirez-Ortiz ZG, Lee CK, Wang JP, Boon L, Specht CA, Levitz SM. A nonredundant role for plasmacytoid dendritic cells in host defense against

the human fungal pathogen *Aspergillus fumigatus*. *Cell Host Microbe* (2011) 9(5):415–24. doi:10.1016/j.chom.2011.04.007

174. Urban CF, Ermert D, Schmid M, Abu-Abed U, Goosmann C, Nacken W, et al. Neutrophil extracellular traps contain calprotectin, a cytosolic protein complex involved in host defense against *Candida albicans*. *PLoS Pathog* (2009) 5(10):e1000639. doi:10.1371/journal.ppat.1000639
175. Loures FV, Rohm M, Lee CK, Santos E, Wang JP, Specht CA, et al. Recognition of *Aspergillus fumigatus* hyphae by human plasmacytoid dendritic cells is mediated by dectin-2 and results in formation of extracellular traps. *PLoS Pathog* (2015) 11(2):e1004643. doi:10.1371/journal.ppat.1004643
176. Joo H, Upchurch K, Zhang W, Ni L, Li D, Xue Y, et al. Opposing roles of dectin-1 expressed on human plasmacytoid dendritic cells and myeloid dendritic cells in Th2 polarization. *J Immunol* (2015) 195(4):1723–31. doi:10.4049/jimmunol.1402276
177. Gavino AC, Chung JS, Sato K, Ariizumi K, Cruz PD Jr. Identification and expression profiling of a human C-type lectin, structurally homologous to mouse dectin-2. *Exp Dermatol* (2005) 14(4):281–8. doi:10.1111/j.0906-6705.2005.00312.x
178. Lundberg K, Rydnert F, Greiff L, Lindstedt M. Human blood dendritic cell subsets exhibit discriminative pattern recognition receptor profiles. *Immunology* (2014) 142(2):279–88. doi:10.1111/imm.12252

Conflict of Interest Statement: The authors declare that the research was conducted in the absence of any commercial or financial relationships that could be construed as a potential conflict of interest.

Copyright © 2017 Maldonado and Fitzgerald-Bocarsly. This is an open-access article distributed under the terms of the Creative Commons Attribution License (CC BY). The use, distribution or reproduction in other forums is permitted, provided the original author(s) or licensor are credited and that the original publication in this journal is cited, in accordance with accepted academic practice. No use, distribution or reproduction is permitted which does not comply with these terms.

frontiers in Immunology

ORIGINAL RESEARCH
published: 28 September 2017
doi: 10.3389/fimmu.2017.01231

Exploitation of Scavenger Receptor, Macrophage Receptor with Collagenous Structure, by *Cryptococcus neoformans* Promotes Alternative Activation of Pulmonary Lymph Node CD11b$^+$ Conventional Dendritic Cells and Non-Protective Th2 Bias

Jintao Xu[1,2†], Adam Flaczyk[2†], Lori M. Neal[1,2], Zhenzong Fa[2], Daphne Cheng[2], Mike Ivey[2], Bethany B. Moore[1,3], Jeffrey L. Curtis[1,2], John J. Osterholzer[1,2] and Michal A. Olszewski[1,2]*

[1] Division of Pulmonary and Critical Care Medicine, Department of Internal Medicine, University of Michigan Health System, Ann Arbor, MI, United States, [2] Department of Veterans Affairs Health System, VA Ann Arbor Healthcare System (VHA), Ann Arbor, MI, United States, [3] Department of Microbiology and Immunology, University of Michigan Medical School, Ann Arbor, MI, United States

Macrophage receptor with collagenous structure (MARCO) contributes to fungal containment during the early/innate phase of cryptococcal infection; however, its role in adaptive antifungal immunity remains unknown. Using a murine model of cryptococcosis, we compared host adaptive immune responses in wild-type and MARCO$^{-/-}$ mice throughout an extended time course post-infection. Unlike in early infection, MARCO deficiency resulted in improved pulmonary fungal clearance and diminished cryptococcal dissemination during the efferent phase. Improved fungal control in the absence of MARCO expression was associated with enhanced hallmarks of protective Th1-immunity, including higher frequency of pulmonary TNF-α-producing T cells, increased cryptococcal-antigen-triggered IFN-γ and TNF-α production by splenocytes, and enhanced expression of M1 polarization genes by pulmonary macrophages. Concurrently, we found lower frequencies of IL-5- and IL-13-producing T cells in the lungs, impaired production of IL-4 and IL-10 by cryptococcal antigen-pulsed splenocytes, and diminished serum IgE, which were hallmarks of profoundly suppressed efferent Th2 responses in MARCO-deficient mice compared to WT mice. Mechanistically, we found that MARCO expression facilitated early accumulation and alternative activation of CD11b$^+$ conventional DC (cDC) in the lung-associated lymph nodes (LALNs), which contributed to the progressive shift of the immune response from Th1 toward Th2 at the priming site (LALNs) and local infection site (lungs) during the efferent phase of cryptococcal infection. Taken together, our study shows that MARCO can be exploited by the fungal pathogen to promote accumulation and alternative activation of CD11b$^+$ cDC in the LALN, which in turn alters Th1/Th2 balance to promote fungal persistence and dissemination.

Keywords: scavenger receptor macrophage receptor with collagenous structure, fungal persistence, Th2 response, CD11b$^+$ conventional DC, *Cryptococcus neoformans*

OPEN ACCESS

Edited by:
Amariliz Rivera, New Jersey Medical School, United States

Reviewed by:
Bing Zhai, Memorial Sloan Kettering Cancer Center, United States
Joshua J. Obar, Dartmouth College, United States
Floyd Layton Wormley, University of Texas at San Antonio, United States

****Correspondence:***
Michal A. Olszewski
olszewsm@umich.edu

[†]These authors have contributed equally to this work.

Specialty section:
This article was submitted to Microbial Immunology, a section of the journal Frontiers in Immunology

Received: *09 June 2017*
Accepted: *19 September 2017*
Published: *28 September 2017*

Citation:
Xu J, Flaczyk A, Neal LM, Fa Z, Cheng D, Ivey M, Moore BB, Curtis JL, Osterholzer JJ and Olszewski MA (2017) Exploitation of Scavenger Receptor, Macrophage Receptor with Collagenous Structure, by Cryptococcus neoformans Promotes Alternative Activation of Pulmonary Lymph Node CD11b$^+$ Conventional Dendritic Cells and Non-Protective Th2 Bias. Front. Immunol. 8:1231. doi: 10.3389/fimmu.2017.01231

INTRODUCTION

Cryptococcus neoformans is an environmental fungal pathogen that causes severe meningoencephalitis with mortality rates of up to 20–60%, despite the availability of antifungal drugs (1). Cryptococcal infections generally manifest in patients compromised due to HIV infection, cancer, or organ transplantation. However, up to 25% of cases reported in the United States and 60% of cases in China occur in patients without recognizable immune-deficiencies (2, 3). Furthermore, Cryptococci can persist within immune competent hosts for an extended period of time and can reactivate following immune-compromise (4). Increasing evidence suggests that both host immune dysfunction and immune modulation induced by *C. neoformans* contributes to fungal persistence (2, 5–8).

One major way through which *C. neoformans* promotes fungal persistence is by altering $CD4^+$ helper T (Th) cell polarization and subsequent macrophage activation status (9, 10). Virulence factors that contribute to the shift of host responses away from protective Th1 to non-protective Th2 bias correlate with invasive fungal disease severity [reviewed in Ref. (2, 11)]. The absence of protective Th1 cytokines (IFN-γ and TNF-α) and enhanced production of Th2 type cytokines (IL-4, IL-5, and IL-13) facilitate alternative activation of macrophages, which enable intracellular survival and growth of *C. neoformans* (12, 13). Th cell differentiation is orchestrated by antigen-presenting cells. During *C. neoformans* infection, pulmonary $CD11b^+$ conventional DC (cDC) are the primary cellular population responsible for non-protective Th2 cell polarization (14, 15). However, the factors that modulate the migration and activation of $CD11b^+$ cDC during fungal infection are not well understood. Although skewing of Th2 responses is one well-established effect of cryptococcal virulence factors (6–8, 12, 15), very few loopholes in the host immune system that can be exploited by *C. neoformans* to promote non-protective responses have been identified (15–17). Identification of host factors that contribute to non-protective responses and enable fungal persistence may reveal new targets for promoting effective T cell responses that are crucial for combat fungal infections.

Macrophage receptor with collagenous structure (MARCO) (human Gene ID: 8685) is a scavenger receptor that plays important roles in host defense against viral, bacterial, and parasitic infections (18). Our recent study showed that MARCO expression contributes to fungal containment during the innate phase of cryptococcal infection by enhancing production of pro-inflammatory cytokines and recruitment of mononuclear phagocytes to the infection sites (19). Besides its well-studied roles in antibacterial and antifungal innate immunity (20–24), the importance of MARCO in regulating adaptive immunity is being increasingly recognized. Notably, MARCO expression has been shown to regulate morphology, gene expression, and migration of dendritic cell (DC) upon stimulation; thus, MARCO may act as an important link for the initiation and polarization of adaptive responses (25–27). Recent studies support this paradigm and showed that MARCO is involved in the development of T cell-mediated immunity during tumor inflammation and allergic airway responses (28, 29). While the role of MARCO in modulation of adaptive immunity to fungi remains unclear, a previous study by our group demonstrated that another scavenger receptor, scavenger receptor-A (SR-A), can be exploited by *C. neoformans* to support Th2 immune polarization during infection (17). Thus, we hypothesized that MARCO also regulates T cell-mediated immunity during fungal infections, possibly through modulation of DC migration and/or activation.

In the current study, we focused on the roles of MARCO in the adaptive immune response during *C. neoformans* infection. Using a murine model of cryptococcosis, we found that MARCO expression shifts both local and systemic Th responses away from protective Th1 toward non-protective Th2 response with impaired classical activation of macrophages. Thus, MARCO expression contributes to fungal growth and dissemination during the efferent phase of cryptococcal infection. Mechanistically, we show that MARCO expression facilitates the accumulation and alternative activation of $CD11b^+$ cDC in the lung-associated lymph nodes (LALN) which promote the priming of a non-protective Th2 response in secondary lymphoid organs during *C. neoformans* infection.

MATERIALS AND METHODS

Mice

C57BL/6 mice (wild type) were obtained from Jackson Laboratories (Bar Harbor, ME, USA). MARCO-deficient ($MARCO^{-/-}$) mice, obtained initially from Dr. Lester Kobzik (21), were bred and housed under specific pathogen-free conditions in the Animal Care Facility at the VA Ann Arbor Healthcare System. Both male and female mice were between the ages of 6–12 week at the time of infection and were humanely euthanized by CO_2 inhalation at the time of data collection. All experiments were approved by the Institutional Animal Committee on Use and Care and the Veterans Administration Institutional Animal Care and Use Committee under protocol # 0512-025 and were carried out according to NIH guidelines and the Guide for the Care and Use of Laboratory Animals.

Cryptococcus neoformans

Cryptococcus neoformans strain 52D was recovered from 10% glycerol frozen stocks stored at −80°C and grown to stationary phase at 37°C using Sabouraud dextrose broth (1% Neopeptone, 2% dextrose; Difco, Detroit, MI, USA) on a shaker. The cultures were centrifuged and washed with non-pyrogenic saline (Travenol, Deerfield, IL, USA). Cells were counted *via* hemocytometer and diluted to 3.3×10^5 yeast/ml in sterile non-pyrogenic saline.

Intratracheal Inoculation of *C. neoformans*

Mice were anesthetized *via* intraperitoneal (i.p.) injection of ketamine (100 mg/kg body weight) plus xylazine (6.8 mg/kg) and were restrained on a foam plate. A small incision was made through the skin covering the trachea. The underlying salivary glands and muscles were separated. A 30-G needle was attached to a 1 ml tuberculin syringe with *C. neoformans* suspension (3.3×10^5 yeast/ml) and infection was performed by intratracheally injecting 30 μl (10^4 CFU) of inoculum into the lungs. After

inoculation, the skin was closed with cyanoacrylate adhesive and the mice were monitored during recovery from the anesthesia.

Lung Leukocyte Isolation

The lungs from each mouse were excised, washed in RPMI 1640 and digested enzymatically as previously described (30). In brief, lungs were minced with scissors followed by Gentle MACS homogenization and incubated at 37°C for 35 min in 5 ml/mouse digestion buffer [RPMI 1640, 5% FBS, penicillin, and streptomycin (Invitrogen, Grand Island, NY, USA); 1 mg/ml collagenase A (Roche Diagnostics, Indianapolis, IN, USA); and 30 µg/ml DNase I]. The cell suspension and tissue fragments were further dispersed by Gentle MACS homogenization and were centrifuged. Erythrocytes in the cell pellets were lysed by addition of 3 ml NH_4Cl buffer (0.829% NH_4Cl, 0.1% $KHCO_3$, and 0.0372% Na_2EDTA, pH 7.4) for 3 min followed by a threefold excess of RPMI 1640. Cells were re-suspended and subjected to syringe dispersion and filtered through a sterile 100-µm nylon screen (Nitex, Kansas City, MO, USA). The filtrate was centrifuged for 30 min at 1,500 × *g* with no brake in the presence of 20% Percoll (Sigma) to separate leukocytes from cell debris and epithelial cells. Leukocyte pellets were re-suspended in complete RPMI 1640 media and enumerated on a hemocytometer after dilution in trypan blue (Sigma).

CFU Assay

For determination of fungal burden, small aliquots of digested lungs, spleens, and brains were collected. Series of 10-fold dilutions of the samples were plated on Sabouraud dextrose agar plates in duplicate 10-µl aliquots and incubated at room temperature. *C. neoformans* colonies were counted 2 days later and the number of CFU was calculated on a per-organ basis.

LALN Leukocyte Isolation

Individual LALN were excised and then dispersed using a 1-ml sterile syringe plunger and flushed through a 70-µm cell strainer (BD Falcon, Bedford, MA, USA) with complete media into a sterile tube. After being centrifuged at 2,500 rpm/min for 5 min, the supernatant was removed and the cell pellets were used for gene expression analysis by quantitative real-time RT-PCR (qRT-PCR) or flow cytometry.

Ag-Specific Cytokine Production by Splenocytes

Spleens were excised and dispersed using a 3-ml sterile syringe plunger and flushed through a 70-µm cell strainer (BD Falcon) with complete media. Isolated spleen cells were cultured in media with heat-killed *C. neoformans* in a ratio of 1:2 in 6-well plates with 2 ml complete RPMI 1640 medium at 37°C and 5% CO2 for 48 h. Supernatants were stored and analyzed for cytokine levels as described earlier. The Ag-specific cytokine production was quantified using a LEGENDplex cytometric bead array (CBA) kit (BioLegend, San Diego, CA, USA) following the manufacturer's specifications and read on an LSRII flow cytometer (Becton, Dickinson Immunocytometry Systems, Mountain View, CA, USA). Analysis was performed using BioLegend's LEGENDplex software.

Total Serum IgE

Serum was obtained from the blood samples collected by severing the vena cava of the mice before lung excision. Blood samples were then allowed to clot and were spun to separate serum. Serum samples were diluted 100-fold and assayed for total IgE levels using a mouse IgE sandwich ELISA kit (BioLegend, San Diego, CA, USA) following the manufacturer's specifications.

RT-qPCR

Total RNA from lung leukocytes was prepared using TRIzol reagent (Invitrogen), and first-strand cDNA was synthesized using Reverse Transcription Kit (Qiagen, Hilden, Germany) according to the manufacturer's instructions. Relative gene expression was quantified with SYBR green-based detection (Alkali Scientific) using a light cycler96 system (Roche) according to the manufacturer's protocols. Relative gene expression was normalized to 18S mRNA using the $2^{-\Delta Ct}$ method. Fold induction of gene expression was normalized to baseline expression in uninfected mice using the $2^{-\Delta\Delta Ct}$ method.

Abs and Flow Cytometric Analysis

Ab cell staining was performed as previously described (17). For extracellular staining, cells were washed in PBS then stained with Live Dead Fixable Aqua (Life Technologies) for 30 min. Cells were stained with extracellular antibodies (see below), washed, and fixed in 2% formaldehyde. For intracellular staining, the cells were stimulated with 50 ng/ml PMA and 1 µg/ml ionomycin (Millipore) for 6 h (lung and LALN leukocytes) or heat-killed *C. neoformans* for 24 h (spleen cells) prior to Ab staining. Brefeldin A and monensin (BioLegend) were added for the last 4 h. The cells were harvested, stained with extracellular, and subsequently intracellular antibodies (see below). Data were collected on a FACS LSR2 flow cytometer using FACSDiva software (Becton Dickinson Immunocytometry Systems, Mountain View, CA, USA) and analyzed using FlowJo software (Tree Star, San Carlos, CA, USA).

The following gating strategy was used to identify leukocyte subsets in the lungs. First, consecutive gates identified singlets, live cells and $CD45^+$ leukocytes. Next, a series of selective gates were used to identify neutrophils ($CD11b^+Ly6G^+$); eosinophils ($SSC^{high}CD11c^{low}/SiglecF^+$); Alveolar macrophages ($CD11c^{high}/SiglecF^+$); and $Ly6C^{high}$ monocytes ($CD11c^-/CD11b^+/Ly6C^{high}$). In cells expressing both CD11c and high levels of MHCII, autofluorescent (AF^+) exudate macrophages were distinguished from non-AF (AF^-) DCs. Thereafter, DC were further separated into moDC, $CD11b^+$ DC and $CD103^+$ DC as follows: moDC were gated as $CD11c^+MHCII^{high}CD64^+$ cells, then remaining $CD11c^+MHCII^{high}CD64^-$ cells were further divided into $CD11b^+$ DC and $CD103^+$ DC based on the expression of SIRPα and XCR1, respectively (31). A similar gating strategy was used for leukocytes in the LALN. To identify $CD4^+$ Th cells, singlet and live cells were first selected and the total numbers of $CD45^+$ leukocytes were identified. Next, the $CD3^+CD4^+$ cells were identified and the expression levels of specific cytokines (IFN-γ, TNF-α, IL-5,

and IL-13) or transcriptional factors (Gata3) were evaluated. Total numbers of each cell population were calculated by multiplying the frequency of the population by the total number of leukocytes (the original hemocytometer count of total cells). Isotype control antibodies were used to set gates for positive events in all flow cytometric analyses.

Calculations and Statistics

All values are reported as mean ± SEM. Unpaired non-parametric test (Mann–Whitney) or two-way ANOVA with a Bonferroni *post hoc* test were used for comparisons of individual means. Statistical calculations were performed using GraphPad Prism version 6.00 (GraphPad Software, San Diego, CA, USA). Means with p values <0.05 were considered significantly different.

RESULTS

MARCO Expression Promotes Fungal Persistence and Systemic Dissemination during the Efferent Phase of *C. neoformans* Infection

Our previous study showed that MARCO contributes to fungal control during the early/afferent phase of *C. neoformans* infection (19). However, whether MARCO expression affects long-term adaptive immunity against *C. neoformans* is unclear. To explore the function of MARCO during the late/efferent phase of cryptococcal infection, we infected WT and MARCO$^{-/-}$ mice with *C. neoformans* strain 52D and analyzed the fungal burden at 35 days post infection (dpi). Whereas our prior results demonstrated that MARCO-deficient mice have increased fungal burden at the early stage of infection (19), we found that MARCO-deficient mice exhibit decreased pulmonary fungal burden at 35 dpi compared to WT mice (**Figure 1A**). Fungal burdens in spleen and brain were also lower in MARCO$^{-/-}$ mice compared to WT mice at 35 dpi (**Figure 1A**). We further evaluated the effects of MARCO on the kinetics of pulmonary fungal growth during the efferent phase of *C. neoformans* infection. While equivalent growth of yeast in the lungs was noted in WT and MARCO$^{-/-}$ mice at 21 dpi, MARCO deficiency resulted in lower fungal burden at 35 and 49 dpi (**Figure 1B**). Together, our results demonstrate that MARCO expression promotes pulmonary fungal persistence and systemic dissemination during the efferent phase of *C. neoformans* infection.

MARCO Expression Promotes Non-Protective Th2 Response in the Lungs during the Efferent Phase of *C. neoformans* Infection

T helper cell polarization in the lungs is strongly correlated with clearance and persistence during the efferent phase of *C. neoformans* infection (32). To determine how MARCO expression affects T cell-mediated responses in the lungs, we analyzed leukocyte populations in the infected lungs of WT and MARCO$^{-/-}$ mice using flow cytometry. The accumulation of total leukocytes and leukocyte subsets, including eosinophils, alveolar macrophages, and total DCs, in the infected lungs were similar between WT and MARCO$^{-/-}$ mice at 21, 35, and 49 dpi (Figure S1 in Supplementary Material).

We next examined the effect of MARCO on T cell polarization during *C. neoformans* infection. There was no difference in the accumulation of CD4$^+$ T cells in the lungs of *C. neoformans*-infected MARCO$^{-/-}$ and WT mice during the efferent phase of cryptococcal infection (**Figure 2A**). However, MARCO deficiency resulted in reduced *Il-5* and *Il-13* mRNA expression, but not *IFN-γ* and *TNF-α* mRNA expression, by total lung leukocytes isolated from infected mice at 35 dpi, suggesting an impaired Th2 response in MARCO-deficient mice (**Figure 2B**). Phenotypes of T helper cells were further analyzed by intracellular staining using

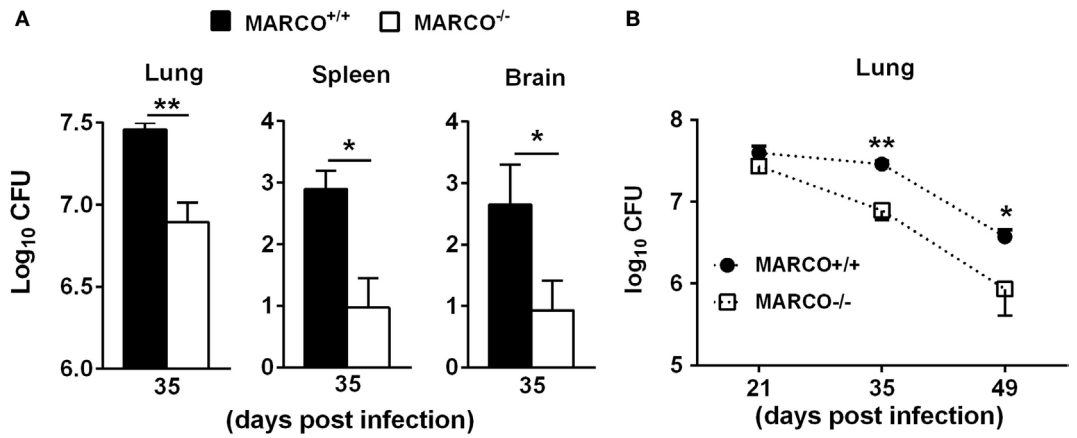

FIGURE 1 | Macrophage receptor with collagenous structure (MARCO) expression contributes to fungal growth and dissemination during the efferent phase of *Cryptococcus neoformans* infection. MARCO$^{+/+}$ and MARCO$^{-/-}$ mice were infected intratracheally with 10^4 *C. neoformans* 52D. **(A)** MARCO expression impaired fungal clearance in the lungs, spleens, and brains at 35 dpi during *C. neoformans* infection. **(B)** Kinetics of pulmonary fungal clearance in the MARCO$^{+/+}$ and MARCO$^{-/-}$ mice during efferent phase of *C. neoformans* infection. Results represent mean ± SEM from one of two separate matched experiments (n = 5 mice for each time point). *p < 0.05, **p < 0.01.

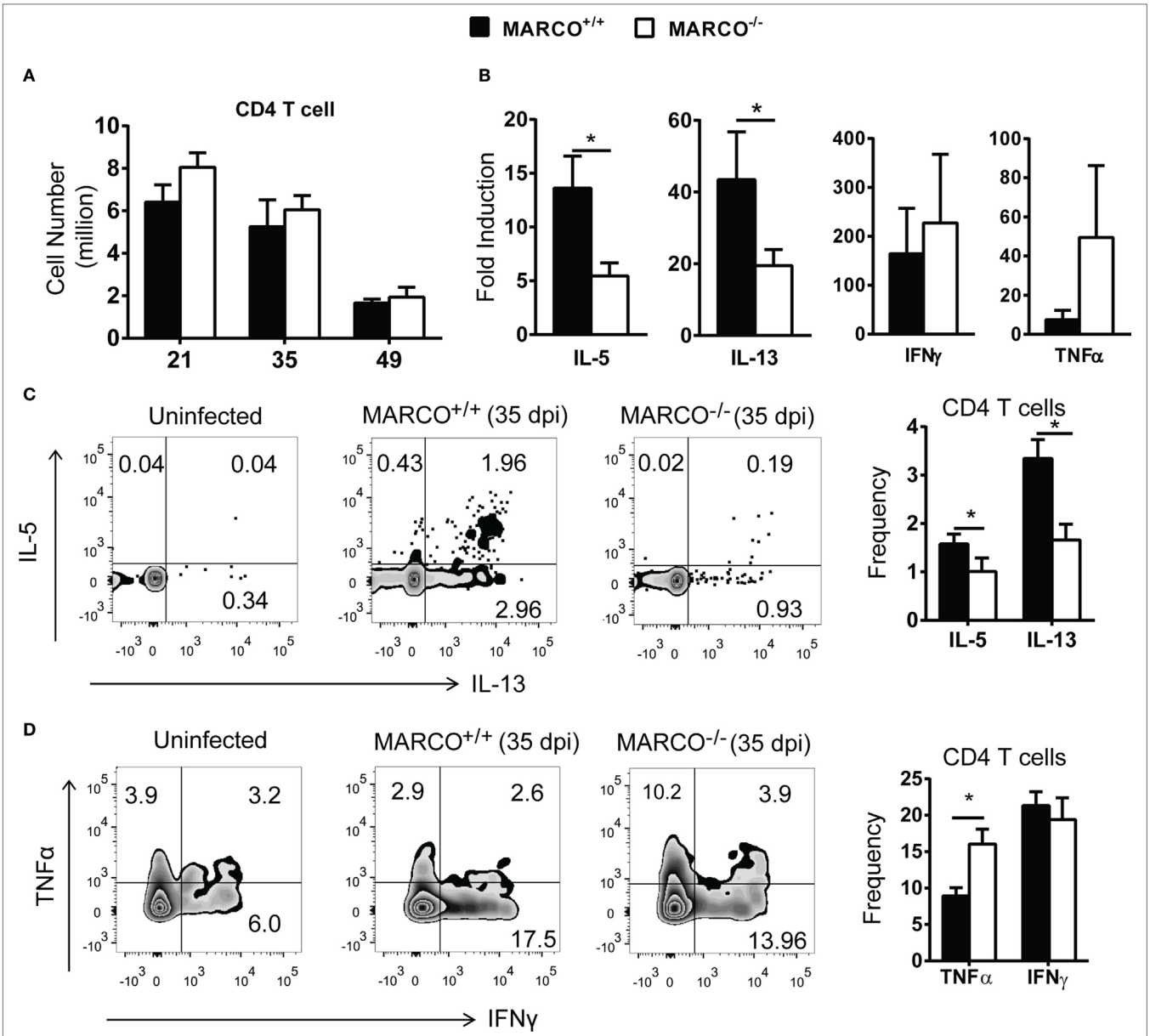

FIGURE 2 | Macrophage receptor with collagenous structure (MARCO) expression promotes Th2 response in the lungs during the efferent phase of *Cryptococcus neoformans* infection. **(A)** MARCO is dispensable for the accumulation of CD4+ T cells in the lungs of *C. neoformans*-infected mice. **(B)** MARCO expression facilitates *IL-5* and *IL-13* but not *IFN-γ* and *TNF-α* mRNA expression by total lung leukocytes at 35 dpi during *C. neoformans* infection. **(C)** MARCO expression promotes IL-5 and IL-13 production by CD4+ T cells in the lungs of *C. neoformans*-infected mice. **(D)** MARCO expression inhibits TNF-α production by CD4+ T cells in the lungs of *C. neoformans*-infected mice. Results represent mean ± SEM ($n = 5$) from one of at least two independent experiments. *$p < 0.05$.

flow cytometry. Frequencies of CD4 T cells expressing IL-5 and IL-13 were significantly lower in MARCO$^{-/-}$ mice compared to WT mice at 35 dpi (**Figure 2C**). By contrast, MARCO deficiency led to higher frequencies of CD4+ T cells expressing TNF-α albeit without affecting those expressing INF-γ at 35 dpi (**Figure 2D**). Collectively, our data demonstrated that MARCO expression did not affect accumulation of lung myeloid or lymphoid cells but altered the balance of T cell polarization away from protective Th1 responses toward non-protective Th2 responses in the lungs during the efferent phase of *C. neoformans* infection.

MARCO Expression Interferes with Classical Activation of Pulmonary Exudate Macrophages during the Efferent Phase of *C. neoformans* Infection

The balance of Th1/Th2 cytokines influences macrophage activation status and their subsequent fungicidal activities (33, 34). Exudate macrophages derived from recruited monocytes during infection have been shown to be the most efficient effector cells in killing *C. neoformans* (35). We next sought to determine whether

MARCO expression affects the activation status of pulmonary macrophages during the efferent phase of *C. neoformans* infection. Equivalent recruitment of exudate macrophages was noted between infected MARCO$^{-/-}$ and WT mice during the efferent phase of *C. neoformans* infection (**Figure 3A**). However, MARCO deficiency resulted in augmented mRNA expression of *iNOS* but not *Arg1* by lung macrophages at 35 dpi (**Figure 3B**). Moreover, we found that MARCO deficiency resulted in significantly increased expression of CD80 and CD86 by exudate macrophages at 35 dpi (**Figures 3C,D**), consistent with improved pulmonary fungal clearance in these mice. Interestingly, expression of CD80, CD86, iNOS, and Arg1 by alveolar macrophages was similar between infected MARCO$^{-/-}$ and WT mice (not shown). Thus, consistent with the diminished efferent Th1 responses, MARCO expression is associated with impaired classical activation of exudate macrophages in the lungs during the efferent phase of *C. neoformans* infection.

MARCO Expression Enhances Non-Protective and Opposes Protective Systemic Responses during the Efferent Phase of *C. neoformans* Infection

Since MARCO affected extra-pulmonary *C. neoformans* dissemination, we next studied its effects on systemic immune responses during the efferent phase of cryptococcal infection. To accomplish this, we evaluated the cytokine production by splenocytes of infected MARCO$^{-/-}$ and WT mice in response to cryptococcal antigen. Consistent with results from the lungs, production of non-protective cytokines, including IL-4 and IL-10, was lower by splenocytes from MARCO$^{-/-}$ compared to WT mice at 21 dpi (**Figure 4A**). The concentration of serum IgE, a hallmark of systemic Th2 response, was also significantly lower in MARCO$^{-/-}$ mice compared to WT mice at 21 and 35 dpi (**Figure 4B**). Furthermore, MARCO deficiency led to elevated production of beneficial Th1 cytokines such as IFN-γ (21 and 35 dpi) and TNF-α (35 dpi) by splenocytes in response to cryptococcal antigen stimulation (**Figure 4C**). We next investigated whether T cells were the major source of antigen-triggered IFN-γ production in splenocyte cultures using intracellular flow cytometric analysis. We identified increased frequencies of IFN-γ-producing CD8$^+$ T cells in MARCO$^{-/-}$ mice compared to WT mice (**Figure 4D**). We also observed a similar, strong trend in increased frequencies of IFN-γ-producing CD4$^+$ T cells in MARCO$^{-/-}$ mice compared to WT mice ($p = 0.1$) (**Figure 4D**), which became significant when splenocyte culture were stimulated with PMA and ionomycin (data not shown). Interestingly, we also found a higher frequency of non-T cell populations (CD4$^-$CD8$^-$) producing IFN-γ in antigen stimulated splenocyte cultures from MARCO$^{-/-}$ mice compared to those from WT mice (**Figure 4D**). These results indicate that MARCO expression also broadly affects IFN-γ production by cells outside the T cell compartment. Collectively, we found that MARCO expression promotes a systemic shift away from protective responses toward non-protective responses during the efferent phase of *C. neoformans* infection.

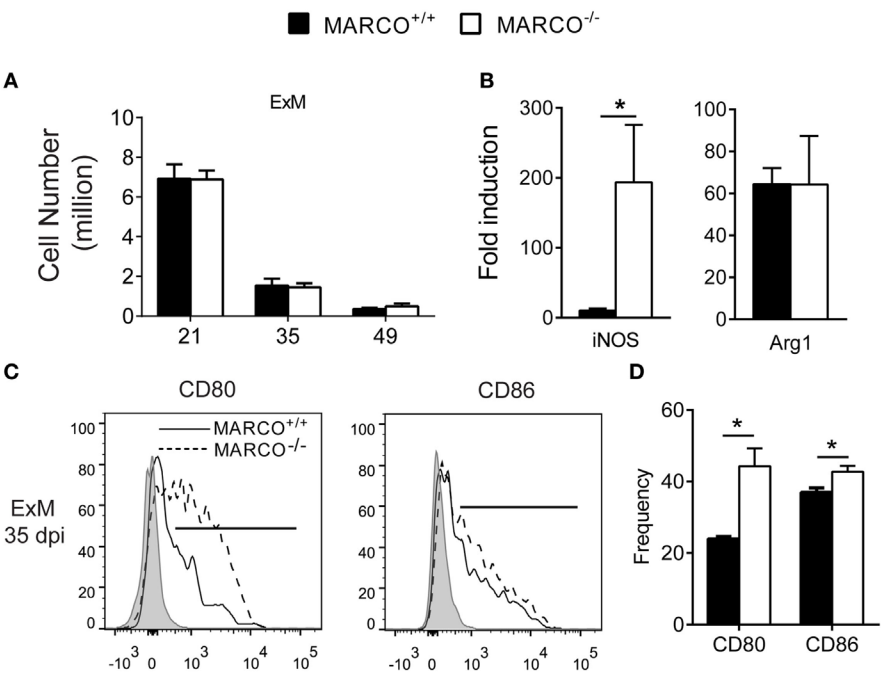

FIGURE 3 | Macrophage receptor with collagenous structure (MARCO) expression impairs classical activation of macrophages in the lungs during the efferent phase of *Cryptococcus neoformans* infection. **(A)** Accumulation of exudate macrophages was not affected by MARCO deletion during *C. neoformans* infection. **(B)** MARCO impairs iNOS expression by adherent macrophages from lungs of infected mice at 35 dpi. **(C,D)** MARCO impairs expression of CD80 and CD86 by lung exudate macrophages at 35 dpi. Results represent mean ± SEM ($n = 5$) from one of two independent experiments. *$p < 0.05$. ExM, exudate macrophages.

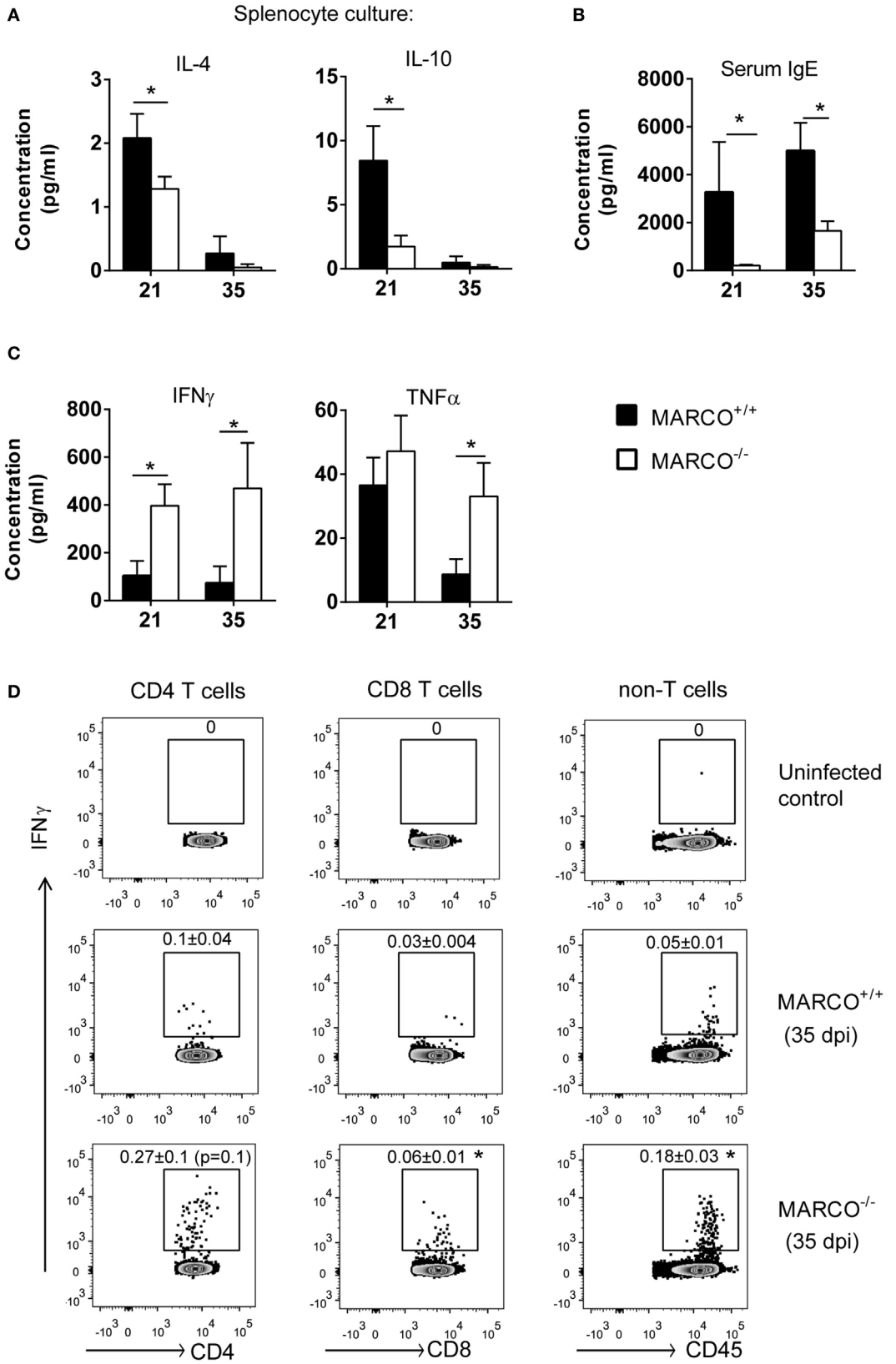

FIGURE 4 | Continued

FIGURE 4 | Continued
Macrophage receptor with collagenous structure (MARCO) expression promotes systemic Th2 response and inhibits Th1 response during the efferent phase of *Cryptococcus neoformans* infection. Spleen leukocytes were isolated from infected MARCO$^{-/-}$ and MARCO$^{+/+}$ mice at 21 and 35 dpi. After stimulated with heat-killed *C. neoformans* for 48 h, cytokine production in the supernatant of cell cultures was analyzed by cytometric bead assay. **(A)** MARCO expression increases IL-4 and IL-10 production by spleen leukocytes at 21 dpi. **(B)** MARCO expression significantly increases serum IgE level in mice infected with *C. neoformans*. **(C)** MARCO expression inhibits production of IFN-γ and TNF-α by spleen leukocytes at 21 or 35 dpi. **(D)** MARCO expression inhibits production of IFN-γ by CD4$^+$ T cells, CD8$^+$ T cells and non-T cells (CD4$^-$CD8$^-$) at 35 dpi. Splenocytes were stimulated with heat-killed *C. neoformans* and analyzed by intracellular flow cytometry. Results represent mean ± SEM ($n > 4$). $^*p < 0.05$.

MARCO Expression Contributes to Th2 Priming in the LALNs during *C. neoformans* Infection

We next dissected the mechanisms by which MARCO modulates Th polarization. T cells are primed in the draining lymph nodes and their polarization is orchestrated by distinct DC subsets during *C. neoformans* infection (36). We, thus, looked at the priming of T cells in the LALN at 10 dpi, an early time point at the onset of T cell polarization. Though MARCO deficiency had no effect on the T cell expansion in LALNs at 10 dpi (**Figure 5A**), we found reduced expression of *IL-13* by the LALN leukocytes of infected MARCO$^{-/-}$ mice compared to WT mice (**Figure 5B**). Furthermore, expression of *IFN-γ* and the transcription factors *T-bet* and *Eomesodermin* by LALN leukocytes were similar between MARCO$^{-/-}$ and WT mice (**Figure 5B** and data not shown). To further assess whether MARCO promotes Th2 priming in the LALN during *C. neoformans* infection, we performed intracellular staining for cytokines and transcription factors in LALN leukocytes. Consistent with our gene expression analysis, we found that MARCO deficiency resulted in reduced frequencies of LALN CD4$^+$ T cells expressing Th2-associated cytokine IL-13 and transcriptional factor Gata3 at 10 dpi (**Figure 5C**). By contrast, MARCO deficiency had no effect on IFN-γ expression by CD4$^+$ T cells in the LALN at 10 dpi. Thus, MARCO expression enhances early Th2 priming but appears to have little or no effect on early Th1 priming in the LALN during *C. neoformans* infection.

MARCO Expression Promotes Accumulation of CD11b$^+$ cDC in the LALN during *C. neoformans* Infection

Pulmonary CD11b$^+$ cDC have been shown to orchestrate the development of non-protective Th2 responses during cryptococcal infection (15). To test whether MARCO expression affects the accumulation of DC in the LALN, we analyzed leukocyte populations in the LALN of infected MARCO$^{-/-}$ and WT mice at 10 dpi. While total leukocyte accumulation in the LALN was not altered in MARCO-deficient mice, MARCO expression significantly promoted the accumulation of migratory DC (CD11c$^+$MHCII^{high}) in the LALN of infected mice (**Figures 6A,B**). We further explored whether MARCO affected the accumulation of specific DC subsets in the LALN during *C. neoformans* infection. Notably, MARCO deficiency selectively impaired accumulation of CD11b$^+$ cDC, but had no effect on the accumulation of CD103$^+$ cDC and moDC subsets in the LALN of *C. neoformans*-infected mice (**Figure 6C**). Thus, MARCO expression is critical for the accumulation of CD11b$^+$ cDC in the LALN during *C. neoformans* infection.

MARCO Expression Promotes Alternative Activation and Inhibits Classical Activation of CD11b$^+$ cDC in LALNs during *C. neoformans* Infection

The activation status of DC in the LALN can be influenced by fungal virulence factors and plays a vital role in the control of T cell polarization (16, 37). We further assessed the effect of MARCO on the activation status of CD11b$^+$ cDC in the LALN during *C. neoformans* infection by analyzing the expression of classical activation markers (CD80 and CD86) as well as alternative activation marker (CD206) on CD11b$^+$ cDC. We found that MARCO deficiency led to increased expression of CD80 and CD86 and decreased expression of CD206 by CD11b$^+$ cDC in the LALN at 10 dpi (**Figures 7A,B**). Interestingly, MARCO deficiency had no effect on the activation status of CD103$^+$ cDC and moDC in LALN of infected mice (not shown). These data show that MARCO expression specifically promotes alternative activation and inhibits classical activation of CD11b$^+$ cDC in the LALN. Collectively, this MARCO-dependent accumulation and alternative activation of CD11b$^+$ cDC in the LALN may represent a critical mechanism through which MARCO promotes the development of a stronger Th2 response and downregulates the Th1 response, leading to fungal persistence during the efferent phase of *C. neoformans* infection (**Figure 8**).

DISCUSSION

Although our previous study demonstrated that scavenger receptor MARCO is involved in the phagocytosis of *C. neoformans* by lung leukocytes and early recruitment of myeloid cells, the function of MARCO in the later stages of adaptive antifungal immunity remains unknown. Here, we demonstrated that MARCO expression ultimately promotes fungal persistence and dissemination by directly or indirectly contributing to the development of non-protective responses during cryptococcal infection. Our immunological analysis mechanistically linked these effects during the adaptive phase with increased pulmonary and systemic Th2 responses and impaired classical activation of macrophages in the lungs. We further show that the upstream accumulation and alternative activation of CD11b$^+$ cDC in LALN of *C. neoformans*-infected mice provides a likely mechanism through which *C. neoformans* exploits MARCO to trigger a shift to Th2 responses. Collectively, our study uncovers novel

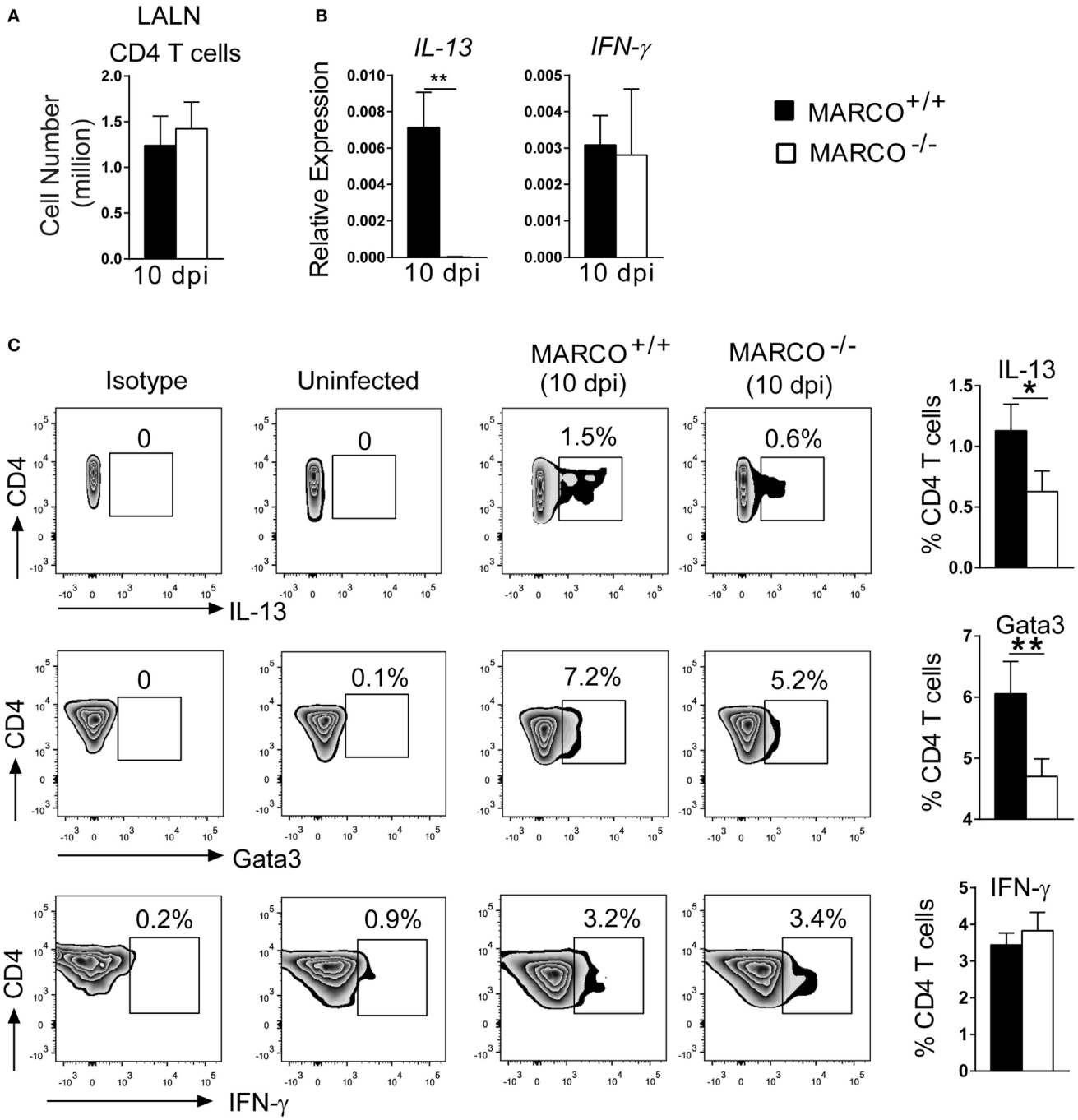

FIGURE 5 | Macrophage receptor with collagenous structure (MARCO) promotes Th2 response in the LALN of *Cryptococcus neoformans*-infected mice. **(A)** MARCO is dispensable for accumulation of CD4+ T cells in the LALN of *C. neoformans*-infected mice at 10 dpi. **(B)** Expression of IL-13 and IFN-γ by total LALN leukocytes from infected MARCO$^{-/-}$ and MARCO$^{+/+}$ mice at 10 dpi were analyzed by RT-qPCR. Note that MARCO enhanced mRNA expression of IL-13 but not IFN-γ by total LALN leukocytes. Expression of each target gene was normalized to the 18S housekeeping gene. **(C)** MARCO expression promotes IL-13 and Gata3 but not IFN-γ protein production by CD4+ T cells in the LALN of *C. neoformans*-infected mice. Results represent mean ± SEM ($n = 5$) with similar results from two independent experiments. *$p < 0.05$.

cellular and molecular pathway through which *C. neoformans* evades host defenses and induces non-protective antifungal immunomodulation.

Our current study revealed the novel observation that MARCO expression significantly promotes fungal persistence and extra-pulmonary dissemination during the efferent phase of

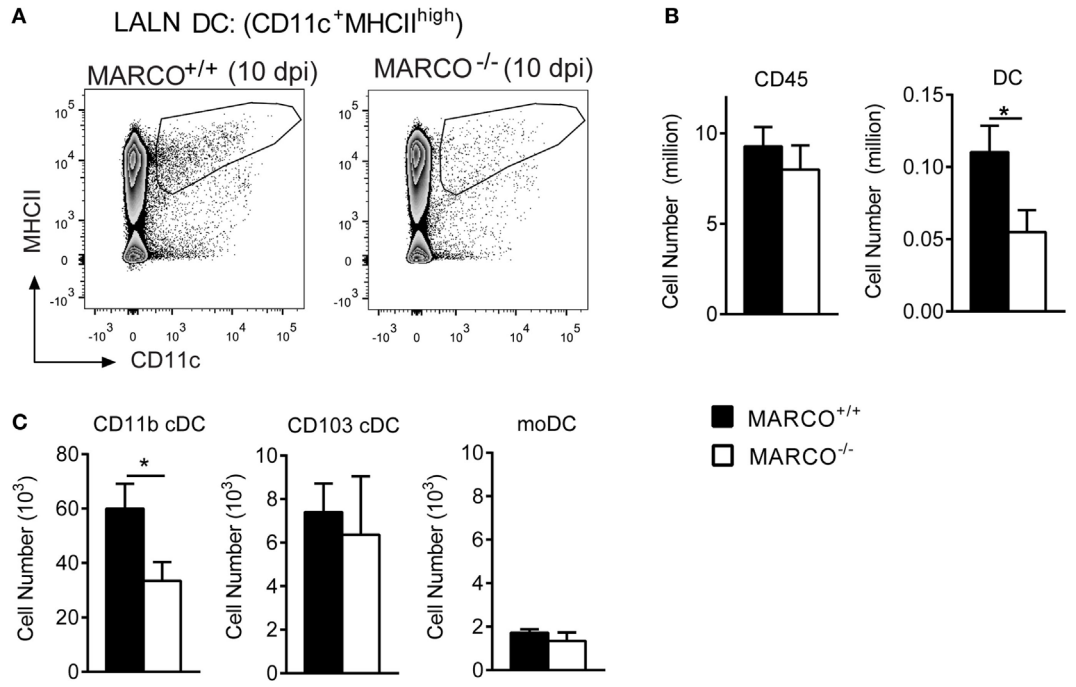

FIGURE 6 | Macrophage receptor with collagenous structure (MARCO) expression promotes the accumulation of CD11b$^+$ cDC in the lung-associated lymph node (LALN) of *Cryptococcus neoformans*-infected mice. **(A,B)** MARCO expression promotes the accumulation of dendritic cell (DC) but not total leukocytes in LALN of *C. neoformans*-infected mice at 10 dpi. **(C)** MARCO expression promotes the accumulation of CD11b$^+$ cDC but not CD103$^+$ cDC and moDC. Results represent mean ± SEM (n = 5), with similar results from two independent experiments. *p < 0.05. cDC, conventional dendritic cells; moDC, monocytes-derived dendritic cells.

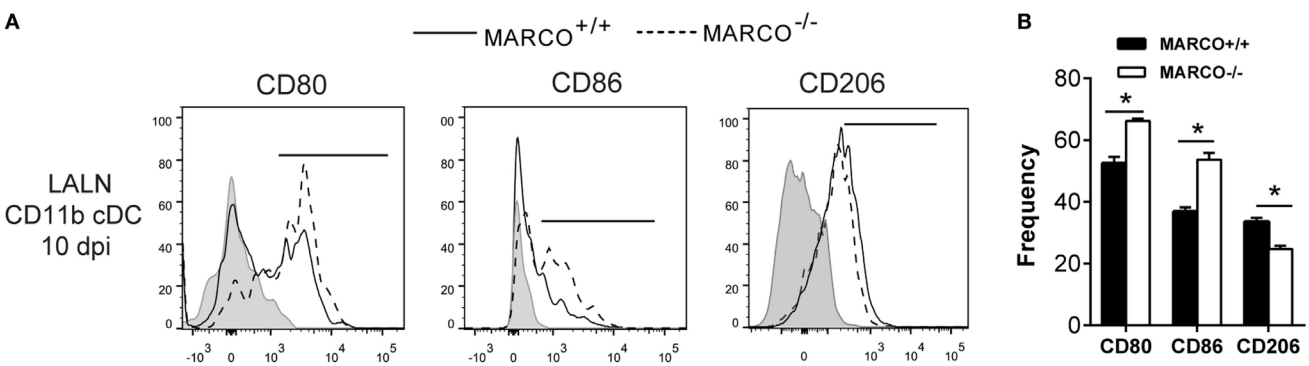

FIGURE 7 | Macrophage receptor with collagenous structure (MARCO) expression promotes alternative activation and inhibits classical activation of CD11b$^+$ conventional DC (cDC) in the lung-associated lymph node (LALN) of *Cryptococcus neoformans*-infected mice. **(A)** Surface expression of CD80, CD86, and CD206 by CD11b$^+$ cDC was analyzed by flow cytometry. **(B)** Bar graphs represent percentage of CD11b$^+$ cDC expressing CD80, CD86, and CD206. Note that CD11b$^+$ cDC from infected MARCO$^{+/+}$ mice exhibited higher expression of CD80 and CD86 but lower levels of CD206 compared to CD11b$^+$ cDC from infected MARCO$^{-/-}$ mice. Results represent mean ± SEM (n = 5), with similar results from two independent experiments. *p < 0.05.

C. neoformans infection. Interestingly, our previous study demonstrated that MARCO orchestrates innate defenses and contributes to fungal containment during initial response to cryptococcal infection by promoting early inflammatory cytokine production in the lungs and phagocytosis by myeloid cells (19). These results show that, in the grand scheme, the initial benefits of MARCO expression during the innate phase were gradually replaced by the non-protective effects induced by MARCO during the efferent phase of *C. neoformans* infection. Collectively, we found that MARCO can play distinct functions in host defenses to pathogens, protective during the relatively short innate phase and then non-protective during subsequent efferent phase.

Distinct roles of specific factors in innate versus adaptive responses, while rare, are not unique to MARCO and can be found in other immune receptors, such as T-cell immunoglobulin domain and mucin domain 3 (TIM3), which was shown to

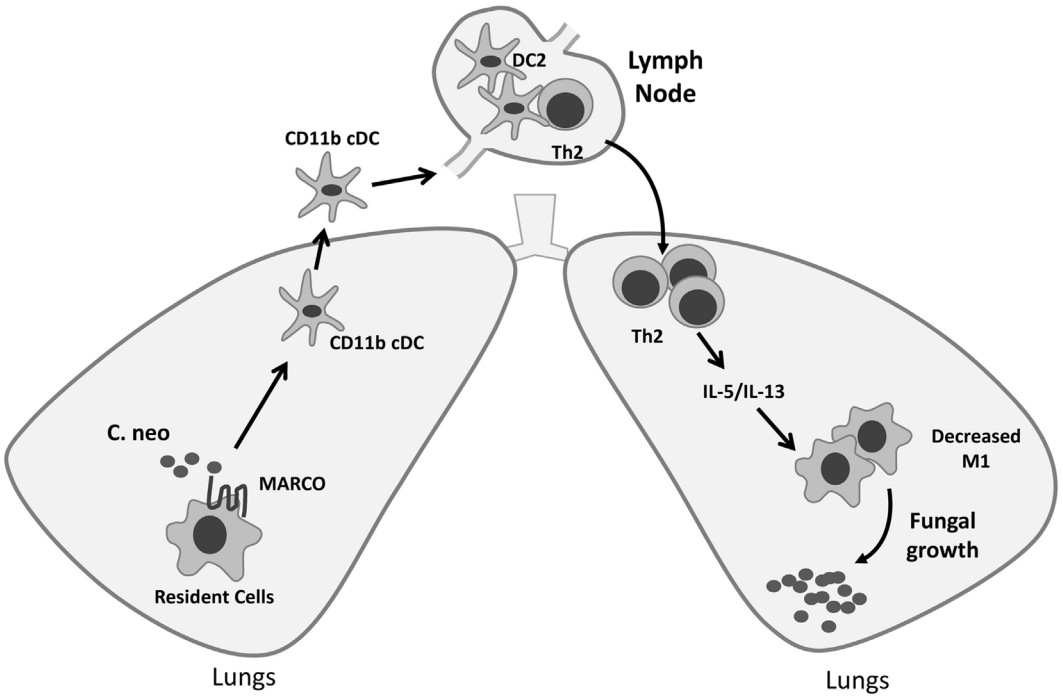

FIGURE 8 | Roles of macrophage receptor with collagenous structure (MARCO) in orchestrating adaptive immunity during fungal infection. MARCO expression contributes to accumulation of CD11b$^+$ conventional DC (cDC) and their alternative activation in the lung-associated lymph node (LALN), which promotes the development of Th2 responses in the LALN and lungs during *Cryptococcus neoformans* infection. Thus, efferent control of fungal growth was impaired along with increased production of type 2 cytokines IL-5 and IL-13, and alternative activation of effector cells in the lungs of MARCO$^{+/+}$ mice.

promote pro-inflammatory innate responses while restraining Th1 responses (38). While it is not uncommon for pathogens to exploit loopholes in the signaling cascades of the immune system and hijack protective pathways, our results showing dual roles of MARCO during cryptococcal infection may provide insights that explain why different genetic variants of MARCO differentially affect health of the human population. In human pulmonary tuberculosis, some genetic variants of MARCO are associated with susceptibility, while other variants are associated with resistance (39). Given the similarities of pathogenicity between *C. neoformans* and *M. tuberculosis* (both can survive and grow intracellularly in the alveolar macrophages and require Th1-cell help for their eradication), it is possible that these distinct variants may affect the magnitude of protective versus non-protective effects of MARCO. Another element of pathogenesis shared by *C. neoformans* and *M. tuberculosis* is their ability to induce latent infections (40, 41). Since, non-protective elements of the immune response contribute to cryptococcal persistence (42, 43), MARCO and other factors exploited by *C. neoformans* may in fact contribute to the development of cryptococcal latency. Thus, possible contribution of MARCO expression to long-term latency of *C. neoformans* infection and whether genetic variants of MARCO are associated with susceptibility to cryptococcosis in humans warrants further study.

The effects of MARCO in the development of adaptive immunity were less well explored compared to its well-studied innate functions in control of infections such as *Mycobacterium tuberculosis, Streptococcus pneumonia, and Leishmania major* (21–23). In this study, we showed that MARCO expression can be later exploited by *C. neoformans* to modulate T cell polarization during the efferent phase of infection. Consistent with the higher fungal burden in WT mice, MARCO expression led to enhancement of non-protective Th2 responses, diminished protective Th1 responses, and impaired classical activation of macrophages in the lungs during the efferent phase of *C. neoformans* infection (**Figure 8**). Interestingly, while the effects of MARCO on induction of systemic and pulmonary Th2 bias were similar (Th2 cytokine production in lungs and spleen and corresponding changes in serum IgE level), divergent functions of MARCO were found when it comes to IFN-γ production. MARCO expression was associated with diminished expression of IFN-γ by both T cells and non-T cells in the spleens, while we did not observe any effects of MARCO on IFN-γ production by the lung and LALN cells. Thus, while our current study substantially advances our understanding of the role of MARCO as an important modulator of host adaptive immunity during fungal infections, future studies are needed to fully characterize the mechanisms by which MARCO plays divergent roles in different organs of the infected host.

Molecular and cellular mechanisms of non-protective Th2 response development during *C. neoformans* infection are incompletely understood. Pathogen virulence factors, such as capsule, chitin, urease, and other lipid mediators, promote Th2 responses during *C. neoformans* infection (8, 44, 45), however, host signaling

pathways exploited by fungal pathogens that contribute to Th2 development are less studied. Though critical roles of pulmonary CD11b$^+$ cDC in Th2 response development during *C. neoformans* infection was demonstrated (15), the underlying mechanisms are not fully elucidated. In our study, we demonstrated that the upstream Th2 priming in the draining lymph nodes was enhanced by MARCO expression. More importantly, our results showed that the accumulation and alternative activation of CD11b$^+$ cDC also depended on MARCO expression. Thus, the increased accumulation and alternative activation of CD11b$^+$ cDC is likely a crucial mechanism by which *C. neoformans* exploits MARCO to promote the Th2 response and downregulate Th1 response during infection. However, at this time, we cannot rule out that other possible cell subsets affected by *C. neoformans* in a MARCO-dependent fashion might also enhance non-protective Th2 responses.

The current study demonstrates that MARCO exhibits some interesting similarities and differences during fungal infections when compared with our previous study on the role of another scavenger receptor, SR-A (17). While our studies demonstrated that *C. neoformans* can exploit multiple scavenger receptors to facilitate its survival in the host by triggering the same type of immunomodulation, there are significant differences between the effects of SR-A and MARCO on DC activation. SR-A promotes the early production of type 2 cytokines in both the lungs and LALN during the afferent phase of *C. neoformans* infection and globally contributed to the alternative activation of DC at both sites (17). By contrast, MARCO contributes to increased early IFN-γ production and classical activation of moDC in the lungs (19), at the same time selectively enhances the accumulation and alternative activation of CD11b$^+$cDC in the LALN of *C. neoformans*-infected mice. These seemingly discrepant effects within mucosal sites and regional lymph nodes demonstrate that MARCO signaling is likely contextual, depending on DC subsets and/or effects of local micro-environments. While future studies are needed to clarify this, our studies indicate that both MARCO and SR-A can promote Th2 polarization during cryptococcal infection possibly *via* different mechanisms.

In summary, our novel findings show that MARCO facilitates cryptococcal persistence in the host through promoting non-protective Th2 responses during the efferent phase of *C. neoformans* infection. We identify MARCO-dependent accumulation and alternative activation of CD11b$^+$ cDC as one mechanism explaining these effects. Thus, this study substantially advances our understanding about the roles of MARCO in the adaptive phase of antifungal immunity.

ETHICS STATEMENT

This study was carried out in accordance with the recommendations of University Committee on the Use and Care of Animals and the Veterans Administration Institutional Animal Care and Use Committee. All experiments and protocol were approved by the University Committee on the Use and Care of Animals and the Veterans Administration Institutional Animal Care and Use Committee.

AUTHOR CONTRIBUTIONS

JX and AF contributed to experimental design, experimental work, data analysis, and manuscript writing. LN, ZF, DC, and MI contributed to experimental work and manuscript editing. BBM, JC, and JO contributed to write and edit manuscript. MO contributed to secure funding, oversee the project, design framework, and experimental work.

ACKNOWLEDGMENTS

MO, JO, and JC were supported by VA Merit grants (I01BX000656, BX002120-01 and I01CX000911, respectively). In addition, MO was supported by VA RCS award (IK6BX003615). BM was supported by NIH grant AI117229, HL127805, and HL119682. LN was supported by T-32 research training grant T32HL07749. The authors wish to thank Enze Xing, Guolei Zhao, Xueli Gao, and Jessica Kolbe for technical assistance and the UROP program at the University of Michigan for their support of undergraduate research.

SUPPLEMENTARY MATERIAL

The Supplementary Material for this article can be found online at http://journal.frontiersin.org/article/10.3389/fimmu.2017.01231/full#supplementary-material.

REFERENCES

1. Brown GD, Denning DW, Gow NA, Levitz SM, Netea MG, White TC. Hidden killers: human fungal infections. *Sci Transl Med* (2012) 4:165rv113. doi:10.1126/scitranslmed.3004404
2. Olszewski MA, Zhang Y, Huffnagle GB. Mechanisms of cryptococcal virulence and persistence. *Future Microbiol* (2010) 5:1269–88. doi:10.2217/fmb.10.93
3. Fang W, Fa Z, Liao W. Epidemiology of *Cryptococcus* and cryptococcosis in China. *Fungal Genet Biol* (2015) 78:7–15. doi:10.1016/j.fgb.2014.10.017
4. Spitzer ED, Spitzer SG, Freundlich LF, Casadevall A. Persistence of initial infection in recurrent *Cryptococcus neoformans* meningitis. *Lancet* (1993) 341:595–6. doi:10.1016/0140-6736(93)90354-J
5. Wager CML, Wormley FL Jr. Is development of a vaccine against *Cryptococcus neoformans* feasible? *PLoS Pathog* (2015) 11:e1004843. doi:10.1371/journal.ppat.1004843
6. He X, Lyons DM, Toffaletti DL, Wang F, Qiu Y, Davis MJ, et al. Virulence factors identified by *Cryptococcus neoformans* mutant screen differentially modulate lung immune responses and brain dissemination. *Am J Pathol* (2012) 181:1356–66. doi:10.1016/j.ajpath.2012.06.012
7. Qiu Y, Davis MJ, Dayrit JK, Hadd Z, Meister DL, Osterholzer JJ, et al. Immune modulation mediated by cryptococcal laccase promotes pulmonary growth and brain dissemination of virulent *Cryptococcus neoformans* in mice. *PLoS One* (2012) 7:e47853. doi:10.1371/journal.pone.0047853
8. Osterholzer JJ, Surana R, Milam JE, Montano GT, Chen G-H, Sonstein J, et al. Cryptococcal urease promotes the accumulation of immature dendritic cells and a non-protective T2 immune response within the lung. *Am J Pathol* (2009) 174:932–43. doi:10.2353/ajpath.2009.080673
9. Rohatgi S, Pirofski LA. Host immunity to *Cryptococcus neoformans*. *Future Microbiol* (2015) 10:565–81. doi:10.2217/fmb.14.132
10. Voelz K, May RC. Cryptococcal interactions with the host immune system. *Eukaryot Cell* (2010) 9:835–46. doi:10.1128/EC.00039-10

11. Gibson JF, Johnston SA. Immunity to *Cryptococcus neoformans* and *C. gattii* during cryptococcosis. *Fungal Genet Biol* (2015) 78:76–86. doi:10.1016/j.fgb.2014.11.006
12. Müller U, Stenzel W, Köhler G, Werner C, Polte T, Hansen G, et al. IL-13 induces disease-promoting type 2 cytokines, alternatively activated macrophages and allergic inflammation during pulmonary infection of mice with *Cryptococcus neoformans*. *J Immunol* (2007) 179:5367–77. doi:10.4049/jimmunol.179.8.5367
13. Zhang Y, Wang F, Tompkins KC, McNamara A, Jain AV, Moore BB, et al. Robust Th1 and Th17 immunity supports pulmonary clearance but cannot prevent systemic dissemination of highly virulent *Cryptococcus neoformans* H99. *Am J Pathol* (2009) 175:2489–500. doi:10.2353/ajpath.2009.090530
14. Iwasaki A, Medzhitov R. Control of adaptive immunity by the innate immune system. *Nat Immunol* (2015) 16:343–53. doi:10.1038/ni.3123
15. Wiesner DL, Specht CA, Lee CK, Smith KD, Mukaremera L, Lee ST, et al. Chitin recognition via chitotriosidase promotes pathologic type-2 helper T cell responses to cryptococcal infection. *PLoS Pathog* (2015) 11:e1004701. doi:10.1371/journal.ppat.1004701
16. Valdez PA, Vithayathil PJ, Janelsins BM, Shaffer AL, Williamson PR, Datta SK. Prostaglandin E2 suppresses antifungal immunity by inhibiting interferon regulatory factor 4 function and interleukin-17 expression in T cells. *Immunity* (2012) 36:668–79. doi:10.1016/j.immuni.2012.02.013
17. Qiu Y, Dayrit JK, Davis MJ, Carolan JF, Osterholzer JJ, Curtis JL, et al. Scavenger receptor A modulates the immune response to pulmonary *Cryptococcus neoformans* infection. *J Immunol* (2013) 191:238–48. doi:10.4049/jimmunol.1203435
18. Canton J, Neculai D, Grinstein S. Scavenger receptors in homeostasis and immunity. *Nat Rev Immunol* (2013) 13:621–34. doi:10.1038/nri3515
19. Xu J, Flaczyk A, Neal LM, Fa Z, Eastman AJ, Malachowski AN, et al. Scavenger receptor MARCO orchestrates early defenses and contributes to fungal containment during cryptococcal infection. *J Immunol* (2017) 198:3548–57. doi:10.4049/jimmunol.1700057
20. Areschoug T, Gordon S. Scavenger receptors: role in innate immunity and microbial pathogenesis. *Cell Microbiol* (2009) 11:1160–9. doi:10.1111/j.1462-5822.2009.01326.x
21. Arredouani M, Yang Z, Ning Y, Qin G, Soininen R, Tryggvason K, et al. The scavenger receptor MARCO is required for lung defense against pneumococcal pneumonia and inhaled particles. *J Exp Med* (2004) 200:267–72. doi:10.1084/jem.20040731
22. Gomes IN, Palma LC, Campos GO, Lima JGB, De Almeida TF, De Menezes JP, et al. The scavenger receptor MARCO is involved in *Leishmania major* infection by CBA/J macrophages. *Parasite Immunol* (2009) 31:188–98. doi:10.1111/j.1365-3024.2009.01093.x
23. Bowdish DM, Sakamoto K, Kim M-J, Kroos M, Mukhopadhyay S, Leifer CA, et al. MARCO, TLR2, and CD14 are required for macrophage cytokine responses to mycobacterial trehalose dimycolate and *Mycobacterium tuberculosis*. *PLoS Pathog* (2009) 5:e1000474. doi:10.1371/journal.ppat.1000474
24. Dorrington MG, Roche AM, Chauvin SE, Tu Z, Mossman KL, Weiser JN, et al. MARCO is required for TLR2-and Nod2-mediated responses to *Streptococcus pneumoniae* and clearance of pneumococcal colonization in the murine nasopharynx. *J Immunol* (2013) 190:250–8. doi:10.4049/jimmunol.1202113
25. Kissick HT, Dunn LK, Ghosh S, Nechama M, Kobzik L, Arredouani MS. The scavenger receptor MARCO modulates TLR-induced responses in dendritic cells. *PLoS One* (2014) 9:e104148. doi:10.1371/journal.pone.0104148
26. Grolleau A, Misek DE, Kuick R, Hanash S, Mulé JJ. Inducible expression of macrophage receptor MARCO by dendritic cells following phagocytic uptake of dead cells uncovered by oligonucleotide arrays. *J Immunol* (2003) 171:2879–88. doi:10.4049/jimmunol.171.6.2879
27. Granucci F, Petralia F, Urbano M, Citterio S, Di Tota F, Santambrogio L, et al. The scavenger receptor MARCO mediates cytoskeleton rearrangements in dendritic cells and microglia. *Blood* (2003) 102:2940–7. doi:10.1182/blood-2002-12-3651
28. Komine H, Kuhn L, Matsushita N, Mulé JJ, Pilon-Thomas S. Examination of MARCO activity on dendritic cell phenotype and function using a gene knockout mouse. *PLoS One* (2013) 8:e67795. doi:10.1371/journal.pone.0067795
29. Arredouani MS, Franco F, Imrich A, Fedulov A, Lu X, Perkins D, et al. Scavenger receptors SR-AI/II and MARCO limit pulmonary dendritic cell migration and allergic airway inflammation. *J Immunol* (2007) 178:5912–20. doi:10.4049/jimmunol.178.9.5912
30. Olszewski MA, Huffnagle GB, McDonald RA, Lindell DM, Moore BB, Cook DN, et al. The role of macrophage inflammatory protein-1 alpha/CCL3 in regulation of T cell-mediated immunity to *Cryptococcus neoformans* infection. *J Immunol* (2000) 165:6429–36. doi:10.4049/jimmunol.165.11.6429
31. Guilliams M, Lambrecht B, Hammad H. Division of labor between lung dendritic cells and macrophages in the defense against pulmonary infections. *Mucosal Immunol* (2013) 6:464–73. doi:10.1038/mi.2013.14
32. Wozniak KL, Hardison S, Olszewski M, Wormley FL Jr. Induction of protective immunity against cryptococcosis. *Mycopathologia* (2012) 173:387–94. doi:10.1007/s11046-011-9505-8
33. Hardison SE, Herrera G, Young ML, Hole CR, Wozniak KL, Wormley FL Jr. Protective immunity against pulmonary cryptococcosis is associated with STAT1-mediated classical macrophage activation. *J Immunol* (2012) 189:4060–8. doi:10.4049/jimmunol.1103455
34. Flaczyk A, Duerr CU, Shourian M, Lafferty EI, Fritz JH, Qureshi ST. IL-33 signaling regulates innate and adaptive immunity to *Cryptococcus neoformans*. *J Immunol* (2013) 191:2503–13. doi:10.4049/jimmunol.1300426
35. Osterholzer JJ, Chen G-H, Olszewski MA, Zhang Y-M, Curtis JL, Huffnagle GB, et al. Chemokine receptor 2-mediated accumulation of fungicidal exudate macrophages in mice that clear cryptococcal lung infection. *Am J Pathol* (2011) 178:198–211. doi:10.1016/j.ajpath.2010.11.006
36. Eastman AJ, Osterholzer JJ, Olszewski MA. Role of dendritic cell-pathogen interactions in the immune response to pulmonary cryptococcal infection. *Future Microbiol* (2015) 10:1837–57. doi:10.2217/fmb.15.92
37. Xu J, Eastman AJ, Flaczyk A, Neal LM, Zhao G, Carolan J, et al. Disruption of early tumor necrosis factor alpha signaling prevents classical activation of dendritic cells in lung-associated lymph nodes and development of protective immunity against cryptococcal infection. *MBio* (2016) 7:e00510–16. doi:10.1128/mBio.00510-16
38. Anderson AC, Anderson DE, Bregoli L, Hastings WD, Kassam N, Lei C, et al. Promotion of tissue inflammation by the immune receptor Tim-3 expressed on innate immune cells. *Science* (2007) 318:1141–3. doi:10.1126/science.1148536
39. Bowdish DM, Sakamoto K, Lack NA, Hill PC, Sirugo G, Newport MJ, et al. Genetic variants of MARCO are associated with susceptibility to pulmonary tuberculosis in a Gambian population. *BMC Med Genet* (2013) 14:47. doi:10.1186/1471-2350-14-47
40. Alanio A, Vernel-Pauillac F, Sturny-Leclère A, Dromer F. *Cryptococcus neoformans* host adaptation: toward biological evidence of dormancy. *MBio* (2015) 6:e02580–14. doi:10.1128/mBio.02580-14
41. Getahun H, Matteelli A, Chaisson RE, Raviglione M. Latent *Mycobacterium tuberculosis* infection. *N Engl J Med* (2015) 372:2127–35. doi:10.1056/NEJMra1405427
42. Arora S, Olszewski MA, Tsang TM, McDonald RA, Toews GB, Huffnagle GB. Effect of cytokine interplay on macrophage polarization during chronic pulmonary infection with *Cryptococcus neoformans*. *Infect Immun* (2011) 79:1915–26. doi:10.1128/IAI.01270-10
43. Hernandez Y, Arora S, Erb-Downward JR, McDonald RA, Toews GB, Huffnagle GB. Distinct roles for IL-4 and IL-10 in regulating T2 immunity during allergic bronchopulmonary mycosis. *J Immunol* (2005) 174:1027–36. doi:10.4049/jimmunol.174.2.1027
44. Almeida GM, Andrade RM, Bento CA. The capsular polysaccharides of *Cryptococcus neoformans* activate normal CD4+ T cells in a dominant Th2 pattern. *J Immunol* (2001) 167:5845–51. doi:10.4049/jimmunol.167.10.5845
45. Vecchiarelli A, Pietrella D, Lupo P, Bistoni F, McFadden DC, Casadevall A. The polysaccharide capsule of *Cryptococcus neoformans* interferes with human dendritic cell maturation and activation. *J Leukoc Biol* (2003) 74:370–8. doi:10.1189/jlb.1002476

Conflict of Interest Statement: The authors declare that the research was conducted in the absence of any commercial or financial relationships that could be construed as a potential conflict of interest.

Copyright © 2017 Xu, Flaczyk, Neal, Fa, Cheng, Ivey, Moore, Curtis, Osterholzer and Olszewski. This is an open-access article distributed under the terms of the Creative Commons Attribution License (CC BY). The use, distribution or reproduction in other forums is permitted, provided the original author(s) or licensor are credited and that the original publication in this journal is cited, in accordance with accepted academic practice. No use, distribution or reproduction is permitted which does not comply with these terms.

frontiers in Immunology

ORIGINAL RESEARCH
published: 08 February 2018
doi: 10.3389/fimmu.2018.00210

Leucine-Rich Repeat Kinase 2 Controls the Ca^{2+}/Nuclear Factor of Activated T Cells/IL-2 Pathway during *Aspergillus* Non-Canonical Autophagy in Dendritic Cells

*Alicia Yoke Wei Wong[1,2], Vasilis Oikonomou[3], Giuseppe Paolicelli[3], Antonella De Luca[3], Marilena Pariano[3], Jan Fric[1,4], Hock Soon Tay[1], Paola Ricciardi-Castagnoli[1,5] and Teresa Zelante[1,3]**

[1]Singapore Immunology Network, Agency for Science, Technology and Research, Singapore, Singapore, [2]National University of Singapore Graduate School for Integrative Sciences and Engineering, National University of Singapore, Singapore, Singapore, [3]Department of Experimental Medicine, University of Perugia, Perugia, Italy, [4]Center for Translational Medicine (CTM), International Clinical Research Center (ICRC), St. Anne's University Hospital Brno, Brno, Czechia, [5]Toscana Life Sciences Foundation, Siena, Italy

OPEN ACCESS

Edited by:
Steven Templeton, Indiana University School of Medicine – Terre Haute, United States

Reviewed by:
Georgios Chamilos, University of Crete, Greece, United States
Eva Maria Carmona, Mayo Clinic Minnesota, United States

***Correspondence:**
Teresa Zelante
teresa.zelante@unipg.it

Specialty section:
This article was submitted to Microbial Immunology, a section of the journal Frontiers in Immunology

Received: 24 August 2017
Accepted: 24 January 2018
Published: 08 February 2018

Citation:
Wong AYW, Oikonomou V, Paolicelli G, De Luca A, Pariano M, Fric J, Tay HS, Ricciardi-Castagnoli P and Zelante T (2018) Leucine-Rich Repeat Kinase 2 Controls the Ca^{2+}/Nuclear Factor of Activated T Cells/IL-2 Pathway during Aspergillus Non-Canonical Autophagy in Dendritic Cells. Front. Immunol. 9:210. doi: 10.3389/fimmu.2018.00210

The Parkinson's disease-associated protein, Leucine-rich repeat kinase 2 (LRRK2), a known negative regulator of nuclear factor of activated T cells (NFAT), is expressed in myeloid cells such as macrophages and dendritic cells (DCs) and is involved in the host immune response against pathogens. Since, the Ca^{2+}/NFAT/IL-2 axis has been previously found to regulate DC response to the fungus *Aspergillus*, we have investigated the role played by the kinase LRRK2 during fungal infection. Mechanistically, we found that in the early stages of the non-canonical autophagic response of DCs to the germinated spores of *Aspergillus*, LRRK2 undergoes progressive degradation and regulates NFAT translocation from the cytoplasm to the nucleus. Our results shed new light on the complexity of the Ca^{2+}/NFAT/IL-2 pathway, where LRRK2 plays a role in controlling the immune response of DCs to *Aspergillus*.

Keywords: leucine-rich repeat kinase 2, nuclear factor of activated T cells, NRON, dendritic cell, *Aspergillus*, autophagy

INTRODUCTION

Leucine-rich repeat kinase 2 (LRRK2) was first discovered in genome-wide linkage studies of patients of Parkinson's disease (1, 2). Since then, the majority of studies on LRRK2 have been focused on linking various point mutations in the various domains of LRRK2 with Parkinson's disease (3), and the contribution of mutated LRRK2 protein to neuronal toxicity (4–6). Studies have also shown a possible involvement of the immune system in Parkinson's disease pathogenesis. Inflammation is thought to lead to the neurodegeneration and neurotoxicity seen in Parkinson's disease (7, 8). Also, it is known that patients of Parkinson's disease are often hospitalized for various types of infections, such as urinary tract infection and pneumonia (9). The involvement of LRRK2 in response to inflammatory stimulus (10), as well as microbes, and pathogen-associated molecular patterns (PAMPs) (11–14), have also been seen in several studies.

Leucine-rich repeat kinase 2 has been reported to negatively regulate the nuclear factor of activated T cells (NFAT) pathway in bone marrow-derived macrophages (BMDMs) *via* the NRON complex. LRRK2 was found to bind 5 of the 11 proteins associated with the NRON complex, and overexpression of LRRK2 increases binding of NFAT with NRON complex members, in particular IQGAP, chromosome segregation 1-like (CSE1L), and transportin-1 (15). This regulation of NFAT by LRRK2 was found to be independent of its kinase function. Given the importance of the NFAT pathway in the regulation of T cell development and function [as reviewed in Ref. (16)], it is of notice that LRRK2 expression is lower in T cells than in BMDMs and bone marrow-derived dendritic cells (BMDCs) (15), underlining a possible role of LRRK2 in innate immunity during infection as supported by other studies (10, 17).

It has been established that the Ca^{2+}/NFAT/IL-2 pathway is activated in DCs in response to live *Candida albicans* and zymosan binding to Dectin-1 leading to the production of cytokines, including IL-2 (18). To this end, we have also shown that NFAT signaling regulates cytokine IL-2 expression in DCs stimulated *in vitro* with *Saccharomyces cereviseae*-derived whole glucan particles (19), and that DC-derived IL-2 expression in lung $CD103^+$ DCs is important for eliciting the appropriate Th17 cell response to *Aspergillus fumigatus* infection (20). In this study, we report that LRRK2 localizes to lysosomic and endosomic structures in DCs at steady state, as well as after *Aspergillus* exposure, and that autophagy is able to influence LRRK2 expression, and subsequently, the activation of Ca^{2+}/NFAT/IL-2 axis in DCs differently from the other NRON complex components. In conclusion, our findings suggest a role for LRRK2 and the NRON complex in the early phases of the immune response to *Aspergillus*.

MATERIALS AND METHODS

Mice

Eight-week-old wild-type C57BL/6 mice used for experiments were bred and kept under specific pathogen-free conditions in the Biomedical Resource Centre, Singapore. All experiments and procedures were approved by the Institutional Animal Care and Use Committee (IACUC) of A*STAR (Biopolis, Singapore) (Authorization No.: IACUC 110626) in accordance with the guidelines of the Agri-Food and Veterinary Authority (AVA) and the National Advisory Committee for Laboratory Animal Research (NACLAR) of Singapore. Z. Liu of Institute of Biophysics Chinese Academy of Sciences provided $LRRK2^{-/-}$ mice bone marrows.

Fungal Cells

Aspergillus fumigatus isolate AF293 (MYA-4609, ATCC, Manassas, VA, USA) was used for cultures. *A. fumigatus* was cultivated for 5 days on potato dextrose agar (Sigma-Aldrich, St. Louis, MO, USA) before conidia were harvested by washing with PBS 0.05% Tween 20. Swollen conidia were obtained by incubating conidia in liquid yeast extract peptone dextrose at 37°C for 4 h on a rotary shaker at 300 rpm. In addition, a red fluorescent protein (RFP)-expressing *A. fumigatus* AF293 strain used in this study was obtained from Prof. Eric Pearlman (Case Western Reserve University, Cleaveland, OH, USA).

Cell Cultures

Bone marrow-derived dendritic cells were generated by culturing mouse bone marrow extracted by flushing the femurs and tibias. The collected bone marrow was treated with ammonium-chloride-potassium lysing buffer. The remaining cells post-lysis were cultured in suspension plates with Iscove's Modified Dulbeccos Medium (IMDM) (HyClone, Thermo Fisher Scientific, Waltham, MA, USA) containing 10% fetal bovine serum (FBS) (Euroclone, Milan, Italy), 2 mM L-glutamine (Gibco, Life Technologies, Carlsbad, CA, USA), 100 U/mL Penicillin/Streptomycin (Gibco, Life Technologies, Carlsbad, CA, USA), supplemented with 10% supernatant from a GM-CSF-producing B16 melanoma cell line to a final concentration of 20 ng/mL GM-CSF to generate BMDCs.

The long-term GM-CSF cytokine-dependent DC cell line, D1 (21), was grown in suspension plates with IMDM containing 10% FBS (Australian origin, Gibco, Life Technologies, Carlsbad, CA, USA) 2 mM L-glutamine, 100 U/mL Penicillin/Streptomycin, and 55 μM β-mercaptoethanol (Gibco, Life Technologies, Carlsbad, CA, USA), supplemented with 30% supernatant from NIH/3T3 cells transfected to produce GM-CSF to a final concentration of 10 ng/mL.

In all stimulation experiments, cells were stimulated with *A. fumigatus* swollen conidia in a 1:10 (fungi:cell) ratio. Pharmaceuticals used in these experiments include 3-methyladenine (3MA) (Sigma-Aldrich, St. Louis, MO, USA), Bafilomycin A (Baf) from *Streptomyces griseus* (Calbiochem, Merck Millipore, Billerica, MA, USA), Cytochalasin D (CytoD) (Sigma-Aldrich, St. Louis, MO, USA), leupeptin hemisulfate (Sigma-Aldrich, St. Louis, MO, USA), and ammonium chloride (Leu/A) (Sigma-Aldrich, St. Louis, MO, USA).

NFAT Nuclear Translocation

D1 nuclear factor of activated T cells translocation-firefly luciferase reporter cells were generated by transducing the D1 cells with Cignal Lenti NFAT Reporter with firefly luciferase (SABiosciences, Qiagen, Venlo, Limburg, Netherlands). NFAT nuclear translocation was detected by ONE-Glo™ Luciferase assay System (Promega, Madison, WI, USA) and the luminescence signal quantified with the GloMax®-Multi Detection System Luminometer module (Promega, Madison, WI, USA).

shRNA Knockdown

MISSION® Lentiviral Particles (Sigma-Aldrich, St. Louis, MO, USA) with the pLKO.1-puro vector containing shRNA sequences targeting NRON, CSE1L, sperm-associated antigen 9 (SPAG9), LRRK2 shRNA, PPP2R1A were used.

Below details includes the gene reference identification number (NM ID) and The RNAi Consortium (TRC) clone identification number (clone ID) for the shRNA-lentiviral particles for targeting these genes (**Table 1**).

NRON shRNA lentiviral particles were custom designed and packaged into lentiviral particles (ACGGTGGGTTTATGACAA ATT and ACGGGTGCTGGATGACATATT) by Sigma-Aldrich

TABLE 1 | Details of commercially purchased MISSION® lentiviral particles.

Gene target	NM ID	The RNAi Consortium (TRC) clone ID
Chromosome segregation 1-like	NM_023565	TRCN0000174506 TRCN0000174691
Sperm-associated antigen 9	NM_027569	TRCN0000176696 TRCN0000177089
Ppp2r1a	NM_016891	TRCN0000012624 TRCN0000012626
Leucine-rich repeat kinase 2	NM_025730	TRCN0000022656 TRCN0000022657

(St. Louis, MO, USA). MISSION® pLKO.1-puro non-target shRNA control transduction particles (Sigma-Aldrich, St. Louis, MO, USA) were used as a transduction control.

For the transduction, D1 cells were seeded and rested overnight in antibiotic-free D1 medium. The next day, the medium was replaced with antibiotic-free D1 medium containing 2 μg/mL SureEntry™ transduction reagent (SABiosciences, Qiagen, Venlo, Limburg, Netherlands). The D1 cells were then transduced with MISSION® lentiviral particles at multiplicity of infection (MOI) 10 and allowed to incubate for 20 h at 37°C in 5% CO_2. After 20 h incubation, the medium containing the lentivirus particles was aspirated out, replaced with complete D1 medium, and allowed to rest for 48 h at 37°C in 5% CO_2. After being allowed to rest, successfully transduced cells were selected 4 days by replacing the medium with D1 medium containing 0.5 μg/mL of puromycin dihydrochloride (Calbiochem, Merck Millipore, Billerica, MA, USA).

For *in vitro* silencing of *Rubcn*, *Nox2,* and *Atg7*, D1 were transfected with 40 nM of the following siRNAs: *Rubcn* (Duplex name mm.Ri.1700021K19Rik.13.1; sense, 5′-GUACUUGACC GCUAGUAAAAUCATT-3′; antisense, 5′-GACAUGAACUGGC GAUCAUUUUAGUAA-3′), Nox2 (Duplex name mm.Ri.Cybb.13.1; sense, 5′-GUUCAAGGUCAGUUUAUUGAAUGAA-3′; antisense, 5′-CACAAGUUCCAGUCAAAUAACUUACUU-3'), Atg7 (Duplex name mm.Ri.Atg7.13.1; sense, 5′CUUGAUCAGUACGAGCGA GAAGGAT-3′; antisense, 5′-AAGAACUAGUCAUGCUCGCU CUUCCUA-3′) (all from IDT). Silencing was performed using TransIT-TKO® Transfection Reagent (Mirus) and incubated for 24 h (as indicated by preliminary experiments performed at 12, 24, or 48 h) at 37°C in 5% CO_2. Transfected cells were exposed to A-sw.

Cytotoxicity Assay

The sensitivity of cells to different inhibitors was determined by 3-(4,5-dimethylthiazol-2-yl)-2,5-diphenyltetrazolium bromide (MTT; Trevigen) assay. Briefly, 2,500 D1 cells were seeded in 180 μL medium in quadruplicate in 96-well tissue culture plates and following overnight incubation with A-sw in a 1:10 (fungi:cell) ratio with or without inhibitors. After 24 h MTT was added and the absorbance of the formazan product was measured on a microplate reader TECAN infinite m200 together with the i-control™ software (Mannedorf, Switzerland) at 600 nm.

Lysosome Isolation

Lysosomes were isolated from D1 cells as described by Graham (22). Briefly, D1 cells were harvested from suspension plates and washed with PBS. The cell pellet was then resuspended in ice cold homogenization medium (0.25 M sucrose, 1 mM EDTA, 10 mM HEPES, pH 7) and homogenized in a Wheaton type Dounce tissue grinder (Wheaton, Millville, NJ, USA) on ice until above 90% cell breakage was observed under the microscope by staining with PBS containing 0.04% v/v Tryphan blue (Sigma-Aldrich, St. Louis, MO, USA). The homogenate was then centrifuged at 800 *g* for 10 min to pellet nuclei and cell debris. The resulting supernatant from the centrifuge was mixed with bovine serum albumin (final proportion of 4% v/v) and Percoll (final proportion of 22% v/v). The mixture was then ultracentrifuged for 30 min at 36,000 × *g* without brake activation. After centrifugation, a visible band of the enriched lysosomes was seen near the bottom of the tube. 400 μL fractions, containing the enriched lysosomes were collected, and Igepal CA-630 (final proportion of 0.5% v/v) was used to solubilize the lysosome membranes. Solubilized fractions were centrifuged at 100,000 × *g* for 2 h to pellet the Percoll, and the resulting supernatants were obtained for analysis by western blotting.

Cytokine Detection

Cell culture medium was assayed for cytokine production by sandwich enzyme-linked immunosorbent assay (ELISA) for IL-2, IL-12/IL-23p40, and IL-23. IL-2 and IL-12/IL-23p40 were assayed using commercially available antibody pairs and standards from BioLegend (San Diego, CA, USA) and eBioscience (San Diego, CA, USA), respectively. Measurements were detected using the TECAN infinite m200 together with the i-control™ software (Mannedorf, Switzerland; measurement wavelength 450 nm, reference wavelength 570 nm). IL-23 was assayed using mouse IL-23 ELISA Ready-SET-Go!® (Second-generation assay) (Affymetric eBioscience, San Diego, CA, USA) according to manufacturer's instructions. In addition, selected supernatant samples were analyzed using the Milliplex Multi Analyte Panels Mouse TH17 Magnetic Bead Panel Immunology Multiplex assay (MTH17MAG-47K) in conjunction with the Luminex MAGPIX® system (Merck Millipore, Billerica, MA, USA).

Western Blot

Whole cell lysates were obtained by lysing cells in radioimmunoprecipitation assay buffer containing 1× cOmplete, EDTA-free Protease Inhibitor Cocktail (Roche, Basel, Switzerland), 1× PhosSTOP Phosphatase Inhibitor Cocktail (Roche, Basel, Switzerland), and 1 mM phenylmethanesulfonylfluoride. The protein concentration in the cell lysates were measured using the Pierce™ 660 nm Protein assay kit (Thermo Scientific, Waltham, MA, USA), and colorimetric readings were obtained by measuring the wavelength at 660 nm using the TECAN infinite m200 together with the i-control™ software (Mannedorf, Switzerland). Protein lysates were diluted with Laemmli buffer containing 2.5% v/v β-mercaptoethanol (Sigma-Aldrich, St. Louis, MO, USA) and heated at 95°C for 10 min prior to separation on sodium dodecyl sulfate (SDS)-polyacrylamide gel electrophoresis (PAGE) in

Tris-glycine-SDS buffer, along side the Precision Plus Protein Dual Color standards protein ladder (Bio-Rad, Hercules, CA, USA). Up to 50 μg of protein was loaded into each well for separation. The SDS-PAGE gel was run at 60 V till all samples entered the resolving gel, before increasing the running voltage to 110 V until the dye front had traveled to the end of the gel. The separated proteins were then transferred to polyvinylidene fluoride membrane in Tris-glycine buffer containing 10% v/v methanol at either 240 mA for 2 h or 200 mA for 4 h. For LRRK2, lysates were first concentrated using the Vivaspin 500 molecular weight cut off 100,000 columns (Sartorius, Goettingen, Germany), and the NuPAGE® large protein analysis system (Life Technologies, Carlsbad, CA, USA) was adopted. Antibodies used for western blot include: LRRK2 rabbit monoclonal antibody, clone: MJFF2 (Epitomics, Abcam, Cambridge, UK), LC3B antibody (cell Signaling Technology, Danvers, MA, USA), Purified anti-mouse CD107a (LAMP-1), clone: 1D4B (Biolegend, San Diego, CA, USA), anti-TATA binding protein (TBP), clone: 1TBP18 (Abcam, Cambridge, UK), Rab5 (C8B1) Rabbit mAb (cell Signaling Technology, Danvers, MA, USA), JIP4/SPAG9 (D72F4) XP® Rabbit mAb (cell Signaling Technology, Danvers, MA, USA), Anti-PPP2R1A antibody [6F9] (Abcam, Cambridge, UK), GAPDH antibody, clone: 6C5 (Merck Millipore, Billerica, MA, USA), DAPK1 mouse polyclonal antibody, clone: RB3033 (antibodies-online.com). For DAPK1, normalization was performed by probing the membrane with mouse monoclonal β-actin antibody, clone: AC-40 (Sigma-Aldrich). Band pixel density was analyzed from the film scans by ImageJ software (NIH, Bethesda, MD, USA).

RNA Extraction, Real-time Quantitative PCR

Cells were lysed with 1 mL of TRIzol® reagent (Ambion, Life Technologies, Carlsbad, CA, USA) and flash frozen on dry ice prior to storage at −80°C. To extract RNA, 200 μL (20% v/v) of chloroform (Merck, Kenilworth, NJ, USA) was added to each sample. Each sample was then shaken vigorously, and then centrifuged at 15,000 rpm, 4°C for 15 min. This separated the sample into a top organic phase containing the RNA, a thin interface containing DNA and a bottom organic phase containing protein. The top supernatant was aspirated and transferred to a new tube. An equal volume of 70% v/v ethanol was added and mixed to the sample. RNA was extracted from this mixture using the RNeasy mini kit (Qiagen, Venlo, Limburg, Netherlands) according to the manufacturer's instructions. Extracted RNA samples were then treated with DNase using the TURBO DNA-free™ kit (Ambion, Life Technologies, Carlsbad, CA, USA) according to manufacturer's instructions. The RNA content of each sample was then quantified using the Nanodrop™ 1000 (Thermo Scientific, Waltham, MA, USA). 2 μg of RNA was retro-transcribed into cDNA using the High Capacity Reverse Transcription Kit (Applied Biosystems, Life Technologies, Carlsbad, CA, USA) according to manufacturer's instruction. The obtained cDNA was then used for real-time quantitative PCR. The Brilliant SYBR® Green QPCR Mastermix and Reference Dye (Stratagene, Agilent Technologies, Santa Clara, CA, USA) was used to set up the real-time quantitative PCR reaction, and the samples were run in the MX3000P instrument (Stratagene, Agilent Technologies, Santa Clara, CA, USA). Gene expression data was analyzed using the MxPro QPCR software (Stratagene, Agilent Technologies, Santa Clara, CA, USA). Primer sequences targeting mouse genes used in this study are listed in **Table 2**.

Immunofluorescence Confocal Microscopy

D1 cells were seeded and stimulated in μ-slide 8-well chambers (Ibidi, Martinsried, Germany). Post-stimulation cells were fixed in 2% paraformaldehyde (Sigma-Aldrich, St. Louis, MO, USA), and permeabilized in PBS containing 0.1% saponin (Sigma-Aldrich, St. Louis, MO, USA), 0.2% gelatin (Fluka Analytical, Sigma-Aldrich, St. Louis, MO, USA), and 5% bovine serum albumin (Merck Millipore, Darmstadt, Germany). Cells were stained and washed using PBS containing 0.01% saponin and 0.2% gelatin. Cells were stained with a primary LC3B antibody (Cell Signaling Technology, Danvers, MA, USA) and a secondary goat α-rabbit IgG antibody conjugated to Alexa Fluor® 488 (Invitrogen, Life Technologies, Carlsbad, CA, USA). In addition, 4',6-diamidino-2-phenylindole (Invitrogen, Life Technologies, Carlsbad, CA, USA) was used to stain the cell nuclei. Images were acquired on an Olympus FV1000 confocal microscope in conjunction with the Fluorview FV1000 software (Olympus, Tokyo, Japan).

For DAPK1 staining, DAPK1 mouse polyclonal antibody, clone: RB3033 (antibodies-online.com) and Alexa Fluor® 488 phalloidin was used for selective labeling of F-actin. After overnight staining with primary antibody, slides were washed and incubated with Rabbit IgG-TRITC antibody (Sigma-Aldrich).

TABLE 2 | List of real-time quantitative PCR primers.

Gene	Forward primer (5′–3′)	Reverse primer (5′–3′)
Chromosome segregation 1-like	GTGGGAAAGGACAGGAAACA	AAACCTTGGTGATCGTTTGC
Gapdh	TTGAGGTCAATGAAGGGGTC	TCGTCCCGTAGACAAAATGG
Leucine-rich repeat kinase 2	GATGTCAGTACGCCCCTGAT	CTGCCAGCGCTATGATGTTA
Nron	CAGTAAAGGAGCAGTAGTGGAAACAG	TGGGGGGAGCGAATGGCATCGGGAAC
Ppp2r1a	CAACCTGGATTGGTGGAACG	GATCCACTAGCCAGGCCATA
Sperm-associated antigen 9	AAACCTCAGGGACTCCAGGT	CCCCACCACTGCTACTTTGT
Rubcn	GUACUUGACCGCUAGUAAAAUCATT	GACAUGAACUGGCGAUCAUUUUAGUAA
Atg7	CUUGAUCAGUACGAGCGAGAAGGAT	AAGAACUAGUCAUGCUCGCUCUUCCUA
Nox2	GUUCAAGGUCAGUUUAUUGAAUGAA	CACAAGUUCCAGUCAAAUAACUUACUU
Dapk1	CGAGUUUGGAUAUGACAAGGAUACA	UGUAUCCUUGUCAUAUCCAAACUCGCC

Images were acquired using a Zeiss Axio Observer. Z1 inverted microscope, equipped with Apotome filter and Axiocam MRm camera detection system Zeiss using a 63×/1.25 oil Plan/neofluar objective.

Transmission Electron Microscopy

Stimulated D1 cells were harvested from the suspension plate with 2 mM EDTA in PBS and washed with 0.2 M sodium cacodylate buffer (pH 7.4). Cells were then fixed in cacodylate fixative buffer (0.1 M sodium cacodylate, 2% paraformaldehyde, and 3% gluteraldehyde) overnight at 4°C. The cells were then washed with 0.2 M sodium cacodylate buffer and dehydrated on an alcohol series (30, 50, 70, 80, 90, and 100%) for 15 min each. Specimens were then embedded into acrylic resin. Ultrafine sections were obtained by cutting into the resin specimens with a glass blade on an ultramicrotome, and mounted on nickel grids. The grids were then washed with PBS and then stained with antibodies LRRK2 rabbit monoclonal antibody clone: MJFF2 (Epitomics, Abcam, Cambridge, UK) and purified anti-mouse CD107a (LAMP-1) clone: 1D4B (Biolegend, San Diego, CA, USA), followed by secondary antibodies that have been conjugated with either 5 or 15 nm gold particles (Cytodiagnostics, Burlington, ON, Canada). All antibody incubations were done in PBS containing 1% bovine serum albumin. After antibody staining, grids were post-fixed with cacodylate fixative buffer for 15 min, and then stained with 2% uranyl acetate. Micrographs were taken with an EM 208 transmission electron microscope (Phillips, Amsterdam, Netherlands).

Graphs and Statistics

Statistical significance of experiments was determined either by Student's *t*-test, one-way ANOVA, or two-way ANOVA as indicated. For statistics generated by one-way ANOVA, the differences between individual groups were compared using the Bonferroni's Multiple Comparison post-test. All graphs and statistics were generated using the Graphpad Prism® software version 6.0 (Graphpad Software, La Jolla, CA, USA).

Flow Cytometry Analysis

At 16 h post-silencing, BMDCs were treated with *Aspergillus* RFP swollen conidia (ratio of 1:1) for 1 h. BMDCs were collected, washed twice with FACS buffer, stained with CD11c-Alexa Fluor 700® (BD) and analyzed by flow cytometry. Data (mean ± SD) represent three independent experiments in which technical triplicates of 100,000 cells per sample were acquired using a Fortessa cytometer (BD). Phagocytosis was calculated using flow cytometry analysis (described above). The percentage of phagocytosis equals the number of BMDCs that have engulfed RFP *A. fumigatus*.

Time Lapse Video

Bone marrow-derived dendritic cells grown in 48-well plates were exposed with shRNA RUBICON or scramble overnight. Cells were then treated with *Aspergillus* swollen conidia for 1 h. Time-lapse imaging was performed over a period of 1 h with a 40× objective using the time-lapse function of the EVOS FL Auto Imaging System with the Invitrogen™ EVOS™ Onstage Incubator.

RESULTS

LRRK2 Is Expressed in DCs and Is Regulated during *A. fumigatus* Infection

Leucine-rich repeat kinase 2 is known to regulate NFAT translocation in response to TLR ligands (15). Since, we have previously shown that *A. fumigatus* swollen conidia, more than ungerminated conidia, induces Ca^{2+}/NFAT/IL-2 pathway in DCs (20), here we went to study the regulation of LRRK2 in response to fungal infection. First, we measured LRRK2 expression at the mRNA and protein level in D1 cells at resting state as well as in D1 cells stimulated with swollen conidia. We found that at resting state, DCs express LRRK2 on both the mRNA (**Figure 1A**) and the protein level (**Figure 1B**). Upon stimulation with swollen conidia, LRRK2 levels were found to be downregulated on both the mRNA as well as the protein level. At 8 h post-stimulation, downregulation of LRRK2 on the gene level was found to be statistically significant, while LRRK2 protein levels decreased further significantly (8 h 0.217 ± 0.1). The downregulation of LRRK2 was further maintained on protein level at 18 h (0.373 ± 0.2), and on gene expression at 24 h post-stimulation, showing that *Aspergillus* is able to influence *Lrrk2* gene expression on both transcriptional and translational level. Interestingly, the downregulation of LRRK2 in DCs responding to *Aspergillus* swollen conidia corresponded to the upregulation of NFAT1 translocation (Figure S1A in Supplementary Material) and IL-2 production (Figure S1B in Supplementary Material).

LRRK2 Intracellular Localization

It has been reported that LRRK2 is degraded in lysosomes (23). In order to understand the subcellular localization of LRRK2 in DCs, lysosomes and early endosomes were enriched from D1 cells by gradient centrifugation protocol (22), and the protein content of the fractions enriched with these organelles were analyzed by western blot (**Figure 2A**). Fraction (lane 1) was harvested and further centrifuged (lane 2), which was negative for the nuclear marker, TBP, indicating that there was no contamination with nuclear material. We found that LRRK2 was present in fractions that expressed lysosomal-associated membrane protein 1 (LAMP-1) and Rab5, which are markers for lysosomes and early endosomes, respectively. This is in line with what was already reported (24, 25). In addition, by electron microscopy, lysosomes were LAMP-1 positive, spherical, enclosed by one membrane, with a diameter of 70–150 nm, homogenous and electron-dense interior. Endosomes were LAMP-1 negative and poorly electron-dense (**Figure 2B**). Interestingly, LRRK2 (**Figure 2C**) was found localized also on endosomic structures. In addition, as endosomes have been proposed to be signaling hubs, where components of signaling pathways can localize and interact (26), the localization of LRRK2 on endosomes implies that the endosomes serve as a possible niche were NFAT signaling pathway is kept under control.

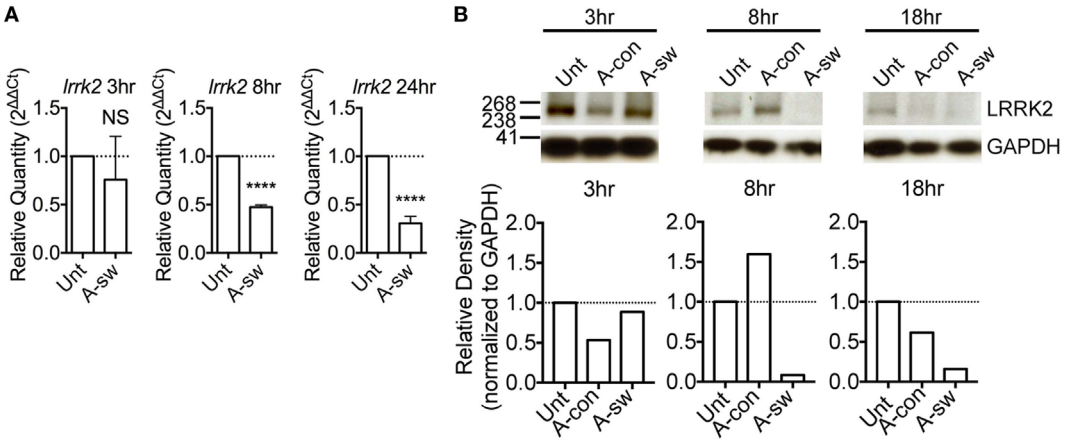

FIGURE 1 | Leucine-rich repeat kinase 2 (LRRK2) is expressed in dendritic cells and is downregulated by *Aspergillus fumigatus*. **(A)** LRRK2 mRNA in D1 cells. Data is displayed as the mean gene expression ± SD of two biological replicates and normalized to the housekeeping protein, GAPDH. Differences found to be statistically significant by one-way ANOVA with Bonferonni's Multiple Comparison post-test are indicated (NS, non-significant; ****, $p < 0.0001$). **(B)** Protein expression level of LRRK2 in whole cell lysates of D1 cells stimulated with *A. fumigatus* condia and swollen conidia. For densitometry analysis, band densities for LRRK2 were normalized to the band density of the housekeeping protein, GAPDH, after which the density of the LRRK2 band of the treated sample was compared with that of the untreated sample. Data is representative of three independent experiments. Abbreviations used: Untreated (Unt); *A. fumigatus* conidia (A-con); *A. fumigatus swollen conidia* (A-sw).

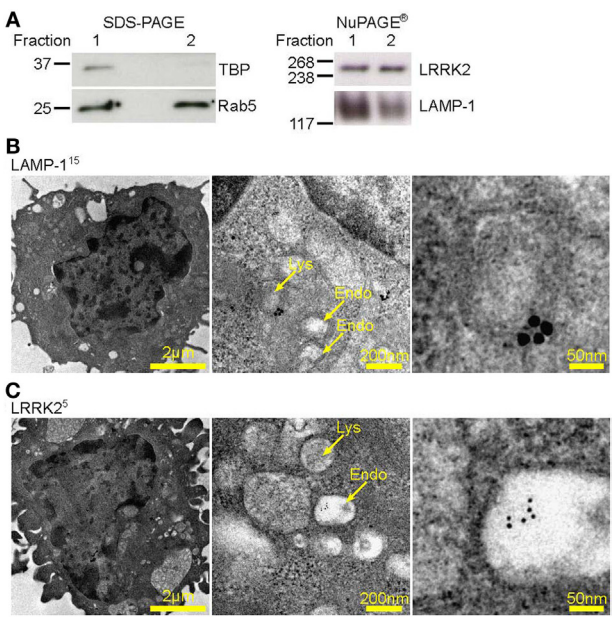

FIGURE 2 | Leucine-rich repeat kinase 2 (LRRK2) is localized on lysosomes and endosomes of dendritic cells. **(A)** Western blot analysis of presence of TATA binding protein, Rab5, LRRK2, and LAMP-1 in a representative protein fraction obtained from the enrichment of lysosomes from D1 cells. Lysate from the protein fraction was run on both sodium dodecyl sulfate-polyacrylamide gel electrophoresis (PAGE) and NuPAGE® to probe for the proteins indicated. Data are representative of three independent experiments **(B–C)**, D1 cells were processed for immune-electron microscopy, stained for LAMP-1 or LRRK2, and labeled with appropriate secondary antibodies conjugated with 5 or 15 nm gold particles (size of particles indicated in superscript). Lysosomic and endosomic structures are as indicated. Electron micrographs of D1 cells show LAMP-1 positive lysosome **(B)**, as well as endosomic structures positive for LRRK2 **(C)**. Size of scale bars are as indicated.

A. fumigatus Swollen Conidia Activate the Non-Canonical Autophagic Pathway in DCs

Lysosomes are known to be involved in the maturation of autophagic vesicles. Given that autophagy is activated by β-glucan (27) and *A. fumigatus* (28, 29), we investigated autophagy in D1 cells stimulated with *Aspergillus* swollen conidia in order to establish a possible role of the autophagic response in the regulation of the NFAT1 translocation. D1 cells stimulated with swollen conidia showed the formation of LC3-positive phagosomes [LC3 associated phagocytosis (LAPosome)] (**Figure 3A**) similar to that induced by β-glucan (27) and *A. fumigatus* (30) in other studies, although germinated A-sw conidia were only partially engulfed. Indeeed, by electron microscopy, it was clear that the resulting membrane cupping was not formed by the double-membranes characteristic of classical autophagy (**Figure 3B**) as previously shown (30). Although images (**Figure 3B**) show partial fungal internalization, time-lapse imaging of DCs demonstrates the bright field on the EVOS FL Auto Cell Imaging System a complete process of phagocytosis (Supplementary Video S1 in Supplementary Material). Taken together, the observations from immunofluorescent staining of LC3 and electron microscopy indicate that the autophagic response induced by *A. fumigatus* swollen conidia in DCs is non-canonical, as reported for conidia (31). LC3-I to LC3-II conversion and higher LC3-II turnover was indeed observed in *A. fumigatus*-stimulated DCs, and p62 was not degraded (**Figure 3C**; Figure S1C in Supplementary Material). Our results indicate that swollen conidia induce non-canonical autophagy in DCs. In addition, we found that there was an increase of subcellular multivesicular structures present in DCs stimulated with swollen conidia as revealed by electron microscopy. Multivesicular structures express LAMP-1 as well as

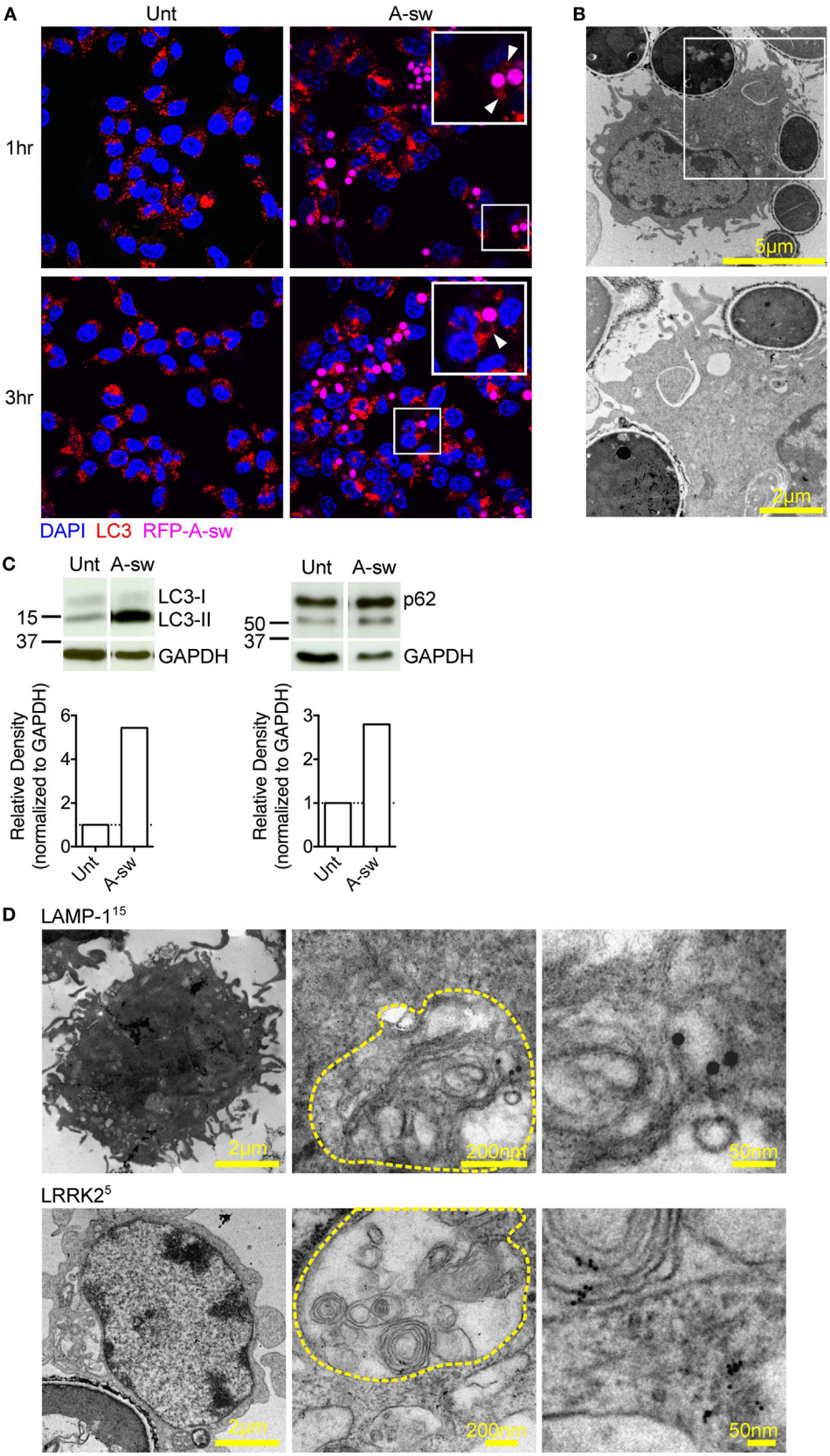

FIGURE 3 | Continued

FIGURE 3 | *Aspergillus fumigatus* swollen conidia activate non-canonical autophagy and the formation of multivesicular bodies in dendritic cells. D1 cells were stimulated with *A. fumigatus* swollen conidia for 3 h. **(A)** Immunofluorescent staining of LC3 (red). Data is representative of two independent experiments. **(B)** Electron micrograph of *Aspergillus* cupping. The bottom panel is zoomed in from the area indicated in the top panel. Data is representative of two independent experiments. **(C)** Expression of LC3 and p62 proteins by western blot in whole cell lysates of D1 cells stimulated for 24 h with *A. fumigatus* swollen conidia. Densitometry for LC3 was performed on the LC3-II band to measure LC3-II turnover, while densitometry analysis of p62 was done on the upper band corresponding to its expected molecular weight of 60kD. Data is representative of two biological replicates**. (D)** Multilamellar bodies (encircled in yellow dashed lines) observed by electron microscopy in *A. fumigatus* swollen conidia-stimulated D1 cells and labeled for LAMP-1 or Leucine-rich repeat kinase 2 with 5 nm or 15 nm gold particles (size of particles indicated in superscript). Cells were incubated with fungi for 3 h. Size of scale bars are as indicated. Abbreviations: Untreated (Unt); *A. fumigatus swollen conidia* (A-sw).

LRRK2 (**Figure 3D**). These structures are lysosomal organelles comprising of multiple concentric layers of membrane, that have been shown to require autophagy for its formation (32). Therefore, taking into account our findings, the germinated form of *Aspergillus* is able to trigger the non-canonical autophagic response together with formation of multivesicular structure formation LRRK2^{+} in DCs.

Ca^{2+}/NFAT/IL-2 Axis Is Affected by Early Autophagic Events, Phagocytosis, and Lysosomal Maturation

Based on the previous findings, two types of autophagy inhibitors, 3MA and Baf were used to investigate whether NFAT1 translocation is mediated by the autophagic response to *A. fumigatus*. As the initiation of autophagosome formation requires Class III PI3 kinase activity, 3MA, a PI3 kinase inhibitor, functions by inhibiting autophagy in the early stages of its initiation. Baf inhibits the last step of autophagosome cargo degradation by preventing the autophagosome–lysosome fusion as well as lysosome acidification (33). We found that NFAT1 translocation and IL-2 cytokine production in DCs stimulated with *Aspergillus* germinated conidia were significantly decreased upon inhibition of the early stages of autophagy by 3-MA, but not with an inhibitor of the late stage of autophagy, Baf (**Figure 4A**). In addition, NFAT pathway in stimulated DCs was also significantly decreased when cells were treated with the phagocytosis inhibitor, CytoD (**Figure 4B**). DCs were also treated with a combination of Leupeptin and ammonium chloride (Leu/A) to inhibit lysosomal maturation by preventing acidification, and it was observed that NFAT1 translocation increased, while IL-2 production unexpectedly decreased in drug-exposed DCs in response to fungi (**Figure 4C**). In order to understand whether those variations were due to a reduced cell viability, we performed the MTT proliferation assay on all the conditions tested above (**Figure 4D**). Pivotally, cells were not affected in terms of viability by the different treatments (**Figure 4D**).

Finally, since more recently, non-canonical autophagy, also defined as LAP, has been extensively described for infection with *A. fumigatus* (29, 31), we performed shRNA of the main key players (*Rubicon*, *Nox2*, *Atg7*) of LAP on D1 cells upon *Aspergillus* treatment and we went to analyze IL-2 transcription as a key response downstream of NFAT translocation (**Figure 4E**; Figure S2 in Supplementary Material). Results here indicate that shRNA of *Rubicon* and *Nox2* mRNA, lead to a significant decrease of IL-2 transcription upon A-sw stimulation. Together, the results show that early events that occur after fungal stimulation, such as phagocytosis and the early part of the autophagy pathway, are important in the activation of the NFAT pathway, but not late-stage autophagy. Moreover, inhibition of LAP is particularly interfering NFAT translocation in DCs although shRNA of *Rubicon* is not affecting the phagocytosis process (Figure S3 in Supplementary Material). Thus, the induction of non-canonical autophagy as well as the downregulation of LRRK2 expression in *A. fumigatus*-stimulated DCs raises the possibility of autophagy being responsible for the degradation of LRRK2, resulting in the activation of NFAT1. This is further supported by the presence of LRRK2 in lysosomic-endosomic structures (**Figure 2C**) and multilamellar bodies (**Figure 3D**).

LRRK2 Deficiency in DCs Leads to Increased NFAT/IL-2 Activation Axis in Response to *A. fumigatus*

Since LRRK2 has been reported as a negative regulator of the NFAT pathway (15), we used LRRK2 $^{-/-}$ BMDCs (Figure S4 in Supplementary Material) to measure IL-2 release as well as other two cytokine regulated by NFAT in DCs (34) upon *Aspergillus* germinated spore stimulation. LRRK2$^{-/-}$ BMDCs showed a significant increase in IL-2 production when stimulated with *Aspergillus* swollen conidia at 8, 18, and 24 h, while cytokine as IL-12/IL-23p40 was significantly increased only at 8 h and IL-23 did not show significant changes (**Figure 5A**). More interestingly, stimulated NFAT-luciferase reporter D1 cells, upon silencing with LRRK2 shRNA and exposed to A-sw showed that NFAT nuclear translocation was also significantly increased (**Figure 5B**). In these settings, IL-2 was also increased upon A-sw stimulation (data not shown). Therefore, LRRK2 regulates the NFAT pathway in response to the fungus *Aspergillus*. Consequently, LRRK2 deficiency may disentangle a possible dysregulation of the NFAT/IL-2 cascade in response to the germinated fungus *Aspergillus*.

The Independent Role of LRRK2 in Regulating the NFAT/IL-2 Axis in *Aspergillus*-Stimulated DCs

It has been reported that LRRK2 physically associates with the NRON complex, and that NRON was important for mediating the regulation of NFAT1 nuclear translocation by LRRK2 (15), hence the expression of four members of the NRON complex; NRON, PPP2R1A, CSE1L, and SPAG9 was investigated in DCs in response to *Aspergillus* swollen conidia. Gene expression analysis shows that components of the NRON complex are expressed in DCs, and are negatively regulated by fungal exposure (Figure S5A in Supplementary Material). On the protein level, the expression of the NRON complex components, including PPP2R1A, CSE1L

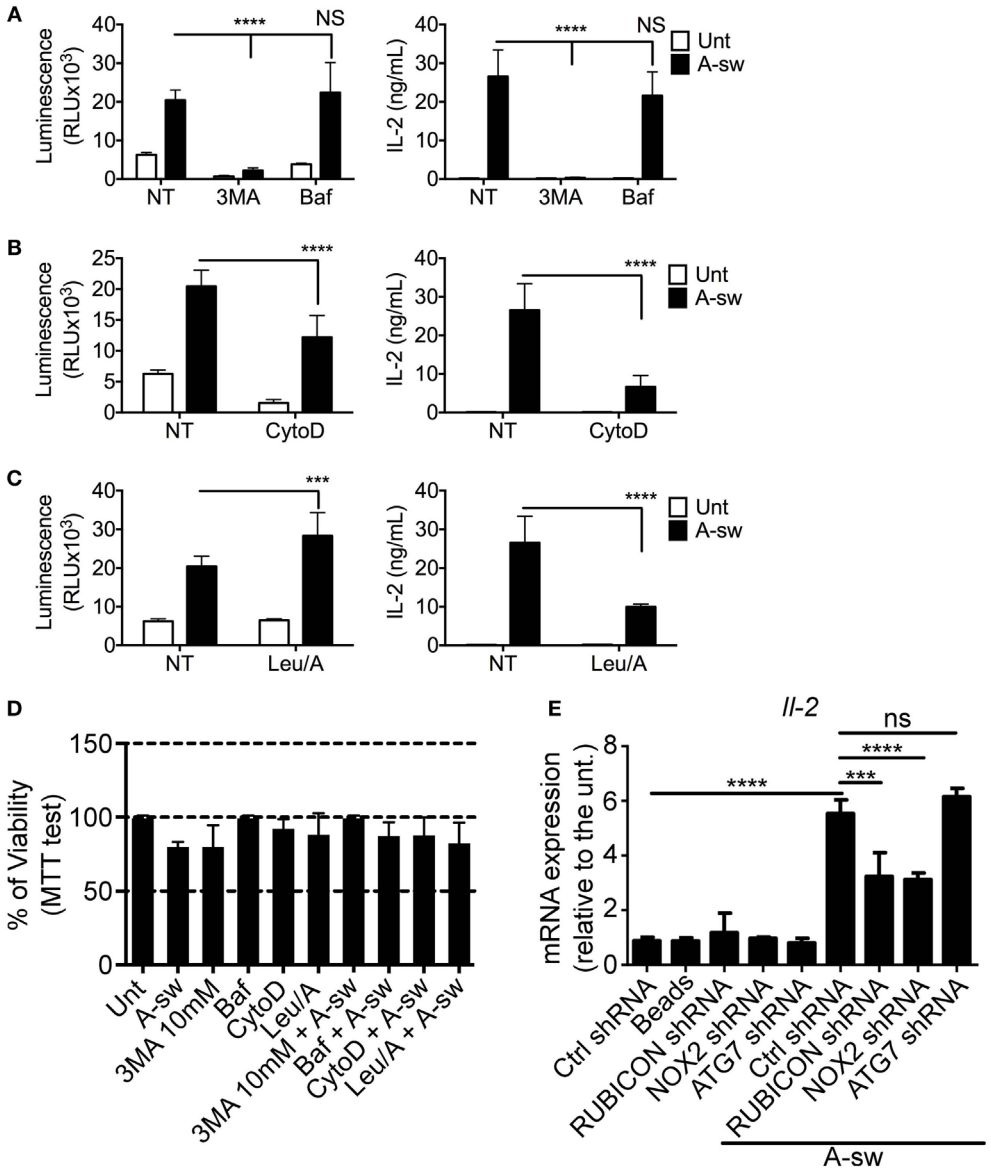

FIGURE 4 | Ca^{2+}-NFAT-IL-2 axis is affected by early autophagic events, phagocytosis and LAP. nuclear factor of activated T cells translocation and IL-2 production of NFAT-luciferase reporter D1 cells that have been stimulated with A-sw for 6 h in the presence and absence of drugs inhibiting specific cellular processes. **(A)** Fungus-stimulated D1 cells in the presence and absence of the type III Phosphatidylinositol 3-kinase inhibitor 3MA, 10 mM, or the vacuolar H + ATPase inhibitor, Baf (50 nM), which inhibits the early and late stage of autophagy respectively. **(B)** Fungus-stimulated D1 cells in the presence or absence of the phagocytosis inhibitor, CytoD (2 μg/mL). **(C)** D1 cells stimulated with fungi in the presence or absence of the lysosomal acidification inhibiting combination of Leu/A. Data is displayed as the mean ± SD of five (in the case of Leu/A) or eight biological replicates. **(D)** Viability of D1 cells treated with fungus, drugs, or a combination of the both. **(E)** mRNA expression of IL-2 in D1 cells silenced for various mRNA regulating LAP in the presence or absence of *A. fumigatus* swollen conidia. Data is displayed as means ± SD of three biological replicates. Differences found to be statistically significant by one-way ANOVA with Bonferroni's Multiple Comparison post-test are indicated (NS, non-significant; ***, $p < 0.001$; ****, $p < 0.0001$). Abbreviations: Untreated (Unt); *A. fumigatus swollen conidia* (A-sw); Vehicle non-treated control (NT); 3-methyladenine (3MA); Bafilomycin (Baf); Cytochalasin D (CytoD), combination of Leupeptin and ammonium chloride (Leu/A).

and SPAG9, could also be detected at basal level. Interestingly, *Aspergillus*-stimulated D1 cells showed marked downregulation of the PPP2R1A protein (Figure S5B in Supplementary Material). Altogether, this shows that *Aspergillus* by inducing phagocytosis and LAP may also influence the expression of other components of the NRON complex as for LRRK2 in DCs. In order to investigate whether the NRON complex in DCs was affecting the NFAT/IL-2 axis as shown for LRRK2, D1 cells were knocked down for NRON, IQGAP, CSE1L, and PPP2R1A (a subunit of the PPP2RA protein), or SPAG9 using shRNA-containing lentiviral particles. Silencing efficiency was investigated and the DC clone was selected accordingly (Figure S6 in Supplementary Material).

Surprisingly, no increase in IL-2 release in response to *Aspergillus* stimulation from silenced D1 cells was observed as we

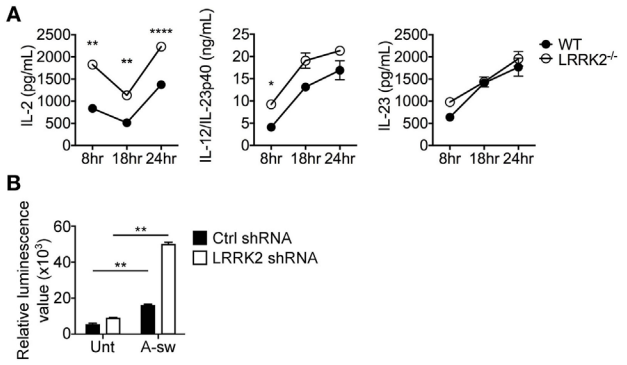

FIGURE 5 | Leucine-rich repeat kinase 2 (LRRK2) deficiency in dendritic cells (DCs) leads to increased IL-2 production and nuclear factor of activated T cells (NFAT) translocation in response to *Aspergillus fumigatus*. **(A)** IL-2, IL-12/IL-23p40, and IL-23 cytokine production of wild-type (closed circles) and LRRK2$^{-/-}$ (open circles) bone marrow-derived DCs in response to fungal stimulation with *A. fumigatus* swollen conidia. Data is displayed as the mean cytokine concentration ± SD of two biological replicates and statistical significance determined by one-way ANOVA with Bonferroni's Multiple Comparison post-test. **(B)** NFAT translocation measured by luminescence signal in A-sw-stimulated NFAT-luciferase reporter D1 cells upon LRRK2 silencing. Data is displayed as the mean luminescence signal ± SD of three biological replicates and statistical significance determined by Student's *t*-test. Differences found to be statistically significant are indicated (*, $p < 0.05$; **, $p < 0.01$; ****, $p < 0.0001$). Abbreviations: Untreated (Unt); *A. fumigatus swollen conidia* (A-sw).

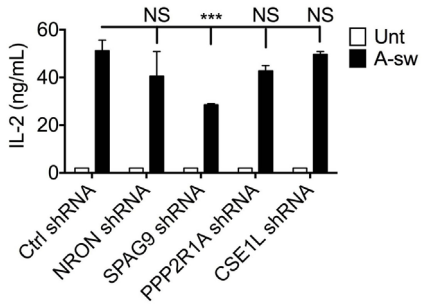

FIGURE 6 | Regulation of IL-2 by NRON complex components. IL-2 cytokine production at 8 h post-exposure from A-sw stimulated D1 cells that were knocked down for NRON, sperm-associated antigen 9, PPP2R1A, or chromosome segregation 1-like through the use of shRNA-lentiviral particles. Data are displayed as the mean ± SD of three replicates. Differences between *Aspergillus*-stimulated cells found to be statistically significant by one-way ANOVA with Bonferroni's Multiple Comparison post-test are indicated (NS, non-significant; ***, $p < 0.001$). Abbreviations: Untreated (Unt); *A. fumigatus swollen conidia* (A-sw).

found in LRRK2 deficiency. Interestingly, other cytokines involved in DC response to infections as IL-1β, IL-6, IL12/IL-23p40, IL-22, IL-23, and TNFα are differently affected by silencing the NRON complex components (Figure S7 in Supplementary Material). Regarding IL-2, only knocking down of SPAG9 led to a decrease of IL-2 production by DCs (**Figure 6**).

Finally, since recently, a mechanism by which inflammation is regulated during LAP through the death-associated protein kinase 1 (DAPK1) has been described in macrophages (31), we investigated a possible cross-regulation between these two proteins during LAP. Moreover, *Dapk1* and *Lrrk2* are both target genes of IFN-γ in myeloid cells (10, 35). Therefore, we have analyzed DAPK1 expression in DCs (**Figures 7A,B**), and we found that DAPK1 protein level increases in response to A-sw (**Figure 7A**) differently from LRRK2 in DCs (**Figure 1A**). However, DCs treated with LRRK2 shRNA (**Figure 7C**), do not show any significant differential expression of *Dapk1* (**Figure 7D**) as well as DAPK1 shRNA treated DCs show similar *Lrrk2* expression than Ctrl shRNA (data not shown). In conclusion, our results underline a more prominent and independent (from NRON components) role of LRRK2 in regulating the NFAT1 translocation to the nucleus and in regulating IL-2 cytokine release in DCs (Figure S8 in Supplementary Material).

DISCUSSION

Leucine-rich repeat kinase 2 was first discovered to play a role in Parkinson's disease (2), and it has been shown to be involved in various signaling pathways and cellular processes. In addition, LRRK2 is genetically associated with other inflammatory diseases (15, 36, 37) and modulated in inflammation by PAMPs (10, 15). Also, LRRK2 was reported to be a negative regulator of the NFAT pathway in BMDMs (15), activated downstream of Dectin-1 by fungi (18). Interestingly, LRRK2 has been investigated recently in immune response to pathogens (10, 17). However, as of now the role of LRRK2 protein in fungal immunity has not been explored.

In support of the observations of *Liu* et al. (15), our study here demonstrates that LRRK2 is indeed involved as a negative regulator of the NFAT pathway in DC response to fungi.

At resting state in DCs, we found that LRRK2 localizes to endosomes, accordingly to recent studies, where LRRK2 interaction with the endocytic network have been recently demonstrated (24, 38, 39). Liu et al. (15) reported LRRK2 to be bound to 5 of the 11 proteins of the NRON complex. In view of these reports, the localization of LRRK2 and possibly also other NRON complex components to endosomes at steady state could serve to regulate NFAT, and this is possibly accomplished by sequestering it at the endosomal membrane.

In this study, four components, including NRON, PPP2R1A, CSE1L, and SPAG9 of the NRON complex were also investigated, and it was found that expression levels of NRON and PPP2R1A in particular, were downregulated in DCs in response to *Aspergillus* stimulation as LRRK2. This is in line with what has been reported that the NRON complex, together with LRRK2, mediates NFAT translocation regulation (15) since a downregulation of NRON complex components would likely lead to a dissociation of this regulatory complex. A knockdown of these components was carried out to investigate whether other than LRRK2 other components may affect NFAT nuclear translocation in DCs. IL-2 production from *Aspergillus*-stimulated DCs knocked down for any of these components was found not to be significantly affected, or was decreased as in the case when SPAG9 was knocked down. This indicates that perhaps NRON, PPP2R1A, and CSE1L alone are not sufficient to regulate the NFAT/IL-2 axis. SPAG9, on the other hand, individually could be positively regulating the NFAT/IL-2 axis, rather than inhibiting it.

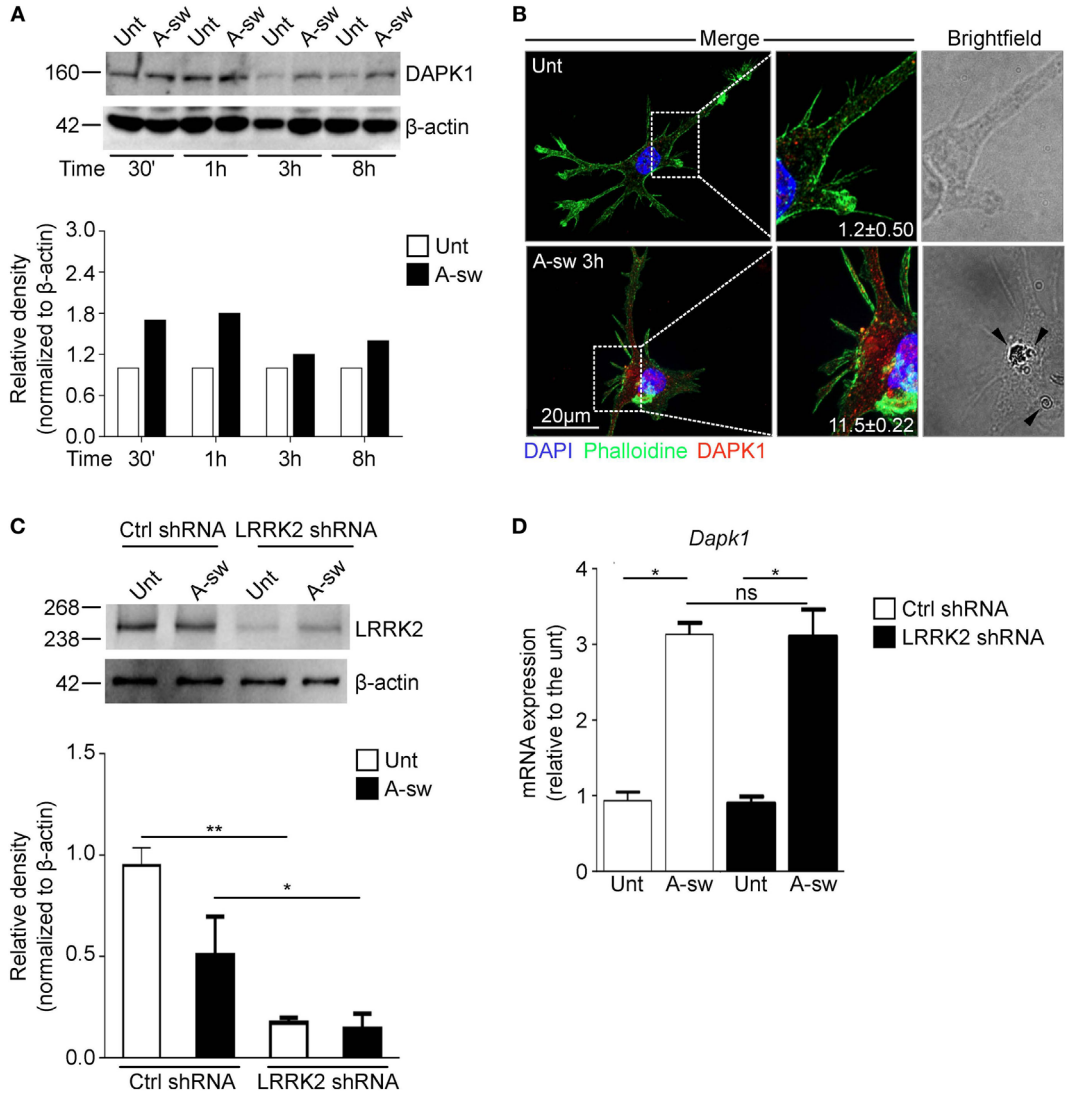

FIGURE 7 | Death-associated protein kinase 1 (DAPK1) expression during LAP is not controlled by Leucine-rich repeat kinase 2 (LRRK2). **(A)** Protein expression of DAPK1 in *A. fumigatus* swollen conidia-stimulated D1 cells. For densitometry analysis, band densities for DAPK1 were normalized to the band density of the housekeeping protein, β-actin, after which the density of the DAPK1 band of the treated sample was compared with that of the untreated sample. Data are representative of three independent experiments. **(B)** Immunofluorescent stanining of DAPK1 and brightfield microscopy of *Aspergillus fumigatus* swollen conidia-stimulated D1 cells. Signal intensity of the DAPK1 was quantified and displayed as mean fluorescence signal ± SD of three biological replicates. Brightfield imaging of the same cell is displayed with arrows indicating the presence of *A. fumigatus* swollen conidia in the cell. **(C)** Knockdown of LRRK2 in D1 cells was assessed by western blot. Data are represented as mean ± SD of three biological replicates and statistical significance determined by two way ANOVA **(D)** mRNA expression of DAPK1 in fungal-treated D1 cells that have been silenced for LRRK2. Data are displayed as the mean mRNA expression ± SD of three biological replicates and statistical significance determined by two way ANOVA. Differences found to be statistically significant are indicated (*, $p < 0.05$; **, $p < 0.01$). Abbreviations: *A. fumigatus swollen conidia* (A-sw); Untreated (Unt); D1 cells transduced with non-targeting control shRNA (Ctrl).

More interestingly, the individual components of the NRON complex were regulating DC cytokine response differently, implying that they may not work in concert.

For SPAG9, CSE1L, and PPP2R1A, besides being known to be part of the NRON complex (15, 40), their reported functions were not originally concerning the immune system. SPAG9 has been proposed as a biomarker for diagnosis in carcinoma of the breast (41), endometrium (42), cervix (43), thyroid (44), and colon (45), and has been proposed to be involved in the tumorogenesis and growth. CSE1L is a nuclear exportin protein that is involved in the cell cycle, and SPAG9 has also been associated with various carcinomas [as reviewed in Behrens et al. (46)]. PPP2R1A is a subunit of protein phosphatase 2A (PP2A). PP2A has been implicated in meiosis and mitosis in numerous studies (47, 48) and is currently being explored as a treatment target for pancreatic cancer (49). More related to the context of this study, PP2A proteins have been shown to interact with signaling pathways, such as the TLR-TRIF signaling (50), Ras signaling (51), as well as Ca^{2+}/Calmodulin-dependent protein kinase B/Akt (52). In relation

to neurological disorders, PP2A has been suggested as a possible treatment target for neurological disorders Alzheimer's disease (53) and has been recently implicated in Tau pathology of Parkinson's disease (54). This study hints that the function of SPAG9, CSE1L, and PPP2R1A may also be related to the immune response to pathogens.

It has been shown that LRRK2 localizes to lysosomes and can be degraded by CMA in neurons (23). In a similar way, this study here shows that LRRK2 is localized to endosomes and lysosomes in steady state DCs, and that *Aspergillus* is able to induce a non-canonical type of autophagy in DCs that is reminiscent of LC3-positive phagosomes, previously reported (27, 30, 31, 55).

The use of transmission electron microscopy allowed the observation of LRRK2-positive multilamellar body formation in *Aspergillus*-stimulated DCs, further strengthening the connection of LRRK2 with lysosomes and autophagy. Multilamellar bodies are reported to be part of the lysosomal pathway and its formation is dependent on autophagy and lysosomal degradation (32), and the localization of LRRK2 to these structures is supported by what has been previously reported in cultured human cells (25).

Interestingly, GSK3-β, a protein involved in phosphorylating NFAT, has also been shown to localize to the endosomal membrane and this is thought to serve to isolate it from interaction with other signaling components (26).

How the NFAT pathway is influenced by the events following the engagement of Dectin-1 by *Aspergillus* in DCs was also investigated here. The dependency of phagocytosis on IL-2 production in response to particulate β-glucan in DCs has been previously demonstrated (19), hence in this study the finding that the NFAT/IL-2 axis in response to *Aspergillus* is also dependent on this cellular process was expected. What was interesting was that early, but not late autophagic events are also required to activate the NFAT/IL-2 pathway.

Autophagy also occurs in macrophages, and with this respect Ma et al. (27) and Kyrmizi et al. (30) have both demonstrated that the formation of LC3-positive phagosomes also occur in macrophages incubated with fungi, and that the recruitment of LC3 is important for macrophage signaling and function in response to fungi. In particular, Kyrmizi, Gresnigt (30) show that the recruitment of LC3 is needed for macrophage ROS production and killing of *Aspergillus* spores.

In this study, we have also evaluated whether DAPK1 may contribute to regulating LRRK2 function (and vice versa), since both are regulated during LAP and concur to the regulation of the inflammatory response during fungal LAP. To this purpose, we have resorted to shRNA of LRRK2 and analyzed DAPK1 expression.

To conclude, our study has shown that DCs express LRRK2 and that it negatively regulates the NFAT pathway activated in response to *Aspergillus*. Upon *Aspergillus* binding to Dectin-1 in DCs, non-canonical autophagy, as well as multilamellar body formation is triggered. Taking into account the findings of previously published reports, the sequestration of LRRK2 in the multilamellar bodies could lead to the dissociation of the NRON complex. Therefore, the role of the NRON complex in immune response of DCs to *Aspergillus* has been shown to be more complex than previously thought, and their interaction with other signaling pathways activated in the immune response will add a new dimension to their currently known cellular functions. Given that DCs have an important role in the immune system as antigen presenting cells and initiating the appropriate adaptive immune response, future *in vivo* studies could elucidate better the immunological function of LRRK2 and the NRON complex eventually in T cell priming. The knowledge obtained from such studies not only sheds light on the control of the NFAT pathway, but also could have implications in other diseases associated with LRRK2, such as Crohn's disease, IBD, and Parkinson's disease.

ETHICS STATEMENT

All experiments and procedures were approved by the IACUC of A*STAR (Biopolis, Singapore) (Authorization No.: IACUC 110626) in accordance with the guidelines of the AVA and the NACLAR of Singapore.

AUTHOR CONTRIBUTIONS

AW designed the study, conducted, analyzed experiments, and wrote the manuscript. VO performed western blotting and immunofluorescence experiments. GP performed qPCR data. AL performed ELISA; MP analyzed western blotting data. JF performed the LRRK2$^{-/-}$ bone marrow expansion experiments. HT generated the D1 NFAT translocation-firefly luciferase reporter cells. PR-C supervised the project. TZ conceived, coordinated the project, and wrote the manuscript.

ACKNOWLEDGMENTS

The authors wish to thank Z. Liu of Institute of Biophysics Chinese Academy of Sciences for LRRK2$^{-/-}$ mice bone marrow; A. Balachander (SIgN) for confocal microscopy; R. Iannitti of the Department of Experimental Medicine, University of Perugia, and P. Rondoni of the Centro Universitario di Microscopia Electtronica (CUME), University of Perugia, for transmission electron microscopy; Prof. A. Milani, S. Pasqua, A. Moriconi of the laboratory E-learning, University of Perugia, Italy for video editing.

FUNDING

This research was funded by the Biomedical Research Council, A*STAR, and the Italian grant "Programma per Giovani Ricercatori – Rita Levi Montalcini 2013." JF was supported by European Social Fund and European Regional Development Fund—Project MAGNET (No. CZ.02.1.01/0.0/0.0/15_003/0000492).

SUPPLEMENTARY MATERIAL

The Supplementary Material for this article can be found online at http://www.frontiersin.org/articles/10.3389/fimmu.2018.00210/full#supplementary-material.

VIDEO S1 | BMDCs phagocytosis of Aspergillus swollen conidia. Representative example of time-lapse imaging data of in vitro mouse BMDCs. BMDCs were infected with Aspergillus swollen conidia and imaged over a period of 1 hour to identify the process of phagocytosis. Images were captured every 2 minutes in the bright field channel on the EVOS FL Auto Cell Imaging System. A movie was then generated from the images at rate of 4 frame/sec.

REFERENCES

1. Paisán-Ruíz C, Jain S, Evans E, Gilks W, Simón J, van der Brug M, et al. Cloning of the gene containing mutations that cause PARK8-linked Parkinson's disease. *Neuron* (2004) 44(4):595–600. doi:10.1016/j.neuron.2004.10.023
2. Funayama M, Hasegawa K, Kowa H, Saito M, Tsuji S, Obata F. A new locus for Parkinson's disease (PARK8) maps to chromosome 12p11.2-q13.1. *Ann Neurol* (2002) 51(3):296–301. doi:10.1002/ana.10113
3. Mata I, Wedemeyer W, Farrer M, Taylor J, Gallo K. LRRK2 in Parkinson's disease: protein domains and functional insights. *Trends Neurosci* (2006) 29(5):286–93. doi:10.1016/j.tins.2006.03.006
4. Jorgensen N, Peng Y, Ho CC-Y, Rideout H, Petrey D, Liu P, et al. The WD40 domain is required for LRRK2 neurotoxicity. *PLoS One* (2009) 4(12):e8463. doi:10.1371/journal.pone.0008463
5. Smith W, Pei Z, Jiang H, Moore D, Liang Y, West A, et al. Leucine-rich repeat kinase 2 (LRRK2) interacts with parkin, and mutant LRRK2 induces neuronal degeneration. *Proc Natl Acad Sci U S A* (2005) 102(51):18676–81. doi:10.1073/pnas.0508052102
6. West A, Moore D, Choi C, Andrabi S, Li X, Dikeman D, et al. Parkinson's disease-associated mutations in LRRK2 link enhanced GTP-binding and kinase activities to neuronal toxicity. *Hum Mol Genet* (2007) 16(2):223–32. doi:10.1093/hmg/ddl471
7. Liu B. Modulation of microglial pro-inflammatory and neurotoxic activity for the treatment of Parkinson's disease. *AAPS J* (2006) 8(3):21. doi:10.1208/aapsj080369
8. Whitton P. Inflammation as a causative factor in the aetiology of Parkinson's disease. *Br J Pharmacol* (2007) 150(8):963–76. doi:10.1038/sj.bjp.0707167
9. Gerlach OH, Winogrodzka A, Weber W. Clinical problems in the hospitalized Parkinson's disease patient: systematic review. *Mov Disord* (2011) 26(2):197–208. doi:10.1002/mds.23449
10. Gardet AS, Benita Y, Li C, Sands B, Ballester I, Stevens C, et al. LRRK2 is involved in the IFN-gamma response and host response to pathogens. *J Immunol* (2010) 185(9):5577–85. doi:10.4049/jimmunol.1000548
11. Hakimi M, Selvanantham T, Swinton E, Padmore R, Tong Y, Kabbach G, et al. Parkinson's disease-linked LRRK2 is expressed in circulating and tissue immune cells and upregulated following recognition of microbial structures. *J Neural Transm (Vienna)* (2011) 118(5):795–808. doi:10.1007/s00702-011-0653-2
12. Moehle M, Webber P, Tse T, Sukar N, Standaert D, DeSilva T, et al. LRRK2 inhibition attenuates microglial inflammatory responses. *J Neurosci* (2012) 32(5):1602–11. doi:10.1523/JNEUROSCI.5601-11.2012
13. Gillardon F, Schmid R, Draheim H. Parkinson's disease-linked leucine-rich repeat kinase 2(R1441G) mutation increases proinflammatory cytokine release from activated primary microglial cells and resultant neurotoxicity. *Neuroscience* (2012) 208:41–8. doi:10.1016/j.neuroscience.2012.02.001
14. Kim B, Yang MS, Choi D, Kim JH, Kim HS, Seol W, et al. Impaired inflammatory responses in murine Lrrk2-knockdown brain microglia. *PLoS One* (2012) 7(4):e34693. doi:10.1371/journal.pone.0034693
15. Liu Z, Lee J, Krummey S, Lu W, Cai H, Lenardo M. The kinase LRRK2 is a regulator of the transcription factor NFAT that modulates the severity of inflammatory bowel disease. *Nat Immunol* (2011) 12(11):1063–70. doi:10.1038/ni.2113
16. Macian F. NFAT proteins: key regulators of T-cell development and function. *Nat Rev Immunol* (2005) 5(6):472–84. doi:10.1038/nri1632
17. Liu W, Liu X, Li Y, Zhao J, Liu Z, Hu Z, et al. LRRK2 promotes the activation of NLRC4 inflammasome during *Salmonella typhimurium* infection. *J Exp Med* (2017) 214(10):3051–66. doi:10.1084/jem.20170014
18. Goodridge HS, Simmons RM, Underhill DM. Dectin-1 stimulation by *Candida albicans* yeast or zymosan triggers NFAT activation in macrophages and dendritic cells. *J Immunol* (2007) 178(5):3107–15. doi:10.4049/jimmunol.178.5.3107
19. Fric J, Zelante T, Ricciardi-Castagnoli P. Phagocytosis of particulate antigens – all roads lead to calcineurin/NFAT signaling pathway. *Front Immunol* (2014) 4:513. doi:10.3389/fimmu.2013.00513
20. Zelante T, Wong AY, Ping TJ, Chen J, Sumatoh HR, Viganò E, et al. CD103(+) dendritic cells control Th17 cell function in the lung. *Cell Rep* (2015) 12(11):1789–801. doi:10.1016/j.celrep.2015.08.030
21. Winzler C, Rovere P, Rescigno M, Granucci F, Penna G, Adorini L, et al. Maturation stages of mouse dendritic cells in growth factor-dependent long-term cultures. *J Exp Med* (1997) 185(2):317–28. doi:10.1084/jem.185.2.317
22. Graham JM. Isolation of lysosomes from tissues and cells by differential and density gradient centrifugation. *Curr Protoc Cell Biol* (2001) Chapter 3:Unit 3.6. doi:10.1002/0471143030.cb0306s07
23. Orenstein S, Kuo SH, Tasset I, Arias E, Koga H, Fernandez-Carasa I, et al. Interplay of LRRK2 with chaperone-mediated autophagy. *Nat Neurosci* (2013) 16(4):394–406. doi:10.1038/nn.3350
24. Schreij AM, Chaineau M, Ruan W, Lin S, Barker PA, Fon EA, et al. LRRK2 localizes to endosomes and interacts with clathrin-light chains to limit Rac1 activation. *EMBO Rep* (2015) 16(1):79–86. doi:10.15252/embr.201438714
25. Alegre-Abarrategui J, Christian H, Lufino M, Mutihac R, Venda L, Ansorge O, et al. LRRK2 regulates autophagic activity and localizes to specific membrane microdomains in a novel human genomic reporter cellular model. *Hum Mol Genet* (2009) 18(21):4022–34. doi:10.1093/hmg/ddp346
26. Pálfy M, Reményi A, Korcsmáros T. Endosomal crosstalk: meeting points for signaling pathways. *Trends Cell Biol* (2012) 22(9):447–56. doi:10.1016/j.tcb.2012.06.004
27. Ma J, Becker C, Lowell C, Underhill D. Dectin-1-triggered recruitment of light chain 3 protein to phagosomes facilitates major histocompatibility complex class II presentation of fungal-derived antigens. *J Biol Chem* (2012) 287(41):34149–56. doi:10.1074/jbc.M112.382812
28. De Luca A, Iannitti R, Bozza S, Beau R, Casagrande A, D'Angelo C, et al. CD4(+) T cell vaccination overcomes defective cross-presentation of fungal antigens in a mouse model of chronic granulomatous disease. *J Clin Invest* (2012) 122(5):1816–31. doi:10.1172/JCI60862
29. Martinez J, Malireddi RK, Lu Q, Cunha LD, Pelletier S, Gingras S, et al. Molecular characterization of LC3-associated phagocytosis reveals distinct roles for Rubicon, NOX2 and autophagy proteins. *Nat Cell Biol* (2015) 17(7):893–906. doi:10.1038/ncb3192
30. Kyrmizi I, Gresnigt MS, Akoumianaki T, Samonis G, Sidiropoulos P, Boumpas D, et al. Corticosteroids block autophagy protein recruitment in *Aspergillus fumigatus* phagosomes via targeting dectin-1/Syk kinase signaling. *J Immunol* (2013) 191(3):1287–99. doi:10.4049/jimmunol.1300132
31. Oikonomou V, Moretti S, Renga G, Galosi C, Borghi M, Pariano M, et al. Noncanonical fungal autophagy inhibits inflammation in response to IFN-gamma via DAPK1. *Cell Host Microbe* (2016) 20(6):744–57. doi:10.1016/j.chom.2016.10.012
32. Hariri M, Millane G, Guimond MP, Guay G, Dennis JW, Nabi IR. Biogenesis of multilamellar bodies via autophagy. *Mol Biol Cell* (2000) 11(1):255–68. doi:10.1091/mbc.11.1.255
33. Mizushima N, Yoshimori T, Levine B. Methods in mammalian autophagy research. *Cell* (2010) 140(3):313–26. doi:10.1016/j.cell.2010.01.028
34. Yu HB, Yurieva M, Balachander A, Foo I, Leong X, Zelante T, et al. NFATc2 mediates epigenetic modification of dendritic cell cytokine and chemokine responses to dectin-1 stimulation. *Nucleic Acids Res* (2015) 43(2):836–47. doi:10.1093/nar/gku1369
35. Gade P, Manjegowda SB, Nallar SC, Maachani UB, Cross AS, Kalvakolanu DV. Regulation of the death-associated protein kinase 1 expression and autophagy via ATF6 requires apoptosis signal-regulating kinase 1. *Mol Cell Biol* (2014) 34(21):4033–48. doi:10.1128/MCB.00397-14
36. Barrett J, Hansoul S, Nicolae D, Cho J, Duerr R, Rioux J, et al. Genome-wide association defines more than 30 distinct susceptibility loci for Crohn's disease. *Nat Genet* (2008) 40(8):955–62. doi:10.1038/ng.175
37. Törkvist L, Halfvarson J, Ong R, Lördal M, Sjöqvist U, Bresso F, et al. Analysis of 39 Crohn's disease risk loci in Swedish inflammatory bowel disease patients. *Inflamm Bowel Dis* (2010) 16(6):907–9. doi:10.1002/ibd.21105
38. Yun HJ, Kim H, Ga I, Oh H, Ho DH, Kim J, et al. An early endosome regulator, Rab5b, is an LRRK2 kinase substrate. *J Biochem* (2015) 157(6):485–95. doi:10.1093/jb/mvv005
39. Gómez-Suaga P, Rivero-Ríos P, Fdez E, Blanca Ramírez M, Ferrer I, Aiastui A, et al. LRRK2 delays degradative receptor trafficking by impeding late endosomal budding through decreasing Rab7 activity. *Hum Mol Genet* (2014) 23(25):6779–96. doi:10.1093/hmg/ddu395
40. Willingham A, Orth A, Batalov S, Peters E, Wen B, Aza-Blanc P, et al. A strategy for probing the function of noncoding RNAs finds a repressor of NFAT. *Science* (2005) 309(5740):1570–3. doi:10.1126/science.1115901

41. Kanojia D, Garg M, Gupta S, Gupta A, Suri A. Sperm-associated antigen 9, a novel biomarker for early detection of breast cancer. *Cancer Epidemiol Biomarkers Prev* (2009) 18(2):630–9. doi:10.1158/1055-9965.EPI-08-0629
42. Yu P, Yan L, Zhang H, Lin X, Zhao X. Expression and clinical significance of sperm-associated antigen 9 in patients with endometrial carcinoma. *Int J Gynecol Cancer* (2012) 22(1):87–93. doi:10.1097/IGC.0b013e3182370f2e
43. Garg M, Kanojia D, Salhan S, Suri S, Gupta A, Lohiya NK, et al. Sperm-associated antigen 9 is a biomarker for early cervical carcinoma. *Cancer* (2009) 115(12):2671–83. doi:10.1002/cncr.24293
44. Garg M, Kanojia D, Suri S, Gupta S, Gupta A, Suri A. Sperm-associated antigen 9: a novel diagnostic marker for thyroid cancer. *J Clin Endocrinol Metab* (2009) 94(11):4613–8. doi:10.1210/jc.2009-0703
45. Kanojia D, Garg M, Gupta S, Gupta A, Suri A. Sperm-associated antigen 9 is a novel biomarker for colorectal cancer and is involved in tumor growth and tumorigenicity. *Am J Pathol* (2011) 178(3):1009–20. doi:10.1016/j.ajpath.2010.11.047
46. Behrens P, Brinkmann U, Wellmann A. CSE1L/CAS: its role in proliferation and apoptosis. *Apoptosis* (2003) 8(1):39–44. doi:10.1023/A:1021644918117
47. Hu WW, Wang ZB, Jiang ZZ, Qi ST, Huang L, Liang QX, et al. Scaffold subunit Aalpha of PP2A is essential for female meiosis and fertility in mice. *Biol Reprod* (2014) 91(1):19. doi:10.1095/biolreprod.114.120220
48. Porter IM, Schleicher K, Porter M, Swedlow JR. Bod1 regulates protein phosphatase 2A at mitotic kinetochores. *Nat Commun* (2013) 4:2677. doi:10.1038/ncomms3677
49. Chien W, Sun QY, Lee KL, Ding LW, Wuensche P, Torres-Fernandez LA, et al. Activation of protein phosphatase 2A tumor suppressor as potential treatment of pancreatic cancer. *Mol Oncol* (2015) 9(4):889–905. doi:10.1016/j.molonc.2015.01.002
50. Woo CW, Kutzler L, Kimball SR, Tabas I. Toll-like receptor activation suppresses ER stress factor CHOP and translation inhibition through activation of eIF2B. *Nat Cell Biol* (2012) 14(2):192–200. doi:10.1038/ncb2408
51. Ory S, Zhou M, Conrads TP, Veenstra TD, Morrison DK. Protein phosphatase 2A positively regulates Ras signaling by dephosphorylating KSR1 and Raf-1 on critical 14-3-3 binding sites. *Curr Biol* (2003) 13(16):1356–64. doi:10.1016/S0960-9822(03)00535-9
52. Fedida-Metula S, Feldman B, Koshelev V, Levin-Gromiko U, Voronov E, Fishman D. Lipid rafts couple store-operated Ca2+ entry to constitutive activation of PKB/Akt in a Ca2+/calmodulin-, Src- and PP2A-mediated pathway and promote melanoma tumor growth. *Carcinogenesis* (2012) 33(4):740–50. doi:10.1093/carcin/bgs021
53. Sontag J-MM, Sontag E. Protein phosphatase 2A dysfunction in Alzheimer's disease. *Front Mol Neurosci* (2014) 7:16. doi:10.3389/fnmol.2014.00016
54. Arif M, Kazim SF, Grundke-Iqbal I, Garruto RM, Iqbal K. Tau pathology involves protein phosphatase 2A in parkinsonism-dementia of Guam. *Proc Natl Acad Sci U S A* (2014) 111(3):1144–9. doi:10.1073/pnas.1322614111
55. Nicola AM, Albuquerque P, Martinez LR, Dal-Rosso RA, Saylor C, Jesus M. De, et al. Macrophage autophagy in immunity to *Cryptococcus neoformans* and *Candida albicans*. *Infect Immun* (2012) 80(9):3065–76. doi:10.1128/IAI.00358-12

Conflict of Interest Statement: The authors declare that the research was conducted in the absence of any commercial or financial relationships that could be construed as a potential conflict of interest.

Copyright © 2018 Wong, Oikonomou, Paolicelli, De Luca, Pariano, Fric, Tay, Ricciardi-Castagnoli and Zelante. This is an open-access article distributed under the terms of the Creative Commons Attribution License (CC BY). The use, distribution or reproduction in other forums is permitted, provided the original author(s) and the copyright owner are credited and that the original publication in this journal is cited, in accordance with accepted academic practice. No use, distribution or reproduction is permitted which does not comply with these terms.

frontiers in Immunology

ORIGINAL RESEARCH
published: 06 December 2017
doi: 10.3389/fimmu.2017.01716

Human and Murine Innate Immune Cell Populations Display Common and Distinct Response Patterns during Their *In Vitro* Interaction with the Pathogenic Mold *Aspergillus fumigatus*

*Anna-Maria Hellmann[1†], Jasmin Lother[1†], Sebastian Wurster[1], Manfred B. Lutz[2], Anna Lena Schmitt[1], Charles Oliver Morton[3], Matthias Eyrich[4], Kristin Czakai[1], Hermann Einsele[1] and Juergen Loeffler[1]**

[1] Medizinische Klinik & Poliklinik II, Universitätsklinikum Würzburg, Würzburg, Germany, [2] Institute of Virology and Immunobiology, University of Würzburg, Würzburg, Germany, [3] School of Science and Health, Western Sydney University, Campbelltown, NSW, Australia, [4] Kinderklinik und Poliklinik, Universitätsklinikum Würzburg, Würzburg, Germany

OPEN ACCESS

Edited by:
Ilse Denise Jacobsen, Leibniz-Institut für Naturstoff-Forschung und Infektionsbiologie, Hans Knöll Institut, Germany

Reviewed by:
Agostinho Carvalho, University of Minho, Portugal
Sven Krappmann, University of Erlangen-Nuremberg, Germany

***Correspondence:**
Juergen Loeffler
loeffler_j@ukw.de

[†]These authors have contributed equally to this work.

Specialty section:
This article was submitted to Microbial Immunology, a section of the journal Frontiers in Immunology

Received: *27 September 2017*
Accepted: *21 November 2017*
Published: *06 December 2017*

Citation:
Hellmann A-M, Lother J, Wurster S, Lutz MB, Schmitt AL, Morton CO, Eyrich M, Czakai K, Einsele H and Loeffler J (2017) Human and Murine Innate Immune Cell Populations Display Common and Distinct Response Patterns during Their In Vitro Interaction with the Pathogenic Mold Aspergillus fumigatus. Front. Immunol. 8:1716. doi: 10.3389/fimmu.2017.01716

Aspergillus fumigatus is the main cause of invasive fungal infections occurring almost exclusively in immunocompromised patients. An improved understanding of the initial innate immune response is key to the development of better diagnostic tools and new treatment options. Mice are commonly used to study immune defense mechanisms during the infection of the mammalian host with *A. fumigatus*. However, little is known about functional differences between the human and murine immune response against this fungal pathogen. Thus, we performed a comparative functional analysis of human and murine dendritic cells (DCs), macrophages, and polymorphonuclear cells (PMNs) using standardized and reproducible working conditions, laboratory protocols, and readout assays. *A. fumigatus* did not provoke identical responses in murine and human immune cells but rather initiated relatively specific responses. While human DCs showed a significantly stronger upregulation of their maturation markers and major histocompatibility complex molecules and phagocytosed *A. fumigatus* more efficiently compared to their murine counterparts, murine PMNs and macrophages exhibited a significantly stronger release of reactive oxygen species after exposure to *A. fumigatus*. For all studied cell types, human and murine samples differed in their cytokine response to conidia or germ tubes of *A. fumigatus*. Furthermore, Dectin-1 showed inverse expression patterns on human and murine DCs after fungal stimulation. These specific differences should be carefully considered and highlight potential limitations in the transferability of murine host–pathogen interaction studies.

Keywords: murine model, humans, *Aspergillus fumigatus*, innate immune response, fungal infection

INTRODUCTION

Humans inhale hundreds of airborne fungal spores daily, including spores from the saprophytic mold *Aspergillus fumigatus*, which is ubiquitous in the environment. While the fungus rarely causes diseases in healthy individuals, disorders of the immune system are associated with a wide spectrum of *Aspergillus*-related diseases (1). Overshooting immune response to the fungus

can lead to hypersensitivity syndromes such as allergic bronchopulmonary aspergillosis, whereas invasive aspergillosis (IA) is a major cause of morbidity and mortality in immunocompromised patients.

The mammalian immune system, evolving under continuous exposure to airborne fungal spores, possesses a vast arsenal of strategies to combat invading fungi including mediating tolerance to commensals and limiting hyperinflammation to prevent tissue damage. In the absence of an effective immune response, *Aspergillus* conidia swell and become invasive by germinating into the lung tissue and entering the blood stream. Alveolar macrophages act as the first line of defense in the airways by phagocytosis of conidia and secretion of pro-inflammatory cytokines and reactive oxygen species (ROS) (2). Neutrophil granulocytes [polymorphonuclear cells (PMNs)] also play a major role in the early immune defense against IA, as they are able to prevent germination and kill fungal hyphae through the release of ROS, phagocytosis, or formation of neutrophil extracellular traps. Dendritic cells (DCs) represent an important bridge between innate and adaptive immunity as they process fungal antigens and subsequently stimulate specific T-cells *via* antigen-presentation by major histocompatibility complex (MHC) I and II molecules. They also orchestrate the immune response by secreting an array of pro- and anti-inflammatory cytokines. Stimulation of pattern recognition receptors (PRRs), such as toll-like receptors (TLR)-2 and -4 (3) and the Dectin-1-receptor, is crucial to the activation of these immune cell subsets (4).

Detailed insights into the pathophysiology of the infection and mechanisms of the host–pathogen interaction are urgently needed to facilitate development of new prophylactic and therapeutic tools and strategies. Due to their easy accessibility, relatively short generation time, and availability of genetically defined strains, mouse models are commonly used to characterize the interaction of *A. fumigatus* with the mammalian host *in vivo* and to evaluate novel therapeutic strategies. There is, however, increasing evidence of major functional differences between the human and murine immune systems, indicating limited application of data obtained in studies employing murine cells or models (5, 6). On one hand, the composition of the murine leukocyte repertoire differs from that of humans; in mice only 7–28% of peripheral blood leukocytes are PMNs in contrast to 35–70% in human blood (7). On the other hand, functional differences, such as the sequence of participating immunological cells after antigen challenge as well as the dose of antigen needed to initiate immunological reaction in delayed type hypersensitivity have been described (5).

So far, little is known about functional differences in the human and murine immune defense against *A. fumigatus*. Thus, this study sought to provide a comparative functional assessment between human and murine innate immune cell subsets routinely employed in host–pathogen interaction studies (8–13). Our data demonstrate that mice and men which differ in their size, habitat, lifespan, genome size, and blood composition possess principle differences in how selected innate immune cell populations specifically interact with the pathogenic mold *A. fumigatus*.

MATERIALS AND METHODS

Fungal Strains and Cultivation Conditions

Aspergillus fumigatus strain American Type Culture Collection 46645 was incubated on beer wort agar (Institute of Hygiene and Microbiology, University of Wuerzburg, Germany) for 72 h at 37°C. Conidial suspensions were prepared by rinsing plates with sterile water and filtered through a 40-µm cell strainer (BD Falcon™ Cell Strainer, BD Biosciences). To generate germ tubes, 1×10^8 resting conidia were inoculated in Rosewell Park Memorial Institute (RPMI) 1640 Medium (Life technologies) and cultured at 37°C until the germ tubes reached a length of about 10–30 µm. To preserve fungal morphotypes during coculture experiments, conidia and germ tubes were inactivated with 100% ethanol (Sigma) for 30 min, washed five times with sterile water, and stored in RPMI at −20°C. For time-lapse microscopy red fluorescent *A. fumigatus* conidia and germ tubes were generated as described before (9).

Isolation and Culture of Human and Murine Immune Cells

Dendritic Cells

Peripheral blood mononuclear cells were isolated from leukocyte concentrates from healthy human donors (Institute of Transfusion Medicine, University Hospital of Wuerzburg) by Ficoll (Biochrome) density centrifugation. After positive magnetic selection of $CD14^+$ cells (CD14 MicroBeads, Miltenyi Biotec), monocytes were cultured for 5 days in RPMI 1640 medium supplemented with 10% fetal calf serum (FCS) (Sigma), rGM-CSF (100 ng/ml, Bayer), and rIL4 (10 ng/ml, Miltenyi Biotec) (9).

Murine bone marrow derived dendritic cells (BMDCs) were generated as described before (14). Briefly, bone marrow from healthy mice was harvested and cultured in R10-medium (RPMI 1640) (GIBCO BRL) with 100 U/ml Penicillin (Sigma), 100 µg/ml Streptomycin (Sigma), 2 mM L-glutamine (Sigma), 50 µM 2-mercaptoethanol (Sigma), 10% FCS (PAA), and 200 U/ml rmGM-CSF (Reprotech/Tebu) for 6 days. The non-adherent cells were harvested and cultured in R10-medium without cytokines.

Polymorphonuclear Cells

To isolate human PMNs anticoagulated blood from healthy human donors was layered on a polysaccharide gradient (Polymorphprep, Axis Shield). After 30 min of centrifugation (500*g*), the PMN interphase was harvested and pelleted for 5 min at 300*g*. Remaining erythrocytes were lysed with EL buffer (Qiagen). Isolation of murine PMNs, which were obtained from bone marrow of C57BL/6NCrl mice, was performed using the EasySep™ Mouse Neutrophil Enrichment Kit (Stem Cell Technologies) according to the manufacturer's protocol. Both murine and human PMNs were cultured in RPMI 1640 Medium with 5% FCS.

Macrophages

Human monocytes obtained from healthy subjects as described above were cultured in RPMI 1640 medium supplemented with 10% FCS and rM-CSF (Immunotools) for 6 days. Only adherent

cells were used for experiments. To generate murine macrophages, bone marrow cells of healthy mice were cultured in R10-medium with M-CSF supernatant [mouse M-CSF (Immunotools) supernatant, L929] for 6 days. Adherent cells were harvested and suspended in R10-medium.

Time-Lapse Video Microscopy

3.5×10^4 human monocyte-derived immature dendritic cells (moDCs) or murine BMDCs were stimulated with 3.5×10^5 *A. fumigatus* (Afu-dTomato) conidia or germ tubes [multiplicity of infection (MOI) = 10]. Polystyrene beads (Sigma) were used as an unspecific stimulus. Image acquisition over a time period of 3 h was performed using a Leica AF6000 time-lapse microscope with a picture frequency of 5/min. Image analysis was conducted with LAS AF lite (Leica), ImageJ1.45s (Wayne Rasband), and Irfan View 4.32 (Irfan Skiljan) software. For each stimulus, phagocytosis activity was analyzed in six independent movies, respectively, following moDCs or BMDCs over a time period of 3 h by separately counting phagocytosed and extracellular particles or fungi, respectively.

Flow Cytometry

Dendritic cells were stimulated with inactivated *A. fumigatus* conidia and germ tubes (MOI = 1), 100 µg/ml zymosan depleted [a yeast cell wall preparation, which was treated with hot alkali to remove all TLR-stimulating properties to selectively activate Dectin-1 (dZym, InvivoGen)] or 1 mg/ml lipopolysaccharid (LPS, Sigma) for 24 h. Subsequently, cells were harvested, washed, and resuspended in cold Hank's balanced salt solution (HBSS, Sigma) containing 2 mM EDTA (Sigma). The following antibodies were used for extracellular staining: HLA-ABC-PE (BD Biosciences), HLA-DR-PE (BD Biosciences), CD1a-APC (BD Biosciences), CD14-FITC (BD Biosciences), CD80-APC (Miltenyi Biotec), CD86-PE (BD Biosciences), Dectin-1-PE (R&D) (human cells) and HLA-$2K^b$-FITC (BD Biosciences), HLA-Ia/I-E-PE (BioLegend), CD11c-APC (BioLegend), CD80-FITC (BioLegend), CD86-PE (BD Biosciences), and Dectin-1-PE (R&D) [murine cells]. 5×10^5 cells were stained for 15 min at 4°C. Subsequently, cells were washed twice and 10^4 viable cells according to FSC-SSC properties were acquired using a FACS Calibur (BD Biosciences) flow cytometer and CellQuest Pro software (version 5.2). Data were analyzed with FlowJo software (Tree Star Inc., Ashland, OR, USA).

ROS Quantification

Polymorphonuclear cells and macrophages were stimulated with inactivated *A. fumigatus* conidia and germ tubes (MOI = 1), 100 µg/ml zymosan depleted or 10 µg/ml phorbol-myristate-acetate [the major endogenous ROS inducer in PMNs and macrophages (PMA, Sigma-Aldrich)]. ROS-formation in human and murine PMNs and macrophages was determined by ROS-dependent CM-H_2DCF oxidation (dichlorfluorescein, Sigma-Aldrich). Excitation was performed at 485 nm, and fluorescence emission was detected at 535 nm (GENios microplate reader, TECAN). PMNs were stimulated at 37°C for 1 h and macrophages for 2.5 h before measuring fluorescence intensity.

Multiplex Cytokine Assays

Polymorphonuclear cells (2×10^6/ml), macrophages (8×10^5/ml), and DCs (1×10^6/ml) were stimulated with *A. fumigatus* conidia and germ tubes (MOI = 1), zymosan depleted (100 µg/ml), LPS (1 µg/ml), or plain culture medium (negative control). Supernatants were harvested after 3 h (PMNs), 12 h (macrophages), or 24 h (DCs) and stored at −20°C. Cytokine concentrations (IL1β, IL4, IL6, huIL8, muGroα, IL10, IL12p70, IL18, IL23, IP10, MCP1, MIP1α, MIP1β, TNFα) were quantified with a human and mouse 13-Plex panel assay (Affymetrix, eBioscience).

Fungicidal Activity of PMNs

Polymorphonuclear cell were isolated from whole blood of four healthy human donors and two mice as described above. PMNs were diluted in colorless RPMI + 10% FCS at a concentration of 2×10^6/ml. 5×10^5 PMNs were seeded per well of a 24-well plate and 5×10^5 vital *A. fumigatus* germ tubes were added (MOI = 1, ideal MOI was determined in a preceding experiment). Control wells containing only PNMs or fungal cells as well as blank wells containing culture medium without cells were prepared. After 2 and 4 h of coculture at 37°C, hypotonic lysis of PMNs was performed by washing wells twice with 1,000 µl cold distilled water, followed by 5 min incubation on ice. Supernatants were carefully removed, and 200 µl HBSS supplemented with 400 µg/ml of 2,3-bis-(2-methoxy-4-nitro-5-sulphenyl)-(2H)-tetrazolium-5-carboxanilide [XTT (Sigma)] and 50 µg/ml of coenzyme (Sigma) were added. After 90 min incubation at 37°C and centrifugation at 300*g* for 5 min, 100 µl supernatant of each well were transferred to a 96-well plate and OD_{450} was measured in a microplate reader. Fold changes of fungal XTT metabolism were calculated according to the following formula: $\text{Fold change} = (OD_{450}^{PMN+Fungus} - OD_{450}^{PMN}) / (OD_{450}^{Fungus} - OD_{450}^{Blank})$.

Statistics

Significance testing was performed using GraphPad Prism 7 (Graphpad Software, Inc.) using different statistical test which are noted in each figure legend. Statistical significance is denoted as follows: $*p < 0.05$, $**p < 0.01$, and $***p < 0.001$.

RESULTS

Murine Neutrophils and Macrophages Show Stronger ROS Release upon Stimulation with *A. fumigatus* Germ Tubes and Depleted Zymosan (dZym)

Reactive oxygen species production by human and murine neutrophils and macrophages cocultured with *A. fumigatus* conidia or germ tubes was quantified and compared. No significant induction of oxidative burst in PMNs or macrophages of either species was observed upon conidial stimulation. *A. fumigatus* germ tubes and dZym (binding exclusively to dectin-1) led to significantly higher ROS release by murine PMNs (**Figure 1A**) and macrophages (**Figure 1B**). By contrast, human PMNs and

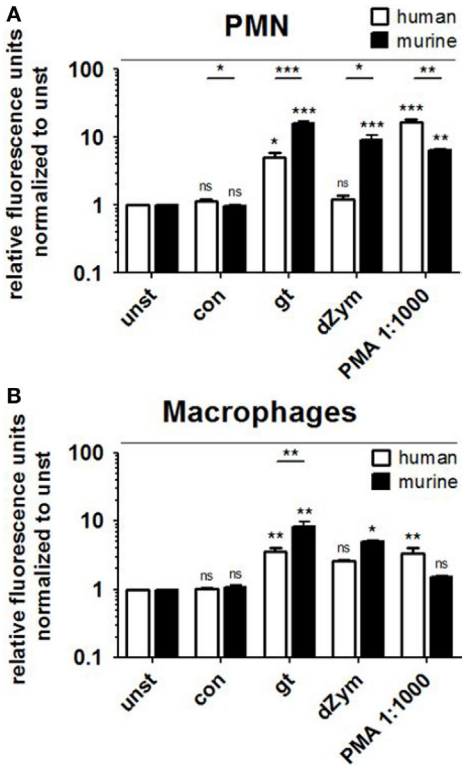

FIGURE 1 | Murine polymorphonuclear cells (PMNs) and macrophages exhibit a stronger reactive oxygen species (ROS) response to *Aspergillus fumigatus* germ tubes and depleted zymosan (dZym). Human and murine PMNs **(A)** or macrophages **(B)** were stimulated with *A. fumigatus* conidia (con), germ tubes (gt), dZym, or phorbol 12-myristate 13-acetate (PMA). ROS production was measured by a dichlorfluorescein-based assay. Mean fold changes of relative fluorescence units after 2 (PMNs) and 3 h (macrophages) are shown. Seven human and three murine samples were analyzed. Significance was calculated as difference to unstimulated with ANOVA and Tukey post-test (stars above of bars) as well as between human and mouse specimens with unpaired *t*-Test, Error bars indicate SDs.

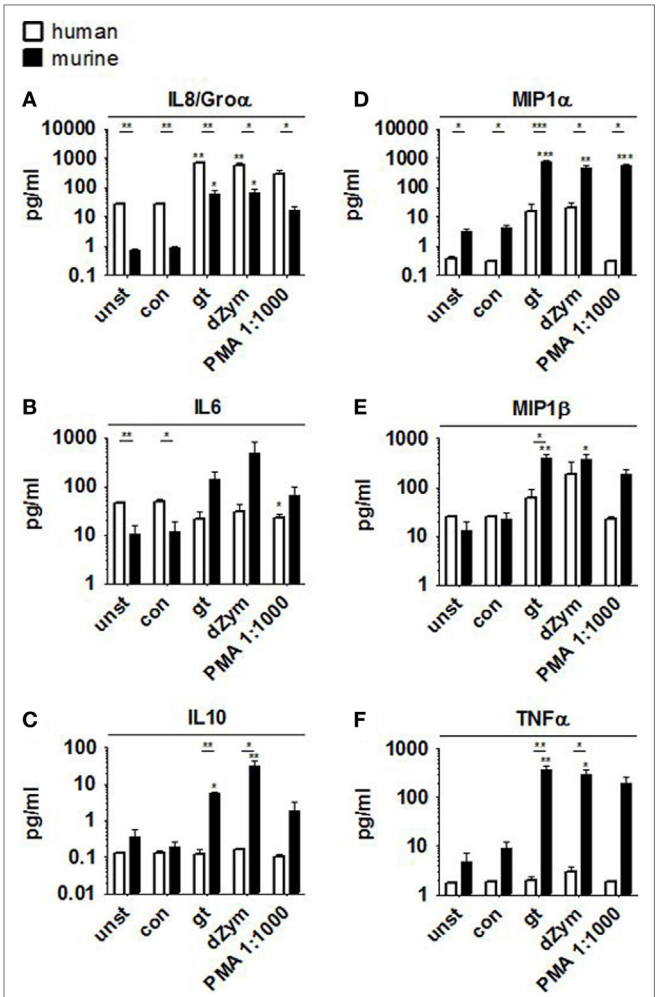

FIGURE 2 | *Aspergillus fumigatus* germ tubes and depleted zymosan (dZym) trigger strong pro-inflammatory cytokine release by murine neutrophils. Murine or human neutrophils were stimulated with *A. fumigatus* conidia, germ tubes, dZym or PMA for a period of 3 h. Subsequently, cytokine concentrations in the culture medium were determined by 13-plex cytokine assays. PMNs obtained from three human donors (white bars) and three mice (black bars) were assessed. Mean concentrations of IL8/Groα **(A)**, IL6 **(B)**, IL10 **(C)**, MIP1α **(D)**, MIP1β **(E)**, and TNFα **(F)** are shown. Error bars indicate standard deviations. Significance was calculated as difference to unstimulated with ANOVA and Tukey post-test (stars above of bars) as well as between human and mouse specimens with unpaired *t*-Test.

macrophages released significantly more ROS after stimulation with the major endogenous ROS inducer PMA.

Murine PMNs Exert Stronger and Broader Pro-inflammatory Cytokine Response to *A. fumigatus* Germ Tubes and dZym

Strong ROS response was paralleled by the secretion of pro-inflammatory cytokines Groα, IL6, MIP1α, MIP1β, and TNFα by murine PMNs after stimulation with *A. fumigatus* germ tubes or dZym, as well as the anti-inflammatory cytokine IL10 (**Figure 2**). Pro-inflammatory cytokine release was also significantly induced by PMA stimulation, whereas coculture with *A. fumigatus* conidia did not result in significant induction of MIP1β or TNFα secretion. Human PMNs showed strongly elevated IL8 release when stimulated with *A. fumigatus* germ tubes, dZym or PMA, while MIP1α and MIP1β secretion was weakly induced by *A. fumigatus* germ tubes and dZym.

Human and Murine Macrophages Release Distinct Cytokine Patterns When Cocultured with *A. fumigatus* or Stimulated with Synthetic Agonists

Pro- and anti-inflammatory cytokine secretion was strongly induced in both murine and human macrophages upon coculture with *A. fumigatus* germ tubes, dZym, or synthetic agonists LPS and Pam3CSK. While human macrophages released higher concentrations of MIP1α, IL8, and IL10 (**Figures 3B,D,E**), fold changes of IL8 and MIP1α were higher in murine samples due to differences in baseline levels. In comparison to murine cells stimulation of human macrophages by *A. fumigatus* germ tubes,

dZym, and Pam3CSK resulted in significantly greater IL1β release (**Figure 3A**). Interestingly, a small but significant increase in MIP1α and TNFα (**Figures 3E,F**) secretion by macrophages of both species was observed upon conidial stimulation. In human macrophages, this was paralleled by an even more pronounced upregulation of IL8 release and minor elevations of IL1β and IL6 (**Figures 3A,C,D**).

Human moDCs Show Higher Phagocytosis Rates of *A. fumigatus* Conidia and Germ Tubes

Live imaging was performed to visualize the interaction between human (**Figure 4A**) or murine DCs (**Figure 4B**) with *A. fumigatus* conidia or germ tubes. Analyzing the number of touches of DCs and fungal cells or the unspecific polystyrene bead control revealed no significant differences between human and murine cells over 3 h (**Figure 4C**). Assessing the percentage of phagocytosed *A. fumigatus* conidia or germ tubes after 3 h, however, human moDCs showed higher phagocytosis rates than murine BMDCs, whereas the internalization of polystyrene beads by human and murine DCs did not differ significantly (**Figure 4D**).

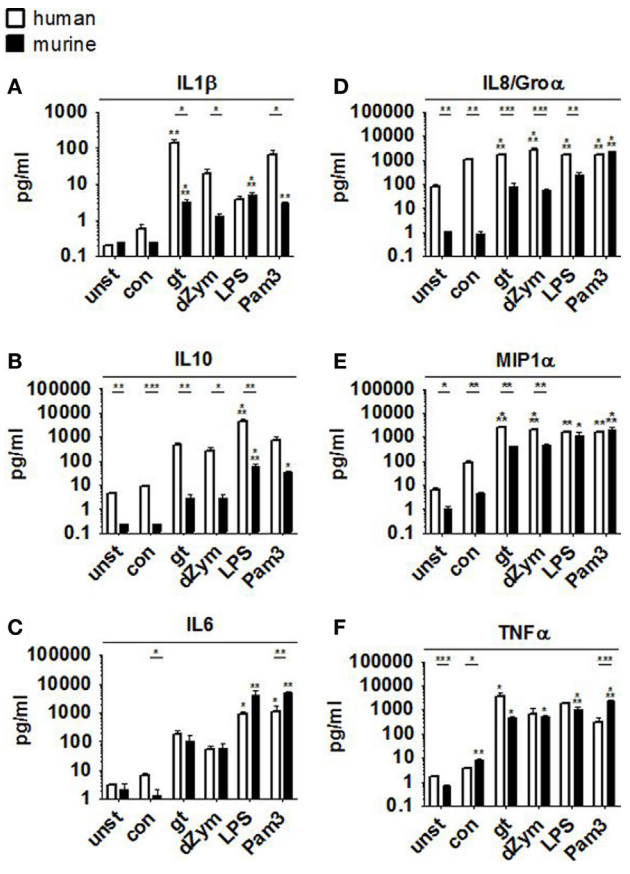

FIGURE 3 | Distinct cytokine response pattern to *Aspergillus fumigatus* by human and murine macrophages. Cytokine patterns in culture supernatants of human and murine macrophages were studied by a 13-plex cytokine assay upon 12 h stimulation with *A. fumigatus* conidia or germ tubes as well as depleted zymosan (dZym), LPS, or Pam3CSK. Four human (white bars) and four murine (black bars) samples were assessed. Mean concentrations of IL1β **(A)**, IL10 **(B)**, IL6 **(C)**, IL8/Groα **(D)**, MIP1α **(E)**, and TNFα **(F)** are shown. Error bars indicate standard deviations. Significance was calculated as difference to unstimulated with ANOVA and Tukey post-test (stars above of bars) as well as between human and mouse specimens with unpaired *t*-test.

Dectin-1 Is Inversely Regulated on Human and Murine DCs after Stimulation with *A. fumigatus* Conidia and Germ Tubes

The transmembrane glycoprotein Dectin-1, also known as C-type lectin domain family member 7A, plays an important role as an *A. fumigatus* phagocytosis receptor (4). Thus, Dectin-1 expression on DCs cocultured with ethanol-inactivated conidia and germ tubes for different periods was assessed and compared with unstimulated DCs. After only 1 h of coculture with both fungal morphotypes, surface expression of Dectin-1 started to decline on human moDCs, with a more pronounced effect after stimulation with germ tubes (**Figure 5A**). By contrast, increased Dectin-1 expression was observed on murine BMDCs stimulated with *A. fumigatus* germ tubes (**Figure 5B**). For each of the coculture periods studied, a significant difference in Dectin-1 surface expression was detected between human and murine DCs stimulated with *A. fumigatus* germ tubes, whereas prolonged exposure (18 h) to inactivated conidia was necessary to observe significantly different expression (**Figures 5C,D**).

Human and Murine DCs Cocultured with *A. fumigatus* Show Distinct Surface Antigen and Cytokine Response Patterns

To further characterize the response patterns of human and murine DCs confronted with resting and germinated stages of *A. fumigatus*, we analyzed the expression of maturation markers (CD80 and CD86) and MHC molecules (MHC-I and MHC-II) on the cell surface. 24 h of stimulation with inactivated *A. fumigatus* germ tubes, dZym, and LPS led to 1.3-fold upregulation of CD80, CD86, MHC-I, and MHC-II on both human and murine DCs (**Figure 6**). Upon coculture with all studied stimuli, significantly greater levels of CD80 and CD86 were observed on human moDCs (**Figures 6A,B**). Coculture with *A. fumigatus* germ tubes led to a significantly higher MHC-I and MHC-II surface expression on human moDCs, whereas conidial stimulation resulted in stronger upregulation of MHC-I in murine BMDCs (**Figures 6C,D**).

Further, cytokine profiles were studied by bead-based multiplex cytokine assays after 24 h coculture of DCs with *A. fumigatus* conidia, germ tubes, dZym, or LPS. Stimulation with *A. fumigatus* germ tubes or LPS led to release of a broad range of pro-inflammatory cytokines by both human moDCs and murine BMDCs. Human moDCs showed significantly stronger TNFα release in response to these stimuli and a trend toward stronger IL12p70 and IL23 induction. By contrast, murine BMDCs released significantly greater amounts of IL6 and IL18 (**Figure 7**).

Conidial stimulation resulted in the release of fewer cytokines and lower concentrations than other stimuli. Murine BMDCs

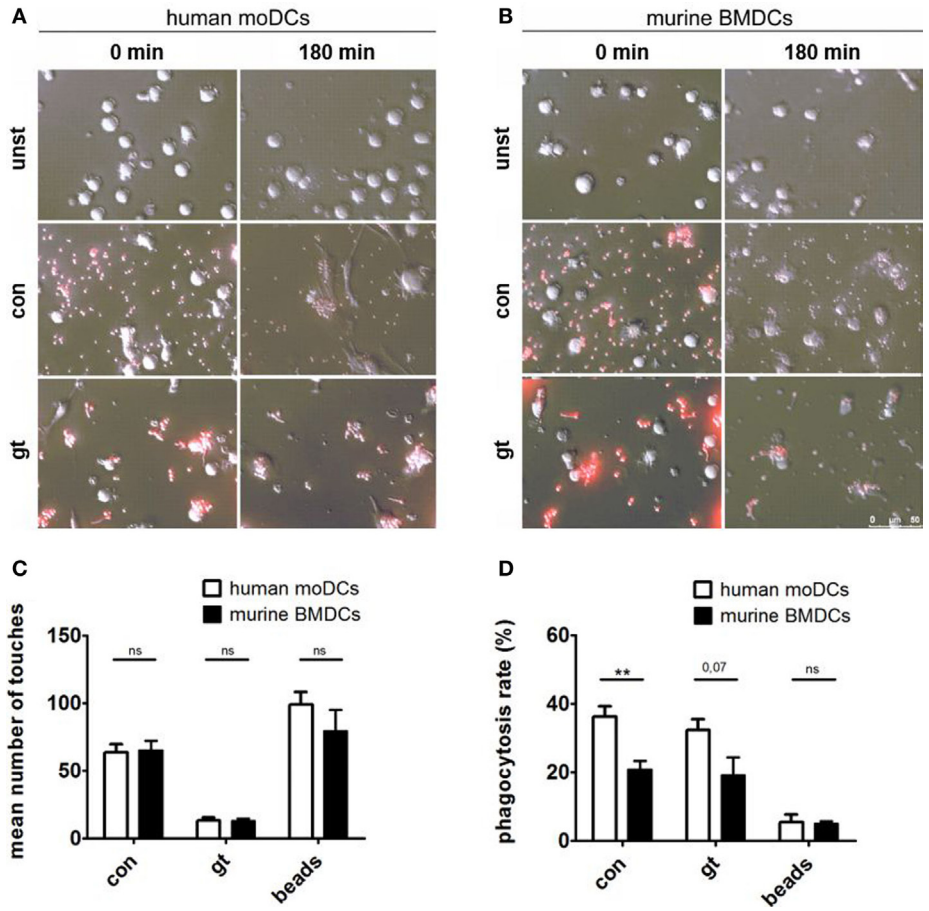

FIGURE 4 | Human dendritic cells (DCs) contact and phagocytose *Aspergillus fumigatus* conidia and germ tubes more effectively. Representative images show phagocytosis of red fluorescent conidia and germ tubes by human **(A)** and murine **(B)** DCs at the indicated time points (duration of coculture). Number of touches **(C)** of human and murine DCs with *A. fumigatus* conidia (con), germ tubes (gt), and polystyrene beads (beads) and phagocytosis rates **(D)** were determined by live imaging analysis. Mean values of touched **(C)** or mean percentage of phagocytosed **(D)** fungal cells or beads after 3 h of coculture are given in the figure. Six human and murine donors were assessed. Significance was calculated with unpaired *t*-Test and error bars indicate SDs.

showed strong and significant induction of the pro-inflammatory cytokines IL1β, IL6, TNFα, but also increased IL10 release after coculture with conidia. Stimulation of murine BMDCs with dZym led to significantly greater release of IL6, IL10, and IL18, whereas a tendency toward greater TNFα release by human moDCs was observed.

Taken together, these results highlight different response patterns of human moDCs and murine BMDCs confronted with *A. fumigatus*, with distinct cytokine profiles and stronger expression of maturation markers and MHC molecules on human moDCs.

Fungicidal Activity of PMNs

Colorimetric analysis of the fungal metabolism revealed that 2 h of *A. fumigatus* germ tube–PMN co-cultivation led to markedly increased fungal metabolism while fungal metabolic activity was decreased again after 4 h, compared to unstimulated control samples. No major difference was observed between human and murine PMNs (Figure S2 in Supplementary Material).

DISCUSSION

Aspergillus fumigatus is the most important cause of invasive fungal infections occurring almost exclusively in immunocompromised patients. A key to understanding *A. fumigatus* pathogenicity is knowledge of the interplay between the fungus and the immune system, in particular with the initial innate immune defense consisting of neutrophils, macrophages, and DCs.

In recent decades, several hundred studies characterized the functions of innate immune cells directed against *A. fumigatus* thereby improving the management and treatment of aspergillosis (15). This intensive work was based on *in vitro* studies involving culturing of primary human immune cells, and cell lines and a large variety of animal models including mice, which are frequently used to model human disease and to mimic scenarios of immunocompromised patients.

This study, the first to our knowledge, provides a comparative functional assessment of murine innate immune cell subsets routinely employed in *A. fumigatus in vitro* interaction studies with

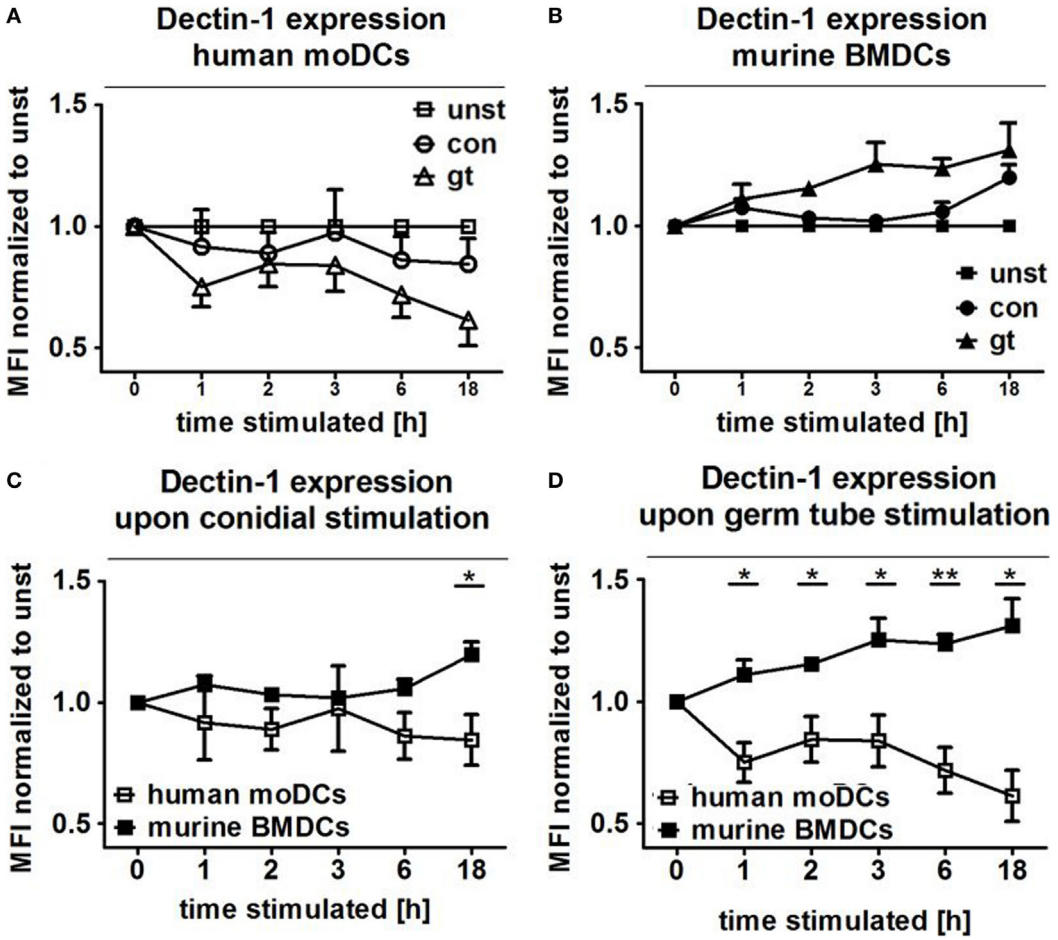

FIGURE 5 | Human and murine dendritic cells show inverse Dectin-1 surface expression patterns after exposure to *Aspergillus fumigatus*. Dectin-1 expression on the cell surface of human moDCs **(A)** and murine bone marrow derived dendritic cells (BMDCs) **(B)** was analyzed by flow cytometry after coculture with *A. fumigatus* conidia and germ tubes for different periods. Mean fold changes (±SDs) of mean fluorescence intensity (MFI) compared to unstimulated cells are given in the figure. Two murine and four human samples were analyzed. The lower panels directly compare Dectin-1 expression following exposure of human moDCs and murine BMDCs to *A. fumigatus* germ tubes **(C)** and conidia **(D)**. Human and murine samples were compared with unpaired *t*-Test, error bars show SDs.

their human counterparts. Humans and mice differ greatly in their size, lifespan, living conditions, and ecological niches. Even the blood composition between different mouse strains varies widely, while C57BL/6 mice contain 10–25% PMNs and 75–90% lymphocytes (16), CD-1 mice exhibit 15–20% PMNs (300–2,000 cells/μl) and 50–70% lymphocytes (1,000–7,000 cells/μl) (17). In contrast, human blood contains 50–70% PMNs (3,500–7,000 cells/μl) and 20–40% lymphocytes (1,400–4,000 cells/μl) (17). In consequence, a direct translation of murine *in vivo* experimental data to human pathological events often fails due to insufficient similarities in the organization of the immune system of both species (18).

In our study, we isolated and cultivated PMNs, macrophages, and DCs from both mammals and challenged them *in vitro* with *A. fumigatus* using standardized and reproducible working conditions, laboratory protocols and readout assays. We are aware that this *in vitro* comparison is restricted due to the isolated use of single immune cell types while well-established murine models allow a complex view of the pathogenesis of IA. However, the chosen comparative *in vitro* study design nicely illustrates the substantial parallel organization of the human and murine immune response against *A. fumigatus* but also provides examples for functional heterogeneity in the defense against the fungus.

Polymorphonuclear cells are among the first line response against *A. fumigatus*. When attracted by chemokines they leave the blood stream and migrate to the site of infection using a large number of PRRs to recognize and respond to the fungus. This includes the release of soluble antimicrobials, reactive metabolites, cytokines, and phagocytosis of conidia (19). In our experiments, murine and human neutrophils were directly isolated from anticoagulated blood using similar protocols (polysaccharide gradient for human blood and the commercial neutrophil enrichment kit for mice). Murine PMNs exhibited a significantly stronger ROS response to *A. fumigatus* and dZym,

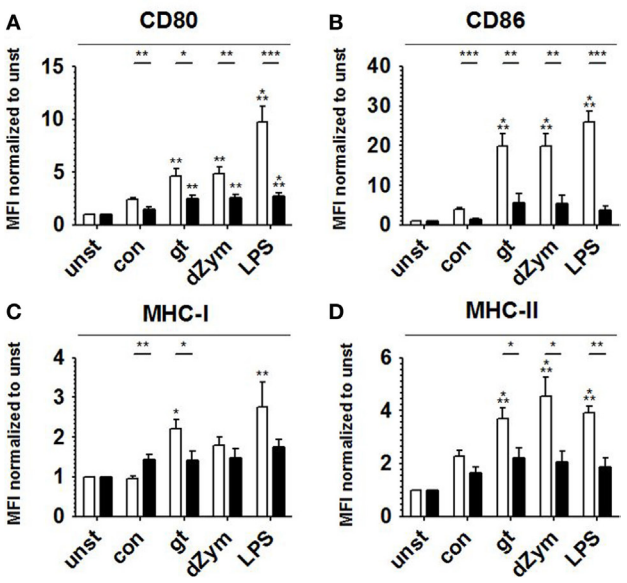

FIGURE 6 | Stronger upregulation of maturation markers and major histocompatibility complex (MHC) molecules upon *Aspergillus fumigatus* stimulation is observed in human moDCs. Surface expression of CD80 **(A)**, CD86 **(B)**, MHC-I **(C)**, and MHC-II **(D)** was analyzed by flow cytometry in human moDCs and murine bone marrow derived dendritic cells after 24 h stimulation with *A. fumigatus* conidia (con) and germ tubes (gt) as well as depleted zymosan (dZym) and LPS. Six human and murine dendritic cell samples were assessed. Mean fold changes of MFI values compared to unstimulated cells (unst) and SDs are shown. Significance between human and mouse specimen was calculated with the unpaired *t*-Test, the comparison to unstimulated specimens is shown as stars above bars and was calculated with ANOVA and Tukey post-test.

a pure dectin-1 agonist, than human PMNs (**Figure 1**). The role of ROS in the immune defense against *A. fumigatus* is rather unclear. While text-book knowledge indicates that ROS is used by PMNs to kill *A. fumigatus*, more recent reports state that they play a regulatory role as signaling molecules and in the activation of antimicrobial enzymes in the phagolysosome (20). Furthermore, it could be demonstrated only recently that murine lung PMNs trigger programmed cell death with apoptosis-like features in *A. fumigatus* conidia (21).

Furthermore, human PMNs showed strongly elevated IL8 release when stimulated with *A. fumigatus* germ tubes and dZym while murine PMNs secreted a much larger variety of cytokines and chemokines, including Groα, IL6, MIP1α, MIP1β, and TNFα, as well as the anti-inflammatory cytokine IL10. While IL8 is the most important chemoattractant for human neutrophil recruitment, an orthologous counterpart is absent in mice (22). In contrast, mice express CXCL15 as an attractant and other functional homologs of IL8, such as Groα (23).

Interestingly, in a preliminary experiment analyzing PMNs from four healthy human donors and two mice by an XTT metabolic assay, we revealed no major differences quantifying fungal metabolism after 2 and 4 h, respectively. We hypothesize that the increase of fungal metabolism after 2 h of co-cultivation with human and murine PMNs might reflect temporarily higher fungal metabolic activity due to early defense mechanisms of *A. fumigatus*.

Human moDCs were generated from $CD14^+$ monocytes using rGM-CSF and rIL4 while murine DCs were derived from bone marrow cultured in R10-medium supplemented with rmGM-CSF. While murine $Ly6C^{high}$ monocytes fail to proliferate (24), proliferating cells mostly represent macrophage-DC progenitors and common monocyte progenitor (25). This observation was described for human $CD14^+$ monocytes undergoing moDC differentiation as well (26). Thereby, GM-CSF has major effects on myelomonocytic cells leading to a massive expansion of macrophage–DC-restricted precursors, but very low effects on common dendritic cell precursors (24). In both, humans and mice, $Ly6C^{high}$ monocytes and moDCs are recruited into tissue under inflammatory and infectious conditions thereby initiating T cell priming in the draining lymph nodes, e.g., in the synovia of rheumatoid arthritis patients (27, 28). Thus, murine BMDCs and human moDCs are highly similar and thus can be considered as functional homologs (29, 30).

Both, human and murine DCs were able to phagocytose *A. fumigatus* conidia and germ tubes. Efficient phagocytosis is a prerequisite for adequate antigen processing and presentation to lymphocytes (31). This characteristic property of DCs in the interplay with *A. fumigatus* underlines their relevance in bridging innate and adaptive immunity during mold infections. The more efficient phagocytosis of *A. fumigatus* conidia in human moDCs might be due to the differential size of human and murine DCs or due to mouse-strain specific variabilities in phagocytosic capacity (32).

Human moDCs secreted substantially more of the pro-inflammatory mediators TNFα, MCP1, IL12p70, and IL1β, indicating their profound role in the broad activation of the innate and adaptive immune response. Murine BMDCs released significantly greater amounts of IL6 and IL18. Cenci et al. showed that IL6(−/−) mice were more susceptible to aspergillosis than the wild-type. Susceptibility was associated with increased inflammatory pathology, decreased antifungal effector functions of phagocytes, and impaired development of protective type 1 responses. Exposure to exogenous IL6 restored antifungal effector activity (33). Similarly, simultaneous neutralization of IL18 and IL12 resulted in a significant increase in *A. fumigatus* CFU in murine lung tissue demonstrating its key role in murine defense against *Aspergillus* infection (34).

Secretion of IL10, which suppresses proliferation, cytokine secretion, and costimulatory molecule expression of pro-inflammatory immune cells, differed markedly between human and murine cells. While *A. fumigatus* germ tubes and dZym led to a 100- and 60-fold induction of the IL10 secretion of human macrophages compared to unstimulated control cells, stimulation of murine macrophages led to lower increases (with germ tubes 14-fold, with dZym 14-fold). Interestingly, basal secretion of IL10 from unstimulated macrophages into the culture medium was over 20-fold higher in human cells than in their murine counterparts. Human and mouse IL10 have roughly 73% sequence homology and are secreted as 178-amino acid proteins (35). It is

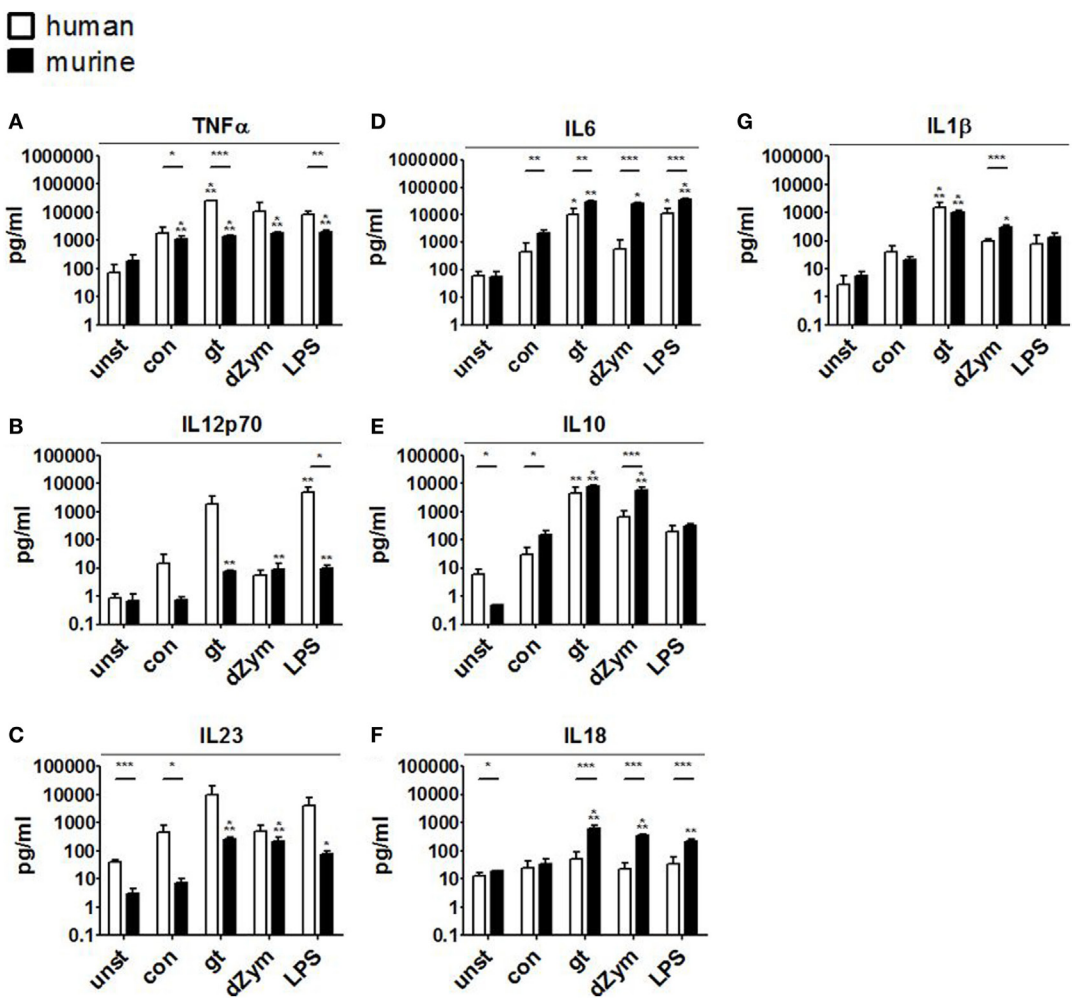

FIGURE 7 | Distinct cytokine response patterns to *Aspergillus fumigatus* are observed in human and murine dendritic cells (DCs). Cytokine concentrations (picograms/milliliter) in culture supernatants of human moDCs and murine bone marrow-derived dendritic cells stimulated with ethanol-inactivated *A. fumigatus* conidia or germ tubes, depleted zymosan (dZym) or LPS were quantified by 13-plex cytokine assays. Four human (white bars) and four murine (black bars) DC samples were assessed. Mean concentrations of TNFα **(A)**, IL12p70 **(B)**, IL23 **(C)**, IL6 **(D)**, IL10 **(E)**, IL18 **(F)**, and IL1β **(G)** are shown. Error bars indicate standard deviations. Significance was calculated as difference to unstimulated specimens with ANOVA and Tukey post-test (stars above of bars) as well as between human and mouse specimens with unpaired *t*-test.

unknown whether both cytokines have identical binding capacity to their receptors, stability, and degradation behavior.

Dectin-1, a β-glucan receptor, is expressed on monocytes, macrophages, DCs, neutrophils, and eosinophils (36). Brown et al. demonstrated that dZym, which was treated with hot alkali to remove its TLR-stimulating properties, triggers expression of pro-inflammatory cytokines *via* Dectin-1 signaling (37). In mice, sensing of *C. albicans* by Dectin-1 results in ingestion and killing of the fungus and the induction of an early inflammatory response, which results in the recruitment and activation of other immune cells to the infection site. Dectin-1 deficiency leads to increased susceptibility to systemic and mucosal candidiasis (38). In contrast, human Dectin-1 deficiency causes diminished cytokine responses, while alternative receptors are then responsible for fungal uptake and subsequent killing. Our results demonstrate inverse Dectin-1 surface expression after exposure to *A. fumigatus*. After 1 h of coculture, surface expression of Dectin-1 decreased on human moDCs, with a more pronounced effect after stimulation with germ tubes (**Figure 5A**). By contrast, increased Dectin-1 expression was observed on murine BMDCs stimulated with *A. fumigatus* germ tubes (**Figure 5B**). We hypothesize that downregulation of Dectin-1 exposure on human moDCs prevents severe and uncontrolled inflammatory reactions while on murine BMDCs, Dectin-1 expression is required for continuous ingestion and killing of the fungus. This is consistent with our previous data showing that anti-Dectin-1 antibody treatment of human moDCs as well as *ex vivo* myeloid DCs subsequently inhibited secretion of pro-inflammatory cytokines after contact with *A. fumigatus*, *C. albicans*, or zymosan (4, 39). This is also consistent with the observation that naïve mice lacking Dectin-1 show reduced killing of conidia and a higher mortality rate than wild-type mice (40).

Taken together, after 65 million years of independent evolution (5), immune systems of both species differ substantially. Mice are perfectly adapted to their relatively short lifespan of 2–3 years and their natural habitat on the ground. In the defense against invading fungi, resistance mechanisms and an efficient control over pathogens dominate in humans, while tolerance determines the immune response in mice (41). Our comparative functional assessment of selected human and murine innate immune cell subsets using standardized and reproducible working conditions, laboratory protocols, and readout assays underlined this hypothesis. We were able to provide examples for functional heterogeneity of mammalian innate immune cell populations in their *in vitro* response against the pathogenic mold *A. fumigatus*. These specific differences should be carefully considered in future comparative discovery and validation studies. Furthermore, they highlight potential limitations in the direct transferability of murine host–pathogen interaction studies. Additional studies are highly warranted comparatively employing murine and human cell populations to further study mold immunopathology and to evaluate new diagnostic and therapeutic strategies. Moreover, work on humanized mouse models or the development of synthetic human models might help to avoid difficulties in translating and harmonizing data across different mammalian species.

ETHICS STATEMENT

Use of whole blood specimens from healthy volunteers was approved by the University Hospital of Wuerzburg Ethical Committee (#302/15). Written informed consent was obtained and data analysis was performed anonymously. Mouse husbandry and experimental procedures were conducted in accordance with institutional guidelines and with the approval of the Committee on Animal Research of the regional government (Regierung von Unterfranken, Wuerzburg, Germany).

AUTHOR CONTRIBUTIONS

A-MH and JaL designed the study, performed experiments, performed data analyzes, and wrote the manuscript. AS performed experiments. SW and ML analyzed the data and contributed to the manuscript. CM, ME, and KC provided discussions, technical assistance and contributed to the manuscript. HE and JuL developed concepts, supervised the study, and wrote the manuscript.

FUNDING

This study was supported by the Deutsche Forschungsgemeinschaft (DFG) within the Collaborative Research Center CRC124 FungiNet "Pathogenic fungi and their human host: Networks of interaction" (project A2 to HE and JuL, A4 to JaL and funding for travel to CM) and by the Interdisciplinary Centre for Clinical Research Wuerzburg (grant Z-3/56 to SW). The authors thank all blood donors for their voluntary donation.

SUPPLEMENTARY MATERIAL

The Supplementary Material for this article can be found online at http://www.frontiersin.org/article/10.3389/fimmu.2017.01716/full#supplementary-material.

FIGURE S1 | Comparison of cytokine response patterns to *Aspergillus fumigatus* germ tubes. Cytokine secretion into the culture medium was analyzed by multiplex bead-based assay upon stimulation of murine or human dendritic cells (DCs), neutrophils [polymorphonuclear cells (PMNs)], or macrophages with *A. fumigatus* germ tubes. Fold changes compared to unstimulated samples are indicated by gray scale. OOR (out of range) indicates that >50% of samples did not meet the limits of detection and thus fold changes could not be calculated reliably.

FIGURE S2 | Impact of human and murine polymorphonuclear cells (PMNs) on fungal XTT metabolism. PMNs were isolated from whole blood of four healthy human donors and two mice as described in the Section "Materials and Methods." After 2 and 4 h of coculture at 37°C, hypotonic lysis of PMNs was performed. Supernatants were carefully removed and 200 µl HBSS supplemented with 400 µg/ml of 2,3-bis-(2-methoxy-4-nitro-5-sulphenyl)-(2 H)-tetrazolium-5-carboxanilide (XTT) and 50 µg/ml of coenzyme were added. After 90 min incubation at 37°C and centrifugation at 300*g* for 5 min, 100 µl supernatant of each well were transferred to a 96-well plate and OD_{450} was measured in a microplate reader. Fold changes of fungal XTT metabolism due to the presence of PMNs was calculated according to the following formula: $\text{Fold change} = (OD_{450}^{PMN+Fungus} - OD_{450}^{PMN}) / (OD_{450}^{Fungus} - OD_{450}^{Blank})$. Individual results for each human and murine PMN sample and mean values (black horizontal bars) are shown in the figure.

REFERENCES

1. Segal BH. Aspergillosis. *N Engl J Med* (2009) 360:1870–84. doi:10.1056/NEJMra0808853
2. Grimm MJ, D'Auria AC, Segal BH. Assessing anti-fungal activity of isolated alveolar macrophages by confocal microscopy. *J Vis Exp* (2014) (89):e51678. doi:10.3791/51678
3. Braedel S, Radsak M, Einsele H, Latge JP, Michan A, Loeffler J, et al. *Aspergillus fumigatus* antigens activate innate immune cells via toll-like receptors 2 and 4. *Br J Haematol* (2004) 125:392–9. doi:10.1111/j.1365-2141.2004.04922.x
4. Mezger M, Kneitz S, Wozniok I, Kurzai O, Einsele H, Loeffler J. Proinflammatory response of immature human dendritic cells is mediated by Dectin-1 after exposure to *Aspergillus fumigatus* germ tubes. *J Infect Dis* (2008) 197:924–31. doi:10.1086/528694
5. Mestas J, Hughes CC. Of mice and not men: differences between mouse and human immunology. *J Immunol* (2004) 172:2731–8. doi:10.4049/jimmunol.172.5.2731
6. Reynolds G, Haniffa M. Human and mouse mononuclear phagocyte networks: a tale of two species? *Front Immunol* (2015) 6:330. doi:10.3389/fimmu.2015.00330
7. Relle M, Thomaidis T, Galle PR, Schwarting A. Comparative aspects of murine proteinase 3. *Rheumatol Int* (2011) 31:1105–11. doi:10.1007/s00296-010-1672-2
8. Park SJ, Burdick MD, Mehrad B. Neutrophils mediate maturation and efflux of lung dendritic cells in response to *Aspergillus fumigatus* germ tubes. *Infect Immun* (2012) 80:1759–65. doi:10.1128/IAI.00097-12
9. Lother J, Breitschopf T, Krappmann S, Morton CO, Bouzani M, Kurzai O, et al. Human dendritic cell subsets display distinct interactions with the pathogenic mould *Aspergillus fumigatus*. *Int J Med Microbiol* (2014) 304:1160–8. doi:10.1016/j.ijmm.2014.08.009
10. Moretti S, Bozza S, Massi-Benedetti C, Prezioso L, Rossetti E, Romani L, et al. An immunomodulatory activity of micafungin in preclinical aspergillosis. *J Antimicrob Chemother* (2014) 69:1065–74. doi:10.1093/jac/dkt457
11. Prufer S, Weber M, Stein P, Bosmann M, Stassen M, Kreft A, et al. Oxidative burst and neutrophil elastase contribute to clearance of *Aspergillus fumigatus* pneumonia in mice. *Immunobiology* (2014) 219:87–96. doi:10.1016/j.imbio.2013.08.010
12. Liu C, Wang M, Sun W, Cai F, Geng S, Su X, et al. PU.1 serves a critical role in the innate defense against *Aspergillus fumigatus* via dendritic cell-associated C-type lectin receptor-1 and toll-like receptors-2 and 4 in THP-1-derived macrophages. *Mol Med Rep* (2017) 15:4084–92. doi:10.3892/mmr.2017.6504

13. Wiemann P, Perevitsky A, Lim FY, Shadkchan Y, Knox BP, Landero Figueora JA, et al. *Aspergillus fumigatus* copper export machinery and reactive oxygen intermediate defense counter host copper-mediated oxidative antimicrobial offense. *Cell Rep* (2017) 19:2174–6. doi:10.1016/j.celrep.2017.05.075
14. Lutz MB, Kukutsch N, Ogilvie AL, Rossner S, Koch F, Romani N, et al. An advanced culture method for generating large quantities of highly pure dendritic cells from mouse bone marrow. *J Immunol Methods* (1999) 223:77–92. doi:10.1016/S0022-1759(98)00204-X
15. Sales-Campos H, Tonani L, Cardoso CR, Kress MR. The immune interplay between the host and the pathogen in *Aspergillus fumigatus* lung infection. *Biomed Res Int* (2013) 2013:693023. doi:10.1155/2013/693023
16. Doeing DC, Borowicz JL, Crockett ET. Gender dimorphism in differential peripheral blood leukocyte counts in mice using cardiac, tail, foot, and saphenous vein puncture methods. *BMC Clin Pathol* (2003) 3:3. doi:10.1186/1472-6890-3-3
17. Haley PJ. Species differences in the structure and function of the immune system. *Toxicology* (2003) 188:49–71. doi:10.1016/S0300-483X(03)00043-X
18. Zschaler J, Schlorke D, Arnhold J. Differences in innate immune response between man and mouse. *Crit Rev Immunol* (2014) 34:433–54. doi:10.1615/CritRevImmunol.2014011600
19. Arnhold J, Flemmig J. Human myeloperoxidase in innate and acquired immunity. *Arch Biochem Biophys* (2010) 500:92–106. doi:10.1016/j.abb.2010.04.008
20. Brakhage AA, Bruns S, Thywissen A, Zipfel PF, Behnsen J. Interaction of phagocytes with filamentous fungi. *Curr Opin Microbiol* (2010) 13:409–15. doi:10.1016/j.mib.2010.04.009
21. Shlezinger N, Irmer H, Dhingra S, Beattie SR, Cramer RA, Braus GH, et al. Sterilizing immunity in the lung relies on targeting fungal apoptosis-like programmed cell death. *Science* (2017) 357:1037–41. doi:10.1126/science.aan0365
22. Zlotnik A, Yoshie O, Nomiyama H. The chemokine and chemokine receptor superfamilies and their molecular evolution. *Genome Biol* (2006) 7:243. doi:10.1186/gb-2006-7-12-243
23. Rossi DL, Hurst SD, Xu Y, Wang W, Menon S, Coffman RL, et al. Lungkine, a novel CXC chemokine, specifically expressed by lung bronchoepithelial cells. *J Immunol* (1999) 162:5490–7.
24. Helft J, Bottcher J, Chakravarty P, Zelenay S, Huotari J, Schraml BU, et al. GM-CSF mouse bone marrow cultures comprise a heterogeneous population of CD11c(+)MHCII(+) macrophages and dendritic cells. *Immunity* (2015) 42:1197–211. doi:10.1016/j.immuni.2015.05.018
25. Hettinger J, Richards DM, Hansson J, Barra MM, Joschko AC, Krijgsveld J, et al. Origin of monocytes and macrophages in a committed progenitor. *Nat Immunol* (2013) 14:821–30. doi:10.1038/ni.2638
26. Romani N, Gruner S, Brang D, Kampgen E, Lenz A, Trockenbacher B, et al. Proliferating dendritic cell progenitors in human blood. *J Exp Med* (1994) 180:83–93. doi:10.1084/jem.180.1.83
27. Randolph GJ, Beaulieu S, Lebecque S, Steinman RM, Muller WA. Differentiation of monocytes into dendritic cells in a model of transendothelial trafficking. *Science* (1998) 282:480–3. doi:10.1126/science.282.5388.480
28. Cheong C, Matos I, Choi JH, Dandamudi DB, Shrestha E, Longhi MP, et al. Microbial stimulation fully differentiates monocytes to DC-SIGN/CD209(+) dendritic cells for immune T cell areas. *Cell* (2010) 143:416–29. doi:10.1016/j.cell.2010.09.039
29. Xu Y, Zhan Y, Lew AM, Naik SH, Kershaw MH. Differential development of murine dendritic cells by GM-CSF versus Flt3 ligand has implications for inflammation and trafficking. *J Immunol* (2007) 179:7577–84. doi:10.4049/jimmunol.179.11.7577
30. Segura E, Touzot M, Bohineust A, Cappuccio A, Chiocchia G, Hosmalin A, et al. Human inflammatory dendritic cells induce Th17 cell differentiation. *Immunity* (2013) 38:336–48. doi:10.1016/j.immuni.2012.10.018
31. Steinman RM, Hemmi H. Dendritic cells: translating innate to adaptive immunity. *Curr Top Microbiol Immunol* (2006) 311:17–58.
32. Maree AF, Komba M, Finegood DT, Edelstein-Keshet L. A quantitative comparison of rates of phagocytosis and digestion of apoptotic cells by macrophages from normal (BALB/c) and diabetes-prone (NOD) mice. *J Appl Physiol (1985)* (2008) 104:157–69. doi:10.1152/japplphysiol.00514.2007
33. Cenci E, Mencacci A, Casagrande A, Mosci P, Bistoni F, Romani L. Impaired antifungal effector activity but not inflammatory cell recruitment in interleukin-6-deficient mice with invasive pulmonary aspergillosis. *J Infect Dis* (2001) 184:610–7. doi:10.1086/322793
34. Brieland JK, Jackson C, Menzel F, Loebenberg D, Cacciapuoti A, Halpern J, et al. Cytokine networking in lungs of immunocompetent mice in response to inhaled *Aspergillus fumigatus*. *Infect Immun* (2001) 69:1554–60. doi:10.1128/IAI.69.3.1554-1560.2001
35. Windsor WT, Syto R, Tsarbopoulos A, Zhang R, Durkin J, Baldwin S, et al. Disulfide bond assignments and secondary structure analysis of human and murine interleukin 10. *Biochemistry* (1993) 32:8807–15. doi:10.1021/bi00085a011
36. Willment JA, Marshall AS, Reid DM, Williams DL, Wong SY, Gordon S, et al. The human beta-glucan receptor is widely expressed and functionally equivalent to murine Dectin-1 on primary cells. *Eur J Immunol* (2005) 35:1539–47. doi:10.1002/eji.200425725
37. Brown GD, Herre J, Williams DL, Willment JA, Marshall AS, Gordon S. Dectin-1 mediates the biological effects of beta-glucans. *J Exp Med* (2003) 197:1119–24. doi:10.1084/jem.20021890
38. Reid DM, Gow NA, Brown GD. Pattern recognition: recent insights from Dectin-1. *Curr Opin Immunol* (2009) 21:30–7. doi:10.1016/j.coi.2009.01.003
39. Hefter M, Lother J, Weiß E, Schmitt AL, Fliesser M, Einsele H, et al. Human primary myeloid dendritic cells interact with the opportunistic fungal pathogen *Aspergillus fumigatus* via the C-type lectin receptor Dectin-1. *Med Mycol* (2016) 55:573–8. doi:10.1093/mmy/myw105
40. Werner JL, Metz AE, Horn D, Schoeb TR, Hewitt MM, Schwiebert LM, et al. Requisite role for the Dectin-1 beta-glucan receptor in pulmonary defense against *Aspergillus fumigatus*. *J Immunol* (2009) 182:4938–46. doi:10.4049/jimmunol.0804250
41. Raberg L, Sim D, Read AF. Disentangling genetic variation for resistance and tolerance to infectious diseases in animals. *Science* (2007) 318:812–4. doi:10.1126/science.1148526

Conflict of Interest Statement: The authors declare that the research was conducted in the absence of any commercial or financial relationships that could be construed as a potential conflict of interest.

Copyright © 2017 Hellmann, Lother, Wurster, Lutz, Schmitt, Morton, Eyrich, Czakai, Einsele and Loeffler. This is an open-access article distributed under the terms of the Creative Commons Attribution License (CC BY). The use, distribution or reproduction in other forums is permitted, provided the original author(s) or licensor are credited and that the original publication in this journal is cited, in accordance with accepted academic practice. No use, distribution or reproduction is permitted which does not comply with these terms.

frontiers in Immunology

ORIGINAL RESEARCH
published: 21 August 2017
doi: 10.3389/fimmu.2017.00949

Th17-Inducing Cytokines IL-6 and IL-23 Are Crucial for Granuloma Formation during Experimental Paracoccidioidomycosis

*Fabrine Sales Massafera Tristão†, Fernanda Agostini Rocha†, Daniela Carlos, Natália Ketelut-Carneiro, Camila Oliveira Silva Souza, Cristiane Maria Milanezi and João Santana Silva**

Department of Biochemistry and Immunology, School of Medicine of Ribeirão Preto, University of São Paulo, Ribeirão Preto, Brazil

Paracoccidioidomycosis (PCM), a chronic granulomatous disease caused by the thermally dimorphic fungus *Paracoccidioides brasiliensis* and *Paracoccidioides lutzii*, has the highest mortality rate among systemic mycosis. The T helper 1-mediated immunity is primarily responsible for acquired resistance during *P. brasiliensis* infection, while susceptibility is associated with Th2 occurrence. Th17 is a population of T CD4$^+$ cells that, among several chemokines and cytokines, produces IL-17A and requires the presence of IL-1, IL-6, and TGF-β for differentiation in mice and IL-23 for its maintenance. Th17 has been described as an arm of the immune system that enhances host protection against several bacterial and fungal infections, as *Pneumocystis carinii* and *Candida albicans*. In this study, we aimed to evaluate the Th17 immune response and the role of Th17-associated cytokines (IL-6, IL-23, and IL-17A) during experimental PCM. First, we observed that *P. brasiliensis* infection [virulent yeast strain 18 of *P. brasiliensis* (Pb18)] increased the IL-17A production *in vitro* and all the evaluated Th17-associated cytokines in the lung tissue from C57BL/6 wild-type mice. In addition, the deficiency of IL-6, IL-23, or IL-17 receptor A (IL-17RA) impaired the compact granuloma formation and conferred susceptibility during infection, associated with reduced tumor necrosis factor-α, IFN-γ, and inducible nitric oxide synthase enzyme expression. Our data suggest that IL-6 production by bone marrow-derived macrophages (BMDMs) is important to promote the Th17 differentiation during Pb18 infection. In accordance, the adoptive transfer of BMDMs from C57BL/6 to infected IL-6$^{-/-}$ or IL-17RA$^{-/-}$ mice reduced the fungal burden in the lungs compared to nontransferred mice and reestablished the pulmonary granuloma formation. Taken together, these results suggest that Th17-associated cytokines are involved in the modulation of immune response and granuloma formation during experimental PCM.

Keywords: paracoccidioidomycosis, Th17, IL-17A, IL-6, IL-23

OPEN ACCESS

Edited by:
Bernhard Hube, Leibniz-Institut für Naturstoff-Forschung und Infektionsbiologie—Hans Knöll Institut, Germany

Reviewed by:
Rebecca Drummond, National Institutes of Health, United States
Mark S. Gresnigt, Radboud University Nijmegen, Netherlands

****Correspondence:***
João Santana Silva
jsdsilva@fmrp.usp.br

†These authors have contributed equally to this work.

Specialty section:
This article was submitted to Microbial Immunology, a section of the journal Frontiers in Immunology

Received: *22 May 2017*
Accepted: *25 July 2017*
Published: *21 August 2017*

Citation:
Tristão FSM, Rocha FA, Carlos D, Ketelut-Carneiro N, Souza COS, Milanezi CM and Silva JS (2017) Th17-Inducing Cytokines IL-6 and IL-23 Are Crucial for Granuloma Formation during Experimental Paracoccidioidomycosis. Front. Immunol. 8:949. doi: 10.3389/fimmu.2017.00949

INTRODUCTION

Paracoccidioidomycosis (PCM), a systemic mycosis characterized by chronic and granulomatous inflammation, is caused by the thermally dimorphic fungus *Paracoccidioides brasiliensis* and *Paracoccidioides lutzii* (1). PCM has high incidence in several countries of Latin America and represents the eighth cause of death among infectious and parasitic diseases. Moreover, it induces

the highest mortality rate (1.45 per million inhabitants) among systemic mycosis, being considered an occupational disease and a serious social problem (2). It affects mainly farm workers and usually leads to the formation of pulmonary dysfunction as a consequence of primary infection progression or reactivation of a latent focus (3).

The infection is acquired after inhalation of fungal propagules that convert into the invasive yeast form once in the lungs (4). The resistance to infection is associated with a potent T helper 1 (Th1) response, which induces activation of macrophages that actively control the fungal growth (5, 6). Otherwise, resistance is associated with a predominantly Th2 and Th9 response, inducing eosinophilia and humoral immune responses (7).

Besides the mentioned Th subtypes, classified by defined phenotypic characteristics and specialized functions in immunity, T cells can also differentiate into Th17, a distinct cell lineage that produces various chemokines and cytokines, such as tumor necrosis factor (TNF)-α, IL-6, IL-21, IL-22, IL-17F, and IL-17A (8, 9). IL-1 signaling in T cells is required for the early Th17 differentiation *in vitro* and *in vivo*, and after polarization, IL-1 also allowed Th17 cells to maintain their cytokine secretion profile (10–12). The murine differentiation of Th17 requires the presence of IL-6, IL-21, and TGF-β, which activate Stat3 and induce the expression of the transcription factor retinoic acid-related orphan receptor (RORγt) (10, 13–15). Although IL-23 is not necessary for Th17 differentiation, it is essential for the maintenance of the differentiated Th17 cells (16).

Notably, Th17 cells are described as an arm of the immune system that enhances host protection against several intracellular and extracellular bacterial infections (17). In addition, fungal infections also have been associated with induction of Th17 immune response, triggering effector mechanisms, as production of antimicrobial peptides (8, 18, 19) and factors important for neutrophil function and recruitment (20–22), promoting the resistance to infection (23–25). In fact, the IL-17A and IL-23 production was important in the protective response during experimental *Pneumocystis carinii* infection (26). In addition, *Candida albicans* recognition by antigen-presenting cells promoted the IL-6 and IL-23 secretion, leading to Th17 differentiation and enhancement of host resistance (27–29). Similarly, *P. brasiliensis* was able to induce Th17 and IL-17-producing $CD8^+$ T cell (Tc17) differentiation (30, 31).

The cytokine IL-17A coordinates tissue inflammation through higher expression of pro-inflammatory cytokines and chemokines, which collectively determine the magnitude of the inflammatory response. The IL-17A receptors (IL-17RAs) are found in the surface of leukocytes, keratinocytes, fibroblasts, epithelial, mesothelial, and vascular endothelial cells, and its action includes granulopoiesis, neutrophil recruitment, and inflammatory responses (21, 22, 32–34). Moreover, IL-17A plays a critical role in the induction of mature granuloma formation during mycobacterial infection (35). Granulomas are immunological structures important in the host defense against fungi. In the course of granuloma maturation, the recruitment of phagocytes and lymphocytes is triggered by various cytokines and chemokines that are initially produced by infected macrophages, as TNF-α (36). In corroboration, our group showed that TNF-α-deficient mice are highly susceptible to *P. brasiliensis* infection, are not able to mount organized granulomas, and have a great amount of fungus in the lesions and high mortality rates (37). Moreover, IL-17-expressing cells have been detected within and around the granulomas in the skin and oral mucosal lesions from PCM patients (38).

Because little is known about the mechanisms involved in the immune response during PCM, we sought here to investigate the role of IL-6, IL-23, and IL-17A during the experimental *P. brasiliensis* infection. Our data suggest that IL-6-production by bone marrow-derived macrophages (BMDMs) is important to promote the IL-17A production and consequent induction of a protective immune response and granuloma formation during *P. brasiliensis* experimental infection.

MATERIALS AND METHODS

Mice

Male 6- to 7-week-old C57BL/6 mice, and genetically deficient ($^{-/-}$) for IL-6, IL-23p19, and IL-17RA, were obtained from our Isogenic Breeding Unit and maintained under specific pathogen-free conditions in microisolator cages in the animal housing facility of the Department of Biochemistry and Immunology, School of Medicine of Ribeirão Preto, São Paulo University, Ribeirão Preto, Brazil. Mice were supplied with sterilized food and water *ad libitum*. Experiments were conducted according to the ethical principles of animal research adopted by the Brazilian College of Animal Experimentation and approved by the Ethical Commission in Animal Research (protocol 095/2010).

Fungus, *In Vitro* and *In Vivo* Infections

The virulent yeast strain 18 of *P. brasiliensis* (Pb18) was cultured (7 days at ~36°C) in Brain Heart Infusion (BHI) agar medium (Oxoid Basingstoke, Hampshire, England) supplemented with gentamicin (100 μg/mL) and 5% fetal bovine serum (FBS; Gibco BRL, Life Technologies, Inc.). After, Pb18 colonies were grown for 24 h (37°C, 150 rpm) in F12 Coon's modified medium (Sigma-Aldrich, St. Louis, MO, USA) containing gentamicin (100 μg/mL). The Pb18 yeast cells were then harvested and washed in sterile phosphate-buffered saline (PBS; pH 7.2), and the fungal viability was determined by fluorescein diacetate-ethidium bromide staining (39). Only high viability suspensions (≥90%) were used in this study. For *in vivo* infection, the concentration of fungal cells was adjusted to 1×10^7 yeasts/mL in PBS and 100 μL of this solution (1×10^6 cells) was intravenously (i.v.) inoculated in each mice. *In vitro* fungal stimulation was performed with a multiplicity of infection (MOI) of 1.

Splenocyte and Pulmonary Cells Isolation and Activation

The spleen from uninfected male C57BL/6 mice were removed, and single-cell suspensions were obtained after red blood cells lysis (1 min) with buffer containing NH_4Cl (0.16 M, 9 parts) and Tris-HCl (0.17 M, 1 part). Splenocytes (1×10^6 cells/well) were cultured for 5 days with 1×10^6 Pb18 yeasts cells in RPMI 1640 supplemented with 5% FBS (Gibco), 0.1 mM non-essential

amino acids, 1 mM sodium pyruvate, L-glutamine (2 mM), 100 U of penicillin/mL, and 100 μg of streptomycin/mL (all from Sigma-Aldrich). Lung lobules were excised from uninfected and Pb18-infected mice, washed in PBS, minced with scissors, and enzyme digested at 37°C for 30–35 min in 1 mL of digestion buffer [RPMI 1640, 2 mg/mL collagenase IV (Sigma) and 1 mg/mL DNase (Sigma)]. Tissue fragments were further homogenized using a 1-mL pipette, crushed through a 50-μm pore size nylon filter (BD Biosciences, San Jose, CA, USA) and then centrifuged (1,300 rpm, 10 min, 4°C). Next, red blood cells were eliminated using lysis buffer, and remaining cells were washed in PBS, centrifuged, and resuspended in RPMI 1640 containing 5% FBS. For splenocytes and pulmonary cells activation, 1×10^6 cells/well were cultured for 4 h with PMA (50 ng/mL), ionomycin (500 ng/mL), and brefeldin A (5 mg/mL), followed by staining for extracellular and intracellular markers and analysis by flow cytometry.

Flow Cytometry

The expression of CD4, CD8, CD19, CD49b, γδ, F4/80, IL-6, and IL-17A was assessed in splenocytes or pulmonary cells by flow cytometry as previously reported (40, 41). The antibodies were conjugated to different fluorochromes (BD Biosciences, eBiosciences, San Diego, CA, USA, and Santa Cruz Biotechnologies, Santa Cruz, CA, USA). For intracellular cytokine staining, cells were previously permeabilized using PBS containing 1% FBS, 0.1% sodium azide, and 0.2% saponin. Data acquisition was performed using a FACSCanto II flow cytometer and FACSDiva software (BD Biosciences). Data were plotted and analyzed using FlowJo software (Tree Star, Ashland, OR, USA).

Measurement of Cytokines in Lung Supernatant

The left lung (42) from uninfected and Pb18-infected mice were removed, weighed, homogenized in sterile PBS-containing protease inhibitor (Complete, Roche), and centrifuged (1,300 rpm, 10 min, 4°C). Supernatants were collected and stored at −20°C. The levels of IL-17A, IL-6, IL-23, TNF-α, and IFN-γ were measured by enzyme-linked immunosorbent assay (ELISA) according to manufacturers' recommendations (BD Pharmingen, San Jose, CA, USA). The reading was held in eMax ELISA reader (Molecular Devices, Sunnyvale, CA, USA) at 450 nm.

Recovery of Colony-Forming Units (CFUs)

The amount of viable yeast cells in the lungs from Pb18-infected mice (3–7 animals per group) was determined after 15 and 30 days postinfection (dpi). Briefly, lung lobules were aseptically collected, weighed, and homogenized using a sterile tissue grinder (IKA®-Werke, Deutschland, Germany). Each homogenate was diluted 1:10 in sterile PBS and plated (100 μL) on BHI agar supplemented with 5% FBS and gentamicin (100 μg/mL). Plates were incubated at 35–37°C for 7 days, and the amount of CFU per gram of tissue was calculated.

Histopathology

Comparative histopathology was conducted with excised lung lobules from C57BL/6, IL-$6^{-/-}$, IL-$23^{-/-}$, and IL-$17RA^{-/-}$ mice at 30 dpi. Tissue was fixed with 10% formalin for 24 h and embedded in paraffin. Next, lung sections (5 μm) were stained by standard procedures with hematoxylin and eosin for lesion analysis, Grocott methenamine silver stain for fungal cell labeling, or silver impregnation (Gomori method) to demonstrate reticulum fibers. Sections were examined with HLIMAGE++ 97 Application Western Vision Software using an optical microscope coupled to a digital camera. Granulomas were visually scored in mature or immature structures according to cellular and reticulin organization and distribution, as described before (43, 44). The percentage of mature granulomas and the granulomatous diameter were calculated. Reticulin measurement was performed in the halo surrounding the granulomas as previously described (45).

Immunohistochemistry

Lungs from C57BL/6, IL-$6^{-/-}$, IL-$23^{-/-}$, and IL-$17RA^{-/-}$ mice were immersed in OCT medium (Sakura Finetek), snap-frozen in liquid nitrogen, and stored at −80°C until analysis. Tissue sections (5 μm) were submitted to an immunohistochemical reaction. Briefly, slides were incubated with anti-mouse IgG as control or rabbit IgG anti-mouse inducible nitric oxide synthase (iNOS) enzyme (Santa Cruz Biotechnology, Santa Cruz, CA, USA) diluted 100 times in PBS 0.01% saponin. At the end, the reaction was followed by Mayer's hematoxylin counterstaining. We measured immunostained areas using Image J software as previously described (41). Briefly, the range of positivity was defined using the IHC Tool box. Next, the images were converted to 8-bit, and the grayscale was converted to binary (black and white). The threshold was adjusted, and the labeled areas became the black portions. Finally, the percentage of stained area was analyzed.

BMDMs Differentiation

Bone marrow cells isolated from femurs and tibias from 7-week-old C57BL/6, IL-$6^{-/-}$, IL-$23^{-/-}$, and IL-$17RA^{-/-}$ naive mice were cultured (7 days, 37°C, 5% CO_2) in RPMI 1640 medium supplemented with 20% FBS and 30% L-929 cell conditioned media, as previously described (46). After differentiation, cells were harvested and infected with *P. brasiliensis* (MOI of 0.04).

Isolation of Naive T $CD4^+$ Cells and Co-Culture with BMDMs

Naive T $CD4^+$ cells were purified from C57BL/6 lymph nodes by using the $CD4^+$ MicroBeads Isolation Kit (Miltenyi Biotec) in conjunction with an AutoMacs separator. Purified naive T cells were cultured for 5 days with *P. brasiliensis*-infected BMDMs from C57BL/6 or IL-$6^{-/-}$ mice (MOI of 0.04). Next, the amount of T $CD4^+$IL-$17A^+$ was analyzed by flow cytometry.

Adoptive Transfer

After adoptive transference of C57BL/6 BMDMs (1×10^6, i.v.) into IL-$6^{-/-}$, IL-$23^{-/-}$, and IL-$17RA^{-/-}$ animals, mice were infected with 1×10^6 *P. brasiliensis* yeast cells, and the CFU was determined at day 30 as described above.

Statistical Analysis

The differences observed between uninfected or Pb18-infected wild-type (WT) group (C57BL/6) and IL-6-, IL-17RA-, or

IL-23-deficient mice were analyzed by applying the ANOVA test followed by multiple comparison using the Bonferroni method (GraphPad Prism, GraphPad Software version 5.0, San Diego, CA, USA). Values are expressed as mean ± SEM. All values were considered significant when $p < 0.05$.

RESULTS

P. brasiliensis Infection Increases IL-17A Production

To evaluate whether fungal cells modulate the IL-17A production, splenocytes from C57BL/6 mice were isolated, cultivated in the presence of or not of *P. brasiliensis*, and the frequency of IL-17A-producing cells was determined 5 days later. Our results showed that the stimulation of spleen cells with viable Pb18 increased the IL-17A expression (**Figure 1A**), and the frequency of IL-17A-producing CD4 T cells (5.5-fold, $p < 0.05$; **Figure 1B**) compared to medium alone. Next, to evaluate whether *P. brasiliensis* modulates the Th17 profile *in vivo*, C57BL/6 mice were infected with Pb18 yeast cells, and the IL-17A production was determined in the lungs at day 30 postinfection. As expected, we observed that Pb18-infected mice exhibited a significant increase (~9.5-fold) in IL-17A production compared to uninfected mice (**Figure 1C**). In addition, at 30 dpi, there was an increase in the number of IL-17A-producing cells (~4.5-fold; **Figure 1D**).

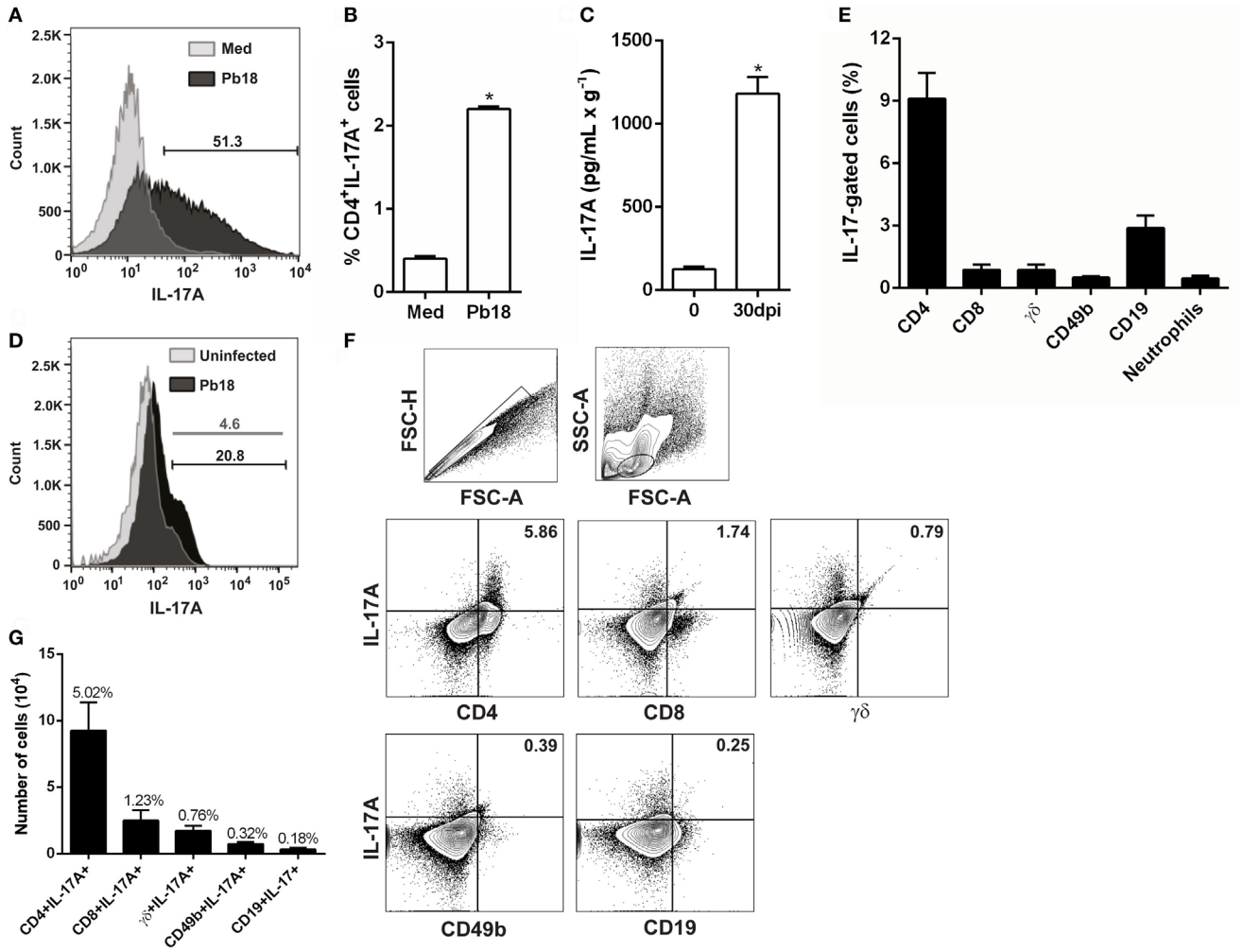

FIGURE 1 | *Paracoccidioides brasiliensis* infection increases the *in vitro* and *in vivo* IL-17A production. **(A,B)** Splenocytes from C57BL/6 mice were isolated and cultivated (1×10^6) in the presence of or not of viable virulent yeast strain 18 of *P. brasiliensis* (Pb18) during 5 days (multiplicity of infection of 1). **(A)** The frequency of IL-17A$^+$-producing cells and **(B)** Th17 (CD4$^+$IL-17A$^+$) cells was determined by flow cytometry. **(C–E)** C57BL/6 mice were infected with 1×10^6 Pb18 yeast cells (intravenously). **(C)** The level of IL-17A was measured by enzyme-linked immunosorbent assay in the whole lung homogenate after 30 days postinfection (dpi). **(D)** The frequency of IL-17A-producing cells was evaluated in the lungs from uninfected and infected (30 dpi) mice. **(E–G)** The frequency of natural killer (CD49b$^+$IL-17A$^+$), Tγδ (γδ$^+$IL-17A$^+$), B (CD19$^+$IL-17A$^+$), IL-17-producing CD8$^+$ T (CD8$^+$IL-17A$^+$), and Th17 cells was assessed in the lungs after 30 dpi. **(E)** Cells were analyzed inside the IL-17-positive gate. **(F)** Lymphocytes were gated inside the singlet population. One representative mice is shown. **(G)** Absolute number (bars) and mean percentage (above bars) of each IL-17-producing cell population gated inside lymphocytes. Bars represent the mean ± SEM of 5 mice. *$p < 0.05$ compared to non-infected control. Similar results were obtained in three independent experiments.

Despite the fact that most of the evidence describes IL-17A as a cytokine secreted by T cells, part of the IL-17A is produced by different cell populations, including innate immune cells (47). To determine the major source of IL-17A in the lungs during the experimental PCM, we evaluated the frequency and absolute number of Th17, Tc17, $\gamma\delta^+$IL-17A$^+$, CD49b$^+$IL-17A$^+$ [natural killer (NK)], and CD19$^+$IL-17A$^+$ (B cells). Initially, we excluded the doublets; delineated a gate comprising lymphocytes, monocytes, and neutrophils; and then a subgate in IL-17-positive cells, which allowed us to evaluate the percentage of each cell subtype (**Figure 1E**). The Th17 population was significantly increased in comparison with other IL-17-producing cells ($p < 0.05$; **Figure 1E**). For better and clear results, we next used a second gate strategy, which consisted of singlets selection in forward scatter height (FSC-H) against forward scatter area (FSC-A) (**Figure 1F**, upper left panel). Next, lymphocytes were gated inside the previous population in side scatter area (SSC-A) against FSC-A (**Figure 1F**, upper right panel), and all analyzed cell populations were gated inside the lymphocyte population. Our data clearly showed the predominance of IL-17A-producing CD4$^+$ cells, both in percentage (~5%, **Figures 1F,G**) or absolute number (~9.2 × 10^4 cells; **Figure 1G**), compared with other IL-17A$^+$ cells subtypes: CD8 (~1.2%, ~2.5 × 10^4 cells), γδ (~0.7%, ~1.7 × 10^4 cells), NK (~0.3%, ~0.7 × 10^4 cells), and B lymphocytes (~0.1%, ~0.3 × 10^4 cells) (**Figures 1F,G**). After evaluating the number and frequency of IL-17-producing neutrophils, we could not see an increase of this cell subtype in the lungs from Pb18-infected mice (data not shown). These findings suggest that Th17 cells are the main source of IL-17A during *P. brasiliensis* infection.

The Absence of IL-6 and IL-23 Impairs the Th17 Immune Response during Experimental *P. brasiliensis* Infection

The Th17 subset differentiation requires the presence of IL-6, and its maintenance is sustained by IL-23 (13, 14, 16). Thus, we evaluated the production of these cytokines in the lungs from naive and Pb18-infected mice at 15 and 30 dpi. Our data showed that at both time points, the IL-6 and IL-23 levels were significantly increased when compared to uninfected mice (**Figure 2A**). To confirm these findings, IL-6$^{-/-}$ and IL-23$^{-/-}$ mice were infected with *P. brasiliensis* yeast cells, and the IL-17A levels were evaluated in the pulmonary tissue after 15 and 30 days. We found that the deficiency of IL-6 or IL-23 impaired the IL-17A-production, which was ~2.5 times smaller than C57BL/6 mice at the same period of infection ($p < 0.05$; **Figure 2B**). Moreover, when compared to WT mice, we found that the frequency and absolute number of IL-17A-producing CD4$^+$ T cells were decreased ($p < 0.05$) in the lung tissue from IL-6$^{-/-}$ and IL-23$^{-/-}$ mice at 30 dpi (**Figure 2C**). These data establish the importance of IL-6 and IL-23 in promoting the late Th17-immune response during the *P. brasiliensis* experimental infection.

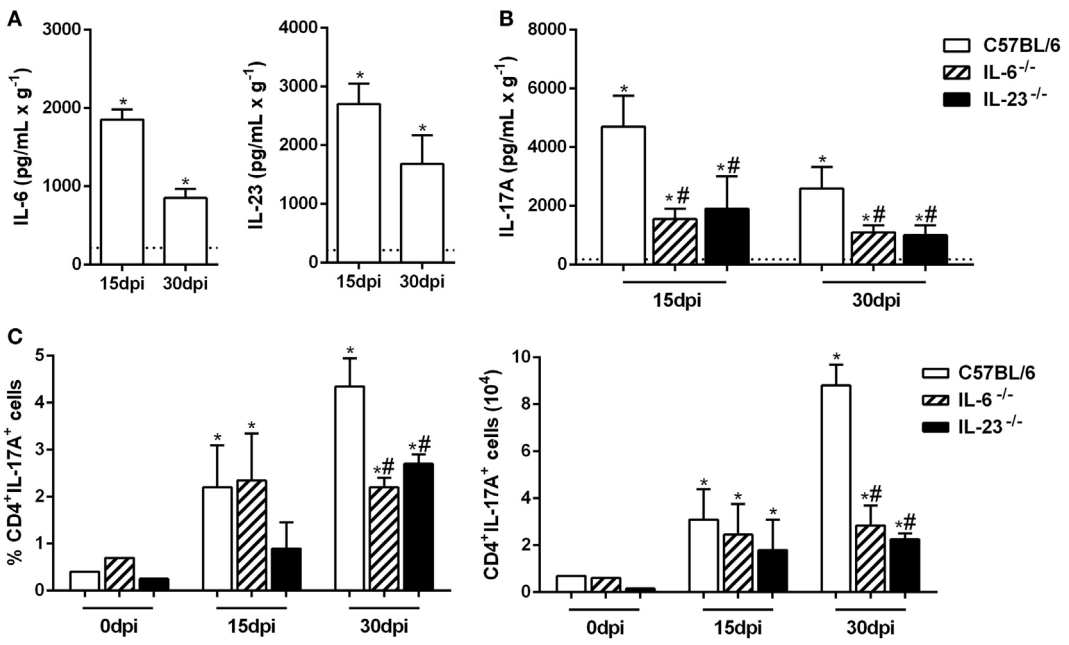

FIGURE 2 | Virulent yeast strain 18 of *Paracoccidioides brasiliensis* (Pb18)-induced IL-6 and IL-23 production improves the establishment of the Th17 profile. **(A–C)** Male C57BL/6, IL-6$^{-/-}$ and IL-23$^{-/-}$ mice were infected with 1 × 10^6 Pb18 yeast cells (intravenously). **(A)** IL-6 and IL-23 productions were quantified in the lung homogenate from uninfected and Pb18-infected C57BL/6 mice, at 15 and 30 days postinfection (dpi). **(B)** The IL-17A production was measured in the lung tissue from C57BL/6-, IL-6-, and IL-23-deficient mice. **(C)** The frequency and absolute number of Th17 (CD4$^+$IL-17A$^+$) cells were evaluated in the pulmonary tissue at 0, 15, and 30 dpi. The data represent the mean ± SEM of five mice and are representative of three independent experiments. Uninfected mice are represented by the dashed line. *$p < 0.05$ compared to uninfected mice. #$p < 0.05$ compared to Pb18-infected C57BL/6 mice at the same time point.

Th17-Associated Cytokines Contribute to Compact Granuloma Formation during the Experimental *P. brasiliensis* Infection

To verify whether *P. brasiliensis*-induced Th17-associated cytokines are important to control the fungal growth and pulmonary infection, we analyzed the amount of CFU and the histopathology of lung tissue from Pb18-infected IL-6-, IL-23-, and IL-17RA-deficient mice. Our data revealed that all deficient mice showed impaired fungal control at both 15 and 30 days after *P. brasiliensis* inoculation when compared to C57BL/6 mice ($p < 0.05$; **Figure 3A**). Likewise, the Grocott stain at 30 dpi corroborated a higher fungal load in the lungs of all deficient mice when compared to infected C57BL/6 mice (**Figure 3B**), suggesting that Th17-associated cytokines, as IL-6 and IL-23, are important to control the fungal growth during the experimental PCM in mice. To better assess the inflammatory process developed during *P. brasiliensis* infection, we analyzed

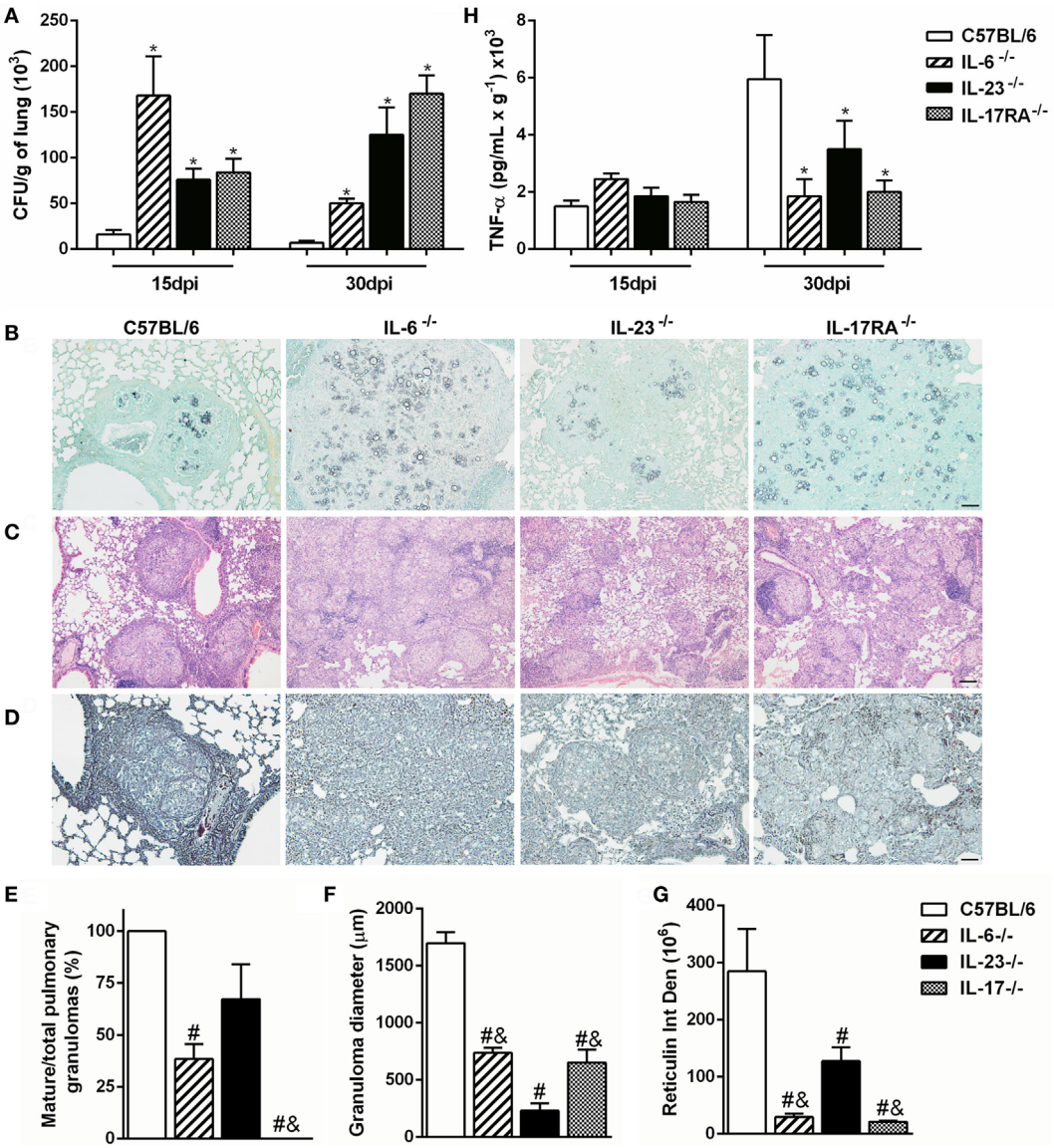

FIGURE 3 | The Th17-associated cytokines contribute to development and organization of granuloma during experimental *Paracoccidioides brasiliensis* infection. **(A–E)** C57BL/6, IL-6$^{-/-}$, IL-23$^{-/-}$, and IL-17 receptor A (IL-17RA)$^{-/-}$ mice were infected with virulent yeast strain 18 of *P. brasiliensis* (Pb18) (1 × 10^6 cells, intravenously). **(A)** The number of colony-forming units (CFUs) was determined in the pulmonary tissue after 15 and 30 days postinfection (dpi). **(B–D)** Lung sections of infected mice were stained with **(B)** Grocott methenamine silver, **(C)** hematoxylin and eosin, or **(D)** silver impregnation (Gomori method) at 30 dpi and analyzed by light microscopy. Scale bar: 50 μm **(B,D)** and 100 μm **(C)**. **(E)** The percentage of mature granulomas and **(F)** diameter of mature and immature granulomas were calculated. **(G)** Integrated density of reticulin present in the halo surrounding the mature granulomas. **(H)** The tumor necrosis factor (TNF)-α production was measured in the lung homogenate from Pb18-infected mice at 15 and 30 dpi. Similar results were obtained in three independent experiments. Data represent the mean ± SEM of five mice. Uninfected mice are represented by the dashed line. $^*p < 0.05$ compared to uninfected mice. $^\#p < 0.05$ compared to Pb18-infected C57BL/6 mice at the same time point. $^\&p < 0.05$ compared to Pb18-infected IL-23$^{-/-}$ mice at the same time point.

the histology of pulmonary tissue at 30 dpi. The C57BL/6 mice showed bigger and mature granulomas characterized by epithelioid and giant cells surrounded by a peripheral mononuclear layer (**Figures 3C,E,F**). In contrast, most of the granulomas from IL-6$^{-/-}$ and IL-17RA$^{-/-}$ mice exhibited an intermediate size and immature profile with few lymphocytes forming the peripheral ring, associated with a diffuse inflammatory process (**Figures 3C,E,F**). Specifically, the IL-23 deficiency induced the formation of numerous well-formed granulomas, but with a smaller diameter compared to all Pb18-infected groups (**Figures 3C,E,F**).

Reticulin fibers are composed of type III collagen; besides very delicate and fine, they form a firm layer linking the connective to the surrounding tissue, being considered a main element of alveolar organization (48). We observed a well-organized and dense reticulin ring contouring the granulomas in the lungs from Pb18-infected C57BL/6 mice (**Figures 3D,G**). In addition, the diminished number of compact granulomas in IL-6$^{-/-}$ and IL-17RA$^{-/-}$ pulmonary tissue was associated with a defective reticulin halo accumulation and formation (**Figures 3D,G**). Moreover, a tiny reticulin layer surrounded the small mature and immature granulomas in the lungs from IL-23-deficient mice at 30 days post-Pb18 infection (**Figures 3D,G**).

Since TNF-α is important to the granuloma formation (36, 37), we also evaluated the expression of this cytokine in the lung tissue from Pb18-infected C57BL/6, IL-6$^{-/-}$, IL-23$^{-/-}$, and IL-17RA$^{-/-}$ mice. Our data showed that *P. brasiliensis* infection increased the TNF-α production at both evaluated time points (**Figure 3H**). There were no differences in TNF-α levels in the various non-infected knock-out mice (data not shown). At 15 dpi, all groups showed similar TNF-α production. However, when compared to C57BL/6 mice, the levels of TNF-α were reduced in all deficient mice at 30 dpi ($p < 0.05$; **Figure 3H**). These results suggest that IL-6, IL-17A, and in less extent, IL-23 modulate the formation of organized and compact granulomas during the experimental *P. brasiliensis* infection.

Th17-Associated Cytokines Promote IFN-γ Production and iNOS Expression during the Experimental *P. brasiliensis* Infection

Several studies have demonstrated that the Th1-type cytokine IFN-γ is implicated in resistance during *P. brasiliensis* infection, inducing cell migration and activation (37, 49). Then, we next evaluated the importance of IL-6, IL-17A, and IL-23 in modulating the IFN-γ-production during the experimental PCM. All naive knock-out mice showed similar IFN- γ levels (data not shown), and these levels were increased after the *P. brasiliensis* infection (**Figure 4A**). At both evaluated time points, 15 and 30 dpi, all deficient mice showed a reduction of IFN-γ levels in the pulmonary tissue in comparison to C57BL/6 group (**Figure 4A**). These findings suggest that Th17-associated cytokines are involved in the IFN-γ production during the experimental PCM in mice.

It was previously demonstrated that IFN-γ is able to induce fungicidal activity in macrophages through nitric oxide (NO) production (50, 51), which is indirectly measured by iNOS expression. At 15 dpi, there was increased iNOS expression inside the granulomatous structure from C57BL/6 mice, in comparison with all analyzed deficient mice at the same time point (**Figures 4B,C**).

Together, these results suggest that the deficiency of Th17-associated cytokines (IL-6 and IL-23) modulates the IFN-γ production and iNOS expression and dampens the fungal death during an experimental PCM model.

Adoptive Transfer of F4/80$^+$ Cells Restores Resistance to *P. brasiliensis* Infection in IL-6- and IL-17RA-Deficient Mice

We first showed that ~38% of F4/80$^+$ cells (macrophages) from splenocytes cultured with Pb18 yeast cells are able to produce IL-6 (**Figure 5A**). Gate strategy consisted of doublets exclusion in FSC-H against FSC-A (data not shown). Next, monocytes were gated in SSC-A against FSC-A (**Figure 5A**, left panel), and then the IL-6-positive cells were selected (**Figure 5A**, middle panel). Finally, the IL-6$^+$F4/80$^+$ population was delimited (**Figure 5A**, right panel). We next evaluated the role of IL-6 in Th17 differentiation during Pb18 infection. The BMDMs from C57BL/6 and IL-6$^{-/-}$ mice were co-cultured with naive CD4$^+$ lymphocytes isolated from C57BL/6 WT mice, in the presence of or not of Pb18 yeast cells. We observed that the frequency and absolute number of Th17 cells induced by WT BMDMs were significantly higher than that of IL-6$^{-/-}$ BMDMs ($p < 0.05$; **Figures 5B,C**, respectively). Overall, these data suggest that the IL-6 produced by F4/80$^+$ macrophages induces Th17 cells during the *P. brasiliensis* infection.

To verify the relevance of Th17-associated cytokines over the macrophage fungicidal activity during *P. brasiliensis* infection, BMDMs from C57BL/6 mice were transferred to IL-6-, IL-23-, and IL-17RA-deficient mice, and the fungal burden was evaluated after 30 dpi. To confirm that transferred cells arrive in the lungs, we labeled BMDMs from GFP$^+$ mice with F4/80, and at day 7 after transference, we tracked these cells. We verified a frequency of ~7.3% of F4/80$^+$GFP$^+$ cells in the pulmonary tissue (data not shown). The IL-6$^{-/-}$ and IL-17RA$^{-/-}$ transferred mice showed diminished number of Pb18 yeast cells in comparison with same genotypes without transfer ($p < 0.05$; **Figure 6A**). However, the adoptive transfer of BMDMs did not change the fungal burden in IL-23$^{-/-}$ mice (**Figure 6A**).

Since resistance to *P. brasiliensis* infection is characterized by the presence of mature granulomas, we evaluated the influence of macrophages in the granuloma formation. Corroborating our previous findings (**Figure 3C**), the Pb18-infected IL-6- and IL-17RA-deficient mice showed diminished capacity to mount organized granulomas at 30 dpi when compared to C57BL/6 group (**Figures 6B,C**). Surprisingly, the adoptive transfer of WT BMDMs restored the ability of IL-6$^{-/-}$ and IL-17RA$^{-/-}$ mice to form mature granulomas in the lung tissue (**Figures 6B,C**). We could not observe histological differences in Pb18-infected IL-23-deficient mice transferred or not with C57BL/6 BMDMs, which continued showing small well-formed granulomas in the lungs after transference (**Figures 6B,D**).

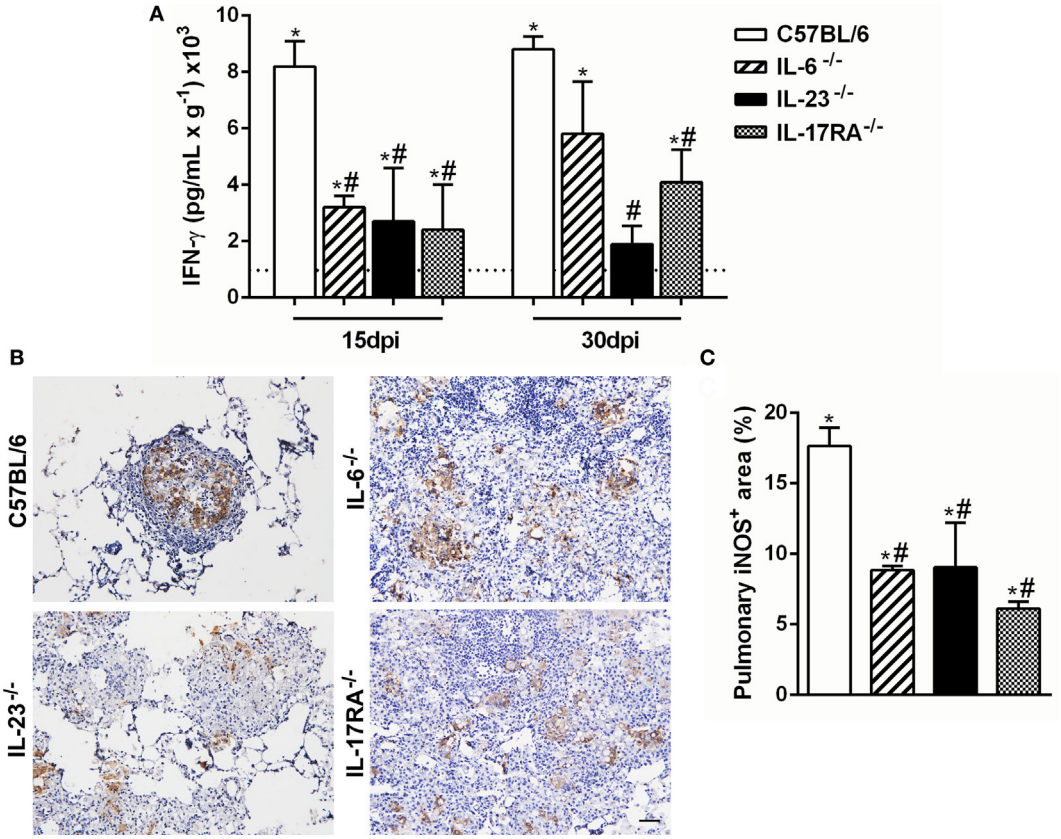

FIGURE 4 | Th17-associated cytokines regulate the IFN-γ production and inducible nitric oxide synthase enzyme (iNOS) expression during the experiment of virulent yeast strain 18 of *Paracoccidioides brasiliensis* (Pb18) infection. **(A,B)** C57BL/6, IL-6$^{-/-}$, IL-23$^{-/-}$, and IL-17 receptor A (IL-17RA)$^{-/-}$ mice were infected (intravenously) with 1 × 10^6 Pb18 yeast cells. **(A)** IFN-γ levels were measured by enzyme-linked immunosorbent assay in the lung homogenate at 15 and 30 days postinfection (dpi). **(B)** Immunohistochemistry was performed in lung tissue to analyze the iNOS expression at 30 dpi. **(C)** The percentage of the pulmonary area containing iNOS$^+$ cells is indicated. Lung sections were stained for iNOS at 30 dpi using immunohistochemistry. Scale bar: 50 μm. Similar results were obtained in three independent experiments. Data represent the mean ± SEM of five mice. Uninfected mice are represented by the dashed line. $^*p < 0.05$ compared to uninfected mice. $^\#p < 0.05$ compared to Pb18-infected C57BL/6 mice at the same time point.

Taken together, our data suggest that Th17-associated cytokines are involved in the modulation of immune response and granuloma formation during experimental PCM.

DISCUSSION

The generation of a protective immune response is essential for human resistance against infectious diseases, including the systemic mycosis caused by *P. brasiliensis*. If the host innate immune response is unable to suppress the infection foci, it is followed by cell-mediated immunity (52). Several studies have demonstrated that the severe PCM occurs due to the inability to develop an effective Th1 response and, therefore, unsuitable for the formation of dense granulomas, while Th2 response is inefficient to contain the spread of infection (53). Since Th17 discovery, these cells have been associated with immune response to fungal diseases and considered one of the main mechanisms that cause resistance to mycosis (23).

In fact, the production of IL-17A is instrumental for protective response in an experimental model of *P. carinii* infection (26). In addition, Th17-associated cytokines improve the host control against *C. albicans* and *Aspergillus fumigatus*, leading to the migration of potentially fungicide neutrophils (54). Moreover, the presence of IL-17A-producing cells in lesions of PCM patients was demonstrated, in an attempt to increase the host immune defenses against fungal cells (38, 55). In agreement, here, we demonstrated the increased expression of Th17-associated cytokines (IL-6, IL-23, and IL-17A) in the lung tissue after the *P. brasiliensis* infection in mice.

Besides Th17, IL-17A is synthesized by NK cells, γδ T cells, neutrophils, and innate lymphoid cells, in a more rapid way than T cells due to the constitutive expression of the Th17-associated transcription factor RORγt in all these cells subtypes (47). During experimental PCM, our results showed that Th17 lymphocytes are the main source of IL-17A in the lungs, followed by CD8$^+$ cells. The presence of Tc17s in the lungs from *P. brasiliensis*-infected mice or in cutaneous and mucosal lesions from PCM patients was showed before (30, 38). Moreover, Tc17 differentiation of naive T lymphocytes was demonstrated *in vitro* after Pb18 infection (31). During *A. fumigatus* infection, neutrophils were positive for

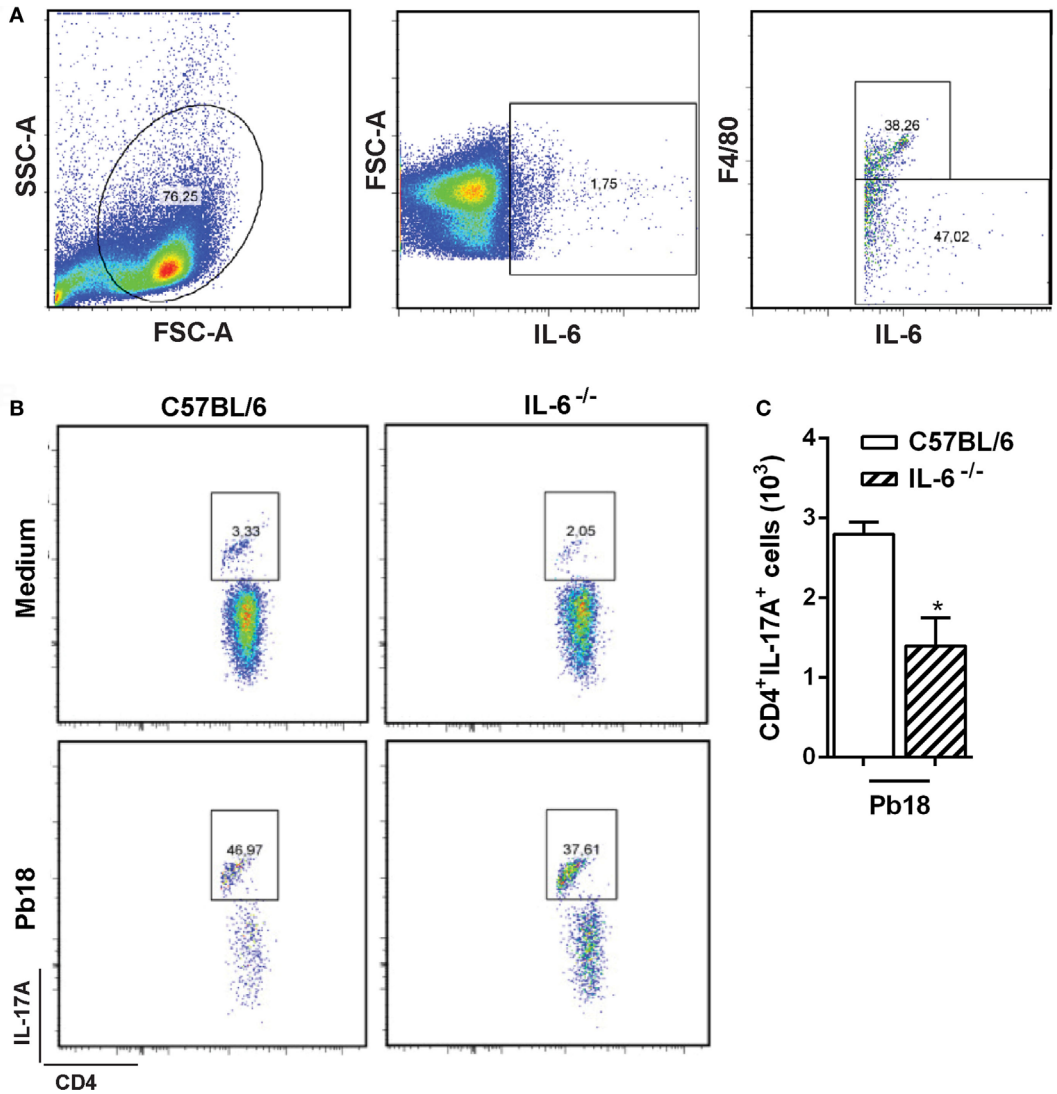

FIGURE 5 | Macrophage-derived IL-6 improves Th17 differentiation during virulent yeast strain 18 of *Paracoccidioides brasiliensis* (Pb18) experimental infection. **(A)** Splenocytes from C57BL/6 mice were isolated and cultivated in the presence of or not of viable Pb18 yeasts cells during 5 days, and the frequency of IL-6-producing F4/80$^+$ macrophages was analyzed by flow cytometry. **(B,C)** Bone marrow-derived macrophages were differentiated from C57BL/6 and IL-6$^{-/-}$ mice and co-cultured with naive T CD4$^+$ cells from C57BL/6 wild-type mice in the presence of or not of Pb18 yeast cells (multiplicity of infection of 0.04) during 5 days. Next, the frequency **(B)** and absolute number **(C)** of Th17 (CD4$^+$IL-17A$^+$) cells were analyzed by flow cytometry. Similar results were obtained in three independent experiments. Data represent the mean ± SEM of five mice. *$p < 0.05$ compared with C57BL/6 mice.

intracellular IL-17A expression and also produced this cytokine in a Dectin-1- and IL-23-dependent manner (56). However, the *P. brasiliensis* infection did not modulate the IL-17-producing neutrophils in the lungs. Moreover, we found that IL-6 is important to the protective response during the infection. Similarly, previous work demonstrated that IL-6 increases murine resistance to *P. brasiliensis* yeast cells (57). Previous work highlighted the critical roles of IL-1 during early Th17 differentiation and expansion/maintenance (11). Our group partially elucidated the mechanisms modulated by IL-1 during PCM (58). We have found that *P. brasiliensis* promoted a NLRP3 inflammasome-dependent caspase-1 activation to release the bioactive IL-1β, and IL-1R1$^{-/-}$ mice displayed a slightly increased survival rate to infection compared with the C57BL/6 mice. Moreover, significantly higher amounts of the fungus were recovered at 30 dpi in the lungs of the IL-1R1-deficient mice, which were contained in organized and compact granulomas (58). These data corroborate the idea that the absence of cytokines associated with Th17 differentiation may increase the susceptibility to experimental PCM.

Granulomas are formed as a consequence of chronic antigen persistence, and their formation involves the interaction between the antigenic organism and host immune cells (48). During primary tuberculosis, IL-17-producing cells are induced, leading to IL-17A synthesis, which is a potent inflammatory cytokine capable of increase chemokines expression that promotes cell recruitment and granuloma organization (59). Similarly, it is

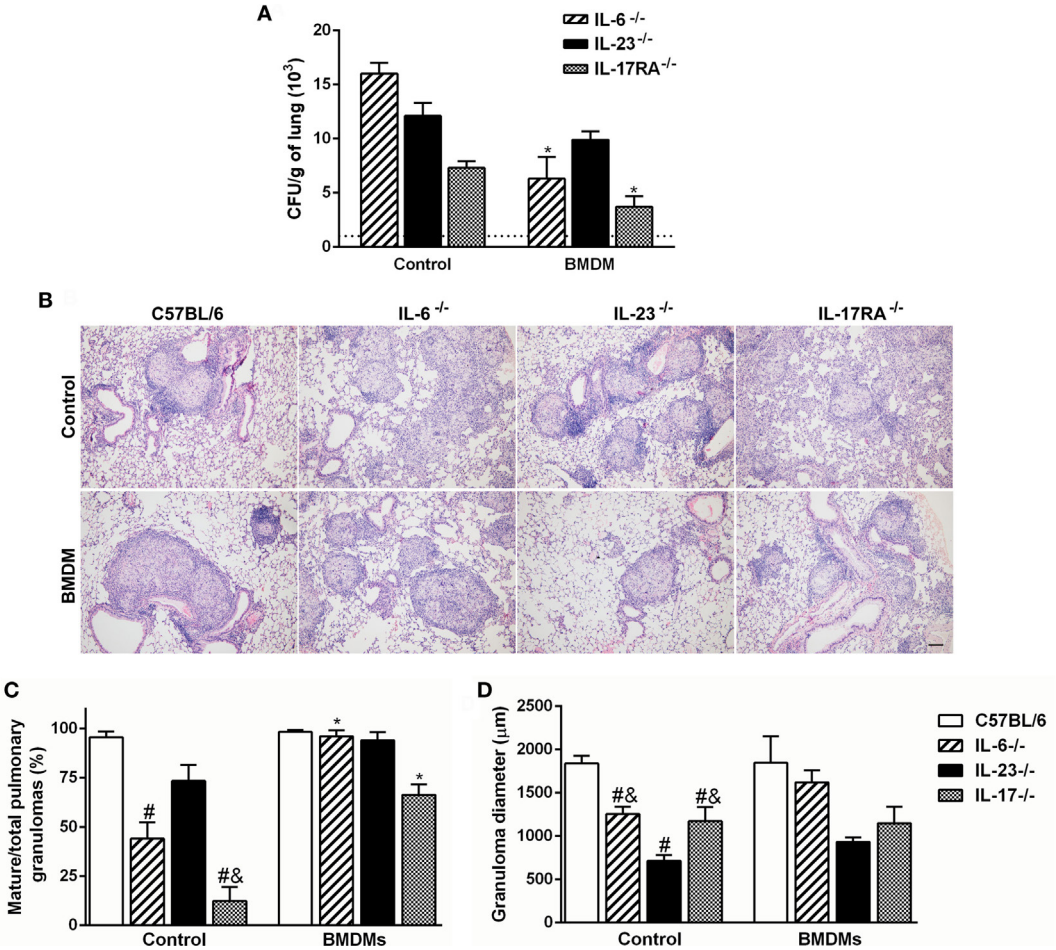

FIGURE 6 | Adoptive transfer of wild-type F4/80+ macrophages restores the granuloma formation and resistance during *Paracoccidioides brasiliensis* infection in susceptible IL-6- and IL-17 receptor A (IL-17RA)-deficient mice. **(A,B)** Macrophages (1×10^6), previously differentiated *in vitro* from C57BL/6 bone marrow-derived macrophages (BMDMs), were adoptively transferred to C57BL/6, IL-$6^{-/-}$, IL-$23^{-/-}$, and IL-$17RA^{-/-}$ mice, followed by the intravenous infection with 1×10^6 virulent yeast strain 18 of *P. brasiliensis* (Pb18). **(A)** The number of colony-forming unit (CFU) was determined in the pulmonary tissue at day 30 postinfection. Dashed line represents the amount of CFU in C57BL/6 mice. **(B)** Lung sections of Pb18-infected mice, transferred or not with wild-type BMDMs, were stained with hematoxylin and eosin. **(C)** The percentage of mature granulomas and **(D)** diameter of mature and immature granulomas was calculated. Scale bar: 100 μm. Similar results were obtained in three independent experiments. Data represent the mean ± SEM of five mice. $^{\#}p < 0.05$ compared to Pb18-infected C57BL/6 mice without BMDMs transfer (control). $^{\&}p < 0.05$ compared to control IL-$23^{-/-}$. $^{*}p < 0.05$ compared with same genotypes without transfer.

possible that IL-17A is leading to cell migration during experimental PCM, contributing to granuloma formation. Moreover, we showed that the Th17-associated cytokine IL-6 constitutes an essential molecule involved in granuloma development during the *P. brasiliensis* infection. Here, we established for the first time the importance of IL-6 and IL-23 for the Th17 induction/expansion during experimental PCM. According to our results, these cytokines play a critical role in the protection against *P. brasiliensis* yeast cells through the induction of mature granuloma formation and control of fungal growth.

The resistance observed in some PCM patients is dependent on cellular activities mediated by IFN-γ and TNF-α. An efficient host immune response and a potent fungicidal activity against *P. brasiliensis* are determined by the synergistic effect between these two cytokines (37, 49). Several studies have demonstrated that Th17 cells can turn into IFN-γ-expressing T cells (60–62). IFN-γ stimulates *P. brasiliensis*-infected macrophages to secrete TNF-α, required for the development and persistence of well-formed granulomas (36) and is important for host resistance against fungal cells (63). Our data showed a diminished IFN-γ and TNF-α production in the pulmonary tissue from IL-$6^{-/-}$, IL-$23^{-/-}$, and IL-$17RA^{-/-}$ mice when compared to C57BL/6 group. The lower production of IFN-γ and TNF-α correlated with impaired granuloma formation in the lung tissue after *P. brasiliensis* infection. In addition, IFN-γ induces inflammatory cells to produce NO, which plays a well-documented role in fungal clearance (64). Besides IFN-γ, the NO production in chronic inflammation is supported by IL-17A (65, 66). This statement justify the decreased iNOS expression inside the granulomatous structures in the lung tissue from *P. brasiliensis*-infected IL-6-, IL-23-, and IL-17RA-deficient mice, associated with increased fungal load.

It is known that IL-17A increases the macrophage activity and survival (67). However, the importance of macrophages in Th17 cell responses is still poorly understood. An inflammatory stimulus is able to increase the expression of IL-17A receptors in macrophages both *in vitro* and *in vivo* (68). Interestingly, mycobacterial infection induces a new type of macrophage population, different from M1/M2 macrophages, that downregulates T cell production of both Th1- and Th2-type cytokines but markedly increases the production of IL-17A and IL-22 through upregulation of Th17 cell expansion, *via* IL-6 and TGF-β, but not IL-21 and IL-23 (69). Similarly, we found that *P. brasiliensis* experimental infection induced IL-6 synthesis even in the early infection, and this cytokine is essential to induce a Th17 immune profile. In corroboration, we showed that IL-6 deficiency in macrophages is associated with abrogated Th17 cell generation, diminished fungal load in the lungs, and absence of organized granulomas. The adoptive transfer of IL-6-competent macrophages restored the resistance in *P. brasiliensis*-infected IL-6- and IL-17RA-deficient mice, but did not change the granuloma formation and fungal clearance in IL-23$^{-/-}$ group.

Taken together, our data suggest that macrophage-produced IL-6 and IL-23 are essential to induce a Th17 immune profile, which positively regulates the TNF-α, IFN-γ, and iNOS expression, contributing to mature granuloma formation and consequent better control of *P. brasiliensis* experimental infection.

ETHICS STATEMENT

Experiments were conducted according to the ethical principles of animal research adopted by the Brazilian College of Animal Experimentation (COBEA) and approved by the Ethical Commission in Animal Research (protocol 095/2010).

AUTHOR CONTRIBUTIONS

FT, FR, DC, NK-C, CS, and CM performed the *in vitro* and *in vivo* experiments. FT, FR, DC, NK-C, and JS designed protocols. FT, FR, and DC conducted data analysis. FT, FR, DC, NK-C, CS, CM, and JS provided scientific input. JS supervised the project. FT reviewed the literature and wrote the manuscript. DC, NK-C, and JS provided comments and corrections of the manuscript.

ACKNOWLEDGMENTS

We are grateful to doctor Marcos Antônio Rossi (*in memoriam*) for precious contribution and to Wander C. R. da Silva and Maria Elena Riul for invaluable technical assistance.

FUNDING

The research leading to these results received funding from Conselho Nacional de Desenvolvimento Científico e Tecnológico (CNPq), Coordenação de Aperfeiçoamento Pessoal de Nível Superior (CAPES), São Paulo Research Foundation (FAPESP) under grant agreement no. 2013/08216-2 (Center for Research in Inflammatory Disease), and from the University of São Paulo NAP-DIN under grant agreement no. 11.1.21625.01.0. The funders had no role in the study design, data collection and analysis, decision to publish, or preparation of this manuscript.

REFERENCES

1. de Oliveira HC, Michaloski JS, da Silva JF, Scorzoni L, de Paula ESAC, Marcos CM, et al. Peptides derived from a phage display library inhibit adhesion and protect the host against infection by *Paracoccidioides brasiliensis* and *Paracoccidioides lutzii*. *Front Pharmacol* (2016) 7:509. doi:10.3389/fphar.2016.00509
2. Coutinho ZF, Silva D, Lazera M, Petri V, Oliveira RM, Sabroza PC, et al. Paracoccidioidomycosis mortality in Brazil (1980–1995). *Cad Saude Publica* (2002) 18(5):1441–54. doi:10.1590/S0102-311X2002000500037
3. Marques SA. Paracoccidioidomycosis. *Clin Dermatol* (2012) 30(6):610–5. doi:10.1016/j.clindermatol.2012.01.006
4. McEwen JG, Bedoya V, Patino MM, Salazar ME, Restrepo A. Experimental murine paracoccidiodomycosis induced by the inhalation of conidia. *J Med Vet Mycol* (1987) 25(3):165–75. doi:10.1080/02681218780000231
5. Calich VL, Vaz CA, Burger E. Immunity to *Paracoccidioides brasiliensis* infection. *Res Immunol* (1998) 149(4–5):407–417; discussion 499–500. doi:10.1016/S0923-2494(98)80764-5
6. Calich VL, da Costa TA, Felonato M, Arruda C, Bernardino S, Loures FV, et al. Innate immunity to *Paracoccidioides brasiliensis* infection. *Mycopathologia* (2008) 165(4–5):223–36. doi:10.1007/s11046-007-9048-1
7. Mamoni RL, Nouer SA, Oliveira SJ, Musatti CC, Rossi CL, Camargo ZP, et al. Enhanced production of specific IgG4, IgE, IgA and TGF-beta in sera from patients with the juvenile form of paracoccidioidomycosis. *Med Mycol* (2002) 40(2):153–9. doi:10.1080/mmy.40.2.153.159
8. Liang SC, Tan XY, Luxenberg DP, Karim R, Dunussi-Joannopoulos K, Collins M, et al. Interleukin (IL)-22 and IL-17 are coexpressed by Th17 cells and cooperatively enhance expression of antimicrobial peptides. *J Exp Med* (2006) 203(10):2271–9. doi:10.1084/jem.20061308
9. Zambrano-Zaragoza JF, Romo-Martinez EJ, Duran-Avelar Mde J, Garcia-Magallanes N, Vibanco-Perez N. Th17 cells in autoimmune and infectious diseases. *Int J Inflam* (2014) 2014:651503. doi:10.1155/2014/651503
10. Chen Z, O'Shea JJ. Th17 cells: a new fate for differentiating helper T cells. *Immunol Res* (2008) 41(2):87–102. doi:10.1007/s12026-007-8014-9
11. Chung Y, Chang SH, Martinez GJ, Yang XO, Nurieva R, Kang HS, et al. Critical regulation of early Th17 cell differentiation by interleukin-1 signaling. *Immunity* (2009) 30(4):576–87. doi:10.1016/j.immuni.2009.02.007
12. Guo L, Wei G, Zhu J, Liao W, Leonard WJ, Zhao K, et al. IL-1 family members and STAT activators induce cytokine production by Th2, Th17, and Th1 cells. *Proc Natl Acad Sci U S A* (2009) 106(32):13463–8. doi:10.1073/pnas.0906988106
13. Bettelli E, Korn T, Kuchroo VK. Th17: the third member of the effector T cell trilogy. *Curr Opin Immunol* (2007) 19(6):652–7. doi:10.1016/j.coi.2007.07.020
14. Stockinger B, Veldhoen M. Differentiation and function of Th17 T cells. *Curr Opin Immunol* (2007) 19(3):281–6. doi:10.1016/j.coi.2007.04.005
15. Wilson NJ, Boniface K, Chan JR, McKenzie BS, Blumenschein WM, Mattson JD, et al. Development, cytokine profile and function of human interleukin 17-producing helper T cells. *Nat Immunol* (2007) 8(9):950–7. doi:10.1038/ni1497
16. Langrish CL, Chen Y, Blumenschein WM, Mattson J, Basham B, Sedgwick JD, et al. IL-23 drives a pathogenic T cell population that induces autoimmune inflammation. *J Exp Med* (2005) 201(2):233–40. doi:10.1084/jem.20041257
17. Graeber KE, Olsen NJ. Th17 cell cytokine secretion profile in host defense and autoimmunity. *Inflamm Res* (2012) 61(2):87–96. doi:10.1007/s00011-011-0419-1
18. Chan YR, Liu JS, Pociask DA, Zheng M, Mietzner TA, Berger T, et al. Lipocalin 2 is required for pulmonary host defense against *Klebsiella* infection. *J Immunol* (2009) 182(8):4947–56. doi:10.4049/jimmunol.0803282

19. Ferreira MC, Whibley N, Mamo AJ, Siebenlist U, Chan YR, Gaffen SL. Interleukin-17-induced protein lipocalin 2 is dispensable for immunity to oral candidiasis. *Infect Immun* (2014) 82(3):1030–5. doi:10.1128/IAI.01389-13
20. Laan M, Cui ZH, Hoshino H, Lotvall J, Sjostrand M, Gruenert DC, et al. Neutrophil recruitment by human IL-17 via C-X-C chemokine release in the airways. *J Immunol* (1999) 162(4):2347–52.
21. Hoshino H, Laan M, Sjostrand M, Lotvall J, Skoogh BE, Linden A. Increased elastase and myeloperoxidase activity associated with neutrophil recruitment by IL-17 in airways in vivo. *J Allergy Clin Immunol* (2000) 105(1 Pt 1):143–9. doi:10.1016/S0091-6749(00)90189-1
22. Ye P, Rodriguez FH, Kanaly S, Stocking KL, Schurr J, Schwarzenberger P, et al. Requirement of interleukin 17 receptor signaling for lung CXC chemokine and granulocyte colony-stimulating factor expression, neutrophil recruitment, and host defense. *J Exp Med* (2001) 194(4):519–27. doi:10.1084/jem.194.4.519
23. Romani L. Immunity to fungal infections. *Nat Rev Immunol* (2011) 11(4): 275–88. doi:10.1038/nri2939
24. Hernandez-Santos N, Gaffen SL. Th17 cells in immunity to *Candida albicans*. *Cell Host Microbe* (2012) 11(5):425–35. doi:10.1016/j.chom.2012.04.008
25. Perez-Nazario N, Rangel-Moreno J, O'Reilly MA, Pasparakis M, Gigliotti F, Wright TW. Selective ablation of lung epithelial IKK2 impairs pulmonary Th17 responses and delays the clearance of *Pneumocystis*. *J Immunol* (2013) 191(9):4720–30. doi:10.4049/jimmunol.1301679
26. Rudner XL, Happel KI, Young EA, Shellito JE. Interleukin-23 (IL-23)-IL-17 cytokine axis in murine *Pneumocystis carinii* infection. *Infect Immun* (2007) 75(6):3055–61. doi:10.1128/IAI.01329-06
27. Netea MG, Brown GD, Kullberg BJ, Gow NA. An integrated model of the recognition of *Candida albicans* by the innate immune system. *Nat Rev Microbiol* (2008) 6(1):67–78. doi:10.1038/nrmicro1815
28. Conti HR, Gaffen SL. Host responses to *Candida albicans*: Th17 cells and mucosal candidiasis. *Microbes Infect* (2010) 12(7):518–27. doi:10.1016/j.micinf.2010.03.013
29. Pandiyan P, Conti HR, Zheng L, Peterson AC, Mathern DR, Hernandez-Santos N, et al. CD4(+)CD25(+)Foxp3(+) regulatory T cells promote Th17 cells in vitro and enhance host resistance in mouse *Candida albicans* Th17 cell infection model. *Immunity* (2011) 34(3):422–34. doi:10.1016/j.immuni.2011.03.002
30. Loures FV, Araujo EF, Feriotti C, Bazan SB, Costa TA, Brown GD, et al. Dectin-1 induces M1 macrophages and prominent expansion of CD8+IL-17+ cells in pulmonary paracoccidioidomycosis. *J Infect Dis* (2014) 210(5):762–73. doi:10.1093/infdis/jiu136
31. Loures FV, Araujo EF, Feriotti C, Bazan SB, Calich VL. TLR-4 cooperates with Dectin-1 and mannose receptor to expand Th17 and Tc17 cells induced by *Paracoccidioides brasiliensis* stimulated dendritic cells. *Front Microbiol* (2015) 6:261. doi:10.3389/fmicb.2015.00261
32. Nakae S, Saijo S, Horai R, Sudo K, Mori S, Iwakura Y. IL-17 production from activated T cells is required for the spontaneous development of destructive arthritis in mice deficient in IL-1 receptor antagonist. *Proc Natl Acad Sci U S A* (2003) 100(10):5986–90. doi:10.1073/pnas.1035999100
33. Koenders MI, Lubberts E, Oppers-Walgreen B, van den Bersselaar L, Helsen MM, Kolls JK, et al. Induction of cartilage damage by overexpression of T cell interleukin-17A in experimental arthritis in mice deficient in interleukin-1. *Arthritis Rheum* (2005) 52(3):975–83. doi:10.1002/art.20885
34. Lu YJ, Gross J, Bogaert D, Finn A, Bagrade L, Zhang Q, et al. Interleukin-17A mediates acquired immunity to pneumococcal colonization. *PLoS Pathog* (2008) 4(9):e1000159. doi:10.1371/journal.ppat.1000159
35. Okamoto Yoshida Y, Umemura M, Yahagi A, O'Brien RL, Ikuta K, Kishihara K, et al. Essential role of IL-17A in the formation of a mycobacterial infection-induced granuloma in the lung. *J Immunol* (2010) 184(8):4414–22. doi:10.4049/jimmunol.0903332
36. Egen JG, Rothfuchs AG, Feng CG, Winter N, Sher A, Germain RN. Macrophage and T cell dynamics during the development and disintegration of mycobacterial granulomas. *Immunity* (2008) 28(2):271–84. doi:10.1016/j.immuni.2007.12.010
37. Souto JT, Figueiredo F, Furlanetto A, Pfeffer K, Rossi MA, Silva JS. Interferon-gamma and tumor necrosis factor-alpha determine resistance to *Paracoccidioides brasiliensis* infection in mice. *Am J Pathol* (2000) 156(5):1811–20. doi:10.1016/S0002-9440(10)65053-5
38. Pagliari C, Fernandes ER, Stegun FW, da Silva WL, Seixas Duarte MI, Sotto MN. Paracoccidioidomycosis: cells expressing IL17 and Foxp3 in cutaneous and mucosal lesions. *Microb Pathog* (2011) 50(5):263–7. doi:10.1016/j.micpath.2010.12.008
39. Calich VL, Purchio A, Paula CR. A new fluorescent viability test for fungi cells. *Mycopathologia* (1979) 66(3):175–7. doi:10.1007/BF00683967
40. Moreira AP, Cavassani KA, Massafera Tristao FS, Campanelli AP, Martinez R, Rossi MA, et al. CCR5-dependent regulatory T cell migration mediates fungal survival and severe immunosuppression. *J Immunol* (2008) 180(5):3049–56. doi:10.4049/jimmunol.180.5.3049
41. Tristao FS, Rocha FA, Moreira AP, Cunha FQ, Rossi MA, Santana Silva J. 5-lipoxygenase activity increases susceptibility to *Paracoccidioides brasiliensis* experimental infection. *Infect Immun* (2013) 81(4):1256–66. doi:10.1128/IAI.01209-12
42. Tristao FS, Rocha FA, Dias FC, Rossi MA, Silva JS. The left lung is preferentially targeted during experimental paracoccidioidomycosis in C57BL/6 mice. *Braz J Med Biol Res* (2013) 46(10):839–43. doi:10.1590/1414-431X20133140
43. Montenegro MR, Franco M. Pathology. In: Franco ML, da Silva Lacaz C, Restrepo-Moreno A, Del Negro G, editors. *Paracoccidioidomycosis*. Boca Raton: CRC Press (1994). p. 131–50.
44. Mariano M. The experimental granuloma. A hypothesis to explain the persistence of the lesion. *Rev Inst Med Trop Sao Paulo* (1995) 37(2):161–76. doi:10.1590/S0036-46651995000200012
45. Lucero HA, Patterson S, Matsuura S, Ravid K. Quantitative histological image analyses of reticulin fibers in a myelofibrotic mouse. *J Biol Methods* (2016) 3(4):e60. doi:10.14440/jbm.2016.152
46. Marim FM, Silveira TN, Lima DS Jr, Zamboni DS. A method for generation of bone marrow-derived macrophages from cryopreserved mouse bone marrow cells. *PLoS One* (2010) 5(12):e15263. doi:10.1371/journal.pone.0015263
47. Cua DJ, Tato CM. Innate IL-17-producing cells: the sentinels of the immune system. *Nat Rev Immunol* (2010) 10(7):479–89. doi:10.1038/nri2800
48. Regev D, Surolia R, Karki S, Zolak J, Montes-Worboys A, Oliva O, et al. Heme oxygenase-1 promotes granuloma development and protects against dissemination of mycobacteria. *Lab Invest* (2012) 92(11):1541–52. doi:10.1038/labinvest.2012.125
49. Alegre AC, Oliveira AF, Dos Reis Almeida FB, Roque-Barreira MC, Hanna ES. Recombinant paracoccin reproduces the biological properties of the native protein and induces protective Th1 immunity against *Paracoccidioides brasiliensis* infection. *PLoS Negl Trop Dis* (2014) 8(4):e2788. doi:10.1371/journal.pntd.0002788
50. Gonzalez A, de Gregori W, Velez D, Restrepo A, Cano LE. Nitric oxide participation in the fungicidal mechanism of gamma interferon-activated murine macrophages against *Paracoccidioides brasiliensis* conidia. *Infect Immun* (2000) 68(5):2546–52. doi:10.1128/IAI.68.5.2546-2552.2000
51. Nishikaku AS, Molina RF, Ribeiro LC, Scavone R, Albe BP, Cunha CS, et al. Nitric oxide participation in granulomatous response induced by *Paracoccidioides brasiliensis* infection in mice. *Med Microbiol Immunol* (2009) 198(2):123–35. doi:10.1007/s00430-009-0113-x
52. Fortes MR, Miot HA, Kurokawa CS, Marques ME, Marques SA. Immunology of paracoccidioidomycosis. *An Bras Dermatol* (2011) 86(3):516–24. doi:10.1590/S0365-05962011000300014
53. Pagliari C, Sotto MN. Dendritic cells and pattern of cytokines in paracoccidioidomycosis skin lesions. *Am J Dermatopathol* (2003) 25(2):107–12. doi:10.1097/00000372-200304000-00003
54. Zelante T, De Luca A, Bonifazi P, Montagnoli C, Bozza S, Moretti S, et al. IL-23 and the Th17 pathway promote inflammation and impair antifungal immune resistance. *Eur J Immunol* (2007) 37(10):2695–706. doi:10.1002/eji.200737409
55. de Castro LF, Ferreira MC, da Silva RM, Blotta MH, Longhi LN, Mamoni RL. Characterization of the immune response in human paracoccidioidomycosis. *J Infect* (2013) 67(5):470–85. doi:10.1016/j.jinf.2013.07.019
56. Werner JL, Gessner MA, Lilly LM, Nelson MP, Metz AE, Horn D, et al. Neutrophils produce interleukin 17A (IL-17A) in a dectin-1- and IL-23-dependent manner during invasive fungal infection. *Infect Immun* (2011) 79(10):3966–77. doi:10.1128/IAI.05493-11
57. Pina A, de Araujo EF, Felonato M, Loures FV, Feriotti C, Bernardino S, et al. Myeloid dendritic cells (DCs) of mice susceptible to paracoccidioidomycosis

suppress T cell responses whereas myeloid and plasmacytoid DCs from resistant mice induce effector and regulatory T cells. *Infect Immun* (2013) 81(4):1064–77. doi:10.1128/IAI.00736-12
58. Ketelut-Carneiro N, Silva GK, Rocha FA, Milanezi CM, Cavalcanti-Neto FF, Zamboni DS, et al. IL-18 triggered by the Nlrp3 inflammasome induces host innate resistance in a pulmonary model of fungal infection. *J Immunol* (2015) 194(9):4507–17. doi:10.4049/jimmunol.1402321
59. Torrado E, Cooper AM. IL-17 and Th17 cells in tuberculosis. *Cytokine Growth Factor Rev* (2010) 21(6):455–62. doi:10.1016/j.cytogfr.2010.10.004
60. Bending D, De la Pena H, Veldhoen M, Phillips JM, Uyttenhove C, Stockinger B, et al. Highly purified Th17 cells from BDC2.5NOD mice convert into Th1-like cells in NOD/SCID recipient mice. *J Clin Invest* (2009) 119(3):565–72. doi:10.1172/JCI37865
61. Lee YK, Turner H, Maynard CL, Oliver JR, Chen D, Elson CO, et al. Late developmental plasticity in the T helper 17 lineage. *Immunity* (2009) 30(1):92–107. doi:10.1016/j.immuni.2008.11.005
62. Shimizu J, Takai K, Fujiwara N, Arimitsu N, Ueda Y, Wakisaka S, et al. Excessive CD4+ T cells co-expressing interleukin-17 and interferon-gamma in patients with Behcet's disease. *Clin Exp Immunol* (2012) 168(1):68–74. doi:10.1111/j.1365-2249.2011.04543.x
63. Figueiredo F, Alves LM, Silva CL. Tumour necrosis factor production in vivo and in vitro in response to *Paracoccidioides brasiliensis* and the cell wall fractions thereof. *Clin Exp Immunol* (1993) 93(2):189–94. doi:10.1111/j.1365-2249.1993.tb07964.x
64. Nascimento FR, Calich VL, Rodriguez D, Russo M. Dual role for nitric oxide in paracoccidioidomycosis: essential for resistance, but overproduction associated with susceptibility. *J Immunol* (2002) 168(9):4593–600. doi:10.4049/jimmunol.168.9.4593
65. Mazzoni A, Bronte V, Visintin A, Spitzer JH, Apolloni E, Serafini P, et al. Myeloid suppressor lines inhibit T cell responses by an NO-dependent mechanism. *J Immunol* (2002) 168(2):689–95. doi:10.4049/jimmunol.168.2.689
66. Miljkovic D, Trajkovic V. Inducible nitric oxide synthase activation by interleukin-17. *Cytokine Growth Factor Rev* (2004) 15(1):21–32. doi:10.1016/j.cytogfr.2003.10.003
67. Sergejeva S, Ivanov S, Lotvall J, Linden A. Interleukin-17 as a recruitment and survival factor for airway macrophages in allergic airway inflammation. *Am J Respir Cell Mol Biol* (2005) 33(3):248–53. doi:10.1165/rcmb.2004-0213OC
68. Barin JG, Baldeviano GC, Talor MV, Wu L, Ong S, Quader F, et al. Macrophages participate in IL-17-mediated inflammation. *Eur J Immunol* (2012) 42(3):726–36. doi:10.1002/eji.201141737
69. Tatano Y, Shimizu T, Tomioka H. Unique macrophages different from M1/M2 macrophages inhibit T cell mitogenesis while upregulating Th17 polarization. *Sci Rep* (2014) 4:4146. doi:10.1038/srep04146

Conflict of Interest Statement: The authors declare that the research was conducted in the absence of any commercial or financial relationships that could be construed as a potential conflict of interest.

Copyright © 2017 Tristão, Rocha, Carlos, Ketelut-Carneiro, Souza, Milanezi and Silva. This is an open-access article distributed under the terms of the Creative Commons Attribution License (CC BY). The use, distribution or reproduction in other forums is permitted, provided the original author(s) or licensor are credited and that the original publication in this journal is cited, in accordance with accepted academic practice. No use, distribution or reproduction is permitted which does not comply with these terms.

frontiers in Immunology

ORIGINAL RESEARCH
published: 19 January 2018
doi: 10.3389/fimmu.2017.01987

Contribution of IL-1RI Signaling to Protection against *Cryptococcus neoformans* 52D in a Mouse Model of Infection

Mitra Shourian[1,2], *Ben Ralph*[3,4], *Isabelle Angers*[2,5], *Donald C. Sheppard*[3,4,6] *and Salman T. Qureshi*[1,2,5,6]*

[1] Division of Experimental Medicine, McGill University, Montreal, QC, Canada, [2] Meakins-Christie Laboratories, McGill University, Montreal, QC, Canada, [3] Program in Infectious Diseases and Immunology in Global Health, Centre for Translational Biology, The Research Institute of the McGill University Health Center (RI-MUHC), Montreal, QC, Canada, [4] Department of Microbiology and Immunology, McGill University, Montreal, QC, Canada, [5] Program in Translational Research in Respiratory Diseases, Department of Critical Care, The Research Institute of the McGill University Health Center (RI-MUHC), Montreal, QC, Canada, [6] Department of Medicine, McGill University, Montreal, QC, Canada

Interleukin-1 alpha (IL-1α) and interleukin-1 beta (IL-1β) are pro-inflammatory cytokines that are induced after *Cryptococcus neoformans* infection and activate the interleukin-1 receptor type I (IL-1RI). To establish the role of IL-1RI signaling in protection against cryptococcal infection, we analyzed wild-type (WT) and IL-1RI-deficient (IL-1RI$^{-/-}$) mice on the BALB/c background. IL-1RI$^{-/-}$ mice had significantly reduced survival compared to WT mice after intratracheal challenge with *C. neoformans* 52D. Microbiological analysis showed a significant increase in the lung and brain fungal burden of IL-1RI$^{-/-}$ compared to WT mice beginning at weeks 1 and 4 postinfection, respectively. Histopathology showed that IL-1RI$^{-/-}$ mice exhibit greater airway epithelial mucus secretion and prominent eosinophilic crystals that were absent in WT mice. Susceptibility of IL-1RI$^{-/-}$ mice was associated with significant induction of a Th2-biased immune response characterized by pulmonary eosinophilia, M2 macrophage polarization, and recruitment of CD4$^+$ IL-13$^+$ T cells. Expression of pro-inflammatory [IL-1α, IL-1β, TNFα, and monocyte chemoattractant protein 1 (MCP-1)], Th1-associated (IFNγ), and Th17-associated (IL-17A) cytokines was significantly reduced in IL-1RI$^{-/-}$ lungs compared to WT. WT mice also had higher expression of KC/CXCL1 and sustained neutrophil recruitment to the lung; however, antibody-mediated depletion of these cells showed that they were dispensable for lung fungal clearance. In conclusion, our data indicate that IL-1RI signaling is required to activate a complex series of innate and adaptive immune responses that collectively enhance host defense and survival after *C. neoformans* 52D infection in BALB/c mice.

Keywords: ***Cryptococcus neoformans*, fungal pneumonia, interleukin-1, interleukin-1 receptor, lung inflammation, cytokines, macrophage polarization, lymphocyte differentiation**

OPEN ACCESS

Edited by:
Amariliz Rivera, New Jersey Medical School, United States

Reviewed by:
Karen L. Wozniak, Oklahoma State University, United States
Michal Adam Olszewski, University of Michigan, United States

***Correspondence:**
Salman T. Qureshi
salman.qureshi@mcgill.ca

Specialty section:
This article was submitted to Microbial Immunology, a section of the journal Frontiers in Immunology

Received: *25 September 2017*
Accepted: *21 December 2017*
Published: *19 January 2018*

Citation:
Shourian M, Ralph B, Angers I, Sheppard DC and Qureshi ST (2018) Contribution of IL-1RI Signaling to Protection against Cryptococcus neoformans 52D in a Mouse Model of Infection. Front. Immunol. 8:1987. doi: 10.3389/fimmu.2017.01987

INTRODUCTION

Cryptococcus neoformans is an encapsulated yeast that is estimated to cause approximately 223,000 cases of meningitis each year and is responsible for 15% of AIDS-related deaths (1). In healthy individuals, inhalation of infectious propagules is usually contained in the lung, but among those with a defective immune response, uncontrolled replication may result in dissemination to other

parts of the body with a tropism for the brain (2, 3). Severe cryptococcal disease occurs primarily in patients with uncontrolled HIV/AIDS and is also found in solid organ transplant recipients, those receiving exogenous immunosuppression, patients with primary or acquired immunodeficiency, and increasingly among immunologically normal hosts (4–7).

The pattern of cytokine expression is a crucial determinant of the pathogenesis of cryptococcal infection (3, 8–11). Th1-type cytokines [interleukin (IL)-12 and IFNγ] promote phagocytosis by dendritic cells (DCs) and polarize macrophages toward a classically activated phenotype (M1), thereby increasing fungal clearance (12–15). On the other hand, Th2-type cytokines (IL-4, IL-5, and IL-13) are associated with a significant eosinophil chemotaxis to the lungs and induction of alternatively activated (M2) macrophages that facilitate cryptococcal proliferation and dissemination (16–18). There is some evidence that Th17-type cytokines (IL-17A and IL-23) contribute to protection against infection with wild-type (WT) *C. neoformans*; however, they appear to be less effective compared to Th1-type cytokines (19–23). Inhibition of IL-17A expression or signaling had no significant effect on M1 macrophage polarization, resolution of infection, or survival in mice infected with *C. neoformans* H99 that has been engineered to express IFNγ (24, 25). Finally, a prospective analysis of HIV-infected humans suggested a potential role for IL-17 in the immunopathogenesis of cryptococcal meningitis; however, further studies are required to confirm this hypothesis (26).

The mechanisms that initiate and regulate the innate immune response against *C. neoformans* infection are not fully understood. The interaction of *C. neoformans* with host cells triggers production of several pro-inflammatory cytokines including TNFα, IL-6, and IL-1 (27–30). Both interleukin-1 alpha (IL-1α) and interleukin-1 beta (IL-1β) are induced during cryptococcal infection *in vitro* (27, 28, 31–34) and *in vivo* (35–40) in a NLRP3-dependent manner, and internalization of opsonized encapsulated cryptococci has been shown to activate the canonical NLRP3–ASC–caspase-1 and non-canonical NLRP3–ASC–caspase-8 inflammasome (34, 41). The magnitude of IL-1 expression between inbred mice with different genetic backgrounds has also been associated with natural resistance or susceptibility to progressive cryptococcal infection (35). After intratracheal infection with *C. neoformans* 52D, the level of IL-1β expression was 11-fold higher in the lungs of resistant SJL/J inbred mice compared to the susceptible C57BL/6 inbred strain. A subsequent analysis of WT and interleukin-1 receptor (IL-1R)-deficient mice on the C57BL/6 genetic background did not identify significant differences in survival or fungal dissemination after intranasal infection with *C. neoformans* H99; however, at day 12 postinfection, the IL-1R$^{-/-}$ mice had a modest elevation of lung fungal burden (37).

Given the essential role for cytokine-mediated inflammation and the evidence for IL-1α and IL-1β induction in response to *C. neoformans*, we hypothesized that the contribution of IL-1R-dependent signaling to host defense may have been underestimated by infection of WT and IL-1R$^{-/-}$ mice on the susceptible C57BL/6 genetic background with a highly virulent *C. neoformans* strain. To test this hypothesis, we performed intratracheal inoculation of inbred BALB/c mice and IL-1R$^{-/-}$ mice on the same genetic background with *C. neoformans* 52D and analyzed fungal burden and immune responses at serial time points. This approach was chosen to model the process of natural infection in a relatively resistant host with a moderately virulent cryptococcal strain. Our findings demonstrate that IL-1RI$^{-/-}$ mice had a significantly higher fungal burden in the lungs and brains as well as a significantly higher mortality compared to BALB/c mice. In IL-1RI$^{-/-}$ mice, *C. neoformans* 52D infection was associated with heightened lung eosinophilia, elevated airway mucus secretion, and a greater percentage of M2 macrophages and CD4^{+} Th2 cells along with significantly fewer lung neutrophils, DCs, Th1, and Th17 cells. Taken together, this study shows that IL-1R-dependent signaling contributes to protection against *C. neoformans* 52D infection in BALB/c mice by triggering a complex innate and adaptive immune response and raises the possibility that modulation of this signaling axis could be a potential therapeutic strategy.

MATERIALS AND METHODS

Mice

Inbred BALB/c mice were purchased from Charles River and maintained in our facility. IL-1RI$^{-/-}$ mice were purchased from Jackson Labs and backcrossed to BALB/c for 10 generations. Mice were provided with sterile food and water and cared for according to the Canadian Council on Animal Care guidelines. All experiments were performed using 7- to 9-week-old male and female mice. Mice were humanely euthanized with CO_2 upon completion of experiments, and every effort was made to minimize suffering. All experimental protocols were reviewed and approved by the McGill University Animal Care Committee.

Cryptococcus neoformans

Cryptococcus neoformans 52D (ATCC 24067) was grown and maintained on Sabouraud dextrose agar (SDA; BD, Becton Dickinson and Company). To prepare an infectious dose, a single colony was suspended in Sabouraud dextrose broth (BD) and grown to early stationary phase (48 h) at room temperature on a rotator. The stationary phase culture was then washed with sterile phosphate-buffered saline (PBS), counted on a hemocytometer, and diluted to 2×10^5 CFU/ml in sterile PBS. The fungal concentration of the experimental dose was confirmed by plating a dilution of the inoculum on SDA and counting the CFU after 72 h of incubation at room temperature.

Intratracheal Infection with *C. neoformans*

For intratracheal administration of *C. neoformans*, mice were anesthetized with 150 mg/kg of ketamine (Ayerst Veterinary Laboratories) and 10 mg/kg of xylazine (Bayer) intraperitoneally. A small skin incision was made below the jaw along the trachea, and the underlying glands and muscle were separated. Infection was performed by intratracheal injection of 10^4 *C. neoformans* in 50 µl PBS through a 22-gauge catheter *via* a 1-ml tuberculin syringe. The incision was closed using the 9-mm EZ clip wound closing kit (Stoelting CO), and mice were monitored daily after surgery.

Tissue Isolation and CFU Assay

After mice were euthanized with CO_2, their lungs, spleen, and brain were excised and placed in sterile, ice-cold PBS. Tissues were then homogenized using a glass tube and pestle attached to a mechanical tissue homogenizer (Glas-Col) and plated at various dilutions on SDA. Plates were incubated at 37°C for 72 h, and CFU were counted. For survival analyses, mice were inoculated as stated above and monitored twice daily for up to 110 days postinfection.

Histopathological Analysis

After euthanasia, lungs were perfused with ice-cold PBS *via* the right ventricle of the heart. Using 10% buffered formalin acetate (Fisher Scientific), the lungs were inflated to a pressure of 25 cm H_2O and fixed overnight. Subsequently, lungs were embedded in paraffin, sectioned at 5 μm, and stained with hematoxylin–eosin (H&E), periodic acid–Schiff (PAS), or mucicarmine reagents at the Histology Facility of the Goodman Cancer Research Centre (McGill University). Representative photographs of lung sections were taken using a BX51 microscope (Olympus), QICAM Fast 1394 digital charge-coupled device camera (QImaging), and Image-Pro Plus software version 7.0.1.658 (Media Cybernetics).

Flow Cytometry

Lungs were excised using sterile technique and placed in RPMI (Gibco, Invitrogen) supplemented with 10% fetal bovine serum (Wisent). Subsequently lungs were minced using surgical blades and incubated with 1 mg/ml collagenase (Sigma) at 37°C for 1 h. After incubation, lung pieces were passed through a 16-gauge needle and filtered through a 70-μm cell strainer (BD). Red blood cells were removed using ACK lysis buffer, cells were counted with a hemacytometer using trypan blue dye, and 5×10^6 cells in 100 μl FACS buffer/well were dispensed in 96-well plates. Fc receptors were blocked with the addition of unlabeled anti-CD16/32 antibodies [93; eBioscience (eBio)], and single-cell suspensions were stained with the following fluorescence-conjugated anti-mouse monoclonal antibodies purchased from eBio, BD, and BioLegend: CD45 (30-F11), B220 (RA3-6B2), CD3e (145-2C11), CD4 (GK1.5), CD8 (53-6.7), CD49b (DX5), γδ TCR (GL3), CD11b (M1/70), CD11c (N418), MHCII (M5/114.15.2), Ly6G (1A8), CD86 (GL1), CD80 (16-10A1), CD64 (X54-5/7.1), CD24 (M1/69), SiglecF (E50-2440), CD103 (2E7), Ly6C (HK1.4), and CD206 (C068C2). Non-viable cells were excluded using a fixable viability dye reagent (eBio). Lineage negative cells (Lin^-) were defined as $CD45^+$ cells that did not express any other surface markers in this panel. Data were acquired using a LSRFortessa flow cytometer (BD) and analyzed using Flow Jo software. The absolute number of leukocytes was determined by multiplying the percentage of $CD45^+$ cells by the total number of counted cells.

Intracellular Staining

Lungs were processed as described above, and 5×10^6 cells/well were dispensed in 96-well plates. For cytokine analysis, cells were stimulated for 4 h with phorbol 12-myristate 13-acetate (PMA) and calcium ionophore (ionomycin) in the presence of brefeldin A (GolgiPlug) for the final 3 h. Cells were then washed, blocked with anti-CD16/32 antibodies, and stained with the surface antibodies. Cells were then fixed, permeabilized, and stained with IL-13 (eBio13A), IFNγ (XMG1.2), and IL-17A (17B7). Intracellular staining for Nos2 (CXNFT) was done as described for cytokines without PMA and ionomycin stimulation. Data were acquired using a LSRFortessa flow cytometer with gating determined by fluorescence-minus-one controls and analyzed using FlowJo software.

Total Lung Cytokine and Chemokine Production

Mice were euthanized and lungs flushed with 10 ml of ice-cold PBS. Whole lungs were homogenized in 2 ml PBS with Halt protease and phosphatase inhibitor cocktail (Fisher Scientific) using a sterilized glass tube and pestle attached to a mechanical tissue homogenizer (Glas-Col) and spun at 12,000 rpm for 20 min. Supernatants were collected, and aliquots were stored at −80°C for further analysis. The following cytokines and chemokines in whole-lung protein samples were analyzed using DuoSet enzyme-linked immunosorbent assay kits (R&D Systems): TNFα (DY410), IL-6 (DY406), IL-1β (DY401), IL-1α (DY400), monocyte chemoattractant protein 1 (MCP-1; MJE00), IL-12/IL-23P40 (DY2398), IFNγ (DY485), CXCL1/KC (DY453), IL-17A (DY421), and IL-13 (DY413).

Neutrophil Depletion

BALB/c mice received an intratracheal inoculum of 1×10^4 CFU of *C. neoformans* strain 52D. Mice were treated with 100 μl of PBS or 200 μg of anti-1A8 antibody (Bio X Cell) in a volume of 100 μl, 1 day before infection and daily during the study. At day 12 postinfection, lungs were excised, and fungal burden was analyzed.

Statistical Analysis

To test the significance of single comparisons, an unpaired Student's *t*-test was applied with a threshold $P \leq 0.05$. For all experiments, the mean and SEM is shown. Survival curves were analyzed by the log-rank test. All statistical analysis was performed with GraphPad Prism software version 6 (GraphPad Software Inc.).

RESULTS

IL-1RI$^{-/-}$ Mice Have Impaired Survival and an Increased Fungal Burden in the Lung, Brain, and Spleen following *C. neoformans* 52D Infection

To investigate the role of IL-1RI-mediated signaling after *C. neoformans* 52D infection, we constructed IL-1RI$^{-/-}$ mice on the BALB/c background by repeated backcrossing. We challenged mice with *C. neoformans* 52D and measured the survival rate and tissue fungal burden. No deaths were observed in WT

mice; however, IL-1RI$^{-/-}$ mice started to die at 40 days postinfection and had a 73% mortality rate at 100 days postinfection (**Figure 1A**). Microbiological analysis also showed a significant increase of fungal burden in IL-1RI$^{-/-}$ mice compared to the WT strain at all time points tested (**Figure 1B**). Importantly, a significant difference in lung fungal burden was observed at 7 days postinfection, suggesting that the IL-1RI signaling affects the initial host response to *C. neoformans* infection. At 35 days postinfection, there was almost a 20-fold increase of lung CFU in the IL-1RI$^{-/-}$ compared to the WT strain. Analysis of the spleen showed a trend toward higher CFU in the IL-1RI$^{-/-}$ mice compared to the WT strain that reached statistical significance at day 14 postinfection (**Figure 1C**). Analysis of the brain showed comparable CFU in both strains at 14 days postinfection; however, at 35 days postinfection, all of the WT mice had cleared the infection, while 10 of 16 (62%) of IL-1RI$^{-/-}$ mice still had detectable fungal growth (**Figure 1D**). Taken together, these data establish a role for IL-1R-mediated signaling in controlling fungal growth in the lungs and brain, limiting organ dissemination, and increasing survival after *C. neoformans* 52D infection.

An Altered Pattern of Pulmonary Inflammation Is Present in IL-1RI$^{-/-}$ Lungs following *C. neoformans* 52D Infection

The significant differences in survival and fungal burden between WT and IL-1RI$^{-/-}$ mice prompted us to investigate the effect of IL-1RI signaling on lung pathology after infection with *C. neoformans* 52D. Histopathological analysis was conducted at 35 days postinfection to correspond with the greatest difference in fungal burden prior to the onset of mortality (**Figures 2A–C**). H&E staining revealed that WT mice displayed abundant lung leukocyte infiltration that was almost absent in the IL-1RI$^{-/-}$ strain. Notably, eosinophilic crystals that have been associated with alternatively activated macrophages in *C. neoformans* 52D infection were clearly observed in IL-1RI$^{-/-}$ lung sections but were absent in the WT. Mucicarmine staining of the cryptococcal cell wall showed that most fungi were located within WT phagocytes with only a few visible extracellular organisms in the parenchyma or airways. In contrast, IL-1RI$^{-/-}$ sections showed lung parenchyma that was filled with heavily encapsulated extracellular cryptococci. PAS staining clearly revealed mucus

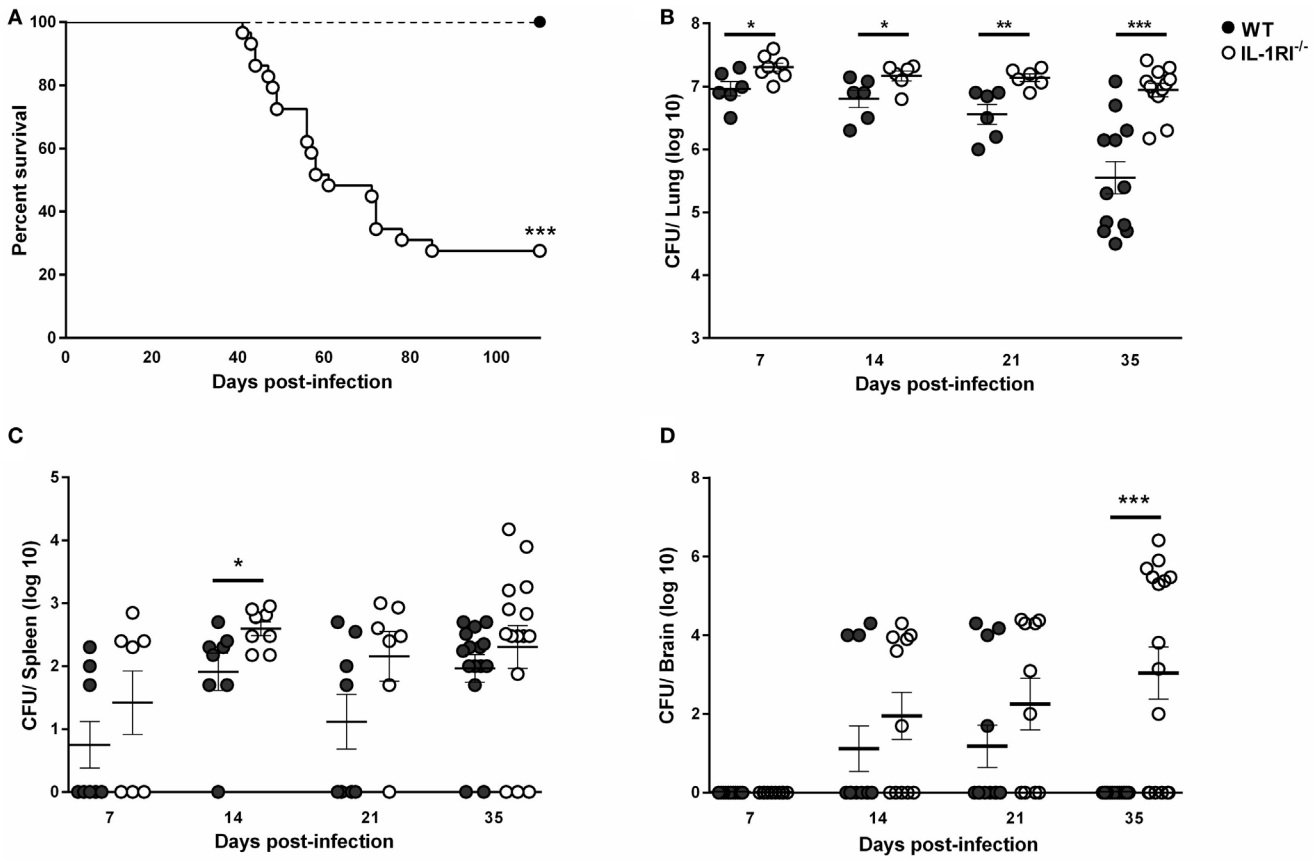

FIGURE 1 | Interleukin-1 receptor type I (IL-1RI) signaling is required for survival and control of fungal burden after infection with *Cryptococcus neoformans* 52D. Wild-type (WT) and IL-1RI-deficient (IL-1RI$^{-/-}$) mice were infected intratracheally with 10^4 CFU of *C. neoformans* strain 52D. **(A)** Mice were observed for up to 110 days for survival analysis (n = 12 mice/strain, using a log-rank test). **(B–D)** Fungal burden in the lung, brain, and spleen at serial time intervals was determined by plating tissue homogenates on Sabouraud dextrose agar. CFU data are shown as mean ± SEM and representative of two independent experiments (n = 6–15 mice/strain/time point). *$P \leq 0.05$, **$P \leq 0.01$, and ***$P \leq 0.001$.

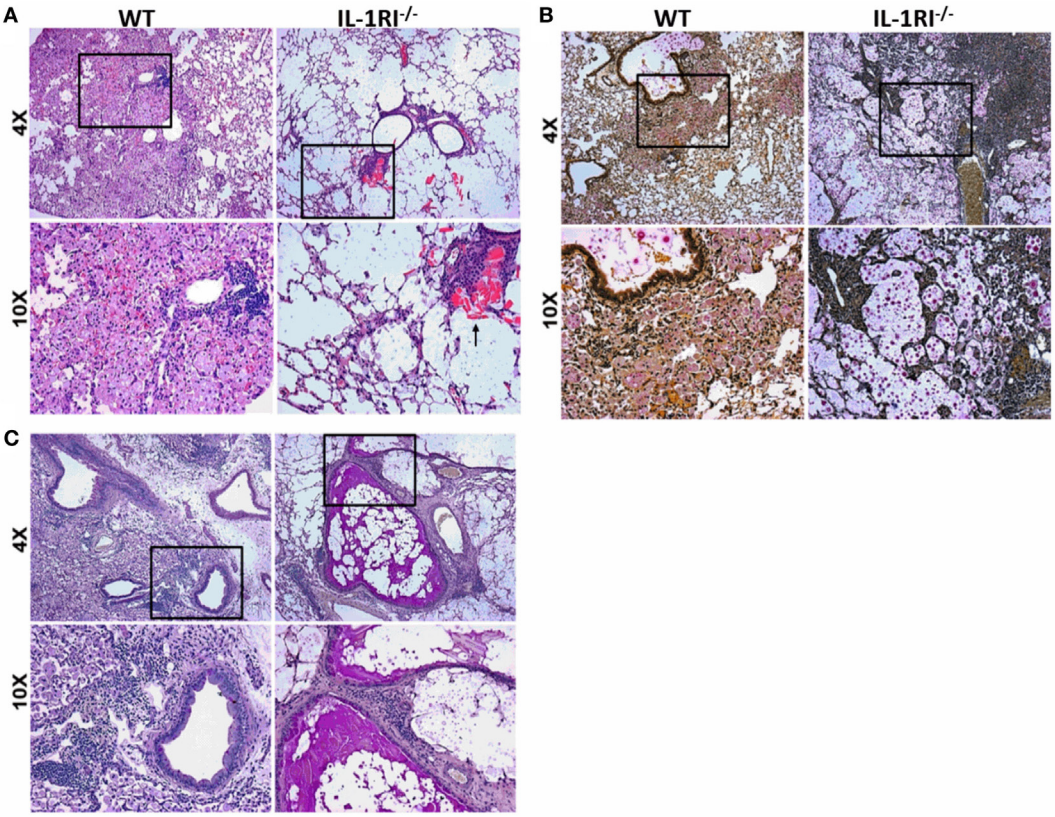

FIGURE 2 | Decreased inflammation in the lungs of interleukin-1 receptor type I-deficient (IL-1RI$^{-/-}$) mice following infection with *Cryptococcus neoformans* 52D. Wild-type (WT) and IL-1RI$^{-/-}$ mice were infected intratracheally with 10^4 CFU of *C. neoformans* 52D. Lungs were harvested at day 35 postinfection; perfused with phosphate-buffered saline; embedded in paraffin; and stained with hematoxylin–eosin (H&E), mucicarmine, or periodic acid–Schiff (PAS). Representative H&E images **(A)** show a significant reduction of inflammation in IL-1RI$^{-/-}$ compared to WT mice; the black arrow points to eosinophilic crystals in IL-1R$^{-/-}$ lung. Mucicarmine staining **(B)** shows numerous heavily encapsulated extracellular *C. neoformans* in the airspaces of IL-1RI$^{-/-}$ mice compared to WT mice. Representative images of lungs stained with PAS **(C)** show goblet cell hyperplasia and mucus in the airways of infected IL-1RI$^{-/-}$ mice compared to WT mice. Each image is representative of 100 fields examined (n = 4 mice/strain from two independent experiments).

secretion by airway epithelial cells in IL-1RI$^{-/-}$ mice that was not observed in the airways of WT mice. Taken together, this histopathological analysis confirmed the results of the lung fungal burden studies and demonstrated reduced inflammation with signs of Th2 polarization in IL-1RI$^{-/-}$ mice compared to the WT strain.

Inflammatory Cytokine and Chemokine Production Is Decreased in the Lungs of IL-1RI$^{-/-}$ Mice following *C. neoformans* 52D Infection

To determine the effect of IL-1RI signaling on the production of soluble inflammatory mediators, WT and IL-1RI$^{-/-}$ mice were infected with *C. neoformans* 52D, and the concentration of pro-inflammatory cytokines (IL-1α, IL-1β, TNFα, and IL-6), chemokines (MCP-1 and KC), Th1-associated cytokines (IFNγ and IL-12), and representative Th2-associated (IL-13) and Th17-associated (IL-17A) cytokines was measured in whole-lung homogenates at serial time points (**Figure 3**). No significant differences in the level of these mediators were observed between two strains prior to infection. In WT mice, both IL-1α and IL-1β were produced in the lungs at day 7 postinfection and continued to increase until day 14 postinfection. Compared to WT, IL-1RI$^{-/-}$ mice had significantly lower production of these two cytokines at day 14 postinfection. The production of TNFα, MCP-1, and KC was significantly higher in WT compared to IL-1RI$^{-/-}$ mice at day 14 postinfection. Significantly greater production of IFNγ and IL-17A was also observed in the lungs of WT mice compared to IL-1RI$^{-/-}$ at day 14 postinfection. IL-13 production did not differ between strains at day 7 and day 14 postinfection, although a modest increase was observed in IL-1R$^{-/-}$ mice compared to WT at day 21 postinfection. In summary, BALB/c mice exhibited significantly greater production of pro-inflammatory, Th1, and Th17 cytokines, as well as chemokines, compared to IL-1RI$^{-/-}$ mice; these findings demonstrate a broad effect of IL-1RI signaling on the lung inflammatory response after *C. neoformans* 52D infection.

IL-1RI$^{-/-}$ Mice Exhibit Reduced Neutrophil and Increased Eosinophil Recruitment to the Lungs following *C. neoformans* 52D Infection

To characterize the effect of IL-1RI signaling on the cellular immune response after *C. neoformans* infection, flow cytometry analysis of whole-lung digests was performed on WT and IL-1RI$^{-/-}$ mice at serial time points postinfection. A comprehensive gating strategy was used for the identification of resident and recruited myeloid cell subsets (**Figure 4**) (42–44). Prior to infection, no significant difference was observed in the total number of lung leukocytes between the two strains. The total number of CD45^{+} cells peaked at day 14 in both strains; however, it was significantly higher in WT compared to IL-1RI$^{-/-}$ mice at 14 and 21 days postinfection (**Figure 5A**). At 7 days postinfection neutrophils (CD11c^{-}, CD11b^{+}, and Ly6G^{high}) were the most frequent leukocyte subset in both strains; however, their percentage and total number was significantly higher in the WT compared to the IL-1RI$^{-/-}$ at 14 and 21 days postinfection (**Figures 5B,C**). Conversely, the percentage and number of lung eosinophils (CD11c^{-}, CD11b^{+}, Siglec F^{+}, and CD24^{+})

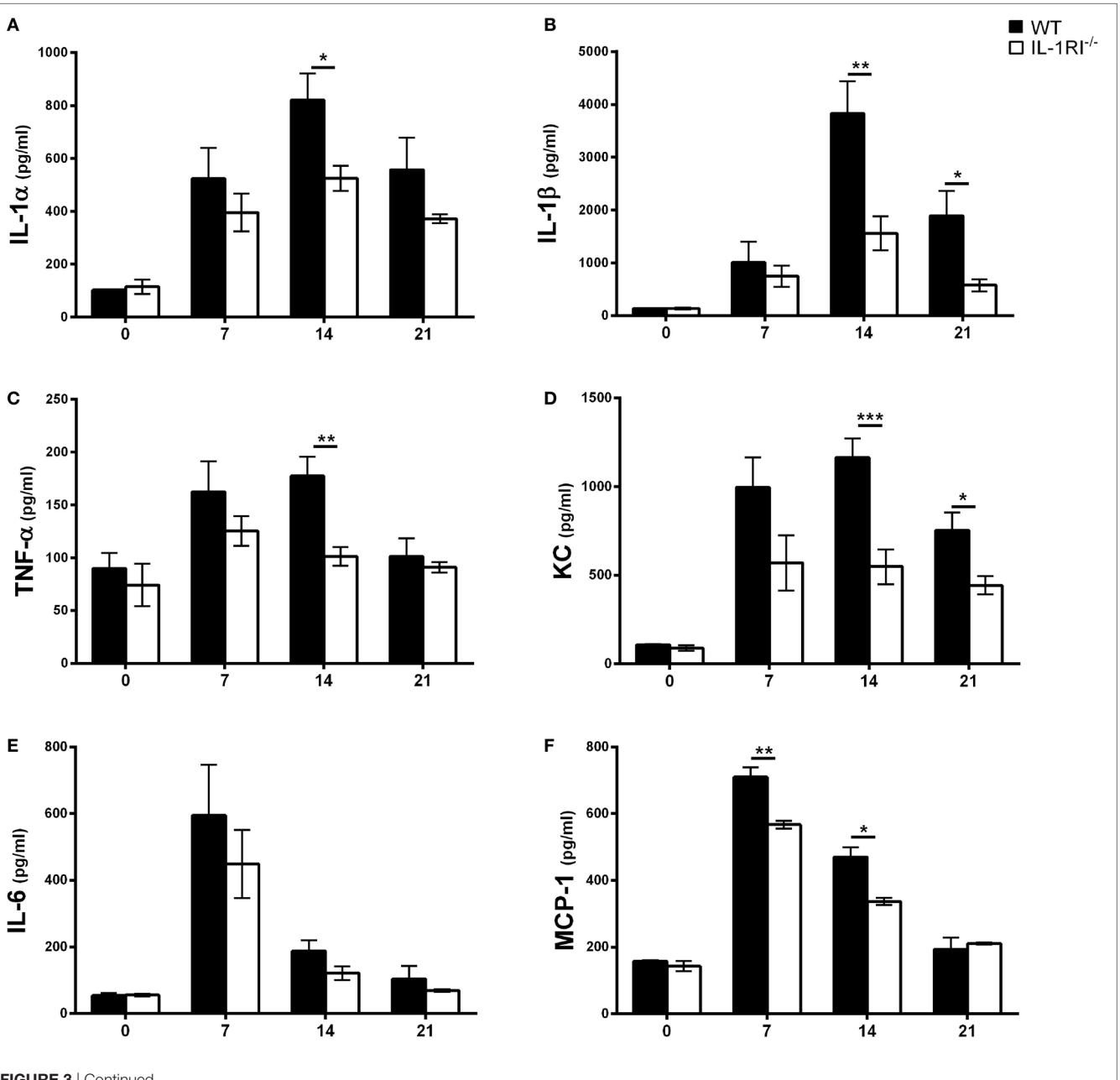

FIGURE 3 | Continued

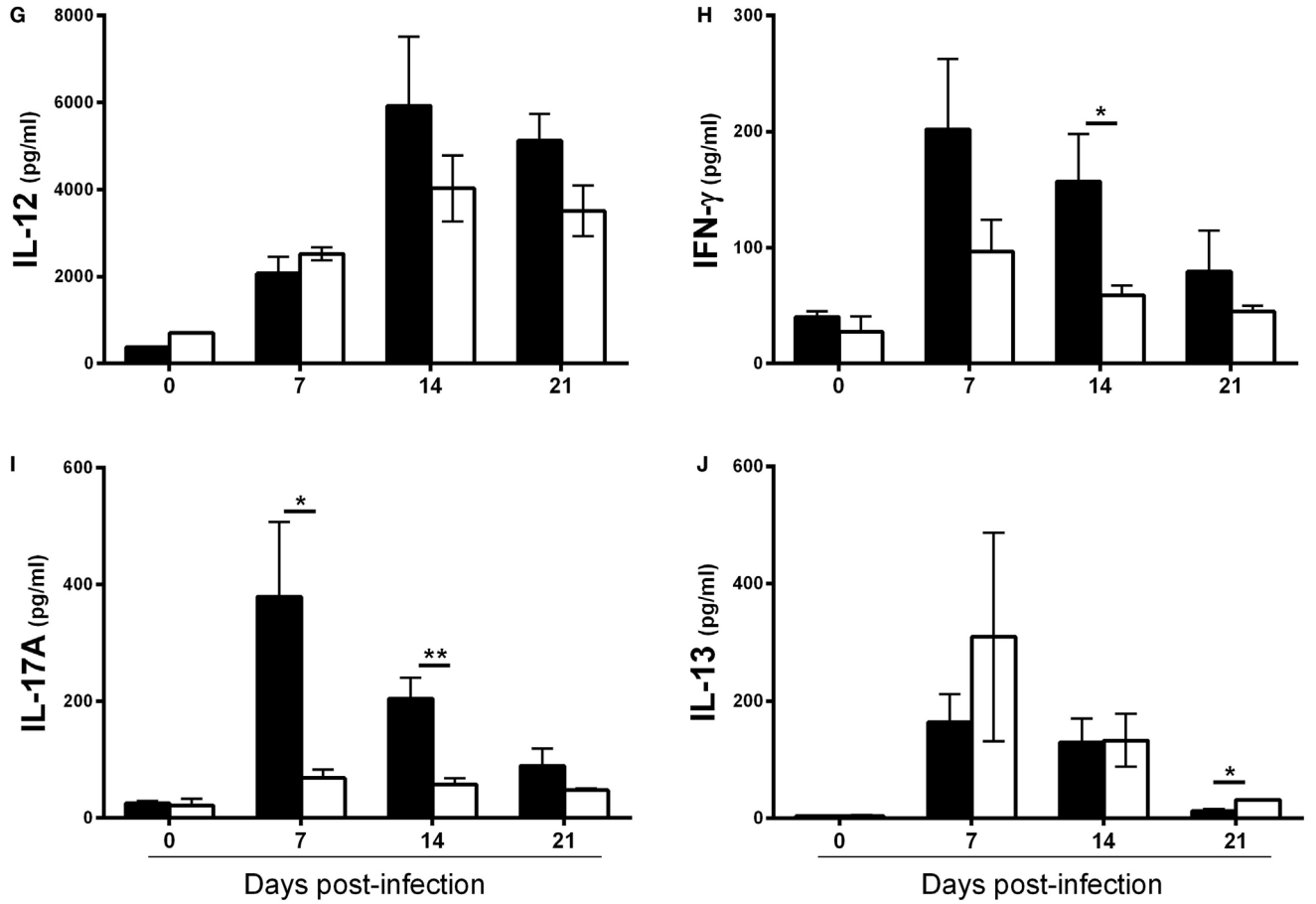

FIGURE 3 | Interleukin-1 receptor type I-deficient (IL-1RI$^{-/-}$) lungs have decreased inflammatory cytokine and chemokine production after *Cryptococcus neoformans* 52D infection. Whole-lung protein was collected at 0, 7, 14, and 21 days postinfection with 10^4 CFU of *C. neoformans* 52D. Enzyme-linked immunosorbent assay was performed to determine the level of pro-inflammatory cytokines **(A–C, E)**, chemokines **(D, F)**, and Th1/Th2/Th17-type cytokines **(G–J)**. Data are shown as mean ± SEM and representative of two independent experiments (n = 4 mice/strain/time point). *$P \leq 0.05$, **$P \leq 0.01$, and ***$P \leq 0.001$. MCP-1, monocyte chemoattractant protein 1.

was significantly higher in IL-1RI$^{-/-}$ mice compared to the WT strain at 14 and 21 days postinfection (**Figures 5D,E**). These data suggest that IL-1R signaling plays an important role in recruitment of neutrophils during the host response to *C. neoformans* 52D infection. In the absence of IL-1R, mice develop significant and sustained lung eosinophilia that is associated with a higher fungal burden.

To evaluate the functional significance of early and sustained neutrophil recruitment to the lungs of BALB/c mice after infection with *C. neoformans* 52D, the effect of antibody-mediated depletion on tissue fungal burden and lung cell infiltration was characterized. Briefly, WT mice received 200 µg of anti-Ly6G antibody (clone 1A8) in a volume of 100 µl *via* intraperitoneal injection 24 h before infection and daily thereafter. To capture the overall effect of neutrophil depletion during the innate and adaptive phases of immunity, lung fungal burden was determined at 12 days postinfection. Interestingly, this analysis showed that neutrophil-depleted mice had a significantly lower cryptococcal burden in the lungs compared to control mice (**Figures 5F–G**).

IL-1RI$^{-/-}$ Mice Recruit Fewer Monocyte-Derived DC and Macrophages to the Lung following *C. neoformans* 52D Infection

Inflammatory monocyte-derived macrophages (ExMs) and DCs are important for protection against *C. neoformans* infection (45, 46). We investigated the effect of IL-1RI signaling on the number of resident and monocyte-derived myeloid cells by harvesting lungs at different times postinfection and analyzing cells by flow cytometry. No significant difference in the percentage of pDCs, CD103$^+$ DCs, and CD11b$^+$ cDCs was observed in the lungs of BALB/c and IL-1R$^{-/-}$ mice after *C. neoformans* 52D infection; however, at day 21 postinfection, there was a significantly higher percentage and number of AMs in BALB/c compared to IL-1R$^{-/-}$ mice (**Figures 6 A,B,D**). As both monocyte-derived ExMs and

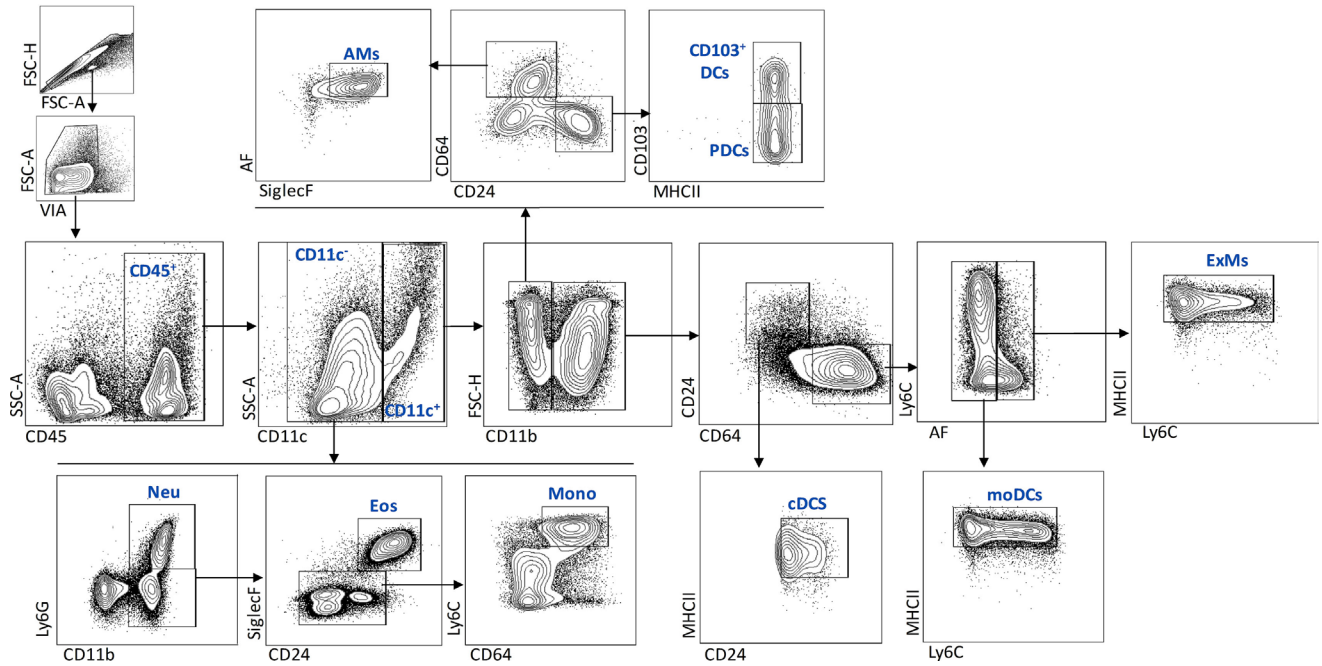

FIGURE 4 | Flow cytometry gating strategy used to identify myeloid cell subsets in the lungs after *Cryptococcus neoformans* 52D infection. Lung cell suspensions were stained with fluorochrome-labeled antibodies and analyzed as described in Section "Materials and Methods." Representative gating plots for CD45$^+$ subsets are shown; neutrophils (CD11c$^-$, CD11b$^+$, and Ly6G^{high}), eosinophils (CD11c$^-$, CD11b$^+$, Ly6G low/negative, CD24$^+$, and SiglecF$^+$), monocytes (CD11c$^-$, CD11b$^+$, Ly6G low/negative, CD64$^+$, and Ly6C^{high}), AMs (CD11c$^+$, CD11b$^-$, CD64$^+$, SiglecF$^+$, and AF$^+$), CD103$^+$DCs (CD11c$^+$, CD11b$^-$, CD24$^+$, CD103$^+$, and MHCII$^+$), pDCs (CD11c$^+$, CD11b$^-$, CD24$^+$, CD103$^-$, and MHCII$^+$), cDCs (CD11c$^+$, CD11b$^+$, CD64$^-$, CD24$^+$, and MHCII$^+$), mDCs (CD11c$^+$, CD11b$^+$, CD24$^-$, CD64$^+$, AF$^-$, MHCII^{high}, and Ly6C$^{+/-}$), and ExMs (CD11c$^+$, CD11b$^+$, CD24$^-$, CD64$^+$, AF$^+$, MHCII$^+$, and Ly6C$^{+/-}$).

DCs are CD11b$^+$, CD11c$^+$, CD24$^-$, MHCII$^+$, and CD64$^+$, we used autofluorescence to distinguish macrophages from DCs (42, 45, 47) (**Figure 4**). This analysis showed comparable recruitment of both cell types between the two strains at day 7 postinfection; however, WT mice had a significantly higher number of inflammatory DCs (days 14 and 21) and ExMs (day 21) compared to IL-1RI$^{-/-}$ mice (**Figures 6C,E**).

The macrophage polarization pattern is also important for protection against cryptococcal infection (8, 48). Classically activated macrophages (M1) that express high levels of pro-inflammatory cytokines and costimulatory molecules, produce high levels of reactive nitrogen and oxygen intermediates, and promote strong IL-12-mediated Th1 responses are efficient killers of *C. neoformans*. In contrast, alternatively activated macrophages (M2) that express chitinase-like 3 (Ym1), found in inflammatory zone (FIZZ1), mannose receptor (CD206), and arginase-1 (Arg1), have reduced pro-inflammatory cytokine secretion and are less microbicidal (3, 9, 42, 43, 47, 49–53). As the number of recruited macrophages peaked at day 14 postinfection in both strains, we characterized polarization at this time point using iNOS and CD206 as representative markers for M1 and M2 macrophages, respectively. At 14 days postinfection, the percentage of M1 macrophages was significantly greater in WT mice compared to IL-1R$^{-/-}$ mice, while the percentage of M2 macrophages was greater in IL-1R$^{-/-}$ compared to WT mice (**Figures 6F,G**). Notably, IL-1RI$^{-/-}$ macrophages showed greater upregulation of the M2-associated marker CD206 at 14 days postinfection (**Figures 6H,I**), while WT macrophages displayed higher expression of the M1-associated marker CD80 (43) at 14 and 21 days postinfection (**Figures 6J,K**). Taken together, these results indicate that IL-1RI signaling has an important role in recruitment of inflammatory DCs and macrophages and increases the ratio of M1/M2-polarized macrophages after *C. neoformans* 52D infection.

T Cells Are the Predominant Sources of IL-17A and IFNγ in WT Lungs Infected with *C. neoformans* 52D

To characterize the mechanism of differential IL-17A and IFNγ expression between WT and IL-1RI$^{-/-}$ lungs, we identified the main sources of these cytokines after *C. neoformans* 52D infection. Compared to IL-1RI$^{-/-}$ mice, WT mice showed significantly more IL-17A-producing cells at 7, 14, and 21 days postinfection and a trend toward a higher number of IFNγ-producing cells at day 21 postinfection (**Figures 7A–C**). Several immune cell types including CD4$^+$ (Th17), CD8$^+$ T (Tc17) cells, NK cells, iNKT cells, γδT cells, B cells, ILCs, DCs, and neutrophils have been shown to produce IL-17 during fungal infection (25, 54–56). In our study, at day 7 postinfection, intracellular cytokine staining of WT lymphocytes showed that CD4$^+$ and γδT cells were the most common IL-17A$^+$ subsets (**Figure 7D**). A similar pattern was observed at

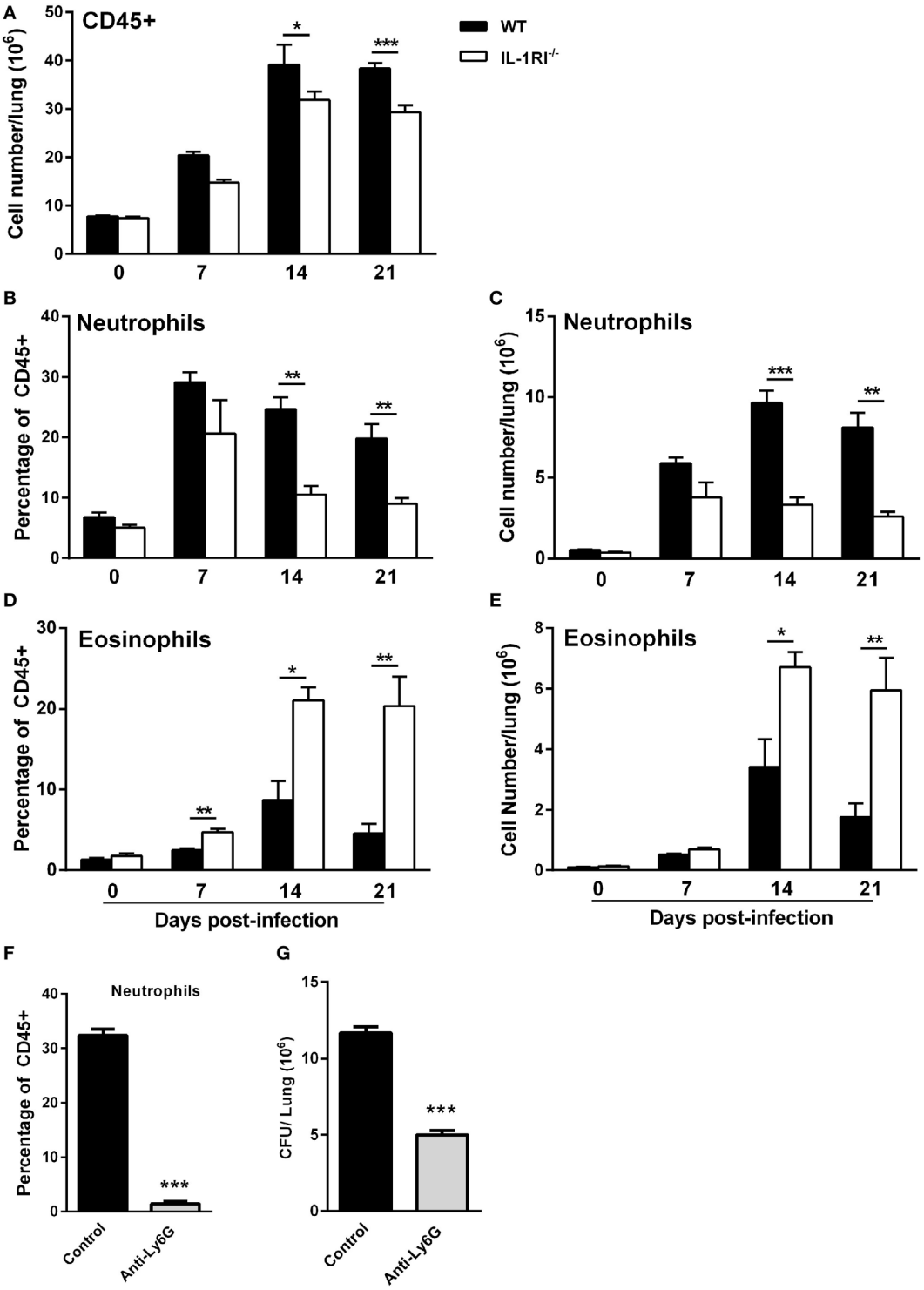

FIGURE 5 | Interleukin-1 receptor type I-deficient (IL-1RI$^{-/-}$) mice have decreased neutrophil and increased eosinophil recruitment to the lungs after *Cryptococcus neoformans* 52D infection. Lung cell suspensions from uninfected and infected wild-type (WT) and IL-1RI$^{-/-}$ mice were stained with fluorochrome-labeled antibodies and analyzed by flow cytometry as described in Section "Materials and Methods." **(A)** Absolute numbers of total CD45^{+} cells in the lungs at 0, 7, 14, and 21 days postinfection. **(B–E)** Percentage and total number of neutrophils and eosinophils at 0, 7, 14, and 21 days postinfection. Data are shown as mean ± SEM and representative of two independent experiments (n = 4 mice/strain/time point). $^{*}P \leq 0.05$, $^{**}P \leq 0.01$, and $^{***}P \leq 0.001$. **(F,G)** BALB/c mice underwent intratracheal infection with 1×10^4 CFU of *C. neoformans* strain 52D. Mice were treated with phosphate-buffered saline or anti-Ly6G antibody 1 day prior to infection and daily during the study. At 12 days postinfection, lungs were excised for analysis of neutrophil recruitment and CFU. **(F)** The number of neutrophils and **(G)** fungal burden is shown. Data are pooled from two independent experiments and shown as mean ± SEM (n = 8 mice/group). $^{***}P \leq 0.001$.

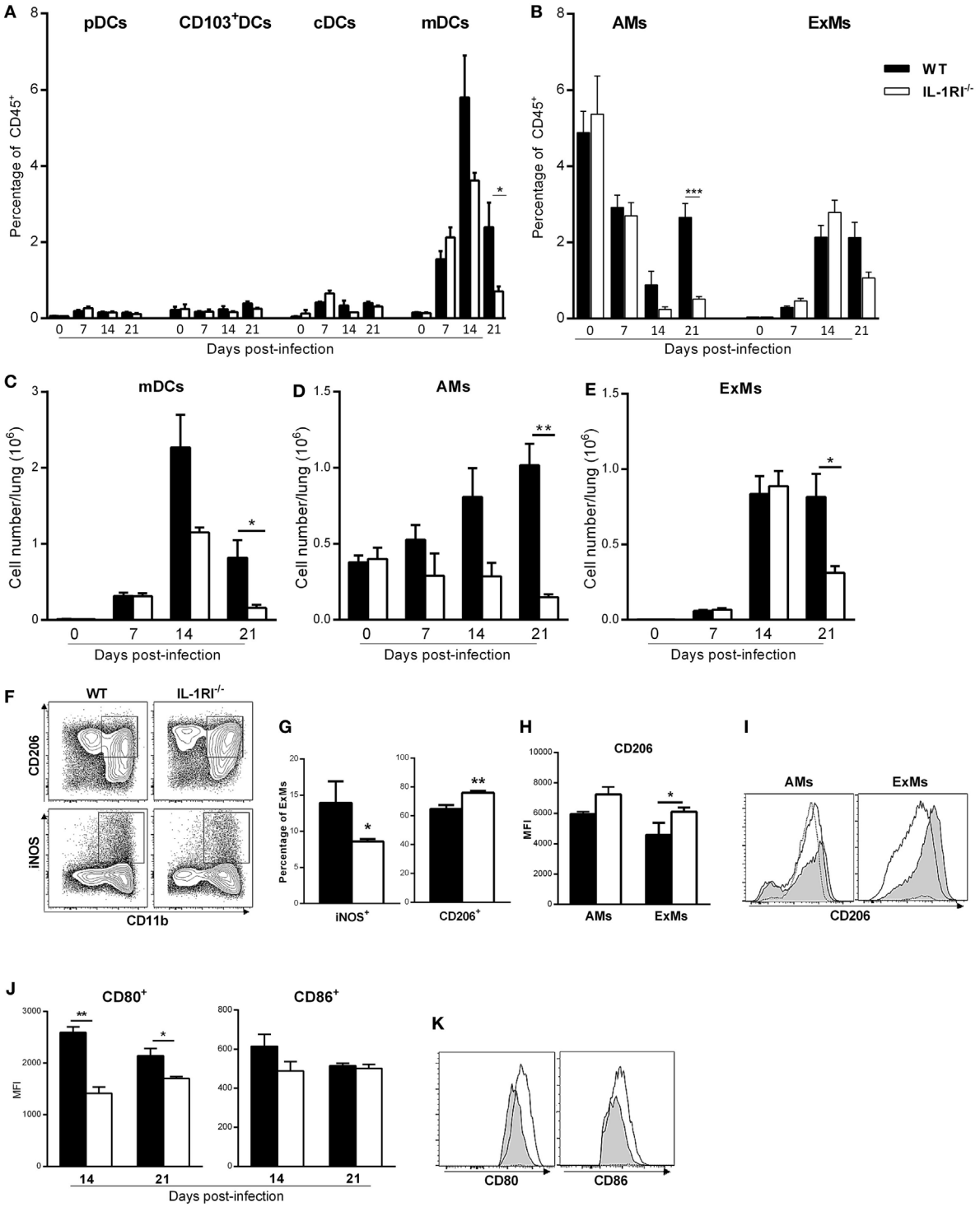

FIGURE 6 | Interleukin-1 receptor type I-deficient (IL-1RI$^{-/-}$) mice have fewer monocyte-derived dendritic cells (DCs) and macrophages in the lungs after *Cryptococcus neoformans* 52D infection. Lung cell suspensions from uninfected and infected mice were stained with fluorochrome-labeled antibodies and analyzed by flow cytometry as described in Section "Materials and Methods." **(A,B)** Percentage of DC and macrophage subsets at 0, 7, 14, and 21 days postinfection. **(C–E)** Total number of mDCs, AMs, and ExMs at 0, 7, 14, and 21 days postinfection. **(F)** Representative plots of M1 (CD11b^{+}, iNOS^{+}) and M2 (CD11b^{+}, CD206^{+}) polarized macrophages in wild-type (WT) and IL-1RI$^{-/-}$ mice at 14 days postinfection. **(G)** Percentage of M1- and M2-polarized macrophages in WT and IL-1RI$^{-/-}$ mice at 14 days postinfection. **(H)** Mean fluorescence intensity (MFI) of CD206 expression on macrophages in WT compared to IL-1RI$^{-/-}$ mice and **(I)** Upregulation of CD206 in AMs and ExMs in IL-1RI$^{-/-}$ compared to WT mice at 14 days postinfection. **(J)** MFI and **(K)** upregulation of CD80- and CD86-positive cells derived from ExMs at 14 days postinfection is shown; **(I,K)** IL-1RI$^{-/-}$, gray filled lines; WT, white filled solid lines; uninfected mice, dashed lines. Data are shown as mean ± SEM and representative of two independent experiments (n = 4 mice/strain/time point). *$P \leq 0.05$, **$P \leq 0.01$, and ***$P \leq 0.001$.

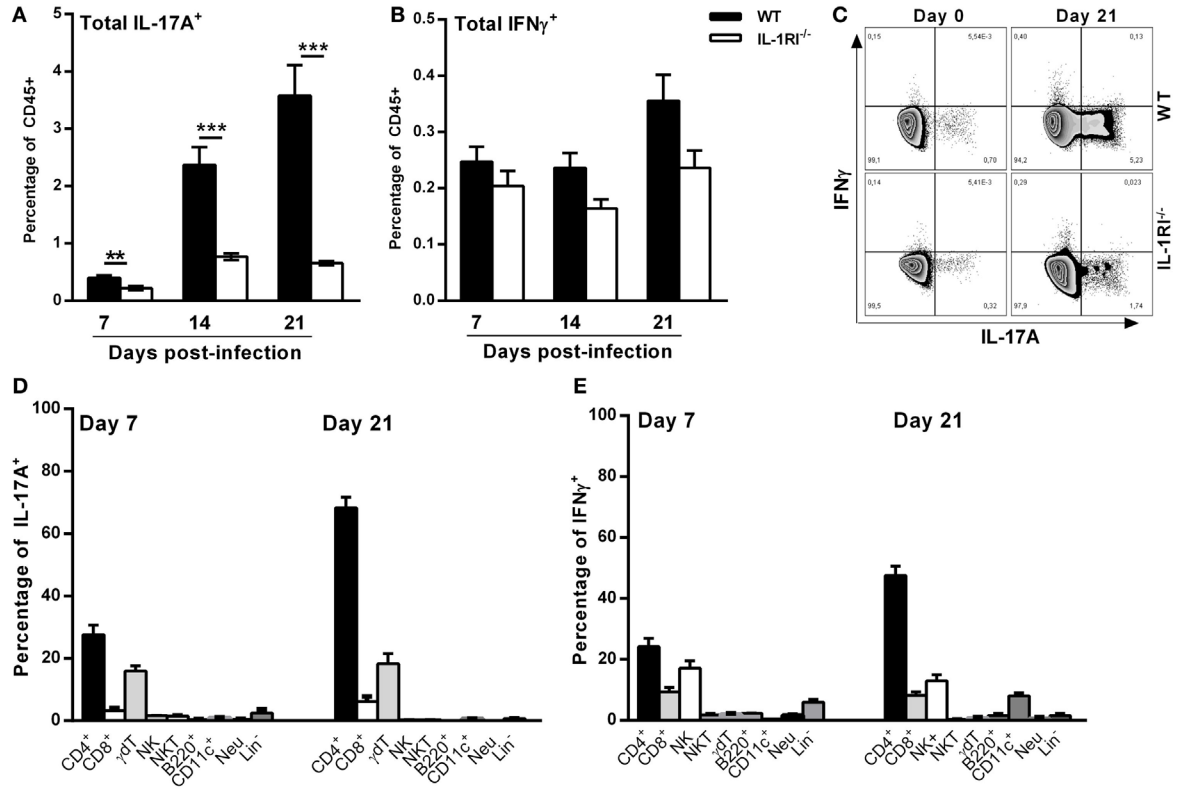

FIGURE 7 | T cells are the predominant sources of interleukin (IL)-17A and IFNγ in BALB/c lungs infected with *Cryptococcus neoformans* 52D. **(A)** Lung cell suspensions from uninfected and infected mice were harvested and restimulated with phorbol 12-myristate 13-acetate (PMA)–ionomycin followed by intracellular staining for IL-17A and IFNγ. **(A,B)** Percentage of total CD45$^+$IFNγ$^+$ and CD45$^+$IL-17A$^+$ cells at 7, 14, and 21 days postinfection. **(C)** Representative flow cytometry plots of lung CD45$^+$ cells from individual mice harvested at 21 days postinfection. **(D,E)** Percentage of IL-17A- and IFNγ-producing cell types in WT mice at 7 and 21 days postinfection is shown. Data are shown as mean ± SEM and representative of two independent experiments (n = 4 mice/strain/time point). $^{**}P \leq 0.01$ and $^{***}P \leq 0.001$.

day 21 postinfection with CD4$^+$ T cells and γδT cells accounting for 60 and 20%, respectively, of IL-17A$^+$ cells. CD4$^+$ and CD8$^+$ T-cells, NK cells, γδT cells, and neutrophils have been shown to produce IFNγ during fungal infection (57–59). In our study, CD4$^+$ T and NK cells were the predominant IFNγ-producing subsets at day 7 and day 21 postinfection (**Figure 7E**).

Effect of IL-1RI Signaling on the Lung Lymphocyte Infiltration following *C. neoformans* 52D Infection

As lymphocytes are necessary for effective clearance of *C. neoformans,* we compared the recruitment of CD4$^+$ or CD8$^+$ T cells, γδT cells, and B cells to the lungs of WT and IL-1RI$^{-/-}$ mice at different time points after infection. Flow cytometry analysis showed that WT mice recruit a significantly higher number of CD4$^+$ cells compared to the IL-1RI$^{-/-}$ strain at 14 and 21 days postinfection (**Figure 8A**). Recruitment of CD8$^+$ T cells was comparable between the two strains at all time points, although WT mice showed a trend toward a higher number of CD8$^+$ T cells at day 21 compared to IL-1RI$^{-/-}$ mice (**Figure 8B**). WT mice demonstrated increased recruitment of γδT cells at day 14 and day 21 postinfection compared to uninfected mice; in contrast, there was no significant increase of this cell type in IL-1RI$^{-/-}$ mice during infection (**Figure 8C**). No differences in the number of B cells recruited to the lungs during infection were observed between the two strains (**Figure 8D**). Taken together, this analysis demonstrates that IL-1RI signaling selectively regulates T lymphocyte recruitment to the lungs during the adaptive phase of immunity against *C. neoformans* 52D infection.

Pulmonary CD4$^+$ T Cells from IL-1RI$^{-/-}$ Mice Display Diminished Th17 and Increased Th2 Cytokine Production following *C. neoformans* Infection

It has been clearly shown that a Th1/Th17 response is protective and a Th2 response is detrimental, respectively, against *C. neoformans* infection (60). To analyze the effect of IL-1R signaling on T cell differentiation during infection, we harvested lungs at serial time points, restimulated the cells with PMA/ionomycin, and stained for intracellular IFNγ, IL-13, and IL-17A as representative cytokines for Th1, Th2, and Th17 polarization states, respectively (**Figure 9**). The results

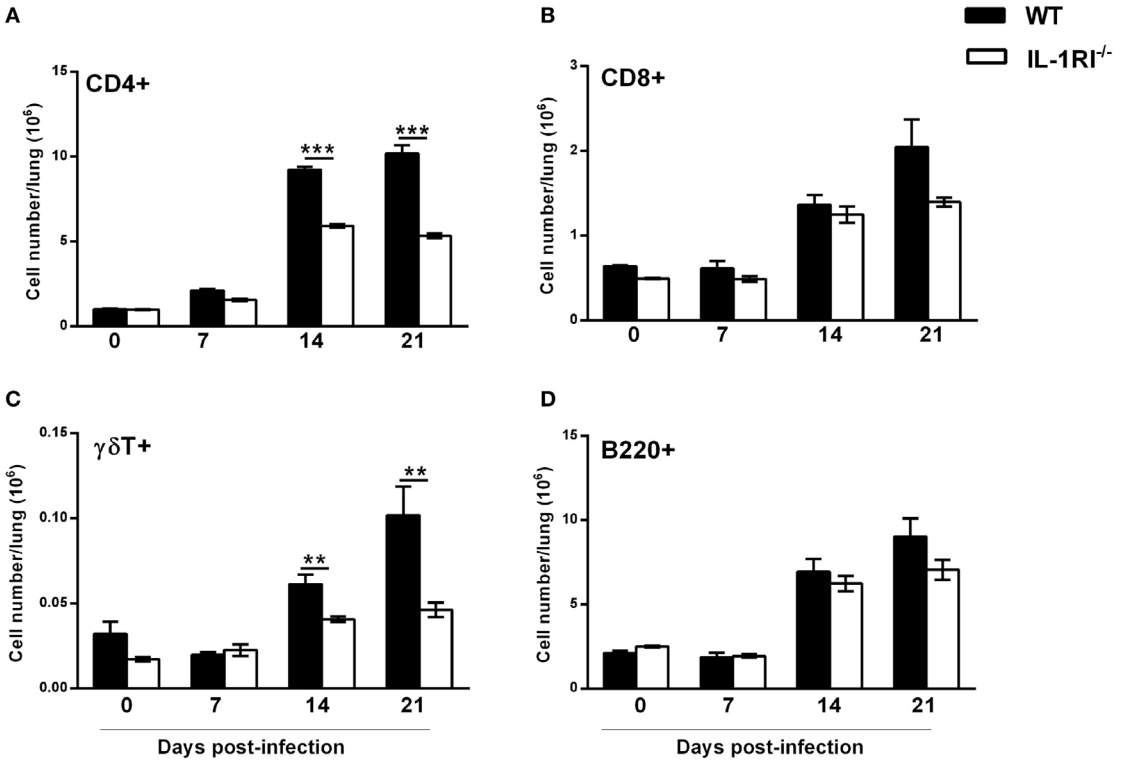

FIGURE 8 | Lungs of interleukin-1 receptor type I-deficient (IL-1RI$^{-/-}$) mice display fewer CD4$^+$ and γδT$^+$ lymphocytes during the adaptive phase of immunity after *Cryptococcus neoformans* 52D infection. Lung cell suspensions from uninfected and infected mice were stained with fluorochrome-labeled antibodies and analyzed by flow cytometry as described in Section "Materials and Methods." **(A–D)** Total number of CD3$^+$CD4$^+$, CD3$^+$CD8$^+$, CD3$^+$γδ$^+$, and B220$^+$ cells in the lungs at 0, 7, 14, and 21 days postinfection. Data are shown as mean ± SEM and representative of two independent experiments (n = 4 mice/strain/time point). $^{**}P \leq 0.01$ and $^{***}P \leq 0.001$.

demonstrated a significantly higher number of CD4$^+$ IFNγ$^+$ cells in the lungs of WT compared to IL-1RI$^{-/-}$ mice at 7 days postinfection with a trend toward more CD4$^+$ IFNγ$^+$ cells at days 14 and 21. Compared to the IL-1RI$^{-/-}$ strain, WT mice showed a trend toward more CD4$^+$ IL-17A$^+$ cells at day 7 with a significant increase of this cell type at days 14 and 21. In contrast, IL-1RI$^{-/-}$ lungs contained a significantly higher percentage of CD4$^+$ IL13$^+$ cells compared to WT lungs at 14 and 21 days postinfection. In summary, these findings demonstrate that after *C. neoformans* infection, IL-1RI signaling significantly increased Th1 differentiation during the early phase of infection and strongly promoted Th17 differentiation during the late phase of infection.

DISCUSSION

Induction of IL-1α/β during mouse cryptococcal infection has been reported, but a clear role for IL-1R-dependent signaling in the host immune response has not been demonstrated (27, 32, 34, 35, 37). Here, we provide evidence that IL-1RI deficiency on the BALB/c background has deleterious effects on the outcome of pulmonary *C. neoformans* 52D infection. The most significant findings of this study are as follows: (1) IL-1RI$^{-/-}$ mice cannot clear moderately virulent *C. neoformans* 52D and develop progressive infection of the lungs and brain resulting in death starting at day 40 postinfection; (2) susceptibility of IL-1RI$^{-/-}$ mice is associated with reduced levels of pro-inflammatory, Th1, and Th17 cytokines; (3) IL-1RI signaling in response to *C. neoformans* 52D infection regulates the recruitment of inflammatory DCs to the lung, contributes to recruitment and M1 polarization of macrophages, and promotes Th1/Th17 differentiation of CD4$^+$ T cells; and (4) lung neutrophil recruitment associated with IL-1R signaling is dispensable for protection against *C. neoformans* 52D infection. Taken together, these data clearly demonstrate that IL-1R-dependent signaling plays a complex and essential role in the control of progressive *C. neoformans* 52D infection.

Previously, intranasal infection of C57BL/6 and IL-1RI$^{-/-}$ mice with 2×10^4 CFU of the virulent *C. neoformans* H99 strain was shown to cause >90% mortality in both groups (37). In the same report, mice lacking MyD88, an intracellular adaptor for IL-1RI, IL-18R, and several Toll-like receptors, had a trend toward reduced survival but no significant difference in fungal burden compared to WT mice after *C. neoformans* challenge (37). Notably, two earlier studies showed that MyD88$^{-/-}$ mice have a significantly shorter survival time and a higher lung fungal burden compared to WT, TLR2$^{-/-}$, and TLR4$^{-/-}$ mice after *C. neoformans* infection (61, 62). These differences may be attributable, at least in part, to variation in the experimental methods that were used including the dose,

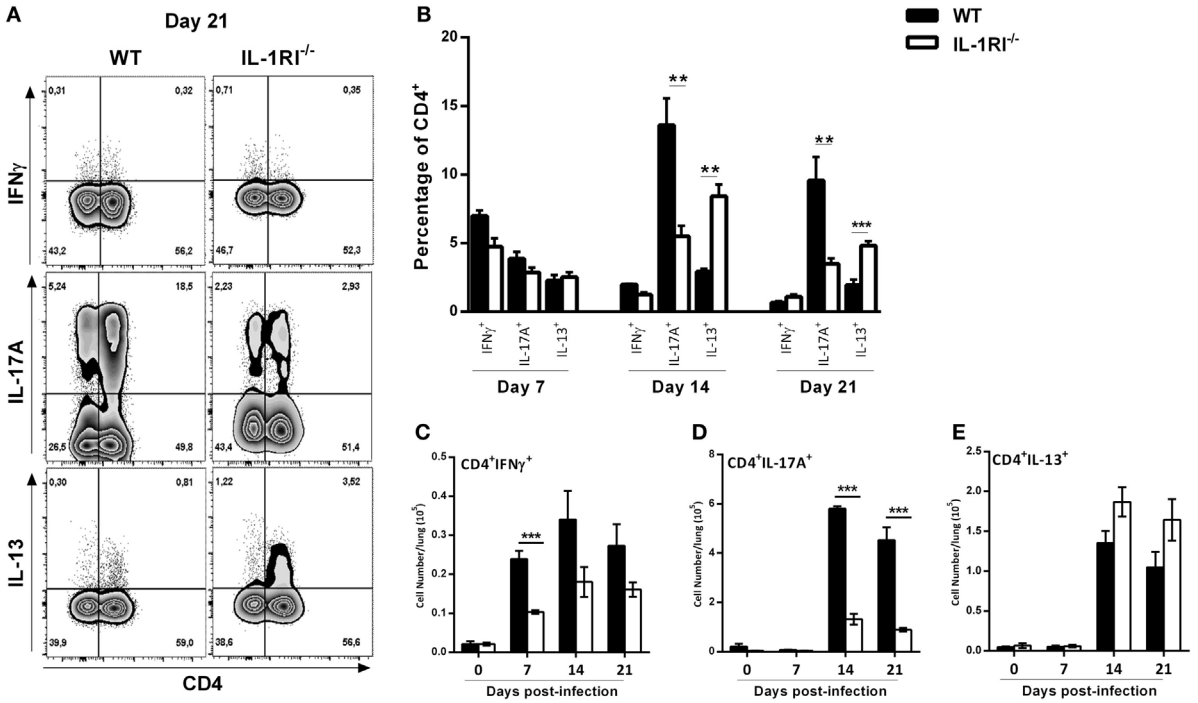

FIGURE 9 | Decreased Th1/Th17 type cytokine expression by CD4+ T cells from interleukin-1 receptor type I-deficient (IL-1RI$^{-/-}$) lungs infected with *Cryptococcus neoformans* 52D. **(A)** Representative flow cytometry plots of lung lymphocytes from individual mice harvested at 14 days postinfection and restimulated with phorbol 12-myristate 13-acetate (PMA)–ionomycin, followed by intracellular staining for IFNγ, IL-17A, and IL-13. **(B)** Percentage and **(C–E)** total numbers of CD4+IFN+, CD4+IL-17A+ and CD4+IL13+ cells are shown. Data are shown as mean ± SEM and representative of two independent experiments (n = 4 mice/strain/time point). *$P \leq 0.05$, **$P \leq 0.01$, and ***$P \leq 0.001$. WT, wild type.

route, and strain of *C. neoformans* (60, 63–65). Furthermore, inbred mouse strains also display marked differences in resistance or susceptibility to a standardized cryptococcal infection, highlighting the importance of the host genetic background in disease pathogenesis (66–68). Our data are consistent with other studies showing that BALB/c mice have a naturally resistant phenotype after respiratory infection with the moderately virulent *C. neoformans* 52D strain. Specifically, BALB/c mice progressively clear pulmonary *C. neoformans* 52D infection in association with numerous hallmarks of a protective Th1 response including tight mononuclear cell infiltrates and classically activated macrophages and do not develop central nervous system dissemination (18, 66, 69, 70). Our observation that both IL-1α and IL-1β were induced in the lungs of BALB/c mice after intratracheal infection with *C. neoformans* 52D is also consistent with earlier reports that associated the induction of IL-1β in lung and brain with resistance to cryptococcal infection (35, 71, 72).

Interleukin-1 is a central mediator of inflammation and links innate and adaptive immune response mechanisms (73). Binding of IL-1α or IL-1β to IL-1RI is followed by the recruitment of the IL-1 receptor accessory protein (IL-1RAcP) and activation of signal transduction pathways that induce the expression of IL-1 responsive genes including IL-6, MCP-1, and TNFα (74–77). Induction of pro-inflammatory cytokines followed by generation of a Th1 adaptive immune response is critical for control of cryptococcosis (8, 11, 78). Compared to the BALB/c strain, IL-1RI$^{-/-}$ mice had significantly reduced expression of KC, TNFα, and MCP-1 that was associated with increased lung fungal burden at day 7 after infection. TNFα is one of the main target genes of the IL-1 signaling cascade (76, 77), and both mediators share downstream pathways that induce pro-inflammatory gene expression (79, 80). TNFα signaling in the afferent phase of cryptococcal infection is associated with optimal DC activation and induction of Th1/Th17 polarization and protective immunity (78, 81–84). MCP1/CCR2 signaling is also responsible for the recruitment of inflammatory DCs and macrophages after cryptococcal infection (45, 46, 85). Thus, the reduced expression of pro-inflammatory cytokines and chemokines is one mechanism that could explain the susceptibility of IL-1RI$^{-/-}$ mice to progressive cryptococcosis.

After *C. neoformans* infection, DCs phagocytose and kill cryptococci by oxidative and non-oxidative mechanisms, play an important role in antigen presentation, and drive protective immune responses by secreting cytokines and chemokines (86–89). Compared to other innate cell types, lung DCs express a high level of IL-1RI and signaling *via* this receptor has been shown to promote the maturation and survival of pulmonary DCs and their CCR7-dependent migration to lymph nodes after Influenza A infection (90). At 21 days postinfection with *C. neoformans*, the total number of moDCs in the lung was significantly lower in IL-1RI$^{-/-}$ compared to WT mice, suggesting that recruitment and activation of DCs in the LALNs may be regulated by IL-1R signaling in this model. In addition to DCs, inflammatory macrophages

that strongly express microbicidal enzymes such as iNOS play a significant role in fungal clearance (45, 46, 69, 91). After *C. neoformans* 52D infection, we observed that lung macrophages of IL-1R$^{-/-}$ mice had reduced expression of the classical activation markers CD80 and iNOS and increased expression of the alternative activation marker CD206 compared to WT, a pattern that is associated with reduced fungal killing capacity. Our findings are similar to a recent study in BALB/c mice infected with *C. neoformans* 52D that correlated an elevated ratio of Arg1/iNOS expression with an increase in fungal burden and showed a reversal of this ratio during the subsequent period of fungal clearance (48).

In addition to monocyte-derived macrophages and DCs, significantly greater neutrophil recruitment was observed in WT compared to IL-1R$^{-/-}$ lungs. Both IL-1α and IL-1β can promote neutrophil migration (92–95), and diminished neutrophil recruitment to the site of infection due to IL-1R deficiency has been associated with increased susceptibility to several bacterial and fungal infections including *Legionella pneumophila*, Group B *Streptococcus*, *Citrobacter rodentium*, and *Candida albicans* (55, 96–100). Inbred mouse strains including SJL/J, CBA/J, and BALB/c are naturally resistant to pulmonary cryptococcal infection and exhibit substantial neutrophil recruitment the lungs; however, the importance of these cells in host protection is not clear (35, 67, 68). For example, an early study of BALB/c mice given a single injection of anti-Gr-1 (anti-Ly6C/6G) antibody showed less inflammatory damage and significantly longer survival compared to controls after *C. neoformans* 52D infection (101). A subsequent study of BALB/c mice that had undergone prior immunization with *C. neoformans* strain H99γ showed that neutrophil depletion with a specific anti-Ly6G antibody did not affect pulmonary fungal burden (102). Finally, a recent report showed that profound neutrophilia in type 2-deficient STAT6$^{-/-}$ mice on a C57BL/6 background was associated with immunopathology and exacerbation of cryptococcal disease (103). To specifically analyze the contribution of neutrophils to resistance against *C. neoformans* 52D, we used anti-Ly6G to deplete these cells in WT BALB/c mice throughout the course of infection (104, 105). In the absence of neutrophil recruitment, we observed a significantly lower lung fungal burden at 12 days postinfection compared to controls. This finding suggests that, despite their abundance in the lung, neutrophils may have a detrimental effect on host defense against moderately virulent *C. neoformans* 52D (101). Several mechanisms may explain this observation, including competition for cryptococcal antigen between neutrophils and antigen-presenting cells, neutrophil secretion of the immunosuppressive cytokine TGFβ1, or production of IL-1 receptor antagonist, a molecule that inhibits IL-1R signaling (100, 106–110). Further research is necessary to precisely establish the physiological mechanisms that control neutrophil recruitment during cryptococcal infection and to determine whether these cells make a positive contribution to host resistance.

Along with reduced pro-inflammatory cytokines, IL-1R$^{-/-}$ mice showed diminished levels of lung IFNγ compared to WT mice at the early (day 7) and late (days 14 and 21) phases of infection. Intracellular cytokine staining identified CD4$^+$ lymphocytes as the most prominent IFNγ-producing cell type. As very few studies have identified IL-1R expression on Th1 cells (111), induction of IFNγ expression by CD4$^+$ T cells appears to be an indirect effect of IL-1RI signaling on DCs and possibly other cell types (90). IFNγ plays a central role in host defense against cryptococci by enhancing the fungal internalization and killing by phagocytes (78, 83). An important role for early IFNγ secretion and the development of a Th1 response against *C. neoformans* 52D infection was previously shown in resistant C.B-17 mice (a BALB/c strain congenic for C57BL/6 immunoglobulin heavy chain gene segment), whereas the absence of this response in the C57BL/6 strain correlated with susceptibility (11).

IL-1 is known to regulate the expression of the transcription factors IRF4 and RORγt, both of which play a major role in the induction of CD4$^+$IL-17$^+$ (Th17) cells in mice and humans (112–114). IL-1 signaling has been shown to be essential for the development of Th17 immunity to infection with *Coccidioides sp* (115), and mice with deletions of IL-17 or IL-17R are susceptible to candidiasis, pulmonary aspergillosis, and histoplasmosis (55). The role of IL-17 during cryptococcal infection has been analyzed using mice with a C57BL/6 genetic background. In one study, IL-17RA deficiency did not impair pulmonary clearance of *C. neoformans* 52D at 1 or 6 weeks postinfection nor did it alter survival compared to WT mice (116). Another study using IL-17A-deficient mice showed that this cytokine does contribute to fungal clearance from the lung but was not essential for 8-week survival (19). In contrast, administration of IL-23, which is essential for the differentiation of Th17 lymphocytes, led to prolonged survival and reduced fungal burden in C57BL/6 mice (22). A Th17-polarized immune response appears to facilitate the resolution of *C. neoformans* 52D infection through several mechanisms including lung recruitment of activated DCs and inflammatory macrophages, induction of IFNγ-producing CD4$^+$ and CD8$^+$ T cells, and enhanced fungal containment within macrophages (19–22). Compared to BALB/c, IL-1R$^{-/-}$ mice display several phenotypes that may be attributable to a diminished Th17 response including reduced recruitment of DCs and inflammatory macrophages and increased recruitment of eosinophils and CD4$^+$IL-13$^+$ cells to the lungs. On the basis of marked difference between WT and IL-1R$^{-/-}$ mice, we speculate that IL-17 plays a non-redundant role in survival after *C. neoformans* 52D infection; however, studies of BALB/c mice that are deficient for IL-17 or IL-17RA would be required to formally test this hypothesis.

In mouse models, IL-1 signaling is protective against infection with a wide spectrum of intracellular pathogens including *Leishmania amazonensis*, *Mycobacterium avium*, *Toxoplasma gondii*, and *Listeria monocytogenes* (117–121). IL-1RI-deficient mice are also highly susceptible to pulmonary challenge with *Aspergillus fumigatus*; in this model, IL-1α has been shown to be crucial for optimal leukocyte recruitment and IL-1β has been shown to be essential for optimal activation of macrophage antifungal activity (122). It has been suggested that polymorphisms in the IL-1 gene cluster might be important in susceptibility or resistance to invasive pulmonary aspergillosis in humans (123, 124). Both IL-1α and IL-1β have also been shown to play an important role in disseminated candidiasis (125–128), and IL-1 signaling has shown to contribute to host resistance against pulmonary histoplasmosis and *Coccidioides sp.* infection (115, 129). This study expands the role of IL-1 in host defense

by demonstrating that IL-1R$^{-/-}$ mice on the Balb/c background are highly susceptible to progressive *C. neoformans* 52D infection of the lungs and brain. IL-1R deficiency in this model results in impaired Th1/Th17 responses and the development of a Th2-biased adaptive immune response. As IL-1α and IL-1β are equally potent activators of IL-1RI signaling yet have different tissue distribution and activation kinetics, future studies that characterize mice that are deficient in either IL-1α or IL-1β or the study of specific cytokine-deficient animals would provide valuable insights into the specific contributions of each cytokine to the development of protective immunity against *C. neoformans* infection.

ETHICS STATEMENT

This study was carried out in accordance with the recommendations of the Canadian Council on Animal Care guidelines. The protocol was approved by the McGill University Animal Care Committee.

AUTHOR CONTRIBUTIONS

MS conceived and performed experiments and wrote/edited the manuscript for important intellectual content. BR and IA performed experiments and edited the manuscript for important intellectual content. DS provided reagents and edited the manuscript for important intellectual content. SQ conceived, designed, and supervised the study and wrote/edited the manuscript for important intellectual content.

ACKNOWLEDGMENTS

We thank the histology core facility of the Bellini Life Sciences Complex for assistance with lung tissue preparation and staining.

FUNDING

This work was supported by grants to the Research Institute of the McGill University Health Centre and a Research Chair (DS) from the Fonds de Recherche Santé Quebec, the Canadian Institutes of Health Research to SQ (MOP-102494) and DS (MOP-81361 and MOP-123306), the Costello Memorial Research Fund (SQ), and the Research Institute and Department of Critical Care of the McGill University Health Centre (SQ).

REFERENCES

1. Rajasingham R, Smith RM, Park BJ, Jarvis JN, Govender NP, Chiller TM, et al. Global burden of disease of HIV-associated cryptococcal meningitis: an updated analysis. *Lancet Infect Dis* (2017) 17(8):873–81. doi:10.1016/S1473-3099(17)30243-8
2. Adams P. Cryptococcal meningitis: a blind spot in curbing AIDS. *Lancet* (2016) 387(10028):1605–6. doi:10.1016/S0140-6736(16)30250-1
3. Hole C, Wormley FL Jr. Innate host defenses against *Cryptococcus neoformans*. *J Microbiol* (2016) 54(3):202–11. doi:10.1007/s12275-016-5625-7
4. Neofytos D, Fishman JA, Horn D, Anaissie E, Chang CH, Olyaei A, et al. Epidemiology and outcome of invasive fungal infections in solid organ transplant recipients. *Transpl Infect Dis* (2010) 12(3):220–9. doi:10.1111/j.1399-3062.2010.00492.x
5. Pappas PG. Cryptococcal infections in non-HIV-infected patients. *Trans Am Clin Climatol Assoc* (2013) 124:61–79.
6. Brizendine KD, Baddley JW, Pappas PG. Predictors of mortality and differences in clinical features among patients with Cryptococcosis according to immune status. *PLoS One* (2013) 8(3):e60431. doi:10.1371/journal.pone.0060431
7. Panackal AA, Wuest SC, Lin YC, Wu T, Zhang N, Kosa P, et al. Paradoxical immune responses in non-HIV cryptococcal meningitis. *PLoS Pathog* (2015) 11(5):e1004884. doi:10.1371/journal.ppat.1004884
8. Arora S, Olszewski MA, Tsang TM, McDonald RA, Toews GB, Huffnagle GB. Effect of cytokine interplay on macrophage polarization during chronic pulmonary infection with *Cryptococcus neoformans*. *Infect Immun* (2011) 79(5):1915–26. doi:10.1128/IAI.01270-10
9. Leopold Wager CM, Wormley FL Jr. Classical versus alternative macrophage activation: the Ying and the Yang in host defense against pulmonary fungal infections. *Mucosal Immunol* (2014) 7(5):1023–35. doi:10.1038/mi.2014.65
10. Koguchi Y, Kawakami K. Cryptococcal infection and Th1-Th2 cytokine balance. *Int Rev Immunol* (2002) 21(4–5):423–38. doi:10.1080/08830180213274
11. Hoag KA, Street NE, Huffnagle GB, Lipscomb MF. Early cytokine production in pulmonary *Cryptococcus neoformans* infections distinguishes susceptible and resistant mice. *Am J Respir Cell Mol Biol* (1995) 13(4):487–95. doi:10.1165/ajrcmb.13.4.7546779
12. Chen GH, McDonald RA, Wells JC, Huffnagle GB, Lukacs NW, Toews GB. The gamma interferon receptor is required for the protective pulmonary inflammatory response to *Cryptococcus neoformans*. *Infect Immun* (2005) 73(3):1788–96. doi:10.1128/IAI.73.3.1788-1796.2005
13. Hoag KA, Lipscomb MF, Izzo AA, Street NE. IL-12 and IFN-gamma are required for initiating the protective Th1 response to pulmonary cryptococcosis in resistant C.B-17 mice. *Am J Respir Cell Mol Biol* (1997) 17(6):733–9. doi:10.1165/ajrcmb.17.6.2879
14. Kawakami K, Qureshi MH, Zhang T, Koguchi Y, Shibuya K, Naoe S, et al. Interferon-gamma (IFN-gamma)-dependent protection and synthesis of chemoattractants for mononuclear leucocytes caused by IL-12 in the lungs of mice infected with *Cryptococcus neoformans*. *Clin Exp Immunol* (1999) 117(1):113–22. doi:10.1046/j.1365-2249.1999.00955.x
15. Pietrella D, Lupo P, Bistoni F, Vecchiarelli A. An early imbalance of interleukin 12 influences the adjuvant effect of mannoproteins of *Cryptococcus neoformans*. *Cell Microbiol* (2004) 6(9):883–91. doi:10.1111/j.1462-5822.2004.00411.x
16. Blackstock R, Murphy JW. Role of interleukin-4 in resistance to *Cryptococcus neoformans* infection. *Am J Respir Cell Mol Biol* (2004) 30(1):109–17. doi:10.1165/rcmb.2003-0156OC
17. Muller U, Stenzel W, Kohler G, Werner C, Polte T, Hansen G, et al. IL-13 induces disease-promoting type 2 cytokines, alternatively activated macrophages and allergic inflammation during pulmonary infection of mice with *Cryptococcus neoformans*. *J Immunol* (2007) 179(8):5367–77. doi:10.4049/jimmunol.179.8.5367
18. Jain AV, Zhang Y, Fields WB, McNamara DA, Choe MY, Chen GH, et al. Th2 but not Th1 immune bias results in altered lung functions in a murine model of pulmonary *Cryptococcus neoformans* infection. *Infect Immun* (2009) 77(12):5389–99. doi:10.1128/IAI.00809-09
19. Murdock BJ, Huffnagle GB, Olszewski MA, Osterholzer JJ. Interleukin-17A enhances host defense against cryptococcal lung infection through effects mediated by leukocyte recruitment, activation, and gamma interferon production. *Infect Immun* (2014) 82(3):937–48. doi:10.1128/IAI.01477-13
20. Valdez PA, Vithayathil PJ, Janelsins BM, Shaffer AL, Williamson PR, Datta SK. Prostaglandin E2 suppresses antifungal immunity by inhibiting interferon regulatory factor 4 function and interleukin-17 expression in T cells. *Immunity* (2012) 36(4):668–79. doi:10.1016/j.immuni.2012.02.013
21. Zhang Y, Wang F, Tompkins KC, McNamara A, Jain AV, Moore BB, et al. Robust Th1 and Th17 immunity supports pulmonary clearance but cannot prevent systemic dissemination of highly virulent *Cryptococcus*

neoformans H99. *Am J Pathol* (2009) 175(6):2489–500. doi:10.2353/ajpath.2009.090530
22. Kleinschek MA, Muller U, Schutze N, Sabat R, Straubinger RK, Blumenschein WM, et al. Administration of IL-23 engages innate and adaptive immune mechanisms during fungal infection. *Int Immunol* (2010) 22(2):81–90. doi:10.1093/intimm/dxp117
23. Kleinschek MA, Muller U, Brodie SJ, Stenzel W, Kohler G, Blumenschein WM, et al. IL-23 enhances the inflammatory cell response in *Cryptococcus neoformans* infection and induces a cytokine pattern distinct from IL-12. *J Immunol* (2006) 176(2):1098–106. doi:10.4049/jimmunol.176.2.1098
24. Hardison SE, Wozniak KL, Kolls JK, Wormley FL Jr. Interleukin-17 is not required for classical macrophage activation in a pulmonary mouse model of *Cryptococcus neoformans* infection. *Infect Immun* (2010) 78(12):5341–51. doi:10.1128/IAI.00845-10
25. Wozniak KL, Hardison SE, Kolls JK, Wormley FL. Role of IL-17A on resolution of pulmonary *C. neoformans* infection. *PLoS One* (2011) 6(2):e17204. doi:10.1371/journal.pone.0017204
26. Marais S, Meintjes G, Lesosky M, Wilkinson KA, Wilkinson RJ. Interleukin-17 mediated differences in the pathogenesis of HIV-1-associated tuberculous and cryptococcal meningitis. *AIDS* (2016) 30(3):395–404. doi:10.1097/QAD.0000000000000904
27. Vecchiarelli A, Retini C, Pietrella D, Monari C, Tascini C, Beccari T, et al. Downregulation by cryptococcal polysaccharide of tumor necrosis factor alpha and interleukin-1 beta secretion from human monocytes. *Infect Immun* (1995) 63(8):2919–23.
28. Retini C, Vecchiarelli A, Monari C, Tascini C, Bistoni F, Kozel TR. Capsular polysaccharide of *Cryptococcus neoformans* induces proinflammatory cytokine release by human neutrophils. *Infect Immun* (1996) 64(8):2897–903.
29. Delfino D, Cianci L, Lupis E, Celeste A, Petrelli ML, Curro F, et al. Interleukin-6 production by human monocytes stimulated with *Cryptococcus neoformans* components. *Infect Immun* (1997) 65(6):2454–6.
30. Levitz SM, Tabuni A, Kornfeld H, Reardon CC, Golenbock DT. Production of tumor necrosis factor alpha in human leukocytes stimulated by *Cryptococcus neoformans*. *Infect Immun* (1994) 62(5):1975–81.
31. Vecchiarelli A, Retini C, Monari C, Tascini C, Bistoni F, Kozel TR. Purified capsular polysaccharide of *Cryptococcus neoformans* induces interleukin-10 secretion by human monocytes. *Infect Immun* (1996) 64(7):2846–9.
32. Schoffelen T, Illnait-Zaragozi MT, Joosten LA, Netea MG, Boekhout T, Meis JF, et al. *Cryptococcus gattii* induces a cytokine pattern that is distinct from other cryptococcal species. *PLoS One* (2013) 8(1):e55579. doi:10.1371/journal.pone.0055579
33. Marroni M, Pericolini E, Cenci E, Bistoni F, Vecchiarelli A. Functional defect of natural immune system in an apparent immunocompetent patient with pulmonary cryptococcosis. *J Infect* (2007) 54(1):e5–8. doi:10.1016/j.jinf.2006.03.018
34. Chen M, Xing Y, Lu A, Fang W, Sun B, Chen C, et al. Internalized *Cryptococcus neoformans* activates the canonical caspase-1 and the noncanonical caspase-8 inflammasomes. *J Immunol* (2015) 195(10):4962–72. doi:10.4049/jimmunol.1500865
35. Guillot L, Carroll SF, Homer R, Qureshi ST. Enhanced innate immune responsiveness to pulmonary *Cryptococcus neoformans* infection is associated with resistance to progressive infection. *Infect Immun* (2008) 76(10):4745–56. doi:10.1128/IAI.00341-08
36. Subramaniam KS, Datta K, Quintero E, Manix C, Marks MS, Pirofski LA. The absence of serum IgM enhances the susceptibility of mice to pulmonary challenge with *Cryptococcus neoformans*. *J Immunol* (2010) 184(10):5755–67. doi:10.4049/jimmunol.0901638
37. Wang JP, Lee CK, Akalin A, Finberg RW, Levitz SM. Contributions of the MyD88-dependent receptors IL-18R, IL-1R, and TLR9 to host defenses following pulmonary challenge with *Cryptococcus neoformans*. *PLoS One* (2011) 6(10):e26232. doi:10.1371/journal.pone.0026232
38. Nakamura K, Miyagi K, Koguchi Y, Kinjo Y, Uezu K, Kinjo T, et al. Limited contribution of Toll-like receptor 2 and 4 to the host response to a fungal infectious pathogen, *Cryptococcus neoformans*. *FEMS Immunol Med Microbiol* (2006) 47(1):148–54. doi:10.1111/j.1574-695X.2006.00078.x
39. Upadhya R, Lam WC, Maybruck B, Specht CA, Levitz SM, Lodge JK. Induction of protective immunity to cryptococcal infection in mice by a heat-killed, chitosan-deficient strain of *Cryptococcus neoformans*. *MBio* (2016) 7(3):e547–516. doi:10.1128/mBio.00547-16
40. Uicker WC, Doyle HA, McCracken JP, Langlois M, Buchanan KL. Cytokine and chemokine expression in the central nervous system associated with protective cell-mediated immunity against *Cryptococcus neoformans*. *Med Mycol* (2005) 43(1):27–38. doi:10.1080/13693780410001731510
41. Lei G, Chen M, Li H, Niu JL, Wu S, Mao L, et al. Biofilm from a clinical strain of *Cryptococcus neoformans* activates the NLRP3 inflammasome. *Cell Res* (2013) 23(7):965–8. doi:10.1038/cr.2013.49
42. Roussey JA, Viglianti SP, Teitz-Tennenbaum S, Olszewski MA, Osterholzer JJ. Anti-PD-1 antibody treatment promotes clearance of persistent cryptococcal lung infection in mice. *J Immunol* (2017) 199(10):3535–46. doi:10.4049/jimmunol.1700840
43. Misharin AV, Morales-Nebreda L, Mutlu GM, Budinger GR, Perlman H. Flow cytometric analysis of macrophages and dendritic cell subsets in the mouse lung. *Am J Respir Cell Mol Biol* (2013) 49(4):503–10. doi:10.1165/rcmb.2013-0086MA
44. Guilliams M, Lambrecht BN, Hammad H. Division of labor between lung dendritic cells and macrophages in the defense against pulmonary infections. *Mucosal Immunol* (2013) 6(3):464–73. doi:10.1038/mi.2013.14
45. Osterholzer JJ, Chen GH, Olszewski MA, Zhang YM, Curtis JL, Huffnagle GB, et al. Chemokine receptor 2-mediated accumulation of fungicidal exudate macrophages in mice that clear cryptococcal lung infection. *Am J Pathol* (2011) 178(1):198–211. doi:10.1016/j.ajpath.2010.11.006
46. Osterholzer JJ, Curtis JL, Polak T, Ames T, Chen GH, McDonald R, et al. CCR2 mediates conventional dendritic cell recruitment and the formation of bronchovascular mononuclear cell infiltrates in the lungs of mice infected with *Cryptococcus neoformans*. *J Immunol* (2008) 181(1):610–20. doi:10.4049/jimmunol.181.1.610
47. Xu J, Flaczyk A, Neal LM, Fa Z, Cheng D, Ivey M, et al. Exploitation of scavenger receptor, macrophage receptor with collagenous structure, by *Cryptococcus neoformans* promotes alternative activation of pulmonary lymph node CD11b(+) conventional dendritic cells and non-protective Th2 bias. *Front Immunol* (2017) 8:1231. doi:10.3389/fimmu.2017.01231
48. Davis MJ, Tsang TM, Qiu Y, Dayrit JK, Freij JB, Huffnagle GB, et al. Macrophage M1/M2 polarization dynamically adapts to changes in cytokine microenvironments in *Cryptococcus neoformans* infection. *MBio* (2013) 4(3):e264–213. doi:10.1128/mBio.00264-13
49. Sica A, Mantovani A. Macrophage plasticity and polarization: in vivo veritas. *J Clin Invest* (2012) 122(3):787–95. doi:10.1172/JCI59643
50. Murray PJ, Allen JE, Biswas SK, Fisher EA, Gilroy DW, Goerdt S, et al. Macrophage activation and polarization: nomenclature and experimental guidelines. *Immunity* (2014) 41(1):14–20. doi:10.1016/j.immuni.2014.06.008
51. May RC, Stone NR, Wiesner DL, Bicanic T, Nielsen K. Cryptococcus: from environmental saprophyte to global pathogen. *Nat Rev Microbiol* (2016) 14(2):106–17. doi:10.1038/nrmicro.2015.6
52. Mantovani A, Sica A, Sozzani S, Allavena P, Vecchi A, Locati M. The chemokine system in diverse forms of macrophage activation and polarization. *Trends Immunol* (2004) 25(12):677–86. doi:10.1016/j.it.2004.09.015
53. Mantovani A, Sozzani S, Locati M, Allavena P, Sica A. Macrophage polarization: tumor-associated macrophages as a paradigm for polarized M2 mononuclear phagocytes. *Trends Immunol* (2002) 23(11):549–55. doi:10.1016/S1471-4906(02)02302-5
54. Veldhoen M. Interleukin 17 is a chief orchestrator of immunity. *Nat Immunol* (2017) 18(6):612–21. doi:10.1038/ni.3742
55. Underhill DM, Pearlman E. Immune interactions with pathogenic and commensal fungi: a two-way street. *Immunity* (2015) 43(5):845–58. doi:10.1016/j.immuni.2015.10.023
56. Gladiator A, Wangler N, Trautwein-Weidner K, LeibundGut-Landmann S. Cutting edge: IL-17-secreting innate lymphoid cells are essential for host defense against fungal infection. *J Immunol* (2013) 190(2):521–5. doi:10.4049/jimmunol.1202924
57. Gozalbo D, Gil ML. IFN-gamma in *Candida albicans* infections. *Front Biosci (Landmark Ed)* (2009) 14:1970–8. doi:10.2741/3356
58. Romani L. Immunity to fungal infections. *Nat Rev Immunol* (2011) 11(4):275–88. doi:10.1038/nri2939
59. Rodrigues DR, Fernandes RK, Balderramas Hde A, Penitenti M, Bachiega TF, Calvi SA, et al. Interferon-gamma production by human neutrophils upon stimulation by IL-12, IL-15 and IL-18 and challenge with *Paracoccidioides brasiliensis*. *Cytokine* (2014) 69(1):102–9. doi:10.1016/j.cyto.2014.05.009

60. Voelz K, May RC. Cryptococcal interactions with the host immune system. *Eukaryot Cell* (2010) 9(6):835–46. doi:10.1128/EC.00039-10
61. Biondo C, Midiri A, Messina L, Tomasello F, Garufi G, Catania MR, et al. MyD88 and TLR2, but not TLR4, are required for host defense against *Cryptococcus neoformans*. *Eur J Immunol* (2005) 35(3):870–8. doi:10.1002/eji.200425799
62. Yauch LE, Mansour MK, Shoham S, Rottman JB, Levitz SM. Involvement of CD14, toll-like receptors 2 and 4, and MyD88 in the host response to the fungal pathogen *Cryptococcus neoformans* in vivo. *Infect Immun* (2004) 72(9):5373–82. doi:10.1128/IAI.72.9.5373-5382.2004
63. Olszewski MA, Zhang Y, Huffnagle GB. Mechanisms of cryptococcal virulence and persistence. *Future Microbiol* (2010) 5(8):1269–88. doi:10.2217/fmb.10.93
64. Urai M, Kaneko Y, Ueno K, Okubo Y, Aizawa T, Fukazawa H, et al. Evasion of innate immune responses by the highly virulent *Cryptococcus gattii* by altering capsule glucuronoxylomannan structure. *Front Cell Infect Microbiol* (2015) 5:101. doi:10.3389/fcimb.2015.00101
65. Montone KT. Regulating the T-cell immune response toward the H99 strain of *Cryptococcus neoformans*. *Am J Pathol* (2009) 175(6):2255–6. doi:10.2353/ajpath.2009.090891
66. Chen GH, McNamara DA, Hernandez Y, Huffnagle GB, Toews GB, Olszewski MA. Inheritance of immune polarization patterns is linked to resistance versus susceptibility to *Cryptococcus neoformans* in a mouse model. *Infect Immun* (2008) 76(6):2379–91. doi:10.1128/IAI.01143-07
67. Carroll SF, Lafferty EI, Flaczyk A, Fujiwara TM, Homer R, Morgan K, et al. Susceptibility to progressive *Cryptococcus neoformans* pulmonary infection is regulated by loci on mouse chromosomes 1 and 9. *Infect Immun* (2012) 80(12):4167–76. doi:10.1128/IAI.00417-12
68. Shourian M, Flaczyk A, Angers I, Mindt BC, Fritz JH, Qureshi ST. The Cnes2 locus on mouse chromosome 17 regulates host defense against cryptococcal infection through pleiotropic effects on host immunity. *Infect Immun* (2015) 83(12):4541–54. doi:10.1128/IAI.00697-15
69. Zhang Y, Wang F, Bhan U, Huffnagle GB, Toews GB, Standiford TJ, et al. TLR9 signaling is required for generation of the adaptive immune protection in *Cryptococcus neoformans*-infected lungs. *Am J Pathol* (2010) 177(2):754–65. doi:10.2353/ajpath.2010.091104
70. Zaragoza O, Alvarez M, Telzak A, Rivera J, Casadevall A. The relative susceptibility of mouse strains to pulmonary *Cryptococcus neoformans* infection is associated with pleiotropic differences in the immune response. *Infect Immun* (2007) 75(6):2729–39. doi:10.1128/IAI.00094-07
71. Blasi E, Barluzzi R, Mazzolla R, Pitzurra L, Puliti M, Saleppico S, et al. Biomolecular events involved in anticryptococcal resistance in the brain. *Infect Immun* (1995) 63(4):1218–22.
72. Maffei CM, Mirels LF, Sobel RA, Clemons KV, Stevens DA. Cytokine and inducible nitric oxide synthase mRNA expression during experimental murine cryptococcal meningoencephalitis. *Infect Immun* (2004) 72(4):2338–49. doi:10.1128/IAI.72.4.2338-2349.2004
73. Garlanda C, Dinarello CA, Mantovani A. The interleukin-1 family: back to the future. *Immunity* (2013) 39(6):1003–18. doi:10.1016/j.immuni.2013.11.010
74. Weber A, Wasiliew P, Kracht M. Interleukin-1 (IL-1) pathway. *Sci Signal* (2010) 3(105):cm1. doi:10.1126/scisignal.3105cm1
75. Casanova JL, Abel L, Quintana-Murci L. Human TLRs and IL-1Rs in host defense: natural insights from evolutionary, epidemiological, and clinical genetics. *Annu Rev Immunol* (2011) 29:447–91. doi:10.1146/annurev-immunol-030409-101335
76. O'Neill LA, Dinarello CA. The IL-1 receptor/toll-like receptor superfamily: crucial receptors for inflammation and host defense. *Immunol Today* (2000) 21(5):206–9. doi:10.1016/S0167-5699(00)01611-X
77. Bethea JR, Gillespie GY, Benveniste EN. Interleukin-1 beta induction of TNF-alpha gene expression: involvement of protein kinase C. *J Cell Physiol* (1992) 152(2):264–73. doi:10.1002/jcp.1041520207
78. Herring AC, Lee J, McDonald RA, Toews GB, Huffnagle GB. Induction of interleukin-12 and gamma interferon requires tumor necrosis factor alpha for protective T1-cell-mediated immunity to pulmonary *Cryptococcus neoformans* infection. *Infect Immun* (2002) 70(6):2959–64. doi:10.1128/IAI.70.6.2959-2964.2002
79. Dinarello CA. Anti-cytokine therapies in response to systemic infection. *J Investig Dermatol Symp Proc* (2001) 6(3):244–50. doi:10.1046/j.0022-202x.2001.00046.x
80. Saperstein S, Chen L, Oakes D, Pryhuber G, Finkelstein J. IL-1beta augments TNF-alpha-mediated inflammatory responses from lung epithelial cells. *J Interferon Cytokine Res* (2009) 29(5):273–84. doi:10.1089/jir.2008.0076
81. Kawakami K, Qifeng X, Tohyama M, Qureshi MH, Saito A. Contribution of tumour necrosis factor-alpha (TNF-alpha) in host defence mechanism against *Cryptococcus neoformans*. *Clin Exp Immunol* (1996) 106(3):468–74. doi:10.1046/j.1365-2249.1996.d01-870.x
82. Milam JE, Herring-Palmer AC, Pandrangi R, McDonald RA, Huffnagle GB, Toews GB. Modulation of the pulmonary type 2 T-cell response to *Cryptococcus neoformans* by intratracheal delivery of a tumor necrosis factor alpha-expressing adenoviral vector. *Infect Immun* (2007) 75(10):4951–8. doi:10.1128/IAI.00176-07
83. Huffnagle GB, Toews GB, Burdick MD, Boyd MB, McAllister KS, McDonald RA, et al. Afferent phase production of TNF-alpha is required for the development of protective T cell immunity to *Cryptococcus neoformans*. *J Immunol* (1996) 157(10):4529–36.
84. Xu J, Eastman AJ, Flaczyk A, Neal LM, Zhao G, Carolan J, et al. Disruption of early tumor necrosis factor alpha signaling prevents classical activation of dendritic cells in lung-associated lymph nodes and development of protective immunity against cryptococcal infection. *MBio* (2016) 7(4):e510–6. doi:10.1128/mBio.00510-16
85. Traynor TR, Kuziel WA, Toews GB, Huffnagle GB. CCR2 expression determines T1 versus T2 polarization during pulmonary *Cryptococcus neoformans* infection. *J Immunol* (2000) 164(4):2021–7. doi:10.4049/jimmunol.164.4.2021
86. Leopold Wager CM, Wormley FL Jr. Is development of a vaccine against *Cryptococcus neoformans* feasible? *PLoS Pathog* (2015) 11(6):e1004843. doi:10.1371/journal.ppat.1004843
87. Wozniak KL, Vyas JM, Levitz SM. In vivo role of dendritic cells in a murine model of pulmonary cryptococcosis. *Infect Immun* (2006) 74(7):3817–24. doi:10.1128/IAI.00317-06
88. Siegemund S, Alber G. *Cryptococcus neoformans* activates bone marrow-derived conventional dendritic cells rather than plasmacytoid dendritic cells and down-regulates macrophages. *FEMS Immunol Med Microbiol* (2008) 52(3):417–27. doi:10.1111/j.1574-695X.2008.00391.x
89. Syme RM, Spurrell JC, Amankwah EK, Green FH, Mody CH. Primary dendritic cells phagocytose *Cryptococcus neoformans* via mannose receptors and Fcgamma receptor II for presentation to T lymphocytes. *Infect Immun* (2002) 70(11):5972–81. doi:10.1128/IAI.70.11.5972-5981.2002
90. Pang IK, Ichinohe T, Iwasaki A. IL-1R signaling in dendritic cells replaces pattern-recognition receptors in promoting CD8(+) T cell responses to influenza A virus. *Nat Immunol* (2013) 14(3):246–53. doi:10.1038/ni.2514
91. Qiu Y, Zeltzer S, Zhang Y, Wang F, Chen GH, Dayrit J, et al. Early induction of CCL7 downstream of TLR9 signaling promotes the development of robust immunity to cryptococcal infection. *J Immunol* (2012) 188(8):3940–8. doi:10.4049/jimmunol.1103053
92. Dinarello CA. Immunological and inflammatory functions of the interleukin-1 family. *Annu Rev Immunol* (2009) 27:519–50. doi:10.1146/annurev.immunol.021908.132612
93. Lee PY, Kumagai Y, Xu Y, Li Y, Barker T, Liu C, et al. IL-1alpha modulates neutrophil recruitment in chronic inflammation induced by hydrocarbon oil. *J Immunol* (2011) 186(3):1747–54. doi:10.4049/jimmunol.1001328
94. Schmitz N, Kurrer M, Bachmann MF, Kopf M. Interleukin-1 is responsible for acute lung immunopathology but increases survival of respiratory influenza virus infection. *J Virol* (2005) 79(10):6441–8. doi:10.1128/JVI.79.10.6441-6448.2005
95. Mascarenhas DP, Pereira MS, Manin GZ, Hori JI, Zamboni DS. Interleukin 1 receptor-driven neutrophil recruitment accounts to MyD88-dependent pulmonary clearance of *Legionella pneumophila* infection in vivo. *J Infect Dis* (2015) 211(2):322–30. doi:10.1093/infdis/jiu430
96. Barry KC, Fontana MF, Portman JL, Dugan AS, Vance RE. IL-1alpha signaling initiates the inflammatory response to virulent *Legionella pneumophila* in vivo. *J Immunol* (2013) 190(12):6329–39. doi:10.4049/jimmunol.1300100
97. Biondo C, Mancuso G, Midiri A, Signorino G, Domina M, Lanza Cariccio V, et al. Essential role of interleukin-1 signaling in host defenses against group B streptococcus. *MBio* (2014) 5(5):e1428–1414. doi:10.1128/mBio.01428-14
98. Lee YS, Yang H, Yang JY, Kim Y, Lee SH, Kim JH, et al. Interleukin-1 (IL-1) signaling in intestinal stromal cells controls KC/CXCL1 secretion, which correlates with recruitment of IL-22-secreting neutrophils at early stages

of *Citrobacter rodentium* infection. *Infect Immun* (2015) 83(8):3257–67. doi:10.1128/IAI.00670-15
99. Altmeier S, Toska A, Sparber F, Teijeira A, Halin C, LeibundGut-Landmann S. IL-1 coordinates the neutrophil response to *C. albicans* in the oral mucosa. *PLoS Pathog* (2016) 12(9):e1005882. doi:10.1371/journal.ppat.1005882
100. Mantovani A, Cassatella MA, Costantini C, Jaillon S. Neutrophils in the activation and regulation of innate and adaptive immunity. *Nat Rev Immunol* (2011) 11(8):519–31. doi:10.1038/nri3024
101. Mednick AJ, Feldmesser M, Rivera J, Casadevall A. Neutropenia alters lung cytokine production in mice and reduces their susceptibility to pulmonary cryptococcosis. *Eur J Immunol* (2003) 33(6):1744–53. doi:10.1002/eji.200323626
102. Wozniak KL, Kolls JK, Wormley FL Jr. Depletion of neutrophils in a protective model of pulmonary cryptococcosis results in increased IL-17A production by gammadelta T cells. *BMC Immunol* (2012) 13:65. doi:10.1186/1471-2172-13-65
103. Wiesner DL, Smith KD, Kashem SW, Bohjanen PR, Nielsen K. Different lymphocyte populations direct dichotomous eosinophil or neutrophil responses to pulmonary cryptococcus infection. *J Immunol* (2017) 198(4):1627–37. doi:10.4049/jimmunol.1600821
104. Daley JM, Thomay AA, Connolly MD, Reichner JS, Albina JE. Use of Ly6G-specific monoclonal antibody to deplete neutrophils in mice. *J Leukoc Biol* (2008) 83(1):64–70. doi:10.1189/jlb.0407247
105. Hasenberg A, Hasenberg M, Mann L, Neumann F, Borkenstein L, Stecher M, et al. Catchup: a mouse model for imaging-based tracking and modulation of neutrophil granulocytes. *Nat Methods* (2015) 12(5):445–52. doi:10.1038/nmeth.3322
106. Barquero-Calvo E, Martirosyan A, Ordonez-Rueda D, Arce-Gorvel V, Alfaro-Alarcon A, Lepidi H, et al. Neutrophils exert a suppressive effect on Th1 responses to intracellular pathogen *Brucella abortus*. *PLoS Pathog* (2013) 9(2):e1003167. doi:10.1371/journal.ppat.1003167
107. Yang CW, Strong BS, Miller MJ, Unanue ER. Neutrophils influence the level of antigen presentation during the immune response to protein antigens in adjuvants. *J Immunol* (2010) 185(5):2927–34. doi:10.4049/jimmunol.1001289
108. Eken C, Gasser O, Zenhaeusern G, Oehri I, Hess C, Schifferli JA. Polymorphonuclear neutrophil-derived ectosomes interfere with the maturation of monocyte-derived dendritic cells. *J Immunol* (2008) 180(2):817–24. doi:10.4049/jimmunol.180.2.817
109. Gasser O, Schifferli JA. Activated polymorphonuclear neutrophils disseminate anti-inflammatory microparticles by ectocytosis. *Blood* (2004) 104(8):2543–8. doi:10.1182/blood-2004-01-0361
110. Bourke E, Cassetti A, Villa A, Fadlon E, Colotta F, Mantovani A. IL-1 beta scavenging by the type II IL-1 decoy receptor in human neutrophils. *J Immunol* (2003) 170(12):5999–6005. doi:10.4049/jimmunol.170.12.5999
111. Santarlasci V, Cosmi L, Maggi L, Liotta F, Annunziato F. IL-1 and T helper immune responses. *Front Immunol* (2013) 4:182. doi:10.3389/fimmu.2013.00182
112. Chung Y, Chang SH, Martinez GJ, Yang XO, Nurieva R, Kang HS, et al. Critical regulation of early Th17 cell differentiation by interleukin-1 signaling. *Immunity* (2009) 30(4):576–87. doi:10.1016/j.immuni.2009.02.007
113. Sutton C, Brereton C, Keogh B, Mills KH, Lavelle EC. A crucial role for interleukin (IL)-1 in the induction of IL-17-producing T cells that mediate autoimmune encephalomyelitis. *J Exp Med* (2006) 203(7):1685–91. doi:10.1084/jem.20060285
114. Sims JE, Smith DE. The IL-1 family: regulators of immunity. *Nat Rev Immunol* (2010) 10(2):89–102. doi:10.1038/nri2691
115. Hung CY, Jimenez-Alzate Mdel P, Gonzalez A, Wuthrich M, Klein BS, Cole GT. Interleukin-1 receptor but not toll-like receptor 2 is essential for MyD88-dependent Th17 immunity to Coccidioides infection. *Infect Immun* (2014) 82(5):2106–14. doi:10.1128/IAI.01579-13
116. Szymczak WA, Sellers RS, Pirofski LA. IL-23 dampens the allergic response to *Cryptococcus neoformans* through IL-17-independent and -dependent mechanisms. *Am J Pathol* (2012) 180(4):1547–59. doi:10.1016/j.ajpath.2011.12.038
117. Xin L, Li Y, Soong L. Role of interleukin-1beta in activating the CD11c(high) CD45RB-dendritic cell subset and priming *Leishmania amazonensis*-specific CD4+ T cells in vitro and in vivo. *Infect Immun* (2007) 75(10):5018–26. doi:10.1128/IAI.00499-07
118. Hunter CA, Chizzonite R, Remington JS. IL-1 beta is required for IL-12 to induce production of IFN-gamma by NK cells. A role for IL-1 beta in the T cell-independent mechanism of resistance against intracellular pathogens. *J Immunol* (1995) 155(9):4347–54.
119. Denis M, Ghadirian E. Interleukin-1 is involved in mouse resistance to *Mycobacterium avium*. *Infect Immun* (1994) 62(2):457–61.
120. Chen W, Havell EA, Moldawer LL, McIntyre KW, Chizzonite RA, Harmsen AG. Interleukin 1: an important mediator of host resistance against *Pneumocystis carinii*. *J Exp Med* (1992) 176(3):713–8. doi:10.1084/jem.176.3.713
121. Juffermans NP, Florquin S, Camoglio L, Verbon A, Kolk AH, Speelman P, et al. Interleukin-1 signaling is essential for host defense during murine pulmonary tuberculosis. *J Infect Dis* (2000) 182(3):902–8. doi:10.1086/315771
122. Caffrey AK, Lehmann MM, Zickovich JM, Espinosa V, Shepardson KM, Watschke CP, et al. IL-1alpha signaling is critical for leukocyte recruitment after pulmonary *Aspergillus fumigatus* challenge. *PLoS Pathog* (2015) 11(1):e1004625. doi:10.1371/journal.ppat.1004625
123. Sainz J, Perez E, Gomez-Lopera S, Jurado M. IL1 gene cluster polymorphisms and its haplotypes may predict the risk to develop invasive pulmonary aspergillosis and modulate C-reactive protein level. *J Clin Immunol* (2008) 28(5):473–85. doi:10.1007/s10875-008-9197-0
124. Wojtowicz A, Gresnigt MS, Lecompte T, Bibert S, Manuel O, Joosten LA, et al. IL1B and DEFB1 polymorphisms increase susceptibility to invasive mold infection after solid-organ transplantation. *J Infect Dis* (2015) 211(10):1646–57. doi:10.1093/infdis/jiu636
125. Romani L. Immunity to fungal infections. *Nat Rev Immunol* (2004) 4(1):1–23. doi:10.1038/nri1255
126. Mayer-Barber KD, Yan B. Clash of the Cytokine Titans: counter-regulation of interleukin-1 and type I interferon-mediated inflammatory responses. *Cell Mol Immunol* (2017) 14(1):22–35. doi:10.1038/cmi.2016.25
127. Van't Wout JW, Van der Meer JW, Barza M, Dinarello CA. Protection of neutropenic mice from lethal *Candida albicans* infection by recombinant interleukin 1. *Eur J Immunol* (1988) 18(7):1143–6. doi:10.1002/eji.1830180728
128. Vonk AG, Netea MG, van Krieken JH, Iwakura Y, van der Meer JW, Kullberg BJ. Endogenous interleukin (IL)-1 alpha and IL-1 beta are crucial for host defense against disseminated candidiasis. *J Infect Dis* (2006) 193(10):1419–26. doi:10.1086/503363
129. Deepe GS Jr, McGuinness M. Interleukin-1 and host control of pulmonary histoplasmosis. *J Infect Dis* (2006) 194(6):855–64. doi:10.1086/506946

Conflict of Interest Statement: The authors declare that the research was conducted in the absence of any commercial or financial relationships that could be construed as a potential conflict of interest.

Copyright © 2018 Shourian, Ralph, Angers, Sheppard and Qureshi. This is an open-access article distributed under the terms of the Creative Commons Attribution License (CC BY). The use, distribution or reproduction in other forums is permitted, provided the original author(s) or licensor are credited and that the original publication in this journal is cited, in accordance with accepted academic practice. No use, distribution or reproduction is permitted which does not comply with these terms.

frontiers in Immunology

ORIGINAL RESEARCH
published: 01 September 2017
doi: 10.3389/fimmu.2017.01055

RIPK3/Fas-Associated Death Domain Axis Regulates Pulmonary Immunopathology to Cryptococcal Infection Independent of Necroptosis

Zhenzong Fa[1,2,3†], Qun Xie[4,5†], Wei Fang[2,6†], Haibing Zhang[5], Haiwei Zhang[5], Jintao Xu[3], Weihua Pan[1,2], Jinhua Xu[6], Michal A. Olszewski[2,3], Xiaoming Deng[4*] and Wanqing Liao[1,2*]*

[1] PLA Key Laboratory of Mycosis, Department of Dermatology and Venereology, Changzheng Hospital, Shanghai, China, [2] Shanghai Key Laboratory of Molecular Medical Mycology, Shanghai Institute of Medical Mycology, Second Military Medical University, Shanghai, China, [3] Division of Pulmonary and Critical Care Medicine, Department of Internal Medicine, University of Michigan Health System, Ann Arbor, MI, United States, [4] Department of Anesthesiology and Intensive Care, Changhai Hospital, Second Military Medical University, Shanghai, China, [5] Key Laboratory of Nutrition and Metabolism, Institute for Nutritional Sciences, Shanghai Institutes for Biological Sciences, Chinese Academy of Sciences, Shanghai, China, [6] Department of Dermatology, Huashan Hospital, Fudan University, Shanghai, China

OPEN ACCESS

Edited by:
Amariliz Rivera, New Jersey Medical School, United States

Reviewed by:
Maziar Divangahi, McGill University, Canada
Floyd Layton Wormley, University of Texas at San Antonio, United States

***Correspondence:**
Michal A. Olszewski olszewsm@med.umich.edu;
Xiaoming Deng deng_x@yahoo.com;
Wanqing Liao liaowanqing@sohu.com

[†]These authors have contributed equally to this work.

Specialty section:
This article was submitted to Microbial Immunology, a section of the journal Frontiers in Immunology

Received: *05 May 2017*
Accepted: *14 August 2017*
Published: *01 September 2017*

Citation:
Fa Z, Xie Q, Fang W, Zhang H, Zhang H, Xu J, Pan W, Xu J, Olszewski MA, Deng X and Liao W (2017) RIPK3/Fas-Associated Death Domain Axis Regulates Pulmonary Immunopathology to Cryptococcal Infection Independent of Necroptosis. Front. Immunol. 8:1055. doi: 10.3389/fimmu.2017.01055

Fas-associated death domain (FADD) and receptor interacting protein kinase 3 (RIPK3) are multifunctional regulators of cell death and immune response. Using a mouse model of cryptococcal infection, the roles of FADD and RIPK3 in anti-cryptococcal defense were investigated. Deletion of RIPK3 alone led to increased inflammatory cytokine production in the *Cryptococcus neoformans*-infected lungs, but in combination with FADD deletion, it led to a robust Th1-biased response with M1-biased macrophage activation. Rather than being protective, these responses led to paradoxical *C. neoformans* expansion and rapid clinical deterioration in *Ripk3*$^{-/-}$ and *Ripk3*$^{-/-}$*Fadd*$^{-/-}$ mice. The increased mortality of *Ripk3*$^{-/-}$ and even more accelerated mortality in *Ripk3*$^{-/-}$*Fadd*$^{-/-}$ mice was attributed to profound pulmonary damage due to neutrophil-dominant infiltration with prominent upregulation of pro-inflammatory cytokines. This phenomenon was partially associated with selective alterations in the apoptotic frequency of some leukocyte subsets, such as eosinophils and neutrophils, in infected *Ripk3*$^{-/-}$*Fadd*$^{-/-}$ mice. In conclusion, our study shows that RIPK3 in concert with FADD serve as physiological "brakes," preventing the development of excessive inflammation and Th1 bias, which in turn contributes to pulmonary damage and defective fungal clearance. This novel link between the protective effect of FADD and RIPK3 in antifungal defense and sustenance of immune homeostasis may be important for the development of novel immunomodulatory therapies against invasive fungal infections.

Keywords: *Cryptococcus neoformans*, immune responses, inflammation, Fas-associated death domain, receptor-interacting serine/threonine kinase 3

INTRODUCTION

Invasive fungal infections have become an increasingly significant challenge to public health due to the ever-increasing population of immunosuppressed patients, associated with aging of the global population, immunosuppressive infections such as HIV, and the growing use of immunosuppressive therapies. Among the major fungal pathogens, *Cryptococcus neoformans* causes life-threatening

invasive infections in both immunocompromised and immunocompetent hosts (1, 2). As supported by evidence from both the clinic and animal infection models, an insufficiency of Th1 and Th17 responses and subsequent classical activation of macrophages are major triggers of cryptococcal infection. However, emerging evidence supports the view that the excessive inflammation and pathology is frequently derived by a Th1 response, which is often initiated during highly active antiretroviral therapy (HAART) in HIV^+ patients with cryptococcosis. This paradoxical response, known as immune reconstitution inflammatory syndrome (IRIS), contributes to worsening symptoms and patient mortality despite ongoing antifungal and HAART treatments (3). This unique clinical problem underscores the importance of immunoregulatory processes during opportunistic fungal infections of which many aspects remain to be elucidated.

Fas-associated death domain protein (FADD) is known as a critical mediator of death receptor-triggered extrinsic apoptosis, which plays a role in removing "no longer needed" inflammatory cells, thereby serving as a crucial immune-regulatory pathway at the site of infection, preventing excessive inflammation (4, 5). Besides its role in apoptosis, FADD also has been shown to function in regulating cell cycle progression (6, 7), cytokine signaling (8, 9), and T-cell activation (10), which are all involved in regulation of immune responses. Targeted deletion of FADD in mice causes embryonic lethality due to spontaneous activation of another programmed cell death (PCD) pathway, necroptosis (11). However, co-deletion of receptor interacting protein kinase 3 (RIPK3), which is an essential serine/threonine kinase for necroptosis, rescues these mice (12). In addition to necroptosis, RIPK3 has also been reported as an important inflammatory signal adaptor because it functions in NF-κB activation, inflammasome activation, and cytokine signaling (13–15) and participates in the pathogenesis of several inflammatory diseases. However, it remains unknown whether these molecules play important roles during immune responses to fungal infections.

Here, we explored the roles of FADD and RIPK3 in a mouse model of cryptococcal infection and identified previously unknown, critical contributions of these molecules in pulmonary immune responses to cryptococcal infection. Deletion of FADD and RIPK3 induced robust Th1 responses, which, paradoxically, led to *C. neoformans* expansion and increased mortality in the infected mice. These effects were attributed to an excessive accumulation of neutrophils, over exuberant inflammatory cytokine production, and development of severe lung pathology. Collectively, these findings establish a novel link between these PCD components and immune response to cryptococcal challenge, demonstrating the crucial importance of FADD and RIPK3 in maintaining immune homeostasis during invasive fungal infection.

MATERIALS AND METHODS

Mice

Female wild-type (WT) C57BL/6 mice were housed in a specific pathogen-free facility. *Ripk3*$^{-/-}$ mice have been previously described (16). *Fadd*$^{+/-}$ mice were generated using the CRISPR–Cas9 mutation system (Shanghai Bioray Laboratory, Inc.). A 100-bp deletion was introduced into exon 1 of the *Fadd* gene (Figure S1 in Supplementary Material). Because ablation of *Fadd* in mice causes embryonic death, we crossed the *Ripk3*$^{-/-}$ mice with *Fadd*$^{+/-}$ mice to obtain *Ripk3*$^{-/-}$*Fadd*$^{-/-}$ mice. All mice genotypes were confirmed by PCR (Figure S1 in Supplementary Material). Mice were 8–10 weeks old at the time of infection and were humanely euthanized by CO_2 inhalation at the time of data collection. Animal experiments were conducted in accordance with the National Institutes of Health Guide for the Care and Use of Laboratory Animals with the approval of the Scientific Investigation Board of Second Military Medical University.

Cryptococcus neoformans

Encapsulated *C. neoformans* strain H99 (serotype A) was recovered from 10% glycerol-frozen stocks stored at −80°C. The strains were cultured on yeast extract-peptone-dextrose agar plates at 30°C. Liquid cultures were grown in Sabouraud dextrose broth at 30°C for 20–24 h in a shaking incubator at 180 rpm. Fungal cells were centrifuged at 2,000 × *g* for 3 min, washed three times, and resuspended in sterile PBS.

Inoculation

Mice were anesthetized by intraperitoneal injection of ketamine (100 mg/kg, Sigma, St. Louis, MO, USA) and secured onto a clean foam board (17). Next, 50 µl [10^5 colony-forming units (CFU)] of the washed yeast (2×10^6 yeast cells/ml in sterile PBS) were used for intranasal infection as previously described (18). After inoculation, the mice were kept warm and monitored during recovery from anesthesia.

Tissue Collection and Lung Leukocyte Isolation

The procedures were performed as previously described with modifications (19). At the time of data collection, the mice were sacrificed and perfused with 5 ml sterile PBS. The lungs were removed, minced with scissors, and added to homogenization gentleMACS C tubes containing proprietary catalysts for mechanical and enzymatic digestion (Miltenyi Biotec, Auburn, CA, USA). This process was followed by lung tissue homogenization using the gentle MACS dissociator (Miltenyi Biotec) and incubation at 37°C for 30 min in 4 ml/mouse digestion buffer (RPMI 1640, 5% fetal bovine serum, penicillin, and streptomycin, Invitrogen, Grand Island, NY, USA), 1 mg/ml collagenase A (Roche Diagnostics, Indianapolis, IN, USA), and 30 g/ml DNase I (Sigma, St. Louis, MO, USA). Erythrocytes were removed using 1× RBC lysis buffer (eBioscience, San Diego, CA, USA). Homogenized tissue was then passed through a 70 µm cell strainer (BD Falcon, Bedford, MA, USA) and centrifuged at 300 × *g* for 10 min to pellet the cells. The filtrate was centrifuged for 25 min at 1,500 × *g* in the presence of 20% Percoll (Sigma, St. Louis, MO, USA) in complete RPMI 1640 medium (RPMI 1640, 5% FBS, penicillin, and streptomycin) with no brake to separate leukocytes from cell debris and epithelial cells. Leukocyte pellets were resuspended in 5 ml complete RPMI 1640 medium

and counted in a hemocytometer using trypan blue staining to exclude dead cells.

Tissue CFU Assay

For determining the fungal burden in the lungs, brains, and spleens, tissues were removed and homogenized in 1 ml sterile PBS. Ten-fold dilutions of the samples were plated in duplicate on Sabouraud dextrose agar plates. Colonies were counted after 48 h of growth at 30°C, and CFU were calculated on a per-gram basis.

Cytokine Analysis

Mouse serum was obtained from blood samples collected by heart puncture before lung excision and centrifugation at 10,000 × *g* for 10 min. Homogenates of lungs were centrifuged, and supernatants were diluted for cytokine analysis. Leukocytes isolated from mice lung were plated at 10^7 cells/ml, and supernatants were collected by centrifugation of the culture medium. Mouse TNFα, IFNγ, IL-1α, IL-1β, IL-4, IL-6, IL-12, IL-17A, and IL-33 ELISA kits were from eBioscience. CXCL1 was from Raybio (Norcross, GA, USA).

Flow Cytometry Analysis of Leukocyte Populations

For the flow cytometry experiments, antibodies were purchased from eBioscience, BioLegend, or BD Biosciences, including anti-murine CD16/CD32; CD45 conjugated to PerCP-Cy5.5; CD3, CD193, CD80, IFNγ, and annexin V conjugated to FITC; CD4, Ly6G, and Siglec F conjugated to APC; CD8, CD11c, CD19, and CD80 conjugated to PE-Cy7; CD19, CD40, F4/80, and IL-4 conjugated to PE; CD11b, CD326, and MHC II conjugated to APC-Cy7; and CD19, CD80, and Ly6C conjugated to BV421.

Leukocytes were isolated from the lung and lymph nodes of mice. Cell surface immunofluorescence staining involved the addition of a fluorochrome-conjugated antibody mixture containing antibodies specific to various leukocyte subpopulations to the staining buffer. Cells were incubated on ice for 30 min in the dark and washed twice with PBS. For intracellular cytokine staining, cells were fixed in IC fixation buffer and stimulated with cell stimulation cocktail (plus protein transportation inhibitors) from eBioscience. Cells were resuspended in permeabilization buffer (eBioscience) and stained with intracellular antibody cocktail. After staining, cells were immediately analyzed by flow cytometry (FACSAria III, BD Biosciences). FlowJo (For Mac OS X, version X 10.0.7r2, Tree Star, San Carlos, CA, USA) was used for data analysis. Leukocyte populations were identified using the following markers as previously described (20, 21): neutrophils ($CD45^+$ $Ly6G^+$ $CD11b^+$), dendritic cells (DCs, $CD45^+$ $CD11c^+$ MHC II high), resident macrophage ($CD45^+$ $CD11b^-$ $Siglec\ F^+$), eosinophils ($CD45^+$ $CD11b^+$ $Siglec\ F^+$), monocyte-derived DCs or macrophages ($CD45^+$ $Ly6C^+$ $CD11c^-$), CD4 T cells ($CD45^+$ $CD3^+$ $CD4^+$), CD8 T cells ($CD45^+$ $CD3^+$ $CD8^+$), and B cells ($CD45^+$ $CD19^+$). DCs in lymph nodes were stained with extracellular CD45, CD11c, and CD80, and intracellular TNFα, IFNγ, and IL-4. Total numbers of each cell population were calculated by multiplying the frequency of the population by the total number of leukocytes (the percentage of $CD45^+$ cells multiplied by the original hemocytometer counts for total cells).

Lung-Associated Lymph Node (LALN) Leukocyte Isolation

Lung-associated lymph node leukocytes were collected as previously described with modifications (22). Lymph nodes were removed from the mediastinum and then mechanically dispersed using an 1-ml sterile syringe plunger to press them through a 70 μm cell strainer (BD Falcon, Bedford, MA, USA) in complete medium. After centrifugation at 2,500 × *g* for 5 min, the supernatant was removed and the cell pellets saved for further use.

Immunoblot Analysis

Lungs were ground up in liquid nitrogen and suspended in lysis buffer containing Tris–HCl (50 mM; pH 8.0), NaCl (150 mM), EDTA (1 mM), NP-40 (1%), PMSF (1 mM; Sigma), phosphatase inhibitor (Sigma), and a protease inhibitor cocktail (Roche Biochemical Laboratories). After incubation on ice for 30 min, the cell lysates were collected after centrifugation (14,000 × *g* for 10 min) at 4°C, and protein concentrations were determined using the Pierce BCA Protein Assay Kit (Thermo Scientific). A total of 30 μg protein was loaded for western blot analysis using the following antibodies: RIPK3 (Prosci) and caspase-3 (Cell Signaling Technology).

Real-time PCR Analysis

Total RNA (10–100 ng, depending on the abundance of the target gene) was purified using TRIzol reagent (Ambion by Life Technologies) for RT-qPCR in a one-step reaction with Reverse Transcriptase (Takara) and SYBR green master mix (Takara) using a 7900 Real-Time PCR system (Applied Biosystems). All primers used for RT-qPCR are listed in Table S1 in Supplementary Material. The qPCR analysis was performed using the $2^{-\Delta Ct}$ method, and target genes were normalized to the housekeeping genes in each strain.

Histology, Immunohistochemistry, and Immunofluorescence

Lungs were instilled with 1 ml 10% neutral-buffered formalin, excised, immersed in 10% neutral-buffered formalin, and embedded in paraffin as described previously (19). Five-micrometer sections were cut and stained with hematoxylin & eosin. Immunohistochemical and immunofluorescent staining was performed using formalin-fixed, paraffin-embedded tissue sections with rabbit anti-RIPK3 (Prosci) antibodies. Sections were photographed by Zeiss light microscopy (ZEISS, AXIO) and Olympus confocal microscopy (FV1000). Lung tissue inflammation and injury score were performed by three different pathologists in a blinded fashion. The quantify criteria is referenced to previous studies with modification (23).

Fungal Killing and Cell Viability Assays

Bone marrow-derived macrophages (BMDMs) were generated as previously described (24, 25). Briefly, marrow was flushed from the C57Bl/6 mouse femurs and tibias and dispersed into a single-cell suspension. The cells were cultured for 7 days in RPMI medium supplemented with 10% FBS and 50 ng/ml M-CSF. The cultures were additionally nourished with M-CSF-containing

medium on the third day of culture. All *in vitro* experiments were performed in RPMI 1640 containing 10% FCS and 5 ng/ml M-CSF.

For the fungal killing assay, freshly isolated BMDMs were diluted to 10^6 cells/ml and plated on a 96-well cell culture plate. *C. neoformans* were washed twice with PBS, resuspended in RPMI medium, and adjusted to 10^5 cells/ml. The yeast cells were further opsonized with anti-GXM antibody for 1 h at 37°C, followed by the addition of 100 µl opsonized *C. neoformans* to each well of the BMDM culture plate and incubation at 37°C with 5% CO_2 for 24 h. BMDM cells were lysed in sterile water for 20 min, mixed with the supernatant, and then diluted and plated on Sabouraud agar plates. CFU were counted after 2 days at 30°C.

Statistical Analysis

All data are expressed as means ± SEMs. The data obtained for the animal survival assays were plotted as Kaplan–Meier survival curves and analyzed with the log-rank test using GraphPad Prism version 6.00 for Windows (GraphPad Software, San Diego, CA, USA). The remaining statistical analyses were conducted with the ANOVA, Student's *t*-test, and Kruskal–Wallis test as well as Dunn's test for non-parametric measures. The results were considered statistically significant when the *P* value was less than 0.05.

RESULTS

RIPK3 and FADD Critically Contribute to Host Defenses against *C. neoformans* Infection

To gain insight into the roles of RIPK3 and FADD during host responses to *C. neoformans* infection, we first evaluated kinetics of RIPK3 and FADD protein expression in the lungs of the infected C57BL6 mice. Immunoblot study results showed that RIPK3 displayed extensive upregulation in the lung tissue at 10 days postinfection (dpi) (**Figure 1A**), further verified by immunochemistry and immunofluorescence assays (**Figures 1B,C**). In contrast, FADD, albeit abundant, appeared to be expressed constitutively throughout the studied time points of infection. Next, to elucidate the relative importance of FADD and RIPK3-related signaling in anti-cryptococcal defense, we compared the survival of infected *Ripk3*$^{-/-}$, *Ripk3*$^{-/-}$*Fadd*$^{-/-}$, and WT mice. As shown in **Figure 1D**, compared with WT mice, infected *Ripk3*$^{-/-}$ mice showed accelerated onset of mortality (8 vs 20 dpi) and reduced median survival (median: 16.5 ± 5.8 vs 21.5 ± 1.4 days). *Ripk3*$^{-/-}$*Fadd*$^{-/-}$ mice showed even greater susceptibility to *C. neoformans* infection compared with either *Ripk3*$^{-/-}$ ($P < 0.05$) or WT mice ($P < 0.001$), exhibiting a drastically shortened median survival

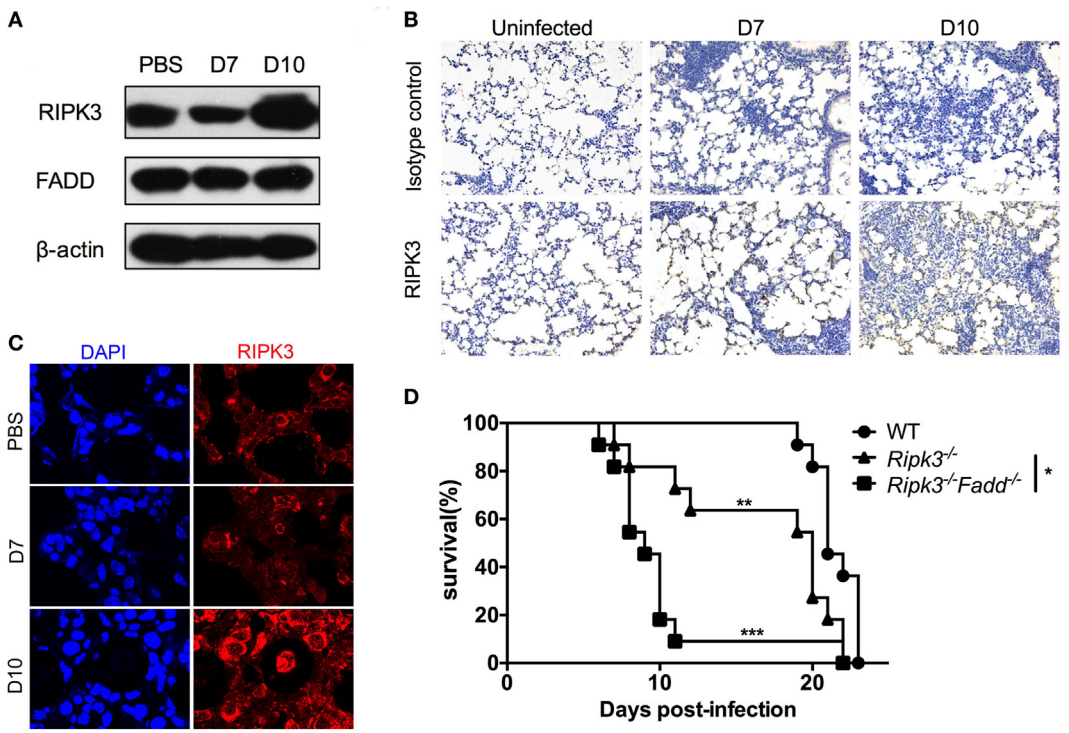

FIGURE 1 | RIPK3 and Fas-associated death domain (FADD) critically contribute to host defenses against *Cryptococcus neoformans* infection. C57BL/6 mice were inoculated intranasally with 10^5 *C. neoformans* strain H99 and sacrificed at 7 or 10 days postinfection. PBS-treated mice were utilized as control. Pulmonary expression of RIPK3 and FADD were examined by western blot analysis in total protein form lung homogenates **(A)**. RIPK3 displayed enhanced expression, while FADD remains unchanged in the lung of infected mice. Fungal infection significantly enhanced the local recruitment of RIPK3 in the lung as shown by immunohistochemistry **(B)** and immunofluorescence **(C)** assays. Wild-type (WT), *Ripk3*$^{-/-}$, *Ripk3*$^{-/-}$*Fadd*$^{-/-}$ mice ($n = 11$ for each group) were infected *via* inhalation to determine effects of RIPK3 and FADD in host defenses against *C. neoformans*. Survival studies showed that *Ripk3*$^{-/-}$ and *Ripk3*$^{-/-}$*Fadd*$^{-/-}$ mice were more susceptible to fungal infection **(D)**. $^*P < 0.05$, $^{**}P < 0.01$, $^{***}P < 0.001$. The survival study was repeated three times independently.

(9.9 ± 4.3 days). These results demonstrate that FADD and RIPK3 signaling critically contribute to host defense against cryptococcal infection, most likely in a synergistic fashion.

RIPK3 or RIPK3/FADD Deletion Reduced Host Ability to Control Fungal Growth and Dissemination

Next, we examined fungal burden in the lung, brain, and spleen in infected mice to assess the effects of RIPK3 and FADD in the control of fungal growth and systemic dissemination. Compared with WT, *Ripk3*$^{-/-}$ mice had a significantly higher pulmonary fungal load at 10 dpi ($P < 0.05$), and RIPK3/FADD double deletions further enhanced the fungal burden in the lungs at both 7 dpi ($P < 0.05$) and 10 dpi (**Figure 2A**, $P < 0.01$). Similar trends in fungal burden were noted in the spleens and brains of *Ripk3*$^{-/-}$ and *Ripk3*$^{-/-}$*Fadd*$^{-/-}$ mice at 10 dpi (**Figures 2B,C**), with frequencies of positive spleen and brain cultures in *Ripk3*$^{-/-}$*Fadd*$^{-/-}$ mice doubling those in the WT mice. Thus, both RIPK3 and FADD significantly contributed fungal containment during pulmonary cryptococcal infection.

RIPK3/FADD Deletions Lead to Severe Lung Pathologies in *C. neoformans*-Infected Mice

Rapid clinical deterioration and the accelerated mortality, especially in the infected *Ripk3*$^{-/-}$*Fadd*$^{-/-}$ mice could not be solely explained by relatively modest increases in fungal burdens at 7 and 10 dpi. Thus, we examined the effects of RIPK3 or RIPK3/FADD on the development of lung inflammation and pathologies post-*C. neoformans* infection. We examined lung sections obtained from sham-infected (PBS) and *C. neoformans*-infected WT and *Ripk3*$^{-/-}$ or *Ripk3*$^{-/-}$*Fadd*$^{-/-}$ mice. Deletion of RIPK3 or RIPK3/FADD induced no visible alterations in uninfected lungs (data not shown), demonstrating that genetic defects in RIPK3 or RIPK3/FADD did not affect baseline pulmonary morphology. Comparative histopathological assessments of lung sections from each group at 10 dpi (**Figure 3**) demonstrated only subtle enhancement of pulmonary leukocyte infiltration in *Ripk3*$^{-/-}$ mice relative to the control mice with largely similar pattern of inflammatory lesions (**Figures 3A–C** vs **Figures 3D–F**). The borders between inflamed regions and normal alveoli remained distinct at 10 dpi in WT and *Ripk3*$^{-/-}$ mice (**Figures 3A–F**). Consistently, blinded pathology score, albeit showing an increasing trend, has not increased significantly (Figure S2 in Supplementary Material). In contrast, *Ripk3*$^{-/-}$*Fadd*$^{-/-}$ mice exhibited progressive pulmonary inflammation with severe tissue damage (**Figures 3G–I**). Less organized inflammatory infiltrates (predominantly neutrophils and lymphocytes) were spread diffusely through bilateral lung fields at 10 dpi. The margins of inflamed regions from uninvolved alveoli were less distinct. Features of suppurative bronchopneumonia, such as airway plugins with polymorphic neutrophil and dense cellular exudate, were observed throughout the lung (**Figures 3H,I**). The blinded pathology score showed that inflammation/pathology score was significantly greater in lungs of *Ripk3*$^{-/-}$*Fadd*$^{-/-}$ mice compared to both WT and *Ripk3*$^{-/-}$ mice (Figure S2 in Supplementary Material), which corroborated well with survival data on day 10 (80% mortality in *Ripk3*$^{-/-}$*Fadd*$^{-/-}$ group, only 20% mortality in *Ripk3*$^{-/-}$ group, and all mice surviving in the WT group at 10 dpi). Collectively, these findings demonstrated that concurrent RIPK3/FADD deletion during *C. neoformans* infection induced severe pulmonary inflammation and tissue damage, potentially explaining the highly accelerated mortality in *Ripk3*$^{-/-}$*Fadd*$^{-/-}$ mice.

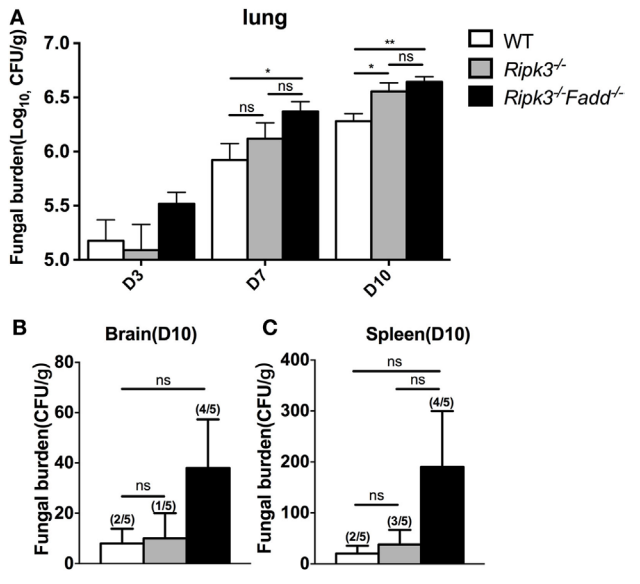

FIGURE 2 | *Ripk3*$^{-/-}$ and *Ripk3*$^{-/-}$*Fadd*$^{-/-}$ mice showed diminished fungal clearance. Pulmonary fungal burden assay revealed diminished fungal clearance of *Ripk3*$^{-/-}$ and *Ripk3*$^{-/-}$*Fadd*$^{-/-}$ mice **(A)** and similar but not significant trends in extra-pulmonary dissemination **(B,C)**. Values represent means and SEMs ($n = 5$ mice for each group); ns, no significant difference, $^{*}P < 0.05$, $^{**}P < 0.01$, between compared groups. The colony-forming units (CFU) assay was repeated three times independently.

RIPK3 and FADD Differentially Modulated Pulmonary Leukocyte Accumulation during *C. neoformans* Infection

To quantify the effects of RIPK3 and FADD deletions on cellular components of the inflammatory response to *C. neoformans*, we compared leukocyte populations isolated from uninfected or infected lungs of WT, *Ripk3*$^{-/-}$, or *Ripk3*$^{-/-}$*Fadd*$^{-/-}$ mice at 10 dpi. Consistent with the histopathological findings, flow cytometric analysis revealed no significant effect of *Ripk3*$^{-/-}$ or *Ripk3*$^{-/-}$*Fadd*$^{-/-}$ mutations in uninfected mice for any of the leukocyte subsets (data not shown). While only a borderline increase in total lung leukocytes counts (CD45^{+} cells) was observed in *Ripk3*$^{-/-}$ mice compared to WT mice at 10 dpi (**Figure 4A**, $P < 0.06$), significant increases in two pulmonary leukocyte subsets were observed. *Ripk3*$^{-/-}$ mice showed increased numbers of neutrophils (**Figure 4B**), increasing trend in macrophages (**Figure 4C**), and elevated CD4^{+} T cells (**Figure 4D**) compared to the infected WT mice.

Ripk3$^{-/-}$*Fadd*$^{-/-}$ mice infected by *C. neoformans* showed more profound alterations in both the magnitude of inflammation

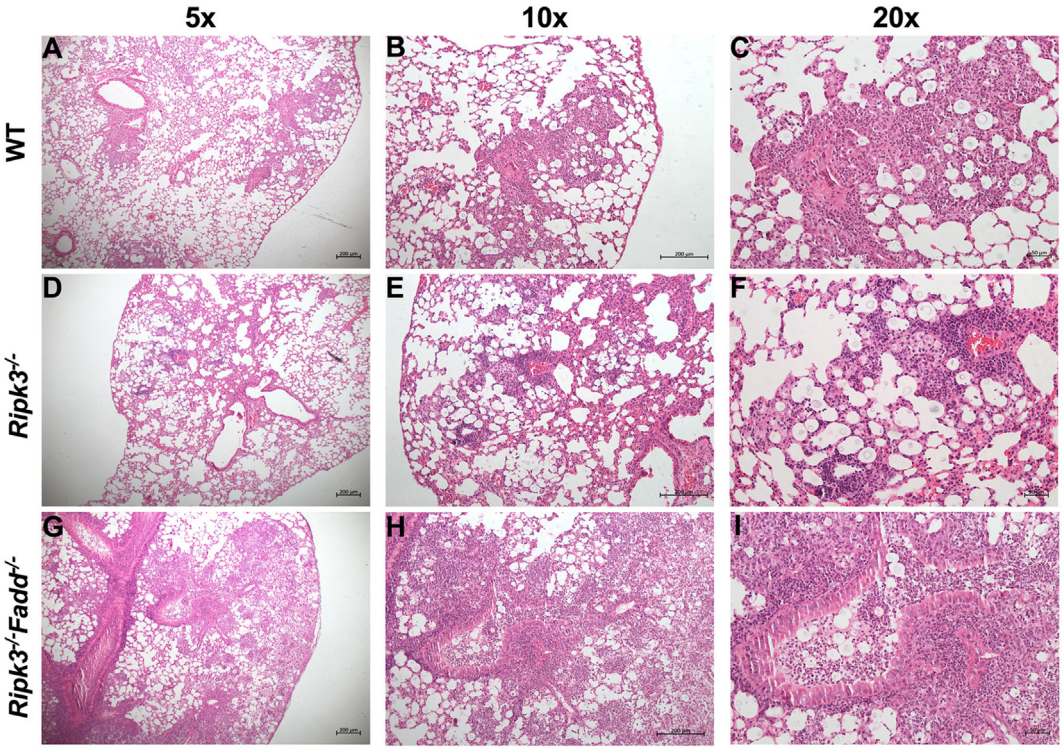

FIGURE 3 | Deletion of RIPK3 and Fas-associated death domain (FADD) resulted in enhanced inflammatory infiltration and tissue injury following pulmonary infection with *Cryptococcus neoformans*. Wild-type (WT) **(A–C)**, *Ripk3*$^{-/-}$ **(D–F)**, or *Ripk3*$^{-/-}$*Fadd*$^{-/-}$ **(G–I)** mice were infected with 10^5 *C. neoformans* strain H99. At 10 days postinfection, lungs were harvested, and the morphological pattern of inflammation was evaluated by light microscopy. Pulmonary representative photomicrographs (hematoxylin and eosin stained) taken from each group were shown [**(A,D,G)** magnification of ×50; **(B,E,H)** magnification of ×100; **(C,F,I)** magnification of ×200]. Compared with WT group, *Ripk3*$^{-/-}$ mice displayed similar pulmonary histological pattern but a slight enhancement in inflammatory infiltration. However, extensive pulmonary inflammation and severe tissue damage were observed in *Ripk3*$^{-/-}$*Fadd*$^{-/-}$ mice, indicating distinct patterns of lung pathology.

and leukocyte composition. There was a significant increase in total leukocyte counts in *Ripk3*$^{-/-}$*Fadd*$^{-/-}$ mice compared with WT group at 10 dpi (**Figure 4A**), mostly driven by a remarkable increase in neutrophil numbers (more than threefold) relative to infected WT (**Figure 4B**) and significantly greater than in the *Ripk3*$^{-/-}$ mice. Significant increases in other myeloid cell subsets (monocytes, **Figure 4E**; DCs, **Figure 4F**) were also detected relative to both WT and *Ripk3*$^{-/-}$ mice. However, the numbers of pulmonary eosinophils observed in abundance in the WT and *Ripk3*$^{-/-}$ mice at 10 dpi were suppressed in *Ripk3*$^{-/-}$*Fadd*$^{-/-}$ mice (**Figure 4G**), suggesting a shift away from a Th2 response in the WT following RIPK3/FADD double deletion. Collectively, these data further support that RIPK3 and more so the RIPK3/FADD double deletion results in an exuberant accumulation of inflammatory cells and immunomodulation that alters the course of inflammatory response implicated in lung injury we observe during *C. neoformans* infection in the absence of these factors.

RIPK3/FADD Deletion Reshaped the Cytokine Responses during Pulmonary *C. neoformans* Infection

Having demonstrated that RIPK3 and RIPK3/FADD deletions altered inflammatory infiltrate compositions, we further examined the roles of RIPK3 and FADD in pulmonary and systemic cytokine levels during cryptococcal infection. Lung homogenates and serum isolated at 10 dpi from *Ripk3*$^{-/-}$, *Ripk3*$^{-/-}$*Fadd*$^{-/-}$, and WT mice were analyzed by ELISA (**Figures 5A–N**). We found that depletion of RIPK3 alone significantly increased pro-inflammatory cytokine production: TNF-α, IL-1α, and IL-1β (**Figures 5A–C**). Non-significant increasing trend in IFN-γ level and decreasing trend in IL-4 production suggested cytokine profile drifting away from Th2 to Th1 pattern (**Figure 5J**), which corresponded to diminished serum IgE accumulation (**Figure 5N**). However, no difference in IL-12p40 or IL-33 have been observed (**Figures 5E,H**), suggesting that the full switch from Th2 to Th1 has not occurred as a result of RIPK3 deletion. Finally, while we observe significant increase in IL-17A, which might have suggested shift toward Th17 response as a result of RIPK3 deletion, there was no concurrent increase in IL-6 or IL-12p40, which would be associated with Th17 response. Most of these trends were reproduced in pulmonary leukocyte cell culture supernatants (Figure S4 in Supplementary Material). Consistently, with lung cytokines, serum cytokine analysis showed somewhat elevated TNFα (**Figure 5K**), suggesting more pronounced inflammatory response levels in infected *Ripk3*$^{-/-}$ mice, but no increase in serum IL-6 or IFNγ (**Figures 5L,M**).

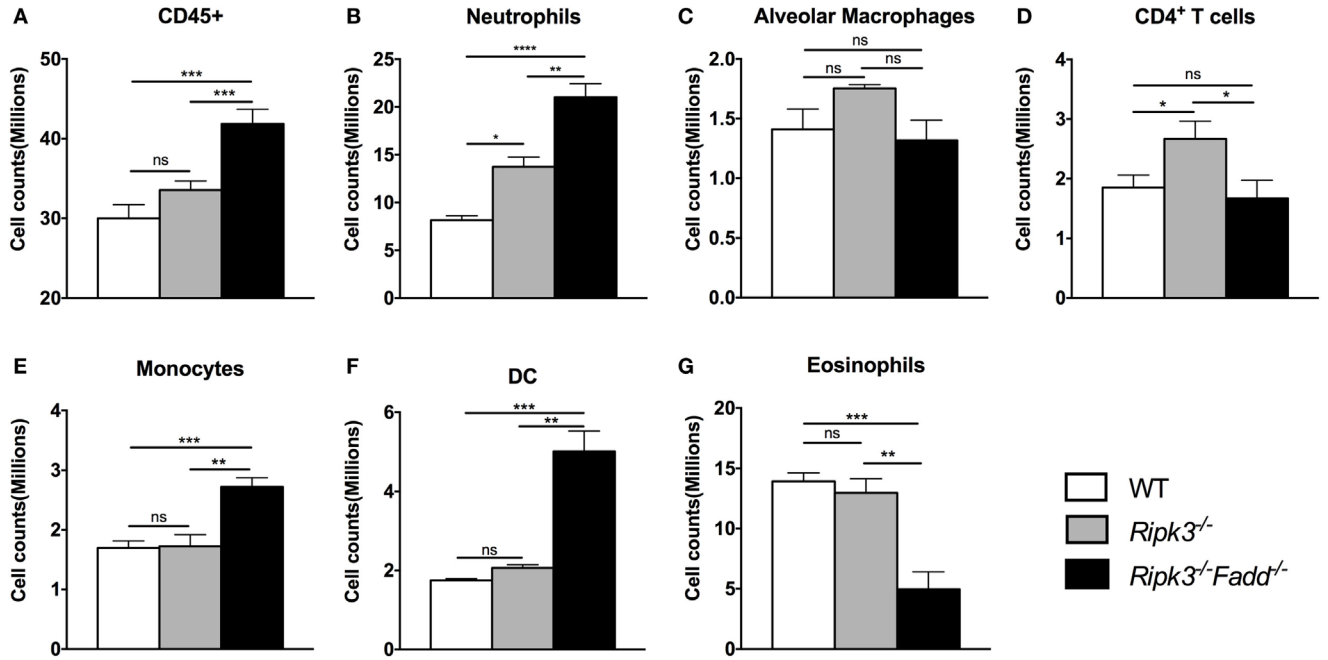

FIGURE 4 | RIPK3 or RIPK3/Fas-associated death domain (FADD) deletions resulted in alteration in pulmonary leukocyte recruitments. Mice were inhalationally infected with 10^5 *Cryptococcus neoformans* strain H99. Lungs were harvested at 10 days postinfection, and total pulmonary leukocytes were isolated from infected lungs after enzymatic digestion. Magnitude and/or leukocyte composition were then analyzed by flow cytometry. Results are illustrated as absolute numbers of each lymphocyte subset **(A–G)** in the total lung sample. Values represent means and SEMs ($n = 6$ mice per group). ns, no significant difference, $^*P < 0.05$, $^{**}P < 0.01$, $^{***}P < 0.001$, $^{****}P < 0.0001$, between compared groups. This experiment was repeated twice.

RIPK3/FADD double deletion further enhanced pro-inflammatory TNFα and IL-6 (**Figures 5A,D**) and showed sustained elevation of IL-1α, IL-1β compared to the WT mice. Furthermore, Th1 cytokines IL-12p40 and IFNγ were significantly elevated relative to WT and RIPK3 mice levels of these cytokines (**Figures 5E,F**), suggesting not only strongly intensified inflammatory response but also shift to a Th1. Consistently, Th2 cytokines (IL-4 and IL-33) were profoundly suppressed (**Figures 5G,H**), and the Th1/Th2 ratio increased more than 300-fold in RIPK3/FADD-depleted relative to WT mice (**Figure 5J**), with corresponding absence of serum IgE accumulation (**Figure 5N**) strongly suggesting the development of a robust Th1 bias in these mice. Interestingly, IL-17 was not elevated as in the *Ripk3*$^{-/-}$ mice but showed level similar to that in the infected WT mice (**Figure 5I**).

To further investigate effects of RIPK3/FADD on T cell polarization, we performed intracellular flow analysis on pulmonary CD4$^+$ T cells from infected *Ripk3*$^{-/-}$ *and Ripk3*$^{-/-}$*Fadd*$^{-/-}$ mice at 10 dpi. Consistent with the cytokine data, percentage of IFNγ$^+$ CD4$^+$ T cells was not different in *Ripk3*$^{-/-}$ mice compared to the WT, but increased in *Ripk3*$^{-/-}$*Fadd*$^{-/-}$ mice compared to WT and *Ripk3*$^{-/-}$ mice (**Figures 6A,B**). Moreover, we found there was a borderline reduction in the frequencies of GATA3 positive CD4$^+$ T cells in *Ripk3*$^{-/-}$ ($P = 0.07$) mice and significant decrease in frequencies of GATA3$^+$ CD4$^+$ T cells in *Ripk3*$^{-/-}$*Fadd*$^{-/-}$ mice relative to WT mice at 10 dpi (**Figures 6C,D**). Interestingly, no increase in IL-17A or RorγT$^+$ CD4 or CD8 T-cells was observed in either *Ripk3*$^{-/-}$ or *Ripk3*$^{-/-}$*Fadd*$^{-/-}$ mice compared to the WT mice (data not shown). Collectively, analysis of cytokine responses and T-cell polarization profile showed that RIPK3 single deletion led to enhanced pro-inflammatory responses, while that additional deletion of FADD further potentiated these effects, leading to a very strong Th1 bias systemic and "cytokine storm" at 10 dpi with *C. neoformans*.

RIPK3 and FADD Deletions Potentiated Classical Activation of Macrophages and Their Fungicidal Responses *In Vitro*

Macrophages are distal effector cells that execute anti-*C. neoformans*-based cytokine responses in infected organs (26, 27). Having determined that RIPK3 increased inflammatory cytokines, including pro-M1 cytokine TNFα and RIPK3/FADD additionally promoted Th1 responses, we assessed the M1/M2 polarization patterns of macrophages in the infected lungs and the fungicidal ability of BMDMs isolated from uninfected mice from each strain. The expression of M1- and M2-associated genes was evaluated by real-time PCR (**Figures 7A–C**). Consistent with absence of major increase in IFNγ production, *Ripk3*$^{-/-}$ mice macrophages did not show significant upregulation of the M1 activation marker iNOS (**Figure 7A**). However, in concert with less pronounced Th2 and more pro-inflammatory environment in the lungs, we observed diminished upregulation of M2 markers arginase Arg1 and Fizz1

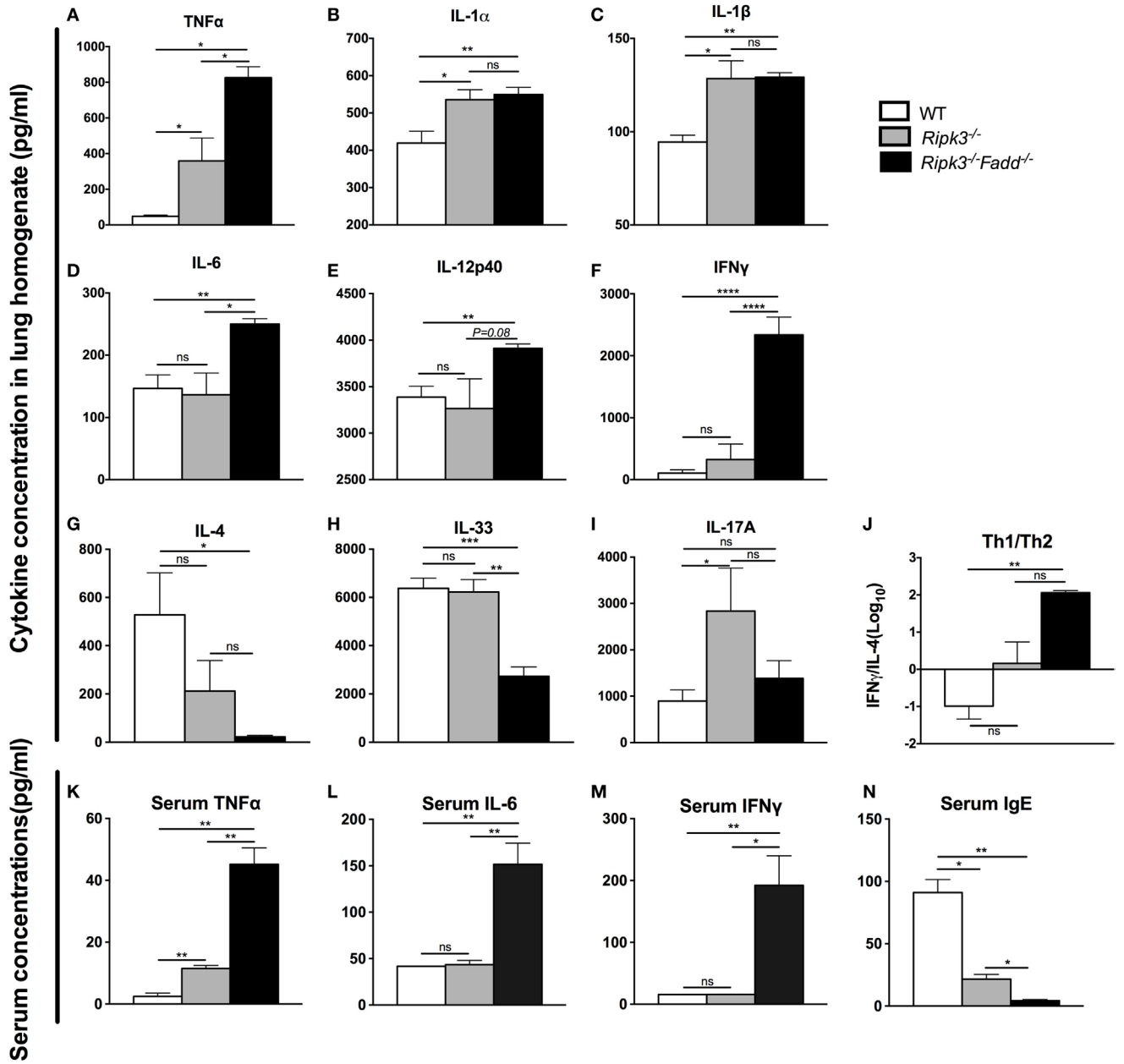

FIGURE 5 | RIPK3 or RIPK3/Fas-associated death domain (FADD) deletions altered Th-polarizing and pro-inflammatory cytokine profiles in local (pulmonary) and systemic response to cryptococcal infection. Total lung tissue **(A–I)** and serum **(K–N)** were harvested from wild-type (WT), *Ripk3*$^{-/-}$, or *Ripk3*$^{-/-}$*Fadd*$^{-/-}$ mice at 10 days postinfection with *Cryptococcus neoformans*. Supernatants of lung tissue homogenates were collected by centrifuging. Cytokine levels were detected in the supernatants and serum by ELISA. Total serum IgE concentrations were also measured by ELISA. Values represent mean cytokine or IgE concentrations [**(A–I)**, **(K–N)**, pg/ml] or **(J)**, the IFNγ/IL-33 ratio (n = 5 mice per group). ns, no statistical significance. *P < 0.05, **P < 0.01, ***P < 0.001. This experiment was repeated twice.

(**Figures 7B,C**), suggesting that macrophages in the infected lung of *Ripk3*$^{-/-}$ mice were less M2 biased. Consistent with the strong Th1-type polarization, expression of the iNOS was significantly upregulated in *Ripk3*$^{-/-}$*Fadd*$^{-/-}$ mice (**Figure 7A**), while Fizz1 expression was diminished (**Figure 7C**) compared to both WT and *Ripk3*$^{-/-}$ mice. Compared with WT mice, arginase1 expression in *Ripk3*$^{-/-}$ *Fadd*$^{-/-}$ mice also showed downward effects (**Figures 7B,C**). To determine whether the fungicidal potential (typically linked to M1/M2 activation) was affected in *Ripk3*$^{-/-}$ and *Ripk3*$^{-/-}$*Fadd*$^{-/-}$ mice, we evaluated the fungicidal effect of the BMDMs after co-incubation with 10^6 CFU of *C. neoformans* (**Figure 7D**). Significantly reduced cryptococcal survival was observed in *Ripk3*$^{-/-}$ and, to an even greater extent, in *Ripk3*$^{-/-}$ *Fadd*$^{-/-}$ macrophages, further demonstrating

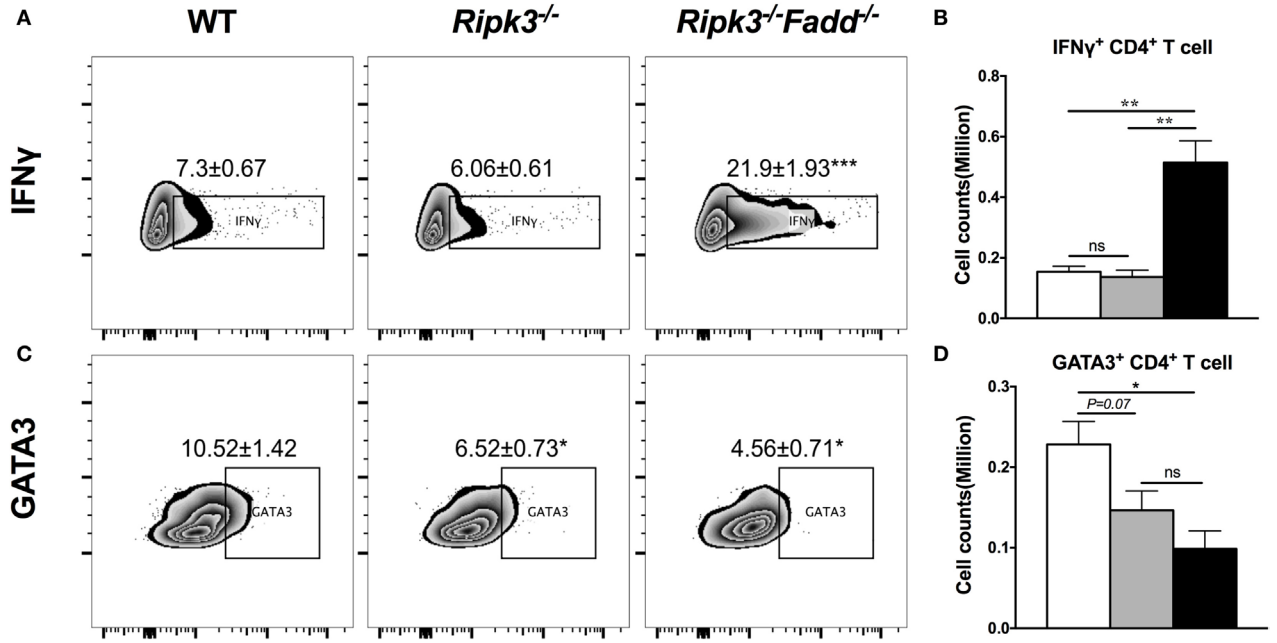

FIGURE 6 | RIPK3 or RIPK3/Fas-associated death domain (FADD) deletions affects Th1/Th2 polarization of CD4 T cells in the lungs of *Cryptococcus neoformans*-infected mice. Leukocytes were isolated from the lungs of infected mice on 9 days postinfection. Intracellular expression of IFNγ, GATA3 in CD4 T cell population was analyzed by flow cytometry. **(A,C)** show the percentage of IFNγ or GATA positive populations in CD4+ cells. **(B,D)** show the cell counts of IFNγ or GATA positive CD4 T cells. Note that there was a significant increase of Th1 markers in the *Ripk3*$^{-/-}$*Fadd*$^{-/-}$ mice compared to the control mice **(A,B)**. Results represent means and SEMs ($n = 4$ mice for each time point). *$P < 0.05$, **$P < 0.01$.

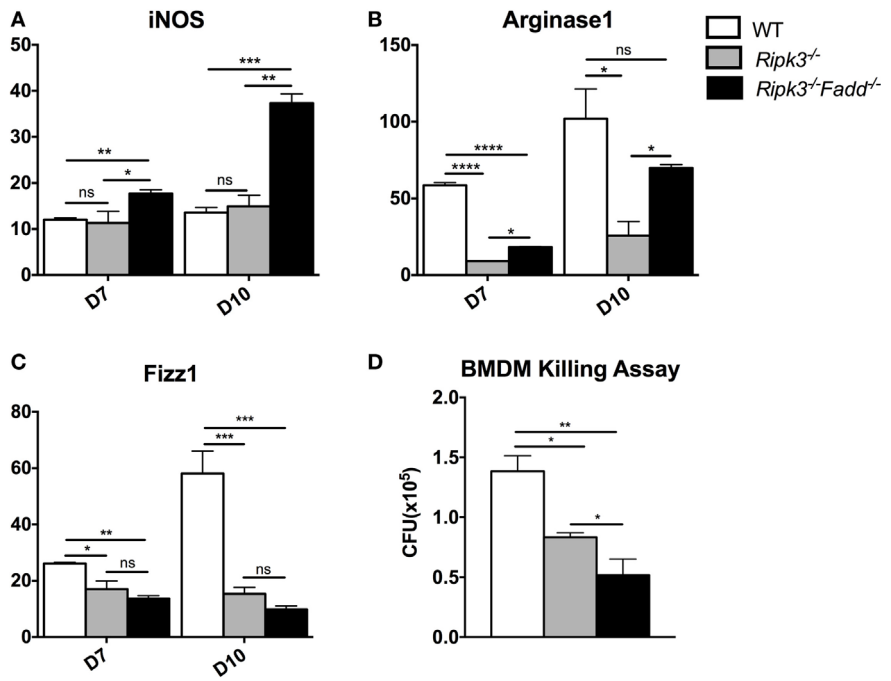

FIGURE 7 | *Ripk3*$^{-/-}$ and *Ripk3*$^{-/-}$*Fadd*$^{-/-}$ mice displayed progressively classical activation and increased fungicidal ability of macrophages. mRNA was isolated from pulmonary macrophages of WT, *Ripk3*$^{-/-}$, or *Ripk3*$^{-/-}$*Fadd*$^{-/-}$ mice at 10 days postinfection. Real-time PCR was performed to determine the expression levels of iNOS [nitric oxide synthase, **(A)**], Arg1 [arginase 1, **(B)**], and Fizz1 **(C)**. Bone marrow-derived macrophages (BMDMs) isolated from uninfected mice were utilized to detect intracellular fungicidal ability **(D)**. ns, no significant difference, *$P < 0.05$, **$P < 0.01$, ***$P < 0.001$, ****$P < 0.0001$, between compared groups. These experiments were repeated three times.

that, at the cellular level, RIPK3 and FADD deletions promoted rather than suppressed fungicidal M1 macrophage polarization. Thus, the effects of RIPK3 and FADD deletion on M1/M2 gene expression were consistent with the cytokine profiles in the *C. neoformans*-infected lungs.

RIPK3 and FADD Deletions Promoted DC Differentiation and Activation in LALNs after Cryptococcal Infection

Having determined that joint RIPK3/FADD deletion promoted a strong shift toward the Th1/M1 response in contrast with single RIPK3 deletion, we analyzed the phenotype of DCs, the central regulators of Th-immune polarization. Flow cytometric analysis of LALN DC was performed to examine the frequency and intensity of CD80, a major co-stimulatory molecule expressed during DC co-stimulatory maturation, and the DC1 phenotypic marker and predictor of Th1 response development (22, 28, 29). Consistent with strong Th1 bias, the frequency and intensity of CD80 expression was significantly enhanced in LALN DC of *Ripk3*$^{-/-}$*Fadd*$^{-/-}$ mice at both 7 and 10 dpi (**Figures 8A–D**) compared to those in the infected WT mice. *Ripk3*$^{-/-}$ mice also did not show this effect on day 7 but displayed some increase of CD80 surface expression at 10 dpi (**Figures 8C,D**). Cytokine expression in LALN DCs was also analyzed by intracellular staining. Again, notable enhancement of IFNγ expression was observed in LALN DCs of *Ripk3*$^{-/-}$*Fadd*$^{-/-}$ mice at day 7 but without significant alteration in IL-4 production (**Figures 8E,F**). However, RIPK3 deletion had no effect on LALN DC cytokine expression. Taken together, these results suggested that RIPK3/FADD deletions synergistically promoted LALN DC maturation and DC1 activation during *C. neoformans* infection, which was consistent with strongly enhanced Th1 responses in these mice, while changes in *Ripk3*$^{-/-}$ DC activation profile was subtle, consistent with subtle

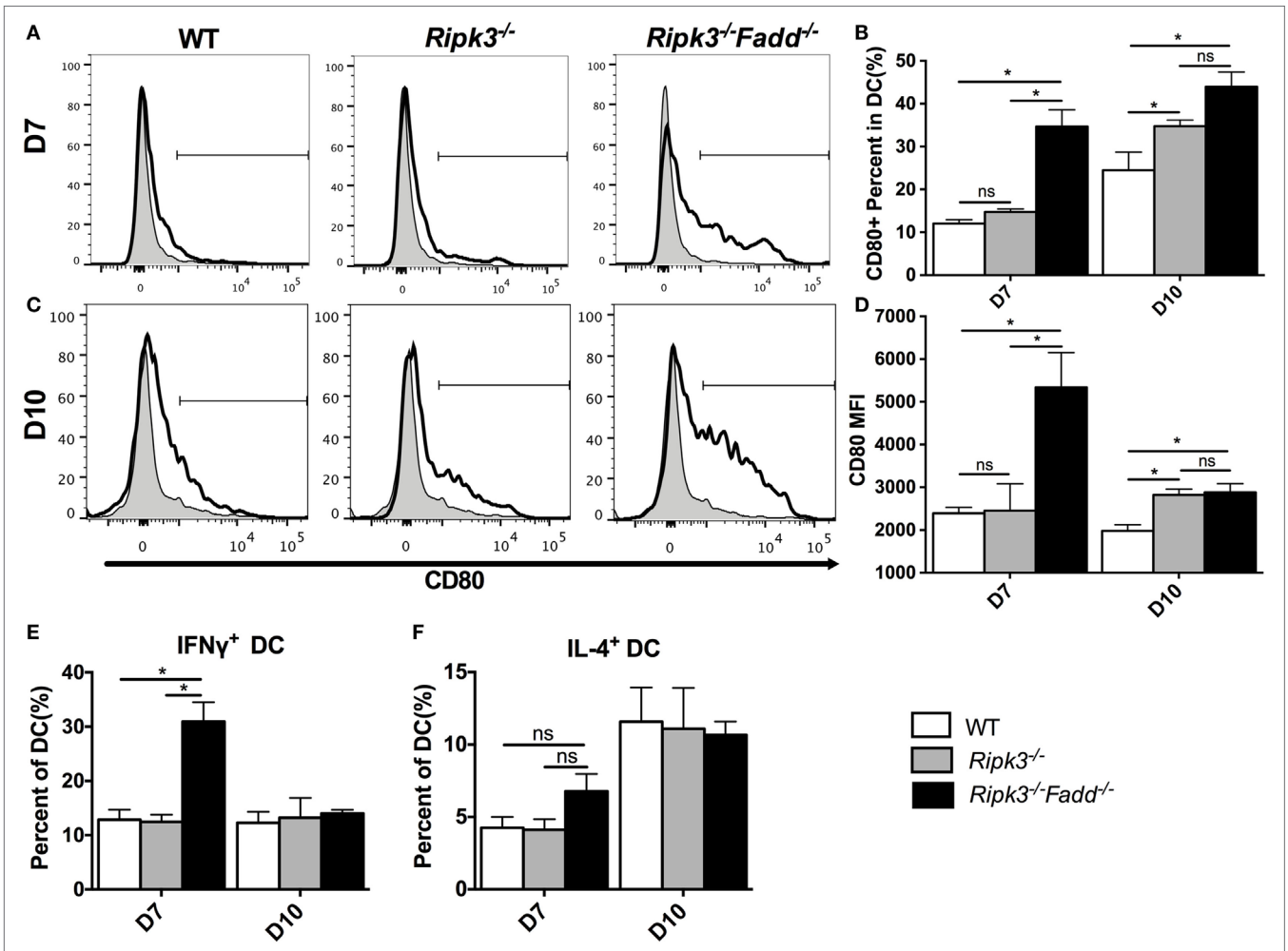

FIGURE 8 | RIPK3 and Fas-associated death domain (FADD) deletion promoted dendritic cells differentiation and activation in lung-associated lymph nodes (LALNs) after cryptococcal infection. LALNs were harvested from wild-type (WT), *Ripk3*$^{-/-}$, and *Ripk3*$^{-/-}$*Fadd*$^{-/-}$ mice at 7 and 10 days postinfection. Dendritic cells (DCs) were stained with CD80 **(A–D)**, IFNγ **(E)**, and IL-4 **(F)** antibodies and then analyzed by flow cytometry. Data are expressed as means and SEMs (n = 3 or more mice per group). ns, no significant difference, *P < 0.05, between compared groups. This experiment was repeated twice.

effects of *Ripk3*$^{-/-}$ Th polarization profile during *C. neoformans* infection.

RIPK3 and FADD Deletions Differentially Affected Apoptosis Rate in Leukocyte Subsets during *C. neoformans* Infection

To further explore the potential mechanisms underlying how RIPK3 and RIPK3/FADD pathways prevent excessive accumulation of inflammatory cells, we next evaluated the apoptotic frequency (APF) of various pulmonary cell subsets in *C. neoformans*-infected lungs. Lungs were dissociated gently, and single-cell suspensions were analyzed by flow cytometry with annexin V. Since different leukocyte subsets have distinct life spans and exploit different cell death pathways (30, 31), we first tested their APF in each group without fungal infection to exclude direct effects of FADD and/or RIPK3 deletions. All three groups exhibited similar rates of apoptosis in all subsets, indicating that FADD and RIPK3 were dispensable for homeostatic survival of these immune cells under physiological condition (data not shown).

Similar APFs in each cell subset at 10 dpi in *Ripk3*$^{-/-}$ compared with WT mouse infected lungs (**Figure 9** and Figure S4 in Supplementary Material) suggested that RIPK3 alone had no effect on inflammatory cell apoptosis during *C. neoformans* infection. However, *C. neoformans* infection significantly reduced eosinophil cell death in WT and *Ripk3*$^{-/-}$ mice (eosinophil APF from uninfected mice: 60.9% ± 1.4% decreasing to 6.6 ± 1.2%

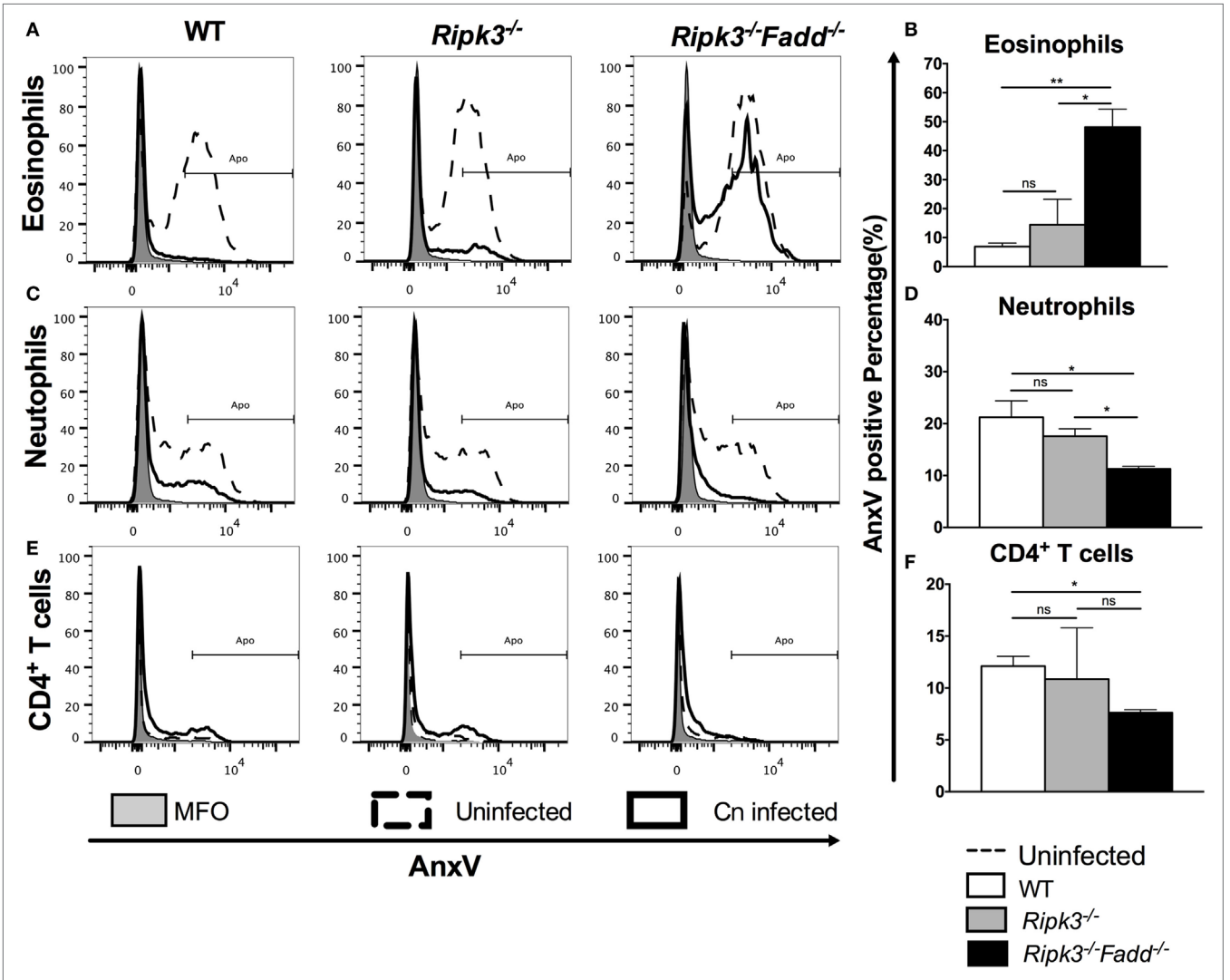

FIGURE 9 | Fas-associated death domain (FADD) deletion differentially regulated the apoptosis of pulmonary leukocyte subsets during *Cryptococcus neoformans* infection. Total pulmonary cells were gently harvested from wild-type (WT), *Ripk3*$^{-/-}$, and *Ripk3*$^{-/-}$*Fadd*$^{-/-}$ mice at 0 or 10 days postinfection. Isolated cells were stained with antibodies specific for annexin V and then analyzed by flow cytometry. After *C. neoformans* infection, eosinophils **(A,B)**, neutrophils **(C,D)**, and CD4$^+$ T cells **(E,F)** displayed significant alteration in apoptosis frequency in the lungs from *Ripk3*$^{-/-}$*Fadd*$^{-/-}$ mice but not *Ripk3*$^{-/-}$ mice. Other pulmonary subsets had no significant difference in apoptosis frequency between WT and genetic-defect mice (see Figure S2 in Supplementary Material). ns, no significant difference, $^*P < 0.05$, $^{**}P < 0.01$, between compared groups. This experiment was repeated twice.

and 16.3 ± 8.0, respectively), whereas the absence of FADD completely abolished this phenomenon (**Figures 9A,B**). A considerable reduction of neutrophil cell death was also detected in each group after fungal infection. Furthermore, consistent with the greatest increase in neutrophil accumulation, the *Ripk3*$^{-/-}$*Fadd*$^{-/-}$ group exhibited significant decrease in the APF of neutrophils (11.0% ± 0.9%) compared with WT (21.5 ± 3.2%, $P < 0.05$) or *Ripk3*$^{-/-}$ mice (17.6 ± 1.5%, **Figures 9C,D**). Among lymphocyte subsets, only CD4^{+} T cells displayed a significant reduction in cell death frequency in *Ripk3*$^{-/-}$*Fadd*$^{-/-}$ mice (12.1 ± 1.7 vs 7.6 ± 0.5%, $P < 0.05$), while other subpopulations did not differ in each group (**Figures 9E,F**). Collectively, these data indicated that *C. neoformans* infection affected apoptotic rates of certain leukocyte subsets, but only the joint FADD/RIPK3 deletion led to detectable alterations in the APF in these leukocyte subsets during fungal infection.

The Effects of RIPK3 and FADD Deletions on Anti-Cryptococcal Defenses Appear to Be Unrelated to Their Role Necroptosis Pathway

RIPK3 and FADD, among other functions, are major intracellular upstream mediators of necroptosis cell death pathway, a PCD resulting in cell lysis, reported to influence mycobacterial-infected macrophages (32) but also to regulate type-I IFN signaling in macrophages independent of necroptosis in influenza-infected macrophages (33). We first asked a question about the global role of necroptosis pathway in anti-cryptococcal host defenses. To asses this, mice with deletion of a distal effector kinase in necroptosis pathway, MLKL along with the WT mice, were infected with *C. neoformans* and mouse survival was monitored. Results show that MLKL deletion had no significant effect on *C. neoformans*-infected mouse survival (**Figure 10A**) demonstrating that the necroptosis cell death pathway is dispensable for mouse resistance to *C. neoformans*.

We next asked, whether *C. neoformans* infection triggers significant level of lytic cell death in macrophages and whether this was affected by RIPK3 and FADD deletion. To address this question, we used LDH release assay on WT, *Ripk3*$^{-/-}$, *Ripk3*$^{-/-}$*Fadd*$^{-/-}$ BMDM following *in vitro* H99-challenge. Results show that *C. neoformans* infection triggered lytic death in a small subset of BMDM (14.3 ± 1.7%, **Figure 10B**), The cell death rate was potentiated when the cells were treated with *C. neoformans* opsonized with M18B7 antibody, which increases cryptococcal uptake by macrophages (34) reaching (21.7 ± 1.6%, **Figure 10B**). However, neither RIPK3 deletion alone nor combined with FADD deletion had effect on the rate of BMDM death. This was in contrast with the positive control, in which lytic cell death triggered by the combined simulation of lipopolysaccharide with pan-caspase inhibition was profoundly reduced *Ripk3*$^{-/-}$, *Ripk3*$^{-/-}$*Fadd*$^{-/-}$ BMDM (**Figure 10B**). Thus, RIPK3 and FADD are not directly involved in regulation lytic cell death of BMDM population infected with *C. neoformans in vitro*, further supporting that the susceptibility of *Ripk3*$^{-/-}$ mice and *Ripk3*$^{-/-}$*Fadd*$^{-/-}$ mice to cryptococcal infection was mechanistically unrelated to the role RIPK3 and FADD in necroptosis pathway.

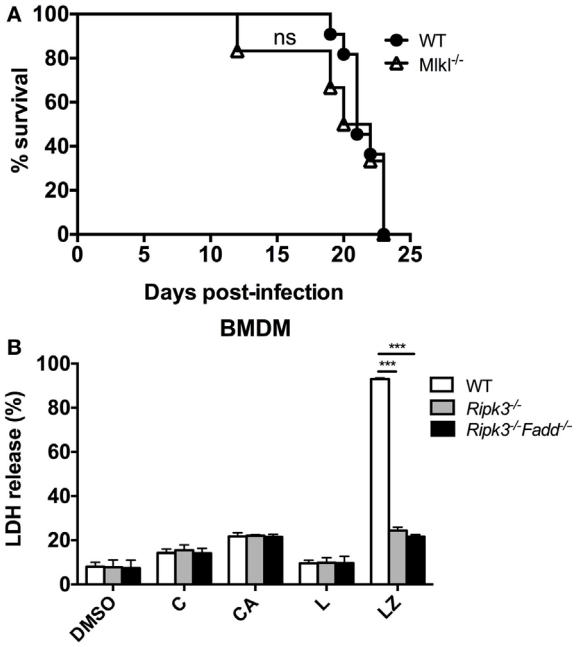

FIGURE 10 | Necroptosis process is not likely a mechanism for RIPK3- and Fas-associated death domain (FADD)-mediated effects on immune responses to *Cryptococcus neoformans*. **(A)** Wild-type (WT) mice and mice with targeted deletion of MLKL gene (distal effector kinase in necroptosis pathway) were infected with *C. neoformans* and analyzed as in **Figure 1D**. MLKL deletion had no effects on survival, unlike RIPK3 and FADD deletions (per **Figure 1D**) ($n = 10$ for each group). **(B)** Bone marrow-derived macrophage (BMDM) cells isolated form WT, *Ripk3*$^{-/-}$, *Ripk3*$^{-/-}$*Fadd*$^{-/-}$ mice were challenged with H99 at MOI = 5:1 and co-incubated for 24 h. Supernatants were collected followed by LDH release detection. In RIPK3 or FADD, deletions had no effect on magnitude of BMDM lytic death in contrast with their effects in positive control (LZ). Study was repeated three times independently. Symbols signify C, *C. neoformans*; A, anti-cryptococcal antibody M18B7; Z, zVAD (pan-caspase inhibitor); L, lipopolysaccharide; ns, no significant difference, ***$P < 0.001$, between compared groups.

DISCUSSION

While PCD pathway components were shown to be important regulators of the immune responses, the role of FADD and RIPK3 in host defenses against fungal infection remained unknown up to this point. This report provides novel data demonstrating that RIPK3 and FADD are crucial for fungal containment and survival of the infected host during *C. neoformans* infection. Here, we show that these factors serve jointly as physiological "brake" that prevents the development of over exuberant inflammation and profound Th1 bias, which in their absence leads to pulmonary damage and rapid deterioration of the infected host.

Our first group of studies elucidated the involvement of both RIPK3 and FADD during cryptococcal infection. Upon *C. neoformans* infection, RIPK3 expression in infected lungs was strongly upregulated and deletion of RIPK3 significantly shortened the survival of the infected mice and impaired fungal clearance. Furthermore, the absence of RIPK3 resulted in upregulation of pro-inflammatory components including, increased T cell numbers and neutrophils and increased inflammatory

cytokines in response to *C. neoformans* (**Figures 5** and **6**). These data provide evidence that RIPK3 exerts an important role in controlling inflammatory responses with some minor effect on Th polarization during *C. neoformans* infection that is at least in part independent of its well-established function in apoptosis and necroptosis pathways (**Figures 9** and **10**).

While FADD expression appeared to be constitutive, RIPK3/FADD double deletion resulted in further enhanced susceptibility to *C. neoformans* infection, demonstrating that joint absence of these factors further potentiated the effects of single RIPK3 deletion at both severity of pathology and upregulation of inflammatory components in the infected lungs. In *Ripk3*$^{-/-}$*Fadd*$^{-/-}$ mice, lung pathology and the effect on mouse survival effects were more severe (**Figures 1–3**; Figure S2 in Supplementary Material) compared to *Ripk3*$^{-/-}$ mice. Our pathology studies further highlighted that in *C. neoformans*-infected lungs RIPK3 and FADD play important roles in protecting infected lungs against the rapid development of severe pathology associated with excessive accumulation and activation of leukocytes. One caveat here could be that the enhanced inflammatory pathology was driven by the increased fungal burden; however, the lung CFU burdens even in the most profoundly affected *Ripk3*$^{-/-}$*Fadd*$^{-/-}$ mice were still relatively modest and could not explain the profound pathological changes and 80% mortality at day 10 in these mice. This, together with very selective amplification of Th1 response, clearly indicates that rather small differences in fungal burdens were not the major driver of the profound changes in the immunophenotype and increase in mouse mortality.

Inflammation is a double-edged sword in the pathogenesis of infectious disease. While suboptimal production of pro-inflammatory cytokines hinders control of *C. neoformans* infection (35–37), highly elevated production of these factors promotes severe inflammatory tissue damage (38). In at least some aspects of host–fungus interactions, a preservation immune strategy denoted "protective tolerance" may be optimal to limit immunopathology while controlling fungal infection (39). This is the first report that RIPK3 and FADD may play jointly important roles by critically fine-tuning "protective tolerance" mechanisms during anti-cryptococcal defense. We show that both of these two molecules are required for optimal control of fungal growth and host protection against the severe inflammatory pathology that develops in lungs in the absence of these factors. Interestingly, the phenotypes that developed in *Ripk3*$^{-/-}$*Fadd*$^{-/-}$ mice mirror many findings in cryptococcosis patients who suffer from IRIS. The development of IRIS (pre-IRIS phase) is specifically characterized by increasing pro-inflammatory responses without efficient clearance of the fungal pathogen (40, 41). Several cohort studies highlighted the relationship of IL-6 signaling and the risk of developing IRIS. For every twofold increase in IL-6 or C-reactive protein, the hazard of IRIS increased by 1.6 and 1.5, respectively (42). Another recent study proposed TNFα, IL-1β, and IL-12 to be predictors of IRIS (43), and these factors found to be elevated as a result of RIPK3 and FADD deletion in *C. neoformans*-infected lungs. Finally, a central IRIS characteristic reproduced in *Ripk3*$^{-/-}$*Fadd*$^{-/-}$ mice is massive systemic elevation of IFNγ, TNFα, and IL-6 (42) (**Figure 5**).

Besides the findings that mimic cytokine profiles of IRIS patients in our models, we also found the elevated induction of IL-1α and neutrophil recruitment in the lungs of both *Ripk3*$^{-/-}$ and *Ripk3*$^{-/-}$*Fadd*$^{-/-}$ mice. Neutrophil recruitment linked to IL-1α upregulation have been shown to contribute to the development of lethal lung pathology during fungal infection with *Aspergillus* (44). Together, these findings document that responses "designed" to be protective in fungal infections can become highly detrimental to the host, and our data demonstrate such detrimental outcomes following RIPK3 and FADD deletion. Collectively, our study shows that RIPK3 and FADD factors are crucial elements of regulatory network that allows protecting the host from pathological effects of inflammation while supporting clearance of the invasive fungal infection.

Another novel finding was that the expression of RIPK3 and FADD proteins was required for the development of Th2 polarization during *C. neoformans* infection. While the deletion of RIPK3 had subtle effect on Th2 polarization, joint deletion of RIPK3 and FADD resulted in a complete switch from strong Th2 to strong Th1 response. Cytokine profile analysis revealed massive reduction in Th2 cytokines (IL-4 and IL-33) in infected lungs of *Ripk3*$^{-/-}$*Fadd*$^{-/-}$ mice. This, together with diminished GATA3 expression by CD4 T cells and the absence of serum IgE accumulation (**Figures 5** and **6**), indicates the loss of Th2 polarization in response to RIPK3 and FADD deletion. Th1 and Th2 responses are known to counterbalance each other. Therefore, it remains to be determined if the primary effect of RIPK3/FADD deletion was the lack of the Th2 development with its subsequent "replacement by Th1," other way around, or else both pathways were subjected to concurrent regulation by joint action of RIPK3 and FADD. While future studies are needed to address these points, our data show that the net effect of RIPK3 and FADD is directly or indirectly counter-regulate Th1 and support Th2 polarization during *C. neoformans* infection. Another highly unexpected finding was that strong Th1 bias and the absence of Th2 rather than being protective (19, 45) resulted in non-protective response in the infected *Ripk3*$^{-/-}$*Fadd*$^{-/-}$ mice. This absence of improved clearance following RIPK3/FADD deletions, despite the robust Th1 polarization, was not due to a defect in macrophage M1 polarization or loss of their intrinsic fungicidal function downstream of robust M1 polarization. Our studies of macrophages from infected lungs and BMDMs revealed neither a defect in macrophage polarization nor a defect in their effector (killing) functions resulting from RIPK3 or FADD deletion (**Figure 7**). In spite of this, we observed paradoxical impairment of pulmonary fungal clearance in both *Ripk3*$^{-/-}$ and *Ripk3*$^{-/-}$*Fadd*$^{-/-}$ mice (**Figure 2**). One explanation for this observation is that the excessive systemic activation of microbicidal factors in macrophages resulted in exhaustion of these effectors cells even before they reached the infection site, which seems to be consistent with our data (**Figures 4** and **7**). Additionally, the excessive accumulation of neutrophils at the infection site interfered with macrophage and T-cell fungicidal functions, since an excessive accumulation of neutrophils have been reported to contribute to tissue damage and defects in the clearance of other fungal organisms (46, 47).

The final observation in our study is quite strong independence of immunoregulatory effects exerted by RIPK3 and FADD

from apoptotic or necroptotic cell death. The diminished apoptosis likely contributed to the excessive accumulation of neutrophils in infected *Ripk3*$^{-/-}$*Fadd*$^{-/-}$ mice (**Figures 3**, **4B** and **9D**) since, granulocytes are typically eliminated *via* extrinsic apoptosis after a brief period of activation (48). However, the enhanced neutrophil accumulation was also observed in *Ripk3*$^{-/-}$ mice without significant effect on neutrophil APF. Likewise, APF in eosinophil population was greatest in the infected *Ripk3*$^{-/-}$*Fadd*$^{-/-}$ mice, demonstrating that eosinophil apoptosis did not require or was positively regulated by FADD or RIPK3. Furthermore, RIPK3 and FADD deletion appeared not to affect APF in T and B cells, monocytes, DCs, or epithelial cells in the infected lungs. Finally, our outcomes do not favor necroptosis as an important pathway defining host–pathogen interactions during *C. neoformans* infection (**Figure 10**). Thus, while future studies are needed to provide definitive answers, our data favor the hypothesis that RIPK3 and FADD can induce immunoregulatory effects during fungal infection in a manner independent of their role in PCD responses, but chiefly by regulating cytokine responses.

In summary, our results demonstrate, for the first time, that RIPK3 and FADD are vital components of the immune responses to fungal pathogens. These molecules are required for fine-tuning of inflammatory responses during infection, acting as powerful regulators of Th1 and Th2 polarization. They contribute to optimal fungal clearance and serve as indispensable "nodes" in immunoregulatory network supporting tissue damage control in fungal-infected host.

ETHICS STATEMENT

This study was carried out in accordance with the recommendations of National Institutes of Health Guide for the Care and Use of Laboratory Animals. The protocol was approved by the Scientific Investigation Board of Second Military Medical University.

AUTHOR CONTRIBUTIONS

ZF, QX, and WF contributed to study concept and design, performing the experiments, and drafting of the manuscript. WL, MO, XD, and HZ (Haibing Zhang) contributed to study concept and design, analysis, and interpretation of data, critical revision of the manuscript, obtained funding, and provided study supervision, administrative, and technical support. HZ (Haiwei Zhang), JX (Jintao Xu), WP, and JX (Jinhua Xu) contributed to data analysis and revision of the manuscript. All listed authors gave final approval of the manuscript.

FUNDING

This study was supported by the National Key Basic Research Programs of China (2013CB531601 and 2013CB531606), the National Natural Science Foundation of China (81401651, 81471926, 81271799, and 81501728), China Postdoctoral Science Foundation Grant (2016M600286), and Shanghai Key Laboratory of Molecular Medical Mycology (14DZ2272900). MO's work is supported by Merit Review Grant 1I01BX000656 and VA Research Career Scientist Award 1K6BX003615 from the US Department of Veterans' Affairs.

SUPPLEMENTARY MATERIAL

The Supplementary Material for this article can be found online at http://journal.frontiersin.org/article/10.3389/fimmu.2017.01055/full#supplementary-material.

REFERENCES

1. Fang W, Fa Z, Liao W. Epidemiology of *Cryptococcus* and cryptococcosis in China. *Fungal Genet Biol* (2015) 78:7–15. doi:10.1016/j.fgb.2014.10.017
2. Heitman J, Kozel TR, Kwon-Chung KJ, Perfect JR, Casadevall A. *Cryptococcus: From Human Pathogen to Model Yeast*. Washington, DC: ASM Press (2010). 275 p.
3. Maziarz EK, Perfect JR. Cryptococcosis. *Infect Dis Clin North Am* (2016) 30(1):179–206. doi:10.1016/j.idc.2015.10.006
4. Greenlee-Wacker MC. Clearance of apoptotic neutrophils and resolution of inflammation. *Immunol Rev* (2016) 273(1):357–70. doi:10.1111/imr.12453
5. Ortega-Gomez A, Perretti M, Soehnlein O. Resolution of inflammation: an integrated view. *EMBO Mol Med* (2013) 5(5):661–74. doi:10.1002/emmm.201202382
6. Scaffidi C, Volkland J, Blomberg I, Hoffmann I, Krammer PH, Peter ME. Phosphorylation of FADD/MORT1 at serine 194 and association with a 70-kDa cell cycle-regulated protein kinase. *J Immunol* (2000) 164(3):1236–42. doi:10.4049/jimmunol.164.3.1236
7. Zhang J, Kabra NH, Cado D, Kang C, Winoto A. FADD-deficient T cells exhibit a disaccord in regulation of the cell cycle machinery. *J Biol Chem* (2001) 276(32):29815–8. doi:10.1074/jbc.M103838200
8. Balachandran S, Thomas E, Barber GN. A FADD-dependent innate immune mechanism in mammalian cells. *Nature* (2004) 432(7015):401–5. doi:10.1038/nature03124
9. Ma Y, Liu H, Tu-Rapp H, Thiesen HJ, Ibrahim SM, Cole SM, et al. Fas ligation on macrophages enhances IL-1R1-toll-like receptor 4 signaling and promotes chronic inflammation. *Nat Immunol* (2004) 5(4):380–7. doi:10.1038/ni1054
10. Zhang J, Cado D, Chen A, Kabra NH, Winoto A. Fas-mediated apoptosis and activation-induced T-cell proliferation are defective in mice lacking FADD/Mort1. *Nature* (1998) 392(6673):296–300. doi:10.1038/32681
11. Varfolomeev EE, Schuchmann M, Luria V, Chiannilkulchai N, Beckmann JS, Mett IL, et al. Targeted disruption of the mouse caspase 8 gene ablates cell death induction by the TNF receptors, Fas/Apo1, and DR3 and is lethal prenatally. *Immunity* (1998) 9(2):267–76. doi:10.1016/S1074-7613(00)80609-3
12. He S, Wang L, Miao L, Wang T, Du F, Zhao L, et al. Receptor interacting protein kinase-3 determines cellular necrotic response to TNF-alpha. *Cell* (2009) 137(6):1100–11. doi:10.1016/j.cell.2009.05.021
13. Kasof GM, Prosser JC, Liu D, Lorenzi MV, Gomes BC. The RIP-like kinase, RIP3, induces apoptosis and NF-kappaB nuclear translocation and localizes to mitochondria. *FEBS Lett* (2000) 473(3):285–91. doi:10.1016/S0014-5793(00)01473-3
14. Moriwaki K, Balaji S, McQuade T, Malhotra N, Kang J, Chan FK. The necroptosis adaptor RIPK3 promotes injury-induced cytokine expression and tissue repair. *Immunity* (2014) 41(4):567–78. doi:10.1016/j.immuni.2014.09.016
15. Shlomovitz I, Zargrian S, Gerlic M. Mechanisms of RIPK3-induced inflammation. *Immunol Cell Biol* (2017) 95(2):166–72. doi:10.1038/icb.2016.124
16. Zhang X, Fan C, Zhang H, Zhao Q, Liu Y, Xu C, et al. MLKL and FADD are critical for suppressing progressive lymphoproliferative disease and activating the NLRP3 inflammasome. *Cell Rep* (2016) 16(12):3247–59. doi:10.1016/j.celrep.2016.06.103

17. Semighini CP, Averette AF, Perfect JR, Heitman J. Deletion of *Cryptococcus neoformans* AIF ortholog promotes chromosome aneuploidy and fluconazole-resistance in a metacaspase-independent manner. *PLoS Pathog* (2011) 7(11):e1002364. doi:10.1371/journal.ppat.1002364
18. Meng Y, Zhang C, Yi J, Zhou Z, Fa Z, Zhao J, et al. Deubiquitinase Ubp5 is required for the growth and pathogenicity of *Cryptococcus gattii*. *PLoS One* (2016) 11(4):e0153219. doi:10.1371/journal.pone.0153219
19. Zhang Y, Wang F, Tompkins KC, McNamara A, Jain AV, Moore BB, et al. Robust Th1 and Th17 immunity supports pulmonary clearance but cannot prevent systemic dissemination of highly virulent *Cryptococcus neoformans* H99. *Am J Pathol* (2009) 175(6):2489–500. doi:10.2353/ajpath.2009.090530
20. Qiu Y, Dayrit JK, Davis MJ, Carolan JF, Osterholzer JJ, Curtis JL, et al. Scavenger receptor A modulates the immune response to pulmonary *Cryptococcus neoformans* infection. *J Immunol* (2013) 191(1):238–48. doi:10.4049/jimmunol.1203435
21. Stevens WW, Kim TS, Pujanauski LM, Hao X, Braciale TJ. Detection and quantitation of eosinophils in the murine respiratory tract by flow cytometry. *J Immunol Methods* (2007) 327(1–2):63–74. doi:10.1016/j.jim.2007.07.011
22. Xu J, Eastman AJ, Flaczyk A, Neal LM, Zhao G, Carolan J, et al. Disruption of early tumor necrosis factor alpha signaling prevents classical activation of dendritic cells in lung-associated lymph nodes and development of protective immunity against cryptococcal infection. *MBio* (2016) 7(4):e00510–16. doi:10.1128/mBio.00510-16
23. Szarka RJ, Wang N, Gordon L, Nation PN, Smith RH. A murine model of pulmonary damage induced by lipopolysaccharide via intranasal instillation. *J Immunol Methods* (1997) 202(1):49–57. doi:10.1016/S0022-1759(96)00236-0
24. Davis MJ, Tsang TM, Qiu Y, Dayrit JK, Freij JB, Huffnagle GB, et al. Macrophage M1/M2 polarization dynamically adapts to changes in cytokine microenvironments in *Cryptococcus neoformans* infection. *MBio* (2013) 4(3):e00264–13. doi:10.1128/mBio.00264-13
25. Davis MJ, Eastman AJ, Qiu Y, Gregorka B, Kozel TR, Osterholzer JJ, et al. *Cryptococcus neoformans*-induced macrophage lysosome damage crucially contributes to fungal virulence. *J Immunol* (2015) 194(5):2219–31. doi:10.4049/jimmunol.1402376
26. Alanio A, Desnos-Ollivier M, Dromer F. Dynamics of *Cryptococcus neoformans*-macrophage interactions reveal that fungal background influences outcome during cryptococcal meningoencephalitis in humans. *MBio* (2011) 2(4):e00158–11. doi:10.1128/mBio.00158-11
27. Arora S, Olszewski MA, Tsang TM, McDonald RA, Toews GB, Huffnagle GB. Effect of cytokine interplay on macrophage polarization during chronic pulmonary infection with *Cryptococcus neoformans*. *Infect Immun* (2011) 79(5):1915–26. doi:10.1128/IAI.01270-10
28. Herring AC, Falkowski NR, Chen GH, McDonald RA, Toews GB, Huffnagle GB. Transient neutralization of tumor necrosis factor alpha can produce a chronic fungal infection in an immunocompetent host: potential role of immature dendritic cells. *Infect Immun* (2005) 73(1):39–49. doi:10.1128/IAI.73.1.39-49.2005
29. Eastman AJ, Osterholzer JJ, Olszewski MA. Role of dendritic cell-pathogen interactions in the immune response to pulmonary cryptococcal infection. *Future Microbiol* (2015) 10(11):1837–57. doi:10.2217/fmb.15.92
30. Hampson P, Hazeldine J, Lord JM. Neutrophil apoptosis and its induction as a potential treatment for chronic inflammatory disease. *Curr Opin Hematol* (2013) 20(1):10–5. doi:10.1097/MOH.0b013e32835b06be
31. Shen ZJ, Malter JS. Determinants of eosinophil survival and apoptotic cell death. *Apoptosis* (2015) 20(2):224–34. doi:10.1007/s10495-014-1072-2
32. Zhao X, Khan N, Gan H, Tzelepis F, Nishimura T, Park SY, et al. Bcl-xL mediates RIPK3-dependent necrosis in *M. tuberculosis*-infected macrophages. *Mucosal Immunol* (2017). doi:10.1038/mi.2017.12
33. Downey J, Pernet E, Coulombe F, Allard B, Meunier I, Jaworska J, et al. RIPK3 interacts with MAVS to regulate type I IFN-mediated immunity to influenza A virus infection. *PLoS Pathog* (2017) 13(4):e1006326. doi:10.1371/journal.ppat.1006326
34. Zebedee SL, Koduri RK, Mukherjee J, Mukherjee S, Lee S, Sauer DF, et al. Mouse-human immunoglobulin G1 chimeric antibodies with activities against *Cryptococcus neoformans*. *Antimicrob Agents Chemother* (1994) 38(7):1507–14. doi:10.1128/AAC.38.7.1507
35. Bauman SK, Huffnagle GB, Murphy JW. Effects of tumor necrosis factor alpha on dendritic cell accumulation in lymph nodes draining the immunization site and the impact on the anticryptococcal cell-mediated immune response. *Infect Immun* (2003) 71(1):68–74. doi:10.1128/IAI.71.1.68-74.2003
36. Siddiqui AA, Shattock RJ, Harrison TS. Role of capsule and interleukin-6 in long-term immune control of *Cryptococcus neoformans* infection by specifically activated human peripheral blood mononuclear cells. *Infect Immun* (2006) 74(9):5302–10. doi:10.1128/IAI.00661-06
37. Axton PJ, Bancroft GJ. In vivo analysis of immune responses to *Cryptococcus neoformans* – role of interferon-gamma in host resistance. *Biochem Soc Trans* (1997) 25(2):276S. doi:10.1042/bst025276s
38. Osterholzer JJ, Milam JE, Chen GH, Toews GB, Huffnagle GB, Olszewski MA. Role of dendritic cells and alveolar macrophages in regulating early host defense against pulmonary infection with *Cryptococcus neoformans*. *Infect Immun* (2009) 77(9):3749–58. doi:10.1128/IAI.00454-09
39. Roussey JA, Olszewski MA, Osterholzer JJ. Immunoregulation in fungal diseases. *Microorganisms* (2016) 4(4):E47. doi:10.3390/microorganisms4040047
40. Skiest DJ, Hester LJ, Hardy RD. Cryptococcal immune reconstitution inflammatory syndrome: report of four cases in three patients and review of the literature. *J Infect* (2005) 51(5):e289–97. doi:10.1016/j.jinf.2005.02.031
41. Wiesner DL, Boulware DR. *Cryptococcus*-related immune reconstitution inflammatory syndrome (IRIS): pathogenesis and its clinical implications. *Curr Fungal Infect Rep* (2011) 5(4):252–61. doi:10.1007/s12281-011-0064-8
42. Boulware DR, Meya DB, Bergemann TL, Wiesner DL, Rhein J, Musubire A, et al. Clinical features and serum biomarkers in HIV immune reconstitution inflammatory syndrome after cryptococcal meningitis: a prospective cohort study. *PLoS Med* (2010) 7(12):e1000384. doi:10.1371/journal.pmed.1000384
43. Sun J, Chen H, Xie Y, Su J, Huang Y, Xu L, et al. Nuclear factor of activated T cells and cytokines gene expression of the T cells in AIDS patients with immune reconstitution inflammatory syndrome during highly active antiretroviral therapy. *Mediators Inflamm* (2017) 2017:1754741. doi:10.1155/2017/1754741
44. Caffrey AK, Lehmann MM, Zickovich JM, Espinosa V, Shepardson KM, Watschke CP, et al. IL-1alpha signaling is critical for leukocyte recruitment after pulmonary *Aspergillus fumigatus* challenge. *PLoS Pathog* (2015) 11(1):e1004625. doi:10.1371/journal.ppat.1004625
45. Holmer SM, Evans KS, Asfaw YG, Saini D, Schell WA, Ledford JG, et al. Impact of surfactant protein D, interleukin-5, and eosinophilia on cryptococcosis. *Infect Immun* (2014) 82(2):683–93. doi:10.1128/IAI.00855-13
46. Zelante T, De Luca A, D'Angelo C, Moretti S, Romani L. IL-17/Th17 in anti-fungal immunity: what's new? *Eur J Immunol* (2009) 39(3):645–8. doi:10.1002/eji.200839102
47. Zelante T, De Luca A, Bonifazi P, Montagnoli C, Bozza S, Moretti S, et al. IL-23 and the Th17 pathway promote inflammation and impair antifungal immune resistance. *Eur J Immunol* (2007) 37(10):2695–706. doi:10.1002/eji.200737409
48. Fox S, Leitch AE, Duffin R, Haslett C, Rossi AG. Neutrophil apoptosis: relevance to the innate immune response and inflammatory disease. *J Innate Immun* (2010) 2(3):216–27. doi:10.1159/000284367

Conflict of Interest Statement: The authors declare that the research was conducted in the absence of any commercial or financial relationships that could be construed as a potential conflict of interest.

Copyright © 2017 Fa, Xie, Fang, Zhang, Zhang, Xu, Pan, Xu, Olszewski, Deng and Liao. This is an open-access article distributed under the terms of the Creative Commons Attribution License (CC BY). The use, distribution or reproduction in other forums is permitted, provided the original author(s) or licensor are credited and that the original publication in this journal is cited, in accordance with accepted academic practice. No use, distribution or reproduction is permitted which does not comply with these terms.

frontiers in Immunology

REVIEW
published: 22 January 2018
doi: 10.3389/fimmu.2017.01996

A Multifaceted Role of Tryptophan Metabolism and Indoleamine 2,3-Dioxygenase Activity in *Aspergillus fumigatus*–Host Interactions

*Tsokyi Choera[1], Teresa Zelante[2], Luigina Romani[2] and Nancy P. Keller[1,3]**

[1] Department of Medical Microbiology and Immunology, University of Wisconsin-Madison, Madison, WI, United States, [2] Department of Experimental Medicine, University of Perugia, Perugia, Italy, [3] Department of Bacteriology, University of Wisconsin-Madison, Madison, WI, United States

Aspergillus fumigatus is the most prevalent filamentous fungal pathogen of humans, causing either severe allergic bronchopulmonary aspergillosis or often fatal invasive pulmonary aspergillosis (IPA) in individuals with hyper- or hypo-immune deficiencies, respectively. Disease is primarily initiated upon the inhalation of the ubiquitous airborne conidia—the initial inoculum produced by *A. fumigatus*—which are complete developmental units with an ability to exploit diverse environments, ranging from agricultural composts to animal lungs. Upon infection, conidia initially rely on their own metabolic processes for survival in the host's lungs, a nutritionally limiting environment. One such nutritional limitation is the availability of aromatic amino acids (AAAs) as animals lack the enzymes to synthesize tryptophan (Trp) and phenylalanine and only produce tyrosine from dietary phenylalanine. However, *A. fumigatus* produces all three AAAs through the shikimate–chorismate pathway, where they play a critical role in fungal growth and development and in yielding many downstream metabolites. The downstream metabolites of Trp in *A. fumigatus* include the immunomodulatory kynurenine derived from indoleamine 2,3-dioxygenase (IDO) and toxins such as fumiquinazolines, gliotoxin, and fumitremorgins. Host IDO activity and/or host/microbe-derived kynurenines are increasingly correlated with many *Aspergillus* diseases including IPA and infections of chronic granulomatous disease patients. In this review, we will describe the potential metabolic cross talk between the host and the pathogen, specifically focusing on Trp metabolism, the implications for therapeutics, and the recent studies on the coevolution of host and microbe IDO activation in regulating inflammation, while controlling infection.

Keywords: *Aspergillus fumigatus*, tryptophan metabolism, IDO, kynurenines, toxins, non-ribosomal peptides, peripheral tolerance, Th17 cells

OPEN ACCESS

Edited by:
Steven Templeton, Indiana University School of Medicine – Terre Haute, United States

Reviewed by:
Mark S. Gresnigt, Radboud University Nijmegen, Netherlands
Sven Krappmann, University of Erlangen-Nuremberg, Germany

****Correspondence:***
Nancy P. Keller
npkeller@wisc.edu

Specialty section:
This article was submitted to Microbial Immunology, a section of the journal Frontiers in Immunology

Received: *02 November 2017*
Accepted: *22 December 2017*
Published: *22 January 2018*

Citation:
Choera T, Zelante T, Romani L and Keller NP (2018) A Multifaceted Role of Tryptophan Metabolism and Indoleamine 2,3-Dioxygenase Activity in Aspergillus fumigatus–Host Interactions. Front. Immunol. 8:1996. doi: 10.3389/fimmu.2017.01996

INTRODUCTION

Aspergillus fumigatus is a saprophytic fungus that has a worldwide distribution. The asexual spores (called conidia) are ubiquitous and individuals inhale hundreds of spores daily. While most inhaled conidia are cleared by individuals with a healthy immune system, *A. fumigatus* can act as an opportunistic human pathogen in individuals with altered immune functions. Disease presentation can vary on the status of the host's immune system; *A. fumigatus* can cause allergic bronchopulmonary aspergillosis, a severe allergenic response, in the hyper-immune, or the fatal invasive growth

invasive pulmonary aspergillosis (IPA) in the hypo-immune, or in individuals with other susceptibilities such as patients unable to mount the necessary oxidative defenses such as in individuals with chronic granulomatous disease (CGD) (1).

The manifestation of disease is dependent not only on the host's immune status but also fungal factors including strain heterogeneity (2). *A. fumigatus* growth in the mammalian lung, following survival of resident pulmonary defenses, requires the fungus to adapt to a hypoxic and nutritionally scarce environment. *Aspergillus* mutants unable to synthesize primary metabolites necessary for growth are generally impaired in virulence. For example, deletion of *cpcA*, a transcription factor that globally modulates amino acid biosynthesis in the fungus led to a less virulent phenotype in a murine model of IPA (3). Additional studies have shown that mutants in sulfur utilization (4), uracil/uridine synthesis (5), zinc uptake, iron acquisition, and many more (6, 7) are also decreased in virulence.

To complicate disease progression further, there is an alarming rise in antifungal resistance strains of *A. fumigatus* (8, 9). Therefore, an understanding of *A. fumigatus* and host metabolic pathways is important in identifying nutrient limitations. One critical metabolic pathway is the biosynthesis of aromatic amino acids [AAAs, tryptophan (Trp), phenylalanine, and tyrosine], which are required not only for growth of *A. fumigatus* but are also precursors for several toxins (**Table 1**). The host relies on dietary sources for all AAAs while *A. fumigatus* synthesizes all three. However, the host and *A. fumigatus* both possess AAA catabolic enzymes. In particular, one key enzyme important in immune homeostasis is indoleamine 2,3-dioxygenase (IDO), which converts Trp to kynurenine and related metabolites in both organisms. Historically, host IDOs activity has been described as an effective antimicrobial control for pathogens that are natural Trp auxotrophs such as *Staphylococcus aureus*, *Chlamydia* spp., and *Toxoplasma gondii*, presumably by Trp starvation (10). However, *A. fumigatus* can synthesize its own Trp and thus the Trp starvation may not be an effective pathogen control for those microbes able to synthesize their own Trp pools. Although, IDOs also play additional roles in host defenses through modifying kynurenine levels and subsequent cytokine responses as described below. In this review, we will summarize the recent studies describing the anabolic and the catabolic pathways of Trp metabolism, the implications for therapeutics, and the host–pathogen interaction.

TABLE 1 | *Aspergillus fumigatus* non-ribosomal peptides containing aromatic amino acids (AAAs) in their peptide structure.

Toxin	AAA[a]	Interaction with host[b-i]
Fumigaclavine C[b]	Tryptophan (Trp)	Downregulation of Th1 cytokines including TNF-α, IL-1β, and IL-17A. Induction of host cell apoptosis Decrease activation of caspase-1
Fumiquinazoline C[c]	Anthranilate Trp	Cytotoxic
Fumisoquin[d]	Tyrosine	Nothing reported
Fumitremorgin[e] Tryprostatin A[f] Verruculogen[g]	Trp	Neurotoxic and produces tremors in mice Tryprostatin causes the inhibition of microtubule assembly Verruculogen causes modification of the electrophysiological properties of HNEC
Gliotoxin[h]	Phenylalanine	Virulent in a steroid murine model of IPA Induction of host cell apoptosis and causes epithelial cell damage Inhibition of phagocytosis and oxidative bursts
Hexadehydroastechrome[i]	Trp	Overexpression resulted in a significantly higher virulence in a neutropenic murine model of IPA[b]

IPA, invasive pulmonary aspergillosis; HNEC, human nasal epithelial cells.
[a]Only the AAA is designated. Other amino acids are also in the structure of these metabolites.
[b–i]Biosynthesis and host interactions based from the following sources: [b](11, 12); [c](13); [d](14); [e](15, 16); [f](17); [g](18, 19); [h](7, 20); [i](21, 22).

Trp SYNTHESIS AND POTENTIAL THERAPEUTIC TARGETING

Chorismic acid derived from the shikimic acid pathway is a key intermediate in producing Trp, phenylalanine (Phe), and tyrosine (Tyr) in microorganisms including *A. fumigatus* (**Figure 1**). Trp and Phe are classified as essential amino acids, whereas mammals acquire them from diet, whereas Tyr is synthesized *via* the hydroxylation of Phe (23, 24). The absence of the AAA biosynthetic enzymes and the low bioavailability of Trp in humans makes the Trp biosynthetic enzymes attractive targets for antifungals (25).

Fungal Trp Anabolic Pathway

Aromatic amino acid synthesis has been extensively studied in *Saccharomyces cerevisiae* and provides the basis for the functional characterization of orthologous enzymes in filamentous fungi (23, 24, 26–28). The shikimic acid pathway is a 7-enzymatic step reaction that initiates with two substrates, phosphoenolpyruvate (PEP) and erythrose-4-phosphate (E4P), which are intermediates of glycolysis and pentose phosphate pathways, respectively (29) (**Figure 1**). The first step of the shikimic acid pathway is catalyzed by 3-deoxy-D-arabinoheptulosonate 7-phosphate (DAHP) synthase to convert PEP and E4P to DAHP. In *S. cerevisiae* and *A. nidulans*, there are two DAHP synthases, Aro3 and Aro4, which are allosterically inhibited by phenylalanine and tyrosine, respectively (24). Steps 2–6 in filamentous fungi such as *A. nidulans* and *A. fumigatus* are completed by the pentafunctional enzyme AroM, or Aro1 in the model organism *S. cerevisiae* (30). The shikimate pathway culminates in the production of chorismic acid synthesized by the enzyme chorismate synthase (AroB) from 5-enolpyruvylshikimate-3-phosphate (EPSP) (31).

The synthesis of Trp from chorismate is initiated by an anthranilate synthase (AS), which converts chorismate to anthranilate, followed by three enzymatic steps as presented in **Figure 1** with the respective functions outlined in **Table 2**. AS(s) in *S. cerevisiae* have been characterized, and it consists of two subunits: anthranilate synthase subunit I (AAS-I), which binds chorismate and is subject to feedback inhibition by Trp and anthranilate synthase

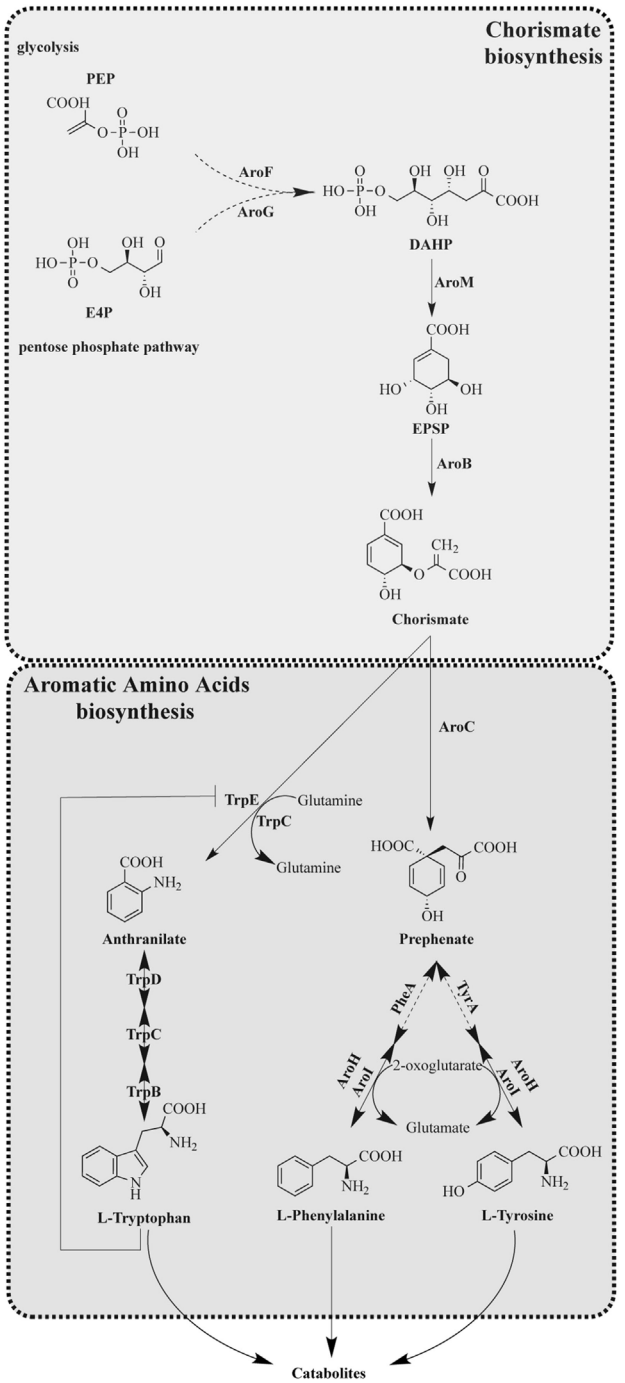

FIGURE 1 | Tryptophan anabolism of *Aspergillus fumigatus*. [Modified from that of Wang et al. (28)]. Solid arrows indicate characterized reaction as being present in *A. fumigatus* with product detected. Dashed arrows indicate uncharacterized reactions; however, putative orthologs are present in *A. fumigatus*.

subunit II (AAS-II) which is a glutamine amidotransferase (32). The *A. nidulans trpC*, an AAS-II encoding gene, was characterized in 1977 (33) and found exchangeable with an *A. fumigatus trpC* in 1994 (34). Wang et al. (28) recently characterized *trpE*, the AAS-I encoding gene in *A. fumigatus*. Wang et al. (28) explored the functions of two putative AAS-Is termed *trpE* and *icsA* by creating null mutants. The deletion of *trpE* led to a Trp auxotrophic strain, whereas the deletion of *icsA* did not. To ensure that *icsA* did not serve a redundant role for Trp synthesis, the group overexpressed *icsA* in a *trpE* deletion and showed that the overexpression of *icsA* does not reverse the Trp auxotrophy concluding that TrpE is the only AS in *A. fumigatus*. Interestingly, the group showed that IcsA is an active enzyme in *A. fumigatus* as the precursor-chorismate pool is altered in the absence or overproduction of IcsA; however, the product is not known (28). Sasse et al. also confirmed that deletion of *trpE* (they termed *trpA*) results in an *A. fumigatus* Trp auxotrophy (31).

The Shikimate Pathway As Potential Antifungal Targets

Currently, there are four major classes of antifungals: azoles and amphotericin B targeting ergosterol, 5-fluorocytosine targeting DNA synthesis, and echinocandins targeting cell wall synthesis. These antifungals either exhibit high toxicity to the mammalian cell (particularly amphotericin B and 5-fluorocytosine) or lose efficacy due to the emergence of drug resistant strains (azoles and echinocandins) (9). With *A. fumigatus* being a eukaryotic pathogen and sharing many proteins with mammalian hosts, there are limitations to developing effective and safe antifungals and therefore a great need for treatments that are fungal specific. Since Trp is a human-essential amino acid and the enzymes in the biosynthesis are fungal specific, several studies have suggested utilizing and finding drugs to target the enzymes of this pathway (35–38).

Targeting essential amino acid pathways have already shown potential for new classes of antifungals. Several groups have explored inhibitors of genes or enzymes involved in methionine biosynthesis. Azoxybacillin, a compound isolated from *B. cereus* targets methionine biosynthesis by interfering with expression of homoserine transacetylase and sulfite reductase encoding genes (39–41). Whereas azoxybacillin displayed a broad spectrum antifungal activity *in vitro*, *in vivo* activity was low possibly due to bioavailability in the host (41). R1-331, a natural product from *Streptomyces akiyoshiensis*, is an effective inhibitor of homoserine dehydrogenase involved in both methionine and threonine biosynthesis (42, 43). Yamaguchi et al. show that R1-331 was active against medically important fungi such as *Candida albicans* and *Cryptoccocus neoformans* and proved to be effective in the treatment of systemic murine candidiasis (42, 44).

Compounds targeting AAA pathways are limited with the most famous being the herbicide Roundup, where the active ingredient glyphosate inhibits EPSP synthase, one of the first enzymes initiating the shikimate pathway (45) (**Figure 1**). Glyphosate has shown to inhibit growth of several fungi including *Candida maltose* (46), *Pneumocystis* (47), and *Cryptococcus neoformans* where glyphosate delayed fungal melanization *in vitro* and *in vivo* and prolonged mice survival during infection (48). Another inhibitor of AAA pathway is a fluorinated anthranilate moiety, 6-FABA, which targets the TrpE enzyme and showed bactericidal activity when used on *Mycobacterium tuberculosis* (49). The studies of

TABLE 2 | *Aspergillus fumigatus* tryptophan (Trp) metabolism genes and putative protein function.

Protein	Ortholog in *Saccharomyces cerevisiae*	Gene name in *A. fumigatus*	Protein function[a]	Ortholog in mammals
Chorismate biosynthesis				
AroF	Aro3	Afu1g02110	DAHP synthase	–
AroG	Aro4	Afu7g04070		
AroM	Aro1	Afu1g13740	EPSP synthase	–
AroB	Aro2	Afu1g06940	Chorismate synthase	–
Aromatic amino acid (AAA) biosynthesis				
TrpE	Trp2	Afu6g12580	Anthranilate synthase	–
TrpC	Trp3	Afu1g13090		
TrpD	Trp4	Afu4g11980	Anthranilate phosphoribosyltransferase	–
TrpC	Trp1	Afu1g13090	Phosphoribosylanthranilate isomerase	–
TrpB	Trp5	Afu2g13250	Trp synthase	–
IcsA	–	Afu6g12110	Isochorismate synthase	–
AroC	Aro7	Afu5g13130	Chorismate mutase	–
PheA	Pha2	Afu5g05690	Prephenate dehydratase	–
TyrA	Tyr1	Afu2g10450	Prephenate dehydrogenase	–
AroH	Aro8	Afu2g13630	AAA transaminase	–
AroI	Aro9	Afu5g02290		
Trp degradation				
IdoA	Bna2	Afu3g14250	Indoleamine 2,3-dioxygenases	IDO1
IdoB	Bna2	Afu4g09830		IDO2
IdoC	Bna2	Afu7g02010		TDO
FmdS	Bna7	Afu1g09960	Kynurenine formamidase	AFMID
Bna4	Bna4	Afu6g07340	Kynureninase	
Bna5	Bna5	Afu4g09840		KYNU
AroH	Aro8	Afu2g13630	AAA transaminase	LAAO
AroI	Aro9	Afu5g02290		
AadA	–	Afu3g02240	Trp carboxylase	AADC
MaoN	–	Afu3g00100	Monoamine oxidase	MAOA
AldA	Ald4	Afu2g00720	Aldehyde dehydrogenase	ALDH
	Ald5	Afu7g01000		
		Afu6g11430		

[a]*Prediction of protein function based on AspGD (http://www.aspgd.org/) and KEGG (http://www.genome.jp/kegg/kegg2.html).*
DAHP synthase, 3-deoxy-D-arabinoheptulosonate 7-phosphate synthase; EPSP synthase, enolpyruvylshikimate-3-phosphate synthase; AFMID, arylformamidase; KYNU, kynureninase; LAAO, L-amino-acid oxidase; AADC, aromatic-L-amino-acid decarboxylase, MAOA, monoamine oxidase; ALDH2, aldehyde dehydrogenase family.

these inhibitors suggest that the Trp biosynthetic pathway could be fruitful in future antifungal drug design.

The value of AAA pathways as drug targets is supported by the findings that AAA auxotrophic mutants are less virulent in animal infection models. Sasse et al. explored the possibility of these pathways as potential drug target by testing the virulence of several AAA auxotrophic mutants in a murine IPA model (31). This study demonstrated that AroM (**Figure 1**) was required for *A. fumigatus* viability. The group also constructed a conditional AroB repression strain that was attenuated virulence. Both a Trp auxotroph (TrpE mutant) and Tyr/Phe auxotroph (AroC mutant) were severely attenuated in virulence for pulmonary infection. Interestingly, the group also unveiled a putative difference in AAA distribution within the host by conducting a systemic infection showing that in a bloodstream infection the TrpE and the AroC mutants although less virulent, can establish some infection (31). Taken together, these results suggest that inhibitors of AAA biosynthetic pathways can potentially be used against *A. fumigatus* as a standalone treatment in a localized pulmonary infection or as an additive treatment in a systemic infection. The result of the bloodstream infection observed by Sasse et al. also suggests that there are mechanisms for the fungus to sense Trp in its environment and utilize it. In *S. cerevisiae*, the Trp specific permease, Tat2, is required for Trp uptake in yeast (50) and its closest homolog in *A. fumigatus* (Afu7g04290) is upregulated during fungal encounters with neutrophils (51) and dendritic cells (52). In *A. nidulans*, the G-protein coupled receptor (Gpr) H may be responsible for sensing Trp and glucose and GprH is conserved in *A. fumigatus* (53, 54). Perhaps, for a systemic infection, inhibition of specific permeases or development of a GprH antagonist would be useful in reducing infections by *Aspergillus*.

CATABOLIC Trp METABOLITES IN FUNGI AND HOST

Although the anabolic Trp pathway is absent in mammals, the common catabolic pathways exist in the mammalian host with possession of the same enzymes as *A. fumigatus* (**Figure 2**). Through the expression of Trp degradation enzymes, immune cells are both controlling inflammation and combating microbial infection. In addition to Trp degradation pathways conserved with animals, *A. fumigatus* can also direct Trp pools to secondary metabolites that may impact host health and response (**Table 1**).

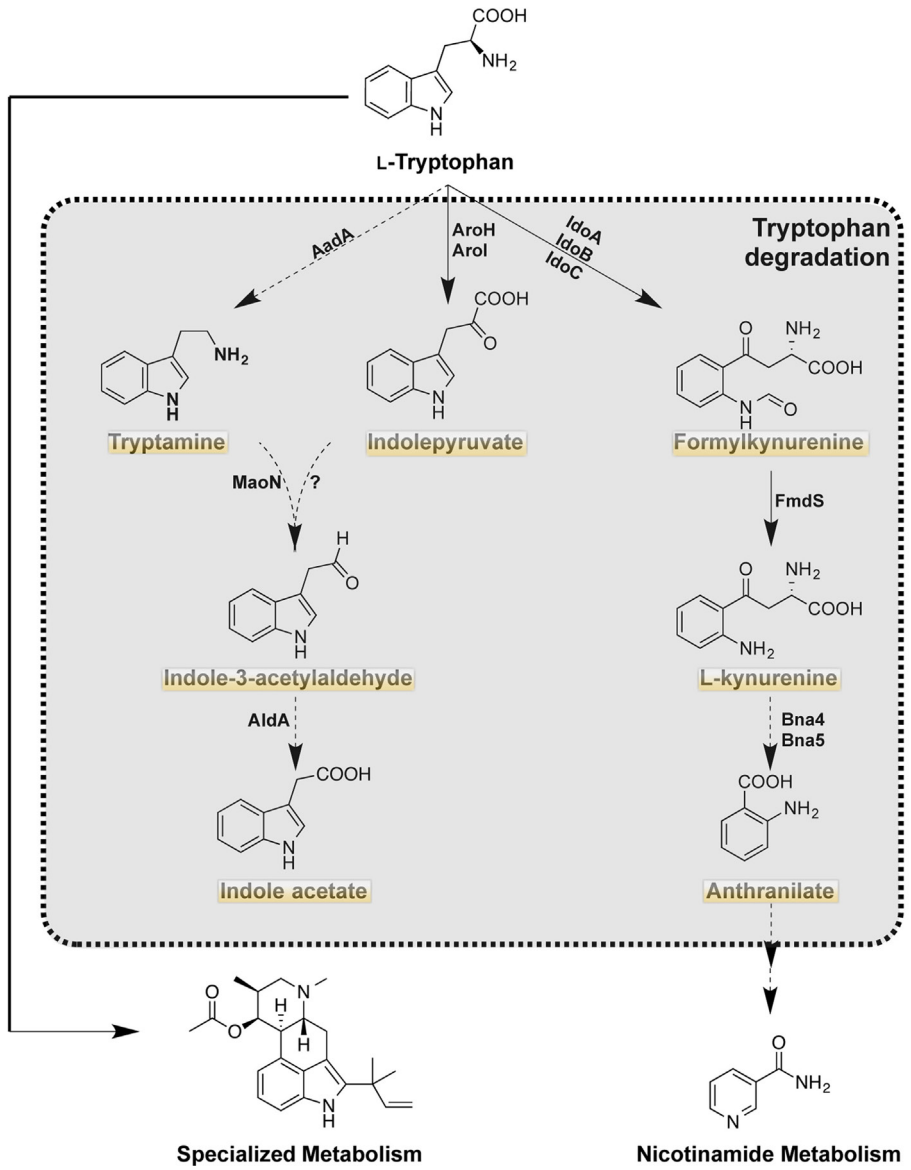

FIGURE 2 | Tryptophan catabolism of *Aspergillus fumigatus*. Highlighted products are putatively produced in the mammalian host as the orthologous enzymes are present in the host (http://www.genome.jp/kegg). Solid arrows indicate characterized reaction as being present in *A. fumigatus* with product detected. Dashed arrows indicate uncharacterized reactions, however putative orthologs are present in *A. fumigatus*.

Fungal Trp Catabolism

There are three putative pathways (**Figure 2**; **Table 2**) for the degradation of Trp in *A. fumigatus*. The kynurenine branch is catalyzed by IDOs that convert Trp into formylkynurenine. In *A. fumigatus*, there are 3 putative *ido* genes: *idoA*, *idoB*, and *idoC*, the orthologs of *A. oryzae ido*α, *ido*β, and *ido*γ, respectively (55). Enzymatic studies of *Aspergillus oryzae* IDO enzymes suggest two of the three enzymes, IDOα, and IDOβ, may participate in Trp degradation as they have a higher affinity of its substrate. However the recent study by Wang et al., suggested IDOb might be the more dominant enzyme than IDOa as determined by gene expression of *A. fumigatus* grown on Trp amended media (28). Additionally, *idoC* gene expression was slightly induced by the addition of Trp, but the authors note that IDOc had a closer relationship to bacterial IDOs than to fungal IDOs (28, 55). In *S. cerevisiae*, formylkynurenine is further oxidized to the immunomodulatory product kynurenine by a kynurenine formamidase denoted as Bna7, which has been described in *A. nidulans* and is predicted to be involved in NAD (+), biosynthesis (56). The kynurenine branch in fungi is involved in the *de novo* biosynthesis of NAD (+), a coenzyme that is required for oxidation-reduction reactions (57).

Tryptophan can also be metabolized via the indole pyruvate pathway, initiated through the transamination of Trp by aromatic

aminotransferases (termed Aro8 and Aro9 in *S. cerevisiae*). These aromatic aminotransferases are also involved in the synthesis of Phe and Tyr in *S. cerevisiae*, and their orthologs are present in *A. fumigatus* (28). In *S. cerevisiae*, the deletion of both Aro8 and Aro9 results in Phe and Tyr auxotrophies (24, 58, 59). In *Candida* spp., where filamentation and pigment production play a role in virulence, the products of these enzymes have been described to influence both phenotypes. The deletion of *aro*8 in *C. glabrata* results in a reduced pigment production and leads to an increased sensitivity to hydrogen peroxide (27). The *aro*8 and *aro*9 mutants of *C. albicans* results in a decreased conversion of Trp to indole acetaldehyde, which is formed via decarboxylation of indole pyruvate. Filamentation of *C. albicans* increased with the exposure to indole acetaldehyde (60).

Indole acetaldehyde can also be produced via the third putative product of Trp degradation: tryptamine. Tryptamine is most famously known as the active compound in psilocybin and for its similarity to serotonins (61). Although the production of tryptamine has yet to be described in *A. fumigatus*, the downstream product of the tryptamine and indole pyruvate pathway, indole acetic acid has been described in several *Aspergillus* spp. including *A. fumigatus* (62, 63). Downstream metabolism of kynurenine, indole pyruvate, and tryptamine has not been explored further, but *A. fumigatus* does possess putative enzymes for the re-synthesis of anthranilate, the precursor to Trp (as denoted in **Figures 1** and **2**).

AAA Incorporation into *Aspergillus* Toxins

Many filamentous fungi, including *A. fumigatus*, produce bioactive small molecules that can have detrimental impacts on human health. Subsets of these toxins are small peptides synthesized by non-ribosomal peptide synthetases (NRPS). Several pathogenic *Aspergillus* species synthesize AAA derived peptides including gliotoxin (*Phe* and serine) (64), fumiquinazoline (*Trp*, *Anthranilate*, and Alanine) (13), fumigaclavine (*Trp*) (65), fumitremorgin (*Trp* and Proline) (66), hexadehydroastechrome (*Trp* and Alanine) (21), fumisoquin (*Tyr*, Serine, and Methionine) (14), DPP-IV inhibitor WYK-1 (*Trp*, *Tyr*, and Leucine) (67), cyclopiazonic acid (*Trp*) (68) and benzomalvin (*Phe* and *Anthranilate*) (69). **Table 1** summarizes the known AAA derived secondary metabolites of *A. fumigatus* and their effect on the host.

Although, fumiquinazolines have yet to be assessed for virulence in an animal model, they are known to have cytotoxic properties (13). Fumigaclavines have been described to have immunosuppressive properties in several studies including the suppression of antifungal cytokines such as TNFα, IL-17, and IFN-γ (12). Fumitremorgin, verruculogen, and tryprostatin—all related products of the fumitremorgin pathway—induce tremorgenic activity in mice and act on the central nervous system (15, 66, 70, 71). Mutants in the hexadehydroastechrome pathway (21) and gliotoxin (20, 21) pathways have altered virulence in murine IPA models. Decreased virulence of the *gliP* mutant (GliP is the NRPS required for gliotoxin synthesis) is dependent on host immune status [reviewed in Ref. (7)]. Overexpression of *hasA* encoding the hexadehydroastechrome transcription factor and thus leading to increased hexadehydroastechrome production was more virulent than wild type *A. fumigatus* in a neutropenic model of IPA (21). Although the exact mechanism underlying the increased virulence of the OE::*hasA* strain is unknown, iron homeostasis and cross talk between metabolic pathways may contribute to the increased virulence of OE::*hasA* (22). These studies highlight the potential contribution of AAA derived toxins in virulence of *A. fumigatus*.

Host Trp Catabolism *via* IDO

The function of host IDO during mammalian infection was originally thought to center on the anti-proliferative effects of pathogenic microorganism via deprivation of Trp exerted by the host. IDO is up-regulated by interferon gamma (IFNγ) and depletes Trp (the least abundant essential amino acid) to inhibit pathogen expansion (72, 73), as demonstrated in the constraint of chlamydial growth (74). Numerous studies have since implicated IDO activity as important in fungal infections and have reported the relative outcomes of IDO expression on disease progression (**Table 3**). Accumulating data continues to support that IDO participates in the host–pathogen interaction in human epithelial cells; therefore, the co-evolution of host and microbe Trp metabolism has been investigated (75). The current consensus is that IDO activation is pivotal in regulating inflammatory processes directly

TABLE 3 | Summary of studies where IDO enzyme activity was found to be implicated in fungal infections.

Fungus	Mouse model	IDO	Outcome	Reference
Candida albicans	Gastrointestinal inf.	Upregulation	Protection of the host against fungus	(76)
C. albicans	Gastrointestinal inf.	Upregulation	Protection of the host against fungus	(77)
C. albicans	Gastrointestinal inf.	Upregulation	Protection of the host against fungus	(78)
C. albicans	*In vitro*	Downregulation	Not done	(79)
Aspergillus fumigatus	Keratitis	Upregulation	Protection of the host against fungus	(80)
A. fumigatus	Allergy	Overexpression	Protection of the host against fungus	(81)
A. fumigatus	IPA	Upregulation	Protection of the host against fungus	(82)
A. fumigatus	IPA in chronic granulomatous disease mice	Upregulation	Protection of the host against fungus	(83)
A. fumigatus	IPA in CF mice	Upregulation	Protection of the host against fungus	(84)
Paracoccidioides brasiliensis	Pulmonary infection	Upregulation	Protection of the host against fungus	(85)
P. brasiliensis	Pulmonary infection	Upregulation	Protection of the host against fungus	(86)
P. brasiliensis	Pulmonary infection	Upregulation	Protection of the host against fungus	(87)
Histoplasma capsulatum	Pulmonary infection	Downregulation	Protection of the host against fungus	(88)
H. capsulatum	Pulmonary infection	Upregulation	Protection of the host against fungus	(89)

via Trp depletion and indirectly via the IDO-mediated release of Trp catabolic secondary metabolites (namely, kynurenines).

Dietary Trp is catabolized by two different IDO protein isoforms, IDO1 and IDO2 that are expressed by immune cells, and TDO (Trp 2,3-dioxygenase) that is mainly expressed in the liver. Cells involved in the innate processes of the anti-microbial defense, such as dendritic cells (DCs), neutrophils, and macrophages express IDO1 upon microbial encounter mainly *via* toll-like receptor stimulation. How fungi specifically induce IDO expression is not known; however, induction by other pathogens is associated with pathogen associated molecular patterns, including lipopolysaccharides and CpG oligodeoxynucleotides (78, 90–92), underlining a role for kynurenine metabolism in microbial-induced inflammatory processes.

IDO-Mediated Tolerance: Impacts on Antimicrobial Responses

Evolutionary studies have shown that the host immune defense against microbes is characterized by three different mechanisms: avoidance, resistance, and tolerance (93). Modules of immunity provide resistance to limit pathogen burden and tolerance and host damage caused by the immune reaction *per se*. However, the inflammatory reaction, although largely considered beneficial for its antimicrobial functions, may also contribute to pathogenicity. Thus, rescue from infection pathology may not only depend on microbial colonization (and inactivation of resistance mechanisms) but also on the resolution of tissue inflammatory pathology through tolerogenic responses to pathogens (94).

Studies using a mouse model of mucosal or invasive *C. albicans* infection found that systemic inhibition of IDO *in vivo* reduced gastrointestinal inflammation and unexpectedly, elevated the levels of fungal colonization compared to control mice (77). Notably, tolerogenic responses toward *C. albicans* were abrogated when IDO was antagonized *in vivo*, as shown in various models of inflammatory disorders (95, 96). As with *C. albicans*, IDO and kynurenine production during *A. fumigatus* infection contributes to fungal pathogen eradication and the regulation of an unacceptable level of tissue damage (97). Indeed, IDO can increase kynurenine host levels to induce adaptive Treg expansion while limiting Th17 polarization (83, 96). In this context, the Th17 pathway, which downregulates Trp catabolism, may instead favor pathology and better explain the paradoxical correlation between fungal infection and chronic inflammation (98).

Another example of this paradox was demonstrated in the context of CGD, in which an NADPH oxidase defect results in reduced host production of antimicrobial ROS and extreme susceptibility to *Aspergillus* infections (1, 83). Although human studies have excluded a role for IDO in CGD (99), further investigations into the IDO pathway are warranted as such studies have failed to demonstrate functional IDO activity at sites of chronic inflammation. Measures of IDO functional activity during IPA have, however, been made in mouse models, and implicate defective IDO activity as a key mediator of chronic inflammation in CGD (83). An exaggerated Th17 pulmonary response was associated with reduced fungal clearance in mouse models of CGD that develop IPA. Here, reduced IDO function was directly related to NADPH/ROS deficiency, as ROS is essential for IDO catalytic activity in mammals (100). ROS deficiency as a result of reduced NADPH function, significantly enhanced IL-17 inflammation and fungal germination in the lung, thus further reducing neutrophil-mediated antimicrobial activities (83).

Since regulation of homeostasis and peripheral tolerance are extremely important in prevention of invasive Aspergillosis or allergy to *Aspergillus* antigens (97, 101), the role of IDO has been extensively studied in this model of fungal infection (81, 82, 102). These studies highlight the induction of the IDO metabolic pathway at different site of fungal colonization as keratinocytes or lung as well as the important anti-inflammatory activity of IDO in the tissue microenvironment (80–82, 84).

Aryl Hydrocarbon Receptor (AhR) Activation by IDO Metabolites in Mammals: Biological Consequences

The AhR is a ligand-activated transcription factor first identified for its role during embryonic development and induction of xenobiotic metabolizing enzymes as a response to environmental toxins, such as dioxin (103). More recently, AhR has been shown to play a critical role in immunity by acting as an immune modulator during fungal infection (85). The connection between the AhR and the immune response lies in part in the endogenous Ahr ligands, which comprise many Trp metabolites, including kynurenine (104). Microbial Trp-derived metabolites can activate the AhR, leading to adjustments in the immune response that may hinder disease development (105). The AhR–IDO axis has been recently demonstrated in fungal infection, highlighting a role for IDO-derived metabolites to trigger AhR target genes (85, 106). For example, one AhR target gene, *Il22*, has been widely studied in the context of fungal/microbial infections (105, 107–109). AhR activation by IDO metabolites can also mediate the expansion of peripheral Treg with anti-inflammatory properties. Using IDO-deficient mice, increased pulmonary disease caused by *Paracoccidioides brasiliensis* was associated with decreased Treg expansion and reduced AhR protein expression (85). In murine models of IPA, distinct Treg populations capable of mediating anti-inflammatory effects expand following exposure to *Aspergillus* conidia (97). Late in infection, tolerogenic adaptive Treg (with shared phenotypic identity with the Treg controlling autoimmune diseases or diabetes) produce IL-10 and TGFβ, inhibit Th2 cells, and prevent an allergic reaction to *Aspergillus* (97).

CONCLUSION

The interplay of Trp metabolic pathways and fungal/host interactions is intriguing with many unanswered questions of the exact nature of crosstalk of shared metabolites and consequences of activation of Trp degradative pathways. In *Aspergillus* infections in particular, not only does the pathogen synthesize and degrade Trp but it also can utilize this amino acid (and its precursor anthranilate or the other two AAAs Tyr and Phe) to yield several potentially damaging toxins (**Table 1**). Also, as both host and *Aspergillus* share catabolic IDO pathways, it is unclear which

organism may generate immunomodulatory Trp degradation products and if they respond to each other's products (e.g., kynurenine). Development of *A. fumigatus* IDO mutants for investigation of disease development could yield valuable information on this front. The research on the expression host IDOs exhibit the importance of an extremely coordinated immune response to mount the right inflammatory response for clearance of spores. However, while an increased IDO expression in the host can control inflammation, the suppression of the IDO-regulated antifungal Th17 responses can favor fungal growth. In this context, it will be critical to explore the entire IDO-mediated innate response, including the specific T cell regulatory subsets affected by IDO activity.

Although the Trp catabolic pathway is shared between host and pathogen, the anabolic pathway is unique to *A. fumigatus.* The antifungals currently used in treatment are becoming increasingly ineffective with emerging drug resistant strains; therefore, drugs targeting essential fungal specific pathways are needed. A proposal for fungal treatment has been highlighted through the studies of essential amino acids. As AAA mutants are auxotrophs and decreased in virulence (28, 31), investigations of drugs targeting these pathway enzymes could lead to novel antifungal compounds. Indeed, a few compounds have exhibited some efficacy in targeting Trp metabolic pathways in *M. tuberculosis* and several fungi and efforts to identify additional inhibitors are warranted.

AUTHOR CONTRIBUTIONS

TC, TZ, and NK have made a substantial, direct, and intellectual contribution to the work and LR provided intellectual insights to the revision. All authors have approved it for publication.

ACKNOWLEDGMENTS

The authors would like to thank support from Dalai Lama Trust MSN178745 to TC, The Italian Grant "Programma per Giovani Ricercatori - Rita Levi Montalcini 2013" to TZ, and NIH 5R01AI065728-10 to NK.

REFERENCES

1. Segal BH, Romani LR. Invasive aspergillosis in chronic granulomatous disease. *Med Mycol* (2009) 47:S282–90. doi:10.1080/13693780902736620
2. Keller NP. Heterogeneity confounds establishment of "a" model microbial strain. *MBio* (2017) 8:e00135–17. doi:10.1128/mBio.00135-17
3. Krappmann S, Bignell EM, Reichard U, Rogers T, Haynes K, Braus GH. The *Aspergillus fumigatus* transcriptional activator CpcA contributes significantly to the virulence of this fungal pathogen. *Mol Microbiol* (2004) 52:785–99. doi:10.1111/j.1365-2958.2004.04015.x
4. Amich J, Dumig M, O'keeffe G, Binder J, Doyle S, Beilhack A, et al. Exploration of sulfur assimilation of *Aspergillus fumigatus* reveals biosynthesis of sulfur-containing amino acids as a virulence determinant. *Infect Immun* (2016) 84:917–29. doi:10.1128/IAI.01124-15
5. D'Enfert C, Diaquin M, Delit A, Wuscher N, Debeaupuis JP, Huerre M, et al. Attenuated virulence of uridine-uracil auxotrophs of *Aspergillus fumigatus*. *Infect Immun* (1996) 64:4401–5.
6. Rhodes JC. *Aspergillus fumigatus*: growth and virulence. *Med Mycol* (2006) 44(Suppl 1):S77–81. doi:10.1080/13693780600779419
7. Dagenais TR, Keller NP. Pathogenesis of *Aspergillus fumigatus* in invasive aspergillosis. *Clin Microbiol Rev* (2009) 22:447–65. doi:10.1128/CMR.00055-08
8. Sanglard D. Emerging threats in antifungal-resistant fungal pathogens. *Front Med* (2016) 3:11. doi:10.3389/fmed.2016.00011
9. Perlin DS, Rautemaa-Richardson R, Alastruey-Izquierdo A. The global problem of antifungal resistance: prevalence, mechanisms, and management. *Lancet Infect Dis* (2017) 17(12):e383–92. doi:10.1016/S1473-3099(17)30316-X
10. Mackenzie CR, Heseler K, Muller A, Daubener W. Role of indoleamine 2,3-dioxygenase in antimicrobial defence and immuno-regulation: tryptophan depletion versus production of toxic kynurenines. *Curr Drug Metab* (2007) 8:237–44. doi:10.2174/138920007780362518
11. Zhu YX, Yao LY, Jiao RH, Lu YH, Tan RX. Enhanced production of fumigaclavine C in liquid culture of *Aspergillus fumigatus* under a two-stage process. *Bioresour Technol* (2014) 152:162–8. doi:10.1016/j.biortech.2013.10.089
12. Guo W, Hu S, Elgehama A, Shao F, Ren R, Liu W, et al. Fumigaclavine C ameliorates dextran sulfate sodium-induced murine experimental colitis via NLRP3 inflammasome inhibition. *J Pharmacol Sci* (2015) 129:101–6. doi:10.1016/j.jphs.2015.05.003
13. Lim FY, Ames B, Walsh CT, Keller NP. Co-ordination between BrlA regulation and secretion of the oxidoreductase FmqD directs selective accumulation of fumiquinazoline C to conidial tissues in *Aspergillus fumigatus*. *Cell Microbiol* (2014) 16:1267–83. doi:10.1111/cmi.12284
14. Baccile JA, Spraker JE, Le HH, Brandenburger E, Gomez C, Bok JW, et al. Plant-like biosynthesis of isoquinoline alkaloids in *Aspergillus fumigatus*. *Nat Chem Biol* (2016) 12:419–24. doi:10.1038/nchembio.2061
15. Suzuki S, Kikkawa K, Yamazaki M. Abnormal behavioral effects elicited by a neurotropic mycotoxin, fumitremorgin A in mice. *J Pharmacobiodyn* (1984) 7:935–42. doi:10.1248/bpb1978.7.935
16. Frisvad JC, Larsen TO. Extrolites of *Aspergillus fumigatus* and other pathogenic species in *Aspergillus* section fumigati. *Front Microbiol* (2015) 6:1485. doi:10.3389/fmicb.2015.01485
17. Usui T, Kondoh M, Cui CB, Mayumi T, Osada H. Tryprostatin A, a specific and novel inhibitor of microtubule assembly. *Biochem J* (1998) 333(Pt 3):543–8. doi:10.1042/bj3330543
18. Khoufache K, Puel O, Loiseau N, Delaforge M, Rivollet D, Coste A, et al. Verruculogen associated with *Aspergillus fumigatus* hyphae and conidia modifies the electrophysiological properties of human nasal epithelial cells. *BMC Microbiol* (2007) 7:5. doi:10.1186/1471-2180-7-5
19. Feng Y, Holte D, Zoller J, Umemiya S, Simke LR, Baran PS. Total synthesis of verruculogen and fumitremorgin A enabled by ligand-controlled C-H borylation. *J Am Chem Soc* (2015) 137:10160–3. doi:10.1021/jacs.5b07154
20. Sugui JA, Pardo J, Chang YC, Zarember KA, Nardone G, Galvez EM, et al. Gliotoxin is a virulence factor of *Aspergillus fumigatus*: *gliP* deletion attenuates virulence in mice immunosuppressed with hydrocortisone. *Eukaryot Cell* (2007) 6:1562–9. doi:10.1128/EC.00141-07
21. Yin WB, Baccile JA, Bok JW, Chen Y, Keller NP, Schroeder FC. A nonribosomal peptide synthetase-derived iron(III) complex from the pathogenic fungus *Aspergillus fumigatus*. *J Am Chem Soc* (2013) 135:2064–7. doi:10.1021/ja311145n
22. Wiemann P, Lechner BE, Baccile JA, Velk TA, Yin WB, Bok JW, et al. Perturbations in small molecule synthesis uncovers an iron-responsive secondary metabolite network in *Aspergillus fumigatus*. *Front Microbiol* (2014) 5:530. doi:10.3389/fmicb.2014.00530
23. Lingens F. Regulation of aromatic amino acid biosynthesis in microorganisms. *Acta Microbiol Acad Sci Hung* (1976) 23:161–6.
24. Braus GH. Aromatic amino acid biosynthesis in the yeast *Saccharomyces cerevisiae*: a model system for the regulation of a eukaryotic biosynthetic pathway. *Microbiol Rev* (1991) 55:349–70.
25. Tagliamonte A, Gessa R, Biggio G, Vargiu L, Gessa GL. Daily changes of free serum tryptophan in humans. *Life Sci* (1974) 14:349–54. doi:10.1016/0024-3205(74)90065-4
26. Pereira SA, Livi GP. Aromatic amino-acid biosynthesis in *Candida albicans*: identification of the ARO4 gene encoding a second DAHP synthase. *Curr Genet* (1996) 29:441–5. doi:10.1007/BF02221512
27. Brunke S, Seider K, Almeida RS, Heyken A, Fleck CB, Brock M, et al. *Candida glabrata* tryptophan-based pigment production via the Ehrlich pathway. *Mol Microbiol* (2010) 76:25–47. doi:10.1111/j.1365-2958.2010.07052.x

28. Wang PM, Choera T, Wiemann P, Pisithkul T, Amador-Noguez D, Keller NP. TrpE feedback mutants reveal roadblocks and conduits toward increasing secondary metabolism in *Aspergillus fumigatus*. *Fungal Genet Biol* (2016) 89:102–13. doi:10.1016/j.fgb.2015.12.002
29. Hawkins AR, Lamb HK, Moore JD, Charles IG, Roberts CF. The pre-chorismate (shikimate) and quinate pathways in filamentous fungi: theoretical and practical aspects. *J Gen Microbiol* (1993) 139:2891–9. doi:10.1099/00221287-139-12-2891
30. Duncan K, Edwards RM, Coggins JR. The pentafunctional AroM enzyme of *Saccharomyces cerevisiae* is a mosaic of monofunctional domains. *Biochem J* (1987) 246:375–86. doi:10.1042/bj2460375
31. Sasse A, Hamer SN, Amich J, Binder J, Krappmann S. Mutant characterization and *in vivo* conditional repression identify aromatic amino acid biosynthesis to be essential for *Aspergillus fumigatus* virulence. *Virulence* (2016) 7:56–62. doi:10.1080/21505594.2015.1109766
32. Graf R, Mehmann B, Braus GH. Analysis of feedback-resistant anthranilate synthases from *Saccharomyces cerevisiae*. *J Bacteriol* (1993) 175:1061–8. doi:10.1128/jb.175.4.1061-1068.1993
33. Kafer E. The anthranilate synthetase enzyme complex and the trifunctional *trpC* gene of *Aspergillus*. *Can J Genet Cytol* (1977) 19:723–38. doi:10.1139/g77-079
34. Borgia PT, Dodge CL, Eagleton LE, Adams TH. Bidirectional gene transfer between *Aspergillus fumigatus* and *Aspergillus nidulans*. *FEMS Microbiol Lett* (1994) 122:227–31. doi:10.1111/j.1574-6968.1994.tb07172.x
35. Hu W, Sillaots S, Lemieux S, Davison J, Kauffman S, Breton A, et al. Essential gene identification and drug target prioritization in *Aspergillus fumigatus*. *PLoS Pathog* (2007) 3:e24. doi:10.1371/journal.ppat.0030024
36. Blanco B, Prado V, Lence E, Otero JM, Garcia-Doval C, Van Raaij MJ, et al. *Mycobacterium tuberculosis* shikimate kinase inhibitors: design and simulation studies of the catalytic turnover. *J Am Chem Soc* (2013) 135:12366–76. doi:10.1021/ja405853p
37. Ianiri G, Idnurm A. Essential gene discovery in the basidiomycete *Cryptococcus neoformans* for antifungal drug target prioritization. *MBio* (2015) 6:e02334–14. doi:10.1128/mBio.02334-14
38. Kaltdorf M, Srivastava M, Gupta SK, Liang C, Binder J, Dietl AM, et al. Systematic identification of anti-fungal drug targets by a metabolic network approach. *Front Mol Biosci* (2016) 3:22. doi:10.3389/fmolb.2016.00022
39. Aoki Y, Kondoh M, Nakamura M, Fujii T, Yamazaki T, Shimada H, et al. A new methionine antagonist that has antifungal activity: mode of action. *J Antibiot (Tokyo)* (1994) 47:909–16. doi:10.7164/antibiotics.47.909
40. Aoki Y, Kamiyama T, Fujii T, Yamamoto M, Ohwada J, Arisawa M. Design of an antifungal methionine inhibitor not antagonized by methionine. *Biol Pharm Bull* (1995) 18:1267–71. doi:10.1248/bpb.18.1267
41. Aoki Y, Yamamoto M, Hosseini-Mazinani SM, Koshikawa N, Sugimoto K, Arisawa M. Antifungal azoxybacilin exhibits activity by inhibiting gene expression of sulfite reductase. *Antimicrob Agents Chemother* (1996) 40:127–32.
42. Yamaguchi M, Yamaki H, Shinoda T, Tago Y, Suzuki H, Nishimura T, et al. The mode of antifungal action of (S)2-amino-4-oxo-5-hydroxypentanoic acid, RI-331. *J Antibiot (Tokyo)* (1990) 43:411–6. doi:10.7164/antibiotics.43.411
43. Jacques SL, Ejim LJ, Wright GD. Homoserine dehydrogenase from *Saccharomyces cerevisiae*: kinetic mechanism and stereochemistry of hydride transfer. *Biochim Biophys Acta* (2001) 1544:42–54. doi:10.1016/S0167-4838(00)00202-8
44. Yamaki H, Yamaguchi M, Nishimura T, Shinoda T, Yamaguchi H. Unique mechanism of action of an antifungal antibiotic RI-331. *Drugs Exp Clin Res* (1988) 14:467–72.
45. Tan S, Evans R, Singh B. Herbicidal inhibitors of amino acid biosynthesis and herbicide-tolerant crops. *Amino Acids* (2006) 30:195–204. doi:10.1007/s00726-005-0254-1
46. Bode R, Melo C, Birnbaum D. Mode of action of glyphosate in *Candida maltosa*. *Arch Microbiol* (1984) 140:83–5. doi:10.1007/BF00409776
47. Chin K, Wyder MA, Kaneshiro ES. Glyphosate reduces organism viability and inhibits growth *in vitro* of *Pneumocystis*. *J Eukaryot Microbiol* (1999) 46:139S–41S.
48. Fernandes JD, Martho K, Tofik V, Vallim MA, Pascon RC. The role of amino acid permease and tryptophan biosynthesis in *Cryptococcus neoformans* survival. *PLoS One* (2015) 10:e0132369. doi:10.1371/journal.pone.0132369
49. Abdel-Rahman HM, El-Koussi NA, Hassan HY. Fluorinated 1,2,4-triazolo[1,5-a]pyrimidine-6-carboxylic acid derivatives as antimycobacterial agents. *Arch Pharm (Weinheim)* (2009) 342:94–9. doi:10.1002/ardp.200800113
50. Forsberg H, Gilstring CF, Zargari A, Martinez P, Ljungdahl PO. The role of the yeast plasma membrane SPS nutrient sensor in the metabolic response to extracellular amino acids. *Mol Microbiol* (2001) 42:215–28. doi:10.1046/j.1365-2958.2001.02627.x
51. Sugui JA, Kim HS, Zarember KA, Chang YC, Gallin JI, Nierman WC, et al. Genes differentially expressed in conidia and hyphae of *Aspergillus fumigatus* upon exposure to human neutrophils. *PLoS One* (2008) 3:e2655. doi:10.1371/journal.pone.0002655
52. Morton CO, Varga JJ, Hornbach A, Mezger M, Sennefelder H, Kneitz S, et al. The temporal dynamics of differential gene expression in *Aspergillus fumigatus* interacting with human immature dendritic cells *in vitro*. *PLoS One* (2011) 6:e16016. doi:10.1371/journal.pone.0016016
53. Grice CM, Bertuzzi M, Bignell EM. Receptor-mediated signaling in *Aspergillus fumigatus*. *Front Microbiol* (2013) 4:26. doi:10.3389/fmicb.2013.00026
54. Brown NA, Dos Reis TF, Ries LN, Caldana C, Mah JH, Yu JH, et al. G-protein coupled receptor-mediated nutrient sensing and developmental control in *Aspergillus nidulans*. *Mol Microbiol* (2015) 98:420–39. doi:10.1111/mmi.13135
55. Yuasa HJ, Ball HJ. The evolution of three types of indoleamine 2,3 dioxygenases in fungi with distinct molecular and biochemical characteristics. *Gene* (2012) 504:64–74. doi:10.1016/j.gene.2012.04.082
56. Fraser JA, Davis MA, Hynes MJ. The formamidase gene of *Aspergillus nidulans*: regulation by nitrogen metabolite repression and transcriptional interference by an overlapping upstream gene. *Genetics* (2001) 157:119–31.
57. Ohashi K, Kawai S, Murata K. Secretion of quinolinic acid, an intermediate in the kynurenine pathway, for utilization in NAD+ biosynthesis in the yeast *Saccharomyces cerevisiae*. *Eukaryot Cell* (2013) 12:648–53. doi:10.1128/EC.00339-12
58. Urrestarazu A, Vissers S, Iraqui I, Grenson M. Phenylalanine- and tyrosine-auxotrophic mutants of *Saccharomyces cerevisiae* impaired in transamination. *Mol Gen Genet* (1998) 257:230–7. doi:10.1007/s004380050643
59. Bulfer SL, Brunzelle JS, Trievel RC. Crystal structure of *Saccharomyces cerevisiae* Aro8, a putative alpha-aminoadipate aminotransferase. *Protein Sci* (2013) 22:1417–24. doi:10.1002/pro.2315
60. Rao RP, Hunter A, Kashpur O, Normanly J. Aberrant synthesis of indole-3-acetic acid in *Saccharomyces cerevisiae* triggers morphogenic transition, a virulence trait of pathogenic fungi. *Genetics* (2010) 185:211–20. doi:10.1534/genetics.109.112854
61. Tylš F, Páleníček T, Horáček J. Psilocybin – summary of knowledge and new perspectives. *Eur Neuropsychopharmacol* (2014) 24:342–56. doi:10.1016/j.euroneuro.2013.12.006
62. Bilkay IS, Karakoç S, Aksoz N. Indole-3-acetic acid and gibberellic acid production in *Aspergillus niger*. *Turk J Biol* (2010) 34:313–8. doi:10.3906/biy-0812-15
63. Pattaeva M, Bakhtiyor R. Growth and phytohormones production by thermophilic *Aspergillus fumigatus* 2 and thermotolerant *Aspergillus terreus* 8 strains in salt stress. *Br J Appl Sci Technol* (2015) 8:305–12. doi:10.9734/BJAST/2015/12292
64. Macdonald JC, Slater GP. Biosynthesis of gliotoxin and mycelianamide. *Can J Biochem* (1975) 53:475–8. doi:10.1139/o75-066
65. Mulinti P, Allen NA, Coyle CM, Gravelat FN, Sheppard DC, Panaccione DG. Accumulation of ergot alkaloids during conidiophore development in *Aspergillus fumigatus*. *Curr Microbiol* (2014) 68:1–5. doi:10.1007/s00284-013-0434-2
66. Yamazaki M, Suzuki S. Toxicology of tremorgenic mycotoxins, fumitremorgin A and B. *Dev Toxicol Environ Sci* (1986) 12:273–82.
67. Imamura K, Tsuyama Y, Hirata T, Shiraishi S, Sakamoto K, Yamada O, et al. Identification of a gene involved in the synthesis of a dipeptidyl peptidase IV inhibitor in *Aspergillus oryzae*. *Appl Environ Microbiol* (2012) 78:6996–7002. doi:10.1128/AEM.01770-12
68. Liu X, Walsh CT. Cyclopiazonic acid biosynthesis in *Aspergillus* sp.: characterization of a reductase-like R* domain in cyclopiazonate synthetase that forms and releases cyclo-acetoacetyl-L-tryptophan. *Biochemistry* (2009) 48:8746–57. doi:10.1021/bi901123r

69. Clevenger KD, Bok JW, Ye R, Miley GP, Verdan MH, Velk T, et al. A scalable platform to identify fungal secondary metabolites and their gene clusters. *Nat Chem Biol* (2017) 13:895–901. doi:10.1038/nchembio.2408
70. Yamazaki M, Fujimoto H, Kawasaki T. Chemistry of tremorogenic metabolites. Fumitremorgin A from *Aspergillus fumigatus*. *Chem Pharm Bull (Tokyo)* (1980) 28:245–54. doi:10.1248/cpb.28.245
71. Cole RJ. Fungal tremorogens. *Prikl Biokhim Mikrobiol* (1993) 29:44–50.
72. Colangelo EJ. Cervicocranium and the aviator's protective helmet. *Aviat Space Environ Med* (1975) 46:1263–4.
73. Zelante T, Fallarino F, Bistoni F, Puccetti P, Romani L. Indoleamine 2,3-dioxygenase in infection: the paradox of an evasive strategy that benefits the host. *Microbes Infect* (2009) 11:133–41. doi:10.1016/j.micinf.2008.10.007
74. Thomas SM, Garrity LF, Brandt CR, Schobert CS, Feng GS, Taylor MW, et al. IFN-gamma-mediated antimicrobial response. Indoleamine 2,3-dioxygenase-deficient mutant host cells no longer inhibit intracellular *Chlamydia* spp. or *Toxoplasma* growth. *J Immunol* (1993) 150:5529–34.
75. Aldajani WA, Salazar F, Sewell HF, Knox A, Ghaemmaghami AM. Expression and regulation of immune-modulatory enzyme indoleamine 2,3-dioxygenase (IDO) by human airway epithelial cells and its effect on T cell activation. *Oncotarget* (2016) 7:57606–17. doi:10.18632/oncotarget.11586
76. De Luca A, Montagnoli C, Zelante T, Bonifazi P, Bozza S, Moretti S, et al. Functional yet balanced reactivity to *Candida albicans* requires TRIF, MyD88, and IDO-dependent inhibition of Rorc. *J Immunol* (2007) 179:5999–6008. doi:10.4049/jimmunol.179.9.5999
77. Bozza S, Fallarino F, Pitzurra L, Zelante T, Montagnoli C, Bellocchio S, et al. A crucial role for tryptophan catabolism at the host/*Candida albicans* interface. *J Immunol* (2005) 174:2910–8. doi:10.4049/jimmunol.174.5.2910
78. Bonifazi P, Zelante T, D'angelo C, De Luca A, Moretti S, Bozza S, et al. Balancing inflammation and tolerance *in vivo* through dendritic cells by the commensal *Candida albicans*. *Mucosal Immunol* (2009) 2:362–74. doi:10.1038/mi.2009.17
79. Cheng SC, Van De Veerdonk F, Smeekens S, Joosten LA, Van Der Meer JW, Kullberg BJ, et al. *Candida albicans* dampens host defense by downregulating IL-17 production. *J Immunol* (2010) 185:2450–7. doi:10.4049/jimmunol.1000756
80. Jiang N, Zhao G, Lin J, Hu L, Che C, Li C, et al. Indoleamine 2,3-dioxygenase is involved in the inflammation response of corneal epithelial cells to *Aspergillus fumigatus* infections. *PLoS One* (2015) 10:e0137423. doi:10.1371/journal.pone.0137423
81. Paveglio SA, Allard J, Foster Hodgkins SR, Ather JL, Bevelander M, Campbell JM, et al. Airway epithelial indoleamine 2,3-dioxygenase inhibits CD4+ T cells during *Aspergillus fumigatus* antigen exposure. *Am J Respir Cell Mol Biol* (2011) 44:11–23. doi:10.1165/rcmb.2009-0167OC
82. De Luca A, Bozza S, Zelante T, Zagarella S, D'angelo C, Perruccio K, et al. Non-hematopoietic cells contribute to protective tolerance to *Aspergillus fumigatus* via a TRIF pathway converging on IDO. *Cell Mol Immunol* (2010) 7:459–70. doi:10.1038/cmi.2010.43
83. Romani L, Fallarino F, De Luca A, Montagnoli C, D'angelo C, Zelante T, et al. Defective tryptophan catabolism underlies inflammation in mouse chronic granulomatous disease. *Nature* (2008) 451:211–5. doi:10.1038/nature06471
84. Iannitti RG, Carvalho A, Cunha C, De Luca A, Giovannini G, Casagrande A, et al. Th17/Treg imbalance in murine cystic fibrosis is linked to indoleamine 2,3-dioxygenase deficiency but corrected by kynurenines. *Am J Respir Crit Care Med* (2013) 187:609–20. doi:10.1164/rccm.201207-1346OC
85. Araujo EF, Feriotti C, Galdino NAL, Preite NW, Calich VLG, Loures FV. The IDO-AhR axis controls Th17/Treg immunity in a pulmonary model of fungal infection. *Front Immunol* (2017) 8:880. doi:10.3389/fimmu.2017.00880
86. Araujo EF, Medeiros DH, Galdino NA, Condino-Neto A, Calich VL, Loures FV. Tolerogenic plasmacytoid dendritic cells control *Paracoccidioides brasiliensis* infection by inducting regulatory T cells in an IDO-dependent manner. *PLoS Pathog* (2016) 12:e1006115. doi:10.1371/journal.ppat.1006115
87. Araujo EF, Loures FV, Bazan SB, Feriotti C, Pina A, Schanoski AS, et al. Indoleamine 2,3-dioxygenase controls fungal loads and immunity in paracoccidioidomicosis but is more important to susceptible than resistant hosts. *PLoS Negl Trop Dis* (2014) 8:e3330. doi:10.1371/journal.pntd.0003330
88. Hage CA, Horan DJ, Durkin M, Connolly P, Desta Z, Skaar TC, et al. *Histoplasma capsulatum* preferentially induces IDO in the lung. *Med Mycol* (2013) 51:270–9. doi:10.3109/13693786.2012.710857
89. George MM, Subramanian Vignesh K, Landero Figueroa JA, Caruso JA, Deepe GS Jr. Zinc induces dendritic cell tolerogenic phenotype and skews regulatory T cell-Th17 balance. *J Immunol* (2016) 197:1864–76. doi:10.4049/jimmunol.1600410
90. Gorski JP, Howard JB. Effect of methylamine on the structure and function of the fourth component of human complement, C4. *J Biol Chem* (1980) 255:10025–8.
91. Jung ID, Lee C-M, Jeong Y-I, Lee JS, Park WS, Han J, et al. Differential regulation of indoleamine 2,3-dioxygenase by lipopolysaccharide and interferon gamma in murine bone marrow derived dendritic cells. *FEBS Lett* (2007) 581:1449–56. doi:10.1016/j.febslet.2007.02.073
92. Fallarino F, Volpi C, Zelante T, Vacca C, Calvitti M, Fioretti MC, et al. IDO mediates TLR9-driven protection from experimental autoimmune diabetes. *J Immunol* (2009) 183:6303–12. doi:10.4049/jimmunol.0901577
93. Rivas FV, Chervonsky AV, Medzhitov R. ART and immunology. *Trends Immunol* (2014) 35:451. doi:10.1016/j.it.2014.09.002
94. Soares MP, Gozzelino R, Weis S. Tissue damage control in disease tolerance. *Trends Immunol* (2014) 35:483–94. doi:10.1016/j.it.2014.08.001
95. Romani L. Cell mediated immunity to fungi: a reassessment. *Med Mycol* (2008) 46:515–29. doi:10.1080/13693780801971450
96. Zelante T, Bozza S, De Luca A, D'angelo C, Bonifazi P, Moretti S, et al. Th17 cells in the setting of *Aspergillus* infection and pathology. *Med Mycol* (2009) 47(Suppl 1):S162–9. doi:10.1080/13693780802140766
97. Montagnoli C, Fallarino F, Gaziano R, Bozza S, Bellocchio S, Zelante T, et al. Immunity and tolerance to *Aspergillus* involve functionally distinct regulatory T cells and tryptophan catabolism. *J Immunol* (2006) 176:1712–23. doi:10.4049/jimmunol.176.3.1712
98. De Luca A, Pariano M, Cellini B, Costantini C, Villella VR, Jose SS, et al. The IL-17F/IL-17RC axis promotes respiratory allergy in the proximal airways. *Cell Rep* (2017) 20:1667–80. doi:10.1016/j.celrep.2017.07.063
99. De Ravin SS, Zarember KA, Long-Priel D, Chan KC, Fox SD, Gallin JI, et al. Tryptophan/kynurenine metabolism in human leukocytes is independent of superoxide and is fully maintained in chronic granulomatous disease. *Blood* (2010) 116:1755–60. doi:10.1182/blood-2009-07-233734
100. Macchiarulo A, Camaioni E, Nuti R, Pellicciari R. Highlights at the gate of tryptophan catabolism: a review on the mechanisms of activation and regulation of indoleamine 2,3-dioxygenase (IDO), a novel target in cancer disease. *Amino Acids* (2009) 37:219–29. doi:10.1007/s00726-008-0137-3
101. Zelante T, De Luca A, Bonifazi P, Montagnoli C, Bozza S, Moretti S, et al. IL-23 and the Th17 pathway promote inflammation and impair antifungal immune resistance. *Eur J Immunol* (2007) 37:2695–706. doi:10.1002/eji.200737409
102. Jiang N, Zhao GQ, Lin J, Hu LT, Che CY, Li C, et al. Expression of indoleamine 2,3-dioxygenase in a murine model of *Aspergillus fumigatus* keratitis. *Int J Ophthalmol* (2016) 9:491–6. doi:10.18240/ijo.2016.04.03
103. Mackowiak B, Wang H. Mechanisms of xenobiotic receptor activation: direct vs. indirect. *Biochim Biophys Acta* (2016) 1859:1130–40. doi:10.1016/j.bbagrm.2016.02.006
104. Hubbard TD, Murray IA, Perdew GH. Indole and tryptophan metabolism: endogenous and dietary routes to Ah receptor activation. *Drug Metab Dispos* (2015) 43:1522–35. doi:10.1124/dmd.115.064246
105. Zelante T, Iannitti RG, Cunha C, De Luca A, Giovannini G, Pieraccini G, et al. Tryptophan catabolites from microbiota engage aryl hydrocarbon receptor and balance mucosal reactivity via interleukin-22. *Immunity* (2013) 39:372–85. doi:10.1016/j.immuni.2013.08.003
106. Bessede A, Gargaro M, Pallotta MT, Matino D, Servillo G, Brunacci C, et al. Aryl hydrocarbon receptor control of a disease tolerance defence pathway. *Nature* (2014) 511:184–90. doi:10.1038/nature13323
107. Goupil M, Cousineau-Cote V, Aumont F, Senechal S, Gaboury L, Hanna Z, et al. Defective IL-17- and IL-22-dependent mucosal host response to *Candida albicans* determines susceptibility to oral candidiasis in mice expressing the HIV-1 transgene. *BMC Immunol* (2014) 15:49. doi:10.1186/s12865-014-0049-9
108. Guo X, Qiu J, Tu T, Yang X, Deng L, Anders RA, et al. Induction of innate lymphoid cell-derived interleukin-22 by the transcription factor STAT3 mediates protection against intestinal infection. *Immunity* (2014) 40:25–39. doi:10.1016/j.immuni.2013.10.021
109. Xu X, Weiss ID, Zhang HH, Singh SP, Wynn TA, Wilson MS, et al. Conventional NK cells can produce IL-22 and promote host defense

in *Klebsiella pneumoniae* pneumonia. *J Immunol* (2014) 192:1778–86. doi:10.4049/jimmunol.1300039

Conflict of Interest Statement: The authors declare that the research was conducted in the absence of any commercial or financial relationships that could be construed as a potential conflict of interest.

Copyright © 2018 Choera, Zelante, Romani and Keller. This is an open-access article distributed under the terms of the Creative Commons Attribution License (CC BY). The use, distribution or reproduction in other forums is permitted, provided the original author(s) or licensor are credited and that the original publication in this journal is cited, in accordance with accepted academic practice. No use, distribution or reproduction is permitted which does not comply with these terms.

frontiers in Immunology

ORIGINAL RESEARCH
published: 13 November 2017
doi: 10.3389/fimmu.2017.01522

Disease Tolerance Mediated by Phosphorylated Indoleamine-2,3 Dioxygenase Confers Resistance to a Primary Fungal Pathogen

*Eliseu Frank de Araújo[1], Flávio Vieira Loures[1], Cláudia Feriotti[1], Tania Costa[1], Carmine Vacca[2], Paolo Puccetti[2], Luigina Romani[2] and Vera Lúcia Garcia Calich[1]**

[1] Department of Immunology, Institute of Biomedical Sciences, University of São Paulo, São Paulo, Brazil,
[2] Department of Experimental Medicine, University of Perugia, Perugia, Italy

Resistance to primary fungal pathogens is usually attributed to the proinflammatory mechanisms of immunity conferred by interferon-γ activation of phagocytes that control microbial growth, whereas susceptibility is attributed to anti-inflammatory responses that deactivate immunity. This study challenges this paradigm by demonstrating that resistance to a primary fungal pathogen such as *Paracoccidiodes brasiliensis* can be mediated by disease tolerance, a mechanism that preserves host fitness instead of pathogen clearance. Among the mechanisms of disease tolerance described, a crucial role has been ascribed to the enzyme indoleamine-2,3 dioxygenase (IDO) that concomitantly controls pathogen growth by limiting tryptophan availability and reduces tissue damage by decreasing the inflammatory process. Here, we demonstrated in a pulmonary model of paracoccidioidomycosis that IDO exerts a dual function depending on the resistant pattern of hosts. IDO activity is predominantly enzymatic and induced by IFN-γ signaling in the pulmonary dendritic cells (DCs) from infected susceptible (B10.A) mice, whereas phosphorylated IDO (pIDO) triggered by TGF-β activation of DCs functions as a signaling molecule in resistant mice. IFN-γ signaling activates the canonical pathway of NF-κB that promotes a proinflammatory phenotype in B10.A DCs that control fungal growth but ultimately suppress T cell responses. In contrast, in A/J DCs IDO promotes a tolerogenic phenotype that conditions a sustained synthesis of TGF-β and expansion of regulatory T cells that avoid excessive inflammation and tissue damage contributing to host fitness. Therefore, susceptibility is unexpectedly mediated by mechanisms of proinflammatory immunity that are usually associated with resistance, whereas genetic resistance is based on mechanisms of disease tolerance mediated by pIDO, a phenomenon never described in the protective immunity against primary fungal pathogens.

Keywords: paracoccidioidomycosis, indoleamine-2,3 dioxygenase, pulmonary dendritic cells, disease tolerance, phosphorylated indoleamine-2,3 dioxygenase, signaling function

OPEN ACCESS

Edited by:
Steven Templeton, Indiana University School of Medicine – Terre Haute, United States

Reviewed by:
Babak Baban, Augusta University, United States
Michael K. Mansour, Massachusetts General Hospital, United States

****Correspondence:***
Vera Lúcia Garcia Calich
vlcalich@icb.usp.br

Specialty section:
This article was submitted to Microbial Immunology, a section of the journal Frontiers in Immunology

Received: *12 August 2017*
Accepted: *26 October 2017*
Published: *13 November 2017*

Citation:
de Araújo EF, Loures FV, Feriotti C, Costa T, Vacca C, Puccetti P, Romani L and Calich VLG (2017) Disease Tolerance Mediated by Phosphorylated Indoleamine-2,3 Dioxygenase Confers Resistance to a Primary Fungal Pathogen. Front. Immunol. 8:1522. doi: 10.3389/fimmu.2017.01522

INTRODUCTION

Indolamine-2,3 dioxygenase (IDO) is an intracellular enzyme of crucial importance in the tryptophan (trp) catabolism acting along the kynurenine (Kyn) pathway (1, 2). Although the cytokine IFN-γ is considered the major inducer of IDO expression, TGF-β, TNF-α, prostaglandins, and toll-like receptor ligands, among others, have also the ability of promoting the expression of the

IDO gene (3–5). Among the cells of myeloid origin, dendritic cells (DCs) express the highest levels of IDO that is, however, also present in macrophages, neutrophils, endothelial cells, and fibroblasts (6–8).

Indolamine-2,3 dioxygenase was primarily associated with host defense against pathogens due to trp starvation caused by its enzymatic activity (9–11). However, the recent recognition of the immunoregulatory function of IDO and Kyn, put IDO to another level of knowledge and relevance (11, 12). Indeed, IDO has been recently described as an intracellular signaling molecule involved in the sustained tolerogenic activity of DCs. This signaling function is mediated by TGF-β signaling that promotes IDO phosphorylation that ultimately activates the non-canonical NF-κB pathway that triggers genes encoding IDO, TGF-β, IFN-α, and IFN-β, that maintain the tolerogenic activity of murine plasmacytoid DCs (12). This likely accounts for the ability of IDO to favor microbial persistence and concomitant control of inflammation during chronic infections (13–15). Therefore, acting *via* trp depletion and Kyn production, IDO can inhibit the proliferation of T cells and induce their apoptosis. Furthermore, through the aryl hydrocarbon receptor (AhR), IDO directs the conversion of naive $CD4^+$ T cells into regulatory $Foxp3^+$ T cells (Tregs) (13, 16, 17).

Paracoccidioidomycosis (PCM), is a granulomatous disease caused by two species of the dimorphic fungus *Paracoccidioides*, *P. brasilienis*, and *P. lutzii* (18). Immunoprotection to PCM is mediated by prevalent Th1/Th17 immunity, whereas Th2 and Th9 responses are associated with severe forms of the disease (19–21). In a murine model of pulmonary infection, A/J and B10.A mice were described, respectively, as resistant and susceptible to PCM. The A/J mouse strain develops a chronic and regressive PCM restricted to the lungs. Its adaptive immunity is mainly mediated by Th1 and Th17 cells that are tightly controlled by elevated numbers and activity of Treg cells. In contrast, B10.A mice develop a progressive disseminated disease associated with large amounts of fungi in non-organized lesions that mimic the severe forms of PCM (22–27).

The immunoregulatory mechanisms that control resistance to PCM are complex and not yet completely solved. In this aspect, our previous studies have shown that in pulmonary PCM, IDO is an important immunoregulatory enzyme that promotes fungal clearance and inhibits T cell immunity but only in susceptible mice IDO inhibition by 1-methyl-DL-tryptophan (1MT) caused progressive tissue pathology and increased mortality rates (28). This difference appeared to be mediated by the opposite innate immunity of resistant and susceptible mice. Indeed, in B10.A mice the innate immunity is preferentially proinflammatory with elevated production of IL-12 and IFN-γ, whereas in A/J mice the predominant TGF-β secretion provides an anti-inflammatory innate response (26–30). These findings led us to hypothesize that IDO has distinct immunoregulatory roles in pulmonary PCM. Here, we could demonstrate that in susceptible mice IDO activity is IFN-γ-dependent and mediated by its catalytic activity, whereas in resistant mice a prevalent TGF-β signaling triggered IDO phosphorylation imparting a signaling and tolerogenic function. The TGF-β-IDO-Treg interplay generates an early pathogen tolerance that allows A/J mice to interact with a primary fungal pathogen as a commensal microbe. Thus, the signaling function of pIDO may lead to an unusual fungus–host interaction that efficiently balances tolerance and resistance mechanisms to the benefit both the pathogen and the host.

MATERIALS AND METHODS

Mice

Susceptible (B10.A) and resistant (A/J) mouse strains to *Paracoccidiodes brasiliensis* infection were obtained from our Isogenic Unit (Immunology Department of Institute of Biomedical Sciences of University of São Paulo, Brazil) and used at 8–11 weeks of age. Specific pathogen free mice were fed with sterilized laboratory chow and water *ad libitum*.

Fungus

Paracoccidiodes brasiliensis 18 (Pb 18) was used throughout this investigation. To ensure the maintenance of its virulence, the isolate was used after three serial animal passages. Pb18 yeast cells were maintained by weekly sub cultivation in semisolid Fava Netto culture medium at 37°C and used on the seventh day of culture. Phosphate-buffered saline (PBS)-washed yeast cells were adjusted to 20×10^6 cells/mL based on hemocytometer counts. Viability was determined with Janus Green B vital dye (Merck) and was always higher than 85%.

1MT Treatment and *In Vivo* Fungal Infection

Mice were anesthetized and submitted to intratracheal (i.t.) *P. brasiliensis* infection as previously described. Briefly, after intraperitoneal (i.p.) anesthesia the animals were infected with 1×10^6 Pb18 yeast cells, contained in 50 μL of PBS, by surgical i.t. inoculation, which allowed dispensing of the fungal cells directly into the lungs. The skins of the animals were then sutured, and the mice were allowed to recover under a heat lamp. Groups of infected B10.A and A/J mice were treated with daily i.p. injections of 5 mg/mL of 1MT or 1 mg/mL of rice starch (Sigma-Aldrich) as control. Mice were sacrificed after 96 h or 2 weeks of infection.

Isolation of Pulmonary $CD11c^+$ Cells

Cell suspensions of the lungs were prepared as previously described (31). The lungs were removed and digested for 60 min in RPMI-1640 medium (Sigma) containing collagenase (2 mg/mL) and DNAse (30 mg/mL). The erythrocytes were lysed with lysis buffer (TRIS + ammonium chloride) and viability determined by the trypan blue exclusion test with viabilities at least to 95%. $CD11c^+$ cells were isolated from total pulmonary cells by magnetic microbeads (Miltenyi Biotec, Cologne, Germany). Pellets of pulmonary cells were counted, washed and the pellet resuspended in 400 μL of buffer (PBS + 0.5% BSA + 2 mM EDTA). The Trypan Blue dye exclusion test was used to determine the number of viable cells present in the DCs cell suspension with viabilities at least to 95%. Then, 100 μL of anti-CD11c coated microspheres were added for each 10^8 cells and incubated for 15 min at 2–8°C. The cells were washed, the supernatant removed and the pellet resuspended in 500 μL of buffer. This suspension

was fractionated using a magnetic separation column, and purified CD11c$^+$ DCs obtained. This fractionation methods resulted in 95% CD11c$^+$ DCs.

Culture of DCs

The viability of the CD11c$^+$ cells was evaluated by the trypan blue exclusion test, and was always higher than 85%. The cell suspensions were then centrifuged at 1,200 rpm at 4°C for 10 min and resuspended in 1.0 mL of culture medium (RPMI-1640 medium) supplemented with 10% fetal bovine serum. The cells were adjusted to 1×10^6/mL and 500 µL were dispensed into each well of 24-well culture plates. The cultures were incubated at 37°C in an incubator containing 5% CO_2–95% air for 24 h. After this period, the cells were removed and used in different assays.

CFU Assay

After 24 h of culture, DCs suspensions were lysed and 100 µL of pellets plated onto BHI-agar medium containing 5% "fungus growth factor" and 4% horse serum (32). The plates were incubated at 35°C and colonies counted daily until no increase in CFU was observed. The numbers (log10) of viable *P. brasiliensis* colonies are expressed as the mean ± SE. Two to three experiments were performed separately.

NO and Cytokines Measurement

Supernatants from DC cultures and lymphoproliferation assays were separated and stored at −70°C. The levels of IL-12, IL-1β, TGF-β, IL-6, IFN-γ, and IL-12 were measured by a capture enzyme-linked immunosorbent assay (ELISA) with antibody pairs purchased from eBioscience. The ELISA procedure was performed according to the manufacturer's protocol, and absorbance was measured with a Versa Max Microplate Reader (Molecular Devices). The concentrations of cytokines were determined based on a standard curve of serial twofold dilutions of murine recombinant cytokines. Nitric oxide production was quantified by the accumulation of nitrite in the supernatants from *in vitro* protocols by a standard Griess reaction (33). All determinations were performed in duplicate, and results were expressed as micromolar concentration of NO.

Determination of IDO Enzymatic Activity

To monitor IDO enzymatic activity, Kyn were measured using a modified spectrophotometric assay (5). The amount of 50 µL of 30% trichloroacetic acid was added to 100 µL of DCs supernatants, vortexed, and centrifuged at 800 *g* for 5 min. A volume of 75 µL of the supernatant was then added to an equal volume of Ehrlich reagent (100 mg P-dimethylbenzaldehyde, 5 mL glacial acetic acid) in a 96-well microtiter plate. Optical density was measured at 492 nm, using a Multiskan MS (Labsystems) microplate reader. A standard curve of defined L-Kyn concentrations (0–100 mM) was used to determine unknown Kyn concentrations.

Flow Cytometry

Pulmonary CD11c$^+$ cells were obtained from 1MT treated and untreated B10.A and A/J mice 96 h and 2 weeks after *P. brasiliensis* infection. For cell surface staining, pulmonary CD11c$^+$ cells were washed and resuspended at a concentration of 1×10^6 cells/mL in staining buffer (PBS 1×, 2% FBS, 0.5% NaN_3). Fc receptors were blocked by the addition of unlabeled anti-CD16/32 (Fc block; BD Biosciences). The DCs cells were then stained for 30 min at 4°C with the optimal dilution of each labeled antibody [phycoerythrin tandem Cy7 (PE-Cy7)-labeled anti-CD11c, phycoerythrin tandem Cy5 (PE-Cy5)-labeled anti-B220, pacific blue (PB)-labeled anti-CD8, phycoerythrin (PE)-labeled anti-CD86, allophycocyanin (APC)-labeled anti-CD40, fluorescein isothiocyanate (FITC)-labeled MHCII (IA^K), and allophycocyanin tandem Cy7 (APC-Cy7)-labeled anti-CD11b] monoclonal antibodies (mAbs) from BD Biociences. Cells were washed twice with staining buffer, fixed with 2% paraformaldehyde (Sigma), and acquired using a FACSCanto II equipment and FACSDiva® software (BD Biosciences) and analyzed by the FlowJo software (Tree-Star, Ashland, OR, USA).

Lymphocyte Proliferation Assay and Lymphocyte Phenotyping

Spleen lymphocytes from normal B10.A and A/J mice were resuspended (1×10^7) in 1 mL PBS-BSA (0.1%) and 1 µL of carboxyfluorescein diacetate, succinimidly ester (CFSE) at a concentration of 5 mM (Molecular Probes, USA). The cells were incubated at room temperature in the dark for 15 min (shaking the tube constantly). The cells were washed two times with 10 mL of supplemented RPMI, counted and resuspended at a concentration of 1×10^6/mL. In parallel, purified DCs from A/J and B10.A of uninfected and infected mice, treated and untreated with 1MT were centrifuged and adjusted to 1×10^6/mL in supplemented medium. Aliquots of 100 µL of DCs were placed in a 96-well plate (U-bottom) in the presence of lymphocytes previously stained with CFSE at a ratio 1:10 (100 µL of DCs + 100 µL of lymphocytes). CFSE stained lymphocytes (treated or not with 1MT), purified DCs and Concanavalin A (Sigma) stimulated lymphocytes were used as controls. The cells were incubated at 37°C in 5% CO_2 for 3 days. After the incubation period the cells were washed and resuspended at a concentration of 1×10^6 cells/mL in staining buffer (PBS 1×, 2% FBS, 0.5% NaN_3). Fc receptors were blocked by the addition of unlabeled anti-CD16/32 (Fc block; BD Biosciences). The leukocytes were then stained for 30 min at 4°C with the optimal dilution of each antibody labeled with the adequate fluorochrome (BD Biosciences). PE-labeled anti-CD44, PE-Cy7-labeled anti-CD8, and PerCP Cy5.5-labeled anti-CD4, and APC-Cy7-labeled anti-CD62L mAbs from BD Biosciences were used. Cells were washed twice with staining buffer, resuspended in 100 µL, and an equal volume of 2% paraformaldehyde was added to fix the cells. A minimum of 50,000 events was acquired on a FACSCanto II flow cytometer using FACSDiva® and FlowJo softwares. Lymphocytes were identified on forward-scatter (FSC) and side-scatter (SSC) analysis. Gated cells were measured for CD4$^+$ and CD8$^+$ expression followed by CD44 expression, and cells expressing high and low levels of this molecule were gated. Gated $CD44^{high}$ cells were then measured for expression of low levels of CD62L identifying the effector/memory $CD4^+CD44^{high}CD62L^{low}$ and $CD8^+CD44^{high}CD62L^{low}$ subpopulations. Gated $CD44^{low}$ cells were then measured for the expression of high levels of CD62L identifying the naive

$CD4^+CD44^{low}CD62L^{high}$ and $CD8^+CD44^{low}CD62L^{high}$ subpopulations (Figure S2A,B in Supplementary Material). Fifty thousand cells were acquired and the data expressed as the frequency of positive cells. The cell division index was calculated and was based on the number of $CFSE^+CD4^+$ or $CFSE^+CD8^+$ T cells found in the stimulated culture/number of $CFSE^+CD4^+$ or $CFSE^+CD8^+$ T cells in the unstimulated culture (34).

Assay to Determine Regulatory $CD4^+CD25^+FoxP3^+$ T Cells

Culture supernatants from lymphoproliferation assays were removed and stored at 70°C for the determination of cytokines according to the manufacturer's protocol. The pellet cells were stained with PE-Cy7-labeled anti-CD4 and PerCP Cy5.5-labeled anti-CD25 for 30 min 4°C. Next, the cells were washed with staining buffer containing 2% fetal bovine serum, 0.1% azide, 100 µL of PBS. The permeabilization of the plasma membrane was made with the addition of 200 µL/well of Cytofix/Cytoperm (Fixation/permeabilization kit BD Biosciences®) at room temperature for 30 min, protected from light. After washing the cells, the nuclear membrane permeabilization was performed using 130 µL/well of solution containing 750 µL of 1× PBS, 250 µL of 4% paraformaldehyde, 5 µL Tween 20 Sigma® and the cells then were incubated for 30 min at room temperature in the dark.

After washing the cells with cold PBS (1×), the nuclear transcription factor FoxP3 was stained with an anti-FoxP3 labeled specific antibody (APC-labeled anti-FoxP3) diluted 1/100 in staining buffer. The cells were incubated for 30 min at 4°C, then washed with ice-cold PBS, fixed with 2% paraformaldehyde and stored at 4°C in the dark until analyzed by flow cytometry. Gates for total lymphocytes, $CD4^+$, $CD4^+CD25^+$, and finally for $TCD4^+CD25^+FoxP3^+$ T lymphocytes were made (Figure S2C in Supplementary Material). Cells were analyzed as above described.

Intracellular Cytokines Measurement

Dendritic cells obtained from the lungs were adjusted to 1×10^6 cells and stimulated for 6 h in complete medium in the presence of 100 ng/mL phorbol 12-myristate 13-acetate, 500 ng/mL ionomycin (both from Sigma-Aldrich; Germany), and monensin (3 mM, eBioscience). Cells were subsequently labeled for surface molecules (PerCP-labeled anti-CD11c) and then treated according to the manufacturer's protocol for intracellular staining using the Cytofix/Cytoperm kit (BD Biosciences). Cells were then stained with Alexa Fluor 488-labeled anti-IDO, PB-labeled anti-IL-10, PE-Cy7-labeled anti-TNF-α, APC-CY7-labeled anti-IL-12, and PE-labeled anti-TGF-β. Cells were washed twice with staining buffer, resuspended in 100 µL, and fixed with an equal volume of 2% paraformaldehyde. The flow cytometry data were acquired and analyzed as above described.

Quantitative Analysis of mRNA Expression

RNA was extracted from DC cultures and the RNA concentrations were determined by spectrophotometer readings at an absorbance of 260 nm. First-strand cDNAs were synthesized from 2 µg RNA using the High Capacity RNA-to-cDNA kit (Applied Biosystems) according to the manufacturer's instructions. Gene expression for the genes of IDO, IFN-γ, janus kinase 1 (JAK1), signal transducer and activator of transcription (STAT1), IL-6, suppressor of cytokine signaling 3 (SOCS3), nitric oxide synthase (NOS2), TGF-β, small mothers against decapentaplegic 2 and 3 (SMAD2 and SMAD3), inositol polyphosphate phosphatase (SHIP), Shp1, Sh22 (tyrosine phosphatases 1 and 2), IFN-α, IFN-β, and the endogenous gene glyceraldehyde 3-phosphate dehydrogenase (GAPDH) was characterized by the real time polymerase chain reaction technique (qPCR) (Applied Biosystems, Foster City, CA, USA). The samples were placed in microcentrifuge tubes for specific qPCR testing of samples containing 2 µL cDNA + 10 µL TaqMan PCR Master Mix (Applied Biosystems, Foster City, CA, USA) according to the following thermal profile: denaturation at 95°C for 15 s, annealing at 60°C for 15 s, and extension at 72°C for 15 s. The sequences of the primers for Indo (Mm00492506_m1), IFN-γ (Mm01168134_m1), Jak1 (Mm00600614_m1), Stat1 (Mm00439531_m1), IL-6 (Mm00446190_m1), SOCS3 (Mm00545913_s1), NOS2 (Mm00440502_m1), TGF-β1 (Mm01178820_m1), Smad2 (Mm00487530_m1), Smad3 (Mm01170760_m1), Inpp5d (Ship—Mm00494987_m1), Nr0b2 (Shp1—Mm00442278_m1), PTPN11 (Shp2—Mm00448434_m1), Ifna1 (Mm03030145_gH), Ifnb1 (Mm00439552_s1), and the gene endogenous transcripts in all cell types, GAPDH (Mm99999915_g1) were obtained from Applied Biosystems ready for testing. Probes were labeled with 6-carboxyfluorescein (FAM) at their 5′-terminal end. Data were normalized to GAPDH gene expression. *Taq*Man PCR assays were performed on a Stratagene MxP3005P QPCR System and data were developed using the MxPro QPCR software (Agilent Technologies, USA).

NF-κB DNA-Binding ELISA-Based Assay

Nuclear extracts from DCs were obtained using the Nuclear Extract Kit (Active Motif, USA). DNA binding activity of NF-κB was measured by an ELISA-based assay using a TransAM NF-κB kit (Active Motif, USA) following manufacturer's instructions. This assay detects binding of p65, p50, p52, and Rel-B proteins to oligonucleotides containing an NF-κB consensus-binding site immobilized onto 96-well plates by specific primary antibodies that recognize an epitope that is accessible only when NF-κB is activated and bound to its target DNA. The binding activity was quantified by spectrophotometry, the OD at 450 nm.

Western Blot Analysis

Dendritic cells were lysed in ice-cold NP40 buffer [1% NP40, 50 mmol/L Tris–HCl (pH 7.4), 150 mmol/L NaCl, 5 mmol/L EDTA containing 5 mmol/L NaF, 2 mmol/L Na_3VO_4, 1 mmol/L phenylmethylsulfonyl fluoride, 5 µg/mL leupeptine, and 5 µg/mL aprotinine], supplemented with a protease inhibitor (Sigma Aldrich). After incubating for 30 min at 4°C, the samples were centrifuged, and the supernatants were kept as the NP40-soluble fraction. The pellets were resuspended in SDS buffer [2% SDS, 80 mmol/L Tris (pH 6.8), 100 mmol/L DTT, and 10% glycerol]. Protein concentration was determined using a BCA assay (Pierce), and 40–60 µg of protein was run on a polyacrylamide gel and transferred to a 0.45 µm nitrocellulose membrane

(Millipore, Bedford, MA, USA). Western blotting was carried out according to a standard procedure using horseradish peroxidase–conjugated secondary antibodies (Thermo Scientific and Sigma Aldrich). mAbs used were as follows: Jak1 (1:500; Sigma-Aldrich), Stat1 (1:500; Sigma-Aldrich), IKK-β (1:1,500; Sigma-Aldrich), IDO1 (1:200; Santa Cruz Biotechnology), Smad2 (1:2,500; Sigma-Aldrich), Ship (1:2,000; Sigma-Aldrich), Shp-2 (1:1,500; Sigma-Aldrich), and IKK-α (1:500; Sigma-Aldrich). Mouse monoclonal antimouse β-tubulin antibody (1:2,000; Sigma-Aldrich) was used as an internal control. The immunoreactive proteins were visualized with ECL plus reagents (ECL Western blotting Detection Reagents; Amersham) and enhanced chemiluminescence apparatus (ImageQuant LAS 4000). Densitometry was performed using ImageQuant TL 8.1 software.

Detection of Phosphorylated IDO1 (pIDO1) by Western Blotting

Lung extracts from susceptible and resistant mice infected with *P. brasiliensis*, treated or not with 1MT were obtained after 96 h and 2 weeks of infection and analyzed by Western Blot for detection of pIDO1. Protein concentration was determined using a BCA assay (Pierce), and 20 µg of protein in Ripa Buffer and Sample buffer 4× were heated at 100°C for 4 min, then on ice for 2 min and loaded 60 µL per well in 10% SDS PAGE, 1.5 mm. Electrophoresis was then performed by transferring the gel to the nitrocellulose membrane with the membranes incubated in blocking solution [5% non-fat dry milk, 0.1% Tween 20 in Tris buffer saline (TBS) for 1 h at room temperature on an orbital shaker]. After two washings steps with TBS-Tween 20 0.1% buffer, the membrane was incubated overnight with polyclonal rabbit antimouse pIDO (CV223 AP8), 2 µg/mL in 5% non-fat dry milk, TBS at 0.1%. The membrane was washed three times for 5 min and incubated with HRP-labeled secondary antibody (anti-rabbit HRP–Pierce) for 1 h at room temperature. The revelation was performed using the ECL chemiluminescent substrate for enzymatic activity detection of peroxidase (HRP) on photographic film. The same method was used with a monoclonal rabbit anti-mouse IDO1 (CV152) and monoclonal antimouse β-tubulin antibody (1:1,000).

Statistical Analysis

Data are expressed as the mean ± SEM. Differences between groups were analyzed by analysis of variance followed by the Bonferroni test. Differences between survival times were determined with the LogRank test. Data were analyzed using GraphPad Prism 6.2 software for Windows (GraphPad). A p value of ≤0.05 was considered statistically significant.

RESULTS

IDO Inhibition Increases the Fungal Loads of DCs from Susceptible and Resistant Mice and Down Regulates NO, Kyn, and IDO mRNA Production

Initially, we sought to investigate the effects of IDO inhibition on the interaction of DCs, from susceptible and resistant mice, with *P. brasiliensis*. To explore the effect of IDO inhibition *in vivo*, A/J and B10.A mice were treated or not with 1MT and subsequently subjected to i.t. infection with *P. brasiliensis* yeasts cells. Pulmonary DCs from both mouse strains were isolated 96 h and 2 weeks after infection and *in vitro* cultivated for 24 h. Using a CFU assay it was verified that in both postinfection periods 1MT-treated DCs presented increased fungal loads than untreated cells (**Figures 1A,B**). The levels of NO and Kyn in the supernatants of 1MT-treated DCs from both mouse strains was significantly lower than those detected in untreated groups (**Figures 1A,B**). In agreement with the reduced levels of Kyn observed, a reduced expression of IDO mRNA was found in 1MT-treated groups of both mouse strains (**Figures 1A,B**). The reduced IDO mRNA expression was further

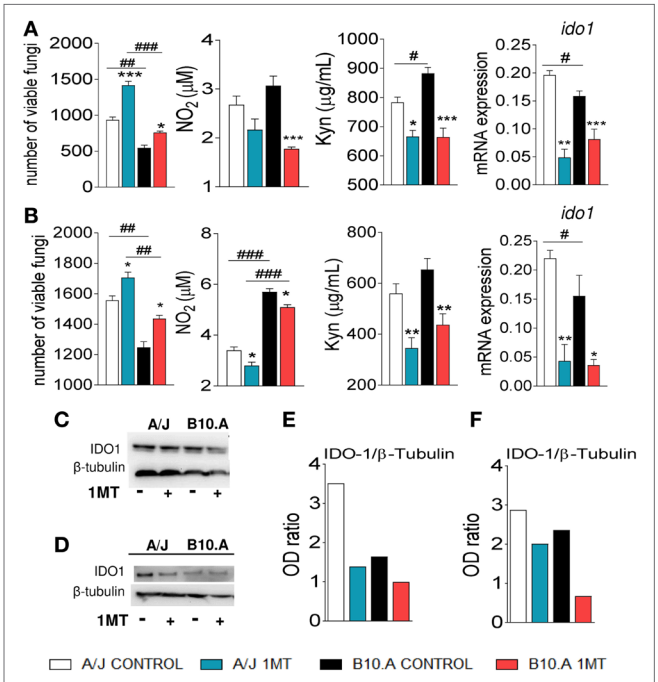

FIGURE 1 | 1-Methyl-DL-tryptophan (1MT) treatment reduces fungicidal activity, NO, kynurenine (Kyn), and indoleamine-2,3 dioxygenase (IDO) production by pulmonary dendritic cells (DCs) of *Paracoccidiodes Brasiliensis*-infected mice. Pulmonary DCs were obtained from 1MT treated or untreated A/J and B10.A mice at 96 h **(A,C,E)** and 2 weeks **(B,D,F)** after infection with 1 × 10^6 yeasts and cultivated for 24 h at 37°C in 5% CO_2. The cells were centrifuged, resuspended in 100 µL of culture medium and assayed for the presence of viable yeasts by a CFU assay. Supernatants from DCs cultures were used to determine the levels of nitrite and Kyn. In the same experimental conditions, DCs of A/J and B10.A mice were mixed with TRizol reagent for RNA extraction. IDO mRNA was measured using TaqMan real-time PCR assay. IDO was also characterized by immunoblotting. DCs were lysed, supernatants supplemented with a protease inhibitor and protein concentration determined by a BCA assay. After electrophoresis in polyacrylamide gel, proteins were transferred to nitrocellulose membranes and stained with anti-IDO antisera. Densitometry of bands was performed using ImageQuant TL 8.1 software. NO production was measured by Griess reagent, and Kyn were evaluated using Ehrlich's reagent. The data represent the mean ± SEM of three independent experiments where the asterisk (*) represents a statistically significant difference between treatments (*$p < 0.05$, **$p < 0.01$, and ***$p < 0.001$) and the hashtag (#) represents the difference between the strains ($^{\#}p < 0.05$, $^{\#\#}p < 0.01$, and $^{\#\#\#}p < 0.001$).

confirmed by the decreased protein production as detected by Western Blotting (**Figures 1C–F**).

IDO Inhibition Promotes Increased Influx and Activation of Pulmonary DCs

We have then asked whether the *in vivo* treatment with 1MT could interfere with the number and activation of pulmonary DCs. We verified that 96 h and 2 weeks after infection, 1MT-treated A/J and B10.A mice presented a higher number of myeloid, lymphoid and plasmacytoid DCs ($CD11c^{high}CD11b^{+}$, $CD11c^{high}CD8^{+}$, and $CD11c^{low}B220^{+}$, respectively) in their lungs than control mice (**Figures 2A,B**; Figure S1 in Supplementary Material). In addition, 1MT treatment increased the expression of MHC class II (IA^{K}) and costimulatory molecules (CD86, CD40, CD11b) in pulmonary DCs obtained at both periods and mouse strains studied (**Figures 2C,D**). Thus, the increased fungal loads induced by 1MT treatment were associated with increased migration and activation of pulmonary DCs.

IDO Inhibition Reduces the Secretion of DCs Cytokines

To better evaluate the function of pulmonary DCs from 1MT-treated and untreated A/J and B10.A mice, the levels of cytokines present in the supernatants of cultivated cells were measured by ELISA. First, we could confirm our previous findings (28, 30) demonstrating that DCs from A/J mice produce higher levels of TGF-β and IL-1β than DCs from B10.A mice that, in contrast, are better producer of IL-12 and IL-6. We have found that 1MT treatment reduced the levels of TGF-β and IL-1β produced by A/J DCs at both postinfection periods. In contrast, reduced levels of IL-12, IL-6, and IL-1β were observed in 1MT-treated B10.A mice at both time points (**Figures 3A,B**).

IDO Inhibition Reduces the Levels of Intracellular IDO and TGF-β in A/J DCs, whereas in B10.A DCs Diminishes the Levels of IDO, IL-12, and IL-6

We have also characterized the effect of IDO inhibition on intracellular cytokine (TGF-β, IL-12, and IL-6) content and IDO. Purified DCs from 1MT-treated and -untreated A/J and B10.A mice obtained at two postinfection periods were cultivated and intracellular proteins analyzed by flow cytometry. Compared with untreated controls, decreased numbers of $TGF\text{-}\beta^{+}$ DCs were observed in the lungs of 1MT treated A/J mice. In contrast, reduced numbers of $IL\text{-}12^{+}$ and $IL\text{-}6^{+}$ DCs were detected in 1MT treated B10A mice (**Figures 4A,B**). In addition, reduced numbers of IDO positive DCs were observed in 1MT-treated DCs from both mouse strains and postinfection periods analyzed (**Figures 4A,B**).

IDO Inhibition Enhances the Immunogenic Activity of DCs

Dendritic cells were isolated from 1MT-treated and untreated A/J and B10.A mice 96 h and 2 weeks after *P. brasiliensis* infection.

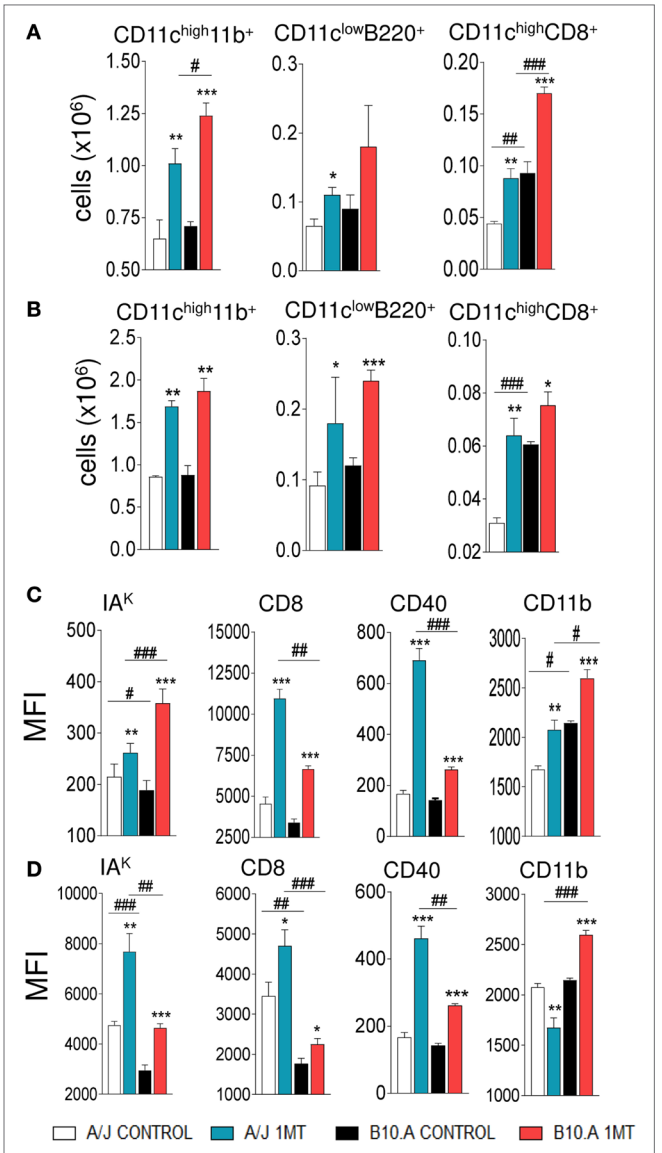

FIGURE 2 | 1-Methyl-DL-tryptophan (1MT) treatment increases the influx of activated dendritic cells (DCs) to the lungs. Number of myeloid ($CD11c^{high}11b^{+}$), plasmacytoid ($CD11c^{low}B220^{+}$), and lymphoid ($CD11c^{high}CD8^{+}$) DCs obtained 96 h **(A)** and 2 weeks **(B)** after infection of 1MT-treated and -untreated A/J and B10.A mice with 1×10^{6} viable *Paracoccidiodes brasiliensis* yeasts. Median fluorescence intensity (MFI) of IA^{K}, CD86, CD11b, and CD40 expressed by DCs obtained from lungs of A/J and B10.A mice 96 h **(C)** and 2 weeks **(D)** after infection. DCs were obtained by fractionation with anti-CD11c magnetic beads and DCs phenotyping determined by flow cytometry. The data represent the mean ± SEM of three independent experiments where the asterisk (*) represents a statistically significant difference between treatments (*$p < 0.05$, **$p < 0.01$, and ***$p < 0.001$) and the hashtag (#) represents the difference between the strains ($^{\#}p < 0.05$, $^{\#\#}p < 0.01$, and $^{\#\#\#}p < 0.001$).

In parallel, splenic lymphocytes from uninfected A/J and B10.A mice were obtained, labeled with CFSE, and cocultured with purified DCs. After 3 days, the proliferation of lymphocytes was analyzed by flow cytometry and the levels of IFN-γ and IL-2 were measured in culture supernatants.

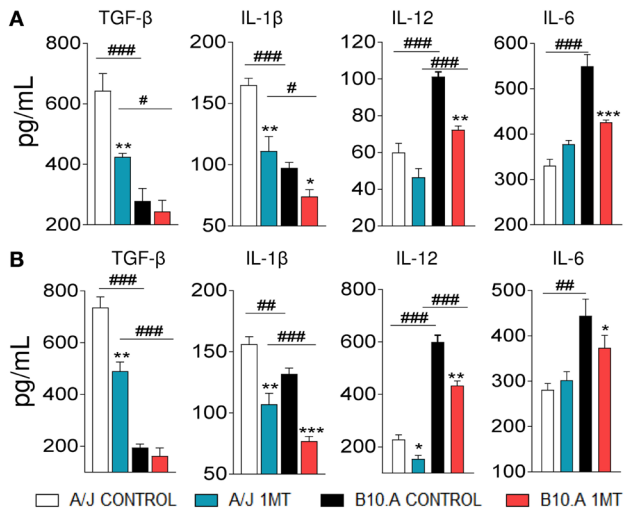

FIGURE 3 | 1-Methyl-DL-tryptophan (1MT) reduces the levels of TGF-β and IL-1β secreted by A/J dendritic cells (DCs), whereas in B10.A DCs 1MT reduces the secretion of IL-12, IL-6, and IL-1β. Pulmonary DCs were purified from lungs of 1MT treated and untreated A/J and B10.A mice 96 h **(A)** and 2 weeks **(B)** after i.t. infection with 1×10^6 *Paracoccidiodes brasiliensis* yeasts cells. DCs were cultivated by 24 h, supernatants collected and analyzed for cytokine content (TGF-β, IL-1β, IL-12, and IL-6) by enzyme-linked immunosorbent assay (ELISA). The data represent the mean ± SEM of three independent determinations where the asterisk (*) represents a statistically significant difference between treatments ($^*p < 0.05$, $^{**}p < 0.01$, and $^{***}p < 0.001$) and the hashtag (#) represents the difference between the strains ($^{\#}p < 0.05$, $^{\#\#}p < 0.01$, and $^{\#\#\#}p < 0.001$).

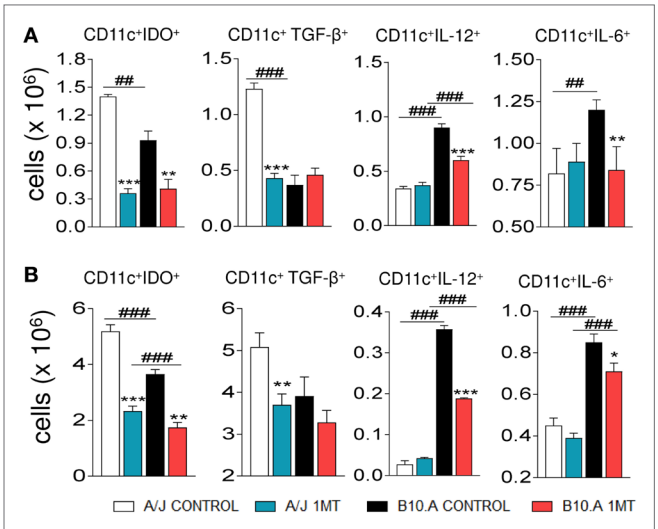

FIGURE 4 | 1-Methyl-DL-tryptophan (1MT) treatment reduces the number of TGF-β$^+$ dendritic cells (DCs) in the lungs of A/J mice but reduces IL-12$^+$ and IL-6$^+$ DCs in B10.A mice. Number of pulmonary DCs expressing intracellular indoleamine-2,3 dioxygenase (IDO), TGF-β, IL-12, and IL-6, 96 h **(A)** and 2 weeks **(B)** after *Paracoccidiodes brasiliensis* infection. Lungs of 1MT treated and untreated A/J and B10.A-infected mice were excised and DCs cells purified by magnetic beads. The expression of intracellular cytokines was analyzed by flow cytometry. The data represent the mean ± SEM of three independent determinations where the asterisk (*) represents a statistically significant difference between treatments ($^*p < 0.05$, $^{**}p < 0.01$, and $^{***}p < 0.001$) and the hashtag (#) represents the difference between the strains ($^{\#\#}p < 0.01$ and $^{\#\#\#}p < 0.001$).

As previously described with untreated pulmonary DCs (30), DCs from 1MT-treated and untreated A/J mice obtained at both postinfection periods induced higher lymphoproliferation than those of B10.A mice (**Figures 5A,B**). However, for both mouse strains at both periods assayed, the inhibition of IDO activity resulted in increased proliferation of lymphocytes. In cultures of 1MT treated or untreated naive lymphocytes no cell proliferation was observed. In the same way, no observe lymphoproliferation were detected when 1MT treated or untreated DCs from uninfected mice were used as APC. The levels of IFN-γ and IL-2 were measured in the supernatants of lymphoproliferation assays. Compared with untreated controls, decreased levels of IFN-γ were observed in 1MT-treated DCs from B10.A mice, whereas increased levels of IL-2 were detected in 1MT-treated DCs of both mouse strains and postinfection periods (**Figures 5A,B**).

IDO Inhibition Expands CD4$^+$ and CD8$^+$ T Cells and Reduces Treg Cells

Treatment of B10.A and A/J mice with 1MT increased the differentiation of T cells induced by isolated DCs. Indeed, increased frequency of naive CD4$^+$ and CD8$^+$ (CD4$^+$CD44^{low}CD62L^{high} and CD8$^+$CD44^{low}CD62L^{high}, respectively) as well as memory/effector CD4$^+$ and CD8$^+$ (CD4$^+$CD44^{high}CD62L^{low} and CD8$^+$CD44^{high}CD62L^{low}) T cells were detected when 1MT-treated DCs were cocultivated with naive lymphocytes (**Figures 6A,B**). Accordingly, reduced frequencies of Treg (CD4$^+$CD25$^+$FoxP3$^+$) cells were observed when DCs were obtained from 1MT-treated resistant and susceptible mice (**Figures 6C,D**).

IDO Is Regulated by IFN-γ in B10.A Mice and TGF-β in A/J Mice

Two opposite pathways were shown to regulate the production and activity of IDO. The IDO-IFN-γ axis is associated with the catalyst function of this enzyme, leads to trp starvation and Kyn production that in turn control pathogen growth and the inflammatory response. In contrast, the TGF-β-IDO axis has been linked with a signaling function of pIDO that promotes the differentiation of tolerogenic DCs and increases the expansion of Treg cells (12, 35, 36).

We speculated that in B10.A mice IDO is mainly catalyst and IFN-γ-regulated, whereas in A/J mice IDO has a predominant signaling function induced by TGF-β. To explore this hypothesis, the expression of genes and proteins related to IFN-γ and TGF-β signaling pathways was characterized in DCs of 1MT-treated and untreated B10.A and A/J mice obtained at 96 h (Figures S3 and S4 in Supplementary Material) and 2 weeks of infection. As shown in **Figure 7A**, DCs from B10.A mice expressed higher levels of mRNA from genes associated with IFN-γ signaling. Therefore, 1MT treatment led to a marked reduction in the expression of IFN-γ, Jak1, Stat1, IL-6, SOCS3, and NOS2 mRNA by DCs from B10.A mice but had a minor effect on DCs of A/J mice (**Figure 7A**).

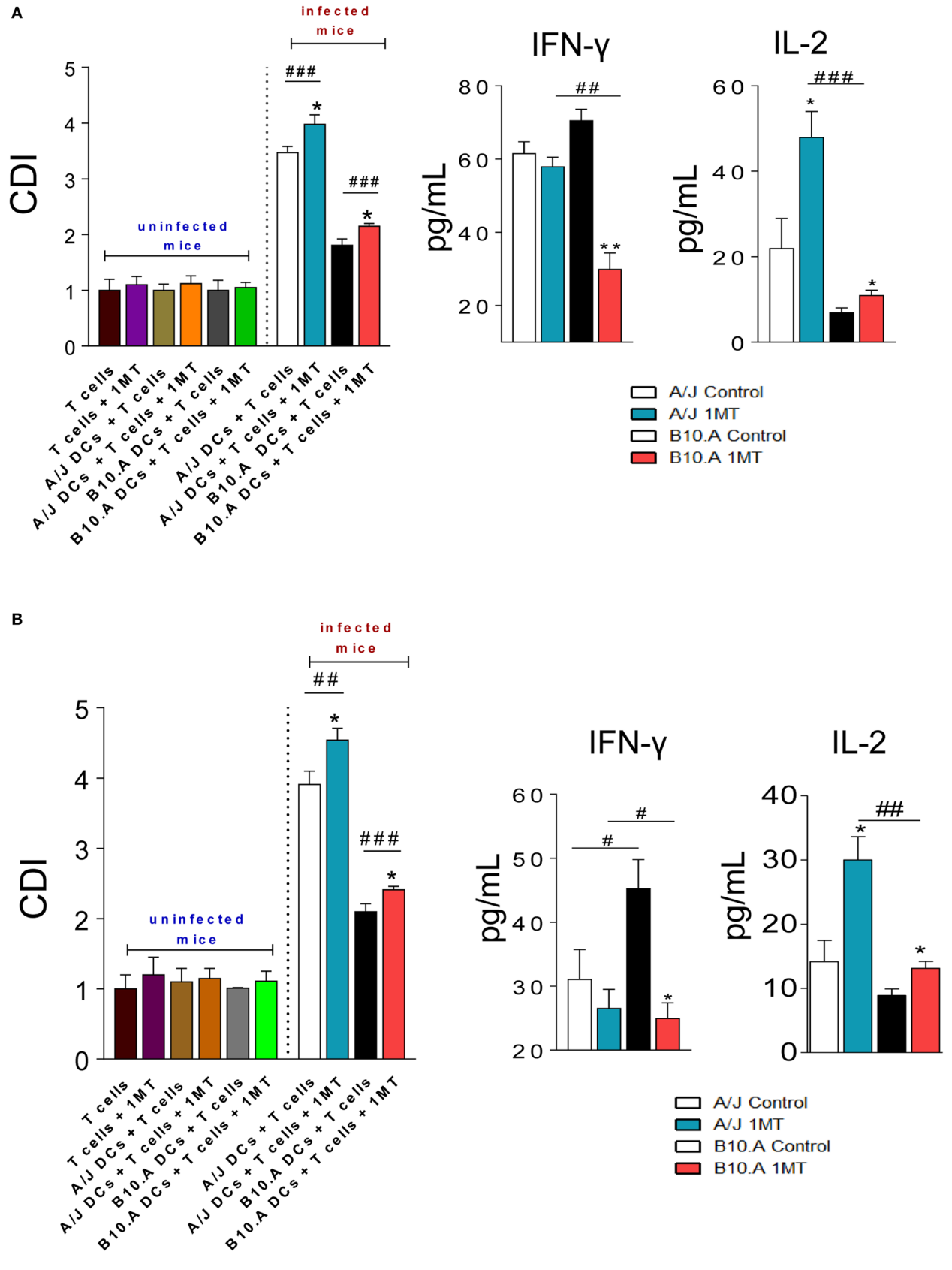

FIGURE 5 | Continued

FIGURE 5 | Continued
1-Methyl-DL-tryptophan (1MT) treatment increases the immunogenicity of dendritic cells (DCs). Pulmonary DCs were obtained from lungs of 1MT-treated and -untreated A/J and B10.A mice 96 h **(A)** and 2 weeks **(B)** after infection with 1 × 10^6 *Paracoccidiodes brasiliensis* yeasts using anti-DC11c magnetic beads. Spleen lymphocytes from non-infected A/J and B10.A mice were obtained, labeled with CFSE (5 mM) and cocultivated with DCs, in a ratio of DC:lymphocyte of 1:10. In parallel, pulmonary DCs from uninfected A/J and B10.A mice were obtained using anti-DC11c magnetic beads and cultured with 1MT treated or untreated naive lymphocytes from non-infected A/J and B10.A mice. After 3 days of cocultivation, the cells were adjusted to 1 × 10^6, labeled with specific anti-CD4 **(A)** and anti-CD8 **(B)** antibodies and analyzed by flow cytometry. The cell division index (CDI) was calculated as previously described by Mannering et al. (34) and was based on the number of CFSE$^+$CD4$^+$ or CFSE$^+$CD8$^+$ T cells found in the stimulated culture/number of CFSE$^+$CD4$^+$ or CFSE$^+$CD8$^+$ T cells in the unstimulated culture. The lymphocyte population was gated by FSC/SSC analysis. Fifty thousand cells were counted, and the data expressed as frequency of positive cells. Results are representative of three independent experiments. Cytokines were measured in culture supernatants by enzyme-linked immunosorbent assay (ELISA). The data represent the mean ± SEM of three independent determinations where the asterisk (*) represents a statistically significant difference between treatments (*$p < 0.05$ and **$p < 0.01$) and the hashtag (#) represents the difference between the strains ($^{\#\#}p < 0.01$ and $^{\#\#\#}p < 0.001$).

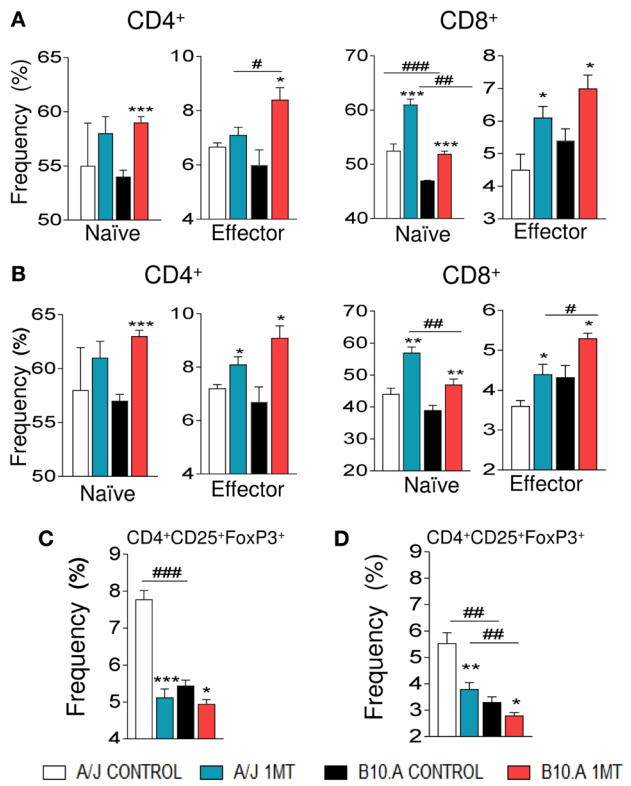

FIGURE 6 | 1-Methyl-DL-tryptophan (1MT) increases proliferation of CD4$^+$ and CD8$^+$ T cells and reduces regulatory T cells (Tregs). Spleen lymphocytes from uninfected A/J and B10.A mice were labeled with CFSE (5 mM) and cocultivated with purified dendritic cells (DCs) obtained from 1MT treated and untreated A/J and B10.A mice infected i.t. with 1 × 10^6 of *Paracoccidiodes brasiliensis* yeasts. DCs were obtained at 96 h and 2 weeks postinfection, and cocultivated with CFSE labeled lymphocytes at a ratio of DC:lymphocyte of 1:10. After 3 days, the cells were adjusted to 1 × 10^6, labeled with specific anti-CD4, -CD8, -CD44, -CD62L, -CD25, and -FoxP3 antibodies. The frequency of naive (CD62L^{high}CD44^{low}) and effector/memory (CD62L^{low}CD44^{high}) CD4$^+$ and CD8$^+$ T cells as well as CD4$^+$CD25$^+$FoxP3 regulatory T cells (Tregs) was measured by flow cytometry. Values are the mean of three independent experiments. The asterisks represent statistically significant differences between treatments (*$p < 0.05$, **$p < 0.01$, and ***$p < 0.05$). The hashtag marks represent statistically significant differences between strains ($^{\#}p < 0.05$, $^{\#\#}p < 0.01$, $^{\#\#\#}p < 0.001$).

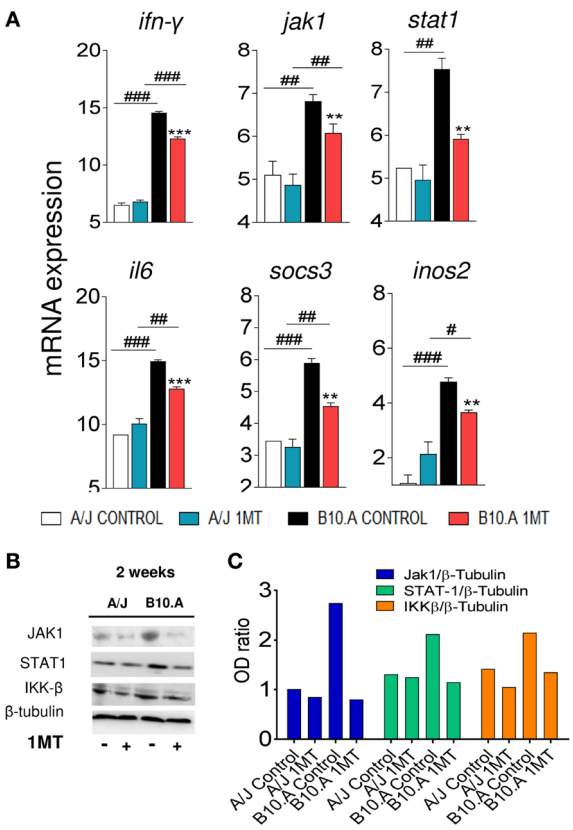

FIGURE 7 | Indoleamine-2,3 dioxygenase (IDO) is regulated by IFN-γ signaling in B10.A dendritic cells (DCs). 1-Methyl-DL-tryptophan (1MT) treated or untreated B10.A and A/J mice were infected i.t. with 1 × 10^6 yeast cells of *P. brasiliensis*, and 2 weeks after infection total lung inflammatory cells were obtained and DCs purified with anti-CD11c magnetic beads. **(A)** The relative expression of mRNA of IFN-γ, Janus kinase 1 (Jak1), signal transducer and activator of transcription (STAT1), IL-6, suppressor of cytokine signaling 3 (SOCS3), and nitric oxide synthase (NOS2) was measured by real-time PCR. **(B)** Presence of Jak1, Stat1, IKK-β, and IDO1 proteins was assessed by western blot in supernatants of lysed DCs. Proteins were estimated by analyzing the intensity of each band normalized by β-tubulin, used as control. **(C)** Densitometry of bands was performed using ImageQuant TL 8.1 software. The asterisks represent statistically significant differences between treatments (*$p < 0.05$, **$p < 0.01$, ***$p < 0.001$). The hash marks represent statistically significant differences between strains ($^{\#}p < 0.05$, $^{\#\#}p < 0.01$, $^{\#\#\#}p < 0.001$).

These findings indicate that in B10.A mice the IDO function is mainly catalyst and regulated by IFN-γ. Immunoblotting assays confirmed these results, and increased amounts of JAK1, STAT-1, and IKK-β proteins were found in DCs extracts of B10.A DCs (**Figures 7B,C**). In contrast to B10.A mice, DCs from A/J mice express higher levels of mRNA from genes associated with TGF-β signaling (**Figure 8**). Compared with B10.A DCs, cells from A/J mice expressed increased levels of TGF-β, SMAD2, SMAD3, SHIP1, SHP1, SHP2, IFN-α, and IFN-β mRNA. 1MT treatment significantly reduced these levels in A/J DCs but had no effect on B10.A cells (**Figure 8A**). Assessing protein production, increased amounts of SMAD2, SHIP1, SHP2, and IKK-α were observed in extracts of A/J DCs (**Figures 8B,C**).

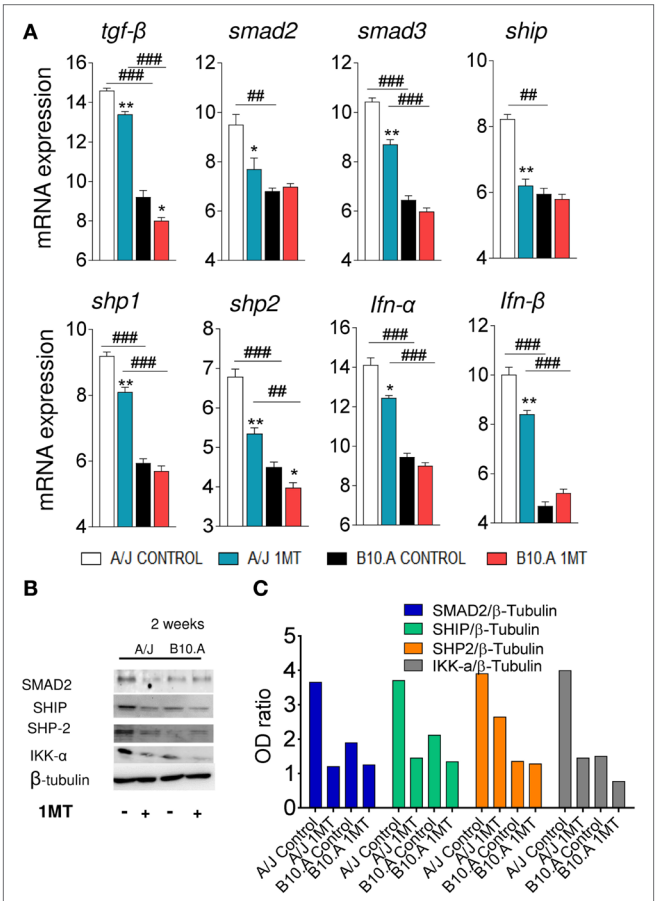

FIGURE 8 | Indoleamine-2,3 dioxygenase (IDO) is regulated by TGF-β signaling in A/J dendritic cells (DCs). 1-Methyl-DL-tryptophan (1MT)-treated or -untreated B10.A and A/J mice were infected i.t. with 1 × 10^6 *Paracoccidiodes brasiliensis* yeasts and 2 weeks after infection total lung inflammatory cells were obtained and DCs purified by anti-CD11c magnetic beads. **(A)** The relative expression of mRNA of TGF-β, Smad2, Smad 3, SHIP, SHP-1, SHP-2, IFN-α, and IFN-β was measured by real-time PCR. **(B)** Smad2, Ship, Shp-2, IKK-α and IDO1, and pIDO protein expression was assessed by western blot in supernatants of lysed DCs. **(C)** Proteins were estimated by analyzing the intensity of each band normalized by β-tubulin, used as control. Densitometry of bands was performed using ImageQuant TL 8.1 software. Values are the mean ± SEM of three independent experiments; the asterisks represent statistically significant differences between treatments (*$p < 0.001$, **$p < 0.01$, ***$p < 0.05$). The hash marks represent statistically significant differences between strains ($^{\#}p < 0.05$, $^{\#\#}p < 0.01$, $^{\#\#\#}p < 0.001$).

A/J Mice pIDO and Use the Non-Canonical Pathway of NF-κB Activation, whereas B10.A Mice Express Non-pIDO and Use the Canonical Pathway of NF-κB Activation

Because IFN-γ signaling is mainly associated with the canonical pathway of NF-κB activation, the transcriptional activity of p65 and p50 were measured by ELISA in the nuclear extracts of 1MT-treated and -untreated DCs. As depicted in **Figure 9A**, DCs from B10.A mice showed increased expression of nuclear

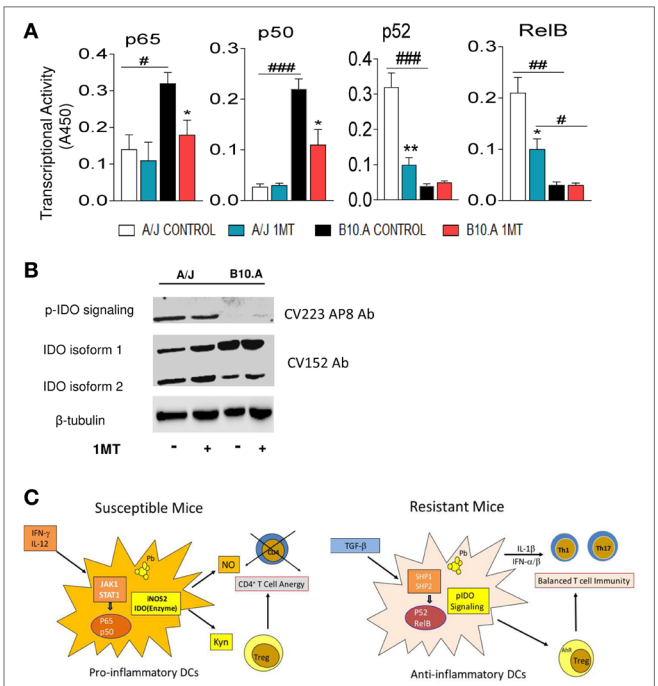

FIGURE 9 | Phosphorylated indoleamine-2,3 dioxygenase (pIDO) of A/J mice activate the non-canonical pathway of NF-κB, whereas in B10.A dendritic cells (DCs) non-phosphorylated IDO use the canonical pathway of NF-κB activation. **(A,B)** Quantitation of p65, p50, p52, and RelB by enzyme-linked immunosorbent assay (ELISA) in nuclear extracts of DCs. Results are presented as absorbance at 450 nm (A450). Values are the mean ± SE of three independent experiments. The asterisks represent statistically significant differences between treatments (*$p < 0.05$, **$p < 0.01$, ***$p < 0.001$). The hash marks represent statistically significant differences between strains ($^{\#}p < 0.05$, $^{\#\#}p < 0.01$, $^{\#\#\#}p < 0.001$). **(C)** Expression of IDO and phosphorylated IDO was assessed by Western blot in lung homogenates of 1MT treated and untreated B10.A and A/J mice i.t. infected with 1 × 10^6 *Paracoccidiodes brasiliensis* yeasts. pIDO was revealed by a specific antibody that recognizes the phosphorylated ITIM moiety of IDO (CV223 AP8) and the enzyme IDO by a specific monoclonal antibody (CV152). **(D)** In susceptible B10.A mice, IDO is induced by IFN-γ that activates the canonical pathway of NF-κB and enhanced iNOS and IDO expression resulting in anergy of T cell immunity. In resistant A/J mice, TGF-β signaling induces the non-canonical pathway of NF-κB activation and continuous synthesis of TGF-β that confers an stable tolerogenic behavior to DCs that control immunity and tissue pathology.

p65 and p50 than those of A/J mice. Furthermore, 1MT treatment reduced this production by B10.A DCs (**Figure 9A**). An equivalent result was observed with DCs obtained at 96 h of infection (Figure S1 in Supplementary Material). The prevalent non-canonical activation of NF-κB by A/J DCs was confirmed by the increased levels of nuclear p52 and RelB produced in comparison with B10.A DCs (**Figure 9A**). Treatment with 1MT caused a significant reduction of p52 and RelB only in A/J DCs. Again, an equivalent result was observed in pulmonary DCs obtained at 96 h of infection (Figure S2 in Supplementary Material). To further confirm the signaling function of IDO, lung extracts from 1MT treated and untreated B10.A and A/J mice were obtained 2 weeks after infection and the expression of pIDO was assessed by immunoblotting using a specific mAb (CV223 AP8 Ab) that recognizes the phosphorylated moiety of ITIM. As depicted in **Figure 9B**, only A/J mice express pIDO and 1MT treatment did not affect the production of this molecule. Using a polyclonal antibody to IDO (CV152 Ab) two isoforms of IDO, and the elevated expression of the isoform 1 by B10.A DCs were seen. The **Figure 9C** summarizes the main findings obtained in this study. In susceptible B10.A mice IDO is induced by IFN-γ that activates the canonical pathway of NF-κB and enhanced iNOS and IDO expression resulting in anergy of T cell immunity. In resistant A/J mice, TGF-β signaling induces the non-canonical pathway of NF-κB activation and continuous synthesis of TGF-β that confers an stable tolerogenic behavior to DCs that control immunity and tissue pathology.

DISCUSSION

The antimicrobial and immunoregulatory functions of IDO have been recognized as central mechanisms used by infected hosts to control pathogen growth and excessive inflammatory responses (37, 38). Both IDO activities were used by resistant and susceptible mice to control pulmonary PCM. However, only in susceptible mice IDO inhibition caused a sustained fungal growth, exacerbated tissue pathology and increased mortality rates. This is the worst scenario for host fitness because it allies uncontrolled pathogen growth with exacerbated, but inefficient, inflammation resulting in warful tissue destruction. These findings led us to further investigate the role of IDO in the resistance mechanisms to pulmonary PCM. We found the IDO inhibitor 1-MT as two stereoisomers, 1-D-MT and 1-L-MT. Most of the studies using the IDO enzyme model employed the racemic mixture 1-DL-MT to inhibit the enzime, independent of the known IDO isoforms, IDO1 and IDO2, as we did in this work. Indeed, recent studies have shown that IDO1 is the preferentially inhibited by1-L-MT, while 1-D-MT inhibits IDO2 (39, 40). These findings directed our subsequent studies on the inhibition of IDO using deficient mice, as we have shown in recent work with IDO1-deficient ($IDO1^{-/-}$) C57BL/6 mice (41). Using isolated pulmonary DCs, we verified that IDO inhibition led to increased recovery of yeasts from both A/J and B10.A cells. This finding could be attributed to the increased trp availability (42–44), but also to the reduced NO production, an important fungicidal mechanism of macrophages and DCs (26, 27, 30).

Interestingly, IDO inhibition by 1MT reduced the typical cytokines that characterize the innate response of B10.A and A/J mice (26, 27, 30). Furthermore, the assessment of intracellular cytokines has further emphasized the higher expression of IDO and TGF-β by A/J DCs, whereas the proinflammatory cytokines IL-12 and IL-6 were more expressed by B10.A DCs. This led us to suppose that IDO activity in B10.A mice was mainly catalytic, whereas in A/J mice was predominantly signaling and involved in signal transduction (12). These investigators clearly demonstrated that TGF-β signaling activates the tyrosine kinase Fyn that phosphorylates ITIM domains of IDO. This promotes the association of IDO with tyrosine phosphatases (SHP1 and SHP2) that results in the activation of the non-canonical NF-κB pathway (p52/RelB), which translocates to the nucleus and induces the production of type I IFNs (IFNα/β), TGF-β, and IDO (12).

An increased number of activated DCs with enhanced immunogenic activity was detected in the lungs of 1MT treated mice. The increased proliferation of naive lymphocytes was concomitant with increased levels of IL-2 in A/J cocultures and decreased IFN-γ production by B10.A cells mirroring the main suppressive mechanisms developed by susceptible and resistant mice (25, 26, 30, 45). This enhanced immunogenic activity was further confirmed by the increased proliferation of naive and effector/memory $CD8^+$ and $CD4^+$ T cells concomitant with a reduced expansion of $CD4^+CD25^+Foxp3^+$ Treg cells, a finding that may be also associated with the reduced levels of suppressive Kyn produced (46, 47). This tolerogenic function of Kyn on T cells has been linked to the activation of the AhR, a ligand activated transcription factor (46, 48) that participates in the pIDO-tolerogenic DCs-Treg loop of immunoregulation.

Further assessing the mechanisms involved in the divergent activities of IDO, a preferential IFN-γ signaling pathway was observed in B10.A DCs which expressed increased levels of IFN-γ and Jak1-Stat1 mRNA. In addition, elevated expression of IL-6, SOCS3, and iNOS2 were also observed indicating a prevalent IFN-γ-mediated catalytic activity. These data were further confirmed by the increased synthesis of Stat1 and IKKβ proteins involved in IFN-γ signaling. The striking expression of IL-6 and SOCS3 suggests that in susceptible mice IDO degradation may occur *via* proteasomal activity (49). Our data have also confirmed the prevalent TGF-β-mediated activation of A/J DCs which express high levels of TGF-β, Smad2, Smad3, Ship1, Shp1, Shp2, IFN-α, and IFN-β mRNA. The high levels of IKK-α, Smad2, Ship1, and Sph-2 proteins expressed by these cells have further confirmed the use of the TGF-β signaling by DCs from resistant mice. These data agree with the signaling cascade that promotes a tolerogenic activity in plasmacytoid DCs previously described (12) and explain the continuous production of TGF-β by A/J mice that favors the conversion of naive $CD4^+$ T cells into Treg cells (25). Interestingly, the inhibition of IDO by 1MT showed little interference with the TGF-β-mediated pathway used by A/J DCs, demonstrating that the signaling function of the IDO has predominance over the catalytic activity.

The predominant expression of p65 and p50 by B10.A DCs and the higher levels of p52 and RelB by A/J DCs showed that B10.A and A/J mice predominantly use, respectively, the canonical and non-canonical pathways of NF-κB activation by their pulmonary

DCs. More importantly, we could demonstrate the presence of pIDO in the lungs of A/J mice, whereas the non-phosphorylated forms of IDO were observed in B10.A mice. Therefore, we could clearly demonstrate that in B10.A mice IDO has a catalytic function, whereas in A/J mice, besides its enzymatic activity, IDO has a signaling function.

Similarly with other infection models, our studies in experimental PCM showed that the balanced activation of the immune system is fundamental for the protection of hosts, and the excessive activation of pro- or anti-inflammatory mechanisms leads to severe disease (23, 29, 50, 51). In susceptible mice, the suppression of adaptive immunity is a consequence of excessive proinflammatory activity of innate immunity, which, however, is able to control the initial fungal burden. In resistant mice, in contrast, an anti-inflammatory, TGF-β dominated activity is observed impairing the initial control of fungal growth. This activity, however, is balanced by the marked dectin-1 and NLRP3 activation and synthesis of TNF-α and IL-1β by A/J macrophages. This pattern of response leads to the subsequent differentiation of Th1/Th17 mixed responses, always strongly controlled by elevated numbers and activity of Treg cells that control tissue pathology (24–27, 29). This is an unusual but interesting model of resistance and susceptibility to a primary fungal pathogen not previously described.

Host defenses are governed by resistance and tolerance mechanisms, the first involved in reducing pathogen burden during infection and the latter associated with mechanisms that protected the hosts from pathogen- or immune-induced damage. These mechanisms are not mutually exclusive and both can contribute to host fitness (52, 53). Our studies clearly demonstrate that the resistance mechanisms used by A/J mice are governed by resistance to disease and not resistance to pathogen growth. Although not intensely explored in infectious diseases, tolerance to disease is well known and described in plant pathology where host protection is not achieved by the elimination of the pathogen, but it is based on the control of host fitness. This response allows pathogen persistence, but its excessive growth is partially controlled by immune mechanisms that are tightly regulated to preserve homeostasis (52). This is also observed in the host responses to commensal fungi such as *Aspergillus fumigatus* and *Candida albicans* that concomitantly control fungal burden and tissue inflammation (50). The important influence of the IDO-AhR-Treg-Th17 axis on the control of this well-balanced response to commensal microorganisms has been well described in the literature (44, 54, 55). The IFN-γ-mediated activation of IDO and Kyn synthesis by tissue DCs confers a tolerogenic profile to these cells that promote the differentiation of naive T cells into Foxp3$^+$ Treg cells *via* activation of AhR that prevents the excessive expansion of Th17 lymphocytes (44, 56). This tightly regulated immunity confers immune homeostasis that results in microbial resistance but avoids tissue pathology. The signaling property of pIDO induced by TGF-β activation of DCs was more recently described and has been viewed as potent immunoregulatory mechanism that confer stable tolerogenic activity to plasmacytoid DCs (12, 36). This tolerogenic mechanism was validated in an *in vivo* model of delayed-type hypersensitivity response and in the protective activity of endotoxin-tolerant state of mice against Gram-positive and Gram-negative infections (12, 54). However, to our knowledge, this mechanism of disease tolerance was never described in the host responses to primary fungal pathogens. Indeed, pIDO-mediated tolerance was poorly explored in infectious pathologies. Therefore, we believe that the findings here described open new perspectives to understand resistance against PCM and other primary fungal pathogens where excessive inflammation has been associated with severe disease (57, 58). Previous results obtained in our experimental model, not well understood when originally obtained, can now be re-evaluated in face of the IDO mediated mechanism here described. The subcutaneous immunization with viable yeasts confers sterile immunity to i.p. challenged B10.A mice but partial immunoprotection in A/J mice that remain with persistent fungal loads (59, 60). We have also previously described that *P. brasiliensis* infection induces an elevated production of TGF-β and M2 differentiation of A/J macrophages which express high levels of arginase (27), another finding which is not in line with the mechanisms of pathogen resistance usually described. However, this finding may now be better appreciated and understood because arginase expression by innate immune cells was reported to be essential for the differentiation of tolerogenic DCs, whose signaling activity is mediated by pIDO (61).

In conclusion, the studies here reported clearly demonstrate that susceptibility to PCM is mainly mediated by the proinflammatory IFN-γ-IDO axis of innate responses, whereas resistance relies on the initial anti-inflammatory TGF-β-pIDO-Treg axis that confers a sustained tolerogenic phenotype in pulmonary DCs allowing A/J mice to interact with a primary fungal pathogen as a commensal microbe. Therefore, the signaling function of pIDO leads to an efficient fungus–-host interaction that conditions advantages to both partners, and may be explored in further innovative anti-fungal therapy.

ETHICS STATEMENT

The experiments were performed in strict accordance with the Brazilian Federal Law 11,794 establishing procedures for the scientific use of animals, and the State Law establishing the Animal Protection Code of the State of São Paulo. All efforts were made to minimize animal suffering. The procedures were approved by the Ethics Committee on Animal Experiments of the Institute of Biomedical Sciences of University of São Paulo (Proc.180/11/CEEA).

AUTHOR CONTRIBUTIONS

EA designed, conducted, and analyzed all experiments. FL, CF, and TC performed and analyzed experiments. CV characterized IDO and IDO phosphorylation. LR provided conceptual help and wrote the article. PP provided conceptual help and precious reagents for IDO analysis. VC planned experiments, supervised the overall study, and wrote the manuscript.

FUNDING

This work was supported by grants from the Fundação de Amparo à Pesquisa do Estado de São Paulo (FAPESP)

research grants no. 2011/51258-2 (VLGC) and 2016/04783-2 (FVL); FAPESP postdoctoral felowships no. 2013/02396-9 (CF) and 2014/18668-0 (EFA); and Conselho Nacional de Pesquisas (CNPq) research grant no. 4713172012 (VLGC).

SUPPLEMENTARY MATERIAL

The Supplementary Material for this article can be found online at http://www.frontiersin.org/article/10.3389/fimmu.2017.01522/full#supplementary-material.

REFERENCES

1. Mellor AL, Munn DH. IDO expression by dendritic cells: tolerance and tryptophan catabolism. *Nat Rev Immunol* (2004) 4:762–74. doi:10.1038/nri1457
2. Grohmann U, Fallarino F, Puccetti P. Tolerance, DCs and tryptophan: much ado about IDO. *Trends Immunol* (2003) 24:242. doi:10.1016/S1471-4906(03)00072-3
3. von Bergwelt-Baildon MS, Popov A, Saric T, Chemnitz J, Classen S, Stoffel MS, et al. CD25 and indoleamine 2,3-dioxygenase are up-regulated by prostaglandin E2 and expressed by tumor-associated dendritic cells *in vivo*: additional mechanisms of T-cell inhibition. *Blood* (2006) 108:228–37. doi:10.1182/blood-2005-08-3507
4. Popov A, Schultze JL. IDO-expressing regulatory dendritic cells in cancer and chronic infection. *J Mol Med* (2008) 86:145–60. doi:10.1007/s00109-007-0262-6
5. Braun D, Longman RS, Albert ML. A two-step induction of indoleamine 2,3 dioxygenase (IDO) activity during dendritic-cell maturation. *Blood* (2005) 106:2375–81. doi:10.1182/blood-2005-03-0979
6. Beutelspacher SC, Tan PH, McClure MO, Larkin DF, Lechler RI, George AJ. Expression of indoleamine 2,3-dioxygenase (IDO) by endothelial cells: implications for the control of alloresponses. *Am J Transplant* (2006) 6:1320–30. doi:10.1111/j.1600-6143.2006.01324.x
7. Uyttenhove C, Pilotte L, Théate I, Stroobant V, Colau D, Parmentier N, et al. Evidence for a tumoral immune resistance mechanism based on tryptophan degradation by indoleamine 2,3-dioxygenase. *Nat Med* (2003) 9:1269–74. doi:10.1038/nm934
8. Wang D, Feng X, Lu L, Konkel JE, Zhang H, Chen Z, et al. A CD8 T cell/indoleamine 2,3-dioxygenase axis is required for mesenchymal stem cell suppression of human systemic lupus erythematosus. *Arthritis Rheumatol* (2014) 66:2234–45. doi:10.1002/art.38674
9. Taylor MW, Feng GS. Relationship between interferon-gamma, indoleamine 2,3-dioxygenase, and tryptophan catabolism. *FASEB J* (1991) 5:2516–22.
10. Sedlmayr P, Blaschitz A, Wintersteiger R, Semlitsch M, Hammer A, MacKenzie CR, et al. Localization of indoleamine 2,3-dioxygenase in human female reproductive organs and the placenta. *Mol Hum Reprod* (2002) 8:385–91. doi:10.1093/molehr/8.4.385
11. Munn DH, Mellor AL. Indoleamine 2,3 dioxygenase and metabolic control of immune responses. *Trends Immunol* (2013) 34:137–43. doi:10.1016/j.it.2012.10.001
12. Pallotta MT, Orabona C, Volpi C, Vacca C, Belladonna ML, Bianchi R, et al. Indoleamine 2,3-dioxygenase is a signaling protein in long-term tolerance by dendritic cells. *Nat Immunol* (2011) 12:870–8. doi:10.1038/ni.2077
13. Barth H, Raghuraman S. Persistent infectious diseases say – IDO. Role of indoleamine-2,3-dioxygenase in disease pathogenesis and implications for therapy. *Crit Rev Microbiol* (2014) 40:360–8. doi:10.3109/1040841X.2012.742037
14. Baban B, Penberthy WT, Mozaffari MS. The potential role of indoleamine 2, 3 dioxygenase (IDO) as a predictive and therapeutic target for diabetes treatment: a mythical truth. *EPMA J* (2010) 1:46–55. doi:10.1007/s13167-010-0009-2
15. Zelante T, Fallarino F, Bistoni F, Puccetti P, Romani L. Indoleamine 2,3-dioxygenase in infection: the paradox of an evasive strategy that benefits the host. *Microbes Infect* (2009) 11:133–41. doi:10.1016/j.micinf.2008.10.007
16. Fallarino F, Grohmann U, You S, McGrath BC, Cavener DR, Vacca C, et al. The combined effects of tryptophan starvation and tryptophan catabolites down-regulate T cell receptor zeta-chain and induce a regulatory phenotype in naive T cells. *J Immunol* (2006) 176:6752–61. doi:10.4049/jimmunol.176.11.6752
17. Sharma MD, Baban B, Chandler P, Hou DY, Singh N, Yagita H, et al. Plasmacytoid dendritic cells from mouse tumor-draining lymph nodes directly activate mature Tregs via indoleamine 2,3-dioxygenase. *J Clin Invest* (2007) 117:2570–82. doi:10.1172/JCI31911
18. Teixeira MM, Theodoro RC, de Carvalho MJ, Fernandes L, Paes HC, Hahn RC, et al. Phylogenetic analysis reveals a high level of speciation in the *Paracoccidioides* genus. *Mol Phylogenet Evol* (2009) 52:273–83. doi:10.1016/j.ympev.2009.04.005
19. De Castro LF, Ferreira MC, da Silva RM, Blotta MH, Longhi LN, Mamoni RL. Characterization of the immune response in human paracoccidioidomycosis. *J Infect* (2013) 67:470–85. doi:10.1016/j.jinf.2013.07.019
20. Mamoni RL, Blotta MH. Kinetics of cytokines and chemokines gene expression distinguishes *Paracoccidioides brasiliensis* infection from disease. *Cytokine* (2005) 32:20–9. doi:10.1016/j.cyto.2005.07.006
21. Benard G, Romano CC, Cacere CR, Juvenale M, Mendes-Giannini MJ, Duarte AJ. Imbalance of IL-2, IFN-gamma and IL-10 secretion in the immunosuppression associated with human paracoccidioidomycosis. *Cytokine* (2001) 13:248–52. doi:10.1006/cyto.2000.0824
22. Calich VL, Singer-Vermes LM, Siqueira AM, Burger E. Susceptibility and resistance of inbred mice to *Paracoccidioides brasiliensis*. *Br J Exp Pathol* (1985) 66:585–94.
23. Calich VLG, Blotta MHSL. Pulmonary paracoccidioidomycosis. 1st ed. In: Fidel P, Huffnagle G, editors. *Fungal Immunology, From an Organ Perspective*. (Vol. 1), New York: Springer (2005). p. 201–28.
24. Cano LE, Singer-Vermes LM, Vaz CAC, Russo M, Calich VL. Pulmonary paracoccidioidomycosis in resistant and susceptible mice: relationship among progression of infection, bronchoalveolar cell activation, cellular immune response, and specific isotype patterns. *Infect Immun* (1995) 63:1777–83.
25. Felonato M, Pina A, de Araujo EF, Loures FV, Bazan SB, Feriotti C, et al. Anti-CD25 treatment depletes Treg cells and decreases disease severity in susceptible and resistant mice infected with *Paracoccidioides brasiliensis*. *PLoS One* (2012) 7:e51071. doi:10.1371/journal.pone.0051071
26. Pina A, Bernardino S, Calich VL. Alveolar macrophages from susceptible mice are more competent than those of resistant mice to control initial *Paracoccidioides brasiliensis* infection. *J Leukoc Biol* (2008) 83:1088–99. doi:10.1189/jlb.1107738
27. Feriotti C, Loures FV, Frank de Araújo E, da Costa TA, Calich VL. Mannosyl-recognizing receptors induce an M1-like phenotype in macrophages of susceptible mice but an M2-like phenotype in mice resistant to a fungal infection. *PLoS One* (2013) 8:e54845. doi:10.1371/journal.pone.0054845
28. Araújo EF, Loures FV, Bazan SB, Feriotti C, Pina A, Schanoski AS, et al. Indoleamine 2,3-dioxygenase controls fungal loads and immunity in paracoccidioidomicosis but is more important to susceptible than resistant hosts. *PLoS Negl Trop Dis* (2014) 8:e3330. doi:10.1371/journal.pntd.0003330
29. Calich VLG, da Costa TA, Felonato M, Arruda C, Bernardino S, Loures FV, et al. Innate immunity to *Paracoccidioides brasiliensis* infection. *Mycopathologia* (2008) 165:223–36. doi:10.1007/s11046-007-9048-1
30. Pina A, de Araujo EF, Felonato M, Loures FV, Feriotti C, Bernardino S, et al. Myeloid dendritic cells (DCs) of mice susceptible to paracoccidioidomycosis suppress T cell responses whereas myeloid and plasmacytoid DCs from resistant mice induce effector and regulatory T cells. *Infect Immun* (2013) 81:1064–77. doi:10.1128/IAI.00736-12
31. Felonato M, Pina A, Bernardino S, Loures FV, de Araujo EF, Calich VLG. CD28 exerts protective and detrimental effects in a pulmonary model of paracoccidioidomycosis. *Infect Immun* (2010) 78:4922–35. doi:10.1128/IAI.00297-10
32. Singer-Vermes LM, Caldeira CB, Burger E, Calich VLG. Experimental murine paracoccidioidomycosis: relationship among dissemination of the infection, humoral and cellular responses. *Clin Exp Immunol* (1993) 94:75–9. doi:10.1111/j.1365-2249.1993.tb05980.x
33. Ding AH, Nathan CF, Stuehr DJ. Release of reactive nitrogen intermediates and reactive oxygen intermediates from mouse peritoneal macrophages. Comparison of activating cytokines and evidence for independent production. *J Immunol* (1988) 141:2407–12.

34. Mannering SI, Morris JS, Jensen KP, Purcell AW, Honeyman MC, van Endert PM, et al. A sensitive method for detecting proliferation of rare autoantigen-specific human T cells. *J Immunol Methods* (2003) 283:173–83. doi:10.1016/j.jim.2003.09.004
35. Orabona C, Pallotta MT, Volpi C, Fallarino F, Vacca C, Bianchi R, et al. SOCS3 drives proteasomal degradation of indoleamine 2,3-dioxygenase (IDO) and antagonizes IDO-dependent tolerogenesis. *Proc Natl Acad Sci U S A* (2008) 105:20828–33. doi:10.1073/pnas.0810278105
36. Orabona C, Pallotta MT, Grohmann U. Different partners, opposite outcomes: a new perspective of the immunobiology of indoleamine 2,3-dioxygenase. *Mol Med* (2012) 18:834–42. doi:10.2119/molmed.2012.00029
37. Bonifazi P, Zelante T, D'Angelo C, De Luca A, Moretti S, Bozza S, et al. Balancing inflammation and tolerance *in vivo* through dendritic cells by the commensal *Candida albicans*. *Mucosal Immunol* (2009) 2:362–74. doi:10.1038/mi.2009.17
38. Araújo EF, Medeiros DH, Galdino NA, Condino-Neto A, Calich VL, Loures FV. Tolerogenic plasmacytoid dendritic cells control *Paracoccidioides brasiliensis* infection by inducting regulatory T cells in an IDO-dependent manner. *PLoS Pathog* (2016) 12:e1006115. doi:10.1371/journal.ppat.1006115
39. Lob S, Konigsrainer A, Zieker D, Brucher BL, Rammensee HG, Opelz G, et al. IDO1 and IDO2 are expressed in human tumors: levo- but not dextro-1-methyl tryptophan inhibits tryptophan catabolism. *Cancer Immunol Immunother* (2009) 58:153–7. doi:10.1007/s00262-008-0513-6
40. Metz R, Duhadaway JB, Kamasani U, Laury-Kleintop L, Muller AJ, Prendergast GC. Novel tryptophan catabolic enzyme IDO2 is the preferred biochemical target of the antitumor indoleamine 2,3-dioxygenase inhibitory compound D-1-methyl-tryptophan. *Cancer Res* (2007) 67:7082–7. doi:10.1158/0008-5472.CAN-07-1872
41. De Araújo EF, Feriotti C, Galdino NAL, Preite NW, Calich VLG, Loures FV. The IDO-AhR axis controls Th17/Treg immunity in a pulmonary model of fungal infection. *Front Immunol* (2017) 8:880. doi:10.3389/fimmu.2017.00880
42. Montagnoli C, Bozza S, Gaziano R, Zelante T, Bonifazi P, Moretti S, et al. Immunity and tolerance to *Aspergillus fumigatus*. *Novartis Found Symp* (2006) 279:66–77. doi:10.1002/9780470035399.ch6
43. Schmidt SV, Schultze JL. New insights into IDO biology in bacterial and viral infections. *Front Immunol* (2014) 5:384–93. doi:10.3389/fimmu.2014.00384
44. Zelante T, Iannitti RG, Fallarino F, Gargaro M, De Luca A, Moretti S, et al. Tryptophan feeding of the IDO1-AhR axis in host-microbial symbiosis. *Front Immunol* (2014) 5:640. doi:10.3389/fimmu.2014.00640
45. Cano LE, Kashino SS, Arruda C, André D, Xidieh CF, Singer-Vermes LM, et al. Protective role of gamma interferon in experimental pulmonary paracoccidioidomycosis. *Infect Immun* (1998) 66:800–6.
46. Mezrich JD, Fechner JH, Zhang X, Johnson BP, Burlingham WJ, Bradfield CA. An interaction between kynurenine and the aryl hydrocarbon receptor can generate regulatory T cells. *J Immunol* (2010) 185:3190–8. doi:10.4049/jimmunol.0903670
47. Puccetti P, Grohmann U. IDO and regulatory T cells: a role for reverse signalling and non-canonical Nf-κB activation. *Nat Rev Immunol* (2007) 7:817–23. doi:10.1038/nri2163
48. Fallarino F, Vacca C, Orabona C, Belladonna ML, Bianchi R, Marshall B, et al. Functional expression of indoleamine 2,3-dioxygenase by murine CD8a+ dendritic cells. *Int Immunol* (2002) 14:1206–12. doi:10.1093/intimm/14.1.65
49. Grohmann U, Fallarino F, Bianchi R, Belladonna ML, Vacca C, Orabona C, et al. IL-6 inhibits the tolerogenic function of CD8α+ dendritic cells expressing indoleamine 2,3-dioxygenase. *J Immunol* (2001) 167:708–14. doi:10.4049/jimmunol.167.2.708
50. Romani L. Immunity to fungal infections. *Nat Rev Immunol* (2011) 11:275–88. doi:10.1038/nri2939
51. Loures FV, Pina A, Felonato M, Araújo EF, Leite KR, Calich VL. Toll-like receptor 4 signaling leads to severe fungal infection associated with enhanced proinflammatory immunity and impaired expansion of regulatory T cells. *Infect Immun* (2010) 78:1078–88. doi:10.1128/IAI.01198-09
52. Read AF, Graham AL, Raberg L. Animal defenses against infectious agents: is damage control more important than pathogen control. *PLoS Biol* (2008) 6:e4. doi:10.1371/journal.pbio.1000004
53. Schneider DS, Ayres JS. Two ways to survive infection: what resistance and tolerance can teach us about treating infectious diseases. *Nat Rev Immunol* (2008) 8:889–95. doi:10.1038/nri2432
54. Bessede A, Gargaro M, Pallotta MT, Matino D, Servillo G, Brunacci C, et al. Aryl hydrocarbon receptor control of a disease tolerance defence pathway. *Nature* (2014) 511:184–90. doi:10.1038/nature13323
55. Romani L, Zelante T, De Luca A, Iannitti RG, Moretti S, Bartoli A, et al. Microbiota control of a tryptophan-AhR pathway in disease tolerance to fungi. *Eur J Immunol* (2014) 44:3192–200. doi:10.1002/eji.201344406
56. Nguyen NT, Kimura A, Nakahama T, Chinen I, Masuda K, Nohara K, et al. Aryl hydrocarbon receptor negatively regulates dendritic cell immunogenicity via a kynurenine-dependent mechanism. *Proc Natl Acad Sci U S A* (2010) 107:19961–6. doi:10.1073/pnas.1014465107
57. Benard G, Costa AN, Ravanini J, Goulart S, Nicodemo EL, Barbas CS, et al. Fatal acute respiratory distress syndrome in a patient with paracoccidioidomycosis: first case report. *Med Mycol* (2010) 48:542–5. doi:10.3109/13693780903330563
58. Gryschek RC, Pereira RM, Kono A, Patzina RA, Tresoldi AT, Shikanai-Yasuda MA, et al. Paradoxical reaction to treatment in 2 patients with severe acute paracoccidioidomycosis: a previously unreported complication and its management with corticosteroids. *Clin Infect Dis* (2010) 50:e56–8. doi:10.1086/652290
59. Arruda C, Kashino SS, Fazioli RA, Calich VL. A primary subcutaneous infection with *Paracoccidioides brasiliensis* leads to immunoprotection or exacerbated disease depending on the route of challenge. *Microbes Infect* (2007) 9:308–16. doi:10.1016/j.micinf.2006.12.005
60. Arruda C, Vaz CA, Calich VL. Aseptic cure of pulmonary paracoccidioidomycosis can be achieved after a previous subcutaneous immunization of susceptible but not resistant mice. *Microbes Infect* (2007) 9:704–13. doi:10.1016/j.micinf.2007.02.014
61. Mondanelli G, Bianchi R, Pallotta MT, Orabona C, Albini E, Iacono A, et al. A relay pathway between arginine and tryptophan metabolism confers immunosuppressive properties on dendritic cells. *Immunity* (2017) 46:233–44. doi:10.1016/j.immuni.2017.01.005

Conflict of Interest Statement: The authors declare that the research was conducted in the absence of any commercial or financial relationships that could be construed as a potential conflict of interest.

Copyright © 2017 de Araújo, Loures, Feriotti, Costa, Vacca, Puccetti, Romani and Calich. This is an open-access article distributed under the terms of the Creative Commons Attribution License (CC BY). The use, distribution or reproduction in other forums is permitted, provided the original author(s) or licensor are credited and that the original publication in this journal is cited, in accordance with accepted academic practice. No use, distribution or reproduction is permitted which does not comply with these terms.

frontiers in Immunology

ORIGINAL RESEARCH
published: 24 July 2017
doi: 10.3389/fimmu.2017.00880

The IDO–AhR Axis Controls Th17/Treg Immunity in a Pulmonary Model of Fungal Infection

Eliseu Frank de Araújo, Claudia Feriotti, Nayane Alves de Lima Galdino, Nycolas Willian Preite, Vera Lúcia Garcia Calich† and Flávio Vieira Loures†*

Departamento de Imunologia, Instituto de Ciências Biomédicas, Universidade de São Paulo, São Paulo, Brazil

In infectious diseases, the enzyme indoleamine 2,3 dioxygenase-1 (IDO1) that catalyzes the tryptophan (Trp) degradation along the kynurenines (Kyn) pathway has two main functions, the control of pathogen growth by reducing available Trp and immune regulation mediated by the Kyn-mediated expansion of regulatory T (Treg) cells *via* aryl hydrocarbon receptor (AhR). In pulmonary paracoccidioidomycosis (PCM) caused by the dimorphic fungus *Paracoccidioides brasiliensis*, IDO1 was shown to control the disease severity of both resistant and susceptible mice to the infection; however, only in resistant mice, IDO1 is induced by TGF-β signaling that confers a stable tolerogenic phenotype to dendritic cells (DCs). In addition, in pulmonary PCM, the tolerogenic function of plasmacytoid dendritic cells was linked to the IDO1 activity. To further evaluate the function of IDO1 in pulmonary PCM, IDO1-deficient ($IDO1^{-/-}$) C57BL/6 mice were intratracheally infected with *P. brasiliensis* yeasts and the infection analyzed at three postinfection periods regarding several parameters of disease severity and immune response. The fungal loads and tissue pathology of $IDO1^{-/-}$ mice were higher than their wild-type controls resulting in increased mortality rates. The evaluation of innate lymphoid cells showed an upregulated differentiation of the innate lymphoid cell 3 phenotype accompanied by a decreased expansion of ILC1 and NK cells in the lungs of infected $IDO1^{-/-}$ mice. DCs from these mice expressed elevated levels of costimulatory molecules and cytokine IL-6 associated with reduced production of IL-12, TNF-α, IL-1β, TGF-β, and IL-10. This response was concomitant with a marked reduction in AhR production. The absence of IDO1 expression caused an increased influx of activated Th17 cells to the lungs with a simultaneous reduction in Th1 and Treg cells. Accordingly, the suppressive cytokines IL-10, TGF-β, IL-27, and IL-35 appeared in reduced levels in the lungs of $IDO1^{-/-}$ mice. In conclusion, the immunological balance mediated by the axis IDO/AhR is fundamental to determine the balance between Th17/Treg cells and control the severity of pulmonary PCM.

Keywords: paracoccidioidomycosis, indolemine 2,3 dioxygenase, aryl hydrocarbon receptor, Th17 cells, regulatory T cells, innate lymphoid cells

OPEN ACCESS

Edited by:
Steven Templeton, Indiana University School of Medicine, United States

Reviewed by:
Anamelia Lorenzetti Bocca, University of Brasília, Brazil
Agostinho Carvalho, University of Minho, Portugal

***Correspondence:**
Flávio Vieira Loures
loures@icb.usp.br

†These authors have contributed equally to this work.

Specialty section:
This article was submitted to Microbial Immunology, a section of the journal Frontiers in Immunology

Received: *19 May 2017*
Accepted: *10 July 2017*
Published: *24 July 2017*

Citation:
de Araújo EF, Feriotti C, Galdino NAdL, Preite NW, Calich VLG and Loures FV (2017) The IDO–AhR Axis Controls Th17/Treg Immunity in a Pulmonary Model of Fungal Infection. Front. Immunol. 8:880. doi: 10.3389/fimmu.2017.00880

INTRODUCTION

Indoleamine 2,3 dioxygenase-1 (IDO1) is an enzyme that catalyzes the degradation of tryptophan (Trp) along the kynurenines (Kyn) pathway. This enzyme plays a critical role to host defenses against a wide range of pathogens by inducing Trp starvation and controlling inflammatory

and immunological reactions. Several types of cells, such as macrophages, epithelial, and dendritic cells (DCs), express IDO1 that can be induced by proinflammatory cytokines (e.g., IFN-γ), toll-like receptor ligands (e.g., lipopolysaccharide), and interactions between immune cells through the engagement of costimulatory molecules (CD80, CD86) on antigen-presenting cells by cytotoxic T-lymphocyte antigen-4 on T cells (1–3). It is known that IDO1 can affect immunity through two non-exclusive mechanisms: (a) establishment of a local response with "amino acid deprivation" that inhibits cell and pathogen proliferation (2); (b) cascade generation of Trp metabolites with specific immunomodulatory or cytotoxic functions that inhibit T cell activation and modulate the differentiation of naïve T cells into regulatory T (Treg) cells (1, 4, 5). Furthermore, Kyn has immunomodulatory effects in the absence of Trp starvation, *via* activation of the transcription factor aryl hydrocarbon receptor (AhR) (6, 7).

Indeed, in fungal infections, IDO1 modulates the mechanisms of host resistance and disease tolerance by inducing Treg cells and inhibiting Th17 differentiation (1, 8–10). Importantly, Treg and Th17 cells share similar developmental pathways (11) and may arise from a common progenitor depending on the balance of inflammatory and anti-inflammatory cytokines (12), presence of retinoic acid (13), and the activation of the AhR, a ligand-activated transcription factor (14, 15).

Paracoccidioidomycosis (PCM), a systemic granulomatous disease caused either by the dimorphic fungi *Paracoccidioides brasiliensis* or *P. lutzii*, is considered the most prevalent deep mycosis in Latin America (16). The inhalation of conidia usually leads to an asymptomatic infection but a few infected individuals evolve to overt disease. The diverse patterns of T cell responses of *P. brasiliensis*-infected individuals are associated with different clinical manifestations. The resistance to infection observed in asymptomatic individuals is mediated by a predominant Th1 response, which is responsible for macrophage activation and fungal killing. The most severe form of the disease, the juvenile form, presents a prevalent Th2/Th9 response and enhanced antibody production. In the chronic inflammatory response characteristic of the adult form of the disease, a prominent Th17 immunity with important participation of Th1 cells was described (17, 18). The polar patterns of the disease could be reproduced in a murine model of pulmonary PCM (19). Resistant mice (A/Sn) develop a chronic regressive disease allied with prevalent Th1/Th17 immunity concomitant with protective $CD8^+$ T cells that synthesize large amounts of IFN-γ. The relative protection of susceptible mice (B10.A) is mediated by $CD8^+$ T cells that, however, are not able to compensate the $CD4^+$ T cell anergy induced by excessive proinflammatory innate response (20–23).

Recent studies of our group have demonstrated that in pulmonary PCM, IDO1 is an important immunoregulatory enzyme that promotes fungal clearance and inhibits T cell immunity and inflammation, with prominent importance to susceptible hosts. Actually, only in the susceptible mouse strain IDO1 inhibition by 1-methyl-dl-tryptophan (1MT) caused progressive tissue pathology and increased mortality rates. In addition, as previously reported in candidiasis and aspergillosis (24, 25), an IDO1-mediated immunomodulatory function of plasmacytoid dendritic cells (pDCs) has been described in pulmonary PCM. The *in vivo* depletion of IDO1 expressing pDCs resulted in less severe disease and increased T cell immunity (26), demonstrating that in pulmonary PCM pDCs have a tolerogenic function as previously described by Pallotta et al. (27). These findings led us to further elucidate the role of IDO1 in pulmonary PCM by comparing the disease developed by IDO1-deficient ($IDO1^{-/-}$) C57BL/6 mice with their normal wild-type (WT) controls. $IDO1^{-/-}$ mice developed a more severe infection with elevated fungal burdens, accompanied by increased inflammatory reactions mediated by prevalent Th17 responses insufficiently controlled by Treg cells. The absence of IDO1 expression has also influenced the expression of AhR and the differentiation of pulmonary innate lymphoid cells (ILCs) by increasing the presence of innate lymphoid cell 3 (ILC3) and reducing NK cells. Both the uncontrolled fungal growth and the exuberant inflammatory reactions appear to have contributed to the exacerbated tissue pathology that resulted in increased mortality rates of $IDO1^{-/-}$ mice.

MATERIALS AND METHODS

Ethics Statement

The experiments were performed in strict accordance with the Brazilian Federal Law 11,794 establishing procedures for the scientific use of animals, and the State Law establishing the Animal Protection Code of the State of São Paulo. All efforts were made to minimize animal suffering. The procedures were approved by the Ethics Committee on Animal Experiments of the Institute of Biomedical Sciences of University of São Paulo (Proc.180/11/CEEA).

Mice

Eight- to twelve-week-old male C57Bl/6 WT and C57Bl/6 $IDO1^{-/-}$ mice originally obtained from Jackson Laboratories and bred as the specific pathogen-free mice at the Isogenic Breeding Unit of the Department of Immunology, Institute of Biomedical Sciences, University of São Paulo were used throughout this study.

Fungus and Infection

The highly virulent *P. brasiliensis* 18 isolate (Pb18) was used throughout this study. Yeast cells were maintained by weekly cultivation in Fava Netto culture medium at 36°C and used on days 6–8 of culture. The viability of fungal suspensions, determined by Janus Green B vital dye (Merck), was always higher than 95%. Mice were anesthetized and submitted to intra-tracheal (i.t.) infection as previously described (19). Briefly, after intraperitoneal (i.p.) injection of ketamine and xylazine, animals were infected with 1×10^6 yeast cells, contained in 50 µL of PBS, by surgical i.t. inoculation, which allowed dispensing of the fungal cells directly into the lungs.

Colony-Forming Unit (CFU) Assays, Mortality Rates, and Histological Analysis

The numbers of viable yeasts in infected organs (lung and liver) were determined by counting the number of CFUs as previously

described (28). Mortality studies were done with groups of 10–12 mice. Deaths were registered daily. For histological examinations, the left lung of infected mice was removed and fixed in 10% formalin. Five-micrometer sections were stained by hematoxylin-eosin for an analysis of the lesions and were silver stained (Grocott stain) for fungal evaluation. Morphometrical analysis was performed using a Nikon DXM 1200c camera and Nikon NIS AR 2.30 software. The areas of lesions were measured (in square micrometers) in 10 microscopic fields per slide in 5 mice per group as previously described (29). Results are expressed as the mean ± SEM of total area of lesions for each mouse.

Assessment of Leukocyte Subpopulations and Flow Cytometric Analysis

The lungs from *P. brasiliensis*-infected WT and IDO1$^{-/-}$ mice were collected after 96 h, 2, and 10 weeks of infection and digested enzymatically for 45 min with collagenase (1 mg/mL; Sigma) in RPMI culture medium (Sigma). Total lung leukocyte numbers were assessed with trypan blue, and viability was always >95%. For cell-surface staining, lung cells were washed and suspended at 1×10^6 cells/mL in staining buffer (PBS, 2% fetal calf serum and 0.1% NaN_3). Fc receptors were blocked by the addition of unlabeled anti-CD16/32 (eBioscience). The cells were then stained in the dark for 20 min at 4°C with the optimal dilution of each monoclonal antibody. To myeloid cells: anti-CD11b, CD11c, CD40, CD80, CD86, and MHC-II; lymphocytes: CD4, CD25, CD8, CD44, and CD62L; NK: NK1.1, CD49b, NPK46, and Eomes; ILC1: CD127, CD49a, IL-12Rβ1, and Tbet; ILC2: CD127, ICOS, IL-17RB, IL-33, and GATA3; ILC3: CD127, IL-23R, IL-22, and RORC (eBiosciences or BioLegend). Cells were washed twice with staining buffer, fixed with 2% paraformaldehyde (PFA; Sigma). For intracellular detection of cytokines, leukocytes obtained from lungs were stimulated for 6 h in complete RPMI medium containing 50 ng/mL phorbol 12-myristate 13-acetate, 500 ng/mL ionomycin (Sigma), and 3 mM monensin (eBioscience). Next, cells were labeled for surface molecules and then treated according to the manufacturer's protocol for intracellular staining using the Cytofix/Cytoperm kit (BD Biosciences) and specifics antibodies anti-17, IL-4, IFN-γ, IL, 22, IL-1β, IL-12, TNF-α, IL-6, TGF-β, FoxP3, IDO1, and AhR. Cells were washed twice with staining buffer, suspended in 100 µL, and an equal volume of PFA was added to fix the cells. A minimum of 50,000 events was acquired on FACScanto II flow cytometer (BD Biosciences) using the FACSDiva software (BD Biosciences). Lymphocytes, myeloid cells, NK cells, and ILCs were gated as judged from forward and side light scatter. For Treg cell characterization, FACS plots or histograms were gated on live CD4$^+$ CD25$^+$ cells and the expression of FoxP3$^+$ were determined. The cell-surface expression of leukocyte markers as well as intracellular cytokine expression was analyzed using the FlowJo software (Tree Star).

RNA Isolation and cDNA Synthesis

Lungs were homogenized in TRIzol reagent using tissue grinders. Phase separation was realized following addition of 0.2 mL chloroform per mL of TRIzol and centrifugation at 12,000 × *g* for 15 min at 4°C. The upper aqueous RNA phase was removed to a new tube and further purified using Ultraclean Tissue and Cells RNA Isolation Kit (MO BIO Laboratories) according to the manufacturer's protocol. RNA purity and concentration were assessed on a NanoDrop ND-1000 spectrophotometer. An amount of 1 µg total RNA was reverse transcribed in a 20 µL reaction mixture using the High Capacity RNA-to-cDNA kit (Applied Biosystems) following the manufacturer's directions.

Real-time Quantitative Polymerase Chain Reaction (RT-PCR)

The cDNA was amplified using TaqMan Universal PCR Master Mix (Applied Biosystems) and pre-developed TaqMan assay primers and probes (*Ahr*, Mm00478932_m1, *Ifng*, Mm001168134_m1, *Tnf*, Mm99999068_m1, *Il-6*, Mm00446190_m1, *Il-10*, Mm00439614_m1, *Tgfb1*, Mm00117882_m1, *Il-17*, Mm00439618_m1, *Il-22*, Mm01226722_m1, *Tbx21*, Mm00450960_m1; *GATA3*, Mm00484683_m1; *Rorc*, Mm01261022_m1; *Foxp3*, Mm 00475162_m1; all from Applied Biosystems). PCR assays were performed on an MxP3000P qPCR System and data were developed using the MxPro qPCR software (Stratagene). The average threshold cycle (C_T) values of samples were normalized to C_T value of *Gapdh* gene. The relative expression was determined by the $2^{-\Delta\Delta}C_T$ method.

Cytokines and Nitric Oxide (NO) Detection

The lungs from *P. brasiliensis*-infected WT and IDO1$^{-/-}$ mice were collected after 96 h, 2, and 10 weeks of infection with one million *P. brasiliensis* yeasts. The organs were aseptically removed and individually disrupted in 7 mL of PBS. Supernatants were separated from cell debris by centrifugation at 3,000 × *g* for 10 min and stored at −80°C. The levels of IL-1β, IL-2, IL-4, IL-6, IL-10, IL-12, IL-17, IL-22, IL-27, IL-35, IL-23, TNF-α, IFN-γ, and TGF-β were measured by capture enzyme-linked immunosorbent assay (ELISA) with antibody pairs purchased from eBioscience or PBL. NO production was quantified by the accumulation of nitrite in the supernatants from *in vitro* protocols by a standard Griess reaction. All determinations were performed in duplicate, and results were expressed as micro molar concentration of NO. Plates were read using a spectrophotometric plate reader (VersaMax, Molecular Devices).

Statistical Analysis

Differences between groups were analyzed by the Student's *t*-test or analysis of variance (ANOVA) followed by the Tukey test. For comparisons of greater than two groups, significance was determined using the one- or two-way ANOVA with Tukey's multiple correction. Differences between survival times were determined with the log-rank test. Calculations were performed using statistical software (GraphPad Prism 7.03). Data are expressed as the mean ± SEM. *p*-Values of ≤0.05 were considered statistically significant.

RESULTS

Absence of IDO1 Increases Mortality Rates Associated With Increased Fungal Loads and Tissue Damage

C57Bl/6 WT and C57Bl/6 IDO1$^{-/-}$ mice were infected with one million yeasts of *P. brasiliensis* by the i.t. route. After 96 h, 2, and 10 weeks, the severity of fungal infection was assessed by a CFU assay. As shown in the **Figure 1**, pulmonary (**Figure 1A**) fungal burdens were increased in IDO1$^{-/-}$ mice at 96 h, 2, and 10 weeks after infection, whereas significant increases in the liver (**Figure 1B**) after 10 weeks of infection showed that the lung of both IDO1$^{-/-}$ mice were concomitant with increased levels of pulmonary NO (**Figure 1C**), considered a potent fungicidal mediator in pulmonary PCM. The histopathology analysis (**Figures 1D–G**) after 10 weeks of infection showed that the lung of both IDO1$^{-/-}$ and WT control mice exhibited large granulomas containing many yeasts and large damaged areas. Comparatively, lung lesions from IDO1$^{-/-}$ were more severe than those of WT mice, involved extensive areas of the lung parenchyma and were composed of isolated or confluent granulomas containing a huge number of fungi (**Figures 1F,G**). To assess the influence of IDO1 deficiency in the disease outcome, the area of lung lesions and mortality of infected mice were evaluated. The absence of IDO1 expression led to increased lung pathology (**Figure 1H**) and mortality rates (**Figure 1I**). At day 127 of infection, all IDO1$^{-/-}$ mice were dead; whereas in the same period, 5 of 10 WT mice were still alive and apparently healthy.

IDO-1 Expression Increases the Expansion of ILC3 but Reduces ILC1 and NK Cells in the Lungs of *P. brasiliensis*-Infected Mice

Innate lymphoid cells are a new family of lymphocytes that lack specific antigen receptors, produce significant amounts of cytokines, and may be cytotoxic upon activation. The distinct ILC subsets exhibit transcription factors and cytokine signatures found in the CD4$^+$ T helper (Th) subpopulations in their responses to specific antigens (30, 31). These features include the shared expression of Tbet and IFN-γ by ILC1 and Th1 cells; GATA-3, IL-5, and IL-13 by Th2 and ILC2 cells; RORC, IL-17, and IL-22 by ILC3 and Th17/Th22 cells, as well as Eomes, IFN-γ, and cytolytic molecules by CD8$^+$ T cells and conventional NK cells (30). The previously described influence of IDO/AhR in the differentiation of T and ILC cells (30–33) led us to investigate the influence of IDO1 in the differentiation of pulmonary ILC subsets after *P. brasiliensis* infection of WT and IDO1$^{-/-}$ mice. Therefore, ILC subpopulations were characterized by their expression of specific surface molecules and transcription factors. The NK cells are classified as NK11$^+$ CD49b$^+$ NKp46$^+$ Eomes$^+$, the ILC1 are CD127$^+$ CD49a$^+$ IL-12Rβ1$^+$ Tbet$^+$, the ILC2 are CD127$^+$ ICOS$^+$ IL-17RB$^+$ IL-33$^+$ GATA3$^+$, and the ILC3 are CD127$^+$ IL-23R$^+$ RORC$^+$, or the so-called NCR$^+$ ILC3$^+$, producing IL-22 that are CD127$^+$ IL-23R$^+$ RORC$^+$ IL-22$^+$. After 96 h and 2 weeks of infection, a significant decrease in NK cells was detected in the lung infiltrating lymphocytes of IDO1$^{-/-}$ mice. However, at all periods of infection studied, a significant increase in the number of ILC3 and NRC IL-22 was observed in the lungs of IDO1$^{-/-}$ mice. Differences in the influx of ILC1 and ILC2 to the lungs were only observed at week 10 postinfection, when ILC1 appeared in reduced numbers whereas ILC2 appeared in increased numbers in the lungs of IDO1$^{-/-}$ mice (**Figure 2**).

IDO1 Controls the Expression of Activation Markers and Intracellular Cytokines of Pulmonary CD11b$^+$ and CD11c$^+$ Cells

IDO1$^{-/-}$ and WT C57BL/6 mice were infected with one million yeasts of *P. brasiliensis* by the i.t. route. After 96 h, 2, and 10 weeks of infection, the lung infiltrating leukocytes were obtained and analyzed for the expression of surface molecules by flow cytometry. We analyzed the expression of some activation molecules (IA^b, CD40, CD80, and CD86) expressed by CD11b$^+$ and CD11c$^+$ (**Figure 3**). When compared with the WT control group, CD11b$^+$ (**Figure 3A**) and CD11c$^+$ (**Figure 3B**) cells from IDO1$^{-/-}$ mice expressed increased levels of IA^b, CD80, and CD86 at all postinfection periods studied. CD40 was also upregulated in CD11b$^+$ cells of IDO1$^{-/-}$ mice.

To better define the activation profile of the lung infiltrating leukocytes of both infected mouse strains, the expression of intracellular cytokines (IL-12, TNF-α, IL-1β, IL-6, TGF-β, and IL-10) was characterized by flow cytometry. At all periods after infection analyzed, a decreased number of CD11b$^+$ cells expressing intracellular IL-12, TNF-α, IL-1β, TGF-β, and IL-10 was detected in the lungs of IDO1$^{-/-}$ mice when compared to the WT counterparts. By contrast, increased numbers of CD11b$^+$ IL-6$^+$ cells were found at all postinfection periods in the lungs of IDO$^{-/-}$ mice (**Figure 4A**). When CD11c$^+$ cells were studied, similar results were obtained (**Figure 4B**), but the differences between IDO1 sufficient and deficient mice was much more evident.

IDO1 Controls the Expression of AhR in CD11b$^+$ and CD11c$^+$ Cells

The influence of IDO1 in the expression of the transcription factor AhR was also investigated in our experimental model. Thus, after 96 h, 2, and 10 weeks of infection with yeasts, the lung infiltrating leukocytes from the IDO1$^{-/-}$ and WT mice were obtained, and the presence of intracellular IDO1 and AhR in CD11b$^+$ and CD11c$^+$ cells detected by flow cytometry. As depicted in **Figure 5**, only WT mice expressed intracellular IDO1. The AhR was detected in both mouse strains, but this transcription factor was markedly downregulated in IDO1$^{-/-}$ mice. These results clearly showed that the expression of AhR is dependent on the enzyme IDO1 (**Figure 5**).

The Absence of IDO1 Increases the Influx of Naïve and Activated TCD4$^+$ and TCD8$^+$ Lymphocytes to the Lungs

We have also assessed whether the absence IDO1 modulates the influx of T cell subpopulations to the lung of *P. brasiliensis*-infected mice. As showed in the **Figure 6**, after 2 and 10 weeks of infection, a higher number of both naive (CD4$^+$ CD44^{low} CD62L^{high}) and effector/activated (CD4$^+$ CD44^{high} CD62L^{low}) CD4$^+$ T cells were found in the lungs of IDO1$^{-/-}$ mice when compared with WT counterparts. Similarly, a larger number of naïve and activated CD8$^+$ T cells (CD8$^+$ CD44^{low} CD62L^{high} and

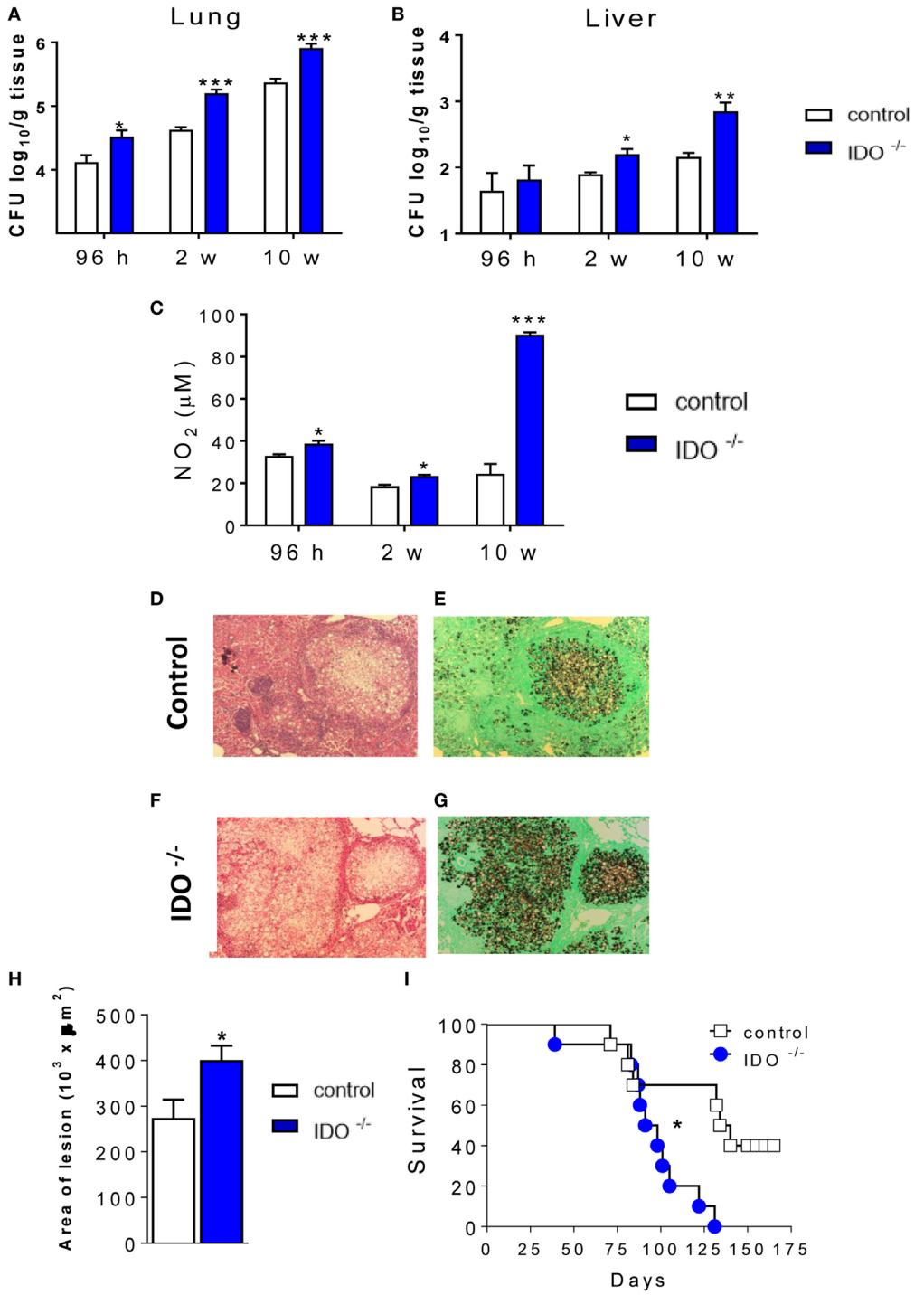

FIGURE 1 | Indoleamine 2,3 dioxygenase-1 (IDO1) controls fungal loads, tissue pathology, and mortality rates. Groups of IDO1$^{-/-}$ and wild-type (WT) C57Bl/6 mice were infected i.t. with 1 × 10^6 of *Paracoccidioides brasiliensis* yeasts. The colony-forming units (CFUs) from lungs **(A)** and liver **(B)** were determined 96 h, 2, and 8 weeks after infection. The bars represent means ± SEs of the mean (SEM) of $\log_{10}$ CFU counts obtained from groups of 4 to 5 mice. **(C)** Supernatants of lung homogenates were obtained from infected mice (n = 4–5/time point) and used to determine the levels of nitrite by the Griess reagent. **(D–G)** Photomicrographs of lung lesions of WT control mice **(D,E)** and IDO1$^{-/-}$ mice **(F,G)** at week 10 of infection. Lesions were stained with hematoxylin-eosin (left panels) and Grocott (right panels). **(H)** Morphometrical analysis of lung lesions. The areas of lesions were measured (in square micrometers) in 10 microscopic fields per slide in five mice per group and results expressed as the mean ± SEM of total area of lesions for each mouse. **(I)** Survival curves of WT and IDO1$^{-/-}$ infected mice (n = 10) were determined in a period of 175 days. Data represent the means ± SEM and are representative of two independent experiments with equivalent results (*p < 0.05; **p < 0.01, and ***p < 0.001).

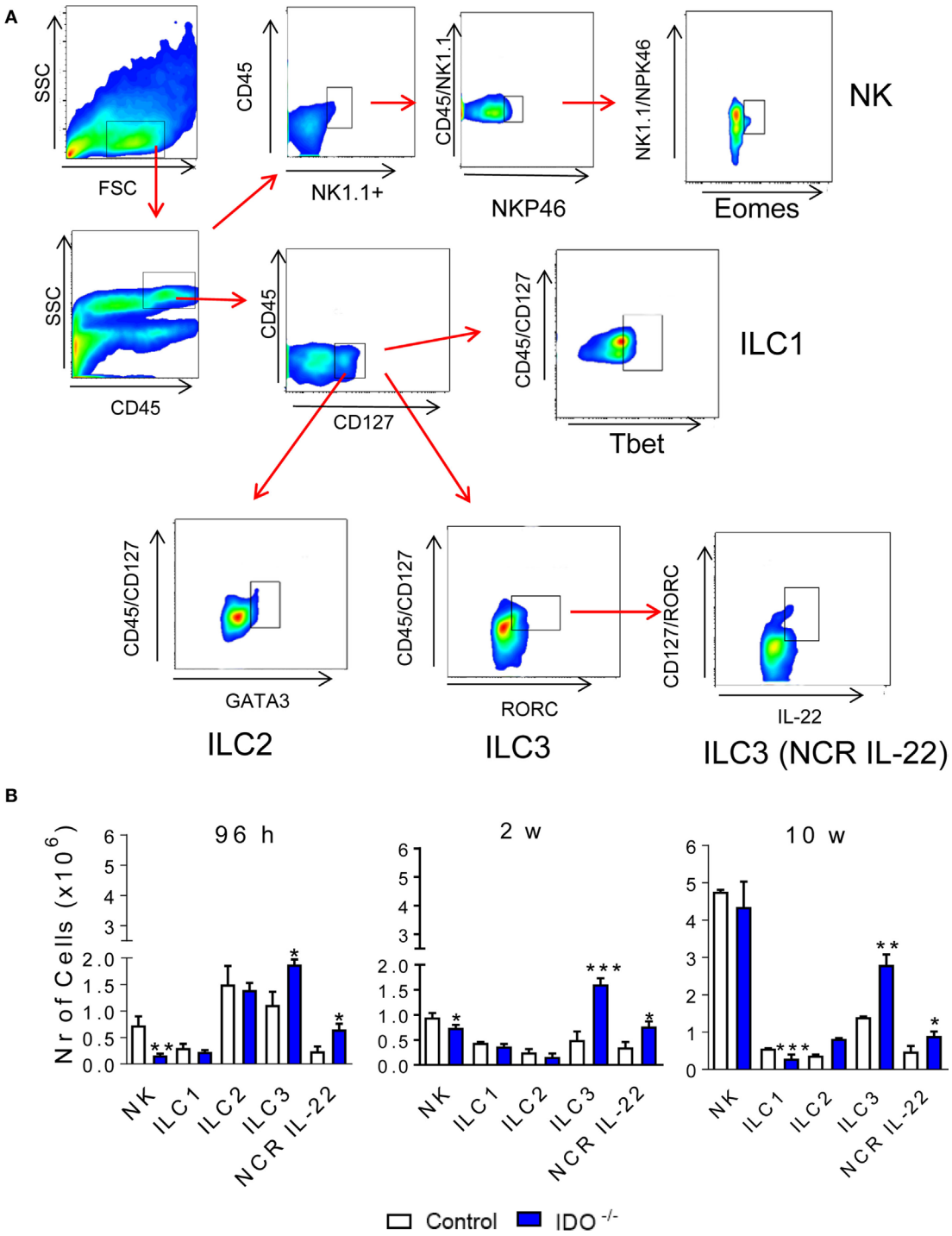

FIGURE 2 | Influence of indoleamine 2,3 dioxygenase-1 (IDO1) expression on the presence of innate lymphoid cells (ILCs) in the lungs of *Paracoccidioides brasiliensis*-infected mice. The phenotypic analysis of ILCs in the lungs of C57Bl/6 wild-type and IDO1$^{-/-}$ mice was performed after 96 h, 2, and 10 weeks after *P. brasiliensis* infection. The lung infiltrating leukocytes were labeled with specific antibodies and analyzed for the phenotypes of NK, ILC1, ILC2, innate lymphoid cell 3 (ILC3), and ILC3 (NCR IL-22) subsets according to the respective markers: for NK: NK1.1, CD49b, NKp46, and Eomes; ILC1: CD127, CD49a, IL-12Rβ1, and Tbet; ILC2: CD127, ICOS, IL-17RB, IL-33, and GATA3; ILC3: CD127, IL-23R, IL-22, and RORC **(A)**. The cell surface and intracellular markers were measured by flow cytometry. One hundred thousand cells were counted and the data expressed by number of positive cells **(B)**. Data are expressed as means ± SEM and are representative of three independent experiments using five mice of each mouse strain per group (*$p < 0.05$; **$p < 0.01$, and ***$p < 0.001$).

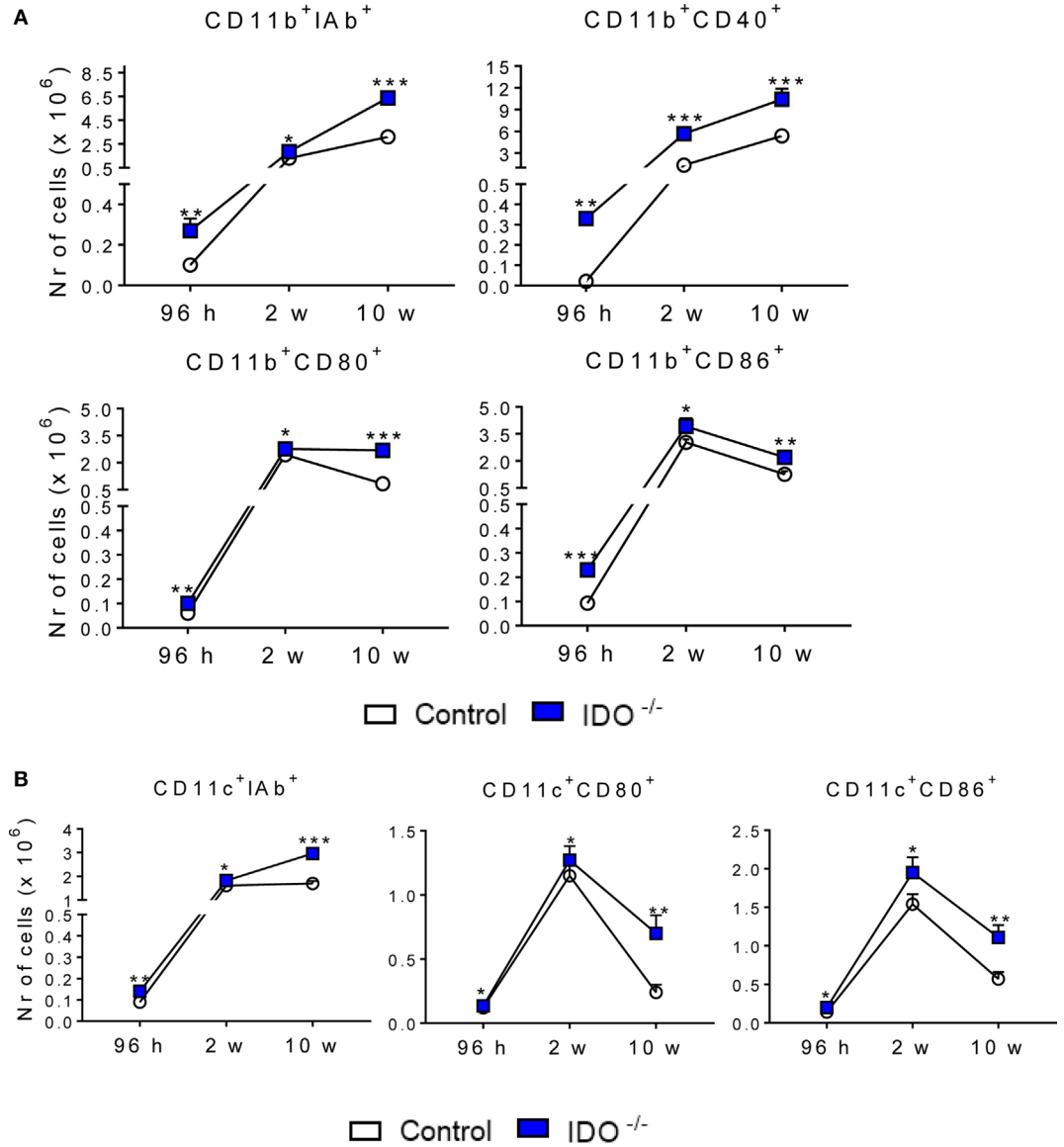

FIGURE 3 | Indoleamine 2,3 dioxygenase-1 (IDO1) controls the expression of activation markers of pulmonary CD11b$^+$ and CD11c$^+$ cells. The activation markers of CD11b$^+$ **(A)** and CD11c$^+$ **(B)** leukocytes were measured in lung infiltrating leukocytes of C57Bl/6 wild-type and IDO1$^{-/-}$ after 96 h, 2, and 10 weeks of infection with 1×10^6 *Paracoccidioides brasiliensis* yeasts. The lung cells were obtained as described in Section "Materials and Methods" and labeled with antibodies conjugated to different fluorochromes. The lung infiltrating leukocytes were gated by FSC/SSC analysis. The cells were gated for CD11b$^+$ or CD11c$^+$ expression and then for the presence of IA^b, CD40, CD80, and CD86. One hundred thousand cells were acquired on FACS CANTO II and, subsequently, analyzed by FlowJo software. Data are expressed as means ± SEM and are representative of three independent experiments using five mice of each mouse strain per group (*$p < 0.05$; **$p < 0.01$, and ***$p < 0.001$).

CD8$^+$ CD44^{high} CD62L^{low}, respectively) were detected in the lungs of IDO1$^{-/-}$ mice when compared with WT controls (**Figure 6**).

IDO1 Controls the Secretion of Pulmonary Cytokines

Lung homogenates were obtained from infected IDO1$^{-/-}$ and control WT mice at 96 h, 2, and 10 weeks of infection. Cytokines were measured by ELISA. Similar patterns of cytokines production were seen at all postinfection periods studied. Most cytokines (TNF-α, IL-1β, IFN-γ, TGF-β, IL-27, IL-10, and IL-35) appeared in decreased levels, whereas IL-2, IL-6, IL-17, and IL-22 were detected in higher concentrations than those detected in WT mice (**Figure 7**).

IDO1 Influences the Expression of Cytokines and Transcription Factors Genes

We have also assayed the gene expression of transcription factors and cytokines involved in Th1, Th2, Th17, Th22, and Treg differentiation as well as the transcription of AhR gene

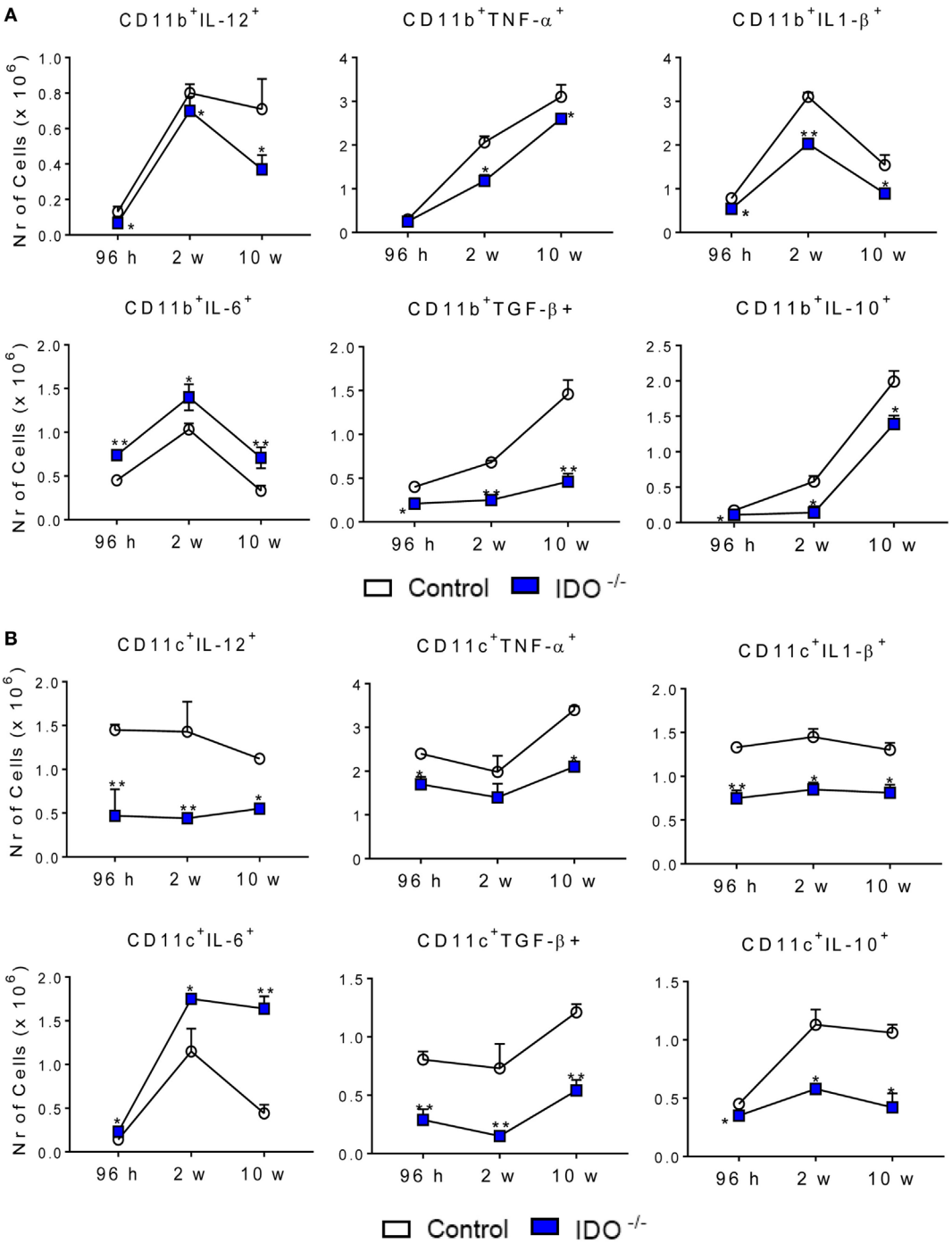

FIGURE 4 | Indoleamine 2,3 dioxygenase-1 (IDO1) expression controls the presence of intracellular cytokines in pulmonary CD11b$^+$ and CD11c$^+$ cells. The intracellular cytokines were determined in CD11b$^+$ **(A)** and CD11c$^+$ **(B)** lung infiltrating leukocytes of wild-type and IDO1$^{-/-}$ C57BL/6 mice after 96 h, 2, and 10 weeks of infection with 1 × 10^6 *Paracoccidioides brasiliensis* yeasts. The lung cells were obtained as described in Section "Materials and Methods" and labeled with antibodies conjugated to different fluorochromes. The lung infiltrating leukocytes were gated by FSC/SSC analysis. The cells were gated for CD11b$^+$ or CD11c$^+$ expression and then for the presence of cytokines IL-12, TNF-α, IL-1β, IL-10, IL-6, and TGF-β. One hundred thousand cells were acquired on FACS CANTO II and subsequently analyzed by FlowJo software. Data are expressed as means ± SEM and are representative of three independent experiments using five mice of each mouse strain per group (*$p < 0.05$; **$p < 0.01$, and ***$p < 0.001$).

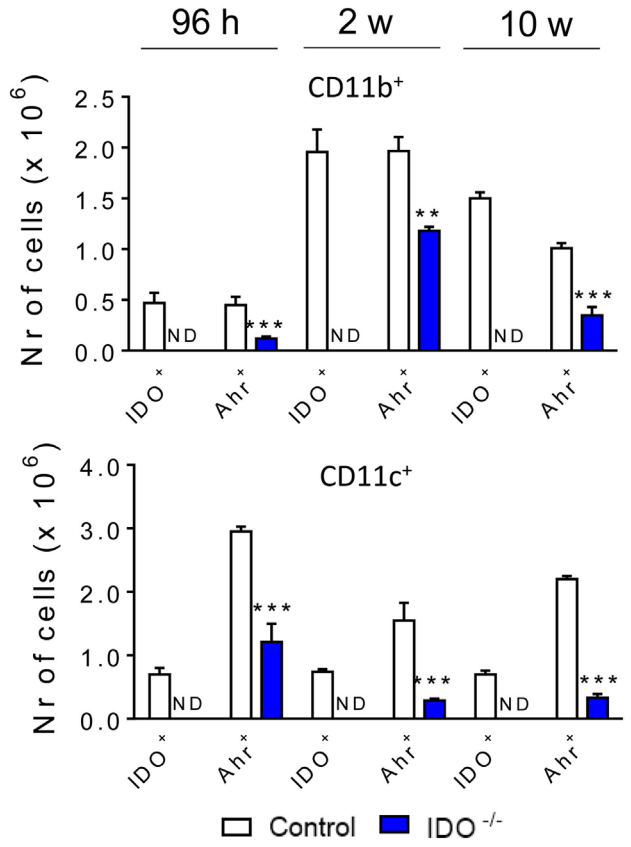

FIGURE 5 | Indoleamine 2,3 dioxygenase-1 (IDO1) expression controls the levels of aryl hydrocarbon receptor (AhR) present in CD11b$^+$ e CD11c$^+$ cells. The number of IDO1 and AhR expressing cells was determined in lung infiltrating leukocytes of wild-type and IDO1$^{-/-}$ mice 96 h, 2, and 10 weeks after infection with 1 × 10^6 viable *Paracoccidioides brasiliensis* yeasts. The lung cells were obtained as described in Section "Materials and Methods" and labeled with antibodies conjugated to different fluorochromes. The lung infiltrating leukocytes were gated by FSC/SSC analysis. The cells were gated for CD11b$^+$ or CD11c$^+$ and then for IDO1 and AhR expression. One hundred thousand cells were acquired on FACS CANTO II and subsequently analyzed by FlowJo software. Data are expressed as means ± SEM and are representative of three independent experiments using five mice of each mouse strain per group (**$p < 0.01$, and ***$p < 0.001$).

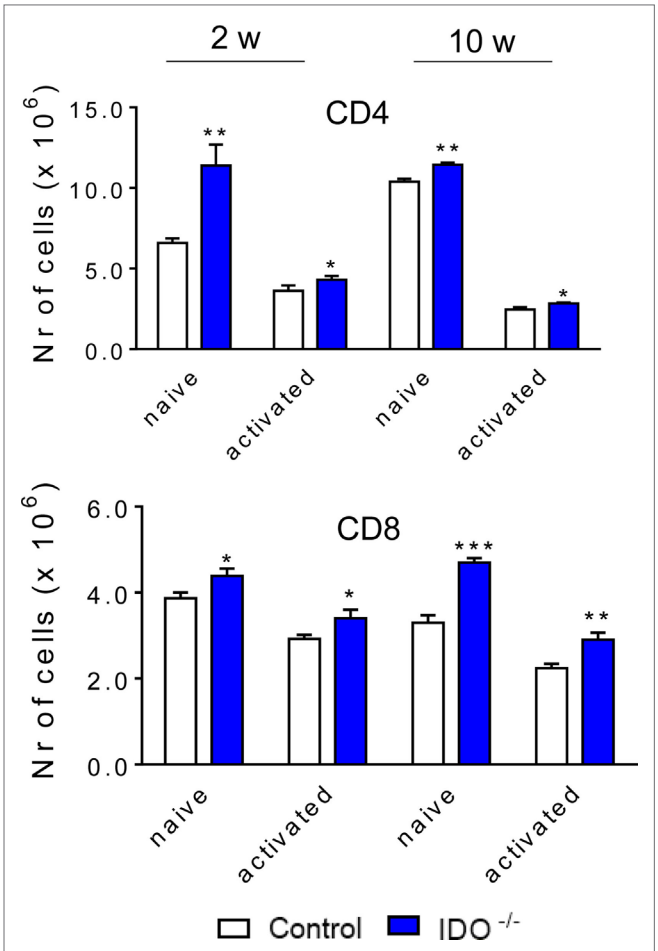

FIGURE 6 | The absence of indoleamine 2,3 dioxygenase-1 (IDO1) induces an increased influx of naïve and activated TCD4$^+$ and TCD8$^+$ lymphocytes to the lungs. The phenotypic analysis of lung infiltrating lymphocytes from wild-type and IDO1$^{-/-}$ mice was performed at 2 and 10 weeks of *Paracoccidioides brasiliensis* infection. The lung cells were obtained as described in Section "Materials and Methods" and labeled with antibodies conjugated to different fluorochromes. The lung infiltrating leukocytes were gated by FSC/SSC analysis. The cells were then gated for CD4$^+$ or CD8$^+$ expression and for membrane markers that characterize naïve and effector/activated cells (CD44^{low} CD62L^{high} and CD44^{high} CD62L^{low}, respectively). For gate strategy, see Figures S1 and S2 in Supplementary Material. One hundred thousand cells were acquired on FACS CANTO II and subsequently analyzed by FlowJo software. Data are expressed as means ± SEM and are representative of three independent experiments using five mice of each mouse strain per group (*$p < 0.05$; **$p < 0.01$, and ***$p < 0.001$).

associated with IDO1 activity. Thus, the mRNA expression in whole lung cells of WT and IDO1$^{-/-}$ mice was determined at weeks 2 and 10 after infection by RT-PCR using appropriate primers. As shown in **Figure 8**, the absence of the IDO1 led to a marked decrease in the relative expression of IFN-γ mRNA, a cytokine associated with the induction and catalytic function of the enzyme. The mRNA expression for IFN-γ, TNF-α, TGF-β, and IL-10 also appeared in decreased levels, whereas IL-6, IL-17 and IL-22 mRNAs were upregulated in IDO1$^{-/-}$ mice. In both postinfection periods, a concomitant decrease in mRNA for AhR and Foxp3 transcription factors were observed in IDO1 deficient mice. By contrast, RORC and GATA3 mRNAs were significantly upregulated IDO1$^{-/-}$ mice, but minor differences were seen in Tbet expression.

The Absence of IDO1 Increases the Number of Th17 but Reduces the Presence of Th1 and Treg Cells

It has been demonstrated in fungal infections the fundamental role of IDO1 in promoting the balance between T cell subpopulations (8, 9). IDO1 and Kyn, have the ability of inducing Treg and inhibit Th17 cells, contributing to the regulatory mechanisms that govern immunity or tolerance to pathogens (1, 2, 10). Therefore, we have also characterized the Th subpopulations in the course of

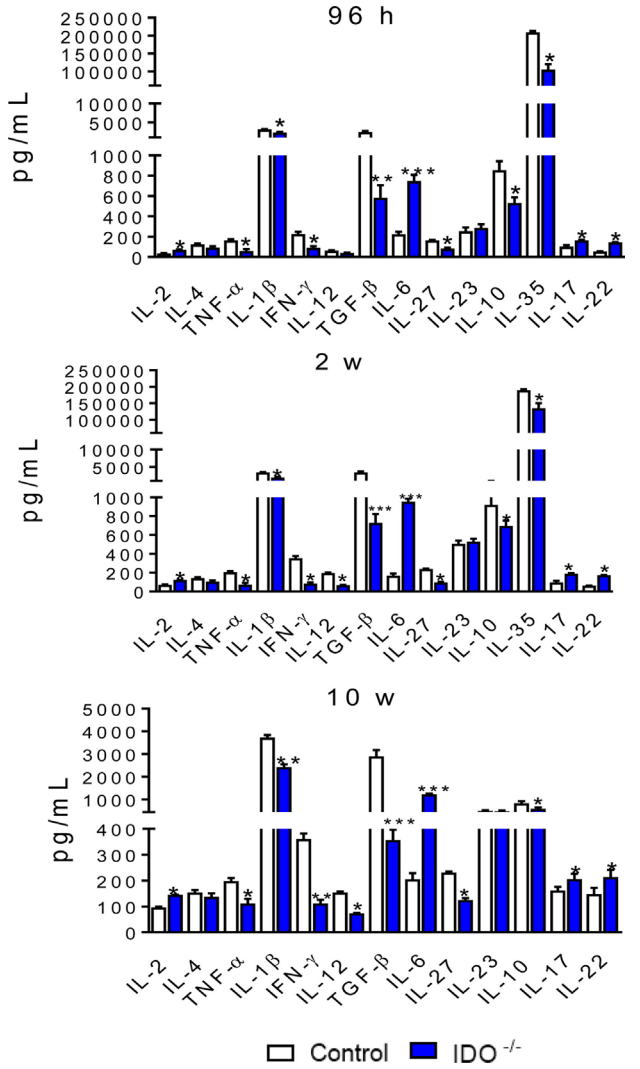

FIGURE 7 | Indoleamine 2,3 dioxygenase-1 (IDO1) regulates the levels of pulmonary cytokines. Quantitation of cytokines in lung homogenates of wild-type and IDO1$^{-/-}$ mice infected with 1 × 10^6 viable *Paracoccidioides brasiliensis* yeasts. The levels of cytokines were measured by enzyme-linked immunosorbent assay in lung homogenates obtained at 96 h, 2, and 10 weeks of infection. Bars show mean ± SEM from at least four mice per group and are representative of two independent experiments (*$p < 0.05$, **$p < 0.01$, and ***$p < 0.001$).

P. brasiliensis infection of IDO1-deficient and -sufficient mice. As depicted in **Figure 9A**, the IDO1 enzyme consistently regulates the differentiation of Th lymphocytes. In the absence of IDO1, decreased numbers of CD4$^+$ IFN-γ$^+$ T cells, which define the Th1 subset, were found. Regarding the Th2 subpopulation, only at the 10th week postinfection, a significant increase in the number of CD4$^+$ IL-4$^+$ cells were detected in the lungs of IDO1$^{-/-}$ mice. After 2 and 10 weeks of infection, CD4$^+$ IL-17$^+$ cells appeared in higher numbers in the lungs of IDO1$^{-/-}$ mice when compared with their WT controls. Furthermore, a marked reduction in pulmonary Treg (CD4$^+$ CD25$^+$ Foxp3$^+$) cells was observed in IDO1$^{-/-}$ mice at weeks 2 and 10 of infection (**Figure 9B**).

DISCUSSION

The characterization of the infectious environment is particularly important to define how the innate immunity influences the subsequent development of adaptive immunity. The regulatory mechanisms that operate at both phases of immunity are also fundamental to determine how the immune response will dictate the severity of an infectious process. In this context, we have explored the regulatory mechanism exerted by IDO1 in both phases of immunity against *P. brasiliensis* infection. It was quite interesting to verify the close association between T cell phenotypes and those of ILCs, a class of innate cells present at the site of infection at the early phase of infection that plays an important role in the further definition of adaptive immunity (34). We could demonstrate for the first time that ILC participate in the immune response against pulmonary PCM. The expansion of these ILCs was influenced by the IDO1 activity that controls the initial cytokines microenvironment and the induction of transcription factors that determine ILC and T cell phenotypes. Reduced Eomes and Tbet led, respectively, to diminished NKp46 and ILC1, whereas increased RORC resulted in increased ILC3, including those associated with increased production of IL-22, despite the reduced AhR mRNA and protein, which were previously shown to be involved in the synthesis of IL-22 (15).

Previous studies demonstrated that IDO1 plays an important role in the immunity against commensal fungi such as *Aspergillus fumigatus* and *Candida albicans* by regulating fungal tolerance mediated by prevalent activity of IDO and Treg cells and fungal immunity mediated by Th1/Th17 cells properly controlled by Treg cells (24, 35, 36). Here, we demonstrated that in pulmonary PCM, IDO1 controls both, fungal burdens and inflammatory reactions, functions that were concomitant with the expression of AhR. The absence of IDO1 expression increases fungal burdens potentiating the expression of activation markers in macrophages and DCs resulting in exacerbated Th17 immunity poorly controlled by Treg cells. This is the worst scenario for a host response where the uncontrolled fungal growth is accompanied by intense but inefficient inflammatory reactions causing exaggerated tissue pathology that ultimately leads to the precocious death of infected mice.

In vaginal candidiasis, the selective deficiency of IDO1 significantly increased fungal loads and tissue damage mediated by inflammatory cells (37) and here a similar result was observed. Our finding of elevated fungal loads may be attributed to the inability of IDO1$^{-/-}$ mice to deplete Trp, which possibly contributed to the enhanced *P. brasiliensis* growth. However, the more severe infection of IDO1$^{-/-}$ mice was accompanied by increased levels of NO, a well-recognized fungicidal mediator in *P. brasiliensis* infection (38–44). Actually, a dual role regarding NO activity has been observed in PCM. It can enhance the killing ability of IFN-γ activated macrophages exerting a protective effect (40–42) but is also suppressive as previously demonstrated (39, 43, 44). Interestingly, Bernardino et al. using iNOS$^{-/-}$ mice clearly showed that absence of NO production is accompanied by an early reduction in fungal loads and increased T cell responses. At the chronic phase of the disease, iNOS$^{-/-}$ mice showed increased numbers of viable yeasts circumscribed, however, by elevated presence of activated

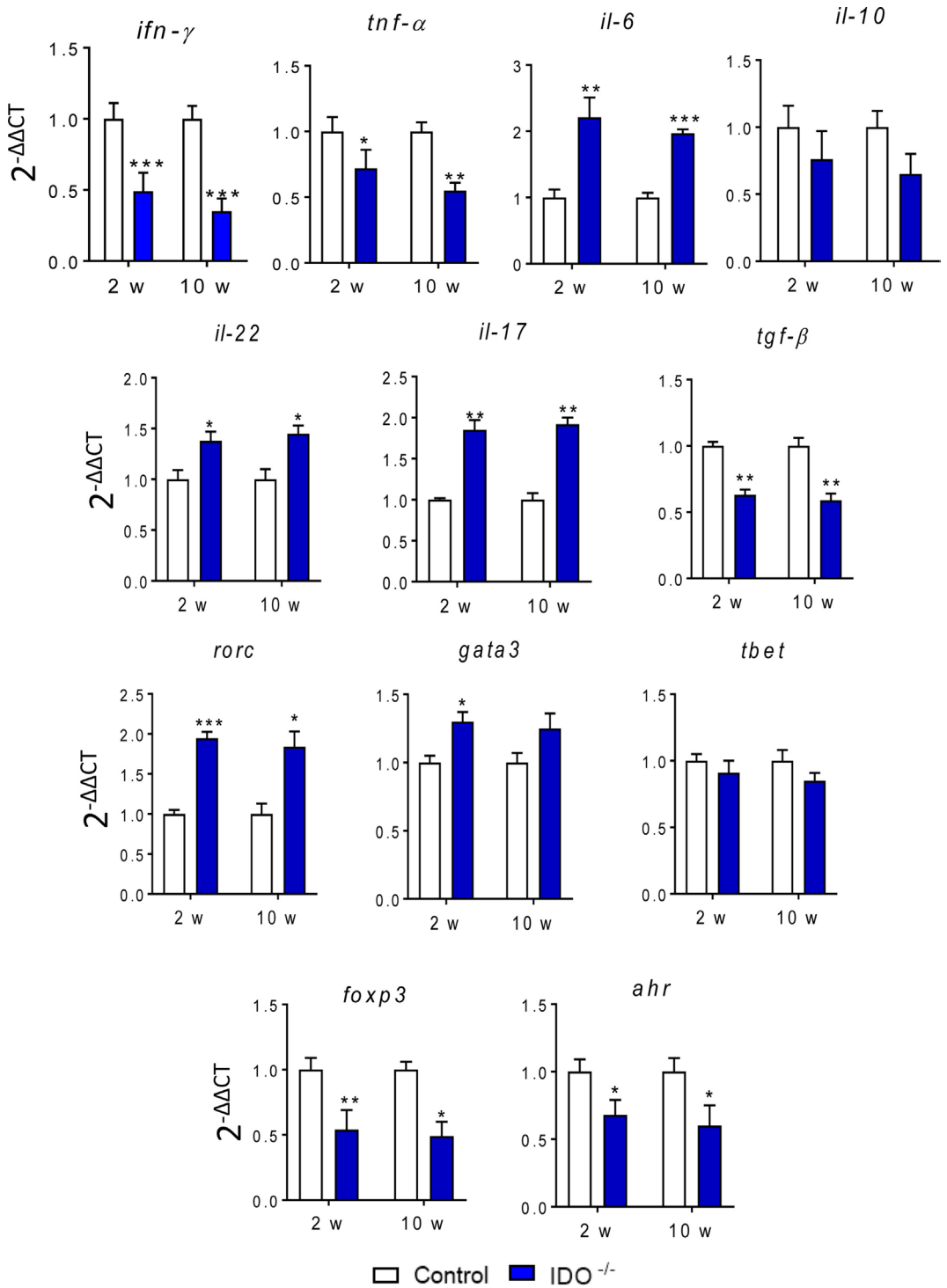

FIGURE 8 | Indoleamine 2,3 dioxygenase-1 (IDO1) influences the gene expression of cytokines and transcription factors. Relative expression of mRNA for aryl hydrocarbon receptor (AhR), IFN-γ, TNF-α, IL-6, RORC, Tbet, GATA3, FoxP3, IL-10, TGF-β, IL-17, and IL-22 in whole lung cells of wild-type and IDO1$^{-/-}$ mice after 10 weeks of *Paracoccidioides brasiliensis* infection. The level of gene transcription was determined by real-time PCR. Bars show mean ± SEM from at least four mice per group and are representative of three independent experiments (*$p < 0.05$; **$p < 0.01$, and ***$p < 0.001$).

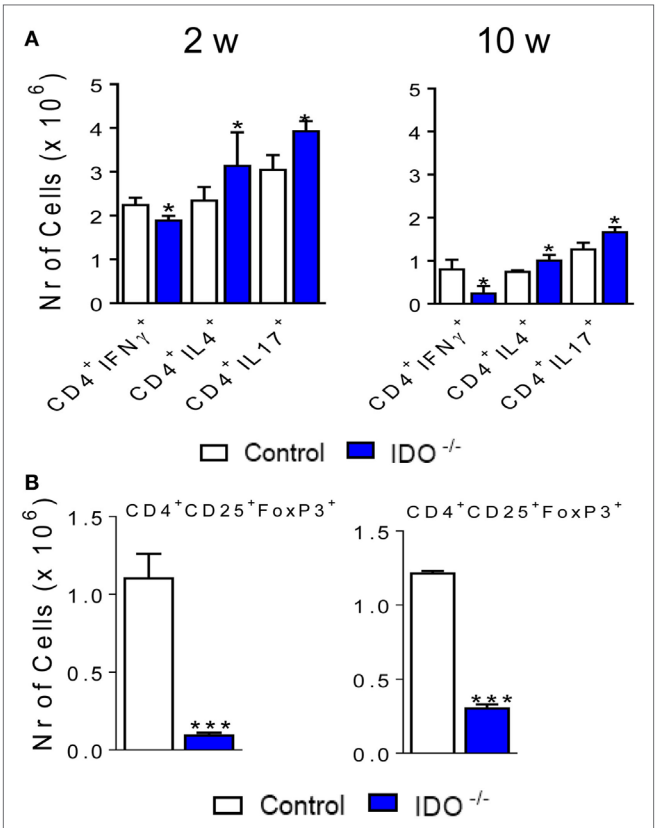

FIGURE 9 | The absence of indoleamine 2,3 dioxygenase-1 (IDO1) increases the number of pulmonary Th17 but reduces the presence of Th1 and regulatory T (Treg) cells. The phenotypic analysis of lung infiltrating lymphocytes from wild-type and IDO1$^{-/-}$ mice was performed at 2 and 10 weeks of *Paracoccidioides brasiliensis* infection. The lung cells were obtained as described in Section "Materials and Methods" and labeled with antibodies conjugated to different fluorochromes. The lung infiltrating leukocytes were gated by FSC/SSC analysis. **(A)** The cells were gated for CD4$^+$ and then for intracellular expression of IL-4, IL-17, IL-22, or IFN-γ. **(B)** For Treg cells characterization, the FoxP3$^+$ cells were counted on CD4$^+$ CD25$^+$ double-positive cells. For gate strategy, see Figure S3 in Supplementary Material. One hundred thousand cells were acquired on FACS CANTO II and subsequently analyzed by FlowJo software. Data are expressed as means ± SEM and are representative of three independent experiments using five mice of each mouse strain per group (*$p < 0.05$ and ***$p < 0.001$).

macrophages and T cells (39). Importantly, the inducible isoform of nitric oxide synthase (iNOS) responsible for NO production and the enzyme IDO1 are induced by IFN-γ (45, 46), but NO and IDO1 are mutually inhibitory (47–49). This reciprocal regulation was here detected, since the absence of IDO1 expression enhanced NO production that, however, was insufficient to control the fungal growth. These results were consistent with our previous studies in resistant and susceptible mice where increased NO synthesis paralleled the IDO1 inhibition by 1MT (50). More than that, these results demonstrate that, contrary to the well accepted paradigm, in murine PCM the control of fungal growth by IDO1 activity is more relevant than that mediated by NO production.

At all postinfection periods analyzed, cells from IDO1$^{-/-}$ mice showed increased levels of activation molecules that can explain the increased expansion of T cell that migrate to the lungs of IDO1$^{-/-}$ mice. Despite its statistical significance, it is difficult to point out the biological relevance of the increased expression of costimulatory molecules by DC11b$^+$ cells. However, our previous report (26) showed that CD11c$^+$ cells from IDO$^{-/-}$ mice have an enhanced ability of inducing T cell proliferation. DCs from IDO$^{-/-}$ mice have an increased ability of expanding CD4$^+$ and CD8$^+$ T lymphocytes in parallel with decreased proliferation of Treg cells (CD4$^+$ CD25$^+$ Foxp3$^+$ T cells). This study has also shown that the CD4$^+$ and CD8$^+$ T cells exhibited an activated phenotype as revealed by the expression of CD25 and DC69. Interestingly, both CD11b$^+$ and CD11c$^+$ cells showed significantly reduced levels of pro- and anti-inflammatory cytokines, in parallel with increased presence of IL-6$^+$ cells. These effects were more prominent in CD11c$^+$ than in CD11b$^+$ cells as expected by the major expression and activity of IDO1 by the former leukocyte subpopulation (2, 51). Furthermore, the new cytokines balance in CD11b$^+$ and CD11c$^+$ cells of IDO1$^{-/-}$ mice led to increased proliferation of ILC3 and Th17 lymphocytes that are known to be expanded by IL-6 and TGF-β signaling, STAT3 phosphorylation, and expression of RORγτ, the molecular signature of IL-17 secreting cells.

It has been reported that IDO1 and AhR expression are mutually regulated (1, 52), and here we could demonstrate the profound impairment of AhR production caused by IDO1 deficiency. These findings can explain the increased inflammatory reactions developed by IDO1$^{-/-}$ mice and the phenotype of T cells and ILC developed by *P. brasiliensis*-infected IDO1$^{-/-}$ mice: increased presence of ILC3 and Th17 cells associated with reduced numbers of Treg cells.

The elevated numbers of naïve and activated lymphocytes found in the lung of IDO1$^{-/-}$ mice were consistent with the higher levels of IL-2 produced by IDO1$^{-/-}$ mice, a fact also observed in our studies with IDO1 inhibition by 1MT (50). In addition, the decreased levels of IL-12, TNF-α, and IFN-γ reflect the reduced expansion of Th1 cells as shown by the low numbers of CD4$^+$ IFN-γ$^+$ lymphocytes present in the lungs of IDO$^{-/-}$ mice. The reduced levels of IL-10, TGF-β, and IL-35 are also concordant with the drastic reduction in the expansion and migration of Treg cells to the lungs of IDO1$^{-/-}$ mice. Furthermore, the blockade of the IDO/AhR axis increased the levels of IL-17 and IL-22 secreted into the lungs parenchyma and reflected the major development of Th17 cells that have the ability of secreting both cytokines. The same shift for the IL-17/IL-22 production was reported by De Luca et al. (37) studying the effect of genetic IDO1 deficiency in vaginal candidiasis.

It is apparently conflicting the elevated levels of IL-22 and reduced presence of AhR observed in the lungs of IDO1$^{-/-}$-infected mice. IL-22 belongs to the IL-10 family of cytokines, is produced by many cell subpopulations, including Th22, Th1, and Th17, classical and non-classical NK cells (NK-22), NKT cells, and ILC3 (15, 53–58). IL-22 plays an important role in fungal infections due to its ability of epithelial tissue repair and the induction of antimicrobial peptides (37, 59–61). Several transcription factors, including STAT3, RORC, and AhR, have been described as essential regulators of IL-22 (15) and AhR$^{-/-}$ mice are highly compromised in terms of IL-22 production (15, 62). By inducing

IL-22-producing ILC, AhR can promote initial fungal clearance, and by expanding Treg cells contributes with disease tolerance but both mechanisms cooperate to maintain host homeostasis (37). The increase in IL-22 here observed could not be ascribed to the effect of AhR on T cells but to the increased influx of IL-22-secreting Th17 and ILC3 into the lungs of IDO1$^{-/-}$ mice. Indeed, besides Th17 cells, an increased presence of ILC3 positive for intracellular IL-22 were seen in the whole course of infection of IDO1$^{-/-}$ mice.

The increased number of effector T cells in the lung cell infiltrates of IDO1-deficient mice was concurrent with a vigorous reduction of CD4^{+} CD25^{+} FoxP3^{+} Treg cells. This decreased expansion can be attributed to the impaired production of Kyn and the reduced activity of AhR, a transcription factor that needs its ligand to upregulate the transcription of FoxP3 necessary to Treg cells differentiation (63, 64). Indeed, the IDO1 enzyme and its catalytic products can act as a bridge between DCs and Treg cells that can use reverse signaling and non-canonical NFκB activation of DCs for its suppressive effector function and self-propagation (3). The low numbers of Treg cells were concomitant with the reduced levels of several suppressive cytokines detected in the lung cell infiltrates of IDO1$^{-/-}$ mice. IL-27 has a wide range of immunomodulatory activities. Although it may promote the development of Th1, IL-27 can suppress T cell responses and the development of pathogenic Th17 cells (65, 66), functions that were possibly impaired in the immune response developed by IDO1$^{-/-}$ mice. Besides IL-27, the low levels of typical Treg cytokines (TGF-β, IL-35, and IL-10) possibly contributed to the enhanced Th17 inflammatory reactions developed by IDO1-deficient mice.

The IDO1 activity has been associated with the tolerogenic function of plasmacytoid DCs (26), a phenomenon also described in our pulmonary model of PCM. We verified that *P. brasiliensis*-infected pDCs enhanced the expansion of Treg cells and reduce the expansion and activation of Th1 and Th17 cells. This finding was not detected when pDCs from IDO1$^{-/-}$ mice were used. More importantly, the *in vivo* depletion of pDC by a specific antibody resulted in reduced levels of IDO1 and regulatory cytokines in the lungs of pDC-depleted mice, once more highlighting the close connection between IDO1 and expression of immunosuppressive cytokines in PCM (26).

Although no studies have directly addressed the role of IL-17 in PCM, several indirect findings have clearly demonstrated that the well-balanced production of pro- and anti-inflammatory cytokines is crucial for establishing protective immunity. Indeed, the absence of TLR2 signaling induces an excessive tissue pathology associated with increased Th17 differentiation and impaired Treg development (67). By contrast, in the case of TLR4 deficiency, the excessive proliferation of Treg cells and reduced Th17 differentiation led to more severe disease due to uncontrolled fungal burden (68). In addition, the immunity mediated by the adoptive transfer of effector T cells without the concomitant presence of Treg cells led to increased Th17 differentiation and tissue pathology (69). These previous findings and those reported here clearly indicate that the balanced differentiation of Th1/Th17/Treg cells is fundamental for achieving protection in pulmonary PCM.

In conclusion, the IDO1–Ahr–Treg axis was strongly impaired in the absence of the IDO1 expression clearly demonstrating that this regulatory loop plays an important role in the control of immunity and severity of pulmonary PCM.

ETHICS STATEMENT

The experiments were performed in strict accordance with the Brazilian Federal Law 11,794 establishing procedures for the scientific use of animals, and the State Law establishing the Animal Protection Code of the State of São Paulo. All efforts were made to minimize animal suffering. The procedures were approved by the Ethics Committee on Animal Experiments of the Institute of Biomedical Sciences of University of São Paulo (Proc.180/11/CEEA).

AUTHOR CONTRIBUTIONS

Conceived and designed experiments: EA, VC, and FL. Contributed with reagent: FL and VC. Performed the experiments: EA, CF, NG, NP, and FL. Analyzed the data: CF, VC, FL, and EA. Wrote the paper: EA, NP, VC, and FL.

ACKNOWLEDGMENTS

We are grateful to Tânia A. Costa for her invaluable technical assistance. We thank Paulo Albe for processing the histological samples.

FUNDING

This work was supported by a grant from the Fundação de Amparo à Pesquisa do Estado de São Paulo (FAPESP-grant to VC 2011/51258-2 and fellowship to EA 2014/18668-2; grant to FL 2014/04783-2) and Conselho Nacional de Pesquisas (CNPq).

SUPPLEMENTARY MATERIAL

The Supplementary Material for this article can be found online at http://journal.frontiersin.org/article/10.3389/fimmu.2017.00880/full#supplementary-material.

REFERENCES

1. Grohmann U, Fallarino F, Puccetti F, Tolerance P. DCs and tryptophan: much ado about IDO. *Trends Immunol* (2003) 24:242–8. doi:10.1016/S1471-4906(03)00072-3
2. Mellor AL, Munn DH. IDO expression by dendritic cells: tolerance and tryptophan catabolism. *Nat Rev Immunol* (2004) 4:762–74. doi:10.1038/nri1457
3. Puccetti P, Grohmann U. IDO and regulatory T cells: a role for reverse signalling and non-canonical NF-kappaB activation. *Nat Rev Immunol* (2007) 7:817–23. doi:10.1038/nri2163
4. Terness P, Bauer TM, Röse L, Dufter C, Watzlik A, Simon H, et al. Inhibition of allogeneic T cell proliferation by indoleamine 2,3-dioxygenase-expressing dendritic cells: mediation of suppression by tryptophan metabolites. *J Exp Med* (2002) 196:447–57. doi:10.1084/jem.20020052

5. Hayashi T, Mo JH, Gong X, Rossetto C, Jang A, Beck L, et al. 3-Hydroxyanthranilic acid inhibits PDK1 activation and suppresses experimental asthma by inducing T cell apoptosis. *Proc Natl Acad Sci U S A* (2007) 104:18619–24. doi:10.1073/pnas.0709261104
6. Grohmann U, Puccetti P. The coevolution of IDO1 and AhR in the emergence of regulatory T-cells in mammals. *Front Immunol* (2015) 6:58. doi:10.3389/fimmu.2015.00058
7. Platten M, Litzenburger U, Wick W. The aryl hydrocarbon receptor in tumor immunity. *Oncoimmunology* (2012) 1:396–7. doi:10.4161/onci.19071
8. Romani L, Puccetti P. Protective tolerance to fungi: the role of IL-10 and tryptophan catabolism. *Trends Microbiol* (2006) 14:183–9. doi:10.1016/j.tim.2006.02.003
9. Romani L, Puccetti P. Controlling pathogenic inflammation to fungi. *Expert Rev Anti Infect Ther* (2007) 5:1007–17. doi:10.1586/14787210.5.6.1007
10. Popov A, Schultze JL. IDO-expressing regulatory dendritic cells in cancer and chronic infection. *J Mol Med* (2008) 86:145–60. doi:10.1007/s00109-007-0262-6
11. Bettelli E, Carrier Y, Gao W, Korn T, Strom TB, Oukka M, et al. Reciprocal developmental pathways for the generation of pathogenic effector TH17 and regulatory T cells. *Nature* (2006) 441:235–8. doi:10.1038/nature04753
12. Mangan PR, Harrington LE, O'Quinn DB, Helms WS, Bullard DC, Elson CO, et al. Transforming growth factor-b induces development of the Th17 lineage. *Nature* (2006) 441:231–4. doi:10.1038/nature04754
13. Mucida D, Park Y, Kim G, Turovskaya O, Scott I, Kronenberg M, et al. Reciprocal Th17 and regulatory T cell differentiation mediated by retinoic acid. *Science* (2007) 317:256–60. doi:10.1126/science.1145697
14. Quintana FJ, Basso AS, Iglesias AH, Korn T, Farez MF, Bettelli E, et al. Control of Treg and TH17 cell differentiation by the aryl hydrocarbon receptor. *Nature* (2008) 453:65–71. doi:10.1038/nature06880
15. Veldhoen M, Hirota K, Westendorf AM, Buer J, Dumoutier L, Renauld JC, et al. The aryl hydrocarbon receptor links TH17-cell-mediated autoimmunity to environmental toxins. *Nature* (2008) 453:106–9. doi:10.1038/nature06881
16. Marques AS. Paracoccidioidomycosis: epidemiological, clinical, diagnostic and treatment up-dating. *An Bras Dermatol* (2013) 88:700–11. doi:10.1590/abd1806-4841.20132463
17. De Castro LF, Ferreira MC, da Silva RM, Blotta MH, Longhi LN, Mamoni RL. Characterization of the immune response in human paracoccidioidomycosis. *J Infect* (2013) 67:470–85. doi:10.1016/j.jinf.2013.07.019
18. Shikanai-Yasuda MA, Telles FQ, Mendes RP, Colombo AL, Moretti ML. Guidelines in paracoccidioidomycosis. *Rev Soc Bras Med Trop* (2006) 39:297–310. doi:10.1590/S0037-86822006000300017
19. Cano LE, Singer-Vermes LM, Vaz CA, Russo M, Calich VL. Pulmonary paracoccidioidomycosis in resistant and susceptible mice: relationship among progression of infection, bronchoalveolar cell activation, cellular immune response, and specific isotype patterns. *Infect Immun* (1995) 63:1777–83.
20. Cano LE, Kashino SS, Arruda C, André D, Xidieh CF, Singer-Vermes LM, et al. Protective role of gamma interferon in experimental pulmonary paracoccidioidomycosis. *Infect Immun* (1998) 66:800–6.
21. Cano LE, Singer-Vermes LM, Costa TA, Mengel JO, Xidieh CF, Arruda C, et al. Depletion of CD8(+) T cells in vivo impairs host defense of mice resistant and susceptible to pulmonary paracoccidioidomycosis. *Infect Immun* (2000) 68:352–9. doi:10.1128/IAI.68.1.352-359.2000
22. Chiarella AP, Arruda C, Pina A, Costa TA, Ferreira RC, Calich VL. The relative importance of CD4+ and CD8+T cells in immunity to pulmonary paracoccidioidomycosis. *Microbes Infect* (2007) 9:1078–88. doi:10.1016/j.micinf.2007.04.016
23. Calich VL, Costa TA, Felonato M, Arruda C, Bernardino S, Loures FV, et al. Innate immunity to *Paracoccidioides brasiliensis* infection. *Mycopathologia* (2008) 165:223–36. doi:10.1007/s11046-007-9048-1
24. Romani L. Immunity to fungal infections. *Nat Rev Immunol* (2011) 11:275–88. doi:10.1038/nri2939
25. Zelante T, Fallarino F, Bistoni F, Puccetti P, Romani L. Indoleamine 2,3-dioxygenase in infection: the paradox of an evasive strategy that benefits the host. *Microbes Infect* (2009) 11:133–41. doi:10.1016/j.micinf
26. Araújo EF, Medeiros DH, Galdino NA, Condino-Neto A, Calich VL, Loures FV. Tolerogenic plasmacytoid dendritic cells control *Paracoccidioides brasiliensis* infection by inducting regulatory T cells in an IDO-dependent manner. *PLoS Pathog* (2016) 12:e1006115. doi:10.1371/journal.ppat.1006115
27. Pallotta MT, Orabona C, Volpi C, Vacca C, Belladonna ML, Bianchi R, et al. Indoleamine 2,3-dioxygenase is a signaling protein in long-term tolerance by dendritic cells. *Nat Immunol* (2011) 12:870–8. doi:10.1038/ni.2077
28. Singer-Vermes LM, Caldeira CB, Burger E, Calich VLG. Experimental murine paracoccidioidomycosis: relationship among dissemination of the infection, humoral and cellular responses. *Clin Exp Immunol* (1993) 94:75–9. doi:10.1111/j.1365-2249.1993.tb05980.x
29. Loures FV, Pina A, Felonato M, Feriotti C, Araújo EF, Calich VL. MyD88 signaling is required for efficient innate and adaptive immune responses to *Paracoccidioides brasiliensis* infection. *Infect Immun* (2011) 79:2470–80. doi:10.1128/IAI.00375-10
30. Huntington ND, Carpentier S, Vivier E, Belz GT. Innate lymphoid cells: parallel checkpoints and coordinate interactions with T cells. *Curr Opin Immunol* (2016) 38:86–93. doi:10.1016/j.coi.2015.11.008
31. Spits H, Artis D, Colonna M, Diefenbach A, Di Santo JP. Innate lymphoid cells – a proposal for uniform nomenclature. *Nat Rev Immunol* (2013) 13:145–9. doi:10.1038/nri3365
32. Lee JS, Cella M, McDonald KG, Garlanda C, Kennedy GD, Nukaya M, et al. AHR drives the development of gut ILC22 cells and postnatal lymphoid tissues via pathways dependent on and independent of Notch. *Nat Immunol* (2011) 13:144–51. doi:10.1038/ni.2187
33. Stockinger B, Hirota K, Duarte J, Veldhoen M. External influences on the immune system via activation of the aryl hydrocarbon receptor. *Semin Immunol* (2011) 23:99–105. doi:10.1016/j.smim.2011.01.008
34. Gronke K, Kofoed-Nielsen M, Diefenbach A. Innate lymphoid cells, precursors and plasticity. *Immunol Lett* (2016) 9:9–18. doi:10.1016/j.imlet.2016.07.004
35. Romani L, Zelante T, De Luca A, Bozza S, Bonifazi P, Moretti S, et al. Indoleamine 2,3-dioxygenase (IDO) in inflammation and allergy to *Aspergillus*. *Med Mycol* (2009) 1:154–61. doi:10.1080/13693780802139867
36. Bonifazi P, Zelante T, D'Angelo C, De Luca A, Moretti S, Bozza S, et al. Balancing inflammation and tolerance in vivo through dendritic cells by the commensal *Candida albicans*. *Mucosal Immunol* (2009) 2:362–74. doi:10.1038/mi.2009.17
37. De Luca A, Carvalho A, Cunha C, Iannitti RG, Pitzurra L, Giovannini G, et al. IL-22 and IDO1 affect immunity and tolerance to murine and human vaginal candidiasis. *PLoS Pathog* (2013) 9:e1003486. doi:10.1371/journal.ppat.1003486
38. Brummer E, Hanson LH, Stevens DA. Gamma-interferon activation of macrophages for killing of *Paracoccidioides brasiliensis* and evidence for nonoxidative mechanisms. *Int J Immunopharmacol* (1988) 10:945–52. doi:10.1016/0192-0561(88)90041-0
39. Bernardino S, Pina A, Felonato M, Costa TA, Frank de Araújo E, Feriotti C, et al. TNF-α and CD8+ T cells mediate the beneficial effects of nitric oxide synthase-2 deficiency in pulmonary paracoccidioidomycosis. *PLoS Negl Trop Dis* (2013) 7:e2325. doi:10.1371/journal.pntd.0002325
40. Livonesi MC, Rossi MA, de Souto JT, Campanelli AP, de Sousa RL, Maffei CM, et al. Inducible nitric oxide synthase-deficient mice show exacerbated inflammatory process and high production of both Th1 and Th2 cytokines during paracoccidioidomycosis. *Microbes Infect* (2009) 11:123–32. doi:10.1016/j.micinf.2008.10.015
41. Batista AC, Soares CT, Lara VS. Failure of nitric oxide production by macrophages and decrease in CD4+ T cells in oral paracoccidioidomycosis: possible mechanisms that permit local fungal multiplication. *Rev Inst Med Trop Sao Paulo* (2005) 47:267–73. doi:10.1590/S0036-46652005000500006
42. Gonzalez A, de Gregori W, Velez D, Restrepo A, Cano LE. Nitric oxide participation in the fungicidal mechanism of gamma interferon-activated murine macrophages against *Paracoccidioides brasiliensis* conidia. *Infect Immun* (2000) 68:2546–52. doi:10.1128/IAI.68.5.2546-2552.2000
43. Bocca AL, Hayashi EE, Pinheiro AG, Furlanetto AB, Campanelli AP, Cunha FQ, et al. Treatment of *Paracoccidioides brasiliensis*-infected mice with a nitric oxide inhibitor prevents the failure of cell-mediated immune response. *J Immunol* (1998) 161:3056–63.
44. Nascimento FR, Calich VL, Rodríguez D, Russo M. Dual role for nitric oxide in paracoccidioidomycosis: essential for resistance, but overproduction associated with susceptibility. *J Immunol* (2002) 168:4593–600. doi:10.4049/jimmunol.168.9.4593
45. Geller DA, Billiar TR. Molecular biology of nitric oxide synthases. *Cancer Metastasis Rev* (1998) 17:7–23. doi:10.1023/A:1005940202801
46. Kleinert H, Schwarz PM, Förstermann U. Regulation of the expression of inducible nitric oxide synthase. *Biol Chem* (2003) 384:1343–64. doi:10.1515/BC.2003.152

47. Alberati-Giani D, Malherbe P, Ricciardi-Castagnoli P, Köhler C, Denis-Donini S, Cesura AM. Differential regulation of indoleamine 2,3-dioxygenase expression by nitric oxide and inflammatory mediators in IFN-gamma-activated murine macrophages and microglial cells. *J Immunol* (1997) 159:419–26.
48. Thomas SR, Mohr D, Stocker R. Nitric oxide inhibits indoleamine 2,3-dioxygenase activity in interferon-gamma primed mononuclear phagocytes. *J Biol Chem* (1994) 269:14457–64.
49. Hucke C, MacKenzie CR, Adjogble KD, Takikawa O, Däubener W. Nitric oxide-mediated regulation of gamma interferon-induced bacteriostasis: inhibition and degradation of human indoleamine 2,3-dioxygenase. *Infect Immun* (2004) 72:2723–30. doi:10.1128/IAI.72.5.2723-2730.2004
50. Araújo EF, Loures FV, Bazan SB, Feriotti C, Pina A, Schanoski AS, et al. Indoleamine 2,3-dioxygenase controls fungal loads and immunity in Paracoccidioidomicosis but is more important to susceptible than resistant hosts. *PLoS Negl Trop Dis* (2014) 8:e3330. doi:10.1371/journal.pntd.0003330
51. Harden JL, Egilmez NK. Indoleamine 2,3-dioxygenase and dendritic cell tolerogenicity. *Immunol Invest* (2012) 41:738–64. doi:10.3109/08820139.2012.676122
52. Vogel CF, Goth SR, Dong B, Pessah IN, Matsumura F. Aryl hydrocarbon receptor signaling mediates expression of indoleamine 2,3-dioxygenase. *Biochem Biophys Res Commun* (2008) 375:331–5. doi:10.1016/j.bbrc.2008.07.156
53. Witte E, Witte K, Warszawska K, Sabat R, Wolk K. Interleukin-22: a cytokine produced by T, NK and NKT cell subsets, with importance in the innate immune defense and tissue protection. *Cytokine Growth Factor Rev* (2010) 21:365–79. doi:10.1016/j.cytogfr.2010.08.002
54. Martin B, Hirota K, Cua DJ, Stockinger B, Veldhoen M. Interleukin-17-producing gammadelta T cells selectively expand in response to pathogen products and environmental signals. *Immunity* (2009) 31:321–30. doi:10.1016/j.immuni.2009.06.020
55. Hughes T, Becknell B, McClory S, Briercheck E, Freud AG, Zhang X, et al. Stage 3 immature human natural killer cells found in secondary lymphoid tissue constitutively and selectively express the TH 17 cytokine interleukin-22. *Blood* (2009) 113:4008–10. doi:10.1182/blood-2008-12-192443
56. Cella M, Fuchs A, Vermi W, Facchetti F, Otero K, Lennerz JK, et al. A human natural killer cell subset provides an innate source of IL-22 for mucosal immunity. *Nature* (2009) 457:722–5. doi:10.1038/nature07537
57. Crellin NK, Trifari S, Kaplan CD, Cupedo T, Spits H. Human NKp44+IL-22+ cells and LTi-like cells constitute a stable RORC+ lineage distinct from conventional natural killer cells. *J Exp Med* (2010) 207:281–90. doi:10.1084/jem.20091509
58. Trifari S, Kaplan CD, Tran EH, Crellin NK, Spits H. Identification of a human helper T cell population that has abundant production of interleukin 22 and is distinct from T(H)-17, T(H)1 and T(H)2 cells. *Nat Immunol* (2009) 10:864–71. doi:10.1038/ni.1770
59. Goupil M, Cousineau-Côté V, Aumont F, Sénéchal S, Gaboury L, Hanna Z, et al. Defective IL-17- and IL-22-dependent mucosal host response to *Candida albicans* determines susceptibility to oral candidiasis in mice expressing the HIV-1 transgene. *BMC Immunol* (2014) 15:49. doi:10.1186/s12865-014-0049-9
60. Delsing CE, Becker KL, Simon A, Kullberg BJ, Bleeker-Rovers CP, van de Veerdonk FL, et al. Th17 cytokine deficiency in patients with *Aspergillus* skull base osteomyelitis. *BMC Infect Dis* (2015) 15:140. doi:10.1186/s12879-015-0891-2
61. Borghi M, De Luca A, Puccetti M, Jaeger M, Mencacci A, Oikonomou V, et al. Pathogenic NLRP3 inflammasome activity during *Candida* infection is negatively regulated by IL-22 via activation of NLRC4 and IL-1Ra. *Cell Host Microbe* (2015) 18:198–209. doi:10.1016/j.chom.2015.07.004
62. Kiss EA, Vonarbourg C, Kopfmann S, Hobeika E, Finke D, Esser C, et al. Natural aryl hydrocarbon receptor ligands control organogenesis of intestinal lymphoid follicles. *Science* (2011) 334:1561–5. doi:10.1126/science.1214914
63. Mezrich JD, Fechner JH, Zhang X, Johnson BP, Burlingham WJ, Bradfield CA. An interaction between kynurenine and the aryl hydrocarbon receptor can generate regulatory T cells. *J Immunol* (2010) 185:3190–8. doi:10.4049/jimmunol.0903670
64. Munn DH, Mellor AL. Indoleamine 2,3 dioxygenase and metabolic control of immune responses. *Trends Immunol* (2013) 34:137–43. doi:10.1016/j.it.2012.10.001
65. Fitzgerald DC, Zhang GX, El-Behi M, Fonseca-Kelly Z, Li H, Yu S, et al. Suppression of autoimmune inflammation of the central nervous system by interleukin 10 secreted by interleukin 27-stimulated T cells. *Nat Immunol* (2007) 8:1372–9. doi:10.1038/ni1540
66. Awasthi A, Carrier Y, Peron JP, Bettelli E, Kamanaka M, Flavell RA, et al. A dominant function for interleukin 27 in generating interleukin 10-producing anti-inflammatory T cells. *Nat Immunol* (2007) 8:1380–9. doi:10.1038/ni1541
67. Loures FV, Pina A, Felonato M, Calich VL. TLR2 is a negative regulator of Th17 cells and tissue pathology in a pulmonary model of fungal infection. *J Immunol* (2009) 183:1279–90. doi:10.4049/jimmunol.0801599
68. Loures FV, Pina A, Felonato M, Araújo EF, Leite KR, Calich VL. Toll-like receptor 4 signaling leads to severe fungal infection associated with enhanced proinflammatory immunity and impaired expansion of regulatory T cells. *Infect Immun* (2010) 78:1078–88. doi:10.1128/IAI.01198-09
69. Bazan SB, Costa TA, de Araújo EF, Feriotti C, Loures FV, Pretel FD, et al. Loss- and gain-of-function approaches indicate a dual role exerted by regulatory T cells in pulmonary paracoccidioidomycosis. *PLoS Negl Trop Dis* (2015) 9:e0004189. doi:10.1371/journal.pntd.0004189

Conflict of Interest Statement: The authors declare that the research was conducted in the absence of any commercial or financial relationships that could be construed as a potential conflict of interest.

Copyright © 2017 de Araújo, Feriotti, Galdino, Preite, Calich and Loures. This is an open-access article distributed under the terms of the Creative Commons Attribution License (CC BY). The use, distribution or reproduction in other forums is permitted, provided the original author(s) or licensor are credited and that the original publication in this journal is cited, in accordance with accepted academic practice. No use, distribution or reproduction is permitted which does not comply with these terms.

frontiers in Immunology

REVIEW
published: 07 February 2018
doi: 10.3389/fimmu.2018.00170

MicroRNA Regulation of Host Immune Responses following Fungal Exposure

Tara L. Croston[1], Angela R. Lemons[1], Donald H. Beezhold[2] and Brett J. Green[1]*

[1] Allergy and Clinical Immunology Branch, Health Effects Laboratory Division, National Institute for Occupational Safety and Health, Centers for Disease Control and Prevention, Morgantown, WV, United States, [2] Health Effects Laboratory Division, National Institute for Occupational Safety and Health, Centers for Disease Control and Prevention, Morgantown, WV, United States

Fungal bioaerosols are ubiquitous in the environment and human exposure can result in a variety of health effects ranging from systemic, subcutaneous, and cutaneous infections to respiratory morbidity including allergy, asthma, and hypersensitivity pneumonitis. Recent research has focused on the role of microRNAs (miRNAs) following fungal exposure and is overlooked, yet important, group of regulators capable of influencing fungal immune responses through a variety of cellular mechanisms. These small non-coding ribose nucleic acids function to regulate gene expression at the post-transcriptional level and have been shown to participate in multiple disease pathways including cancer, heart disease, apoptosis, as well as immune responses to microbial hazards and occupational allergens. Recent animal model studies have characterized miRNAs following the exposure to inflammatory stimuli. Studies focused on microbial exposure, including bacterial infections, as well as exposure to different allergens have shown miRNAs, such as miR-21, miR-146, miR-132, miR-155, and the let-7 family members, to be involved in immune and inflammatory responses. Interestingly, the few studies have assessed that the miRNA profiles following fungal exposure have identified the same critical miRNAs that have been characterized in other inflammatory-mediated and allergy-induced experimental models. Review of available *in vitro*, animal and human studies of exposures to *Aspergillus fumigatus*, *Candida albicans*, *Cryptococcus neoformans*, *Paracoccidioides brasiliensis*, and *Stachybotrys chartarum* identified several miRNAs that were shared between responses to these species including miR-125 a/b (macrophage polarization/activation), miR-132 [toll-like receptor (TLR)2-mediated signaling], miR-146a (TLR mediated signaling, alternative macrophage activation), and miR-29a/b (natural killer cell function, C-leptin signaling, inhibition of Th1 immune response). Although these datasets provide preliminary insight into the role of miRNAs in fungal exposed models, interpretation of miRNA datasets can be challenging for researchers. To assist in navigating this rapidly evolving field, the aim of this review is to describe miRNAs in the framework of host recognition mechanisms and provide initial insight into the regulatory pathways in response to fungal exposure.

Keywords: fungal exposure, microRNA, fungi, immune response, inflammatory response

OPEN ACCESS

Edited by:
Amariliz Rivera, New Jersey Medical School, United States

Reviewed by:
Agostinho Carvalho, University of Minho, Portugal
Joshua J. Obar, Dartmouth College, United States

****Correspondence:***
Tara L. Croston
xzu9@cdc.gov

Specialty section:
This article was submitted to Microbial Immunology, a section of the journal Frontiers in Immunology

Received: *30 October 2017*
Accepted: *19 January 2018*
Published: *07 February 2018*

Citation:
Croston TL, Lemons AR, Beezhold DH and Green BJ (2018) MicroRNA Regulation of Host Immune Responses following Fungal Exposure. Front. Immunol. 9:170. doi: 10.3389/fimmu.2018.00170

Abbreviations: Clec7a, C-type lectin domain family 7 member A; IL, interleukin; LPS, lipopolysaccharide; RNA, ribose nucleic acid; RNAi, RNA interference; mRNA, messenger RNA; miRNA, microRNA; TLRs, Toll-like receptors.

INTRODUCTION

Fungi are ubiquitous eukaryotic microorganisms that can be prevalent in indoor, outdoor, and occupational environments. A small portion of 1.5 million fungal species estimated to exist (1) are primary or opportunistic pathogens, whereas the vast majority is ubiquitous saprophytes that obtain nutrients from organic matter. Fungi are composed of membrane bound organelles that are encased by a rigid cell wall but do not contain chlorophyll. The cell wall is composed of ergosterol, chitin, glucans, such as (1 → 3)-β-d-glucan, and mannose proteins (2). Fungal lifeforms broadly vary from unicellular yeasts to multicellular filamentous hyphae that include the production of mitotic or meiotically produced spores. In some cases, fungi are dimorphic and share both lifecycles. Upon disturbance, fungal spores can be aerosolized and in some occupational environments the airborne concentrations may exceed 1×10^5 spores/m^3 (3).

Personal exposure to fungal species has been associated with a broad variety of adverse health effects that range from pulmonary, sinus, and subcutaneous infections to respiratory morbidities that may include hypersensitivity pneumonitis, allergy, and asthma (3). Each of these health effects is dependent on the host's immune responsiveness and fungal species exposed (4). In specific geographical regions, dimorphic fungi that cause endemic mycoses exist as either a filamentous fungus in the environment or as a pathogenic yeast in the host. In the environment, the filamentous hyphae grow in soil at ambient temperatures and produce infectious spores (5, 6). Soil disturbance can aerosolize spores that can be inhaled by a mammalian host. In a process that is thermoregulated, the spores can germinate into a pathogenic yeast phase that helps these fungi avoid the hosts' immune responses. For example, *Blastomyces dermatitidis* can proliferate on the respiratory mucosa, *Histoplasma capsulatum* modulates the monocyte phagolysosome compartment, and *Coccidioides immitis* develops a large spherule containing endospores that is resistant to phagocytosis. These dimorphic fungal species as well as others, including *Paracoccidioides brasiliensis* (paracoccidioidomycosis) and *Talaromyces* (*Penicillium*) *marneffei* (talaromycosis), affect the lungs, although the latter can also affect the liver and mouth.

By contrast, opportunistic fungal pathogens consist of fungi that are environmentally ubiquitous and affect those who are immunocompromised, especially patients who have received a transplant or undergoing chemotherapy or corticosteroid therapy. Examples of fungi that are commonly implicated in opportunistic infections include, *Candida albicans* (candidiasis), *Pneumocystis jirovecii* (*Pneumocystis* pneumonia), *Cryptococcus neoformans/gattii* (cryptococcosis), and *Aspergillus fumigatus* (aspergillosis). Infections can be acquired through the inhalation of conidia or yeast depending on the species and can result in systemic mycoses. With the increase in broad-spectrum antibiotic usage and other medical and therapeutic strategies, invasive opportunistic fungal infections are of particular concern in the hospital setting, as nosocomial infections may be life-threatening for critically ill individuals (7).

The World Health Organization and the Institute of Medicine have published consensus documents that report respiratory morbidities are associated with damp indoor environments (8, 9). Recent epidemiological evidence has further built on these consensus findings and shown exposure to mold in damp indoor environments to be associated with adverse respiratory health effects (10, 11). Following recent natural disasters and flooding events associated with Hurricanes Harvey, Irma, and Maria, water-infiltrated occupational, and residential buildings are environments where mold can grow and proliferate on water damaged building materials. Returning to these environments and disturbing contaminated building materials can result in the aerosolization of fungal spores (12) that can pose a significant health risk especially if the person is immunocompromised. Fungi associated with colonizing wet building materials include, *Aspergillus versicolor*, *Ulocladium chartarum*, *Chaetomium globosum*, and *Stachybotrys chartarum* that are hydrophilic and require a high water activity for growth and proliferation. Of these hydrophilic fungal contaminants, *S. chartarum* is the most widely studied and many reports have identified exposure to contribute to negative health effects (12–15).

Due to increased community concern regarding personal exposure to these pathogenic fungi and the potential result of life-threatening health outcomes, it is important to characterize the mechanisms that contribute to the host innate and adaptive immune responses. Previous research has focused on host responses in fungal exposure models by analyzing functional, histological, and immunological endpoints; however, research examining the molecular mechanisms that underlie these responses remains unclear for many clinically relevant fungal species. Although many studies have been published that have explored pulmonary immunological responses to acute and chronic fungal spores exposures, the microRNAs (miRNAs) that regulate these deficiencies have not been fully characterized. In this review, the state-of-knowledge of miRNAs characterized in various animal models, including those that have evaluated fungal exposures, will be reviewed with emphasis placed on the mechanistic insights that these studies have provided in relation to the host response following fungal exposure.

MICRORNAs

MicroRNAs are an important group of regulators capable of influencing gene expression through different mechanisms (16–20). Consisting of short, single stranded noncoding ribose nucleic acids (RNAs), miRNAs bind to target messenger RNA (mRNA) to downregulate gene expression post-transcriptionally through RNA silencing or RNA degradation (21, 22). Depending on the complementarity of base pairing, gene expression is repressed, as observed in humans and animals, or mRNA is cleaved, as observed in plants (23–25). More recently, studies have shown that miRNA can also activate the translation of certain target mRNA (17, 18, 26). Providing insight into how altered miRNA profiles affect upstream processes can be methodologically challenging. For example, a single miRNA can regulate from one to multiple genes, whereas studies have also shown that multiple miRNAs can regulate the same gene (27–30). Several miRNAs, as well as miRNA families, have been extensively studied and have been characterized in models of cancer, heart disease, aging, apoptosis, and immune responses to inflammatory stimuli (19, 20, 31–34).

Influence of miRNAs on IL-13-Mediated Allergic Responses

The *let-7* family is the most abundant pulmonary miRNAs and has been identified in cancer, diabetes, and aging studies (35–39). The *let-7* family members have been shown to target interleukin (IL)-13 in *in vivo* and *in vitro* models, although the regulatory *in vivo* mechanisms of *let-7* are complex (20, 40). miR-21 is another widely studied miRNA and has been shown to participate in the inflammatory response elicited by different stimuli, including doxycycline-induced allergic airway inflammation (41), as well as viral, bacterial and protozoan infections (42–44). One of the most upregulated miRNAs in human patients with allergic eosinophilic esophagitis is miR-21 (45, 46), which correlates with studies that reported miR-21 and miR-223 as regulators of eosinophilic development in an *ex vivo* model of bone-derived eosinophils (47, 48). miR-375 has also been reported to be downregulated in epithelial cells derived from patients with eosinophilic esophagitis, as well as in IL-13 stimulated epithelial cells indicating the role of miR-375 as a regulator of IL-13-mediated responses (21).

miRNA Involvement in Allergy-Induced Asthma

In rodent models exposed to house dust mite allergen, increased miR-126, miR-106a, and miR-145 expression have been shown to contribute to allergic inflammation (49–51). Studies involving airborne pollutants, such as cigarette smoke, reported a down-regulation in let-7c, let-7f, miR-34b, miR-34c, and miR-222, all of which contributed to pulmonary inflammation in rodent models (52–54). Research examining aberrant miRNA profiles in asthmatic hosts has also revealed novel miRNAs that contribute to allergic airway disease. Examination of $CD4^+$ T cells isolated from the bronchoalveolar lavage fluid from asthmatic human patients revealed that miR-19a had the highest expression (55), which promoted a Th2-mediated cell response, a known response contributing to allergic asthma. In another study, miR-221 and miR-485-3p were upregulated in peripheral blood from pediatric asthmatic human patients compared with controls, suggesting that these miRNAs contribute to the development of asthma (56). In a chemical allergen model examining the murine miRNA profile following dermal exposure to toluene 2,4-diisocyanate, miR-21, miR-22, miR-27b, miR-31, miR-126, miR-155, miR-210, and miR-301a expression were increased (57). While this study identified miRNAs that are known to participate in the immune response associated with asthma (miR-21, miR-31, miR-126, and miR-155), new miRNAs were proposed as potential biomarkers for allergic sensitization to toluene 2,4-diisocyanate (miR-22, miR-27b, miR-301a, and miR-210).

miRNA Regulation on Adaptive Immunity

MicroRNAs critically influence the development and responses of the immune system, but the contributing biological mechanisms are poorly characterized (22, 58–60). Overexpression of the miR-17-92 cluster and miR-181 enhanced B-cell proliferation, while miR-150 regulated B-cell differentiation (61–64). When overexpressed, miR-181 has been shown to decrease T-cell numbers (61), but enhance T-cell receptor signaling (65). When T cells are activated, the miRNA expression profiles are altered (66–68). T-cell activation has additionally been found to induce the miR-17~92 family members (69), as well as the gene that encodes miR-155 (70). miR-155 has also been reported to regulate antigen presentation (71) and to negatively regulate toll-like receptor (TLR) and cytokine signaling (72). The miR-17-92 cluster promotes Th1 type immune responses along with inhibiting regulatory T-cell differentiation (69). Rodriquez et al. showed that miR-155 is required for normal functioning of B and T lymphocytes as well as dendritic cells (73).

Macrophage Development and TLR Signaling

In human macrophages, miR-155 targets and subsequently decreases IL-13Rα1, modulating the IL-13 pathway and the switching between classic and alternatively activated macrophages (74). Macrophage polarization is transcriptionally controlled by either miR-146b or miR-34a, directing an M1 macrophage polarization, whereas miR-18a/miR-34a, miR-130b, or miR-125-5p dictates an M2 macrophage phenotype (75). miR-21 has also been reported to direct macrophage polarization from an M1 phenotype toward an M2 phenotype (75). Alveolar macrophages isolated from a fibrotic mouse model showed significantly increased miR-let-7c levels compared with control and that overexpression of this miRNA regulated macrophage polarization (76). Expression of miR-124 and miR-223 in macrophages has also been reported to contribute to macrophage polarization (77, 78).

Located on the surface of sentinel cells, such as macrophages, TLRs play a critical role in the innate immune system by recognizing pathogen-associated molecular patterns expressed on pathogens and signaling for the production of cytokine to elicit an immune response. These TLRs participate in macrophage activation and have been shown to induce miR-155, miR-146, miR-147, miR-9, and miR-21 (79, 80). An upregulation of miR-21 has been observed in both primary human airway epithelial cells (41) and in an IL-13 transgenic mouse model with the latter study identifying that the observed miR-21 upregulation was through an IL-13Rα1-dependent mechanism (81). This increase in miR-21 was also associated with inhibited Th1 cytokine signaling (41). Using an ovalbumin-induced miR-21 deficient mouse model, Th1 cytokines were found to be increased (82), supporting the contribution of miR-21 in Th2 type immune responses. One study confirmed that miR-21 expression inhibited murine pulmonary inflammation by suppressing TLR2 signaling (81). When secreted from tumor cells, miR-21 and miR-29a have also been reported to interact with TLRs, specifically TLR7 and TLR8, respectively (83). Upon lipopolysaccharide (LPS) stimulation, miR-146a/b was shown to be induced and predicted to negatively regulate TLR and cytokine signaling (72).

Influence of miRNA on T-Helper Cell Responses

Macrophage surface activation is induced in the presence of overexpressed miR-125b (84) and in an eosinophilic rhinosinusitis animal model, miR-125b is increased resulting in increased interferon gamma and a Th1 type immune response (85). miR-19a has

also been shown to be critical in regulating Th1 type responses through the production of interferon gamma following antigen stimulation in a mouse model (69). Upregulation of miR-19a also caused increased inflammation and promoted a Th2 type response (55). miR-19a is a member of the miR-17–92 cluster, which has been reported to be upregulated during T-cell activation (69, 86). Th17 cell differentiation has also been shown to be regulated by the miR-106-363 cluster (87) and in an experimental autoimmune encephalomyelitis model, Th17 cell-mediated inflammation was shown to be induced by both miR-326 and miR-21 (88, 89).

In summary, multiple studies have characterized the role of miRNAs on immune processes in a variety of diverse animal models of inflammation, but few studies have evaluated the miRNA profiles following fungal exposures (**Figure 1**). Investigation of these miRNA profiles could provide insight into the immune mechanisms and regulatory pathways involved in the host response to fungal exposure.

FUNGAL EXPOSURE: ROLE OF miRNAs

Several research studies have focused on the miRNA profiles following acute or chronic fungal exposures (**Figure 1**). **Table 1** shows 10 studies that have preliminarily characterized differentially expressed miRNAs following exposure to five clinically relevant fungal species including *A. fumigatus* (22, 90, 91), *C. albicans* (22, 92–94), *C. neoformans* (95), *P. brasiliensis* (96, 97), and *S. chartarum* (98). The paucity of research investigating the regulation of miRNAs on pulmonary and systemic responses to fungal exposure highlights the need for research examining the role miRNAs play in the immunological mechanisms associated with endemic, opportunistic, and environmental fungal exposures.

miRNA Profiles following *P. brasiliensis* Infection

Paracoccidioidomycosis, caused by the dimorphic fungus *P. brasiliensis*, is a public health burden in Latin America (117). This fungus can be isolated in the form of yeast from infected individuals and armadillos, and has also been sporadically isolated from soil, dog food, and bat feces (118, 119). The disease begins with the inhalation of spores into the lungs that germinate into yeast and cause a primary lung infection or disseminate systemically resulting in oral and cutaneous lesions. To date, two studies have evaluated differentially expressed miRNAs following *P. brasiliensis* exposure in a murine model and in a human model. Turini Gonzales Marioto et al. (97) evaluated the miRNA profiles in mice intravenously administered *P. brasiliensis* and showed that the most upregulated miRNAs at 28 days included miR-126a-5p, miR-340-5p, miR-30b-5p, miR-19b-3p, miR-221-3p, miR-20a-5p, miR-130a-3p, and miR-301a-3p, whereas after 56 days, miRNAs from the let-7 family, as well as miR-26b-5p, and miR-369-3p were the greatest upregulated miRNAs (97). The only miRNA that was upregulated at both time points was miR-466k (**Table 1**). This study identified differentially expressed miRNAs that are known to contribute to the immune response through T cell function and proliferation, as well as monocyte and erythrocyte differentiation. The contribution of miR-466k on the immune response is unknown; however, this miRNA has been identified in prostate cancer and graft rejection studies (120, 121). Another study examined the miRNA profile in the serum of human patients infected with *P. brasiliensis* and found that of the 752 miRNAs analyzed, 8 were differentially expressed (96). The upregulated miRNAs included miR-132-3p, miR-604, miR-186-5p, miR-29b-3p, miR-125b-5p, miR-376c-3p, and miR-30b-5p, where the only downregulated miRNA was miR-423-3p

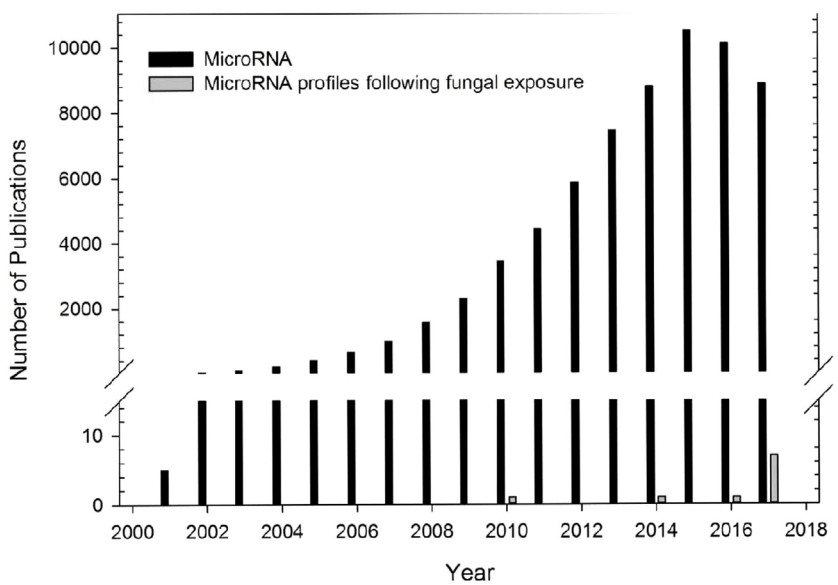

FIGURE 1 | Number of microRNA (miRNA) publications. Number of publications examining miRNA profiles from different diseased models (black bars) or following fungal exposure (gray bars). Data obtained from PubMed search using term "microRNA" for publications using different diseased models. One study in 1972 was not included. Number of publications using a fungal exposed model were obtained from studies included in this review.

TABLE 1 | Differentially expressed microRNAs following fungal exposure.

miRNA	Regulation	Fungal species	Exposure model	Function in immune response[a]	Reference
let-7 family	↑	*Paracoccidioides brasiliensis*	Inv	Regulator of TLR mediated signaling; Involved in IL-13 production	(97, 99)
miR-125a	↑	*Candida albicans*	Cc	Regulator of macrophage polarization; Enhances classical activation of macrophages	(92, 100)
miR-125b	↑	*P. brasiliensis*	Hu		(96, 101)
miR-126a	↑	*P. brasiliensis*	Inv	Promoter of Th2 immune response	(49, 97)
miR-129	↑	*C. albicans* with *Aspergillus fumigatus*	Cc	Regulation of cell cycle	(22, 102)
miR-130a	↑	*P. brasiliensis*	Inv	Involved in $CD8^+$T cell activation	(97, 103)
miR-132	↑	*P. brasiliensis*	Hu	Regulator of TLR2 mediated signaling; induces alternative activation of macrophages	(96, 104)
	↑	*A. fumigatus*	Cc		(90, 101)
	↑	*C. albicans* with *A. fumigatus*	Cc		(22)
miR-146a	↑	*C. albicans*	Cc	Negative regulator of TLR mediated signaling; Induces alternative activation of macrophages	(92, 94)
	↑	*Cryptococcus neoformans*	Cc		(95, 101, 105)
miR-155	↑	*C. albicans*	Cc	Regulator of TLR mediated signaling; Enhances classical activation of macrophages; Promoter of Th2 immune response	(92, 93, 100, 101, 105)
miR-186	↑	*P. brasiliensis*	Hu	Involved in TLR2 mediated signaling	(96, 106)
miR-19b	↑	*P. brasiliensis*	Inv	Promoter of Th17 immune response; T cell proliferation	(97, 107)
miR-20a	↑	*P. brasiliensis*	Inv	Negatively regulates monocyte differentiation	(97, 108)
miR-210	↑	*C. albicans*	Cc	Involved in Th1 and Th17 cell differentiation	(94, 109)
miR-21a	↑	*Stachybotrys chartarum*	Inh	Regulator of TLR mediated signaling; Involved in monocyte, dendritic, macrophage, and Th2 cell differentiation; Involved in macrophage activation	(98, 109, 110)
miR-212	↑	*C. albicans* with *A. fumigatus*	Cc	Involved in B-cell development and Th17 cell differentiation	(22, 111)
miR-23	↓	*A. fumigatus*	Inh	Involved in cell differentiation of B cells; Mediate macrophage polarization	(91, 109)
miR-26b	↑	*P. brasiliensis*	Inv	Increases regulatory T cells	(97, 107)
miR-29a	↓	*A. fumigatus*	Inh	Regulator of natural killer cell function; Involved in C-leptin signaling; Inhibition of Th1 immune response	(91, 112)
miR-29b	↑	*P. brasiliensis*	Hu		(96, 100)
miR-30	↑	*C. albicans*	Cc	Involved in natural killer cell function and B cell activation; Involved in cell function of cytotoxic T cells	(94, 109)
miR-30b	↑	*P. brasiliensis*	Inv, Hu		(96, 97)
miR-301a	↑	*P. brasiliensis*	Inv	Promoter of Th17 immune response; Regulator of TLR mediated signaling	(97, 100, 113)
miR-340	↑	*P. brasiliensis*	Inv	Unknown	(97)
miR-369	↑	*P. brasiliensis*	Inv	Activation of protein translation	(26, 97)
miR-376c	↑	*P. brasiliensis*	Hu	Unknown	(96)
miR-423	↓	*P. brasiliensis*	Hu	Regulator of chemokine expression	(96, 114)
miR-455	↑	*C. albicans*	Cc	Involved in nuclear factor-kappaB signaling	(92, 115)
miR-466k	↑	*P. brasiliensis*	Inv	Unknown	(97)
miR-604	↑	*P. brasiliensis*	Hu	Unknown	(96)
miR-706	↑	*S. chartarum*	Inh	Promotes granulocyte production	(98, 116)

[a]*Immune responses are compiled from different studies utilizing a variety of diseased models and not necessarily from fungal exposure studies. Exposure model abbreviations are Inv, Intravenous administration or through; Inh, Inhalation using a mouse model; Cc, cell culture; Hu, Human patients.*

(**Table 1**). These miRNAs are known to mediate macrophage polarization or are involved in TLR2 signaling, indicative of a Th1 immune response. Interestingly, both studies reported an upregulation in miR-30b-5p, suggesting a possible biomarker for *P. brasiliensis* infection.

miR-132 Is Induced by *A. fumigatus* Exposure

Aspergillus fumigatus is a commonly encountered pathogenic fungal species and is often found in the soil, occupational environments [i.e., biowaste containment facilities (122, 123)] or indoor environments [i.e., hospitals (124, 125)]. Inhalation of *A. fumigatus* unicellular spores can result in varying degrees of infection, known as aspergillosis, depending on the preexisting conditions of the host. miR-132 has been shown to be induced in human monocytes and dendritic cells following stimulation with *A. fumigatus* compared with control, LPS (90). These datasets suggest a Th2-mediated response, which is further supported by other recent animal models of inhalation exposure to *A. fumigatus* (91).

Upregulation of miR-146 in *Candida* and *C. neoformans*

Candidiasis, an infection caused by several endogenous *Candida* species, results in varying symptoms depending on the site of infection (126, 127). Candidiasis is among the most common opportunistic fungal infections localized in the gastrointestinal tract (thrush), occluded regions of the hands, feet, and groin, or can develop into invasive candidiasis and disseminate systemically in the blood (candidemia), heart, brain, eyes, and bones. Invasive candidiasis is the most common type of fungal infection in critically ill patients, with approximately 46,000 healthcare-associated cases occurring each year in the United

States (126–128). Although *Candida* infections are typically resolved by antifungal therapy, some *Candida* species are resistant or are becoming resistant, such as *C. auris* (129). In murine macrophages stimulated by 10^6 cells/mL heat killed *C. albicans,* miR-146a and miR-155, as well as miR-455 and miR-125a were upregulated (92), indicative of the involvement of these miRNAs in macrophage polarization.

Similar to the findings of Monk et al. (92), miR-146a was also shown to be upregulated in human monocytic THP-1 cells exposed to *C. neoformans*, inhibiting nuclear factor-κB activation and the release of inflammatory cytokines (95). *C. neoformans* is one of two pathogenic *Cryptococcus* species, and along with *C. gatti*, typically live in the soil surrounding trees and are capable of causing infection following inhalation. Exposure to *Cryptococcus* species usually causes adverse respiratory health effects; however, it can affect other parts of the body such as the brain, known as cryptococcal meningitis (130, 131).

miRNA Profiles following a Mixed Fungal Exposure

In a model of mixed fungal exposure, Dix et al. co-cultured human monocyte-derived dendritic cells with *A. fumigatus, C. albicans,* and LPS and showed that differentially expressed miRNAs were increased after 6 and 12 h, with a stronger regulation observed after 12 h (22). Twenty six miRNAs were identified to be differently expressed in response to the exposure. The authors also showed that strongly modified miRNAs after exposure to fungi clustered separately from the strongly modified miRNAs exposed to LPS. This clustering pattern suggests that examination of miRNA profiles could distinguish between fungal and bacterial exposure. For example, miR-132 and miR-212-5p were specific to fungal exposure at 6 h time point, whereas miR-132, miR-212, and miR-129-5p were specific to fungal exposure at 12 h time point.

C-Leptin Receptors and Associated miRNAs

Critical to antifungal innate immunity, Dectin-1 is a surface receptor that recognizes (1,3)-β-D-glucan found on the cell wall of germinating conidia (91, 132). To date, several studies have attempted to explore the regulatory mechanisms involving miRNAs that underlie Dectin-1 associated immune responses. In a murine model of subchronic *A. fumigatus* inhalation exposure, Croston et al. showed that significantly downregulated miR-29a-3p was predicted to regulate C-type lectin domain family 7 member A, the gene that codes for Dectin-1 (91). A recent study found that following exposure to *C. albicans*, Dectin-1 is required for the upregulation of miR-155 in murine macrophages (93). Along with an increase in miR-30-5p and miR-210-3p in THP-1 cells treated with β-glucan isolated from *C. albicans*, Du et al. found that miR-146a was increased upon Dectin-1 stimulation and negatively regulated the resultant inflammatory response (94). Results from the Croston et al. study using a murine model of subchronic *A. fumigatus* inhalation exposure also determined that significantly downregulated miR-23b-3p and miR-145a-5p was predicted to regulate the mannose receptor gene, *Mrc1* (data not reported).

miRNA Profiles following Exposure to Occupationally Relevant Fungal Species

In order to elucidate the influence of germination on the ensuing immune response, Croston et al. utilized an acoustical generator system to deliver dry fungal spores to mice housed in a multi-animal nose-only inhalation chamber (91). This murine inhalation model reproduces exposures that could be encountered in contaminated indoor or occupational environments (133). Furthermore, this study included a heat inactivated conidia group that was used as a biological control to examine the influence of germination on the miRNA profiles. Along with a downregulation of miR-29a-3p, miR-23b-3p, a miRNA predicted to target *SMAD2,* as well as genes involved in IL-13 and IL-33 responses, was also downregulated following subchronic exposure to a dry aerosol containing viable *A. fumigatus* conidia (91). Furthermore, out of 415 miRNAs detected, approximately 50% were altered in mice exposed to viable versus heat inactivated conidia 48 h post fungal exposure. Taken together, these results demonstrate that *A. fumigatus* germination is an important variable that can lead to the induction of allergic inflammation in the lungs, potentially through an IL-13/IL-33-driven mechanism.

Stachybotrys chartarum is a hydrophilic fungal species prevalent in water infiltrated occupational and residential environments. Exposure to *S. chartarum* is currently of heightened public health interest following recent natural disasters, such as floods and hurricanes, that can lead to the contamination of indoor building materials. Following the consensus reports published by the IOM and WHO, the immunological mechanisms that contribute to the host response to fungal contaminant exposure require further elucidation. Recent studies have attempted to characterize critical interactions that influence these pulmonary immunological responses. Croston et al. found that miR-21a was the only miRNA upregulated in murine whole lung homogenate 48 h following subchronic exposure to *S. chartarum* (98) (**Figure 2**). Although miR-21a is known to promote a Th2 phenotype, a more dominant Th1 phenotype was evident. Since then, miR-706 was also discovered to be upregulated at the same time point. Interestingly, out of 468 miRNA evaluated, only 2 were upregulated with no downregulated miRNAs. These preliminary results suggest that miRNA regulation mechanisms induced by *S. chartarum* vary from *A. fumigatus* in these studies using the same exposure system and the pulmonary immunological responses to this species require further evaluation.

Figure 2 depicts a disease pathway generated by Ingenuity Pathway Analysis (IPA) that includes predicted miRNAs involved in the inflammation of organs. Once miRNA data are uploaded into IPA, the integrated knowledge base predicts associations between miRNAs from the dataset and different disease pathways or biological functions. These predictions are primarily based on previously publish datasets derived from a broad diversity of animal models. The miRNA dataset included in **Figure 2** was obtained from murine whole lung homogenate 48 h following subchronic exposure to *S. chartarum* (98). When analyzing the top diseases and biological functions of the miRNAs included in the dataset, a handful were predicted to be involved in an inflammatory response, specifically in organ inflammation,

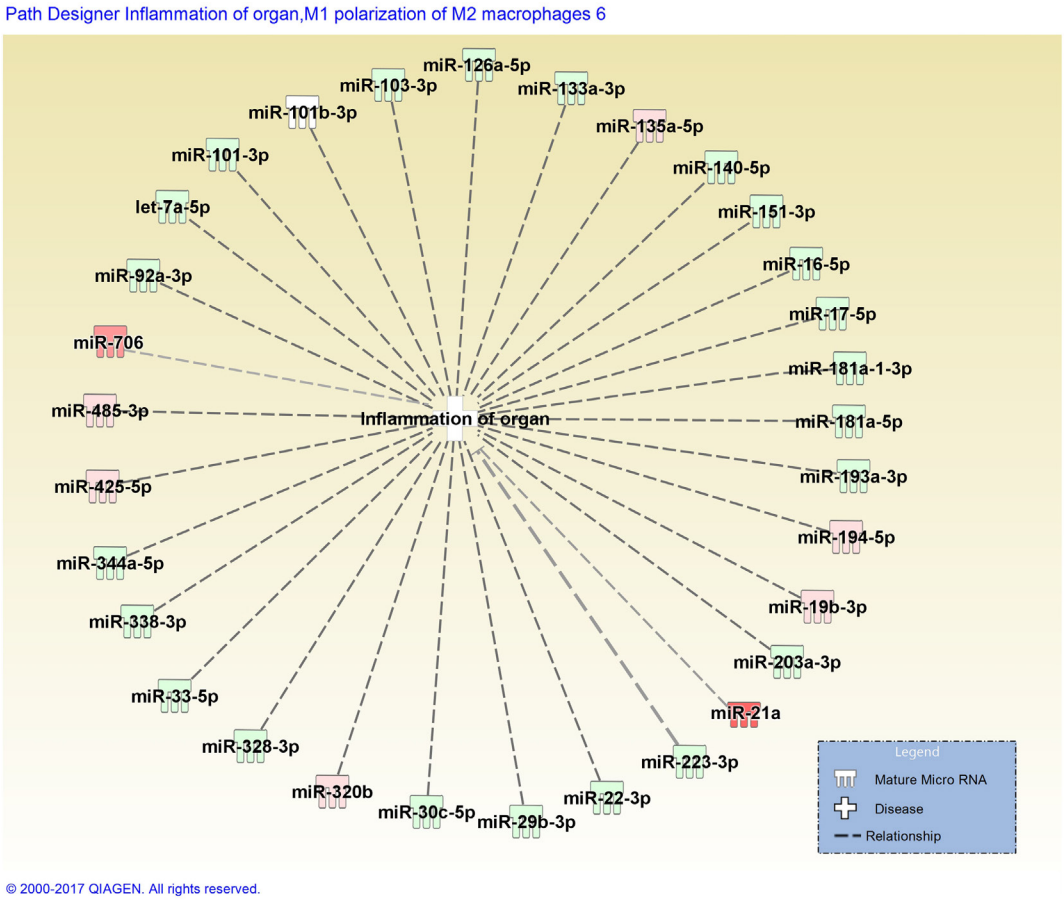

FIGURE 2 | Disease network map generated by Ingenuity Pathway Analysis depicting miRNAs involved in the inflammation of organs. miRNAs are color-coded (red or green for up- and downregulation, respectively) for the expression of miRNAs in *Stachybotrys chartarum* exposed versus control at 13 weeks, 48 h post-exposure. Gray dotted lines represent predicted regulated relationship.

illustrated in **Figure 2**. The miRNAs are color-coded depending on the respective expression level (red or green for up- and down-regulation, respectively). The absence of confirmed associations between miRNAs, evidenced by gray dotted lines, supports the lack of miRNA profile studies following fungal exposure.

To date, only a handful of studies have examined the altered miRNA profiles following fungal exposure; therefore, more researches are required to fully understand the mechanistic influence miRNAs have on the immune response. With the increased interest in studying miRNAs, methodological approaches are becoming more advanced by using next-generation sequencing methods that examine miRNA profiles in more depth and at a higher precision compared with miRNA arrays. Once the more influential miRNAs are identified, strategies can be developed in order to manipulate the host response. With the use of transgenic or knockout animal models, the functionality of miRNAs or genes can be elucidated; however, the manipulation of the genome may in fact alter normal miRNA production or function, contributing to the phenotype of the disease (134). Targeting miRNAs that are upregulated or replacing the expression of miRNAs that are downregulated are potential strategies that could be tested in animal models as a new therapeutic strategy to treat fungal infections and diseases. This targeting strategy could be completed through the use of an anti-miR or a miRNA mimic (135), and may allow for the manipulation of a group of genes or proteins that participate in the progression of the infection or disease. Ultimately, these targeting strategies will help bridge the knowledge gap between the identification of miRNAs and the host responses to fungal exposure, potentially leading to advanced therapeutics to combat adverse effects resulting from exposure to pathogenic fungi.

CONCLUSION

In this review, the identification and influence of miRNAs on the host immune responses following fungal exposure were examined. Compared with existing datasets examining miRNA profiles in allergic and inflammatory models, some common differentially expressed miRNAs were identified in fungal exposed models. Influential miRNAs altered in different disease models, such as miR-132, functions to maintain a normal hematopoietic output during an immune response and regulates genes at the beginning of an immune response to regain homeostasis of the immune system. Other common miRNAs identified in

multiple inflammatory disease models, including miR-155 and miR-146a, regulates critical genes involved in the host defense system through opposing mechanisms. For example, miR-146a is known to decrease cytokine production and inhibits Th1 cells following an inflammatory stimulus, as well as induces alternative activation of macrophages, whereas miR-155 stimulates both Th1 and Th17 immune responses and induces classical activation of macrophages. Taken together, these miRNAs act in concert to defend the host from infection. In addition to common miRNAs identified in multiple diseased models, the miRNAs that were observed to be differentially expressed specifically in fungal exposed models could potentially serve as biomarkers for fungal exposures.

Recent discoveries in miRNA biology have heightened the research community's interest in examining the altered genetic profiles in different disease models; however, only a few studies have examined miRNA profiles following fungal exposure. As such, the description of the immune responses to the corresponding miRNAs listed in **Table 1** was not all compiled from fungal exposure studies due to the lack of research examining the influence of miRNAs on the immune responses following fungal exposure. Although advancements made in this field have helped elucidate mechanisms underlying host responses to a variety of infections and diseases, further examination of miRNA profiles, specifically in fungal exposed models, is required in order to provide greater mechanistic insight into the immunological response to clinically and environmentally relevant fungal species.

AUTHOR CONTRIBUTIONS

TC and BG designed the manuscript; TC drafted the manuscript and prepared figures/tables; TC, AL, DB, and BG revised and edited the manuscript; TC, AL, DB, and BG approved the final version of the manuscript and agree to be accountable for the content of the work.

ACKNOWLEDGMENTS

The findings and conclusions in this report are those of the author(s) and do not necessarily represent the official position of the National Institute for Occupational Safety and Health, Centers for Disease Control and Prevention. The author declares no conflict of interest.

REFERENCES

1. Hawksworth DL. The magnitude of fungal diversity: the 1.5 million species estimate revised. *Mycol Res* (2001) 105:1422–32. doi:10.1017/S0953756201004725
2. Cannon R, Firth N. Fungi and fungal infections of the oral cavity. In: Lamont R, Burne R, Lantz M, LeBlanc D, editors. *Oral Microbiology and Immunology* Washington, DC: ASM Press (2006). p. 333–48.
3. Eduard W. Fungal spores: a critical review of the toxicological and epidemiological evidence as a basis for occupational exposure limit setting. *Crit Rev Toxicol* (2009) 39(10):799–864. doi:10.3109/10408440903307333
4. Benedict K, Park BJ. Invasive fungal infections after natural disasters. *Emerg Infect Dis* (2014) 20(3):349–55. doi:10.3201/eid2003.131230
5. Klein BS, Tebbets B. Dimorphism and virulence in fungi. *Curr Opin Microbiol* (2007) 10(4):314–9. doi:10.1016/j.mib.2007.04.002
6. Gauthier GM. Dimorphism in fungal pathogens of mammals, plants, and insects. *PLoS Pathog* (2015) 11(2):e1004608. doi:10.1371/journal.ppat.1004608
7. Bajwa SJ, Kulshrestha A. Fungal infections in intensive care unit: challenges in diagnosis and management. *Ann Med Health Sci Res* (2013) 3(2):238–44. doi:10.4103/2141-9248.113669
8. IoM. *Damp Indoor Spaces and Health*. Washington, DC, USA: National Academies Press (2004).
9. WHO. *WHO Guidelines for Indoor Air Quality: Dampness and Mould*. Geneva: WHO Regional Office for Europe (2009).
10. Mendell MJ, Mirer AG, Cheung K, Tong M, Douwes J. Respiratory and allergic health effects of dampness, mold, and dampness-related agents: a review of the epidemiologic evidence. *Environ Health Perspect* (2011) 119(6):748–56. doi:10.1289/ehp.1002410
11. Quansah R, Jaakkola MS, Hugg TT, Heikkinen SA, Jaakkola JJ. Residential dampness and molds and the risk of developing asthma: a systematic review and meta-analysis. *PLoS One* (2012) 7(11):e47526. doi:10.1371/journal.pone.0047526
12. Kuhn DM, Ghannoum MA. Indoor mold, toxigenic fungi, and *Stachybotrys chartarum*: infectious disease perspective. *Clin Microbiol Rev* (2003) 16(1):144–72. doi:10.1128/CMR.16.1.144-172.2003
13. Johanning E, Biagini R, Hull D, Morey P, Jarvis B, Landsbergis P. Health and immunology study following exposure to toxigenic fungi (*Stachybotrys chartarum*) in a water-damaged office environment. *Int Arch Occup Environ Health* (1996) 68(4):207–18. doi:10.1007/s004200050052
14. Andersson MA, Nikulin M, Koljalg U, Andersson MC, Rainey F, Reijula K, et al. Bacteria, molds, and toxins in water-damaged building materials. *Appl Environ Microbiol* (1997) 63(2):387–93.
15. Pestka JJ, Yike I, Dearborn DG, Ward MD, Harkema JR. *Stachybotrys chartarum*, trichothecene mycotoxins, and damp building-related illness: new insights into a public health enigma. *Toxicol Sci* (2008) 104(1):4–26. doi:10.1093/toxsci/kfm284
16. Bartel DP. MicroRNAs: genomics, biogenesis, mechanism, and function. *Cell* (2004) 116(2):281–97. doi:10.1016/S0092-8674(04)00045-5
17. Li L-C, Okino ST, Zhao H, Pookot D, Place RF, Urakami S, et al. Small dsRNAs induce transcriptional activation in human cells. *Proc Natl Acad Sci U S A* (2006) 103(46):17337–42. doi:10.1073/pnas.0607015103
18. Janowski BA, Younger ST, Hardy DB, Ram R, Huffman KE, Corey DR. Activating gene expression in mammalian cells with promoter-targeted duplex RNAs. *Nat Chem Biol* (2007) 3(3):166–73. doi:10.1038/nchembio860
19. Place RF, Li L-C, Pookot D, Noonan EJ, Dahiya R. MicroRNA-373 induces expression of genes with complementary promoter sequences. *Proc Natl Acad Sci U S A* (2008) 105(5):1608–13. doi:10.1073/pnas.0707594105
20. Lu TX, Rothenberg ME. Diagnostic, functional, and therapeutic roles of microRNA in allergic diseases. *J Allergy Clin Immunol* (2013) 132(1):3–13; quiz 14. doi:10.1016/j.jaci.2013.04.039
21. Lu TX, Lim E-J, Wen T, Plassard AJ, Martin LJ, Aronow BJ, et al. miR-375 is down-regulated in epithelial cells after IL-13 stimulation and regulates an IL-13 induced epithelial transcriptome. *Mucosal Immunol* (2012) 5(4):388–96. doi:10.1038/mi.2012.16
22. Dix A, Czakai K, Leonhardt I, Schäferhoff K, Bonin M, Guthke R, et al. Specific and novel microRNAs are regulated as response to fungal infection in human dendritic cells. *Front Microbiol* (2017) 8:270. doi:10.3389/fmicb.2017.00270
23. Lewis BP, Shih IH, Jones-Rhoades MW, Bartel DP, Burge CB. Prediction of mammalian microRNA targets. *Cell* (2003) 115(7):787–98. doi:10.1016/S0092-8674(03)01018-3
24. Lewis BP, Burge CB, Bartel DP. Conserved seed pairing, often flanked by adenosines, indicates that thousands of human genes are microRNA targets. *Cell* (2005) 120(1):15–20. doi:10.1016/j.cell.2004.12.035
25. Carthew RW, Sontheimer EJ. Origins and mechanisms of miRNAs and siRNAs. *Cell* (2009) 136(4):642–55. doi:10.1016/j.cell.2009.01.035

26. Vasudevan S, Tong Y, Steitz JA. Switching from repression to activation: microRNAs can up-regulate translation. *Science* (2007) 318(5858):1931–4. doi:10.1126/science.1149460
27. Krek A, Grun D, Poy MN, Wolf R, Rosenberg L, Epstein EJ, et al. Combinatorial microRNA target predictions. *Nat Genet* (2005) 37(5):495–500. doi:10.1038/ng1536
28. Rajewsky N. MicroRNA target predictions in animals. *Nat Genet* (2006) 38:S8–13. doi:10.1038/ng1798
29. Bartel DP. MicroRNA target recognition and regulatory functions. *Cell* (2009) 136(2):215–33. doi:10.1016/j.cell.2009.01.002
30. Friedman RC, Farh KK-H, Burge CB, Bartel DP. Most mammalian mRNAs are conserved targets of microRNAs. *Genome Res* (2009) 19(1):92–105. doi:10.1101/gr.082701.108
31. van Rooij E, Olson EN. MicroRNAs: powerful new regulators of heart disease and provocative therapeutic targets. *J Clin Invest* (2007) 117(9):2369–76. doi:10.1172/JCI33099
32. Hackl M, Brunner S, Fortschegger K, Schreiner C, Micutkova L, Muck C, et al. miR-17, miR-19b, miR-20a, and miR-106a are down-regulated in human aging. *Aging Cell* (2010) 9(2):291–6. doi:10.1111/j.1474-9726.2010.00549.x
33. Leopold JA, Maron BA. Molecular mechanisms of pulmonary vascular remodeling in pulmonary arterial hypertension. *Int J Mol Sci* (2016) 17(5):761. doi:10.3390/ijms17050761
34. Posch W, Heimdörfer D, Wilflingseder D, Lass-Flörl C. Invasive candidiasis: future directions in non-culture based diagnosis. *Expert Rev Anti Infect Ther* (2017) 15:829–38. doi:10.1080/14787210.2017.1370373
35. Frost RJA, Olson EN. Control of glucose homeostasis and insulin sensitivity by the Let-7 family of microRNAs. *Proc Natl Acad Sci U S A* (2011) 108(52):21075–80. doi:10.1073/pnas.1118922109
36. Jen-Liang S, Pai-Sheng C, Gunnar J, Min-Liang K. Function and regulation of let-7 family microRNAs. *Microrna* (2012) 1(1):34–9. doi:10.2174/2211536611201010034
37. Jun-Hao ET, Gupta RR, Shyh-Chang N. Lin28 and let-7 in the metabolic physiology of aging. *Trends Endocrinol Metab* (2016) 27(3):132–41. doi:10.1016/j.tem.2015.12.006
38. Brennan E, Wang B, McClelland A, Mohan M, Marai M, Beuscart O, et al. Protective effect of let-7 miRNA family in regulating inflammation in diabetes-associated atherosclerosis. *Diabetes* (2017) 66(8):2266. doi:10.2337/db16-1405
39. Pal AS, Kasinski AL. Animal models to study microRNA function. *Adv Cancer Res* (2017) 135:53–118. doi:10.1016/bs.acr.2017.06.006
40. Polikepahad S, Knight JM, Naghavi AO, Oplt T, Creighton CJ, Shaw C, et al. Proinflammatory role for let-7 microRNAS in experimental asthma. *J Biol Chem* (2010) 285(39):30139–49. doi:10.1074/jbc.M110.145698
41. Lu TX, Munitz A, Rothenberg ME. MicroRNA-21 is up-regulated in allergic airway inflammation and regulates IL-12p35 expression. *J Immunol* (2009) 182(8):4994–5002. doi:10.4049/jimmunol.0803560
42. Zhou R, Hu G, Liu J, Gong AY, Drescher KM, Chen XM. NF-kappaB p65-dependent transactivation of miRNA genes following *Cryptosporidium parvum* infection stimulates epithelial cell immune responses. *PLoS Pathog* (2009) 5(12):e1000681. doi:10.1371/journal.ppat.1000681
43. Eulalio A, Schulte L, Vogel J. The mammalian microRNA response to bacterial infections. *RNA Biol* (2012) 9(6):742–50. doi:10.4161/rna.20018
44. Chen Y, Chen J, Wang H, Shi J, Wu K, Liu S, et al. HCV-induced miR-21 contributes to evasion of host immune system by targeting MyD88 and IRAK1. *PLoS Pathog* (2013) 9(4):e1003248. doi:10.1371/journal.ppat.1003248
45. Lu S, Mukkada VA, Mangray S, Cleveland K, Shillingford N, Schorl C, et al. MicroRNA profiling in mucosal biopsies of eosinophilic esophagitis patients pre and post treatment with steroids and relationship with mRNA targets. *PLoS One* (2012) 7(7):e40676. doi:10.1371/journal.pone.0040676
46. Lu TX, Sherrill JD, Wen T, Plassard AJ, Besse JA, Abonia JP, et al. MicroRNA signature in patients with eosinophilic esophagitis, reversibility with glucocorticoids, and assessment as disease biomarkers. *J Allergy Clin Immunol* (2012) 129(4):1064–75.e9. doi:10.1016/j.jaci.2012.01.060
47. Lu TX, Lim E-J, Besse JA, Itskovich S, Plassard AJ, Fulkerson PC, et al. miR-223 deficiency increases eosinophil progenitor proliferation. *J Immunol* (2013) 190(4):1576–82. doi:10.4049/jimmunol.1202897
48. Lu TX, Lim E-J, Itskovich S, Besse JA, Plassard AJ, Mingler MK, et al. Targeted ablation of miR-21 decreases murine eosinophil progenitor cell growth. *PLoS One* (2013) 8(3):e59397. doi:10.1371/journal.pone.0059397
49. Mattes J, Collison A, Plank M, Phipps S, Foster PS. Antagonism of microRNA-126 suppresses the effector function of T(H)2 cells and the development of allergic airways disease. *Proc Natl Acad Sci U S A* (2009) 106(44):18704–9. doi:10.1073/pnas.0905063106
50. Collison A, Mattes J, Plank M, Foster PS. Inhibition of house dust mite-induced allergic airways disease by antagonism of microRNA-145 is comparable to glucocorticoid treatment. *J Allergy Clin Immunol* (2011) 128(1):160–167.e4. doi:10.1016/j.jaci.2011.04.005
51. Sharma A, Kumar M, Ahmad T, Mabalirajan U, Aich J, Agrawal A, et al. Antagonism of mmu-mir-106a attenuates asthma features in allergic murine model. *J Appl Physiol (1985)* (2012) 113(3):459–64. doi:10.1152/japplphysiol.00001.2012
52. Izzotti A, Bagnasco M, Cartiglia C, Longobardi M, Balansky RM, Merello A, et al. Chemoprevention of genome, transcriptome, and proteome alterations induced by cigarette smoke in rat lung. *Eur J Cancer* (2005) 41(13):1864–74. doi:10.1016/j.ejca.2005.04.011
53. Izzotti A, Calin GA, Arrigo P, Steele VE, Croce CM, De Flora S. Downregulation of microRNA expression in the lungs of rats exposed to cigarette smoke. *FASEB J* (2009) 23(3):806–12. doi:10.1096/fj.08-121384
54. Izzotti A, Calin GA, Steele VE, Croce CM, De Flora S. Relationships of microRNA expression in mouse lung with age and exposure to cigarette smoke and light. *FASEB J* (2009) 23(9):3243–50. doi:10.1096/fj.09-135251
55. Simpson LJ, Patel S, Bhakta NR, Choy DF, Brightbill HD, Ren X, et al. A microRNA upregulated in asthma airway T cells promotes TH2 cytokine production. *Nat Immunol* (2014) 15(12):1162–70. doi:10.1038/ni.3026
56. Liu F, Qin HB, Xu B, Zhou H, Zhao DY. Profiling of miRNAs in pediatric asthma: upregulation of miRNA-221 and miRNA-485-3p. *Mol Med Rep* (2012) 6(5):1178–82. doi:10.3892/mmr.2012.1030
57. Anderson SE, Beezhold K, Lukomska E, Richardson J, Long C, Anderson K, et al. Expression kinetics of miRNA involved in dermal toluene 2,4-diisocyanate sensitization. *J Immunotoxicol* (2014) 11(3):250–9. doi:10.3109/1547691X.2013.835891
58. Carissimi C, Fulci V, Macino G. MicroRNAs: novel regulators of immunity. *Autoimmun Rev* (2009) 8(6):520–4. doi:10.1016/j.autrev.2009.01.008
59. Xiao C, Rajewsky K. MicroRNA control in the immune system: basic principles. *Cell* (2009) 136(1):26–36. doi:10.1016/j.cell.2008.12.027
60. Gracias DT, Katsikis PD. MicroRNAs: key components of immune regulation. In: Pulendran B, Katsikis PD, Schoenberger SP, editors. *Crossroads between Innate and Adaptive Immunity III*. New York, NY: Springer (2011). p. 15–26.
61. Chen CZ, Li L, Lodish HF, Bartel DP. MicroRNAs modulate hematopoietic lineage differentiation. *Science* (2004) 303(5654):83–6. doi:10.1126/science.1091903
62. Xiao C, Calado DP, Galler G, Thai TH, Patterson HC, Wang J, et al. miR-150 controls B cell differentiation by targeting the transcription factor c-Myb. *Cell* (2007) 131(1):146–59. doi:10.1016/j.cell.2007.07.021
63. Xiao C, Srinivasan L, Calado DP, Patterson HC, Zhang B, Wang J, et al. Lymphoproliferative disease and autoimmunity in mice with elevated miR-17-92 expression in lymphocytes. *Nat Immunol* (2008) 9(4):405–14. doi:10.1038/ni1575
64. Lu L-F, Liston A. MicroRNA in the immune system, microRNA as an immune system. *Immunology* (2009) 127(3):291–8. doi:10.1111/j.1365-2567.2009.03092.x
65. Li Q-J, Chau J, Ebert PJR, Sylvester G, Min H, Liu G, et al. miR-181a is an intrinsic modulator of T cell sensitivity and selection. *Cell* (2007) 129(1):147–61. doi:10.1016/j.cell.2007.03.008
66. Monticelli S, Ansel KM, Xiao C, Socci ND, Krichevsky AM, Thai T-H, et al. MicroRNA profiling of the murine hematopoietic system. *Genome Biol* (2005) 6(8):R71–71. doi:10.1186/gb-2005-6-8-r71
67. Wu H, Neilson JR, Kumar P, Manocha M, Shankar P, Sharp PA, et al. miRNA profiling of naïve, effector and memory CD8 T cells. *PLoS One* (2007) 2(10):e1020. doi:10.1371/journal.pone.0001020
68. Jeker LT, Bluestone JA. MicroRNA regulation of T-cell differentiation and function. *Immunol Rev* (2013) 253(1):65–81. doi:10.1111/imr.12061
69. Jiang S, Li C, Olive V, Lykken E, Feng F, Sevilla J, et al. Molecular dissection of the miR-17-92 cluster's critical dual roles in promoting Th1 responses and preventing inducible Treg differentiation. *Blood* (2011) 118(20):5487–97. doi:10.1182/blood-2011-05-355644

70. Haasch D, Chen Y-W, Reilly RM, Grace Chiou X, Koterski S, Smith ML, et al. T cell activation induces a noncoding RNA transcript sensitive to inhibition by immunosuppressant drugs and encoded by the proto-oncogene, BIC. *Cell Immunol* (2002) 217(1):78–86. doi:10.1016/S0008-8749(02)00506-3
71. Pedersen I, David M. MicroRNAs in the immune response. *Cytokine* (2008) 43(3):391–4. doi:10.1016/j.cyto.2008.07.016
72. Taganov KD, Boldin MP, Chang K-J, Baltimore D. NF-κB-dependent induction of microRNA miR-146, an inhibitor targeted to signaling proteins of innate immune responses. *Proc Natl Acad Sci U S A* (2006) 103(33):12481–6. doi:10.1073/pnas.0605298103
73. Rodriguez A, Vigorito E, Clare S, Warren MV, Couttet P, Soond DR, et al. Requirement of bic/microRNA-155 for normal immune function. *Science* (2007) 316(5824):608–11. doi:10.1126/science.1139253
74. Martinez-Nunez RT, Louafi F, Sanchez-Elsner T. The interleukin 13 (IL-13) pathway in human macrophages is modulated by microRNA-155 via direct targeting of interleukin 13 receptor α1 (IL13Rα1). *J Biol Chem* (2011) 286(3):1786–94. doi:10.1074/jbc.M110.169367
75. Roy S. miRNA in macrophage development and function. *Antioxid Redox Signal* (2016) 25(15):795–804. doi:10.1089/ars.2016.6728
76. Banerjee S, Xie N, Cui H, Tan Z, Yang S, Icyuz M, et al. MicroRNA let-7c regulates macrophage polarization. *J Immunol* (2013) 190(12):6542–9. doi:10.4049/jimmunol.1202496
77. Zhuang G, Meng C, Guo X, Cheruku PS, Shi L, Xu H, et al. A novel regulator of macrophage activation clinical perspective miR-223 in obesity-associated adipose tissue inflammation. *Circulation* (2012) 125(23):2892–903. doi:10.1161/CIRCULATIONAHA.111.087817
78. Veremeyko T, Siddiqui S, Sotnikov I, Yung A, Ponomarev ED. IL-4/IL-13-dependent and independent expression of miR-124 and its contribution to M2 phenotype of monocytic cells in normal conditions and during allergic inflammation. *PLoS One* (2013) 8(12):e81774. doi:10.1371/journal.pone.0081774
79. O'Connell RM, Rao DS, Chaudhuri AA, Baltimore D. Physiological and pathological roles for microRNAs in the immune system. *Nat Rev Immunol* (2010) 10(2):111–22. doi:10.1038/nri2708
80. O'Neill LA, Sheedy FJ, McCoy CE. MicroRNAs: the fine-tuners of toll-like receptor signalling. *Nat Rev Immunol* (2011) 11(3):163–75. doi:10.1038/nri2957
81. Case SR, Martin RJ, Jiang D, Minor MN, Chu HW. MicroRNA-21 inhibits toll-like receptor 2 agonist-induced lung inflammation in mice. *Exp Lung Res* (2011) 37(8):500–8. doi:10.3109/01902148.2011.596895
82. Lu TX, Hartner J, Lim EJ, Fabry V, Mingler MK, Cole ET, et al. MicroRNA-21 limits in vivo immune response-mediated activation of the IL-12/IFN-gamma pathway, Th1 polarization, and the severity of delayed-type hypersensitivity. *J Immunol* (2011) 187(6):3362–73. doi:10.4049/jimmunol.1101235
83. Chen X, Liang H, Zhang J, Zen K, Zhang CY. MicroRNAs are ligands of toll-like receptors. *RNA* (2013) 19(6):737–9. doi:10.1261/rna.036319.112
84. Chaudhuri AA, So AY, Sinha N, Gibson WS, Taganov KD, O'Connell RM, et al. MicroRNA-125b potentiates macrophage activation. *J Immunol* (2011) 187(10):5062–8. doi:10.4049/jimmunol.1102001
85. Zhang XH, Zhang YN, Li HB, Hu CY, Wang N, Cao PP, et al. Overexpression of miR-125b, a novel regulator of innate immunity, in eosinophilic chronic rhinosinusitis with nasal polyps. *Am J Respir Crit Care Med* (2012) 185(2):140–51. doi:10.1164/rccm.201103-0456OC
86. Podshivalova K, Salomon DR. MicroRNA regulation of T lymphocyte immunity: modulation of molecular networks responsible for T cell activation, differentiation and development. *Crit Rev Immunol* (2013) 33(5):435–76. doi:10.1615/CritRevImmunol.2013006858
87. Kastle M, Bartel S, Geillinger-Kastle K, Irmler M, Beckers J, Ryffel B, et al. MicroRNA cluster 106a~363 is involved in T helper 17 cell differentiation. *Immunology* (2017) 152:402–13. doi:10.1111/imm.12775
88. Liston A, Lu LF, O'Carroll D, Tarakhovsky A, Rudensky AY. Dicer-dependent microRNA pathway safeguards regulatory T cell function. *J Exp Med* (2008) 205(9):1993–2004. doi:10.1084/jem.20081062
89. Murugaiyan G, da Cunha AP, Ajay AK, Joller N, Garo LP, Kumaradevan S, et al. MicroRNA-21 promotes Th17 differentiation and mediates experimental autoimmune encephalomyelitis. *J Clin Invest* (2015) 125(3):1069–80. doi:10.1172/JCI74347
90. Das Gupta M, Fliesser M, Springer J, Breitschopf T, Schlossnagel H, Schmitt AL, et al. *Aspergillus fumigatus* induces microRNA-132 in human monocytes and dendritic cells. *Int J Med Microbiol* (2014) 304(5–6):592–6. doi:10.1016/j.ijmm.2014.04.005
91. Croston TL, Nayak AP, Lemons AR, Goldsmith WT, Gu JK, Germolec DR, et al. Influence of *Aspergillus fumigatus* conidia viability on murine pulmonary microRNA and mRNA expression following subchronic inhalation exposure. *Clin Exp Allergy* (2016) 46(10):1315–27. doi:10.1111/cea.12783
92. Monk CE, Hutvagner G, Arthur JSC. Regulation of miRNA transcription in macrophages in response to *Candida albicans*. *PLoS One* (2010) 5(10):e13669. doi:10.1371/journal.pone.0013669
93. Agustinho DP, de Oliveira MA, Tavares AH, Derengowski L, Stolz V, Guilhelmelli F, et al. Dectin-1 is required for miR155 upregulation in murine macrophages in response to *Candida albicans*. *Virulence* (2017) 8(1):41–52. doi:10.1080/21505594.2016.1200215
94. Du L, Chen X, Duan Z, Liu C, Zeng R, Chen Q, et al. miR-146a negatively regulates dectin-1-induced inflammatory responses. *Oncotarget* (2017) 8(23):37355–66. doi:10.18632/oncotarget.16958
95. Chen H, Jin Y, Chen H, Liao N, Wang Y, Chen J. MicroRNA-mediated inflammatory responses induced by *Cryptococcus neoformans* are dependent on the NF-kappaB pathway in human monocytes. *Int J Mol Med* (2017) 39(6):1525–32. doi:10.3892/ijmm.2017.2951
96. De Lacorte Singulani J, De Fátima Da Silva J, Gullo FP, Costa MC, Fusco-Almeida AM, Enguita FJ, et al. Preliminary evaluation of circulating microRNAs as potential biomarkers in paracoccidioidomycosis. *Biomed Rep* (2017) 6(3):353–7. doi:10.3892/br.2017.849
97. Turini Gonzales Marioto D, Navarro Dos Santos Ferraro AC, Goulart de Andrade F, Barros Oliveira M, Itano EN, Petrofeza S, et al. Study of differential expression of miRNAs in lung tissue of mice submitted to experimental infection by *Paracoccidioides brasiliensis*. *Med Mycol* (2017) 55:774–84. doi:10.1093/mmy/myw135
98. Croston TL, Nayak AP, Lemons AR, Goldsmith WT, Germolec DM, Beezhold DH, et al. Pulmonary immune response following subchronic *Stachybotrys chartarum* exposure. *J Allergy ClinImmunol* (2017) 139(2):AB75. doi:10.1016/j.jaci.2016.12.291
99. Kumar M, Ahmad T, Sharma A, Mabalirajan U, Kulshreshtha A, Agrawal A, et al. Let-7 microRNA-mediated regulation of IL-13 and allergic airway inflammation. *J Allergy ClinImmunol* (2011) 128(5):1077–85.e1–10. doi:10.1016/j.jaci.2011.04.034
100. Liu G, Abraham E. MicroRNAs in immune response and macrophage polarization. *Arterioscler Thromb Vasc Biol* (2013) 33(2):170–7. doi:10.1161/ATVBAHA.112.300068
101. Essandoh K, Li Y, Huo J, Fan G-C. miRNA-mediated macrophage polarization and its potential role in the regulation of inflammatory response. *Shock* (2016) 46(2):122–31. doi:10.1097/SHK.0000000000000604
102. Rivera A, Barr T, Rais M, Engelmann F, Messaoudi I. MicroRNAs regulate host immune response and pathogenesis during influenza infection in rhesus macaques. *Viral Immunol* (2016) 29(4):212–27. doi:10.1089/vim.2015.0074
103. Zhang N, Bevan MJ. Dicer controls CD8(+) T-cell activation, migration, and survival. *Proc Natl Acad Sci U S A* (2010) 107(50):21629–34. doi:10.1073/pnas.1016299107
104. Nahid MA, Yao B, Dominguez-Gutierrez PR, Kesavalu L, Satoh M, Chan EK. Regulation of TLR2-mediated tolerance and cross-tolerance through IRAK4 modulation by miR-132 and miR-212. *J Immunol* (2013) 190(3):1250–63. doi:10.4049/jimmunol.1103060
105. Testa U, Pelosi E, Castelli G, Labbaye C. miR-146 and miR-155: two key modulators of immune response and tumor development. *Noncoding RNA* (2017) 3(3):22. doi:10.3390/ncrna3030022
106. Suman S, Jones-Reed DZZ, Schmidt ML, Clark GJ, Klinge C, Barve S, et al. Alteration of miR-186 expression modifies inflammatory markers in normal epithelial and prostate cancer cell models. *FASEB J* (2017) 31(1 Suppl):757.716. doi:10.1096/fasebj.31.1_supplement.757.16
107. Liu S-Q, Jiang S, Li C, Zhang B, Li Q-J. miR-17-92 cluster targets phosphatase and tensin homology and Ikaros family zinc finger 4 to promote T(H)17-mediated inflammation. *J Biol Chem* (2014) 289(18):12446–56. doi:10.1074/jbc.M114.550723
108. Fontana L, Pelosi E, Greco P, Racanicchi S, Testa U, Liuzzi F, et al. MicroRNAs 17-5p-20a-106a control monocytopoiesis through AML1 targeting and

M-CSF receptor upregulation. *Nat Cell Biol* (2007) 9(7):775–87. doi:10.1038/ncb1613
109. Paladini L, Fabris L, Bottai G, Raschioni C, Calin GA, Santarpia L. Targeting microRNAs as key modulators of tumor immune response. *J Exp Clin Cancer Res* (2016) 35(1):103. doi:10.1186/s13046-016-0375-2
110. Quinn SR, O'Neill LA. A trio of microRNAs that control toll-like receptor signalling. *Int Immunol* (2011) 23(7):421–5. doi:10.1093/intimm/dxr034
111. Mehta A, Baltimore D. MicroRNAs as regulatory elements in immune system logic. *Nat Rev Immunol* (2016) 16(5):279–94. doi:10.1038/nri.2016.40
112. Ma F, Xu S, Liu X, Zhang Q, Xu X, Liu M, et al. The microRNA miR-29 controls innate and adaptive immune responses to intracellular bacterial infection by targeting interferon-[gamma]. *Nat Immunol* (2011) 12(9):861–9. doi:10.1038/ni.2073
113. Huang L, Liu Y, Wang L, Chen R, Ge W, Lin Z, et al. Down-regulation of miR-301a suppresses pro-inflammatory cytokines in toll-like receptor-triggered macrophages. *Immunology* (2013) 140(3):314–22. doi:10.1111/imm.12139
114. Vegh P, Magee DA, Nalpas NC, Bryan K, McCabe MS, Browne JA, et al. MicroRNA profiling of the bovine alveolar macrophage response to *Mycobacterium bovis* infection suggests pathogen survival is enhanced by microRNA regulation of endocytosis and lysosome trafficking. *Tuberculosis* (2015) 95(1):60–7. doi:10.1016/j.tube.2014.10.011
115. Warg LA, Oakes JL, Burton R, Neidermyer AJ, Rutledge HR, Groshong S, et al. The role of the E2F1 transcription factor in the innate immune response to systemic LPS. *Am J Physiol Lung Cell Mol Physiol* (2012) 303(5):L391–400. doi:10.1152/ajplung.00369.2011
116. Wong JJL, Ritchie W, Gao D, Lau KA, Gonzalez M, Choudhary A, et al. Identification of nuclear-enriched miRNAs during mouse granulopoiesis. *J Hematol Oncol* (2014) 7:42. doi:10.1186/1756-8722-7-42
117. Goldani LZ, Wirth F. Animal models and antifungal agents in paracoccidioidomycosis: an overview. *Mycopathologia* (2017) 182(7):633–43. doi:10.1007/s11046-017-0130-z
118. Terçarioli GR, Bagagli E, Reis GM, Theodoro RC, Bosco Sde M, Macoris SA, et al. Ecological study of *Paracoccidioides brasiliensis* in soil: growth ability, conidia production and molecular detection. *BMC Microbiol* (2007) 7(1):92. doi:10.1186/1471-2180-7-92
119. Bagagli E, Theodoro RC, Bosco SM, McEwen JG. *Paracoccidioides brasiliensis*: phylogenetic and ecological aspects. *Mycopathologia* (2008) 165(4–5):197–207. doi:10.1007/s11046-007-9050-7
120. Seo M, Choi J-S, Rho CR, Joo C-K, Lee SK. MicroRNA miR-466 inhibits lymphangiogenesis by targeting prospero-related homeobox 1 in the alkali burn corneal injury model. *J Biomed Sci* (2015) 22(1):3. doi:10.1186/s12929-014-0104-0
121. Colden M, Dar AA, Saini S, Dahiya PV, Shahryari V, Yamamura S, et al. MicroRNA-466 inhibits tumor growth and bone metastasis in prostate cancer by direct regulation of osteogenic transcription factor RUNX2. *Cell Death Dis* (2017) 8(1):e2572. doi:10.1038/cddis.2017.15
122. Wéry N. Bioaerosols from composting facilities—a review. *Front Cell Infect Microbiol* (2014) 4:42. doi:10.3389/fcimb.2014.00042
123. Pearson C, Littlewood E, Douglas P, Robertson S, Gant TW, Hansell AL. Exposures and health outcomes in relation to bioaerosol emissions from composting facilities: a systematic review of occupational and community studies. *J Toxicol Environ Health B Crit Rev* (2015) 18(1):43–69. doi:10.1080/10937404.2015.1009961
124. Symoens F, Burnod J, Lebeau B, Viviani MA, Piens MA, Tortorano AM, et al. Hospital-acquired *Aspergillus fumigatus* infection: can molecular typing methods identify an environmental source? *J Hosp Infect* (2002) 52(1):60–7. doi:10.1053/jhin.2002.1263
125. Kauffman CA, Nicolasora NP. Epidemiology of invasive pulmonary aspergillosis. In: Comarú Pasqualotto A, editor. *Aspergillosis: From Diagnosis to Prevention*. Dordrecht, Netherlands: Springer (2010). p. 329–44.
126. CDC. *Fungal Diseases: Candidiasis*. (2017). Available from: https://www.cdc.gov/fungal/diseases/candidiasis/index.html
127. CDC. *Fungal Diseases: Invasive Candidiasis Statistics*. (2017). Available from: https://www.cdc.gov/fungal/diseases/candidiasis/invasive/statistics.html
128. Epelbaum O, Chasan R. Candidemia in the intensive care unit. *Clin Chest Med* (2017) 38(3):493–509. doi:10.1016/j.ccm.2017.04.010
129. CDC. *Fungal Diseases: General Information about Candida auris*. (2016). Available from: https://www.cdc.gov/fungal/diseases/candidiasis/candida-auris-qanda.html
130. CDC. *Fungal Diseases: C. gattii Infection*. (2015). Available from: https://www.cdc.gov/fungal/diseases/cryptococcosis-gattii/index.html
131. CDC. *Fungal Diseases: C. neoformans Infection*. (2015). Available from https://www.cdc.gov/fungal/diseases/cryptococcosis-neoformans/index.html
132. Brown GD. Dectin-1: a signalling non-TLR pattern-recognition receptor. *Nat Rev Immunol* (2006) 6(1):33–43. doi:10.1038/nri1745
133. Buskirk AD, Green BJ, Lemons AR, Nayak AP, Goldsmith WT, Kashon ML, et al. A murine inhalation model to characterize pulmonary exposure to dry *Aspergillus fumigatus* conidia. *PLoS One* (2014) 9(10):e109855. doi:10.1371/journal.pone.0109855
134. Bhaskaran M, Mohan M. MicroRNAs: history, biogenesis, and their evolving role in animal development and disease. *Vet Pathol* (2014) 51(4):759–74. doi:10.1177/0300985813502820
135. Gibson NW. Engineered microRNA therapeutics. *J R Coll Physicians Edinb* (2014) 44(3):196–200. doi:10.4997/JRCPE.2014.302

Conflict of Interest Statement: The authors declare that the research was conducted in the absence of any commercial or financial relationships that could be construed as a potential conflict of interest.

Copyright © 2018 Croston, Lemons, Beezhold and Green. This is an open-access article distributed under the terms of the Creative Commons Attribution License (CC BY). The use, distribution or reproduction in other forums is permitted, provided the original author(s) and the copyright owner are credited and that the original publication in this journal is cited, in accordance with accepted academic practice. No use, distribution or reproduction is permitted which does not comply with these terms.

frontiers in Immunology

ORIGINAL RESEARCH
published: 14 July 2017
doi: 10.3389/fimmu.2017.00820

Autoimmune Regulator Deficiency Results in a Decrease in STAT1 Levels in Human Monocytes

*Ofer Zimmerman[1], Lindsey B. Rosen[1], Muthulekha Swamydas[1], Elise M. N. Ferre[1], Mukil Natarajan[1], Frank van de Veerdonk[2], Steven M. Holland[1] and Michail S. Lionakis[1]**

[1] Laboratory of Clinical Infectious Diseases, National Institute of Allergy and Immunology, National Institutes of Health, Bethesda, MD, United States, [2] Department of Internal Medicine, Radboud University Medical Center, Radboud Institute for Molecular Life Sciences (RILMS), Nijmegen, Netherlands

OPEN ACCESS

Edited by:
Steven Templeton, Indiana University School of Medicine – Terre Haute, United States

Reviewed by:
Claudio Pignata, University of Naples Federico II, Italy
Partha Sarathi Biswas, University of Pittsburgh, United States

***Correspondence:**
Michail S. Lionakis
lionakism@niaid.nih.gov

Specialty section:
This article was submitted to Microbial Immunology, a section of the journal Frontiers in Immunology

Received: 15 May 2017
Accepted: 29 June 2017
Published: 14 July 2017

Citation:
Zimmerman O, Rosen LB, Swamydas M, Ferre EMN, Natarajan M, van de Veerdonk F, Holland SM and Lionakis MS (2017) Autoimmune Regulator Deficiency Results in a Decrease in STAT1 Levels in Human Monocytes. Front. Immunol. 8:820. doi: 10.3389/fimmu.2017.00820

Autoimmune polyendocrinopathy-candidiasis-ectodermal dystrophy (APECED) is a rare primary immunodeficiency disorder typically caused by biallelic autoimmune regulator (*AIRE*) mutations that manifests with chronic mucocutaneous candidiasis (CMC) and autoimmunity. Patients with *STAT1* gain-of-function (GOF) mutations also develop CMC and autoimmunity; they exhibit increased STAT1 protein levels at baseline and STAT1 phosphorylation (pSTAT1) upon interferon (IFN)-γ stimulation relative to healthy controls. AIRE interacts functionally with a protein that directly regulates STAT1, namely protein inhibitor of activated STAT1, which inhibits STAT1 activation. Given the common clinical features between patients with *AIRE* and *STAT1* GOF mutations, we sought to determine whether APECED patients also exhibit increased levels of STAT1 protein and phosphorylation in $CD14^+$ monocytes. We obtained peripheral blood mononuclear cells from 8 APECED patients and 13 healthy controls and assessed the levels of STAT1 protein and STAT1 tyrosine phosphorylation at rest and following IFN-γ stimulation, as well as the levels of *STAT1* mRNA. The mean STAT1 protein levels in $CD14^+$ monocytes exhibited a ~20% significant decrease in APECED patients both at rest and after IFN-γ stimulation relative to that of healthy donors. Similarly, the mean peak value of IFN-γ-induced pSTAT1 level was ~20% significantly lower in APECED patients compared to that in healthy controls. The decrease in STAT1 and peak pSTAT1 in APECED patients was not accompanied by decreased *STAT1* mRNA or anti-IFN-γ autoantibodies; instead, it correlated with the presence of autoantibodies to type I IFN and decreased $AIRE^{-/-}$ monocyte surface expression of IFN-γ receptor 2. Our data show that, in contrast to patients with *STAT1* GOF mutations, APECED patients show a moderate but consistent and significant decrease in total STAT1 protein levels, associated with lower peak levels of pSTAT1 molecules after IFN-γ stimulation.

Keywords: STAT1, phosphorylation, chronic mucocutaneous candidiasis, *AIRE*, APECED, $CD14^+$ monocytes, IFN-γ

Abbreviations: APECED, autoimmune polyendocrinopathy-candidiasis-ectodermal dystrophy; APS-1, autoimmune polyglandular syndrome type-1; CC, coiled-coil; CMC, chronic mucocutaneous candidiasis; DB, DNA binding; GOF, gain-of-function; LOF, loss-of-function; PBMC, peripheral blood mononuclear cells; STAT, signal transducer and activator of transcription.

INTRODUCTION

Autoimmune polyendocrinopathy-candidiasis-ectodermal dystrophy (APECED) or autoimmune polyglandular syndrome type-1 (APS-1; OMIM 240300) is a monogenic disorder caused by biallelic mutations in the autoimmune regulator (*AIRE*) gene, a thymus-enriched transcription regulator that promotes central immune tolerance *via* the expression of peripheral tissue self-antigens in medullary thymic epithelial cells (1, 2). Additional AIRE functions have recently been proposed to also contribute to immunological tolerance (3–6). In addition, heterozygous dominant-negative *AIRE* mutations in the plant homeodomain 1 domain have also been described, associated with organ-specific APECED-associated autoimmune manifestations and/or chronic mucocutaneous candidiasis (CMC) (7–9). APECED patients manifest with a characteristic constellation of CMC and autoimmunity that involves both endocrine and non-endocrine tissues (10–12). In fact, APECED is the only CMC-associated primary immunodeficiency disorder in which CMC is the sole consistent infectious disease phenotype. In addition to the breakdown in mechanisms of T-cell tolerance, AIRE-deficient patients also have high titers of neutralizing autoantibodies against Th17 cytokines and tissue-specific autoantigens, which have been shown to correlate with the development of CMC and organ-specific autoimmune manifestations, respectively (13–15). In addition, APECED patients exhibit a decreased frequency of peripheral blood IL-17-producing $CD4^+$ T cells following PMA/ionomycin stimulation [(3, 15), Lionakis, unpublished observations].

Heterozygous *STAT1* gain-of-function (GOF) mutations were initially implicated in causing autosomal-dominant CMC (16, 17) but have thereafter also been associated with the development of autoimmunity that can involve endocrine and non-endocrine tissues (16–19); beyond these common clinical features between APECED and *STAT1* GOF mutations, patients with *STAT1* GOF mutations also develop a broad-spectrum of infectious, inflammatory, and vascular manifestations not seen in APECED (19). These *STAT1* mutations are considered GOF because of enhanced phosphorylated STAT1 molecules upon interferon (IFN)-γ stimulation (17, 20). Impaired production of Th17 cytokines by T-cells has been implicated in the pathogenesis of CMC in these patients (17, 19, 20).

Due to the overlap in CMC and other clinical features between patients with APECED and *STAT1* GOF mutations, and because AIRE interacts functionally with a protein inhibitor of activated STAT1 (PIAS1), which inhibits STAT1 activation (21, 22), we aimed to study STAT1 protein level and phosphorylation upon IFN-γ stimulation in patients with *AIRE* mutations and determine whether human AIRE deficiency phenocopies the cell-intrinsic enhanced STAT1 levels seen in patients with *STAT1* GOF mutations.

MATERIALS AND METHODS

Study Participants

Eight APECED patients were enrolled (2015–2017) on a NIAID IRB-approved protocol and provided written informed consent. All eight had a clinical diagnosis of APECED based on the development of any two manifestations within the classic triad of CMC, hypoparathyroidism, and adrenal insufficiency. The most common clinical manifestations among the eight APECED patients included CMC (88%), hypoparathyroidism (100%), adrenal insufficiency (88%), and enamel hypoplasia (100%). The full list and frequencies of clinical manifestations of the eight APECED patients are outlined in **Table 1**. The most common *AIRE* mutant allele in these eight patients was c.967_979del13 (60%), followed by c.769C>T (13%). Two patients were compound heterozygous for c.967_979del13 and c.769C>T, while the remaining six patients had six different *AIRE* genotypes. Samples from a patient carrying the c.1057G>A E353K *STAT1* GOF mutation and a patient with the autosomal dominant form of IFN-γ receptor 1 deficiency carrying the 818del4 mutation were also collected under a NIAID IRB-approved protocol and provided written informed consent. Healthy volunteer blood samples from 13 individuals were obtained for STAT1 protein evaluation and from 10 individuals for *STAT1* mRNA level determination under IRB-approved protocols through the Department of Transfusion Medicine, at the NIH Clinical Center. The study was conducted in accordance with the Helsinki Declaration.

Peripheral Blood Mononuclear Cells (PBMC) Isolation and Intracellular Staining for STAT1 and pSTAT1

STAT1 protein and pSTAT1 levels were examined using flow cytometry in paired APECED patients and healthy control individuals in seven independent experiments at rest and up to 60 min after IFN-γ stimulation. Each patient and healthy donor was evaluated only once. In six of the seven independent experiments, a single APECED patient was evaluated along with

TABLE 1 | Clinical manifestations of the eight autoimmune polyendocrinopathy-candidiasis-ectodermal dystrophy patients included in this study.

Manifestation[a]	Number of affected patients	% of affected patients
Adrenal insufficiency	7	88
Asplenia	1	13
Autoimmune hepatitis	2	25
Alopecia	1	13
B12 deficiency	3	38
Chronic mucocutaneous candidiasis	7	88
Enamel hypoplasia	8	100
Gastritis	3	38
Gonadal failure	3	38
Early-onset hypertension	4	50
Hypoparathyroidism	8	100
Hypothyroidism	3	38
Intestinal dysfunction	6	75
Keratoconjunctivitis	1	13
Nail dystrophy	1	13
Tubulointerstitial nephritis	1	13
Pneumonitis	2	25
Sjogren's-like syndrome	3	38
Urticarial eruption	3	38
Vitiligo	1	13

[a]*The manifestations are presented in alphabetical order.*

two accompanying healthy donors, and in one experiment two APECED patients were evaluated together with one accompanying healthy donor.

PBMC were isolated by density-gradient centrifugation using lymphocyte separation media (Lonza) and resuspended in RPMI culture media (Gibco), supplemented with pyruvate (100 mM, Sigma Aldrich), glutamate (200 mM, Life Technologies), penicillin/streptomycin (100 U/100 µg/ml, Life Technologies), 10% fetal bovine serum (Serum Source International) and HEPES (20 mM, General Electric).

Intracellular phosphorylated STAT1 (pSTAT1) and total STAT1 were determined by FACS analysis, as previously described (18, 23). Freshly isolated PBMC were resuspended at 10^6 cells per 100 µl in RPMI and were serum starved for 30 min, in polystyrene round-bottom tubes (Becton Dickinson Falcon). Cells were then incubated with FITC-conjugated anti-human CD14 (Becton Dickinson cat# 555397). Cells were then stimulated with IFN-γ (800 U/ml) for 15, 30, or 60 min at 37°C, fixed with 2% Paraformaldehyde (Electron Microscopy Sciences) at 37°C for 10 min, permeabilized with 100% methanol in dark on ice for 30 min, washed with PBS/2%FBS, and incubated for 1 h in the dark at 4°C with combinations of PerCP–Cy5.5-conjugated anti-human pSTAT1 (Y701) (Becton Dickinson cat# 560113) and Alexa Fluor 647-conjugated anti-human N-terminus STAT1 (Becton Dickinson cat# 558560) with Fix and Perm Medium B (Life technologies). Alexa Fluor 647-conjugated IgG1 isotype control (Becton Dickinson cat# 557783) was used. Baseline pSTAT1 levels were used as a control for the specificity of the PerCP–Cy5.5-conjugated anti-human pSTAT1 antibody, by comparing between pSTAT1 levels as expressed in geometric mean of fluorescence-at rest and after stimulation. Samples were washed once with PBS/2%FBS and resuspended in 1% Paraformaldehyde. All data were collected with LSR Fortessa or LSRII (Becton Dickinson) and analyzed with FlowJo software (Treestar, Ashland, OR, USA).

IFN-α, IFN-ω, and IFN-γ Autoantibody Detection

A particle-based multiplex assay was used to detect IFN-α, IFN-ω, and IFN-γ autoantibodies in the serum or plasma samples from the eight APECED patients and compared with healthy control subjects ($n = 100$) enrolled through the NIH Blood Bank, as previously described (24).

IFN-γ Receptors 1 and 2 Expression on Monocytes

Frozen PBMC from eight APECED patients and eight healthy donors were used for measuring IFN-γ receptors 1 and 2 levels on $CD14^+$ monocytes. Cells were resuspended at 10^6 cells per 100 µl in PBS and incubated with LIVE/DEAD® Fixable Aqua Dead Cell Stain Kit (ThermoFisher) in 4°C followed by staining with FITC-conjugated anti-human CD14 (Becton Dickinson cat# 555397), PE-conjugated anti CD119 (IFN-γ receptor 1; IFN-γR1; Becton Dickinson cat# 558937), or APC-conjugated anti-IFN-γ receptor 2 (IFN-γR2; R&D cat# FAB773A) for 30 min. PE-conjugated IgG2b κ isotype control (Cat# 555058) and APC-conjugated IgG isotype control (R&D cat# IC108A) were used for control staining. Cells were then washed with PBS/2%FBS and fixed with 1% PFA. Data were collected with LSRII (Becton Dickinson) and analyzed with FlowJo software (Treestar, Ashland, OR, USA). The geometric mean fluorescence intensity on monocytes for each receptor was calculated after subtracting the geometric mean fluorescence intensity of the corresponding isotype control staining.

STAT1 mRNA Expression Determination

Frozen PBMC from the 8 APECED patients and 10 healthy donors were used for measuring *STAT1* mRNA expression by quantitative PCR (qPCR). To determine the percent of live $CD14^+$ monocytes within PBMC, an aliquot of the PBMC was incubated with LIVE/DEAD® Fixable Violet Dead Cell Stain Kit (ThermoFisher) in 4°C followed by staining with FITC-conjugated anti-human CD14 (Becton Dickinson cat# 555397). Data were collected with LSRII (Becton Dickinson) and analyzed with FlowJo software (Treestar, Ashland, OR, USA). Among the live PBMC, the mean percentage of $CD14^+$ monocytes was similar in the patient and healthy donor groups: 7.2 ± 0.8 vs. 7.7 ± 1.7, respectively ($p = 0.75$). For mRNA extraction, the RNeasy kit (Qiagen) was used, according to the manufacturer's instructions. To convert mRNA to cDNA, the high-capacity cDNA reverse transcription kit (Applied Biosystems) was used. qPCR was then performed with TaqMan detection (TaqMan® Universal Master Mix II, with UNG; ThermoFisher), using the 7,500 real-time PCR system (Applied Biosystems) and predesigned primer and probe mixes for glyceraldehyde-3-phosphate dehydrogenase (GAPDH; ThermoFisher) or STAT1 (ThermoFisher). All qPCR assays were performed in duplicate and results were normalized to GAPDH transcript levels using the threshold cycle (Ct) method.

AIRE Sequencing

Genomic DNA was extracted from whole blood, amplified and sequenced for *AIRE* exons and flanking splice sites as previously described (25).

Statistical Analysis

The geometric mean of fluorescence for pSTAT1 or STAT1 protein levels was calculated using the FlowJo software and the values obtained from APECED patients were normalized to the values obtained from the same-day healthy control samples. All results were expressed as mean ± SEM unless otherwise indicated. Statistical analyses were performed by Student's *t*-test or Mann–Whitney U test, where appropriate, using the GraphPad Prism 7 software (La Jolla, CA, USA). A p value of less than 0.05 was considered significant.

RESULTS

We enrolled eight APECED patients from eight non-consanguineous families with clinical and genetic diagnosis of APECED. Two (25%) were male and six (75%) were female. The mean patient age was 22 years (range, 9–56 years); 3 (38%) were children, with a mean age of 11 years. Thirteen healthy donors were enrolled for same-day harvesting and comparative analyses

of STAT1 and pSTAT1 protein levels. A *STAT1* GOF patient was tested as control for enhanced STAT1 protein and pSTAT1 levels [patient 1 in Ref. (20)], and a patient with the autosomal dominant form of IFN-γR1 deficiency [patient described in the case report in Ref. (26)] was tested as control for absent IFN-γ-induced pSTAT1 stimulation (**Figures 1A,B**).

We examined STAT1 protein and pSTAT1 levels in paired APECED patients and healthy control individuals, at rest and up to 60 min after IFN-γ stimulation. We focused on IFN-γ because it induces STAT1 phosphorylation and homo-dimerization without the involvement of other STAT molecules as in the case of STAT1–STAT2 heterodimer formation induced by IFN-α stimulation (27, 28). We also focused on CD14$^+$ monocytes because of their relatively high levels of IFN-γ receptors 1 and 2, which allows for detection of rapid activation of STAT1 (29).

In all the eight tested APECED patients, STAT1 protein levels were lower than the same-day healthy donors mean levels (**Figure 1C**). The eight patients' mean CD14$^+$ monocyte STAT1 protein level at rest was ~80% of that observed in healthy donors ($p = 0.003$). After IFN-γ stimulation, the significant decrease in CD14$^+$ monocyte mean STAT1 protein level of APECED patients persisted at all examined time-points throughout the 60 min of the experiment (**Figure 1C**).

Consistent with previous reports (23), we found that pSTAT1 induction peaked 15 min after IFN-γ stimulation and started to decline toward baseline at 30 min after stimulation in all 13 healthy donor monocytes (**Figure 1A**). Similar kinetics of pSTAT1 induction peak and decline were observed in all eight APECED patients (**Figure 1A**). APECED patient monocytes' mean pSTAT1 levels at rest were not significantly different compared to healthy

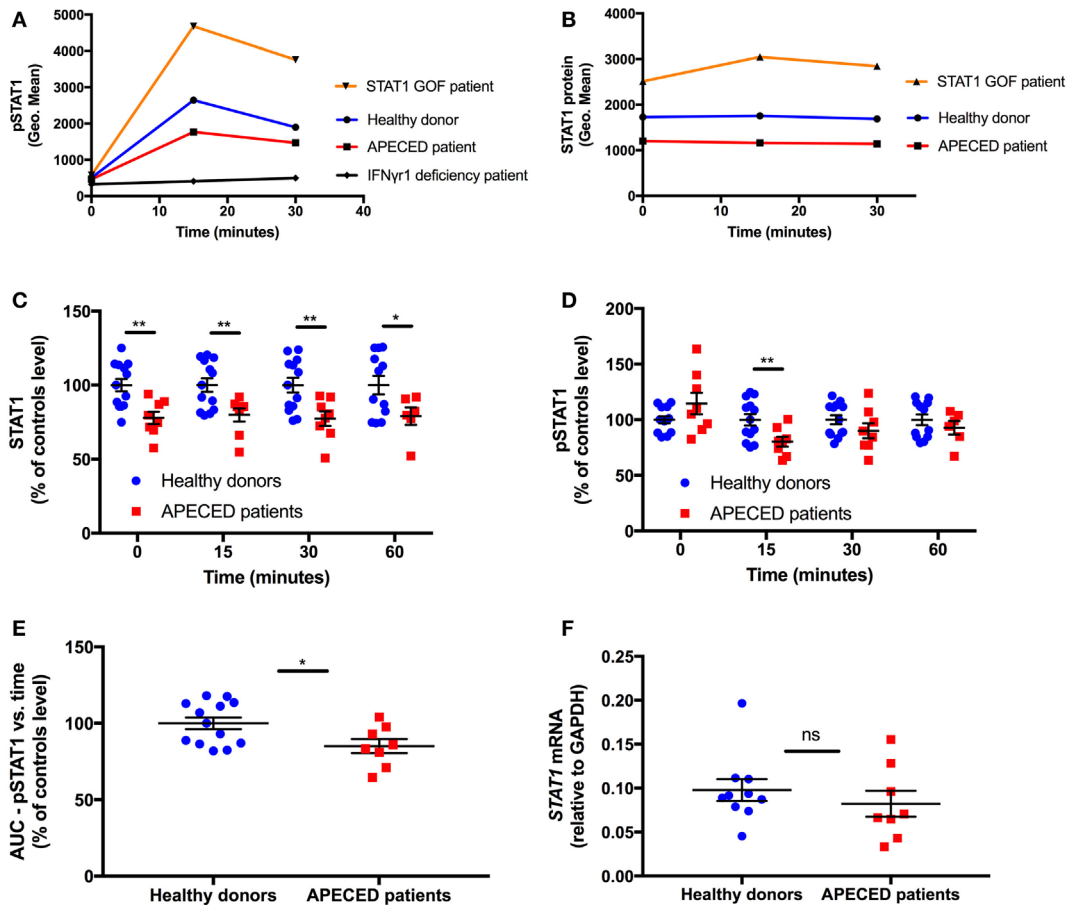

FIGURE 1 | Autoimmune regulator deficiency results in a decrease in STAT1 protein levels in human monocytes. **(A)** Representative depiction of pSTAT1 level at rest and up to 30 min after interferon (IFN)-γ stimulation in CD14$^+$ cells of a *STAT1* gain-of-function (GOF) patient (orange), an autoimmune polyendocrinopathy-candidiasis-ectodermal dystrophy (APECED) patient (red), a patient with the autosomal dominant form of IFN-γR1 deficiency (black) and a healthy donor (blue) **(B)** Representative depiction of STAT1 protein level at rest and up to 30 min after IFN-γ stimulation in CD14$^+$ cells of a *STAT1* GOF patient (orange), an APECED patient (red), and a healthy donor (blue). Protein and phosphorylation levels are expressed in geometric mean of fluorescence (Geo. Mean), as measured by flow cytometry. STAT1 total protein **(C)** and pSTAT1 **(D)** levels in CD14$^+$ cells of APECED patients ($n = 8$; red dots) and healthy donors ($n = 13$; blue dots) at rest (time 0) and up to 60 min after IFN-γ stimulation. Total protein and phosphorylation levels are expressed in % of the same-day control average values, for each time point—0, 15, 30, and 60 min, separately. **(E)** Area under the curve of CD14$^+$ cells STAT1 phosphorylation vs. time in APECED patients ($n = 8$; red dots) and healthy donors ($n = 13$; blue dots). **(F)** *STAT1* mRNA level, relative to glyceraldehyde-3-phosphate dehydrogenase, in peripheral blood mononuclear cells of healthy donors ($n = 10$) and APECED patients ($n = 8$) at rest. ns, not significant. $^*p < 0.05$; $^{**}p < 0.01$, by *t*-test. Quantitative data represent mean ± SEM.

donor levels at rest (108.7 ± 9.2% vs. 100 ± 2.83%, respectively, $p = 0.29$; **Figure 1D**). However, the mean peak pSTAT1 level of the APECED patients was 20% decreased compared to that seen in healthy donors at 15 min (80 ± 4.5% vs. 100 ± 4.5%, respectively. $p = 0.008$). Thereafter, at 30 min after IFN-γ stimulation, the patients' mean pSTAT1 level was lower than healthy donors (87 ± 5.1% vs. 100 ± 3.9%, respectively), and the difference was close to statistical significance ($p = 0.06$), whereas at 60 min after IFN-γ stimulation the differences in pSTAT1 levels between the patients and healthy donors groups were not significant (91 ± 5.5% vs. 100 ± 4.3%, respectively, $p = 0.25$; **Figure 1D**). We also calculated the area under the curve (AUC) of STAT1 phosphorylation (expressed as geometric mean of fluorescence) vs. time (expressed as minutes) for up to 60 min after IFN-γ stimulation in both groups and compared patient AUC level to the same-day healthy donor average. Consistent with the mean peak pSTAT1 values, APECED patients mean AUC levels were ~15% decreased relative to those seen in healthy controls ($p = 0.025$, **Figure 1E**). Because Th17 cells are decreased in peripheral blood of APECED [(3, 15), Lionakis, unpublished observations] and STAT1 GOF patients (17, 19, 20), our findings collectively indicate that the Th17 frequency decrease in AIRE deficiency is not caused by a STAT1 GOF state in peripheral blood monocytes.

Because among the eight APECED patients, seven different *AIRE* genotypes were observed, reflecting the greater genetic diversity of APECED in North America (25), we were not able to examine whether there is a correlation between specific *AIRE* mutations and the degree of pSTAT1 and total STAT1 levels in AIRE-deficient monocytes.

Given the decreased STAT1 protein levels seen in APECED patients, we asked whether *STAT1* is also decreased at the mRNA level in APECED patients. Thus, we compared *STAT1* mRNA levels by qPCR in PBMC of 8 APECED patients and 10 healthy donors and found them to be similar ($p = 0.32$) (**Figure 1F**).

Because APECED patients are known to have autoantibodies against cytokines, we examined whether autoantibodies to type I IFNs or IFN-γ were present in the serum of the eight APECED patients, which could potentially affect the levels of pSTAT1 in the patients group, after IFN-γ stimulation. All eight tested patients had autoantibodies to IFN-α and IFN-ω, while no patient had autoantibodies to IFN-γ (**Figure 2A**).

Given the decreased peak pSTAT1 level after IFN-γ stimulation in AIRE-deficient monocytes, we also asked whether the surface expression of IFN-γ receptors 1 and 2 is decreased in the monocytes of the eight APECED patients using flow cytometry. We found no difference in the expression of IFN-γR1 between healthy donor and APECED monocytes but a significant ~40% decrease in surface expression of IFN-γR2 in patient monocytes (mean fluorescence intensity 186.4 ± 14.61 vs. 117.3 ± 10.68, $p = 0.002$, respectively, **Figure 2B**).

DISCUSSION

Because of the similarities in clinical presentation of CMC and autoimmunity and decreased peripheral blood Th17 frequencies between patients with APECED and *STAT1* GOF mutations, our study examined STAT1 protein and phosphorylation levels in patients with APECED and shows that APECED patient monocytes do not share the same cell-intrinsic increase in STAT1 protein and phosphorylation levels as cells from patients with *STAT1* GOF mutations. In fact, our findings reveal a moderate but consistent and significant decrease in STAT1 protein and phosphorylation levels in APECED $CD14^+$ monocytes at rest and after IFN-γ stimulation.

Until recently, it had been postulated that impaired nuclear dephosphorylation is the underlying cause of increase in pSTAT1 levels in patients with *STAT1* GOF mutations (17, 19, 20). Nonetheless, recent reports have described normal dephosphorylation rates in some patients with a *STAT1* GOF mutations; for example, Sobh et al. (30), Meesilpavikkai et al. (31), and Weinacht et al. (32) described three new *STAT1* GOF mutations in the SH2 (p.H629Y and p.V653I) and linker (p.E545K) domains with enhanced pSTAT1 levels but normal dephosphorylation. In addition, Tabellini and colleagues recently reported high levels of STAT1 protein in NK cells from seven patients carrying five different CC or DNA binding (DB) domain *STAT1* GOF mutations (23). Similarly, high STAT1 protein levels were found in $CD14^+$ monocytes and $CD3^+$ T cells of 12 patients with 10 different CC, DB, or SH2 domain *STAT1* GOF mutations (Zimmerman and Holland, submitted manuscript). After controlling the *STAT1* GOF patients' pSTAT1 levels for the corresponding total STAT1 protein levels, STAT1 phosphorylation levels were normal (Zimmerman and Holland, submitted manuscript). These findings collectively support the hypothesis that high resting and IFN-γ-stimulated total STAT1 protein levels may serve as a background against which high pSTAT1 levels occur in some patients with *STAT1* GOF mutations. Alternatively, the pSTAT1 levels may not directly correlate with total STAT1 levels, as indicated in other reports (33). Future studies using more STAT1 GOF and STAT1 loss-of-function (LOF) patients will be needed to determine the temporal dynamics and correlation of total and pSTAT1 molecules.

In our study, based on the presence of CMC and other shared clinical features between APECED and *STAT1* GOF mutation patients, we tested the hypothesis that AIRE deficiency enhances STAT1 cellular responses as a result of enhanced STAT1 protein and phosphorylation levels. Instead, we found a ~20% decrease in STAT1 protein and peak pSTAT1 levels in APECED patients; the decrease in total STAT1 levels could indicate that the decreased STAT1 protein level may be a determining factor for the decreased peak STAT1 phosphorylation levels observed in APECED $CD14^+$ monocytes, although it could be accounted for by alternative factors that remain to be elucidated.

The molecular mechanism behind our finding is currently unknown. One possible explanation could have been that AIRE is involved in the regulation of STAT1 transcription; however, we found no significant difference in *STAT1* mRNA levels between healthy donor and APECED PMBCs. Alternatively, AIRE may regulate STAT1 post-transcriptionally at the level of degradation or SUMOylation or other process directly or indirectly *via* known (e.g., PIAS1) or yet-unknown protein partners (21, 22). Alternatively, APECED patient autoantibodies against type I IFNs, which have been shown to exhibit the ability to neutralize and block IFN-α activity, STAT1 phosphorylation, and the expression of interferon-stimulated genes (34, 35), may adversely affect tonic

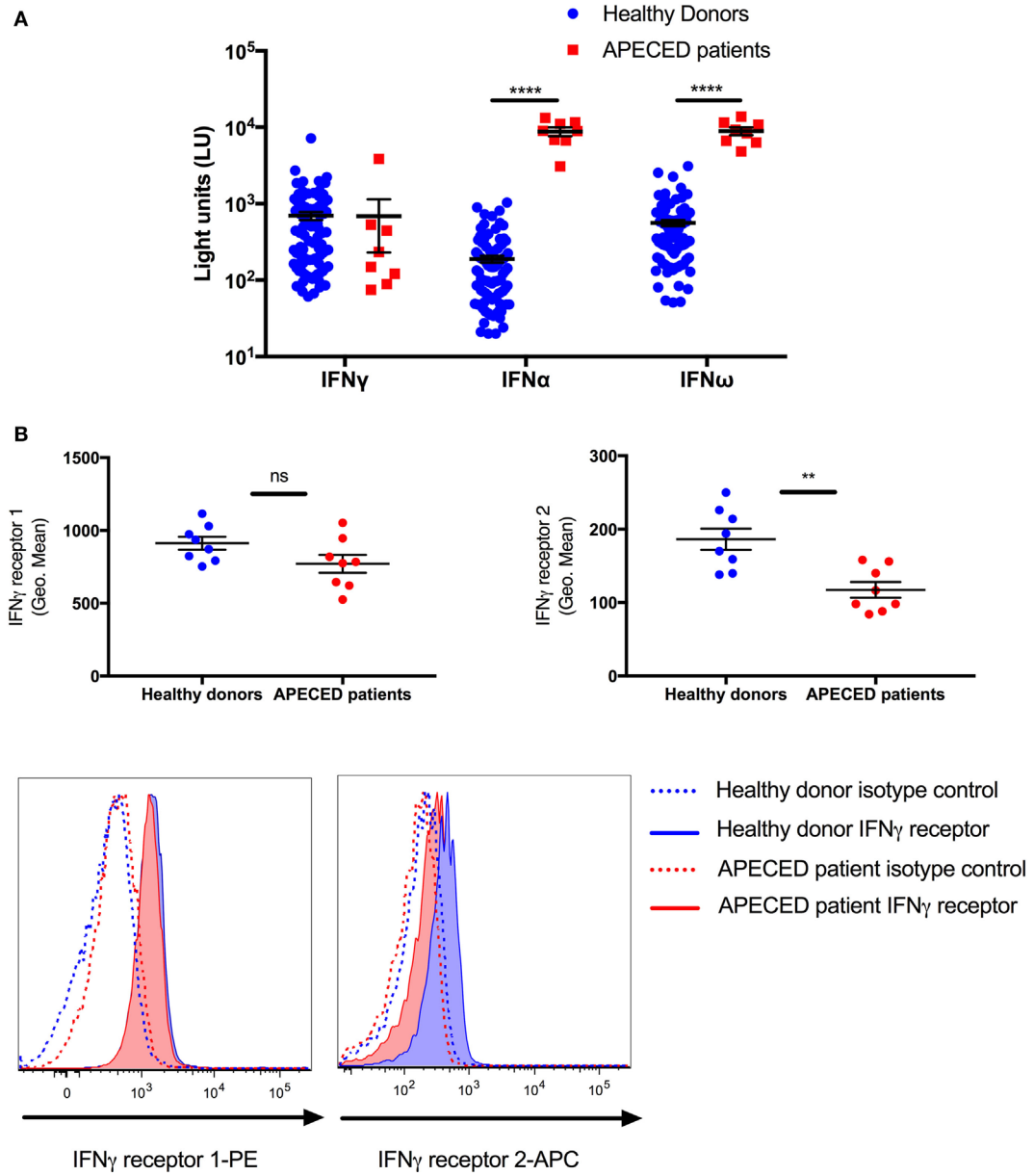

FIGURE 2 | The decrease in STAT1 protein and pSTAT1 levels seen in autoimmune polyendocrinopathy-candidiasis-ectodermal dystrophy (APECED) patients correlates with lower monocyte interferon (IFN)-γR2 receptor expression and the presence of type I IFN autoantibodies. **(A)** Sera from 8 APECED patients and 100 healthy donors were evaluated for the presence of autoantibodies against IFN-γ, IFN-α, and IFN-ω. Shown is autoantibody immunoreactivity against the indicated cytokines expressed as fluorescence intensity using a particle-based multiplex assay. **(B)** IFN-γ receptor 1 and 2 levels were measured in $CD14^+$ monocytes of healthy donors ($n = 8$) and APECED patients ($n = 8$). Summary data on mean fluorescence intensity and representative histogram FACS plots are shown. $^{**}p < 0.01$; $^{****}p < 0.0001$, by Mann–Whitney U test **(A)** or *t*-test **(B)**. Quantitative data represent median ± SEM.

STAT1 expression in blood monocytes. The decrease in IFN-γR2 expression on $CD14^+$ monocytes may be a contributor to the decreased peak pSTAT1 levels in APECED patients' cells. Future studies will be required to further examine this hypothesis as well as molecules and functional responses downstream of STAT1.

Impaired STAT1-dependent responses in patients with LOF *STAT1* mutations or in patients with defects in the IFN-γ receptor signaling axis, underlie Mendelian susceptibility to mycobacterial disease (36). The defect in STAT1 levels post-IFN-γ stimulation that we observed in our APECED patients is modest relative to the complete absence of STAT1 phosphorylation following IFN-γ stimulation in patients with IFN-γ receptor deficiency [(23); **Figure 1A**]. Therefore, significant residual STAT1 signaling is functional in APECED patients to prevent the development of mycobacterial infections in these patients. Whether the decrease in STAT1 protein and phosphorylation that we identified is a contributing factor to the development of viral infections in some APECED patients [(37); Lionakis, unpublished observations]

remains to be elucidated. However, the decrease in STAT1 levels is unlikely to contribute to the pathogenesis of CMC as patients with defects in the IFN-γ receptor signaling axis do not have Th17 defects and do not develop CMC (36). Hence, at this point, the biological and clinical implications of the decreased STAT1 levels in patients' monocytes are unclear.

In summary, we describe an association between AIRE deficiency and a decrease in STAT1 protein level in primary human monocytes that is not accompanied by decreased *STAT1* mRNA levels but correlates with the presence of type I IFN autoantibodies and decreased monocyte surface expression of IFN-γR2. The mechanism behind this finding and its clinical and biological implications in APECED patients require further investigation.

ETHICS STATEMENT

Eight APECED patients were enrolled (2015–2017) on a NIAID IRB-approved protocol and provided written informed consent. Samples from a patient carrying the c.1057G>A E353K STAT1 GOF mutation and a patient with the autosomal dominant form of IFN-γ receptor 1 deficiency carrying the 818del4 mutation were also collected under a NIAID IRB-approved protocol and provided written informed consent. Healthy volunteer blood samples from 13 individuals were obtained for STAT1 protein evaluation and from 10 individuals for STAT1 mRNA level determination under IRB-approved protocols through the Department of Transfusion Medicine, at the NIH Clinical Center. The study was conducted in accordance with the Helsinki Declaration.

AUTHOR CONTRIBUTIONS

ML conceived the project and contributed to the design and supervision of the experiments. OZ and ML wrote the manuscript. OZ, LR, and MS conducted experiments and generated manuscript figures. OZ, LR, MN, FV, and ML contributed to the interpretation of the data. EF contributed to healthy donor enrollment. SH provided patient care contributed patients' samples critical for the study execution.

FUNDING

This research was supported by the Division of Intramural Research, NIAID, NIH. The content of this article are those of the authors and do not reflect the official policy of the Department of Health and Human Services, nor does mention of trade names, commercial products, or organizations imply endorsement by the US government.

REFERENCES

1. Anderson MS, Venanzi ES, Klein L, Chen Z, Berzins SP, Turley SJ, et al. Projection of an immunological self shadow within the thymus by the aire protein. *Science* (2002) 298(5597):1395–401. doi:10.1126/science.1075958
2. Mathis D, Benoist C. Aire. *Annu Rev Immunol* (2009) 27:287–312. doi:10.1146/annurev.immunol.25.022106.141532
3. Fujikado N, Mann AO, Bansal K, Romito KR, Ferre EM, Rosenzweig SD, et al. Aire inhibits the generation of a perinatal population of interleukin-17A-producing γδ T cells to promote immunologic tolerance. *Immunity* (2016) 45(5):999–1012. doi:10.1016/j.immuni.2016.10.023
4. Yang S, Fujikado N, Kolodin D, Benoist C, Mathis D. Immune tolerance. Regulatory T cells generated early in life play a distinct role in maintaining self-tolerance. *Science* (2015) 348(6234):589–94. doi:10.1126/science.aaa7017
5. Gardner JM, Devoss JJ, Friedman RS, Wong DJ, Tan YX, Zhou X, et al. Deletional tolerance mediated by extrathymic Aire-expressing cells. *Science* (2008) 321(5890):843–7. doi:10.1126/science.1159407
6. Malchow S, Leventhal DS, Lee V, Nishi S, Socci ND, Savage PA. Aire enforces immune tolerance by directing autoreactive T cells into the regulatory T cell lineage. *Immunity* (2016) 44(5):1102–13. doi:10.1016/j.immuni.2016.02.009
7. Oftedal BE, Hellesen A, Erichsen MM, Bratland E, Vardi A, Perheentupa J, et al. Dominant mutations in the autoimmune regulator AIRE are associated with common organ-specific autoimmune diseases. *Immunity* (2015) 42(6):1185–96. doi:10.1016/j.immuni.2015.04.021
8. Cetani F, Barbesino G, Borsari S, Pardi E, Cianferotti L, Pinchera A, et al. A novel mutation of the autoimmune regulator gene in an Italian kindred with autoimmune polyendocrinopathy-candidiasis-ectodermal dystrophy, acting in a dominant fashion and strongly cosegregating with hypothyroid autoimmune thyroiditis. *J Clin Endocrinol Metab* (2001) 86(10):4747–52. doi:10.1210/jcem.86.10.7884
9. Su MA, Giang K, Zumer K, Jiang H, Oven I, Rinn JL, et al. Mechanisms of an autoimmunity syndrome in mice caused by a dominant mutation in Aire. *J Clin Invest* (2008) 118(5):1712–26. doi:10.1172/JCI34523
10. Ahonen P, Myllärniemi S, Sipilä I, Perheentupa J. Clinical variation of autoimmune polyendocrinopathy-candidiasis-ectodermal dystrophy (APECED) in a series of 68 patients. *N Engl J Med* (1990) 322(26):1829–36. doi:10.1056/NEJM199006283222601
11. Perheentupa J. Autoimmune polyendocrinopathy-candidiasis-ectodermal dystrophy. *J Clin Endocrinol Metab* (2006) 91(8):2843–50. doi:10.1210/jc.2005-2611
12. Wolff AS, Erichsen MM, Meager A, Magitta NF, Myhre AG, Bollerslev J, et al. Autoimmune polyendocrine syndrome type 1 in Norway: phenotypic variation, autoantibodies, and novel mutations in the autoimmune regulator gene. *J Clin Endocrinol Metab* (2007) 92(2):595–603. doi:10.1210/jc.2006-1873
13. Consortium TF-GA. An autoimmune disease, APECED, caused by mutations in a novel gene featuring two PHD-type zinc-finger domains. *Nat Genet* (1997) 17(4):399–403. doi:10.1038/ng1297-399
14. Puel A, Doffinger R, Natividad A, Chrabieh M, Barcenas-Morales G, Picard C, et al. Autoantibodies against IL-17A, IL-17F, and IL-22 in patients with chronic mucocutaneous candidiasis and autoimmune polyendocrine syndrome type I. *J Exp Med* (2010) 207(2):291–7. doi:10.1084/jem.20091983
15. Kisand K, Boe Wolff AS, Podkrajsek KT, Tserel L, Link M, Kisand KV, et al. Chronic mucocutaneous candidiasis in APECED or thymoma patients correlates with autoimmunity to Th17-associated cytokines. *J Exp Med* (2010) 207(2):299–308. doi:10.1084/jem.20091669
16. van de Veerdonk FL, Plantinga TS, Hoischen A, Smeekens SP, Joosten LA, Gilissen C, et al. STAT1 mutations in autosomal dominant chronic mucocutaneous candidiasis. *N Engl J Med* (2011) 365(1):54–61. doi:10.1056/NEJMoa1100102
17. Liu L, Okada S, Kong XF, Kreins AY, Cypowyj S, Abhyankar A, et al. Gain-of-function human STAT1 mutations impair IL-17 immunity and underlie chronic mucocutaneous candidiasis. *J Exp Med* (2011) 208(8):1635–48. doi:10.1084/jem.20110958
18. Uzel G, Sampaio EP, Lawrence MG, Hsu AP, Hackett M, Dorsey MJ, et al. Dominant gain-of-function STAT1 mutations in FOXP3 wild-type immune dysregulation-polyendocrinopathy-enteropathy-X-linked-like syndrome. *J Allergy Clin Immunol* (2013) 131(6):1611–23. doi:10.1016/j.jaci.2012.11.054
19. Toubiana J, Okada S, Hiller J, Oleastro M, Lagos Gomez M, Aldave Becerra JC, et al. Heterozygous STAT1 gain-of-function mutations underlie an unexpectedly broad clinical phenotype. *Blood* (2016) 127(25):3154–64. doi:10.1182/blood-2015-11-679902
20. Sampaio EP, Hsu AP, Pechacek J, Bax HI, Dias DL, Paulson ML, et al. Signal transducer and activator of transcription 1 (STAT1) gain-of-function

mutations and disseminated coccidioidomycosis and histoplasmosis. *J Allergy Clin Immunol* (2013) 131(6):1624–34. doi:10.1016/j.jaci.2013.01.052
21. Liu B, Liao J, Rao X, Kushner SA, Chung CD, Chang DD, et al. Inhibition of Stat1-mediated gene activation by PIAS1. *Proc Natl Acad Sci U S A* (1998) 95(18):10626–31. doi:10.1073/pnas.95.18.10626
22. Ilmarinen T, Kangas H, Kytömaa T, Eskelin P, Saharinen J, Seeler JS, et al. Functional interaction of AIRE with PIAS1 in transcriptional regulation. *Mol Immunol* (2008) 45:1847–62. doi:10.1016/j.molimm.2007.10.045
23. Tabellini G, Vairo D, Scomodon O, Tamassia N, Ferraro RM, Patrizi O, et al. Impaired natural killer cell functions in patients with signal transducer and activator of transcription 1 (STAT1) gain-of-function mutations. *J Allergy Clin Immunol* (2017). doi:10.1016/j.jaci.2016.10.051
24. Ding L, Mo A, Jutivorakool K, Pancholi M, Holland SM, Browne SK. Determination of human anticytokine autoantibody profiles using a particle-based approach. *J Clin Immunol* (2012) 32(2):238–45. doi:10.1007/s10875-011-9621-8
25. Ferre EMN, Rose SR, Rosenzweig SD, Burbelo PD, Romito KR, Niemela JE, et al. Redefined clinical features and diagnostic criteria in autoimmune polyendocrinopathy-candidiasis-ectodermal dystrophy. *JCI Insight* (2016) 1(13):e88782. doi:10.1172/jci.insight.88782
26. Vinh DC, Masannat F, Dzioba RB, Galgiani JN, Holland SM. Refractory disseminated coccidioidomycosis & mycobacteriosis in interferon-γ receptor 1 deficiency. *Clin Infect Dis* (2009) 49(6):e62–5. doi:10.1086/605532
27. Shuai K, Horvath CM, Huang LH, Qureshi SA, Cowburn D, Darnell JE Jr. Interferon activation of the transcription factor Stat1 involves dimerization through SH2-phosphotyrosyl peptide interactions. *Cell* (1994) 76(5):821–8. doi:10.1016/0092-8674(94)90357-3
28. Au-Yeung N, Mandhana R, Horvath CM. Transcriptional regulation by STAT1 and STAT2 in the interferon JAK-STAT pathway. *JAKSTAT* (2013) 2(3):e23931. doi:10.4161/jkst.23931
29. Bernabei P, Coccia EM, Rigamonti L, Bosticardo M, Forni G, Pestka S, et al. Interferon-γ receptor 2 expression as the deciding factor in human T, B, and myeloid cell proliferation or death. *J Leukoc Biol* (2001) 70(6):950–60.
30. Sobh A, Chou J, Schneider L, Geha RS, Massaad MJ. Chronic mucocutaneous candidiasis associated with an SH2 domain gain-of-function mutation that enhances STAT1 phosphorylation. *J Allergy Clin Immunol* (2016) 138(1):297–9. doi:10.1016/j.jaci.2015.12.1320
31. Meesilpavikkai K, Dik WA, Schrijver B, Nagtzaam NM, van Rijswijk A, Driessen GJ, et al. A novel heterozygous mutation in the STAT1 SH2 domain causes chronic mucocutaneous candidiasis, atypically diverse infections, autoimmunity, and impaired cytokine regulation. *Front Immunol* (2017) 8:274. doi:10.3389/fimmu.2017.00274
32. Weinacht KG, Charbonnier LM, Alroqi F, Plant A, Qiao Q, Wu H, et al. Ruxolitinib reverses dysregulated T helper cell responses and controls autoimmunity caused by a novel signal transducer and activator of transcription 1 (STAT1) gain-of-function mutation. *J Allergy Clin Immunol* (2017) 139:1629–40.e2. doi:10.1016/j.jaci.2016.11.022
33. Kong XF, Ciancanelli M, Al-Hajjar S, Alsina L, Zumwalt T, Bustamante J, et al. A novel form of human STAT1 deficiency impairing early but not late responses to interferons. *Blood* (2010) 116(26):5895–906. doi:10.1182/blood-2010-04-280586
34. Kisand K, Link M, Wolff AS, Meager A, Tserel L, Org T, et al. Interferon autoantibodies associated with AIRE deficiency decrease the expression of IFN-stimulated genes. *Blood* (2008) 112(7):2657–66. doi:10.1182/blood-2008-03-144634
35. Meyer S, Woodward M, Hertel C, Vlaicu P, Haque Y, Kärner J, et al. AIRE-deficient patients harbor unique high-affinity disease-ameliorating autoantibodies. *Cell* (2016) 166(3):582–95. doi:10.1016/j.cell.2016.06.024
36. Boisson-Dupuis S, Kong XF, Okada S, Cypowyj S, Puel A, Abel L, et al. Inborn errors of human STAT1: allelic heterogeneity governs the diversity of immunological and infectious phenotypes. *Curr Opin Immunol* (2012) 24(4):364–78. doi:10.1016/j.coi.2012.04.011
37. Nagafuchi S, Umene K, Yamanaka F, Oohashi S, Shindo M, Kurisaki H, et al. Recurrent herpes simplex virus infection in a patient with autoimmune polyendocrinopathy-candidiasis-ectodermal dystrophy associated with L29P and IVS9-1G>C compound heterozygous autoimmune regulator gene mutations. *J Intern Med* (2007) 261(6):605–10. doi:10.1111/j.1365-2796.2007.01786.x

Conflict of Interest Statement: The authors declare that the research was conducted in the absence of any commercial or financial relationships that could be construed as a potential conflict of interest.

Copyright © 2017 Zimmerman, Rosen, Swamydas, Ferre, Natarajan, van de Veerdonk, Holland and Lionakis. This is an open-access article distributed under the terms of the Creative Commons Attribution License (CC BY). The use, distribution or reproduction in other forums is permitted, provided the original author(s) or licensor are credited and that the original publication in this journal is cited, in accordance with accepted academic practice. No use, distribution or reproduction is permitted which does not comply with these terms.

frontiers in Immunology

REVIEW
published: 10 January 2018
doi: 10.3389/fimmu.2017.01968

The Interface between Fungal Biofilms and Innate Immunity

*John F. Kernien[1], Brendan D. Snarr[2], Donald C. Sheppard[2,3] and Jeniel E. Nett[1,4]**

[1] Department of Medicine, University of Wisconsin, Madison, WI, United States, [2] Department of Microbiology and Immunology, McGill University, Montreal, QC, Canada, [3] Department of Medicine, McGill University, Montreal, QC, Canada, [4] Department of Medical Microbiology and Immunology, University of Wisconsin, Madison, WI, United States

Fungal biofilms are communities of adherent cells surrounded by an extracellular matrix. These biofilms are commonly found during infection caused by a variety of fungal pathogens. Clinically, biofilm infections can be extremely difficult to eradicate due to their resistance to antifungals and host defenses. Biofilm formation can protect fungal pathogens from many aspects of the innate immune system, including killing by neutrophils and monocytes. Altered immune recognition during this phase of growth is also evident by changes in the cytokine profiles of monocytes and macrophages exposed to biofilm. In this manuscript, we review the host response to fungal biofilms, focusing on how these structures are recognized by the innate immune system. Biofilms formed by *Candida*, *Aspergillus*, and *Cryptococcus* have received the most attention and are highlighted. We describe common themes involved in the resilience of fungal biofilms to host immunity and give examples of biofilm defenses that are pathogen-specific.

Keywords: biofilm, matrix, fungi, neutrophil extracellular trap, innate immunity, neutrophil, *Aspergillus*, *Candida*

OPEN ACCESS

Edited by:
Steven Templeton, Indiana University School of Medicine – Terre Haute, United States

Reviewed by:
Teresa Zelante, University of Perugia, Italy
Luis R. Martinez, University of Texas at El Paso, United States

****Correspondence:***
Jeniel E. Nett
jenett@medicince.wisc.edu

Specialty section:
This article was submitted to Microbial Immunology, a section of the journal Frontiers in Immunology

Received: *07 November 2017*
Accepted: *19 December 2017*
Published: *10 January 2018*

Citation:
Kernien JF, Snarr BD, Sheppard DC and Nett JE (2018) The Interface between Fungal Biofilms and Innate Immunity. Front. Immunol. 8:1968. doi: 10.3389/fimmu.2017.01968

INTRODUCTION

Fungi frequently flourish as biofilms, which are aggregated communities encased in a protective extracellular matrix (1, 2). Many clinically relevant fungi have been shown to form biofilms, such as *Candida* spp., *Aspergillus* spp., *Cryptococcus neoformans*, *Fusarium* spp., *Blastoschizomyces capitatus*, *Malassezia pachydermatis*, *Pneumocystis* spp., *Trichosporon asahii*, *Rhizopus* spp., and *Rhizomucor* spp (3–13). In the clinical setting, fungal biofilms can propagate on artificial medical devices, such as catheters, as well as on epithelial and endothelial surfaces (3, 14–19) (**Figure 1A**). In addition, during invasive infection, fungal pathogens can proliferate as non-surface associated microcolonies embedded in extracellular matrix (18) (**Figure 1B**). Biofilms resist antifungal therapies and host defenses, making them notoriously difficult to eradicate (4, 20–36). One defining trait of biofilm formation is the production of a microbial-produced extracellular matrix, or the "glue" necessary for adhesion, which also serves as a shield that creates protected reservoirs of infection (4, 5, 20, 33, 37). As investigations reveal the complex composition of the extracellular matrix for several fungal pathogens, it has become increasing clear that this material is distinct from the cell wall (4, 5, 18, 38–41). Therefore, biofilm growth provides a means to present unique moieties and conceal cell wall ligands. Studies are just beginning to shed light on how biofilm formation and matrix production influence host recognition (5, 15, 27, 29–32, 42–50). In this review, we examine the innate immune response to fungal biofilms, highlighting how production of the extracellular matrix alters immunity. While a variety of fungal pathogens have been shown to produce biofilms, investigations examining host interactions have primarily utilized model pathogens *Candida albicans*, *Aspergillus fumigatus*, and *C. neoformans*, which will be the focus of our discussion.

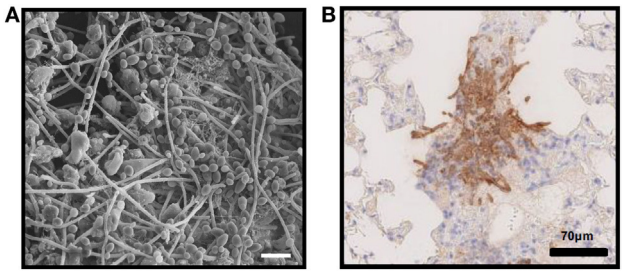

FIGURE 1 | *In vivo* fungal biofilms. **(A)** *Candida albicans* biofilm growing on the luminal surface of a rat venous catheter for 24 h. Scanning electron microscopy reveals adherent organisms growing within in an extracellular matrix. **(B)** Immunohistochemistry of pulmonary tissue from an immunocompromised mouse infected with *Aspergillus fumigatus* and stained with an anti-galactosaminogalactan antibody. Brown indicates accumulation of galactosaminogalactan-containing biofilm matrix surrounding hyphae growing within pulmonary tissues.

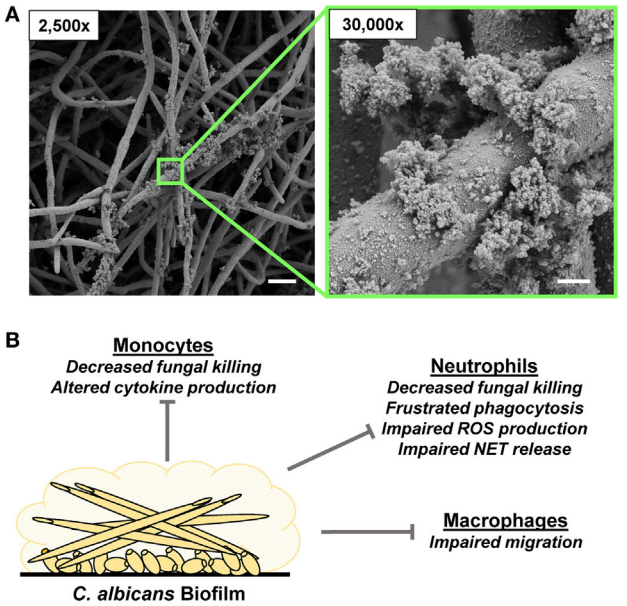

FIGURE 2 | *Candida albicans* biofilm formation and innate immune response. **(A)** Scanning electron microscopy images reveal *C. albicans* biofilms grown on coverslips. Biofilms were grown for 48 h. Measurement bars represent 10 and 1 μm for 2,500× and 30,000×, respectively. **(B)** Summary of innate immune responses impaired by *C. albicans* biofilms.

Candida BIOFILMS

Biofilm Formation

Candida spp., commensal fungi of the gastrointestinal tract, can cause severe, disseminated disease with high mortality, particularly in patients with implanted medical devices or compromised immune systems (17, 51–57). The vast majority of these infections involve biofilm formation on either an artificial or a biotic surface (13, 58, 59) (**Figure 2**). Clinical *Candida* biofilms grow on diverse medical devices, including central venous catheters, urinary catheters, prosthetic valves, left ventricular assist devices, and oral devices, such as dentures (3, 60). Both vaginal and oral mucosal surfaces promote biofilm formation as well (16, 61). The majority of the *in vitro* and *in vivo* biofilm studies have utilized *C. albicans*, the most widespread species. However, non-*albicans* species, including *Candida tropicalis*, *Candida parapsilosis*, and *Candida glabrata*, similarly produce clinically relevant biofilms (3, 62–68). In addition, this virulence trait has been described for the emerging pathogen *Candida auris* (69). *Candida* biofilm formation involves the adherence of yeast to a substrate, the proliferation of cells to form a fungal community, and the production of an extracellular matrix (37, 70–72). *C. albicans* biofilm development often involves the production of hyphae, although the degree of filamentation varies among strains and niches. Non-*albicans* strains lacking the ability to filament produce biofilms composed of layers of yeast embedded in an extracellular matrix (73).

Matrix Composition

Upon encounter with biofilm, immune cells are first confronted with the extracellular matrix covering the fungal cells. A combination of both *in vitro* and *in vivo* models has been integral for the dissection of *Candida* biofilm matrix assembly and composition (20, 22, 39, 40, 58, 67, 70, 74–79). For *C. albicans*, *in vitro* studies have revealed that the mature biofilm matrix consists of a variety of macromolecules, including protein (55%), carbohydrate (25%), lipid (15%), and DNA (5%) (23, 38, 40, 80). Interestingly, many of the matrix components vastly differ from the cell wall components that would be initially recognized by immune cells in the absence of biofilm (40). For example, the main polysaccharide of *C. albicans* biofilm matrix is α-1,2-branched α-1,6 mannan, which is found in high molecular weight structures of approximately 12,000 residues. In contrast, mannans of the outer cell wall layer are 5- to 10-fold smaller. Furthermore, the matrix mannans associate with β-1,6 glucans, forming a mannan–glucan complex that assembles extracellularly, and this structure has not been identified in the cell wall of *C. albicans* (40, 75). In addition, matrix β-1,6 glucan exists in a linear conformation, while the β-1,6 glucan of the cell wall is highly branched (81). Proteomic analysis of *in vitro* biofilms shows some similarities between matrix-associated proteins and those released into the media during planktonic growth (79). However, the extracellular matrix lacks many of the proteins associated with the cell wall (40, 82). *In vivo*, host proteins contribute to the construction of biofilm, with an astonishing majority (>95%) of the matrix-associated proteins of host origin (76). This finding demonstrates variation in the content of fungal biofilm matrix *in vivo* and highlights the importance of including animal models for investigation of *Candida* biofilms.

Neutrophil–*Candida* Biofilm Interactions

Neutrophils are primary responders to *C. albicans* infection, with neutropenic patients prone to severe, lethal candidiasis (83–86). Neutrophils respond to chemokines and other signals during recruitment to the site of infection. Upon pathogen encounter,

neutrophils elicit various responses important for control of infection, including phagocytosis, degranulation, reactive oxygen species (ROS) production, and neutrophil extracellular trap (NET) release (87). In the context of *C. albicans* biofilms, neutrophils are the primary leukocyte recruited to the site of infection (15, 76, 88–90). In fact, neutrophil recruitment has been observed in animal models mimicking diverse clinical biofilms, including catheter-related infections (vascular and urinary), denture stomatitis, oral candidiasis, and vaginal candidiasis (15, 76, 91). Despite their presence at the site of infection, neutrophils fail to eradicate *Candida* biofilms. Pioneering studies with human neutrophils revealed that *C. albicans* biofilms resist neutrophil attack, in comparison to their planktonic counterparts (29, 30). Intact biofilm structure is required for this resistance, as resuspension of the biofilm cells reverses the phenotype (29). Furthermore, biofilm impairment of neutrophils is robust, persisting despite neutrophil priming by IFN-γ or G-CSF (92).

The ability of *Candida* biofilms to withstand immune attack appears to vary by strain and species. For *C. albicans*, biofilms are approximately twofold to fivefold more resistant to killing when compared to planktonic cells (29–31, 92). Investigation of *C. parapsilosis* found a similar trend, but did not identify a significant difference in susceptibility to neutrophils between biofilms and planktonic organisms (43, 93). The lack of statistical significance was attributed to the heterogeneity of biofilm formation, resulting in high assay variability. A recent investigation found *C. glabrata* biofilms also resist neutrophil killing, exhibiting a threefold higher resistance for biofilm over planktonic organisms (45).

For killing and containment of *C. albicans*, neutrophils release NETs, which are structures of DNA, histones, and antimicrobial proteins (94, 95). These structures are particularly well-suited to combat large organisms, such as hyphae, which are unable to be ingested by phagocytosis (95). As *C. albicans* biofilms consist of aggregated cells and hyphal elements, NETosis would seemingly be an efficient method of attack. However, a recent study has revealed that neutrophils fail to release NETs in the presence of *C. albicans* biofilms (31). This phenomenon is conserved across a variety of *C. albicans* strains exhibiting differing degrees of filamentation and biofilm architecture (44). This inhibitory pathway appears to be closely linked to the production of an extracellular matrix, as physical or genetic disruption of this process restores NET release (31). Remarkably, when neutrophils are induced to generate NETs prior to biofilms exposure, biofilm inhibition is observed (31). This suggests that inhibition of NETosis is an adaptation by *C. albicans* biofilms to prevent killing by neutrophils. Other species appear to employ this mechanism as well. For example, *C. glabrata* biofilms also impair NET release, although the inhibition is not as pronounced (45).

Recent studies have begun to shed light on the planktonic *C. albicans* cell surface components that induce NET release. The process appears to be multifactorial, as β-glucan, mannan, and secreted aspartic proteases all variably trigger NETosis (93, 96, 97). NET inhibition by biofilm likely involves concealment of cell surface ligands by the extracellular matrix, as disruption of this process permits NET release (31). In particular, disruption of the matrix mannan–glucan complex in a *pmr1*Δ/Δ mutant strain reverses the NET inhibition phenotype, suggesting a role for this unique polysaccharide complex (31, 75). In addition, studies by Zawrotniak et al. show that NET induction by cell wall mannan is concentration-dependent, with higher concentrations failing to trigger NETosis *in vitro* (97). Further investigation would be of interest to explore a similar pattern for polysaccharides of the biofilm matrix in NET inhibition.

Upon encounter with *C. albicans* biofilms, the generation of ROS by neutrophils is dampened compared to the response observed for planktonic organisms (30, 31, 44). Multiple pathways govern NET release and a subset of these depend on ROS production (96, 98–103). In response to planktonic *C. albicans*, both ROS-dependent and ROS-independent pathways trigger NETosis, which may not be surprising given the numerous cell surface ligands expected to be involved (96, 97, 103). While further investigation is needed to dissect pathways impairing neutrophil function by biofilms, inhibition of ROS production is likely involved. A study of *C. glabrata*–neutrophil interactions demonstrates a similar neutrophil response, with reduced ROS production upon encounter with biofilm (45). Taken together, these studies show that *C. albicans* biofilms inhibit the release of NETs and resist killing by neutrophils. The pathway appears to involve the production of an extracellular matrix and dampening of neutrophil ROS production. Based on studies with *C. glabrata*, it may be conserved, in part, among *Candida* spp.

Monocytes and Macrophages Interactions with *Candida* Biofilms

Chandra et al. first demonstrated that *Candida* biofilms resist attack by monocytes and can alter their cytokine profile (42). Peripheral blood mononuclear cells (PBMCs) fail to phagocytose biofilm-associated *C. albicans*, in contrast to planktonic organisms (42). However, these cells remain viable, migrating within the biofilm, even providing a stimulus for biofilm proliferation through an unknown mechanism (29, 42). Compared to planktonic organisms, *C. albicans* biofilms are twofold to threefold more resistant to killing by monocytes (29).

Encounter with *Candida* biofilms influences cytokine release by mononuclear cells. One of the more intriguing alterations is the downregulation of TNF-α, a cytokine which facilitates phagocyte activation. Compared to planktonic organisms, exposure to *C. albicans* biofilms significantly diminishes the production of TNF-α by monocytic cell line THP-1 (29). Not only is this predicted to impact phagocyte function in the host but the alteration in production of TNF-α may also have a direct impact on the biofilm. Application of exogenous TNF-α has been shown to prevent *C. albicans* biofilm formation, through a TNF receptor-independent pathway (104). Furthermore, this activity is blocked by preincubation of TNF-α with *N*,*N*′-diacetylchitobiose, a major carbohydrate component of *C. albicans* cell wall (104). Therefore, inhibition of TNF-α by biofilms may represent an evolutionary adaption and mechanism of immune evasion. However, much remains a mystery about how the cytokine response influences the host response to biofilm infection. For example, when compared to planktonic cells, PBMCs exposed to *C. albicans* biofilms produce elevated

levels of IL-1β, IL-10, and MCP-1 and reduced levels of IL-6 and MIP1β (42). How these combinations of both pro- and anti-inflammatory cytokines are triggered and their influence on host response to biofilm infection is unknown.

Recent work by Alonso et al. revealed that formation of *C. albicans* biofilm impairs the migratory capacity of macrophages (105). Upon exposure to biofilm, the migration of murine macrophages (J774.1 cell line) is reduced approximately twofold when compared to encounter with planktonic organisms. A *pmr1*Δ/Δ mutant similarly impaired macrophage migration during biofilm growth. As this biofilm is deficient in matrix mannan production, the macrophage inhibition is likely related to another factor, such as physical structure (75, 105). Therefore, *Candida* biofilms may elicit distinct inhibitory pathways for neutrophils and macrophages (31, 105).

Aspergillus BIOFILMS

Biofilm Formation

Aspergillus spp. grow ubiquitously in the environment and individuals are constantly exposed to their spores, which are released into the air (106). Immunocompetent individuals clear these spores after inhalation, but those with impaired immunity are at risk for development of severe disease. *Aspergillus* spp. can cause a variety of clinical diseases, including invasive, chronic, and allergic forms (106). The chronic form of disease typically involves formation of an aspergilloma, or fungal ball, in the sinus or lung cavity. These dense structures consist of agglutinated hyphae with occasional conidial heads growing as a biofilm encased in an adhesive extracellular matrix (18) (**Figure 3**). As the community matures, the inner cells loose viability, likely due to starvation. *A. fumigatus* also produces extracellular matrix material during invasive pulmonary aspergillosis (18). However, during this mode of growth, the hyphae remain separated without an inner core of decaying fungal mass. *In vitro*, *A. fumigatus* forms biofilms on agar medium in aerial, static conditions that mimic the host niches for aspergilloma formation (4).

Matrix Production

Aspergillus fumigatus produces a unique extracellular matrix during biofilm growth *in vitro* and *in vivo* (4, 18, 107). By biochemical analysis, this material consists of 40% protein, 43% carbohydrates, 14% lipids, and 3% aromatic-containing compounds, as well as DNA (108–110). The polysaccharides of the extracellular matrix exhibit cohesion properties and provide immune protection. The main matrix polysaccharides include galactomannan and galactosaminogalactan (GAG), of which, GAG has received the most attention (18). *A. fumigatus* strains deficient in GAG production lack the capacity to form biofilms or produce extracellular matrix (47). GAG is an α-1,4-linked linear heteroglycan composed of variable combinations of galactose and *N*-acetyl-galactosamine (GalNAc) (111, 112). GalNAc residues within the GAG polymer are partially deacetyated by the secreted enzyme Agd3, rendering mature GAG polycationic (113). Deacetylation is required for GAG to mediate adhesion between hyphae and other anionic surfaces such as host cells, plastic, and glass (113). GAG production has also been reported for other *Aspergillus* spp., including *Aspergillus parasiticus*, *Aspergillus niger*, and *Aspergillus nidulans*, although the relative proportion of galactose and GalNAc varies between strains and likely influences matrix function as detailed below (114–117). While galactomannan and GAG are universally present in *A. fumigatus* matrix, key differences exist between the clinical niche biofilms. For example, aspergilloma biofilms produce a thicker extracellular matrix, which contains α-glucan, a polysaccharide absent in biofilms formed during invasive aspergillosis (18). Aspergilloma biofilms also produce melanin, an immune modulator (4, 18, 33, 118). However, its specific role during biofilm formation is unknown.

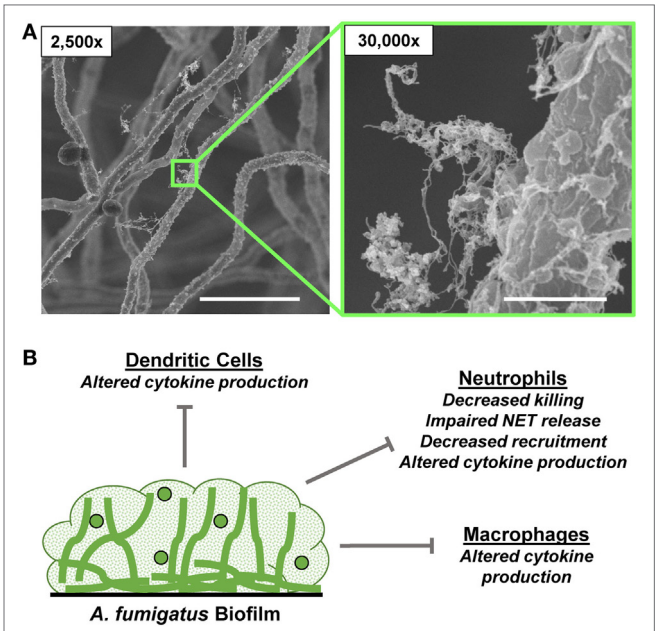

FIGURE 3 | *Aspergillus fumigatus* biofilm formation and innate immune response. **(A)** Scanning electron microscopy images reveal *A. fumigatus* biofilms grown on coverslips. Biofilms were grown for 24 h. Measurement bars represent 10 and 1 μm for 2,500× and 30,000×, respectively. **(B)** Summary of innate immune responses impaired by *A. fumigatus* biofilms.

Innate Immunity to *Aspergillus* Biofilms

Neutrophils are key players in the innate immune defense against *Aspergillus*. Neutropenia, often in the face of chemotherapy or hematologic malignancy, places patients at high risk factor for invasive pulmonary aspergillosis, which can progress to disseminated lethal disease (119, 120). Neutrophils are recruited to *Aspergillus* spores *in vivo* and are critical for their engulfment through phagocytosis (121–123). Neutrophils also release NETs in response to hyphal elements (46, 124–126). While NETs lack significant activity against conidia, they exhibit modest inhibitory activity against the larger hyphal forms of *A. fumigatus* (46, 126). Production of an extracellular matrix shields *A. fumigatus* from neutrophil attack and much of this protection is attributed to GAG (32). *A. fumigatus* mutants deficient in GAG synthesis or deacetylation exhibit attenuated

virulence (47, 113), and treatment with recombinant glycoside hydrolases that degrade GAG reduces fungal growth in a murine model of aspergillosis (127).

Studies of differences in GAG composition between *A. fumigatus* and *A. nidulans* have suggested that protection against neutrophil attack is mediated by hyphal-associated GalNAc-rich GAG (32). Unlike *A. fumigatus*, *A. nidulans* produces GalNAc-poor GAG, which contains over fivefold higher levels of galactose and produces poorly adherent biofilms containing minimal extracellular matrix. *A. nidulans* is also less virulent in a murine model of pulmonary aspergillosis and more than twofold more susceptible to killing by human neutrophils. Heterologous expression of the *A. fumigatus uge3* gene encoding a GalNAc-epimerase in *A. nidulans* results in the production of *A. fumigatus*-like GalNAc-rich GAG (32). Unlike wild-type *A. nidulans*, the GalNAc-rich GAG-producing strain of *A. nidulans* forms biofilm, produces extracellular matrix, and resists killing by neutrophils. The protective effects of GAG are dependent on NADPH oxidase and likely involve defense against NETs released through activation of this pathway. It has been hypothesized that GAG-mediated protection against NETs is mediated by electrostatic repulsion between this partially deacetylated cationic polysaccharide and cationic antimicrobial peptides or histones contained within NETs (32).

The immunomodulatory effects of GAG during biofilm formation are likely multifactorial. Hyphal-associated GAG masks β-glucans on the cell wall of hyphae (47, 128) and alters recognition by murine bone marrow-derived dendritic cells *in vitro* (47). Genetic disruption of GAG synthesis leads to increased pro-inflammatory cytokine release through Dectin-1 signaling (47). In a non-neutropenic murine model of pulmonary aspergillosis, genetic disruption of GAG synthesis results in production of a non-protective, hyper-inflammatory response marked by increased neutrophil recruitment (47). This observation suggests that GAG impairs neutrophil recruitment during biofilm growth and is consistent with the reports that soluble GAG can modulate immunity through induction of apoptosis in neutrophils and stimulation of anti-inflammatory IL-1Ra production by macrophages *in vitro* (49, 129). Further, *in vivo* studies are needed to evaluate the relative role of these functions of GAG in invasive and chronic *Aspergillus* infections.

Recent studies have begun to shed light on the mechanisms involved in NET release in response to fungi (32, 46, 93, 97, 124–126, 130). Specific ligands triggering this response to *Aspergillus* remain largely unknown, and how the extracellular matrix may influence these pathways is of great interest. For example, NET production is reduced in response to resting conidia when compared to hyphae (46). This inhibition is linked to RodA, a hydrophobin on the surface of conidia that masks pathogen-associated molecular patterns, including β-glucan (46, 48). As transcriptional analysis shows abundance of *RodA* during *A. fumigatus* biofilm growth when compared to planktonic conditions, it is interesting to postulate a role for RodA production in immune evasion during biofilm growth (131). Also, as melanin production has been described for some *Aspergillus* biofilms, investigation of a role for this immune modulator is also intriguing (4, 18, 33, 118).

Cryptococcus BIOFILMS

Biofilm Formation

Cryptococcus spp. are opportunistic environmental fungal pathogens that cause life-threatening meningoencephalitis, particularly in patients with suppressed immunity in the setting of HIV or organ transplantation (132). Following inhalation of spores from the environment, *C. neoformans* disseminates from the lungs, with a propensity for the central nervous system. *C. neoformans* also exhibits a predilection for artificial surfaces and forms biofilms on medical devices, such as cerebrospinal fluid shunts, vascular catheters, and prosthetic dialysis fistulae (133–136). These adherent communities are composed of yeast encased in an extracellular matrix (5, 41, 137). *In vitro*, *C. neoformans* biofilms mature in 24–48 h and display a multiple-drug-resistance phenotype (5).

Matrix Production

Cryptococcus neoformans produces a protective polysaccharide capsule composed of glucuronoxylomannan (GXM), galactoxylomannan, and mannoprotein (137, 138). During biofilm growth, these capsular polysaccharides are shed into the surrounding milieu, ultimately providing extracellular matrix material for surface adhesion and cell–cell cohesion (5). Acapsular *C. neoformans* mutants are unable to form biofilms (5). Martinez and Casadevall identified GXM as the principle polysaccharide of the *C. neoformans* biofilm matrix (41). This polysaccharide has received the most attention due to its immunomodulatory properties and high abundance in the biofilm matrix (5, 138–141). However, biochemical analysis also shows the presence of sugars not found in GXM, suggesting that the biofilm matrix contains additional polysaccharides (41). Little is known about the structure of these polysaccharides and how they may influence immunity to *Cryptococcus* biofilms.

Innate Immunity to *Cryptococcus* Biofilms

While studies have begun to dissect the impact of biofilm formation on immunity to *Cryptococcus*, much of this host–fungal interaction remains a mystery. Production of a GXM-rich extracellular matrix appears to be the key defense against host immunity. Genetic or antibody-mediated disruption of GXM impairs biofilm formation and diminishes virulence (5, 141). As a capsule polysaccharide, GXM is responsible for a multifaceted inhibition of neutrophil function, impeding chemotaxis, phagocytosis, NET production, and antifungal activity (138, 139, 142, 143). Similar mechanisms of diminished neutrophil function are anticipated in response to *C. neoformans* biofilms and may even be augmented given the high GXM content of biofilm matrix (41). Furthermore, capsular GXM can impair phagocytosis by monocytes and macrophages (138). However, it is unknown if phagocytosis would be an effective response against *Cryptococcus* biofilms, given the large structure of cohesive, aggregated yeast (41).

In addition to the immunomodulatory activity of the extracellular matrix, *C. neoformans* biofilms also resist antimicrobial host defenses. Compared to planktonic *C. neoformans*, biofilms tolerate higher concentrations of defensins, including PG-1, β-defensin-1, and β-defensin-3 (27). This resistance is even further augmented when biofilms are induced to produce melanin through L-Dopa

supplementation. Biofilm formation also protects *C. neoformans* from oxidative stress induced by a variety of stimuli (27). Taken together, these studies show that *Cryptococcus* biofilms withstand innate immunity through both immune modulation and resistance to immune attack.

CONCLUSION

Adoption of a biofilm lifestyle during fungal infection is increasingly recognized as a mechanism to avoid host immune attack and provide a protective niche. In this environment, the extracellular matrix can shield the fungal cell wall from host cellular recognition, modulating the immune response. In addition, the extracellular matrix can provide protection from antimicrobial defenses, such as defensins, oxidative stress, and NETs. Furthermore, biofilm formation produces an aggregated community that may resist engulfment by phagocytosis.

While it is clear that biofilm formation significantly influences immunity, studies are just beginning to shed light on the many mechanisms underlying this modulation of host response. As biofilms are heterogeneous structures with variations in architecture and composition based on their environmental niche, mechanisms impairing immunity likely vary among clinical biofilms. Therefore, inclusion of conditions closely mimicking the host and animal models of biofilm infection remains critical for future studies. While recent studies have revealed the influence of biofilm formation on the innate immune response, still little is known about how these structures may modulate adaptive immunity.

Fungal biofilms are among the most difficult infections to treat due to their high tolerance of antifungals and immune evasion strategies. The incidence of fungal biofilm infections is likely to rise given the growing number of patients with artificial medical devices and immunocompromising conditions. Anti-biofilm therapies are urgently needed. Understanding the dynamics of biofilm formation, matrix production, and how these processes induce resistance to multiple facets of the innate immune system may lead to biofilm-specific antifungal strategies.

AUTHOR CONTRIBUTIONS

JK, DS, and JN wrote the manuscript. JK and BS constructed the figures.

FUNDING

JN is supported by the National Institutes of Health (K08 AI108727), the Burroughs Wellcome Fund (1012299), and the Doris Duke Charitable Foundation (112580130). BS has been supported by graduate scholarships from CFC and CIHR. DS is supported by a Research Chair from the Fonds de Recherche Quebec Santé.

REFERENCES

1. Donlan RM. Biofilm formation: a clinically relevant microbiological process. *Clin Infect Dis* (2001) 33(8):1387–92. doi:10.1086/322972
2. Hoyle BD, Jass J, Costerton JW. The biofilm glycocalyx as a resistance factor. *J Antimicrob Chemother* (1990) 26(1):1–5. doi:10.1093/jac/26.1.1
3. Kojic EM, Darouiche RO. *Candida* infections of medical devices. *Clin Microbiol Rev* (2004) 17(2):255–67. doi:10.1128/CMR.17.2.255-267.2004
4. Beauvais A, Schmidt C, Guadagnini S, Roux P, Perret E, Henry C, et al. An extracellular matrix glues together the aerial-grown hyphae of *Aspergillus fumigatus*. *Cell Microbiol* (2007) 9(6):1588–600. doi:10.1111/j.1462-5822.2007.00895.x
5. Martinez LR, Casadevall A. Specific antibody can prevent fungal biofilm formation and this effect correlates with protective efficacy. *Infect Immun* (2005) 73(10):6350–62. doi:10.1128/iai.73.10.6350-6362.2005
6. Imamura Y, Chandra J, Mukherjee PK, Lattif AA, Szczotka-Flynn LB, Pearlman E, et al. *Fusarium* and *Candida albicans* biofilms on soft contact lenses: model development, influence of lens type, and susceptibility to lens care solutions. *Antimicrob Agents Chemother* (2008) 52(1):171–82. doi:10.1128/aac.00387-07
7. D'Antonio D, Parruti G, Pontieri E, Di Bonaventura G, Manzoli L, Sferra R, et al. Slime production by clinical isolates of *Blastoschizomyces capitatus* from patients with hematological malignancies and catheter-related fungemia. *Eur J Clin Microbiol Infect Dis* (2004) 23(10):787–9. doi:10.1007/s10096-004-1207-4
8. Cannizzo FT, Eraso E, Ezkurra PA, Villar-Vidal M, Bollo E, Castella G, et al. Biofilm development by clinical isolates of *Malassezia pachydermatis*. *Med Mycol* (2007) 45(4):357–61. doi:10.1080/13693780701225767
9. Cushion MT, Collins MS, Linke MJ. Biofilm formation by *Pneumocystis* spp. *Eukaryot Cell* (2009) 8(2):197–206. doi:10.1128/ec.00202-08
10. Di Bonaventura G, Pompilio A, Picciani C, Iezzi M, D'Antonio D, Piccolomini R. Biofilm formation by the emerging fungal pathogen *Trichosporon asahii*: development, architecture, and antifungal resistance. *Antimicrob Agents Chemother* (2006) 50(10):3269–76. doi:10.1128/aac.00556-06
11. Singh R, Shivaprakash MR, Chakrabarti A. Biofilm formation by zygomycetes: quantification, structure and matrix composition. *Microbiology* (2011) 157(Pt 9):2611–8. doi:10.1099/mic.0.048504-0
12. Sun Y, Chandra J, Mukherjee P, Szczotka-Flynn L, Ghannoum MA, Pearlman E. A murine model of contact lens-associated *Fusarium* keratitis. *Invest Ophthalmol Vis Sci* (2010) 51(3):1511–6. doi:10.1167/iovs.09-4237
13. Nobile CJ, Johnson AD. *Candida albicans* biofilms and human disease. *Annu Rev Microbiol* (2015) 69:71–92. doi:10.1146/annurev-micro-091014-104330
14. Escande W, Fayad G, Modine T, Verbrugge E, Koussa M, Senneville E, et al. Culture of a prosthetic valve excised for streptococcal endocarditis positive for *Aspergillus fumigatus* 20 years after previous *A. fumigatus* endocarditis. *Ann Thorac Surg* (2011) 91(6):e92–3. doi:10.1016/j.athoracsur.2011.01.102
15. Dongari-Bagtzoglou A, Kashleva H, Dwivedi P, Diaz P, Vasilakos J. Characterization of mucosal *Candida albicans* biofilms. *PLoS One* (2009) 4(11):e7967. doi:10.1371/journal.pone.0007967
16. Harriott MM, Lilly EA, Rodriguez TE, Fidel PL Jr, Noverr MC. *Candida albicans* forms biofilms on the vaginal mucosa. *Microbiology* (2010) 156(Pt 12):3635–44. doi:10.1099/mic.0.039354-0
17. Ganguly S, Mitchell AP. Mucosal biofilms of *Candida albicans*. *Curr Opin Microbiol* (2011) 14(4):380–5. doi:10.1016/j.mib.2011.06.001
18. Loussert C, Schmitt C, Prevost MC, Balloy V, Fadel E, Philippe B, et al. In vivo biofilm composition of *Aspergillus fumigatus*. *Cell Microbiol* (2010) 12(3):405–10. doi:10.1111/j.1462-5822.2009.01409.x
19. Seidler MJ, Salvenmoser S, Muller FM. *Aspergillus fumigatus* forms biofilms with reduced antifungal drug susceptibility on bronchial epithelial cells. *Antimicrob Agents Chemother* (2008) 52(11):4130–6. doi:10.1128/aac.00234-08
20. Al-Fattani MA, Douglas LJ. Biofilm matrix of *Candida albicans* and *Candida tropicalis*: chemical composition and role in drug resistance. *J Med Microbiol* (2006) 55(Pt 8):999–1008. doi:10.1099/jmm.0.46569-0
21. Mukherjee PK, Chandra J, Kuhn DM, Ghannoum MA. Mechanism of fluconazole resistance in *Candida albicans* biofilms: phase-specific role of efflux pumps and membrane sterols. *Infect Immun* (2003) 71(8):4333–40. doi:10.1128/IAI.71.8.4333-4340.2003

22. Nett J, Lincoln L, Marchillo K, Massey R, Holoyda K, Hoff B, et al. Putative role of beta-1,3 glucans in *Candida albicans* biofilm resistance. *Antimicrob Agents Chemother* (2007) 51(2):510–20. doi:10.1128/aac.01056-06
23. Ramage G, Vandewalle K, Wickes BL, Lopez-Ribot JL. Characteristics of biofilm formation by *Candida albicans*. *Rev Iberoam Micol* (2001) 18(4):163–70.
24. Mowat E, Butcher J, Lang S, Williams C, Ramage G. Development of a simple model for studying the effects of antifungal agents on multicellular communities of *Aspergillus fumigatus*. *J Med Microbiol* (2007) 56(Pt 9):1205–12. doi:10.1099/jmm.0.47247-0
25. Seidler MJ, Salvenmoser S, Müller FMC. *Aspergillus fumigatus* forms biofilms with reduced antifungal drug susceptibility on bronchial epithelial cells. *Antimicrob Agents Chemother* (2008) 52(11):4130–6. doi:10.1128/aac.00234-08
26. Mowat E, Lang S, Williams C, McCulloch E, Jones B, Ramage G. Phase-dependent antifungal activity against *Aspergillus fumigatus* developing multicellular filamentous biofilms. *J Antimicrob Chemother* (2008) 62(6):1281–4. doi:10.1093/jac/dkn402
27. Martinez LR, Casadevall A. *Cryptococcus neoformans* cells in biofilms are less susceptible than planktonic cells to antimicrobial molecules produced by the innate immune system. *Infect Immun* (2006) 74(11):6118–23. doi:10.1128/iai.00995-06
28. Ramage G, Rajendran R, Sherry L, Williams C. Fungal biofilm resistance. *Int J Microbiol* (2012) 2012:528521. doi:10.1155/2012/528521
29. Katragkou A, Kruhlak MJ, Simitsopoulou M, Chatzimoschou A, Taparkou A, Cotten CJ, et al. Interactions between human phagocytes and *Candida albicans* biofilms alone and in combination with antifungal agents. *J Infect Dis* (2010) 201(12):1941–9. doi:10.1086/652783
30. Xie Z, Thompson A, Sobue T, Kashleva H, Xu H, Vasilakos J, et al. *Candida albicans* biofilms do not trigger reactive oxygen species and evade neutrophil killing. *J Infect Dis* (2012) 206(12):1936–45. doi:10.1093/infdis/jis607
31. Johnson CJ, Cabezas-Olcoz J, Kernien JF, Wang SX, Beebe DJ, Huttenlocher A, et al. The extracellular matrix of *Candida albicans* biofilms impairs formation of neutrophil extracellular traps. *PLoS Pathog* (2016) 12(9):1–23. doi:10.1371/journal.ppat.1005884
32. Lee MJ, Liu H, Barker BM, Snarr BD, Gravelat FN, Al Abdallah Q, et al. The fungal exopolysaccharide galactosaminogalactan mediates virulence by enhancing resistance to neutrophil extracellular traps. *PLoS Pathog* (2015) 11(10):e1005187. doi:10.1371/journal.ppat.1005187
33. Beauvais A, Latge JP. *Aspergillus* biofilm in vitro and in vivo. *Microbiol Spectr* (2015) 3(4):1–10. doi:10.1128/microbiolspec.MB-0017-2015
34. Chandra J, Mukherjee PK. *Candida* biofilms: development, architecture, and resistance. *Microbiol Spectr* (2015) 3(4):1–14. doi:10.1128/microbiolspec.MB-0020-2015
35. Desai JV, Mitchell AP, Andes DR. Fungal biofilms, drug resistance, and recurrent infection. *Cold Spring Harb Perspect Med* (2014) 4(10):1–18. doi:10.1101/cshperspect.a019729
36. Nett JE. Future directions for anti-biofilm therapeutics targeting *Candida*. *Expert Rev Anti Infect Ther* (2014) 12(3):375–82. doi:10.1586/14787210.2014.885838
37. Fox EP, Nobile CJ. A sticky situation: untangling the transcriptional network controlling biofilm development in *Candida albicans*. *Transcription* (2012) 3(6):315–22. doi:10.4161/trns.22281
38. Baillie GS, Douglas LJ. Matrix polymers of *Candida* biofilms and their possible role in biofilm resistance to antifungal agents. *J Antimicrob Chemother* (2000) 46(3):397–403. doi:10.1093/jac/46.3.397
39. Hawser SP, Baillie GS, Douglas LJ. Production of extracellular matrix by *Candida albicans* biofilms. *J Med Microbiol* (1998) 47(3):253–6. doi:10.1099/00222615-47-3-253
40. Zarnowski R, Westler WM, Lacmbouh GA, Marita JM, Bothe JR, Bernhardt J, et al. Novel entries in a fungal biofilm matrix encyclopedia. *MBio* (2014) 5(4):e1333–1314. doi:10.1128/mBio.01333-14
41. Martinez LR, Casadevall A. *Cryptococcus neoformans* biofilm formation depends on surface support and carbon source and reduces fungal cell susceptibility to heat, cold, and UV light. *Appl Environ Microbiol* (2007) 73(14):4592–601. doi:10.1128/aem.02506-06
42. Chandra J, McCormick TS, Imamura Y, Mukherjee PK, Ghannoum MA. Interaction of *Candida albicans* with adherent human peripheral blood mononuclear cells increases *C. albicans* biofilm formation and results in differential expression of pro- and anti-inflammatory cytokines. *Infect Immun* (2007) 75(5):2612–20. doi:10.1128/iai.01841-06
43. Katragkou A, Chatzimoschou A, Simitsopoulou M, Georgiadou E, Roilides E. Additive antifungal activity of anidulafungin and human neutrophils against *Candida parapsilosis* biofilms. *J Antimicrob Chemother* (2011) 66(3):588–91. doi:10.1093/jac/dkq466
44. Kernien J, Johnson C, Nett J. Conserved inhibition of neutrophil extracellular trap release by clinical *Candida albicans* biofilms. *J Fungi (Basel)* (2017) 3(3):49. doi:10.3390/jof3030049
45. Johnson CJ, Kernien JF, Hoyer AR, Nett JE. Mechanisms involved in the triggering of neutrophil extracellular traps (NETs) by *Candida glabrata* during planktonic and biofilm growth. *Sci Rep* (2017) 7(1):13065. doi:10.1038/s41598-017-13588-6
46. Bruns S, Kniemeyer O, Hasenberg M, Aimanianda V, Nietzsche S, Thywissen A, et al. Production of extracellular traps against *Aspergillus fumigatus* in vitro and in infected lung tissue is dependent on invading neutrophils and influenced by hydrophobin RodA. *PLoS Pathog* (2010) 6(4):e1000873. doi:10.1371/journal.ppat.1000873
47. Gravelat FN, Beauvais A, Liu H, Lee MJ, Snarr BD, Chen D, et al. *Aspergillus* galactosaminogalactan mediates adherence to host constituents and conceals hyphal beta-glucan from the immune system. *PLoS Pathog* (2013) 9(8):e1003575. doi:10.1371/journal.ppat.1003575
48. de Jesus Carrion S, Leal SM, Ghannoum MA, Pearlman E. The RodA hydrophobin on *Aspergillus fumigatus* spores masks Dectin-1 and Dectin-2 dependent responses and enhances fungal survival in vivo. *J Immunol* (2013) 191(5):2581–8. doi:10.4049/jimmunol.1300748
49. Gresnigt MS, Bozza S, Becker KL, Joosten LA, Abdollahi-Roodsaz S, van der Berg WB, et al. A polysaccharide virulence factor from *Aspergillus fumigatus* elicits anti-inflammatory effects through induction of interleukin-1 receptor antagonist. *PLoS Pathog* (2014) 10(3):e1003936. doi:10.1371/journal.ppat.1003936
50. Chai LY, Netea MG, Sugui J, Vonk AG, Van De Sande WW, Warris A, et al. *Aspergillus fumigatus* conidial melanin modulates host cytokine response. *Immunobiology* (2010) 215(11):915–20. doi:10.1016/j.imbio.2009.10.002
51. Achkar JM, Fries BC. *Candida* infections of the genitourinary tract. *Clin Microbiol Rev* (2010) 23(2):253–73. doi:10.1128/cmr.00076-09
52. Kennedy MJ, Volz PA. Ecology of *Candida albicans* gut colonization: inhibition of *Candida* adhesion, colonization, and dissemination from the gastrointestinal tract by bacterial antagonism. *Infect Immun* (1985) 49(3):654–63.
53. Kumamoto CA. *Candida* biofilms. *Curr Opin Microbiol* (2002) 5(6):608–11. doi:10.1016/S1369-5274(02)00371-5
54. Kumamoto CA. Inflammation and gastrointestinal *Candida* colonization. *Curr Opin Microbiol* (2011) 14(4):386–91. doi:10.1016/j.mib.2011.07.015
55. Webb BC, Thomas CJ, Willcox MD, Harty DW, Knox KW. *Candida*-associated denture stomatitis. Aetiology and management: a review. Part 2. Oral diseases caused by *Candida* species. *Aust Dent J* (1998) 43(3):160–6. doi:10.1111/j.1834-7819.1998.tb00172.x
56. Vazquez JA. Options for the management of mucosal candidiasis in patients with AIDS and HIV infection. *Pharmacother J Hum Pharmacol Drug Ther* (1999) 19(1):76–87. doi:10.1592/phco.19.1.76.30509
57. Launay O, Lortholary O, Bouges-Michel C, Jarrousse B, Bentata M, Guillevin L. Candidemia: a nosocomial complication in adults with late-stage AIDS. *Clin Infect Dis* (1998) 26(5):1134–41. doi:10.1086/520291
58. Douglas LJ. *Candida* biofilms and their role in infection. *Trends Microbiol* (2003) 11(1):30–6. doi:10.1016/S0966-842X(02)00002-1
59. Kumamoto CA, Vinces MD. Alternative *Candida albicans* lifestyles: growth on surfaces. *Annu Rev Microbiol* (2005) 59:113–33. doi:10.1146/annurev.micro.59.030804.121034
60. Uppuluri P, Pierce CG, Lopez-Ribot JL. *Candida albicans* biofilm formation and its clinical consequences. *Future Microbiol* (2009) 4(10):1235–7. doi:10.2217/fmb.09.85
61. Dongari-Bagtzoglou A. Mucosal biofilms: challenges and future directions. *Expert Rev Anti Infect Ther* (2008) 6(2):141–4. doi:10.1586/14787210.6.2.141
62. Shin JH, Kee SJ, Shin MG, Kim SH, Shin DH, Lee SK, et al. Biofilm production by isolates of *Candida* species recovered from nonneutropenic patients: comparison of bloodstream isolates with isolates from other sources. *J Clin Microbiol* (2002) 40(4):1244–8. doi:10.1128/jcm.40.4.1244-1248.2002

63. Bizerra FC, Nakamura CV, de Poersch C, Estivalet Svidzinski TI, Borsato Quesada RM, Goldenberg S, et al. Characteristics of biofilm formation by *Candida tropicalis* and antifungal resistance. *FEMS Yeast Res* (2008) 8(3):442–50. doi:10.1111/j.1567-1364.2007.00347.x
64. Kuhn DM, Chandra J, Mukherjee PK, Ghannoum MA. Comparison of biofilms formed by *Candida albicans* and *Candida parapsilosis* on bioprosthetic surfaces. *Infect Immun* (2002) 70(2):878–88. doi:10.1128/IAI.70.2.878-888.2002
65. Jain N, Kohli R, Cook E, Gialanella P, Chang T, Fries BC. Biofilm formation by and antifungal susceptibility of *Candida* isolates from urine. *Appl Environ Microbiol* (2007) 73(6):1697–703. doi:10.1128/aem.02439-06
66. Lewis RE, Kontoyiannis DP, Darouiche RO, Raad II, Prince RA. Antifungal activity of amphotericin B, fluconazole, and voriconazole in an in vitro model of *Candida* catheter-related bloodstream infection. *Antimicrob Agents Chemother* (2002) 46(11):3499–505. doi:10.1128/AAC.46.11.3499-3505.2002
67. Thein ZM, Samaranayake YH, Samaranayake LP. In vitro biofilm formation of *Candida albicans* and non-*albicans Candida* species under dynamic and anaerobic conditions. *Arch Oral Biol* (2007) 52(8):761–7. doi:10.1016/j.archoralbio.2007.01.009
68. Tumbarello M, Posteraro B, Trecarichi EM, Fiori B, Rossi M, Porta R, et al. Biofilm production by *Candida* species and inadequate antifungal therapy as predictors of mortality for patients with candidemia. *J Clin Microbiol* (2007) 45(6):1843–50. doi:10.1128/jcm.00131-07
69. Sherry L, Ramage G, Kean R, Borman A, Johnson EM, Richardson MD, et al. Biofilm-forming capability of highly virulent, multidrug-resistant *Candida auris*. *Emerg Infect Dis* (2017) 23(2):328–31. doi:10.3201/eid2302.161320
70. Chandra J, Kuhn DM, Mukherjee PK, Hoyer LL, McCormick T, Ghannoum MA. Biofilm formation by the fungal pathogen *Candida albicans*: development, architecture, and drug resistance. *J Bacteriol* (2001) 183(18):5385–94. doi:10.1128/JB.183.18.5385-5394.2001
71. Ramage G, Mowat E, Jones B, Williams C, Lopez-Ribot J. Our current understanding of fungal biofilms. *Crit Rev Microbiol* (2009) 35(4):340–55. doi:10.3109/10408410903241436
72. Ramage G, Saville SP, Thomas DP, López-Ribot JL. *Candida* biofilms: an update. *Eukaryot Cell* (2005) 4(4):633–8. doi:10.1128/ec.4.4.633-638.2005
73. Silva S, Henriques M, Martins A, Oliveira R, Williams D, Azeredo J. Biofilms of non-*Candida albicans Candida* species: quantification, structure and matrix composition. *Med Mycol* (2009) 47(7):681–9. doi:10.3109/13693780802549594
74. Mitchell KF, Taff HT, Cuevas MA, Reinicke EL, Sanchez H, Andes DR. Role of matrix β-1,3 glucan in antifungal resistance of non-*albicans Candida* biofilms. *Antimicrob Agents Chemother* (2013) 57(4):1918–20. doi:10.1128/aac.02378-12
75. Mitchell KF, Zarnowski R, Sanchez H, Edward JA, Reinicke EL, Nett JE, et al. Community participation in biofilm matrix assembly and function. *Proc Natl Acad Sci U S A* (2015) 112(13):4092–7. doi:10.1073/pnas.1421437112
76. Nett JE, Zarnowski R, Cabezas-Olcoz J, Brooks EG, Bernhardt J, Marchillo K, et al. Host contributions to construction of three device-associated *Candida albicans* biofilms. *Infect Immun* (2015) 83(12):4630–8. doi:10.1128/iai.00931-15
77. Martins M, Henriques M, Lopez-Ribot JL, Oliveira R. Addition of DNase improves the in vitro activity of antifungal drugs against *Candida albicans* biofilms. *Mycoses* (2012) 55(1):80–5. doi:10.1111/j.1439-0507.2011.02047.x
78. Nett JE, Sanchez H, Cain MT, Ross KM, Andes DR. Interface of *Candida albicans* biofilm matrix-associated drug resistance and cell wall integrity regulation. *Eukaryot Cell* (2011) 10(12):1660–9. doi:10.1128/EC.05126-11
79. Thomas DP, Bachmann SP, Lopez-Ribot JL. Proteomics for the analysis of the *Candida albicans* biofilm lifestyle. *Proteomics* (2006) 6(21):5795–804. doi:10.1002/pmic.200600332
80. Martins M, Uppuluri P, Thomas DP, Cleary IA, Henriques M, Lopez-Ribot JL, et al. Presence of extracellular DNA in the *Candida albicans* biofilm matrix and its contribution to biofilms. *Mycopathologia* (2010) 169(5):323–31. doi:10.1007/s11046-009-9264-y
81. Klis FM, de Groot P, Hellingwerf K. Molecular organization of the cell wall of *Candida albicans*. *Med Mycol* (2001) 39(Suppl 1):1–8. doi:10.1080/mmy.39.1.1.8-0
82. Chaffin WL, López-Ribot JL, Casanova M, Gozalbo D, Martínez JP. Cell wall and secreted proteins of *Candida albicans*: identification, function, and expression. *Microbiol Mol Biol Rev* (1998) 62(1):130–80.
83. Edwards JE Jr, Lehrer RI, Stiehm ER, Fischer TJ, Young LS. Severe candidal infections: clinical perspective, immune defense mechanisms, and current concepts of therapy. *Ann Intern Med* (1978) 89(1):91–106. doi:10.7326/0003-4819-89-1-91
84. Fidel PL Jr. Immunity to *Candida*. *Oral Dis* (2002) 8(Suppl 2):69–75. doi:10.1034/j.1601-0825.2002.00015.x
85. Erwig LP, Gow NA. Interactions of fungal pathogens with phagocytes. *Nat Rev Microbiol* (2016) 14(3):163–76. doi:10.1038/nrmicro.2015.21
86. Pappas PG, Kauffman CA, Andes DR, Clancy CJ, Marr KA, Ostrosky-Zeichner L, et al. Clinical practice guideline for the management of candidiasis: 2016 update by the Infectious Diseases Society of America. *Clin Infect Dis* (2016) 62(4):e1–50. doi:10.1093/cid/civ933
87. Kolaczkowska E, Kubes P. Neutrophil recruitment and function in health and inflammation. *Nat Rev Immunol* (2013) 13(3):159–75. doi:10.1038/nri3399
88. Nett JE. The host's reply to *Candida* biofilm. *Pathogens* (2016) 5(1):1–10. doi:10.3390/pathogens5010033
89. Yano J, Noverr MC, Fidel PL Jr. Cytokines in the host response to *Candida* vaginitis: identifying a role for non-classical immune mediators, S100 alarmins. *Cytokine* (2012) 58(1):118–28. doi:10.1016/j.cyto.2011.11.021
90. Nieminen MT, Hernandez M, Novak-Frazer L, Kuula H, Ramage G, Bowyer P, et al. DL-2-hydroxyisocaproic acid attenuates inflammatory responses in a murine *Candida albicans* biofilm model. *Clin Vaccine Immunol* (2014) 21(9):1240–5. doi:10.1128/CVI.00339-14
91. Fidel PL, Barousse M, Espinosa T, Ficarra M, Sturtevant J, Martin DH, et al. An intravaginal live *Candida* challenge in humans leads to new hypotheses for the immunopathogenesis of vulvovaginal candidiasis. *Infect Immun* (2004) 72(5):2939–46. doi:10.1128/iai.72.5.2939-2946.2004
92. Katragkou A, Simitsopoulou M, Chatzimoschou A, Georgiadou E, Walsh TJ, Roilides E. Effects of interferon-gamma and granulocyte colony-stimulating factor on antifungal activity of human polymorphonuclear neutrophils against *Candida albicans* grown as biofilms or planktonic cells. *Cytokine* (2011) 55(3):330–4. doi:10.1016/j.cyto.2011.05.007
93. Branzk N, Lubojemska A, Hardison SE, Wang Q, Gutierrez MG, Brown GD, et al. Neutrophils sense microbe size and selectively release neutrophil extracellular traps in response to large pathogens. *Nat Immunol* (2014) 15(11):1017–25. doi:10.1038/ni.2987
94. Brinkmann V, Reichard U, Goosmann C, Fauler B, Uhlemann Y, Weiss DS, et al. Neutrophil extracellular traps kill bacteria. *Science* (2004) 303(5663):1532–5. doi:10.1126/science.1092385
95. Urban CF, Reichard U, Brinkmann V, Zychlinsky A. Neutrophil extracellular traps capture and kill *Candida albicans* yeast and hyphal forms. *Cell Microbiol* (2006) 8(4):668–76. doi:10.1111/j.1462-5822.2005.00659.x
96. Byrd AS, O'Brien XM, Johnson CM, Lavigne LM, Reichner JS. An extracellular matrix-based mechanism of rapid neutrophil extracellular trap formation in response to *Candida albicans*. *J Immunol* (2013) 190(8):4136–48. doi:10.4049/jimmunol.1202671
97. Zawrotniak M, Bochenska O, Karkowska-Kuleta J, Seweryn-Ozog K, Aoki W, Ueda M, et al. Aspartic proteases and major cell wall components in *Candida albicans* trigger the release of neutrophil extracellular traps. *Front Cell Infect Microbiol* (2017) 7:414. doi:10.3389/fcimb.2017.00414
98. Kenny EF, Herzig A, Kruger R, Muth A, Mondal S, Thompson PR, et al. Diverse stimuli engage different neutrophil extracellular trap pathways. *Elife* (2017) 6:e24437. doi:10.7554/eLife.24437
99. Bjornsdottir H, Welin A, Michaelsson E, Osla V, Berg S, Christenson K, et al. Neutrophil NET formation is regulated from the inside by myeloperoxidase-processed reactive oxygen species. *Free Radic Biol Med* (2015) 89:1024–35. doi:10.1016/j.freeradbiomed.2015.10.398
100. Stoiber W, Obermayer A, Steinbacher P, Krautgartner WD. The role of reactive oxygen species (ROS) in the formation of extracellular traps (ETs) in humans. *Biomolecules* (2015) 5(2):702–23. doi:10.3390/biom5020702
101. Gray RD, Lucas CD, Mackellar A, Li F, Hiersemenzel K, Haslett C, et al. Activation of conventional protein kinase C (PKC) is critical in the generation of human neutrophil extracellular traps. *J Inflamm (Lond)* (2013) 10(1):12. doi:10.1186/1476-9255-10-12

102. Hogan D, Wheeler RT. The complex roles of NADPH oxidases in fungal infection. *Cell Microbiol* (2014) 16(8):1156–67. doi:10.1111/cmi.12320
103. Metzler KD, Fuchs TA, Nauseef WM, Reumaux D, Roesler J, Schulze I, et al. Myeloperoxidase is required for neutrophil extracellular trap formation: implications for innate immunity. *Blood* (2011) 117(3):953–9. doi:10.1182/blood-2010-06-290171
104. Rocha FAC, Alves A, Rocha MFG, Cordeiro RA, Brilhante RSN, Pinto A, et al. Tumor necrosis factor prevents *Candida albicans* biofilm formation. *Sci Rep* (2017) 7(1):1206. doi:10.1038/s41598-017-01400-4
105. Alonso M, Gow N, Erwig L, Bain J. Macrophage migration is impaired within *Candida albicans* biofilms. *J Fungi* (2017) 3(3):31. doi:10.3390/jof3030031
106. Patterson TF, Thompson GR III, Denning DW, Fishman JA, Hadley S, Herbrecht R, et al. Practice guidelines for the diagnosis and management of aspergillosis: 2016 update by the infectious diseases society of America. *Clin Infect Dis* (2016) 63(4):e1–60. doi:10.1093/cid/ciw326
107. Sheppard DC, Howell PL. Biofilm exopolysaccharides of pathogenic fungi: lessons from bacteria. *J Biol Chem* (2016) 291(24):12529–37. doi:10.1074/jbc.R116.720995
108. Reichhardt C, Ferreira JA, Joubert LM, Clemons KV, Stevens DA, Cegelski L. Analysis of the *Aspergillus fumigatus* biofilm extracellular matrix by solid-state nuclear magnetic resonance spectroscopy. *Eukaryot Cell* (2015) 14(11):1064–72. doi:10.1128/ec.00050-15
109. Rajendran R, Williams C, Lappin DF, Millington O, Martins M, Ramage G. Extracellular DNA release acts as an antifungal resistance mechanism in mature *Aspergillus fumigatus* biofilms. *Eukaryot Cell* (2013) 12(3):420–9. doi:10.1128/EC.00287-12
110. Shopova I, Bruns S, Thywissen A, Kniemeyer O, Brakhage AA, Hillmann F. Extrinsic extracellular DNA leads to biofilm formation and colocalizes with matrix polysaccharides in the human pathogenic fungus *Aspergillus fumigatus*. *Front Microbiol* (2013) 4:141. doi:10.3389/fmicb.2013.00141
111. Fontaine T, Delangle A, Simenel C, Coddeville B, van Vliet SJ, van Kooyk Y, et al. Galactosaminogalactan, a new immunosuppressive polysaccharide of *Aspergillus fumigatus*. *PLoS Pathog* (2011) 7(11):e1002372. doi:10.1371/journal.ppat.1002372
112. Lee MJ, Gravelat FN, Cerone RP, Baptista SD, Campoli PV, Choe SI, et al. Overlapping and distinct roles of *Aspergillus fumigatus* UDP-glucose 4-epimerases in galactose metabolism and the synthesis of galactose-containing cell wall polysaccharides. *J Biol Chem* (2014) 289(3):1243–56. doi:10.1074/jbc.M113.522516
113. Lee MJ, Geller AM, Bamford NC, Liu H, Gravelat FN, Snarr BD, et al. Deacetylation of fungal exopolysaccharide mediates adhesion and biofilm formation. *MBio* (2016) 7(2):1–14. doi:10.1128/mBio.00252-16
114. Ruperez P, Leal JA. Extracellular galactosaminogalactan from *Aspergillus parasiticus*. *Trans Br Mycol Soc* (1981) 77(3):621–5. doi:10.1016/S0007-1536(81)80111-8
115. Bardalaye PC, Nordin JH. Galactosaminogalactan from cell walls of *Aspergillus niger*. *J Bacteriol* (1976) 125(2):655–69.
116. Gorin PA, Eveleigh DE. Extracellular 2-acetamido-2-deoxy-D-galacto-D-galactan from *Aspergillus nidulans*. *Biochemistry* (1970) 9(25):5023–7. doi:10.1021/bi00827a029
117. Leal JA, Rupérez P. Extracellular polysaccharide production by *Aspergillus nidulans*. *Trans Br Mycol Soc* (1978) 70(1):115–20. doi:10.1016/S0007-1536(78)80180-6
118. Akoumianaki T, Kyrmizi I, Valsecchi I, Gresnigt MS, Samonis G, Drakos E, et al. *Aspergillus* cell wall melanin blocks LC3-associated phagocytosis to promote pathogenicity. *Cell Host Microbe* (2016) 19(1):79–90. doi:10.1016/j.chom.2015.12.002
119. Feldmesser M. Role of neutrophils in invasive aspergillosis. *Infect Immun* (2006) 74(12):6514–6. doi:10.1128/iai.01551-06
120. Gerson SL, Talbot GH, Hurwitz S, Strom BL, Lusk EJ, Cassileth PA. Prolonged granulocytopenia: the major risk factor for invasive pulmonary aspergillosis in patients with acute leukemia. *Ann Intern Med* (1984) 100(3):345–51. doi:10.7326/0003-4819-100-3-345
121. Bonnett CR, Cornish EJ, Harmsen AG, Burritt JB. Early neutrophil recruitment and aggregation in the murine lung inhibit germination of *Aspergillus fumigatus* conidia. *Infect Immun* (2006) 74(12):6528–39. doi:10.1128/iai.00909-06
122. Sturtevant J, Latge JP. Participation of complement in the phagocytosis of the conidia of *Aspergillus fumigatus* by human polymorphonuclear cells. *J Infect Dis* (1992) 166(3):580–6. doi:10.1093/infdis/166.3.580
123. Behnsen J, Narang P, Hasenberg M, Gunzer F, Bilitewski U, Klippel N, et al. Environmental dimensionality controls the interaction of phagocytes with the pathogenic fungi *Aspergillus fumigatus* and *Candida albicans*. *PLoS Pathog* (2007) 3(2):e13. doi:10.1371/journal.ppat.0030013
124. Jaillon S, Peri G, Delneste Y, Fremaux I, Doni A, Moalli F, et al. The humoral pattern recognition receptor PTX3 is stored in neutrophil granules and localizes in extracellular traps. *J Exp Med* (2007) 204(4):793–804. doi:10.1084/jem.20061301
125. Bianchi M, Hakkim A, Brinkmann V, Siler U, Seger RA, Zychlinsky A, et al. Restoration of NET formation by gene therapy in CGD controls aspergillosis. *Blood* (2009) 114(13):2619–22. doi:10.1182/blood-2009-05-221606
126. McCormick A, Heesemann L, Wagener J, Marcos V, Hartl D, Loeffler J, et al. NETs formed by human neutrophils inhibit growth of the pathogenic mold *Aspergillus fumigatus*. *Microbes Infect* (2010) 12(12–13):928–36. doi:10.1016/j.micinf.2010.06.009
127. Snarr BD, Baker P, Bamford NC, Sato Y, Liu H, Lehoux M, et al. Microbial glycoside hydrolases as antibiofilm agents with cross-kingdom activity. *Proc Natl Acad Sci U S A* (2017) 114(27):7124–9. doi:10.1073/pnas.1702798114
128. Gravelat FN, Ejzykowicz DE, Chiang LY, Chabot JC, Urb M, Macdonald KD, et al. *Aspergillus fumigatus* MedA governs adherence, host cell interactions and virulence. *Cell Microbiol* (2010) 12(4):473–88. doi:10.1111/j.1462-5822.2009.01408.x
129. Robinet P, Baychelier F, Fontaine T, Picard C, Debre P, Vieillard V, et al. A polysaccharide virulence factor of a human fungal pathogen induces neutrophil apoptosis via NK cells. *J Immunol* (2014) 192(11):5332–42. doi:10.4049/jimmunol.1303180
130. Rohm M, Grimm MJ, D'Auria AC, Almyroudis NG, Segal BH, Urban CF. NADPH oxidase promotes neutrophil extracellular trap formation in pulmonary aspergillosis. *Infect Immun* (2014) 82(5):1766–77. doi:10.1128/IAI.00096-14
131. Gibbons JG, Beauvais A, Beau R, McGary KL, Latge JP, Rokas A. Global transcriptome changes underlying colony growth in the opportunistic human pathogen *Aspergillus fumigatus*. *Eukaryot Cell* (2012) 11(1):68–78. doi:10.1128/ec.05102-11
132. Perfect JR, Dismukes WE, Dromer F, Goldman DL, Graybill JR, Hamill RJ, et al. Clinical practice guidelines for the management of cryptococcal disease: 2010 update by the infectious diseases society of America. *Clin Infect Dis* (2010) 50(3):291–322. doi:10.1086/649858
133. Walsh TJ, Schlegel R, Moody MM, Costerton JW, Salcman M. Ventriculoatrial shunt infection due to *Cryptococcus neoformans*: an ultrastructural and quantitative microbiological study. *Neurosurgery* (1986) 18(3):373–5. doi:10.1227/00006123-198603000-00025
134. Bach MC, Tally PW, Godofsky EW. Use of cerebrospinal fluid shunts in patients having acquired immunodeficiency syndrome with cryptococcal meningitis and uncontrollable intracranial hypertension. *Neurosurgery* (1997) 41(6):1280–2; discussion 2–3. doi:10.1097/00006123-199712000-00008
135. Braun DK, Janssen DA, Marcus JR, Kauffman CA. Cryptococcal infection of a prosthetic dialysis fistula. *Am J Kidney Dis* (1994) 24(5):864–7. doi:10.1016/S0272-6386(12)80683-4
136. Banerjee U, Gupta K, Venugopal P. A case of prosthetic valve endocarditis caused by *Cryptococcus neoformans* var. *neoformans*. *J Med Vet Mycol* (1997) 35(2):139–41. doi:10.1080/02681219780001031
137. Martinez LR, Casadevall A. Biofilm formation by *Cryptococcus neoformans*. *Microbiol Spectr* (2015) 3(3):1–11. doi:10.1128/microbiolspec.MB-0006-2014
138. Vecchiarelli A. Immunoregulation by capsular components of *Cryptococcus neoformans*. *Med Mycol* (2000) 38(6):407–17. doi:10.1080/714030973
139. Dong ZM, Murphy JW. Intravascular cryptococcal culture filtrate (CneF) and its major component, glucuronoxylomannan, are potent inhibitors of leukocyte accumulation. *Infect Immun* (1995) 63(3):770–8.
140. Baena-Monroy T, Moreno-Maldonado V, Franco-Martinez F, Aldape-Barrios B, Quindos G, Sanchez-Vargas LO. *Candida albicans*, *Staphylococcus aureus* and *Streptococcus mutans* colonization in patients wearing dental prosthesis. *Med Oral Patol Oral Cir Bucal* (2005) 10(Suppl 1):E27–39.
141. Martinez LR, Christaki E, Casadevall A. Specific antibody to *Cryptococcus neoformans* glucurunoxylomannan antagonizes antifungal drug action

against cryptococcal biofilms in vitro. *J Infect Dis* (2006) 194(2):261–6. doi:10.1086/504722

142. Rocha JD, Nascimento MT, Decote-Ricardo D, Corte-Real S, Morrot A, Heise N, et al. Capsular polysaccharides from *Cryptococcus neoformans* modulate production of neutrophil extracellular traps (NETs) by human neutrophils. *Sci Rep* (2015) 5:8008. doi:10.1038/srep08008
143. Monari C, Casadevall A, Retini C, Baldelli F, Bistoni F, Vecchiarelli A. Antibody to capsular polysaccharide enhances the function of neutrophils from patients with AIDS against *Cryptococcus neoformans*. *AIDS* (1999) 13(6):653–60. doi:10.1097/00002030-199904160-00005

Conflict of Interest Statement: The authors declare that the research was conducted in the absence of any commercial or financial relationships that could be construed as a potential conflict of interest.

Copyright © 2018 Kernien, Snarr, Sheppard and Nett. This is an open-access article distributed under the terms of the Creative Commons Attribution License (CC BY). The use, distribution or reproduction in other forums is permitted, provided the original author(s) or licensor are credited and that the original publication in this journal is cited, in accordance with accepted academic practice. No use, distribution or reproduction is permitted which does not comply with these terms.

frontiers in Microbiology

PERSPECTIVE
published: 12 December 2017
doi: 10.3389/fmicb.2017.02477

Fungal Microbiota in Chronic Airway Inflammatory Disease and Emerging Relationships with the Host Immune Response

Irene Zhang[1], *Steven D. Pletcher*[2], *Andrew N. Goldberg*[2], *Bridget M. Barker*[1] *and Emily K. Cope*[1]*

[1] *Pathogen and Microbiome Institute, Northern Arizona University, Flagstaff, AZ, United States,* [2] *Department of Otolaryngology Head and Neck Surgery, University of California, San Francisco, San Francisco, CA, United States*

The respiratory tract is a complex system that is inhabited by niche-specific communities of microbes including bacteria, fungi, and viruses. These complex microbial assemblages are in constant contact with the mucosal immune system and play a critical role in airway health and immune homeostasis. Changes in the composition and diversity of airway microbiota are frequently observed in patients with chronic inflammatory diseases including chronic rhinosinusitis (CRS), cystic fibrosis, allergy, and asthma. While the bacterial microbiome of the upper and lower airways has been the focus of many recent studies, the contribution of fungal microbiota to inflammation is an emerging research interest. Within the context of allergic airway disease, fungal products are important allergens and fungi are potent inducers of inflammation. In addition, murine models have provided experimental evidence that fungal microbiota in peripheral organs, notably the gastrointestinal (GI) tract, influence pulmonary health. In this review, we explore the role of the respiratory and GI microbial communities in chronic airway inflammatory disease development with a specific focus on fungal microbiome interactions with the airway immune system and fungal-bacterial interactions that likely contribute to inflammatory disease. These findings are discussed in the context of clinical and immunological features of fungal-mediated disease in CRS, allergy, and asthmatic patients. While this field is still nascent, emerging evidence suggests that dysbiotic fungal and bacterial microbiota interact to drive or exacerbate chronic airway inflammatory disease.

Keywords: airway microbiome, airway fungal microbiome, mycobiome, host-microbiome interactions, bacterial-fungal interactions, biofilm

OPEN ACCESS

Edited by:
Steven Templeton,
Indiana University School of Medicine - Terre Haute, United States

Reviewed by:
Jeniel E. Nett,
University of Wisconsin-Madison, United States
Iliyan Iliev,
Weill Cornell Medical College, Cornell University, United States

***Correspondence:**
Emily K. Cope
emily.cope@nau.edu

Specialty section:
This article was submitted to Microbial Immunology, a section of the journal Frontiers in Microbiology

Received: *01 October 2017*
Accepted: *29 November 2017*
Published: *12 December 2017*

Citation:
Zhang I, Pletcher SD, Goldberg AN, Barker BM and Cope EK (2017) Fungal Microbiota in Chronic Airway Inflammatory Disease and Emerging Relationships with the Host Immune Response. Front. Microbiol. 8:2477. doi: 10.3389/fmicb.2017.02477

INTRODUCTION

Microbial communities associated with host mucosal surfaces play essential and diverse roles in biological processes from metabolism to immune regulation and homeostasis. In return, host inflammatory responses can shape the microbial community by supporting the growth of some microbes while inhibiting others (Kumamoto, 2016). Most studies of host-associated microbiota in health and disease have focused on the bacterial microbiota, despite fungal diseases incurring a substantial infectious disease burden (Huffnagle and Noverr, 2013). Because of this, relatively little is known about the importance and function of the fungal microbiota (mycobiota). Recent

advances in culture-independent sequencing approaches have helped elucidate the fungal diversity, burden, and functions associated with mucosal surfaces such as the human intestinal tract, oral cavity, skin, and respiratory tract.

In virtually every body habitat studied to date, niche-specific microbial communities have been identified, including the gastrointestinal and respiratory tracts (Human Microbiome Project Consortium, 2012). Fungi live in host niches as commensals and interact with bacteria and the host as members of the healthy microbiome. While fungal microbiota are numerically small, they are diverse, have large genomes, and potentially act as important keystone species in the microbiome (Huffnagle and Noverr, 2013). Studies have shown that disrupting commensal fungi can affect both local and peripheral immune responses and enhance disease states. In addition, members of the mycobiome can switch from commensalism to pathogenicity, often dependent upon co-colonizing microbial taxa (Cohen et al., 1969; Peleg et al., 2010). Recent studies suggest a role for airway microbial communities in maintaining airway health (Abreu et al., 2012). In this perspective, we focus on the potential role of fungal interactions with the host and bacterial co-colonizers chronic rhinosinusitis (CRS) and lower airway comorbidities.

RESPIRATORY TRACT PHYSIOLOGY

Like the GI tract (Jeraldo et al., 2012), the respiratory tract is composed of distinct environments that vary according to mucosal architecture and immune responses. Reflective of this, the microbial communities that inhabit the respiratory tract exhibit niche specificity; compositionally distinct communities exist between the nares, sinuses, oral cavity, oropharynx and lower airway in healthy individuals (Lemon et al., 2010; Bassis et al., 2015). The sinonasal cavity, nasopharynx, and trachea are lined with a pseudostratified columnar ciliated epithelium and mucus-producing goblet cells. Lung bronchi and bronchioles are covered by stratified columnar ciliated epithelia and few goblet cells. Mucus secretion and immune effector molecules protect the host from insults by trapping and removing inhaled pathogens and irritants, a process orchestrated by ciliary beating (Cohen, 2006). Airway epithelial cells express pattern recognition receptors (PRRs), including toll-like receptors (TLR) and non-TLR PRRs such as Dectin-1, that can recognize and respond to components of microorganisms (Ryu et al., 2013; Liu et al., 2015).

CHRONIC INFLAMMATORY DISEASES OF THE UPPER AND LOWER AIRWAYS

Chronic airway inflammatory diseases including asthma, rhinosinusitis, and rhinitis are substantial health problems resulting in significant healthcare expenditures. Chronic rhinosinusitis (CRS) alone affects approximately 15% of the adult population annually; recent estimates suggest that costs associated with CRS exceed $65 billion each year accounting for 5% of the US healthcare budget (Caulley et al., 2015). Several epidemiological studies suggest that concomitant upper and lower airway disease result from shared pathophysiologic mechanisms (Passalacqua et al., 2001; Ciprandi et al., 2012; Licari et al., 2014).

CRS is clinically defined by duration of symptoms and endoscopic or radiographic evidence of sinus inflammation. Multiple subtypes of CRS have been described based on clinical (Akdis et al., 2013; Orlandi et al., 2016), immunological (Tomassen et al., 2016) and microbiological (Cope et al., 2017) heterogeneity. The role of fungi in the pathophysiology of CRS has long been controversial. While some authors argued that fungi drove inflammation in nearly all CRS patients (Ponikau et al., 2000), this finding has been recently disputed (Orlandi and Marple, 2010; Fokkens et al., 2012). Fungi clearly play a central role in several discrete subtypes of CRS, such as allergic fungal sinusitis and development of fungus balls (deShazo et al., 1997). Fungi found in culture-based studies of CRS patients include members of *Aspergillus*, *Alternaria*, *Candida*, *Cladosporium*, and *Penicillium* (Ponikau et al., 1999). Molecular studies have expanded this list to include fastidious fungi *Malassezia*, *Curvularia, Schizophyllum*, and *Neocosmospora* (Cleland et al., 2014; Gelber et al., 2016; Zhao et al., 2017). While there are few studies on host-fungal interactions in the upper airways, recent research suggests that defects in epithelial genes might compromise immune barrier function and lead to dysfunctional host immune responses to bacterial or fungal colonization (Tieu et al., 2009). Additionally, fungal glycans (e.g., β-glucan) interact with airway epithelial cells via surface receptors and can act as determinants of allergenicity or induce inflammation (Roy and Klein, 2013). In allergic bronchopulmonary aspergillosis (ABPA), structural abnormalities in the airway epithelium allow fungal spores to breach immune defenses and germinate into hyphae (Chaudhary and Marr, 2011). Upon germination, fungal spores secrete proteases which can disrupt epithelial barrier integrity (Chen et al., 2011). Epithelial barrier dysfunction is frequently observed in CRS and asthma (Tieu et al., 2009; Lambrecht and Hammad, 2012). The presence of bacterial and fungal biofilms increased mucosal IgE in CRS patients, suggesting that these biofilms interact with the host immune system and perpetuate chronic inflammation (Foreman et al., 2012).

CRS is phenotypically classified into two groups based on the presence or absence of nasal polyps. This clinical classification of CRS patients was initially reflected immunologically with a predominance of T_H2 cells and eosinophils in CRS patients with polyps (CRSwNP) and a predominance of T_H1 cells and neutrophils in CRS patients without polyps (CRSsNP). However, recent studies using molecular methods have demonstrated up to 10 distinct endotypes of patients using markers of T_H1, T_H2, T_H17, eosinophil, and neutrophil activation (Tomassen et al., 2016). A separate study found four distinct groups of CRS patients characterized by distinct bacterial communities, each conferring a unique immune response (Cope et al., 2017). *Corynebacteriaceae*-dominated communities conferred increased *IL-5* gene expression and a higher risk for nasal polyps. While these findings are helpful, it is also important to understand how the sinus microbiota drive or exacerbate observed inflammatory endotypes so new therapeutics can target the initiation of disease.

Unified Airway Hypothesis

CRS often exists in the setting of concomitant lower airway disease, including asthma, and is frequently preceded by rhinitis. Upper respiratory infections can exacerbate asthma symptoms; bronchial hyperresponsiveness often occurs along with rhinitis (Leynaert et al., 2000; Passalacqua et al., 2001). Between 20 and 60% of CRS patients with nasal polyps have asthma (Larsen, 1996; Klossek et al., 2005). These observations have led to the "unified airway" hypothesis, which treats the respiratory tract as one organ rather than distinct organs affected by specific diseases. Supporting this hypothesis, medical and surgical treatment in the upper airways for CRS frequently results in reduced asthma symptoms. Therefore, respiratory inflammatory disease can be considered a disorder of the entire respiratory tract. Dysbiotic (altered) microbial communities have been described in the upper airways of CRS patients and in the lower airways of asthmatic patients, however, the microbiota of these two sites have not yet been examined in parallel. Below, we will discuss recent findings in CRS and asthmatic microbiota and potential interactions between these important microbial populations.

AIRWAY BACTERIAL MICROBIOME

The upper and lower airways harbor niche-specific microbial communities that relate to health status (Lemon et al., 2010; Huang and Boushey, 2014). Recent studies of the sinonasal microbiome generally demonstrate a loss of bacterial diversity and concomitant enrichment of pathobionts, resident microbes with pathogenic potential, in the sinuses of patients with CRS (Biswas et al., 2015; Cope et al., 2017; Lal et al., 2017; Wagner Mackenzie et al., 2017). Abreu and colleagues found that the sinus microbiome was characterized by reduced microbial richness and depletion of taxa associated with healthy individuals, such as lactic acid bacteria (Abreu et al., 2012). This depleted CRS microbiome was enriched with the pathobiont *Corynebacterium tuberculostearicum.* In a murine model, *C. tuberculostearicum* increased host mucin secretion, potentially increasing factors such as nutrient availability and adherence. Larger studies of upper airway microbiota in CRS patients demonstrate a heterogeneous, compositionally distinct microbiota which relate to distinct host immune responses (Cope et al., 2017; Lal et al., 2017). Studies comparing the lung microbiome of asthmatics and healthy controls found increased bacterial burden and diversity among asthmatics and a compositional shift in the bacterial microbiome composition characterized by enriched *Proteobacteria* (Huang et al., 2011; Han et al., 2012; Durack et al., 2017). Polymicrobial biofilms consisting of bacteria and fungi have been observed on sinonasal mucosa using fluorescence *in situ* hybridization, demonstrating that these taxa exist in mixed-species mucosal communities (Sanderson et al., 2006; Doble et al., 2007). More research is required on the upper and lower airway microbiota, and, in particular, on the relationship between sinonasal and pulmonary microbiota and mycobiota. The function and composition of these communities may shed light on the heterogeneity observed in CRS.

AIRWAY FUNGAL MICROBIOME

While the bacterial communities in airway inflammatory disease have been more extensively studied, fungal microbiota are still poorly characterized. This is due, in part, to the challenges faced by researchers who study the airway mycobiome. Low fungal biomass in the airways and databases that are curated from GI or environmental sources affect sample collection, DNA extraction, library preparation, and sequence analysis. In other body sites such as the GI tract, fungal dysbiosis has been implicated in diseases including inflammatory bowel disease. Although outside the scope of this perspective, gut mycobiome dysbiosis and interaction with the host immune response has been extensively reviewed (Underhill and Iliev, 2014; Mukherjee et al., 2015). In the airways, similarities between allergic fungal rhinosinusitis and ABPA illustrate the ability of fungi to act as antigens and invade the respiratory tract.

Studies on the fungal microbiome in CRS and asthma suggest that fungal communities in the airways likely influence host health. *Malassezia*, a known pathobiont on skin (Findley et al., 2013), is the predominant fungal genus in the sinonasal cavity in healthy individuals, CRS patients, and patients with allergic rhinitis (Cleland et al., 2014; Jung et al., 2015; Gelber et al., 2016). Lower abundance fungi in the sinuses of CRS patients include *Aspergillus*, *Alternaria*, *Fusarium*, and *Saccharomyces* (Cleland et al., 2014). A recent study using ITS gene sequencing found fungal presence in the sinuses of 63% of CRS patients and the predominant fungal genus in this study was *Aspergillus* (Zhao et al., 2017). PCR evaluations of *Aspergillus*, however, have demonstrated the presence of this fungus only in the sinuses of CRS patients with a known fungal subtype of CRS (Gelber et al., 2016). These discrepancies may be due to challenges related to fungal databases for human-associated ITS sequences. Analysis of the nasal vestibule of patients with AR and healthy individuals demonstrated increased diversity of fungal communities in AR characterized by preponderance of *Malassezia* (91–99% of 18S rRNA gene sequences) with lower abundance *Aspergillus* and *Alternaria* (Jung et al., 2015). In asthma, the lung mycobiome composition is altered between patients with severe asthma, ABPA, asthma with fungal sensitization (SAFS), and mild asthmatics. In ABPA, *Pseudomonas* abundance and fungal diversity both increased. Severe asthmatics were characterized by enrichment of *Aspergillus;* the relative abundance of *Aspergillus* increased approximately 15-fold compared to mild asthmatics (Chishimba et al., 2015). These results suggest that bacterial and fungal communities change in parallel in subsets of human disease. Future studies examining paired upper and lower airway microbiota (bacterial and fungal) in individuals with CRS and asthma are warranted.

Aspergillus fumigatus is often involved in the development of allergic fungal rhinosinusitis (AFRS) specific subtype CRS that accounts for an estimated 6–9% of all CRS patients undergoing surgery (Schubert, 2004). Patients with AFRS present with hyperplastic sinus disease, characterized by chronic eosinophilic-lymphocytic inflammation and nasal polyps. In

AFRS, fungal hyphae are found within allergic mucin. Sinus cultures obtained in surgical patients reveal the presence of fungal taxa such as *Bipolaris spicifera*, *Alternaria*, and *Aspergillus*. AFRS bears many similarities to ABPA in its immunopathology, treatment, and outcomes. ABPA and AFS patients have elevated levels of serum IgE, and ABPA patients have elevated *A. fumigatus*-specific IgE and IgG. Allergic mucin in AFRS patients is histologically identical to the bronchial mucus plugs in ABPA patients (Schubert, 2004). In ABPA, immunological hypersensitivity is higher relative to AFS, possibly due to differences in the diseased organ or etiological fungus.

Concurrent upper and lower airway disease may be a singular inflammatory process caused or mediated by microbial communities. Microbes or their metabolites might translocate between the upper and lower airways. Interactions between microbes, the environment, and the host inflammatory response could alter the mucus-associated microbial communities, causing dysbiosis. Fungi involved in these allergic fungal disorders, along with associated bacteria such as *S. aureus*, viruses, or other microbes, may act as the source of microbial T-cell superantigens. Fungal contributions to chronic inflammatory airway diseases are an emerging research interest, one which may advance the understanding of such unified airway disorders and treatment for patients with allergic airway disease.

FUNGAL-HOST AND FUNGAL-BACTERIAL INTERACTIONS AND HOST HEALTH

Bacteria and fungi co-inhabit the human body and mounting evidence suggests that microbial interactions in a given niche can influence human health and disease. Bacterial co-colonizers can directly affect fungal morphology (Peters et al., 2012), survival (Romano and Kolter, 2005; Harriott and Noverr, 2009), growth (Kerr et al., 1999), virulence (Schlecht et al., 2015), and attachment to host epithelia or other microbes (El-Azizi et al., 2004; Morales and Hogan, 2010). Current investigations have focused on bacterial interactions with the opportunistic pathogen *Candida albicans*. In the oral cavity, *C. albicans* selectively attaches to the bacterium *Streptococcus gordonii* to increase attachment and growth of the fungi (Holmes et al., 1996). *In vitro* experimental studies have demonstrated that *S. aureus* and *P. aeruginosa* selectively attach to *C. albicans* hyphae but not yeast (Peters et al., 2012; Schlecht et al., 2015), and these interactions have distinct outcomes. *S. aureus* attachment to *Candida* hyphae results in increased invasion of tissue (Schlecht et al., 2015), while *P. aeruginosa* forms biofilms on the hyphal cells, killing the fungus (Hogan and Kolter, 2002). Physical sensing and Quorum sensing (QS) through small molecules that allow microbes to respond to environmental stimuli play important roles in mediating these interactions. For example, the *C. albicans* QS molecule farnesol inhibits *Pseudomonas* quinolone signal (PQS) and virulence factor production (Cugini et al., 2010). *C. albicans* can respond to *P. aeruginosa* QS molecules, specifically 3-3-oxo-C12 homoserine lactone, which prevents hyphal formation in the fungus (Hogan et al., 2004). These species-specific interactions through physical contact and QS molecules likely affect microbial virulence or biofilm formation in host upper or lower airways. Ongoing research in our lab seeks to explore these interactions.

We are interested in interactions between sinonasal-associated fungi and bacterial co-colonizers, including *Malassezia* sp. (Mowat et al., 2010; Jung et al., 2015; Gelber et al., 2016). *Malassezia*, a dimorphic yeast implicated in a variety of conditions including dandruff and atopic dermatitis, is present in the upper airways (Cleland et al., 2014; Gelber et al., 2016). *Malassezia* species are known to be immunomodulatory and encode at least 13 different allergens; these fungi can exist as commensals and can be immunosuppressive (Ashbee and Evans, 2002) or as pathobionts and can become immunostimulatory (Gaitanis et al., 2012). Similar to CRS, *Malassezia dermatis* often co-occurs with *S. aureus* in atopic dermatitis, perhaps interacting with bacteria in driving skin inflammation. Further research is required to identify these *Malassezia* at the species or strain level and to compare populations between healthy subjects and those with allergic airway disease. Mechanistic studies are needed to reveal the interactions between *Malassezia*, bacterial community members, and the host immune system.

Airway epithelial cells and phagocytes express pattern recognition receptors, including C-type lectins, that sense and respond to components of the fungal cell wall. Dectin-1, a pattern recognition receptor expressed by dendritic cells, neutrophils, and macrophages, recognizes the fungal polysaccharide β-1,3 glucan motif found on fungal cell walls. Dectin-1 may mediate host immune responses to these fungi. In mice, loss of dectin-1 resulted in more severe colitis compared to wild-type mice. DSS-induced colitis was associated with increased *Candida* and *Trichosporon* and decreased *Saccharomyces*. Fungi were also found to invade inflamed tissues in dectin-1 KO mice, but not in wild-type mice. When given the antifungal fluconazole, dectin-1 KO mice had milder symptoms (Iliev et al., 2012). These results indicate that fungi contribute to the aggravation of inflammatory responses in colitis, and dectin-1 is an immune mechanism that regulates fungal community composition. Another C-type lectin that specifically recognizes *Malassezia* has recently been described (Yamasaki et al., 2009). When expressed on macrophages, Mincle (also called Clec4e and Clecsf9) sensing of *Malassezia* induces pro-inflammatory responses (Yamasaki et al., 2009), although this receptor has also been implicated in T_H2-polarization upon activation (Geijtenbeek and Gringhuis, 2016). Mincle-deficient mice showed a 2-4 fold reduction of IL-10, TNF-alpha, and MIP1 when challenged with *Malassezia* but not *A. fumigatus* (Yamasaki et al., 2009) Host-associated commensal fungi, therefore, specifically interact with the mucosal immune system, maintaining host and microbial homeostasis.

Fungal microbial communities in the GI tract can also affect the development of respiratory disease. Mice treated with antifungals exhibited increased development of allergic airway disease along with increased disease severity in models of colitis (Wheeler et al., 2016). The microbiomes of these mice revealed a restructuring of fungal and bacterial communities

characterized by decreased *Candida* (2.25-fold) and increased *Aspergillus* (2.5-fold), *Wallemia* (6-fold), and *Epicoccum* (4-fold). Oral supplements of *A. amstelodami*, *W. sebi*, and *E. nigrum* recapitulated the effects of antifungal drugs to exacerbate allergic airway disease as measured by increased pulmonary eosinophils and lymphocytes and elevated serum IgE (Wheeler et al., 2016). Colonization of the gut by *Candida albicans* has also previously been shown to influence allergic airway disease and asthma in a mouse model, perhaps through secretion of prostaglandin-like immunomodulatory molecules (Noverr et al., 2005; Huffnagle, 2010; Marsland and Salami, 2015). Thus, fungal dysbiosis in the gut can affect disease development and exacerbation in the respiratory tract, indicating that a healthy mycobiome mediates immune responses throughout the body. Whether these effects reflect a direct action of fungi on the host or occur indirectly by altering the bacterial microbiome composition is unknown. Further studies are needed to elucidate the mechanisms for these responses and to determine whether fungal communities in other organs can influence allergic airway disease.

FUTURE DIRECTIONS

The evidence for the influence of dysbiotic fungal and bacterial microbiota interactions to drive or exacerbate chronic airway inflammatory disease is compelling. These findings open up the potential for targeted manipulation of the airway or gastrointestinal tract microbiota to improve airway health and manage airway disease in patients with CRS, asthma, and cystic fibrosis, among others. Current mycobiome studies focus on comparisons in healthy vs. diseased models, but more research needs to occur to understand the interactions between fungal and bacterial communities with the host immune system in host body sites. Fungi produce diverse secondary metabolites that can affect bacteria, while bacteria can keep the mycobiome in check by producing substances that inhibit the yeast to hyphae transition of fungal pathobionts such as in *C. albicans*.

Additional research is needed to define the functional effects of the mycobiome (**Figure 1**). Rather than focusing on taxonomic diversity, studies comparing microbial community function are potentially more useful. Further understanding of the contribution of the mycobiome and bacterial-fungal interactions should move beyond the GI tract into respiratory tract, where fungal dysbiosis has been shown to influence disease development and exacerbate symptoms. A variety of methods, combining metagenomics and sequencing approaches, experimental models, and functional studies should be used to clarify mechanisms by which the mycobiome impacts health and disease. In particular, focusing on microbial interactions with mucosal surfaces and their influence on local immune response

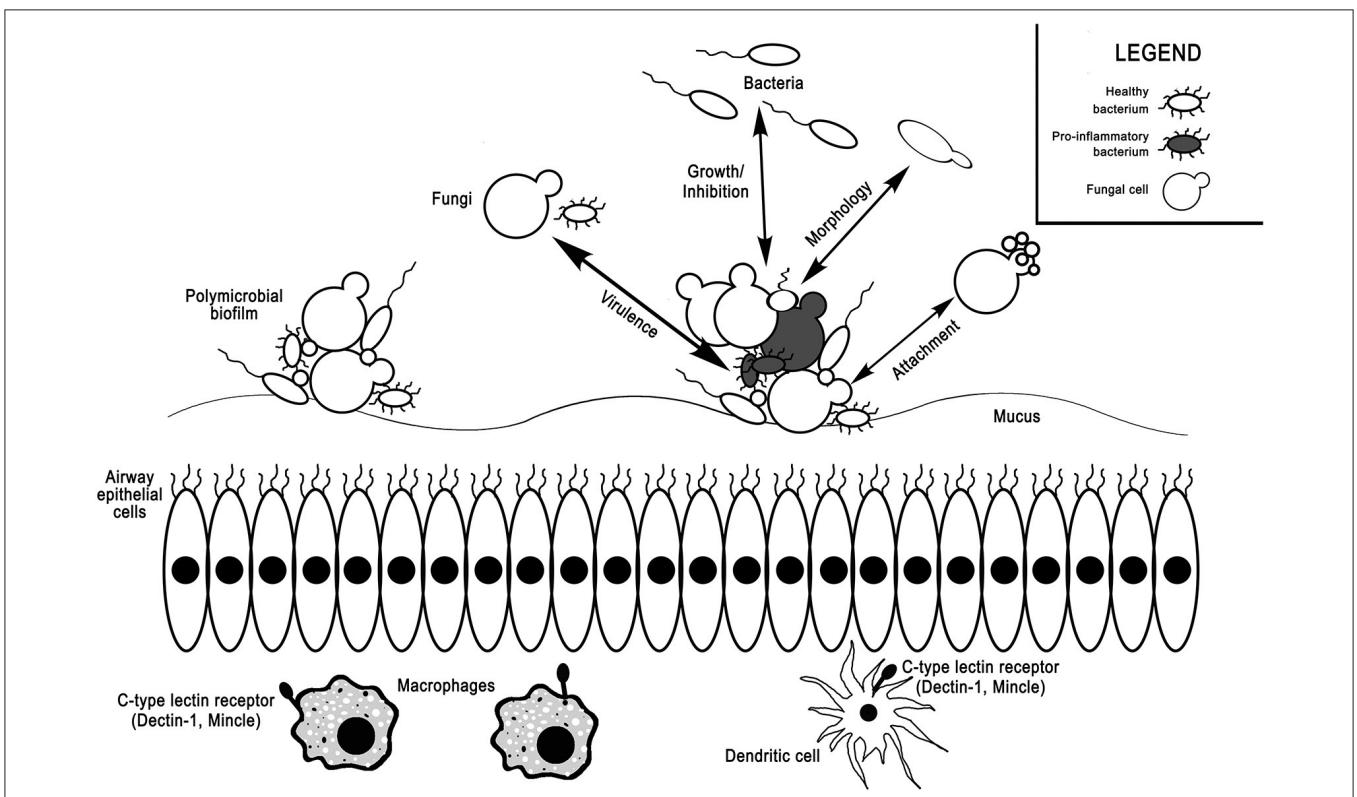

FIGURE 1 | Interactions between the bacterial microbiome, mycobiome, and host immune system in the airways. Bacteria and fungi coexist in mucosa-attached polymicrobial biofilms in the airways. Fungi can selectively induce or inhibit growth of various bacterial taxa, increase bacterial virulence factors, alter bacterial morphology, or act as attachment sites for bacteria. Vice versa, bacteria can also alter fungal growth, virulence, morphology, and attachment. C-type lectin receptors on macrophages and dendritic cells, such as dectin-1 and Mincle, can sense fungi and mediate host inflammatory responses.

likely will provide additional insights into the role of microbes in inflammatory disease of the upper and lower airways. Because fungal dysbiosis can have as great an effect on the host as bacterial dysbiosis, we cannot overlook the contributions of these largely unexplored fungal communities in our search to understand the microbial mechanisms behind health and disease.

AUTHOR CONTRIBUTIONS

IZ drafted and revised the manuscript. EC conceived, wrote, and revised the manuscript. BB conceived, wrote and revised the manuscript. AG conceived and revised the manuscript. SP conceived, wrote, and revised the manuscript.

REFERENCES

Abreu, N. A., Nagalingam, N. A., Song, Y., Roediger, F. C., Pletcher, S. D., Goldberg, A. N., et al. (2012). Sinus microbiome diversity depletion and *Corynebacterium tuberculostearicum* enrichment mediates rhinosinusitis. *Sci. Transl. Med.* 4:151ra124. doi: 10.1126/scitranslmed.3003783

Akdis, C. A., Bachert, C., Cingi, C., Dykewicz, M. S., Hellings, P. W., Naclerio, R. M., et al. (2013). Endotypes and phenotypes of chronic rhinosinusitis: a PRACTALL document of the european academy of allergy and clinical immunology and the american academy of allergy, asthma & immunology. *J. Allergy Clin. Immunol.* 131, 1479–1490. doi: 10.1016/j.jaci.2013.02.036

Ashbee, H. R., and Evans, E. G. V. (2002). Immunology of diseases associated with *Malassezia* species. *Clin. Microbiol. Rev.* 15, 21–57. doi: 10.1128/CMR.15.1.21-57.2002

Bassis, C. M., Erb-Downward, J. R., Dickson, R. P., Freeman, C. M., Schmidt, T. M., Young, V. B., et al. (2015). Analysis of the upper respiratory tract microbiotas as the source of the lung and gastric microbiotas in healthy individuals. *MBio* 6:e00037-15. doi: 10.1128/mBio.00037-15

Biswas, K., Hoggard, M., Jain, R., Taylor, M. W., and Douglas, R. G. (2015). The nasal microbiota in health and disease: variation within and between subjects. *Front. Microbiol.* 9:134. doi: 10.3389/fmicb.2015.00134

Caulley, L., Thavorn, K., Rudmik, L., Cameron, C., and Kilty, S. J. (2015). Direct costs of adult chronic rhinosinusitis by using 4 methods of estimation: results of the US medical expenditure panel survey. *J. Allergy Clin. Immunol.* 136, 1517–1522. doi: 10.1016/j.jaci.2015.08.037

Chaudhary, N., and Marr, K. A. (2011). Impact of *Aspergillus fumigatus* in allergic airway diseases. *Clin. Transl. Allergy* 1:4.doi: 10.1186/2045-7022-1-4

Chen, J.-C., Chuang, J.-G., Su, Y.-Y., Chiang, B.-L., Lin, Y.-S., and Chow, L.-P. (2011). The protease allergen Pen c 13 induces allergic airway inflammation and changes in epithelial barrier integrity and function in a murine model. *J. Biol. Chem.* 286, 26667–26679. doi: 10.1074/jbc.M110.193987

Chishimba, L., Niven, R., Fraczek, M., Bowyer, P., Smyth, L., Simpson, A., et al. (2015). Lung microbiome is associated with asthma severity in fungal associated asthma. *Eur. Respir. J.* 46:OA1462. doi: 10.1183/13993003.congress-2015.OA1462

Ciprandi, G., Caimmi, D., Miraglia Del Giudice, M., La Rosa, M., Salpietro, C., and Marseglia, G. L. (2012). Recent developments in United airways disease. *Allergy Asthma Immunol. Res.* 4, 171–177. doi: 10.4168/aair.2012.4.4.171

Cleland, E. J., Bassiouni, A., Bassioni, A., Boase, S., Dowd, S., Vreugde, S., et al. (2014). The fungal microbiome in chronic rhinosinusitis: richness, diversity, postoperative changes and patient outcomes. *Int. Forum Allergy Rhinol.* 4, 259–265. doi: 10.1002/alr.21297

Cohen, N. A. (2006). Sinonasal mucociliary clearance in health and disease. *Ann. Otol. Rhinol. Laryngol. Suppl.* 196, 20–26. doi: 10.1177/00034894061150S904

Cohen, R., Roth, F. J., Delgado, E., Ahearn, D. G., and Kalser, M. H. (1969). Fungal flora of the normal human small and large intestine. *N. Engl. J. Med.* 280, 638–641.doi: 10.1056/NEJM196903202801204

Cope, E. K., Goldberg, A. N., Pletcher, S. D., and Lynch, S. V. (2017). Compositionally and functionally distinct sinus microbiota in chronic rhinosinusitis patients have immunological and clinically divergent consequences. *Microbiome* 5:53. doi: 10.1186/s40168-017-0266-6

Cugini, C., Morales, D. K., and Hogan, D. A. (2010). *Candida albicans*-produced farnesol stimulates *Pseudomonas* quinolone signal production in LasR-defective *Pseudomonas aeruginosa* strains. *Microbiology* 156, 3096–3107.doi: 10.1099/mic.0.037911-0

Doble, P., Kern, R. C., Healy, D. Y., Leid, J., Sanderson, A. R., and Hunsaker, D. H. (2007). 11:06: biofilms with fungi in chronic rhinosinusitis. *Otolaryngol. Head Neck Surg.* 137, P40–P40. doi: 10.1016/j.otohns.2007.06.033

Durack, J., Lynch, S. V., Nariya, S., Bhakta, N. R., Beigelman, A., Castro, M., Dyer, A.-M., Israel, E., Kraft, M., Martin, R. J., et al. (2017). Features of the bronchial bacterial microbiome associated with atopy, asthma, and responsiveness to inhaled corticosteroid treatment. *J. Allergy Clin. Immunol.* 140, 63–75. doi: 10.1016/j.jaci.2016.08.055

El-Azizi, M. A., Starks, S. E., and Khardori, N. (2004). Interactions of *Candida albicans* with other *Candida* spp. and bacteria in the biofilms. *J. Appl. Microbiol.* 96, 1067–1073. doi: 10.1111/j.1365-2672.2004.02213.x

Findley, K., Oh, J., Yang, J., Conlan, S., Deming, C., Meyer, J. A., Schoenfeld, D., Nomicos, E., and Park, M. (2013). NIH intramural sequencing center comparative sequencing program, et al. topographic diversity of fungal and bacterial communities in human skin. *Nature* 498, 367–370. doi: 10.1038/nature12171

Fokkens, W. J., van Drunen, C., Georgalas, C., and Ebbens, F. (2012). Role of fungi in pathogenesis of chronic rhinosinusitis: the hypothesis rejected. *Curr. Opin. Otolaryngol. Head Neck Surg.* 20, 19–23. doi: 10.1097/MOO.0b013e32834e9084

Foreman, A., Boase, S., Psaltis, A., and Wormald, P.-J. (2012). Role of bacterial and fungal biofilms in chronic rhinosinusitis. *Curr. Allergy Asthma Rep.* 12, 127–135. doi: 10.1007/s11882-012-0246-7

Gaitanis, G., Magiatis, P., Hantschke, M., Bassukas, I. D., and Velegraki, A. (2012). The Malassezia genus in skin and systemic diseases. *Clin. Microbiol. Rev.* 25, 106–141. doi: 10.1128/CMR.00021-11

Geijtenbeek, T. B. H., and Gringhuis, S. I. (2016). C-type lectin receptors in the control of T helper cell differentiation. *Nat. Rev. Immunol.* 16, 433–448. doi: 10.1038/nri.2016.55

Gelber, J. T., Cope, E. K., Goldberg, A. N., and Pletcher, S. D. (2016). Evaluation of *Malassezia* and common fungal pathogens in subtypes of chronic rhinosinusitis. *Int. Forum Allergy Rhinol.* 6, 950–955. doi: 10.1002/alr.21777

Han, M. K., Huang, Y. J., Lipuma, J. J., Boushey, H. A., Boucher, R. C., Cookson, W. O., et al. (2012). Significance of the microbiome in obstructive lung disease. *Thorax* 67, 456–463. doi: 10.1136/thoraxjnl-2011-201183

Harriott, M. M., and Noverr, M. C. (2009). *Candida albicans* and *Staphylococcus aureus* form polymicrobial biofilms: effects on antimicrobial resistance. *Antimicrob. Agents Chemother.* 53, 3914–3922. doi: 10.1128/AAC.00657-09

Hogan, D. A., and Kolter, R. (2002). *Pseudomonas-candida* interactions: an ecological role for virulence factors. *Science* 296, 2229–2232.doi: 10.1126/science.1070784

Hogan, D. A., Vik, Å., and Kolter, R. (2004). A *Pseudomonas aeruginosa* quorum-sensing molecule influences *Candida albicans* morphology. *Mol. Microbiol.* 54, 1212–1223.doi: 10.1111/j.1365-2958.2004.04349.x

Holmes, A. R., McNab, R., and Jenkinson, H. F. (1996). *Candida albicans* binding to the oral bacterium *Streptococcus gordonii* involves multiple adhesin-receptor interactions. *Infect. Immun.* 64, 4680–4685.

Huang, Y. J., and Boushey, H. A. (2014). The microbiome and asthma. *Ann. Am. Thorac. Soc.* 11, S48–S51. doi: 10.1513/AnnalsATS.201306-187MG

Huang, Y. J., Nelson, C. E., Brodie, E. L., Desantis, T. Z., Baek, M. S., Liu, J., et al. (2011). Airway microbiota and bronchial hyperresponsiveness in patients with suboptimally controlled asthma. *J. Allergy Clin. Immunol.* 127, 372–381.e1–3. doi: 10.1016/j.jaci.2010.10.048

Huffnagle, G. B. (2010). The microbiota and allergies/asthma. *PLoS Pathog.* 6:e1000549. doi: 10.1371/journal.ppat.1000549

Huffnagle, G. B., and Noverr, M. C. (2013). The emerging world of the fungal microbiome. *Trends Microbiol.* 21, 334–341. doi: 10.1016/j.tim.2013.04.002

Human Microbiome Project Consortium (2012). Structure, function and diversity of the healthy human microbiome. *Nature* 486, 207–214. doi: 10.1038/nature11234

Iliev, I. D., Funari, V. A., Taylor, K. D., Nguyen, Q., Reyes, C. N., Strom, S. P., et al. (2012). Interactions between commensal fungi and the C-type lectin receptor Dectin-1 influence colitis. *Science* 336, 1314–1317. doi: 10.1126/science.1221789

Jeraldo, P., Sipos, M., Chia, N., Brulc, J. M., Dhillon, A. S., Konkel, M. E., et al. (2012). Quantification of the relative roles of niche and neutral processes in structuring gastrointestinal microbiomes. *Proc. Natl. Acad. Sci. U.S.A.* 109, 9692–9698. doi: 10.1073/pnas.1206721109

Jung, W. H., Croll, D., Cho, J. H., Kim, Y. R., and Lee, Y. W. (2015). Analysis of the nasal vestibule mycobiome in patients with allergic rhinitis. *Mycoses* 58, 167–172. doi: 10.1111/myc.12296

Kerr, J. R., Taylor, G. W., Rutman, A., Høiby, N., Cole, P. J., and Wilson, R. (1999). *Pseudomonas aeruginosa* pyocyanin and 1-hydroxyphenazine inhibit fungal growth. *J. Clin. Pathol.* 52, 385–387.

Klossek, J. M., Neukirch, F., Pribil, C., Jankowski, R., Serrano, E., Chanal, I., et al. (2005). Prevalence of nasal polyposis in France: a cross-sectional, case-control study. *Allergy* 60, 233–237. doi: 10.1111/j.1398-9995.2005.00688.x

Kumamoto, C. A. (2016). The fungal mycobiota: small numbers, large impacts. *Cell Host Microbe* 19, 750–751. doi: 10.1016/j.chom.2016.05.018

Lal, D., Keim, P., Delisle, J., Barker, B., Rank, M. A., Chia, N., et al. (2017). Mapping and comparing bacterial microbiota in the sinonasal cavity of healthy, allergic rhinitis, and chronic rhinosinusitis subjects. *Int. Forum Allergy Rhinol.* 7, 561–569. doi: 10.1002/alr.21934

Lambrecht, B. N., and Hammad, H. (2012). The airway epithelium in asthma. *Nat. Med.* 18, 684–692. doi: 10.1038/nm.2737

Larsen, K. (1996). The clinical relationship of nasal polyps to asthma. *Allergy Asthma Proc.* 17, 243–249. doi: 10.2500/108854196778662255

Lemon, K. P., Klepac-Ceraj, V., Schiffer, H. K., Brodie, E. L., Lynch, S. V., and Kolter, R. (2010). Comparative analyses of the bacterial microbiota of the human nostril and oropharynx. *MBio* 1. doi: 10.1128/mBio.00129-10

Leynaert, B., Neukirch, F., Demoly, P., and Bousquet, J. (2000). Epidemiologic evidence for asthma and rhinitis comorbidity. *J. Allergy Clin. Immunol.* 106, S201–S205. doi: 10.1067/mai.2000.110151

Licari, A., Caimmi, S., Bosa, L., Marseglia, A., Marseglia, G. L., and Caimmi, D. (2014). Rhinosinusitis and asthma: a very long engagement. *Int. J. Immunopathol. Pharmacol.* 27, 499–508. doi: 10.1177/039463201402700405

Liu, Z.-C., Wang, M., Sun, W.-K., Xia, D., Tan, M.-M., Ding, Y., et al. (2015). Up-regulation of Dectin-1 in airway epithelial cells promotes mice defense against invasive pulmonary aspergillosis. *Int. J. Clin. Exp. Med.* 8, 17489–17497.

Marsland, B. J., and Salami, O. (2015). Microbiome influences on allergy in mice and humans. *Curr. Opin. Immunol.* 36, 94–100. doi: 10.1016/j.coi.2015.07.005

Morales, D. K., and Hogan, D. A. (2010). *Candida albicans* interactions with bacteria in the context of human health and disease. *PLoS Pathog.* 6:e1000886. doi: 10.1371/journal.ppat.1000886

Mowat, E., Rajendran, R., Williams, C., McCulloch, E., Jones, B., Lang, S., et al. (2010). *Pseudomonas aeruginosa* and their small diffusible extracellular molecules inhibit *Aspergillus fumigatus* biofilm formation. *FEMS Microbiol. Lett.* 313, 96–102. doi: 10.1111/j.1574-6968.2010.02130.x

Mukherjee, P. K., Sendid, B., Hoarau, G., Colombel, J.-F., Poulain, D., and Ghannoum, M. A. (2015). Mycobiota in gastrointestinal diseases. *Nat. Rev. Gastroenterol. Hepatol.* 12, 77–87. doi: 10.1038/nrgastro.2014.188

Noverr, M. C., Falkowski, N. R., McDonald, R. A., McKenzie, A. N., and Huffnagle, G. B. (2005). Development of allergic airway disease in mice following antibiotic therapy and fungal microbiota increase: role of host genetics, antigen, and interleukin-13. *Infect. Immun.* 73, 30–38. doi: 10.1128/IAI.73.1.30-38.2005

Orlandi, R. R., Kingdom, T. T., and Hwang, P. H. (2016). International consensus statement on allergy and rhinology: rhinosinusitis executive summary. *Int. Forum Allergy Rhinol.* 6(Suppl. 1), S3–S21. doi: 10.1002/alr.21694

Orlandi, R. R., and Marple, B. F. (2010). Fungus and chronic rhinosinusitis: weighing the evidence. *Otolaryngol. Head Neck Surg.* 143, 611–613. doi: 10.1016/j.otohns.2010.07.002

Passalacqua, G., Ciprandi, G., and Canonica, G. W. (2001). The nose-lung interaction in allergic rhinitis and asthma: united airways disease. *Curr. Opin. Allergy Clin. Immunol.* 1, 7–13.

Peleg, A. Y., Hogan, D. A., and Mylonakis, E. (2010). Medically important bacterial–fungal interactions. *Nat. Rev. Microbiol.* 8, 340–349. doi: 10.1038/nrmicro2313

Peters, B. M., Ovchinnikova, E. S., Krom, B. P., Schlecht, L. M., Zhou, H., Hoyer, L. L., et al. (2012). *Staphylococcus aureus* adherence to *Candida albicans* hyphae is mediated by the hyphal adhesin Als3p. *Microbiology* 158, 2975–2986. doi: 10.1099/mic.0.062109-0

Ponikau, J. U., Sherris, D. A., and Kern, E. B. (2000). Role of fungi in allergic fungal sinusitis and chronic Rhinosinusitis: in response. *Mayo Clin. Proc.* 75, 540–541. doi: 10.4065/75.5.540-a

Ponikau, J. U., Sherris, D. A., Kern, E. B., Homburger, H. A., Frigas, E., Gaffey, T. A., et al. (1999). The diagnosis and incidence of allergic fungal sinusitis. *Mayo Clin. Proc.* 74, 877–884. doi: 10.4065/74.9.877

deShazo, R. D., Chapin, K., and Swain, R. E. (1997). Fungal sinusitis. *N. Engl. J. Med.* 337, 254–259. doi: 10.1056/NEJM199707243370407

Romano, J. D., and Kolter, R. (2005). *Pseudomonas-Saccharomyces* interactions: influence of fungal metabolism on bacterial physiology and survival. *J. Bacteriol.* 187, 940–948. doi: 10.1128/JB.187.3.940-948.2005

Roy, R. M., and Klein, B. S. (2013). Fungal glycan interactions with epithelial cells in allergic airway disease. *Curr. Opin. Microbiol.* 16, 404–408. doi: 10.1016/j.mib.2013.03.004

Ryu, J.-H., Yoo, J.-Y., Kim, M.-J., Hwang, S.-G., Ahn, K. C., Ryu, J.-C., et al. (2013). Distinct TLR-mediated pathways regulate house dust mite-induced allergic disease in the upper and lower airways. *J. Allergy Clin. Immunol.* 131, 549–561. doi: 10.1016/j.jaci.2012.07.050

Sanderson, A. R., Leid, J. G., and Hunsaker, D. (2006). Bacterial biofilms on the sinus mucosa of human subjects with chronic rhinosinusitis. *Laryngoscope* 116, 1121–1126. doi: 10.1097/01.mlg.0000221954.05467.54

Schlecht, L. M., Peters, B. M., Krom, B. P., Freiberg, J. A., Hänsch, G. M., Filler, S. G., et al. (2015). Systemic *Staphylococcus aureus* infection mediated by *Candida albicans* hyphal invasion of mucosal tissue. *Microbiology* 161, 168–181. doi: 10.1099/mic.0.083485-0

Schubert, M. S. (2004). Allergic fungal sinusitis: pathogenesis and management strategies. *Drugs* 64, 363–374. doi: 10.2165/00003495-200464040-00002

Tieu, D. D., Kern, R. C., and Schleimer, R. P. (2009). Alterations in epithelial barrier function and host defense responses in chronic rhinosinusitis. *J. Allergy Clin. Immunol.* 124, 37–42. doi: 10.1016/j.jaci.2009.04.045

Tomassen, P., Vandeplas, G., Van Zele, T., Cardell, L.-O., Arebro, J., Olze, H., et al. (2016). Inflammatory endotypes of chronic rhinosinusitis based on cluster analysis of biomarkers. *J Allergy Clin Immunol* 137, 1449–1456.e4. doi: 10.1016/j.jaci.2015.12.1324

Underhill, D. M., and Iliev, I. D. (2014). The mycobiota: interactions between commensal fungi and the host immune system. *Nat. Rev. Immunol.* 14, 405–416. doi: 10.1038/nri3684

Wagner Mackenzie, B., Waite, D. W., Hoggard, M., Douglas, R. G., Taylor, M. W., and Biswas, K. (2017). Bacterial community collapse: a meta-analysis of the sinonasal microbiota in chronic rhinosinusitis. *Environ. Microbiol.* 19, 381–392. doi: 10.1111/1462-2920.13632

Wheeler, M. L., Limon, J. J., Bar, A. S., Leal, C. A., Gargus, M., Tang, J., et al. (2016). Immunological consequences of intestinal fungal dysbiosis. *Cell Host Microbe* 19, 865–873. doi: 10.1016/j.chom.2016.05.003

Yamasaki, S., Matsumoto, M., Takeuchi, O., Matsuzawa, T., Ishikawa, E., Sakuma, M., et al. (2009). C-type lectin mincle is an activating receptor for pathogenic fungus, Malassezia. *Proc. Natl. Acad. Sci. U.S.A.* 106, 1897–1902. doi: 10.1073/pnas.0805177106

Zhao, Y. C., Bassiouni, A., Tanjararak, K., Vreugde, S., Wormald, P.-J., and Psaltis, A. J. (2017). Role of fungi in chronic rhinosinusitis through ITS sequencing. *Laryngoscope*. doi: 10.1002/lary.26702. [Epub ahead of print].

Conflict of Interest Statement: The authors declare that the research was conducted in the absence of any commercial or financial relationships that could be construed as a potential conflict of interest.

Copyright © 2017 Zhang, Pletcher, Goldberg, Barker and Cope. This is an open-access article distributed under the terms of the Creative Commons Attribution License (CC BY). The use, distribution or reproduction in other forums is permitted, provided the original author(s) or licensor are credited and that the original publication in this journal is cited, in accordance with accepted academic practice. No use, distribution or reproduction is permitted which does not comply with these terms.

frontiers in Immunology

MINI REVIEW
published: 22 November 2017
doi: 10.3389/fimmu.2017.01614

Host Responses to *Malassezia* spp. in the Mammalian Skin

Florian Sparber and Salomé LeibundGut-Landmann**

Section of Immunology, Vetsuisse Faculty, University of Zürich, Zürich, Switzerland

The skin of mammalian organisms is home for a myriad of microbes. Many of these commensals are thought to have beneficial effects on the host by critically contributing to immune homeostasis. Consequently, dysbiosis can have detrimental effects for the host that may manifest with inflammatory diseases at the barrier tissue. Besides bacteria, fungi make an important contribution to the microbiota and among these, the yeast *Malassezia* widely dominates in most areas of the skin in healthy individuals. There is accumulating evidence that *Malassezia* spp. are involved in a variety of skin disorders in humans ranging from non- or mildly inflammatory conditions such as dandruff and pityriasis versicolor to more severe inflammatory skin diseases like seborrheic eczema and atopic dermatitis. In addition, *Malassezia* is strongly linked to the development of dermatitis and otitis externa in dogs. However, the association of *Malassezia* spp. with such diseases remains poorly characterized. Until now, studies on the fungus–host interaction remain sparse and they are mostly limited to experiments with isolated host cells *in vitro*. They suggest a multifaceted crosstalk of *Malassezia* spp. with the skin by direct activation of the host *via* conserved pattern recognition receptors and indirectly *via* the release of fungus-derived metabolites that can modulate the function of hematopoietic and/or non-hematopoietic cells in the barrier tissue. In this review, we discuss our current understanding of the host response to *Malassezia* spp. in the mammalian skin.

Keywords: *Malassezia*, commensalism, opportunistic pathogenic fungi, skin disorders, innate immunity, adaptive immunity, allergic response, indoles

OPEN ACCESS

Edited by:
Bernhard Hube,
Hans Knöll Institut, Germany

Reviewed by:
Ruth Ashbee,
University of Leeds, United Kingdom
Annika Elisabet Scheynius,
Karolinska Institute (KI), Sweden
Peter Mayser,
Justus Liebig Universität
Gießen, Germany

****Correspondence:***
Florian Sparber
florian.sparber@uzh.ch;
Salomé LeibundGut-Landmann
salome.leibundgut-landmann@uzh.ch

Specialty section:
This article was submitted to Microbial Immunology, a section of the journal Frontiers in Immunology

Received: *28 September 2017*
Accepted: *08 November 2017*
Published: *22 November 2017*

Citation:
Sparber F and LeibundGut-Landmann S (2017) Host Responses to Malassezia spp. in the Mammalian Skin. Front. Immunol. 8:1614. doi: 10.3389/fimmu.2017.01614

INTRODUCTION

Malassezia spp. are lipophilic yeasts, which are part of the skin microbiota of many mammals and birds. In fact, the genus *Malassezia* is by far the most abundant eukaryotic member of the microbial flora of the skin in these organisms (1). Most *Malassezia* spp. have a predilection for seborrheic skin sites such as the scalp and the trunk. They rely on exogenous fatty acid sources for their nutritive requirements because of their lack of genes encoding for the fatty acid synthase and genes involved in carbohydrate metabolism (2–4). In agreement, the cell wall of *Malassezia* spp. is particularly rich in lipids (5).

The genus *Malassezia* currently comprises 17 species, three of which have only recently been proposed (6–8). *Malassezia globosa*, *Malassezia restricta*, and *Malassezia sympodialis* are most frequently isolated from the healthy human skin with distinct relative frequencies at specific body sites (1, 9). The age of the host and geographic factors also influence their distribution (10). *Malassezia pachydermatis*, *Malassezia nana*, and *Malassezia caprae* are found predominantly in non-human hosts (6). Surprisingly, the microbial communities of the skin are astonishingly stable and

maintained over time, despite the skin's exposure to the external environment (11). It is currently unknown whether *Malassezia* spp. play a mutualistic role and may thus contribute to immune homeostasis of the host.

Apart from their commensal nature, *Malassezia* spp. are also associated with common skin disorders such as pityriasis versicolor and seborrheic dermatitis as well as more severe inflammatory skin pathologies including atopic eczema and atopic dermatitis in humans (10) and dermatitis and otitis externa in animals, most frequently in dogs (12). The composition of the skin mycobiome can vary under pathological conditions and some species of *Malassezia* such as *M. sympodialis* and *Malassezia furfur* are found to be enriched in certain skin disorders (10). To date, a causative link between *Malassezia* and disease development has only been made for Pityriasis versicolor, while the role of the yeast in other pathologies remains correlative (10, 13, 14). Changes in the degree of colonization in diseased compared to healthy skin have been documented in dogs (15) but remain uncertain in humans (16).

The pathophysiology of *Malassezia*-associated skin conditions is largely unknown. The lack of knowledge on the cellular and molecular interactions between *Malassezia* spp. and the host preclude a better understanding of the factors determining commensalism versus disease. Herein, we review the current knowledge with regard to how the host recognizes *Malassezia* spp. and responds to it (**Figure 1**).

SENSING OF *Malassezia* spp. BY THE HOST

Through their localization in the skin, *Malassezia* spp. interact primarily with keratinocytes, tissue-resident dendritic cells (DCs), and macrophages, as well as with myeloid cells that are recruited to the skin under inflammatory conditions. Activation of DCs is key for induction of adaptive immunity and memory formation. The fungus is recognized by the host either directly through interaction of fungal cell wall components with membrane bound pattern recognition receptors (PRRs) or indirectly through soluble metabolites that are released by *Malassezia* spp. The set of receptors expressed by the hematopoietic and the non-hematopoietic compartment are largely distinct.

Direct Recognition of *Malassezia* spp. by Surface-Bound Receptors

The fungal cell wall is rich in carbohydrates and glycoproteins that are recognized by PRRs of the family of Syk-coupled C-type lectin receptor (CLR), which are expressed primarily by myeloid cells (17, 18). Binding to these receptors results in ligand internalization and activation of multiple signaling pathways, including the MAPK, NF-κB, and NFAT pathways as well as the inflammasome.

The polysaccharides of the *Malassezia* cell wall are organized differently than in other fungal species analyzed to date (19, 20).

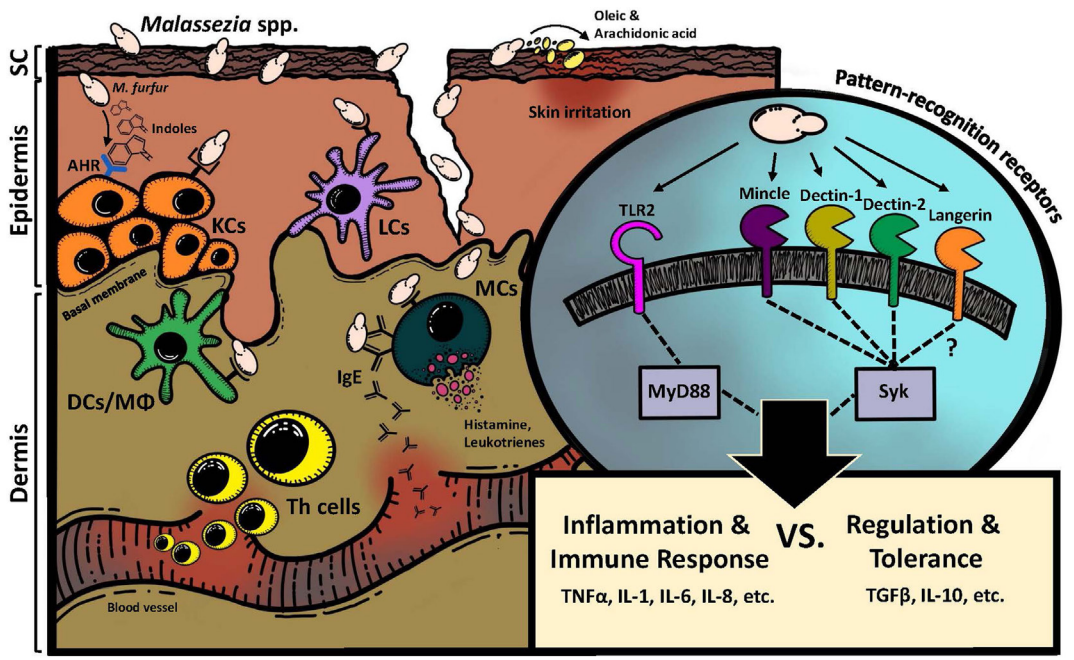

FIGURE 1 | Interaction of *Malassezia* spp. with the mammalian skin. Direct interactions involve various PRRs, which recognize fungal cell wall constituents and are distinctly expressed on the surface of non-hematopoietic (i.e., keratinocytes) and hematopoietic cells (i.e., Langerhans cells, mast cells) of the skin. Spatial and temporal signal integration of different PRR signals results in the induction of inflammation and immunity or, alternatively, in the regulation and tolerance of the host toward *Malassezia* spp. Indirect interactions of *Malassezia* spp. with the skin include fungus-derived metabolites such as irritant fatty acids on the one hand and indoles that are potent agonists for the AhR, which is expressed by various skin cells, on the other hand. KCs, keratinocytes; LCs, Langerhans cells; DCs, dendritic cells; Mϕ, macrophages; MCs, mast cells; SC, stratum corneum; AhR, aryl hydrocarbon receptor.

Moreover, the cell wall is surrounded by a lipid-rich outer layer (21). Several CLRs have been shown to respond to *Malassezia* spp. *in vitro*. The two FcRγ-associated receptors Dectin-2 and Mincle sense *Malassezia* spp., albeit through recognition of distinct ligands (22). While Mincle binds to two distinct glycolipids in *Malassezia*, Dectin-2 recognizes the fungus through α-1,2-linked mannose. High-mannose binding is a general feature of Dectin-2, which is reported to recognize a variety of fungi, including *Candida albicans*, *Saccharomyces cerevisiae*, *Blastomyces dermatitidis*, *Aspergillus fumigatus*, *Cryptococcus neoformans*, and *Fonsecaea pedrosoi* (23). In contrast, *Malassezia* spp. were initially found to be unique agonists of Mincle when a large panel of 50 different fungi was tested in a glycoconjugate microarray (24). More recently, other fungi such as *Pneumocystis carinii*, *F. pedrosoi*, and *Fonsecaea monomorpha* were also reported to engage Mincle (25–27), in addition to bacterial ligands (28–32), mammalian alarmins released from damaged cells (33, 34) and even cholesterol crystals (35, 36). Mincle is thus a highly pleiotropic receptor, which can bind chemically and structurally distinct ligands through at least two complementary binding sites (37–40). The β-glucan receptor Dectin-1, which was the first member of the family of Syk-coupled CLRs to be identified (41), was also found to sense *Malassezia* and was linked to the activation of the NLRP3 inflammasome (42). Finally, Langerin was suggested to act as a receptor for *Malassezia* in the skin due to its prominent expression by epidermal Langerhans cells and by a subset of dermal DCs. Direct binding of the fungus to recombinant Langerin was indeed observed (43, 44).

Activation of myeloid cells by *Malassezia* spp. *via* these different CLRs was shown to induce the secretion of proinflammatory cytokines. However, the relative contribution of individual receptors to fungal control *in vivo* during commensalism and in infectious settings remains to be determined. At least partial redundancy of receptors that signal *via* the same pathway may occur, similarly to what was found for other fungi (45, 46). Dissecting the role of Mincle in the context of *Malassezia* spp. in more detail will also be interesting in light of its reported antagonizing activity, e.g., in response to *Fonsacaea* spp. (27), and thus this receptor may also mediate regulatory or inhibitory responses to *Malassezia* spp.

In addition to CLRs, Toll-like receptors (TLRs), and in particular TLR2, also contribute to fungal recognition by the host. TLR2 was implicated in sensing of *Malassezia* spp. and inducing a proinflammatory response characterized by the release of cytokines, chemokines and antimicrobial peptides by keratinocytes (47–50).

The proinflammatory response is generally enhanced by lipid removal from the yeast to enhance exposure of fungal cell wall carbohydrates (51, 52). In contrast, thymic stromal lymphopoietin secretion from keratinocytes was found to be induced specifically by the lipid layer components of *M. restricta* and *M. globosa* but not by yeasts that were depleted of lipids (53).

Indirect Interaction

Specific products of *Malassezia* metabolic pathways are thought to act as virulence factors promoting inflammation and pathology, while others downregulate the production of inflammatory mediators and thereby contribute to immune regulation. Fungal strains with altered production of such factors have been linked to *Malassezia*-associated skin disorders (54–56).

Malassezia-derived lipases and phospholipases, which are required to assimilate host-derived lipids, can initiate an inflammatory response in the skin by releasing unsaturated free fatty acids from the sebum lipids (57–60). Oleic acid has irritant and desquamative effects on keratinocytes (61–63), whereas arachidonic acid produces proinflammatory eicosanoids and leads to inflammation and damage to the stratum corneum, thereby contributing to the disruption of the epithelial barrier function and induction of abnormal keratinization (64).

Malassezia furfur is able to convert tryptophan into a variety of indole alkaloids. This pathway is mainly active if tryptophan is the sole source of nitrogen (65). *M. furfur*-derived indoles including malassezin, indirubin, and indolo [3,2-b] carbazole (ICZ) serve as potent ligands for the host aryl hydrocarbon receptor (AhR) and thereby potentially modify the function of all cells in the epidermis expressing this receptor (54, 55, 66, 67). For example, some tryptophan metabolites can promote apoptosis of melanocytes (68) or inhibit the respiratory burst in neutrophils (69). Given the broad spectrum of biological responses that are influenced by AhR activity, *M. furfur* may engage this pathway to modulate inflammation and/or promote skin immune homeostasis (70) but may also promote skin pathology (71) or even contribute to carcinogenesis (72). The significance of yeast-derived indoles in each of these contexts remains to be demonstrated *in vivo*.

INNATE IMMUNITY TO *Malassezia* spp.

The majority of what is currently known about the host response to *Malassezia* spp. is based on *in vitro* studies with isolated myeloid cells or keratinocyte cell lines. Stimulation of these cells with *Malassezia* yeast leads to the induction of mainly proinflammatory cytokines, chemokines, and antimicrobial peptides (22, 24, 47–52, 73–76). In line with an inflammatory character of the innate response to the fungus, the intraperitoneal injection of *Malassezia* into mice results in the recruitment of neutrophils to the peritoneum (24). Only few studies have examined regulatory cytokines such as IL-10 and TGF-β by the yeast (24, 49, 51, 74, 77), but these may be relevant with regard to the role of *Malassezia* spp. as a skin commensal.

Given the association of *Malassezia* spp. with inflammatory skin disorders and allergic responses, the fungus may also interact with mast cells. Progenitor cell-derived mast cells from atopic patients show increased release of proinflammatory cytokines upon stimulation with *Malassezia* (76) and are enriched in the skin of atopic eczema patients where they are positioned in the superficial dermis and can interact with the fungus (78). Mast cell activation in response to *Malassezia* spp. has also been reported in studies with bone-marrow-derived mast cells. These cells are directly activated by the fungus in a TLR2-dependent manner and release inflammatory mediators and cytokines (79). Moreover, the crosslinking of the high-affinity IgE receptor (FcεRI) by antigen-bound IgE can induce mast cell degranulation (79). Therefore, mast cells may contribute to further barrier disruption and thereby amplify the inflammatory response.

The access of *Malassezia* to immune cells in the skin may be facilitated by disruption of the epithelial barrier as it frequently occurs during chronic inflammation. Moreover, *Malassezia* spp. were reported to release nanovesicles/exosomes that contain immunogenic proteins and trigger increased release of cytokines by DCs (80).

ADAPTIVE IMMUNITY TO *Malassezia* spp.

As a commensal, *Malassezia* interacts continuously with the immune system. Therefore, cellular and humoral immune memory to the fungus can be evidenced in healthy individuals (81). Although there are fewer studies related to dogs when compared with humans, dogs also develop cellular and humoral immune responses to their commensal yeast, *M. pachydermatis* (82–84). Generally, the adaptive immune responses are heightened and qualitatively distinct in patients with *Malassezia*-associated diseases.

Humoral Responses

During steady state, *Malassezia*-specific antibodies are predominantly of the IgG and IgM isotypes (81). In contrast, although *Malassezia*-specific IgE is not usually detected in healthy individuals, it is common in atopic patients (85). A positive correlation was found between the sensitization to *Malassezia*-specific IgE and the severity of atopic dermatitis (86, 87). Similar observations were made in atopic dogs (83, 84). However, whether the IgE response plays a pathogenic role in atopic and other *Malassezia*-associated inflammatory disorders or rather serves as a marker for the severity of disease remains unclear.

T Cell Responses

Patients with atopic dermatitis often show positive skin prick test and atopic patch test reactions to *Malassezia* (85). T cell-responsiveness to *Malassezia* in such patients was associated with a Th2 response (88), in line with the classical paradigm of Th2-polarized allergic T cells. GATA3$^+$ T cells were identified in pityriasis versicolor lesions (89) and likewise *Malassezia*-specific T cell in allergic dogs were found to be strongly polarized toward a type 2 response (82). More recently, other T helper cell subsets such as Th17 and Th22 cells have been found enriched in allergic individuals (90, 91) as well as in non-allergic immune-mediated skin diseases such as psoriasis (92). Consistent with this notion, *Malassezia*-reactive skin homing T cells from *Malassezia*-sensitized atopic dermatitis patients comprise not only Th1 and Th2 subsets but also IL-17- and IL-22-secreting cells (93). Of note, IL-4/IL-17 coproducers have also been described in the context of atopic eczema especially in children (94). Importantly, Th17 differentiation is a hallmark of T cell responses induced by CLR signaling (46) and T cells directed against other fungi, in particular *Candida* spp., belong predominantly to the Th17 subset (95). Whether and how IL-17 and/or IL-22 may contribute to pathogenicity in atopic dermatitis remains to be determined. It is also unknown to which subset *Malassezia*-specific T cells belong in healthy individuals and to what extent T cell plasticity contributes to sensitization.

Malassezia Allergens

To date, 13 *Malassezia*-derived allergens have been identified from *M. furfur* and *M. sympodialis* (3, 96). Interestingly, more allergens are released from *M. sympodialis* when cultured at the increased pH conditions of atopic skin compared with culture at the pH of healthy skin (97). Several of the known allergens belong to a class of phylogenetically highly conserved proteins and display a high degree of homology with the corresponding mammalian proteins. Cross-reactivity between *Malassezia*-derived allergens and endogenous human proteins (e.g., thioredoxin, manganese-dependent superoxide dismutase) has been indeed demonstrated (93, 98, 99). Therefore, the induction of autoreactive T cells by *Malassezia* allergens may play a role in sustained inflammation.

CONCLUSION

Malassezia spp. have been implicated in various pathologies. Yet, direct evidence for a causal relationship between *Malassezia* spp. and the mammalian host remains elusive. For instance, it is unclear whether *Malassezia* actively promotes atopic dermatitis or whether the inflammatory environment in the atopic skin triggers a dysregulated immune response toward the fungus.

At the basis of this is the key question of what determines the balance between commensalism and pathogenicity of *Malassezia* spp. The answer likely relates to changes occurring in both the fungus (55) (e.g., variable secretion of AhR agonists) and in the host (e.g., barrier defects, changes in immune polarization) which are responsible for promoting the development of pathology. Changes in the environment such as seasonal variations in sebum production have also been linked to altered disease prevalence (100).

Inter-species variations in the skin mycobiome may further contribute as different species of *Malassezia* can induce variable inflammatory responses (51, 75, 101). Moreover, *Malassezia* spp. have been shown to display a large intra-species diversity (73) similarly to what is known for other opportunistic fungal pathogens (102), and thus the exact composition of *Malassezia* strains and species present in an individual at a given time may contribute to different outcomes in the interaction between the fungus and the host. The recently completed assembly and detailed annotation of the genome of *M. sympodialis* makes an important contribution to approach this complexity (103). Future research will help fill the important gaps in our knowledge on the pathophysiology of and the host response to *Malassezia in vivo*. Enhanced understanding of host-*Malassezia* interactions may contribute to improved diagnostic and therapeutic options for patients affected by *Malassezia*-associated pathologies.

AUTHOR CONTRIBUTIONS

Both authors listed have made a substantial, direct, and intellectual contribution to the work and approved it for publication.

FUNDING

This work was supported by the University of Zürich.

REFERENCES

1. Findley K, Oh J, Yang J, Conlan S, Deming C, Meyer JA, et al. Topographic diversity of fungal and bacterial communities in human skin. *Nature* (2013) 498:367–70. doi:10.1038/nature12171
2. Wu G, Zhao H, Li C, Rajapakse MP, Wong WC, Xu J, et al. Genus-wide comparative genomics of *Malassezia* delineates its phylogeny, physiology, and niche adaptation on human skin. *PLoS Genet* (2015) 11:e1005614. doi:10.1371/journal.pgen.1005614
3. Gioti A, Nystedt B, Li W, Xu J, Andersson A, Averette AF, et al. Genomic insights into the atopic eczema-associated skin commensal yeast *Malassezia sympodialis*. *mBio* (2013) 4: e00572–12. doi:10.1128/mBio.00572-12
4. Park M, Cho Y-J, Lee YW, Jung WH. Whole genome sequencing analysis of the cutaneous pathogenic yeast *Malassezia restricta* and identification of the major lipase expressed on the scalp of patients with dandruff. *Mycoses* (2017) 60:188–97. doi:10.1111/myc.12586
5. Thompson E, Colvin JR. Composition of the cell wall of *Pityrosporum ovale* (Bizzozero) Castellani and Chalmers. *Can J Microbiol* (1970) 16:263–5. doi:10.1139/m70-048
6. Cabanes FJ. *Malassezia* yeasts: how many species infect humans and animals? *PLoS Pathog* (2014) 10:e1003892. doi:10.1371/journal.ppat.1003892
7. Honnavar P, Prasad GS, Ghosh A, Dogra S, Handa S, Rudramurthy SM. *Malassezia arunalokei* sp. nov., a novel yeast species isolated from seborrheic dermatitis patients and healthy individuals from India. *J Clin Microbiol* (2016) 54:1826–34. doi:10.1128/JCM.00683-16
8. Cabanes FJ, Coutinho SDA, Puig L, Bragulat MR, Castella G. New lipid-dependent *Malassezia* species from parrots. *Rev Iberoam Micol* (2016) 33: 92–9. doi:10.1016/j.riam.2016.03.003
9. Jo J-H, Kennedy EA, Kong HH. Topographical and physiological differences of the skin mycobiome in health and disease. *Virulence* (2017) 8:324–33. doi: 10.1080/21505594.2016.1249093
10. Prohic A, Jovovic Sadikovic T, Krupalija-Fazlic M, Kuskunovic-Vlahovljak S. *Malassezia* species in healthy skin and in dermatological conditions. *Int J Dermatol* (2016) 55:494–504. doi:10.1111/ijd.13116
11. Oh J, Byrd AL, Park M, Kong HH, Segre JA. Temporal stability of the human skin microbiome. *Cell* (2016) 165:854–66. doi:10.1016/j.cell.2016.04.008
12. Bond R, Guillot J, Cabañes FJ. *Malassezia* yeasts in animal disease. In: Boekhout T, Mayser P, Guého-Kellermann E, Velegraki A, editors. *Malassezia and the Skin: Science and Clinical Practice*. Berlin, Heidelberg: Springer (2010). p. 271–99.
13. Johansson C, Eshaghi H, Linder MT, Jakobson E, Scheynius A. Positive atopy patch test reaction to *Malassezia furfur* in atopic dermatitis correlates with a T helper 2-like peripheral blood mononuclear cells response. *J Invest Dermatol* (2002) 118:1044–51. doi:10.1046/j.1523-1747.2002.01758.x
14. Casagrande BF, Fluckiger S, Linder MT, Johansson C, Scheynius A, Crameri R, et al. Sensitization to the yeast *Malassezia sympodialis* is specific for extrinsic and intrinsic atopic eczema. *J Invest Dermatol* (2006) 126:2414–21. doi:10.1038/sj.jid.5700431
15. Cafarchia C, Gallo S, Romito D, Capelli G, Chermette R, Guillot J, et al. Frequency, body distribution, and population size of *Malassezia* species in healthy dogs and in dogs with localized cutaneous lesions. *J Vet Diagn Invest* (2005) 17:316–22. doi:10.1177/104063870501700403
16. Sandstrom Falk MH, Tengvall Linder M, Johansson C, Bartosik J, Back O, Sarnhult T, et al. The prevalence of *Malassezia* yeasts in patients with atopic dermatitis, seborrhoeic dermatitis and healthy controls. *Acta Derm Venereol* (2005) 85:17–23. doi:10.1080/00015550410022276
17. Underhill DM, Pearlman E. Immune interactions with pathogenic and commensal fungi: a two-way street. *Immunity* (2015) 43:845–58. doi:10.1016/j.immuni.2015.10.023
18. Dambuza IM, Brown GD. C-type lectins in immunity: recent developments. *Curr Opin Immunol* (2015) 32:21–7. doi:10.1016/j.coi.2014.12.002
19. Stalhberger T, Simenel C, Clavaud C, Eijsink VGH, Jourdain R, Delepierre M, et al. Chemical organization of the cell wall polysaccharide core of *Malassezia restricta*. *J Biol Chem* (2014) 289:12647–12656.
20. Kruppa MD, Lowman DW, Chen YH, Selander C, Scheynius A, Monteiro MA, et al. Identification of (1 – >6)-beta-D-glucan as the major carbohydrate component of the *Malassezia sympodialis* cell wall. *Carbohydr Res* (2009) 344:2474–9. doi:10.1016/j.carres.2009.09.029
21. Mittag H. Fine structural investigation of *Malassezia furfur*. II. The envelope of the yeast cells. *Mycoses* (1995) 38:13–21. doi:10.1111/j.1439-0507.1995.tb00003.x
22. Ishikawa T, Itoh F, Yoshida S, Saijo S, Matsuzawa T, Gonoi T, et al. Identification of distinct ligands for the C-type lectin receptors Mincle and Dectin-2 in the pathogenic fungus *Malassezia*. *Cell Host Microbe* (2013) 13:477–88. doi:10.1016/j.chom.2013.03.008
23. Brown GD, Crocker PR. Lectin receptors expressed on myeloid cells. *Microbiol Spectr* (2016) 4(5):MCHD-0036-2016. doi:10.1128/microbiolspec.MCHD-0036-2016
24. Yamasaki S, Matsumoto M, Takeuchi O, Matsuzawa T, Ishikawa E, Sakuma M, et al. C-type lectin Mincle is an activating receptor for pathogenic fungus, *Malassezia*. *Proc Natl Acad Sci U S A* (2009) 106:1897–902. doi:10.1073/pnas.0805177106
25. Kottom TJ, Hebrink DM, Jenson PE, Nandakumar V, Wuthrich M, Wang H, et al. The interaction of pneumocystis with the C-type lectin receptor Mincle exerts a significant role in host defense against infection. *J Immunol* (2017) 198:3515–25. doi:10.4049/jimmunol.1600744
26. Sousa MdG., Reid DM, Schweighoffer E, Tybulewicz V, Ruland J, Langhorne J, et al. Restoration of pattern recognition receptor costimulation to treat chromoblastomycosis, a chronic fungal infection of the skin. *Cell Host Microbe* (2011) 9:436–43. doi:10.1016/j.chom.2011.04.005
27. Wevers BA, Kaptein TM, Zijlstra-Willems EM, Theelen B, Boekhout T, Geijtenbeek TBH, et al. Fungal engagement of the C-type lectin mincle suppresses dectin-1-induced antifungal immunity. *Cell Host Microbe* (2014) 15:494–505. doi:10.1016/j.chom.2014.03.008
28. Iborra S, Martinez-Lopez M, Cueto FJ, Conde-Garrosa R, Del Fresno C, Izquierdo HM, et al. *Leishmania* uses Mincle to target an inhibitory ITAM signaling pathway in dendritic cells that dampens adaptive immunity to infection. *Immunity* (2016) 45:788–801. doi:10.1016/j.immuni.2016.09.012
29. Rabes A, Zimmermann S, Reppe K, Lang R, Seeberger PH, Suttorp N, et al. The C-type lectin receptor Mincle binds to Streptococcus pneumoniae but plays a limited role in the anti-pneumococcal innate immune response. *PLoS One* (2015) 10:e0117022. doi:10.1371/journal.pone.0117022
30. Devi S, Rajakumara E, Ahmed N. Induction of Mincle by *Helicobacter pylori* and consequent anti-inflammatory signaling denote a bacterial survival strategy. *Sci Rep* (2015) 5:15049. doi:10.1038/srep15049
31. Schick J, Etschel P, Bailo R, Ott L, Bhatt A, Lepenies B, et al. Toll-like receptor 2 and Mincle cooperatively sense corynebacterial cell wall glycolipids. *Infect Immun* (2017) 85:e00075–17. doi:10.1128/IAI.00075-17
32. Matsunaga I, Moody DB. Mincle is a long sought receptor for mycobacterial cord factor. *J Exp Med* (2009) 206:2865–8. doi:10.1084/jem.20092533
33. Yamasaki S, Ishikawa E, Sakuma M, Hara H, Ogata K, Saito T. Mincle is an ITAM-coupled activating receptor that senses damaged cells. *Nat Immunol* (2008) 9:1179–88. doi:10.1038/ni.1651
34. Nagata M, Izumi Y, Ishikawa E, Kiyotake R, Doi R, Iwai S, et al. Intracellular metabolite beta-glucosylceramide is an endogenous Mincle ligand possessing immunostimulatory activity. *Proc Natl Acad Sci U S A* (2017) 114:E3285–94. doi:10.1073/pnas.1618133114
35. Kiyotake R, Oh-Hora M, Ishikawa E, Miyamoto T, Ishibashi T, Yamasaki S. Human Mincle binds to cholesterol crystals and triggers innate immune responses. *J Biol Chem* (2015) 290:25322–32. doi:10.1074/jbc.M115.645234
36. Kostarnoy AV, Gancheva PG, Lepenies B, Tukhvatulin AI, Dzharullaeva AS, Polyakov NB, et al. Receptor Mincle promotes skin allergies and is capable of recognizing cholesterol sulfate. *Proc Natl Acad Sci U S A* (2017) 114:E2758–65. doi:10.1073/pnas.1611665114
37. Feinberg H, Jegouzo SAF, Rowntree TJW, Guan Y, Brash MA, Taylor ME, et al. Mechanism for recognition of an unusual mycobacterial glycolipid by the macrophage receptor mincle. *J Biol Chem* (2013) 288:28457–65. doi:10.1074/jbc.M113.497149
38. Jegouzo SAF, Harding EC, Acton O, Rex MJ, Fadden AJ, Taylor ME, et al. Defining the conformation of human mincle that interacts with mycobacterial trehalose dimycolate. *Glycobiology* (2014) 24:1291–300. doi:10.1093/glycob/cwu072
39. Feinberg H, Rambaruth NDS, Jegouzo SAF, Jacobsen KM, Djurhuus R, Poulsen TB, et al. Binding sites for acylated trehalose analogs of glycolipid

ligands on an extended carbohydrate recognition domain of the macrophage receptor Mincle. *J Biol Chem* (2016) 291:21222–33.
40. Furukawa A, Kamishikiryo J, Mori D, Toyonaga K, Okabe Y, Toji A, et al. Structural analysis for glycolipid recognition by the C-type lectins Mincle and MCL. *Proc Natl Acad Sci U S A* (2013) 110:17438–43. doi:10.1073/pnas.1312649110
41. Brown GD, Gordon S. Immune recognition. A new receptor for beta-glucans. *Nature* (2001) 413:36–7. doi:10.1038/35092620
42. Kistowska M, Fenini G, Jankovic D, Feldmeyer L, Kerl K, Bosshard P, et al. *Malassezia* yeasts activate the NLRP3 inflammasome in antigen-presenting cells via Syk-kinase signalling. *Exp Dermatol* (2014) 23:884–9. doi:10.1111/exd.12552
43. de Jong MA, Vriend LE, Theelen B, Taylor ME, Fluitsma D, Boekhout T, et al. C-type lectin Langerin is a beta-glucan receptor on human Langerhans cells that recognizes opportunistic and pathogenic fungi. *Mol Immunol* (2010) 47:1216–25. doi:10.1016/j.molimm.2009.12.016
44. Tateno H, Ohnishi K, Yabe R, Hayatsu N, Sato T, Takeya M, et al. Dual specificity of Langerin to sulfated and mannosylated glycans via a single C-type carbohydrate recognition domain. *J Biol Chem* (2010) 285:6390–400. doi:10.1074/jbc.M109.041863
45. Robinson MJ, Osorio F, Rosas M, Freitas RP, Schweighoffer E, Gross O, et al. Dectin-2 is a Syk-coupled pattern recognition receptor crucial for Th17 responses to fungal infection. *J Exp Med* (2009) 206:2037–51. doi:10.1084/jem.20082818
46. LeibundGut-Landmann S, Gross O, Robinson MJ, Osorio F, Slack EC, Tsoni SV, et al. Syk- and CARD9-dependent coupling of innate immunity to the induction of T helper cells that produce interleukin 17. *Nat Immunol* (2007) 8:630–8. doi:10.1038/ni1460
47. Angrisano T, Pero R, Paoletti I, Keller S, Lembo L, Baroni A, et al. Epigenetic regulation of IL-8 and beta-defensin genes in human keratinocytes in response to *Malassezia furfur*. *J Invest Dermatol* (2013) 133:2104–2104. doi:10.1038/jid.2013.143
48. Buommino E, De Filippis A, Parisi A, Nizza S, Martano M, Iovane G, et al. Innate immune response in human keratinocytes infected by a feline isolate of *Malassezia pachydermatis*. *Vet Microbiol* (2013) 163:90–6. doi:10.1016/j.vetmic.2012.12.001
49. Donnarumma G, Perfetto B, Paoletti I, Oliviero G, Clavaud C, Del Bufalo A, et al. Analysis of the response of human keratinocytes to *Malassezia globosa* and restricta strains. *Arch Dermatol Res* (2014) 306:763–8. doi:10.1007/s00403-014-1479-1
50. Baroni A, Orlando M, Donnarumma G, Farro P, Iovene MR, Tufano MA, et al. Toll-like receptor 2 (TLR2) mediates intracellular signalling in human keratinocytes in response to *Malassezia furfur*. *Arch Dermatol Res* (2006) 297:280–8. doi:10.1007/s00403-005-0594-4
51. Thomas DS, Ingham E, Bojar RA, Holland KT. In vitro modulation of human keratinocyte pro- and anti-inflammatory cytokine production by the capsule of *Malassezia* species. *FEMS Immunol Med Microbiol* (2008) 54:203–14. doi:10.1111/j.1574-695X.2008.00468.x
52. Kesavan S, Holland KT, Ingham E. The effects of lipid extraction on the immunomodulatory activity of *Malassezia* species in vitro. *Med Mycol* (2000) 38:239–47. doi:10.1080/mmy.38.3.239.247
53. Ishibashi Y, Sugawara K, Sugita T, Nishikawa A. Secretion of thymic stromal lymphopoietin from human keratinocytes in response to *Malassezia* yeasts. *J Dermatol Sci* (2011) 62:124–8. doi:10.1016/j.jdermsci.2011.02.012
54. Magiatis P, Pappas P, Gaitanis G, Mexia N, Melliou E, Galanou M, et al. *Malassezia* yeasts produce a collection of exceptionally potent activators of the Ah (dioxin) receptor detected in diseased human skin. *J Invest Dermatol* (2013) 133:2023–30. doi:10.1038/jid.2013.92
55. Gaitanis G, Magiatis P, Stathopoulou K, Bassukas ID, Alexopoulos EC, Velegraki A, et al. AhR ligands, malassezin, and indolo[3,2-b]carbazole are selectively produced by *Malassezia furfur* strains isolated from seborrheic dermatitis. *J Invest Dermatol* (2008) 128:1620–5. doi:10.1038/sj.jid.5701252
56. Cafarchia C, Otranto D. Association between phospholipase production by *Malassezia pachydermatis* and skin lesions. *J Clin Microbiol* (2004) 42:4868–9. doi:10.1128/JCM.42.10.4868-4869.2004
57. Riciputo RM, Oliveri S, Micali G, Sapuppo A. Phospholipase activity in *Malassezia furfur* pathogenic strains. *Mycoses* (1996) 39:233–5. doi:10.1111/j.1439-0507.1996.tb00131.x
58. Plotkin LI, Squiquera L, Mathov I, Galimberti R, Leoni J. Characterization of the lipase activity of *Malassezia furfur*. *J Med Vet Mycol* (1996) 34:43–8. doi:10.1080/02681219680000071
59. Lee YW, Lee SY, Lee Y, Jung WH. Evaluation of expression of lipases and phospholipases of *Malassezia restricta* in patients with seborrheic dermatitis. *Ann Dermatol* (2013) 25:310–4. doi:10.5021/ad.2013.25.3.310
60. Ortiz G, Martin MC, Carrillo-Muñoz AJ, Paya MJ. [Phospholipase and proteinase production by *Malassezia pachydermatis* isolated in dogs with and without otitis]. *Rev Iberoam Micol* (2013) 30:235–8. doi:10.1016/j.riam.2013.01.006
61. DeAngelis YM, Gemmer CM, Kaczvinsky JR, Kenneally DC, Schwartz JR, Dawson TL Jr. Three etiologic facets of dandruff and seborrheic dermatitis: *Malassezia* fungi, sebaceous lipids, and individual sensitivity. *J Investig Dermatol Symp Proc* (2005) 10:295–7. doi:10.1111/j.1087-0024.2005.10119.x
62. Katsuta Y, Iida T, Hasegawa K, Inomata S, Denda M. Function of oleic acid on epidermal barrier and calcium influx into keratinocytes is associated with N-methyl D-aspartate-type glutamate receptors. *Br J Dermatol* (2009) 160:69–74. doi:10.1111/j.1365-2133.2008.08860.x
63. Katsuta Y, Iida S, Fau-Inomata T, Inomata M, Fau-Denda S, Denda M. Unsaturated fatty acids induce calcium influx into keratinocytes and cause abnormal differentiation of epidermis. *J Investig Dermatol* (2005) 124:1008–13. doi:10.1111/j.0022-202X.2005.23682.x
64. Plotkin LI, Mathov I, Squiquera L, Leoni J. Arachidonic acid released from epithelial cells by *Malassezia furfur* phospholipase A2: a potential pathophysiologic mechanism. *Mycologia* (1998) 90:163–9. doi:10.2307/3761291
65. Mayser P, Wille G, Imkampe A, Thoma W, Arnold N, Monsees T. Synthesis of fluorochromes and pigments in *Malassezia furfur* by use of tryptophan as the single nitrogen source. *Mycoses* (1998) 41:265–71. doi:10.1111/j.1439-0507.1998.tb00336.x
66. Mexia N, Gaitanis G, Velegraki A, Soshilov A, Denison MS, Magiatis P. Pityriazepin and other potent AhR ligands isolated from *Malassezia furfur* yeast. *Arch Biochem Biophys* (2015) 571:16–20. doi:10.1016/j.abb.2015.02.023
67. Mayser P, Schafer U, Kramer HJ, Irlinger B, Steglich W. Pityriacitrin – an ultraviolet-absorbing indole alkaloid from the yeast *Malassezia furfur*. *Arch Dermatol Res* (2002) 294:131–4. doi:10.1007/s00403-002-0294-2
68. Kramer HJ, Podobinska M, Bartsch A, Battmann A, Thoma W, Bernd A, et al. Malassezin, a novel agonist of the aryl hydrocarbon receptor from the yeast *Malassezia furfur*, induces apoptosis in primary human melanocytes. *Chembiochem* (2005) 6:860–5. doi:10.1002/cbic.200400247
69. Kramer HJ, Kessler D, Hipler UC, Irlinger B, Hort W, Bodeker RH, et al. Pityriarubins, novel highly selective inhibitors of respiratory burst from cultures of the yeast *Malassezia furfur*: comparison with the bisindolylmaleimide arcyriarubin A. *Chembiochem* (2005) 6:2290–7. doi:10.1002/cbic.200500163
70. Vlachos C, Schulte BM, Magiatis P, Adema GJ, Gaitanis G. *Malassezia*-derived indoles activate the aryl hydrocarbon receptor and inhibit toll-like receptor-induced maturation in monocyte-derived dendritic cells. *Br J Dermatol* (2012) 167:496–505. doi:10.1111/j.1365-2133.2012.11014.x
71. Tauchi M, Hida A, Negishi T, Katsuoka F, Noda S, Mimura J, et al. Constitutive expression of aryl hydrocarbon receptor in keratinocytes causes inflammatory skin lesions. *Mol Cell Biol* (2005) 25:9360–8. doi:10.1128/MCB.25.21.9360-9368.2005
72. Gaitanis G, Velegraki A, Magiatis P, Pappas P, Bassukas ID. Could *Malassezia* yeasts be implicated in skin carcinogenesis through the production of aryl-hydrocarbon receptor ligands? *Med Hypotheses* (2011) 77:47–51. doi:10.1016/j.mehy.2011.03.020
73. Buommino E, Nocera FP, Parisi A, Rizzo A, Donnarumma G, Mallardo K, et al. Correlation between genetic variability and virulence factors in clinical strains of *Malassezia pachydermatis* of animal origin. *New Microbiol* (2016) 39:216–23.
74. Donnarumma G, Paoletti I, Buommino E, Orlando M, Tufano MA, Baroni A. *Malassezia furfur* induces the expression of beta-defensin-2 in human keratinocytes in a protein kinase C-dependent manner. *Arch Dermatol Res* (2004) 295:474–81. doi:10.1007/s00403-003-0445-0
75. Watanabe S, Kano R, Sato H, Nakamura Y, Hasegawa A. The effects of *Malassezia yeasts* on cytokine production by human keratinocytes. *J Invest Dermatol* (2001) 116:769–73. doi:10.1046/j.1523-1747.2001.01321.x
76. Ribbing C, Engblom C, Lappalainen J, Lindstedt K, Kovanen PT, Karlsson MA, et al. Mast cells generated from patients with atopic eczema have enhanced

levels of granule mediators and an impaired Dectin-1 expression. *Allergy* (2011) 66:110–9. doi:10.1111/j.1398-9995.2010.02437.x
77. Baroni A, Paoletti I, Ruocco E, Agozzino M, Tufano MA, Donnarumma G. Possible role of *Malassezia furfur* in psoriasis: modulation of TGF-beta1, integrin, and HSP70 expression in human keratinocytes and in the skin of psoriasis-affected patients. *J Cutan Pathol* (2004) 31:35–42. doi:10.1046/j.0303-6987.2004.0135.x
78. Jarvikallio A, Naukkarinen A, Harvima IT, Aalto ML, Horsmanheimo M. Quantitative analysis of tryptase- and chymase-containing mast cells in atopic dermatitis and nummular eczema. *Br J Dermatol* (1997) 136:871–7. doi:10.1111/j.1365-2133.1997.tb03927.x
79. Selander C, Engblom C, Nilsson G, Scheynius A, Andersson CL. TLR2/MyD88-dependent and -independent activation of mast cell IgE responses by the skin commensal yeast *Malassezia sympodialis*. *J Immunol* (2009) 182:4208–16. doi:10.4049/jimmunol.0800885
80. Gehrmann U, Qazi KR, Johansson C, Hultenby K, Karlsson M, Lundeberg L, et al. Nanovesicles from *Malassezia sympodialis* and host exosomes induce cytokine responses – novel mechanisms for host-microbe interactions in atopic eczema. *PLoS One* (2011) 6:e21480. doi:10.1371/journal.pone.0021480
81. Ashbee HR, Bond R. *Malassezia* species and immunity: host–pathogen interactions. In: Boekhout T, Mayser P, Guého-Kellermann E, Velegraki A, editors. *Malassezia and the Skin: Science and Clinical Practice*. Berlin, Heidelberg: Springer (2010). p. 139–73.
82. Valli JL, Williamson A, Sharif S, Rice J, Shewen PE. In vitro cytokine responses of peripheral blood mononuclear cells from healthy dogs to distemper virus, *Malassezia* and Toxocara. *Vet Immunol Immunopathol* (2010) 134:218–29. doi:10.1016/j.vetimm.2009.09.023
83. Kang MH, Kim HJ, Jang HJ, Park HM. Sensitization rates of causative allergens for dogs with atopic dermatitis: detection of canine allergen-specific IgE. *J Vet Sci* (2014) 15:545–50. doi:10.4142/jvs.2014.15.4.545
84. Chen TA, Halliwell RE, Pemberton AD, Hill PB. Identification of major allergens of *Malassezia pachydermatis* in dogs with atopic dermatitis and *Malassezia* overgrowth. *Vet Dermatol* (2002) 13:141–50. doi:10.1046/j.1365-3164.2002.00291.x
85. Johansson C, Sandstrom MH, Bartosik J, Sarnhult T, Christiansen J, Zargari A, et al. Atopy patch test reactions to *Malassezia* allergens differentiate subgroups of atopic dermatitis patients. *Br J Dermatol* (2003) 148:479–88. doi:10.1046/j.1365-2133.2003.05093.x
86. Glatz M, Buchner M, von Bartenwerffer W, Schmid-Grendelmeier P, Worm M, Hedderich J, et al. *Malassezia* spp.-specific immunoglobulin E level is a marker for severity of atopic dermatitis in adults. *Acta Derm Venereol* (2015) 95:191–6. doi:10.2340/00015555-1864
87. Zhang E, Tanaka T, Tajima M, Tsuboi R, Kato H, Nishikawa A, et al. Anti-*Malassezia*-specific IgE antibodies production in Japanese patients with head and neck atopic dermatitis: relationship between the level of specific ige antibody and the colonization frequency of cutaneous *Malassezia* species and clinical severity. *J Allergy (Cairo)* (2011) 2011:645670. doi:10.1155/2011/645670
88. Johansson C, Ahlborg N, Andersson A, Lundeberg L, Karlsson MA, Scheynius A, et al. Elevated peripheral allergen-specific T cell response is crucial for a positive atopy patch test reaction. *Int Arch Allergy Immunol* (2009) 150:51–8. doi:10.1159/000210380
89. Levy JMS, Magro C. Atrophying pityriasis versicolor as an idiosyncratic T cell-mediated response to *Malassezia*: a case series. *J Am Acad Dermatol* (2017) 76:730–5. doi:10.1016/j.jaad.2016.08.062
90. Eyerich S, Eyerich K, Pennino D, Carbone T, Nasorri F, Pallotta S, et al. Th22 cells represent a distinct human T cell subset involved in epidermal immunity and remodeling. *J Clin Invest* (2009) 119:3573–85. doi:10.1172/JCI40202
91. Cavani A, Pennino D, Eyerich K. Th17 and Th22 in skin allergy. *Chem Immunol Allergy* (2012) 96:39–44. doi:10.1159/000331870
92. Di Cesare A, Di Meglio P, Nestle FO. The IL-23/Th17 axis in the immunopathogenesis of psoriasis. *J Invest Dermatol* (2009) 129:1339–50. doi:10.1038/jid.2009.59
93. Balaji H, Heratizadeh A, Wichmann K, Niebuhr M, Crameri R, Scheynius A, et al. *Malassezia* sympodialis thioredoxin-specific T cells are highly cross-reactive to human thioredoxin in atopic dermatitis. *J Allergy Clin Immunol* (2011) 128: 92–9.e4. doi:10.1016/j.jaci.2011.02.043
94. Esaki H, Brunner PM, Renert-Yuval Y, Czarnowicki T, Huynh T, Tran G, et al. Early-onset pediatric atopic dermatitis is TH2 but also TH17 polarized in skin. *J Allergy Clin Immunol* (2016) 138:1639–51. doi:10.1016/j.jaci.2016.07.013
95. Sparber F, LeibundGut-Landmann S. Interleukin 17-mediated host defense against *Candida albicans*. *Pathogens* (2015) 4:606–19. doi:10.3390/pathogens4030606
96. Gaitanis G, Magiatis P, Hantschke M, Bassukas ID, Velegraki A. The *Malassezia* genus in skin and systemic diseases. *Clin Microbiol Rev* (2012) 25:106–41. doi:10.1128/CMR.00021-11
97. Selander C, Zargari A, Mollby R, Rasool O, Scheynius A. Higher pH level, corresponding to that on the skin of patients with atopic eczema, stimulates the release of *Malassezia sympodialis* allergens. *Allergy* (2006) 61:1002–8. doi:10.1111/j.1398-9995.2006.01108.x
98. Schmid-Grendelmeier P, Fluckiger S, Disch R, Trautmann A, Wuthrich B, Blaser K, et al. IgE-mediated and T cell-mediated autoimmunity against manganese superoxide dismutase in atopic dermatitis. *J Allergy Clin Immunol* (2005) 115:1068–75. doi:10.1016/j.jaci.2005.01.065
99. Glaser AG, Limacher A, Fluckiger S, Scheynius A, Scapozza L, Crameri R. Analysis of the cross-reactivity and of the 1.5 A crystal structure of the *Malassezia sympodialis* Mala s 6 allergen, a member of the cyclophilin pan-allergen family. *Biochem J* (2006) 396:41–9. doi:10.1042/BJ20051708
100. Youn SW, Na JI, Choi SY, Huh CH, Park KC. Regional and seasonal variations in facial sebum secretions: a proposal for the definition of combination skin type. *Skin Res Technol* (2005) 11:189–95. doi:10.1111/j.1600-0846.2005.00119.x
101. Kim SY, Kim SH, Kim SN, Kim AR, Kim YR, Kim MJ, et al. Isolation and identification of *Malassezia* species from Chinese and Korean patients with seborrheic dermatitis and in vitro studies on their bioactivity on sebaceous lipids and IL-8 production. *Mycoses* (2016) 59:274–80. doi:10.1111/myc.12456
102. Schonherr FA, Sparber F, Kirchner FR, Guiducci E, Trautwein-Weidner K, Gladiator A, et al. The intraspecies diversity of *C. albicans* triggers qualitatively and temporally distinct host responses that determine the balance between commensalism and pathogenicity. *Mucosal Immunol* (2017) 10:1335–50. doi:10.1038/mi.2017.2
103. Zhu Y, Engstrom PG, Tellgren-Roth C, Baudo CD, Kennell JC, Sun S, et al. Proteogenomics produces comprehensive and highly accurate protein-coding gene annotation in a complete genome assembly of *Malassezia sympodialis*. *Nucleic Acids Res* (2017) 45:2629–43.

Conflict of Interest Statement: The authors declare that the research was conducted in the absence of any commercial or financial relationships that could be construed as a potential conflict of interest.

Copyright © 2017 Sparber and LeibundGut-Landmann. This is an open-access article distributed under the terms of the Creative Commons Attribution License (CC BY). The use, distribution or reproduction in other forums is permitted, provided the original author(s) or licensor are credited and that the original publication in this journal is cited, in accordance with accepted academic practice. No use, distribution or reproduction is permitted which does not comply with these terms.

frontiers in Immunology

REVIEW
published: 30 April 2018
doi: 10.3389/fimmu.2018.00855

Mechanisms of *Cryptococcus neoformans*-Mediated Host Damage

Arturo Casadevall[1]*, *Carolina Coelho*[1] and *Alexandre Alanio*[1,2,3]

[1] Department of Molecular Microbiology and Immunology, Johns Hopkins School of Public Health, Baltimore, MD, United States, [2] Institut Pasteur, Molecular Mycology Unit, CNRS UMR2000, Paris, France, [3] Laboratoire de Parasitologie-Mycologie, Hôpital Saint-Louis, Groupe Hospitalier Lariboisière, Saint-Louis, Fernand Widal, Assistance Publique-Hôpitaux de Paris (AP-HP), Université Paris Diderot, Sorbonne Paris Cité, Paris, France

Cryptococcus neoformans is not usually considered a cytotoxic fungal pathogen but there is considerable evidence that this microbe can damage host cells and tissues. In this essay, we review the evidence that *C. neoformans* damages host cells and note that the mechanisms involved are diverse. We consider *C. neoformans*-mediated host damage at the molecular, cellular, tissue, and organism level. Direct mechanisms of cytotoxicity include lytic exocytosis, organelle dysfunction, phagolysosomal membrane damage, and cytoskeletal alterations. Cytotoxicity contributes to pathogenesis by interfering with immune effector cell function and disrupting endothelial barriers thus allowing dissemination. When *C. neoformans*-mediated and immune-mediated host damage is sufficient to affect homeostasis, cryptococcosis occurs at the organism level.

Keywords: *Cryptococcus*, cryptococcosis, disease, damage, macrophage, cytotoxicity

OPEN ACCESS

Edited by:
Bernhard Hube,
Hans Knöll Institut, Germany

Reviewed by:
David L. Moyes,
King's College London,
United Kingdom
Ana Traven,
Monash University, Australia
Elizabeth R. Ballou,
University of Birmingham,
United Kingdom

***Correspondence:**
Arturo Casadevall
acasade1@jhu.edu

Specialty section:
This article was submitted to Microbial Immunology, a section of the journal Frontiers in Immunology

Received: *24 January 2018*
Accepted: *06 April 2018*
Published: *30 April 2018*

Citation:
Casadevall A, Coelho C and Alanio A (2018) Mechanisms of Cryptococcus neoformans-Mediated Host Damage. Front. Immunol. 9:855. doi: 10.3389/fimmu.2018.00855

Anyone with expertise in routine laboratory tissue culture knows that fungal contamination rapidly kills mammalian cells *in vitro*. However, *Cryptococcus neoformans* is unusual among fungi in that it has minimal toxicity for animal cells in tissue culture, such that it is possible to maintain yeast cells and macrophages for days without major cytotoxicity for the latter. Macrophage-like cells that have phagocytosed *C. neoformans* are capable of replicating and divide their yeast cargo among daughter cells (1). This implies that *C. neoformans* does not release major cytotoxic products, at least *in vitro*. Consistent with this notion, cryptococcal infections are not associated with tissue necrosis as seen in infections caused by other fungal pathogens, such as those caused by *Aspergillus* or Mucorales spp. In fact, cryptococcosis often shows many features of a chronic infection, and host death is often due to the effects of physical compression of tissue, and defects in resorption of cerebrospinal fluid (CSF) (possibly due to increased viscosity from fungal polysaccharide shedding into CSF) and overwhelming brain edema (2). While these observations might lead to the conclusion that *C. neoformans* infections are associated with minimal host damage, a review of available knowledge reveals otherwise. In this essay, we survey the available evidence that *C. neoformans* is capable of inflicting direct damage on host cells and tissues. We note that host damage following cryptococcal infection can come from microbe and the host (3, 4), with the latter culminating in a dramatic pathology known as Immune Reconstitution Inflammatory Syndrome (IRIS).

We consider damage at four levels of scale: molecular, cellular, tissue, and organism level. Molecular damage is that caused by enzymes or molecules produced by *C. neoformans,* which induces modifications of host molecules and cells and manifests itself at the molecular or organelle level. Cellular damages are those causing modifications of the architecture and structure of the host cells due to the toxic action of *C. neoformans*. Tissue damages cause anatomical and functional disorganization beyond cellular injury. Together, these combine to produce the disease of cryptococcosis at the organism level. We recognize that these are not independent, since molecular damage leads

to cellular damage, cellular damage leads to tissue damage, and all three combine to produce organismal damage. Furthermore, we note that a process of *C. neoformans* can damage the host at more than one level. For example, cryptococcal phospholipase can cause molecular damage by destroying surfactant molecules (5) while also being a potential cause of cellular damage at the level of macrophage (6). Despite these important caveats, these mechanisms are sufficiently distinct that it is possible to discuss them separately. Our goal is integrating them to produce a holistic view of *C. neoformans*-mediated host damage into a new synthesis for approaching cryptococcal pathogenesis (**Figure 1**).

MOLECULAR DAMAGE

In the section for molecular damage, we consider how cryptococcal products damage host molecules (**Figure 1**). *C. neoformans*-mediated molecular damage enhances its likelihood of survival in tissues. As a soil-dwelling organism that obtains its nutrition from digesting material in the environment, *C. neoformans* secretes a large suite of enzymes with the potential to degrade host molecules (7). Among all enzymes produced by the fungus, the major candidates as mediators of host toxicity at the molecular level are proteases, urease, phospholipase, and nuclease (7). *C. neoformans* can metabolize immunoglobulins and complement proteins for growth as these compounds are presumably degraded by released proteases (8). Hence, proteases may interfere with host defense mechanisms by cleaving immunologically important molecules and directly damaging effector cells. Cryptococcal serine proteases promote increased blood–brain barrier (BBB) permeability (9), which may help in the process of brain infection. Although not directly related to host damage *C. neoformans* releases a protease that cleaves a peptide, which functions as quorum-sensing molecule to increase virulence (10). Urease is a virulence factor for *C. neoformans* (11), which is important for brain invasion (12). The mechanism by which urease promotes brain invasion could involve catalyzing the hydrolysis of urea to ammonia to locally damage endothelial cells in the brain vasculature. Another group of enzymes involved in the pathogenesis of *C. neoformans*

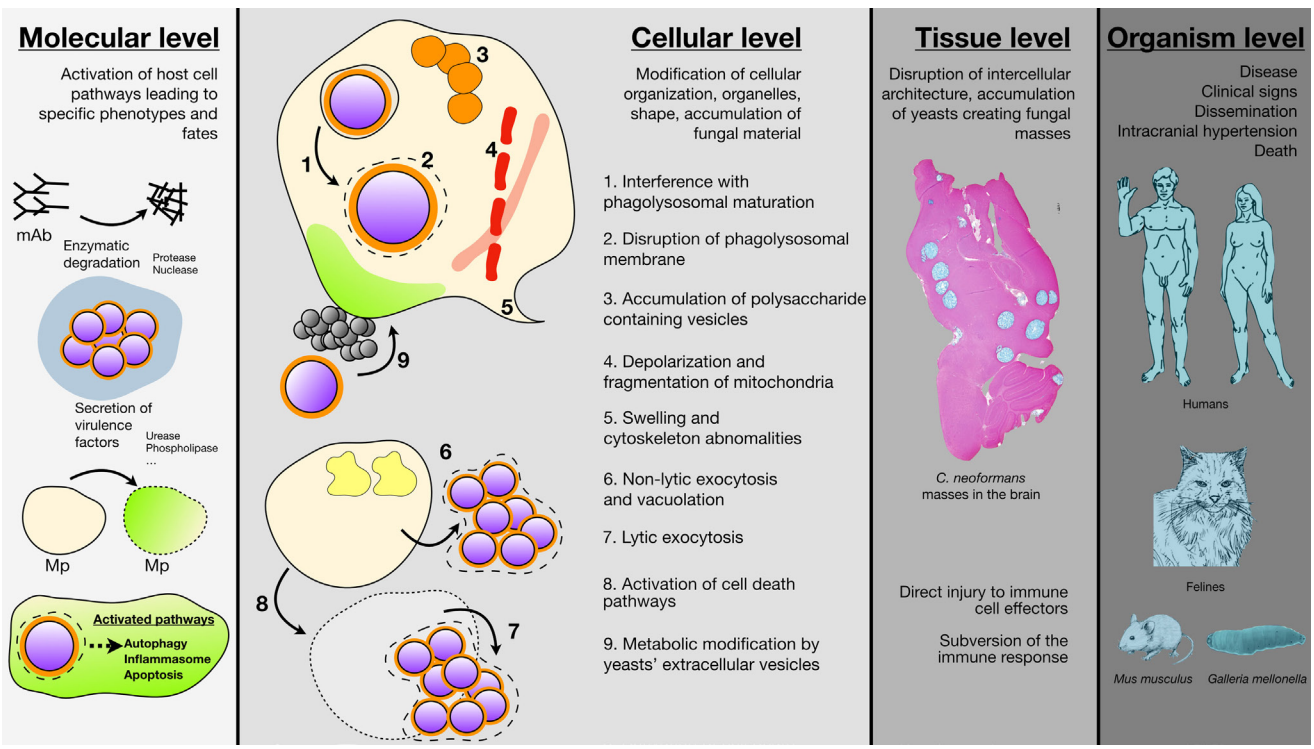

FIGURE 1 | Schematic representation of the different *Cryptococcus neoformans*-mediated cell host damages are various scales. Damage at the molecular level results from the secretion of various enzyme by *C. neoformans* (proteases, nuclease, urease, phospholipase) that degrade host molecules such as antibodies and/or modify cells membranes. *C. neoformans* ingestion is also able to trigger autophagy, apoptosis, and cell death in the host (mAb, monoclonal antibodies; Mp, macrophages). Damage at the cellular level involves modification of cellular compartments such as accumulation of polysaccharide vacuoles (1), inhibition of phagolysosomal maturation (2), phagolysosomal leakage (3), mitochondrial fission and depolarization (4), swelling and cytoskeleton abonomalities (5) or metabolic modification due to *C. neoformans* vesicles secretions (6), *C. neoformans* engulfment resulted also in non-lytic (7), or lytic (8) exocytosis. Damage at the tissue level consisted typical cryptococcal lesions in the brain parenchyma after intravenous inoculation of *C. neoformans* to outbred mice (sacrifice seven days after inoculation). No granuloma and accumulation of yeast masses without inflammatory cells can be observed engendering tissue disorganization. Coloration Alcian Blue (magnification 4×). Damage at the organism level combines to produce the clinical signs associated with cryptococcal diseases in humans with dissemination and neurological abnormalities as the most severe clinical presentation leading to death. Felines are also naturally susceptible to cryptococcosis with localized to disseminate infections. *Mus musculus* and *Galleria mellonella* are well established organisms for experimental models of infection that help understanding the pathophysiology of the disease and the biology of the yeast in relation to the host.

are phospholipases. *C. neoformans* produces both phospholipase B and C (6, 13–17). Phospholipases cleave phospholipids, which in turn allow them to damage membranes. Phospholipase-deficient *C. neoformans* manifest delayed intracellular replication, which could result in better maintenance of phagosomal membrane integrity and subsequent enhanced fungal control (6). *In vitro* phospholipase-mediated cleaves surfactant and promotes the attachment of *C. neoformans* to human lung epithelial cells, a process *in vivo* could promote pulmonary infection (5). Ingestion of *C. neoformans* results in the activation of autophagy initiation complex pathways, which results in a global reprogramming of host kinase signaling (18).

CELLULAR DAMAGE

By cellular damage, we consider mechanisms for cytotoxicity. *C. neoformans*-mediated cytotoxicity contributes to establishment of disease *via* at least two major mechanisms. First, damage to host immune system in tissue, which inflicts damage to immune system, the surrounding tissues and may cause symptoms to the host while ultimately allowing persistence of infection. Second, damage to the endothelial cells in the brain vasculature (possibly in other organs as well), precedes invasion of the central nervous system to cause meningoencephalitis, the most common life-threatening form of cryptococcosis. Interaction of *C. neoformans* with the epithelial barriers is transient, and internalization of *C. neoformans* by epithelial cells is rarely observed. The airway epithelium is critical to trigger initial inflammatory response to the inhaled spores or yeast (19) and can produce surfactant, which agglutinates yeast cells (20). Potentially important to the pathogenesis of disease are interactions of *C. neoformans* with neurons or (micro)glial cells and their potential to cause neurological dysfunction but so far this remains an enigma (21). Therefore, we focus our discussion on cytotoxic damage primarily on phagocytic cells and endothelial cells and describe several forms of damage that can be inflicted on host cells (**Figure 1**).

1. *Interference with phagolysosomal maturation:* after ingestion of *C. neoformans* by macrophage, yeasts resides in an acidic phagosome that has maturation markers such as Lamp1 (22). Initially, *C. neoformans* was thought to not interfere with phagosome maturation similar to other intracellular pathogens such as *Mycobacterium tuberculosis*. However, recent studies indicate that ingestion of live but not dead *C. neoformans* cells is associated with the early removal of phagosome maturation markers Rab5 and Rab11 and interference with proteolytic activity and calcium fluxes (23). Interference with phagolysosome maturation would have the effect of interfering with its microbicidal activity, which in turn would promote fungal intracellular replication.
2. *Phagolysosomal leakage:* electron microscopic studies revealed damaged membranes in phagosomes containing *C. neoformans* (24). Phagolysosomal leakage was confirmed with fluorescence labeled microscopy (25). Leakage of phagosome components into the cytoplasm interferes with microbicidal activity of this organelle but may also trigger the inflammasome (26). The amount of phagosomal leakage is modulated by IFN gamma (27), and likely other cytokines, with consequences to the amount of host cell damage and death.
3. *Accumulation of polysaccharide-containing vesicles in macrophage: C. neoformans* infection in macrophage is accompanied by the accumulation of vesicles, which contain fungal polysaccharide (24). The presence of large numbers of vesicles in the macrophage cytoplasm can give the impression of "holes" and these cells were named "hueco cells" after the Spanish term for hole (24). These intracytoplasmic vesicles appear to bud from the cryptococcal phagolysosome (24). Whether vesicle accumulation causes direct damage to the host cell is not known but their presence crowds out the cytoplasm and could impair cellular function. In addition, the generation of such large number of vesicles must tax lipid reserves (as composed of lipid bilayer), which could put a stress on membrane generation and repair.
4. *Interference with organelle function:* upon detection of intruder pathogenic microbes, macrophage undergo a series of concerted metabolic changes ranging from shift to a glycolytic metabolism to adaptation of the rate of protein synthesis or autophagy. Cellular quality control is a method to detect pathogen interference with organelle and cellular function and, therefore, is a mechanism of immune surveillance. When *C. neoformans* infects murine macrophage mitochondria potential is decreased and protein synthesis is impaired (28, 29). The presence of extracellular yeast could also lead to chromosomal aberrations and cell cycle impairment in murine macrophage (28).
5. *Host cell swelling and cytoskeleton alterations:* several decades ago, cryptococcal polysaccharide was reported to produce direct swelling effects on host cells (30–32). Although the biochemical pathway is still unknown, there is evidence that *C. neoformans* can induce changes in the cellular cytoskeleton. Human brain microvascular endothelial cells exposed to *C. neoformans* manifested changes in membrane ruffling, morphological changes in the nucleus, and swelling of the mitochondria and endoplasmic reticulum (33). These changes were associated with dephosphorylation of cofilin and actin changes (33). Similarly, changes to the cell cytoskeleton are apparent after *C. neoformans* infection of *Drosophila* cells (34). Another example of close interaction, and possible manipulation of host cytoskeleton, is that in human endothelial cells transcytosis requires CD44 receptor, which triggers the movement of actin to membrane lipid rafts that presumably aid in cellular entry (35). Changes to the cytoskeleton are apparent before non-lytic exocytosis in the form of actin flashes (36).
6. *Non-lytic exocytosis and vacuolation:* non-lytic exocytosis is generally considered a relatively benign process on the host cell given that cells from which *C. neoformans* has exited can replicate (37, 38). However, it is likely that any interference in the process of non-lytic exocytosis will trigger lytic exocytosis (discussed below). In this regard, macrophage deficient in annexin A2, a protein that is involved in a myriad of cellular functions including membrane fusion and plasma membrane repair, manifested increased lytic exocytosis, possibly due to problems in membrane fusion during the process of exocytosis (39). Non-lytic exocytosis results in the formation of large vacuoles in the cytoplasm of macrophage from which *C. neoformans* exited (40). Although the mechanism and

etiology of the formation of these large vacuoles is not known they represent an anatomic cellular abnormality that could interfere with cell homeostasis.

7. *Lytic exocytosis*: unchecked replication of *C. neoformans* inside macrophage can lead to rupture of the host cell with the release of fungal cells. This process, known as lytic exocytosis results in the death of the host cell. Host cell lysis by *C. neoformans* is also triggered by a mechanism that is dependent on cell wall mannosylation of cell wall and does not require the viability of the fungal cell (41).
8. *Activation of cell death pathways*: the toxic presence of *C. neoformans* may culminate in host cellular death. However, a study of death pathways activated in murine macrophage upon *C. neoformans* infection did not find a specific pathway predominantly activated. In contrast, in dendritic cells *C. neoformans* caused robust inflammasome activation and cell death, which was critically dependent of caspase-1, or caspase-8 in the absence of caspase-1 (28, 29). *C. neoformans* polysaccharides glucuronoxylomannan and galactoxylomannan can mediate direct cytoxicity to macrophage by activation of Fas ligand and triggering apoptosis (42, 43). Galatoxylomannan trigger B cell death leading to lymphocyte depletion and abrogating effective antibody responses (44).
9. *Extracellular vesicle (EV) effects. C. neoformans* like all other fungi that have been examined produces EVs (45). In the case of *C. neoformans*, these vesicles contain many fungal products associated with virulence, including fungal secreted polysaccharides and laccase (46). EVs are not directly toxic to host cells but they can have powerful stimulatory effects on host macrophage (47). In fact, incubation of macrophage with *C. neoformans* EVs led to activation changes that increased the antifungal activity (47). Although at this time EVs are not linked directly to cryptococcal pathogenesis there is considerable indirect evidence for an important role in virulence. For example, capsular polysaccharides have been implicated in negative effects on immune function, and this material is exported across the cryptococcal cell wall in EVs (5, 48). In addition to capsular polysaccharides, EVs have been shown to carry numerous short RNA molecules raising the possibility that these microbial RNAs are involved in modulating host cell function (49).

TISSUE AND ORGAN DAMAGE

Immune System Damage

The immune system is damaged during *C. neoformans* infection by direct injury to its effector cells and by interference with effective immunity. The outcome of the *C. neoformans*–macrophage interaction is a critical determinant for the fate of the microbe and host during infection. The ability of *C. neoformans* to replicate inside macrophage correlated with mice and rat susceptibility to infection (50, 51). In humans, the capacity of *C. neoformans* strains to replicate in macrophage to higher intracellular burden correlated with worse clinical outcomes (52, 53). Hence, the available evidence suggests that factors and interventions that modulate macrophage function, in particular when T-cell function is impaired, could control cryptococcal disease, whereas the capacity of the yeast to efficiently replicate intracellularly is associated with progression of infection. In this light, it is apparent that mechanisms that damage macrophage are likely to impair the antifungal capacity of these cells, which in turn facilitates intracellular growth. Hence, mitochondrial damage, phagosomal damage, and induction of programmed cellular pathways can be expected to directly aid in fungal survival *in vivo* through impairment of monocyte mononuclear macrophage as well as other innate immune cells. Damage to other immune cells has been less studied, but for example direct effects of shed polysaccharides on adaptive cellular responses (54) will magnify the impairment to macrophage function by providing inadequate activation of microbicidal capacity. A last point is that shear physical force of capsule and cell body growth, to dimensions surpassing 10 μm, may exhaust intracellular membranes of the host and that this fungal gigantism could physically damage host cell (55, 56), as seen with capsule growth and titan cell formation.

The second form of damage to the immune system is interference with its ability to organize an effective response. Here, the damage is multifaceted and originates from the cellular damage described above as well direct effects of cryptococcal components that affect the response of immune cells, which in turn interfere with effective immunity. The major cryptococcal polysaccharides have protean effects on the function of immune cells, which contribute to dysregulated process [reviewed in Ref. (57)]. In addition, to polysaccharide-mediated effects, the presence of the *C. neoformans* urease in the lung promotes the accumulation of immature dendritic cells and the emergence of a non-protective T2 polarized inflammatory response (58). *C. neoformans* produces a variety of prostaglandins and leukotrienes, which have direct effects on inflammatory cells and thus may have a major effect in altering the local immune response to infection (3, 41). Synthesis of eicosanoids is dependent on phospholipase activity thus implicating this enzyme in several different possible mechanism of virulence (47). Cryptococcal polysaccharides interfere with leukocyte migration toward chemoattractants (59). The mechanism for this effect includes induction of L-selectin shedding from neutrophils (60). Interference with leukocyte migration could account for the notoriously poor inflammatory responses observed in many individuals (61).

The immune response to *C. neoformans* can also mediate host damage. This phenomenon was first when HIV-infected individuals successfully treated for cryptococcosis manifested a worsening of symptoms after the initiation of antiretroviral therapy (62, 63). What came to be known as "immune reconstitution inflammatory syndrome" was the result of immune system recovery reacting to residual cryptococcal antigens in tissue, which resulted in inflammation and local organ damage (63). Recently, T cells have been associated with immune injury in experimental murine cryptococcosis establishing a mechanism by which immune dysregulation in response to infection can produce host damage (3). The contribution of immune-mediated damage to the pathogenesis of cryptococcosis could help explain the paradoxical observation that the prognosis of cryptococcal meningitis if more favorable in patients with HIV infection and severe immunodeficiency than in those without obvious immune impairment (4). There is also some evidence that cryptococcal infection in the lung predisposes

the host to develop allergic inflammation that could progress to hyperreactive airway diseases, such as asthma (64–66).

Damage to BBB

The major cause of mortality and morbidity during cryptococcosis is meningoencephalitis. For *C. neoformans* to invade the central nervous system yeast cells must cross the BBB. *C. neoformans* crosses the BBB by two mechanisms: transcytosis, whereby yeast cells transit directly through endothelial cells and a Trojan Horse-like mechanism involving carriage inside an infected macrophage (67–69). The former mechanism involves undermining the integrity of the BBB (70) and is enhanced by brain inositol (71). The yeasts are trapped in the brain capillaries because of their size, allowing for active transcytosis (12). For the efficient Trojan horse crossing, *C. neoformans* must survive inside macrophage and, as noted above, fungal-mediated damage to the phagocytic cell enhances intracellularly cryptococcal survival. However, it is still poorly understood if the crossing of the BBB merely causes a transient disruption in integrity of the BBB or whether it has more pernicious consequences. One could hypothesize that entrapment of yeast in brain capillaries cause ischemia to surrounding tissues but this issue has not been formally addressed.

Tissue Masses

A distinctive feature of many cases of cryptococcal meningoencephalitis is the formation of masses of yeast cells in the brain with little or no inflammation (**Figure 1**). This feature distinctively distinguishes these structures from granuloma where inflammation and immune response are well organized. These structures are so distinctive that they have been referred as "soap bubbles" as they are composed of gelatinous pseudocysts composed of packed *C. neoformans* cells with a particular appearance in magnetic resonance imaging (72). For masses of *C. neoformans* to form in the brain, they must grow in a manner that displaces or destroys brain tissue to create the space for the fungal mass. Given the propensity of *C. neoformans* to replicate inside cells and trigger host cell death such soap bubble anatomic lesions could be the result of progressive lysis of host cells at the fungal–brain interface. In this regard, *C. neoformans* can replicate inside microglial cells, the brain resident macrophage population (73). Alternatively, it is possible that such lesions represent fungal replication that creates spaces in the brain through compression of brain tissue through the force generated by fungal replication. Hence, irrespective of the mechanism of formation, soap bubble lesions represent *prima facie* evidence of direct fungal damage to brain tissue.

ORGANISM DAMAGE

At the organism level the combination of molecular, cellular, and tissue damage leads to cryptococcosis (**Figure 1**). The damage–response framework of microbial pathogenesis posits that disease occurs when host damage is sufficient to affect hemostasis, which in turn produces clinical symptoms (74). For *C. neoformans* infections, host damage can come from both the microbe, as reviewed in this essay, and from the immune response (3, 4, 75). Although a discussion of how tissue damage results in clinical signs and symptoms that can ultimately lead to death is beyond the scope of this review, there is a clear connection between the types of damage discussed here and the disease.

RELATION OF CYTOTOXICITY TO ENVIRONMENTAL SELECTION PRESSURES—AMOEBA

Evolution of *C. neoformans* virulence, virulence being defined as capacity to survive or to cause disease in mammalian hosts, was proposed to arise from selection pressures in the environment by phagocytic predators such as amoeba (76, 77). According to this view, *C. neoformans* virulence factors needed for animal pathogenicity function emerged as characteristics that protect fungal cells against phagocytic predators. For example, the capsule, melanin, and phospholipase each contribute to fungal cell survival when preyed upon by amoeba (76). The outcome of amoeba–*C. neoformans* interactions is highly dependent on the conditions of the experiment. In conditions where there are minimal nutrients such as phosphate-buffered saline, *C. neoformans* is ascendant but the reverse occurs when there are nutrients for amoeba (48). The presence of extracellular Ca^{2+} and Mg^{2+} is enough to tilt the balance of the host–*C. neoformans* and allow amoeba to kill a significant portion of *C. neoformans* (78). Although far less is known about how *C. neoformans* damages amoeba than for mammalian cells, it is likely to have parallels in the mechanisms for cytotoxicity. In this regard, accumulation of polysaccharide-containing vesicles was observed in the cytoplasm of amoeba that ingested *C. neoformans* (76).

A SYNTHESIS FOR *C. neoformans*-MEDIATED HOST DAMAGE

For the purposes of this essay, we have considered host damage as a function of size scales but it is important to stress that damage is continuous from the molecular to organism level (**Figure 1**). Disseminated cryptococcosis is a rare disease in hosts with intact immunity, which means that host defense mechanisms are highly effective at confiding damage form inhaled *C. neoformans* to the molecular and cellular level in the lungs, such that damage does not rise to the level where homeostasis is affected and clinical symptoms ensue. Since cryptococcal infection is common and diseases is rare, and *C. neoformans* are common in the environment, it is likely that repeated cycles of macrophage infection occur in the lives of human hosts. Although we do not know the sequence of events that follow these interactions, the fact that these are asymptomatic suggests fungal control in the lung with minimal tissue damage. However, once there is impairment to the immune system, commonly following immunosuppression, HIV infection or iatrogenic, cryptococcal infection transforms from silent or latent, to a slow but inexorable progressive condition that invariably kills the host without aggressive therapy. However, more than a half century after the introduction of the first antifungal agent in the form of amphotericin B, the mortality and morbidity of cryptococcosis remains stubbornly high. Improvements in therapy may require a better understanding of the mechanisms of host damage that will

allow the development of new therapeutic interventions. A critical synthesis of how the various types of host damage synergize to impair tissue function is an important next step for understanding the pathogenesis of cryptococcosis.

AUTHOR CONTRIBUTIONS

All authors listed have made a substantial, direct, and intellectual contribution to the work and approved it for publication.

ACKNOWLEDGMENTS

The authors thank Françoise Dromer, for providing the picture of the whole brain of infected mouse. The authors also credit the histopathology and models unit at the Institute Pasteur, Paris. AC was supported by grants 5R01HL059842, 5R01AI033774, 5R37AI033142, and 5R01AI052733. AA was supported by a Fullbright and Monahan fellowship and a grant from the Philippe Foundation.

REFERENCES

1. Luo Y, Alvarez M, Xia L, Casadevall A. The outcome of phagocytic cell division with infectious cargo depends on single phagosome formation. *PLoS One* (2008) 3:e3219. doi:10.1371/journal.pone.0003219
2. Robertson EJ, Najjuka G, Rolfes MA, Akampurira A, Jain N, Anantharanjit J, et al. *Cryptococcus neoformans* ex vivo capsule size is associated with intracranial pressure and host immune response in HIV-associated cryptococcal meningitis. *J Infect Dis* (2014) 209:74–82. doi:10.1093/infdis/jit435
3. Neal LM, Xing E, Xu J, Kolbe JL, Osterholzer JJ, Segal BM, et al. CD4(+) T cells orchestrate lethal immune pathology despite fungal clearance during *Cryptococcus neoformans* meningoencephalitis. *MBio* (2017) 8:e01415–7. doi:10.1128/mBio.01415-17
4. Pirofski LA, Casadevall A. Immune-mediated damage completes the parabola: *Cryptococcus neoformans* pathogenesis can reflect the outcome of a weak or strong immune response. *MBio* (2017) 8:e02063-17. doi:10.1128/mBio.02063-17
5. Ganendren R, Carter E, Sorrell T, Widmer F, Wright L. Phospholipase B activity enhances adhesion of *Cryptococcus neoformans* to a human lung epithelial cell line. *Microbes Infect* (2006) 8:1006–15. doi:10.1016/j.micinf.2005.10.018
6. Cox GM, Mcdade HC, Chen SC, Tucker SC, Gottfredsson M, Wright LC, et al. Extracellular phospholipase activity is a virulence factor for *Cryptococcus neoformans*. *Mol Microbiol* (2001) 39:166–75. doi:10.1046/j.1365-2958.2001.02236.x
7. Almeida F, Wolf JM, Casadevall A. Virulence-associated enzymes of *Cryptococcus neoformans*. *Eukaryot Cell* (2015) 14:1173–85. doi:10.1128/EC.00103-15
8. Chen L-C, Blank E, Casadevall A. Extracellular proteinase activity of *Cryptococcus neoformans*. *Clin Diagn Lab Immunol* (1996) 3:570–4.
9. Xu CY, Zhu HM, Wu JH, Wen H, Liu CJ. Increased permeability of blood-brain barrier is mediated by serine protease during *Cryptococcus* meningitis. *J Int Med Res* (2014) 42:85–92. doi:10.1177/0300060513504365
10. Homer CM, Summers DK, Goranov AI, Clarke SC, Wiesner DL, Diedrich JK, et al. Intracellular action of a secreted peptide required for fungal virulence. *Cell Host Microbe* (2016) 19:849–64. doi:10.1016/j.chom.2016.05.001
11. Cox GM, Mukherjee J, Cole GT, Casadevall A, Perfect JR. Urease as a virulence factor in experimental cryptococcosis. *Infect Immun* (2000) 68:443–8. doi:10.1128/IAI.68.2.443-448.2000
12. Shi M, Li SS, Zheng C, Kim KS, Zhou H, Kubes P, et al. Real-time imaging of trapping and urease-dependent transmigration of *Cryptococcus* in the brain. *J Clin Invest* (2010) 120:1683–93. doi:10.1172/JCI41963
13. Chen SC, Wright LC, Santangelo RT, Muller M, Moran VR, Kuchel PW, et al. Identification of extracellular phospholipase B, lysophospholipase, and acyltransferase produced by *Cryptococcus neoformans*. *Infect Immun* (1997) 65:405–11.
14. Santangelo R, Zoellner H, Sorrell T, Wilson C, Donald C, Djordjevic J, et al. Role of extracellular phospholipases and mononuclear phagocytes in dissemination of cryptococcosis in a murine model. *Infect Immun* (2004) 72:2229–39. doi:10.1128/IAI.72.4.2229-2239.2004
15. Shea JM, Kechichian TB, Luberto C, Del Poeta M. The cryptococcal enzyme inositol phosphosphingolipid-phospholipase C confers resistance to the antifungal effects of macrophages and promotes fungal dissemination to the central nervous system. *Infect Immun* (2006) 74:5977–88. doi:10.1128/IAI.00768-06
16. Chayakulkeeree M, Sorrell TC, Siafakas AR, Wilson CF, Pantarat N, Gerik KJ, et al. Role and mechanism of phosphatidylinositol-specific phospholipase C in survival and virulence of *Cryptococcus neoformans*. *Mol Microbiol* (2008) 69:809–26. doi:10.1111/j.1365-2958.2008.06310.x
17. Djordjevic JT. Role of phospholipases in fungal fitness, pathogenicity, and drug development – lessons from *Cryptococcus neoformans*. *Front Microbiol* (2010) 1:125. doi:10.3389/fmicb.2010.00125
18. Pandey A, Ding SL, Qin QM, Gupta R, Gomez G, Lin F, et al. Global reprogramming of host kinase signaling in response to fungal infection. *Cell Host Microbe* (2017) 21:637–49.e636. doi:10.1016/j.chom.2017.04.008
19. Taylor-Smith LM. *Cryptococcus*-epithelial interactions. *J Fungi (Basel)* (2017) 3:E53. doi:10.3390/jof3040053
20. Schelenz S, Malhotra R, Sim RB, Holmskov U, Bancroft GJ. Binding of host collectins to the pathogenic yeast *Cryptococcus neoformans*: human surfactant D acts as an agglutinin for acapsular cells. *Infect Immun* (1995) 63:3360–6.
21. Drummond RA. Neuro-immune mechanisms of anti-cryptococcal protection. *J Fungi (Basel)* (2017) 4:E4. doi:10.3390/jof4010004
22. Levitz SM, Nong SH, Seetoo KF, Harrison TS, Speizer RA, Simons ER. *Cryptococcus neoformans* resides in an acidic phagolysosome of human macrophages. *Infect Immun* (1999) 67:885–90.
23. Smith LM, Dixon EF, May RC. The fungal pathogen *Cryptococcus neoformans* manipulates macrophage phagosome maturation. *Cell Microbiol* (2015) 17:702–13. doi:10.1111/cmi.12394
24. Feldmesser M, Kress Y, Novikoff P, Casadevall A. *Cryptococcus neoformans* is a facultative intracellular pathogen in murine pulmonary infection. *Infect Immun* (2000) 68:4225–37. doi:10.1128/IAI.68.7.4225-4237.2000
25. Tucker SC, Casadevall A. Replication of *Cryptococcus neoformans* in macrophages is accompanied by phagosomal permeabilization and accumulation of vesicles containing polysaccharide in the cytoplasm. *Proc Natl Acad Sci U S A* (2002) 99:3165–70. doi:10.1073/pnas.052702799
26. Chen M, Xing Y, Lu A, Fang W, Sun B, Chen C, et al. Internalized *Cryptococcus neoformans* activates the canonical caspase-1 and the noncanonical caspase-8 inflammasomes. *J Immunol* (2015) 195:4962–72. doi:10.4049/jimmunol.1500865
27. Davis MJ, Eastman AJ, Qiu Y, Gregorka B, Kozel TR, Osterholzer JJ, et al. *Cryptococcus neoformans*-induced macrophage lysosome damage crucially contributes to fungal virulence. *J Immunol* (2015) 194:2219–31. doi:10.4049/jimmunol.1402376
28. Ben-Abdallah M, Sturny-Leclere A, Ave P, Louise A, Moyrand F, Weih F, et al. Fungal-induced cell cycle impairment, chromosome instability and apoptosis via differential activation of NF-kappaB. *PLoS Pathog* (2012) 8:e1002555. doi:10.1371/journal.ppat.1002555
29. Coelho C, Souza AC, Derengowski Lda S, De Leon-Rodriguez C, Wang B, Leon-Rivera R, et al. Macrophage mitochondrial and stress response to ingestion of *Cryptococcus neoformans*. *J Immunol* (2015) 194:2345–57. doi:10.4049/jimmunol.1402350
30. Hirano A, Zimmerman HM, Levine S. Fine structure of cerebral fluid accumulation. V. Transfer of fluid from extracellular compartments in acute phase of cryptococcal polysaccharide lesions. *Arch Neurol* (1964) 11:632–41. doi:10.1001/archneur.1964.00460240064009
31. Hirano A, Zimmerman HM, Levine S. The fine structure of cerebral fluid accumulation. III. Extracellular spread of cryptococcal polysaccharides in the acute stage. *Am J Pathol* (1964) 45:1–19.
32. Hirano A, Zimmerman HM, Levine S. The fine structure of cerebral fluid accumulation. VII. Reactions of astrocytes to cryptococcal polysaccharide implantation. *J Neuropathol Exp Neurol* (1965) 24:386–96. doi:10.1097/00005072-196507000-00002

33. Chen SH, Stins MF, Huang SH, Chen YH, Kwon-Chung KJ, Chang Y, et al. *Cryptococcus neoformans* induces alterations in the cytoskeleton of human brain microvascular endothelial cells. *J Med Microbiol* (2003) 52:961–70. doi:10.1099/jmm.0.05230-0
34. Qin QM, Luo J, Lin X, Pei J, Li L, Ficht TA, et al. Functional analysis of host factors that mediate the intracellular lifestyle of *Cryptococcus neoformans*. *PLoS Pathog* (2011) 7:e1002078. doi:10.1371/journal.ppat.1002078
35. Jong A, Wu CH, Shackleford GM, Kwon-Chung KJ, Chang YC, Chen HM, et al. Involvement of human CD44 during *Cryptococcus neoformans* infection of brain microvascular endothelial cells. *Cell Microbiol* (2008) 10:1313–26. doi:10.1111/j.1462-5822.2008.01128.x
36. Johnston SA, May RC. The human fungal pathogen *Cryptococcus neoformans* escapes macrophages by a phagosome emptying mechanism that is inhibited by Arp2/3 complex-mediated actin polymerisation. *PLoS Pathog* (2010) 6:e1001041. doi:10.1371/journal.ppat.1001041
37. Alvarez M, Casadevall A. Phagosome fusion and extrusion, and host cell survival following *Cryptococcus neoformans* phagocytosis by macrophages. *Curr Biol* (2006) 16:2161–5. doi:10.1016/j.cub.2006.09.061
38. Ma H, Croudace JE, Lammas DA, May RC. Expulsion of live pathogenic yeast by macrophages. *Curr Biol* (2006) 16:2156–60. doi:10.1016/j.cub.2006.09.032
39. Stukes S, Coelho C, Rivera J, Jedlicka AE, Hajjar KA, Casadevall A. The membrane phospholipid binding protein annexin A2 promotes phagocytosis and nonlytic exocytosis of *Cryptococcus neoformans* and impacts survival in fungal infection. *J Immunol* (2016) 197(4):1252–61. doi:10.4049/jimmunol.1501855
40. Alvarez M, Casadevall A. Cell-to-cell spread and massive vacuole formation after *Cryptococcus neoformans* infection of murine macrophages. *BMC Immunol* (2007) 8:16. doi:10.1186/1471-2172-8-16
41. O'Meara TR, Veri AO, Ketela T, Jiang B, Roemer T, Cowen LE. Global analysis of fungal morphology exposes mechanisms of host cell escape. *Nat Commun* (2015) 6:6741. doi:10.1038/ncomms7741
42. Pericolini E, Cenci E, Monari C, De Jesus M, Bistoni F, Casadevall A, et al. *Cryptococcus neoformans* capsular polysaccharide component galactoxylomannan induces apoptosis of human T-cells through activation of caspase-8. *Cell Microbiol* (2006) 8:267–75. doi:10.1111/j.1462-5822.2005.00619.x
43. Monari C, Paganelli F, Bistoni F, Kozel TR, Vecchiarelli A. Capsular polysaccharide induction of apoptosis by intrinsic and extrinsic mechanisms. *Cell Microbiol* (2008) 10:2129–37. doi:10.1111/j.1462-5822.2008.01196.x
44. De JM, Nicola AM, Frases S, Lee IR, Mieses S, Casadevall A. Galactoxylomannan-mediated immunological paralysis results from specific B cell depletion in the context of widespread immune system damage. *J Immunol* (2009) 183:3885–95. doi:10.4049/jimmunol.0900449
45. Rodrigues ML, Nimrichter L, Oliveira DL, Frases S, Miranda K, Zaragoza O, et al. Vesicular polysaccharide export in *Cryptococcus neoformans* is a eukaryotic solution to the problem of fungal trans-cell wall transport. *Eukaryot Cell* (2007) 6:48–59. doi:10.1128/EC.00318-06
46. Rodrigues ML, Nakayasu ES, Oliveira DL, Nimrichter L, Nosanchuk JD, Almeida IC, et al. Extracellular vesicles produced by *Cryptococcus neoformans* contain protein components associated with virulence. *Eukaryot Cell* (2008) 7:58–67. doi:10.1128/EC.00370-07
47. Oliveira DL, Freire-De-Lima CG, Nosanchuk JD, Casadevall A, Rodrigues ML, Nimrichter L. Extracellular vesicles from *Cryptococcus neoformans* modulate macrophage functions. *Infect Immun* (2010) 78:1601–9. doi:10.1128/IAI.01171-09
48. Garcia-Solache MA, Izquierdo-Garcia D, Smith C, Bergman A, Casadevall A. Fungal virulence in a lepidopteran model is an emergent property with deterministic features. *MBio* (2013) 4:e00100–13. doi:10.1128/mBio.00100-13
49. Peres da Silva R, Puccia R, Rodrigues ML, Oliveira DL, Joffe LS, Cesar GV, et al. Extracellular vesicle-mediated export of fungal RNA. *Sci Rep* (2015) 5:7763. doi:10.1038/srep07763
50. Shao X, Mednick A, Alvarez M, Van Rooijen N, Casadevall A, Goldman DL. An innate immune system cell is a major determinant of species-related susceptibility differences to fungal pneumonia. *J Immunol* (2005) 175:3244–51. doi:10.4049/jimmunol.175.5.3244
51. Zaragoza O, Alvarez M, Telzak A, Rivera J, Casadevall A. The relative susceptibility of mouse strains to pulmonary *Cryptococcus neoformans* infection is associated with pleiotropic differences in the immune response. *Infect Immun* (2007) 75:2729–39. doi:10.1128/IAI.00094-07
52. Alanio A, Desnos-Ollivier M, Dromer F. Dynamics of *Cryptococcus neoformans*-macrophage interactions reveal that fungal background influences outcome during cryptococcal meningoencephalitis in humans. *MBio* (2011) 2:e00158–111. doi:10.1128/mBio.00158-11
53. Sabiiti W, Robertson E, Beale MA, Johnston SA, Brouwer AE, Loyse A, et al. Efficient phagocytosis and laccase activity affect the outcome of HIV-associated cryptococcosis. *J Clin Invest* (2014) 124:2000–8. doi:10.1172/JCI72950
54. Yauch LE, Lam JS, Levitz SM. Direct inhibition of T-cell responses by the *Cryptococcus* capsular polysaccharide glucuronoxylomannan. *PLoS Pathog* (2006) 2:e120. doi:10.1371/journal.ppat.0020120
55. Zaragoza O, García-Rodas R, Nosanchuk JD, Cuenca-Estrella M, Rodriguez-Tudela JL, Casadevall A. Fungal cell gigantism during mammalian infection. *PLoS Pathog* (2010) 6:e1000945. doi:10.1371/journal.ppat.1000945
56. Hommel B, Mukaremera L, Cordero RJB, Coelho C, Desjardins CA, Sturny-Leclère A, et al. Titan cells formation in *Cryptococcus neoformans* is finely tuned by environmental conditions and modulated by positive and negative genetic regulators. *PLoS Pathog* (2018) (in press).
57. Vecchiarelli A, Pericolini E, Gabrielli E, Kenno S, Perito S, Cenci E, et al. Elucidating the immunological function of the *Cryptococcus neoformans* capsule. *Future Microbiol* (2013) 8:1107–16. doi:10.2217/fmb.13.84
58. Osterholzer JJ, Surana R, Milam JE, Montano GT, Chen GH, Sonstein J, et al. Cryptococcal urease promotes the accumulation of immature dendritic cells and a non-protective T2 immune response within the lung. *Am J Pathol* (2009) 174:932–43. doi:10.2353/ajpath.2009.080673
59. Ellerbroek PM, Walenkamp AME, Hoepelman AIM, Coenjaerts FEJ. Effects of the capsular polysaccharides of Cryptococcus neoformans on phagocyte migration and inflammatory mediators. *Curr Med Chem* (2004) 11(2):253–66.
60. Dong ZM, Murphy JW. Cryptococcal polysaccharides induce L-selectin shedding and tumor necrosis factor receptor loss from the surface of human neutrophils. *J Clin Invest* (1996) 97:689–98. doi:10.1172/JCI118466
61. Casadevall A, Perfect JR. *Cryptococcus Neoformans*. Washington, DC: ASM Press (1998).
62. Lortholary O, Fontanet A, Memain N, Martin A, Sitbon K, Dromer F, et al. Incidence and risk factors of immune reconstitution inflammatory syndrome complicating HIV-associated cryptococcosis in France. *AIDS* (2005) 19:1043–9. doi:10.1097/01.aids.0000174450.70874.30
63. Beatty GW. Immune reconstitution inflammatory syndrome. *Emerg Med Clin North Am* (2010) 28:393–407. doi:10.1016/j.emc.2010.01.004
64. Goldman DL, Davis J, Bommartio F, Shao X, Casadevall A. Enhanced allergic inflammation and airway responsiveness in rats with chronic *Cryptococcus neoformans* infection suggests a potential role for fungal pulmonary infection in the pathogenesis of asthma. *J Infect Dis* (2006) 193:1178–86. doi:10.1086/501363
65. Goldman DL, Vicencio AG. The chitin connection. *MBio* (2012) 3:e00056–12. doi:10.1128/mBio.00056-12
66. Grahnert A, Muller U, Von Buttlar H, Treudler R, Alber G. Analysis of asthma patients for cryptococcal seroreactivity in an urban German area. *Med Mycol* (2015) 53:576–86. doi:10.1093/mmy/myv024
67. Charlier C, Nielsen K, Daou S, Brigitte M, Chretien F, Dromer F. Evidence of a role for monocytes in dissemination and brain invasion by *Cryptococcus neoformans*. *Infect Immun* (2009) 77:120–7. doi:10.1128/IAI.01065-08
68. Sorrell TC, Juillard PG, Djordjevic JT, Kaufman-Francis K, Dietmann A, Milonig A, et al. Cryptococcal transmigration across a model brain blood-barrier: evidence of the Trojan horse mechanism and differences between *Cryptococcus neoformans* var. grubii strain H99 and *Cryptococcus gattii* strain R265. *Microbes Infect* (2016) 18:57–67. doi:10.1016/j.micinf.2015.08.017
69. Santiago-Tirado FH, Onken MD, Cooper JA, Klein RS, Doering TL. Trojan horse transit contributes to blood-brain barrier crossing of a eukaryotic pathogen. *MBio* (2017) 8:e2183–2116. doi:10.1128/mBio.02183-16
70. Chang YC, Stins MF, Mccaffery MJ, Miller GF, Pare DR, Dam T, et al. Cryptococcal yeast cells invade the central nervous system via transcellular penetration of the blood-brain barrier. *Infect Immun* (2004) 72:4985–95. doi:10.1128/IAI.72.11.6753.2004
71. Liu TB, Kim JC, Wang Y, Toffaletti DL, Eugenin E, Perfect JR, et al. Brain inositol is a novel stimulator for promoting *Cryptococcus* penetration of the blood-brain barrier. *PLoS Pathog* (2013) 9:e1003247. doi:10.1371/journal.ppat.1003247

72. Vieira MA, Costa CH, Ribeiro JC, Nunes-Filho LP, Rabelo MG, Almeida-Neto WS. Soap bubble appearance in brain magnetic resonance imaging: cryptococcal meningoencephalitis. *Rev Soc Bras Med Trop* (2013) 46:658–9. doi:10.1590/0037-8682-0142-2013
73. Lee SC, Kress Y, Zhao M-L, Dickson DW, Casadevall A. *Cryptococcus neoformans* survive and replicate in spacious phagosomes in human microglia. *Lab Invest* (1995) 73:871–9.
74. Casadevall A, Pirofski L. The damage-response framework of microbial pathogenesis. *Nat Microbiol Rev* (2003) 1:17–24. doi:10.1038/nrmicro732
75. Panackal AA, Williamson KC, Van De Beek D, Boulware DR, Williamson PR. Fighting the monster: applying the host damage framework to human central nervous system infections. *MBio* (2016) 7:e1906–15. doi:10.1128/mBio.01906-15
76. Steenbergen JN, Shuman HA, Casadevall A. *Cryptococcus neoformans* interactions with amoebae suggest an explanation for its virulence and intracellular pathogenic strategy in macrophages. *Proc Natl Acad Sci U S A* (2001) 18:15245–50. doi:10.1073/pnas.261418798
77. Casadevall A. Amoeba provide insight into the origin of virulence in pathogenic fungi. *Adv Exp Med Biol* (2012) 710:1–10. doi:10.1007/978-1-4419-5638-5_1
78. Fu MS, Casadevall A. Divalent metal cations potentiate the predatory capacity of amoeba for *Cryptococcus neoformans*. *Appl Environ Microbiol* (2017) 84(3):e01717. doi:10.1128/AEM.01717-17

Conflict of Interest Statement: The authors declare that the research was conducted in the absence of any commercial or financial relationships that could be construed as a potential conflict of interest.

Copyright © 2018 Casadevall, Coelho and Alanio. This is an open-access article distributed under the terms of the Creative Commons Attribution License (CC BY). The use, distribution or reproduction in other forums is permitted, provided the original author(s) and the copyright owner are credited and that the original publication in this journal is cited, in accordance with accepted academic practice. No use, distribution or reproduction is permitted which does not comply with these terms.

frontiers in Immunology

MINI REVIEW
published: 04 April 2018
doi: 10.3389/fimmu.2018.00651

Immunology of Cryptococcal Infections: Developing a Rational Approach to Patient Therapy

*Waleed Elsegeiny[1], Kieren A. Marr[2] and Peter R. Williamson[1]**

[1] Laboratory of Clinical Immunology and Microbiology (LCIM), National Institute of Allergy and Infectious Diseases (NIAID), National Institutes of Health (NIH), Bethesda, MD, United States, [2] Johns Hopkins University, Baltimore, MD, United States

Cryptococcal meningoencephalitis is responsible for upwards of 15% of HIV-related deaths worldwide and is currently the most common cause of non-viral meningitis in the US, affecting both previously healthy and people with immune suppression caused by cancer chemotherapy, transplantation, and biologic therapies. Despite a continued 30–50% attributable mortality, recommended therapeutic strategies have remained largely unchanged since the 1950s. Recent murine models and human studies examining the role of the immune system in both susceptibility to the infection as well as host damage have begun to influence patient care decisions. The Damage Framework Response, originally proposed in 1999, was recently used to discuss dichotomous etiologies of host damage in cryptococcal disease. These include patients suffering microbiological damage with low host immunity (especially those immunosuppressed with HIV) and those having low (live) microbiological burden but high immune-mediated damage (HIV-related immune reconstitution syndrome and non-HIV-related postinfectious inflammatory response syndrome). Cryptococcal disease in previously healthy hosts, albeit rare, has been known for a long time. Immunophenotyping and dendritic cell-T cell signaling studies on cerebral spinal fluid of these rare patients reveal immune capacity for recognition and T-cell activation pathways including increased levels of HLA-DR and CD56. However, despite effective T-cell signals, brain biopsy and autopsy specimens demonstrated an M2 alternative macrophage polarization and poor phagocytosis of fungal cells. These studies expand the paradigm for cryptococcal disease susceptibility to include a prominent role for immune-mediated damage and suggest a need for careful individual consideration of immune activation during therapy of cryptococcal disease in diverse hosts.

Keywords: ***Cryptococcus*, cryptococcal, meningoencephalitis, meningitis, neurology, infection, fungus**

OPEN ACCESS

Edited by:
Steven Templeton, Indiana University School of Medicine – Terre Haute, United States

Reviewed by:
Liise-anne Pirofski, Albert Einstein College of Medicine, United States
Simon Andrew Johnston, University of Sheffield, United Kingdom
Floyd Layton Wormley, University of Texas at San Antonio, United States

****Correspondence:***
Peter R. Williamson
williamsonpr@mail.nih.gov

Specialty section:
This article was submitted to Microbial Immunology, a section of the journal Frontiers in Immunology

Received: *04 January 2018*
Accepted: *16 March 2018*
Published: *04 April 2018*

Citation:
Elsegeiny W, Marr KA and Williamson PR (2018) Immunology of Cryptococcal Infections: Developing a Rational Approach to Patient Therapy. Front. Immunol. 9:651. doi: 10.3389/fimmu.2018.00651

INTRODUCTION

Cryptococcus is an opportunistic fungus, which most frequently presents as a pulmonary infection or meningoencephalitis. Cryptococcosis has a high impact on immunocompromised populations such as patients with HIV-AIDS and a wide array of non-HIV patients including those with hematopoietic malignancies, autoimmune diseases, or genetic immunodeficiency syndromes, as well as patients receiving immunosuppressive cancer-therapies, undergoing transplant conditioning, in combination with age-related immunosenescence (1–5). HIV-related cryptococcal meningitis (CM) is one

the most common causes of adult meningitis with an estimated 223,100 cases and 181,100 deaths in 2014, globally (6, 7). In countries with access to optimal medical care, non-HIV CM accounts for at least 25% of all CM-related hospitalization and deaths and is currently the leading cause of non-viral meningitis in the U.S. (2, 8–10). Interestingly, there are rare reports that as much as 30% of non-HIV patients with cryptococcal infection were previously healthy with no known underlying condition (11).

Cryptococcus is a basidiomycete yeast with over 30 known species; however, the majority of human infections are caused by either *Cryptococcus neoformans* and *Cryptococcus gattii*. *C. neoformans* is the main source of infections in CM patients with CD4+ T-cell deficiency while *C. gattii* is a predominant species in the previously healthy (12, 13). *C. neoformans* and *C. gattii* both can both be found in the vicinity of a variety of trees, and *C. neoformans* can also be found in soils and bird feces (14). Although the life-cycle of *Cryptococcus* is not dependent on an animal host, *C. neoformans* has the potential to infect a wide range of warm- and cold-blooded species (15). Cryptococci are considered sapronotic due to their ability to cause an opportunistic infection without coevolution of a host–parasite virulence (16) although molecular optimization of virulence has been noted in environmental strains after mammalian residence (17). Key to infecting such a wide-ranging host population is its adaptation to environmental conditions and defenses against innate plant defenses as well as phagocytic predators such as parasites and insects (18–21).

CRYPTOCOCCAL INFECTION

Cryptococcal infection is believed to be transmitted by inhalation of infective particles such as yeast cells and/or spores from an environmental source. It is believed that humans encounter the organism early in life, evident by the gradual increase of cryptococcal-specific antibodies in humans with age (22) and isolation of infective strain types from the country of origin in immigrant patients later presenting with HIV/AIDS-related CM (23). As most immunocompetent humans are asymptomatic and resolve the infection, there are limited observations as to the mechanism in which infection is cleared. *Cryptococcus* spp. has a unique repertoire of immune reactivity from other fungi because of distinguishing attributes such as a large polysaccharide capsule that limits exposure to immune dominant carbohydrate epitopes (20), immunomodulatory enzymes such as a phenol oxidizing and cytokine-inducing laccase (24), and a robust tolerance to low nutrient conditions such as within brain tissues (25, 26).

INNATE RECOGNITION

Although no single pattern recognition receptor (PRR) has been shown to be required for binding of *Cryptococcus*, it is hypothesized that alveolar macrophages recognize *Cryptococcus* and initialize the immune response through multiple receptors such as Dectin-1, Mincle, mannose receptor, CD14, and toll-like receptors (TLRs) (**Figure 1**.1) (27–30). The role of AMs and phagocytosis is believed to be critical during early infection, as observed *in vivo* imaging studies and animal models demonstrating enhanced susceptibility after AM depletion (31, 32). The complexity of how PRRs impact the immune response to cryptococcal infection is still being studied as there may be redundancy among them. For example, TLRs 2, 4, and 9 individually appear to play only a minor role, although the use of agonists *in vitro* enhances the proinflammatory responses by microglial cells to *Cryptococcus* (33). NOD-like receptor family pyrin domain containing 3 (NLRP3) is another cryptococcal recognizing PRR and has been shown in mice to be involved with leukocyte infiltration in the lung during infection (34). Interestingly, *in vitro*, NLRP3 activation appears to be inhibited by capsulated cryptococcal cells further suggesting that PRRs may have a more important role during early infection (35). Some PRRs have been linked to specific immune responses such as scavenger receptors B1 and SR-B3, which appear to be important for the induction of IL-1β (36). Macrophage receptor with collagenous structure (MARCO) is also a scavenger receptor which plays a role in cellular recruitment to the lung, cytokine production, and pathogen uptake by mononuclear phagocytes during early stages of cryptococcal infection (37). However, during the adaptive phase of infection, mice deficient in MARCO have improved fungal clearance which is marker by a type-I skewed immune response. Although MARCO plays an important role initially during infection, it is believed that *Cryptococcus* is capable of exploiting MARCO to polarize toward a non-protective immune response (38). There are other recognition receptors such as scavenger receptor A (SR-A) that are also associated with poorer response to *Cryptococcus*. SR-A-deficient mice show enhanced fungal clearance, which was correlated with decreased production of IL-4 and IL-13 (39). This may be linked to the unique cell wall composition of *C. neoformans* compared to other fungi, which contains high levels of acetylated chitin and deacetylated chitosan polymers (40). Furthermore, the binding of PRRs will become hindered as the infectious propagule starts forming the polysaccharide capsule, thus, it is believed that the successful phagocytosis of *Cryptococcus* also requires antibody- or complement-type opsonins (41, 42).

INITIATION OF THE IMMUNE RESPONSE

Although recognition and phagocytosis are important in induction of the immune response to *Cryptococcus*, the processes and pathways involved in breaking down and clearing pathogens and their antigens are also critical steps to mounting an optimal immune response. One clinical study observed that *in vitro* macrophage phagocytosis was directly correlated with clinical outcome (43). This suggests that other factors including phagocyte polarization and lysosomal activity may also need to be regulated for successful clearance.

Unlike other intracellular pathogens such as *Mycobacterium tuberculosis*, cryptococci do not interfere with phagosome formation or maturation; however, they are capable of surviving within vesicles or escaping by phagosome permeabilization or vesicular release (44–47). *C. neoformans* is thus capable of using macrophages as a host for immune evasion, and can escape through expulsion, lysis, or rupture due to excessive intracellular proliferation (47, 48). Alveolar macrophages are required; however, to recruit monocytes and dendritic cells (DCs) primarily through

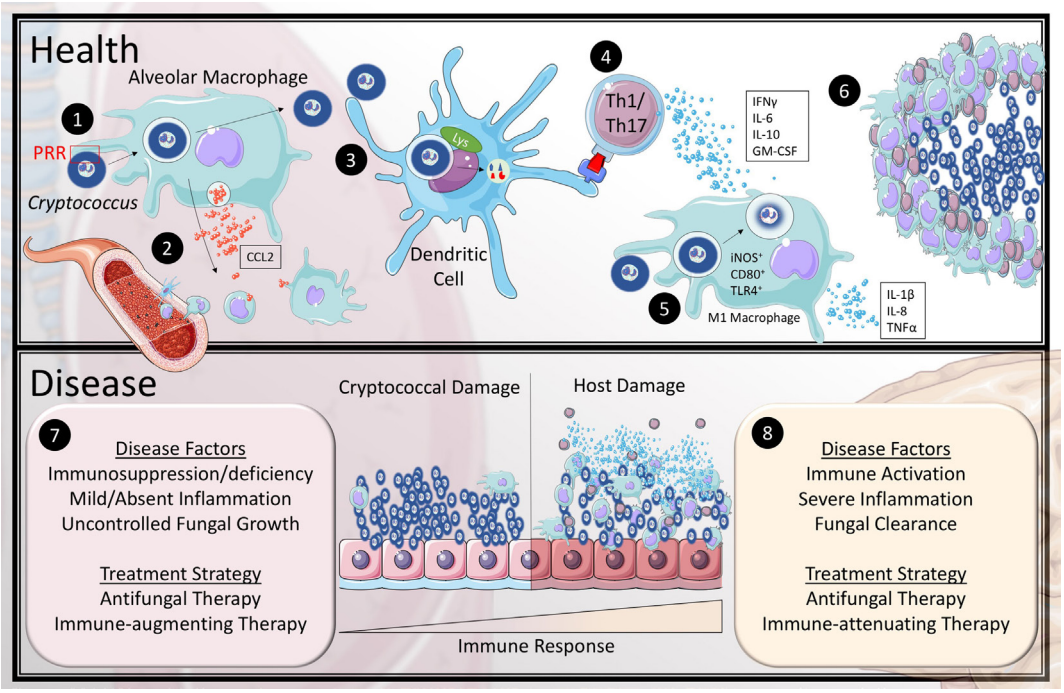

FIGURE 1 | Current model of the immune response to *Cryptococcus* in health and disease. In health (1) inhaled cryptococcal spores are recognized by alveolar macrophages through pattern recognition receptors (PRR). (2) This stimulates the macrophages to release CCL2 to recruit monocytes and dendritic cells (DCs) to the lung. (3) Recruited DCs are capable of breaking down cryptococcal lifeforms and present antigen to CD4+ T-cells. (4) Activated T helper 1 and Th17 T-cells secrete IFNγ, IL-6, IL-10, and granulocyte-macrophage colony stimulating factor (GM-CSF) to recruit and differentiate classical (M1) macrophages. (5) The exact mechanism of fungicidal activity by M1 macrophages against *Cryptococcus* is still unclear in humans; however, they are known to upregulate iNOS, CD80, and TLR4 as well as produce IL-1β, IL-8, and TNFα. (6) The cytokine and chemokine mileu organize the leukocytes to encapsulate and eliminate cryptococcal organisms within granulomas. The most common association with cryptococcal disease (7) is the absence or dysfunction of at least one aspect of the healthy immune response, which leads to uncontrolled fungal growth. (8) However, some patients develop a skewed hyper-immune response to the pathogen that causes inflammatory damage to the host tissue even with fungal clearance.

the production of macrophage chemotactic protein 1 (MCP1). In rats, MCP1 (also known as CCL2) and its receptor, CCR2, are essential for the recruitment of DCs, formation of granulomas, antigen presentation, and T-cell responses (**Figure 1**.2) (49, 50). Granulomas are a sign for control of infections and are composed of macrophages and giant multinucleated cells that contain cryptococcal cells, as well as CD4+ T-cells. These granulomas encompass the fungi and often resolve without additional medical assistance, but treatment with antifungal therapy or surgical removal of the lesions may expedite recovery. It has also been suggested that cryptococci may also be able to latently persist within granulomas and macrophages without degradation (51, 52). In patients with HIV-related pulmonary cryptococcosis, multinucleated giant cells are still present; however, the cryptococci are mainly extracellular and propagate within alveolar spaces (53). DCs are considered the primary antigen-presenting cell (APC) in the context of cryptococcal infection and have an advantage over macrophages in stimulating T-cell proliferation (54). Recruited DCs phagocytose cryptococcal bodies, which then are passaged through lysosomes to be degraded by both oxidative and non-oxidative mechanisms (**Figure 1**.3) (54, 55). For example, cathepsin-B has a non-enzymatic role to fracture the cell wall through osmotic lysis. Degraded components are then loaded onto major histocompatibility complex class II to initiate the adaptive immune response through CD4+ T-cell stimulation (**Figure 1**.4) (56). Eosinophils from a rat model of cryptococcosis have also been demonstrated to have the ability to phagocytose cryptococci and prime of CD4+ and CD8+ T-cells, *in vitro* (57) although their role in human infections is less clear. Their ability to function as APCs is associated with a decrease in nitric oxide and hydrogen peroxide production, followed by migration to the lymphatic system (58). However, their involvement in priming the adaptive immune response is associated with increased fungal burden and lung pathology by skewing immunity toward a type-II response (59, 60).

THE ADAPTIVE IMMUNE RESPONSE

Involvement of the adaptive immune compartment is critical for control of a cryptococcal infection; however, it may also have a detrimental affect depending on the type of response. In draining lymphoid tissues, APCs carrying cryptococcal antigens stimulate several types of lymphocytes including CD4+ T cells, CD8+ T cells, and natural killer T cells. Once activated, CD4+ T-cells can further differentiate into unique effector subsets with distinctive cytokine profiles including: T helper 1 (Th1), Th2, and

Th17 cells. Cxcr5+ T follicular helper cells are also induced and primarily function to stimulate B cell maturation and antibody production, as well as activate inflammatory macrophages (61, 62). Th1 and Th17 cells are recognized by their production of IFNγ and IL-17, respectively, and both help mediate the resolution of cryptococcal infection. On the other hand, Th2 cells, which are described as producers of IL-4, IL-5, and IL-13, are associated with more of a detrimental outcome such as increases in inflammation, worsened pathology, and increased risk of dissemination. In both humans and experimental murine models, deficiencies in type-II responses is linked with enhanced control of fungal burden and diminished eosinophilia, inflammation, airway damage, and dissemination (63, 64).

Interestingly, patients with HIV infection will gradually shift from a type-I to a type-II immune response profile, thus developing an increased vulnerability to cryptococcal infection (65). Profiling studies performed by Jarvis et al. on the cytokines and chemokines produced by stimulated peripheral blood mononuclear cells (PBMCs)-derived CD4+ T-cell as well as within cerebral spinal fluid (CSF) of patients with HIV-related CM have provided some immunological associations with survival (66, 67). Increased levels of IL-6, IL-8, IL-10, IL-17, IFN-γ, tumor necrosis factor (TNF), and CCL5 within the CSF correlated with high white cell counts, macrophage activation, reduced cryptococcal burden, and survival. A high proportion of IFN-γ and TNF double producing PBMC-derived CD4+ T-cells was also associated with survival (68). This study corroborates the critical importance of maintaining a Th1/Th17 profile in both cryptococcal pulmonary infection and meningoencephalitis. Most CM studies have been performed in the context of HIV patients and *C. neoformans*; however, little is known about the immune profile in patients with non-HIV CM, particularly those with *C. gattii* infection.

HUMORAL IMMUNITY TO *Cryptococcus*

As previously mentioned, serum antibodies to *Cryptococcus* can be detected in early life. However, immunocompromised patients at risk for cryptococcal infection appear to have a defect in antibody responses, such as loss of glucuronoxylomannan (GXM), a capsular component reactive B-cells, as well as overall lower levels of peripheral blood memory IgM B cells (69, 70). Lower serum GXM-IgM antibody levels in both HIV+ as well as HIV− solid organ transplant patients is also associated with increased risk for development of cryptococcosis (71–73). Antibody-mediated phagocytosis may be important as the increase in capsular size has been shown to reduce complement-mediated phagocytosis (74). Furthermore, murine studies have demonstrated that the murine equivalent of IgM memory B cells, B-1 cells, can dampen fungal growth *in vitro* and *in vivo*, by inducing an earlier T-cell response, reducing dissemination, and enhancing macrophage phagocytosis (75–78). Additionally, adoptive transfer of IgM-sufficient wild-type mouse serum into $Rag1^{-/-}$ mice demonstrated enhanced alveolar macrophage phagocytosis and a reduction in early dissemination compared to mice treated with IgM-deficient serum. The use of vaccines or antibody therapy to boost antifungal titers may thus provide protection against the development of cryptococcal disease (79–81).

CRYPTOCOCCAL ELIMINATION

The primary mechanism for pulmonary clearance is the formation and resolution of granulomas by macrophages. However, as previously mentioned, *Cryptococcus* is capable of surviving within resident alveolar macrophages, thus the macrophages required for clearance must be recruited and activated by CD4+ T-cell signals. Macrophages stimulated under Th1/Th17 or Th2 cytokine profiles become skewed toward either classical or alternative activation, respectively. Classically activated (M1) macrophages are primarily induced by IFNγ and lipopolysaccharide, while type-2 cytokines including IL-4 and IL-13 induce alternatively activated (M2) macrophages and function through production of proline and polyamines (82). M1 and M2 macrophages *in vitro* have demonstrated different outcomes during intracellular parasitism by *C. neoformans* with type-1/type-17 conditions having enhanced fungicidal activity (**Figure 1**.5) (83). Furthermore, STAT1-deficient mice, which are deficient in M1 macrophages due to an inability to generate a strong Th1 profile, have a defect in anti-cryptococcal activity, which correlated with a decrease in NO production (84). In the previously mentioned cohort of non-HIV patients with CM, although there were intact Th1 signaling found in the CSF, autopsy results revealed an overrepresentation of M2 macrophages within central nervous system (CNS) tissues (85). Similarly, patients with granulocyte-macrophage colony stimulating factor (GM-CSF) autoantibodies are also at risk for CM and have an abundance of Th1 CD4+ T-cells, but also have a skewed M2 macrophage phenotype (86, 87). Activated M1 macrophages, with CD4+ T-cells, resolve the infection by entrapping and degrading the cryptococcal propagules through the formation of granulomas (**Figure 1**.6).

BRAIN DISSEMINATION

Uncontrolled cryptococcal infection will inevitably disseminate into the (CNS) leading to a life-threatening CM. There are currently three known methods of cryptococcal dissemination from the lung: (1) the disruption of blood vesicle integrity allowing passive transport into the blood stream, (2) intact endothelial cells may phagocytose the spores from the lung and expulse them into the blood stream, (3) macrophages may act as a Trojan Horse by transporting phagocytosed spores to the brain, and regurgitating the spores in a process known as vomocytosis. Both microbial and host factors have been identified to be involved in CNS invasion, including cryptococcal matrix metalloprotease, production of a urease enzyme (88), and increases in host brain inositol levels (89, 90).

NON-HIV FACTORS OF SUSCEPTIBILITY

Over 1,000 cases of CM are reported to occur in previously healthy people in the U.S. annually. Studying this population reveals unique vulnerability risks, including previously undiagnosed, rare immune-associated monogenic disorders or

autoimmune diseases. Patients with autoantibodies to (GM-CSF) and interferon-gamma (IFNγ) were recently demonstrated to be susceptible to CM, emphasizing the T-cell/monocyte signaling pathway that is required for a successful immune response (86, 87, 91). Interestingly, poor macrophage function was also demonstrated in a cohort of clinically refractory patients by a lack of iNOS expression and intact M2-related CD200R1 expression using immunohistochemistry of infected brain tissue (85). Further studies also demonstrated defective CSF activated macrophage TNF-α secretion, which may explain a lack of symptomatology and diagnostic delays in non-HIV related CM.

Historically, the most common syndrome associated with risk for CM is an idiopathic CD4 lymphopenia (ICL) that presents as a non-HIV-associated reduction or loss of CD4+ T-cells. The tremendous impact of CM on AIDS patients makes the importance of CD4 T-cells self-evident. However, ICL is a very heterogeneous disorder that has been implicated as a serious risk factor (92, 93) but many patients with ICL remain healthy. Recently, the concept of a "two hit" hypothesis was advanced by the finding of two ICL patients with CM who had additional autoantibodies to GMCSF or an otherwise benign, but functionally significant mutation in the IKBKG/NEMO gene, with reductions in NFKB T-cell signaling (94). Similarly, patients with monocytopenia, such as patients with a GATA2 deficiency, also have increased risk of developing CM (95–97). Monogenic disorders such as X-linked CD40L deficiency, chronic granulomatous disease, and Job syndrome are also associated with susceptibility to CM (98–100). T-cell suppressing biological therapy such as natalizumab or fingolimod is also a risk factor (101, 102).

CRYPTOCOCCAL DISEASE: A REFLECTION OF HOST AND MICROBIOLOGICAL FACTORS

Recently, there has been a greater appreciation that host damage can occur from either the toxic products of an overwhelming microbial infection or a pathological inflammatory response to the invading pathogen (**Figure 1**.7 and **Figure 1**.8), recently termed the damage-framework response (103). Cryptococcal disease is a classic example of this phenomenon, often occurring within the same patient during different stages of treatment (104, 105). For example, in the setting of HIV infection, clinical outcomes of primary therapy are related to clearance of the fungus (106, 107). However, a paradoxical immune reconstitution syndrome can also be seen in these same patients whereby, in the setting of microbiological control, reconstitution of the immune system after initiation of antiretroviral therapy (ART) results in a pathological central nervous system inflammatory response (7, 108–110). HIV-related CM further exemplifies differences in disease at these polar extremes of immune response—a recent study of 90 HIV patients with cryptococcal disease found that high levels of Th1-related cytokines INF-gamma and IL-6 were predictive of 2-week initial survival when pathogen load was high; whereas, the development of symptomatic cIRIS was associated with elevated activation with increased macrophage-related cytokines such as CCL2/MCP-1, CCL3/MIP1a, and GM-CSF (67).

Similar to HIV-related disease, in the initial stages of therapy of non-HIV patients, failure to achieve negative CSF fungal cultures at 2 weeks is associated with clinical failure (107). However, many more such patients develop refractory symptoms and/or clinical deterioration despite microbiological control, recently described in previously healthy patients as a postinfectious inflammatory response syndrome. Similar to that encountered with cIRIS in HIV, these patients have an activated CD4+ T-cell intrathecal compartment with minimal Th2 presence (85). Additionally, these patients have high levels of CD4+ T-cells in the CSF and within the intracranial Virchow–Robin channels, which displayed an activated phenotype, as measured by HLA-DR4 and CD56 positivity. Elevated Th1 CSF soluble cytokines such as INF-gamma and interferon-related CXCL10 confirmed the activated T-cell phenotype. In addition, a strong relationship between the T-cell activation marker, sCD27, and elevations of the axonal damage marker, neurofilament light chain protein, suggest that such inflammation is not a benign event, but pathological (85, 111). These observations were surprising as these conditions typically define a successful immune response, as understood from susceptibility studies in HIV-related disease. However, as described above, many of the previously healthy have defects in macrophage polarization, allowing disease susceptibility in the face of unrestrained T-cell-mediated host damage. Such findings also highlight the limitations of applying disease principles from one host to another without careful consideration.

TREATMENT: TOWARD A MORE RATIONAL APPROACH TO ADJUNCTIVE THERAPY

Treatment strategies for patients with CM should be developed to address damage caused by both the microbe and the pathological immune response; the disease framework is a useful guide (**Figure 1**.7 and **Figure 1**.8) (104). In the initial therapy of all patients, treatment with antifungals with a fungicidal agent such as amphotericin B is paramount and is typically continued with oral azole therapy to prevent relapse after initial negative CSF cultures (112–114). Those with low immunity (HIV prior to ART or patients with a skewed Th2 response to *Cryptococcus*), may benefit from potential immune adjuvants such as IFNγ to accelerate microbiological control (115). In these cases, rates of clearance of CSF fungal cultures (early fungicidal activity) may be an important parameter (67, 106, 107). However, in HIV patients who have developed cryptococcal immune reconstitution inflammatory syndrome (cIRIS) or in refractory non-HIV patients after microbiological control, attention needs to be drawn to the host damage side of the disease model—to minimize pathological effects of a dysregulated host response. In this setting, application of immune enhancers such as IFNγ therapy (116) may lead to exacerbated inflammation and potentially cause irreparable neurological damage (85). In these patients, use of adjunctive immunosuppression including corticosteroids is increasingly reported to suppress pathological inflammatory responses and control cerebral

edema, improving clinical response (85, 115–120). In the previously healthy CM patient, for example, successful application of adjunctive corticosteroids in refractory disease or after clinical deterioration requires a personalized strategy. When resources are available, CSF culture negativity and measures of CSF inflammation such as sCD27, CSF glucose, or choroid plexitis or ependymitis by MRI imaging can provide specific biomarkers of the relative contributions of microbe and host toward understanding an individual patient's condition (85, 120, 121). Biomarkers may also be useful guides during corticosteroid tapers to prevent exacerbations.

However, applying this type of therapy successfully requires careful attention to concurrent microbial control, as corticosteroids suppress innate and acquired immune responses needed to maintain fungal clearance (122, 123). Indeed, corticosteroids can have a deleterious effect when applied without pre-established microbial control during primary therapy of HIV-related CM (**Figure 1**.7) (124). The complex heterogeneity of clinical pathologies that occur in various patients during HIV-related CM requires a thoughtful approach that considers the evolving damage caused by both the fungus and the immune response within defined sub-groups. In resource-limited regions, more studies are needed to understand the damage-response framework as it relates to CM in poorly controlled HIV infection, and to identify markers that can tailor resource appropriate therapies. Strategies to prevent CM in HIV (125) and to diagnose or empirically treat co-infections (126) may have tremendous impact on outcomes given the high prevalence of disease in some geographic regions (8). Risks for co-infections, such as tuberculosis and bacterial infections can be exacerbated without specific therapy in the presence of corticosteroids (127).

Other populations with risks for CM such as solid organ transplant recipients also require tailored approaches to prevention and treatment. In populations other than HIV, the feasibility of prevention strategies is limited due to a lower prevalence of disease. Much more attention is needed to better define appropriate therapeutic strategies. Since diagnosis typically occurs late, fungal burden can be high at diagnosis; at the same time, relatively intact and variable inflammatory responses can lead to exuberant inflammatory neurological damage similar to cIRIS (128). In these patients, attention needs to be focused on personalizing therapies according to which side of the host damage framework is most responsible for neurological pathology (128, 129).

AUTHOR CONTRIBUTIONS

The bulk of this manuscript was written by WE under the guidance of PW. PW and KM provided revisional comments and suggestions on both content and organization of this manuscript.

ACKNOWLEDGMENTS

The introduction diagram was designed using Servier Medical Art. Link to Creative Commons License: https://creativecommons.org/licenses/by/3.0/legalcode.

FUNDING

This research was supported by NIH/NIAID extramual grants AI109657 as well as funding from the NIAID intramural program, AI001123, and AI001124.

REFERENCES

1. Sloan DJ, Parris V. Cryptococcal meningitis: epidemiology and therapeutic options. *Clin Epidemiol* (2014) 6:169–82. doi:10.2147/CLEP.S38850
2. Pyrgos V, Seitz AE, Steiner CA, Prevots DR, Williamson PR. Epidemiology of cryptococcal meningitis in the US: 1997-2009. *PLoS One* (2013) 8(2):e56269. doi:10.1371/journal.pone.0056269
3. Durski KN, Kuntz KM, Yasukawa K, Virnig BA, Meya DB, Boulware DR. Cost-effective diagnostic checklists for meningitis in resource-limited settings. *J Acquir Immune Defic Syndr* (2013) 63(3):e101–8. doi:10.1097/QAI.0b013e31828e1e56
4. Rajasingham R, Rhein J, Klammer K, Musubire A, Nabeta H, Akampurira A, et al. Epidemiology of meningitis in an HIV-infected Ugandan cohort. *Am J Trop Med Hyg* (2015) 92(2):274–9. doi:10.4269/ajtmh.14-0452
5. Jarvis JN, Meintjes G, Williams A, Brown Y, Crede T, Harrison TS. Adult meningitis in a setting of high HIV and TB prevalence: findings from 4961 suspected cases. *BMC Infect Dis* (2010) 10:67. doi:10.1186/1471-2334-10-67
6. Park BJ, Wannemuehler KA, Marston BJ, Govender N, Pappas PG, Chiller TM. Estimation of the current global burden of cryptococcal meningitis among persons living with HIV/AIDS. *AIDS* (2009) 23(4):525–30. doi:10.1097/QAD.0b013e328322ffac
7. Williamson PR, Jarvis JN, Panackal AA, Fisher MC, Molloy SF, Loyse A, et al. Cryptococcal meningitis: epidemiology, immunology, diagnosis and therapy. *Nat Rev Neurol* (2017) 13(1):13–24. doi:10.1038/nrneurol.2016.167
8. Rajasingham R, Smith R, Park B, Jarvis J, Govender NP, Chiller T, et al. Global Burden of Disease of HIV-associated cryptococcal meningitis: an updated analysis. *Lancet Infect Dis* (2017) 17(8):873–81. doi:10.1016/S1473-3099(17)30243-8
9. Pappas PG, Perfect JR, Cloud GA, Larsen RA, Pankey GA, Lancaster DJ, et al. Cryptococcosis in human immunodeficiency virus-negative patients in the era of effective azole therapy. *Clin Infect Dis* (2001) 33(5):690–9. doi:10.1086/322597
10. Brizendine KD, Baddley JW, Pappas PG. Predictors of mortality and differences in clinical features among patients with cryptococcosis according to immune status. *PLoS One* (2013) 8(3):e60431. doi:10.1371/journal.pone.0060431
11. Zhu LP, Wu JQ, Xu B, Ou XT, Zhang QQ, Weng XH. Cryptococcal meningitis in non-HIV-infected patients in a Chinese tertiary care hospital, 1997-2007. *Med Mycol* (2010) 48(4):570–9. doi:10.3109/13693780903437876
12. Farrer RA, Desjardins CA, Sakthikumar S, Gujja S, Saif S, Zeng Q, et al. Genome evolution and innovation across the four major lineages of *Cryptococcus gattii*. *MBio* (2015) 6(5):e868–815. doi:10.1128/mBio.00868-15
13. Hagen F, Khayhan K, Theelen B, Kolecka A, Polacheck I, Sionov E, et al. Recognition of seven species in the *Cryptococcus gattii/Cryptococcus neoformans* species complex. *Fungal Genet Biol* (2015) 78:16–48. doi:10.1016/j.fgb.2015.02.009
14. Reimão JQ, Drummond ED, Terceti Mde S, Lyon JP, Franco MC, de Siqueira AM. Isolation of *Cryptococcus neoformans* from hollows of living trees in the city of Alfenas, MG, Brazil. *Mycoses* (2007) 50(4):261–4. doi:10.1111/j.1439-0507.2007.01374.x
15. Casadevall A, Steenbergen JN, Nosanchuk JD. 'Ready made' virulence and 'dual use' virulence factors in pathogenic environmental fungi – the *Cryptococcus neoformans* paradigm. *Curr Opin Microbiol* (2003) 6(4):332–7. doi:10.1016/S1369-5274(03)00082-1
16. Kuris AM, Lafferty KD, Sokolow SH. Sapronosis: a distinctive type of infectious agent. *Trends Parasitol* (2014) 30(8):386–93. doi:10.1016/j.pt.2014.06.006
17. Hu G, Chen SH, Qiu J, Bennett JE, Myers TG, Williamson PR. Microevolution during serial mouse passage demonstrates FRE3 as a virulence adaptation gene in *Cryptococcus neoformans*. *MBio* (2014) 5(2):e941–914. doi:10.1128/mBio.00941-14

18. Warpeha KM, Park YD, Williamson PR. Susceptibility of intact germinating *Arabidopsis thaliana* to human fungal pathogens *Cryptococcus neoformans and C. gattii*. *Appl Environ Microbiol* (2013) 79(9):2979–88. doi:10.1128/AEM.03697-12
19. McDonald T, Wiesner DL, Nielsen K. Cryptococcus. *Curr Biol* (2012) 22(14):R554–5. doi:10.1016/j.cub.2012.05.040
20. Zaragoza O, Rodrigues ML, De Jesus M, Frases S, Dadachova E, Casadevall A. The capsule of the fungal pathogen *Cryptococcus neoformans*. *Adv Appl Microbiol* (2009) 68:133–216. doi:10.1016/S0065-2164(09)01204-0
21. Steenbergen JN, Casadevall A. The origin and maintenance of virulence for the human pathogenic fungus *Cryptococcus neoformans*. *Microbes Infect* (2003) 5(7):667–75. doi:10.1016/S1286-4579(03)00092-3
22. Goldman DL, Khine H, Abadi J, Lindenberg DJ, Pirofski L, Niang R, et al. Serologic evidence for *Cryptococcus neoformans* infection in early childhood. *Pediatrics* (2001) 107(5):E66. doi:10.1542/peds.107.5.e66
23. Dromer F, Ronin O, Dupont B. Isolation of *Cryptococcus neoformans* var. gattii from an Asian patient in France: evidence for dormant infection in healthy subjects. *J Med Vet Mycol* (1992) 30(5):395–7. doi:10.1080/02681219280000511
24. Valdez PA, Vithayathil PJ, Janelsins BM, Shaffer AL, Williamson PR, Datta SK. Prostaglandin E2 suppresses antifungal immunity by inhibiting interferon regulatory factor 4 function and interleukin-17 expression in T cells. *Immunity* (2012) 36(4):668–79. doi:10.1016/j.immuni.2012.02.013
25. Waterman S, Hacham M, Hu G, Zhu X, Park Y, Shin S, et al. Role of a CUF1-CTR4 copper regulatory axis in the virulence of *Cryptococcus neoformans*. *J Clin Invest* (2007) 117:794–802. doi:10.1172/JCI30006
26. Hu G, Hacham M, Waterman SR, Panepinto J, Shin S, Liu X, et al. PI3K signaling of autophagy is required for starvation tolerance and virulenceof *Cryptococcus neoformans*. *J Clin Invest* (2008) 118(3):1186–97. doi:10.1172/JCI32053
27. Garcia-Rodas R, Zaragoza O. Catch me if you can: phagocytosis and killing avoidance by *Cryptococcus neoformans*. *FEMS Immunol Med Microbiol* (2012) 64(2):147–61. doi:10.1111/j.1574-695X.2011.00871.x
28. Levitz SM. Innate recognition of fungal cell walls. *PLoS Pathog* (2010) 6(4):e1000758. doi:10.1371/journal.ppat.1000758
29. Walsh NM, Wuthrich M, Wang H, Klein B, Hull CM. Characterization of C-type lectins reveals an unexpectedly limited interaction between *Cryptococcus neoformans* spores and Dectin-1. *PLoS One* (2017) 12(3):e0173866. doi:10.1371/journal.pone.0173866
30. Mansour MK, Reedy JL, Tam JM, Vyas JM. Macrophage *Cryptococcus* interactions: an update. *Curr Fungal Infect Rep* (2014) 8(1):109–15. doi:10.1007/s12281-013-0165-7
31. Shao X, Mednick A, Alvarez M, van Rooijen N, Casadevall A, Goldman DL. An innate immune system cell is a major determinant of species-related susceptibility differences to fungal pneumonia. *J Immunol* (2005) 175(5):3244–51. doi:10.4049/jimmunol.175.5.3244
32. Bojarczuk A, Miller KA, Hotham R, Lewis A, Ogryzko NV, Kamuyango AA, et al. *Cryptococcus neoformans* intracellular proliferation and capsule size determines early macrophage control of infection. *Sci Rep* (2016) 6:21489. doi:10.1038/srep21489
33. Redlich S, Ribes S, Schütze S, Eiffert H, Nau R. Toll-like receptor stimulation increases phagocytosis of *Cryptococcus neoformans* by microglial cells. *J Neuroinflammation* (2013) 10:71. doi:10.1186/1742-2094-10-71
34. Lei G, Chen M, Li H, Niu JL, Wu S, Mao L, et al. Biofilm from a clinical strain of *Cryptococcus neoformans* activates the NLRP3 inflammasome. *Cell Res* (2013) 23(7):965–8. doi:10.1038/cr.2013.49
35. Guo C, Chen M, Fa Z, Lu A, Fang W, Sun B, et al. Acapsular *Cryptococcus neoformans* activates the NLRP3 inflammasome. *Microbes Infect* (2014) 16(10):845–54. doi:10.1016/j.micinf.2014.08.013
36. Means TK, Mylonakis E, Tampakakis E, Colvin RA, Seung E, Puckett L, et al. Evolutionarily conserved recognition and innate immunity to fungal pathogens by the scavenger receptors SCARF1 and CD36. *J Exp Med* (2009) 206(3):637–53. doi:10.1084/jem.20082109
37. Xu J, Flaczyk A, Neal LM, Fa Z, Eastman AJ, Malachowski AN, et al. Scavenger receptor MARCO orchestrates early defenses and contributes to fungal containment during cryptococcal infection. *J Immunol* (2017) 198(9):3548–57. doi:10.4049/jimmunol.1700057
38. Xu J, Flaczyk A, Neal LM, Fa Z, Cheng D, Ivey M, et al. Exploitation of scavenger receptor, macrophage receptor with collagenous structure, by *Cryptococcus neoformans* promotes alternative activation of pulmonary lymph node CD11b(+) conventional dendritic cells and non-protective Th2 bias. *Front Immunol* (2017) 8:1231. doi:10.3389/fimmu.2017.01231
39. Qiu Y, Dayrit JK, Davis MJ, Carolan JF, Osterholzer JJ, Curtis JL, et al. Scavenger receptor a modulates the immune response to pulmonary *Cryptococcus neoformans* infection. *J Immunol* (2013) 191(1):238–48. doi:10.4049/jimmunol.1203435
40. Wiesner DL, Specht CA, Lee CK, Smith KD, Mukaremera L, Lee ST, et al. Chitin recognition via chitotriosidase promotes pathologic type-2 helper T cell responses to cryptococcal infection. *PLoS Pathog* (2015) 11(3):e1004701. doi:10.1371/journal.ppat.1004701
41. Dan JM, Wang JP, Lee CK, Levitz SM. Cooperative stimulation of dendritic cells by *Cryptococcus neoformans* mannoproteins and CpG oligodeoxynucleotides. *PLoS One* (2008) 3(4):e2046. doi:10.1371/journal.pone.0002046
42. Voelz K, May RC. Cryptococcal interactions with the host immune system. *Eukaryot Cell* (2010) 9(6):835–46. doi:10.1128/EC.00039-10
43. Sabiiti W, Robertson E, Beale MA, Johnston SA, Brouwer AE, Loyse A, et al. Efficient phagocytosis and laccase activity affect the outcome of HIV-associated cryptococcosis. *J Clin Invest* (2014) 124(5):2000–8. doi:10.1172/JCI72950
44. Johnston SA, May RC. The human fungal pathogen *Cryptococcus neoformans* escapes macrophages by a phagosome emptying mechanism that is inhibited by Arp2/3 complex-mediated actin polymerisation. *PLoS Pathog* (2010) 6(8):e1001041. doi:10.1371/journal.ppat.1001041
45. Levitz SM, Nong SH, Seetoo KF, Harrison TS, Speizer RA, Simons ER. *Cryptococcus neoformans* resides in an acidic phagolysosome of human macrophages. *Infect Immun* (1999) 67(2):885–90.
46. Vandal OH, Nathan CF, Ehrt S. Acid resistance in mycobacterium tuberculosis. *J Bacteriol* (2009) 191(15):4714–21. doi:10.1128/JB.00305-09
47. Tucker SC, Casadevall A. Replication of *Cryptococcus neoformans* in macrophages is accompanied by phagosomal permeabilization and accumulation of vesicles containing polysaccharide in the cytoplasm. *Proc Natl Acad Sci U S A* (2002) 99(5):3165–70. doi:10.1073/pnas.052702799
48. Alvarez M, Casadevall A. Cell-to-cell spread and massive vacuole formation after *Cryptococcus neoformans* infection of murine macrophages. *BMC Immunol* (2007) 8:16. doi:10.1186/1471-2172-8-16
49. He W, Casadevall A, Lee SC, Goldman DL. Phagocytic activity and monocyte chemotactic protein expression by pulmonary macrophages in persistent pulmonary cryptococcosis. *Infect Immun* (2003) 71(2):930–6. doi:10.1128/IAI.71.2.930-936.2003
50. Osterholzer JJ, Curtis JL, Polak T, Ames T, Chen GH, McDonald R, et al. CCR2 mediates conventional dendritic cell recruitment and the formation of bronchovascular mononuclear cell infiltrates in the lungs of mice infected with *Cryptococcus neoformans*. *J Immunol* (2008) 181(1):610–20. doi:10.4049/jimmunol.181.1.610
51. Garcia-Hermoso D, Janbon G, Dromer F. Epidemiological evidence for dormant *Cryptococcus neoformans* infection. *J Clin Microbiol* (1999) 37(10):3204–9.
52. Goldman DL, Lee SC, Mednick AJ, Montella L, Casadevall A. Persistent *Cryptococcus neoformans* pulmonary infection in the rat is associated with intracellular parasitism, decreased inducible nitric oxide synthase expression, and altered antibody responsiveness to cryptococcal polysaccharide. *Infect Immun* (2000) 68(2):832–8. doi:10.1128/IAI.68.2.832-838.2000
53. Shibuya K, Hirata A, Omuta J, Sugamata M, Katori S, Saito N, et al. Granuloma and cryptococcosis. *J Infect Chemother* (2005) 11(3):115–22. doi:10.1007/s10156-005-0387-X
54. Syme RM, Spurrell JC, Amankwah EK, Green FH, Mody CH. Primary dendritic cells phagocytose *Cryptococcus neoformans* via mannose receptors and Fcgamma receptor II for presentation to T lymphocytes. *Infect Immun* (2002) 70(11):5972–81. doi:10.1128/IAI.70.11.5972-5981.2002
55. Mansour MK, Latz E, Levitz SM. *Cryptococcus neoformans* glycoantigens are captured by multiple lectin receptors and presented by dendritic cells. *J Immunol* (2006) 176(5):3053–61. doi:10.4049/jimmunol.176.5.3053
56. Hole CR, Bui H, Wormley FL Jr, Wozniak KL. Mechanisms of dendritic cell lysosomal killing of *Cryptococcus*. *Sci Rep* (2012) 2:739. doi:10.1038/srep00739
57. Garro AP, Chiapello LS, Baronetti JL, Masih DT. Rat eosinophils stimulate the expansion of *Cryptococcus neoformans*-specific CD4(+) and CD8(+) T cells with a T-helper 1 profile. *Immunology* (2011) 132(2):174–87. doi:10.1111/j.1365-2567.2010.03351.x

58. Garro AP, Chiapello LS, Baronetti JL, Masih DT. Eosinophils elicit proliferation of naive and fungal-specific cells in vivo so enhancing a T helper type 1 cytokine profile in favour of a protective immune response against *Cryptococcus neoformans* infection. *Immunology* (2011) 134(2):198–213. doi:10.1111/j.1365-2567.2011.03479.x
59. Huffnagle GB, Boyd MB, Street NE, Lipscomb MF. IL-5 is required for eosinophil recruitment, crystal deposition, and mononuclear cell recruitment during a pulmonary *Cryptococcus neoformans* infection in genetically susceptible mice (C57BL/6). *J Immunol* (1998) 160(5):2393–400.
60. Holmer SM, Evans KS, Asfaw YG, Saini D, Schell WA, Ledford JG, et al. Impact of surfactant protein D, interleukin-5, and eosinophilia on cryptococcosis. *Infect Immun* (2014) 82(2):683–93. doi:10.1128/IAI.00855-13
61. Luckheeram RV, Zhou R, Verma AD, Xia B. CD4(+)T cells: differentiation and functions. *Clin Dev Immunol* (2012) 2012:925135. doi:10.1155/2012/925135
62. Gibson JF, Johnston SA. Immunity to *Cryptococcus neoformans and C. gattii* during cryptococcosis. *Fungal Genet Biol* (2015) 78:76–86. doi:10.1016/j.fgb.2014.11.006
63. Zhang Y, Wang F, Tompkins KC, McNamara A, Jain AV, Moore BB, et al. Robust Th1 and Th17 immunity supports pulmonary clearance but cannot prevent systemic dissemination of highly virulent *Cryptococcus neoformans* H99. *Am J Pathol* (2009) 175(6):2489–500. doi:10.2353/ajpath.2009.090530
64. Flaczyk A, Duerr CU, Shourian M, Lafferty EI, Fritz JH, Qureshi ST. IL-33 signaling regulates innate and adaptive immunity to *Cryptococcus neoformans*. *J Immunol* (2013) 191(5):2503–13. doi:10.4049/jimmunol.1300426
65. Altfeld M, Addo MM, Kreuzer KA, Rockstroh JK, Dumoulin FL, Schliefer K, et al. T(H)1 to T(H)2 shift of cytokines in peripheral blood of HIV-infected patients is detectable by reverse transcriptase polymerase chain reaction but not by enzyme-linked immunosorbent assay under non-stimulated conditions. *J Acquir Immune Defic Syndr* (2000) 23(4):287–94. doi:10.1097/00042560-200004010-00001
66. Jarvis JN, Casazza JP, Stone HH, Meintjes G, Lawn SD, Levitz SM, et al. The phenotype of the *Cryptococcus*-specific CD4 + memory T-cell response is associated with disease severity and outcome in HIV-associated cryptococcal meningitis. *J Infect Dis* (2013) 207(12):1817–28. doi:10.1093/infdis/jit099
67. Jarvis JN, Meintjes G, Bicanic T, Buffa V, Hogan L, Mo S, et al. Cerebrospinal fluid cytokine profiles predict risk of early mortality and immune reconstitution inflammatory syndrome in HIV-associated cryptococcal meningitis. *PLoS Pathog* (2015) 11(4):e1004754. doi:10.1371/journal.ppat.1004754
68. Scriven JE, Rhein J, Hullsiek KH, von Hohenberg M, Linder G, Rolfes MA, et al. Early ART after cryptococcal meningitis is associated with cerebrospinal fluid pleocytosis and macrophage activation in a multisite randomized trial. *J Infect Dis* (2015) 212(5):769–78. doi:10.1093/infdis/jiv067
69. Pirofski LA. Polysaccharides, mimotopes and vaccines for fungal and encapsulated pathogens. *Trends Microbiol* (2001) 9(9):445–51. doi:10.1016/S0966-842X(01)02134-5
70. Subramaniam K, Metzger B, Hanau LH, Guh A, Rucker L, Badri S, et al. IgM(+) memory B cell expression predicts HIV-associated cryptococcosis status. *J Infect Dis* (2009) 200(2):244–51. doi:10.1086/599318
71. Deshaw M, Pirofski LA. Antibodies to the *Cryptococcus neoformans* capsular glucuronoxylomannan are ubiquitous in serum from HIV + and HIV-individuals. *Clin Exp Immunol* (1995) 99(3):425–32. doi:10.1111/j.1365-2249.1995.tb05568.x
72. Subramaniam K, French N, Pirofski LA. *Cryptococcus neoformans*-reactive and total immunoglobulin profiles of human immunodeficiency virus-infected and uninfected Ugandans. *Clin Diagn Lab Immunol* (2005) 12(10):1168–76. doi:10.1128/CDLI.12.10.1168-1176.2005
73. Jalali Z, Ng L, Singh N, Pirofski LA. Antibody response to *Cryptococcus neoformans* capsular polysaccharide glucuronoxylomannan in patients after solid-organ transplantation. *Clin Vaccine Immunol* (2006) 13(7):740–6. doi:10.1128/CVI.00139-06
74. Zaragoza O, Taborda CP, Casadevall A. The efficacy of complement-mediated phagocytosis of *Cryptococcus neoformans* is dependent on the location of C3 in the polysaccharide capsule and involves both direct and indirect C3-mediated interactions. *Eur J Immunol* (2003) 33(7):1957–67. doi:10.1002/eji.200323848
75. Fleuridor R, Zhong Z, Pirofski L. A human IgM monoclonal antibody prolongs survival of mice with lethal cryptococcosis. *J Infect Dis* (1998) 178(4):1213–6. doi:10.1086/515688
76. Subramaniam KS, Datta K, Quintero E, Manix C, Marks MS, Pirofski LA. The absence of serum IgM enhances the susceptibility of mice to pulmonary challenge with *Cryptococcus neoformans*. *J Immunol* (2010) 184(10):5755–67. doi:10.4049/jimmunol.0901638
77. Szymczak WA, Davis MJ, Lundy SK, Dufaud C, Olszewski M, Pirofski LA. X-linked immunodeficient mice exhibit enhanced susceptibility to *Cryptococcus neoformans* Infection. *MBio* (2013) 4(4):e265–213. doi:10.1128/mBio.00265-13
78. Rohatgi S, Pirofski LA. Molecular characterization of the early B cell response to pulmonary *Cryptococcus neoformans* infection. *J Immunol* (2012) 189(12):5820–30. doi:10.4049/jimmunol.1201514
79. Chaturvedi AK, Hameed RS, Wozniak KL, Hole CR, Leopold Wager CM, Weintraub ST, et al. Vaccine-mediated immune responses to experimental pulmonary *Cryptococcus gattii* infection in mice. *PLoS One* (2014) 9(8):e104316. doi:10.1371/journal.pone.0104316
80. Mirza Z, Soto ER, Dikengil F, Levitz SM, Ostroff GR. Beta-glucan particles as vaccine adjuvant carriers. *Methods Mol Biol* (2017) 1625:143–57. doi:10.1007/978-1-4939-7104-6_11
81. Spero D, Levitz L, De Groot AS. Report from the field: overview of the sixth annual vaccine renaissance conference. *Hum Vaccin Immunother* (2013) 9(7):1555–7. doi:10.4161/hv.24833
82. Classen A, Lloberas J, Celada A. Macrophage activation: classical versus alternative. *Methods Mol Biol* (2009) 531:29–43. doi:10.1007/978-1-59745-396-7_3
83. Voelz K, Lammas DA, May RC. Cytokine signaling regulates the outcome of intracellular macrophage parasitism by *Cryptococcus neoformans*. *Infect Immun* (2009) 77(8):3450–7. doi:10.1128/IAI.00297-09
84. Leopold Wager CM, Hole CR, Wozniak KL, Olszewski MA, Wormley FL Jr. STAT1 signaling is essential for protection against *Cryptococcus neoformans* infection in mice. *J Immunol* (2014) 193(8):4060–71. doi:10.4049/jimmunol.1400318
85. Panackal AA, Wuest SC, Lin YC, Wu T, Zhang N, Kosa P, et al. Paradoxical immune responses in non-HIV cryptococcal meningitis. *PLoS Pathog* (2015) 11(5):e1004884. doi:10.1371/journal.ppat.1004884
86. Saijo T, Chen J, Chen SC, Rosen LB, Yi J, Sorrell TC, et al. Anti-granulocyte-macrophage colony-stimulating factor autoantibodies are a risk factor for central nervous system infection by *Cryptococcus gattii* in otherwise immunocompetent patients. *MBio* (2014) 5(2):e912–4. doi:10.1128/mBio.00912-14
87. Rosen LB, Freeman AF, Yang LM, Jutivorakool K, Olivier KN, Angkasekwinai N, et al. Anti-GM-CSF autoantibodies in patients with cryptococcal meningitis. *J Immunol* (2013) 190(8):3959–66. doi:10.4049/jimmunol.1202526
88. Cox G, Mukherjee J, Cole G, Casadeval lA, Perfect J. Urease as a virulence factor in experimental cryptococcosis. *Infect Immun* (2000) 68:443–8. doi:10.1128/IAI.68.2.443-448.2000
89. Liu TB, Kim JC, Wang Y, Toffaletti DL, Eugenin E, Perfect JR, et al. Brain inositol is a novel stimulator for promoting *Cryptococcus* penetration of the blood-brain barrier. *PLoS Pathog* (2013) 9(4):e1003247. doi:10.1371/journal.ppat.1003247
90. Santiago-Tirado FH, Onken MD, Cooper JA, Klein RS, Doering TL. Trojan horse transit contributes to blood-brain barrier crossing of a eukaryotic pathogen. *MBio* (2017) 8(1). doi:10.1128/mBio.02183-16
91. Browne SK, Burbelo PD, Chetchotisakd P, Suputtamongkol Y, Kiertiburanakul S, Shaw PA, et al. Adult-onset immunodeficiency in Thailand and Taiwan. *N Engl J Med* (2012) 367(8):725–34. doi:10.1056/NEJMoa1111160
92. Ahmad DS, Esmadi M, Steinmann WC. Idiopathic CD4 lymphocytopenia: spectrum of opportunistic infections, malignancies, and autoimmune diseases. *Avicenna J Med* (2013) 3(2):37–47. doi:10.4103/2231-0770.114121
93. Gorska MM, Alam R. A mutation in the human Uncoordinated 119 gene impairs TCR signaling and is associated with CD4 lymphopenia. *Blood* (2012) 119(6):1399–406. doi:10.1182/blood-2011-04-350686
94. Panackal AA, Rosen LB, Uzel G, Davis MJ, Hu G, Adeyemo A, et al. Susceptibility to cryptococcal meningoencephalitis associated with idiopathic CD4(+) lymphopenia and secondary germline or acquired defects. *Open Forum Infect Dis* (2017) 4(2):ofx082. doi:10.1093/ofid/ofx082
95. Vinh DC, Patel SY, Uzel G, Anderson VL, Freeman AF, Olivier KN, et al. Autosomal dominant and sporadic monocytopenia with susceptibility to mycobacteria, fungi, papillomaviruses, and myelodysplasia. *Blood* (2010) 115(8):1519–29. doi:10.1182/blood-2009-03-208629
96. Hsu AP, Sampaio EP, Khan J, Calvo KR, Lemieux JE, Patel SY, et al. Mutations in GATA2 are associated with the autosomal dominant and sporadic

monocytopenia and mycobacterial infection (MonoMAC) syndrome. *Blood* (2011) 118(10):2653–5. doi:10.1182/blood-2011-05-356352
97. Spinner MA, Sanchez LA, Hsu AP, Shaw PA, Zerbe CS, Calvo KR, et al. GATA2 deficiency: a protean disorder of hematopoiesis, lymphatics, and immunity. *Blood* (2014) 123(6):809–21. doi:10.1182/blood-2013-07-515528
98. Jacobs DH, Macher AM, Handler R, Bennett JE, Collen MJ, Gallin JI. Esophageal cryptococcosis in a patient with the hyperimmunoglobulin E-recurrent infection (Job's) syndrome. *Gastroenterology* (1984) 87(1):201–3.
99. Holland SM, DeLeo FR, Elloumi HZ, Hsu AP, Uzel G, Brodsky N, et al. STAT3 mutations in the hyper-IgE syndrome. *N Engl J Med* (2007) 357(16):1608–19. doi:10.1056/NEJMoa073687
100. Winkelstein JA, Marino MC, Ochs H, Fuleihan R, Scholl PR, Geha R, et al. The X-linked hyper-IgM syndrome: clinical and immunologic features of 79 patients. *Medicine (Baltimore)* (2003) 82(6):373–84. doi:10.1097/01.md.0000100046.06009.b0
101. Forrestel AK, Modi BG, Longworth S, Wilck MB, Micheletti RG. Primary cutaneous *Cryptococcus* in a patient with multiple sclerosis treated with fingolimod. *JAMA Neurol* (2016) 73(3):355–6. doi:10.1001/jamaneurol.2015.4259
102. Valenzuela RM, Pula JH, Garwacki D, Cotter J, Kattah JC. Cryptococcal meningitis in a multiple sclerosis patient taking natalizumab. *J Neurol Sci* (2014) 340(1–2):109–11. doi:10.1016/j.jns.2014.03.007
103. Casadevall A, Pirofski LA. Host-pathogen interactions: redefining the basic concepts of virulence and pathogenicity. *Infect Immun* (1999) 67(8):3703–13.
104. Pirofski LA, Casadevall A. Immune-mediated damage completes the parabola: *Cryptococcus neoformans* pathogenesis can reflect the outcome of a weak or strong immune response. *MBio* (2017) 8(6):e02063-17. doi:10.1128/mBio.02063-17
105. Panackal AA, Williamson KC, van de Beek D, Boulware DR, Williamson PR. Fighting the monster: applying the host damage framework to human central nervous system infections. *MBio* (2016) 7(1):e1906–15. doi:10.1128/mBio.01906-15
106. Bicanic T, Meintjes G, Wood R, Hayes M, Rebe K, Bekker L, et al. Fungal burden, early fungicidal activity, and outcome in cryptococcal meningitis in antiretroviral-naive or antiretroviral-experienced patients treated with amphotericin B or fluconazole. *Clin Infect Dis* (2007) 45:76–80. doi:10.1086/518607
107. Montezuma-Rusca JM, Powers JH, Follmann D, Wang J, Sullivan B, Williamson PR. Early fungicidal activity as a candidate surrogate endpoint for all-cause mortality in cryptococcal meningitis: a systematic review of the evidence. *PLoS One* (2016) 11(8):e0159727. doi:10.1371/journal.pone.0159727
108. Jenny-Avital E, Abadi M. Immune reconstitution cryptococcosis after initiation of successful highly active antiretroviral therapy. *Clin Infect Dis* (2002) 35:e128–33. doi:10.1086/344467
109. Longley N, Harrison TS, Jarvis JN. Cryptococcal immune reconstitution inflammatory syndrome. *Curr Opin Infect Dis* (2013) 26(1):26–34. doi:10.1097/QCO.0b013e32835c21d1
110. Bahr NC, Wallace J, Frosch AE, Boulware DR. Unmasking cryptococcal meningitis immune reconstitution inflammatory syndrome due to granulocyte colony-stimulating factor use in a patient with a poorly differentiated germ cell neoplasm. *Case Rep Oncol* (2014) 7(1):1–5. doi:10.1159/000357666
111. Bacioglu M, Maia LF, Preische O, Schelle J, Apel A, Kaeser SA, et al. Neurofilament light chain in blood and CSF as marker of disease progression in mouse models and in neurodegenerative diseases. *Neuron* (2016) 91(1):56–66. doi:10.1016/j.neuron.2016.05.018
112. Dismukes WE, Cloud G, Gallis HA, Kerkering TM, Medoff G, Craven PC, et al. Treatment of cryptococcal meningitis with combination amphotericin B and flucytosine for four as compared with six weeks. *N Engl J Med* (1987) 317(6):334–41. doi:10.1056/NEJM198708063170602
113. Sarosi GA, Parker JD, Doto IL, Tosh FE. Amphotericin B in cryptococcal meningitis. Long-term results of treatment. *Ann Intern Med* (1969) 71(6):1079–87. doi:10.7326/0003-4819-71-6-1079
114. Diamond RD, Bennett JE. Prognostic factors in cryptococcal meningitis. A study in 111 cases. *Ann Intern Med* (1974) 80(2):176–81. doi:10.7326/0003-4819-80-2-176
115. Jarvis JN, Meintjes G, Rebe K, Williams GN, Bicanic T, Williams A, et al. Adjunctive interferon-gamma immunotherapy for the treatment of HIV-associated cryptococcal meningitis: a randomized controlled trial. *AIDS* (2012) 26(9):1105–13. doi:10.1097/QAD.0b013e3283536a93
116. Perfect JR, Dismukes WE, Dromer F, Goldman DL, Graybill JR, Hamill RJ, et al. Clinical practice guidelines for the management of cryptococcal disease: 2010 update by the infectious diseases society of america. *Clin Infect Dis* (2010) 50(3):291–322. doi:10.1086/649858
117. Pappas PG, Bustamante B, Ticona E, Hamill RJ, Johnson PC, Reboli A, et al. Recombinant interferon-gamma 1b as adjunctive therapy for AIDS-related acute cryptococcal meningitis. *J Infect Dis* (2004) 189(12):2185–91. doi:10.1086/420829
118. Chen SC, Korman TM, Slavin MA, Marriott D, Byth K, Bak N, et al. Antifungal therapy and management of complications of cryptococcosis due to *Cryptococcus gattii*. *Clin Infect Dis* (2013) 57(4):543–51. doi:10.1093/cid/cit341
119. Mehta GU, Panackal AA, Murayi R, Bennett JE, Williamson PR, Chittiboina P. Corticosteroids for shunted previously healthy patients with non-HIV cryptococcal meningoencephalitis. *J Neurol Neurosurg Psychiatry* (2017). doi:10.1136/jnnp-2017-315830
120. Panackal AA, Komori M, Kosa P, Khan O, Hammoud DA, Rosen LB, et al. Spinal arachnoiditis as a complication of cryptococcal meningoencephalitis in non-HIV previously healthy adults. *Clin Infect Dis* (2017) 64(3):275–83. doi:10.1093/cid/ciw739
121. Hammoud DA, Mahdi E, Panackal AA, Wakim P, Sheikh V, Sereti I, et al. Choroid plexitis and ependymitis by magnetic resonance imaging are biomarkers of neuronal damage and inflammation in HIV-negative cryptococcal meningoencephalitis. *Sci Rep* (2017) 7(1):9184. doi:10.1038/s41598-017-09694-0
122. Collins JV, Tong D, Bucknall RG, Warin AP. Cryptococcal meningitis as a complication of systemic lupus erythematosus treated with systemic corticosteroids. *Postgrad Med J* (1972) 48(555):52–5. doi:10.1136/pgmj.48.555.52
123. Rinehart JJ, Balcerzak SP, Sagone AL, LoBuglio AF. Effects of corticosteroids on human monocyte function. *J Clin Invest* (1974) 54(6):1337–43. doi:10.1172/JCI107880
124. Beardsley J, Wolbers M, Kamali A, Cuc NT, Chierakul W, Chan AK, et al. Adjunctive Corticosteroids in HIV-associated cryptococcal meningitis: a randomised controlled trial in African and Southeast Asian Adults. *55th Interscience Conference on Antimicrobial Agents and Chemotherapy*. San Diego, CA (2015).
125. Meya DB, Manabe YC, Castelnuovo B, Cook BA, Elbireer AM, Kambugu A, et al. Cost-effectiveness of serum cryptococcal antigen screening to prevent deaths among HIV-infected persons with a CD4 + cell count < or = 100 cells/microL who start HIV therapy in resource-limited settings. *Clin Infect Dis* (2010) 51(4):448–55. doi:10.1086/655143
126. Hakim J, Musiime V, Szubert AJ, Mallewa J, Siika A, Agutu C, et al. Enhanced prophylaxis plus antiretroviral therapy for advanced HIV infection in Africa. *N Engl J Med* (2017) 377(3):233–45. doi:10.1056/NEJMoa1615822
127. Beale MA, Sabiiti W, Robertson EJ, Fuentes-Cabrejo KM, O'Hanlon SJ, Jarvis JN, et al. Genotypic diversity is associated with clinical outcome and phenotype in cryptococcal meningitis across Southern Africa. *PLoS Negl Trop Dis* (2015) 9(6):e0003847. doi:10.1371/journal.pntd.0003847
128. Sun HY, Singh N. Opportunistic infection-associated immune reconstitution syndrome in transplant recipients. *Clin Infect Dis* (2011) 53(2):168–76. doi:10.1093/cid/cir276
129. Sun HY, Wagener MM, Singh N. Cryptococcosis in solid-organ, hematopoietic stem cell, and tissue transplant recipients: evidence-based evolving trends. *Clin Infect Dis* (2009) 48(11):1566–76. doi:10.1086/598936

Conflict of Interest Statement: The authors declare that the research was conducted in the absence of any commercial or financial relationships that could be construed as a potential conflict of interest.

Copyright © 2018 Elsegeiny, Marr and Williamson. This is an open-access article distributed under the terms of the Creative Commons Attribution License (CC BY). The use, distribution or reproduction in other forums is permitted, provided the original author(s) and the copyright owner are credited and that the original publication in this journal is cited, in accordance with accepted academic practice. No use, distribution or reproduction is permitted which does not comply with these terms.

frontiers in Immunology

ORIGINAL RESEARCH
published: 30 October 2017
doi: 10.3389/fimmu.2017.01359

Induction of Broad-Spectrum Protective Immunity against Disparate *Cryptococcus* Serotypes

*Marley C. Caballero Van Dyke[1,2], Ashok K. Chaturvedi[1,2], Sarah E. Hardison[1,2], Chrissy M. Leopold Wager[1,2], Natalia Castro-Lopez[1,2], Camaron R. Hole[1,2], Karen L. Wozniak[1,2] and Floyd L. Wormley Jr.[1,2]**

[1] Department of Biology, The University of Texas at San Antonio, San Antonio, TX, United States, [2] The South Texas Center for Emerging Infectious Diseases, The University of Texas at San Antonio, San Antonio, TX, United States

Cryptococcosis is a fungal disease caused by multiple *Cryptococcus* serotypes; particularly *C. neoformans* (serotypes A and D) and *C. gattii* (serotypes B and C). To date, there is no clinically available vaccine to prevent cryptococcosis. Mice given an experimental pulmonary vaccination with a *C. neoformans* serotype A strain engineered to produce interferon-γ, denoted H99γ, are protected against a subsequent otherwise lethal experimental infection with *C. neoformans* serotype A. Thus, we determined the efficacy of immunization with *C. neoformans* strain H99γ to elicit broad-spectrum protection in BALB/c mice against multiple disparate *Cryptococcus* serotypes. We observed significantly increased survival rates and significantly decreased pulmonary fungal burden in H99γ immunized mice challenged with *Cryptococcus* serotypes A, B, or D compared to heat-killed H99γ (HKH99γ) immunized mice. Results indicated that prolonged protection against *Cryptococcus* serotypes B or D in H99γ immunized mice was $CD4^+$ T cell dependent and associated with the induction of predominantly Th1-type cytokine responses. Interestingly, immunization with H99γ did not elicit greater protection against challenge with the *Cryptococcus* serotype C tested either due to low overall virulence of this strain or enhanced capacity of this strain to evade host immunity. Altogether, these studies provide "proof-of-concept" for the development of a cryptococcal vaccine that provides cross-protection against multiple disparate serotypes of *Cryptococcus*.

Keywords: *Cryptococcus neoformans*, *Cryptococcus gattii*, cryptococcosis, host–fungal interaction, fungal vaccines, fungal immunology

OPEN ACCESS

Edited by:
Amariliz Rivera, New Jersey Medical School, United States

Reviewed by:
Liliane Mukaremera, University of Minnesota Twin Cities, United States
Chaoyang Xue, Rutgers University–Newark, United States

***Correspondence:**
Floyd L. Wormley Jr.
floyd.wormley@utsa.edu

Specialty section:
This article was submitted to Microbial Immunology, a section of the journal Frontiers in Immunology

Received: *25 May 2017*
Accepted: *04 October 2017*
Published: *30 October 2017*

Citation:
Van Dyke MCC, Chaturvedi AK, Hardison SE, Leopold Wager CM, Castro-Lopez N, Hole CR, Wozniak KL and Wormley FL Jr. (2017) Induction of Broad-Spectrum Protective Immunity against Disparate Cryptococcus Serotypes. Front. Immunol. 8:1359. doi: 10.3389/fimmu.2017.01359

INTRODUCTION

Cryptococcosis is a worldwide fungal disease caused by species in the *Cryptococcus neoformans*/*Cryptococcus gattii* species complex (1). *C. neoformans* and *C. gattii* cause pneumonia in immunocompromized and immunocompetent individuals and can disseminate to the central nervous system resulting in life-threatening meningoencephalitis. Cryptococcal meningoencephalitis is the most common disseminated fungal disease in AIDS patients (2) and is responsible for 15% of AIDS-related deaths (3). The former species *C. neoformans* is divided into two species, *C. neoformans* and *C. deneoformans*. *C. neoformans* (serotype A) is distributed worldwide with the highest amount of disease cases occurring in sub-Saharan Africa where approximately 21.7 million people

currently live with AIDS, and *C. deneoformans* (serotype D) is predominantly geographically restricted to Europe and Latin America (3–5). Conversely, *C. gattii* (serotype B *C. deuterogattii* and serotype C *C. bacillisporus*) predominantly occurs in tropical and subtropical climates (6–8). However, cryptococcosis due to *C. gattii* is also observed in more temperate climates including British Columbia, Canada, and southwest, southeast, northwest, and northeast regions of the USA and in Mediterranean Europe (9–16). Species in the *C. neoformans*/*C. gattii* complex can cause disease in both apparently healthy individuals and immunocompromized hosts such as AIDS patients, individuals on prolonged treatment with corticosteroids, and in patients on immunosuppressive drugs to prevent rejection of solid organ transplants [reviewed by Kwon-Chung et al. (17)] (7, 8, 18–20). There is a higher occurrence of *C. gattii* disease in immunocompetent individuals compared to *C. neoformans* (20–22). Currently, there is no vaccine clinically available to prevent cryptococcosis and current drug therapies are often rendered ineffective due to the development of drug resistance by *Cryptococcus* or drug toxicity (23). Thus, the overall incidence of disease and mortality associated with cryptococcosis and the potential expanded geographic distribution of the pathogen indicates an urgent need for immunotherapies and/or vaccines to combat cryptococcosis.

Results from multiple studies in both humans and animal models suggest that cell-mediated immunity (CMI) by Th1-type $CD4^+$ T cells is the primary host defense against cryptococcosis (24, 25). However, studies suggest that the host immune response against *C. gattii* and *C. neoformans* differ in that *C. gattii* infection appears to be more immune suppressive, which may explain the disparate clinical presentation displayed by these different species (26–31). Differences in the host response to various *Cryptococcus* serotypes complicate efforts to devise a vaccine that can provide broad-spectrum protection against cryptococcosis caused by disparate *Cryptococcus* serotypes.

Historically, several approaches have been employed to develop an anti-*Cryptococcus* vaccine that generates protective antibody mediated and/or cell-mediated immune responses against *Cryptococcus* [reviewed in Ref. (32).]. Recently, studies have demonstrated that mice given an immunization with glucan particles (GPs) packaged with alkaline extracts from mutant *C. neoformans* or *C. gattii* strains develop increased survival against cryptococcosis (33). Other, studies showed cross-protection of mice immunized with a heat-killed chitosan deficient *C. neoformans* strain against challenge with *C. neoformans* or *C. gattii* (34). Rella and colleagues showed that mice vaccinated with a *C. neoformans* mutant strain that lacks the enzyme sterylglucosidase (Δ*sgl*1) are protected against challenge with both *C. neoformans* H99 and *C. gattii* R265 strains (35).

Studies have shown that mice immunized with a *C. neoformans* strain H99, serotype A, engineered to produce murine interferon (IFN)-γ, denoted H99γ, develop protective Th1-type immune responses against a subsequent otherwise lethal pulmonary challenge with wild-type *C. neoformans* strain H99 (25, 36–40). The presence of $CD4^+$ and/or $CD8^+$ T cells are required for protection during the immunization phase with H99γ but not during subsequent challenge with *C. neoformans* strain H99 (40). These results and those by Rella et al. highlight that protection against pulmonary cryptococcosis in immunocompetent hosts can be maintained in immunosuppressed hosts and that the development of a prophylactic vaccine against cryptococcosis is feasible. Nonetheless, no studies have shown that protection elicited following immunization with one *Cryptococcus* serotype provides similar levels of cross-protection against all four *Cryptococcus* serotypes.

Consequently, the objective of these studies was to determine the potential for an anti-cryptococcal vaccine to provide broad-spectrum protection against multiple disparate *Cryptococcus* serotypes. We therefore determined the efficacy of immunization with *C. neoformans* strain H99γ to elicit protection against experimental pulmonary challenge with disparate cryptococcal serotypes in mice. We demonstrate that immunization with *C. neoformans* strain H99γ, serotype A, elicits a predominantly protective Th1-type immune response against challenge with different serotypes of *Cryptococcus*. These data support the premise that development of a broad-spectrum prophylactic vaccine against cryptococcosis is achievable.

MATERIALS AND METHODS

Mice

Female BALB/c (National Cancer Institute/Charles River Laboratories) 4–6 weeks of age were used throughout these studies. Mice were housed at the University of Texas at San Antonio Small Animal Laboratory Vivarium and all animal experiments were conducted following NIH guidelines for housing and care of laboratory animals and in accordance with protocols approved by the Institutional Animal Care and Use Committee (protocol number MU021) of the University of Texas at San Antonio.

Strains and Media

Cryptococcus neoformans strains H99 (serotype A, mating type α), *C. deuterogattii* strain R265 (serotype B; a kind gift from Dr. Joseph Heitman of Duke University Medical Center in Durham, NC, USA), *C. bacillisporus* strain WSA87 (serotype C), and *C. deneoformans* strain R4247 (serotype D) (each kind gifts from Dr. Brian Wickes of the UT Health San Antonio, San Antonio, TX, USA), and H99γ [an IFN-gamma producing *C. neoformans* strain derived from H99 (38)] were recovered from 15% glycerol stocks stored at −80°C prior to use in the experiments described herein. The strains were maintained on yeast-extract-peptone-dextrose (YPD) media (1% yeast extract, 2% peptone, 2% dextrose, and 2% Bacto agar). Yeast cells were grown for 16 h at 30°C with shaking in YPD broth, collected by centrifugation, washed three times with sterile PBS, and viable yeasts were quantified using trypan blue dye exclusion on a hemacytometer.

Pulmonary Cryptococcal Infections

Cryptococcal infections were initiated as previously described (25, 41). Briefly, mice were anesthetized with 2% isoflurane using a rodent anesthesia device (Eagle Eye Anesthesia, Jacksonville, FL, USA) and given an intranasal inoculation with 1×10^4 CFU of *Cryptococcus* strains H99, R265, WSA87, or R4247 in 50 µl of sterile PBS. Alternatively, mice were given an intranasal immunization

with 1×10^4 CFU of *C. neoformans* strain H99γ or heat-killed H99γ (HKH99γ) yeasts in 50 µl of sterile PBS, allowed 70 days to resolve the infection and subsequently given an intranasal challenge with 1×10^4 CFU of H99, R265, WSA87, or R4247 in 50 µl of sterile PBS. The inocula used for immunizations and challenges were verified by quantitative culture on YPD agar. The mice were monitored by inspection twice daily. Mice were euthanized on pre-determined days post challenge and lung tissues excised using aseptic technique. Tissues were homogenized in 1 ml of sterile PBS followed by culture of 10-fold dilutions of each tissue on YPD agar supplemented with chloramphenicol (Mediatech Inc., Herndon, VA, USA). CFU were enumerated following incubation at 30°C for 48 h. Alternatively, mice intended for survival analysis were monitored by inspection twice daily and euthanized if they appeared to be in pain or moribund (weight loss, ataxia, listlessness, or failure to groom). Mice were euthanized using CO_2 inhalation followed by cervical dislocation.

T Cell Depletion

Mice were immunized with 1×10^4 CFU of *C. neoformans* strain H99γ as described above. After 70 days of rest, mice were depleted of $CD4^+$ T cells, $CD8^+$ T cells, or both $CD4^+/CD8^+$ T cell subsets *via* intraperitoneal administration of anti-CD4 (clone GK1.5) and anti-CD8 (clone 2.43) antibodies (**Table 1**) (each from Cell Culture Company/NCCC, Minneapolis, MN, USA) or given isotype control antibody (rat IgG_{2b}) (BioXCell, Lebanon, NH, USA). Each mouse received 200 µg of GK1.5 and/or 2.43 or control rat IgG_{2b} antibodies in a volume of 200 µl PBS 48 h prior to challenge with H99, R265, WSA87, or R4247 and weekly thereafter during the observation period. The efficiency of T cell depletion in lungs and spleens was assessed by flow cytometric analysis using anti-CD4 and anti-CD8 antibodies that bind epitopes of the CD4 and CD8 protein at locations distinct from GK1.5 and 2.43. Efficiency was determined to be >98% at each anatomic location for each depletion via comparison of T cell subsets in treated mice with those in control animals.

TABLE 1 | Antibodies used in flow cytometry.

mAb	Clone	Manufacturer
CD45R (B220)-PE	RA3-6B2	BD Biosciences
CD11c-Pe-Cy7	N418	eBiosciences
CD11c-PE	N418	eBiosciences
CD11b-Pe-Cy7	M1170	eBiosciences
CD45-APC	30-F11	eBiosciences
CD45-Pe-Cy7	30-F11	eBiosciences
F4/80-APC	BM8	Life Technologies
Ly6G-PE	1A8	BD Biosciences
T cell mix-CD8a APC, CD3e, Pe-Cy7, CD4 PE	CD8a 53-6.7, CD3e-145-2C11, CD4 RM4-5	BD Biosciences
CD19-PE	1D3	BD Biosciences
Siglec-F-PE	E50-2440	BD Biosciences
CD3e-Pe-Cy7	145-2C11	eBiosciences
CD4-PE	RM4-5	BD Biosciences
Intracellular flow		
Interferon-γ-APC	XMG1.2	eBiosciences
IL-4-APC	11B11	eBiosciences
IL-17A-APC	eBio17B7	eBiosciences
Depletion antibodies		
Anti-CD4	GK1.5	Cell Culture Company
Anti-CD8	2.43	Cell Culture Company

Cytokine Analysis

As previously described (25, 41), cytokine levels in lung tissues were analyzed using the Bio-Plex protein array system (Luminex-based technology; Bio-Rad Laboratories, Hercules, CA, USA). Briefly, the left lobe of the lung was excised and homogenized in ice-cold sterile PBS (1 ml). An aliquot (50 µl) was taken to quantify the pulmonary fungal burden and an anti-protease buffer solution containing PBS, protease inhibitors (inhibiting cysteine, serine, and other metalloproteinases), and 0.05% Triton X-100 was added to the homogenate and then clarified by centrifugation ($800 \times g$) for 10 min. Supernatants from pulmonary homogenates were assayed for the presence of IL-1α, IL-1β, IL-1, IL-3, IL-4, IL-5, IL-6, IL-9, IL-10, IL-12(p40), IL-12(p70), IL-13, IL-17A, CCL5/RANTES, CCL11/Eotaxin, CXCL1/KC, CCL3/MIP-1α, CCL4/MIP-1β, CCL2/MCP-1, G-CSF, GM-CSF, TNF-α, and IFN-γ.

Pulmonary Leukocyte Isolation

Lungs were excised on days 3, 7, and 14 post challenge and digested enzymatically at 37°C for 30 min in 10 ml of digestion buffer (RPMI 1640 and 1 mg/ml of collagenase type IV) (Sigma Chemical Co., St. Louis, MO, USA) with intermittent (every 10 min) stomacher homogenizations as previously described (25, 41). The digested tissues were then filtered through sterile nylon filters of various pore sizes (70 and 40 µm; BD Biosciences) and washed with sterile HBSS to enrich for leukocytes. Erythrocytes were lysed by incubation in NH_4Cl buffer (0.859% NH_4Cl, 0.1% $KHCO_3$, 0.0372% Na_2EDTA pH 7.4) for 3 min on ice followed by the addition of a twofold excess of PBS. The leukocyte population was then washed twice with sterile PBS, suspended in sterile PBS + 2% heat-inactivated fetal bovine serum (FACS buffer), and enumerated in a hemacytometer using trypan blue dye exclusion. Flow cytometry analysis was used to determine the percentage of each leukocyte population as well as the absolute number of total leukocytes ($CD45^+$) within the lung cell suspension for standardization of hemacytometer counts.

Flow Cytometry

Standard methodology was employed for the direct immunofluorescence of pulmonary leukocytes (25, 41). Briefly, in 96-well U-bottom plates, 100 µl containing 1×10^6 cells in PBS plus 2% FBS (FACS buffer) were incubated with Fc block (BD Biosciences) diluted in FACS buffer for 5 min to block nonspecific binding of antibodies to cellular Fc receptors. An optimal concentration of fluorochrome-conjugated antibodies (0.125—1 µg/1×10^6 cells) as listed in **Table 1** was added in various combinations to allow for dual or triple staining, and cells were then incubated for 30 min at 4°C. Cells were washed three times with FACS buffer and fixed in 200 µl of 2% ultrapure formaldehyde (Polysciences) diluted in FACS buffer (fixation buffer). Cells analyzed for intracellular cytokine staining were fixed in fixation buffer for 10 min in the dark at room temp. The cells were then permeabilized with 0.1% saponin (diluted in FACS buffer) and incubated for 10 min in the dark at room temperature. Antibodies listed in

Table 1 were subsequently added at optimal concentrations, and cells incubated at 4°C for 30 min. Following incubation, cells were washed three times with 0.1% saponin buffer and resuspended in fixation buffer. Cells incubated with either FACS buffer alone or single fluorochrome-conjugated Abs were used to determine positive staining and spillover/compensation calculations, and background fluorescence determined with FlowJo Software (FlowJo, LLC, Ashland, OR, USA). Raw data were collected with the BD FACSArray flow cytometer (BD Biosciences) and then analyzed using FlowJo Software. Dead cells were excluded on the basis of forward angle and 90° light scatter. For data analyses, 30,000 events (cells) were evaluated from a predominantly leukocyte population identified by back gating from $CD45^+$ stained cells. The absolute number of total leukocytes was quantified by multiplying the total number of cells observed by hemacytometer counting by the percentage of $CD45^+$ cells determined by flow cytometry. The absolute number of leukocytes ($CD45^+$ cells), T cells ($CD4^+/CD3^+$ and $CD8^+/CD3^+$), $CD19^+/CD45^+$, $Ly6G^+/CD45^+$, $F4/80^+/CD45^+$, $CD11b^{int}/CD11c^+/CD45^+$, $CD11b^{hi}CD11c^+/CD45^+$, and Siglec-F^+/$CD11b^+$ was determined by multiplying the percentage of each gated population by the total number of $CD45^+$ cells. Gating strategies are provided as supplemental materials. Intracellular cytokine staining is represented in histograms with unstained cells as a control.

Statistical Analysis

The unpaired Student's *t* test (two-tailed) was used to analyze the immunization studies fungal burden, pulmonary cell populations, and cytokine/chemokine data where appropriate using GraphPad Prism version 5.00 for Windows (GraphPad Prism Software, San Diego, CA, USA). Survival data were analyzed using the log-rank test (GraphPad Software). Significant differences were defined as $^*p < 0.05$, $^{**}p < 0.005$, or $^{***}p < 0.0001$.

RESULTS

Immunization with *C. neoformans* Strain H99γ Elicits Protection against Disparate *Cryptococcus* Serotypes

Previous studies in our lab demonstrated that experimental pulmonary infection with *C. neoformans* strain H99γ in mice results in clearance of the acute infection and induction of protective immunity against a subsequent otherwise lethal challenge with a WT *C. neoformans* strain H99 that does not produce IFN-γ (25, 36–40). Nevertheless, studies to date have not demonstrated that protective immunity generated against one serotype of *Cryptococcus* affords protection against multiple disparate *Cryptococcus* serotypes. Consequently, we sought to determine the level of cross-protection that is generated in mice immunized with *C. neoformans* strain H99γ, a serotype A strain, against pulmonary infection with disparate serotypes of *Cryptococcus*. To establish a baseline prior to evaluating if immunization with *Cryptococcus* strain H99γ, serotype A, enhanced protection against challenge with disparate *Cryptococcus* serotypes, we first determined the relative virulence of each serotype in non-immunized mice. To do this, BALB/c mice were given an experimental pulmonary infection with either *Cryptococcus* strain H99 (serotype A), R265 (serotype B), WSA87 (serotype C), or R4247 (serotype D) and evaluated for mortality (**Figure 1A**). As shown in **Figure 1A**, experimental pulmonary infection with *Cryptococcus* strains H99, R265, and R4247 resulted in 100% mortality with median survival times of 28, 32, and 33 days, respectively. In contrast, we observed 87.5% survival in mice given an experimental pulmonary infection with WSA87. *Cryptococcus* strain WSA87, serotype C, appeared to be significantly less virulent compared to all the other strains tested during our analysis.

Next, we tested the potential of mice immunized with *C. neoformans* strain H99γ (serotype A) to be protected against challenge with *Cryptococcus* serotypes B, C, or D. For this, mice were immunized with *C. neoformans* strain H99γ or heat-killed H99γ (HKH99γ), rested for 70 days, and separate groups subsequently given an experimental pulmonary challenge with each *Cryptococcus* serotype. We observed a 100% survival rate in mice immunized with H99γ and challenged with H99, while the HKH99γ immunized mice challenged with H99 demonstrated a median survival time of 28 days post challenge (**Figure 1B**), confirming our previous observations (38, 40). Mice immunized with H99γ and then challenged with either R265 (*C. gattii* serotype B) or R4247 (*C. deneoformans* serotype D) exhibited median survival times of 59 and 72 days post challenge, respectively, and significantly increased survival rates compared to HKH99γ immunized mice challenged with the same strain (median survival of 33 and 34.5 days in R265 and R4247 challenged mice, respectively; **Figure 1B**). Additionally, we observed a 20% survival rate in protectively immunized mice challenged with R4247 at 100 days post challenge. **Figure 1B** shows that no significant difference in mortality was observed in H99γ immunized mice challenged with WSA87 (median survival time of 90.5 days) compared to HKH99γ immunized mice challenged with the same strain (median survival time of 87.5 days). The mortality of mice immunized with HKH99γ and challenged with each *Cryptococcus* serotype mirrored the mortality rates of non-immunized mice given an experimental infection with each serotype and provided no additional protection (**Figures 1A,B**).

Pulmonary fungal burden was also quantified at days 3, 7, and 14 post challenge in H99γ or HKH99γ immunized mice challenged with each individual serotype (**Figure 1C**). Mice immunized with HKH99γ and challenged with each species showed progressive growth of each serotype in the lungs. In contrast, we observed significantly less pulmonary fungal burden as early as day 3 in H99γ immunized mice challenged with R265 and WSA87 compared to HKH99γ immunized mice (**Figure 1C**). Additionally, H99γ immunized mice showed significantly less pulmonary fungal burden following challenge with all serotypes on days 7 and 14 post challenge compared to HKH99γ immunized mice challenged with the same strain. Brain fungal burden was also quantified at day 14 post challenge and a trend (although not statistically significant) toward a reduction of brain fungal burden together with the number of mice negative for *Cryptococcus* in the brain was observed in

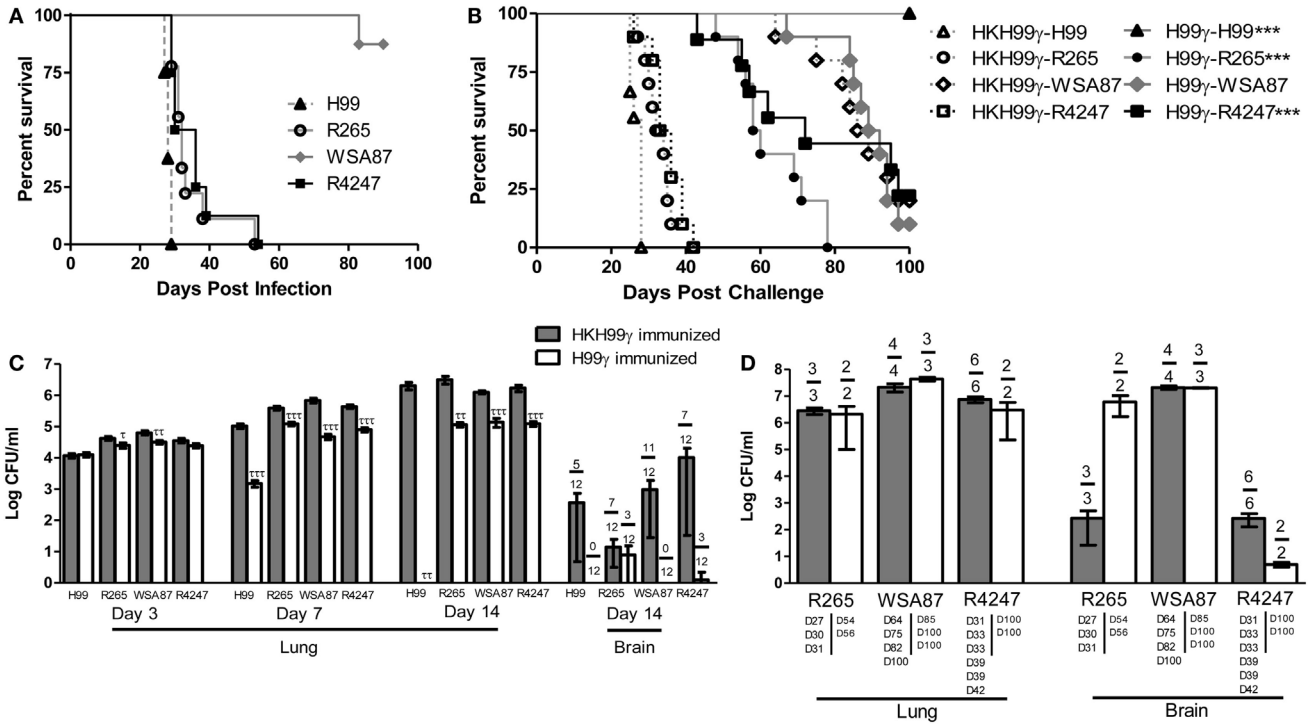

FIGURE 1 | Virulence of disparate *Cryptococcus* serotypes in non-immunized or serotype A immunized mice. BALB/c mice received an intranasal inoculation **(A)** with 1×10^4 CFU of *Cryptococcus* strain H99 (serotype A), R265 (serotype B), WSA87 (serotype C), or R4247 (serotype D). Mice were observed for up to 90 days for mortality analysis. Alternatively, BALB/c mice received an intranasal immunization **(B)** with 1×10^4 CFU of either H99γ or HKH99γ, allowed 70 days to resolve the infection, and subsequently challenged with individual serotypes of *Cryptococcus*. Mice were observed for up to 100 days post challenge for survival analysis **(B)** or, alternatively pulmonary and brain fungal burden determined at days 3, 7, and 14 post challenge **(C)**. Pulmonary and brain fungal burden were analyzed from mice that appeared moribund or sacrificed at 100 days post challenge with the day the mice were sacrificed indicated below the bars **(D)**. Survival data shown are from one experiment, using 8–10 mice per group. Fungal burden data are cumulative of three experiments using 4 mice per group per time point. Numbers above the bars represent the number of mice positive for *Cryptococcus*. $^*p < 0.05$, $^{**}p < 0.005$, $^{***}p < 0.0001$. *Significant increase compared to HKH99γ; $^{\tau}p < 0.05$, $^{\tau\tau}p < 0.005$, $^{\tau\tau\tau}p < 0.0001$. $^{\tau}$Significant decrease compared to HKH99γ.

H99γ immunized mice challenged with each serotype compared to their HKH99γ immunized counterparts (**Figure 1C**). Overall, our data show that mice immunized with H99γ, serotype A, display significant protection against challenge with serotypes A, B, or D of *Cryptococcus*.

Figure 1D demonstrates the fungal burden of moribund mice or mice sacrificed at the conclusion of the study. The HKH99γ immunized mice challenged with R265 appeared to have similar pulmonary fungal burden and less brain fungal burden at time of death compared to H99γ immunized mice challenged with R265 (**Figure 1D**). No significant differences in pulmonary or brain fungal burden were observed between H99γ and HKH99γ immunized mice challenged with WSA87 (**Figure 1D**). Both groups of mice immunized with HKH99γ or H99γ and challenged with R4247 appear to have similar pulmonary fungal burden and lower brain fungal burden at sacrifice with the H99γ immunized mice surviving longer. However, we cannot definitively state if the mice succumbed to pulmonary and/or brain fungal burden. Overall, immunization with H99γ appeared to prolong the survival of mice challenged with each serotype.

Pulmonary Leukocyte Recruitment during Pulmonary Cryptococcosis Is Increased in H99γ Immunized Mice Challenged with Each *Cryptococcus* Serotype

Our next goal was to examine the pulmonary inflammatory response in immunized mice during infection with the various representative *Cryptococcus* serotypes. We observed a significant increase in the total number of leukocytes recruited to the lungs of H99γ immunized mice challenged with H99 at days 3 and 7 post challenge compared to HKH99γ immunized mice (**Figure 2A**). Additionally, we observed significant increases in leukocyte recruitment to the lungs of H99γ immunized mice challenged with R265 on days 7 and 14 post challenge, H99γ immunized mice challenged with WSA87 on days 3 and 7 post challenge, and H99γ immunized mice challenged with R4247 at each time point post challenge compared to their HKH99γ immunized counterparts (**Figure 2A**). We observed an increased total cell number of $F4/80^+$ cells in the lungs of H99γ immunized mice challenged with H99 at day 3, R4247 at days 3 and 7, and WSA87 at day 14 post challenge compared

to HKH99γ immunized mice (**Figure 2B**). We observed a significant increase in the total number of CD11b^{hi}/CD11c^{+} cells recruited to the lungs of H99γ immunized mice challenged with H99, WSA87, or R4247 at day 3, each serotype at day 7 post challenge, and in H99γ immunized mice challenged with WSA87 at day 14 post challenge compared to HKH99γ immunized mice challenged with the same serotype (**Figure 2C**). **Figure 2C** also shows a significant increase in the percentage

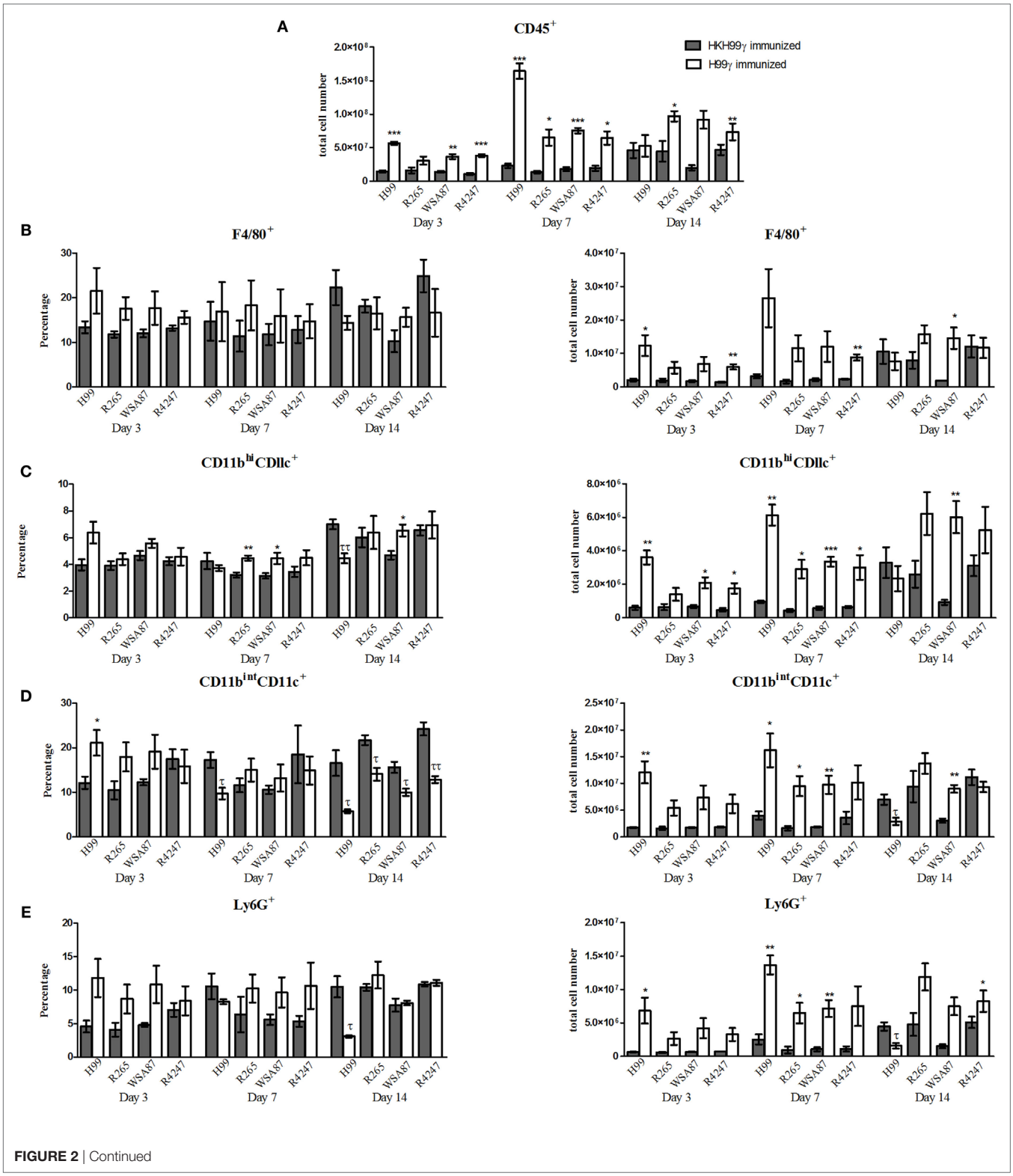

FIGURE 2 | Continued

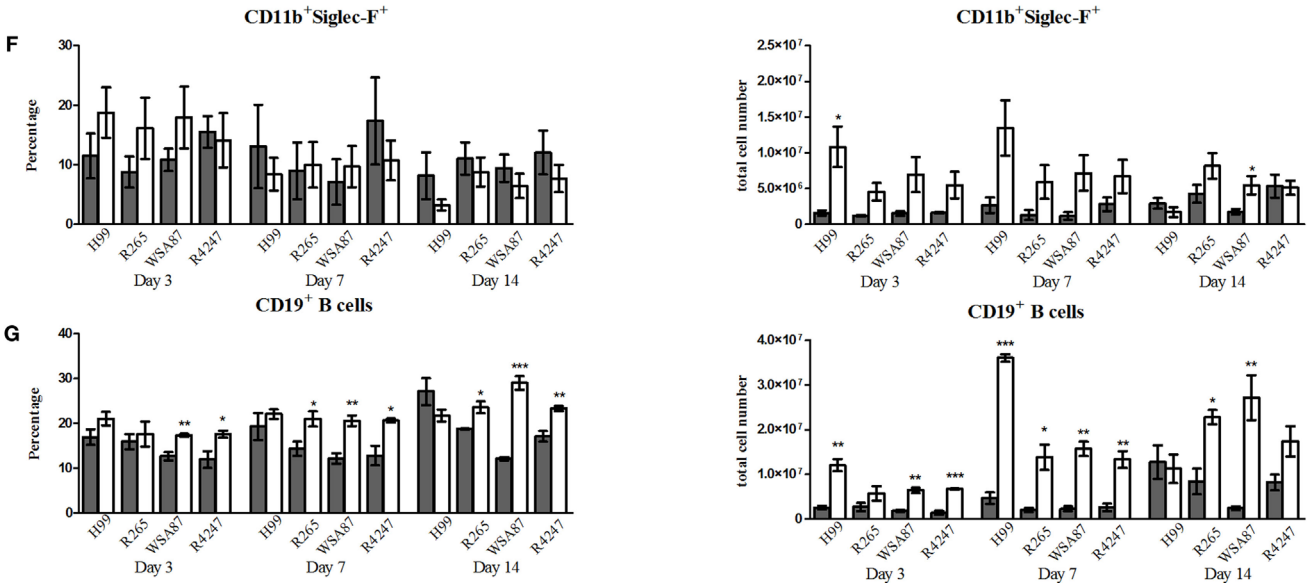

FIGURE 2 | Pulmonary leukocyte populations in immunized mice challenged with different serotypes of *Cryptococcus*. BALB/c mice were immunized intranasally with 1×10^4 CFU of either H99γ or HKH99γ, allowed 70 days to resolve the infection, and subsequently challenged with individual serotypes of *Cryptococcus*. At days 3, 7, and 14 post challenge, lungs were excised, tissues digested, and pulmonary infiltrates were analyzed by flow cytometry. Leukocytes were labeled with anti-CD45 **(A)** or dual labeled with anti-CD45 and antibodies for specific cell types **(B–G)** and analyzed by flow cytometry. Data shown are the mean ± SEM of absolute cell numbers or percentage from three independent experiments performed using 4 mice per group per experiment. $^*p < 0.05$, $^{**}p < 0.005$, $^{***}p < 0.0001$. *Significant increase compared to HKH99γ; $^{\tau}p < 0.05$, $^{\tau\tau}p < 0.005$, $^{\tau\tau\tau}p < 0.0001$. $^{\tau}$Significant decrease compared to HKH99γ.

of CD11b^{hi}/CD11c$^+$ cells in H99γ immunized mice challenged with R265 or WSA87 at day 7, and WSA87 at day 14 post challenge. There was also a significant increase in the total number of CD11b^{int}CD11c$^+$ cells in H99γ immunized mice challenged with H99 at days 3 and 7, R265 at day 7 post challenge, and WSA87 at days 7 and 14 post challenge (**Figure 2D**). **Figure 2D** also shows a significant increase in CD11b^{int}CD11c$^+$ cells in H99γ immunized mice challenged with H99 at day 3, while we observe a significant decrease in these cells at day 7 in H99 challenged mice, and across each serotype at day 14 post challenge. The recruitment of Ly6G$^+$ cells to the lungs was significantly higher in H99γ immunized mice challenged with H99 at days 3 and 7 post challenge, R265 or WSA87 at day 7 post challenge, and in H99γ immunized mice challenged with R4247 on day 14 post challenge compared to their HKH99γ immunized counterparts (**Figure 2E**). While mice immunized with H99γ and challenged with H99 are clearing the infection, these mice show a significant decrease in the total number and percentage of Ly6G$^+$ cells at day 14 post infection compared to HKH99γ immunized mice (**Figure 2E**). We observed a significant increase in the total number of Siglec-F$^+$ cells in mice immunized with H99γ and challenged with H99 at day 3 post challenge and WSA87 challenged mice at day 14 post challenge (**Figure 2F**). We observed a significant increase in the total number of B cells in mice immunized with H99γ and challenged with H99, WSA87, or R4247 at day 3 post challenge, across each serotype at day 7 post challenge, and R265 or WSA87 at day 14 post challenge (**Figure 2G**). For the percentage of B cells, we observed a significant increase in H99γ immunized mice challenged with WSA87 or R4247 across each time point and in mice challenged with R265 at days 7 and 14 post challenge (**Figure 2G**). Overall, our data show significantly increased pulmonary recruitment of F4/80$^+$ cells, CD11b$^+$/CD11c$^+$ cells, B cells, and Ly6G$^+$ cells in mice immunized with the serotype A *Cryptococcus* strain H99γ following challenge with various other *Cryptococcus* serotypes which, altogether, may contribute to the increased protective responses observed in these mice.

Immunization with H99γ Elicits Elevated Proinflammatory and a Predominant Th1-Type Cytokine Response following Challenge with Disparate *Cryptococcus* Serotypes

The pulmonary fungal burden and mortality analysis suggested that mice immunized with H99γ were able to mount protective responses against challenge with disparate *Cryptococcus* serotypes. Therefore, we evaluated cytokine levels in the lungs of H99γ or HKH99γ immunized mice following challenge with each *Cryptococcus* serotype. Lung homogenates were prepared from pulmonary tissues of mice on days 3, 7, and 14 post challenge with *Cryptococcus* serotypes A, B, C, or D, and the levels of Th1 associated (IFN-γ, IL-2, IL-12p70), Th2 associated (IL-4 and IL-5), immunoregulatory (IL-10 and G-CSF), and proinflammatory (IL-1α, IL-1β, IL-17A, and TNF-α) cytokines and chemokines (CCL3, CCL4, CCL2, CXCL1, and CCL5) were determined. We observed that H99γ immunized

mice challenged with *C. neoformans* strain H99 exhibited a significant increase in Th1 associated cytokines (IFN-γ, IL-2, and IL-12p70) as early as day 3 post challenge that remained significantly elevated, except IL-2, through day 7 post challenge compared to HKH99γ immunized mice challenged with H99 (**Tables 2** and **3**). However, we observed significantly less Th1 associated cytokine (IL-12p70 and IFN-γ) production at day 14 post challenge in H99γ immunized mice compared to HKH99γ immunized mice (**Table 4**). Also, proinflammatory (IL-1α and IL-1β) and immunoregulatory (G-CSF) cytokines and chemokine levels (CCL3, CCL4, CCL2, and CXCL1) in H99γ immunized mice challenged with H99 were significantly less compared to levels observed in HKH99γ immunized mice challenged with H99 at day 14 post challenge (**Table 4**). The significant decrease in Th1 associated and proinflammatory cytokine and chemokine levels in H99γ immunized mice challenged with H99 at day 14 post challenge compared to levels observed in HKH99γ immunized mice likely coincides with the significant reduction in pulmonary fungal burden observed in the H99γ immunized mice; whereas, the HKH99γ immunized mice are experiencing progressive disease (**Figure 1C**). Th1 associated cytokine levels in the lungs of H99γ immunized mice challenged with each other serotype were generally elevated at day 3 post challenge and remained significantly elevated at days 7 and 14 post challenge, particularly cytokines IFN-γ and IL-12p70, compared to their HKH99γ immunized counterparts (**Tables 2–4**). For Th2-associated cytokines, we observed a significant increase at day 3 post challenge in mice that were immunized with H99γ and challenged with each serotype [H99 (IL-4 and IL-5), R265, WSA87, or R4247 (IL-5)] (**Table 2**). At day 7 post challenge in mice immunized with H99γ, we observed an increase in IL-4 in mice challenged with R265 or R4247 (**Table 3**). By day 14 post challenge, there was a statistically significant decrease in Th2 associated cytokines (IL-4 and IL-5) across each serotype except for WSA87 challenged mice that showed significantly increased IL-5 levels across days 7 and 14 post challenge (**Tables 3** and **4**). We also observed an overall trend toward significantly increased proinflammatory cytokine (IL-1α, IL-1β, and IL-17A), immunoregulatory cytokine (G-CSF), and chemokine (CCL3, CCL4, CCL2, CXCL1, and CCL5) production as early as day 3 post challenge that remained elevated through day 7 post challenge in H99γ immunized mice challenged with each serotype compared to similarly challenged mice immunized using HKH99γ (**Tables 2** and **3**). We observed an overall trend toward significantly higher levels of proinflammatory cytokine (IL-1α, IL-1β, IL-17A, and TNF-α), immunoregulatory cytokine (G-CSF), and chemokine levels (CCL3, CCL4, CCL2, CXCL1, and RANTES) was observed in H99γ immunized mice challenged with R265, WSA87, or R4247 compared to similarly challenged HKH99γ immunized at day 14 post challenge except for CCL3 and CXCL1 for R265 challenged mice, and CCL3 and CCL2 for R4247 challenged mice (**Table 4**). Altogether, the cytokine results suggest that immunization with *C. neoformans* strain H99γ elicits a heightened cytokine anamnestic response against multiple disparate serotypes of *Cryptococcus* compared to HKH99γ immunized mice.

Vaccine-Mediated Protection against Pulmonary Cryptococcosis Is Associated with Enhanced Th1-Type Immune Responses

We next evaluated T cell responses in the lungs of immunized mice following challenge with the various *Cryptococcus* serotypes. Flow cytometry analysis was utilized to determine levels of $CD4^+$ and $CD8^+$ T cell infiltration to the lungs on days 3, 7, and 14 post challenge. Also, intracellular cytokine staining of $CD4^+$ T cells for representative T helper (Th) 1, Th2, and Th17-type cytokines IFN-γ, IL-4, and IL-17A, respectively, and subsequent flow cytometry analysis was used to access the $CD4^+$ Th cell phenotype during the anamnestic response to pulmonary cryptococcosis. We observed an overall trend toward increased total numbers of $CD4^+$ and $CD8^+$ T cells in H99γ immunized mice compared to HKH99γ immunized mice following challenge with each serotype as the infection progressed (**Figures 3A,B**). The total number of $CD4^+$ T cells was significantly increased in H99γ immunized mice challenged with H99, R265, or R4247 at day 3 post challenge, and in mice challenged with H99 at day 7 post challenge compared to their HKH99γ immunized counterparts (**Figure 3A**). However, there was no significant difference in percentage of $CD4^+$T cells between groups. We also observed an increase in the total number of $CD8^+$ T cells in H99γ immunized mice challenged with H99, WSA87, or R4247 at day 3 post challenge, in mice challenged with H99, R265, or WSA87 at day 7 post challenge, and in R265 or WSA87 challenged mice at day 14 post challenge compared to HKH99γ immunized mice challenged with their equivalent serotype (**Figure 3B**). A significant increase in the percentage of $CD8^+$ T cells was observed in mice immunized with H99γ and challenged with R265 or R4247 at day 14 post challenge compared to their HKH99γ immunized counterparts.

Overall, we observed significant increases in the total number of $CD4^+$/IFN-γ^+ T cells followed by $CD4^+$/IL-$17A^+$ T cells and then $CD4^+$/IL-4^+ T cells at day 7 post challenge in H99γ immunized mice challenged with each serotype compared to HKH99γ immunized mice challenged with the corresponding serotype (**Figures 3C–E**). We observed greater total $CD4^+$/IFN-γ^+ T cell numbers in H99γ immunized mice challenged with H99 compared to H99γ immunized mice challenged with R265, WSA87, or R4247 at day 7 post challenge (**Figure 3C**). These results suggest that mice immunized with H99γ are capable of eliciting a predominantly Th1-type anamnestic response upon challenge with each disparate *Cryptococcus* serotype. These data show that mice immunized with the serotype A strain exhibit an increased putatively protective Th1-type immune response following challenge with other disparate serotypes.

Protection Afforded by Immunization with H99γ against Serotypes B and D of *Cryptococcus* Requires $CD4^+$ T Cells

Previous studies in our lab demonstrated that H99γ immunized mice depleted of $CD4^+$ or $CD8^+$ T cells were completely protected against an otherwise lethal challenge with the non-IFN-γ producing *C. neoformans* strain H99 (40). Also, H99γ immunized

TABLE 2 | Cytokine levels within lung homogenates of H99γ and HKH99γ immunized mice infected with each serotype.

	Day 3 post challenge							
	HKH99γ	**H99γ**	**HKH99γ**	**H99γ**	**HKH99γ**	**H99γ**	**HKH99γ**	**H99γ**
	H99		**R265**		**WSA87**		**R4247**	
Th1 associated								
Interferon (IFN)-γ	5.88 ± 1.45	**12.57 ± 1.84***	4.26 ± 1.07	6.461 ± 0.9474	5.59 ± 1.55	5.94 ± 0.68	3.22 ± 0.71	**6.40 ± 0.89***
IL-2	26.03 ± 6.49	**109.30 ± 18.96****	17.98 ± 3.66	21.3 ± 2.35	22.15 ± 6.41	35.64 ± 4.94	15.09 ± 3.28	**27.58 ± 4.31***
IL-12p70	13.51 ± 0.72	**69.90 ± 8.56*****	14.95 ± 0.58	**27.9 ± 1.754*****	16.04 ± 4.42	**34.21 ± 3.23****	9.91 ± 1.08	**29.20 ± 3.97*****
Th2 associated								
IL-4	4.15 ± 1.40	**34.58 ± 6.29*****	4.36 ± 1.33	5.873 ± 1.514	4.58 ± 1.31	9.25 ± 2.39	4.22 ± 1.27	6.02 ± 1.42
IL-5	2.49 ± 0.24	**10.96 ± 0.94*****	2.26 ± 0.30	**4.729 ± 0.4244*****	2.91 ± 0.63	**6.32 ± 0.52*****	2.00 ± 0.19	**5.43 ± 0.27*****
Proinflammatory								
IL-1α	142.40 ± 25.02	**20.86 ± 3.38**¤¤¤**	16.60 ± 1.85	18.53 ± 0.9751	18.45 ± 3.08	**37.21 ± 4.70****	15.58 ± 1.69	**23.42 ± 2.61***
IL-1β	45.79 ± 4.72	**815.70 ± 124.40*****	46.04 ± 6.80	**105.9 ± 8.724*****	45.37 ± 2.90	**248.90 ± 40.52*****	37.11 ± 1.94	**120.40 ± 18.97*****
IL-17A	2.56 ± 0.41	**501.70 ± 83.71*****	2.72 ± 0.25	**44.56 ± 8.306*****	3.09 ± 0.44	**195.50 ± 43.31*****	2.41 ± 0.30	**52.92 ± 12.55****
TNF-α	45.64 ± 5.51	64.35 ± 7.17	40.39 ± 4.26	48.37 ± 3.266	38.08 ± 4.85	**53.17 ± 4.03***	30.81 ± 2.78	**48.19 ± 4.99****
Immunoregulatory								
IL-10	5.15 ± 0.61	**23.05 ± 1.96*****	4.25 ± 0.76	**11.18 ± 1.105*****	4.30 ± 0.51	**12.78 ± 0.81*****	3.93 ± 0.55	**8.90 ± 1.09****
G-CSF	5.22 ± 1.25	**510.90 ± 64.82*****	5.27 ± 1.19	**45.88 ± 5.85*****	5.62 ± 1.30	**135.90 ± 24.62*****	4.76 ± 1.21	**64.73 ± 12.34*****
Chemokine								
CCL3/MIP-1α	43.41 ± 5.17	**452.80 ± 49.90*****	45.01 ± 3.49	**111.60 ± 9.96*****	68.20 ± 24.17	**194.70 ± 18.11*****	37.94 ± 1.68	**122.20 ± 12.11*****
CCL4/MIP-1β	6.64 ± 0.81	**79.97 ± 13.09*****	6.27 ± 0.53	**16.58 ± 1.97*****	6.35 ± 0.70	**35.92 ± 6.91*****	4.72 ± 0.21	**17.78 ± 1.94*****
CCL2/MCP-1	57.51 ± 8.79	**934.30 ± 88.77*****	64.73 ± 4.93	**189.30 ± 21.11*****	64.70 ± 6.91	**411.70 ± 95.02****	56.65 ± 6.29	**183.00 ± 17.56*****
CXCL1/KC	26.76 ± 1.74	**971.50 ± 94.97*****	34.39 ± 4.76	**189.70 ± 31.80*****	32.66 ± 2.49	**460.40 ± 79.29*****	26.03 ± 1.98	**211.60 ± 31.00*****
CCL5/RANTES	152.90 ± 19.47	**1241.00 ± 127.50*****	166.60 ± 11.56	**321.00 ± 42.19****	273.70 ± 118.80	**560.70 ± 49.99***	156.00 ± 10.44	**375.60 ± 38.23*****

Data shown are expressed as mean ± SEM and are cumulative of three experiments using four mice per group per time point.

Bolded values indicate significance either increased or decreased compared to HKH99γ.

**p < 0.05, **p < 0.005, ***p < 0.0001 significant increase compared to HKH99γ.*

¤¤¤p < 0.0001 significant decrease compared to HKH99γ.

TABLE 3 | Cytokine levels within lung homogenates of H99γ and HKH99γ immunized mice infected with each serotype.

	Day 7 post challenge							
	HKH99γ	**H99γ**	**HKH99γ**	**H99γ**	**HKH99γ**	**H99γ**	**HKH99γ**	**H99γ**
	H99		**R265**		**WSA87**		**R4247**	
Th1 associated								
IFN-γ	5.23 ± 0.79	**13.28 ± 0.88*****	4.83 ± 0.54	**10.36 ± 1.08*****	5.29 ± 0.95	**10.40 ± 0.42*****	5.70 ± 1.46	**9.61 ± 0.62***
IL-2	19.69 ± 5.12	31.41 ± 3.14	24.52 ± 8.36	35.83 ± 4.22	20.02 ± 4.53	**37.75 ± 5.55***	24.48 ± 6.46	38.61 ± 4.57
IL-12p70	27.22 ± 5.78	**139.60 ± 30.20****	14.19 ± 3.31	**77.97 ± 15.14****	13.12 ± 2.53	**75.36 ± 5.15*****	16.58 ± 4.11	**61.84 ± 6.50*****
Th2 associated								
IL-4	30.90 ± 14.04	12.87 ± 3.31	1.98 ± 1.30	**8.46 ± 1.58****	0.33 ± 0.12	5.19 ± 2.53	0.45 ± 0.16	**4.86 ± 1.29****
IL-5	12.51 ± 2.74	8.41 ± 0.72	8.08 ± 2.36	6.89 ± 0.39	0.96 ± 0.37	**5.73 ± 1.47****	7.05 ± 0.83	6.97 ± 1.16
Proinflammatory								
IL-1α	31.91 ± 5.40	**353.40 ± 95.66****	20.30 ± 5.94	**109.40 ± 17.98*****	15.39 ± 1.78	**152.30 ± 35.52****	18.42 ± 2.24	**95.36 ± 17.63*****
IL-1β	123.10 ± 23.21	**1816.00 ± 409.20****	46.24 ± 4.47	**782.00 ± 137.60*****	29.71 ± 3.71	**942.80 ± 206.40*****	49.95 ± 7.70	**647.60 ± 121.60*****
IL-17A	6.84 ± 2.27	**663.20 ± 90.46*****	0.62 ± 0.24	**454.60 ± 83.45*****	0.47 ± 0.18	**669.40 ± 210.30****	0.77 ± 0.23	**481.50 ± 112.00*****
TNF-α	39.17 ± 3.51	**84.68 ± 5.97*****	34.34 ± 1.70	**66.83 ± 3.35*****	37.01 ± 3.59	**66.90 ± 3.61*****	40.08 ± 4.15	**59.52 ± 3.14****
Immunoregulatory								
IL-10	7.31 ± 0.84	**40.08 ± 5.68*****	5.30 ± 0.92	**25.05 ± 3.14*****	4.02 ± 0.51	**27.08 ± 2.55*****	3.87 ± 0.78	**21.09 ± 2.47*****
G-CSF	64.74 ± 13.03	**408.90 ± 99.61****	5.92 ± 0.85	**211.10 ± 44.00*****	3.22 ± 0.34	**298.50 ± 89.68****	13.12 ± 2.22	**189.40 ± 53.74****
Chemokine								
CCL3/MIP-1α	138.00 ± 31.56	**354.40 ± 36.93*****	44.37 ± 3.16	**226.90 ± 15.24*****	29.94 ± 2.05	**255.40 ± 53.29*****	34.75 ± 5.91	**207.70 ± 37.53*****
CCL4/MIP-1β	29.95 ± 6.78	**66.32 ± 14.73***	8.82 ± 1.72	**40.40 ± 4.68*****	6.86 ± 1.17	**43.55 ± 6.54*****	6.77 ± 1.42	**31.96 ± 3.67*****
CCL2/MCP-1	372.60 ± 95.97	**962.50 ± 152.70****	89.06 ± 14.96	**713.00 ± 127.20*****	38.46 ± 5.58	**636.00 ± 64.17*****	116.90 ± 28.72	**474.90 ± 58.73*****
CXCL1/KC	268.20 ± 47.52	**1055.00 ± 169.70*****	58.81 ± 7.29	**774.70 ± 118.20*****	45.73 ± 14.61	**782.60 ± 140.60*****	86.95 ± 15.98	**643.10 ± 111.40*****
CCL5/RANTES	246.70 ± 31.91	**1407.00 ± 156.60*****	135.20 ± 6.51	**621.90 ± 59.09*****	105.80 ± 8.11	**880.10 ± 183.90*****	86.45 ± 11.71	**607.50 ± 110.20*****

Data shown are expressed as mean ± SEM and are cumulative of three experiments using four mice per group per time point.
Bolded values indicate significance either increased or decreased compared to HKH99γ.
**p < 0.05, **p < 0.005, ***p < 0.0001 significant increase compared to HKH99γ*

TABLE 4 | Cytokine levels within lung homogenates of H99γ and HKH99γ immunized mice infected with each serotype.

	Day 14 post challenge							
	HKH99γ	**H99γ**	**HKH99γ**	**H99γ**	**HKH99γ**	**H99γ**	**HKH99γ**	**H99γ**
	H99		**R265**		**WSA87**		**R4247**	
Th1 associated								
IFN-γ	8.37 ± 0.60	**6.33 ± 0.54**$^{\tau}$	7.09 ± 0.74	**11.71 ± 0.88****	4.61 ± 0.57	**10.52 ± 0.66*****	4.80 ± 0.23	**10.82 ± 0.94*****
IL-2	15.67 ± 1.19	15.87 ± 3.17	14.14 ± 0.43	**28.83 ± 2.17*****	13.21 ± 4.47	**28.20 ± 1.48****	9.67 ± 1.21	**28.49 ± 1.09*****
IL-12p70	78.16 ± 10.72	**30.11 ± 2.46**$^{\tau\tau\tau}$	62.74 ± 9.46	**130.30 ± 23.33***	21.28 ± 2.23	**127.10 ± 20.38*****	41.41 ± 3.31	**135.10 ± 21.07*****
Th2 associated								
IL-4	190.30 ± 33.23	**1.37 ± 0.37**$^{\tau\tau\tau}$	102.40 ± 17.90	**14.11 ± 4.43**$^{\tau\tau\tau}$	6.38 ± 2.57	4.96 ± 0.96	68.98 ± 7.51	**12.23 ± 2.89**$^{\tau\tau\tau}$
IL-5	23.74 ± 5.57	**1.83 ± 0.70**$^{\tau\tau}$	73.75 ± 21.66	**8.24 ± 0.98**$^{\tau\tau}$	4.95 ± 1.27	**8.88 ± 1.09***	74.35 ± 13.94	**7.35 ± 0.86**$^{\tau\tau\tau}$
Proinflammatory								
IL-1α	151.60 ± 18.96	**20.36 ± 2.50**$^{\tau\tau\tau}$	122.20 ± 12.17	**380.80 ± 84.73****	29.50 ± 6.28	**337.90 ± 46.85*****	105.90 ± 14.39	**471.00 ± 39.58*****
IL-1β	862.80 ± 218.50	**87.04 ± 8.71**$^{\tau\tau}$	398.20 ± 71.61	**2434.00 ± 519.10****	82.79 ± 21.65	**2346.00 ± 383.20*****	315.20 ± 53.03	**2645.00 ± 322.50*****
IL-17A	55.84 ± 10.26	33.87 ± 6.83	17.10 ± 4.86	**959.40 ± 178.60*****	3.24 ± 1.27	**897.10 ± 105.60*****	6.65 ± 2.03	**968.90 ± 83.29*****
TNF-α	52.10 ± 2.22	46.05 ± 3.00	45.81 ± 2.05	**80.03 ± 6.04*****	32.51 ± 2.89	**76.46 ± 4.20*****	38.77 ± 1.57	**71.21 ± 4.29*****
Immunoregulatory								
IL-10	26.14 ± 1.78	**11.61 ± 0.93**$^{\tau\tau\tau}$	27.59 ± 3.00	**40.29 ± 4.54***	7.96 ± 0.98	**39.11 ± 3.23*****	17.97 ± 1.63	**40.08 ± 3.30*****
G-CSF	62.52 ± 15.47	**5.02 ± 0.42**$^{\tau\tau}$	42.48 ± 4.68	**81.41 ± 13.82***	13.80 ± 2.37	**110.50 ± 20.14*****	35.52 ± 4.65	**88.34 ± 10.39*****
Chemokine								
CCL3/MIP-1α	1023.00 ± 252.10	**99.74 ± 21.77**$^{\tau\tau}$	515.30 ± 77.06	362.80 ± 47.70	73.85 ± 15.04	**346.10 ± 41.46*****	286.90 ± 44.40	366.10 ± 23.44
CCL4/MIP-1β	40.83 ± 8.61	**8.71 ± 1.24**$^{\tau\tau}$	21.83 ± 4.15	**40.93 ± 4.74****	8.96 ± 2.82	**36.65 ± 4.08*****	18.59 ± 1.98	**40.43 ± 2.62*****
CCL2/MCP-1	542.50 ± 117.10	**93.71 ± 11.92**$^{\tau\tau}$	1244.00 ± 213.40	**516.20 ± 71.17**$^{\tau\tau}$	183.80 ± 51.99	**585.40 ± 61.80*****	827.00 ± 188.20	486.40 ± 35.50
CXCL1/KC	533.10 ± 57.85	**80.39 ± 10.84**$^{\tau\tau\tau}$	496.70 ± 65.65	655.90 ± 70.33	297.00 ± 67.81	**751.40 ± 77.80*****	345.20 ± 55.87	**625.50 ± 31.55*****
CCL5/RANTES	582.60 ± 114.80	305.40 ± 71.84	285.20 ± 27.58	**1402.00 ± 240.60*****	201.50 ± 39.46	**1623.00 ± 219.30*****	214.70 ± 45.55	**1377.00 ± 162.90*****

Data shown are expressed as mean ± SEM and are cumulative of three experiments using four mice per group per time point.

Bolded values indicate significance either increased or decreased compared to HKH99γ.

**p < 0.05, **p < 0.005, ***p < 0.0001 significant increase compared to HKH99γ.*

$^{\tau}$p < 0.05, $^{\tau\tau}$p < 0.005, $^{\tau\tau\tau}$p < 0.0001 significant decrease compared to HKH99γ.

mice that were subsequently depleted of both $CD4^+$ and $CD8^+$ T cells were shown to have an 80% survival rate following challenge with *C. neoformans* strain H99. Therefore, we sought to determine the necessity of T cells in protection against cryptococcosis caused by the different serotypes of *Cryptococcus* in H99γ immunized mice. For this, BALB/c mice were immunized with *C. neoformans* strain H99γ and allowed 70 days to resolve the infection. Mice were then depleted of $CD4^+$ and/or $CD8^+$ T cells or received isotype control antibody two days prior to challenge and weekly thereafter during the observation period. H99γ immunized mice depleted of both $CD4^+$ and $CD8^+$ T cells prior to and during challenge with H99 demonstrated an 87.5% survival rate upon the conclusion of the study (**Figure 4A**) as previously demonstrated (40). **Figure 4** shows that H99γ immunized mice treated with isotype control antibodies and challenged with R265 (**Figure 4B**) or R4247 (**Figure 4D**) had similar prolonged survival (median survival times of 65 and 64.5 days for R265 and R4247 challenged mice, respectively); similar to observations demonstrated in **Figure 1B**. In contrast, we observed 100% mortality in H99γ immunized mice depleted of $CD4^+$ T cells alone during challenge with R265 (median survival of 35.5 days) or depleted of $CD4^+$ and $CD8^+$ T cells (median survival of 34 days; **Figure 4B**). Interestingly, H99γ immunized mice depleted of $CD8^+$ T cells alone and challenged with R265 showed increased, although not statistically significant, survival (median survival of 80 days) compared to that observed in isotype control-treated mice (median survival of 65 days). We also observed that H99γ immunized mice challenged with R4247 while depleted of $CD4^+$ T cells alone experienced 87.5% mortality (median survival time of 30.5 days) and 100% mortality upon depletion of both $CD4^+$ and $CD8^+$ T cells (median survival time of 31.5 days; **Figure 4D**). Additionally, H99γ immunized mice depleted of $CD8^+$ T cells alone and challenged with R4247 had increased survival although not statistically significant (median survival of 75.5 days) compared to the isotype control-treated mice (median survival of 64.5 days). Mice immunized with H99γ and subsequently depleted of $CD4^+$ T and/or $CD8^+$ T cells prior to and during challenge with WSA87 did not show any difference in survival compared to the isotype control-treated mice (**Figure 4C**). Overall, we observed that depletion of $CD4^+$ T cells resulted in a significant loss of protection against challenge with R265 (serotype B) or R4247 (serotype D) in H99γ (serotype A) immunized mice, indicating that $CD4^+$ T cells are required for broad-spectrum protection against these serotypes.

DISCUSSION

While the overwhelming majority of *Cryptococcus* exposures do not progress to life-threatening illness, the ubiquitous presence of *Cryptococcus* in the environment world-wide indicates that exposure to persons predicted to be at an exceptionally high risk for developing cryptococcosis (i.e., patients scheduled to receive organ transplants, otherwise healthy HIV^+ persons, and immune competent persons in areas observed to contain *C. gattii*) is inevitable and supports the need for development of a prophylactic and/or therapeutic vaccine that provides broad-spectrum protection against multiple *Cryptococcus* serotypes (9–16, 42). We have previously shown that mice immunized with *C. neoformans* strain H99γ, serotype A, are protected against a subsequent otherwise lethal challenge with wild-type *C. neoformans* strain H99 (25, 36–38, 40, 41, 43–45). Herein, we demonstrate the potential for achieving broad-spectrum protection against multiple clinically relevant strains of *Cryptococcus* serotypes following vaccination with a *Cryptococcus* serotype A strain previously shown to elicit protective immunity against *C. neoformans*. Specifically, we demonstrated that mice immunized with *Cryptococcus* strain H99γ, serotype A, develop significant protection against challenge with serotypes A, B, or D of *Cryptococcus.* Our data are in line with a similar study showing that mice vaccinated with an avirulent chitosan-deficient *C. neoformans* strain also created from a serotype A background strain exhibited significantly delayed mortality when challenged with serotype B *C. gattii* strains R265 or WM276 (34). Altogether, these studies clearly demonstrate that significant cross-protection can be developed following vaccination with a *Cryptococcus* strain of a disparate serotype and provide further proof-of-principle for the development of a prophylactic vaccine that can protect against multiple disparate *Cryptococcus* serotypes.

Both clinical and experimental studies have shown that Th1-type $CD4^+$ T CMI is critical for protection against cryptococcosis (24, 25, 46). We observed a predominantly Th1-type and proinflammatory cytokine profile and increased survival in H99γ immunized mice following challenge with representative *Cryptococcus* serotypes B or D. Additionally, intracellular cytokine staining of $CD4^+$ T cells showed that H99γ immunized mice were capable of eliciting a predominantly Th1-type anamnestic immune response upon subsequent challenge with the other *Cryptococcus* serotypes. These studies indicated that a Th1-type cell-mediated immune response was responsible for the increased survival observed in H99γ immunized mice challenged with *Cryptococcus* strains from serotypes B or D. We also observed increases in some Th2-type cytokines in H99γ immunized mice; however, the overall low levels observed are unlikely to be biologically relevant and were not as significant as the levels observed in HKH99γ immunized mice at day 14 post challenge. These findings do suggest that a Th1-Th2 balance may be important to achieve an optimal host immune response against *Cryptococcus* (47). Additionally, we observed an overall increase in the total number of infiltrating leukocytes in H99γ immunized mice compared to HKH99γ immunized mice challenged with their equivalent serotypes. Dendritic cells are known to play a vital role in the initial response against *C. neoformans* with the ability to phagocytose and kill the fungal organisms (48, 49). The significant increase in the infiltration of $CD11b^+/CD11c^+$ cells in mice given the H99γ immunization prior to challenge with the different serotypes compared to HKH99γ immunized mice correlates with reduced fungal burden in these mice. We did observe an increase in $F4/80^+$ cells in H99γ immunized mice. However, previous studies in our laboratory has demonstrated that quantity of macrophages does not correlate with clearance, rather the ability of $F4/80^+$ cells to polarize to a classically activated, M1 phenotype promotes clearance of *C. neoformans* (36, 41, 43, 50). The increase in infiltrating $Ly6G^+$ cells correlates with significant increases in known neutrophil chemoattractants

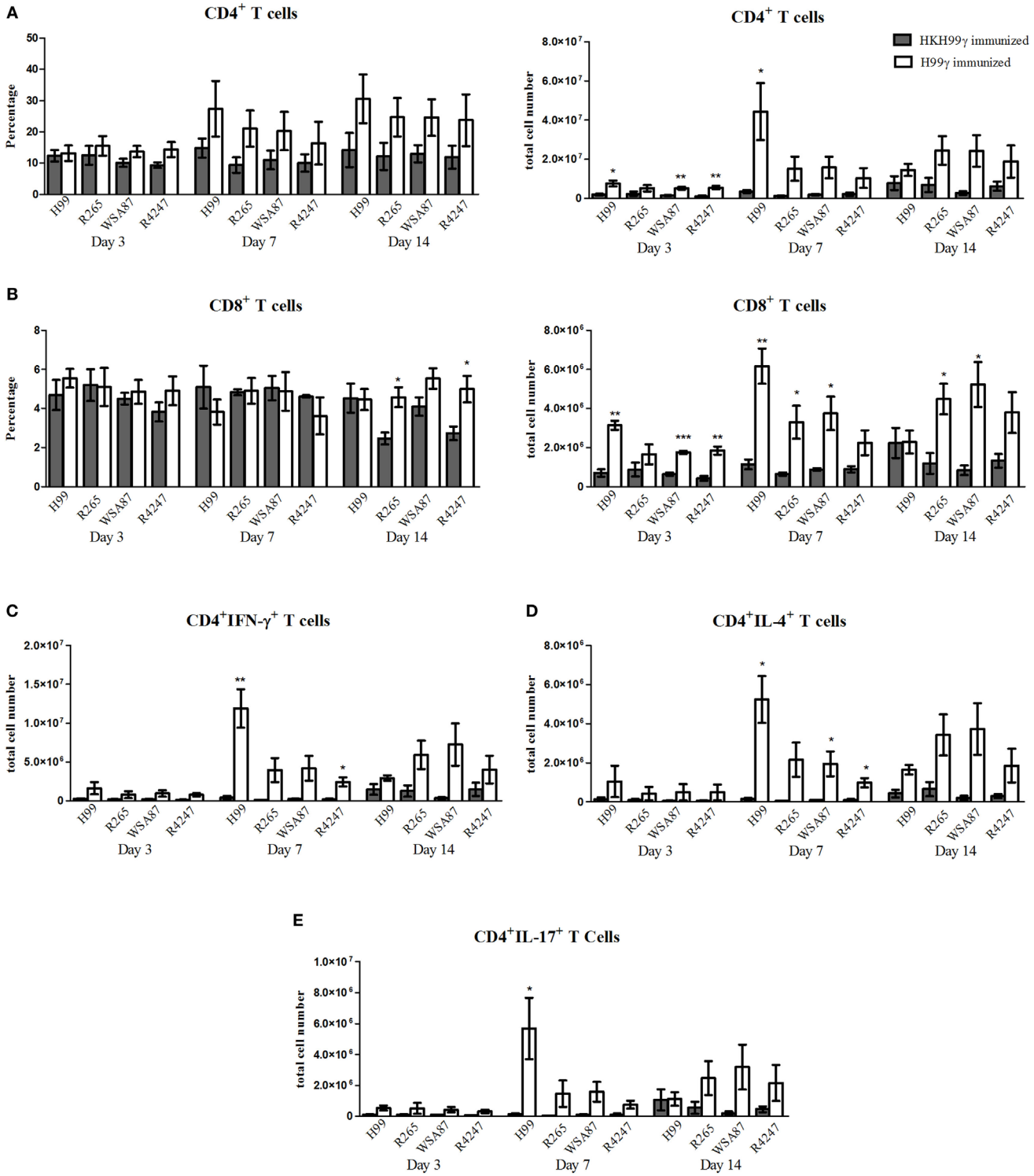

FIGURE 3 | Pulmonary T cell recruitment in immunized mice challenged with disparate serotypes of *Cryptococcus*. BALB/c mice were immunized intranasally with 1×10^4 CFU of either H99γ or HKH99γ, allowed 70 days to resolve the infection, and subsequently challenged with one serotype of *Cryptococcus*. At days 3, 7, and 14 post challenge, lungs were excised, tissues digested, and pulmonary immune cell infiltrates were analyzed by flow cytometry **(A,B)** as described previously in **Figure 2** or further permeabilized to stain for intracellular cytokines **(C–E)**. Data shown are the mean ± SEM of absolute cell numbers or percentage from three independent experiments performed using 4 mice per group per experiment. *$p < 0.05$, **$p < 0.005$, ***$p < 0.0001$. *Significant increase compared to HKH99γ.

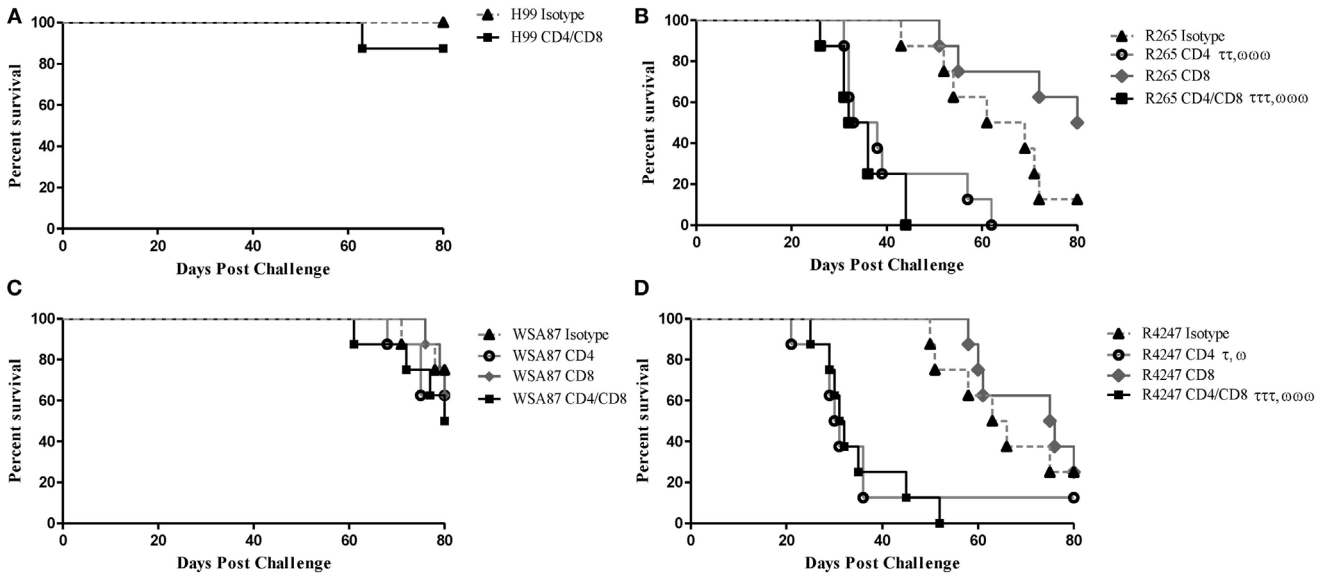

FIGURE 4 | Protection mediated by immunization with *C. neoformans* strain H99γ, serotype A, appears to be predominantly CD4+ T cell-mediated. BALB/c mice were immunized intranasally with 1×10^4 CFU of H99γ and allowed 70 days to rest. Mice were depleted of CD4+ T cells, CD8+ T cells, or both CD4+/CD8+ T cell subsets or received isotype control antibody two days prior to challenge with one serotype of *Cryptococcus* and weekly thereafter during the observation period. Mice were observed for up to 80 d post challenge for survival analysis. Survival data shown are from one experiment each, using 8 mice per group. However, the results are shown for individual groups and mice challenged with H99 **(A)**, R265 **(B)**, WSA87 **(C)** or R4247 **(D)** for simplicity. $^{\tau}p < 0.05$, $^{\tau\tau}p < 0.005$, $^{\tau\tau\tau}p < 0.0001$. τ = significant decrease compared to isotype; $^{\omega}p < 0.05$, $^{\omega\omega}p < 0.005$, $^{\omega\omega\omega}p < 0.0001$. ω = significant decrease compared to CD8+ T cell depleted.

[IL-17A, G-CSF (indirect chemotaxis), and CXCL1/KC] in the H99γ immunized mice (51, 52). However, previous studies from our lab demonstrate that neutrophils are not critical for clearance of *C. neoformans* strain H99 in H99γ immunized mice (44).

The vast majority of patients who acquire cryptococcosis due to *C. neoformans* are severely immunocompromized while those who acquire *C. gattii* infections appear to have little to no known immunodeficiency (53–55). Nonetheless, the protection observed in H99γ immunized mice challenged with serotypes B or D appeared to be CD4+ T cell-dependent. Interestingly, depletion of CD8+ T cells appeared to partially enhance survival in H99γ immunized mice challenged with serotypes B or D. We hypothesize that this additional protection may be attributed to a reduction in putative deleterious CD8+ T cell-mediated inflammatory responses or regulatory function in CD8+ T cell depleted mice challenged with serotypes B or D; however, this hypothesis will need to be confirmed in follow-up studies. In contrast, significant protection was evident in H99γ immunized mice rendered CD4+ and CD8+ T cell deficient and challenged with the serotype A *Cryptococcus* strain, H99. These studies demonstrate that immunization with H99γ produces memory T cells that allow for a rapid response against the invading cryptococcal strain as previously shown in our studies (40). Subtle species-specific differences in an antigen's peptide sequence and/or structure in the different serotypes tested may account for the lack of complete protection observed in our studies. Without the memory T cells present, there is no delay in onset of disease and the CD4+ T cell deficient mice challenged with serotypes B or D succumb to infection at a rate similar to the mice that were immunized with HKH99γ. Recent studies have shown increased protection against *C. neoformans* and *C. gattii* using a vaccine formulation comprised of antigens extracted from capsule or chitosan deficient *Cryptococcus* strains by treatment with an alkaline solution and packaged into GPs (33). The source of antigens for each vaccine formulation was specifically tailored to each challenge (i.e., *C. neoformans* antigens for *C. neoformans* challenge), and thus, the efficacy for the formulations to provide cross-protection was not determined. However, these studies also suggested that the protection induced following immunization with the *Cryptococcus* antigen/GP formulation against *C. neoformans* challenge was dependent on T CMI (33). The protection observed in T cell-deficient, H99γ immunized mice against a subsequent serotype A challenge may be antibody-mediated or may be suggestive of a trained innate cell population that compensates for the lack of T cells. Although we did observe an increase in the total number of B cells in H99γ immunized mice compared to HKH99γ immunized mice on days 7 and 14 post challenge, previous studies from our lab show that B cells are not required for the generation of protective immunity against cryptococcosis in H99γ immunized mice suggesting that antibody-mediated protection in the absence of T cells is unlikely (25). Overall, immunization with H99γ resulted in a non-T cell dependent protective immune response to challenge with a serotype A *Cryptococcus* strain showing that long-term protection in immunocompromized hosts can be generated. However, our results showing that CD4+ T cells are required for the protection observed in H99γ immunized mice challenged with serotypes B and D suggests that a vaccine formulation designed to induce complete protection against multiple *Cryptococcus* serotypes

should include antigens specific to each serotype or contain antigens with significant homology across the serotypes.

Our studies also showed that the serotype C *Cryptococcus* strain used herein, WSA87, is less virulent or remains latent in mice compared to all the other strains tested. When H99γ immunized mice were subsequently challenged with WSA87, we observed a statistically significant increase in immune cell infiltrates at day 7 post challenge compared to HKH99γ immunized mice which correlated with the significant decrease of fungal burden in H99γ immunized mice. However, survival during challenge with serotype C was similar regardless of the immunization strategy most likely due to the initial low virulence of this strain or the strain's ability to remain latent with mice not succumbing to infection until almost day 90 post challenge. Also, depletion of $CD4^+$ and/or $CD8^+$ T cells was observed to have no impact on the survival of H99γ immunized mice challenged with WSA87. The results suggest that WSA87 suppresses T CMI or that protection against WSA87 is not dependent on T CMI. The serotype C strain chosen for this study was a clinical isolate that caused human disease; however, virulence due to this strain appeared to be relatively low in mice. *Cryptococcus* strains of the same serotype are known to exhibit significant variability in virulence within murine models. Thus, it is inappropriate to suggest that the serotypes utilized in our study are completely representative of all *Cryptococcus* strains within their serotype. However, these specific results suggest an unfortunate and perhaps unavoidable reality that developing vaccine formulations that target the more pathogenic *Cryptococcus* strains may still allow for less virulent strains of *Cryptococcus* to slip under the host's immunological radar resulting in disease and mortality.

While no fungal vaccines are clinically available, an ideal vaccine would mirror the results of the currently available vaccines against other microbial pathogens that can protect against multiple serotypes. The quadrivalent meningococcal conjugate vaccine (MenACWY-D; Menactra®, Sanofi Pasteur, Swiftwater, PA, USA), for example, contains polysaccharides from serotypes A, C, Y, and W-135 meningococci conjugated to a diphtheria protein carrier (56) and provides broad-spectrum protection against those serotypes that cause the majority of meningococcal disease. While the studies presented herein determined the efficacy of vaccination with one serotype to provide cross-protection against other serotypes, our results suggest that the identification and inclusion of multiple cross-protective $CD4^+$ T cell-dependent antigens will be critical for the development of a vaccine formulation that elicits broad-spectrum protection against *Cryptococcus* strains that cause the majority of clinical disease. Although much work remains toward the development of a cross-protective cryptococcal vaccine, these studies provide a foundation for understanding the protective host immune response to multiple clinically relevant strains of *Cryptococcus* and the need to identify protective $CD4^+$ T cell epitopes that can be incorporated into a vaccine formulation that provides broad-spectrum protection against cryptococcosis.

ETHICS STATEMENT

This study was carried out in accordance with the recommendations of the Institutional Animal Care and Use Committee (protocol number MU021) of the University of Texas at San Antonio.

AUTHOR CONTRIBUTIONS

FW designed study, performed statistical analysis, interpreted study results, and participated in drafting and editing of manuscript. MD assisted in study design, performed experiments and statistical analysis, participated in interpretation of results, and drafted manuscript. AC, SH, CW, NC-L, CH, and KW performed experiments and statistical analysis, participated in interpretation of results and manuscript revision.

ACKNOWLEDGMENTS

The funders had no role in study design, data collection and analysis, decision to publish, or preparation of the manuscript.

FUNDING

Supported by research grants 2RO1AI071752 (FW) and 2RO1AI071752-08S1 (MD) from the National Institute of Allergy and Infectious Diseases (NIAID) of the National Institutes of Health (NIH) and grant GM060655 (MD) from the National Institute of General Medical Sciences of the NIH.

SUPPLEMENTARY MATERIAL

The Supplementary Material for this article can be found online at http://www.frontiersin.org/article/10.3389/fimmu.2017.01359/full#supplementary-material.

REFERENCES

1. Hagen F, Khayhan K, Theelen B, Kolecka A, Polacheck I, Sionov E, et al. Recognition of seven species in the *Cryptococcus gattii/Cryptococcus neoformans* species complex. *Fungal Genet Biol* (2015) 78:16–48. doi:10.1016/j.fgb.2015.02.009
2. Vibhagool A, Sungkanuparph S, Mootsikapun P, Chetchotisakd P, Tansuphaswaswadikul S, Bowonwatanuwong C, et al. Discontinuation of secondary prophylaxis for cryptococcal meningitis in human immunodeficiency virus-infected patients treated with highly active antiretroviral therapy: a prospective, multicenter, randomized study. *Clin Infect Dis* (2003) 36(10):1329–31. doi:10.1086/374849
3. Rajasingham R, Smith RM, Park BJ, Jarvis JN, Govender NP, Chiller TM, et al. Global burden of disease of HIV-associated cryptococcal meningitis: an updated analysis. *Lancet Infect Dis* (2017) 17(8):873–81. doi:10.1016/S1473-3099(17)30243-8
4. Maziarz EK, Perfect JR. Cryptococcosis. *Infect Dis Clin North Am* (2016) 30(1):179–206. doi:10.1016/j.idc.2015.10.006
5. Perez C, Dolande M, Moya M, Rosello A, de Capriles CR, Landaeta ME, et al. *Cryptococcus neoformans, Cryptococcus gattii*: serotypes in Venezuela. *Mycopathologia* (2008) 166(3):149–53. doi:10.1007/s11046-008-9132-1
6. Kwon-Chung KJ, Bennett JE. Epidemiologic differences between the two varieties of *Cryptococcus neoformans*. *Am J Epidemiol* (1984) 120(1):123–30. doi:10.1093/oxfordjournals.aje.a113861
7. Lizarazo J, Escandon P, Agudelo CI, Firacative C, Meyer W, Castaneda E. Retrospective study of the epidemiology and clinical manifestations of *Cryptococcus gattii* infections in Colombia from 1997-2011. *PLoS Negl Trop Dis* (2014) 8(11):e3272. doi:10.1371/journal.pntd.0003272

8. MacDougall L, Fyfe M, Romney M, Starr M, Galanis E. Risk factors for *Cryptococcus gattii* infection, British Columbia, Canada. *Emerg Infect Dis* (2011) 17(2):193–9. doi:10.3201/eid1702.101020
9. Byrnes EJ, Heitman J. *Cryptococcus gattii* outbreak expands into the Northwestern United States with fatal consequences. *F1000 Biol Rep* (2009) 1:62. doi:10.3410/B1-62
10. Byrnes EJ III, Li W, Lewit Y, Perfect JR, Carter DA, Cox GM, et al. First reported case of *Cryptococcus gattii* in the Southeastern USA: implications for travel-associated acquisition of an emerging pathogen. *PLoS One* (2009) 4(6):e5851. doi:10.1371/journal.pone.0005851
11. Datta K, Bartlett KH, Baer R, Byrnes E, Galanis E, Heitman J, et al. Spread of *Cryptococcus gattii* into pacific northwest region of the United States. *Emerg Infect Dis* (2009) 15(8):1185–91. doi:10.3201/eid1508.081384
12. Datta K, Bartlett KH, Marr KA. *Cryptococcus gattii*: emergence in Western North America: exploitation of a novel ecological niche. *Interdiscip Perspect Infect Dis* (2009) 2009:176532. doi:10.1155/2009/176532
13. Galanis E, Macdougall L, Kidd S, Morshed M; British Columbia Cryptococcus gattii Working Group. Epidemiology of *Cryptococcus gattii*, British Columbia, Canada, 1999-2007. *Emerg Infect Dis* (2010) 16(2):251–7. doi:10.3201/eid1602.090900
14. Hagen F, Colom MF, Swinne D, Tintelnot K, Iatta R, Montagna MT, et al. Autochthonous and dormant *Cryptococcus gattii* infections in Europe. *Emerg Infect Dis* (2012) 18(10):1618–24. doi:10.3201/eid1810.120068
15. McCulloh RJ, Phillips R, Perfect JR, Byrnes EJ III, Heitman J, Dufort E. *Cryptococcus gattii* genotype VGI infection in New England. *Pediatr Infect Dis J* (2011) 30(12):1111–4. doi:10.1097/INF.0b013e31822d14fd
16. Walraven CJ, Gerstein W, Hardison SE, Wormley F, Lockhart SR, Harris JR, et al. Fatal disseminated *Cryptococcus gattii* infection in New Mexico. *PLoS One* (2011) 6(12):e28625. doi:10.1371/journal.pone.0028625
17. Kwon-Chung KJ, Fraser JA, Doering TL, Wang Z, Janbon G, Idnurm A, et al. *Cryptococcus neoformans* and *Cryptococcus gattii*, the etiologic agents of cryptococcosis. *Cold Spring Harb Perspect Med* (2014) 4(7):a019760. doi:10.1101/cshperspect.a019760
18. Chen SC, Slavin MA, Heath CH, Playford EG, Byth K, Marriott D, et al. Clinical manifestations of *Cryptococcus gattii* infection: determinants of neurological sequelae and death. *Clin Infect Dis* (2012) 55(6):789–98. doi:10.1093/cid/cis529
19. Ngamskulrungroj P, Chang Y, Sionov E, Kwon-Chung KJ. The primary target organ of *Cryptococcus gattii* is different from that of *Cryptococcus neoformans* in a murine model. *mBio* (2012) 3(3):e00103-12. doi:10.1128/mBio.00103-12
20. Speed B, Dunt D. Clinical and host differences between infections with the two varieties of *Cryptococcus neoformans*. *Clin Infect Dis* (1995) 21(1):28–34; discussion 5–6. doi:10.1093/clinids/21.1.28
21. Lomes NR, Melhem MS, Szeszs MW, Martins Mdos A, Buccheri R. Cryptococcosis in non-HIV/non-transplant patients: a Brazilian case series. *Med Mycol* (2016) 54(7):669–76. doi:10.1093/mmy/myw021
22. Mitchell DH, Sorrell TC, Allworth AM, Heath CH, McGregor AR, Papanaoum K, et al. Cryptococcal disease of the CNS in immunocompetent hosts: influence of cryptococcal variety on clinical manifestations and outcome. *Clin Infect Dis* (1995) 20(3):611–6. doi:10.1093/clinids/20.3.611
23. Perfect JR, Cox GM. Drug resistance in *Cryptococcus neoformans*. *Drug Resist Updat* (1999) 2(4):259–69. doi:10.1054/drup.1999.0090
24. Olszewski MA, Zhang Y, Huffnagle GB. Mechanisms of cryptococcal virulence and persistence. *Future Microbiol* (2010) 5(8):1269–88. doi:10.2217/fmb.10.93
25. Wozniak KL, Ravi S, Macias S, Young ML, Olszewski MA, Steele C, et al. Insights into the mechanisms of protective immunity against *Cryptococcus neoformans* infection using a mouse model of pulmonary cryptococcosis. *PLoS One* (2009) 4(9):e6854. doi:10.1371/journal.pone.0006854
26. Angkasekwinai P, Sringkarin N, Supasorn O, Fungkrajai M, Wang YH, Chayakulkeeree M, et al. *Cryptococcus gattii* infection dampens Th1 and Th17 responses by attenuating dendritic cell function and pulmonary chemokine expression in the immunocompetent hosts. *Infect Immun* (2014) 82(9):3880–90. doi:10.1128/IAI.01773-14
27. Cheng PY, Sham A, Kronstad JW. Cryptococcus gattii isolates from the British Columbia cryptococcosis outbreak induce less protective inflammation in a murine model of infection than *Cryptococcus neoformans*. *Infect Immun* (2009) 77(10):4284–94. doi:10.1128/IAI.00628-09
28. Dong ZM, Murphy JW. Effects of the two varieties of *Cryptococcus neoformans* cells and culture filtrate antigens on neutrophil locomotion. *Infect Immun* (1995) 63(7):2632–44.
29. Huston SM, Li SS, Stack D, Timm-McCann M, Jones GJ, Islam A, et al. *Cryptococcus gattii* is killed by dendritic cells, but evades adaptive immunity by failing to induce dendritic cell maturation. *J Immunol* (2013) 191(1):249–61. doi:10.4049/jimmunol.1202707
30. Wright L, Bubb W, Davidson J, Santangelo R, Krockenberger M, Himmelreich U, et al. Metabolites released by *Cryptococcus neoformans* var. *neoformans* and var. *gattii* differentially affect human neutrophil function. *Microbes Infect* (2002) 4(14):1427–38. doi:10.1016/S1286-4579(02)00024-2
31. Urai M, Kaneko Y, Ueno K, Okubo Y, Aizawa T, Fukazawa H, et al. Evasion of innate immune responses by the highly virulent *Cryptococcus gattii* by altering capsule glucuronoxylomannan structure. *Front Cell Infect Microbiol* (2015) 5:101. doi:10.3389/fcimb.2015.00101
32. Hole CR, Wormley FL Jr. Vaccine and immunotherapeutic approaches for the prevention of cryptococcosis: lessons learned from animal models. *Frontiers Microbiol* (2012) 3:291. doi:10.3389/fmicb.2012.00291
33. Specht CA, Lee CK, Huang H, Tipper DJ, Shen ZT, Lodge JK, et al. Protection against experimental cryptococcosis following vaccination with glucan particles containing *Cryptococcus* alkaline extracts. *mBio* (2015) 6(6):e1905–15. doi:10.1128/mBio.01905-15
34. Upadhya R, Lam WC, Maybruck B, Specht CA, Levitz SM, Lodge JK. Induction of protective immunity to cryptococcal infection in mice by a heat-killed, chitosan-deficient strain of *Cryptococcus neoformans*. *mBio* (2016) 7(3):e00547-16. doi:10.1128/mBio.00547-16
35. Rella A, Mor V, Farnoud AM, Singh A, Shamseddine AA, Ivanova E, et al. Role of sterylglucosidase 1 (Sgl1) on the pathogenicity of *Cryptococcus neoformans*: potential applications for vaccine development. *Frontiers Microbiol* (2015) 6:836. doi:10.3389/fmicb.2015.00836
36. Hardison SE, Herrera G, Young ML, Hole CR, Wozniak KL, Wormley FL Jr. Protective immunity against pulmonary cryptococcosis is associated with STAT1-mediated classical macrophage activation. *J Immunol* (2012) 189(8):4060–8. doi:10.4049/jimmunol.1103455
37. Hardison SE, Ravi S, Wozniak KL, Young ML, Olszewski MA, Wormley FL Jr. Pulmonary infection with an interferon-gamma-producing *Cryptococcus neoformans* strain results in classical macrophage activation and protection. *Am J Pathol* (2010) 176(2):774–85. doi:10.2353/ajpath.2010.090634
38. Wormley FL Jr, Perfect JR, Steele C, Cox GM. Protection against cryptococcosis by using a murine gamma interferon-producing *Cryptococcus neoformans* strain. *Infect Immun* (2007) 75(3):1453–62. doi:10.1128/IAI.00274-06
39. Wozniak KL, Hardison S, Olszewski M, Wormley FL Jr. Induction of protective immunity against cryptococcosis. *Mycopathologia* (2012) 173(5–6):387–94. doi:10.1007/s11046-011-9505-8
40. Wozniak KL, Young ML, Wormley FL Jr. Protective immunity against experimental pulmonary cryptococcosis in T cell-depleted mice. *Clin Vaccine Immunol* (2011) 18(5):717–23. doi:10.1128/CVI.00036-11
41. Leopold Wager CM, Hole CR, Wozniak KL, Olszewski MA, Mueller M, Wormley FL Jr. STAT1 signaling within macrophages is required for antifungal activity against *Cryptococcus neoformans*. *Infect Immun* (2015) 83(12):4513–27. doi:10.1128/IAI.00935-15
42. Park BJ, Wannemuehler KA, Marston BJ, Govender N, Pappas PG, Chiller TM. Estimation of the current global burden of cryptococcal meningitis among persons living with HIV/AIDS. *AIDS* (2009) 23(4):525–30. doi:10.1097/QAD.0b013e328322ffac
43. Leopold Wager CM, Hole CR, Wozniak KL, Olszewski MA, Wormley FL Jr. STAT1 signaling is essential for protection against *Cryptococcus neoformans* infection in mice. *J Immunol* (2014) 193(8):4060–71. doi:10.4049/jimmunol.1400318
44. Wozniak KL, Kolls JK, Wormley FL Jr. Depletion of neutrophils in a protective model of pulmonary cryptococcosis results in increased IL-17A production by gammadelta T cells. *BMC Immunol* (2012) 13:65. doi:10.1186/1471-2172-13-65
45. Wozniak KL, Hardison SE, Kolls JK, Wormley FL. Role of IL-17A on resolution of pulmonary *C. neoformans* infection. *PLoS One* (2011) 6(2):e17204. doi:10.1371/journal.pone.0017204
46. Chaturvedi AK, Wormley FL Jr. *Cryptococcus* antigens and immune responses: implications for a vaccine. *Expert Rev Vaccines* (2013) 12(11):1261–72. doi:10.1586/14760584.2013.840094

47. Koguchi Y, Kawakami K. Cryptococcal infection and Th1-Th2 cytokine balance. *Int Rev Immunol* (2002) 21(4–5):423–38. doi:10.1080/08830180213274
48. Osterholzer JJ, Milam JE, Chen GH, Toews GB, Huffnagle GB, Olszewski MA. Role of dendritic cells and alveolar macrophages in regulating early host defense against pulmonary infection with *Cryptococcus neoformans*. *Infect Immun* (2009) 77(9):3749–58. doi:10.1128/IAI.00454-09
49. Wozniak KL, Levitz SM. *Cryptococcus neoformans* enters the endolysosomal pathway of dendritic cells and is killed by lysosomal components. *Infect Immun* (2008) 76(10):4764–71. doi:10.1128/IAI.00660-08
50. Arora S, Olszewski MA, Tsang TM, McDonald RA, Toews GB, Huffnagle GB. Effect of cytokine interplay on macrophage polarization during chronic pulmonary infection with *Cryptococcus neoformans*. *Infect Immun* (2011) 79(5):1915–26. doi:10.1128/IAI.01270-10
51. Mellett M, Atzei P, Horgan A, Hams E, Floss T, Wurst W, et al. Orphan receptor IL-17RD tunes IL-17A signalling and is required for neutrophilia. *Nat Commun* (2012) 3:1119. doi:10.1038/ncomms2127
52. Yong KL. Granulocyte colony-stimulating factor (G-CSF) increases neutrophil migration across vascular endothelium independent of an effect on adhesion: comparison with granulocyte-macrophage colony-stimulating factor (GM-CSF). *Br J Haematol* (1996) 94(1):40–7. doi:10.1046/j.1365-2141.1996.d01-1752.x
53. Chen SC-A, Meyer W, Sorrell TC. *Cryptococcus gattii* infections. *Clin Microbiol Rev* (2014) 27(4):980–1024. doi:10.1128/cmr.00126-13
54. Rosen LB, Freeman AF, Yang LM, Jutivorakool K, Olivier KN, Angkasekwinai N, et al. Anti-GM-CSF autoantibodies in patients with cryptococcal meningitis. *J Immunol* (2013) 190(8):3959–66. doi:10.4049/jimmunol.1202526
55. Saijo T, Chen J, Chen SC, Rosen LB, Yi J, Sorrell TC, et al. Anti-granulocyte-macrophage colony-stimulating factor autoantibodies are a risk factor for central nervous system infection by *Cryptococcus gattii* in otherwise immunocompetent patients. *mBio* (2014) 5(2):e912–4. doi:10.1128/mBio.00912-14
56. Pace D, Pollard AJ, Messonier NE. Quadrivalent meningococcal conjugate vaccines. *Vaccine* (2009) 27(Suppl 2):B30–41. doi:10.1016/j.vaccine.2009.05.003

Conflict of Interest Statement: The authors declare that the research was conducted in the absence of any commercial or financial relationships that could be construed as a potential conflict of interest.

Copyright © 2017 Van Dyke, Chaturvedi, Hardison, Leopold Wager, Castro-Lopez, Hole, Wozniak and Wormley. This is an open-access article distributed under the terms of the Creative Commons Attribution License (CC BY). The use, distribution or reproduction in other forums is permitted, provided the original author(s) or licensor are credited and that the original publication in this journal is cited, in accordance with accepted academic practice. No use, distribution or reproduction is permitted which does not comply with these terms.

frontiers in Immunology

REVIEW
published: 27 April 2018
doi: 10.3389/fimmu.2018.00897

The Elusive Anti-*Candida* Vaccine: Lessons From the Past and Opportunities for the Future

*Gloria Hoi Wan Tso†, Jose Antonio Reales-Calderon† and Norman Pavelka**

*Singapore Immunology Network (SIgN), Agency of Science, Technology and Research (A*STAR), Singapore, Singapore*

Candidemia is a bloodstream fungal infection caused by *Candida* species and is most commonly observed in hospitalized patients. Even with proper antifungal drug treatment, mortality rates remain high at 40–50%. Therefore, prophylactic or preemptive antifungal medications are currently recommended in order to prevent infections in high-risk patients. Moreover, the majority of women experience at least one episode of vulvovaginal candidiasis (VVC) throughout their lifetime and many of them suffer from recurrent VVC (RVVC) with frequent relapses for the rest of their lives. While there currently exists no definitive cure, the only available treatment for RVVC is again represented by antifungal drug therapy. However, due to the limited number of existing antifungal drugs, their associated side effects and the increasing occurrence of drug resistance, other approaches are greatly needed. An obvious prevention measure for candidemia or RVVC relapse would be to immunize at-risk patients with a vaccine effective against *Candida* infections. In spite of the advanced and proven techniques successfully applied to the development of antibacterial or antiviral vaccines, however, no antifungal vaccine is still available on the market. In this review, we first summarize various efforts to date in the development of anti-*Candida* vaccines, highlighting advantages and disadvantages of each strategy. We next unfold and discuss general hurdles encountered along these efforts, such as the existence of large genomic variation and phenotypic plasticity across *Candida* strains and species, and the difficulty in mounting protective immune responses in immunocompromised or immunosuppressed patients. Lastly, we review the concept of "trained immunity" and discuss how induction of this rapid and nonspecific immune response may potentially open new and alternative preventive strategies against opportunistic infections by *Candida* species and potentially other pathogens.

Keywords: *Candida*, candidemia, candidiasis, vaccine, trained immunity, opportunistic infections, immunocompromised patients

OPEN ACCESS

Edited by:
Steven Templeton, Indiana University School of Medicine-Terre Haute, United States

Reviewed by:
Jeniel E. Nett, University of Wisconsin-Madison, United States
Rebecca Drummond, National Institutes of Health (NIH), United States

****Correspondence:***
Norman Pavelka
norman_pavelka@immunol.a-star.edu.sg

†These authors have contributed equally as first authors.

Specialty section:
This article was submitted to Microbial Immunology, a section of the journal Frontiers in Immunology

Received: *15 February 2018*
Accepted: *11 April 2018*
Published: *27 April 2018*

Citation:
Tso GHW, Reales-Calderon JA and Pavelka N (2018) The Elusive Anti-Candida Vaccine: Lessons From the Past and Opportunities for the Future. Front. Immunol. 9:897. doi: 10.3389/fimmu.2018.00897

INTRODUCTION

Due to advances in medicine and surgery, over the past century there has been a rising population of immunocompromised patients, which are at an elevated risk to suffer from opportunistic infections (1, 2). While hospital-acquired fungal infections are less frequent than bacterial ones, they disproportionately account for higher mortality rates, longer hospitalization times and increased healthcare costs (3). Risk factors for fungal infections are very broad and nonspecific, and they include chronic respiratory disease, cancer, HIV infection, organ transplantation, neutropenia, presence of central venous catheters, prolonged hospital stay, administration of total parenteral nutrition, exposure to invasive procedures, chemotherapy, hemodialysis, gastric acid suppression,

and use of broad-spectrum antibiotics (4, 5). Candidiasis (caused by *Candida* species) is the most common opportunistic fungal infection and the fourth most common nosocomial bloodstream infection (6, 7). Despite the best available standards of care, the incidence of candidemia, a sign of invasive or systemic candidiasis, is on the rise in the US (8) and mortality rates often exceed 50% despite use of antifungal drugs (9). This is especially true in intensive care units and in immunocompromised patients, where *Candida* bloodstream infections are estimated to strike ~400,000 patients a year, with an associated mortality of 46–75% (10). For all these reasons, and because the hospitalization and treatment cost of these patients is very high (3, 11), CDC guidelines recommend prophylactic or preemptive antifungal treatment in patients considered at high risk of candidemia (12).

Mucosal fungal infections, though almost never life-threatening, are much more common than invasive ones and can be associated with high morbidity, socioeconomic impact, and low quality of life. The most common infection sites are the oral cavity and the genitourinary tract (13). Vulvovaginal candidiasis (VVC) is the most common mucosal fungal infection, with different studies estimating that 50–70% of women suffer an episode of VVC at least once in their lifetime and 5–8% of women suffer from recurrent VVC (RVVC) (14). To this date, there still exists no definitive cure for RVVC, which is commonly treated with over-the-counter antifungal medications but continues to relapse ≥4 times a year for the rest of a woman's life (15).

Antifungal agents available for the treatment of systemic or mucosal candidiasis are restricted to only a few classes of compounds, such as azoles, polyenes, allylamines, and echinocandins (16). However, adverse side effects, toxicity, and emergence of drug resistance limit the use of these drugs (10). In particular, various *Candida* species can acquire resistance to different antifungals or, even worse, to more than one drug (17–20). In fact, the emergence of drug resistance in *Candida* spp. has been on a growing trend over the past decade (21), with multidrug-resistant *Candida* spp. now being reported all over the world (22, 23). Finally, the recent discovery of a novel multidrug resistant species of *Candida* (*C. auris*) poses a further threat to our ability to use antifungal drugs to treat candidiasis (24).

To reduce the incidence and mortality of opportunistic fungal infections, experts agree that we need (i) improved diagnostics to allow more rapid implementation of appropriate therapies, (ii) more effective antifungal agents associated with less severe side effects, and (iii) to develop immunotherapies based on our mounting knowledge of antifungal immunity (10, 25). These same strategies could be used also to reduce the recurrence and severity of RVVC episodes. We hereby argue that an anti-*Candida* vaccine, as long as it was effective in the populations of patients it is intended to protect, could help reduce the global burden of both systemic and vaginal candidiasis bringing about substantial socioeconomic benefits.

In this review, we first provide an up-to-date overview of various efforts that have been attempted so far in the quest of an anti-*Candida* vaccine, which has remained elusive. We next critically assess potential common problems that might have hindered such efforts and finally propose a few tentative solutions to overcoming those problems.

CURRENT ANTI-*CANDIDA* VACCINE LANDSCAPE

In the last decades, several different anti-*Candida* vaccines have been proposed but only few of them have been tested in clinical trials (**Table 1**). Here, we will summarize the current anti-*Candida* vaccine landscape and discuss advantages and disadvantages of each vaccination strategy.

TABLE 1 | Summary of past and current anti-*Candida* vaccine candidates.

Vaccine category	Description	Clinical trial stage	Protection (*C. albicans* infection site)	Cross-protection (non-*C. albicans* organisms)	Reference
LA	Hyphal-defective *C. albicans* strain PCA-2		SYS	*Staphylococcus aureus*	(26)
LA	MAP kinase-defective *hog1*Δ *C. albicans* strain CNC13		SYS		(27)
LA	Cell wall-defective *ecm33*Δ *C. albicans* strain RML2U		SYS		(28)
LA	Filamentation-repressible *C. albicans* strain tet-NRG1		SYS		(29)
LA	Yeast-locked *C. albicans* strain *cph1*Δ/*efg1*Δ		SYS		(30)
LA	Heat-killed or live *Saccharomyces cerevisiae* clinical strains		SYS	*Aspergillus fumigatus, Cryptococcus grubii, and Coccidioides posadasii*	(31–34)
REC	Recombinant N-terminus of *C. albicans* Als1p		SYS, VAG, OR		(35, 36)
REC	Recombinant N-terminus of *C. albicans* Als3p		SYS, VAG	*S. aureus*	(37, 38)
REC	Recombinant N-terminus of *C. albicans* Als3p plus alum adjuvant (NDV-3)	Phase II	SYS, VAG	*S. aureus*	(39)
REC	Recombinant *C. albicans* Sap2p		VAG		(40)
REC	Recombinant *C. albicans* Sap2p (PEV-7)	Phase I	VAG		(41)
REC	Recombinant *C. albicans* Hsp90p (Mycograb)		SYS		(42)
REC	Recombinant *C. albicans* Hyr1p		SYS	*C. glabrata, C. krusei, C. parapsilosis and C. tropicalis*	(43)
EX	Crude cell wall extract		SYS		(44)
GC	Mannans and peptide conjugates		SYS		(45, 46)
GC	β-glucan conjugated with MF59 adjuvant		VAG		(47)
GC	Laminarin conjugated with diphtheria toxoid (Lam-CRM197)		SYS, VAG	*A. fumigatus*	(48)

LA, live attenuated; REC, recombinant; EX, extract; GC, glycoconjugate; SYS, systemic; VAG, vaginal; OR, oral.

Historically, vaccines are developed to boost antigen-specific immune responses and elicit protective immunological memory against specific pathogenic strains. In the case of *Candida* species, most of the efforts have been focused around the most common species, *C. albicans*. Different strategies have been used to immunize hosts against candidiasis: (i) live-attenuated strains, (ii) recombinant proteins, and (iii) glycoconjugates.

Live-Attenuated Vaccines

The first ever reported vaccine, Edward Jenner's famous vaccinia virus, was a live virus causing cowpox in cattle but protecting humans against smallpox (49). By all definitions, it was a live-attenuated vaccine, which caused only a very mild form of the disease in humans while at the same time raising long-lasting protective immune memory. Up to this date, most currently available antiviral vaccines (e.g., yellow fever, measles, varicella) and some antibacterial ones (e.g., BCG) are essentially live-attenuated versions of their pathogenic counterparts. Because of this long history of success, it is not surprising that several studies have ascribed various attenuated strains of *C. albicans* the ability to confer protection against candidiasis.

The morphogenetic transition between the conidial (yeast) and hyphal (filamentous) form is one of the most important virulence factors in *C. albicans* (50); for this reason, the absence of filamentation is a common characteristic of attenuated strains of this species. Several *C. albicans* mutants associated with no or low virulence, including PCA-2 (incapable of yeast-hyphae conversion), CNC13 (deleted in the MAP kinase *HOG1*), RML2U [deleted in the cell wall protein (CWP) gene *ECM33*], and tet-NRG1 (in which the filamentation repressor *NRG1* can be overexpressed by doxycycline), have been used to immunize mice and shown to protect them from a subsequent lethal systemic infection with a virulent strain (26–29). Also, the *C. albicans* double-mutant *cph1*/*efg1*, which is severely impaired in hyphal morphogenesis, partially protects mice from systemic infection by a wild-type *C. albicans* strain (30).

Not only *C. albicans* attenuated strains have been used to protect against systemic candidiasis, but also the generally regarded-as-safe baker's yeast *Saccharomyces cerevisiae* has been successfully used to this end. Stevens and colleagues have described the use of heat-killed or live *S. cerevisiae* as a protective vaccine against *C. albicans* infection, but also against *A. fumigatus*, *Cryptococcus grubii*, and *Coccidioides* infection in a dose-dependent manner (31–34).

Despite these success stories at the basic research level, none of these vaccine candidates has progressed to clinical trials. Possible reasons include the fact that characterization of these strains is complex, that the stability of the virulence-attenuating mutations is not guaranteed, and that the use of live-attenuated vaccines is currently not recommended in immunocompromised patients due to their weaker immune defense and the higher probability to develop a disease.

Recombinant Proteins

In contrast to live *Candida* vaccines (how attenuated they may be), recombinant vaccines are generally perceived as potentially safer to the human host, because they do not contain any infectious agent. This characteristic makes recombinant protein vaccines more suitable especially for the immunocompromised individuals that would most benefit from such a vaccine. In general, this strategy has focused on proteins expressed on the surface of the fungus, such as CWPs or adhesion proteins, to ensure that epitopes would be easily accessible and "visible" by the immune system. Efforts also often concentrated on proteins critical to virulence, such as hyphal-specific effectors, in order to mount immune responses specifically against the pathogenic forms of the fungus. Besides, current work has shown that the strongest adaptive immune memory responses are often directed toward hyphal-associated proteins.

Agglutinin-Like Sequence Proteins

Agglutinin-like sequence (Als) proteins are located at the surface of *C. albicans* and play important roles in the adhesion to human endothelial cells and in the development of invasive candidiasis (51). Because these proteins are both exposed on the fungal surface and important for invasion of host cells, several vaccines have been proposed against invasive candidiasis using recombinant versions of various Als proteins, including Als1p and Als3p, formulated with or without adjuvants.

The recombinant N-terminus of Als1 (rAls1p-N) was produced and purified from *S. cerevisiae* and used in combination with Complete Freund's Adjuvant (CFA) subcutaneously and boosted with different doses of rAls1p-N with Incomplete Freund's Adjuvant (IFA) at day 21 post-immunization; lethal challenge with live *C. albicans* showed a survival rate of 50–57% and a decrease in fungal burden (36). This vaccine was deemed effective and improved survival in both immunocompetent and neutropenic mice and in murine models of oropharyngeal candidiasis and *Candida* vaginitis (35).

Vaccination with the recombinant N-terminus of Als3 (rAls3p-N) induced a stronger antibody response and survival rate compared with the rAls1p-N vaccine, and was more effective than rAls1p-N in the murine model of oropharyngeal and vaginal candidiasis (37). Interestingly, it showed also protection against *S. aureus* infection (38), suggesting the existence of shared immune epitopes between these distantly related species; consistently, *Candida* Als3p is structurally similar to a clumping factor of *S. aureus* (52).

Bar et al. identified an antigenic peptide by immunoproteomic approaches called pAls, widely conserved in many non-*Candida* species; this epitope mediates T-cell-dependent protection from invasive candidiasis. This pAls epitope is found in the Als3 protein and the authors suggest an implication of this epitope in the protective effect of the Als3 vaccine (53).

NDV-3A, a rAls3p-N vaccine formulated with Alhydrogel adjuvant, has been tested in a phase-I clinical trial. The trial was performed on 40 healthy volunteers and showed an increase in antibody titers at two different doses, as well as increased cytokine responses and IgG and IgA_1 titers in the revaccinated subjects (39). A few adverse events have been described, but overall the vaccine was well tolerated by the subjects and hence the results were deemed as promising. Like the version of rAls3p-N vaccine without adjuvant, NDV-3 also showed activity against *S. aureus* infection, further corroborating the idea that the vaccination with *Candida* antigens containing epitope homologs found in other

organisms can be harnessed to generate "convergent immunity." NDV-3A is now in a phase-II clinical trial to test the immunotherapeutic effect of the vaccine in women with RVVC.[1]

Secreted Aspartil Proteases

Secreted Aspartil Proteases (SAP) constitute a family of 10 proteins secreted by *C. albicans*, which are required for adhesion, epithelial, and endothelial invasion and fungal cell metabolism (54, 55). Sap2p is the most abundantly expressed SAP in *C. albicans* and its recombinant form has been used to immunize rats intravaginally or intranasally, either using cholera toxin as an adjuvant or without an adjuvant; the vaccination resulted in the clearance of the *Candida* vaginal infection (40). The same research group also developed PEV7, a truncated version of Sap2p (amino acids 77–400) incorporated into the lipid bilayer of influenza virosomes. Because preclinical data demonstrated that intramuscularly vaccinated rats showed protection against vaginal candidiasis (41), PEV7 has progressed to clinical trials as a therapeutic vaccine for the treatment of RVVC. In a randomized phase-I trial, the subjects, whether immunized *via* intramuscular injections or by intravaginal capsules, showed a strong B-cell-mediated immune response in vaginal and cervical samples. All volunteers showed a mucosal immune response with consistently high titers across the groups, the response was dose-dependent and no serious adverse events were reported.[2]

Heat Shock Protein 90 (Hsp90p)

Heat shock protein 90 is a highly conserved stress-induced chaperone, with key functions in setting cellular responses to stressful stimuli, which is indispensable for yeast viability and located in the cell wall of *C. albicans*. The 47-kDa carboxyl fragment of *C. albicans* Hsp90 had been identified as a *Candida* antigen in different studies (56). This antigen is very abundant and immunogenic, and the presence of antibodies against Hsp90 correlates with good prognosis, whereas low levels are associated with mortality (57). Various Hsp90 epitopes (LSREM, LKVIRK, and DEPAGE) have been identified using a phage-display library and shown to induce Hsp90-specific serum antibodies and to prolong survival in a mouse model of systemic candidiasis (42). A recombinant protein called Mycograb, consisting of cross-linked Hsp90 NKILKVIRKNIVKK peptide-binding variable domains of human antibody heavy and light chains, was constructed and expressed in *Escherichia coli*. When combined with amphotericin B, Mycograb produced significant improvement in patients with invasive candidiasis (58, 59). However, the drug was refused by the European Medicines Agency on the grounds of product safety and quality, and its ability to potentiate the effects of amphotericin B were later found to be non Hsp90-specific (60).

Hyphally Regulated Proteins

Hyphally regulated 1 (Hyr1) is a glycosyl phosphatidylinositol (GPI)-anchor mannoprotein that is expressed during hyphal formation on the cell wall of *C. albicans*. A recombinant version of the N-terminus of Hyr1 (rHyr1p-N) was produced in *E. coli* and used to immunize mice *via* subcutaneous injection with either CFA or aluminum hydroxide and boosted on day 21 with IFA. After 2 weeks, vaccinated mice were challenged with a lethal dose of *C. albicans* and non-albicans *Candida* (NAC) species. The vaccine was effective against infections by *C. albicans*, *C. glabrata, C. krusei*, *C. parapsilosis*, and *C. tropicalis* in both immunocompetent and neutropenic mice (43).

CWP Extracts

Not only purified recombinant proteins, but also crude *C. albicans* cell wall extracts, seem to be effective to protect against invasive candidiasis. In fact, subcutaneous immunization with β-mercaptoethanol-extracted *C. albicans* CWPs in combination with Ribi Adjuvant System (RAS) R-700 followed by a booster injected 21 days after the first immunization, conferred protection in 75% of immunized mice after a lethal challenge with *C. albicans* (44). However, such crude preparations are unlikely to progress to clinical trials due to the difficulty in characterizing and standardizing such complex vaccine formulations.

Glycoconjugates

An alternative to protein-based vaccines is to use glycans commonly found in fungal cell walls but absent in host cells. In fact, the *Candida* cell wall represents a hub of pathogen-associated molecular pattern (PAMP)–pathogen recognition receptor (PRR) interactions that dictate downstream immune responses (61). For these reasons, various cell wall polysaccharides have been tested as vaccine targets against systemic candidiasis.

Mannans and Derivative Peptide Conjugates

Mannans are polymers of *O*-linked or *N*-linked mannosides attached to CWPs and constitute the outermost, and hence most accessible, layer of the *C. albicans* cell wall. While *O*-mannans are predominately recognized by TLR4 (62), *N*-mannans are recognized by a multitude of receptors, including the Mannose Receptor (MR), DC-SIGN, Dectin-2, Galectin-3, and Mincle (63). Classically, *Candida* mannans have been attributed immunesuppressive properties (64); but the discovery that *N*-linked mannans are critically required for recognition by DC-SIGN and MR on human dendritic cells (DCs) has established a rational for conjugating them to antigenic peptides. Consistent with this idea, mannosylated antigens were shown to be presented more effectively than non-mannosylated forms (65).

In one example, researchers have used computational epitope searches to select 6 peptides in *C. albicans* CWPs (fructose-bisphosphate aldolase; methyltetrahydropteroyltriglutamate; hyphal wall protein-1; enolase; glyceraldehyde-3-phosphate dehydrogenase; and phosphoglycerate kinase) and conjugated these peptides with β-mannans to generate the first series of fully synthetic glycopeptide vaccines against systemic candidiasis. Depending on the specific peptide, the immunized mice showed 80–100% survival and reduced kidney fungal burden after the challenge with *C. albicans* (45).

More recent studies showed than the vaccination with BSA-based conjugates bearing synthetic α-1,6-branched oligomannosides induced humoral responses in mice and induced production of potentially protective antibodies (46). Immunization with

[1]https://www.clinicaltrials.gov/ct2/show/NCT01926028 (Accessed: April 17, 2018).
[2]https://www.clinicaltrials.gov/ct2/show/NCT01067131 (Accessed: April 17, 2018).

Candida mannan-derived branched 3,6-di-*O*-substituted α-oligomannosides conjugated to BSA (M5-BSA and M6-BSA conjugates) induced similar levels of $CD19^+$ B lymphocytes, but the candidacidal activity of polymorphonuclear leukocytes induced by opsonization with M6-BSA antisera was higher than that with M5-BSA, thus revealing some important differences in their ability to induce an effective and protective immune response against *Candida* infection (66). A better mechanistic understanding of the type of immune responses elicited by various *Candida* mannans is therefore required before these compounds can progress to clinical studies.

β-Glucan and Derivative Conjugate Vaccines

Directly underneath mannans lies a hidden layer of β-glucans, which is an essential component of the *Candida* cell wall (67) and elicits Dectin-1-dependent innate immune responses that are critical for host protection against fungi (68). Moreover, β-glucans from the *C. albicans* cell wall are highly immunogenic, leading to epigenetic and metabolic reprogramming of monocytes/macrophages, elevated cytokine responses and to innate host protection against systemic candidiasis (69–71). This phenomenon was termed "trained immunity" (72) and is discussed further in Section "Trained Immunity—Toward the Next Generation of Vaccines?"

When used in combination with the MF59 adjuvant (oil-in-water emulsion of squalene oil), fungal-derived β-glucan showed protection against murine vaginal candidiasis but is currently not approved for use in humans (47). The conjugation of the β-glucan preparation Laminarin (a soluble Dectin-1 ligand derived from seaweed) with diphtheria toxoid (Lam-CRM197) resulted, in murine models, in significant protection against systemic candidiasis, as well as cross-protection against aspergillosis (48). In further studies, researchers conjugated the diphtheria toxoid with various other β-glucan preparations, such as curdlan (a high-molecular-weight β-1,3-linked polymer produced by bacteria) or synthetic oligosaccharides that contained either only linear β-1,3 linkages or also branched β-1,6 linkages, and combined it with the MF59 adjuvant. Interestingly, conjugates raising antibodies against β-1,3-glucans were protective in a mouse model of systemic candidiasis, while anti-β-1,6-antibodies appeared to reverse this effect (73). Overall these studies reveal the high immunogenicity of β-glucans but also a surprisingly complex relationship between antifungal immune responses and host protection against fungal infections. Moreover, different *Candida* species expose β-glucan on their surface to different degrees (74), questioning how broadly protective such vaccines would be against various candidiasis-causing agents. These complexities will need to be better understood, before these polysaccharides can be translated into safe and effective antifungal vaccines for human use.

COMMON CHALLENGES FACED SO FAR

The fact that *C. albicans* is thought to have coevolved with humans for at least the past 2,000 years (75), that it is a lifelong inhabitant of humans that colonizes the gastrointestinal (GI) tract since birth (76) and that is then transmitted between family members (77), poses a few conceptual and technical challenges in the development of an anti-*Candida* vaccine. On one hand, this long interaction history with the human GI tract suggests that these fungi might have evolved a series of mechanisms to escape various host immune defenses, including a high genetic, phenotypic and morphological plasticity (78). On the other hand, humans might have learned to recognize *Candida* species as commensals and might have therefore developed immune tolerance toward them—breaking this tolerance is expected to be both difficult and in some cases even counterproductive (79). Lastly, the highest risk group for *Candida*-related infections is represented by immunocompromised and immunosuppressed patients, i.e., a class of individuals that is intrinsically less responsive to immunization. Here, we will outline each of these issues in greater detail, and later we will attempt to offer some possible ways forward based on recent learning points.

Zeroing in on a Moving Target

Morphological and Phenotypic Plasticity of *C. albicans*

A first difficulty encountered when designing an anti-*Candida* vaccine lies in the morphological and phenotypic plasticity of these fungi (**Figure 1**), which makes them almost "moving targets." In fact, *C. albicans* is a polymorphic fungus that can reversibly transition between yeast, pseudohyphal and hyphal forms—a property that is closely linked to its evolutionary adaptation to life inside the human host. When *C. albicans* grows in its unicellular yeast form, it is commonly regarded as a harmless colonizer, while its switching to the hyphal form is related to pathogenesis, in that hyphae adhere to and invade epithelial cells resulting in extensive damage to host cells (80).

Interestingly, *C. albicans* isolated from the blood of patients with candidiasis often matches those recovered from the GI tract of the same patients (81), suggesting that *C. albicans* invades the bloodstream directly from the GI tract. How exactly the GI barrier is crossed is currently not completely understood, but it is thought to be mediated by or facilitated by epithelial tissue damage; and that *C. albicans* hyphal formation might be critical for this ability (82). Therefore, hyphal-specific or hyphal-associated CWPs such as Hyr1, Hwp2, Plb5, and Sod5 have all been proposed as vaccine target candidates (83).

However, vaccines against hyphal CWPs alone may not be sufficient to provide immune protection. While direct penetration into the mucosal surfaces by the hyphal form is important for invasion, widespread dissemination through the bloodstream and to the organs is thought to be facilitated by the yeast form (84). As both yeast and hyphae are detected in patients with candidiasis (85), and some mutants defective in filamentation displayed similar virulence as the wild type (86), it is the plasticity of this morphological switch, rather than the hyphal form alone, that appears to critically underlie the virulence of *C. albicans*. The variety of different forms of *C. albicans* that exist in various organs may represent a further challenge in vaccine development. For example, in mouse infection models, while *C. albicans* is mainly observed in the hyphal form in the kidney, it actually persists as a yeast in the spleen and the liver (87). To achieve sterile protection, the ideal vaccine should be able to stimulate clearance of the fungus not only in the former but also in the latter organs.

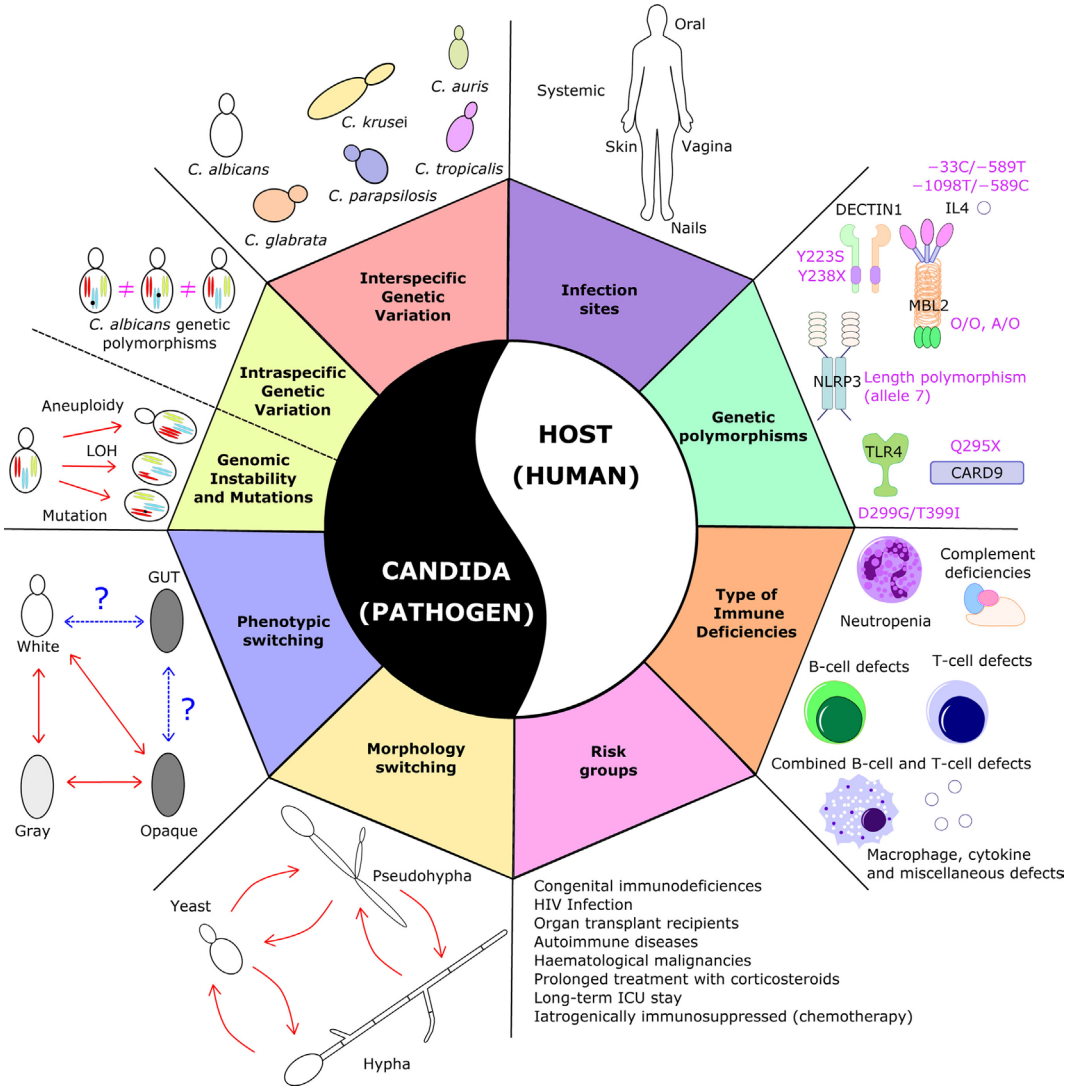

FIGURE 1 | Sources of variability in *Candida*-related infections. The figure illustrates the plethora of variations at the level of the pathogen and the host, which pose serious challenges in the development of an antifungal vaccine. On the pathogen side, *Candida* species display large phenotypic, morphological, and genetic variation and dynamics; on the host side, candidiasis can occur in different types of patients, with different types of immune system dysfunction or carrying different genetic polymorphisms, and in different anatomical sites. Taken together, this broad and diverse clinical spectrum of the disease makes it difficult to design a "one-size-fits-all" vaccine that would protect all these different patients from all these different types of fungal infection.

A second form of plasticity in *C. albicans* is a heritable white-to-opaque phenotypic switch. Smooth and white colonies are observed during the white phase, while elongated and rod-like cells giving rise to flattened gray colonies appear in the opaque phase (88). Opaque cells are less virulent than white cells in mouse bloodstream infection model (89, 90) and undergo filamentation in response to stimuli that are distinct form white cells (91). The switching between white and opaque phenotypes may facilitate *C. albicans* to evade from host immune response, as opaque cells are less susceptible to be phagocytosed by macrophages (92) and also capable to evade killing by neutrophils (93).

Another phenotypic switch, known as gastrointestinally induced transition (GUT) and found as a result of *WOR1* overexpression, was recently described to confer increased fitness of *C. albicans* in the GI tract of antibiotic-treated mice (94). While GUT cells share some resemblance with opaque cells, such as a reduced virulent in mouse bloodstream infections, they appear to be transcriptionally distinct from both white and opaque cells, therefore likely representing an independent epigenetic state. Whether GUT cells also arise in mucosal or systemic infections in humans and whether these cells express specific factors that are important for disease remains to be determined, but their discovery nonetheless sheds light on additional layers of complexity in the morphological and phenotypic plasticity of this fungal pathogen.

As a whole, morphological and phenotypic plasticity renders *C. albicans* a "skilled transformer" (78). Therefore, vaccines directed against single targets expressed only in a particular fungal form may not be sufficient to raise protective immune responses

against the entire arsenal of antigens and virulence factors that are dynamically presented to the host in different organs at different times.

Genomic Plasticity of *Candida albicans*

Candida albicans, apart from morphological and phenotypic transitions, also displays a high degree of genomic plasticity including gross chromosome rearrangement, aneuploidy and loss of heterozygosity when exposed to different stresses. Such genomic changes equip *C. albicans* to rapidly adapt to an adverse environment by changing the copy number of specific genes on a given chromosome (95). One of the well-known examples is the identification of an isochromosome composed of two copies of the left arm of chromosome 5, which is associated with azole resistance (17) due to amplification of two resistance genes, *ERG11* and *TAC1* (96). Genomic variations are commonly observed in clinical *C. albicans* isolates, which includes copy number variations, chromosomal inversions, subtelomeric hypervariation, loss of heterozygosity and aneuploidy (97). Moreover, *C. albicans* with increased DNA content (aneuploidy) occurs at a higher frequency in clinical blood isolates when compared with mucosal isolates (98). This suggests that acquisition of aneuploidy, and the consequent copy number alteration of specific genes, may provide a rapid mechanism to modify the expression pattern of certain antigens that were originally targeted by a certain vaccine.

Non-albicans *Candida* Species

The genus *Candida* represents a highly heterogeneous group of >50 known species. Nevertheless, >90% of the invasive *Candida* infections are caused by *C. albicans*, *C. glabrata*, *C. parapsilosis*, *C. tropicalis* or *C. krusei* (99). While this figure has remained largely unchanged, the relative ranking between these species has seen significant shifts in different regions over the past decades (100). While *C. albicans* is still considered the most common species causing candidemia, increasing rates of NAC species in candidemia have been reported worldwide (18, 101, 102). Moreover, significant variations of *Candida* species are detected in different patient groups and geographical regions (103). For instance, *C. glabrata* has emerged as an important pathogen in northern Europe, the United States and Canada with a higher rate of incidence in adults than in children, and lower in neonates (104). *C. parapsilosis*, instead, is more prominent in southern Europe, Asia, and South America and is mostly associated with low-birth-weight neonates and transplant recipients (105). Finally, *C. tropicalis* constitutes 20–45% of *Candida* isolates in the Asia-Pacific region (18) and invasive candidiasis due to this species is commonly associated with patients with neutropenia and malignancy (106). Recently, the emergence of *C. auris*, first reported in 2009 in Japan, highlights a new challenge of antifungal treatment, as *C. auris* is often multi-drug resistant and also difficult to be diagnosed with standard laboratory methods, which is contributing to its rapid spreading over multiple countries (107). In addition to NAC, multispecies candidemia is also emerging as a threat (108). Taken together, these observations suggest that vaccines specifically against *C. albicans* alone may not be sufficient to provide protection against candidiasis caused by other emerging NAC species or mixed *Candida* species infections.

Breaking Immune Tolerance Toward Fungi

A microbial ecosystem in the human intestine, known as the gut microbiome, harbors more than 100 trillion microorganisms and thus immunological tolerogenic responses are required in order to maintain gut homeostasis and prevent chronic inflammation (109). Immune tolerance toward human gut commensals, such as *Bacteroides fragilis* and certain *Clostridia* species, is maintained by regulatory T (Treg) cell responses (110–112). Apart from bacteria, *Candida* species are the most common fungal species found in the GI tract; it is therefore reasonable to assume that similar tolerance mechanisms might have evolved to regulate the commensal relationship between humans and fungi. One such mechanism, which likely resulted from the coevolution of bacterial microbiota, commensal fungi and host immune system, relies on the metabolic tryptophan-AhR pathway and 2,3-indoleamine dioxygenase (IDO) (113, 114). *C. albicans*, being a lifelong inhabitant of humans that colonizes the GI tract since birth (76), is able to induce IDO expression in DCs. IDO-expressing DCs then promote tolerogenic Treg responses, probably facilitating the switch from pathogenicity to commensalism in *C. albicans* (115).

The existence of immunological tolerance toward *C. albicans* and probably other *Candida* species poses two serious challenges for anti-*Candida* vaccine development. First, unlike obligate pathogens with no commensal relationship with humans, this tolerance represents an additional hurdle toward establishment of effective and protective immunological memory. Second, much of the clinical manifestations of *Candida*-related infections are more due to host-derived immunopathology than to pathogen-derived host damage (116, 117). For instance, mice lacking the chemokine receptor Ccr1, which is critical for neutrophil recruitment, display improved renal function during invasive candidiasis (118) and administration of Ccr1 antagonists reduces renal tissue injury and improves survival in mice challenged with systemic candidiasis (119).

It has thus been argued that a careful balance between immunity and tolerance must be established to maintain commensalism (79). Breaking host tolerance against fungi and the self-regulated equilibrium between Th17 and Treg responses might lead to undesired consequences, such as exacerbating fungal disease progression or other underlying inflammatory or autoimmune conditions.

Vaccinating Patients With No Immunity

Fungal infections, especially invasive ones, most frequently occur in individuals with compromised or suppressed immunity. Hence, it appears that the patients that would mostly benefit from a future antifungal vaccine are also those least likely to respond to it. Is such an effort then even justified? Or is it doomed to fail from the start? Answers to these questions are more complex than one might expect.

Efficacy and safety are always a primary concern in any vaccine development effort, and especially so in vulnerable subjects such as patients with lowered immune defenses. As mentioned, the risk of *Candida* infection is especially high in patients with neutropenia, hematological malignancies, solid-organ transplants, prolonged treatment with corticosteroids, long-term ICU stay, chemotherapy and HIV infection (120). The ideal anti-*Candida*

vaccine should possess all of the following properties: (i) zero risk of causing a *Candida*-related infection or to exacerbate the immunopathology associated with an ongoing or future fungal infection, (ii) be immunogenic enough to elicit protection in patients with little or no immunity, (iii) do not increase the risk of aggravating any underlying disease. While this may sound like a "catch-22," vaccinating immunocompromised patients has been attempted with various degrees of success in the past for other kinds of infection.

For instance, a single-dose of the pneumococcal vaccine was recently deemed safe and immunogenic in children under active immunosuppressive therapy (121). However, low immunogenicity of the meningococcal vaccine was reported in solid-organ transplant recipients (122). Lower immunogenicity against the influenza vaccine is generally reported in immunocompromised patients when compared with healthy individuals (123). However, using a high-dose influenza vaccine was reported to be more immunogenic than the standard dose in children and young adults with leukemia or solid tumors, although not in those with HIV (124).

What is progressively becoming clearer is that a "one-size-fits-all" anti-*Candida* vaccine may never see the light. For example, a vaccine effective in preventing candidemia in neutropenic cancer patients might not be effective in T-cell-deficient HIV or transplant patients and *vice versa*. As a whole, one of the greatest challenges of any antifungal vaccine will be to deal with the large diversity of underlying disease states and of the associated types of immunosuppression that characterizes this highly heterogeneous risk group (**Figure 1**).

BACK TO THE FUTURE: NEW VACCINE STRATEGIES ON THE HORIZON?

Multivalent Vaccines

Some monovalent vaccines, i.e., those directed against a single strain or a single antigen, are very effective. A good example is represented by the measles vaccine, which has almost completely eradicated the disease in countries where it has been employed consistently throughout the population (125). However, the most recent vaccines tend to be multivalent, i.e., they carry multiple antigens of two or more strains/serotypes of the same pathogen. An example is the quadrivalent meningococcal vaccine that protects against 4 serogroups (A, C, W-135, and Y) of meningococci. The quadrivalent vaccine was shown to be more effective in reducing invasive meningococcal disease incidence when compared with the monovalent C vaccine (126). Another example is the 13-valent pneumococcal conjugate vaccine (PCV13) containing antigens from 13 serotypes of pneumococci. A replacement of the seven-valent pneumococcal conjugate vaccine (PCV7) with PCV13 covering additional six of the most prevalent serotypes that are not included in PCV7 successfully reduced the burden of pneumococcal disease in pediatric populations (127).

As *C. albicans* itself expresses a range of virulence factors and several NAC species also carry their own species-specific virulence factors, the recent development of univalent subunit vaccines may face practical obstacles. Considering above success stories of multivalent vaccines applied to bacterial infections, it has been argued that a better approach toward the development of an anti-*Candida* vaccine would be to simultaneously target multiple unrelated virulence-associated antigens (78). The predicted advantages include the lower probability of selecting "escape mutants" and a higher selectively against the pathogenic form of *C. albicans*, thus sparing the commensal—and perhaps beneficial—form of this gut inhabitant. In particular, it was proposed to combine a few of the univalent vaccines that have so far progressed furthest in clinical trials, such as the Als3 and the Sap2 vaccines (78).

More recently, a study reported that a newly identified cytolytic peptide toxin, Candidalysin, is secreted from *C. albicans* to induce epithelial cell damage and inflammation and to facilitate tissue invasion (128). Intriguingly, the mechanism of action of this novel virulence factor is partially uncoupled from the hyphal morphogenesis program, suggesting that a vaccine targeting both the former and the latter would be more effective than one targeting only one or the other. In general, as more knowledge is gained on the pathogenesis of *C. albicans*, further targets could be added to the list of antigens to be included in a multivalent formulation. At the same time, we can also predict that as the complexity of the vaccine increases, so will regulatory hurdles and manufacturing challenges. Nevertheless, testing the efficacy and safety of a combination of more and more antigens is likely going to be crucial for better vaccines against *Candida* infections.

Trained Immunity—Toward the Next Generation of Vaccines?

The classic vaccination paradigm is based on adaptive immunity and the raising of long-lasting, protective B- and/or T-cell memory responses (129). As mentioned above, mounting protective antibodies or T-cell responses across different *Candida* strains and species may be challenging due to their large genetic, phenotypic and morphological variation and plasticity. In addition, the capacity to mount B- and T-memory responses may be impaired in immunocompromised or immunosuppressed patients such as HIV/AIDS or transplant recipients who are among the highest risk groups for candidiasis. Though innate immunity lacks most of the properties of classical immunological memory, various studies have demonstrated that certain vaccines induce a type of innate immune memory known as "trained immunity" (**Figure 2**), which is mediated by monocytes, macrophages or NK cells (72). For instance, BCG vaccination reduces mortality in low-birth-weight children (130, 131) and vaccination against measles reduces all-cause mortality in childhood (132), suggesting non-specific cross-protection against other infections (133).

Testing whether such innate memory responses could be stimulated also in adults, PBMCs obtained 2 weeks or 3 months after BCG vaccination were found to produce higher levels of pro-inflammatory cytokines such as TNF-α and IL-1β when restimulated *in vitro* with *C. albicans* (134). Such increased cytokine production capacity involved epigenetic changes mediated by increased H3K4 trimethylation in monocytes and was dependent on NOD2 and Rip2. Similarly, SCID mice vaccinated by BCG are protected against lethal *C. albicans* infection through a T and B lymphocyte-independent mechanism (134). Apart from the increased production of pro-inflammatory cytokines in monocytes, another study reported that BCG vaccination also

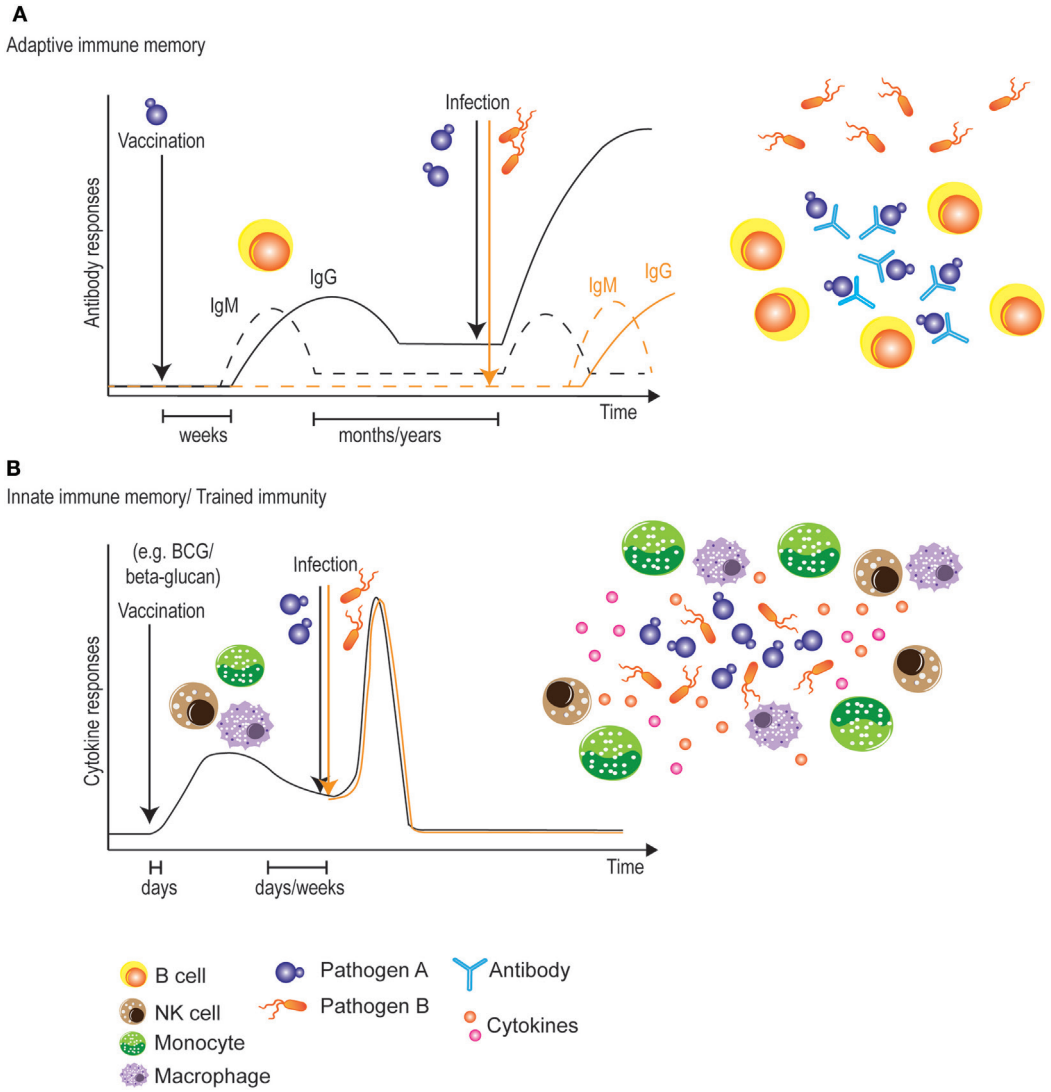

FIGURE 2 | Vaccination strategies targeting adaptive or innate immune memory. **(A)** Classical vaccines initially induce a slow adaptive immune response. During this primary response, however, adaptive immune memory is raised, allowing for a more rapid and stronger secondary response upon encounter of the targeted pathogen. This protection is very long-lived, but is limited to the antigens present in the vaccine. **(B)** Most vaccines also induce a very rapid innate immune response. During this primary response, some vaccines also "train" innate immune cells, allowing for a stronger secondary innate response against pathogens. One advantage of this innate immune memory is the non-specificity of the secondary response, which could potentially lead to broadly cross-protective vaccines. A potential disadvantage would be the relatively shorter time window of protection.

enhances IL-1β production in human NK cells when stimulated with *C. albicans*. BCG-induced protection against disseminated *C. albicans* infection was shown to be partially dependent on NK cells in NOD-SCID-IL2Rγ$^{-/-}$ mice (135). These studies warrant clinical trials to test if BCG vaccination could reduce the risk of candidiasis in high-risk patients.

Consistent with what reviewed in Section "Live-Attenuated Vaccines," systemic infection of mice with an avirulent *C. albicans* strain was shown by Antonio Cassone's group to confer protection against a subsequent challenge with a pathogenic *C. albicans* strain (26). The protection was shown to be non-specific, as cross-protection against *C. tropicalis* and *Staphylococcus aureus* was equally observed, and to be mediated by macrophage-like cells, as adoptive transfer of "plastic-adherent" cells was sufficient to confer protection against subsequent challenge with a virulent strain of *C. albicans*. Several years later, Mihai Netea's group demonstrated that vaccination of both wild-type and RAG1$^{-/-}$ mice, but not CCR2$^{-/-}$ mice that lack circulating monocytes, with a sublethal dose of a virulent *C. albicans* strain similarly affords protection against reinfection with a lethal dose of the same strain, and dubbed the phenomenon "trained immunity" (69). Increased TNF-α and IL-6 levels from the trained monocytes were induced by β-glucan found in the *C. albicans* cell wall and sensed by Dectin-1 on host cells. In another study, mice trained with *Candida*-derived β-glucan showed increased serum levels of TNF-α and IL-6 when challenged by LPS four days later, but the

response was transient and diminished after 20 days (136). To test the possibility of using β-glucan as a vaccine or "immune trainer" in humans, a pilot study was conducted by orally administrating β-glucan to healthy volunteers and subsequently testing innate immune responses in PBMCs restimulated *in vitro* with *C. albicans* (137). Enhanced innate immune responses as in the mouse model, however, were unfortunately not observed in this human study. This may probably be due to the solubility of β-glucan and the absorbability of β-glucan in the human GI tract. Further studies using different administration routes are still worth exploring, in order to establish whether β-glucan could one day be used as a vaccine to induce trained immunity against subsequent *Candida* infections (**Figure 2**).

CONCLUDING REMARKS

With the increasing reports of multidrug resistance in several *Candida* species, prophylactic vaccination of at-risk patients likely represents a more effective long-term measure to reduce the growing incidence of *Candida*-related infections. The main challenges faced by *Candida* vaccine developers are the large variation and plasticity of these fungi, the existence of preestablished immunological tolerance and the difficulty in raising protective memory responses in patients with impaired adaptive immunity. In addition to multivalent vaccines, we propose that future vaccine development efforts should harness the growing mechanistic understanding of trained innate immunity, which might provide not only protection against candidiasis but also potentially cross-protection against a wide range of opportunistic infections. Further research on the mechanism, efficacy, and safety of raising trained immunity especially in immunocompromised patients would pave the way toward the development of a new generation of vaccines against *Candida*-related and other nosocomial infections.

AUTHOR CONTRIBUTIONS

GT and JR-C contributed equally as first authors. GT and JR-C conducted literature review and drafted the manuscript. NP conceptualized and oversaw the study and revised the manuscript. All authors read and approved the submitted version.

ACKNOWLEDGMENTS

The authors are thankful to all authors of the cited literature for their invaluable contributions and apologize for any omissions that were due to lack of space.

FUNDING

This work was supported by an A*STAR Investigatorship to NP (JCO/1437a00117) and by core funding by the Singapore Immunology Network (SIgN), A*STAR.

REFERENCES

1. Fishman JA. Infection in solid-organ transplant recipients. *N Engl J Med* (2007) 357:2601–14. doi:10.1056/NEJMra064928
2. Teoh F, Pavelka N. How chemotherapy increases the risk of systemic candidiasis in cancer patients: current paradigm and future directions. *Pathogens* (2016) 5:6. doi:10.3390/pathogens5010006
3. Menzin J, Meyers JL, Friedman M, Perfect JR, Langston AA, Danna RP, et al. Mortality, length of hospitalization, and costs associated with invasive fungal infections in high-risk patients. *Am J Health Syst Pharm* (2009) 66:1711–7. doi:10.2146/ajhp080325
4. Pfaller MA, Diekema DJ. Epidemiology of invasive candidiasis: a persistent public health problem. *Clin Microbiol Rev* (2007) 20:133–63. doi:10.1128/CMR.00029-06
5. Richardson M, Lass-Florl C. Changing epidemiology of systemic fungal infections. *Clin Microbiol Infect* (2008) 14(Suppl 4):5–24. doi:10.1111/j.1469-0691.2008.01978.x
6. Wisplinghoff H, Bischoff T, Tallent SM, Seifert H, Wenzel RP, Edmond MB. Nosocomial bloodstream infections in US hospitals: analysis of 24,179 cases from a prospective nationwide surveillance study. *Clin Infect Dis* (2004) 39:309–17. doi:10.1086/421946
7. Peman J, Canton E, Quindos G, Eraso E, Alcoba J, Guinea J, et al. Epidemiology, species distribution and in vitro antifungal susceptibility of fungaemia in a Spanish multicentre prospective survey. *J Antimicrob Chemother* (2012) 67:1181–7. doi:10.1093/jac/dks019
8. Cleveland AA, Farley MM, Harrison LH, Stein B, Hollick R, Lockhart SR, et al. Changes in incidence and antifungal drug resistance in candidemia: results from population-based laboratory surveillance in Atlanta and Baltimore, 2008-2011. *Clin Infect Dis* (2012) 55:1352–61. doi:10.1093/cid/cis697
9. Eliakim-Raz N, Babaoff R, Yahav D, Yanai S, Shaked H, Bishara J. Epidemiology, microbiology, clinical characteristics, and outcomes of candidemia in internal medicine wards-a retrospective study. *Int J Infect Dis* (2016) 52:49–54. doi:10.1016/j.ijid.2016.09.018
10. Brown GD, Denning DW, Gow NA, Levitz SM, Netea MG, White TC. Hidden killers: human fungal infections. *Sci Transl Med* (2012) 4:165rv113. doi:10.1126/scitranslmed.3004404
11. Smith PB, Morgan J, Benjamin JD, Fridkin SK, Sanza LT, Harrison LH, et al. Excess costs of hospital care associated with neonatal candidemia. *Pediatr Infect Dis J* (2007) 26:197–200. doi:10.1097/01.inf.0000253973.89097.c0
12. Pappas PG, Kauffman CA, Andes DR, Clancy CJ, Marr KA, Ostrosky-Zeichner L, et al. Clinical practice guideline for the management of candidiasis: 2016 update by the Infectious Diseases Society of America. *Clin Infect Dis* (2016) 62:e1–50. doi:10.1093/cid/civ1194
13. Havlickova B, Czaika VA, Friedrich M. Epidemiological trends in skin mycoses worldwide. *Mycoses* (2008) 51(Suppl 4):2–15. doi:10.1111/j.1439-0507.2008.01606.x
14. Sobel JD. Vulvovaginal candidosis. *Lancet* (2007) 369:1961–71. doi:10.1016/S0140-6736(07)60917-9
15. Sobel JD, Faro S, Force RW, Foxman B, Ledger WJ, Nyirjesy PR, et al. Vulvovaginal candidiasis: epidemiologic, diagnostic, and therapeutic considerations. *Am J Obstet Gynecol* (1998) 178:203–11. doi:10.1016/S0002-9378(98)80001-X
16. Cannon RD, Lamping E, Holmes AR, Niimi K, Baret PV, Keniya MV, et al. Efflux-mediated antifungal drug resistance. *Clin Microbiol Rev* (2009) 22:291–321. doi:10.1128/CMR.00051-08
17. Selmecki A, Forche A, Berman J. Aneuploidy and isochromosome formation in drug-resistant *Candida albicans*. *Science* (2006) 313:367–70. doi:10.1126/science.1128242
18. Pfaller MA, Diekema DJ, Gibbs DL, Newell VA, Ellis D, Tullio V, et al. Results from the ARTEMIS DISK Global Antifungal Surveillance Study, 1997 to 2007: a 10.5-year analysis of susceptibilities of *Candida* species to fluconazole and voriconazole as determined by CLSI standardized disk diffusion. *J Clin Microbiol* (2010) 48:1366–77. doi:10.1128/JCM.02117-09
19. Alexander BD, Johnson MD, Pfeiffer CD, Jimenez-Ortigosa C, Catania J, Booker R, et al. Increasing echinocandin resistance in *Candida glabrata*: clinical failure correlates with presence of FKS mutations and elevated minimum inhibitory concentrations. *Clin Infect Dis* (2013) 56:1724–32. doi:10.1093/cid/cit136
20. Reales-Calderon JA, Molero G, Gil C, Martinez JL. The fungal resistome: a risk and an opportunity for the development of novel antifungal therapies. *Future Med Chem* (2016) 8:1503–20. doi:10.4155/fmc-2016-0051
21. Fadda ME, Podda GS, Pisano MB, Deplano M, Cosentino S. Prevalence of *Candida* species in different hospital wards and their susceptibility to

antifungal agents: results of a three year survey. *J Prev Med Hyg* (2008) 49:69–74. doi:10.15167/2421-4248/jpmh2008.49.2.119
22. Vermitsky JP, Edlind TD. Azole resistance in *Candida glabrata*: coordinate upregulation of multidrug transporters and evidence for a Pdr1-like transcription factor. *Antimicrob Agents Chemother* (2004) 48:3773–81. doi:10.1128/AAC.48.10.3773-3781.2004
23. Vermitsky JP, Earhart KD, Smith WL, Homayouni R, Edlind TD, Rogers PD. Pdr1 regulates multidrug resistance in *Candida glabrata*: gene disruption and genome-wide expression studies. *Mol Microbiol* (2006) 61:704–22. doi:10.1111/j.1365-2958.2006.05235.x
24. Navalkele BD, Revankar S, Chandrasekar P. *Candida auris*: a worrisome, globally emerging pathogen. *Expert Rev Anti Infect Ther* (2017) 15(9):819–27. doi:10.1080/14787210.2017.1364992
25. Denning DW, Perlin DS, Muldoon EG, Colombo AL, Chakrabarti A, Richardson MD, et al. Delivering on antimicrobial resistance agenda not possible without improving fungal diagnostic capabilities. *Emerg Infect Dis* (2017) 23:177–83. doi:10.3201/eid2302.152042
26. Bistoni F, Vecchiarelli A, Cenci E, Puccetti P, Marconi P, Cassone A. Evidence for macrophage-mediated protection against lethal *Candida albicans* infection. *Infect Immun* (1986) 51:668–74.
27. Fernandez-Arenas E, Molero G, Nombela C, Diez-Orejas R, Gil C. Low virulent strains of *Candida albicans*: unravelling the antigens for a future vaccine. *Proteomics* (2004) 4:3007–20. doi:10.1002/pmic.200400929
28. Martinez-Lopez R, Nombela C, Diez-Orejas R, Monteoliva L, Gil C. Immunoproteomic analysis of the protective response obtained from vaccination with *Candida albicans* ecm33 cell wall mutant in mice. *Proteomics* (2008) 8:2651–64. doi:10.1002/pmic.200701056
29. Saville SP, Lazzell AL, Chaturvedi AK, Monteagudo C, Lopez-Ribot JL. Efficacy of a genetically engineered *Candida albicans* tet-NRG1 strain as an experimental live attenuated vaccine against hematogenously disseminated candidiasis. *Clin Vaccine Immunol* (2009) 16:430–2. doi:10.1128/CVI.00480-08
30. Yang YL, Wang CW, Chen CT, Wang MH, Hsiao CF, Lo HJ. Non-lethal *Candida albicans* cph1/cph1 efg1/efg1 mutant partially protects mice from systemic infections by lethal wild-type cells. *Mycol Res* (2009) 113:388–90. doi:10.1016/j.mycres.2008.11.016
31. Capilla J, Clemons KV, Liu M, Levine HB, Stevens DA. *Saccharomyces cerevisiae* as a vaccine against coccidioidomycosis. *Vaccine* (2009) 27:3662–8. doi:10.1016/j.vaccine.2009.03.030
32. Liu M, Capilla J, Johansen ME, Alvarado D, Martinez M, Chen V, et al. *Saccharomyces* as a vaccine against systemic aspergillosis: 'the friend of man' a friend again? *J Med Microbiol* (2011) 60:1423–32. doi:10.1099/jmm.0.033290-0
33. Liu M, Clemons KV, Johansen ME, Martinez M, Chen V, Stevens DA. *Saccharomyces* as a vaccine against systemic candidiasis. *Immunol Invest* (2012) 41:847–55. doi:10.3109/08820139.2012.692418
34. Majumder T, Liu M, Chen V, Martinez M, Alvarado D, Clemons KV, et al. Killed *Saccharomyces cerevisiae* protects against lethal challenge of *Cryptococcus grubii*. *Mycopathologia* (2014) 178:189–95. doi:10.1007/s11046-014-9798-5
35. Spellberg BJ, Ibrahim AS, Avenissian V, Filler SG, Myers CL, Fu Y, et al. The anti-*Candida albicans* vaccine composed of the recombinant N terminus of Als1p reduces fungal burden and improves survival in both immunocompetent and immunocompromised mice. *Infect Immun* (2005) 73:6191–3. doi:10.1128/IAI.73.9.6191-6193.2005
36. Ibrahim AS, Spellberg BJ, Avanesian V, Fu Y, Edwards JE Jr. The anti-*Candida* vaccine based on the recombinant N-terminal domain of Als1p is broadly active against disseminated candidiasis. *Infect Immun* (2006) 74:3039–41. doi:10.1128/IAI.74.5.3039-3041.2006
37. Spellberg BJ, Ibrahim AS, Avanesian V, Fu Y, Myers C, Phan QT, et al. Efficacy of the anti-*Candida* rAls3p-N or rAls1p-N vaccines against disseminated and mucosal candidiasis. *J Infect Dis* (2006) 194:256–60. doi:10.1086/504691
38. Lin L, Ibrahim AS, Xu X, Farber JM, Avanesian V, Baquir B, et al. Th1-Th17 cells mediate protective adaptive immunity against *Staphylococcus aureus* and *Candida albicans* infection in mice. *PLoS Pathog* (2009) 5:e1000703. doi:10.1371/journal.ppat.1000703
39. Schmidt CS, White CJ, Ibrahim AS, Filler SG, Fu Y, Yeaman MR, et al. NDV-3, a recombinant alum-adjuvanted vaccine for *Candida* and *Staphylococcus aureus*, is safe and immunogenic in healthy adults. *Vaccine* (2012) 30:7594–600. doi:10.1016/j.vaccine.2012.10.038
40. De Bernardis F, Boccanera M, Adriani D, Girolamo A, Cassone A. Intravaginal and intranasal immunizations are equally effective in inducing vaginal antibodies and conferring protection against vaginal candidiasis. *Infect Immun* (2002) 70:2725–9. doi:10.1128/IAI.70.5.2725-2729.2002
41. De Bernardis F, Amacker M, Arancia S, Sandini S, Gremion C, Zurbriggen R, et al. A virosomal vaccine against candidal vaginitis: immunogenicity, efficacy and safety profile in animal models. *Vaccine* (2012) 30:4490–8. doi:10.1016/j.vaccine.2012.04.069
42. Yang Q, Wang L, Lu DN, Gao RJ, Song JN, Hua PY, et al. Prophylactic vaccination with phage-displayed epitope of *C. albicans* elicits protective immune responses against systemic candidiasis in C57BL/6 mice. *Vaccine* (2005) 23:4088–96. doi:10.1016/j.vaccine.2004.07.005
43. Luo G, Ibrahim AS, French SW, Edwards JE Jr, Fu Y. Active and passive immunization with rHyr1p-N protects mice against hematogenously disseminated candidiasis. *PLoS One* (2011) 6:e25909. doi:10.1371/journal.pone.0025909
44. Thomas DP, Viudes A, Monteagudo C, Lazzell AL, Saville SP, Lopez-Ribot JL. A proteomic-based approach for the identification of *Candida albicans* protein components present in a subunit vaccine that protects against disseminated candidiasis. *Proteomics* (2006) 6:6033–41. doi:10.1002/pmic.200600321
45. Xin H, Dziadek S, Bundle DR, Cutler JE. Synthetic glycopeptide vaccines combining beta-mannan and peptide epitopes induce protection against candidiasis. *Proc Natl Acad Sci U S A* (2008) 105:13526–31. doi:10.1073/pnas.0803195105
46. Paulovicova L, Paulovicova E, Karelin AA, Tsvetkov YE, Nifantiev NE, Bystricky S. Effect of branched alpha-oligomannoside structures on induction of anti-*Candida* humoral immune response. *Scand J Immunol* (2013) 77:431–41. doi:10.1111/sji.12044
47. Pietrella D, Rachini A, Torosantucci A, Chiani P, Brown AJ, Bistoni F, et al. A beta-glucan-conjugate vaccine and anti-beta-glucan antibodies are effective against murine vaginal candidiasis as assessed by a novel in vivo imaging technique. *Vaccine* (2010) 28:1717–25. doi:10.1016/j.vaccine.2009.12.021
48. Torosantucci A, Bromuro C, Chiani P, De Bernardis F, Berti F, Galli C, et al. A novel glyco-conjugate vaccine against fungal pathogens. *J Exp Med* (2005) 202:597–606. doi:10.1084/jem.20050749
49. Smith KA. Edward Jenner and the small pox vaccine. *Front Immunol* (2011) 2:21. doi:10.3389/fimmu.2011.00021
50. Lo HJ, Kohler JR, Didomenico B, Loebenberg D, Cacciapuoti A, Fink GR. Nonfilamentous *C. albicans* mutants are avirulent. *Cell* (1997) 90:939–49. doi:10.1016/S0092-8674(00)80358-X
51. Hoyer LL, Cota E. *Candida albicans* agglutinin-like sequence (Als) family vignettes: a review of Als protein structure and function. *Front Microbiol* (2016) 7:280. doi:10.3389/fmicb.2016.00280
52. Spellberg B, Ibrahim AS, Yeaman MR, Lin L, Fu Y, Avanesian V, et al. The antifungal vaccine derived from the recombinant N terminus of Als3p protects mice against the bacterium *Staphylococcus aureus*. *Infect Immun* (2008) 76:4574–80. doi:10.1128/IAI.00700-08
53. Bar E, Gladiator A, Bastidas S, Roschitzki B, Acha-Orbea H, Oxenius A, et al. A novel Th cell epitope of *Candida albicans* mediates protection from fungal infection. *J Immunol* (2012) 188:5636–43. doi:10.4049/jimmunol.1200594
54. Hube B, Naglik J. *Candida albicans* proteinases: resolving the mystery of a gene family. *Microbiology* (2001) 147:1997–2005. doi:10.1099/00221287-147-8-1997
55. Naglik JR, Challacombe SJ, Hube B. *Candida albicans* secreted aspartyl proteinases in virulence and pathogenesis. *Microbiol Mol Biol Rev* (2003) 67:400–28, table of contents. doi:10.1128/MMBR.67.3.400-428.2003
56. Matthews R, Burnie J. Cloning of a DNA sequence encoding a major fragment of the 47 kilodalton stress protein homologue of *Candida albicans*. *FEMS Microbiol Lett* (1989) 51:25–30. doi:10.1016/0378-1097(89)90071-2
57. Matthews RC, Burnie JP, Tabaqchali S. Isolation of immunodominant antigens from sera of patients with systemic candidiasis and characterization of serological response to *Candida albicans*. *J Clin Microbiol* (1987) 25:230–7.
58. Matthews RC, Rigg G, Hodgetts S, Carter T, Chapman C, Gregory C, et al. Preclinical assessment of the efficacy of mycograb, a human recombinant antibody against fungal HSP90. *Antimicrob Agents Chemother* (2003) 47:2208–16. doi:10.1128/AAC.47.7.2208-2216.2003

59. Pachl J, Svoboda P, Jacobs F, Vandewoude K, van der Hoven B, Spronk P, et al. A randomized, blinded, multicenter trial of lipid-associated amphotericin B alone versus in combination with an antibody-based inhibitor of heat shock protein 90 in patients with invasive candidiasis. *Clin Infect Dis* (2006) 42:1404–13. doi:10.1086/503428
60. Richie DL, Ghannoum MA, Isham N, Thompson KV, Ryder NS. Nonspecific effect of Mycograb on amphotericin B MIC. *Antimicrob Agents Chemother* (2012) 56:3963–4. doi:10.1128/AAC.00435-12
61. Netea MG, Brown GD, Kullberg BJ, Gow NA. An integrated model of the recognition of *Candida albicans* by the innate immune system. *Nat Rev Microbiol* (2008) 6:67–78. doi:10.1038/nrmicro1815
62. Netea MG, Gow NA, Munro CA, Bates S, Collins C, Ferwerda G, et al. Immune sensing of *Candida albicans* requires cooperative recognition of mannans and glucans by lectin and toll-like receptors. *J Clin Invest* (2006) 116:1642–50. doi:10.1172/JCI27114
63. Hall RA, Gow NA. Mannosylation in *Candida albicans*: role in cell wall function and immune recognition. *Mol Microbiol* (2013) 90:1147–61. doi:10.1111/mmi.12426
64. Nelson RD, Shibata N, Podzorski RP, Herron MJ. *Candida* mannan: chemistry, suppression of cell-mediated immunity, and possible mechanisms of action. *Clin Microbiol Rev* (1991) 4:1–19. doi:10.1128/CMR.4.1.1
65. Tan MC, Mommaas AM, Drijfhout JW, Jordens R, Onderwater JJ, Verwoerd D, et al. Mannose receptor-mediated uptake of antigens strongly enhances HLA class II-restricted antigen presentation by cultured dendritic cells. *Eur J Immunol* (1997) 27:2426–35. doi:10.1002/eji.1830270942
66. Paulovicova L, Paulovicova E, Karelin AA, Tsvetkov YE, Nifantiev NE, Bystricky S. Immune cell response to *Candida* cell wall mannan derived branched alpha-oligomannoside conjugates in mice. *J Microbiol Immunol Infect* (2015) 48:9–19. doi:10.1016/j.jmii.2013.08.020
67. Douglas CM, D'ippolito JA, Shei GJ, Meinz M, Onishi J, Marrinan JA, et al. Identification of the FKS1 gene of *Candida albicans* as the essential target of 1,3-beta-D-glucan synthase inhibitors. *Antimicrob Agents Chemother* (1997) 41:2471–9.
68. Taylor PR, Tsoni SV, Willment JA, Dennehy KM, Rosas M, Findon H, et al. Dectin-1 is required for beta-glucan recognition and control of fungal infection. *Nat Immunol* (2007) 8:31–8. doi:10.1038/ni1408
69. Quintin J, Saeed S, Martens JHA, Giamarellos-Bourboulis EJ, Ifrim DC, Logie C, et al. *Candida albicans* infection affords protection against reinfection via functional reprogramming of monocytes. *Cell Host Microbe* (2012) 12:223–32. doi:10.1016/j.chom.2012.06.006
70. Cheng SC, Quintin J, Cramer RA, Shepardson KM, Saeed S, Kumar V, et al. mTOR- and HIF-1alpha-mediated aerobic glycolysis as metabolic basis for trained immunity. *Science* (2014) 345:1250684. doi:10.1126/science.1250684
71. Saeed S, Quintin J, Kerstens HH, Rao NA, Aghajanirefah A, Matarese F, et al. Epigenetic programming of monocyte-to-macrophage differentiation and trained innate immunity. *Science* (2014) 345:1251086. doi:10.1126/science.1251086
72. Netea MG, Joosten LA, Latz E, Mills KH, Natoli G, Stunnenberg HG, et al. Trained immunity: a program of innate immune memory in health and disease. *Science* (2016) 352:aaf1098. doi:10.1126/science.aaf1098
73. Bromuro C, Romano M, Chiani P, Berti F, Tontini M, Proietti D, et al. Beta-glucan-CRM197 conjugates as candidates antifungal vaccines. *Vaccine* (2010) 28:2615–23. doi:10.1016/j.vaccine.2010.01.012
74. Sem X, Le GT, Tan AS, Tso G, Yurieva M, Liao WW, et al. Beta-glucan exposure on the fungal cell wall tightly correlates with competitive fitness of *Candida* species in the mouse gastrointestinal tract. *Front Cell Infect Microbiol* (2016) 6:186. doi:10.3389/fcimb.2016.00186
75. Barnett JA. A history of research on yeasts 12: medical yeasts part 1, *Candida albicans*. *Yeast* (2008) 25:385–417. doi:10.1002/yea.1595
76. Fujimura KE, Sitarik AR, Havstad S, Lin DL, Levan S, Fadrosh D, et al. Neonatal gut microbiota associates with childhood multisensitized atopy and T cell differentiation. *Nat Med* (2016) 22:1187–91. doi:10.1038/nm.4176
77. Bougnoux ME, Diogo D, Francois N, Sendid B, Veirmeire S, Colombel JF, et al. Multilocus sequence typing reveals intrafamilial transmission and microevolutions of *Candida albicans* isolates from the human digestive tract. *J Clin Microbiol* (2006) 44:1810–20. doi:10.1128/JCM.44.5.1810-1820.2006
78. Cassone A. Development of vaccines for *Candida albicans*: fighting a skilled transformer. *Nat Rev Microbiol* (2013) 11:884–91. doi:10.1038/nrmicro3156
79. Carvalho A, Cunha C, Bozza S, Moretti S, Massi-Benedetti C, Bistoni F, et al. Immunity and tolerance to fungi in hematopoietic transplantation: principles and perspectives. *Front Immunol* (2012) 3:156. doi:10.3389/fimmu.2012.00156
80. Kumamoto CA, Vinces MD. Contributions of hyphae and hypha-co-regulated genes to *Candida albicans* virulence. *Cell Microbiol* (2005) 7:1546–54. doi:10.1111/j.1462-5822.2005.00616.x
81. Miranda LN, van der Heijden IM, Costa SF, Sousa AP, Sienra RA, Gobara S, et al. *Candida* colonisation as a source for candidaemia. *J Hosp Infect* (2009) 72:9–16. doi:10.1016/j.jhin.2009.02.009
82. Koh AY, Kohler JR, Coggshall KT, Van Rooijen N, Pier GB. Mucosal damage and neutropenia are required for *Candida albicans* dissemination. *PLoS Pathog* (2008) 4:e35. doi:10.1371/journal.ppat.0040035
83. Heilmann CJ, Sorgo AG, Siliakus AR, Dekker HL, Brul S, De Koster CG, et al. Hyphal induction in the human fungal pathogen *Candida albicans* reveals a characteristic wall protein profile. *Microbiology* (2011) 157:2297–307. doi:10.1099/mic.0.049395-0
84. Saville SP, Lazzell AL, Monteagudo C, Lopez-Ribot JL. Engineered control of cell morphology in vivo reveals distinct roles for yeast and filamentous forms of *Candida albicans* during infection. *Eukaryot Cell* (2003) 2:1053–60. doi:10.1128/EC.2.5.1053-1060.2003
85. Di Carlo P, Di Vita G, Guadagnino G, Cocorullo G, D'arpa F, Salamone G, et al. Surgical pathology and the diagnosis of invasive visceral yeast infection: two case reports and literature review. *World J Emerg Surg* (2013) 8:38. doi:10.1186/1749-7922-8-38
86. Noble SM, French S, Kohn LA, Chen V, Johnson AD. Systematic screens of a *Candida albicans* homozygous deletion library decouple morphogenetic switching and pathogenicity. *Nat Genet* (2010) 42:590–8. doi:10.1038/ng.605
87. Lionakis MS, Lim JK, Lee CC, Murphy PM. Organ-specific innate immune responses in a mouse model of invasive candidiasis. *J Innate Immun* (2011) 3:180–99. doi:10.1159/000321157
88. Lohse MB, Johnson AD. White-opaque switching in *Candida albicans*. *Curr Opin Microbiol* (2009) 12:650–4. doi:10.1016/j.mib.2009.09.010
89. Kvaal CA, Srikantha T, Soll DR. Misexpression of the white-phase-specific gene WH11 in the opaque phase of *Candida albicans* affects switching and virulence. *Infect Immun* (1997) 65:4468–75.
90. Kvaal C, Lachke SA, Srikantha T, Daniels K, Mccoy J, Soll DR. Misexpression of the opaque-phase-specific gene PEP1 (SAP1) in the white phase of *Candida albicans* confers increased virulence in a mouse model of cutaneous infection. *Infect Immun* (1999) 67:6652–62.
91. Si H, Hernday AD, Hirakawa MP, Johnson AD, Bennett RJ. *Candida albicans* white and opaque cells undergo distinct programs of filamentous growth. *PLoS Pathog* (2013) 9:e1003210. doi:10.1371/journal.ppat.1003210
92. Lohse MB, Johnson AD. Differential phagocytosis of white versus opaque *Candida albicans* by *Drosophila* and mouse phagocytes. *PLoS One* (2008) 3:e1473. doi:10.1371/journal.pone.0001473
93. Sasse C, Hasenberg M, Weyler M, Gunzer M, Morschhauser J. White-opaque switching of *Candida albicans* allows immune evasion in an environment-dependent fashion. *Eukaryot Cell* (2013) 12:50–8. doi:10.1128/EC.00266-12
94. Pande K, Chen C, Noble SM. Passage through the mammalian gut triggers a phenotypic switch that promotes *Candida albicans* commensalism. *Nat Genet* (2013) 45:1088–91. doi:10.1038/ng.2710
95. Selmecki A, Forche A, Berman J. Genomic plasticity of the human fungal pathogen *Candida albicans*. *Eukaryot Cell* (2010) 9:991–1008. doi:10.1128/EC.00060-10
96. Selmecki A, Gerami-Nejad M, Paulson C, Forche A, Berman J. An isochromosome confers drug resistance in vivo by amplification of two genes, ERG11 and TAC1. *Mol Microbiol* (2008) 68:624–41. doi:10.1111/j.1365-2958.2008.06176.x
97. Hirakawa MP, Martinez DA, Sakthikumar S, Anderson MZ, Berlin A, Gujja S, et al. Genetic and phenotypic intra-species variation in *Candida albicans*. *Genome Res* (2015) 25:413–25. doi:10.1101/gr.174623.114
98. Mandelblat M, Frenkel M, Abbey D, Ben Ami R, Berman J, Segal E. Phenotypic and genotypic characteristics of *Candida albicans* isolates from bloodstream and mucosal infections. *Mycoses* (2017) 60:534–45. doi:10.1111/myc.12623
99. Pfaller MA, Diekema DJ. Epidemiology of invasive mycoses in North America. *Crit Rev Microbiol* (2010) 36:1–53. doi:10.3109/10408410903241444
100. Falagas ME, Apostolou KE, Pappas VD. Attributable mortality of candidemia: a systematic review of matched cohort and case-control studies. *Eur J Clin Microbiol Infect Dis* (2006) 25:419–25. doi:10.1007/s10096-006-0159-2

101. Eggimann P, Garbino J, Pittet D. Epidemiology of *Candida* species infections in critically ill non-immunosuppressed patients. *Lancet Infect Dis* (2003) 3:685–702. doi:10.1016/S1473-3099(03)00801-6
102. Bassetti M, Merelli M, Righi E, Diaz-Martin A, Rosello EM, Luzzati R, et al. Epidemiology, species distribution, antifungal susceptibility, and outcome of candidemia across five sites in Italy and Spain. *J Clin Microbiol* (2013) 51:4167–72. doi:10.1128/JCM.01998-13
103. Pfaller MA, Castanheira M, Messer SA, Moet GJ, Jones RN. Variation in *Candida* spp. distribution and antifungal resistance rates among bloodstream infection isolates by patient age: report from the SENTRY Antimicrobial Surveillance Program (2008-2009). *Diagn Microbiol Infect Dis* (2010) 68:278–83. doi:10.1016/j.diagmicrobio.2010.06.015
104. Guinea J. Global trends in the distribution of *Candida* species causing candidemia. *Clin Microbiol Infect* (2014) 20(Suppl 6):5–10. doi:10.1111/1469-0691.12539
105. Trofa D, Gacser A, Nosanchuk JD. *Candida* parapsilosis, an emerging fungal pathogen. *Clin Microbiol Rev* (2008) 21:606–25. doi:10.1128/CMR.00013-08
106. Nucci M, Colombo AL. Candidemia due to *Candida tropicalis*: clinical, epidemiologic, and microbiologic characteristics of 188 episodes occurring in tertiary care hospitals. *Diagn Microbiol Infect Dis* (2007) 58:77–82. doi:10.1016/j.diagmicrobio.2006.11.009
107. Spivak ES, Hanson KE. *Candida auris*: an emerging fungal pathogen. *J Clin Microbiol* (2018) 56:e01588-17. doi:10.1128/JCM.01588-17
108. Nace HL, Horn D, Neofytos D. Epidemiology and outcome of multiple-species candidemia at a tertiary care center between 2004 and 2007. *Diagn Microbiol Infect Dis* (2009) 64:289–94. doi:10.1016/j.diagmicrobio.2009.03.010
109. Nutsch KM, Hsieh CS. T cell tolerance and immunity to commensal bacteria. *Curr Opin Immunol* (2012) 24:385–91. doi:10.1016/j.coi.2012.04.009
110. Round JL, Mazmanian SK. Inducible Foxp3+ regulatory T-cell development by a commensal bacterium of the intestinal microbiota. *Proc Natl Acad Sci U S A* (2010) 107:12204–9. doi:10.1073/pnas.0909122107
111. Atarashi K, Tanoue T, Oshima K, Suda W, Nagano Y, Nishikawa H, et al. Treg induction by a rationally selected mixture of clostridia strains from the human microbiota. *Nature* (2013) 500:232–6. doi:10.1038/nature12331
112. Furusawa Y, Obata Y, Fukuda S, Endo TA, Nakato G, Takahashi D, et al. Commensal microbe-derived butyrate induces the differentiation of colonic regulatory T cells. *Nature* (2013) 504:446–50. doi:10.1038/nature12721
113. Zelante T, Iannitti RG, Cunha C, De Luca A, Giovannini G, Pieraccini G, et al. Tryptophan catabolites from microbiota engage aryl hydrocarbon receptor and balance mucosal reactivity via interleukin-22. *Immunity* (2013) 39:372–85. doi:10.1016/j.immuni.2013.08.003
114. Romani L, Zelante T, De Luca A, Iannitti RG, Moretti S, Bartoli A, et al. Microbiota control of a tryptophan-AhR pathway in disease tolerance to fungi. *Eur J Immunol* (2014) 44:3192–200. doi:10.1002/eji.201344406
115. Bonifazi P, Zelante T, D'angelo C, De Luca A, Moretti S, Bozza S, et al. Balancing inflammation and tolerance in vivo through dendritic cells by the commensal *Candida albicans*. *Mucosal Immunol* (2009) 2:362–74. doi:10.1038/mi.2009.17
116. Duggan S, Leonhardt I, Hunniger K, Kurzai O. Host response to *Candida albicans* bloodstream infection and sepsis. *Virulence* (2015) 6:316–26. doi:10.4161/21505594.2014.988096
117. Carpino N, Naseem S, Frank DM, Konopka JB. Modulating host signaling pathways to promote resistance to infection by *Candida albicans*. *Front Cell Infect Microbiol* (2017) 7:481. doi:10.3389/fcimb.2017.00481
118. Lionakis MS, Fischer BG, Lim JK, Swamydas M, Wan W, Richard Lee CC, et al. Chemokine receptor Ccr1 drives neutrophil-mediated kidney immunopathology and mortality in invasive candidiasis. *PLoS Pathog* (2012) 8:e1002865. doi:10.1371/journal.ppat.1002865
119. Lionakis MS, Albert ND, Swamydas M, Lee CR, Loetscher P, Kontoyiannis DP. Pharmacological blockade of the chemokine receptor CCR1 protects mice from systemic candidiasis of hematogenous origin. *Antimicrob Agents Chemother* (2017) 61:e02365-16. doi:10.1128/AAC.02365-16
120. Kullberg BJ, Arendrup MC. Invasive candidiasis. *N Engl J Med* (2015) 373:1445–56. doi:10.1056/NEJMra1315399
121. Hung TY, Kotecha RS, Blyth CC, Steed SK, Thornton RB, Ryan AL, et al. Immunogenicity and safety of single-dose, 13-valent pneumococcal conjugate vaccine in pediatric and adolescent oncology patients. *Cancer* (2017) 123:4215–23. doi:10.1002/cncr.30764
122. Wyplosz B, Derradji O, Hong E, Francois H, Durrbach A, Duclos-Vallee JC, et al. Low immunogenicity of quadrivalent meningococcal vaccines in solid organ transplant recipients. *Transpl Infect Dis* (2015) 17:322–7. doi:10.1111/tid.12359
123. Zbinden D, Manuel O. Influenza vaccination in immunocompromised patients: efficacy and safety. *Immunotherapy* (2014) 6:131–9. doi:10.2217/imt.13.171
124. Hakim H, Allison KJ, Van de Velde LA, Tang L, Sun Y, Flynn PM, et al. Immunogenicity and safety of high-dose trivalent inactivated influenza vaccine compared to standard-dose vaccine in children and young adults with cancer or HIV infection. *Vaccine* (2016) 34:3141–8. doi:10.1016/j.vaccine.2016.04.053
125. Holzmann H, Hengel H, Tenbusch M, Doerr HW. Eradication of measles: remaining challenges. *Med Microbiol Immunol* (2016) 205:201–8. doi:10.1007/s00430-016-0451-4
126. Vickers DM, Anonychuk AM, De Wals P, Demarteau N, Bauch CT. Evaluation of serogroup C and ACWY meningococcal vaccine programs: projected impact on disease burden according to a stochastic two-strain dynamic model. *Vaccine* (2015) 33:268–75. doi:10.1016/j.vaccine.2013.09.034
127. Daniels CC, Rogers PD, Shelton CM. A review of pneumococcal vaccines: current polysaccharide vaccine recommendations and future protein antigens. *J Pediatr Pharmacol Ther* (2016) 21:27–35. doi:10.5863/1551-6776-21.1.27
128. Moyes DL, Wilson D, Richardson JP, Mogavero S, Tang SX, Wernecke J, et al. Candidalysin is a fungal peptide toxin critical for mucosal infection. *Nature* (2016) 532:64–8. doi:10.1038/nature17625
129. Zepp F. Principles of vaccine design-lessons from nature. *Vaccine* (2010) 28(Suppl 3):C14–24. doi:10.1016/j.vaccine.2010.07.020
130. Aaby P, Roth A, Ravn H, Napirna BM, Rodrigues A, Lisse IM, et al. Randomized trial of BCG vaccination at birth to low-birth-weight children: beneficial nonspecific effects in the neonatal period? *J Infect Dis* (2011) 204:245–52. doi:10.1093/infdis/jir240
131. Biering-Sorensen S, Aaby P, Napirna BM, Roth A, Ravn H, Rodrigues A, et al. Small randomized trial among low-birth-weight children receiving bacillus Calmette-Guerin vaccination at first health center contact. *Pediatr Infect Dis J* (2012) 31:306–8. doi:10.1097/INF.0b013e3182458289
132. Aaby P, Martins CL, Garly ML, Bale C, Andersen A, Rodrigues A, et al. Non-specific effects of standard measles vaccine at 4.5 and 9 months of age on childhood mortality: randomised controlled trial. *BMJ* (2010) 341:c6495. doi:10.1136/bmj.c6495
133. Benn CS, Netea MG, Selin LK, Aaby P. A small jab––a big effect: non-specific immunomodulation by vaccines. *Trends Immunol* (2013) 34:431–9. doi:10.1016/j.it.2013.04.004
134. Kleinnijenhuis J, Quintin J, Preijers F, Joosten LA, Ifrim DC, Saeed S, et al. Bacille Calmette-Guerin induces NOD2-dependent nonspecific protection from reinfection via epigenetic reprogramming of monocytes. *Proc Natl Acad Sci U S A* (2012) 109:17537–42. doi:10.1073/pnas.1202870109
135. Kleinnijenhuis J, Quintin J, Preijers F, Joosten LA, Jacobs C, Xavier RJ, et al. BCG-induced trained immunity in NK cells: role for non-specific protection to infection. *Clin Immunol* (2014) 155:213–9. doi:10.1016/j.clim.2014.10.005
136. Garcia-Valtanen P, Guzman-Genuino RM, Williams DL, Hayball JD, Diener KR. Evaluation of trained immunity by beta-1, 3 (d)-glucan on murine monocytes in vitro and duration of response in vivo. *Immunol Cell Biol* (2017) 95:601–10. doi:10.1038/icb.2017.13
137. Leentjens J, Quintin J, Gerretsen J, Kox M, Pickkers P, Netea MG. The effects of orally administered beta-glucan on innate immune responses in humans, a randomized open-label intervention pilot-study. *PLoS One* (2014) 9:e108794. doi:10.1371/journal.pone.0108794

Conflict of Interest Statement: The authors are inventors on a patent application related to the topic of this article.

Copyright © 2018 Tso, Reales-Calderon and Pavelka. This is an open-access article distributed under the terms of the Creative Commons Attribution License (CC BY). The use, distribution or reproduction in other forums is permitted, provided the original author(s) and the copyright owner are credited and that the original publication in this journal is cited, in accordance with accepted academic practice. No use, distribution or reproduction is permitted which does not comply with these terms.

frontiers in Immunology

REVIEW
published: 08 January 2018
doi: 10.3389/fimmu.2017.01939

Methods of Controlling Invasive Fungal Infections Using CD8+ T Cells

Pappanaicken R. Kumaresan[1], Thiago Aparecido da Silva[1] and Dimitrios P. Kontoyiannis[2]**

[1] Department of Pediatrics, The University of Texas MD Anderson Cancer Center, Houston, TX, United States, [2] Department of Infectious Diseases, The University of Texas MD Anderson Cancer Center, Houston, TX, United States

Invasive fungal infections (IFIs) cause high rates of morbidity and mortality in immunocompromised patients. Pattern-recognition receptors present on the surfaces of innate immune cells recognize fungal pathogens and activate the first line of defense against fungal infection. The second line of defense is the adaptive immune system which involves mainly CD4+ T cells, while CD8+ T cells also play a role. CD8+ T cell-based vaccines designed to prevent IFIs are currently being investigated in clinical trials, their use could play an especially important role in acquired immune deficiency syndrome patients. So far, none of the vaccines used to treat IFI have been approved by the FDA. Here, we review current and future antifungal immunotherapy strategies involving CD8+ T cells. We highlight recent advances in the use of T cells engineered using a Sleeping Beauty vector to treat IFIs. Recent clinical trials using chimeric antigen receptor (CAR) T-cell therapy to treat patients with leukemia have shown very promising results. We hypothesized that CAR T cells could also be used to control IFI. Therefore, we designed a CAR that targets β-glucan, a sugar molecule found in most of the fungal cell walls, using the extracellular domain of Dectin-1, which binds to β-glucan. Mice treated with D-CAR+ T cells displayed reductions in hyphal growth of *Aspergillus* compared to the untreated group. Patients suffering from IFIs due to primary immunodeficiency, secondary immunodeficiency (e.g., HIV), or hematopoietic transplant patients may benefit from bioengineered CAR T cell therapy.

Keywords: fungal infection, immunotherapy, chimeric antigen receptor, D-CAR+ T cells, cell therapy, Sleeping Beauty, CD8+ T cells, adoptive T cell therapy

OPEN ACCESS

Edited by:
Steven Templeton, Indiana University School of Medicine, United States

Reviewed by:
Ana Serezani, Vanderbilt University Medical Center, United States
Agostinho Carvalho, University of Minho, Portugal

****Correspondence:***
Pappanaicken R. Kumaresan
pkumaresan@mdanderson.org;
Dimitrios P. Kontoyiannis
dkontoyi@mdanderson.org

Specialty section:
This article was submitted to Microbial Immunology, a section of the journal Frontiers in Immunology

Received: *31 October 2017*
Accepted: *15 December 2017*
Published: *08 January 2018*

Citation:
Kumaresan PR, da Silva TA and Kontoyiannis DP (2018) Methods of Controlling Invasive Fungal Infections Using CD8+ T Cells. Front. Immunol. 8:1939. doi: 10.3389/fimmu.2017.01939

INTRODUCTION

Opportunistic invasive fungal infections (IFIs) are a major threat to the immunocompromised individual; neutropenia is a major risk factor for these infections (1, 2). Patients who require prolonged immunosuppressive therapy, for example, those who have undergone solid organ transplantation or hematopoietic stem-cell transplantation (HSCT) and those who have severe autoimmune diseases are also highly susceptible to IFIs (3–7). Other risk factors include long-term stays in an intensive care unit, the use of indwelling catheters, chemotherapy, or broad-spectrum antibiotics. The main causative agents of IFI are *Aspergillus* spp., *Candida* spp., and *Cryptococcus* spp. The incidence of IFI is increasing worldwide (2, 8, 9) (**Table 1**), and the worldwide crude mortality rate of invasive aspergillosis and invasive candidiasis has been estimated to be 0.4 deaths per 100,000 people. However, mortality rates associated with IFIs in immunocompromised patients are considerably higher, reaching 60–85% for invasive aspergillosis. The emergence of fungal strains that are resistant to currently available antifungal drugs such as polyenes, triazoles, and echinocandins poses a dangerous

TABLE 1 | Incidence and patterns of fungal infections worldwide.

Fungal infection	Incidence per year	Reference	Main routes	Comments
Invasive aspergillosis (*Aspergillus*)	>300,000	(15)	Pulmonary	
Invasive candidiasis (*Candida*)	8–10 cases/100,000	(16, 17)	Cutaneous Oropharyngeal Gastrointestinal Genitourinary	
Mucormycosis (*Mucorales*)	1.7 cases/1000,000	(18)	Sinopulmonary Disseminated	
Cryptococcus	~1,000,000	(19)	Pulmonary	
Pneumocystis pneumonia	In the US, 9% among hospitalized HIV/acquired immune deficiency syndrome patients and 1% among solid organ transplant recipients	(20, 21)	Pulmonary	In immunocompromised patients, the mortality rate ranges from 5 to 40% in those who receive treatment. The mortality rate approaches 100% without therapy

CNS, central nervous system.
Since there is a lack of epidemiological data in many countries, the world incidence rate may be overestimated.

problem (10) and immune-based treatments are giving new hope to combat these deadly fungal infections (11–14).

The host response to fungal infection depends on several factors, including the host immune status, site of infection, fungal morphotype (yeast or hyphae), cell wall complexity, and virulence traits, such as the production of fungal exotoxins (22–25). The routes of various fungal infections are listed in **Table 1**; the majority occurs *via* the sinopulmonary and gastrointestinal routes (22). The host immune response to fungal infection occurs in a coordinated way *via* both innate and adaptive immune cells. Innate effector cells, mainly macrophages and neutrophils, are the first line of defense against inhaled fungal spores (11, 26). As a result, most initial fungal encounters go unnoticed (27). Pattern-recognition receptors (PRRs) are a family of receptors that is composed of the C-type lectin receptors (CLRs), toll-like receptors (TLRs), Nod-like receptors, and other receptors that initiate immune responses against invading fungal pathogens. Cellular expression and signaling mechanism of the PRRs have been reviewed previously (28–30).

Most of the sugars present on the fungal cell wall are recognized by the receptors from the CLR family, underscoring the constant vigil of the host innate immune system against invading fungal pathogens (28, 31–33). CLRs recognize the various carbohydrate glycoprotein components of the fungal cell wall, such as β-glucan or α-mannan, which trigger downstream signaling cascades that are essential for inducing protective immunity against fungi (34–37). When the fungal insult cannot be quickly controlled, adaptive immune cells, mainly $CD4^+$ T cells, activate other cellular responses and antibody production. Adaptive immune cells produce cytokines to activate B cells, which in turn secrete antibodies against fungal antigens and activate the release of antimicrobial peptides from endothelial cells. Recent comprehensive reviews have already detailed the mechanisms of $CD4^+$ T cells and surveyed current immunotherapeutic strategies to control fungal diseases (12, 38, 39). Despite having intact innate immune systems, patients with acquired immune deficiency syndrome (AIDS) are highly susceptible to fungal infections, highlighting the importance of the adaptive immune system. When $CD4^+$ T cell counts are low, as in patients with AIDS, $CD8^+$ T cells have a heightened role in controlling fungal infections (40). In this review, we focus on the functional role of $CD8^+$ T cells in the immune response to fungal infections. We then discuss a new method of combating fungal infections, engineering T cells with the "Sleeping Beauty" (SB) vector system.

CURRENT AND FUTURE STRATEGIES TO CONTROL FUNGAL INFECTIONS

Drug Therapy

Antifungal drugs have had only modest success in reducing the high mortality rates associated with IFIs. In large part, this is because diagnosis of fungal infection and identification of the responsible organism is often delayed, leading to a delay in the administration of directed antifungal therapy. The use of available antifungal drugs is also restricted by their route of administration, spectrum of activity, and bioavailability in target tissues such as the brain (41). Additional issues include toxicity, undesirable drug interactions, and drug resistance. Use of the triazoles, for example, is limited by their interactions with statins, corticosteroids, and other drugs (42).

Despite tremendous improvements in the response rates of aspergillosis to modern antifungal agents, fatality rates of 40% are common in contemporary real life cohorts of unselected patients with leukemia and transplant recipients (43). The high rate of mortality following *A. fumigatus* infection is a result of the suboptimal diagnostic tools available, leading to late diagnosis. Other factors include rising *Aspergillus* resistance, and even more importantly, the relative ineffectiveness of existing antifungal drugs against established *Aspergillus* infections (44).

The development of effective and safe immune enhancement therapies is a major unmet need. Some patients with candidiasis struggle with poor outcomes, although this is less common in the era of widespread azole prophylaxis given to high-risk patients. Randomized controlled studies typically exclude high-risk immunosuppressed patients by use of their inclusion criteria (45).

Immunotherapy

Innate Immune Cells

Immunotherapy, which comprises cell-based therapies, such as the adoptive transfer of T cells, dendritic cells (DCs), or neutrophils, and other humoral approaches, such as antibodies and recombinant pentraxins, is a viable option for control of IFIs. Among immunocompetent individuals, the innate immunity efficiently prevents and clears IFIs (26). Alveolar macrophages are the first line of fungal defense; they recognize, phagocytize, and destroy fungal spores (46). Neutrophils also play a key role in killing fungal hyphae. They eliminate fungal hyphae by inducing an oxidative burst and by forming neutrophil extracellular traps (NETs) (47). Neutrophils utilize NETs to trap the invading pathogens by releasing chromatin fibers to form a meshwork adorned with cytoplasmic granules containing the antimicrobial enzymes myeloperoxidase, cathepsin G and neutrophil elastase that destroy trapped pathogens. The whole process is called NETosis (48).

To date, immunotherapeutic strategies to combat IFIs have primarily focused on augmenting the number of granulocytes, since these cells are known to have fungicidal activity. Granulocyte-focused immunotherapies include granulocyte transfusions (49), infusion of growth factors [granulocyte colony-stimulating factor (G-CSF), or granulocyte macrophage colony-stimulating factor (GM-CSF)] to increase granulocyte numbers (50), and the administration of cytokines such as interferon (IFN)-γ (51) and/or interleukin (IL)-15, the latter of which promotes the production of IL-8 (52), to augment phagocytic and cytotoxic function. However, the reconstitution of granulocytes is hampered by an inability to numerically expand large numbers of cells *ex vivo*. Moreover, after infusion, reconstituted granulocytes exhibit poor persistence owing to increased apoptosis, weak potency, and a propensity to become trapped in the pulmonary vasculature (53).

Natural Killer (NK) Cells

Natural killer cells are another type of innate immune cell reported to be involved in controlling fungal infections. NK cells make up from 5 to 15% of the peripheral blood mononuclear cells (PBMCs) of healthy individuals; the NK cell population is made up of $CD56^+$ and $CD3^-$ cells (54). NK cells are activated when signals from activating receptors outweigh signals from inhibitory receptors, leading to cytotoxicity directed against tumor cells and virus-infected cells. NK cells also recognize infectious fungal pathogens, including *A. fumigatus*, *C. albicans*, *C. neoformans,* and *Mucorales* species (31, 55–58). Recently, CD56 has been identified as a PRR that can bind directly to both germ tubes and hyphae of *Aspergillus fumigatus* (59). Upon recognition, NK cells either induce lysis of these pathogens by secreting perforin and granulysin or trigger activation of other immune cells by releasing IFN-γ (60). Fungal pathogen-specific NK cell receptors and their mechanism of action has been reviewed (61, 62).

Dendritic Cells

Dendritic cells are professional antigen presenting cells (APCs) that can recognize and phagocytize fungal conidia and hyphae through PRRs and degrade them by fusing with lysosome vesicles (63). PRRs activate DCs to secrete cytokines, such as IL-12, IL-6, IL-4, and IL-1β that induce T-cell differentiation in the lymph nodes. During *A. fumigatus* infection, pulmonary DCs secrete IL-12 upon exposure to conidia, while IL-4 and IL-10 are secreted after exposure to hyphae. Therefore, IL-12 signaling generates a T helper (Th) 1 cell response, while IL-4 and IL-10 signaling generates a Th2 response. DCs also secrete tumor necrosis factor (TNF)-α and the chemokine CXCL8 which recruit neutrophils to the infection site (64).

In conventional DCs, β-glucan-induced Dectin-1-mediated signaling promotes secretion of the cytokines IL-2 and IL-23. The release of IL-23 induces Th17 differentiation but it is tightly regulated by IL-2 (65, 66). These data suggest that DCs direct naïve T cells to mature into functional T-cell sub types by secreting specific cytokines in the microenvironment based upon stimuli received by PRRs from different forms of fungi.

$CD4^+$ T Cells

Even though DCs help to reduce the fungal burden to some extent through fusion with lysosome vesicles, the major function of DCs is to present fungal antigens to naive T-cells. DCs present processed antigens *via* major histocompatibility complex (MHC) class I or class II molecules and interact with naive T cells through formation of an immunological synapse. T cells are broadly classified into helper $CD4^+$ T cells and cytotoxic $CD8^+$ T cells. In fungal infections, both $CD4^+$ and $CD8^+$ T cells participate in the elimination of fungal pathogens (67, 68). On the basis of their function and cytokine secretion profile, $CD4^+$ T cells are classified into several subsets: Th1, Th2, Th9, Th17, Th22, regulatory T cells, and follicular helper T cells. The activity of $CD4^+$ T cells against fungal infection in immunocompetent individuals has been very well characterized. The most important $CD4^+$ T cells in the antifungal immune response are the Th1 and Th17 helper T cells. After priming by DCs, $CD4^+$ T cells differentiate into Th1 and Th17 helper T cells. Th1 helper T cells secrete the cytokines IFN-γ and TNF-α which activate innate immune cells, such as neutrophils, macrophages, DCs, and inflammatory monocytes, to fight against invading fungi and bacteria (12, 27). The cytokines secreted by Th1 cells also activate B cells, leading to the secretion of antigen-specific antibodies against fungi. IL-17 secreted by Th17 cells controls fungal infection by mobilizing neutrophils and protecting mucosal body sites by inducing epithelial cells to secrete defensin (69). IL-17 deficiency has been shown to enhance susceptibility to *Candida albicans* infections at mucosal sites (70).

$CD8^+$ T Cells

Like $CD4^+$ T cells, $CD8^+$ T cells also have sub types, namely Tc1, Tc2, and Tc17 (**Figure 1**). APCs, mainly DCs, cross-present fungal antigens to $CD8^+$ T cells. $CD8^+$ T cells can be primed to recognize fungi by utilizing a "cross-presentation" and "cross-priming" approach, in which exogenous or fungal antigens are presented on MHC-I molecules (71). DCs internalize exogenous fungal products by CLRs and scavenger receptors for processing and presenting to MHC-I, and this process is called cross-presentation. Along with cross-presentation, some of the CLRs, for example, Dectin-1 activates DCs *via* Syk kinase signaling to produce IL-12, which favors Tc1 differentiation (72). Curdlan

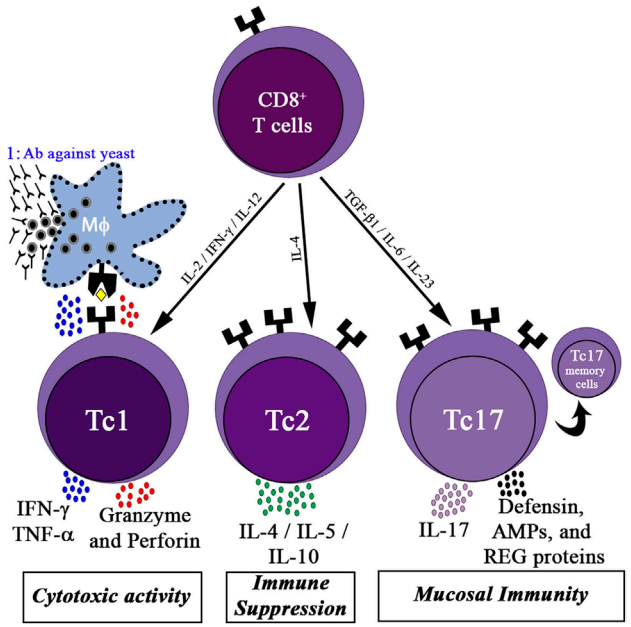

FIGURE 1 | CD8+ T cells activity in the immune response. Differentiation of CD8+ T cells into three functional subsets: the cytotoxic cells (Tc1) cells, producing high levels of interferon (IFN)-γ, tumor necrosis factor (TNF)-α, granzyme, and perforin, which contribute to the killing of yeast infected host cells; Tc1 kills fungal infected macrophages and allows the participation of humoral immunity (marked as 1); Tc2 cells, release high amounts of interleukin (IL)-4 and IL-10, promoting immune suppression; Tc17 cells secrete IL-17, which activates mucosal immunity by inducing epithelial cells to secrete defensin, antimicrobial peptides (AMPs), and regenerating proteins (REG). Some of the activated Tc17 cells may differentiate into memory Tc17 cells.

has been demonstrated to stimulate the Dectin-1-syk-CARD pathway, producing IL-23 to boost the differentiation of Th17 cells (73).

Upon recognition of fungal peptides presented by APCs, CD8+ T cells differentiate into Tc1 cells and Tc17 cells (CD8+ T cells that secrete IL-17A), depending on the cytokines present in the environment. Several reports highlighted the role of Tc1 and Tc17 cells in protecting humans from fungal infection (74, 75). Tc1 cells act indirectly by secreting cytokines such as IFN-γ, TNF-α, and GM-CSF to activate innate immune cells such as neutrophils and macrophages involved in antifungal defense. Furthermore, Tc1 cells directly kill unresponsive fungal-infected macrophages by secreting cytotoxic factors such as perforin, granulysin, and granzyme K (76). DCs uptake fungal breakdown products from apoptotic macrophages by endocytosis to cross prime CD8+ Tc1 cells. CD8+ Tc17 cells, like CD4+ Th17 cells, secrete IL-17A cytokines to activate epithelial cells (mucosal immunity) to secrete antimicrobial products such as defensin to fight against fungal infections (**Figure 1**).

The Tc1 and Tc17 subtypes can be divided into effector T cells and effector memory T cells on the basis of their expression of surface receptors. The cell-surface markers used for phenotypical characterization of Tc1 and Tc17 cells are shown in **Table 2**. Tc1 cells that express C–X–C motif chemokine receptor 3 migrate

TABLE 2 | Phenotypic characterization of CD8+ Tc1 and Tc17 cell subtypes.

Cell-surface markers/ cytokines	Expression in Tc1	Expression in Tc17	Transcription factors/ secretory granules	Expression in Tc1	Expression in Tc17
CCR6	N.I.	High	TCF-1	High	High
CXCR3	High	Low	T-bet	Low/High	Low
CD62L	Low/high	Low	Eomes	High	
CD27	High	Low/ intermediate	Ror (γ)t	Low	High
KLRG-1	Low	Low			
IFN-γ	+	–	Perforin	+	–
TNF-α	+	–	Granulysin	+	–
IL-2	+	–			
GM-CSF	+	–			
IL-17	–	+			

CCR6, C–C motif chemokine receptor 6; CXCR3, C–X–C motif chemokine receptor 3; CD62L, cluster of differentiation 62L;CD27, cluster of differentiation 27; KLRG-1, co-inhibitory receptor killer-cell lectin-like receptor G1; IFN, interferon; TNF, tumor necrosis factor; IL-2, interleukin-2; GM-CSF, Granulocyte macrophage colony-stimulating factor; IL-17, interleukin-17; TCF-1, T cell factor 1; T-bet, T-box transcription factor; ROR-γt, RAR-related orphan receptor gamma; N.I., no information.

to the lungs during pulmonary infections, such as pneumocystis (77). Tc17 cells have increased levels of effector memory phenotype markers on the cell surface ($CD62L^{lo}$ and $CD27^{it/lo}$) as compared with Tc1 cells, suggesting that Tc17 cells may play a role in preserving long-term antifungal immunity in the host. Cytokines secreted by CD8+ Tc1 and Tc17 cells boost the innate immune system as well as the mucosal immune system to give protection from IFI (**Figure 1**).

CD8+ T cells share many cellular functional mechanisms with NK cells, such as releasing cytolytic granules and cytokines. As indicated above, in the absence of CD4+ T cells, CD8+ T cells also play a major role in controlling fungal infection. Immunotherapy could take advantage of several properties of CD8+ T cells, they can kill pathogen infected cells, be propagated in large numbers *ex vivo*, be genetically modified to recognize particular antigens, and contribute to immunologic memory.

THE ROLE OF CD8+ T CELLS IN THE ANTIFUNGAL IMMUNE RESPONSE

The immune response to fungi elicited by CD8+ T cells can broadly classified into two processes: (1) T-cell receptor (TCR) mediated and (2) TLR and scavenger receptor mediated.

TCR-Mediated CD8+ T Cell Activation

Vaccines are a promising avenue for the treatment and prevention of IFIs (78–84) mediated through TCR receptors. The vaccine candidates developed against fungal antigens typically activate CD4+ T cells and Th17 cells. Several highly immunogenic and protective vaccine formulations for candidiasis are currently undergoing clinical trials (84, 85). It is worth noting that vaccination against fungi has mainly focused on yeast pathogens, such as *Candida* spp. and *Cryptococcus* spp. (80), and endemic mycoses that infect immunocompetent individuals, such as *Coccidioides* spp. (86), *Blastomyces* spp., and *Histoplasma* spp. It remains to

be seen whether similar strategies will be as effective against opportunistic fungi, such as *Aspergillus*. In preclinical studies, vaccination using both crude and recombinant *Aspergillus* antigens improved the survival of immunocompromised mice following inhalation and intravenous administration of *Aspergillus fumigatus* (87).

Direct killing by $CD8^+$ T cells has not been widely explored in the development of an immunotherapy against fungi, even though studies demonstrated the essential role of the $CD8^+$ T-cell response in controlling fungal infections after vaccination (74, 75, 88–92) (**Table 3**). However, the presence of *Aspergillus*-specific $CD8^+$ T cells has been shown in both mice and humans (93–96). Moreover, *Mucorales* (97) and *Fusarium*-specific T-cells (98) were reported in hematologic patients with IFI. Type I $CD8^+$ T-cells (Tc1) were shown to provide protection against pneumocystis in mice (99). Preclinical studies demonstrated that the direct effect of $CD8^+$ T cell-mediated cytotoxic activity and TNF-α and IFN-γ production were necessary to clear infected macrophages containing *H. capsulatum* (76), and provided full protection against coccidioidomycosis (88, 89). The activation of $CD8^+$ T cells also contributed a protective response during *Cryptococcus neoformans* infection; involvement of Type 1 $CD8^+$ T (Tc1) cells was triggered through immunization with the cytosolic proteins of the pathogens (90). Moreover, $CD8^+$ T-cells secrete IL-17A to give protection against lethal fungal diseases, such as *Blasotomyces dermatitidis* and *Histoplasma capsulatum*, by supporting neutrophil activity (74) (**Figure 1**).

However, there are limitations for vaccine therapy. Currently, no FDA-approved vaccines are available to prevent the major opportunistic fungal infections, specifically candidiasis, aspergillosis, and cryptococcosis. Several reasons underlie the paucity of viable candidates. First, these infections are relatively uncommon, compared to viral and bacterial infections and typically occur in severely ill patients. Thus, finding sizable niche patient population who can benefit from a cost-effective vaccine strategy is difficult and not an area of priority for development by the pharmaceutical industry. Second, high-risk patients have pleiotropic and ever-evolving defects in both innate and adaptive immunity. As responses to fungi depend on both arms of the immune response, and because such responses are complex, depending on the site of infection (mucosal vs systemic infection) and the type of fungus (e.g., *Candida* or *Cryptococcus* vs a mold), much more groundwork needs to be done to decipher the key elements of a successful vaccine. In addition, there are questions regarding the efficacy and feasibility of using a vaccine in immunocompromised patients, since they are incapable of mounting a complete immune response (105).

TLR-Mediated $CD8^+$ T Cell Activation

Toll-like receptors of the innate immune system play a major role in recognizing fungal cell wall carbohydrates, cell wall breakdown products, RNA, and DNA (13, 106–108) and thereby activate immune cells. One possible mechanism TLRs use to augment T-cell activation is when DCs activate fungal-specific $CD8^+$ T cells by cross-presenting fungal antigens. TLR3 plays a crucial role in this process by sensing fungal RNA derived from necrotic cells and activating $CD8^+$ memory T cells along with DCs. Indeed, $TLR3^{-/-}$ mice are more susceptible to *Aspergillus* infection than are control mice (101), and people with mutations in key TLR3 and TLR4 signaling components are susceptible to various fungal infections (109–111).

T-Cell Activation Mediated by Scavenger Receptors and Other Receptors

The scavenger receptor proteins are a highly heterogeneous set of proteins expressed on the cell surface that are involved in the uptake of modified low-density lipoproteins and a variety of microbes. One of the scavenger receptors, CD5, has been shown to bind β-glucan, a fungal cell wall sugar moiety, as well as many strains of yeast cells (112). CD5 is expressed on T cells and a small subset of mature B cells, where it associates with antigen receptors. Upon stimulation with zymosan (a protein-sugar moiety derived from the yeast cell wall), a CD5-transfected cell line produces IL-8, suggesting that CD5 has a pro-inflammatory role in fungal infection (112).

Besides TLRs, T cells have other receptors such as CD23 and CD56 for direct recognition of fungal antigens. CD23 is an

TABLE 3 | Fungal vaccine candidates and their $CD8^+$ T-cell mechanisms of action.

Fungal infection	Candidate	$CD8^+$ T cell responses	Model	Reference
Aspergillosis	Recombinant fungal antigens Pep1p, Gel1p, and Crh1p	Cytotoxic activity	Murine	(100)
	Live *A. fumigatus* conidia or *A. fumigatus* cell wall glucanase Crf1p	Cytotoxic activity	Murine	(101)
Blastomycosis	Attenuated mutant lacking BAD1	Tc17 cells	Murine	(74, 91)
	Attenuated mutant lacking WI-1 adhesin	TNF-α, IFN-γ, and GM-CSF production; $CD8^+$ T cell memory	Murine	(75, 92)
Coccidioidomycosis	Arthroconidia of the 95–291 strain	Cytotoxic activity; TNF-α production	Murine	(88)
	Live spores of the Δcts2/ard1/cts3 strain	IFN-γ production	Murine	(89)
Candidiasis	Candidal adhesin (rAls3p-N) plus aluminum hydroxide adjuvant	Cytotoxic activity	Murine	(102)
	Candida dubliniensis mannan–human serum albumin conjugate	Upregulation	Rabbit	(103)
	Cytosolic antigens entrapped in liposomes	Upregulation	Murine	(104)
Paracoccidioidomycosis	N.I.	N.I.	N.I.	N.I.
Cryptococcosis	Cytosolic proteins	Tc1 cells	Murine	(90)

TNF, tumor necrosis factor; IFN, interferon; GM-CSF, granulocyte macrophage colony-stimulating factor; N.I., no information.

inducible low-affinity receptor for immunoglobulin (Ig)E (113). It can recognize both β-glucan and α-mannan sugar moieties and thereby targets both yeast and hyphae forms of *Candida* (114), and upon activation, it upregulates nitric oxide production to destroy invading *Candida.* C-Jun N-terminal kinases (JNK1) activation suppresses the expression of CD23, which increases susceptibility of fungal infection. This was verified in JNK1 KO mice which showed resistance to *Candida* infection when compared to control mice (114). CD56 is a NK cell receptor that has been shown to bind to *Aspergillus* hyphae in a concentration-dependent manner. Blocking of CD56 reduced fungal-mediated NK cell activation (59). Activated T-cells expresses high levels of CD56 and its expression level directly correlates with T-cell effector functions (115). However, additional studies are warranted to verify that the CD56 mediated $CD8^+$ T cells are activated during fungal infection.

ADOPTIVE T-CELL THERAPY

Over the years, several immunotherapies have been used to treat fungal infection. One such immunotherapy, adoptive T-cell therapy (ACT), is a promising therapeutic strategy not only for cancer but also for treating viral and fungal infections (38, 116–118). ACT involves the isolation and *ex vivo* expansion of autologous T cells in an antigen-specific manner; these expanded T cells are later infused into the patient. ACT has been shown to be effective in controlling viral infections, such as cytomegalovirus (119) and fungal infections, such as *Aspergillus* in HSCT patients (120). Immunocompromised patients, especially patients undergoing allogeneic HSCT, are highly susceptible to IFIs (7). The mortality rate from IFI in this patient population remains unacceptably high, partly due to the long-lasting immunosuppression in patients after HSCT (3, 121). Most IFIs in these patients occur after engraftment of the innate immune system, which suggests that adaptive cellular immunity plays a major role in controlling IFIs. In fact, adoptive transfer of $CD4^+$ Th1 cells elicited significant protection against invasive aspergillosis in haploidentical HSCT settings (120). These findings have generated a growing interest in restoring adaptive immunity against fungal pathogens by infusing donor-derived antifungal T cells and in various *ex vivo* methods of propagating clinical-grade *Aspergillus*-specific T cells (38, 122). Recently, the FDA-approved chimeric antigen receptor (CAR) T-cell therapy to treat B-cell malignancies. CAR T cell technology can be applied to redirect T cell specificity to target fungal pathogens.

Three approaches are used to redirect T-cell specificity against a particular antigen (123).

1. Gene modification with antigen-specific TCRs in which the α and β chains of the TCR are cloned from tumor-associated antigen-specific T-cell clones (124, 125).
2. Gene modification using natural receptors other than TCRs, such as the Dectin-1 receptor (126).
3. Introduction of a CAR that recognizes tumor-associated antigens through a single-chain variable region (scFv) derived from the corresponding monoclonal antibody (127). Currently, there are no reports in the literature of scFv-derived CAR T-cells targeting fungal antigens. Therefore, in the current review, it was added for comparison analysis with $D\text{-}CAR^+$ T cells (**Figure 2**).

Gene Modification Using Pathogen-Specific TCRs

T-cell receptors are found on the surface of T cells as heterodimers of α and β chains and they recognize antigens presented by the MHC receptors of the APCs. For ACT, genes of tumor

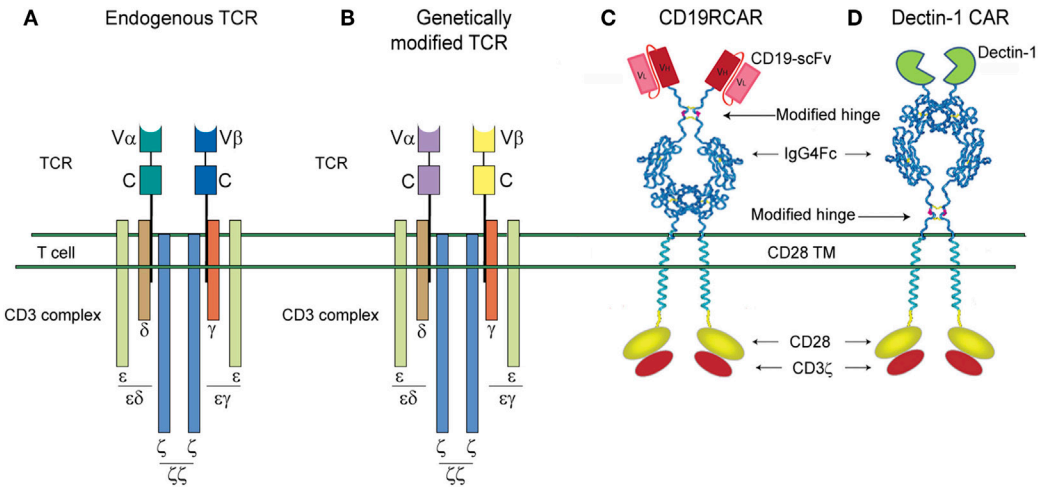

FIGURE 2 | Schematic representations of the T-cell receptor (TCR) complex and second-generation single-chain variable region (scFv)-chimeric antigen receptor (CAR) and D-CAR. **(A)** Unmodified endogenous TCR complex and **(B)** genetically modified TCR complex. The α and β chains are highlighted in different colors. **(C)** The CD19R-CAR derived from a scFv region of a CD19 antigen-specific mouse monoclonal antibody and **(D)** the $D\text{-}CAR^+$ derived from an extracellular domain of the Dectin-1 receptor. CD19R-CAR and D-CARs shown here have the same signaling domains, derived from costimulatory molecules, such as CD28 and CD3-ζ.

antigen-specific TCRs are isolated from patients and engineered into T cells using a viral or non-viral-based vector system (128, 129). These T cells are expanded *ex vivo* to generate large numbers for infusion. Improvements in vector design have recently increased the efficiency of this approach, and the avidity of the TCR has been improved by substituting amino acids in its complementarity determining region and introducing cysteines to form disulfide bonds, thereby preventing α- and β-chain mispairing. TCR-mediated T-cell responses to fungal antigens have been documented in both *in vitro* and *in vivo* studies (130, 131).

In colon cancer studies, TCR-driven ACT was effective in reducing tumor volume (132), but a high incidence of toxicity was reported, especially when high-avidity TCRs were used (133). Moreover, TCR-specific therapy is MHC restricted; if tumor cells lose antigen expression by downregulating MHC, they can evade the T cell attack (134). Hence, TCR-specific T-cell recognition is restricted to a single type of MHC molecule that presents the targeted antigen (135). In order to circumvent this problem, CAR-based therapy was developed. With CAR-based T-cell therapy, the tumor recognition of the CAR is not dependent on MHC (136).

Engineered CAR T-Cell Therapy

Engineered T-cell therapy involving the introduction of a CAR, which recognizes tumor-associated antigens through its scFv, is derived from the corresponding monoclonal antibody. CAR-based therapy involves the genetically engineered fusion of a variable light chain and a variable heavy chain that are specific for a cell-surface antigen and are tailored to produce an activating signal to host immune cells upon antigen engagement (137). CAR-based T-cell therapy has several key advantages. First, a CAR-based approach can be used in all tumor conditions expressing the antigen and is not MHC restricted. Second, tumor cells have no protection against CAR-based immunoediting. Finally, a varied range of tumor antigens can be targeted using this system, including glycoproteins and lipids (138, 139).

The CAR has been structurally refined over three generations of development. CAR's structure consists of four elements: an antigen-targeting domain, an extracellular linker/spacer, a membrane-spanning (transmembrane) domain, and an intracellular signaling domain. The antigen-specific domain is usually derived from the scFv of the monoclonal antibody targeting the antigen. The linker makes the CAR flexible so that it can reach the antigen. A mutated IgG derived Fc sequence incapable of activating innate immune cells is commonly used because of its stability in expressing the CAR on the cell surface (140). In first-generation CARs, the transmembrane domain used CD4 or CD8, while CD28 was used in second-generation CARs (141). The intracellular signaling domain of second-generation CARs used CD3-ζ along with the costimulatory signaling domain CD28 (142). Tumor clearance and persistence is better in second- and third-generation CAR^+ T cells than in the first generation (140, 141, 143, 144).

SB, a Non-Viral-Based Vector

Several vector systems have been used to introduce the CAR transgene into T cells. Of these, mammalian transposon/transposase-based vectors produce the most robust integration, have low immunogenicity, and allow for easy manipulation of plasmids. Multiple vectors have been studied in mammalian systems, including the SB transposon (derived from the fish, *Tanichthys albonubes*), the PiggyBac element (from the moth, *Trichoplusia ni)*, Frog Prince (from the frog, *Rana pipiens*), Himar1 (from the horn fly, *Haematobia irritans*), Tol2 (from the fish, *Oryzias latipes*), and Passport (from the flatfish, *Pleuronectes platessa)* (145, 146).

Among all of the elements with activity in mammalian cells, the SB transposon is one of the most widely studied for use in gene transfer (147, 148). The SB transposase was derived by combining inactive transposase sequences from the genome of salmonid fish and then reversing the termination codon to activate transposase activity. A typical SB vector consists of 230-base pair (bp) regions containing long inverted and direct repeats (IR/DR) flanking the target gene sequence. These IR/DR sites bind with SB transposase to transfer the target gene to the host genome. In addition to the IR/DR sites, SB transposase also contains a DNA-recognition site, a nuclear localization signal, and a catalytic domain. Gene transfer using the SB transposon/transposase involves a cut-and-paste mechanism. The SB transposase protein is translated and accumulated in the cytoplasm, which is then imported into the nucleus using the nuclear localization signal. The SB transposase protein binds to the IR/DR sequence of the transposon, causing DNA breaks around the gene of interest.

The integration site of the gene cut from the SB transposon in the T cell genome depends on the presence of a TA dinucleotide site, DNA flexibility, and proximity of the donor and receiver (local hopping). More than 25% of integrations occur within a 200-bp region between the donor and receiver sites of the gene, and more than 75% of integrations are located in a single chromosome. CD19R-CAR T cells were developed using the SB vector and successfully used in clinical trials to treat acute myeloid leukemia and chronic lymphocytic leukemia (127, 149).

Dectin-1 CAR T-Cells to Target β-Glucan-Expressing Fungi

We modified this prototypical CAR to recognize carbohydrates by utilizing the pattern-recognition properties of Dectin-1 (126, 150, 151). It is specific for β-glucan, a glucose polymer consisting of β-1, 3-glucan and β-1, 6-glucan that is expressed on the cell wall of all known fungi (152–155). We hypothesized that the extracellular portion of Dectin-1 could be adapted as the specificity domain for a CAR (D-CAR) on T cells to redirect their specificity to β-glucan expressing fungi such as *Aspergillus*. Using the extracellular domain of Dectin-1, we engineered a CAR with specificity for the fungal cell wall sugar moiety β-glucan. This CAR was fused in frame to a modified human IgG4 hinge/Fc stalk (156), CD28 transmembrane domain, and a combination of CD28 and CD3ζ intracellular domains. This design is similar to that of our second-generation CD19-specific CAR (designated CD19RCD28), which is currently being employed in clinical trials to treat B-cell leukemia (157) (**Figure 2**).

Since this was the first time that a PRR was adapted to redirect T-cell specificity, we employed multiple assays [cell viability

assay (XTT), cytokine production, upregulation of CD107a, and microscopy] to compare the ability of D-CAR$^+$ T cells to target germinating *Aspergillus* hyphae with that of CD19-specific T cells. All of these assays demonstrated that the D-CAR activated the cytolytic machinery of the genetically modified T cells and probably their perforin/granzyme pathway as well (126). The production of IFN-γ by the D-CAR$^+$ T cells may further augment innate immunity to IFIs. Treatment with recombinant IFN-γ or IFN-γ derived from CD4$^+$ helper T cells or NK cells has been shown to augment anti-*Aspergillus* activity (55, 122). It remains to be determined whether the D-CAR-dependent production of IFN-γ contributes directly to the clearance of fungal infections or whether this activity works indirectly through the activation of granulocytes. Other cytokines, such as IL-17, may also participate in antifungal immunity. Reports indicate that IL-17 can activate neutrophils in a similar manner to IFN-γ (158), though increased levels of IL-17 are associated with mortality (153, 159–162) (**Figure 3**).

The use of combination therapies may supplement the antifungal efficacy of D-CAR$^+$ T cells. For example, in *Aspergillus* pre-exposed to Caspofungin, β-glucan residues in the cell wall were unmasked, enhancing antifungal activity mediated by neutrophils (163). In HSCT patients, innate immune cells are present in the blood within 2 weeks of the stem-cell transplant, whereas it takes, on average, 7–12 months for NK, B, and T cells to be produced. Most IFIs occur during this period because no cellular immune system exists to support the innate immune system (7, 164). One clinical application for the add-back of donor-derived D-CAR$^+$-T cells after allogeneic HSCT is to provide protection from IFIs by the recognition of β-glucan moieties present in all opportunistic fungi.

Bioengineered Dual CAR T Cells to Target B-Cell Leukemia and IFI

CD19-specific CAR T-cells have been used successfully to treat acute lymphoblastic leukemia (ALL) by eliminating both malignant and normal B-cells, since CD19 is also expressed on normal cells. However, total elimination of B-cells resulted in B-cell aplasia as a side effect (165). Therefore, patients undergoing CAR T cell therapy are typically given intravenous Ig to control bacterial and fungal infections. Also, high incidences

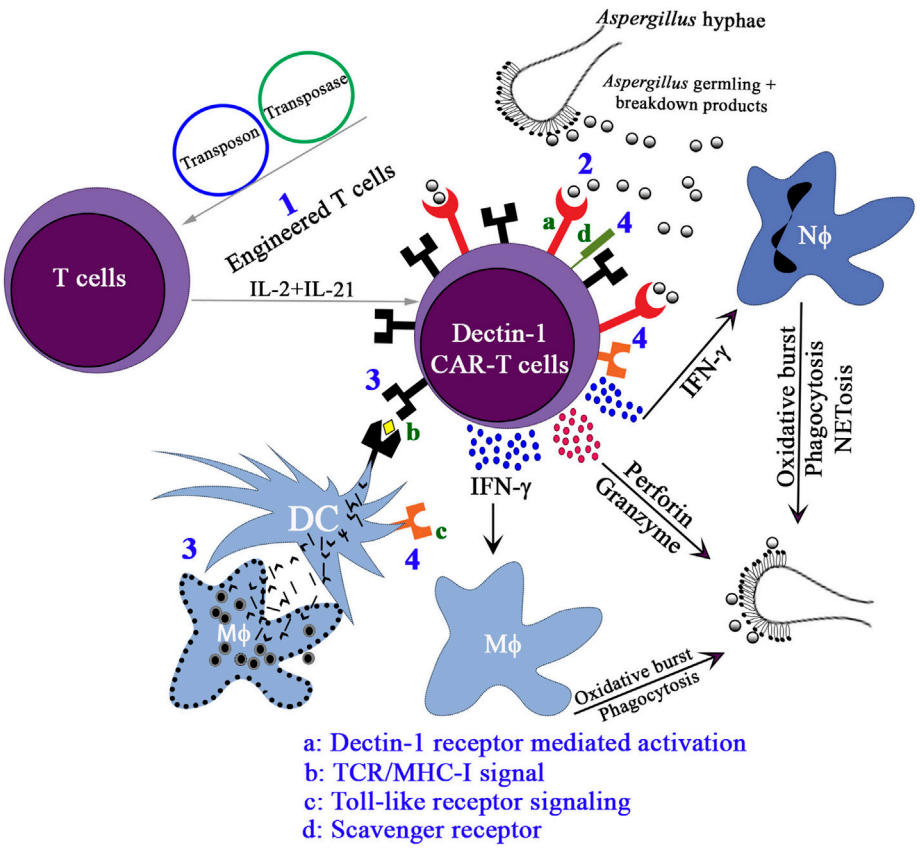

FIGURE 3 | The proposed activation pathways of Engineered T cells. (1) Expression of D-CAR$^+$ using Sleeping Beauty system, namely, D-CAR$^+$ T cells; (2) the β-glucan expressing *Aspergillus* germlings are recognized by D-CAR$^+$-T cells and induce the production of interferon (IFN)-γ, which favors the microbicidal activity of macrophages and neutrophils. Activated D-CAR$^+$-T cells also secrete granzyme and perforin to degrade fungal cell walls. (3) The activation of the D-CAR$^+$-T cells can also occur by cross-presentation of dendritic cells (DCs) and recognition by specific T-cell receptor (TCR), and (4) direct interaction of fungal breakdown products with toll-like receptors and scavenger receptor-ligands.

of IFI are found in patients diagnosed with pediatric ALL (166, 167). These patients will gain additional benefits if CAR T cells can be engineered to destroy both IFI and tumor cells. With this goal in mind, we developed a novel gene therapy approach using dual CAR T cells to prevent IFIs such as *Aspergillus* and *Candida* and also treat B-cell leukemia. To target fungal infections, we adapted the PRR Dectin-1 to activate T cells *via* chimeric CD28 and CD3-ζ upon binding with β-1,3-gucan carbohydrate present in the fungal cell wall. The D-CAR$^+$ T cells exhibited specificity for β-1,3-gucan and led to damage to fungal hyphae and inhibition of hyphal growth of *Aspergillus* and *Candida* upon testing in both *in vitro* and mouse models. To target B-cell leukemia, we adapted chimeric CD19R-CD28-CD3-ζ T-cells that are currently being used in clinical trials (149). The D-CAR$^+$ T cells do not kill the yeast form of *Candida* so there should not be any reactions to normal commensals that live in the gut microbiota. Also, D-CAR T cells can control *Aspergillus* infections in the presence of immunosuppressive drugs at physiological concentrations (168). Thus, we propose utilizing the clinically appealing dual CAR T cells to control both leukemia and IFIs.

Future Directions for CAR T-Cell Therapy

The recent breakthroughs in bioengineered CAR T-cell therapy for cancer have opened up new horizons for targeting infectious disease-causing organisms, such as viruses, bacteria, and fungi. This approach promises to be especially useful in immunocompromised patients or those requiring long-term immunosuppressive drug therapy, such as solid organ transplant recipients. CAR T-cell therapy offers not only an immediate cure of the disease, but also long-term benefits because memory CAR T cells will protect the host from future attack by foreign invaders. This therapy will also give new hope to patients suffering from drug-resistant IFIs such as aspergillosis. An advantage of D-CAR T cell therapy is that it can be used with antifungal therapy such as Caspofungin and Amphotericin-B, thereby reducing drug-related toxicity such as nephrotoxicity associated with Amphotericin-B.

Several factors limit the immediate clinical applications of CAR T-cell therapy. Cytokine storm and neurotoxicity are the major side effects of CAR T-cell therapy and the good news is that now clinicians are successfully addressing these symptoms (169). Since D-CAR$^+$-T cells are activated by the β-glucan sugar moiety which is not present in the mammalian system, off-target related toxicities may be minimal. At present, we cannot rule out the possibility of other toxicities such as macrophage activation syndrome or GvHD that are observed in CAR T therapy to treat cancers (170).

At present, CAR T-cell therapy is a personalized therapy; more CAR T-cell manufacturing centers are needed to produce clinical-grade T cells in a cost-effective way. The therapeutic success of any form of ACT depends on infusing sufficient numbers of T cells that lack replicative senescence and terminal differentiation and have the desired specificity (171). The CAR T-cell therapy used in current clinical trials requires the use of a Good Manufacturing Practice (GMP)-compliant facility to generate the T cells; it takes 2–4 weeks to propagate enough CAR T cells for infusion into the patient. However, the length of time T cells spend in culture, especially if they are propagated under non-physiological conditions, may erode the quality of the product despite increasing its quantity. Thus, a technique to generate T cells that can be harvested from peripheral blood, minimally manipulated, and infused within a few days of collection is appealing. Pharmaceutical and biotechnology companies are actively evaluating methods for generating CAR T cells in less than a week by automating the cell culture process. Automation has immediate appeal, as it avoids the expense and risk of contamination associated with prolonged culture and reduces human labor-associated error. Rapid production may in fact improve the therapeutic potential of the manufactured T cells by allowing them to avoid the replication senescence and terminal differentiation that causes them to lose *in vivo* persistence.

Approaches to generating T cells in compliance with GMPs are based on the *ex vivo* use of reagents to identify antigen-specific T cells. One approach is to use fluorescence-labeled or paramagnetic-labeled probes that bind TCRs to identify T cells with the desired specificity. The labeled T cells are subsequently subjected to fluorescence-activated cell sorting or magnetic selection to generate a homogeneously tagged product that can be immediately infused upon meeting release criteria (172, 173). The success of this approach is measured in terms of the time needed to identify antigen-specific T cells and the specificity of the harvested product. In another approach, antigen-specific T cells are isolated from donor PBMCs using a cytokine-capture system. In this process, donor PBMCs are incubated with a peptide antigen for 4 h; the activated T cells secrete IFN-γ, which is captured by a magnetic bead-conjugated bi-specific antibody. One arm of the bi-specific antibody is specific to IFN-γ, and the other arm is specific for the cell-surface CD45. T cells that secrete IFN-γ are then separated by passing them through a column. However, this approach is limited by the number of antigen-specific T cells in the donor. If more than one donor is available, prescreening of T cells (obtained from potential donors by simple venipuncture) for antigen-specific secretion of IFN-γ will determine the most suitable donor.

Despite these limitations, adoptive transfer of viral-antigen-specific T cells that have been modified for minimal manipulation and immediate infusion has been successful in clinical trials (174). TCR sequences can be identified from these antigen-specific T cells and can be used to generate TCR CAR T cells (175). Some clinical applications, such as infusion of allogeneic antigen-specific T cells after HSCT, are not possible because the initial donor may be unavailable or anonymous. In these cases, however, potential recipients may benefit from infusion of "captured" T cells from third-party donors that can recognize antigens *via* a human leukocyte antigen molecule shared by the recipient and the donor. These "off-the-shelf" T cells could be premanufactured and cryopreserved for infusion on demand. This approach might be better for prophylaxis in high-risk patients than for treatment in patients with recalcitrant IFIs. A precedent for this approach was reported, in which third-party Epstein–Barr virus-specific T cells and multivirus-specific T cells were infused (119, 176, 177). This approach could be adapted to treat or prevent IFIs.

CONCLUSION

Adoptive T-cell therapy could play a key role in controlling IFI. The GMP grade protocols for isolation of fungal-specific T cells are well characterized. Fungal-specific $CD8^+$ T-cells protect the host by activating the host innate immune system (Tc1 mediated) and mucosal immune system (Tc17 mediated) against IFI. For direct control, D-CAR^+ T-cells have been developed by fusing the extra cellular domain of Dectin-1 and cytoplasmic domains of CD3 and CD28 receptors. It can target various fungi, such as *Aspergillus* and *Candida* (126), and such treatment is highly warranted to combat IFI infections in immunocompromised patients. We have also developed Bi-specific CARs to target both B-cell malignancies and IFI by expressing CD19R-CAR and D-CAR in the same T-cell. The high costs involved with providing CAR T-cell therapy may prohibit many patients from receiving this potentially life-saving therapy, especially those located in the developing world, where fungal infections are highly prevalent. To reduce the manufacturing costs, off-the-shelf products are being developed which can be adapted for treating IFI in near future.

AUTHOR CONTRIBUTIONS

DPK wrote the introduction and back ground. TAS wrote $CD8^+$ T cell vaccines and PRK wrote engineered T-cells and Dectin1-CAR T cells. All authors have equally contributed for the tables. TAS and PRK contributed equally for figures.

ACKNOWLEDGMENTS

The authors thank Dr. Paul Hauser in the Pediatric Department and Dr. Amy Ninetto, Scientific Editor, Department of Scientific Publications for their assistance with proofreading this article.

FUNDING

National Institute of Allergy and Infectious Diseases grants R21 (AI127381-01), R33 (CA116127), P01 (CA148600); Burroughs Wellcome Fund; Cancer Prevention and Research Institute of Texas; CLL Global Research Foundation; DARPA (Defense Sciences Office); Department of Defense; Estate of Noelan L. Bibler; Gillson Longenbaugh Foundation; Harry T. Mangurian, Jr., Fund for Leukemia Immunotherapy; Institute of Personalized Cancer Therapy; Leukemia and Lymphoma Society; Lymphoma Research Foundation; MD Anderson Cancer Center's Sister Institution Network Fund; Miller Foundation; Mr. Herb Simons; Mr. and Mrs. Joe H. Scales; Mr. Thomas Scott; National Foundation for Cancer Research; Pediatric Cancer Research Foundation; William Lawrence and Blanche Hughes Children's Foundation. DK acknowledges the Texas 4000 Endowed Professorship for Cancer Research. Visiting scientist salary, Thiago Aparecido da Silva, was supported by funds received from Fundação de Amparo a Pesquisa do Estado de São Paulo (2016/23044-1).

REFERENCES

1. Perfect JR, Pfaller MA, Ostrosky-Zeichner L, Kontoyiannis DP. Invasive mycoses: evolving challenges and opportunities in antifungal therapy (multimedia activity). *Am J Med* (2011) 124:S2–3. doi:10.1016/j.amjmed.2011.08.001
2. Pfaller MA, Diekema DJ. Epidemiology of invasive mycoses in North America. *Crit Rev Microbiol* (2010) 36:1–53. doi:10.3109/10408410903241444
3. Neofytos D, Horn D, Anaissie E, Steinbach W, Olyaei A, Fishman J, et al. Epidemiology and outcome of invasive fungal infection in adult hematopoietic stem cell transplant recipients: analysis of multicenter prospective antifungal therapy (PATH) alliance registry. *Clin Infect Dis* (2009) 48:265–73. doi:10.1086/595846
4. Wirk B, Wingard JR. Current approaches in antifungal prophylaxis in high risk hematologic malignancy and hematopoietic stem cell transplant patients. *Mycopathologia* (2009) 168:299–311. doi:10.1007/s11046-009-9188-6
5. Person AK, Kontoyiannis DP, Alexander BD. Fungal infections in transplant and oncology patients. *Infect Dis Clin North Am* (2010) 24:439–59. doi:10.1016/j.idc.2010.01.002
6. Martino R, Subira M, Rovira M, Solano C, Vazquez L, Sanz GF, et al. Invasive fungal infections after allogeneic peripheral blood stem cell transplantation: incidence and risk factors in 395 patients. *Br J Haematol* (2002) 116:475–82. doi:10.1046/j.1365-2141.2002.03259.x
7. Kontoyiannis DP, Marr KA, Park BJ, Alexander BD, Anaissie EJ, Walsh TJ, et al. Prospective surveillance for invasive fungal infections in hematopoietic stem cell transplant recipients, 2001–2006: overview of the transplant-associated infection surveillance network (TRANSNET) database. *Clin Infect Dis* (2010) 50:1091–100. doi:10.1086/651263
8. Groll AH, Schrey D, Tragiannidis A, Bochennek K, Lehrnbecher T. Invasive aspergillosis in children and adolescents. *Curr Pharm Des* (2013) 19:3545–68. doi:10.2174/13816128113199990311
9. Tragiannidis A, Roilides E, Walsh TJ, Groll AH. Invasive aspergillosis in children with acquired immunodeficiencies. *Clin Infect Dis* (2012) 54:258–67. doi:10.1093/cid/cir786
10. Kontoyiannis DP. Antifungal prophylaxis in hematopoietic stem cell transplant recipients: the unfinished tale of imperfect success. *Bone Marrow Transplant* (2011) 46:165–73. doi:10.1038/bmt.2010.256
11. Lionakis MS, Iliev ID, Hohl TM. Immunity against fungi. *JCI Insight* (2017) 2:93156. doi:10.1172/jci.insight.93156
12. Wuthrich M, Deepe GS, Klein B. Adaptive immunity to fungi. *Annu Rev Immunol* (2012) 30:115–48. doi:10.1146/annurev-immunol-020711-074958
13. Romani L. Immunity to fungal infections. *Nat Rev Immunol* (2011) 11:275–88. doi:10.1038/nri2939
14. Armstrong-James D, Brown GD, Netea MG, Zelante T, Gresnigt MS, van de Veerdonk FL, et al. Immunotherapeutic approaches to treatment of fungal diseases. *Lancet Infect Dis* (2017) 17:e393–e402. doi:10.1016/S1473-3099(17)30442-5
15. Global Action Found for Fugal Disease. *Burden of Common Life-Threatening Fungal Infections*. Global Action Found for Fugal Disease (2017). Available from: https://www.gaffi.org/why/fungal-disease-frequency/
16. Gudlaugsson O, Gillespie S, Lee K, Berg JV, Hu JF, Messer S, et al. Attributable mortality of nosocomial candidemia, revisited. *Clin Infect Dis* (2003) 37:1172–7. doi:10.1086/378745
17. Hajjeh RA, Sofair AN, Harrison LH, Lyon GM, Arthington-Skaggs BA, Mirza SA, et al. Incidence of bloodstream infections due to *Candida* species and in vitro susceptibilities of isolates collected from 1998 to 2000 in a population-based active surveillance program. *J Clin Microbiol* (2004) 42:1519–27. doi:10.1128/JCM.42.4.1519-1527.2004
18. Gomes MZR, Lewis RE, Kontoyiannis DP. Mucormycosis caused by unusual mucormycetes, non-*Rhizopus*, -*Mucor*, and -*Lichtheimia* species. *Clin Microbiol Rev* (2011) 24:411. doi:10.1128/CMR.00056-10
19. Park BJ, Wannemuehler KA, Marston BJ, Govender N, Pappas PG, Chiller TA. Estimation of the current global burden of cryptococcal meningitis among persons living with HIV/AIDS. *AIDS* (2009) 23:525–30. doi:10.1097/QAD.0b013e328322ffac
20. Harris K, Maroun R, Chalhoub M, Elsayegh D. Unusual presentation of pneumocystis pneumonia in an immunocompetent patient diagnosed by open lung biopsy. *Heart Lung Circ* (2012) 21:221–4. doi:10.1016/j.hlc.2011.10.006

21. Harris JR, Marston BJ, Sangrujee N, DuPlessis D, Park B. Cost-effectiveness analysis of diagnostic options for pneumocystis pneumonia (PCP). *PLoS One* (2011) 6:e23158. doi:10.1371/journal.pone.0023158
22. Cottier F, Pavelka N. Complexity and dynamics of host-fungal interactions. *Immunol Res* (2012) 53:127–35. doi:10.1007/s12026-012-8265-y
23. Brunke S, Mogavero S, Kasper L, Hube B. Virulence factors in fungal pathogens of man. *Curr Opin Microbiol* (2016) 32:89–95. doi:10.1016/j.mib.2016.05.010
24. Gow NAR, Latge JP, Munro CA. The fungal cell wall: structure, biosynthesis, and function. *Microbiol Spectr* (2017) 5:1–25. doi:10.1128/microbiolspec.FUNK-0035-2016
25. Ibrahim AS. Host cell invasion in mucormycosis: role of iron. *Curr Opin Microbiol* (2011) 14:406–11. doi:10.1016/j.mib.2011.07.004
26. Espinosa V, Rivera A. First line of defense: innate cell-mediated control of pulmonary aspergillosis. *Front Microbiol* (2016) 7:272. doi:10.3389/fmicb.2016.00272
27. LeibundGut-Landmann S, Wuthrich M, Hohl TM. Immunity to fungi. *Curr Opin Immunol* (2012) 24:449–58. doi:10.1016/j.coi.2012.04.007
28. Plato A, Hardison SE, Brown GD. Pattern recognition receptors in antifungal immunity. *Semin Immunopathol* (2015) 37:97–106. doi:10.1007/s00281-014-0462-4
29. Claes AK, Zhou JY, Philpott DJ. NOD-like receptors: guardians of intestinal mucosal barriers. *Physiology (Bethesda)* (2015) 30:241–50. doi:10.1152/physiol.00025.2014
30. Kawai T, Akira S. The roles of TLRs, RLRs and NLRs in pathogen recognition. *Int Immunol* (2009) 21:317–37. doi:10.1093/intimm/dxp017
31. Hoving JC, Wilson GJ, Brown GD. Signalling C-type lectin receptors, microbial recognition and immunity. *Cell Microbiol* (2014) 16:185–94. doi:10.1111/cmi.12249
32. Underhill DM, Pearlman E. Immune interactions with pathogenic and commensal fungi: a two-way street. *Immunity* (2015) 43:845–58. doi:10.1016/j.immuni.2015.10.023
33. Naglik RJ. *Candida* immunity. *N J Sci* (2014) 2014:27. doi:10.1155/2014/390241
34. Brown GD, Taylor PR, Reid DM, Willment JA, Williams DL, Martinez-Pomares L, et al. Dectin-1 is a major beta-glucan receptor on macrophages. *J Exp Med* (2002) 196:407–12. doi:10.1084/jem.20020470
35. Robinson MJ, Osorio F, Rosas M, Freitas RP, Schweighoffer E, Gross O, et al. Dectin-2 is a Syk-coupled pattern recognition receptor crucial for Th17 responses to fungal infection. *J Exp Med* (2009) 206:2037–51. doi:10.1084/jem.20082818
36. Saijo S, Ikeda S, Yamabe K, Kakuta S, Ishigame H, Akitsu A, et al. Dectin-2 recognition of alpha-mannans and induction of Th17 cell differentiation is essential for host defense against *Candida albicans*. *Immunity* (2010) 32:681–91. doi:10.1016/j.immuni.2010.05.001
37. Zhu LL, Zhao XQ, Jiang C, You Y, Chen XP, Jiang YY, et al. C-type lectin receptors Dectin-3 and Dectin-2 form a heterodimeric pattern-recognition receptor for host defense against fungal infection. *Immunity* (2013) 39:324–34. doi:10.1016/j.immuni.2013.05.017
38. Papadopoulou A, Kaloyannidis P, Yannaki E, Cruz CR. Adoptive transfer of *Aspergillus*-specific T cells as a novel anti-fungal therapy for hematopoietic stem cell transplant recipients: progress and challenges. *Crit Rev Oncol Hematol* (2016) 98:62–72. doi:10.1016/j.critrevonc.2015.10.005
39. Castellano-Gonzalez G, Clancy LE, Gottlieb D. Prospects for adoptive T-cell therapy for invasive fungal disease. *Curr Opin Infect Dis* (2017) 30(6):518–27. doi:10.1097/QCO.0000000000000403
40. van de Veerdonk FL, Netea MG. T-cell subsets and antifungal host defenses. *Curr Fungal Infect Rep* (2010) 4:238–43. doi:10.1007/s12281-010-0034-6
41. Roemer T, Krysan DJ. Antifungal drug development: challenges, unmet clinical needs, and new approaches. *Cold Spring Harb Perspect Med* (2014) 4:a019703. doi:10.1101/cshperspect.a019703
42. Vermeulen E, Lagrou K, Verweij PE. Azole resistance in *Aspergillus fumigatus*: a growing public health concern. *Curr Opin Infect Dis* (2013) 26:493–500. doi:10.1097/QCO.0000000000000005
43. Heo ST, Tatara AM, Jimenez-Ortigosa C, Jiang Y, Lewis RE, Tarrand J, et al. Changes in in vitro susceptibility patterns of *Aspergillus* to triazoles and correlation with aspergillosis outcome in a tertiary care cancer center, 1999–2015. *Clin Infect Dis* (2017) 65:216–25. doi:10.1093/cid/cix297
44. Kontoyiannis DP, Selleslag D, Mullane K, Cornely OA, Hope W, Lortholary O, et al. Impact of unresolved neutropenia in patients with neutropenia and invasive aspergillosis: a post hoc analysis of the SECURE trial. *J Antimicrob Chemother* (2017) 1–17. doi:10.1093/jac/dkx423
45. Kontoyiannis DP. Echinocandin-based initial therapy in fungemic patients with cancer: a focus on recent guidelines of the infectious diseases society of America. *Clin Infect Dis* (2009) 49:638–39; author reply 639–40. doi:10.1086/603585
46. Waldorf AR, Levitz SM, Diamond RD. In vivo bronchoalveolar macrophage defense against *Rhizopus oryzae* and *Aspergillus fumigatus*. *J Infect Dis* (1984) 150:752–60. doi:10.1093/infdis/150.5.752
47. Amulic B, Cazalet C, Hayes GL, Metzler KD, Zychlinsky A. Neutrophil function: from mechanisms to disease. *Annu Rev Immunol* (2012) 30:459–89. doi:10.1146/annurev-immunol-020711-074942
48. Kaplan MJ, Radic M. Neutrophil extracellular traps: double-edged swords of innate immunity. *J Immunol* (2012) 189:2689–95. doi:10.4049/jimmunol.1201719
49. Mousset S, Hermann S, Klein SA, Bialleck H, Duchscherer M, Bomke B, et al. Prophylactic and interventional granulocyte transfusions in patients with haematological malignancies and life-threatening infections during neutropenia. *Ann Hematol* (2005) 84:734–41. doi:10.1007/s00277-005-1055-z
50. Grigull L, Beilken A, Schmid H, Kirschner P, Sykora KW, Linderkamp C, et al. Secondary prophylaxis of invasive fungal infections with combination antifungal therapy and G-CSF-mobilized granulocyte transfusions in three children with hematological malignancies. *Support Care Cancer* (2006) 14:783–6. doi:10.1007/s00520-005-0910-8
51. Gil-Lamaignere C, Winn RM, Simitsopoulou M, Maloukou A, Walsh TJ, Roilides E. Inteferon gamma and granulocyte-macrophage colony-stimulating factor augment the antifungal activity of human polymorphonuclear leukocytes against *Scedosporium* spp.: comparison with *Aspergillus* spp. *Med Mycol* (2005) 43:253–60. doi:10.1080/13693780412331271072
52. Winn RM, Gil-Lamaignere C, Roilides E, Simitsopoulou M, Lyman CA, Maloukou A, et al. Effects of interleukin-15 on antifungal responses of human polymorphonuclear leukocytes against *Fusarium* spp. and *Scedosporium* spp. *Cytokine* (2005) 31:1–8. doi:10.1016/j.cyto.2004.07.016
53. Valentini CG, Farina F, Pagano L, Teofili L. Granulocyte transfusions: a critical reappraisal. *Biol Blood Marrow Transplant* (2017) 23:2034–41. doi:10.1016/j.bbmt.2017.07.029
54. Robertson MJ, Ritz J. Biology and clinical relevance of human natural killer cells. *Blood* (1990) 76:2421–38.
55. Bouzani M, Ok M, McCormick A, Ebel F, Kurzai O, Morton CO, et al. Human NK cells display important antifungal activity against *Aspergillus fumigatus*, which is directly mediated by IFN-gamma release. *J Immunol* (2011) 187:1369–76. doi:10.4049/jimmunol.1003593
56. Schmidt S, Schneider A, Demir A, Lass-Florl C, Lehrnbecher T. Natural killer cell-mediated damage of clinical isolates of mucormycetes. *Mycoses* (2016) 59:34–8. doi:10.1111/myc.12431
57. Schmidt S, Tramsen L, Hanisch M, Latge JP, Huenecke S, Koehl U, et al. Human natural killer cells exhibit direct activity against *Aspergillus fumigatus* hyphae, but not against resting conidia. *J Infect Dis* (2011) 203:430–5. doi:10.1093/infdis/jiq062
58. Voigt J, Hunniger K, Bouzani M, Jacobsen ID, Barz D, Hube B, et al. Human natural killer cells acting as phagocytes against *Candida albicans* and mounting an inflammatory response that modulates neutrophil antifungal activity. *J Infect Dis* (2014) 209:616–26. doi:10.1093/infdis/jit574
59. Ziegler S, Weiss E, Schmitt AL, Schlegel J, Burgert A, Terpitz U, et al. CD56 is a pathogen recognition receptor on human natural killer cells. *Sci Rep* (2017) 7:6138. doi:10.1038/s41598-017-06238-4
60. Li SS, Kyei SK, Timm-McCann M, Ogbomo H, Jones GJ, Shi M, et al. The NK receptor NKp30 mediates direct fungal recognition and killing and is diminished in NK cells from HIV-infected patients. *Cell Host Microbe* (2013) 14:387–97. doi:10.1016/j.chom.2013.09.007
61. Ogbomo H, Mody CH. Granule-dependent natural killer cell cytotoxicity to fungal pathogens. *Front Immunol* (2016) 7:692. doi:10.3389/fimmu.2016.00692
62. Schmidt S, Condorelli A, Koltze A, Lehrnbecher T. NK cells and their role in invasive mold infection. *J Fungi* (2017) 8:1623. doi:10.3389/fimmu.2017.01623

63. Fidan I, Kalkanci A, Yesilyurt E, Erdal B. In vitro effects of *Candida albicans* and *Aspergillus fumigatus* on dendritic cells and the role of beta glucan in this effect. *Adv Clin Exp Med* (2014) 23:17–24. doi:10.17219/acem/37016
64. Bozza S, Gaziano R, Spreca A, Bacci A, Montagnoli C, di Francesco P, et al. Dendritic cells transport conidia and hyphae of *Aspergillus fumigatus* from the airways to the draining lymph nodes and initiate disparate Th responses to the fungus. *J Immunol* (2002) 168:1362–71. doi:10.4049/jimmunol.168.3.1362
65. Thakur R, Anand R, Tiwari S, Singh AP, Tiwary BN, Shankar J. Cytokines induce effector T-helper cells during invasive aspergillosis; what we have learned about T-helper cells? *Front Microbiol* (2015) 6:429. doi:10.3389/fmicb.2015.00429
66. Zelante T, Wong AY, Ping TJ, Chen J, Sumatoh HR, Vigano E, et al. CD103(+) dendritic cells control Th17 cell function in the lung. *Cell Rep* (2015) 12:1789–801. doi:10.1016/j.celrep.2015.08.030
67. Cutler JE, Deepe GS Jr, Klein BS. Advances in combating fungal diseases: vaccines on the threshold. *Nat Rev Microbiol* (2007) 5:13–28. doi:10.1038/nrmicro1537
68. Chen K, Kolls JK. T cell-mediated host immune defenses in the lung. *Annu Rev Immunol* (2013) 31:605–33. doi:10.1146/annurev-immunol-032712-100019
69. Hernandez-Santos N, Gaffen SL. Th17 cells in immunity to *Candida albicans*. *Cell Host Microbe* (2012) 11:425–35. doi:10.1016/j.chom.2012.04.008
70. Huppler AR, Bishu S, Gaffen SL. Mucocutaneous candidiasis: the IL-17 pathway and implications for targeted immunotherapy. *Arthritis Res Ther* (2012) 14:217. doi:10.1186/ar3893
71. Backer R, van Leeuwen F, Kraal G, den Haan JM. CD8-dendritic cells preferentially cross-present *Saccharomyces cerevisiae* antigens. *Eur J Immunol* (2008) 38:370–80. doi:10.1002/eji.200737647
72. Leibundgut-Landmann S, Osorio F, Brown GD, Reis e Sousa C. Stimulation of dendritic cells via the dectin-1/Syk pathway allows priming of cytotoxic T-cell responses. *Blood* (2008) 112:4971–80. doi:10.1182/blood-2008-05-158469
73. LeibundGut-Landmann S, Gross O, Robinson MJ, Osorio F, Slack EC, Tsoni SV, et al. Syk- and CARD9-dependent coupling of innate immunity to the induction of T helper cells that produce interleukin 17. *Nat Immunol* (2007) 8:630–8. doi:10.1038/ni1460
74. Nanjappa SG, Heninger E, Wuthrich M, Gasper DJ, Klein BS. Tc17 cells mediate vaccine immunity against lethal fungal pneumonia in immune deficient hosts lacking CD4+ T cells. *PLoS Pathog* (2012) 8:e1002771. doi:10.1371/journal.ppat.1002771
75. Nanjappa SG, Heninger E, Wuthrich M, Sullivan T, Klein B. Protective antifungal memory CD8(+) T cells are maintained in the absence of CD4(+) T cell help and cognate antigen in mice. *J Clin Invest* (2012) 122:987–99. doi:10.1172/JCI58762
76. Lin JS, Yang CW, Wang DW, Wu-Hsieh BA. Dendritic cells cross-present exogenous fungal antigens to stimulate a protective CD8 T cell response in infection by *Histoplasma capsulatum*. *J Immunol* (2005) 174:6282–91. doi:10.4049/jimmunol.174.10.6282
77. McAllister F, Ruan S, Steele C, Zheng M, McKinley L, Ulrich L, et al. CXCR3 and IFN protein-10 in pneumocystis pneumonia. *J Immunol* (2006) 177:1846–54. doi:10.4049/jimmunol.177.3.1846
78. Nanjappa SG, Klein BS. Vaccine immunity against fungal infections. *Curr Opin Immunol* (2014) 28:27–33. doi:10.1016/j.coi.2014.01.014
79. Reichard U, Herrmann S, Asif AR. Vaccination approaches against opportunistic fungal infections caused by *Aspergillus fumigatus*. *Curr Protein Pept Sci* (2014) 15:424–9. doi:10.2174/1389203715666140512122037
80. Chaturvedi AK, Wormley FL. *Cryptococcus* antigens and immune responses: implications for a vaccine. *Expert Rev Vaccines* (2013) 12:1261–72. doi:10.1586/14760584.2013.840094
81. Bocca AL, Amaral AC, Teixeira MM, Sato P, Shikanai-Yasuda MA, Soares Felipe MS. Paracoccidioidomycosis: eco-epidemiology, taxonomy and clinical and therapeutic issues. *Future Microbiol* (2013) 8:1177–91. doi:10.2217/fmb.13.68
82. Nguyen C, Barker BM, Hoover S, Nix DE, Ampel NM, Frelinger JA, et al. Recent advances in our understanding of the environmental, epidemiological, immunological, and clinical dimensions of coccidioidomycosis. *Clin Microbiol Rev* (2013) 26:505–25. doi:10.1128/CMR.00005-13
83. Levitz SM, Huang H, Ostroff GR, Specht CA. Exploiting fungal cell wall components in vaccines. *Semin Immunopathol* (2015) 37:199–207. doi:10.1007/s00281-014-0460-6
84. Edwards JE Jr. Fungal cell wall vaccines: an update. *J Med Microbiol* (2012) 61:895–903. doi:10.1099/jmm.0.041665-0
85. Cassone A, Casadevall A. Recent progress in vaccines against fungal diseases. *Curr Opin Microbiol* (2012) 15:427–33. doi:10.1016/j.mib.2012.04.004
86. Yoon HJ, Clemons KV. Vaccines against *Coccidioides*. *Korean J Intern Med* (2013) 28:403–7. doi:10.3904/kjim.2013.28.4.403
87. Ito JI, Lyons JM, Hong TB, Tamae D, Liu YK, Wilczynski SP, et al. Vaccinations with recombinant variants of *Aspergillus fumigatus* allergen Asp f 3 protect mice against invasive aspergillosis. *Infect Immun* (2006) 74:5075–84. doi:10.1128/IAI.00815-06
88. Fierer J, Waters C, Walls L. Both CD4+ and CD8+ T cells can mediate vaccine-induced protection against *Coccidioides immitis* infection in mice. *J Infect Dis* (2006) 193:1323–31. doi:10.1086/502972
89. Hung CY, Gonzalez A, Wuthrich M, Klein BS, Cole GT. Vaccine immunity to coccidioidomycosis occurs by early activation of three signal pathways of T helper cell response (Th1, Th2, and Th17). *Infect Immun* (2011) 79:4511–22. doi:10.1128/IAI.05726-11
90. Khan AA, Jabeen M, Chauhan A, Owais M. Vaccine potential of cytosolic proteins loaded fibrin microspheres of *Cryptococcus neoformans* in BALB/c mice. *J Drug Target* (2012) 20:453–66. doi:10.3109/1061186X.2012.685474
91. Nanjappa SG, Hernandez-Santos N, Galles K, Wuthrich M, Suresh M, Klein BS. Intrinsic MyD88-Akt1-mTOR signaling coordinates disparate Tc17 and Tc1 responses during vaccine immunity against fungal pneumonia. *PLoS Pathog* (2015) 11:e1005161. doi:10.1371/journal.ppat.1005161
92. Wuthrich M, Filutowicz HI, Warner T, Deepe GS Jr, Klein BS. Vaccine immunity to pathogenic fungi overcomes the requirement for CD4 help in exogenous antigen presentation to CD8+ T cells: implications for vaccine development in immune-deficient hosts. *J Exp Med* (2003) 197:1405–16. doi:10.1084/jem.20030109
93. Templeton SP, Buskirk AD, Law B, Green BJ, Beezhold DH. Role of germination in murine airway CD8+ T-cell responses to *Aspergillus* conidia. *PLoS One* (2011) 6:e18777. doi:10.1371/journal.pone.0018777
94. Chaudhary N, Staab JF, Marr KA. Healthy human T-cell responses to *Aspergillus fumigatus* antigens. *PLoS One* (2010) 5:e9036. doi:10.1371/journal.pone.0009036
95. Cui N, Wang H, Long Y, Liu D. CD8(+) T-cell counts: an early predictor of risk and mortality in critically ill immunocompromised patients with invasive pulmonary aspergillosis. *Crit Care* (2013) 17:R157. doi:10.1186/cc12836
96. Sun Z, Zhu P, Li L, Wan Z, Zhao Z, Li R. Adoptive immunity mediated by HLA-A*0201 restricted Asp f16 peptides-specific CD8+ T cells against *Aspergillus fumigatus* infection. *Eur J Clin Microbiol Infect Dis* (2012) 31:3089–96. doi:10.1007/s10096-012-1670-2
97. Potenza L, Vallerini D, Barozzi P, Riva G, Forghieri F, Zanetti E, et al. Mucorales-specific T cells emerge in the course of invasive mucormycosis and may be used as a surrogate diagnostic marker in high-risk patients. *Blood* (2011) 118:5416–9. doi:10.1182/blood-2011-07-366526
98. Vallerini D, Forghieri F, Lagreca I, Riva G, Barozzi P, Quadrelli C, et al. Detection of *Fusarium*-specific T cells in hematologic patients with invasive fusariosis. *J Infect* (2017) 74:314–8. doi:10.1016/j.jinf.2016.12.008
99. McAllister F, Steele C, Zheng M, Young E, Shellito JE, Marrero L, et al. T cytotoxic-1 CD8+ T cells are effector cells against pneumocystis in mice. *J Immunol* (2004) 172:1132–8. doi:10.4049/jimmunol.172.2.1132
100. De Luca A, Iannitti RG, Bozza S, Beau R, Casagrande A, D'Angelo C, et al. CD4(+) T cell vaccination overcomes defective cross-presentation of fungal antigens in a mouse model of chronic granulomatous disease. *J Clin Invest* (2012) 122:1816–31. doi:10.1172/JCI60862
101. Carvalho A, De Luca A, Bozza S, Cunha C, D'Angelo C, Moretti S, et al. TLR3 essentially promotes protective class I-restricted memory CD8(+) T-cell responses to *Aspergillus fumigatus* in hematopoietic transplanted patients. *Blood* (2012) 119:967–77. doi:10.1182/blood-2011-06-362582
102. Spellberg B, Ibrahim AS, Lin L, Avanesian V, Fu Y, Lipke P, et al. Antibody titer threshold predicts anti-candidal vaccine efficacy even though the mechanism of protection is induction of cell-mediated immunity. *J Infect Dis* (2008) 197:967–71. doi:10.1086/529204
103. Paulovicova E, Machova E, Tulinska J, Bystricky S. Cell and antibody mediated immunity induced by vaccination with novel *Candida dubliniensis* mannan immunogenic conjugate. *Int Immunopharmacol* (2007) 7:1325–33. doi:10.1016/j.intimp.2007.05.014

104. Chauhan A, Swaleha Z, Ahmad N, Farazuddin M, Vasco A, Abida M, et al. Escheriosome mediated cytosolic delivery of *Candida albicans* cytosolic proteins induces enhanced cytotoxic T lymphocyte response and protective immunity. *Vaccine* (2011) 29:5424–33. doi:10.1016/j.vaccine.2011.05.066
105. Hamad M. Universal fungal vaccines: could there be light at the end of the tunnel? *Hum Vaccin Immunother* (2012) 8:1758–63. doi:10.4161/hv.21838
106. Meier A, Kirschning CJ, Nikolaus T, Wagner H, Heesemann J, Ebel F. Toll-like receptor (TLR) 2 and TLR4 are essential for *Aspergillus*-induced activation of murine macrophages. *Cell Microbiol* (2003) 5:561–70. doi:10.1046/j.1462-5822.2003.00301.x
107. Shoham S, Huang C, Chen JM, Golenbock DT, Levitz SM. Toll-like receptor 4 mediates intracellular signaling without TNF-alpha release in response to *Cryptococcus neoformans* polysaccharide capsule. *J Immunol* (2001) 166:4620–6. doi:10.4049/jimmunol.166.7.4620
108. Calich VL, Pina A, Felonato M, Bernardino S, Costa TA, Loures FV. Toll-like receptors and fungal infections: the role of TLR2, TLR4 and MyD88 in paracoccidioidomycosis. *FEMS Immunol Med Microbiol* (2008) 53:1–7. doi:10.1111/j.1574-695X.2008.00378.x
109. Firinu D, Pisanu M, Piras B, Meleddu R, Lorrai MM, Manconi PE, et al. Genetic susceptibility to *Candida* infection: a new look at an old entity. *Chin Med J (Engl)* (2013) 126:378–81.
110. Nahum A, Dadi H, Bates A, Roifman CM. The biological significance of TLR3 variant, L412F, in conferring susceptibility to cutaneous candidiasis, CMV and autoimmunity. *Autoimmun Rev* (2012) 11:341–7. doi:10.1016/j.autrev.2011.10.007
111. Bochud PY, Chien JW, Marr KA, Leisenring WM, Upton A, Janer M, et al. Toll-like receptor 4 polymorphisms and aspergillosis in stem-cell transplantation. *N Engl J Med* (2008) 359:1766–77. doi:10.1056/NEJMoa0802629
112. Vera J, Fenutria R, Canadas O, Figueras M, Mota R, Sarrias MR, et al. The CD5 ectodomain interacts with conserved fungal cell wall components and protects from zymosan-induced septic shock-like syndrome. *Proc Natl Acad Sci U S A* (2009) 106:1506–11. doi:10.1073/pnas.0805846106
113. Acharya M, Borland G, Edkins AL, Maclellan LM, Matheson J, Ozanne BW, et al. CD23/FcepsilonRII: molecular multi-tasking. *Clin Exp Immunol* (2010) 162:12–23. doi:10.1111/j.1365-2249.2010.04210.x
114. Zhao X, Guo Y, Jiang C, Chang Q, Zhang S, Luo T, et al. JNK1 negatively controls antifungal innate immunity by suppressing CD23 expression. *Nat Med* (2017) 23:337–46. doi:10.1038/nm.4260
115. Van Acker HH, Capsomidis A, Smits EL, Van Tendeloo VF. CD56 in the immune system: more than a marker for cytotoxicity? *Front Immunol* (2017) 8:892. doi:10.3389/fimmu.2017.00892
116. McLaughlin LP, Gottschalk S, Rooney CM, Bollard CM. EBV-directed T cell therapeutics for EBV-associated lymphomas. *Methods Mol Biol* (2017) 1532:255–65. doi:10.1007/978-1-4939-6655-4_19
117. Kumaresan P, Figliola M, Moyes JS, Huls MH, Tewari P, Shpall EJ, et al. Automated cell enrichment of cytomegalovirus-specific T cells for clinical applications using the cytokine-capture system. *J Vis Exp* (2015) 104:e52808. doi:10.3791/52808
118. Krishnamurthy J, Rabinovich BA, Mi T, Switzer KC, Olivares S, Maiti SN, et al. Genetic engineering of T cells to target HERV-K, an ancient retrovirus on melanoma. *Clin Cancer Res* (2015) 21:3241–51. doi:10.1158/1078-0432.CCR-14-3197
119. Tzannou I, Papadopoulou A, Naik S, Leung K, Martinez CA, Ramos CA, et al. Off-the-shelf virus-specific T cells to treat BK virus, human herpesvirus 6, cytomegalovirus, Epstein-Barr virus, and adenovirus infections after allogeneic hematopoietic stem-cell transplantation. *J Clin Oncol* (2017) 35:3547–57. doi:10.1200/JCO.2017.73.0655
120. Perruccio K, Tosti A, Burchielli E, Topini F, Ruggeri L, Carotti A, et al. Transferring functional immune responses to pathogens after haploidentical hematopoietic transplantation. *Blood* (2005) 106:4397–406. doi:10.1182/blood-2005-05-1775
121. Pagano L, Caira M, Nosari A, Van Lint MT, Candoni A, Offidani M, et al. Fungal infections in recipients of hematopoietic stem cell transplants: results of the SEIFEM B-2004 study – Sorveglianza Epidemiologica Infezioni Fungine Nelle Emopatie Maligne. *Clin Infect Dis* (2007) 45:1161–70. doi:10.1086/522189
122. Beck O, Topp MS, Koehl U, Roilides E, Simitsopoulou M, Hanisch M, et al. Generation of highly purified and functionally active human TH1 cells against *Aspergillus fumigatus*. *Blood* (2006) 107:2562–9. doi:10.1182/blood-2005-04-1660
123. Shi H, Liu L, Wang Z. Improving the efficacy and safety of engineered T cell therapy for cancer. *Cancer Lett* (2013) 328:191–7. doi:10.1016/j.canlet.2012.09.015
124. Stauss HJ, Morris EC, Abken H. Cancer gene therapy with T cell receptors and chimeric antigen receptors. *Curr Opin Pharmacol* (2015) 24:113–8. doi:10.1016/j.coph.2015.08.006
125. Klebanoff CA, Rosenberg SA, Restifo NP. Prospects for gene-engineered T cell immunotherapy for solid cancers. *Nat Med* (2016) 22:26–36. doi:10.1038/nm.4015
126. Kumaresan PR, Manuri PR, Albert ND, Maiti S, Singh H, Mi T, et al. Bioengineering T cells to target carbohydrate to treat opportunistic fungal infection. *Proc Natl Acad Sci U S A* (2014) 111:10660–5. doi:10.1073/pnas.1312789111
127. Singh H, Huls H, Kebriaei P, Cooper LJ. A new approach to gene therapy using Sleeping Beauty to genetically modify clinical-grade T cells to target CD19. *Immunol Rev* (2014) 257:181–90. doi:10.1111/imr.12137
128. Dembic Z, Haas W, Weiss S, McCubrey J, Kiefer H, von Boehmer H, et al. Transfer of specificity by murine alpha and beta T-cell receptor genes. *Nature* (1986) 320:232–8. doi:10.1038/320232a0
129. Zhao Y, Zheng Z, Cohen CJ, Gattinoni L, Palmer DC, Restifo NP, et al. High-efficiency transfection of primary human and mouse T lymphocytes using RNA electroporation. *Mol Ther* (2006) 13:151–9. doi:10.1016/j.ymthe.2005.07.688
130. Hohl TM. Immune responses to invasive aspergillosis: new understanding and therapeutic opportunities. *Curr Opin Infect Dis* (2017) 30:364–71. doi:10.1097/QCO.0000000000000381
131. Grazziutti M, Przepiorka D, Rex JH, Braunschweig I, Vadhan-Raj S, Savary CA. Dendritic cell-mediated stimulation of the in vitro lymphocyte response to *Aspergillus*. *Bone Marrow Transplant* (2001) 27:647–52. doi:10.1038/sj.bmt.1702832
132. Robbins PF, Morgan RA, Feldman SA, Yang JC, Sherry RM, Dudley ME, et al. Tumor regression in patients with metastatic synovial cell sarcoma and melanoma using genetically engineered lymphocytes reactive with NY-ESO-1. *J Clin Oncol* (2011) 29:917–24. doi:10.1200/JCO.2010.32.2537
133. Parkhurst MR, Yang JC, Langan RC, Dudley ME, Nathan DA, Feldman SA, et al. T cells targeting carcinoembryonic antigen can mediate regression of metastatic colorectal cancer but induce severe transient colitis. *Mol Ther* (2011) 19:620–6. doi:10.1038/mt.2010.272
134. Garrido F, Ruiz-Cabello F, Cabrera T, Perez-Villar JJ, Lopez-Botet M, Duggan-Keen M, et al. Implications for immunosurveillance of altered HLA class I phenotypes in human tumours. *Immunol Today* (1997) 18:89–95. doi:10.1016/S0167-5699(96)10075-X
135. Kershaw MH, Teng MW, Smyth MJ, Darcy PK. Supernatural T cells: genetic modification of T cells for cancer therapy. *Nat Rev Immunol* (2005) 5:928–40. doi:10.1038/nri1729
136. Eshhar Z. Tumor-specific T-bodies: towards clinical application. *Cancer Immunol Immunother* (1997) 45:131–6. doi:10.1007/s002620050415
137. Kuwana Y, Asakura Y, Utsunomiya N, Nakanishi M, Arata Y, Itoh S, et al. Expression of chimeric receptor composed of immunoglobulin-derived V regions and T-cell receptor-derived C regions. *Biochem Biophys Res Commun* (1987) 149:960–8. doi:10.1016/0006-291X(87)90502-X
138. Dotti G, Gottschalk S, Savoldo B, Brenner MK. Design and development of therapies using chimeric antigen receptor-expressing T cells. *Immunol Rev* (2014) 257:107–26. doi:10.1111/imr.12131
139. Johnson LA, June CH. Driving gene-engineered T cell immunotherapy of cancer. *Cell Res* (2017) 27:38–58. doi:10.1038/cr.2016.154
140. Hombach A, Hombach AA, Abken H. Adoptive immunotherapy with genetically engineered T cells: modification of the IgG1 Fc 'spacer' domain in the extracellular moiety of chimeric antigen receptors avoids 'off-target' activation and unintended initiation of an innate immune response. *Gene Ther* (2010) 17:1206–13. doi:10.1038/gt.2010.91
141. Bridgeman JS, Hawkins RE, Bagley S, Blaylock M, Holland M, Gilham DE. The optimal antigen response of chimeric antigen receptors harboring the CD3zeta transmembrane domain is dependent upon incorporation of the receptor into the endogenous TCR/CD3 complex. *J Immunol* (2010) 184:6938–49. doi:10.4049/jimmunol.0901766

142. Finney HM, Lawson AD, Bebbington CR, Weir AN. Chimeric receptors providing both primary and costimulatory signaling in T cells from a single gene product. *J Immunol* (1998) 161:2791–7.
143. Savoldo B, Ramos CA, Liu E, Mims MP, Keating MJ, Carrum G, et al. CD28 costimulation improves expansion and persistence of chimeric antigen receptor-modified T cells in lymphoma patients. *J Clin Invest* (2011) 121:1822–6. doi:10.1172/JCI46110
144. Porter DL, Levine BL, Kalos M, Bagg A, June CH. Chimeric antigen receptor-modified T cells in chronic lymphoid leukemia. *N Engl J Med* (2011) 365:725–33. doi:10.1056/NEJMoa1103849
145. Hackett PB, Largaespada DA, Cooper LJN. A transposon and transposase system for human application. *Mol Ther* (2010) 18:674–83. doi:10.1038/mt.2010.2
146. Hackett PB, Ekker SC, Largaespada DA, McIvor RS. Sleeping Beauty transposon-mediated gene therapy for prolonged expression. *Adv Genet* (2005) 54:189–232. doi:10.1016/S0065-2660(05)54009-4
147. Hudecek M, Izsvak Z, Johnen S, Renner M, Thumann G, Ivics Z. Going non-viral: the Sleeping Beauty transposon system breaks on through to the clinical side. *Crit Rev Biochem Mol Biol* (2017) 52:355–80. doi:10.1080/10409238.2017.1304354
148. Kebriaei P, Izsvak Z, Narayanavari SA, Singh H, Ivics Z. Gene therapy with the Sleeping Beauty transposon system. *Trends Genet* (2017) 33:852–70. doi:10.1016/j.tig.2017.08.008
149. Kebriaei P, Singh H, Huls MH, Figliola MJ, Bassett R, Olivares S, et al. Phase I trials using Sleeping Beauty to generate CD19-specific CAR T cells. *J Clin Invest* (2016) 126:3363–76. doi:10.1172/JCI86721
150. Brown GD, Herre J, Williams DL, Willment JA, Marshall AS, Gordon S. Dectin-1 mediates the biological effects of beta-glucans. *J Exp Med* (2003) 197:1119–24. doi:10.1084/jem.20021890
151. Gringhuis SI, den Dunnen J, Litjens M, van der Vlist M, Wevers B, Bruijns SC, et al. Dectin-1 directs T helper cell differentiation by controlling noncanonical NF-kappaB activation through Raf-1 and Syk. *Nat Immunol* (2009) 10:203–13. doi:10.1038/ni.1692
152. Bowman SM, Free SJ. The structure and synthesis of the fungal cell wall. *Bioessays* (2006) 28:799–808. doi:10.1002/bies.20441
153. Werner JL, Metz AE, Horn D, Schoeb TR, Hewitt MM, Schwiebert LM, et al. Requisite role for the dectin-1 beta-glucan receptor in pulmonary defense against *Aspergillus fumigatus*. *J Immunol* (2009) 182:4938–46. doi:10.4049/jimmunol.0804250
154. Taylor PR, Brown GD, Reid DM, Willment JA, Martinez-Pomares L, Gordon S, et al. The beta-glucan receptor, dectin-1, is predominantly expressed on the surface of cells of the monocyte/macrophage and neutrophil lineages. *J Immunol* (2002) 169:3876–82. doi:10.4049/jimmunol.169.7.3876
155. Willment JA, Marshall AS, Reid DM, Williams DL, Wong SY, Gordon S, et al. The human beta-glucan receptor is widely expressed and functionally equivalent to murine Dectin-1 on primary cells. *Eur J Immunol* (2005) 35:1539–47. doi:10.1002/eji.200425725
156. Cooper LJ, Topp MS, Serrano LM, Gonzalez S, Chang WC, Naranjo A, et al. T-cell clones can be rendered specific for CD19: toward the selective augmentation of the graft-versus-B-lineage leukemia effect. *Blood* (2003) 101:1637–44. doi:10.1182/blood-2002-07-1989
157. Singh H, Manuri PR, Olivares S, Dara N, Dawson MJ, Huls H, et al. Redirecting specificity of T-cell populations for CD19 using the Sleeping Beauty system. *Cancer Res* (2008) 68:2961–71. doi:10.1158/0008-5472.CAN-07-5600
158. Ouyang W, Kolls JK, Zheng Y. The biological functions of T helper 17 cell effector cytokines in inflammation. *Immunity* (2008) 28:454–67. doi:10.1016/j.immuni.2008.03.004
159. Zelante T, De Luca A, Bonifazi P, Montagnoli C, Bozza S, Moretti S, et al. IL-23 and the Th17 pathway promote inflammation and impair antifungal immune resistance. *Eur J Immunol* (2007) 37:2695–706. doi:10.1002/eji.200737409
160. Ivanov II, McKenzie BS, Zhou L, Tadokoro CE, Lepelley A, Lafaille JJ, et al. The orphan nuclear receptor RORgammat directs the differentiation program of proinflammatory IL-17$^+$ T helper cells. *Cell* (2006) 126:1121–33. doi:10.1016/j.cell.2006.07.035
161. Ivanov II, Zhou L, Littman DR. Transcriptional regulation of Th17 cell differentiation. *Semin Immunol* (2007) 19:409–17. doi:10.1016/j.smim.2007.10.011
162. Yang XO, Pappu BP, Nurieva R, Akimzhanov A, Kang HS, Chung Y, et al. T helper 17 lineage differentiation is programmed by orphan nuclear receptors ROR alpha and ROR gamma. *Immunity* (2008) 28:29–39. doi:10.1016/j.immuni.2007.11.016
163. Lamaris GA, Lewis RE, Chamilos G, May GS, Safdar A, Walsh TJ, et al. Caspofungin-mediated beta-glucan unmasking and enhancement of human polymorphonuclear neutrophil activity against *Aspergillus* and non-*Aspergillus* hyphae. *J Infect Dis* (2008) 198:186–92. doi:10.1086/589305
164. Ogonek J, Kralj Juric M, Ghimire S, Varanasi PR, Holler E, Greinix H, et al. Immune reconstitution after allogeneic hematopoietic stem cell transplantation. *Front Immunol* (2016) 7:507. doi:10.3389/fimmu.2016.00507
165. Bonifant CL, Jackson HJ, Brentjens RJ, Curran KJ. Toxicity and management in CAR T-cell therapy. *Mol Ther Oncolytics* (2016) 3:16011. doi:10.1038/mto.2016.11
166. Pana ZD, Roilides E, Warris A, Groll AH, Zaoutis T. Epidemiology of invasive fungal disease in children. *J Pediatric Infect Dis Soc* (2017) 6:S3–11. doi:10.1093/jpids/pix046
167. Bochennek K, Hassler A, Perner C, Gilfert J, Schoning S, Klingebiel T, et al. Infectious complications in children with acute myeloid leukemia: decreased mortality in multicenter trial AML-BFM 2004. *Blood Cancer J* (2016) 6:e382. doi:10.1038/bcj.2015.110
168. Pappanaicken RK, Nathaniel A, Harjeet S, Simon O, Sourindra NM, Tiejuan M, et al. Bioengineered Dectin-1 CAR$^+$ T cells to control invasive fungal infection. *Inaugural International Cancer Immunotherapy Conference*. New York (2016). Abstract A193.
169. Brudno JN, Kochenderfer JN. Toxicities of chimeric antigen receptor T cells: recognition and management. *Blood* (2016) 127:3321–30. doi:10.1182/blood-2016-04-703751
170. Neelapu SS, Tummala S, Kebriaei P, Wierda W, Gutierrez C, Locke FL, et al. Chimeric antigen receptor T-cell therapy – assessment and management of toxicities. *Nat Rev Clin Oncol* (2018) 15:47–62. doi:10.1038/nrclinonc.2017.148
171. DiGiusto D, Cooper L. Preparing clinical grade Ag-specific T cells for adoptive immunotherapy trials. *Cytotherapy* (2007) 9:613–29. doi:10.1080/14653240701650320
172. Yee C. Adoptive T-cell therapy for cancer: boutique therapy or treatment modality? *Clin Cancer Res* (2013) 19:4550–2. doi:10.1158/1078-0432.CCR-13-1367
173. Casati A, Varghaei-Nahvi A, Feldman SA, Assenmacher M, Rosenberg SA, Dudley ME, et al. Clinical-scale selection and viral transduction of human na < ve and central memory CD8(+) T cells for adoptive cell therapy of cancer patients. *Cancer Immunol Immunother* (2013) 62:1563–73. doi:10.1007/s00262-013-1459-x
174. Leen AM, Bollard CM, Mendizabal AM, Shpall EJ, Szabolcs P, Antin JH, et al. Multicenter study of banked third-party virus-specific T cells to treat severe viral infections after hematopoietic stem cell transplantation. *Blood* (2013) 121:5113–23. doi:10.1182/blood-2013-02-486324
175. Park TS, Rosenberg SA, Morgan RA. Treating cancer with genetically engineered T cells. *Trends Biotechnol* (2011) 29:550–7. doi:10.1016/j.tibtech.2011.04.009
176. Cruz CRY, Micklethwaite KP, Savoldo B, Ramos CA, Lam S, Ku S, et al. Infusion of donor-derived CD19-redirected virus-specific T cells for B-cell malignancies relapsed after allogeneic stem cell transplant: a phase 1 study. *Blood* (2013) 122:2965–73. doi:10.1182/blood-2013-06-506741
177. Barker JN, Doubrovina E, Sauter C, Jaroscak JJ, Perales MA, Doubrovin M, et al. Successful treatment of EBV-associated posttransplantation lymphoma after cord blood transplantation using third-party EBV-specific cytotoxic T lymphocytes. *Blood* (2010) 116:5045–9. doi:10.1182/blood-2010-04-281873

Conflict of Interest Statement: Some of the technology described was advanced to clinic through research conducted at MD Anderson Cancer Center by PK and DK. A patent application based on research reported in this manuscript has been filed.

Copyright © 2018 Kumaresan, da Silva and Kontoyiannis. This is an open-access article distributed under the terms of the Creative Commons Attribution License (CC BY). The use, distribution or reproduction in other forums is permitted, provided the original author(s) or licensor are credited and that the original publication in this journal is cited, in accordance with accepted academic practice. No use, distribution or reproduction is permitted which does not comply with these terms.

Advantages of publishing in Frontiers

OPEN ACCESS
Articles are free to read for greatest visibility and readership

FAST PUBLICATION
Around 90 days from submission to decision

HIGH QUALITY PEER-REVIEW
Rigorous, collaborative, and constructive peer-review

TRANSPARENT PEER-REVIEW
Editors and reviewers acknowledged by name on published articles

Frontiers
Avenue du Tribunal-Fédéral 34
1005 Lausanne | Switzerland

Visit us: www.frontiersin.org
Contact us: info@frontiersin.org | +41 21 510 17 00

REPRODUCIBILITY OF RESEARCH
Support open data and methods to enhance research reproducibility

DIGITAL PUBLISHING
Articles designed for optimal readership across devices

FOLLOW US
@frontiersin

IMPACT METRICS
Advanced article metrics track visibility across digital media

EXTENSIVE PROMOTION
Marketing and promotion of impactful research

LOOP RESEARCH NETWORK
Our network increases your article's readership